Y 3. At 7: 16/20-17

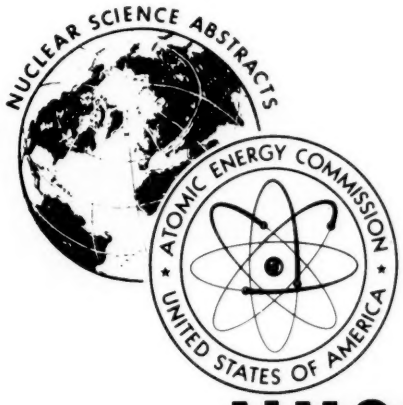

NUCLEAR SCIENCE ABSTRACTS

OCT 3 1966

Volume 20 Number 17

Abstracts 30960–32891

September 15, 1966

MIAMI UNIVERSITY LIBRARY

UNITED STATES ATOMIC ENERGY COMMISSION
Division of Technical Information

USAEC DEPOSITORY LIBRARIES

Collections of USAEC reports are maintained in the libraries of the organizations listed below for reference use by the general public. Facilities for making photocopies are available. The USAEC also makes available through these libraries atomic energy reports of countries other than the U. S. that are abstracted in *Nuclear Science Abstracts*.

ALABAMA
Auburn, Auburn University
ALASKA
College, University of Alaska
ARIZONA
Tucson, University of Arizona
ARKANSAS
Fayetteville, University of Arkansas
CALIFORNIA
Berkeley, University of California
Davis, University of California
Los Angeles, University of California
San Diego, Public Library
Stanford, Stanford University
COLORADO
Boulder, University of Colorado
Denver, Public Library
CONNECTICUT
New Haven, Yale University
DELAWARE
Newark, University of Delaware
DISTRICT OF COLUMBIA
Washington, Library of Congress
FLORIDA
Coral Gables, University of Miami
Gainesville, University of Florida
Tallahassee, The Florida State University
GEORGIA
Atlanta, Georgia Institute of Technology
HAWAII
Honolulu, University of Hawaii
ILLINOIS
Chicago, John Crerar Library
Chicago, University of Chicago
Evanston, Northwestern University
Urbana, University of Illinois
INDIANA
Bloomington, Indiana University
Lafayette, Purdue University
IOWA
Ames, Iowa State University
KANSAS
Manhattan, Kansas State University
KENTUCKY
Lexington, University of Kentucky
Louisville, University of Louisville
LOUISIANA
Baton Rouge, Louisiana State University
New Orleans, Tulane University
MARYLAND
Baltimore, Johns Hopkins University
College Park, University of Maryland
MASSACHUSETTS
Cambridge, Harvard University
Cambridge, Massachusetts Institute of Technology
MICHIGAN
Ann Arbor, University of Michigan
Detroit, Public Library
East Lansing, Michigan State University
MINNESOTA
Minneapolis, University of Minnesota
MISSISSIPPI
State College, Mississippi State University
MISSOURI
Kansas City, Linda Hall Library
Rolla, University of Missouri School of Mines and Metallurgy
St. Louis, Washington University
MONTANA
Bozeman, Montana State College
NEVADA
Las Vegas, Nevada Southern University
Reno, University of Nevada
NEW JERSEY
Princeton, Princeton University
Teaneck, Fairleigh Dickinson University
NEW MEXICO
Albuquerque, University of New Mexico
NEW YORK
Albany, The University of the State of New York
Buffalo, State University of New York at Buffalo
Ithaca, Cornell University
New York, Atomic Industrial Forum, Inc.
New York, Columbia University
New York, New York University
Rochester, University of Rochester
Schenectady, Union College
Syracuse, Syracuse University
Troy, Rensselaer Polytechnic Institute
NORTH CAROLINA
Charlotte, Public Library of Charlotte and Mecklenburg County
Durham, Duke University
Raleigh, North Carolina State College
NORTH DAKOTA
Grand Forks, University of North Dakota
OHIO
Cincinnati, University of Cincinnati
Cleveland, Public Library
OHIO (CONT.)
Columbus, Ohio State University
Toledo, University of Toledo
Youngstown, Youngstown University
OKLAHOMA
Norman, University of Oklahoma
Stillwater, Oklahoma State University
OREGON
Corvallis, Oregon State University
Portland, Reed College
PENNSYLVANIA
Philadelphia, University of Pennsylvania
Pittsburgh, Carnegie Library
University Park, Pennsylvania State University
PUERTO RICO
Rio Piedras, University of Puerto Rico
RHODE ISLAND
Providence, Brown University
SOUTH CAROLINA
Columbia, University of South Carolina
TENNESSEE
Knoxville, University of Tennessee
Memphis, Public Library
Nashville, Joint University Libraries
Oak Ridge, Oak Ridge Associated Universities
TEXAS
Austin, University of Texas
College Station, Texas A & M University
Dallas, Southern Methodist University
Houston, Rice University
Lubbock, Texas Technological College
San Antonio, Public Library
UTAH
Salt Lake City, University of Utah
VIRGINIA
Blacksburg, Virginia Polytechnic Institute
Charlottesville, University of Virginia
Norfolk, Old Dominion College
WASHINGTON
Pullman, Washington State University
Seattle, University of Washington
WEST VIRGINIA
Morgantown, West Virginia University
WISCONSIN
Madison, University of Wisconsin
Milwaukee, Public Library
WYOMING
Laramie, University of Wyoming

Volume 20, Number 17, September 15, 1966

NUCLEAR SCIENCE ABSTRACTS

A semimonthly publication of the USAEC Division of Technical Information, Edward J. Brunenkant, Director.
Published by the USAEC Division of Technical Information Extension, Robert L. Shannon, Extension Manager.

Nuclear Science Abstracts covers the international literature on nuclear science and technology and provides the only comprehensive abstracting and indexing of this body of information. Published twice each month since 1947, *NSA* covers technical reports of the U. S. Atomic Energy Commission and its contractors, technical reports of U. S. Government agencies and other governments, universities, industrial and research organizations, as well as patents, books, and journal literature on a world-wide basis. Nearly 350,000 abstracts have appeared in *NSA* through Volume 19. The subject matter covered in *NSA* is described in issue Number 1 and in TID-4552, *Subject Scope of Nuclear Science Abstracts*, available free from the U. S. Atomic Energy Commission, Division of Technical Information Extension, P. O. Box 62, Oak Ridge, Tennessee 37830.

Abstracts are arranged according to a number of subject categories and subcategories. Definitions of categories appear in issues Number 1 and 13. If the language of the original item is not English, the language will be indicated. Translations are not abstracted where an abstract of the original item has appeared in *NSA*.

INDEXES TO NSA

Corporate author, personal author, subject, and report number indexes appear in each issue and are cumulated quarterly, semiannually, and annually. Multi-volume cumulations have been issued as indicated on the following page. Report number indexes for all volumes (1–18) were issued at the end of Vol. 18. At the end of Vol. 19, the indexes for Vols. 1–15 were reissued to include additional public availability information. This cumulation will be a permanent shelf item and will not be reissued. Report number indexes for Vol. 19 are included as a cumulation beginning with Vol. 16.

AVAILABILITY OF PUBLICATIONS ABSTRACTED

The public availability of all U. S. Atomic Energy Commission reports is indicated in the report number indexes. The availability of other reports, when known, is also indicated. The availability of some unnumbered reports is given in the abstract.

Dissertations abstracted in *Dissertation Abstracts* and included in *NSA* are available from University Microfilms, Inc., 315 N. First Street, Ann Arbor, Michigan 48103.

Most of the published literature abstracted in *NSA* is on deposit at the Library, Oak Ridge Associated Universities, Oak Ridge, Tennessee, (a USAEC depository library) and is available through interlibrary loan. When requesting papers from this source, it is important that *NSA* volume and abstract number be cited.

HOW TO OBTAIN NUCLEAR SCIENCE ABSTRACTS

NSA is available on an exchange basis to universities, research institutions, industrial firms, and publishers of scientific information. Inquiries should be directed to the U. S. Atomic Energy Commission, Division of Technical Information Extension, P. O. Box 62, Oak Ridge, Tennessee 37830.

Government agencies may obtain *NSA* free of charge.

NSA is available to the general public on a subscription basis from the Superintendent of Documents, U. S. Government Printing Office, Washington, D. C. 20402, as follows:

For the 24 regular issues, $30.00 domestic, $37.00 foreign. A single issue costs $1.75, plus 25 per cent for foreign mailing. Domestic rates apply to the United States, Canada, Mexico, and Central and South American countries except Argentina, Brazil, Guyana and French Guiana, Surinam, and British Honduras. Foreign rates apply to the countries excepted above and to all other countries throughout the world.

For the quarterly, semiannual, and annual indexes, $22.00 domestic, $25.00 foreign.

Multivolume subject and author indexes are available as follows:

Vols. 1–4 (1948–1950) Johnson Reprint Corporation, 111 Fifth Avenue, New York, N. Y. 10003, $30.00.

Vols. 5–10 (1951–1956) Superintendent of Documents, U. S. Government Printing Office, Washington, D. C. 20402, $5.25.

Vols. 11–15, Subjects, Superintendent of Documents, U. S. Government Printing Office, Washington, D. C. 20402, $19.00.

Vols. 11–15, Personal Authors, Superintendent of Documents, U. S. Government Printing Office, Washington, D. C. 20402, $14.25.

Vols. 11–15, Corporate Authors, Superintendent of Documents, U. S. Government Printing Office, Washington, D. C. 20402, $2.50.

Cumulative Report Number Index, Vols. 1–15, Revised, is available from the Superintendent of Documents, U. S. Government Printing Office, Washington, D. C. 20402, $4.00.

Cumulative Report Number Index, Vols. 16–19, is available from the Superintendent of Documents, U. S. Government Printing Office, Washington, D. C. 20402, $2.50.

Annual Indexes are available separately from the U. S. Government Printing Office as follows:

Vol. 16, Subject and Authors, $9.75.
Vol. 17, Subject and Authors, $12.25.
Vol. 18, Subject and Authors, $12.50.
Vol. 19, Subject and Authors, $12.50.

ACKNOWLEDGMENTS

Agreements between the United States Atomic Energy Commission and the following organizations with regard to providing continuing services and specific literature coverage for *Nuclear Science Abstracts* are gratefully acknowledged:

American Institute of Physics; Atomic Energy of Canada Limited; Atomic Energy Research Establishment, United Kingdom; European Atomic Energy Community (EURATOM); Gmelin Institute; International Atomic Energy Agency; Japan Atomic Energy Bureau — Japan Atomic Energy Research Institute; Netherlands Patent Office; Reactor Centrum Nederland.

TABLE OF CONTENTS

Volume 20, Number 17, September 15, 1966

Category	*Page*
BIOLOGY AND MEDICINE	3775
General	3775
Ecology	3775
Metabolism, Tissue Distribution, and Toxicology	3775
Radiation Effects on Biochemicals	3779
Radiation Effects on Tissues	3783
Radiation Effects Therapy and Countermeasures	3797
Radiation Hazards and Protection	3800
Radiotherapy and Radiodiagnosis	3800
CHEMISTRY	3803
General	3803
Analytical Procedures	3803
Inorganic and Physical Chemistry	3808
Organic Chemistry	3813
Radiation Chemistry	3814
Radiochemistry	3819
Separation Processes and Procedures	3820
ENGINEERING	3822
General	3822
Applications of Nuclear Explosions	3823
Facilities and Equipment	3823
Heat Transfer and Fluid Flow	3823
Materials Testing	3825
Space Propulsion	3826
Vacuum Engineering	3831
GEOLOGY, METEOROLOGY, AND MINERALOGY	3832
General	3832
Natural Radioactivity and Fallout	3832
Site Survey and Selection	3835
Techniques and Equipment	3836
Thorium and Uranium Minerals	3837
HEALTH AND SAFETY	3838
INSTRUMENTATION	3843
General	3843
Radiation Detection	3845
Radiation Effects	3856
ISOTOPE TECHNOLOGY	3858
General	3858
Industrial Applications	3858
Power Application	3859
Separation and Production	3859
MATHEMATICS AND COMPUTERS	3861
METALS, CERAMICS, AND OTHER MATERIALS	3864
General	3864
Corrosion	3865
Fabrication	3867
Properties and Structure	3869
Radiation Effects	3877
PHYSICS	3881
General	3881
Accelerators	3881
Astrophysics and Cosmology	3885
Atomic Physics	3890
Cosmic Radiation	3896
Direct Energy Conversion	3897
Elementary Particles and Radiations	3900
Field Theory, Scattering Theory, and Symmetries	3912
Fluid Physics and Thermodynamics	3923
Geophysics	3925
Gravitation, Quantum Mechanics, and Relativity Theory	3931
Low Temperature Physics	3933
Neutron Physics	3937
Nuclear Properties and Reactions	3939
Plasma Physics and Thermonuclear Processes	3960
Shielding	3973
Solid State Physics	3974
REACTOR TECHNOLOGY	3982
General	3982
Auxiliaries and Components	3982
Criticality Studies	3984
Design and Feasibility	3987
Fuels	3987
Power and Power-Breeder Reactors	3988
Process Heat Reactors	3992
Propulsion and Space	3993
Research and Test Reactors	3994
WASTE DISPOSAL AND PROCESSING	3998
GENERAL AND MISCELLANEOUS	3999
CORPORATE AUTHOR INDEX	INDEX-1
PERSONAL AUTHOR INDEX	INDEX-7
SUBJECT INDEX	INDEX-49
REPORT NUMBER INDEX	INDEX-122

STAFF OF NUCLEAR SCIENCE ABSTRACTS

MANAGING EDITOR

John W. Norris

ASSISTANT MANAGING EDITOR

Donald D. Davis

ASSOCIATE EDITORS

Lawrence T. Whitehead
David E. Bost
Robert C. Kelly
Lee M. Thompson

SUBJECT INDEX EDITOR

Everett J. Hoffman

EVALUATORS

William D. Matheny
John H. Mitchell
Mary H. Newman

ABSTRACTORS

F. S. Armstrong (AECL)
Jane G. Buchanan
D. Lamar Cason
Bennie G. Di Bona
Helen G. Donald
James R. Dulaney
Wells L. Green
Mary Catherine Grissom
Fernando J. Hamilton
Phyllis C. Hansen
Carolyn D. Houston
Rose V. Jermain
Betty L. McDowell
Jean F. Peckham
Mona H. Raridon
Julia S. Redford
Francis L. Sachs
Lila B. Smith
Charles E. Stuber
Martha J. Thomas
Anne G. Ward
David C. West
Milton O. Whitson
Gabriel O. Ycaza

SUBJECT HEADING SPECIALIST

Robert E. Upchurch

CORPORATE AUTHOR SPECIALIST

Clara L. Fox

DESCRIPTIVE CATALOGING SPECIALIST

J. Paul Meredith

SCHEDULING AND PUBLISHING COORDINATOR

Brainard L. Patton

Communication concerning the editorial policy and content of *NSA* should be addressed to the Managing Editor, *Nuclear Science Abstracts*, AEC Division of Technical Information Extension, P. O. Box 62, Oak Ridge, Tennessee 37830.

Use of funds for printing this publication approved by the Director of the Bureau of the Budget, June 28, 1966.

Volume 20, Number 17 September 15, 1966

NUCLEAR SCIENCE ABSTRACTS

BIOLOGY AND MEDICINE

General

30960 (BNWL–235-4, pp 22-5) ANIMAL ACTIVITY MONITOR DEVELOPMENT. Wilbur, R. L. (Battelle-Northwest, Richland, Wash. Pacific Northwest Lab.).

A method is being developed to monitor the physical activity of animals in physiological experiments by providing X-Y position data and time. A system is described consisting of two animal cages with floor transducers to monitor the animals positions. One cage is used as the control while the second monitors animals under test. The signals provide either digital readouts or magnetic tape readouts for later use on a computer. (J.R.D.)

30961 (BNWL–235-4, pp 25-9) ANIMAL PHYSIOLOGICAL FUNCTION TELEMETRY DEVELOPMENTS. Hoitink, N. C.; Porter, N. S.; Ratcliffe, C. A. (Battelle-Northwest, Richland, Wash. Pacific Northwest Lab.).

A measurement and telemetry system was developed to provide continuous monitoring of several physiological functions of free-ranging animals. The system comprises appropriate sensors, three channels of FM/FM telemetry, and appropriate receiving and readout instruments. Body temperature, respiration rate, and heart rate are monitored. Successful operation can be achieved over a 200-ft range with the equipment. (auth)

30962 (JPRS–35315) STUDIES IN HIGHER NERVOUS ACTIVITY. Translated from Zh. Vyssh. Nerv. Deyatel'nosti im. I. P. Pavlova, 16: 34-51; 62-6; 82-7; 96-101; 103-11; 117-23; 125-30; 134-5(1966). 89p. (TT–66-31751). CFSTI $3.00 cy, $0.75 mn.

Translations of 10 articles that discuss various aspects of higher nervous activity are presented. A separate abstract was prepared on one article. (C.H.)

For an abstract of the individual paper see: 31037.

30963 PHYSICAL APPROACH TO THE VISUAL RECEPTOR PROCESS. Rosenberg, Barnett (Michigan State Univ., East Lansing). Contract Nonr-2587(96). Advance. Radiat. Biol., 2: 193-241(1966).

The detailed mechanism which converts the optical excitation of a visual pigment into a discharge of the optic nerve is not known. Theories and model systems that have been proposed are reviewed. The solid state biophysical approach to problems of the functioning of the visual receptor structure is discussed in detail. Topics discussed include photoreceptor ultrastructure, a solid state theory of the receptor, the photoconduction theory of the receptor process, model systems, photoconduction in β-carotene, photovoltaic effects in carotenoid pigments, the role of the triplet state, photoconduction as a process competitive with photoisomerism, photoconductivity as an amplifying process, color responses in photoconductive carotenoid cells, the relation of color responses in carotenoid cells to electrophysiological data, and conductivity in proteins and photoreceptors. (80 references.) (C.H.)

30964 LYSOSOMAL MODIFICATIONS AFTER ADMINISTRATION OF RADIOPROTECTIVE DRUGS. Hugon, J.; Maisin, J. R.; Borgers, M. (CEN, Mol, Belg.). Experientia, 22: 235-6(1966).

Morphologic effects of a mixture of AET, glutathione, and serotonin were investigated in stem cells of the duodenal crypt in mice. Dense vacuoles increasing greatly in the first hours following injection were presumed to be lysosomes. In sections treated for acid phosphatase activity, the number of reactive sites was much higher than in the controls. Observations showed that radioprotective drugs are not easily metabolized by cells. In the mixture studied, it is likely that the drug liable for the increased lytic activity is AET for neither glutathione nor serotonin, given separately, provoked similar lesions. (H.G.D.)

30965 RADIOISOTOPE APPLICATIONS IN MEDICINE. (International Atomic Energy Agency, Vienna). pp 101-14 of STI-DOC–10/53.

Radioisotope investigations of the cause of endemic goiter in various places in the Philippines are discussed. Studies of the metabolism of iodinated amino acids in humans are reported. (M.C.G.)

30966 ULTRAFINE STRUCTURE OF RADIORESISTANT FLEXNER BACILLI. Pavlova, I. B.; Pershina, Z. G. (Gamalin Inst. of Epidemology and Microbiology, Moscow). Zh. Mikrobiol. Epidemiol. Immunobiol., No. 3, 8-10(Mar. 1966). (In Russian).

The ultrastructure of Flexner bacilli is described. Cell wall structure was particularly distinctive and complex intracytoplasmic membranous structures were noted around the nucleus and at the periphery of the cell. The nucleus, occupying an insignificant portion of the cell, was often represented by agglomerates of its fibrillar component. The cytoplasm was composed of granules about the size of ribosomes. Mitosis was similar to that in gram-positive organisms. (H.G.D.)

Ecology

30967 (TID–3910(Suppl.4)) TERRESTRIAL AND FRESHWATER RADIOECOLOGY. A Selected Bibliography. Klement, Alfred W. Jr.; Schultz, Vincent (Division of Biology and Medicine (AEC), Washington, D. C.). Jan. 1966. 130p. Dep. mn. CFSTI $1.50 cy, $1.00 mn.

References are presented to 1291 recent publications on terrestrial and freshwater ecology. Emphasis is placed on publications reporting the cycling of fallout fission products in ecological systems. (C.H.)

Metabolism, Tissue Distribution, and Toxicology

Refer also to abstracts 31441, 31442, and 31444.

30968 (BNWL–SA–11) WHOLE-BODY COUNTING OF PLUTONIUM IN DOGS. Swinth, K. L.; Griffin, B. I.;

Park, J. F. (Battelle-Northwest, Richland, Wash. Pacific Northwest Lab.). May 19, 1965. Contract AT(45-1)-1830. 19p. Dep. mn. CFSTI $1.00 cy, $0.50 mn.

Thin NaI(Tl) scintillation counters were used for the assessment of body burdens in dogs exposed to ^{239}Pu aerosol. Experiments were made with both a dog phantom and live dogs. The count rate was affected by changes in dog size, isotopic composition of the plutonium, and by plutonium distribution in the body. A 50% change in dog weight made a change of a factor of two in counting efficiency in some experiments. The sensitivity for a typical dog when counting the x rays emitted is 2.1 cpm/nC and 14.0 cpm/nC when counting both x rays and 60 kev gamma rays. This sensitivity is based on body burdens determined by post-mortem alpha counting analysis of the tissues of several dogs. Data are included on 30 exposed dogs, which had body burdens ranging from 0.12 to 2.9 μC. (auth)

30969 (BNWL-SA-45) THE UPTAKE AND RETENTION OF ^{32}P AND ^{65}Zn FROM THE CONSUMPTION OF COLUMBIA RIVER FISH. Honstead, John F.; Brady, David N. (Battelle-Northwest, Richland, Wash. Pacific Northwest Lab.). June 7, 1965. Contract At(45-1)-1830. 19p. Dep. mn. CFSTI $1.00 cy, $0.50 mn.

The uptake and whole-body retention of ^{32}P and ^{65}Zn was studied in subjects whose diet contained measured quantities of Columbia River fish. The ^{32}P and ^{65}Zn content of duplicate fish samples was measured. An instrument developed for measuring ^{32}P in vivo gave good agreement with whole-body counting data. Preliminary results indicated that all subjects absorbed more than 95% of the ^{32}P available in the fish while ^{65}Zn absorption ranged from 31 to 50% of that available in the fish. The effective half-life of ^{65}Zn was 150 days. There appeared to be greater variation in the metabolic parameters of fractional absorption and effective half-life in the case of ^{65}Zn than was apparent for ^{32}P. (C.H.)

30970 (COO-1170-5) COMPARATIVE TOXICITY OF STABLE RARE EARTH COMPOUNDS. Technical Progress Report for 1964. (Iowa State Univ. of Science and Technology, Ames. Veterinary Medical Research Inst.). Dec. 31, 1964. Contract AT(11-1)-1170. 72p. ORAU.

Progress is reported in studies of the toxic effects of stable rare earth compounds in laboratory animals. Data are included on the chronic, life-time effects of subcutaneous implants of Gd, Dy, Pr, Ce, and Yb in mice; the tissue distribution of intratracheally administered oxides and citrates of Ce, Gd, Nd, Dy, Y, and Yb in guinea pigs and rats; the pathological effects resulting from breathing an aerosol of stable Nd_2O_3 of known particle size range and concentration in mice and guinea pigs; and the effects of breathing moderate concentrations of Y_2O_3 in Rhesus monkeys and dogs. A study in mice indicated a statistically significant difference in hematological values associated with sex and with aging. (C.H.)

30971 (ORINS-45) LABELING OF MYELOMA CELLS AND LEUKEMIC LEUKOCYTES IN SHORT-TERM CULTURE WITH TAGGED PRECURSORS OF NUCLEIC ACID AND PROTEIN. Saito, Hiroshi; Nagai, Teruo (Oak Ridge Inst. of Nuclear Studies, Inc., Tenn.). Aug. 1964. Contract AT(40-1)-Gen-33. 18p. Dep. mn. CFSTI $1.00 cy, $0.50 mn.

The metabolism of nucleic acids and proteins was studied in cultured bone marrow cells from patients with multiple myeloma, lymphatic leukemia, and mild polycythemia by means of microscopic autoradiography and precursors labeled with ^{14}C, ^{3}H, or ^{35}S. Infrequent DNA synthesis by myeloma cells was suggested by the fact that uptake of thymidine was seen only in a small percentage. Extranuclear grains over myeloma cells after a longer incubation interval with thymidine possibly indicated cytoplasmic DNA synthesis. The RNA and protein synthesis in myeloma cells seemed very active. Use of formate for the synthesis of protein in myeloma cells was suggested. No uptake of thymidine was observed in two cases of chronic lymphocytic leukemia cells. This suggests exceedingly low DNA synthesis. (28 references.) (C.H.)

30972 (TID-22027) ^{90}Sr IN BEAGLE HAIR. Della Rosa, R. J.; Peterson, G.; Gielow, F. (California Univ., Davis. School of Veterinary Medicine). [1963]. Contract AT(04-3)-472. 10p. Dep. mn. CFSTI $1.00 cy, $0.50 mn.

Hair clippings obtained at various times during the chronic ingestion of ^{90}Sr by beagles indicate that in the transfer from diet to hair, the mean $^{90}Sr/Ca$ ratio of hair was 0.42 that of the diet, and the mean $^{90}Sr/Ca$ ratio of plasma to hair was 1.0. Following the end of ^{90}Sr feeding, the mean $^{90}Sr/Ca$ ratio of hair taken at 100 day intervals, relative to plasma was consistently greater than unity, and was 1.5 to 2.0 times that of plasma at one-year post-feeding. The ^{90}Sr content of hair can be used to estimate the radionuclide concentration of the diet and plasma and, indirectly, the portion of the labeled skeleton undergoing remodeling. (auth)

30973 MECHANISM OF STRONTIUM DEPOSITION IN BONE TISSUE. Berger, H. J.; Eger, W. (Univ., Goettingen, Ger.). Acta Histochem., 22: 298-308(1965). (In German).

In vitro studies of Sr uptake by bone were conducted in distal femur tissue decalcified electrolytically. The bone was incubated in 0.1, 0.01, and 0.001M solutions of $SrCl_2$ for one hr, and the Sr uptake by bone was demonstrated histochemically with Na N,N-naphthylhydroxylamine and by Na rhodizonate. Strontium was found by this means to be preferentially taken up in the growth zone and epiphyseal cartilage; little Sr appeared in the metaphysis. Thus, Sr showed the same predilection for developing bone ground substances as Ca. These sites were high in acid mucopolysaccharides, as shown by histochemical tests for these ground substance components. Strontium was not adsorbed by fully developed bone tissue, where neutral polysaccharides (periodic acid-Schiff-positive) predominate. Uptake of Sr was rapid, reaching a maximum in a few minutes with 0.01M $SrCl_2$ solution. When $CaCl_2$ solutions were present simultaneously at equal concentrations, more Sr than Ca was taken up by developing bone tissue. It was concluded that Sr is preferentially taken up in osteoid seams by newly formed ground substance mucopolysaccharides. (BBB)

30974 STUDY OF LABILE STATES OF BIOLOGICAL MOLECULES WITH FLASH PHOTOLYSIS. Grossweiner, Leonard I. (Illinois Inst. of Tech., Chicago). Contract AT(11-1)-1052. Advance. Radiat. Biol., 2: 83-133(1966).

Flash photolysis is an experimental method in which a substance is irradiated with an intense light flash and the short-lived photochemical intermediates produced by the light are identified and followed by fast measurements of their optical absorption spectra. Applications of the technique in investigations of the labile states of proteins, amino acids, visual pigments, chlorophyll, and sensitizing dyes are reported. Factors that influence the path of optical excitation are discussed. (225 references.) (C.H.)

30975 ULTRASTRUCTURAL ALTERATIONS IN DEUTERIUM INTOXICATION. Zunker, Heinz O. H.; McKay, Donald G. (Columbia Univ., New York). Contracts AT(30-1)-1803; Nonr-4259(02). Arch. Pathol., 82: 18-26(July 1966).

Deuterium intoxication was studied in three groups of animals that ingested 75% D_2O-drinking water. In one group, four pregnant rats were given deuterium, starting the tenth day of gestation. Histologic study revealed areas of pyknotic nuclei in renal tubules and basement membrane thickening of salivary gland acini. Another group, given deuterium starting the 15th day of gestation, were sacrificed five days later. Electron microscopic study showed an increase of large vacuoles and electron-dense cytoplasmic bodies in the cells of the proximal convoluted tubule. Enlargement of the endothelial and epithelial glomerular cells resulted in partial obliteration of capillary lumina. Degradation of the endoplasmic structures was seen in the cells of the salivary gland acini. In the third group, two mice received deuterium for nine to ten days. Alterations were more pronounced, with varying degrees of degeneration present in the cells of the proximal convoluted tubules.

Observations suggest an effect of deuterium on organs concerned with water transfer. (auth)

30976 STUDIES ON THE METABOLISM OF ISOLATED CELLS. INVESTIGATION OF FACTORS ACTING ON THE INCORPORATION OF RADIOPHOSPHORIC ACID IN THE RNA OF THE RAT HEPATOCYTES. Mallevais, Jean-Pierre; Segard, Emile; Montreuil, Jean (Institut de Recherches sur le Cancer, Lille). Compt. Rend., Ser. D, 262: 1892-5(Apr. 25, 1966). (In French).

A systematic study was made of the influence of different factors on the in vitro incorporation of radiophosphates into the RNA of isolated rat liver, using an original procedure. The optimum conditions of incubation were defined. The regulatory action of various mineral ions was also studied and a relation between the synthesis of RNA and the respiratory phenomena was established. The significant inhibiting effect of calcium salts and of ceric compounds, whose nature is still unknown, was emphasized. (tr-auth)

30977 THE RELATION BETWEEN THE EXCRETION OF RADIOSTRONTIUM AND THE INTAKE OF Na PHYTATE. Gotoh, Shiroh; Seki, Hiromaro; Hayami, Hiroshi (Tokyo-to Labs. for Medical Sciences, Tokyo). Eiyo To Shokuryo, 16: 522-4(1964). (In Japanese).

The amount of ^{90}Sr excreted by rats fed radiostrontium with a high calcium diet was greater than that of a low-calcium diet group. The relation between the Na phytate intake and the excretion of ^{90}Sr and Ca was investigated, because of the known interference of phytic acid on calcium absorption. When the amount of ^{90}Sr excreted in feces and urine and the uptake of femur were observed, there was no significant difference between two groups fed on Na phytate diet and control diet. Rats were fed a synthetic basal diet containing 0.625% Ca, to which ^{90}Sr was added at the level 0.82 μC/day. When phytate was fed, the daily excretion of ^{90}Sr in the urine dropped from a control level of 1.0 to 0.8% of the injected dose and in the feces from 2.5 to 2.1%, but these changes were not significant. The Ca content of femur decreased from 156.4 in controls to 154.0 mg/100 g in phytate-fed animals while the ^{90}Sr content rose from 8.7 to 9.3% (of the injected dose). These changes were not significant either. (BBB)

30978 ^{86}Rb ACCUMULATION AND DULCITOL DISTRIBUTIONS IN LENSES OF GALACTOSE-FED RATS. Cotlier, Edward; Becker, Bernard (Washington Univ., St. Louis). Exp. Eye Res., 4: 340-5(Dec. 1965).

An early decrease in ^{86}Rb uptake was found in lenses of galactose-fed rats. Dissections in normal rat lenses showed that ^{86}Rb accumulation occurred in areas closer to the lens epithelium. The decreased uptake in lenses of galactosemic rats occurred in all lens areas; however, these lenses recovered in ability to accumulate ^{86}Rb following galactose withdrawal from the diet. High dulcitol (galactitol) levels were found in lenses of galactose-fed rats. Dulcitol accumulations in the lens suggested a possible inhibitory role of this metabolite on the concentrating mechanisms of cations and amino acids in the lens during the development of galactose cataract in rats. The accumulation of dulcitol by rat lenses is explained in terms of a deficiency of a polyol dehydrogenase for this metabolite. There were marked concentration differences of dulcitol between the lens and aqueous humor of galactosemic rats. Only traces (1–2 mmoles/liter) of dulcitol were detectable in aqueous humor and plasma of rats with early galactose lens changes. At the time nuclear opacities were visible, however, dulcitol concentrations decreased markedly in the lens and increased in the aqueous humor. Lens Na^+ concentrations and ^{22}Na uptakes were also altered in lenses of galactose-fed rats. Decreased concentrations of free amino acids in lenses of rats as early as 4 days after starting a galactose diet suggests a similar early defect in the amino acid pumps. (BBB)

30979 WASHOUT OF INTRAARTERIALLY INJECTED ^{85}Kr FROM THE INTESTINE OF THE CAT. Lundgren, O.; Kampp, M. (Univ., Goteborg). Experientia, 22: 268-70(1966).

Tissue clearance techniques were used to study ^{85}Kr metabolism in the intestine of cats. Gamma radiation was recorded by an external scintillation detector collimated in such a way that only radiation from the intestine was registered. In most experiments beta activity was also recorded by means of a Geiger-Mueller tube placed either in the lumen of the intestine or against the outside of the gut in such a way that only activity from the intestinal wall was registered. The radioactivity decay was multiexponential and was the sum of four monoexponential components. Localization and functional significance of these components are as yet not completely known. Data suggest that the fourth component is located outside the intestinal wall, the third in the muscularis of the intestine, and that the first two are shunted between the arterial and venous ends of the capillary loops. (H.G.D.)

30980 PREDICTING THE TOTAL PROJECTED INTAKE OF RADIOIODINE FROM MILK BY MAN. I. THE SITUATION WHERE NO COUNTER MEASURES ARE TAKEN. Lengemann, F. W. (Cornell Univ., Ithaca, N. Y.). Contract AT(30-1)-2147. Health Phys., 12: 825-30(June 1966).

A method of predicting the total intake commitment of radioiodine by an average member of the human population after a single contamination of pastures is presented. Equations for the radioiodine transfer to milk with time are presented for cows given twice-daily doses of radioiodine. These curves are then modified to account for intake of radioiodine by the cow, radioactive decay, residence time of the radioisotope on vegetation, time delay from production to consumption, and the volume of milk consumed by the average individual. This is then integrated to calculate total radioiodine intake commitment by the human population. Ratios were then calculated by dividing the total intake of radioiodine from 0 to infinite time by the concentration of radioiodine in milk from day 1 to day 15. From a table of these ratios it is possible to predict the total radioiodine intake of an average individual knowing the level of radioiodine in a sample of milk and the time relation of that sample to the initial contamination of the pastures. This method makes it possible to estimate the radioiodine consumed by the human population without estimating the intake of radioiodine by the dairy cow. (auth)

30981 PREDICTING THE TOTAL PROJECTED INTAKE OF RADIOIODINE FROM MILK BY MAN. II. THE SITUATION WHERE COUNTER MEASURES ARE EMPLOYED. Lengemann, F. W. (Cornell Univ., Ithaca, N. Y.). Contract AT(30-1)-2147. Health Phys., 12: 831-5(June 1966).

Data from cows given single doses of radioiodine and from cows given radioiodine for 14 consecutive days showed that the decline in milk radioactivity after ingestion of radioiodine ceases is influenced by the number of days of radioiodine intake. An equation was developed to estimate the rate of decline after any given number of days of radioiodine intake by the cow. This equation was then used to estimate the intake of radioiodine from milk by humans after the change of cattle to stored feeds. These intakes are added to the radioiodine consumed before the protective action is operative and this sum in turn is expressed as a percentage of the projected total intake if no action is instituted. From a graph of these values it is possible to estimate the reduction of radioiodine intake as a function of when action is begun. The chart also compares the effectiveness of the procedure of changing cattle to uncontaminated feed to that of entirely eliminating radioactive milk from the human diet. (auth)

30982 ESTIMATION OF STABLE SULPHUR IN HUMAN TISSUE. Minski, Margaret; Cleary, J. J. (Radiological Protection Service, Belmont, Eng.). Health Phys., 12: 837-42(June 1966).

The estimation of sulfur in human testes and several other organs of the body is described. The concentration in most tissues, including testes, falls in the range 1 to 2 mg/g, but the concentration in cartilage is higher, namely, 5.5 mg/g, while that in bone marrow is less. No change in sulfur concentration of testes with age was

found. The mean concentration of stable sulfur in adult human tissues was 1.7 mg S/g wet weight and for testes was 1.3 mg S/g wet weight. It was concluded that when considering intake of ^{35}S the whole body rather than testes should be considered as the critical organ. The new estimates for tissue concentration, together with information on the daily sulfur intake, are consistent with a biological half-time for sulfur in the whole body of 90 days, in agreement with the value reported in the Recommendations of the International Commission on Radiological Protection. (auth)

30983 CREATININE IN URINE AS AN INDEX OF URINARY EXCRETION RATE. Jackson, S. (United Kingdom Atomic Energy Authority, Harwell, Eng.). Health Phys., 12: 843-50(June 1966). (AHSB(RP)M-37).

When internal contamination with a radionuclide is investigated by the analysis of urine, it is essential to know the period of metabolic activity represented by each sample of urine. A genuine 24-hr sample is the ideal, but it is not always possible to be certain that complete accurately timed 24-hr collections of urine have been made. The best internal standard appears to be the normal creatinine content of urine. A comprehensive consideration of the literature on human creatinine excretion is presented. The creatinine excretion rate of an individual person is almost constant and is correlated with the potassium content of the body. When the excretion of an individual has not been measured, standard values for creatinine excretion rate of 1.7 g/day for men and 1.0 g/day for women may be used but from these values, the sample time is only reliable to within a factor of 0.5 to 1.5 (95 per cent limits of confidence). (auth)

30984 EFFECT OF CYSTAMINE ON RESPIRATION, OXIDATIVE PHOSPHORYLATION, AND ULTRASTRUCTURE OF RAT MITOCHONDRIA. Firket, H.; Lelievre, P. (Univ., Liege). Int. J. Radiat. Biol., 10: 403-15(1966). (In French).

The effects of cystamine on the ultrastructure of rat liver, spleen, lymph nodes, and thymus and on respiration and oxidative phosphorylation of mitochondria isolated from liver and spleen were studied. Modifications in the ultrastructure of mitochondria in hematopoietic tissues were observed shortly after injection of cystamine. No change was seen in the liver. Cystamine caused inhibition of respiration and oxidative phosphorylation of mitochondria isolated from both spleen and liver. Results are correlated with respiration of whole animals and the duration of the radioprotective effect of cystamine in rats. (C.H.)

30985 EFFECTS OF SOIL FRACTIONS ON UPTAKE OF ^{90}Sr INTO THE PLANTS. Gulyakin, I. V.; Yudintseva, E. V.; Korovkina, A. V. Izv. Timiryazevsk. Sel'skokhoz. Akad., No. 4, 36-47(1965). (In Russian).

The results of studies on the effects of different mechanical properties in soils on the uptake of ^{90}Sr by plants and its accumulation in crops indicate that of the soil components slime decreases the radiostrontium uptake and accumulation the most. The slime used in these tests contained calcium in the absorbed state and was very similar to the muddy fractions of natural soils. It strongly fixed the absorbed ^{90}Sr and by its effect with respect to the decrease of the accumulation of this radioisotope in the harvest approached that of natural soil. The slime fractions, from which the calcium was removed, also significantly decreased the accumulation of ^{90}Sr in the harvest. (tr-auth)

30986 CELL DIVISION: PRESSURE-INDUCED REVERSAL OF THE ANTI-MEIOTIC EFFECTS OF HEAVY WATER IN THE ÖOCYTES OF THE STARFISH, ASTERIAS FORBESI. Marsland, Douglas; Hiramoto, Yukio (Marine Biological Lab., Woods Hole, Mass.). J. Cell. Physiol., 67: 13-22(Feb. 1966).

Meiotic activity in the öocytes of the starfish, Asterias forbesi, may be blocked by immersion in deuterated sea water (60% or more) as is judged by a stoppage in the breakdown of the germinal vesicles and a failure of the cells to form persistent polar bodies. These anti-meiotic effects of heavy water were reversed in significant degree by application of suitable intensities (3,000 to 6,000 psi) of hydrostatic pressure. In this regard meiosis resembles mitosis, as studied previously in the first cleavage division of the sea urchin, Strongylocentrotus purpuratus. In studying germinal vesicle breakdown, immersion of the öocytes in the deuterated (60, 70, and 80% D_2O) sea water was initiated ten minutes after shedding and pressurization was established six minutes later. None of the non-pressurized deuterated cells showed complete breakdown of the germinal vesicle, whereas complete breakdown was observed in a significant percentage of the pressurized deuterated specimen. In studying their capacity to form and maintain polar bodies, the öocytes were deuterated 60 minutes after shedding and pressurized six minutes later. Maximum release from deuterational blockage, as judged by the percentage of persistent polar bodies after one hour of treatment, was as follows: 85% at 2,000 psi for 50% D_2O; 65% at 2,500 psi, for 60%; 77% at 3,000 psi for 70%; 55% at 3,500 psi for 80% and 65% at 3,500 psi for 90%. Persistence of polar bodies in the non-pressurized deuterated cells did not exceed 15% in any medium containing 60% or more of D_2O and the average persistence in such media was only 2.5%. Basic mechanisms which may account for the observed effects are discussed. (auth)

30987 EFFECT OF GREEN TEA AND RELATED SUBSTANCES ON THE GASTROINTESTINAL ABSORPTION OF ^{90}Sr. Ukai, Teiji; Hayashi, Eiichi; Saito, Shigeko; Tamamura, Shozo; Inohara, Sumiko; Tamemasa, Osamu; Tao, Atake; Okada, Shoji (Shizuoka Coll. of Pharmacy, Japan). J. Radiat. Res. (Jap.), 6: 55-63(June 1965).

The effect of green tea and related substances on ^{90}Sr absorption through the intestine was examined in rats. It was concluded that green tea acts inhibitorily on the absorption of ^{90}Sr through the intestine and that the effect is partly due to the astringent action and the reduction of the intestinal movement caused by green tea. (auth)

30988 CESIUM TURNOVER IN MAN FOLLOWING SINGLE ADMINISTRATION OF ^{132}Cs. 1. WHOLE-BODY RETENTION AND EXCRETION PATTERN. Iinuma, Takeshi; Nagai, Teruo; Ishihara, Tomio; Watari, Kazuo; Izawa, Masami (National Inst. of Radiological Sciences, Chiba, Japan). J. Radiat. Res. (Jap.), 6: 73-81(June 1965).

Four Japanese subjects (three males and a female) were measured for their whole-body retention and excretion rate following oral administration of ^{132}Cs. For the retention and distribution studies, a whole body counter-scanner was used. Short- and long-term biological half-lives, daily urinary and fecal excretion rates, and the calibration constants for ^{137}Cs in the body are reported. Although the excretion patterns obtained were quite similar to those already reported by others, the mean long-term biological half-life for the three male subjects, (73 days ranging from 65.5 to 82.0 days) was rather smaller than other values. The short-term half-life is caused by a large excretion rate in urine in a few days following the administration. (auth)

30989 NATURAL CONTENT AND DISTRIBUTION OF THORIUM IN THE HUMAN ORGANISM. Pavlovskaya, N. A. (Inst. of Industrial Hygiene and Occupational Diseases Academy of Medical Sciences, USSR). Med. Radiol., 11: No. 5, 28-30(May 1966). (In Russian).

Data were obtained on the natural content and distribution of thorium isotopes in the human organism. The average ^{232}Th content in the skeletons of human beings in the age group from 19 to 70 years, not exposed to occupational contacts with thorium-containing preparations, was 4 to 5 times higher than in liver, kidneys, spleen, brain, and muscles. The content in lungs was 2 to 3 times higher than that of other soft tissues. (C.H.)

30990 STABLE BROMINE AND ACTIVATION ANALYSIS IN PROTEIN TRACER STUDIES. Fireman, Philip; Borg, Donald; Gitlin, David (Univ. of Pittsburgh. Brookhaven National Lab., Upton, N. Y.). Nature, 210: 547-8(Apr. 30, 1966). (BNL-9320).

The feasibility of using stable brominated proteins and neutron activation analysis for the study of plasma protein

metabolism was demonstrated in preliminary studies in mice. It is suggested that the technique is particularly applicable to studies in infants and pregnant women where exposure of the subject to even small amounts of radiation may be harmful. (C.H.)

30991 CALCIUM METABOLISM IN A FRESHWATER MOLLUSK: QUANTITATIVE IMPORTANCE OF WATER AND FOOD AS SUPPLY FOR CALCIUM DURING GROWTH. Van Der Borght, O.; Van Puymbroeck, S. (CEN, Mol, Belg.). Nature, 210: 791-3(May 21, 1966).

The direct diffusion of Ca ions from water to mollusks was demonstrated in young snails (Lymnaea stagnalis) placed in beakers of tapwater containing measured amounts of ^{45}Ca and fed only lettuce. The animals were ashed and measurements of ^{45}Ca uptake were made at various times up to 74 days. The importance of this method of Ca uptake on the uptake of Sr in radiocontaminated aquatic ecosystems is discussed. (C.H.)

30992 EFFECT OF CALCIUM AND STRONTIUM ON THE PREFERENTIAL FORMATION OF AN ADENOSINE TRIPHOSPHATASE IN WHEAT ROOTS. Johnson, Ray E.; Jackson, W. A. (North Carolina State Coll., Raleigh). Nature, 210: 869-70(May 21, 1966).

Results are reported from a study of the effects of the inorganic cations Ca and Sr on the selective formation of adenosine triphosphatase in wheat roots. Results indicate that Ca and Sr behave the same in one enzyme system (ATPase formation) while their effects on the hydrolysis at ATP are directly opposite. (C.H.)

30993 ESTIMATION OF THE TOTAL HYDROGEN CONTENT OF THE HUMAN BODY. Rundo, J.; Bunce, L. J. (Atomic Energy Research Establishment, Harwell, Eng.). Nature, 210: 1023-4(June 4, 1966).

A method is described for estimating the whole-body hydrogen content of man that is based on the emission of 2.23-Mev γ rays when hydrogen atoms capture thermal neutrons. The γ rays are measured by scintillation spectrometry with thallium-activated sodium iodide. The possibility of using cosmic radiation as a source of fast neutrons which are first moderated by, and then captured in the body, for measurements of hydrogen content was investigated in phantoms and humans. The average hydrogen content was estimated as 9.47% of the body weight for men and 8.65% of the body weight for women. (C.H.)

30994 UPTAKE AND LOSS OF Na^+, Rb^+, AND Cs^+ IN RELATION TO AN ACTIVE MECHANISM FOR EXTRUSION OF Na^+ IN SCENEDESMUS. Kylin, Anders (Univ. of California, Riverside). Plant Physiol., 41: 579-84(Apr. 1966).

The mechanism for extrusion of Na^+ from Scenedesmus cells is characterized physiologically. It is stimulated by phosphate but oxygen is not necessary. Rb^+ and Cs^+ may also be extruded, but in the presence of Na^+ they cannot compete for the sites on the inside of the transport system. When Na^+ is extruded, Rb^+ and, by inference, K^+ seems to be transported as counter ion from the outside, and sodium ions compete only weakly for this external site. The parallelism between these findings and the Na^+-K^+-activated adenosine triphosphatases known from animal tissues is pointed out. With low additions of phosphate, the extrusion mechanism can keep the cells practically free from Na^+. Increasing the concentrations of external phosphate stimulates uptake more than extrusion, and a net uptake occurs. As for Rb^+ and Cs^+, they are taken up in the absence of external phosphate, but additions of P will greatly enhance the amounts absorbed. Two different ways of uptake are indicated. (auth)

30995 PANCREATIC LIPASE ACTIVITY IN DEUTERIUM OXIDE. Thomson, John F.; Bush, Karen J.; Nance, Sharron L. (Argonne National Lab., Ill.). Proc. Soc. Exp. Biol. Med., 122: 502-5(June 1966).

The activity of purified pancreatic lipase, with tributyrin emulsified in gum arabic as the substrate, was studied in ordinary water and in varying concentrations of D_2O up to 100%. Estimates of maximum reaction velocities indicate that the degree of inhibition increases linearly with increasing D_2O. At low substrate concentrations, however, the inhibition produced by D_2O was much less, an indication that there is a stronger solvent effect on enzyme-substrate binding than on the rate of hydrolysis itself. (auth)

30996 RETENTION OF FOLIAR APPLICATIONS OF ^{85}Sr BY SEVERAL PLANT SPECIES AS AFFECTED BY TEMPERATURE AND RELATIVE HUMIDITY OF THE AIR. Ambler, J. E.; Menzel, R. G. (Dept. of Agriculture, Beltsville, Md.). Radiat. Bot., 6: 219-23(June 1966).

Absorption of radiostrontium by leaves was found to vary widely among different plant species. Absorption increased with increasing relative humidity and temperature of the air to which leaves were exposed for 24 hr after the applied radiostrontium solution became dry. Differences between species were related to differences in wettability of the leaves. (auth)

30997 LIQUID SCINTILLATION COUNTING. Quimby, G. H. (Rayonier, Inc., Shelton, Wash.); Denison, J. G.; Stein, J. E. Water Sewage Works, 112: 72-3(Feb. 1965).

A procedure for measuring primary production in enriched environment by the use of liquid scintillation counting is described in detail. The procedure employing ^{14}C, as described by Steemann Nielsen, was found to be complicated by bacterial activity and different amounts of suspended material. A solution sufficiently clear for high counting efficiency was found when a membrane filter was dissolved in dimethylformamide. It is concluded that the procedure described is also superior to determination of primary production by the evolution of oxygen, especially in cases where interfering chemicals reduce the accuracy of standard analytical methods. (Pub. Health Abstr.)

Radiation Effects on Biochemicals

See also CHEMISTRY — Radiation Chemistry

30998 (BNWL-SA-709) THE RADIATION CHEMISTRY OF AGAROSE JELLIES. Kalkwarf, D. R. (Battelle-Northwest, Richland, Wash. Pacific Northwest Lab.). May 23, 1966. Contract AT(45-1)-1830. 10p. (CONF-660615-3). Dep. mn. CFSTI $1.00 cy, $0.50 mn.

From American Chemical Society, Northwest Regional Meeting, Vancouver, B. C.

The sensitivities of aqueous jellies in living tissue to ionizing radiation and methods for protecting them by chemical means were studied. The agarose used in the study is a linear polysaccharide consisting of alternate D-galactose and 3,6-anhydro-L-galactose units. Jelly solutions of known concentration were prepared by melting together weighed quantities of agarose and water at 90°C and cooling rapidly to room temperature. A Gamma cell-200 with a dose rate of 3000 rads per minute was used for irradiation studies. Liquefaction of the jellies was found to be an easily determined and reasonably precise measure of radiation damage. It was concluded that pure agarose jellies are very radiation resistant. Both the low reactivity of hydrated electrons with all carbohydrate structures and the low reactivity of hydroxyl radicals with carbohydrate polymers, particularly in the jelly state, are shown to account for the radiation stability of agarose jellies. The protective effects of food coloring were studied and found to offer substantial protection. (M.C.G.)

30999 (UCB-34P95-7) RADIATION OF HEME PROTEINS. Progress Report, October 1, 1964–September 30, 1965. Brown, W. D. (California Univ., Berkeley). Contract AT(11-1)-34. 12p. Dep. mn. CFSTI $1.00 cy, $0.50 mn.

The effects of radiation on heme proteins found in fish, cooked meats, and cured meats were studied. The rate for formation of nitrosyl myoglobin was followed spectrophotometrically in irradiated and non-irradiated myoglobin exposed to doses of 500 kR. Results indicate that, at least up

to the point of radioinduced precipitation, the changes that occur in myoglobins following irradiation can best be explained by relatively slight alterations in molecular shape and size. (C.H.)

31000 EXTRACORPOREAL IRRADIATION OF THE BLOOD IN HUMANS: EFFECTS UPON ERYTHROCYTE SURVIVAL. Schiffer, Lewis M.; Atkins, Harold L.; Chanana, Arjun D.; Cronkite, Eugene P.; Greenberg, Michael L.; Johnson, Horton A.; Robertson, James S.; Stryckmans, Pierre A. (Brookhaven National Lab., Upton, N. Y.). Blood, 27: 831-43(June 1966). (BNL-9484).

Autologous erythrocytes were γ irradiated at doses of 35,000 to 200,000 rads, chromated, and red cell survival studied. The 24-hour loss of labeled-cells and subsequent apparent erythrocyte survival times were found to be functions of the radiation dose. ECIB-produced red cell hemolysis of a mild degree is to be expected during courses of therapy, as demonstrated by clinical findings. However, there is no doubt that acute, severe, hemolysis could be produced by administering large radiation doses to patients over a short period of time. (auth)

31001 QUANTITATIVE REGULARITIES OF QUINONE FORMATION IN GAMMA-IRRADIATED PLANT TISSUE. Kuzin, A. M.; Narbaev, N. (Inst. of Biological Physics, Academy of Sciences, USSR). Dokl. Akad. Nauk SSSR, 164: 1409-12(Oct. 21, 1965). (In Russian).

Potato tubers were exposed to a ^{137}Cs γ source at a dose rate of 700 R/min. The oxidation potential (Eh) was determined before and at several periods after the exposure in the upper, 3-mm-deep layer. It was found that Eh decreased within 15 minutes after exposure as a result of the radiation-chemical oxidation reactions and the reduction of the free oxygen concentration. A clear correlation was established between Eh and the dose up to a total dose of 20 kR; there were no changes in the value of Eh beyond 50 kR. At later periods, the radiation activated polyphenol oxidase system began to exert its action and the oxidant was accumulated in the tissue, resulting in an increase of Eh as a linear function of the dose for 24 hours, becoming exponential within 72 hours. Polarographic tests of the extracted products indicated that the toxic quinone is formed in the plant tissue as the result of a first-order, reversible reaction. It is suggested that the usually observed exponential character of radiobiological survival curves be attributed to the formation of toxic products. (TTT)

31002 EFFECT OF PHYSIOLOGICALLY ACTIVE COMPOUNDS AND IONIZING RADIATION ON METABOLISM IN WHEAT. Il'ina, G. V.; Kuznetsova, N. N.; Rydkii, S. G. (Moscow State Univ.). Fiziol. Rast., 12: 424-31 (1965). (In Russian).

Wheat seeds soaked in solutions of 0.01M cysteine or 0.01% P-46 [2-hydroxy-4-[4-(α-pyridylsulfonamido) phenylimino]-1,4-naphthoquinone] were irradiated with 1500 R ^{60}Co and then grown to maturity in nutrient medium. The changes in carbohydrate and N fractions of plants grown from the treated seeds were compared with plants grown from radiated and nontreated seeds. The metabolic changes were related to both radiation and the effects of the chemicals. Results indicated that radiation of the seeds produces favorable conditions for a more rapid participation of the chemicals in metabolism. (C.H.)

31003 EFFECT OF METAL IONS ON FREE RADICAL FORMATION AND REACTIONS IN IRRADIATED PROTEINS. Singh, B. B.; Ormerod, M. G. (Royal Military Coll. of Science, Shrivenham, Eng.). Int. J. Radiat. Biol., 10: 369-78(1966).

The effect of different metal ions (Co, Cu, Fe, and Hg) on free radical formation and reactions in gamma-irradiated bovine serum albumin and trypsin in the solid state was studied using electron spin resonance spectroscopy. The metal ions lowered the radical concentration as observed at 77°K, and markedly reduced the concentration of $-CH_2-S\cdot$ radicals formed at room temperature. The results were interpreted in terms of the reaction of radiation-produced electrons with the metal ions, and they confirm the postulate that, at 77°K, electrons are trapped on cystine residues in proteins and that the resultant cystine anion reacts at higher temperatures to give the $-CH_2-S\cdot$ radical. The ESR results were correlated with the results of Butler and Robins, who found that metal ions protected trypsin against high-energy radiation. (auth)

31004 AN INDUCED ENZYME IN X-IRRADIATED ESCHERICHIA COLI: COMPARISON WITH LETHAL EFFECTS. Moore, J. L. (Hammersmith Hospital, London). J. Gen. Microbiol., 41: 119-26(Oct. 1965).

The effects of x rays on the synthesis of induced β-D-galactosidase was examined with Escherichia coli strain B and three of its mutants, BS, B/r, and B/H. In E. coli B, the extent of radioinduced lethal damage depended on conditions of culture after irradiation, whereas radioinduced inhibition of β-D-galactosidase was unaffected by the composition of the culture medium. The sensitivity of radiation damage to induction of β-D-galactosidase was about the same for strains B, B/r, and B/H, the dose required to give 37% survival being 42 ± 6 krad. Enzyme induction was one-half to one-third as radiosensitive as viability for the strains B/r, B/H, and BS. Oxygen enhancement ratios for lethal effects were always smaller than those for inhibition of enzyme synthesis. The relatively high oxygen enhancement ratios in experiments with inducible systems may indicate that damage to some part of the induction system other than DNA is responsible. Attempts were made to estimate target size from the dose required (D_{37}) to give an average of one damaging event per cell. The D_{37} value of 42 krad for inhibition of β-D-galactosidase in three strains of E. coli was similar to that reported for lysine decarboxylase. On the basis of the doses of radiation to reduce the surviving fraction to 37% for enzyme induction, the site responsible for induction has a molecular weight of 25 million, similar to that deduced for induction of lysine decarboxylase. Further evidence is presented to show that not only damage to DNA takes place, but that some other form of damage is responsible for the high values of oxygen enhancement ratio. (TCO)

31005 EFFECT OF X RAYS IN COMBINATION WITH NOVOEMBICHIN ON EXTRACELLULAR ACCUMULATION OF AMINO ACIDS IN MYCOBACTERIUM CYANEUM 416. Zarin', D. (Kirkhenshtein Inst. of Microbiology, Academy of Sciences, Latvian SSR). Latv. PSR Zinat. Akad. Vestis, No. 3, 67-72(1966). (In Russian).

By treating Mycobacterium cyaneum 416 with x-rays and novoembichine, mutants with increased capability for extracellular accumulation of alanine and aspartic acid were obtained. The highest amount of amino acids was excreted on a medium containing glucose, urea, and fish extract. Cultivation of the seeding material on molasses agar ensured high yields of amino acids, whereas cultivation on MPA led to complete absence of extracellular accumulation. (auth)

31006 EXPERIMENTAL OBSERVATIONS ON THE BEHAVIOR OF THE SERUM CHOLESTEROL AFTER IRRADIATION. Villani, G.; Migliorini, M.; Titta, L.; Lertora, M. (Spedali Riuniti S. Shiara, Pisa, Italy). Minerva Radiol., Fisioterap. Radiobiol., 10: 616-22(Dec. 1965). (In Italian).

The principal bibliographic sources of the subject are reviewed and then the experimental concepts and results are reported. The guinea pig was exposed to γ irradiation doses of 500, 200, and 2000 R with whole-body exposure, cephalic segment exposure, and exposure of the lower extremities. The results show that the total serum cholesterol increased by small doses which affect the trunk. Hypotheses are advanced with respect to the behavior of cholesterol fractions and cholesterol joined with β and α proteins which do not behave in an identical way. It is postulated that the two larger doses either in whole-body irradiation or in radiation on segments and the smaller doses in the cephalic and podalic region do not cause an increase in the cholesterol. (tr-auth)

31007 REGIONAL CHANGES IN BRAIN SEROTONIN AFTER HEAD X-IRRADIATION AND ITS SIGNIFICANCE

IN THE POTENTIATION OF BARBITURATE HYPNOSIS. Nair, V. (Chicago Medical School). Nature, 208: 1293-4(Dec. 25, 1965).

The effects of cephalic x-irradiation on brain serotonin were studied in male rats given single doses of 500 or 10,000 R. Serotonin was determined in the whole brain as well as in the hypothalamus and medulla. The amine level in the brain began to rise about 48 hrs post-irradiation, reaching a peak value after about 72 to 96 hrs and subsequently returning to normal by 144 hrs. Of particular interest was the absence of increased serotonin in the hypothalamus at 75 hrs, at which time a significant increase in serotonin was noted in the medulla. Radioinduced changes in brain levels of serotonin are discussed in relation to barbiturate hypnosis. (H.G.D.)

31008 EFFECTS OF IRRADIATION ON SYNTHESIS OF DEOXYRIBONUCLEIC ACID AND MITOSIS IN SYNCHRONOUS CULTURES OF HELA CELLS. Brent, T. P.; Butler, J. A. V.; Crathorn, A. R. (Royal Cancer Hospital, London). Nature, 210: 393-5(Apr. 23, 1966).

The effects of gamma radiation on DNA synthesis at different stages of the cell cycle were examined in HeLa cells given doses ranging from 500 to 1000 rads. Measurements on the rates of DNA synthesis were made at various times during two complete cell cycles. As the rate of thymidine incorporation fell immediately after irradiation, it was assumed that the rate of DNA synthesis in cells that are in the DNA synthetic phase must be immediately affected by irradiation. Only when the cells were irradiated during the S-period was there a marked effect on DNA synthesis during the same cell cycle. During the second cycle the rate of DNA synthesis was depressed irrespective of the time of irradiation. Some signs of recovery were noted near the end of the synthetic period after irradiation during the earlier part of the same period. It was concluded that two kinds of damage may be distinguished: that to the mitotic apparatus or its precursor; and that to the DNA in relation to its replication. During mitosis the former was clearly more radiosensitive than the latter, but sensitivity of the mitotic process during replication could not be clearly differentiated. (H.G.D.)

31009 ELECTRON SPIN RESONANCE STUDY OF THERMAL EFFECTS IN IRRADIATED DEOXYRIBONUCLEIC ACID. Cook, J. B.; Wyard, S. J. (Guy's Hospital Medical School, London). Nature, 210: 526-7(Apr. 30, 1966).

A dry specimen of DNA, extracted from salmon sperm, was exposed to 1 mrad ^{60}Co γ radiation at 77°K and the electron spin resonance spectrum was recorded on an electron spin resonance spectrometer. The sample was brought to various temperatures between 77° and 300°K and the electron spin resonance measured. Changes in the spectrum were irreversible and were found to be dependent on the annealing temperature and the annealing time at a given temperature. Results indicated that energy transfer occurred at three different temperatures as the specimen was warmed from 77 to 300°K. Annealing experiments performed with polycrystalline thymine, thymidine, and thymidine monophosphate irradiated and measured at various temperatures gave spectra that could not be explained on the basis of either temperature or chemical structure. (C.H.)

31010 NUCLEIC ACIDS AND PHOSPHATASE ACTIVITY IN CEREBRAL NERVE CELLS IN RATS IN THE COURSE OF ACUTE POSTRADIATION DISEASE. Ojak, Maria (Inst. of Pathology, Warsaw). Patol. Pol., 15: 561-71(Oct.-Dec. 1964). (In Polish).

Histochemical and cytochemical studies on DNA, RNA and acid phosphatase were conducted during acute postradiation disease induced in 36 rats of the Wistar strain by a single 1000-R dose of x rays. Changes in nerve cells in the course of acute radiation disease were studied histochemically. In the early stage of the disease a shift of RNA and phosphatase toward the nuclear and cell membranes was observed. Changes in the localization of DNA were minor. In later stages of acute postirradiation disease (from the third day) signs of tigrolysis were observed in the neurons throughout many of the ganglia of the central nervous system. The early changes in postirradiation disease are discussed in relation to the concept of damage of cell membranes by ionizing radiation. Radioinduced depolymerization of RNA and DNA was also considered as contributing to the observed histochemical changes in neurons. (BBB)

31011 BIOSYNTHESIS OF CORTICOSTEROIDS IN THE ADRENAL TISSUE OF IRRADIATED HYPOPHYSECTOMIZED RATS, AND ELECTROLYTE METABOLISM. Grodzenskii, D. E.; Ivanenko, T. I.; Bagramyan, E. R.; Aleshina, L. V. (All-Union Inst. of Experimental Endocrinology, Moscow). Probl. Endokrinol. Gormonoterap., 11: No. 5, 77-81(1965). (In Russian).

Rats were subjected to hypophysectomy and some of the animals were exposed to an x ray dose of 750 R 48 hrs later. The animals were sacrificed 48 hrs following the hypophysectomy or 3 hrs following irradiation, and their adrenals analyzed for corticosterone and aldosterone by a combined chromatographic-spectrophotometric technique. The Na and K contents of the blood serum at the time the rats were sacrificed were determined and the urinary excretion of Na and K was followed in both groups. It was concluded that the effect of irradiation on the synthesis of aldosterone by the adrenals and on the metabolism of Na and K is not necessarily dependent on the pituitary tropic hormones. (C.H.)

31012 GENETICS OF ENZYME LOCATIONAL SPECIFICITY. Munkres, K. D.; Woodward, D. O. (Stanford Univ., Calif.). Proc. Nat. Acad. Sci. U. S., 55: 1217-24 (May 1966).

Results are reported from experiments on the locational specificity of Neurospora malate dehydrogenase in malate mutants isolated following exposure to uv or x radiation. Histochemical localization of malate dehydrogenase in thin sections of mycelia by electron microscopy indicated that most of the enzyme activity was associated with mitochondria. The kinetics of malate oxidation by isolated mitochondria and the function of mitochondrial-bound and membrane- or protein-bound enzyme were determined. Results led to the conclusion that the physiological phenotype of malate mutants of Neurospora is primarily a consequence of the genetic alteration of the structure of malate dehydrogenase and secondarily an expression of functional and conformational alterations of mutant enzymes associated with mitochondrial membrane and structural protein. (C.H.)

31013 RADIATION-INDUCED CHANGES IN THE PROPERDIN SYSTEM OF THE DOG AND A CRITICAL ANALYSIS OF THE GENERAL PROBLEM. Michaelson, Sol M.; Shively, James N.; Haydock, Irene C. (Univ. of Rochester, N. Y.). Contract W-7401-49; DASAMD 960. Radiat. Res., 28: 60-70(May 1966).

In whole-body irradiated dogs (360 to 470 R Co or 594 R, 1000 kvp x rays), there was a progressive decline in properdin titer. Among decedents, properdin levels decreased much more rapidly than among survivors. Dogs exposed to 594 R of x rays had an earlier properdin decrease than did animals exposed to 360 to 470 R of ^{60}Co irradiation. There was no correlation between the properdin titer and the presence or absence of bacteremia. Dogs treated with chlortetracycline hydrochloride showed a significant delay in properdin decline in comparison with comparably irradiated but untreated dogs; these animals also had a significantly increased survival time. Injection of zymosan (5 mg/kg intravenously) resulted in an increase in properdin titer in normal dogs and a delayed decline in properdin level among dogs irradiated 1 day after zymosan injection. (auth)

31014 RADIATION SENSITIVITY OF CELLS AND BASE COMPOSITION OF DNA: AN ELECTRON SPIN RESONANCE STUDY. Pihl, Alexander; Sanner, Tore (Norsk Hydro's Inst. for Cancer Research, Oslo). Radiat. Res., 28: 96-108(May 1966).

The yield of x radioinduced radicals in DNA samples isolated from different sources was largely independent of the base composition and was unrelated to the radiosensitivity of the parent bacteria. The yield and stability of

the radicals were similar in the DNA preparations and in corresponding molecular mixtures of the four mononucleotides. In the nucleic acid components in general, the yield and stability of radioinduced radicals increased in the order base, nucleoside, nucleotide. No consistent differences were found between ribose and deoxyribose derivatives. The yield of radicals at 77°K was considerably higher in guanine and cytosine than in adenine and thymine. Futhermore, the radicals in the former base pair were less stable, indicating that they are more reactive than radicals induced in the adenine–thymine base pair. The number of radicals stabilized in bromouracil and iodouracil was greater than in thymine after irradiation at 77°K, and the radicals induced in the halogenated derivatives were less stable than those in the parent compound. It is suggested that absorption of radiation energy in the guanine–cytosine base pair results more frequently in crosslinking than does energy absorption in the adenine–thymine pair, and that this may account for the seemingly higher radiosensitivity of guanine–cytosine-rich DNA. A similar explanation is offered for the radiosensitizing effect of halogenated base derivatives. (auth)

31015 X-RAY-INDUCED DEGRADATION OF DEOXYRIBONUCLEIC ACID IN A POLYAUXOTROPHIC BACTERIUM. Frampton, E. W.; Billen, D. (Univ. of Texas, Houston). Radiat. Res., 28: 109-20(May 1966).

Postirradiation DNA degradation was determined in E. coli requiring thymine and amino acids by measuring the loss of radioactivity from cells previously labeled with thymine-2-^{14}C. Omission of the required amino acids from the postirradiation growth medium amplified the loss of DNA and allowed the detection of DNA degradation after irradiation of the bacteria with 2 kR. Completion of chromosome synthesis and temporary loss of DNA-synthetic capacity before irradiation resulted in the loss of less DNA. Restoration of DNA-synthetic capacity before irradiation did not restore the rate and extent of DNA degradation to the type observed in cells removed from cultures in logarithmic growth. Bacteria having one strand of DNA substituted with tritiated 5-bromouracil and the other with thymine-^{14}C showed almost equal rates of strand degradation after irradiation. No evidence of denaturation was detected in the DNA remaining after a period of postirradiation incubation. (auth)

31016 INCORPORATION OF DIETARY LINOLEIC ACID INTO TRIGLYCERIDES OF IRRADIATED BONE MARROW. Bollinger, J. N. (Oak Ridge Associated Universities, Tenn.). Radiat. Res., 28: 121-31(May 1966).

A study was made on rats to show that dietary fat readily influences the fatty acid composition of triglycerides in bone marrow. Whole-body irradiation (800 R) produced extremely fatty marrow regardless of the level or type of fat in the diet and greatly increased the rate and amount of linoleic acid incorporated into marrow triglycerides when diets containing 10 to 30% safflower oil were fed. By substituting coconut oil for safflower oil in the diet, it was determined that the large quantity of triglycerides remaining in bone marrow 1 to 3 weeks after irradiation are capable of undergoing a change in fatty acid composition. There was a significant increase in the level of stearic acid and a concomitant decrease in arachidonic acid in the phospholipid fraction of the bone marrow, liver, and plasma lipids 1 week after irradiation; however, there appeared to be no direct correlation between these changes and the increased synthesis of triglycerides in bone marrow. (auth)

31017 EFFECTS OF ADDED AGAR ON THE RADIATION SENSITIVITY OF TRYPSIN IN SOLUTION. Holladay, Wendell; Augenstein, Elizabeth; Augenstein, Leroy (Michigan State Univ., East Lansing). Radiat. Res., 28: 132-42 (May 1966).

Mixtures of trypsin (0.7 to 5 μM) and agar (0.001 to 0.005%) were irradiated with 250-kvp x rays at 4°C to investigate further the inactivation of an enzyme in a heterogeneous system which may simulate some cellular conditions. Even in such a relatively simple system, three classes of trypsin molecules with widely differing properties can be demonstrated: some molecules require inactivation doses only slightly larger than those for trypsin in solution alone; another class of molecules has a greatly decreased radiosensitivity; and some trypsin activity is lost completely during mixing. The occurrence of trypsin–agar complexes can be readily inferred from the appearance of scattering spectra which are monotonically correlated with concentration. A number of factors, such as the order of mixing, time of mixing, and the method of assay, influences the extent of class 2 and class 3 molecules. These results raise important questions concerning the relevance of studies in model systems to an understanding of radiobiological mechanisms in cells. (auth)

31018 EXPLORATORY INVESTIGATION ON THE INHIBITION OF SELECTED PHOTOSENSITIZERS BY AGENTS OF VARYING ANTIOXIDANT ACTIVITY. Epstein, Samuel S.; Forsyth, Jeannette; Saporoschetz, Inna B.; Mantel, Nathan (Harvard Medical School, Boston. National Cancer Inst., Bethesda, Md.). Radiat. Res., 28: 322-35(June 1966).

The interactions between twenty-five selected antioxidants and four photosensitizing agents were investigated over a wide concentration range at log-fold increments, by means of a previously established in vivo bioassay for antioxidants based on their ability to protect Tetrahymena pyriformis against the oxygen-dependent effects of photodynamic toxicity. These data have been topologically characterized by families of contours of constant response (isobols), the importance of whose general pattern, rather than whose individual locations and slopes, is stressed. Protective effects, in general, increase progressively with increasing antioxidant concentrations and with decreasing photosensitizer concentrations; they are similar for a given antioxidant, irrespective of against which photosensitizer it is tested. Antioxidant and photosensitizer dose-response slopes are a function of the width of horizontal and vertical separations, respectively, between adjacent isobols. No characteristic isobol pattern is seen for primary or secondary antioxidants, nor indeed for antioxidants within a particular group, such as the hindered phenols or amines. Observed differences in antioxidant activities are unlikely to be determined by solubility or permeability factors. (auth)

31019 EFFECTS OF PRELIMINARY γ-IRRADIATION OF COTTONSEEDS ON THE CHANGE OF DNA IN SUCCEEDING GENERATIONS. Khalikov, D. R.; Ibragimov, A. P.; Turkakulov, Ya. Kh. Uzb. Biol. Zh., 9: No. 3, 9-12 (1965). (In Russian).

In DNA, isolated from cotton seeds after γ irradiation (500 to 2000 R), the content of thymine and cytosine was decreased in 3 generations in comparison with the control. The content of guanine and adenine remained practically unchanged. (C.H.)

31020 EFFECT OF ^{60}Co RAYS ON HYPERWEAK LUMINESCENCE OF THE ROOT SYSTEM OF THE MALT SPROUT. Veselovskii, V. A.; Tarusov, B. N. Vestn. Moskov. Univ. Ser. VI, Biol., Pochvoved., 20: No. 4, 65-8 (1965). (In Russian).

Five-day-old embryos of barley used for malt sprout were γ irradiated from a ^{60}Co source by doses of 3000 and 30,000 R. Chemoluminescence was observed 1 to 2 hrs, 1, 2, 3, 4, 5, and 6 days after irradiation. An increased degradation of luminescence was noted at these time intervals. A decreased luminescence 2 days after the irradiation correlated with the inhibition of the growth of the roots. The treatment of the root system with 0.01M cysteine or 0.02M mercaptoethylamine resulted in a large drop of the luminescence. (C.H.)

31021 AMINO ACID COMPOSITION OF SERUM α_3-PROTEIN OF IRRADIATED AND NONIRRADIATED DOGS. Chudinovskikh, A. V. (Inst. of Biological and Medical Chemistry, Moscow). Vop. Med. Khim., 11: No. 3, 53-7 (1965). (In Russian).

The amino acid composition of serum α_3-protein was determined in 3 dogs of which 2 were irradiated with a dose of 700 R. No significant difference in the amino acid composition of serum α_3-protein of irradiated and nonirradiated dogs was noted. (C.H.)

31022 EFFECT OF EXTERNAL IONIZING RADIATION (GAMMA-RAYS OF THE BETATRON) ON THE BIOLOGICAL ACTIVITY OF PENICILLIN. I. Yakim, S. M. Vrach. Delo, No. 7, 76-9(1965). (In Russian).

The effect of γ rays from a betatron on the biological activity of the K and Na salt of penicillin was studied. The irradiation was made on the samples in glass flasks wrapped in Al at a distance of 25 cm from the source. The doses were 100, 250, 500, 1000, 10,000 and 100,000 R. at an energy of 12.5 Mev. and 100, 250, 500, 1000, 10,000, 100,000, 600,000, and 1,500,000 R. at the maximum energy of the betatron of 25 Mev. The rate of the absorbed dose was 18.7 R/min at 12.5 Mev, and 187 R/min at 25 Mev. The biological activity was determined by a microbiological method with Staphylococcus at 24 hrs, 1, 6, and 12 months after irradiation. The specific activity of penicillin irradiated with various doses of γ rays was higher than that of nonirradiated samples at 12.5 Mev., and there was no difference between the effects of the various doses. At 25 Mev the biological activity was destroyed. The changes in the shape of penicillin crystals and the appearance of induced radioactivity in penicillin were studied. The penicillin samples were irradiated with γ rays from a betatron at 8, 10, 12.5, 18, and 25 Mev. Below 15 Mev no activity was induced. Above that value the activity was retained for 35 to 40 min. The shape of the crystals was studied by micrographs. Nonirradiated penicillin had long needles intersecting at right or acute angles. Irradiated penicillin showed clumps which stuck together. (C.H.)

31023 THE EFFECT OF X-IRRADIATION ON ESCHERICHIA COLI B. I. EFFECT ON THE NUCLEIC ACIDS IN ESCHERICHIA COLI B. Kuo, Chieh-yen; Chou, Te-ch'ing; Li, Chun-ying (Fu Tan Univ., China). Yuan Tzu Neng, No. 2, 150-5(1965).

The survival curve of Escherichia coli B following x irradiation was found to be of the exponential type; the LD_{50}'s of the two components having different sensitivity levels were 2.5 and 4.5 kiloroentgens, respectively. Among the three classes of biological materials, DNA was found to be most sensitive to radiation, RNA was somewhat less sensitive and protein was least affected. The length of time for which the bacteria were kept at 37°C after irradiation also had varied effects on the content of DNA, RNA and protein within the cell. The DNA content was found to decrease progressively with an increase in the warming period. The RNA content decreased similarly but to a lesser degree. The protein content, on the other hand, only showed a slight decrease in the initial 40 min and thereafter remained unchanged. It was also found that, along with the decrease in DNA content, there was an accompanying increase in the content of nucleotides. This evidence further strengthened the hypothesis that DNA, upon x irradiation, is degraded into acid-soluble forms of nucleotides. The degradation of DNA is closely related to temperature; thus, the DNA content showed almost no change when the bacteria were kept at 0°C following x irradiation. (ATD)

31024 BIOLOGICAL VARIATIONS IN AGRICULTURAL SEEDS DURING STORAGE AFTER GAMMA IRRADIATION. Liu, Chao; Hsu, Mei-ch'i; Liu, Chin-t'ao; Chao, Kuang (Honan Agricultural Coll., China). Yuan Tzu Neng, No. 3, 280-4(1965).

The biological variations in agricultural seeds after γ irradiation (500 to 60,000 R from ^{60}Co) were found to differ corresponding to the amount of radiation and the length of time in storage. Analysis showed that low amounts of radiation stimulate growth and development, physiological process and the biochemical synthesis of the essential substances in the plant, such as vitamins B_1 and C, phosphatides, RNA and DNA, while higher amounts of radiation inhibit. After treatment with small doses of radiation, the longer the time in storage, the less will be the stimulating effect on vitamins B_1 and C, but the difference in effect is not so significant with respect to DNA and RNA. After treatment with higher doses of radiation, the inhibitory effect increases with length of time in storage. The inhibitory effect on vitamins B_1 and C, and RNA, after various amounts of radiation was different after 30 and 60 days in storage, but no significant variation in effect was found for phosphatides and DNA after 60 days in storage. (ATD)

Radiation Effects on Tissues

31025 (AD-631690) LONG-TERM STUDY OF INHALED PLUTONIUM IN DOGS. Bair, William J.; Park, James F.; Clarke, William J. (Battelle-Northwest, Richland, Wash. Pacific Northwest Lab.). Mar. 1966. Contract DO-29-601-62-1507. 58p. (AFWL-TR-65-214). CFSTI $3.00 cy, $0.50 mn.

To determine the long-term translocation and biological effects of inhaled plutonium, 40 beagle dogs were given a single 10- to 30-minute exposure to $^{239}PuO_2$ aerosols. Thirteen dogs died or were sacrificed when clinical signs indicated death was imminent 29 to 66 months postexposure. The body burdens at death ranged from 0.5 to 3 μC with 40 to 75 per cent of the body burden in the lungs, and 20 to 50 per cent in the bronchial and mediastinal lymph nodes. The liver contained 2 to 21 per cent, and the skeleton, 1 to 7 per cent. Cardiopulmonary insufficiency and lymphopenia were primary clinical signs. Pathology in the lungs consisted of severe fibrosis followed by alveolar cell hyperplasia, and bronchiolar and squamous types of metaplasia. Seven of the 13 animals showed bronchiolo-alveolar carcinomas, an incidence of 18 per cent as compared to a reported canine primary lung-tumor incidence of 0.2 per cent. The bronchial lymph nodes were composed of dense sclerotic connective tissue devoid of any lymphoid element. Metastases of the pulmonary tumor to the bronchial lymph nodes were seen in three animals. Twenty-three dogs with body burdens of 0.3 to 1 μC survived 4 to 6 yr after exposure. (auth)

31026 (AD-633606) INJURY ACCUMULATION IN SHEEP DURING PROTRACTED GAMMA RADIATION. Leong, G. F.; Page, N. P.; Ainsworth, E. J.; Hanks, G. E. (Naval Radiological Defense Lab., San Francisco, Calif.). Mar. 24, 1966. 17p. (USNRDL-TR-998). CFSTI $1.00 cy, $0.50 mn.

The relationship between γ radiation exposure rate and injury accumulation in sheep given a total protracted exposure to 165 R was evaluated. The method used was the split-dose technique wherein the animals were first subjected to protracted exposure and immediately thereafter were acutely exposed for LD_{50} determination. The end point used, therefore, was mortality within 60 days. Using this method, the extent to which the LD_{50} is lower than the LD_{50} for normal animals is a reflection of the amount of injury accumulated during the protracted exposure. The following protraction schedules (of 165 R) and exposure rates were used in the present experiments: ~14 days, 0.5 R/hr.; ~7 days, 0.95 R/hr.; ~3.5 days, 1.85 R/hr.; ~1.7 days, 3.9 R/hr. The data indicate that with a total exposure of 165 R, the threshold exposure rate for significant injury accumulation lies between 1.0 and 1.8 R/hr. Recovery from injury accumulated during protracted exposure at rates of 1.85 and 3.9 R/hr. appeared to be rapid, and a significant radioresistance was detected at 15 days after the conclusion of protracted exposure at 1.85 R/hr. (auth)

31027 (AECD/AG-14) MUTATION TYPES IN THE IRRADIATED POPULATION OF JUTE. Mia, M. M.; Ali, S. M.; Shaikh, A. Q. (Atomic Energy Centre, Dacca (Pakistan). [Agriculture Div.]). Feb. 1966. 14p. Dep. mn.

Dry healthy seeds of two commercial species of jute, C. capsularis, var.-D-154 and C. olitorius var. C.G. were irradiated with gamma rays of varied intensities ranging from 70 kR to 100 kR. Both M_1 and M_2 generations were studied in the years 1964 and 1965. M_1 variants were mostly chimeric. Some of them died at the early stage of growth but many survived to maturity. In the M_2 generation changed types apparently induced by mutation included plants with flat stems having turf of leaves (fertile), dwarf plants otherwise normal, very early flowering (fertile), and various other stem and leaf abnormalities which were sterile. (auth)

31028 (AECL-2409) EFFECTS OF INTERNALLY DEPOSITED RADIONUCLIDES ON THE THERMAL TOLERANCE OF FISH. Ophel, I. L.; Judd, J. M. (Atomic Energy of Canada Ltd., Chalk River (Ontario)). Apr. 1966. 12p. Dep. mn. AECL $0.50.

The effects of body burdens of ^{90}Sr and ^{131}I on the ability of goldfish (Carassius auratus) to withstand lethal temperatures were studied. In 15 of 17 experiments, the radioactive fish survived longer than control fish. Possible explanations are discussed. (C.H.)

31029 (BNL-10221) HEMATOLOGICAL EFFECTS OF SPACE RADIATION. Conard, Robert A. (Brookhaven National Lab., Upton, N. Y.). [1965]. Contract AT(30-2)-Gen-16. 31p. Dep. mn. CFSTI $2.00 cy, $0.50 mn.

Available data on the hematological effects of space radiation on man are reviewed. The data indicate that the bone marrow is, under most circumstances, the most critical organ for damage from radiation. The blood forming tissues possibly do not have the regenerative or renewal capacity that the gastrointestinal epithelium has, and will, in most cases, be the limiting factor for survival. Neutrophil and platelet levels will be of primary importance in regard to the fitness and survival of the astronaut from the hematological point of view. Peripheral blood counts, both preflight and in-flight, for total white cell count (with neutrophil and lymphocyte levels) offer the best index of prognosis from the point of view of hematopoietic damage. Lymphopenia must be interpreted with caution, since dose distribution patterns and abscopal effects from partial body irradiation may give lower values than indicative of general bone marrow damage. The development of fever, infection, bleeding are signs of severe bone marrow damage. Abortion of a mission is indicated if an accumulated whole body dose of radiation of greater than 150 rads in a 48 hour period occurs; white blood counts drop below 2000 cells per cubic mm and neutrophils below 1000 cells per cubic mm; or if associated fever, infections, or bleeding occur. Very large doses of partial body radiation may be tolerated without lethal depression of circulating blood cells. Shielding part of the bone marrow may be an important factor in preventing serious hematological depression. It is recommended that serious consideration be given to providing shielding of part of the bone marrow of the astronaut. A lead apron over the pelvic region would shield about 40% of his bone marrow, and he could then withstand considerably larger doses of radiation to the remainder of his body. The dose rate and depth-dose distribution patterns of space radiation are the most important physical considerations in determining total bone marrow damage. High proton flux irradiation associated with solar flares presents the most serious radiation hazard. Based on limited data, the quality of radiation delivered to the bone marrow does not appear to present any special hazards, since the RBE appears to be about 1 or only slightly above for most space radiations that penetrate to the depth of the bone marrow. (auth)

31030 (BNWL-SA-39) THE TREATMENT AND EVALUATION OF INTERNAL DEPOSITION FROM A PLUTONIUM WOUND. Baumgartner, W. V.; Larson, H. V.; Crook, G. H.; Newton, C. E. Jr. (Battelle-Northwest, Richland, Wash. Pacific Northwest Lab.). June 10, 1965. Contract AT(45-1)-1830. 16p. Dep. mn. CFSTI $1.00 cy, $0.50 mn.

Fragments of plutonium with activity exceeding 10 mC, resulting from an explosive disintegration of plutonium metal, penetrated a hood glove and lodged in the left upper arm of an employee. The health physics and medical aspects of the incident were followed rigorously; urine samples continuously analyzed for plutonium activity; blood samples obtained and analyzed prior to the administration of some 70 intravenous injections of diethylenetriaminepentaacetic acid (DTPA); and the activity in the wound measured frequently. Observations on modifications of prior methods of treatment are presented, i.e., washing open wound with solutions of DTPA and effect of intramuscular injections of DTPA into the wound site. Discussions are presented that include methods of evaluating the internal deposition. These include a comparative study of past deposition cases that were also complicated with the administration of chelating agents and trends from this study which help to establish estimations of internal depositions from very early bioassay results even when the data are influenced by DTPA treatment. The use of digital and analog computer techniques using the standard models with observed data is analyzed and the value of the analog computer for aiding the understanding of excretion patterns from plutonium deposition cases discussed. (auth)

31031 (BNWL-SA-201) HEMATOPOIETIC TISSUE NEOPLASMS IN ANIMALS ADMINISTERED ^{90}Sr. McClellan, R. O. (Battelle-Northwest, Richland, Wash. Pacific Northwest Lab.). May 27, 1965. Contract AT(45-1)-1350. 10p. Dep. mn. CFSTI $1.00 cy, $0.50 mn.

Twelve cases of hematopoietic tissue neoplasms were observed in long term radiostrontium toxicity studies with dogs or miniature swine where the animals had chronic exposure to ^{90}Sr starting early in life. In these experimental groups relatively few bone neoplasms were observed. In contrast, dogs which received acute exposures to ^{90}Sr showed a large number of bone neoplasms, but no hematopoietic tissue neopiasms. (C.H.)

31032 (CEA-R-2953) ATMOSPHERE PLAQUETTAIRE: ETUDE DES FACTEURS II ET VII. MODIFICATIONS APPORTEES PAR LES RAYONS X. (Platelet Environment: Study of Factors II and VII. Modifications Brought About by X Rays). Hollard, Daniel; Darnault, Jean; Rambaud, Francoise; Suscillon, Michel; Marcille Genevieve (Commissariat a l'Energie Atomique, Grenoble (France). Centre d'Etudes Nucleaires). Mar. 1966. 8p. Dep. mn.

Factors affecting blood coagulation were studied using blood platelets exposed to various environmental factors and doses of 0 to 70,000 R x radiation. Applications of the findings in clinical studies are discussed. (C.H.)

31033 (NASA-CR-59196) [CELLULAR BIOPHYSICS: A STUDY OF THE STRUCTURE AND FUNCTION OF LIVING CELLS]. Progress Report, Period Ending July 1, 1964. (Pennsylvania State Univ., University Park. Dept. of Biophysics). [1964]. Contract NsG-324. 49p. CFSTI $2.00 cy, $0.50 mn.

Research was completed on a study of the effect of ionizing radiation on genetic transcription. Arrhenius plots for the rate of transcription and the rate of decay are given, and the activation energies measured are in the range of 16,000 cal/mole. The cessation of transcription is linked to the degradation, possibly of only one strand of DNA. Another completed study on the mutation rate in cells grown in D_2O disposed the hypothesis that the mutagenic process consists of a tunneling of a hydrogen nucleus from one DNA base to another. Progress is reported on the centrifugation of E. coli, work on the mutagenic effect of tritium decay, and the high intrinsic velocity machine. Studies on radiation effects on bacteria included thymine labeling, uracil uptake, enzyme induction, and experiments involving the physical nature of DNA. Preliminary work on the design of a spectrophotometric method for studying single cells was begun. (H.G.D.)

31034 (RLO-1780-7) EFFECTS OF IONIZING RADIATION ON THE TESTICULAR FUNCTION OF MAN. First Yearly Progress Report, June 1, 1963–May 31, 1964. Heller, Carl G. (Pacific Northwest Research Foundation, Seattle, Wash.). Mar. 4, 1964. Contract AT(45-1)-1780. 52p. Dep. mn. CFSTI $3.00 cy, $0.75 mn.

Results are reported for developments in: design and use of x-ray apparatus for uniform irradiation of human testes; scheme for subject irradiation; effects of various x-ray doses on seminal fluid and sperm counts; effects of graded doses of x irradiation on the germinal epithelium; and effects of x irradiation on gonadal and gonadotropic hormones. (H.G.D.)

31035 (RLO-1780-8) EFFECTS OF IONIZING RADIATION ON THE TESTICULAR FUNCTION OF MAN. Second Yearly Progress Report, June 1, 1964–May 31, 1965. Heller, Carl G. (Pacific Northwest Research Foundation, Seattle, Wash.). Mar. 15, 1965. Contract

AT(45-1)-1780. 35p. Dep. mn. CFSTI $2.00 cy, $0.50 mn.

Progress is reported on: design and use of x-ray apparatus for uniform irradiation of human testes; hormonal evaluations; seminal fluid counts; quantitation of the germinal epithelium; assessing Leydig cell function; chromosomal studies; and tritium labeling in x-ray studies. Hormonal evaluations were made on subjects that received 5, 15, 20, 25, 50, 100, 300, 400, or 600 R. Estrogen, ICSH, and 17-ketosteroid data revealed no apparent changes after radiation compared to that of the control period. There was, however, a highly significant rise in gonadotropins following irradiation for every dose level and every subject. Of the subjects undergoing testicular biopsy, only 39% experienced a drop in sperm count, and this decrease always occurred within the first ten weeks. A technique was devised for evaluating the structural changes in Leydig cells and relating these to observed hormonal changes, or lack of changes. Problems inherent in the study of pachytene bivalents are discussed. Preliminary studies were conducted on two individuals to determine if labeled sperm could be detected through the depletion period following irradiation, and therefore, to prove that the preleptotene spermatocyte is not as radiosensitive as the spermatogonia. The two individuals were injected with ^{3}H-thymidine just prior to irradiation, and smears of their seminal fluid were followed by radioautography. Labeled sperm appeared after 46 days and continued until the tubules were empty and the subjects zoospermic as determined by routine seminal fluid counts. (H.G.D.)

31036 (SAN-529-3) ESTIMATION OF SENSITIVITY OF DROSOPHILA MELANOGASTER TO RADIATION USING A THIRD-ORDER ROTABLE DESIGN. Three Year Comprehensive Report. Ratty, F. J. (San Diego State Coll., Calif.). [1966]. Contract AT(04-3)-529. 24p. Dep. mn. CFSTI $1.00 cy, $0.50 mn.

Results are reported from a series of studies on the relation between survival of first instar larvae of Drosophila melanogaster and dose and time of x radiation exposure. Radiosensitivity was estimated in 3 lines of inbred flies and the hybrids formed between them. Data are included on the correlation of larvae survival to x radiation with chromosome puffing pattern; the relation between age and non-disjunction in irradiated parents; mutation induction in Drosophila cultured on aged and non-aged medium supplemented with DNA irradiated with 150 kR; the mutability of loci in an x-chromosome duplication; and mutation induction in Drosophila cultured on a medium exposed to 150, 500, or 3,000 kR γ radiation. (C.H.)

31037 (JPRS-35315, pp 65-75) PRIMARY POTENTIALS IN ANIMALS IRRADIATED DURING THE ANTENATAL PERIOD. Ivanitskii, A. M. Translated from Zh. Vyssh. Nerv. Deyatel'nosti im. I. P. Pavlova, 16: 117-23(1966).

Analysis of electrical activity of the visual cortex of the brain in rabbits x irradiated on the 15th and 23rd day of embryonic development yielded a number of characteristic alterations of primary potentials. The shape of the primary potential in animals irradiated in the middle of embryogenesis was not substantially altered, there being only a slight increase in the latent period and amplitude of the potential with a predominance of its positive phase. In contrast, in the case of rabbits irradiated in late embryogenesis, there was disturbance in the shape of the potential with significant reduction in its positive phase. The latent period and amplitude of the response was diminished. Analysis of the evoked activity confirms the previously made conclusion concerning a different localization of the dominant defect in antenatally irradiated animals, depending on the time of irradiation. (27 references.) (tr-auth)

31038 ADVANCES IN RADIATION BIOLOGY. VOLUME 2. Augenstein, Leroy G.; Mason, Ronald; Zelle, Max (eds.). New York, Academic Press, 1966. 380p. $15.00.

Separate abstracts were prepared on the six chapters in this volume. (C.H.)

For abstracts of individual chapters see: 30963, 30974, and 31039–31042.

31039 REACTIVATION AFTER PHOTOBIOLOGICAL DAMAGE. Rupert, Claud S. (Johns Hopkins Univ., Baltimore); Harm, Walter. Advance. Radiat. Biol., 2: 1-81 (1966).

General considerations concerning ultraviolet inactivation of the reproductive process in bacteria and viruses and the evolution of recovery processes are reviewed. The phenomenon of photoreactivation, host-cell reactivation and uv reactivation phenomenon, the genetic control of reactivation, indirect reactivation phenomenon, and multiplicity and cross reactivation are discussed. Emphasis is placed on uv damage to nucleic acids and recovery mechanisms. (250 references.) (C.H.)

31040 REPAIR OF PREMUTATIONAL DAMAGE. Kimball, R. F. (Oak Ridge National Lab., Tenn.). Advance. Radiat. Biol., 2: 135-66(1966). (ORNL-P-983).

Present concepts of repair mechanisms in bacteria, paramecium, and metozoan germ cells exposed to uv or x radiation are reviewed. Emphasis is placed on mechanisms involved in the repair of premutational damage including the reunion of broken chromosomes, the repair of DNA, enzymatic repair of DNA, temporal relationships, other mutation systems, photoreversal, the site of uv and x radiation induced mutations, modifying treatments, dose-rate effects, and repair in sperm. It is concluded that radioinduced mutation induction in microorganisms arises from initially reparable damage and that the final end point beyond which there is no repair is the first post-radiation DNA synthesis. Little agreement exists as to specific phenomena involved. In metazoa the mixture of cells of different sensitivity to mutation induction and reproductive death makes the analysis of premutational damage even more difficult. (160 references.) (C.H.)

31041 GENETIC CONTROL OF RADIATION SENSITIVITY IN MICROORGANISMS. Adler, Howard I. (Oak Ridge National Lab., Tenn.). Advance. Radiat. Biol., 2: 167-91(1966). (ORNL-P-1012).

The radiosensitivity of microorganisms is greatly dependent on environmental conditions before, during, and after irradiation but the range of responses possible for each organism is determined by its genetic constitution. Differences in the response of Escherichia coli grown under standardized conditions to γ, x, and uv radiations are summarized. Topics discussed include the influence of DNA composition on radiosensitivity; genetic alterations affecting radiation response of protozoa, yeast, bacteriophages, and bacteria; and bacterial conjugation techniques and their application in studies of the radiosensitivity of E. coli. (85 references.) (C.H.)

31042 ROLE OF GENETIC DAMAGE IN RADIATION-INDUCED CELL LETHALITY. Davies, D. R. (Wantage Research Lab., Eng.); Evans, H. J. Advance. Radiat. Biol., 2: 243-353(1966).

Data are reviewed from a number of studies of the role of genetic damage in radioinduced cell lethality. It is pointed out that a multitude of different effects are involved in the response of a wide variety of cell types that range from the simplest virus to the most complex of animals to uv or x radiations and that the first problem in such studies is the definition of the end point. Emphasis in the discussion is placed on proliferating cells since they allow genetic investigation. Topics discussed include the role of the nucleus and of the cytoplasm in radiation death; chromosome aberrations; recovery and modification of radiation damage; the effect of purine or pyrimidine haloanalog incorporation on radiation response; mutation and cell death; and patterns of cell death. (520 references.) (C.H.)

31043 EFFECT OF AGE OF THE DOG ON IMMUNOGENIC EFFICIENCY OF DOUBLE VACCINATION WITH X-IRRADIATED ANCYLOSTOMA CANINUM LARVAE. Miller, T. A. (Univ. Coll., Nairobi, Kenya). Amer. J. Vet. Res., 26: 1383-90(Oct. 1965).

The administration of one or two doses of x-irradiated Ancylostoma caninum infective larvae, preferably by subcutaneous inoculation, to 3- to 5-month-old pups stimulated satisfactory resistance to subsequent challenge of immunity with normal larvae. Double vaccination was more than twice

as effective as single vaccination in dogs that were 3 months old when the first dose of x-irradiated larvae were given. Experiments were devised to determine the quality of immune responses of dogs of different ages. Subcutaneous inoculation with 2 doses of 40 kR-irradiated A. caninum infective larvae successfully protected dogs of different ages against a challenge inoculation with normal larvae. There were significant reductions in challenge worm establishment and little adverse hematologic changes and clinical signs in vaccinated dogs when compared with the changes in unvaccinated challenge control groups. Vaccination of pups was effective when started as early as 72 hr after birth. Several uses are suggested for the larval vaccine, depending upon intensity of infection in dog hookworm enzootic areas. The most beneficial effects would probably be gained by vaccinating as early as is possible in the pup's life. Consideration would also have to be given to the influences of prenatal infection, early neonatal exposure in a contaminated environment, and probable need for early and repeated anthelmintic medication. (BBB)

31044 DIRECT IRRADIATION OF LYMPH NODES WITH ^{131}I TAGGED ETHIODOL. Tilak, S. P.; Salak, W. W.; Howard, John M. (Hahnemann Medical Coll., Philadelphia). Ann. Surg., 163: 67-73(Jan. 1966).

An experimental study was made on dogs to determine whether selective irradiation of lymph nodes might be of value in conditioning the host for reception of a homograft or in the treatment of lymphomas or metastatic malignant disease. The ^{131}I-tagged Ethiodol used as a source of irradiation contained 10 mC/ml. The dose of ^{131}I varied in different experiments in dogs from 0.54 to 3.0 mC in each hind limb. Shrinkage of the lymph nodes following irradiation was striking, being observed by the end of the first week and continuing for about 3 months at which time they were about one fifth the original volume. Serial blood counts demonstrated a reduction in lymphocyte counts during the second to the fourth week with no reduction in neutrophil counts. Effects on the general health of the animal appeared to be transient. Depilation and reduction in body weight was observed during the first month. Thereafter, each animal regained its preoperative condition, although the texture of the hair remained permanently altered. Histologic studies showed changes that varied with the dose of irradiation administered and the lapse of time before biopsy. It was concluded that the technique produces a significant degree of destruction of lymph nodes within the path of injection and might prove of value in conditioning a host to receive a homograft or for selective irradiation of lymphomas or nodal metastases. (TCO)

31045 REPARATIVE REGENERATION OF TISSUES UNDER THE EFFECT OF IONIZING RADIATION. Mikhailov, V. P. Arkh. Anat. Gistol. Embriol., 48: No. 2, 3-16(1965). (In Russian).

The course of reparative regeneration in various mammalian and avian tissues after exposure to single total-body irradiation in doses from 500 to 1000 R or to single local irradiation in doses from 1000 to 6000 R were studied. The regeneration of epithelial tissues (epithelium of jejunum and rectum, glandular portion of the stomach, liver, uterus, cortical substance of adrenals, peritoneum, thymus), muscular tissues (cross-striated musculature of skeletal type, smooth muscles of uterus and intestine), and connective tissues (lymphoid tissue of thymus, loose connective tissue from various parts of the body, granulation tissue) was followed. The tissues maintained their inherent and philogenetically conditioned histioblastic potencies after the irradiation. In acute irradiation sickness produced by total exposure to 1000 R the tissues under study maintained their high ability of mitotic division on which the restoration processes are based. Physiologic regeneration of the adrenal cortex and reparative regeneration of the liver show that the diurnal rhythm of mitoses is maintained at the climax of the radiation sickness. The causes of retarded healing of similar wounds and tissues in different conditions of irradiation and of different tissues in the similar conditions (acute irradiation sickness) were analyzed. The delayed course of regeneration in the acute radiation sickness is due not so much to the impairment of the proliferative ability of the given tissue by irradiation exposure but mainly to various disturbances of functions of the whole organism and complications connected therewith. In case of local irradiation with sufficiently large doses the radiation lesion of the tissue and resulting disturbance of intertissue coordinated relationships become most manifested. (C.H.)

31046 CONTROL OF FRUIT FLIES BY GAMMA RAYS. Huque, Heshamul; Ahmed, Hafiz (Radioisotope and Radiation Lab., Karachi, Pakistan). Food Irradiat., 6: No. 3, 28-32(Jan.-Mar. 1966).

The possibilities of control of Tephritid (Diptera) flies (Dacus cucurbitae) by sterile male release techniques are considered. A ^{60}Co source of 1800°C emitting a dose of 2.96×10^5 R/hr was used. The dose rate within the irradiation chamber varies from 100 to 70 and from 100 to 115 on vertical and horizontal axis, respectively. At a dose of 7,000 and 9,000 R, the flies were sterile and so did not produce viable eggs. The role of anoxia in the irradiation chamber is discussed. (M.C.G.)

31047 COMPARATIVE FREQUENCY OF X-RAY INDUCED CROSSOVER-SUPPRESSING ABERRATIONS RECOVERED FROM OOCYTES AND SPERM OF DROSOPHILA MELANOGASTER. Thomas, Ruth E.; Roberts, Paul A. (Oak Ridge National Lab., Tenn.). Genetics, 53: 855-62(May 1966). (ORNL-P-1654).

One thousand chromosome arms from x irradiated oocytes of Drosophila melanogaster (stage 7 and earlier) were screened for crossover-suppressing aberrations; two such aberrations were recovered, but neither was an inversion. The yield of intrachromosomal rearrangements recovered from oocytes was an order of magnitude below that recovered from sperm given the same radiation exposure. Possible explanations for the differences in aberration yield from the two germ-cell stages and their relation to the problem of dominant lethality in oocytes are considered. (auth)

31048 HERITABLE RADIATION EFFECTS ON MOUSE BODY AND ORGAN WEIGHTS, FAT DEPOSITION, CELLULAR ENZYMES, AND BLOOD. Chaffee, R. R. J.; Hensley, J. C.; Spalding, J. F. (Los Alamos Scientific Lab., N. Mex.). Genetics, 53: 875-82(May 1966). (LA-DC-7588).

Six to eight-month-old offspring of white mice whose male ancestors received whole-body x ray exposures of 200 rads over 25 to 37 successive generations had lower body weights, less omental and uterine associated fat, but higher kidney weights than controls. There were no differences in the weights of the heart, liver, spleen, or scapular brown fat pads. There were no differences in the mean weights for the two mouse lines at age 75 or 90 days; only body weights were measured on mice of this age. There were no differences in the oxidative enzyme systems assayed in adults. The irradiated line mice had a lower total white blood cell count which was primarily due to fewer lymphocytes. There was a somewhat higher erythrocyte mean cell volume in the irradiated line, but erythrocyte counts were not different. The amino acid composition of the hemoglobin in the two lines of mice was indistinguishable, but preliminary studies indicated that the electrophoretic migration patterns of the hemoglobins in the two lines may be quite different. Blood oxygen and CO_2 levels were different in the two lines, as was blood sodium, but blood glucose levels were the same. The results of these experiments should be useful in indicating where some definable and transmissible changes take place for future studies on mutagenic effects of irradiation. (auth)

31049 EVOLUTION OF FITNESS. I. IMPROVEMENT IN THE PRODUCTIVITY AND SIZE OF IRRADIATED POPULATIONS OF DROSOPHILA SERRATA AND DROSOPHILA BIRCHII. Ayala, Francisco Jose (Rockefeller Univ., New York). Contract AT(30-1)-3096-f. Genetics, 53: 883-95(May 1966).

Drosophila serrata and D. birchii flies were x irradiated

with 2000 R per generation for three generations. Two experimental populations of irradiated flies and one control population were started for each species at 25°C. After 51 days a sample of 300 flies was taken from each population to start six other populations at 19°C. The populations were maintained under conditions of intense competition, both among the larvae and among the adults. At 25°C, the irradiated populations of D. serrata decreased in size and in productivity during the first few weeks of the experiment. From the 6th to the 15th week they increased greatly in size and in productivity, and maintained their superiorities until the end of the experiment. The equilibrium levels were 50 or more percent higher than that of the control. At 19°C the two irradiated populations of D. serrata were also superior to the control in productivity and in size from the 13th week until the end of the experiment. The two irradiated populations of D. birchii at 25°C increased in size steadily from the 5th week until the end of the experiment, exceeding the control population in productivity and in size by more than 50%. At 19°C there is no marked difference between the control and the irradiated population. Regression analysis showed that there was a continuous differential increase in the fitness of the irradiated populations of D. serrata at both temperatures, and in those of D. birchii at 25°C. It is concluded that an increase in genetic variability produced by high frequency radiation may, with natural selection, result in an increase in the rate of evolution of the population, and finally of the fitness of the population in new environments. (auth)

31050 INDUCTION OF MUTATIONS BY REPEATED IRRADIATION OF SUCCESSIVE GENERATIONS IN BARLEY AND RICE. **Yamaguchi, Hikoyuki** (Tokyo Univ.). Ikushugaku Zasshi, 12: 141-7(1962). (In Japanese).

Techniques were developed for inducing mutagenesis in various characters and for selecting desirable mutations from many induced mutant lines. Dormant seeds of barley and rice were γ or x irradiated regularly with a constant dose in successive generations to determine the effect of recurrent irradiation on fertility and genotype frequency in the population. Fertility of the populations did not decrease with repeated irradiation. A striking improvement in seed fertility for the X_2 population as compared with that for X_1 was found. Thus, with repeated irradiation the seeds did not become more sensitive to the treatment as regards fertility. Effects of treatment upon mutation in rice were marked in increasing frequency and extending the spectra of mutations. An increase in the frequency of mutation was obtained particularly in the population irradiated repeatedly with 10,000 R, but the increase was slight after treatment recurrently with 30,000 R. A possible explanation for the smaller increase of mutations in the latter population could be their lowered viability caused by the higher dose of irradiation. From analysis of the genetic constitution of a group of individuals treated with x irradiation, the proportion of heterozygotes involved and the frequency of mutation newly induced in $X_{1/2/3}$ populations were estimated. The frequency of mutation newly induced in $X_{1/2/3}$ was of the same magnitude as that produced in X_1. This indicates that neither an increase nor decrease occurred in radiosensitivity of the seed from repeatedly irradiated populations. (TCO)

31051 DIVISION DELAY IN HeLa CELLS AND CHINESE HAMSTER CELLS. A TIME-LAPSE STUDY. **Froese, Gerd** (Manitoba Cancer Treatment and Research Foundation, Winnipeg, Can.). Int. J. Radiat. Biol., 10: 353-67(1966).

Division delay after ^{60}Co irradiation was studied in HeLa cells by hourly observations of sister cell pairs, well separated from each other, and in hamster cells by time-lapse photomicrography of small colonies. A maximum delay was observed if HeLa cells were irradiated toward the end and hamster cells during the middle of their life cycle. A fraction of the post-irradiated generation of hamster cells was delayed but this was unrelated to the delay in the previous generation. The response of sister cells was then investigated in order to eliminate the stage of development during irradiation as a variable quantity. The results suggest that biologically alike cells (i.e., sister cells) may show a variation in their division delay; this delay, however, is modified to approach a common value if the cells remain in proximity. Cell disintegration was found to be more extensive during the post-irradiated generation. (auth)

31052 X-RAY EFFECTS ON BARLEY ROOTS. I. CONTINUOUS EXPOSURE. **Kiefer, Juergen** (Inst. of Biophysics, Giessen, Ger.). Int. J. Radiat. Biol., 10: 379-90(1966).

The growth of barley roots under continuous exposure of 50 kv x rays was investigated. A model is described which can explain the behavior qualitatively and quantitatively. A survival curve for the meristem cells could be derived showing an exponential shape within the range investigated. (auth)

31053 THE EFFECT OF ^{131}I ON THE ABERRATION RATE OF CHROMOSOMES FROM CHINESE HAMSTER THYROIDS. **Moore, W. Jr.; Colvin, M.** (Dept. of Health, Education, and Welfare, Montgomery, Ala.). Int. J. Radiat. Biol., 10: 391-401(1966).

The effects of ^{131}I on the chromosomal aberration-rate of thyroid cells from the Chinese hamster were studied. The animals were given a single injection of ^{131}I intraperitoneally, and after selected intervals of time the thyroids were removed and the cells grown in tissue culture. It was found that thyroid cells are sensitive to irradiation as indicated by chromosome damage at dose-levels as low as 6 rad. There was also an increase in the number of cells containing aberrations over the time-intervals studied, suggesting a persistence of these cells for long periods of time. Dicentrics and other forms of the chromosome type of aberration occurred most frequently, indicating that most of the injury took place while the thyroid cells were in the G_1 stage of the cell cycle. (auth)

31054 RADIOSENSITIVITY OF TWO VARIETIES OF VICIA FABA L. AND OF THEIR HYBRID. **Remmelg, H.** (Inst. of Experimental Biology, Academy of Sciences, Estonian SSR). Izv. Akad. Nauk Est. SSR, Ser. Biol., 14: 475-84(1965). (In Russian).

Radiosensitivity was determined in two parental varieties of Vicia faba and in one hybrid of the two. Scoring of various characters revealed differences in the radiosensitivities of the parental varieties, the radiosensitivity of hybrid being intermediate between the two. Genetic control of radiosensitivity was analyzed, but no heterosis was observed. (H.G.D.)

31055 EFFECTS OF A SINGLE EXPOSURE TO X RAYS ON THE FUNCTION AND ULTRASTRUCTURE OF AN ISOLATED SYMPATHETIC GANGLION. **Posternak, J. M.; Tinguely, H.; Forssmann, W. G.** (Organisation Romande de Recherches Neurophysiologiques, Geneva). J. Physiol. (Paris), 57: 683-4(Sept.-Oct. 1965). (In French).

The effects of 6200 R of x irradiation, administered in 0.5 hr on the superior cervical ganglion of the rat suspended in Krebs solution were studied. The ganglion was arranged so that it could be electrically stimulated preganglionically. Irradiation reduced the survival of the ganglion significantly when the suspension medium was altered by addition of NaCl or sucrose. The results suggested that irradiation increased the permeability of the ganglion. Electron microscope studies of the cells of the ganglion showed injuries which became apparent very early and increased rapidly with time. (BBB)

31056 EFFECTS OF X-RAY RADIATION ON HeLa CELLS. **Kanno, Iwao; Fukushi, Kazue; Yamaguchi, Junji; Utagawa, Keiji; Umehara, Eiju; Sato, Kazuo; Ito, Yasuhiko** (Tohoku Univ., Sendai). J. Radiat. Res. (Jap.), 6: 82-95 (June 1965).

Observations on the effect of single x irradiation at 100 to 1,000 R on HeLa cells are reported. The metabolism was disturbed in HeLa cells in culture in test tubes by x irradiation at more than 300 R. With over 300 R, the proliferation of the number of cell nuclei was restrained. This effect was especially pronounced with irradiation by 1,000 R. Examination by Giemsa staining revealed only the disturbance in mitotic cells in x irradiation at less than 200 R, but the disturbance in the resting cells was pronounced in x irradiation at over 500 R. Histochemical observation by means of Feul-

gen reaction revealed that more than 20% of the stickiness of chromosome was produced in 3 to 7 days after x irradiation by 500 to 1,000 R. Observation of electron-microscopic pictures revealed that the cytoplasm of HeLa cells grew larger with the increase of the amount of x irradiation and that round degenerations were present locally. Both cytoplasm and nucleoplasm became scarce. No remarkable changes were observed in mitochondria, endoplasmic reticulum and nucleolus. The double structure of the nuclear membrane remained undisturbed. The inhibitions of about 18% in the respiratory action and 29% in glycolysis were observed 24 hours after x irradiation at 1,000 R. There was hardly any change in the amount of nucleic acid (both RNA-P and DNA-P) 15 hours after x irradiation at 1,000 R, but the incorporation of ^{32}P into nucleic acid-P was clearly inhibited. Also about 50% inhibition of the mononucleotide of the RNA was observed. No remarkable difference in incorporation was observed among the mononucleotides in the groups. (auth)

31057 SITE DISTRIBUTION PARAMETER FOR RADIATION-INDUCED CHROMOSOME EXCHANGES. Savage, John R. K.; Papworth, D. G. (Medical Research Council Radiobiological Research Unit, Harwell, Eng.). J. Theoret. Biol., 11: 1-9(May 1966).

The distribution between cells of radiation induced chromosome exchange aberrations in a number of species conforms to the terms of a binomial $[p + (1 - p)]^n$. The current explanation for this observation is that there are only a few placed (termed sites) within the nucleus, where the participating chromosomal threads come close enough together for exchange to take place. p is taken as representing the probability of obtaining an exchange in a site, and n the number of sites in the cell available for exchange. Mathematical consideration is given to the case where not all cells in the population have the same number of sites, and it is concluded that n is a distribution parameter indicating the way in which cells with different numbers of sites are distributed in the population, and that it does not indicate directly the mean number of sites available. This conclusion is illustrated by calculated exchange distributions for a number of hypothetical populations having cells in the different site categories distributed in a known manner. It follows from this conclusion that different types of aberration may have different mean numbers of sites, but the same distribution parameter; and a Poissonian distribution of aberrations does not necessarily indicate that the mean number of sites per cell is unlimited or even large. Applications in studies of radioinduced chromosome aberrations in Tradescentia paludosa microspores are included. (auth)

31058 EFFECTS OF SPACEFLIGHT FACTORS ON WHEAT SEEDS AND PLANTS GROWN FROM THEM. Il'ina, G. V.; Kuznetsova, N. N.; Rydkil, S. G.; Vysotskii, V. G. Kosm. Issled., 4: 320-3(Mar.-Apr. 1966). (In Russian).

The growth and development of wheat plants subjected to the action of space-flight factors on the satellites Vostok-5 and Vostok-6 were studied. Some tendency toward depression of germination was found. Substantial changes in carbohydrate and protein exchange of the plants in the vegetation period and also in the chemical composition of the grain as a function of the factors investigated were not observed. (tr-auth)

31059 EFFECT OF LONG-WAVE AND SHORT-WAVE SUPPLEMENTAL UV RADIATION ON GROWTH AND ACCUMULATION OF PIGMENTS IN CUCUMBER AND TOMATO PLANTS UNDER CONDITIONS OF GLASS-COVERED GROUND. Godnev, T.; Selga, M. (Inst. of Biology, Academy of Sciences, Latvian SSR). Latv. PSR Zinat. Akad. Vestis, No. 3, 58-66(1966). (In Russian).

The effects of long and short wavelengths of uv radiation on growth and pigmentation were studied in cucumbers and tomatoes. Stimulated growth of plants and foliar surface increment were enhanced by the short wave. Short-wave uv-irradiation impeded the aforesaid processes. Characteristic alterations in the pigment system induced by uv light were preserved after discontinuation of serial lighting of plants. This refers to both long-wave and short-wave uv radiation and bears evidence to the strength and long duration of the after-effect of uv light on the plant organism. The experimental findings reported are indicative of the interrelation between accumulation of carotenoids and chlorophylls that may be due to the community of the initial stages in the development of the phytol part of the chlorophyll molecule and of the carotenoids up to the formation of C-20 compounds. (H.G.D.)

31060 RADIATION EFFECTS IN IRRADIATION OF DIFFERENT AREAS OF THE HEAD. Skoropad, Yu. D. Med. Radiol., 9: No. 12, 35-40(Dec. 1964). (In Russian).

Doses of 1760 R were given to the entire head or the cerebral or facial regions of dogs. Clinical manifestations were most severe for entire head exposure, less for cerebral region exposure, and still less for facial exposure. One animal died. The clinical manifestations are discussed from the viewpoint of the values of tissue doses and the nature of dose distribution in areas of the head. (D.E.B.)

31061 ACTION OF HORMONES ON THE REPARATIVE PROCESSES IN THE SKIN EXPOSED TO GAMMA IRRADIATION. Bukhonova, A. I. (Inst. of Medical Radiology, Academy of Medical Sciences, USSR). Med. Radiol., 11: No. 5, 38-43(May 1966). (In Russian).

The effect produced by somatotrophic hormone (STH) and desoxycorticosterone acetate (DOCA) on the healing of experimental wounds in rats (30 species of the Wistar line and 30 of the August line), subjected to a single whole-body gamma-irradiation in doses of 500 R and 300 R, was studied. The hormonal preparations were administered also to non-irradiated animals. The biopsy-material from the wound-edges was submitted to a histological and histochemical examination. The irradiation inhibited for the most part the development of the granulation tissue; macrophages and fibroblasts showed reduced RNP content, with a relatively high succinate dehydrogenase activity. In irradiated animals STH stimulated but weakly the development of granulation tissue poor in cells and fiber structure. Desoxycorticosterone acetate enhances the glycogen and RNP content, activating the growth of the young connective tissue cells. The regenerating epithelium of irradiated animals showed increased succinate dehydrogenase and acid phosphatase activity. STH, and particularly desoxycorticosterone acetate, stimulated proliferation of the young epithelium and the glycogen and RNP enrichment of the cells, with a very feeble activity of the succinate dehydrogenase and thiol (sulfhydryl) compounds. The stimulation of the reparative process in irradiated animals was stronger under the influence of desoxycorticosterone acetate than under that of STH. (auth)

31062 SENSITIZATION OF ESCHERICHIA COLI TO RADIATION BY BROMOURACIL: EXCESSIVE POST-IRRADIATION BREAKDOWN OF DEOXYRIBONUCLEIC ACID WITHOUT CONCOMITANT SYNTHESIS. Aoki, Susan; Boyce, Richard P.; Howard-Flanders, Paul (Yale Univ., New Haven). Nature, 209: 686-8(Feb. 12, 1966).

Carbon-14-labeled thymidine was used to study the processes of DNA breakdown and synthesis in bromouracil-substituted E. coli after exposure to ultraviolet light. Results indicated that irradiated DNA containing bromouracil (BU) was extensively degraded and that DNA synthesis was inhibited. Hence DNA containing BU was not effectively repaired. (H.G.D.)

31063 DEPLETION OF MOUSE SPERMATOGONIA FOLLOWING EXPOSURE TO ^{210}Po. Samuels, L. D. (Harvard Univ., Boston). Nature, 210: 434-5(Apr. 23, 1966).

The effects of ^{210}Po on spermatogenesis were studied in stage VII tubules in mouse testes. Autoradiography confirmed the localization of the ^{210}Po in the intertubular spaces such that the basement membrane of the tubules was exposed to a maintained flux of alpha particles. Preliminary investigations of the functional effects of the exposure suggest that overall fertility of the mouse was not

grossly impaired by ^{210}Po exposure although the systematic effects of larger doses of ^{210}Po impaired the general vigor of the animals and appeared to depress their reproductive activity. (H.G.D.)

31064 CELLULAR CONTROL SYSTEMS AND RADIOSENSITIVITY. Orr, J. S. (Western Regional Hospital Board, Glasgow); Hope, C. S.; Laurie, Jean; Stark, J. M. Nature, 210: 699-700(May 14, 1966).

The relation between cellular control systems and radiosensitivity is discussed. Results of recent publications are reviewed that suggest that cells do not necessarily respond to radiation as individual autonomous units that local interactions controlling proliferation of normal cells in tissues can be altered. It is concluded that theory and experiment together reveal a strong association between temporal properties of cellular control systems and radiosensitivity. (C.H.)

31065 RELATION BETWEEN EXTRAPOLATION NUMBER AND APICAL CELL NUMBER IN GEMMAE OF MARCHANTIA POLYMORPHA L. Miller, Morton W. (Brookhaven National Lab., Upton, N. Y.). Nature, 210: 748-9 (May 14, 1966). (BNL-9135).

The gemmae of the liverwort Marchantia polymorpha are approximately discoidal with two apical notches and both apical cells are active in DNA synthesis and mitosis. Results of studies of cell survival after exposure of gemmae of Marchantia to 250 kvp x radiation indicate that both apical cells must be inactivated to halt apical survival. (C.H.)

31066 PREVIOUS REPRODUCTIVE HISTORY AND THE SUSCEPTIBILITY TO X-RAY-INDUCED CONGENITAL ANOMALIES. Rugh, Roberts; Wohlfromm, Marlis (Columbia Univ., New York). Nature, 210: 969-70 (May 28, 1966).

Frequency of anomalous offspring was compared in irradiated (150 R x rays) and non-irradiated primiparous and multiparous mice. Anomalies observed besides resorption and death were: exencephaly, cephalic blisters, microcephaly, brain hemorrhage, eye and jaw defects, persistent exteriorized intestines, and stunting. No attempt was made to determine inner histological alterations. Little difference in the condition of the fetuses was noted among the controls except that a higher (3.3%) incidence of anomalies occurred among the primiparous than among the multiparous (1.5%) females. Primiparous females irradiated on the 8th day of gestation produced more anomalies (34.7%) than the irradiated multiparous females (29.5%). With regard to sex ratios, it was found that among unirradiated fetuses there were 52% males to 48% females, but among both x-irradiated groups the percentage of males was significantly higher (57.1 and 58.3%). (H.G.D.)

31067 PROLIFERATION OF HUMAN LYMPHOCYTES IN CULTURE. Sasaki, M. S.; Norman, Amos (Univ. of California, Los Angeles). Nature, 210: 913-14(May 28, 1966).

Three series of experiments were performed with leukocytes separated from peripheral blood in order to study proliferation of human leukocytes in culture. In the first set of experiments chromosomes were labeled with tritiated thymidine added to the cultures at various times after the start of incubation. Cells were treated with colcemide for $1\frac{1}{2}$ hr prior to analysis. Whether metaphase cells were in the first or second division following irradiations was based on the chromosome labeling pattern. In the second experimental series, cells were incubated for 20 hrs and then treated with colcemide and tritiated thymidine labeling index and mitotic index were determined from counts of 1000 to 3000 mononuclear cells. The third set of experiments was based on the observation that the small fraction of acentric chromosomes produced by x rays that survive cell division appears in the daughter proportion of cells as double sets of acentric chromosomes. Results showed that; more than 30% of the original mononuclear cells begin DNA synthesis by 72 hrs; transformation of the cells is essentially completed in 24 to 48 hrs; after transformation the cells proliferate with a generation time of 22 hrs; the increase in frequency of cells synthesizing DNA from 48 to 72 hrs is due almost entirely to cell proliferation; and 70 to 80 per cent of the cells in metaphase at 72 hrs are in at least their second division in culture. X-ray doses up to 500 rads given before culture did not delay the onset of the 1st DNA synthesis, nor did they alter the duration of the G, S, G_2, or M phases. (H.G.D.)

31068 SITE OF LETHAL DAMAGE BY IONIZING RADIATION IN ESCHERICHIA COLI B/r GROWING EXPONENTIALLY IN MINIMAL MEDIUM. Munson, R. J.; Bridges, B. A. (Medical Research Council Radiobiological Research Unit, Harwell, Eng.). Nature, 210: 922-5 (May 28, 1966).

Mechanisms of radiation injury in E. coli B/r are hypothesized. It was concluded that the inactivation by ionizing radiation of E. coli B/r in minimal medium is due to the inactivation of discrete units (targets) within the organism, which segregate from one another at cell division. A bacterium that possesses only inactivated targets is unable to undergo further division. Evidence is presented that the target is the bacterial chromatid that is itself inactivated with one-hit kinetics. The inactivating lesions must therefore prevent both strands of the DNA from passing on viable information during replication. (H.G.D.)

31069 LIBERATION OF 5-HYDROXYTRYPTAMINE IN THE BRAIN STEM OF ADRENALECTOMIZED RATS AFTER X-IRRADIATION. Palaic, Djuro; Supek, Zlatko (Ruder Boskovic Inst., Zagreb). Nature, 210: 970-1 (May 28, 1966).

Total, basic and acidic 5-OR indoles (where R is a hydrogen atom or an aryl or alkyl group) were examined in the brain stem of adrenalectomized rats after x-irradiation (900 R). By simultaneous determination of these compounds it was possible to measure the rate of biosynthesis, release, and metabolism of 5-hydroxytryptamine (5-HT). Irradiation of controls produced a significant increase of total 5-OR indoles, as was the case with sham-operated animals. In adrenalectomized rats there was an increase of total and basic 5-OR indoles on the first day after operation. After irradiation such animals showed a statistically significant increase of total and acidic 5-OR indoles in comparison with adrenalectomized and non-irradiated ones. It is suggested that increase of 5-HT content of the brain of adrenalectomized rats is probably a consequence of increased 5-HT biosynthesis. (H.G.D.)

31070 SOME CONSIDERATIONS ON THE MECHANISM OF RECOVERY OF THE IRRADIATED YOSHIDA ASCITES TUMOR CELLS. Tai, Yukimitsu (Tokyo Univ.). Nippon Acta Radiol., 25: 115-23(May 1965). (In Japanese).

Fifty male Wister rats were inoculated intraperitoneally with 2 million Yoshida ascites prior to whole-body x-ray exposures to 100, 300, 500, 700, or 1000 R. Five types of recovery curve were obtained using the data calculated from the number of mitotic figures, mitosis was observed to depend on dose and recovery. The concept of Hit Theory was used to interpret the recovery curve. As a regeneration number, the values of five, six, seven, and eight were statistically obtained respectively for 300, 500, 700, and 1000 R exposure groups. The results described show that the degree of radiation damage is demonstrated by the regeneration number "u" also. (TCO)

31071 RADIOSENSITIVITY OF BONE MARROW CELLS IN MOUSE STRAINS WITH DIFFERENT LD50. Sugahara, Tsutomu; Tanaka, Tomizo (Kyoto Univ.). Nippon Igaku Hoshasen Gakkai Zasshi, 25: 1255-9(Feb. 1966). (In Japanese).

Radiosensitivity of bone marrow cells of strains of mice with different LD_{50} (30 days), RF and C57BL/6, was studied using two different techniques. In the first technique, bone marrow cells from the two strains were transfered to CF#1 mice previously exposed to 800 R of x rays and the spleen weight of the recipient was measured 7 days after the transfer. Difference in spleen weight was statistically significant, higher in C57BL than in RF, when the bone marrow cells were irradiated in the donor but not when irradiated in the recipient. In the second technique, spleen weights and nod-

ules after graded doses of x radiation were measured in the two strains of mice. Both values for RF were higher than for C57BL/6 at almost all dose levels. Since LD_{50} is higher in C57BL/6 than in RF, the results of the experiments of the first technique may indicate that the radiosensitivity of bone marrow cells are in accord with whole-body exposures, but those of the second technique appear to be contrary. The apparent contradiction may be explained by assuming the difference in the level of stimulating factors for bone marrow cell multiplication induced by radiation. (auth)

31072 RELATIVE BIOLOGICAL EFFECTIVENESS OF 15-Mev BETATRON X RAYS AND 200 kv X RAYS FOR LETHALITY IN MICE. Fujino, Moriji; Nakatsuka, Haruo (Osaka City Univ.). Nippon Igaku Hoshasen Gakkai Zasshi, 25: 1304-7(Feb. 1966).

The relative biological effectiveness of 15-Mev x rays from a Betatron with reference to 200-kv x rays: (primary HVL Cu 1.72 mm) was determined by using the lethal effect on mice. The RBE was estimated to be 0.66 for 15-Mev betatron x radiation for LD_{50} of mice. When a definite method of dosimetry for high energy betatron x rays is established, the RBE value tentatively derived in the present study may be subject to some changes. (auth)

31073 EFFECT OF X-IRRADIATED TUMOR BED ON TUMOR CELLS. PART I. EFFECT OF TUMOR BED ON TUMOR GROWTH AND HOST SURVIVAL. Urano, Muneyasu (Kyoto Prefectural Univ. of Medicine). Nippon Igaku Hoshasen Gakkai Zasshi, 25: 1326-36(Feb. 1966).

The effect of pretransplant irradiation of the tumor bed on mouse tumor growth and host survival time was investigated with mouse Takizawa-sarcoma. The tumor bed effect (TBE) as demonstrated in these experiments may be summarized as: (1) prolongation of host survival time, (2) reduction of tumor growth and (3) smaller maximum volume of tumor; i.e., the final size of tumors causing death of animals was smaller in X-irradiated than in non-irradiated tumor beds. A TBE was observed when the tumor bed was irradiated with more than 1,000 R three days before transplantation. Prolongation of host survival time was almost constant without any relation to x-ray dosage up to 4500 R. A negative corelation with x-ray dosage was noted, however, with maximum tumor volumes and up to 3,000 R of irradiation. When the tumor bed was irradiated with 2,000 R at various periods (3 hours to 84 days) before transplantation, the TBE was constant, regardless of the interval between x-irradiation and transplantation. That is, TBE persisted for at least eighty-four days. When tumor cells grown slowly in tumor beds irradiated before transplantation were reinoculated to normal beds, their growth curve was essentially similar to that of normal tumor cells. (auth)

31074 EFFECTS OF CONTINUOUS LOW-DOSE IRRADIATION ON MICE. I. EFFECTS ON THE POSTNATAL DEVELOPMENT OF THE SUCKLINGS AND THE GROWTH AFTER BIRTH. Muramatsu, Susumu; Hayakawa, Junichiro (National Inst. Radiological Sciences, Chiba, Japan). Nippon Igaku Hoshasen Gakkai Zasshi, 25: 1365-73(Mar. 1966). (In Japanese).

An effort was made to demonstrate the somatic effects of radiation on mice under continuous low dose-rate irradiation for 83 to 125 days between conception and full growth. Male and female mice were irradiated with ^{60}Co gamma rays during their reproductive period. The dose-rate was about 6R/day, and the total accumulated dose was 498 to 750 R for each mouse. CF1-JCL mice were used. The stage when external ears opened, fur appeared, lower incisors erupted, and vagina opened was observed for both a control and an irradiated group. Results indicate that continuous irradiation at a low dose hastens the appearance of these external characteristics, and the differences between both series are statistically highly significant. The observation of the body weight, head-body length, and tail length from birth to nine weeks old was carried out as indication of the growing process. Body weight, head-body length, and tail length in earlier period after birth were not much different in the two series, but growth in the irradiated series was slightly lower in later weeks. At the ninth week tail length showed statistical significance. The lengths of long bones, i.e., humerus, ulna, radius, femur, and tibia were measured between 35 to 105 days old. Bone length was smaller in the irradiated series than in the control, but statistical significance was not clearly demonstrated. (TCO)

31075 ESR OF THE HUMAN BLACK HAIR. Asai, Takuo; Shono, Yoshihiko (Radiation Center of Osaka Prefecture, Japan). Nippon Igaku Hoshasen Gakkai Zasshi, 25: 1380-4(Mar. 1966). (In Japanese).

The shape and intensity of the spectra of human black hair were studied under various conditions. Some of the results suggest possible practical applications of the ESR spectra for instance in the fields of horensic science. The typical ESR spectra of the human black hair are presented and are so stable that there are no significant differences in shape in those obtained for irradiated and unirradiated hair. Within 2 or 3 months after collecting, the spectra were intensified by irradiation with gamma rays from a ^{60}Co source, were more intense in male than female, and the intensity was independent of age. After storage of the hair in either water or air for as much as a year, the intensity of the spectra decreased; and after air storage for 22 years, the decrease of intensity is remarkable. The decrease over long periods of time parallels the length of time but is not parallel to blackness. (TCO)

31076 THE EFFECT OF ACUTE IRRADIATION IN AIR, N_2 AND CO_2 ON THE GROWTH OF THE SHOOT APEX AND INTERNODES OF KALANCHOE CV BRILLIANT STAR. Stein, O. L. (Montana State Univ., Missoula); Sparrow, A. H. Radiat. Bot., 6: 187-201(June 1966). (BNL-9570).

Acute irradiation with moderate x-ray exposures (1500 to 2000 R) of Kalanchoë seedlings resulted in temporary inhibition of leaf production. Within two weeks new leaves were formed, and at a slightly greater than normal rate. Thus, ultimately, the irradiated plants showed as many as or more leaves than the control material. Internodes that were meristematic during irradiation became severely inhibited, but the subsequently formed internode showed a considerable increase in length over control internodes. The changes in length of internodes were the result of altered cell number rather than cell size. Efforts to determine 3-indoleacetic acid involvement in this phenomenon proved inconclusive. Either internode lengths or frequency of abnormal phyllotaxies are suitable for quantitative assays of radiation effect. Use of the latter to test the effect of various gases and atmospheric pressures showed that this species is more tolerant to irradiation in a N_2 atmosphere than in air, and that sensitivity increased as the atmospheric pressure of air was increased. Irradiation in a CO_2 atmosphere gave results similar to irradiation in N_2 but an increase of CO_2 pressure in the presence of 1 atmosphere of air increased radiation sensitivity tremendously. Irradiation of the apical meristem proper with β rays from a $^{90}Sr/^{90}Y$ point source gave results similar to those obtained with x-irradiation of the entire shoot tip area. Thus the internode pattern of development observed must be under the control of the apical meristem itself. (auth)

31077 EFFECTS OF CHRONIC EXPOSURES TO ^{60}Co RADIATION ON PINUS RIGIDA SEEDLINGS. Mergen, Francois (Yale Univ., New Haven. Brookhaven National Lab., Upton, N. Y.); Thielges, Bart A. Radiat. Bot., 6: 203-10(June 1966). (BNL-9579).

An experiment was designed to test effects of differential exposures to ionizing radiations at various stages of development and periods of growth on the survival, height growth, productivity, and cytology of Pinus rigida Mill. Seedlings were exposed to radiation at 9 levels (0 to 20 R/20 hr day) in the Gamma Field at the Brookhaven National Laboratory. Radiation had a marked effect on terminal shoot growth inhibition and in the stimulation of sprouting. Shoot growth decreased, and flushing was delayed with increasing exposure, while sprouting increased. Sprouting was responsible for the survival of

many of the seedlings. Increased exposure to radiation also resulted in a decrease in subterminal bud formation and, at the higher levels (15 and 20 R/day), no axial primordia developed and the apical primordia were damaged. Needle length decreased with increasing exposure but cell damage in the needle meristems was slight. Two microsporangiate strobili were produced in 1 month on a sprout from a seedling that had been exposed to a total of 6800 R at a rate of 20 R/day, representing a considerable shortening of the normal phenology. Observations of sprouting in the spring of 1963 showed that in seedlings exposed to higher levels of radiation, sprouting was suppressed, probably as a result of the general weakening of the plants. Stem sprouting was inhibited to a greater extent than was basal sprouting. Basal sprouting was probably the result of partial shielding of the root collars by soil. (auth)

31078 RADIOBIOLOGICAL STUDIES IN PLANTS. XI. FURTHER STUDIES ON SOMATIC MUTATIONS INDUCED BY X RAYS AT THE al LOCUS OF DIPLOID OATS. Nishiyama, Ichizo; Ikushima, Takaji; Ichikawa, Sadao (Kyoto Univ.). Radiat. Bot., 6: 211-18(June 1966).

The effects of x-ray dose rate, fractionated exposure, and DNP treatment on somatic mutation frequency were studied using a mutant strain of diploid oats heterozygous for the albino gene. Various x-ray treatments were conducted on both the dry and 24-hr pre-soaked seeds. Higher dose rates were more effective in inducing mutations than lower dose rates. Fractionated exposure induced less mutations than non-fractionated exposure. Similar fractionated exposure but accompanied with a DNP treatment had about the same efficiency as the non-fractionated exposure. Consequently, it was concluded that many of the induced somatic mutations were induced by chromosomal deficiencies. The number of white stripes per leaf decreased with the progress of leaf order. This phenomenon appears to be due to the difference in numbers of the primordial or initial cells at the time of irradiation. A similar relationship was observed between the average ratio of white stripe width to leaf width and leaf order. It seems possible to consider that a considerable elimination of mutant cells occurred in the course of leaf development. Distinct white stripes were observed in leaf 3 and upper leaves but never in leaf 1 and 2 after irradiations of dry seeds. However, such distinct stripes were also observed in leaf 2 after irradiations of 24-hr presoaked seeds. This phenomenon is discussed giving two possible explanations. (auth)

31079 DIURNAL AND ANNUAL PERIOD OF RADIATION RESISTANCE OF PLANT CELLS. Biebl, R.; Hofer, K. (Univ., Vienna). Radiat. Bot., 6: 225-50(June 1966). (In German).

The outer and inner epidermises of red onion scales of Allium cepa and leaflets of the moss Mnium cuspidatum showed a marked diurnal rhythm of their resistance toward α- and uv rays. In the onion epidermis α-radiation resistance reached its maximum at 12 noon, its minimum at 8 p.m. Mnium cuspidatum showed the maximum of the α-radiation resistance at midnight and the minimum between noon and 4 p.m. In addition the diurnal changes of nuclear sizes of the inner epidermises of onion scales were measured (maximum: 12 noon, minimum: 8 p.m.). Both the cells of the onion scale and those of the leaflets of various mosses and liverworts also showed a marked annual rhythm of resistance to α- and uv-radiation. The bryophytes reached their maxima of radiation resistance in June and their minima in December, the onion epidermises were most sensitive to radiation in June and most resistant in December. The nuclear size of the inner epidermises of onion scales showed also an annual rhythm beside the diurnal rhythm. The nuclei reached maximum size in summer, minimum size in winter. While in the diurnal rhythm of the inner epidermises of onion scales the maxima of nuclear size coincided with the maximum radiation resistance of the cells, in the annual rhythm the cells showed their greatest radiation resistance when the nuclei were smallest and their greatest sensitivity when the nuclei were largest. The survival curves of α-irradiated outer epidermises of onion scales show a rapid drop within 24 hr after intensive irradiation, while inner epidermises exposed to lower doses of radiation death occurred only after some days. The etiology of cell death is discussed. Results are compared with those of similar studies, and hypotheses are advanced to explain annual variations in radiosensitivity. (H.G.D.)

31080 RADIATION GENETICS IN WHEAT. IX. DIFFERENCES IN EFFECTS OF GAMMA RAYS AND 14 Mev, FISSION, AND FAST NEUTRONS FROM Po–Be. Matsumura, Seiji (National Inst. of Genetics, Misima, Japan). Radiat. Bot., 6: 275-83(June 1966).

Dry seeds of Triticum monococcum were exposed to ^{137}Cs γ rays or to monoenergetic 14 Mev neutrons obtained from the T(d,n) reaction in a neutron generator. For both radiations the higher the dose, the more delayed the seedling growth and the more reduced both survival rate and seed fertility. However the frequency of chlorophyll mutations increased with increase in dose. In general, T. monococcum (n = 7) was the most sensitive to fission neutrons and γ rays. There was, as expected, no significant difference between T. durum (n = 14) and T. vulgare (n = 21). The higher the dose of fission neutrons and γ rays, the more delayed were germination and seedling growth, and the more reduced was seed fertility. As expected, the higher the ploidy, the lower the frequency of chlorophyll mutations. For seedling height the RBE value of fission neutrons to that of γ rays was found to be 10 ~ 15 in the three ploidy series. For seed fertility the RBE was about 10 for diploids and about 50 for tetra- and hexaploids and for chlorophyll mutations an RBE of 25 or more was determined for di- and tetraploids. In general, the RBE value was higher for the characters observed at maturity than in earlier stages, especially in polyploids. Fast neutrons of mean energy 4.7 Mev were obtained from a Po–Be source. Doses of 75 ~ 125 rad were not markedly effective in inhibiting seed germination and seedling growth or decreasing survival and seed fertility in T. monococcum, but were effective in inducing chlorophyll mutations. It was concluded that these neutrons are more effective than 14 Mev and fission neutrons, and that the RBE value for chlorophyll mutation frequency is about 40 against γ rays. (auth)

31081 EFFECTS OF WHOLE-BODY IRRADIATION ON THE TRANSFER CAPACITY OF RAT SMALL INTESTINE. Perris, A. D.; Jervis, E. L.; Smyth, D. H. (Univ. of Sheffield, Eng.). Radiat. Res., 28: 13-29(May 1966).

Intestinal transfer of glucose and fluid was studied in sacs of everted intestine made from rats that had received whole-body x irradiation. For this purpose the combined jejunum and ileum was divided into five parts, and the third and fifth segments were used. The effects can be divided into: indirect effects due to diminished presentation of food to the epithelial cells; and direct effects due to irradiation changes in the cells. Both direct and indirect effects reduced the transfer capacity of the intestine. In the third segment the capacity for transfer of both glucose and fluid was reduced, whereas in the fifth segment the capacity for fluid transfer was reduced. The time course of the indirect effects was the same in the third and fifth sacs. These effects were seen best on the second day after irradiation. The direct effects varied in the third and fifth segments. In the third segment the greatest effects appeared on the third day after irradiation, whereas in the fifth segment the greater effects appeared on the second day. The difference in the time relationships of the effects of irradiation in different parts of the intestine may reflect differences in the kinetics of the cell population in the jejunum and ileum. (auth)

31082 COMPARISON OF THE EFFECTS OF X IRRADIATION AND COLCHICINE ON THE INTESTINAL MUCOSA OF THE MOUSE. Hampton, James C. (Northwestern Univ., Chicago). Contract AT(11-1)-1244. Radiat. Res., 28: 37-59(May 1966).

Mice were injected with 0.04 mg of colchicine once daily

and sacrificed at intervals from 2 hours to 4 days. The effects on the intestinal epithelium were compared to those found after similar intervals in mice that had received 3 krads of x radiation. The characteristic loss of epithelium, the reduction in number and the abnormal appearance of mitochondria, and the depletion of ribosomes observed in irradiated mice failed to develop in drug-treated animals. Additionally, extreme shortening of crypts and villi did not occur in mice treated with colchicine. These observations suggest that the effects produced by ionizing radiation cannot be attributed only to blockage of mitosis and interference with cell renewal but that undifferentiated post-mitotic cells are irreversibly damaged, thus producing a cell population that is functionally incompetent. (auth)

31083 EFFECTS OF IONIZING RADIATION ON THE FINE STRUCTURE OF PANETH CELLS OF THE MOUSE. Hampton, James C. (Northwestern Univ., Chicago). Contract AT(11-1)-1244. Radiat. Res., 28: 71-83(May 1966).

Mice were subjected to 3 krads of x radiation, and changes in Paneth cells were studied at intervals of ½ hour to 5 days. Obvious changes occurred at 1 day, when it was noticed that structures regarded as stages in Paneth cell granule synthesis no longer appeared. At the 3- to 5-day intervals progressive loss of ribosomes and other signs of degeneration were observed, but Paneth cells containing secretory granules were still present until day 5 in surviving animals. Survival of Paneth cells versus loss of villus epithelial cells was attributed to the apparent long turnover time and hence longer life span of mature Paneth cells as compared to villus cells. The role of the undifferentiated cell and of the renewal time for a given cell population in intestinal radiation death was emphasized as an important cofactor with blockage of mitosis. (auth)

31084 SURVIVAL OF SYNCHRONIZED L CELLS AFTER ULTRAVIOLET IRRADIATION. Rauth, A. M.; Whitmore, G. F. (Univ. of Toronto). Radiat. Res., 28: 84-95(May 1966).

Survival curves for colony-forming ability of synchronized populations of mouse L cells were obtained after exposure of the cells to various doses of uv radiation. The D_{37} and D_0 values of these curves were strongly dependent on the age of the cell in the cell cycle at the time of irradiation, varying at the extremes by a factor of approximately 2. Cells in early S phase were most sensitive; cells in late S or early G_2 were least sensitive. The age-dependence of the sensitivity of L cells exposed to uvl radiation was found to be qualitatively and quantitatively different from the age-dependence observed when the same population of cells was exposed to ionizing radiation. (auth)

31085 STUDIES ON SYNCHRONIZED CELLS: RADIATION-INDUCED DIVISION DELAY IN THE FLAGELLATE ASTASIA LONGA. Padilla, George M.; Van Dreal, Paul A.; Anderson, Norman G. (Oak Ridge National Lab., Tenn.). Radiat. Res., 28: 157-65(May 1966). (ORNL-P-118).

The protozoan flagellate Astasia longa, dividing both exponentially and synchronously, was exposed to x radiation. Exponentially dividing cells were insensitive to doses of 105 R, but showed a 1.5-hour division delay when exposed to 495 to 1000 R, after which they resumed a normal rate of division. At larger doses, 2000 and 10,000 R, there was an immediate cessation of cytokinesis for an extended period, after which the cells resumed cytokinesis at a rate slower than that of the control. Synchronized cells were exposed to 400 to 1000 R at various times during the cycle, and the delay in the time of cell burst was noted. Sensitivity to radiation was variable over the cell cycle. It gradually increased during the latter portions of the cold period, reaching a maximum level 1 hr after the warm period began. It decreased during the time of mitosis and then increased again during the rest of the warm period. This same sensitive period corresponded to the periods when synthesis of DNA, RNA, and protein was taking place. (auth)

31086 AUTORADIOGRAPHIC STUDIES OF LYMPHOID CELLS IN BLOOD AND BONE MARROW OF NORMAL AND IRRADIATED DOGS. Keiser, G.; Bryant, B. J.; Bond, V. P. (Brookhaven National Lab., Upton, N. Y.). Radiat. Res., 28: 166-80(May 1966). (BNL-9299).

The migration, fate, and turnover of lymphoid cells in blood and bone marrow of four irradiated and four non-irradiated dogs were studied by serial autoradiography with clamping of the hind legs during the plasma clearance time of ^{3}H-thymidine injected into an anterior vein. In irradiated dogs, the ^{3}H-thymidine injection procedure was carried out during the early recovery phase after 250 R of whole-body x irradiation. The results on two irradiated and two normal dogs are described in detail. Migration of lymphoid cells from blood to marrow parenchyma was confirmed in the irradiated dogs. Conclusive evidence of transformation of these cells into hemopoietic precursors was not found. The relative number of large lymphoid cells, labeling index of the whole population of lymphoid cells, and that of small lymphoid cells were increased in irradiated marrow; few initially labeled small lymphoid cells could also be observed. Data indicate that the pattern of proliferation of lymphoid cells is changed in irradiated regenerating bone marrow. Possible interpretations of these changes are discussed. (auth)

31087 KINETIC MODEL OF BIOLOGICAL RADIATION RESPONSE. Dienes, G. J. (Brookhaven National Lab., Upton, N. Y.). Radiat. Res., 28: 183-202(June 1966). (BNL-9366; BNL-9389).

A model for biological radiation response is presented that postulates that on irradiation a series of reactions takes place, these reactions remaining unspecified in the model, which leads to a final product that is lethal to the biological system. It is assumed for simplicity that all the reactions are first-order. Thus, this treatment is a linear treatment in the sense that all the differential equations describing the rate process are linear. There is no conceptual difficulty in introducing bimolecular, or higher-order, reactions, but the mathematical difficulties become severe, and the equations must be handled by numerical techniques. Applications presented include a simple case with no recovery, a simple case of dose-rate dependence and recovery, and retrogressive recovery behavior. The model was in good agreement with experimentally demonstrated behavior. (C.H.)

31088 EFFECT OF X IRRADIATION ON DNA SYNTHESIS IN THE UTERINE EPITHELIUM. Perrotta, Carmie A. (Brookhaven National Lab., Upton, N. Y.). Radiat. Res., 28: 232-42(June 1966). (BNL-9012).

The effects of x irradiation on the presynthetic and synthetic phases of the uterine epithelial cells with respect to DNA synthesis were investigated in mice by varying the timing of irradiation and tritiated thymidine injection relative to the time of estrogen administration. Whole-body doses of 100 to 400 rads at a time when the epithelium was in the presynthetic phase delayed most of the cells from making the transition from the G_1 phase to the S phase, whereas 2000 rads prevented them from ever making the transition during the observational period. Whole-body doses of 200 to 2000 rads at a time when the epithelium was in the synthetic state reduced DNA synthesis in S phase cells by about one-half. These results suggest that the mechanisms affected by irradiation of S phase cells are different from those affected in the presynthetic period. The different possible natures of the G_1 and S effects are discussed. (auth)

31089 THE EFFECTS OF 250-kv X RAYS ON THE DOG'S PANCREAS: MORPHOLOGICAL AND FUNCTIONAL CHANGES. Archambeau, John; Griem, Melvin; Harper, Paul (Argonne Cancer Research Hospital, Chicago). Radiat. Res., 28: 243-56(June 1966).

The pancreas of 9 dogs was surgically isolated to the right side of the abdomen and irradiated with a total dose of 4500 to 5000 rads x radiation fractionated over 30 days. At the end of irradiation and at 1 month, 2 months, and 5 months after irradiation, the histological changes demonstrated a progressive interstitial fibrosis and scarring which distorted the regular architecture. The acini were

separated by fibrosis but were morphologically intact. The islets showed no histological change. Beta and alpha cells were present. One dog with a modified total pancreatic fistula survived 2 weeks after receiving a tissue dose of 4500 rads to the pancreas fractioned over 24 days. The total 24-hour secretory volume and the secretory volumes after secretin and mecholyl stimulation were unchanged during and after irradiation. The serum and pancreatic secretion electrolytes, fasting blood sugars, and glucose tolerance determinations were within normal limits. However, the elevated serum amylase decreased, whereas the concentration of amylase in the pancreatic secretion increased. These studies are consistent with the morphological findings, indicating that the function of the pancreas is not markedly altered by the dose and time schedule of irradiation used in this study. (auth)

31090 HISTOCHEMICAL OBSERVATIONS OF OXIDATIVE ENZYMES IN IRRADIATED TESTIS AND EPIDIDYMIS. Ito, Minoru (Osaka Univ. Dental School). Radiat. Res., 28: 266-77 (June 1966).

The histochemical distribution of oxidative enzyme systems was observed in testes and epididymides of mice that had received a single whole-body irradiation or a single local irradiation with x rays or γ rays. The enzymatic activities of succinic, α-glycerophosphate, and glucose-6-phosphate dehydrogenases in the germinal epithelia showed a progressive decrease postirradiation, particularly after whole-body exposure. Irradiated testes and epididymides exhibited the histochemical changes associated with morphological damages irrespective of the kind of radiation used. In the degenerated seminiferous tubules of the testes, succinic dehydrogenase activity in immature cells such as spermatogonia conspicuously decreased after whole-body x irradiation. α-Glycerophosphate dehydrogenase activity of spermia in the shrunken testicular tubules and epididymal canals was low, with some variation during a few days after whole-body irradiation. Glucose-6-phosphate dehydrogenase was absent in all testicular cells on the first day, but it remained normal in interstitial Leydig cells of the degenerating testes. The histochemical dehydrogenase activities examined showed a more rapid and marked decrease after whole-body exposure than those obtained after local exposure. In tissues γ irradiated by local exposure, the maximal decrease in the enzyme activities which occurred about the sixteenth day was followed by a recovery toward the end of the experiment, especially in glucose-6-phosphate dehydrogenase activity. The significance of these alterations suggests that testicular oxidative metabolism generally decreases after irradiation, but the specific nature of these changes and their causes still remain unclear. (auth)

31091 FREQUENCY OF LIVE BIRTHS AMONG SURVIVORS OF HIROSHIMA AND NAGASAKI ATOMIC BOMBINGS. Seigel, Daniel G. (Atomic Bomb Casualty Commission, Nagasaki). Radiat. Res., 28: 278-88 (June 1966). (TID-22640).

Koseki data through 1961 were checked for the live birth experience of approximately 24,000 persons in Nagasaki and Hiroshima, and comparisons were made among groups at various distances from the atomic bomb in 1945. Although the investigation was motivated by an interest in the relationship between radiation and fertility, no information is available on comparative birth control practices in these study populations, and hence no inferences are made concerning any stage of reproduction prior to the live birth itself. Among those with married status in 1945, the percentage with no births from 1945 to 1961 was the same in each distance group. This was also true for the subgroups with no births previous to 1945. Among those with first marriage from 1946 to 1950, the percentage with no births up to 1961 did not show any extraordinary variation by distance from the bomb; the same is true for persons with first marriage from 1946 to 1950. The ratio of live births to person-years of marriage during 1946 to 1961 was unrelated to comparison group. (auth)

31092 ENERGY REQUIREMENTS AND RELATIVE BIOLOGICAL EFFECTIVENESS FOR PRODUCING A CYTOGENETIC PHENOMENON IN MAIZE BY IRRADIATING SEEDS WITH X-RAYS AND MONOENERGETIC NEUTRONS. Smith, Harold H.; Rossi, Harald H. (Brookhaven National Lab., Upton, N. Y.). Contract AT(30-1)-2740. Radiat. Res., 28: 302-21 (June 1966). (BNL-9633).

The frequency of occurrence of yellow-green (yg_2) sectors in seedling leaves that develop from irradiated Yg_2/yg_2 maize seeds was used as a criterion of radiation effect. The yg_2 phenomenon is due mainly to a break in chromosome 9 between the centromere and the Yg_2 locus, with loss of the Yg_2-containing segment. The dose-response curves for 250-kvp x rays (1,420 to 14,250 rads) and for monoenergetic neutrons (0.43, 1.25, 1.80, and 14.7 Mev) were linear (or indistinguishable from linearity) and were independent of dose rate (with x rays from 10.3 to 1758 rads/min), thus indicating that breakage of the chromosome, with loss of Yg_2, may be due to a single charged particle. X ray-induced yg_2 mutation rates were 16.4×10^{-7} and 8.3×10^{-7} per rad for cells of leaves 4 and 5, respectively. The mutation rates per rad for neutrons were dependent on the leaf scored and the neutron energies employed. For leaf 5 the range was from 3.9×10^{-5} (1.80 Mev) to 6.8×10^{-5} (0.43 Mev). The effective volume was assumed to be a sphere and, based on microdosimetric concepts, was computed to have a diameter of 1.35 microns in leaf 4 and 1.10 microns in leaf 5. The corresponding estimates arrived at by cytological methods were 1.52 microns and 1.38 microns, respectively. The results can be accounted for both relatively and absolutely on the assumption that the interphase chromosome is broken, to cause the occurrence of a yg_2 sector, when a single charged particle delivers an energy of approximately 93 kev or more to a spherical region of the seed embryo cell nucleus that is approximately 1 micron in diameter but proportional to nuclear diameter. The relative biological effectiveness of the neutron irradiations used, compared to 250-kvp x rays, ranged from 47 to 102. (auth)

31093 DRY T_1 BACTERIOPHAGE IN MEASUREMENT OF LARGE DOSES OF IONIZING RADIATION. Fluke, Donald J. (Duke Univ., Durham, N. C.). Radiat. Res., 28: 336-51 (June 1966).

Dry films of T_1 bacteriophage in nutrient broth irradiated in a vacuum at room temperature are useful in dosimetry and physical characterization of accelerated particle beams. The intrinsic sensitivity of the phage under prescribed circumstances appears to be 570 ± 15 krads for survival e^{-1} for γ rays or positive ions. For fast electron irradiations the same figure appears to be applicable, although for some series the physical description of the irradiation process must be presumed to be incomplete. Phage films can be employed for range measurements by Bragg curves and for developing dose-depth relations more generally. (auth)

31094 EFFECTS OF WHOLE-BODY IRRADIATION ON THE ADRENAL OF THE GOLDFISH CARASSIUS AURATUS L. Sathyanesan, A. G.; Chavin, Walter (Wayne State Univ., Detroit). Radiat. Res., 28: 352-64 (June 1966).

Whole-body irradiated (^{137}Cs γ) goldfish (Carassius auratus L.) showed little mortality after 1 to 2 kR for the experimental period of 90 days. The LD_{50} at 2.5 kR occurred at 15 days; 38% survived for 30 days, and 8% for 90 days. With 10 kR, the LD_{100} was achieved at 17 days. Significant adrenal alterations were present 4 days postirradiation at all dose levels. The sequence of changes occurring with time at the 2.5-kR dose level included hypertrophy, hyperplasia, atrophy, degeneration, and cyst formation. Adrenocortical phospholipid granulation was reduced after irradiation. A numerical increase in medullary cells also occurred. Blood vessel alterations ranged from dilation and rupture to occlusion. In some cases, adrenal cells appeared in the lumina of the blood vessels after rupture. In other cases, microhemorrhage and edema were present. The adrenal alterations in response to irradiation were generally comparable to those described in similarly treated mammals. (auth)

31095 PROTONS AND SPACE TRAVEL: AN INTRODUCTION. Dalrymple, Glenn V.; Lindsay, Ian R.

(Brooks Air Force Base, Tex.). Radiat. Res., 28: 365-71(June 1966).

The radiations found in space can be grouped into four major categories: (1) electromagnetic radiations, (2) electrons, (3) protons, and (4) nuclei of elements with atomic number (Z number) greater than 1. The electrons and electromagnetic radiations have sufficiently low energy (and subsequently low penetration power) that they do not represent a great hazard to the occupant of a space vehicle as long as he remains inside, because the shielding provided by the vehicle walls would be thick enough to absorb these radiations. The protons and heavier nuclei, however, do represent a very real danger because a large number of them have sufficient energy to penetrate the thickest shielding, either available now or planned for years to come. Of these particles, the protons are by far the most hazardous to the space traveler because of the weight of their numbers. Of all the charged particles (excluding electrons) found in space, the protons make up well over 90% of the total. Available data on the origin of protons in space and the reactions of protons in tissue are reviewed. The biological effects of the complex space proton spectrum are discussed. (C.H.)

31096 WHOLE-BODY IRRADIATION OF PRIMATES WITH PROTONS OF ENERGIES TO 400 Mev. Williams, Gwilym H.; Hall, James D.; Morgan, Ira L. (Texas Nuclear Corp., Austin, Tex.). Contract AF41(609)-2418. Radiat. Res., 28: 372-89(June 1966).

The physical and dosimetric aspects of the whole-body irradiation of small primates (Macaca mulatta) with 400-, 250-, 138-, 55-, and 32-Mev protons are described. Doses varying from 25 to 7000 rads were given, about 100 animals being exposed at each energy. Details of the experimental procedures are given and the dosimetry problems are discussed. Biological results of these exposures are described in the references. (auth)

31097 SOME EFFECTS OF WHOLE-BODY 32-Mev PROTON IRRADIATIONS ON PRIMATES. Dalrymple, Glenn V.; Lindsay, Ian R.; Ghidoni, John J.; Kundel, Harold L.; Still, Ed T.; Jacobs, Robert; Morgan, Ira L. (Brooks Air Force Base, Tex.). Radiat. Res., 28: 406-33(June 1966).

Seventy-six primates (Macaca mulatta) were irradiated with spaced doses of 32-Mev protons (280 to 6700 rads). The highest doses (5200 to 6700 rads) produced severe central nervous system disease with convulsions. Intermediate doses (1440 to 4250 rads) caused marked cutaneous destruction with extensive ulceration and secondary infection. Mortality patterns, blood counts, ^{59}Fe ferrokinetics, clinical manifestations, and histopathological studies showed no evidence of either gastrointestinal or hematological radiation changes. This situation was anticipated, since the average transverse diameter of the primate (10 cm) was considerably larger than the range of the protons (1 cm in soft tissue). Because of the absence of injury to the bone marrow or gastrointestinal tract, mortality was relatively delayed after irradiation. An $LD_{50(80)}$ of 1595 ± 101 (S.E.) rads was estimated from the cumulative mortality data. The postirradiation course of those animals dying from a cutaneous mechanism was in many ways similar to that found following third-degree thermal burns. All survivors (1440 to 1880 rads) had collections of edema fluid which appeared as a delayed finding after the eighth postirradiation week. Lower doses (560 to 990 rads) caused no cutaneous destruction but did produce transient edema. No clinical abnormalities were noted in the lowest dose group (280 rads). Serum lactic dehydrogenase (LDH) and glutamic oxalacetic transaminase (SGOT) levels were markedly elevated following irradiation, the degree of elevation being correlated with dose. (auth)

31098 EDEMA: A DELAYED COMPLICATION OF TOTAL-BODY 32-Mev PROTON IRRADIATION. Dalrymple, Glenn V.; Ghidoni, John J.; Kundel, Harold L.; Wolfle, Thomas L.; Lindsay, Ian R. (Brooks Air Force Base, Tex.). Radiat. Res., 28: 434-45(June 1966).

Severe edema of the head and, to a lesser degree, edema of the anterior abdominal wall and perineum occurred approximately 8 weeks after 32-Mev proton irradiation of Macaca mulatta. A group of 11 primates were irradiated with a large dose of 32-Mev protons (2350 rads); some of the animals were treated with antibiotics in an effort to decrease mortality during periods of acute cutaneous infection. Of the original 11 irradiated animals, the 5 survivors of the acute effects of the radiation developed edema. Several diagnostic studies suggest that increased capillary and/or lymphatic permeability in conjunction with a moderate hypoalbuminemia is probably the etiology of the edema. (auth)

31099 SOME EFFECTS OF 55-Mev PROTONS ON PRIMATES. Lindsay, Ian R.; Dalrymple, Glenn V.; Ghidoni, John J.; Mitchell, John C.; Morgan, Ira L. (Brooks Air Force Base, Tex.). Radiat. Res., 28: 446-64(June 1966).

Seventy-four primates (Macaca mulatta) were given spaced doses of 55-Mev protons to the whole-body surface. The mortality data, hematological measurements, and LDH and SGOT concentrations demonstrate an effect intermediate between that of poorly penetrating 32-Mev protons and that of radiation that completely penetrates the primate. In addition, 12 animals received partial-body exposures of 55-Mev protons in single spaced doses to the abdominal area. These exposures produced the gastrointestinal syndrome with no accompanying hematological injury, and a linear relationship between survival time and dose was demonstrated. (auth)

31100 THE KINETICS OF RECUPERATION FOLLOWING 55-Mev PROTON IRRADIATION. Dalrymple, Glenn V.; Lindsay, Ian R.; Mitchell, John C.; Hall, James D.; Morgan, Iral L. (Brooks Air Force Base, Tex.). Radiat. Res., 28: 465-70(June 1966).

The kinetics of recuperation of mice following initial doses of 470 rads of 55-Mev protons and 350 rads of ^{60}Co γ radiation were investigated by means of the paired-dose method. By use of semilog plots, recovery half-times of 4.85 ± 0.85 days and 2.02 ± 0.45 days were found after initial doses of the protons and ^{60}Co γ radiation, respectively. (auth)

31101 SOME EFFECTS OF 138-Mev PROTONS ON PRIMATES. Dalrymple, Glenn V.; Lindsay, Ian R.; Ghidoni, John J.; Hall, James D.; Mitchell, John C.; Kundel, Harold L.; Morgan, Ira L. (Brooks Air Force Base, Tex.). Radiat. Res., 28: 471-88(June 1966).

A total of 102 primates (Macaca mulatta) were irradiated with spaced doses of 138-Mev protons ranging from 105 to 1220 rads, an $LD_{50(30)}$ of 516 ± 0.09 (S.E.) for the mortality RBE. Adjusting the 2-Mev x ray $LD_{50(30)}$ to correspond to the 138-Mev proton dose rate gives an RBE of 1.0. Changes in total leukocyte count, lymphocyte count, neutrophil count, platelet count, hemoglobin concentration, hematocrits, LDH concentrations, and SGOT concentrations indicate an RBE of 1 for 138-Mev protons as compared to 2-Mev x rays. The only findings that were significantly different between these qualities of radiation were clinical. Considerably more pronounced signs of gastrointestinal injury and hemorrhage were produced by 138-Mev protons as compared to equivalent doses of 2-Mev x rays. (auth)

31102 THE RELATIVE BIOLOGICAL EFFECTIVENESS OF 138-Mev PROTONS AS COMPARED TO ^{60}Co GAMMA RADIATION. Dalrymple, Glenn V.; Lindsay, Ian R.; Hall, James D.; Mitchell, John C.; Ghidoni, John J.; Kundel, Harold L.; Morgan, Ira L. (Brooks Air Force Base, Tex.). Radiat. Res., 28: 489-506(June 1966).

Adult female white Swiss Webster mice were irradiated with single spaced doses of either 138-Mev protons or ^{60}Co γ radiation delivered at 86, 256, and 550 rads/min; the doses were so spaced as to bracket the $LD_{50(30)}$. Clinically, doses of 865 rads and above of the protons produced relatively more gastrointestinal injury than did doses of the same size of ^{60}Co γ radiation. Total mortality through 30 days, however, was the same for both types of radiation. Comparison of the $LD_{50(30)}$'s at all three dose rates provided estimates of the proton to ^{60}Co γ ray RBE of approximately

1. The RBE's determined by comparison of the $LD_{50(6)}$'s were 10% to 20% higher than those found at 30 days. No dose-rate dependence was found. The results are compared to published data from similar experiments. (auth)

31103 SOME EFFECTS OF 400-Mev PROTONS ON PRIMATES. Dalrymple, Glenn V.; Lindsay, Ian R.; Ghidoni, John J.; Mitchell, John C.; Morgan, Ira L. (Brooks Air Force Base, Tex.). Radiat. Res., 28: 507-28 (June 1966).

Primates (Macaca mulatta) were given spaced doses of 400-Mev protons. From the mortality data an $LD_{50(30)}$ of 585 ± 33 (S.E.) rads was calculated. Hematological measurements, LDH, and SGOT concentrations, ^{59}Fe ferrokinetics, and histopathological findings indicate that the effects produced by the protons are virtually identical to those produced by equivalent doses of 2-Mev x rays. The only differences in response were clinical; relatively more intense gastrointestinal and hemorrhagic signs occurred after proton irradiation than after similar doses of x rays. (auth)

31104 EFFECT OF HIGH-ENERGY PROTON IRRADIATION ON THE CARDIOVASCULAR SYSTEM OF THE RHESUS MONKEY. Kundel, Harold L. (Brooks Air Force Base, Tex.). Radiat. Res., 28: 529-37 (June 1966).

During the first 24 hours after total-body irradiation of the rhesus monkey (Macaca mulatta) with 3680 rads of 138- or 400-Mev protons, there is a decrease in mean arterial pressure similar to that observed in monkeys irradiated with an equivalent dose of ^{60}Co γ radiation. Irradiation of monkeys with the same dose of 55-Mev protons also causes a decrease in mean arterial pressure, but of much lesser magnitude than at the higher energies. After irradiation with 32-Mev protons, although there is an immediate decrease of mean arterial pressure, recovery occurs by 6 hours postirradiation. The response of the mean arterial pressure to small intravenous doses of norepinephrine is diminished immediately after irradiation with 55-, 138-, or 400-Mev protons. The animals in the 138-Mev and 400-Mev proton-irradiated groups showed recovery by 24 hours, a pattern similar to that seen in the ^{60}Co γ irradiated animals. The abnormality persisted in the 55-Mev proton-irradiated animals. The 32-Mev proton-irradiated animals showed only a minimal decrease in responsiveness to norepinephrine immediately after irradiation. The differences in response of the rhesus monkeys to the same surface dose of different proton energies is attributed to differences in depth-dose distribution of the protons. At energies of 138 and 400 Mev, where deposition of energy is relatively uniform, the effects are similar to those of ^{60}Co γ irradiation, and it is suggested that the RBE for these effects approximates 1. At lower energies, where only the outer portion of the volume of the body is irradiated, the effect on the blood pressure is not as great. Because of difference in depth-dose distribution, an RBE cannot be validly calculated. (auth)

31105 EFFECT OF GAMMA AND PROTON IRRADIATION ON LACTIC DEHYDROGENASE ISOENZYMES. Hawrylewicz, Ervin J.; Blair, William H. (Illinois Inst. of Tech., Chicago). Contract AF41(609)-2021. Radiat. Res., 28: 538-47 (June 1966).

Exposure of monkeys (Macaca mulatta) to γ and proton radiation causes marked alterations in the serum and the tissue LDH enzyme activity. The increase of serum activity is a reflection of an immediate increase in the M-LDH isoenzymes, and subsequently an inversion and crossover point are observed. At this point the H-LDH isoenzyme activity predominates. The extent of the increase, the rate of the increase, and the extent of alteration of the isoenzyme ratios are functions of dose, energy level, and type of radiation. Gamma radiation produces the most rapid and severest response. (auth)

31106 ESTIMATE OF THE BIOLOGICAL EFFECTS OF THE SPACE PROTON ENVIRONMENT. Dalrymple, Glenn V.; Lindsay, Ian R.; Ghidoni, John J.; Mitchell, John C.; Morgan, Ira L. (Brooks Air Force Base, Tex.). Radiat. Res., 28: 548-66 (June 1966).

Small primates (Macaca mulatta) were irradiated with relatively low doses (25 to 400 rads) of either 55- or 250-Mev protons. The biological changes which were demonstrated were directly related to the depth of penetration of the protons as well as to the size of the doses. A summary of the results of the present and prior studies is presented, together with some published physical measurements of the space proton spectrum. Predictions of the biological effects of the protons on man as a space traveler are given. In general, the effects produced by protons are very similar to those produced by supervoltage electromagnetic radiations, when allowance is made for depth-dose distribution. (auth)

31107 RELATIVE BIOLOGICAL EFFICIENCY OF 200 kv X-RAYS, ^{60}Co RAYS AND 14 Mev NEUTRONS IN ESCHERICHIA COLI INACTIVATION. Bollini, Vincenzo; Babini, Lucio; Bernardi, Zena; Cecchetti, Ervedo; Corinaldesi, Alberto; Gavelli, Gian Paolo; Petralia, Stefano; Zanetti, Mario (Univ., Bologna). Ric. Sci. Riv., 36: 243-5 (Apr. 1966). (In Italian).

The values of the relative biological efficiency of x rays of 200 kv and neutrons of 14 Mev in comparison with γ rays from ^{60}Co were determined. Inactivation of Escherichia coli was chosen for a biological test. The RBE of x rays is 0.92 and of neutrons is 0.85. (auth)

31108 RADIATION BIOLOGY. (International Atomic Energy Agency, Vienna). pp 59-75 of STI-DOC-10/53.

Mutation rates at specific autosomal loci in different species of irradiated Drosophila, phosphate metabolism of Escherichia coli and baker's yeast, tissue therapy after irradiation, selective protection against damages induced by x-irradiation and radiomimetic drugs, the relation between radioresistance and immunoresistance, factors influencing the radiation resistance of food spoilage fungi, and mechanisms of initial radiation effects at cellular levels are discussed. (M.C.G.)

31109 RADIOISOTOPE APPLICATIONS IN AGRICULTURE. (International Atomic Energy Agency, Vienna). pp 87-100 of STI-DOC-10/53.

Topics covered include: induction of genetic mutation by irradiation in plant species of economic importance, selection methods for induced small mutations in higher plants with special regard to mutations of yielding capacity, control of the Mediterranean fruit fly by liberation of adult males irradiated with gamma rays, relations between the biochemistry of latex and the mineral nutrition and productivity of Hevea brasiliensis, maize fertility studies using fertilizer containing labeled nutrient elements, and field experiments for control or elimination of local populations of Queensland fruit fly, Dacus tryoni. (M.C.G.)

31110 EFFECT OF IRRADIATION OF SEEDS BY ^{60}Co γ-RAYS ON THE FORMS OF WATER IN CORN AND WHEAT LEAVES. Reshetnikov, A. E. Uzb. Biol. Zh., 99: No. 4, 10-11(1965). (In Russian).

Seeds of wheat and corn received 1500 R of γ rays from a ^{60}Co source, following which they were planted, and sections of leaves appearing at various age intervals analyzed for free and bound water. While irradiation caused a 3 to 5% higher yield of corn, the total water content of the leaves was at all times below that of the controls, and the leaves of the experimental plants contained more free water as compared with normal leaves, the difference tending to level off towards blooming time. (C.H.)

31111 KINETICS OF ACCUMULATION AND ELIMINATION OF RADIOACTIVE CESIUM FROM THE RESPIRATORY ORGANS. Korolev, G. K. (Inst. of Medical Radiology, Obninsk, SSSR). Vestn. Akad. Med. Nauk SSSR, 20: No. 9, 58-65(1965). (In Russian).

Rapid absorption followed the inhalation of ^{137}Cs by rats. On the 1st day, almost 90% of the incorporated activity was removed from the lungs; the absorption occurred exponentially, and the half-elimination period was 2 days. The greatest quantity of ^{137}Cs was deposited in the muscles (46% of the incorporated activity), and the liver was 2nd with 10%. The highest content of the isotope was observed in the 1st day in the kidneys, liver, and heart. No substantial differ-

ences in the content of ^{137}Cs in the internal organs arose subsequently. Under the influence of ^{137}Cs at a dose of 0.4 $\mu c/g$ in the lungs (absorbed dose, 226 rads) on the 10th day after the inhalation of the isotope there developed extensive hemorrhage, perivascular edema, and degenerative changes in the endothelium of the vessels, the epithelium of the bronchi and muscles. Subsequently, inflammatory and degenerative changes were replaced by proliferative processes. (C.H.)

31112 IMMUNOPATHOLOGY IN A CHRONIC EXPOSURE TO ^{65}Zn. Filatov, P. P.; Gaidova, E. S. Vestn. Akad. Med. Nauk SSSR, 20: No. 9, 65-70(1965). (In Russian).

$^{65}ZnCl_2$ was administered orally to rabbits daily for 18 months in a daily dose of 10 $\mu c/kg$ body weight. After 12 to 16 months of treatment autoantibodies against tissues were detected by immunodiffusion. After 9 months the protein content of the blood serum showed changes; the albumin decreased by 29% and the β- and γ-globulin levels increased by 45 to 48%. After 16 to 18 months there was evidence of reticular tissue hyperplasia in the hemopoietic organs, extramedullary hemopoietic foci in the spleen and lymph nodes, and the presence of plasma cells and amyloid in the spleen and kidneys. The data suggest that an autoimmune mechanism plays an important role in the pathogenesis of chronic radiation injury by ^{65}Zn. (C.H.)

31113 EFFECT OF GAMMA RADIATION ON SEEDS IN THE SECOND GENERATION. Liu, Chao; Chao, Juang; Hsu, Chao mei; Liu, Chin-t'ao; Wang, Chan-t'ien; Liu, Ching-hsiang; Kuo, An-hsi (Honan Agricultural Coll., China). Yuan Tzu Neng, No. 2, 169-71(1965).

It is well known that γ irradiation of wheat and corn with doses of 750 to 2500 and 1000 to 3000 R, respectively, helps to increase production, which is decreased after doses of 10,000 R. The results are presented of a study of the effect of radiation on the second generation of wheat and corn. The stimulatory effect on the first generation was found to be continued in the second generation, but the inhibitory effect was greatly weakened. After irradiation, the rate of tillering and the number of ears of wheat were increased, and correspondingly favorable results were also found in the case of corn. With the strain of the plants taken into account, the effects of γ irradiation evidently helped the growth of the second generation. A physiological analysis showed that the metabolism in the second generation is better, as indicated by the higher catalase activity in the second generation sprouts. Therefore, it is concluded that the application of the proper amount of radiation to seeds may stimulate growth and increase production in the second generation. (ATD)

31114 A PRELIMINARY STUDY OF THE BIOLOGICAL EFFECT OF GAMMA RAYS ON PEAS. I. THE EFFECT OF THE GROWTH AND DEVELOPMENT OF PEAS. T'ang, Tse-sheng; Yang, Ch'ang-yu; Yu, Shao-hua (Nan-ch'ung Normal Coll., China). Yuan Tzu Neng, No. 2, 177-81(1965).

The results are presented that were obtained in experimental work with peas subjected to different amounts of γ radiation from ^{60}Co. The results showed that a stimulating effect can be produced by radiation doses below 4000 R, while doses over 10,000 R cause inhibition. However, no inhibitory effect was observed on sprouts even at relatively high radiation doses up to 80,000 R; this may be due to the fact that the radiation does not penetrate the skin of the sprouts. The most favorable radiation dosage, yielding the best increase in germination rate, is between 100 and 4000 R. Doses over 10,000 R definitely reduce the productivity, and doses over 50,000 R kill the pea seeds. (ATD)

31115 EFFECT OF IONIZING RADIATION ON THE METABOLISM AND RESPIRATION OF SEEDLINGS. Li, Yu; Liu, Ts'un-te. Yuan Tzu Neng, No. 3, 265-71(1965).

Experiments carried out on the effect of x ray on respiration in seedlings showed inhibition of respiration proportional to the dose of radiation. Respiration was found to be more sensitive to radiation in the presence of oxygen than without it. There is a latent period in the effect of radiation, so that no obvious effect can be measured immediately after irradiation, and respiration continues even after lethal doses of radiation. Dry seeds can withstand stronger radiation doses than sprouts, so that larger amounts of radiation are required to prevent germination of dry seeds. Some protection against radiation may be obtained by the lowering of the metabolic rate at low temperatures. Ionizing radiation delays maturation of the seed toward the embryonic stage, and even after transformation into an embryo, the proper seedling structure may not be produced. It is also pointed out that the inhibition of respiration cannot be utilized as a means of decreasing the content of metabolic intermediates. It is proposed that further studies should be devoted to the complicated enzymatic reactions in plant respiration and the effects on the processes of oxidative phosphorylation. (ATD)

31116 EFFECT OF GAMMA RADIATION FROM ^{60}Co ON THE SURVIVAL REPRODUCTION AND RATE OF INFECTION OF WATERSNAILS. Yeh, Chia-fu; Sun, Ch'ing-ch'i. Yuan Tzu Neng, No. 3, 272-9(1965).

Experiments showed that the death rate of water snails after treatment with 500 to 30,000 R of γ-radiation (65 to 99 r/min) is comparable to that in controls, but dosages above 40,000 R cause the prompt death of water snails, and a dosage range of 33,040 to 35,150 R causes death in 95%, with a latent period of 60 to 70 days. Sixty days after treatment of the male snail with 500 R, its testicles begin to atrophy, reaching a maximum at 90 days, with gradual recovery after 120 days, but active sperm are still present in the vas deferens, and there is no change in appearance of the genitalia. When a male snail which has been treated with 1000 R is brought together with a normal female snail, the fertilization rate of the eggs laid by the female apparently drops, starting about 20 days after breeding, due to the degeneration of the male sperm. After treatment of the female with 500 R, its ovaries wither, beginning 20 days after treatment and reaching a maximum at 90 days, after which they recover gradually, and mature eggs are found in the ovaries if the female is treated with doses below 15,000 R. The number of eggs laid decreases with an increase in the amount of radiation treatment, and the fertilization rate also drops correspondingly. When the female is treated with doses over 15,000 R, the time of egg laying is postponed about 20 days, and it ceases about 1 month earlier; moreover, the eggs are impossible to fertilize. As far as infection is concerned, the water snails can still be infected by schistosomes. (ATD)

31117 STUDY ON THE DAMAGE AND RECOVERY OF THE SPERMATOCYTES OF MONKEYS FOLLOWING X AND GAMMA RADIATION. Hsu, Feng-tsao. Yuan Tzu Neng, No. 4, 314-19(1965).

The results are reported of three experiments on the effects of x and gamma radiation on monkeys. A total of 13 male monkeys (Macaca mulatta Zimmermann) were used. The dosages for whole-body radiation varied from 200 to 600 R, and the reproductive organs were examined 8 days to 1 year following irradiation. These preliminary studies showed that severe damage to the sperm cells resulted from this dose of radiation. The damage was evidenced by a decrease in the number of cell divisions as well as by cell mortality, which could be seen by the shrinkage or disappearance of the nuclei. The sterilization dosage of x rays or γ rays for these animals was 300 to 400 R. The radiation damage to the reproductive organs was often localized, so that certain areas in this organ were left completely unaffected. A possible recovery of the reproductive function from these unharmed parts is postulated. (ATD)

31118 FINE STRUCTURAL STUDIES ON THE EFFECT OF X RAYS ON THE RETINA OF GUINEA PIGS. Becher, H.; Themann, H. (Anatomisches Institut, Muenster, Ger.). Z. Mikroskop.-Anat. Forsch., 71: 587-608(1964). (In German).

The morphologically highly differentiated fine structure of the guinea pig retina was studied after localized x irradiation with 500, 1000, 1500, 3000, and 6000 R, administered at a rate of 500 R/min. The retinas were studied at inter-

vals of 1, 2, 3, 4, 5, and 6 days after irradiation. The generally high radioresistance of the retinal tissues that has been reported previously from studies made with the light microscope was confirmed by studies made with an electron microscope. No changes were observed in the fine structure of the retina after irradiation with 100, 300, and 1000 R at the various time intervals. At higher doses the effect of irradiation was shown predominantly by degeneration and complete destruction of the external elements which was followed by similar effects on the internal elements. There was a marked increase in the glycogen content of the internal receptor elements with mitochondrial swelling, and some quantitative decrease in the mitochondria. These results suggested that the mitochondria had not lost their capacity to synthesize glycogen, but that the use of glycogen had been decreased. In other layers of the retina there was only slight evidence of irradiation injury. This consisted of appearance of lipid deposits, reduction of glycogen content of supporting fibers, and the infrequent appearance of myelin particles in the reticular layers. (BBB)

31119 EFFECTS OF X-RAYS ON THE ORCHITIS DEVELOPMENT IN RABBITS AND THE ANTIGEN PROPERTY FOR THE REACTION OF TREPONEMA PALLIDUM IMMOBILIZATION. Butovetskii, L. D. Zh. Mikrobiol. Epidemiol. Immunobiol., No. 3, 131-4(Mar. 1966). (In Russian).

Orchitis was enhanced in rabbits exposed to x-ray doses of 350 to 400 R 10 days after infection with the Budapest strain of Treponema pallidum. Antigen quality was best in animals killed 10 to 14 days after infection. In animals given 500 R doses, clinical development of orchitis was inhibited and the antigen contained an insufficient number of treponemata. (H.G.D.)

31120 TISSUE GRAFTING AND RADIATION. Micklem, H. S.; Loutit, John F. American Institute of Biological Sciences and U. S. Atomic Energy Commission Monograph Series on Radiation Biology. New York, Academic Press, 1966. 228p. $7.00.

The field of transplantation immunity and tolerance is reviewed and the various ways in which the two disciplines of radiation biology and transplantation are used together to study problems of immune reactions and radiobiology are described. The effects of x radiation on the rejection of homografts and the subsequent humoral antibody formation are discussed with emphasis on the underlying cellular events. A detailed discussion of radiation chimeras is included and the establishment and survival of chimeras and the use of chimeras to study the potentialities of injected cell populations carrying abnormal marker chromosomes, hematological, and immunological problems are described. Recent progress in clinical organ transplantation and clinical uses of radiation and immunosuppressive drugs is reviewed. Techniques of chromosome analysis are described. Author and subject indexes are included. (735 references.) (C.H.)

Radiation Effects Therapy and Countermeasures

31121 CHEMICAL PROTECTION AGAINST THE GENETIC EFFECT OF SMALL DOSES OF IONIZING RADIATION. Dubinin, N. P.; Dubinina, L. G. (Inst. of Biological Physics, Academy of Sciences, USSR). Dokl. Akad. Nauk SSSR, 164: 1405-6(Oct. 21, 1965). (In Russian).

The radioprotective actions of AET, streptomycin, and serotonin, were examined on human tissue cultures exposed to 50 and 100 R of ^{60}Co γ radiation. Protective effects on chromosomes were most marked during the prophase and during the synthesis phase, subsequently decreasing during the postsynthesis phase. However, surprisingly though none of the radioprotectors was effective at 25 R doses. The inability of chromosomes to avail themselves of the protective action was clearly demonstrated in an irradiation series at 38 R. The effects of thiourea and serotonin were also examined on tissue cultures of embryonic cells of Macaca mulatta, exposed to x radiation. No protective effect was noted at a dose of 12.5 R, although both agents were effective at higher doses. A definite threshold effect was thus indicated. (TTT)

31122 STUDIES OF MECHANISMS OF CHEMICAL RADIATION PROTECTION IN VIVO. III. CHANGES IN FLUORESCENCE OF INTRACELLULAR PYRIDINE NUCLEOTIDES AND MODIFICATION BY EXTRACELLULAR HYPOXIA. Jamieson, Dana; van den Brenk, H. A. S. (Cancer Inst. Board, Melbourne). Int. J. Radiat. Biol., 10: 223-41(1966).

Changes in the fluorescent signal emitted by the pyridine nucleotide co-enzyme system were recorded from rat tissues in vivo and from ascites tumour cells in vitro. The degree of reduction of this component of the electron transport chain has been shown to be a sensitive index of intercellular oxygen tensions. The effect of selected radioprotective chemicals on the fluorescent emission signal has been studied in rats respiring oxygen at pressures from zero to 760 mm Hg. Similar observations for changes in pO2 have been made for ascites cells treated with protective agents. A quantitative analysis has been made of the redox state of this respiratory coenzyme system. Results obtained support the view that the radioprotective action of sulfydryl derivatives, cysteamine and AET (and possibly cystamine and cysteine) is independent of intracellular tissue pO2 levels. That of dimethyl sulfoxide appeared similarly independent of pO2 change. Results with 5-hydroxytryptamine were equivocal. The agents chlorpromazine and paraaminopropiophenone were found to cause a degree of intracellular anoxia in vivo but not in vitro, which adequately explained their protective action. The results are discussed in relation to mechanisms of radioprotective chemical action. (auth)

31123 THE EFFECT OF OXYGEN ON IMPAIRMENT OF THE PROLIFERATIVE CAPACITY OF HUMAN CELLS IN CULTURE BY IONIZING RADIATIONS OF DIFFERENT LET. Barendsen, G. W. (Radiobiological Inst. TNO, Rijswijk, Netherlands); Koot, C. J.; van Kersen, G. R.; Bewley, D. K.; Field, S. B.; Parnell, C. J. Int. J. Radiat. Biol., 10: 317-27(1966).

Oxygen-enhancement ratios (OER) were determined for the inhibition of clone-formation by cultured cells of human origin irradiated with α particles and deuterons of different energies, fast neutrons, and 250 kvp x rays. The results of experiments with mono-energetic charged particles, whereby narrow distributions of linear energy transfer (LET) are obtained, show that the OER decreases with increasing LET from about 2.6 at a LET of 5.6 kev/μ of unit density tissue to a value of 2.05 at 61 kev/μ, followed by a more rapid decrease to 1.0 at 165 kev/μ. With fast neutrons, produced by bombarding Be with 16 Mev deuterons, an OER of 1.6 was obtained and with 250 kvp x rays the OER was 2.7. The relation between the relative biological effectiveness (RBE), the OER, and the LET is discussed. (auth)

31124 THE EFFECT OF SULPHOGUANIDINE AND p-NITROBENZOIC ACID ON THE CHROMOSOME BREAKAGE-REUNION PROCESS BY γ-, X- AND β-IRRADIATION IN VICIA FABA. Lazanyi, Andrei (Center of Biological Researches, Cluj). Int. J. Radiat. Biol., 10: 329-43(1966).

Primary roots of Vicia faba seedlings were irradiated with γ, x, and beta rays in a sulfoguanidine solution. Analysis of anaphase aberrations showed that the breakage-reunion index (which is the number of anaphase fragments per bridges) in the middle of the first mitosis after irradiation, is constant, and at low doses is independent of the intensity and quality of ionizing radiation. The breakage-reunion index indicates that after irradiation in the presence of sulfoguanidine, twice as many breaks enter into reunion as in distilled water. This cytological effect of the sulfoguanidine was suspended by p-aminobenzoic acid, folic acid, arginine, and guanine, as well as by 2,4-dinitrophenol and chloramphenicol. Therefore, the sulfoguanidine effect seems to be connected with the chromosomal histone and DNA synthesis. p-Nitrobenzoic acid has the same effect as the sulfoguanidine. The cytological effect of these compounds was linked

with a radiosensitizing effect, manifested in root-growth inhibition. (auth)

31125 EFFECT OF RADIOPROTECTIVE COMPOUNDS ON THE INCORPORATION OF TRITIATED THYMIDINE INTO MAMMALIAN CELLS. Simons, H. A. B.; Davis, Elizabeth M. (Royal Free Hospital School of Medicine, London). Int. J. Radiat. Biol., 10: 343-52(1966).

The effect of radioprotective compounds on the rate of DNA synthesis in bone marrow and intestinal epithelium of Swiss albino mice was investigated, using tritiated thymidine and an autoradiographic technique. A significant depression in the grain count and fraction of labeled cells was found to occur for myelocytes from mice injected with good radioprotectors of the sulfhydryl group. The magnitude of the effects observed was to some degree correlated with the protective ability of the compound: no similar effect was seen for intestinal epithelium although the presence of the radioprotector in these cells was checked using S-labeled AET. No effect on grain count and fraction of labeled cells was found in mice in which cellular anoxia was produced by keeping the mice in an atmosphere of low oxygen-content. (auth)

31126 FRACTIONATION OF BONE MARROW SUSPENSIONS AND THEIR USE TO PROTECT AGAINST LETHAL IRRADIATION. Harris, P. F.; Joseph, S. (Univ. of Sheffield, Eng.). J. Physiol. (London), 182: 7P-8P(Jan. 1966).

Suspensions of whole bone marrow from guinea pigs were fractionated prior to testing the radioprotective capacity of the various fractions. Cell fractions were separated by differential centrifugation in a gradient comprising various concentrations of bovine plasma albumin (BPA). Tests were performed to determine whether recombined fractions would protect guinea pigs against lethal irradiation (720 R, $LD_{100/14}$). Using bone marrow from inbred litter mates, an average of 400×10^6 nucleated cells were transfused. The transfusion was completely successful, with rapid recovery of leukocyte levels and no detectable depression of erythrocyte count in any of the recipients. (TCO)

31127 INHIBITION OF RADIATION-INDUCED LEUKAEMIA BY THE INJECTION OF HAEMATOPOIETIC TISSUE: A STUDY OF CHIMAERISM. Wallis, Valerie; Davies, A. J. S.; Koller, P. C. (Royal Cancer Hospital, London). Nature, 210: 500-4(Apr. 30, 1966).

The hypothesis that leukemia development in mice is inhibited when injected bone marrow cells survive and proliferate in the irradiated host was investigated using two cytologically marked mouse strains as host and donor. Mice $(C57BLXCBA/T6T6)F_1$, were given 4 doses of 200 R x radiation at weekly intervals starting when one month old. Within 1.5 hr after the last radiation dose the mice were injected intravenously with either CBA bone marrow cells, CBA spleen cells, CBA lymph node cells, or BALB strain bone marrow cells. Mice were killed at various times during the latent period and after leukemia developed and cytological preparations were examined. Either the spleen or thymus of leukemic mice was transplanted into host and tissue-donor strain mice and chromosome analyses were made of bone marrow, spleen, and thymus of leukemic mice in an effort to determine whether the leukemia had arisen from the irradiated host cells or the unirradiated injected cells. Results indicate that the injection of syngenic bone marrow or spleen cells results in a greatly decreased incidence of leukemia while allogenic bone marrow and parental lymph node cells were ineffective in reducing the incidence of leukemia below control levels. It was not determined whether the inhibition of leukemia development in mice injected with parental bone marrow and spleen cells was due to cell repopulation of hematopoietic tissues or the liberation of some humoral factor that is anti-leukemogenic by the bone marrow. (C.H.)

31128 ULTRASTRUCTURAL ASPECTS OF DUODENAL CRYPTS IN X-IRRADIATED MICE AFTER CHEMICAL PROTECTION. Hugon, J.; Maisin, J. R.; Borgers, M. (CEN, Mol, Belg.). Nature, 210: 749-50(May 14, 1966).

The protective effects of a mixture of glutathione, AET, and serotonin against radiation injuries of the cells of duodenal crypt of mice exposed to 1,350 R x radiation were evaluated 30, 60, 180, and 300 min after irradiation. A marked protective effect was noted for undifferentiated stem cells of the duodenal crypt in irradiated mice protected by the chemical mixture. (C.H.)

31129 AMINO-ACID PROTECTION OF ULTRAVIOLET-IRRADIATED BACILLUS SUBTILIS. Hunt, Dale E. (C. V. Chapin Hospital, Providence). Nature, 210: 761-2(May 14, 1966).

Cultivation of Bacillus subtilis in a defined acidic broth medium supplemented with phenylalanine, proline, glycine, or serine markedly increased the resistance of this organism to inactivation by uv exposure. Possible reaction mechanisms involved are discussed. (C.H.)

31130 RADIOSENSITIZATION OF HUMAN TUMOR CELLS IN VITRO BY N-ETHYLMALEINIMIDE UNDER HYPOXIC CONDITIONS. Klimek, M. (Inst. of Biophysics, Brno). Neoplasma, 13: 31-4(1966).

Cells of the HeLa S3 strain grown in single cell culture under deep anoxic conditions were used as model cells resembling the conditions in a tumor. The question was, whether such cells, which probably are responsible for the tumor radioresistence, might be selectively sensitized by N-ethylmaleinimide, which in bacteria has been shown to sensitize under anoxic conditions only. Experiments showed that a 2 μM concentration is not toxic. This concentration was used in radiosensitization experiments using x radiation and hypoxia was checked by polarographic method. It was shown that under these conditions NEM exerted the radiosensitizing effect with a DMF equal to 1.5. The mechanism of the effect and the possibilities of tumor sensitization are discussed. (auth)

31131 COMBINED EFFECT OF RADIATION AND ANTITUMOR AGENTS MEASURED BY MOUSE SPLENIC AND THYMIC WEIGHT. Miura, Takashi; Hamada, Tatsumi (Osaka Univ.). Nippon Igaku Hoshasen Gakkai Zasshi, 25: 1405-9(Mar. 1966). (In Japanese).

An attempt was made to demostrate graphically whether combined x irradiation and antitumor agents have synergistic effects on mouse splenic and thymic weight. Whole-body x irradiation and intraperitoneal administration of Mitomycin C and Endoxan were used. As the shape of each dose–response curve is similar, doses of two agents having the same effect are plotted on a common abscissa to get a single curve for both. The results indicate the combined effect of x irradiation and Mitomycin C or Endoxan is synergistic, on the other hand, that of Mitomycin C and Endoxan is merely additive. (auth)

31132 TRANSPLANTATION OF HOMOLOGOUS BONE MARROW AND INTRAVENOUS INJECTION OF WHOLE BLOOD TO DOGS IRRADIATED WITH SUPRALETHAL DOSES. Maksimenko, A. S. (Inst. of Hematology and Blood Transfusion, Moscow). Probl. Gematol. Pereliv. Krovi, 11: No. 2, 26-31(Feb. 1966). (In Russian).

Bone marrow transplants in superlethally irradiated dogs (1000 R) stimulated transformation of hematopoietic tissue into lymphocytes, the graft-vs-host reaction. A similar phenomenon was observed following blood transfusions, where small blood lymphocytes allegedly undergo lymphoid transformation at the expense of the hemopoietic stem cells present in the blood. Results of blood transfusion experiments were related to the problem of bone marrow transplantation. (H.G.D.)

31133 POSSIBILITY OF THERAPEUTIC APPLICATION OF BONE MARROW AUTOTRANSPLANTATION IN UNEVEN IRRADIATION. Strelin, G. S.; Shmidt, N. K.; Sil'chenko, N. N. Probl. Gematol. Pereliv. Krovi, 11: No. 2, 38-41 (Feb. 1966). (In Russian).

In order to develop a therapeutic tool for combatting radiation-induced complications encountered during radiation treatment of tumors, experiments were carried out with autotransplanted bone-marrow from slightly exposed portions of an unevenly exposed body. The male rats used for the experiments were protected by means of a lead collar at the thigh bone, the collar being removed before com-

pleting the exposure. The whole-body dose of x radiation was thus 650 to 700 R and the femoral dose about 200 R. Bone marrow cells from the thigh bone were introduced in a citrate-containing physiological solution into the caudal vein of the same animal within 30 to 40 minutes after completing the exposure. The results indicated that the autograft of bone marrow from the partially shielded area is more efficient as a clinical tool than shielding alone without transplantation. The number of leukocytes, which decrease strongly after the exposure, was regenerated in the surviving animals. The uneven exposure definitely increased the survival rate; the autograft enhanced this effect. (TTT)

31134 TREATMENT OF RADIATION LEUKOPENIA BY BONE MARROW AUTOTRANSPLANTATION. Gabelov, A. A.; Koiro, M. A.; Prilipko, L. G.; Pushnitsina, A. D.; Khachkuzova, E. S.; Shmidt, N. K. Probl. Gematol. Pereliv. Krovi, 11: No. 2, 41-4(Feb. 1966). (In Russian).

Bone marrow autotransplantation was used for treating radioinduced leukopenia, resulting from the therapeutic irradiation of gynecological patients. The autotransplantation method elaborated at the clinic was applied in the treatment of 31 patients. Data are presented on the changes of leukocyte count index in the peripheral blood following the autotransplantation. This method proved to be highly effective both for prevention and treatment of radiation leukopenia in these patients. (auth)

31135 USE OF CADAVER BONE MARROW IN THE TREATMENT OF RADIATION INJURIES. Butomo, N. V. (Kirov Military-Medical Academy, Leningrad). Probl. Gematol. Pereliv. Krovi, 11: No. 2, 54-9(Feb. 1966). (In Russian).

At present, transfusion of bone marrow cells is the most promising treatment for counteracting the effects of lethal radiation exposure. For humans, up to 4×10^{10} cells must be used; this large amount makes the donor system difficult. Therefore, experiments were made with transplants from cadavers, as it has been found earlier that the bone marrow cells are able to survive for periods up to ten to twenty hours after death. Results obtained with mice exposed to 700 R of x radiation indicated that in order to obtain the same regenerative effect of myeloid hemopoiesis as fresh bone marrow, the number of cells from the cadavers had to be increased by a factor of 2 to 4. Under such conditions, the effect on the survival rate and lengthening of life was identical. Administration of bone marrow from cadavers helped the recipients to pass through the crisis period of radiation sickness. Secondary unfavorable effects may arise but they have not yet been investigated. (TTT)

31136 POST-IRRADIATION MODIFICATION OF BIOLOGICAL EFFECTS OF NEUTRONS. I. EFFECT OF MYLERAN ON CHROMOSOMAL ABERRATIONS IN NEUTRON-IRRADIATED SEEDS. Moutschen-Dahmen, M.; Moutschen, J.; Ehrenberg, L. (Univ., Liege. Univ., Stockholm). Radiat. Bot., 6: 251-64(June 1966).

In experiments with barley and Vicia seeds it was demonstrated that a certain type of neutron induced lesion, one-hit chromosome aberrations (chiefly isolocus breaks), is affected by Myleran in the same way as the corresponding γ-ray effect: for both types of radiations the frequencies of breaks are increased by about 75 per cent by a post irradiation treatment of seeds with Myleran. In these experiments Myleran was given at a low concentration giving only few aberrations in unirradiated seeds. The same treatment decreased strongly γ-ray produced two-hit aberrations, whereas the neutron produced aberrations of this two-hit type were not (or much less) affected. The Myleran effect may be described formally as a decrease of completeness of exchanges; it was further indicated that neutron induced inter- and intrachanges may be produced by another mechanism than γ-ray induced breaks and exchanges and neutron induced breaks. Myleran treatment decreased the frequencies of neutron induced mutations. It was indicated that neutron induced mutation is affected by Myleran in the same way as breaks. (auth)

31137 COMPARATIVE STUDIES ON THE PROTECTION SHOWN BY α-AMINOTHIOACETAMIDE, CYSTEINE, AND ANOXIA AGAINST THE ACTION OF GAMMA RAYS ON ALLIUM CEPA. Elkhalifa, M. D. (Univ. of Khortoum, Sudan). Radiat. Bot., 6: 285-8(June 1966).

Primary roots of Allium cepa were used to investigate and compare the protective effect of certain substances as well as anoxia in pre-treatment against the action of gamma-rays. Survival of roots and chromosome damage were taken as measures of radiation effect. Anoxic condition was found to be superior in protection to that shown by cysteine or α-aminothioacetamide. Protective factors obtained through such pre-treatments were comparable to protective factors obtained in an earlier study where the rate of growth of Allium cepa roots was the measure of radiation effect. (auth)

31138 EFFECT OF L-TRIIODOTHYRONINE ON RADIATION-INDUCED PULMONARY FIBROSIS IN DOGS. Tyree, Ella B.; Glicksman, Arvin S.; Nickson, James J. (Sloan-Kettering Inst. for Cancer Research, New York). Radiat. Res., 28: 30-6(May 1966).

Male beagle dogs, having received a fibrosis-inducing dose of ^{60}Co γ irradiation, were treated with daily pharmacological doses of L-triiodothyronine (T-3). Lung compliance was the parameter employed to evaluate the condition of the lungs in the post-irradiation state. The radiation damage appeared to be less severe in the animals receiving T-3 postirradiation than in those in the radiation control group. No harmful effect was noted in the dogs receiving T-3 only. (auth)

31139 THE INTERNAL HYDROGEN ION CONCENTRATION OF THIOBACILLUS THIO-OXIDANS AND SURVIVAL AFTER IRRADIATION. Dewey, D. L.; Beecher, Jean (Mount Vernon Hospital, Middlesex, Eng.). Radiat. Res., 28: 289-95(June 1966).

A suspension of Thiobacillus thio-oxidans was adjusted to either pH 4 or pH 1.5 and given various doses of x rays. The bacteria were irradiated in neat oxygen and in pure nitrogen; 2.8 times the dose was required in nitrogen to simulate the effect in oxygen. No significant effect of pH was observed in either gas. Anoxic bacteria irradiated in M glycerol were protected; in 0.3 mM N-ethyl-maleimide they were sensitized. Again there was no significant effect of pH on radiosensitivity. A thick suspension of bacteria was disrupted in a French press. The results indicated that the bulk internal hydrogen ion concentration was probably independent of the external pH. (auth)

31140 POSSIBILITY OF ISOLATING RADIATION PROTECTION AGENTS ON THE BASIS OF THE TOTAL QUANTITY OF DICHE-POSITIVE COMPOUNDS IN URINE. Davydova, S. A.; Dorofeev, V. M.; Yakovlev, V. G. Radiobiologiya, 6: 93-6(1966). (In Russian).

An attempt was made to establish a correlation between the biological protective effect and the capacity of protective agents to influence the production of Diche-positive compounds (DPC) in the urine of irradiated organisms. Earlier researchers noted a considerable DPC increase in the urine of irradiated animals and suggested that this reaction was a specific feature of radiation sickness; they also suggested that the reaction could be used to diagnose and isolate radiation protection agents. In order to check these theories, rats of both sexes were exposed to ^{60}Co γ rays (700 rad), after having received protective doses of 1 of 24 preparations (sulfur-containing radiation protective agents, high molecular compounds, indole derivatives, and others). It was found that irradiation increased DPC production in the urine by 58% over the initial level. The authors conclude that the rise in the DPC level in the urine of irradiated animals is not a feature specific to ionizing radiation and that the amount of DPC is not a reliable criterion for isolating radiation protection agents. The effect of the 24 preparations on DPC production in the irradiated rats is presented in tabular form. (CFSTI)

31141 DETERMINATION OF RADIATION EFFECT IN THE BODY. I. THE SH PROTECTIVE AGENTS AGAINST RADIATION AND FREE RADICALS. Seki, Takakazu (Nippon Dental Coll., Tokyo). Radioisotopes (Tokyo), 15: 132-8(1966). (In Japanese).

Interaction of sulfhydryl groups with radioinduced free

radicals was studied by electron spin resonance, and the radioprotective properties were investigated in liver and tumor tissues of mice irradiated with ^{60}Co gamma rays (600 R). A seven-fold increase in free radicals was found in irradiated mouse liver, compared to non-irradiated controls. Similar results were obtained with tumor tissue, though free radicals were produced to a lesser extent. Glutathione, MEA, and cystine were successful in removing free radicals from liver when they were administered 30 min prior to irradiation. Glutathione also moderated radiation injury in tumorous tissues, but not as effectively as in liver tissue. (H.G.D.)

31142 HEALTH PHYSICS AND RADIATION PROTECTION. (International Atomic Energy Agency, Vienna). pp 25-58 of STI-DOC-10/53.

Topics covered include: influence of chemical radiation protectors on the effects of x-ray therapy of spontaneous and grafted cancer in mice, chemical protection against radiopathological effects due to deposition of ^{140}Ba in the aortic wall in experimental animals and in humans, influence of disorders of thyroid on calcium metabolism of human beings, radionuclide content (^{90}Sr and ^{137}Cs) of human bones and tissues in Finland in relation to pathological findings, metabolism and clinical effects of ^{90}Sr and radium in humans, uptake of radioactive substances from air by plants, transfer mechanisms of artificial radionuclides in the placentae of humans and animals as influenced by inactive carriers, combined use of chemical compounds and bone marrow in lethally irradiated mammals, distribution of common and radioactive cesium in nature and in man, role of protective substances during irradiation, damage to bacteriophage and reparation after the effect of radiation and radiomimetics, and deposition of inhaled fission products in lungs and pulmonary lymph nodes of human beings. (M.C.G.)

31143 EFFECT OF CYSTAMINE AND S-β-AMINOETHYLISOTHIURONIUM ON THE ACTIVITY OF DNASE II IN THE SPLEEN AND THYMUS OF IRRADIATED RATS. Libikova, N. I. (Military Medical Academy, Leningrad). Vop. Med. Khim., 11: No. 5, 65-8(1965). (In Russian).

An increase in activity of DNase II was observed in the spleen and thymus of irradiated (700 R) rats. The maximum activity of DNase II was reached 24 hrs after irradiation. Pretreatment by cystamine or S-β-aminoethylisothiuronium (intraperitoneally) decreased the changes in DNase II activity. (C.H.)

31144 THE EFFECT OF X-IRRADIATION ON ESCHERICHIA COLI B. II. INHIBITING THE ROLE OF DEOXYRIBONUCLEASE (DNAase) IN THE DEGRADATION OF DNA IN ESCHERICHIA COLI AFTER X-IRRADIATION. Kuo, Chieh-yen; Chou, Te-ch'ing; Li, Chun-ying (Futan Univ., Shanghai). Yuan Tzu Neng, No. 3, 245-50(1965).

Experiments showed that sodium citrate, sodium fluoride, disodium ethylenediaminetetraacetate, sodium sulfite, sodium acetoacetate, and copper sulfate of appropriate concentration prevent or reduce the degradation of deoxyribonucleic acid (DNA) in E. coli cells under the influence of x ray. All of the above substances, with the exception of sodium acetoacetate which is a little less effective, inhibit the DNA degradation in E. coli after radiation almost completely. The DNA degradation is inhibited immediately as soon as the sodium citrate, sodium fluoride, or sodium sulfide is added after x irradiation. It is pointed out that the degradation of DNA in E. coli after irradiation may be due to the effect of enzymolysis, and that a high concentration of sodium citrate (0.5 M) may reduce the lethal effect of x ray to a certain extent, and thus increase the percentage survival of E. coli cells after irradiation. (ATD)

Radiation Hazards and Protection

See also HEALTH AND SAFETY

31145 ALPHA RADIOACTIVITY OF HUMAN BLOOD. Hasson, V.; Cherry, R. D. (Univ. of Cape Town). Nature, 210: 591-3(May 7, 1966).

Measurements of α activity in samples of normal human blood showed a mean α activity of 54 pC/kg. Measurements were made on whole blood, red cells, and plasma. (C.H.)

31146 ESTIMATION OF EXPOSURE DOSE TO FETUS FROM FETAL RADIOGRAPHY USING A FLUOROGLASS DOSIMETER. Antoku, Shigetoshi; Tabuchi, Akira (Hiroshima Univ.). Nippon Igaku Hoshasen Gakkai Zasshi, 25: 1390-7(Mar. 1966). (In Japanese).

Estimations of gonadal, spine (bone marrow), and volume doses to fetuses from radiography were made using measured dose distributions in an advanced pregnancy phantom and the posture and position of the fetus in radiographs. Fluoroglass plates (FD-P8, 8 × 8 × 4.7 mm) were put in planes at 0, 3, 6, 9, 12, and 15-cm depths in the phantom and exposed to x rays. Dose distributions are shown as functions of depth, tube voltage, and filtration. Exposure parameters in fetal radiography were collected in a survey of fourteen hospitals in Hiroshima and neighboring prefectures. Gonadal and volume doses to the fetus, based on measured doses with the phantom, ranged from 0.41 to 2.5 R/examination and from 690 to 3900g · R/examination with the average values for the fourteen hospitals equal to 0.92R/examination and 1600g · R/examination, respectively. These values vary with the position of the fetus, output of the x-ray machine, film sensitivity, fluoroscreen efficiency, etc. However, the values obtained agreed in general with those reported by others. (auth)

Radiotherapy and Radiodiagnosis

31147 (CNEA-168) UN NUEVO COLOIDE DE ^{99m}Tc EN CENTELLOGRAFIA HEPATICA. (A New Colloid of ^{99m}Tc in Scintillation Scanning of the Liver). Seeber, Jose Martinez; Pecorini, Victorio; Degrossi, Osvaldo; Olivari, Americo; Chwojnik, Abraham (Comision Nacional de Energia Atomica, Buenos Aires Argentina)). 1966. 9p. Dep. mn.

Experience obtained in scintillation scanning of the liver using a new colloid of antimony sulfide labelled with ^{99m}Tc is presented. The excellent resolution of the tracer and the lower body radiation dose are characteristics of the nuclide used. (tr-auth)

31148 (CNEA-170) CENTELLOGRAFIA DEL RINON. (Scintillation Scanning in Kidneys). Olivari, A. J.; Pecorini, V.; Chwojnik, A.; Garcia del Rio, H.; Testa, H. (Comision Nacional de Energia Atomica, Buenos Aires (Argentina)). 1966. 18p. Dep. mn.

The technique of scintillation scanning in kidneys using ^{203}Hg- and ^{197}Hg-labeled compounds is described. The equipment and methods, radiation dose received by the patient, and interpretation of the graphs are discussed. Typical graphs showing normal and diseased conditions are given. (J.S.R.)

31149 (TID-22969) I. INTRACELLULAR PICKUP OF RADIOACTIVE PHOSPHORUS BY PROSTATIC EPITHELIAL CELLS. II. ANCILLARY PROJECT: ABSORPTION OF RADIOPHOSPHORUS FROM THE CANINE URINARY BLADDER IN THE PRESENCE OF DMSO AND OTHER HYPERTONIC SOLUTIONS. Final Technical Report. (Oregon Univ., Portland. Medical School). [1965]. Contract AT(45-1)-1755. 7p. Dep. mn. CFSTI $1.00 cy, $0.50 mn.

Solutions of ^{32}P have been used by intravenous injection for deposition in metastatic prostatic cancer to bring relief of pain, presumably by shrinking cancer cells and relieving pressure on sensory nerves. Results are reported from studies in dogs of humoral factors influencing the uptake of ^{32}P by the prostate gland when solutions of sodium phosphate, colloidal chromic phosphate, diethylstilbestrol diphosphate, 1-naphthol phosphate, or sodium 2-glycerol phosphate were used as carriers for ^{32}P. The rate of ^{32}P absorption from the canine bladder was also measured and was shown to be directly proportional to the osmolarity of the solution within the bladder. (C.H.)

31150 (UCRL-16691) SCINTILLATION PHOTOGRAPHY OF INTRAVASCULAR CLOTS IN VIVO WITH ^{131}I-LABELED PLASMINOGEN. Berger, William C. (Lawrence

Radiation Lab., Univ. of California, Berkeley). Feb. 9, 1966. Contract W-7405-eng-48. 15p. Dep. mn. CFSTI $1.00 cy, $0.50 mn.

The injection of 5 μC of ^{131}I-labeled human plasminogen (SK activated) demonstrated within 5 minutes the presence of a fresh, experimentally made intravenous clot in an otherwise intact living rabbit. The Anger scintillation camera was used to produce photographic representation of the clot. (auth)

31151 EVIDENCE FOR A TUMORICIDAL DOSE LEVEL IN THE RADIOTHERAPY OF HODGKIN'S DISEASE. Kaplan, Henry S. (Stanford Univ. School of Medicine, Palo Alto, Calif.). Cancer Res., 26: 1221-4(June 1966).

A review of the available evidence indicates that Hodgkin's disease tends to recur in a treated field with a frequency which is inversely related to the radiation dose and approaches zero at a dose of approximately 4000 rads, delivered at the rate of about 1000 rads/week. Such doses make the use of megavoltage x ray beams mandatory to avoid severe skin reactions, but are otherwise well tolerated by the normal tissues. The inverse relationship of recurrence rate to radiation dose has important implications for the radiotherapy of Hodgkin's disease, which are supported by the limited data thus far available relating radiation dose to long term survival in Hodgkin's disease. (auth)

31152 NUCLEAR MEDICINE: A NEW DISCIPLINE. Vetter, Herbert. Int. At. Energy Agency Bull., 8: No. 2, 7-13(June 1966).

The present status and likely future of nuclear medicine, the use of radioisotopes for diagnosis and treatment of disease and in clinical research work, are discussed. (M.C.G.)

31153 SIX OBSERVATIONS ON THE TREATMENT OF PATIENTS WITH METASTASIZED MAMMARY CARCINOMAS BY MEANS OF TREATMENT OF THE HYPOPHYSIS WITH RADIOACTIVE YTTRIUM. Coenegracht, J. M.; Lankester, J.; van der Plaats, G. J. Jr.; de Lange, S. A.; Touber, J. L.; Frenkel, M.; van der Werf, A. J. M. Jaarb. Kankeronderz. Kankerbestrijding Ned., 13: 75-88(1963). (In Dutch).

A discussion on results of destruction of the hypophysis by ^{90}Y implantation and comparison of these results with hypophysectomy in patients with metastasis of mammary carcinoma is reported. Tables of the effect of the treatment in conjunction with hormonal treatment are given for 33 patients. Of eight patients who were treated without success with corticosteroids, three were treated successfully by ^{90}Y implantation. Morphology of the hypophysis after ^{90}Y treatment is illustrated. Yttrium-90 dosimetry and source placement for maximum benefit are discussed. (TCO)

31154 ON THE HYPERFUNCTIONING SOLITARY THYROID NODULE. Molnar, Goerge D.; Wilber, Robert D.; Lee, Robert E.; Woolner, Lewis B.; Keating, F. Raymond Jr. (Mayo Clinic, Rochester, Minn.). Mayo Clin. Proc., 40: 665-84(Sept. 1965).

Thirty-four cases of scintigraphically documented hyperfunctioning, solitary thyroid nodules are reported. Data showed that routine ^{131}I-uptake studies are potentially misleading without simultaneous scintigraphy. Twenty patients were treated surgically and 12 were treated with radioiodine. Surgically treated patients presented no special therapeutic problems, unlike some of the patients treated with ^{131}I. Magnitude of ^{131}I dosage and scintigrams after therapy are discussed. Clinically and by scintigram, no difference could be detected between results after 20-mC doses and those after the smaller doses. The results did not agree with the recommendation for a minimum of 20 mC of ^{131}I to be administered as treatment of solitary hyperfunctioning thyroid nodule. The feasibility of radioiodine therapy in thyrotoxic patients with diffusely hyperfunctioning glands is considered in view of recent findings that are more favorable to thyroid radiotherapy. (TCO)

31155 ELECTRONIC COMPUTERS AND METHODS OF LINEAR PROGRAMMING IN THE CHOICE OF OPTIMAL CONDITIONS FOR RADIATION TELETHERAPY. Klepper, L. Ya. (Inst. of Medical Radiology, Academy of Medical Sciences, USSR). Med. Radiol., 11: No. 5, 8-15(May 1966). (In Russian).

The task of selecting optimal conditions for irradiation of malignant tumors can be divided into two successive stages. First, it is necessary to gain information about the dosage distribution for different conditions of irradiation and then to determine the optimal conditions of irradiation. The task is an extremely complicated one and for its solution, an electronic computer, along with the methods of linear programming, were used. Fundamental conditions are formulated attending the dosage distribution in the body and a mathematical interpretation in terms of linear programming is included. (auth)

31156 AN EXPERIMENTAL INQUIRY INTO DOSAGE IN THE GONAD REGION IN SHORT-RANGE X-RAY THERAPY OF ANGIOMAS IN CHILDREN. Podlyashuk, E. L.; Khrushchov, M. M. (Inst. of Roentgen Radiology, Moscow). Med. Radiol., 11: No. 5, 15-21(May 1966). (In Russian).

Measurement of a scattered radiation dose in water-equivalent phantoms of children aged 1 and 3 months and 1 year under a short-range x ray therapy of hemangiomas demonstrated the radiation load on individual vital organs capable of reaching several thousand mR and thus to be fraught with the danger of somatic complications. During irradiation of the head the scattered radiation doses to the gonad vary within a range of from 2.8 up to 13 mR, with an exposure dose of 500 R, being dependent upon the field siting, its magnitude, the hardness of radiation, and direction of the primary beam. The reduction of the dose at individual points of the phantom is secured by the protection from external scattered radiation (from walls and objects). At the same time the diminution of the scattered radiation emerging in the phantom itself can be brought about only by changing technical conditions and, first of all, by lowering the tension of the primary beam generation and by sparing use of the areas under irradiation. (auth)

31157 IMPROVED DOSIMETRIC TECHNIQUE IN ALPHA THERAPY. Andreev, S. V.; Abramov, V. I.; Vyrubova, A. V. Med. Radiol., 11: No. 5, 44-9(May 1966). (In Russian).

By using the principle of ^{222}Rn adsorption in activated coal, cooled down to −90°C, a multichannel unit was designed to determine small ^{222}Rn concentrations in air. A study of ^{222}Rn passage from the human organism through the lungs and the skin after taking radon baths, effected by means of the above-mentioned unit, was used for verification of the integral absorbed dose. The investigation helped to demonstrate the importance of skin in ^{222}Rn excretion in this form of alpha-therapy (up to 40% of the total amount of the isotope that found its way into the organism). (auth)

31158 STUDIES ON THE QUANTITATIVE MEASUREMENT OF RADIOISOTOPES IN THE HUMAN BODY BY LINEAR SCANNING. Mori, Tomoyuki (Chiba Univ., Japan). Nippon Acta Radiol., 25: 57-65(Apr. 1965). (In Japanese).

A simple method is presented for externally measuring the dose and distribution of radioisotopes within the body. (TCO)

31159 RADIATION THERAPY OF THE MAXILLARY SINUS. STUDIES ON CONFORMATION RADIOTHERAPY. REPORT 14. STUDIES ON TELECOBALT THERAPY. REPORT 25. Morita, Kozo (Nagoya Univ., Japan). Nippon Igaku Hoshasen Gakkai Zasshi, 25: 1260-8(Feb. 1966). (In Japanese).

Eighty-four cases of cancer of the maxillary sinus were treated in the Radiological Department of Nagoya University Hospital from 1954 to 1963. The method of treatment, survival rate, and complications are discussed. Treatment consisted chiefly of radical maxillectomy combined with postoperative external irradiation using ^{60}Co (more than 5000 R). Forty-one cases were treated by conformation irradiation, Three-year and five-year survival rates were 36.0 and 28.6%, respectively. Since, the conformation irradiation technique has been applied, the three-year survival rate has risen 62.6%. Complications in addition to those already existing have never been seen. (auth)

31160 VARIOUS PROBLEMS IN STOMACH SCANNING. Tatsumo, Ikuro; Okimura, Tetsuro (National Kanazawa Hospital, Japan). Nippon Igaku Hoshasen Gakkai Zasshi, 25: 1269-77(Feb. 1966). (In Japanese).

The salivary glands and stomach are known to concentrate ionic iodine almost immediately following intravenous injection. The mechanism of ^{131}I concentration in the stomach and salivary glands is different from that in the thyroid in that excessive iodine ingestion prevents thyroid uptake, but does not interfere with uptake in either the stomach or the salivary glands. (auth)

31161 THYROID ANTIBODIES IN EUTHYROID SUBJECTS AFTER ^{131}I THERAPY. Einhorn, J.; Fagraeus, Astrid; Jonsson, J. (Radiumhemmel and Statens Bakteriologiska Laboratorium, Stockholm). Radiat. Res., 28: 296-301(June 1966).

It is known that circulating thyroid cytoplasmic antibodies increase after 131 iodine treatment for hyperthyroidism. In an investigation of 31 euthyroid patients receiving radioiodine therapy, the therapy was followed by an increase in the thyroid cytoplasmic antibodies ($P < 0.05$) and thyroglobulin antibodies ($P < 0.01$). The antibodies were present in fairly low titers. Thyroid cytoplasmic antibodies were not found after intensive irradiation that did not involve the thyroid gland. It cannot be excluded that the increase in thyroglubulin antibodies is due to a general stimulation of the antibody-forming organs resulting from tissue destruction by local irradiation. (auth)

31162 CURRENT TOPICS IN THYROID RESEARCH. Proceedings of the Fifth International Thyroid Conference, Rome, 1965. Cassano, C.; Andreoli, M. (eds). New York, Academic Press, 1965. 1243p. $42.00. (CONF-650551).

Advances in the field of thyroid biochemistry, pathology, and therapy are discussed in 124 papers. The papers discuss the heterogenicity of the thyroid gland; the biochemistry of thyroid particulate fractions; iodide peroxidase and the biochemistry of iodination reactions; techniques for electron microscopy and autoradiography; iodine kinetics and particulate iodoproteins; thyroid iodoproteins; iodine metabolism and the secretion and properties of calcitonin and goitrogens; the effects and metabolism of thyroid hormones; thyroid-heart relationships; the biochemistry and physiology of thyrotropic factors; thyrotropin assay and the action of thyrotropin; thyrotropic factors neuro-endocrine interaction in Graves' disease; thyroxine-protein interactions; the metabolism and physiological significance of thyroxine-binding prealbumin in man; fetal thyroid function and diagnostic tests in humans; thyroid autoimmunity; endemic and congenital goiter; thyroid nodules; experimental thyroid tumors; thyroid cancer; the metabolic aspects of thyroid diseases; adrenal-thyroid relationships, and radioactive iodine therapy in the treatment of thyrotoxicosis. Tracer techniques using radioisotopes for studies of thyroid physiology are described. (C.H.)

31163 X RAY DAMAGE AFTER THERAPEUTIC IRRADIATIONS IN THE VICINITY OF JOINTS. Soballa, G. Munich, Univ., 1964. 80p. $2.00 Gmelin, AED-Diss. 64-1050.

Changes of blood vessels in the vicinity of joints after x irradiation were studied. After single whole-body irradiation with 500 R no changes were observed. Marked changes were detected after 1000 to 4000 R. (Gmelin Inst.)

CHEMISTRY

General

Refer also to abstract 32804.

31164 (ANL–7175) CHEMICAL ENGINEERING DIVISION RESEARCH HIGHLIGHTS, MAY 1965–APRIL 1966. (Argonne National Lab., Ill.). Contract W-31-109-eng-38. 242p. Dep. mn. CFSTI $6.00 cy, $1.25 mn.

Research and development progress is summarized in eight sections. Separate abstracts were prepared for each section. Lists of publications by Chemical Engineering Division Personnel are included. (J.R.D.)

For abstracts of individual sections see: 31167, 31213–31316, 31440, 31959, and 32370.

31165 (HMI-B–46) JAHRESBERICHT, 1965. (Annual Report, 1965). (Hahn-Meitner-Institut fuer Kernforschung, Berlin (West Germany)). May 1966. 117p. Dep. mn.

Work done in nuclear chemistry, mathematics, nuclear physics, radiochemistry, electronics, and reactor physics, is reported. Publications by the various sections are listed, and abstracts of some of them are given. Backgrounds of new studies initiated during the year are reviewed. Training sessions and symposia held by the different sections are tabulated. (J.S.R.)

31166 (UCRL–16658, pp 89-92) NUCLEAR SCIENCE. (Lawrence Radiation Lab., Univ. of California, Berkeley).

Results of investigations are presented concerning reactions of Cl_2 and UCl_4 in fused LiCl–KCl, Ge–I_2 reactions, reactor coolant-loss temperature transients, graphite-H_2 reaction kinetics, extraction of fission products from U fuels, and diffusion in liquid metals. Lists of 1965 publications are included, and research plans for 1966 are outlined. (J.R.D.)

Analytical Procedures

See also Separation Processes and Procedures

Refer also to abstracts 31355, 31423, and 31541.

31167 (ANL–7175, pp 217-25) ANALYTICAL RESEARCH AND DEVELOPMENT. (Argonne National Lab., Ill.).

Work devoted to analytical support of research and development groups of the Chemical Engineering Division is summarized. Information is included on elemental chemical analysis, atomic absorption spectrometry, x-ray spectroscopy, x-ray diffraction, electron probe microscopy, gas analysis and determination of burnup in fast reactors. (J.R.D.)

31168 (CONF-660611–1) THE APPLICATION OF A SPUTTERING ION SOURCE TO THE MASS ANALYSIS OF NANOGRAM SOLID SAMPLES. McHugh, James A. (Knolls Atomic Power Lab., Schenectady, N. Y.). May 23, 1966. Contract W-31-109-eng-52. 22p. Dep. mn. CFSTI $1.00 cy, $0.50 mn.

From Society of Applied Spectroscopy Meeting, Chicago.

The process of generating secondary ions of a material by ion bombardment was applied to small solid-sample analyses. A compact ion source employing this technique was constructed and is described. The application of this source to the analysis of iodine and beryllium is discussed. The isotopic abundance analysis of nanogram quantities of iodine was achieved. The sensitivity of the method was sufficiently high that 10^{-13} gram of a given iodine isotope can be detected in a sample. The quantitative determination of Be at the subnanogram level was shown to be possible with this source and a sample-standard technique. The determination of 10^{-13} gram of Be^9 is possible. (auth)

31169 (D–1-82-0508) NEW TYPE OF LOW-RESOLUTION MASS SPECTROMETER. Dayton, I. E.; Saari, J. M.; Schoen, R. I. (Boeing Scientific Research Labs., Seattle, Wash. Geo-Astrophysics Lab.). Mar. 1966. 37p.

A pulsed, low-resolution, slitless mass spectrometer of a new type is discussed. Mass analysis is achieved by scanning the energies of ions which were given equal momentum increments. The chief advantages of the design lies in the large ionization volume available. The possibility of using this kind of mass spectrometer for photoionization, ion-molecule reaction, and energetic ion studies is pointed out. Mass spectra obtained by electron ionization and photoionization are presented. Resolution of at least one mass unit in 15 is demonstrated and a sensitivity of 3 amp/(amp Torr) for electron ionization in nitrogen is shown. (auth)

31170 (ISO-SA–16) A DIFFERENTIAL SPECTROPHOTOMETRIC DETERMINATION OF PLUTONIUM(III) USING COLORED GLASS FILTERS. Winkle, L. W. (Isochem Inc., Richland, Wash.). May 3, 1966. Contract AT(45-1)-1851. 10p. (CONF-660615–2). Dep. mn. CFSTI $1.00 cy, $0.50 mn.

From American Chemical Society, Northwest Regional Meeting, Vancouver, B. C.

A procedure is described for the precise spectrophotometric determination of plutonium(III) in the 10 to 15 g/l range. The method is similar to that reported by Phillips, except that the relative absorbance of the sample solution is measured against a colored glass filter instead of a standard plutonium solution. The concentration range that gives maximum precision was determined for a double-beam spectrophotometer (Beckman DK-2A) and the influence of extraneous elements was evaluated. The standard deviation for 10 samples using a filter as a reference was the same as that reported earlier by Phillips for aqueous standards (± 0.05%). (auth)

31171 (ORO–596) A DISSOLVED-OXYGEN ANALYZER FOR OCEANOGRAPHIC USE. Final Report. Gillespie, Arthur S. Jr.; Roberts, Kenneth F. (Research Triangle Inst., Durham, N. C. Measurement and Controls Lab.). Dec. 31, 1965. Contract AT(40-1)-2513. 54p. Dep. mn. CFSTI $3.00 cy, $0.50 mn.

An instrumental dissolved oxygen analyzer was developed for in situ measurements down to a mile in the sea. The instrument is based on the radio release principle in which aqueous dissolved oxygen reacts with radioactive thallium metal in a column to release radioactive thallous ions. ^{204}Tl beta detectors studied included plastic scintillators and a special high-pressure Geiger counter developed in this study. The plastic scintillator was abandoned because of severe cracking and crazing of the polyvinyltoluene based plastic under the high hydrostatic pressures. The Geiger tubes were constructed with a thin-walled, small-diameter stainless steel sample flow tube running lengthwise through the counter. These counters detect ^{204}Tl beta radiation (0.7 Mev maximum) with an efficiency of about 1%. Instrument response is linear with respect to dissolved oxygen and is independent of pressure up to at least 2,500 lbs/in^2. Results of field testing the instrument on an oceanographic vessel were most encouraging. (auth)

31172 (SGAE-BL-17/1966) NEUTRONENAKTIVIERUNGSANALYTISCHE BESTIMMUNG VON RADIOSENSIBILISATOREN. (Neutron Activation Analysis Determination of Radiosensitizers). Altmann, H.; Frischauf, H.; Adamiker, D.; Kaindl, K. (Oesterreichische Studiengesellschaft fuer Atomenergie G.m.b.H., Seibersdorf). 1966. 10p. Dep. mn.

Neutron activation analysis was used to investigate the effective mechanism of the radiosensitizers 5-bromouracil, 5-chlorouracil, 5-iodouracil, 5-bromodesoxycytidine, 1-bromo-2-naphthol, 6-bromo-2-naphthol, iodobenzoic acid, p-iodophenol, p-bromophenol, p-chlorophenol, iodoacetamide, iodoacetic acid, phenylmercuric acetate, p-chloromercuric benzoate, and p-hydroxymercuric benzoate. The methods using neutron activation analysis for determination

of the halogens, Cl, Br, I, and for Hg are described. The results indicated that neutron activation analysis can be used for the determination of radiosensitizers. (J.S.R.)

31173 (SGAE-BL–18/1966) ZUR BESTIMMUNG VON JOD IM GESAMTSERUM UND IM SERUMEIWEISS MIT DER NEUTRONENAKTIVIERUNGSANALYSE. (Determination of Iodine in Whole Serum and in Blood Protein with Neutron Activation Analysis). Frischauf, H.; Altmann, H. (Oesterreichische Studiengesellschaft fuer Atomenergie G.m.b.H., Seibersdorf). 1966. 6p. Dep. mn.

Studies showed that the determination of iodine in blood proteins and serum by means of activation analysis is simple and rapid. The time necessary for the chemical processing and measurement and for calculation of the results was 15 to 20 minutes for two persons per determination. By automation this time could be significantly shortened. The method can be used for the determination of iodine in tissues or other biological materials difficult to process and is suitable as an independent measurement for the comparison of the results obtained with chemical methods. (tr-auth)

31174 (WAPD-T–1905) ENRICHED URANIUM SCRAP ASSAY GAGE. Moss, H. D.; McNamara, W. G.; Zontek, D. E. (Bettis Atomic Power Lab., West Mifflin, Pa.). June 1966. Contract AT(11-1)-Gen-14. 39p. (CONF-660616–1). Dep. mn. CFSTI $2.00 cy, $0.50 mn.

From 7th Annual Inst. of Nuclear Materials Management Meeting, Columbus, Ohio.

The enriched uranium scrap assay gage was designed and built for use as a nondestructive method of measuring the ^{235}U content in combustible waste and air exhaust filters, which contain up to 350 g of ^{235}U. The gage monitors gamma radiation (at 0.130 to 0.240 Mev) from the source under investigation by use of 8 detector heads mounted at the 8 corners of the counting chamber. The source is counted for 80 sec to give the desired gage precision and counts from the 8 detector heads are integrated and appear as one value on the counter. Uses in criticality control and accountability programs are discussed. (M.C.G.)

31175 TRACE ELEMENTS IN HUMAN MYOCARDIAL INFARCTION DETERMINED BY NEUTRON ACTIVATION ANALYSIS. Wester, P. O. (Karolinska Inst., Stockholm). Acta Med. Scand., 178: 765-88(Dec. 1965).

A recently developed ion-exchange technique combined with neutron activation analysis and subsequent γ spectrometry was used to determine simultaneously a large number of trace elements in injured and uninjured heart tissue from patients who died soon after myocardiac infarction. In the infarcted tissue calculations on a wet weight basis showed a decrease in Co, Cs, K, Mo, P, Rb, and Zn, and an increase in Br, Ca, Ce, La, Na, Sb, and Sm. The differences in Ca, La, Mo, P, and Zn were dependent on the age of the myocardial infarction, and the regression lines for these elements are given. In the normal material, none of the elements studied varied significantly with age, but differences in As, Ce, Cu, and Mo in uninjured tissue from infarcted hearts were correlated with age. In the group of trace elements with known biological function, Ca was found to be highly enriched in the injured tissue, the median value of Ca in injured tissue being $2\frac{1}{2}$ times that in uninjured tissue. Among the trace elements without known biological function, increased amounts of Sb and of the lanthanides Ce, La, and Sm were found in the injured tissue. The La enrichment varied with the age of the myocardial infarction. (TCO)

31176 TRACE ELEMENTS IN THE CONDUCTIVE TISSUE OF BEEF HEART DETERMINED BY NEUTRON ACTIVATION ANALYSIS. Wester, P. O. (Karolinska Inst., Stockholm). Acta Med. Scand., 178: 789-800(Dec. 1965).

A recently developed ion-exchange technique, neutron activation analysis, and subsequent γ spectrometry were used to determine simultaneously a large number of trace elements in a very small sample. The amounts of Ag, As, Au, Ba, Br, Ca, Cd, Ce, Co, Cr, Cs, Cu, Fe, Hg, K, La, Mo, Na, P, Rb, Sb, Sc, Se, Sm, W, and Zn were estimated in the conductive tissue and adjacent muscle tissue of the beef heart. Samples of four beef hearts taken from the bundle of His and adjacent ventricular muscle, and AV node, and adjacent atrial muscle were studied. In the conductive tissue compared to adjacent muscle tissue, calculations on a wet weight basis showed lower concentrations of Cs, Cu, Fe, K, P, Rb, and Zn in the former, and higher concentrations of Ag, Au, Br, Ca, and Na. The mean differences ($\mu g/g$ wet tissue), as well as their degree of significance, between the bundle of His and adjacent tissue from the ventricular septum, between the AV node and adjacent atrial muscle, between the ventricular septum and the right atrium, and between the bundle of His and the AV node are given for the elements Cu, Fe, K, Na, P and Zn. Cerium, La, and Sm like the other lanthanides determined, were found to occur in the same concentration, or a slightly higher one, in the conductive tissue compared with adjacent muscle tissue. (TCO)

31177 COMPUTER PROGRAM FOR CALCULATION OF LIQUID SCINTILLATION SPECTROMETRY DATA FROM DUAL-LABELED SAMPLES CORRECTED FOR QUENCHING BY DUAL INTERNAL STANDARDIZATION. Matthijssen, Charles (Southwest Foundation for Research and Education, San Antonio). Anal. Biochem., 15: 382-5 (June 1966).

A computer program was written in FORTRAN II language for the calculation of liquid scintillation spectrometry data from dual-labeled samples corrected for quenching by dual internal standardization. The individual data are statistically evaluated and the precision is stated as the relative standard error (one tail 95% confidence limits). (auth)

31178 DETERMINATION OF ^{14}C-LACTATE ADAPTED TO LIQUID SCINTILLATION COUNTING. Leunissen, R. L. A.; Piatnek-Leunissen, D. A. (Hahnemann Medical Coll., Philadelphia). Anal. Biochem., 15: 409-20(June 1966).

A method is presented for determination of the radioactivity in the 1-carbon and the 2,3-carbon moieties of lactic acid adapted to liquid scintillation counting. The lactic acid is oxidized by ceric sulfate to acetaldehyde and CO_2, which are carried over into a series of traps by means of a CO_2-free and carbonyl-free air stream. The acetaldehyde is trapped as its semicarbazone and assayed spectrophotometrically. The CO_2 is trapped as its Hyamine-carbonate and measured by difference titration. Radiochemical assays are performed directly using Bray's solution as the counting system. A description is given of the distillation-degradation setup and of the CO_2-carbonyl scrub train used. Optimal conditions of air flow, temperature, and duration of the reaction are given. The method can be used in the range of 15 to 60 μmoles and is reproducible and accurate. (auth)

31179 DETERMINATION OF RADIOACTIVITY IN AGAR BLOCKS BY LIQUID SCINTILLATION TECHNIQUES. Lagerstedt, H. B.; Langston, R. (Texas Agricultural and Mechanical Univ., College Station). Anal. Biochem., 15: 448-53(June 1966).

Two methods were developed for liquid scintillation counting of radioactivity in aqueous solutions prepared in agar. One method involves breaking down the structure of the agar while the second involves extraction of the sample. Both methods employ absolute ethanol as a cosolvent in order to achieve miscibility between the aqueous-agar sample and the toluene-based scintillator solution. A 1:7 absolute ethanol:toluene solution was found to be most efficient in extracting three different types of ^{14}C-containing solutes from aqueously prepared agar blocks. These techniques yielded greater sensitivity and better counting efficiency than was previously possible because a liquid scintillation spectrometer can be employed for the assay. (auth)

31180 RAPID ESTIMATION OF IMPORTANT RADIONUCLIDES ^{89}Sr, ^{90}Sr, ^{131}I, AND ^{137}Cs IN FOOD AND WATER. [PART] II. Bergner, K. G.; Jagerhuber, P. Deut. Lebensm.-Rundsch., 60: 207-10; 253-5(1964).

Analytical procedures are discussed for the accurate routine control and rapid emergency testing of the effect of fallout on foods and water. Use of the γ-spectrometer

is recommended for the estimation of ^{131}I and ^{137}Cs; measurement of the β-radiation at 2 definite time intervals is recommended for the estimation of ^{89}Sr and ^{90}Sr. (Pub. Health Abstr.)

31181 COMPLEXOMETRIC MICRODETERMINATION OF HEAVY METALS WITH ^{60}Co AS THE RADIOACTIVE INDICATOR. Fuchs, A. (Univ., Zurich). Helv. Chim. Acta, 49: 1023-9(1966). (In German).

Nanogram masses of cobalt and other heavy metals can be determined complexometrically with ^{60}Co as the radioactive indicator. In the method described the cation and chelate are separated by paper electrophoresis. (tr-auth)

31182 PROGRAMMED ANALYSIS FOR COUNTING OF AQUEOUS SAMPLES CONTAINING TWO RADIOACTIVE ISOTOPES. Ninomiya, R. (Univ. of Toronto). Int. J. Appl. Radiat. Isotop., 17: 355-8(June 1966).

A computer program was written in Fortran IV to carry out the computations involved in the method proposed by Hendler for the simultaneous measurement of radioactivity of quenched samples containing 2 different β-emitting isotopes such as ^{14}C and ^{3}H. The program is assembled to accept an unlimited number of counting jobs with each job accommodating up to 100 samples. It is used on an IBM 7094 system. The total computation time for 100 vials is about 1 min. (M.C.G.)

31183 DETERMINATION OF COPPER IN QUARTZ BY NEUTRON ACTIVATION ANALYSIS. Hoffmeister, W. (IBM Labs., Boeblingen, Ger.). Int. J. Appl. Radiat. Isotop., 17: 360-1(June 1966).

Four types of commercially available quartz were analyzed for their copper concentration by neutron activation followed by a chemical separation. The 0.51-Mev peak of ^{64}Cu annihilation radiation was used for the measurements. The count rate ranged from 200 to 900 counts/min. The detection limit for copper was 5×10^{-10} g. Normal quartz was found to have a copper content of 10^{-8} g/g whereas in synthetic quartz the copper content was on the order of 10^{-9} g/g. (M.C.G.)

31184 THE ASSAY OF β-EMITTING RADIOISOTOPES USING CHERENKOV COUNTING. Parker, R. P.; Elerick, R. H. (Inst. of Cancer Research, Sutton, Eng.). Int. J. Appl. Radiat. Isotop., 17: 361-2(June 1966).

An automatic liquid scintillation counter was used to study the Cherenkov counting method for beta-emitting radioisotopes. It was found that reasonable efficiencies can be achieved by the Cherenkov method. The effects of chemical quenching were studied using ^{32}P-labeled sodium orthophosphate in perchloric acid and found to be less than 1%. Color quenching was found to be significant for pigmented samples. (M.C.G.)

31185 NEW OXYGEN FLASK APPARATUS FOR THE ASSAY OF TRITIUM AND ^{14}C. Dobbs, H. E. (Reckitt and Sons Ltd., Hull Yorks, Eng.). Int. J. Appl. Radiat. Isotop., 17: 363-4(June 1966).

The use of screwcap seals for oxygen flask apparatus in determination of ^{14}C and tritium is discussed. This modification and other changes increased the sensitivity of the method for assay of tritium and reduced the overall time per assay. (M.C.G.)

31186 QUANTITATIVE DETERMINATION OF RADIONUCLIDES USING GAMMA SPECTRA. Santholzer, Vilem (Charles Univ., Prague). Jad. Energ., 12: 143-5(1966). (In Czech).

Literature (26 references) on the determination of radionuclides from their gamma spectra is reviewed. The individual nuclides may often be determined by a combination of radiochemical separation and identification of the gamma spectra. The simplest method for determining an element from its gamma spectrum depends on finding the area under the photopeak, taking as the base of the area the abscissal distance between the "valleys" on either side of the peak. The number of curies of the nuclide present can then be calculated from a formula. This value may be converted to the absolute beta activity by a conversion coefficient. In a mixture of radionuclides, each may be determined individually by calculation from the gamma spectra. In the subtraction method the spectrum is analyzed differentially. By the graphic method, on log-log paper, two nuclides, e.g., ^{134}Cs and ^{137}Cs, may be determined individually; three may also be determined. The effect of beta radiation on measurements made with a well counter is shown in a Fermi-Curie plot. (TTT)

31187 A METHOD OF ^{210}Po DETERMINATION IN HUMAN URINE SAMPLES. Tibor, Zh.; Arpad, T.; Aladar, U. Med. Radiol., 11: No. 5, 56-60(May 1966). (In Russian).

Conditions governing the isolation of ^{210}Po from urine solutions onto a nickel plate, such as temperature, acidity, the volume of solution, precipitation time, etc., were studied. The data formed a basis for a method of ^{210}Po estimation in urine, enabling measurements of concentrations from 0.3^{10-12} C/l (liter) (with collection of 2 liters of the urine) and above. Concentrations of ^{210}Po, in the urine of 16 persons not exposed to radon irradiation were determined and these yielded an average background value of 0.4^{10-12} C/l (liter). Data from literature sources on the polonium content in the urine of diverse persons (over 200) are cited. (auth)

31188 RESOLUTION OF ^{89}Sr AND ^{90}Sr IN ENVIRONMENTAL MEDIA BY AN INSTRUMENTAL TECHNIQUE. Velten, R. J. (Robert A. Taft Sanitary Engineering Center, Cincinnati). Nucl. Instrum. Methods, 42: 169-72(June 1966).

The beta emissions of ^{89}Sr and ^{90}Sr are resolved by observing the ingrowth of the ^{90}Y and decay of ^{89}Sr. The ratio of count rate of the ^{90}Sr and the ingrown ^{90}Y to that of the parent ^{90}Sr at any time is predetermined. Two measurements of the total radiostrontium fractions are made at an interval of 7 to 14 days. Relating this ratio and the decay factor for ^{89}Sr with these two measurements, two equations can be set up and solved simultaneously to express the individual count rate of the two strontium isotopes. The count rate of the ^{90}Sr is corrected for self-absorption losses by relating the overall detection efficiency of ^{90}Sr to that of ^{90}Y, an energetic beta emitter with no sample absorption losses at the thickness studied. This technique differs from conventional methods in that neither additional chemistry nor the use of absorbers is required as a differentiating tool. (auth)

31189 RADIOCHEMICAL DETERMINATION OF ^{235}U ABUNDANCES BY ACTIVATION ANALYSIS. Kjelberg, A.; Pappas, A. C.; Westgaard, L. (Univ. of Oslo). Radiochim. Acta, 5: 104-9(May 1966).

The feasibility of using ^{99}Mo for the determination of ^{235}U abundances was investigated and a radiochemical procedure for its isolation from fission mixture given. The interference from secondary reactions was investigated, and it is shown that these are negligible in most cases or can be made so by use of proper techniques. Some results obtained with the suggested method are presented. (auth)

31190 ERRORS IN ACTIVATION ANALYSIS DUE TO VARIATIONS IN ISOTOPIC RATIO. de Goeij, J. J. M.; Houtman, J. P. W.; Kanij, J. B. W. (Reactor Instituut, Delft, Netherlands). Radiochim. Acta, 5: 117-18(May 1966).

In investigations of a lithium alloy, the results of activation analysis were quite different from those of the classical flame-photometric determination. It was found that the ^{6}Li abundance was only 4.9% instead of the normal (natural) 7.4%. (M.C.G.)

31191 PRELIMINARY REPORT ON THE DETERMINATION OF RADIUM IN RIVER WATERS. Hataye, Itsuhachiro; Oocho, Emiko; Aoyama, Hideo. Rep. Fac. Sci., Shizuoka Univ., 1: 35-41(Dec. 1965).

The content of radium in river waters was studied by coprecipitation of radium with barium sulfate, ferric hydroxide, and calcium carbonate. This method was compared with results from direct radioactivity measurements on nonprocessed and evaporated samples. It was found that coprecipitation of radium with $CaCO_3$ and the conditions that 10 g of $CaCl_2$ as carrier was added to

the solution whose pH value was 10.0 is the most suitable method for concentration of radium. (M.C.G.)

31192 WATER PROBLEM AND DESALINATION. Hunter, J. (Office of Saline Water, Washington, D. C.). pp 17-28 of STI-DOC-10/51.

The basics of water desalination are discussed. The energy requirements for six desalination processes are given. Processes such as electrodialytic and electrochemical or briefly described. Several demonstration plants are described. (M.O.W.)

31193 FRESH WATER FROM THE SEA. Silver, R. S. (Dept. of Engineering, Heriot-Watt Coll., Edinburgh). pp 29-51 of STI-DOC-10/51.

Separate discussions of the following aspects of water desalination are presented: relation between water and power consumptions, seawater conversion and power, energy costs in seawater conversion, multistage flash distillation process, possible improvements in distillation, cost possibilities of other processes, and stability and control problem in flash distillation. (M.O.W.)

31194 EXPERIENCE WITH ELECTRODIALYSIS. Minken, J. W. (International Atomic Energy Agency, Vienna). pp 52-8 of STI-DOC-10/51.

The principle of the electrodialysis method for water desalination is described. The performance of the method is described. (M.O.W.)

31195 ION EXCHANGE SEPARATION OF URANIUM, THORIUM, AND LANTHANIDES IN MIXED AND NON-AQUEOUS SOLVENTS. Korkisch, J. (Univ. of Vienna). pp 121-4 of STI-DOC-10/53.

An ion exchange method was developed for use in the spectrophotometric determination of uranium, thorium, and rare earths in organic solvent–acid media. (M.C.G.)

31196 TITRIMETRIC DETERMINATION OF SOME ORGANIC ACIDS BY XENON TRIOXIDE OXIDATION. Jaselskis, Bruno; Krueger, R. H. (Loyola Univ., Chicago). Talanta, 13: 945-9(July 1966).

Aqueous xenon trioxide in acidic or neutral solutions oxidizes carboxylic acids quantitatively to carbon dioxide and water. Micro and semimicro amounts of carboxylic acids may be determined by the iodometric titration of the excess of xenon trioxide remaining in the reaction mixture. The optimum time and temperature for the reaction depend on the structure of the acid; dicarboxylic and hydroxycarboxylic acids react faster than corresponding monocarboxylic acids. Oxalic and polyhydroxy acids are oxidized within 20 min at room temperature while acetic, maleic, succinic, malonic acids require 2 hr at 40°C. Carboxylic acids in amounts less than 100 μg are determined with a coefficient of variation of 4%, which decreases to 1% for amounts over 250 μg. (auth)

31197 ADVANCES IN MASS SPECTROMETRY. VOLUME 3. Proceedings of a Conference held in Paris, September 1964. Mead, W. L. (ed.). Advance. Mass Spectrometry, 3: Proc. Conf. Paris, 1964, 1-1064(1966). (CONF-520).

Separate abstracts were prepared for twenty-eight of the seventy-four papers presented. Three papers were previously abstracted for NSA 18: 39057; 19: 4353, 42411. The remaining papers deal with theory of mass spectra and uses of mass spectrometry in analysis of solids and measurements of isotopic abundances and in studies of ionization phenomena, ion-molecule reactions, molecular structure, chemical reactions, and thermodynamics. A bibliography on mass spectrometry covering the period mainly from Jan. 1961 to Dec. 1962 is included. (A.G.W.)

For abstracts of individual papers see: 31198–31209, 31224–31227, 31270, 31271, 31399–31401, 31723, 31808, 31905–31907, 32385, and 32386.

31198 PRODUCTION OF FIELD IONIZATION MASS SPECTRA WITH A SHARP EDGE. Robertson, A. J. B.; Viney, B. W. (King's Coll., London). Advance. Mass Spectrometry, 3: Proc. Conf. Paris, 1964, 23-34(1966).

Positive ions were produced by field ionization at the sharp edge of an ordinary razor blade. Two simple ion sources employing a razor blade were investigated. With a source with three slit plates ion currents approaching 10^{-11} amp were obtained as resolved ion beams; a sample pressure of 10^{-4} mm Hg and voltages less than 10 kv were used. The assignment of mass to peaks in a mass spectrum from the ion accelerating voltage is discussed. Mass spectra were obtained with some ketones, olefins, and alcohols, and with propane and diethyl ether. Generally the parent ion was predominant. Fragment ions produced could usually be accounted for by simple processes of dissociation. With all the ketones investigated the same simple dissociation processes were observed. However some fragment ions appeared, which were not accounted for by simple dissociation. With some substances ions were produced of mass greater than that of the parent ion. A reaction involving a condensed film is probably involved. (auth)

31199 ADVANCES IN EXPERIMENTAL TECHNIQUES, APPLICATIONS, AND THEORY OF FIELD ION MASS SPECTROMETRY. Beckey, H. D.; Knoeppel, H.; Metzinger, G.; Schulze, P. (Univ., Bonn). Advance. Mass Spectrometry, 3: Proc. Conf. Paris, 1964, 35-67(1966).

Work done at the University of Bonn since 1961 on field ion mass spectrometry is reviewed. New experimental techniques include use of thin wires or sharp metal edges for field ionization. A multiwire field ion source, quartz filaments covered with metals, and a combined electron impact and field ion source are described. Applications of the method to analysis of hydrocarbon mixtures and to structural analysis of solid natural products (e.g., steroids) are discussed. A general model describing the mechanisms of fragment ion formation after field ionization was developed. The model is compared with results of several experiments. (A.G.W.)

31200 MICROANALYSIS BY SECONDARY ION EMISSION. Castaing, Raymond; Slodzian, Georges (Faculte des Sciences, Orsay, France). Advance. Mass Spectrometry, 3: Proc. Conf. Paris, 1964, 91-8(1966). (In French).

Characteristic secondary ions emitted from a massive sample by primary ion bombardment are focused to give an image of the surface of the object by means of suitable ion optics. From this image as many images as there are elements (and isotopes) present in the sample may be extracted by a magnetic filter. Each of these images gives the distribution of the element to which it corresponds with a resolving power of the order of a micron. The analysis obtained is semiquantitative. The samples may be insulators or conductors and the secondary ions used positive or negative. (auth)

31201 ANALYSIS OF SOLIDS BY MASS SPECTROMETRY. Honig, Richard E. (RCA Labs., Princeton, N. J.). Contract AF19(628)-446. Advance. Mass Spectrometry, 3: Proc. Conf. Paris, 1964, 101-29(1966).

The various mass spectrometric methods in use today for bulk and surface analyses of solids are reviewed. Suitable ion sources are discussed from the standpoint of the underlying physical processes, with particular emphasis on the more recent vacuum discharge methods. The systems of ion detection available at this time are briefly evaluated, followed by a detailed discussion of the different factors that make up elemental sensitivities. The limited analytical accuracy achieved to date is illustrated by typical results obtained with r-f spark source instruments. (62 references) (auth)

31202 QUANTITATIVE ANALYSIS BY SPARK SOURCE MASS SPECTROMETRY. Halliday, J. S.; Swift, P.; Wolstenholme, W. A. (Associated Electrical Industries Ltd., Manchester, Eng.). Advance. Mass Spectrometry, 3: Proc. Conf. Paris, 1964, 143-61(1966).

The accuracy of analysis obtained with an r-f spark source can be as good as 10 per cent when the source conditions are maintained constant and relative sensitivity factors are established with a sample of the same matrix examined under the same source conditions. The linearity

of the technique over an impurity concentration range of 10^5 to 1, extending down to a few parts in 10^9, has been established. The worst variation in sensitivity relative to the matrix when large changes were made in the ion accelerating voltage, the r-f spark voltage, or the pulse repetition rate was about a factor five to one for certain elements in steel. These variations are much smaller than those reported by Franzen and Hintenberger, probably because the energy spread of ions transmitted to the spectrum was three times larger in the AEI MS 7 mass spectrometer. A direct correlation between sample inhomogeneity and poor reproducibility was established by x-ray microanalysis. With homogeneous metallic and nonmetallic materials the reproducibility on repeat analyses is usually between 20 and 30 per cent, and can be as good as 10 per cent. (auth)

31203 CONTRIBUTION TO THE INVESTIGATION OF BACKGROUND EFFECTS IN SPARK SOURCE MASS SPECTROGRAPHY. Mai, H. (Institut fuer Angewandte Physik, Dresden). Advance. Mass Spectrometry, 3: Proc. Conf. Paris, 1964, 163-8(1966).

Attempts to reduce the background blackening of mass spectra caused by reactions of the principal parts of the ion beam with the photographic plate (halo) are described. It was found that a strong influence on the halo was obtained only if the mean value of the instantaneous monitor current remained below 3×10^{-10} amp. The use of different types of conducting and nonconducting target materials failed to yield the success hoped for. By cutting out those parts of the photographic plate that normally intercept the most intensive lines due to the matrix, it was possible to suppress the halo entirely. The resulting improvement in the limits of detection of impurities in Al in some cases ran to one order of magnitude for elements in the mass range 20 to 120. (A.G.W.)

31204 NEW MASS SPECTROMETER ION SOURCE FOR SOLIDS. Cobic, B.; Perovic, B.; Tosic, D. (Boris Kidric Inst. of Nuclear Sciences, Belgrade). Advance. Mass Spectrometry, 3: Proc. Conf. Paris, 1964, 179-81 (1966).

A mass-spectrometer ion source with cathode sputtering of charge materials was developed for analysis of low-vapor-pressure materials. The ion source has a magnetron geometry with axial hot cathode and cylindrical anode. The material to be analyzed is fixed to the cathode filament by coating the central part of the cathode with an emulsion of powdered material, acetone, and colodium. The cathode is then heated and argon is introduced into the source. Ion collector currents obtained are in the range 10^{-12} to 10^{-11} amp. The energy spread of the magnetron ion source is of the same order as that of Nier's ion source. (A.G.W.)

31205 MEASUREMENT OF RELATIVE ABUNDANCE AND PRODUCTION CROSS SECTIONS OF LITHIUM ISOTOPES IN METALLIC TARGETS BY HIGH-ENERGY PROTONS. Klapisch, R.; Gradsztajn, E.; Yiou, F.; Epherre, M.; Bernas, R. (Faculte des Sciences, Orsay, France). Advance. Mass Spectrometry, 3: Proc. Conf. Paris, 1964, 547-52(1966). (In French).

An experimental method is described, which is particularly adapted for the measurement of micro-trace amounts of stable isotopes in various elements and which was developed for lithium isotopes produced in nuclear reactions. It includes a new thermionic ion source with three independently demountable and accurately adjusted filaments. Extraction of the nuclear reaction products is done only by physical means: either by the use of a high-temperature oven and condensation of the products on a liquid nitrogen-cooled filament or by the direct use of the spectrometer filament as the accelerator target. An all-metal 60° mass spectrometer equipped with a high-gain multiplier (5×10^8) and employing pulse-counting techniques is used for the measurements. Lithium isotope ratios were obtained from targets of C, V, Nb, Ta, and Pt bombarded by protons of energies varying from 40 Mev to 25 Bev. Absolute cross sections are obtained by using as tracer the ^{7}Li produced from the decay of ^{7}Be (half life 53 days) formed during the same irradiation. (auth)

31206 TANDEM MASS SPECTROMETER FOR ISOTOPIC ANALYSIS. Ridley, R. G. (Atomic Weapons Research Establishment, Aldermaston, Eng.); Munro, R.; Young, W. A. P.; Hayes, R.; Hardy, R. W. D.; Wilson, H. W. Advance. Mass Spectrometry, 3: Proc. Conf. Paris, 1964, 553-68(1966).

A two-stage, 25-inch radius, magnetic mass spectrometer with a resolution of 1500 and a mass range of 5–300 is described. A new all-metal vacuum lock is attached to the source, which may operate for positive ions at +25 kv or negative ions at −12 kv. An electron multiplier detector for ion counting, with a background of 0.003 counts per second, is used at the end of the spectrometer with source voltage sweeping or switching. Simultaneous collection is available between a center Faraday cup or multiplier and the final detector giving facilities that retain the high abundance sensitivity. A multiplier after the center-defining slit allows the beam from the first stage to be monitored and is useful for measurement with magnetic field sweeping or switching when high abundance sensitivity is not required or when a large mass range is necessary or when in the low mass region to avoid a large source discrimination. In the uranium region the abundance sensitivity on the low mass side and on the high mass side respectively of the major peak for the single stage is 2.5×10^{-6} and 1.3×10^{-6} and for the two stages 1.3×10^{-6} and 3.6×10^{-8}. (auth)

31207 SOME PROBLEMS RELATING TO THE THERMAL EMISSION OF IONS IN THE MASS SPECTROMETRIC DETERMINATION OF ISOTOPIC ABUNDANCES FOR NEUTRON CROSS-SECTION MEASUREMENTS. Baldock, Russell (Oak Ridge National Lab., Tenn.). Advance. Mass Spectrometry, 3: Proc. Conf. Paris, 1964, 749-54 (1966).

Some greatly improved yields of metal ions from submicrogram samples of uranium and californium, obtained by the use of properly shaped single filaments, are reported. Isotopic analyses of samples of bismuth, which normally tend to flake off filaments and samples of enriched isotopes of palladium and ruthenium normally available as a fine metal powder were successfully obtained by use of these shaped ovens. By employing these ovens and enriched isotopes of palladium, the yield was determined for the procedures developed to measure the ^{105}Pd and ^{106}Pd produced by the neutron activation of enriched ^{104}Ru and the amounts of the ^{105}Pd and ^{106}Pd produced. (auth)

31208 INS MASS SPECTROMETER (A NEW MASS SPECTROMETER). Sakai, Mitsuo (Tokyo Univ.); Goto, Masayuki. Advance. Mass Spectrometry, 3: Proc. Conf. Paris, 1964, 791-6(1966).

The construction of a new mass spectrometer with high resolution and high luminosity was based on the theoretical prediction that a special setting of the source and the detector (deflection angle $\theta = (2\sqrt{2}/3)\pi$ and distance between the source and the boundary of the magnetic field $= \sqrt{2}\rho \tan \pi/12$ in an inhomogeneous magnetic field with field coefficients $\alpha = \frac{1}{2}$ and $\beta = \frac{1}{4}$) should have excellent focusing properties. The main radius is 20 cm. A resolving power of 340 cm was obtained. (auth)

31209 RESULTS ON A NEW ELECTROSTATIC TIME-OF-FLIGHT MASS SPECTROMETER DEVELOPED AT THE REACTOR CENTER, SEIBERSDORF. Higatsberger, M. J.; Viehboeck, F. P.; Ruedenauer, F.; Buschbeck, F. (Oesterreichische Studiengesellschaft fuer Atomenergie, Seibersdorf, Austria). Advance. Mass Spectrometry, 3: Proc. Conf. Paris, 1964, 803-20(1966).

A new type of electrostatic r-f time-of-flight mass spectrometer is described, which employs parabolic flight paths for energy selection. Mathematical treatment of such a system is given. Details of the analyzer and the electron circuit of a prototype instrument are reported. First experimental tests were performed and the results obtained are in good agreement with theory. (auth)

31210 PROCESS GAS CHROMATOGRAPH FOR THE MEASUREMENT OF IMPURITIES IN HELIUM. Richardson, Robert D. (Thermco Instrument Corp., La Porte, Ind.). 10p. (CONF-650311-5). ORAU.

From Conference on Analytical Chemistry and Applied Spectroscopy, Pittsburgh.

A continuously operating gas chromatograph was developed to measure the impurities in the blanketing gas over the reacting fluid in a nuclear reactor. In the specific application described, helium is used over a heavy water bath in a neutron-producing reactor. The sample is drawn by vacuum from the reactor, the deuterium oxide is removed, and the sample is passed through the chromatograph at a vacuum of 24 in. of Hg. The operation of the instrument is checked every six hours by automatic insertion of a standard gas. Nitrogen, oxygen, deuterium, and other gases that may appear in the blanketing helium are detected. (A.G.W.)

31211 COMBINATION NEUTRON EXPERIMENT FOR REMOTE ANALYSIS. Caldwell, R. L.; Mills, W. R.; Allen, L. S.; Bell, P. R.; Heath, R. L. 19p. (CONF-651140–1). ORAU. Gmelin, AED-CONF-65-399-1.

From Society of Exploration Geophysicists, 35th Annual International Meeting, Dallas.

A neutron analysis technique suitable for unmanned lunar and planetary surface exploration is described. The technique consists essentially of bombarding the surface with bursts of neutrons and measuring the energies of the resulting prompt, capture, and activation gamma rays. The rate at which the capture gamma rays die away is also measured. All four measurements are carried out with a single instrument and the data are telemetered to earth for analysis. Results of preliminary experiments on granite and basalt are shown. It is expected that rock type, water content, and near-surface layering can be determined. (A.G.W.)

31212 DISTRIBUTION OF PLUTONIUM DIOXIDE IN URANIUM DIOXIDE BY AUTORADIOGRAPHY. Jeffs, A. T. (Atomic Energy of Canada Ltd., Chalk River, Ontario). 10p. (CONF-650841–1). ORAU. Gmelin, AED-CONF-65-277-3.

From Conference of Metallurgists, Ottawa.

Autoradiographic techniques for study of the distribution of plutonium in PuO_2-UO_2 pellets are described. A resolution of about 20μ was obtained by a dry exposure process employing Kodak AR 10 stripping emulsion pressed onto the specimen surface by a sponge rubber backing. Higher resolution was obtained by interposition between specimen and emulsion of a heavy-element foil of thickness just less than the range of Pu alphas in it. A Pt foil 3×10^{-4} in. thick was used. To minimize thickness variations the foil was moved slowly during exposure. (A.G.W.)

Inorganic and Physical Chemistry

Refer also to abstracts 31440 and 31959.

31213 (ANL–7175, pp 119-58) MATERIALS CHEMISTRY AND THERMODYNAMICS. (Argonne National Lab., Ill.).

Activities in a program directed toward development of reactor materials for use at 1500 to 3000°C are reported. Emphasis during the report period was placed on phase studies of $U-UO_2$ systems. Results of investigations are included concerning ceramic fuel preparation, colorimetric determination of high-temperature materials thermodynamic properties, liquid Na chemistry, and chemistry of other liquid metals. (J.R.D.)

31214 (CEA–R–2859) ETUDE CINETIQUE DE LA FLUORATION PAR LE FLUOR DE QUELQUES COMPOSES DE L'URANIUM ET DU PLUTONIUM. (Kinetic Study of the Fluorination by Fluorine of Some Uranium and Plutonium Compounds). Vandenbussche, Gerard (Commissariat a l'Energie Atomique, Fontenay-aux-Roses (France). Centre d'Etudes Nucleaires). Dec. 17, 1964. 92p. Dep. mn.

Thesis. Submitted to Paris Univ. (France). Faculte des Sciences.

The fluorination reactions of uranium and plutonium compounds with elementary fluorine were studied using a thermogravimetric method. These reactions are heterogeneous ones, and of the following type: $S_{Solid} + G_{1\ gas} \rightarrow G_{2\ gas}$. The kinetics of these reactions correspond to a uniform attack of the entire surface of the sample. If α is the degree of completion of the reaction, k_{rel}, the relative rate of penetration of the reaction interface, and t, the time, the relation, $(1-\alpha)^{1/3} = 1 - k_{rel}\,t$, is evaluated. The mechanism of the reaction varies according to the nature of the compound. With uranium tetrafluoride, the reaction proceeds in a single step. With uranium oxides, the reaction proceeds in two steps with uranium oxyfluoride as the intermediate compound. With plutonium oxide, the reaction proceeds in two steps with plutonium tetrafluoride as the intermediate compound. With uranium trichloride, the mechanism is complex. Chlorine trifluoride is formed. (auth)

31215 (LA–3507) BIBLIOGRAPHY ON KINETICS OF THE OXIDATION-REDUCTION REACTIONS OF URANIUM, NEPTUNIUM, PLUTONIUM, AND AMERICIUM IN AQUEOUS SOLUTIONS. Treiman, Marilyn (Los Alamos Scientific Lab., Univ. of California, N. Mex.). Mar. 9, 1966. Contract W-7405-eng-36. 12p. Dep. mn. CFSTI $1.00 cy, $0.50 mn.

Seventy-six references from NSA, 1958 to March 1966, on kinetics of the oxidation-reduction reactions of uranium, neptunium, plutonium, and americium in aqueous solutions are presented. The references are listed numerically by NSA abstract number. (M.C.G.)

31216 (LA-DC–7659) A SHOCK WAVE STUDY OF RECOMBINATION IN NEAR-STOICHIOMETRIC HYDROGEN–OXYGEN MIXTURES. Getzinger, Richard W. (Los Alamos Scientific Lab., Univ. of California, N. Mex.). [1965]. Contract W-7405-eng-36. 26p. (CONF-660802–1). Dep. mn. CFSTI $2.00 cy, $0.50 mn.

For Presentation at 11th International Symposium on Combustion, Berkeley, Calif.

Recombination in very dilute hydrogen–oxygen–argon mixtures with H_2/O_2 ratios of 3:1 and 2.2:1 was studied in a shock tube at 1307–1846°K and 1.3–6.1 atm. The progress of the reaction was followed by OH ultraviolet line absorption. It was determined that recombination was third order in total pressure and that reactions (I)–(III) were sufficient to account for the total rate of species disappearance. $H + H + M \rightarrow H_2 + M$ (I), $H + O_2 + M \rightarrow HO_2 + M$ (II), and $H + OH + M \rightarrow H_2O + M$ (III). In the course of this analysis the rate coefficient of reaction (III), k_{III}(M = Ar), was determined to be $5.4 \pm 50\% \times 10^{15}$ cc^2/mole^2 sec at these temperatures. The results of this work and of previous recombination studies indicate that throughout the regime $8 \geq H_2/O_2 \geq 0.33$ recombination can be satisfactorily accounted for by only reactions (I)–(III). (auth)

31217 (LA-DC–7661) POST-INDUCTION KINETICS IN SHOCK INITIATED H_2–O_2 REACTIONS. Hamilton, Charles W.; Schott, Garry L. (Los Alamos Scientific Lab., Univ. of California, N. Mex.). [1966]. Contract W-7405-eng-36. 33p. (CONF-660802–2). Dep. mn. CFSTI $2.00 cy, $0.50 mn.

For Presentation at 11th International Symposium on Combustion, Berkeley, Calif.

The course of the shock initiated hydrogen–oxygen reaction after the induction period, during the transition to partial equilibrium, was investigated by computer integration of the rate equations, and approximate analytic descriptions of particular aspects are developed. $H_2:O_2$ ratios far from stoichiometric are considered. An earlier suggestion by one of the authors that partial equilibrium conditions with no recombination represent a practical upper limit to the transient atom and radical concentrations is contradicted, and attention is focused on the pronounced "spike" in oxygen atom concentration that modern rate coefficient data predict to occur in fuel-rich mixtures at the time of maximum reaction rates and most rapid O_2 depletion. Failure of measured OH concentrations to exhibit such "spikes" in rich mixtures is used to establish an upper limit to the ratio of rate coefficients k_a/k_c, $H + O_2 \xrightarrow{k_a} OH + O$ and $OH + H_2 \xrightarrow{k_c} H_2O + H$, over the range $1156° \leq T \leq 1884°K$. (auth)

31218 (UCRL–16658, pp 1-9) INORGANIC CHEMISTRY. (Lawrence Radiation Lab., Univ. of California, Berkeley).

Results of investigations are reported on water exchange on metal ions, polymerization of chromic ions, synthesis of silanes and germanes, reactions of atomic N with sulfur compounds, proton magnetic resonance spectra of cobalt ammine complexes, kinetics of metal-ammonia solutions, nuclear magnetic resonance of weak acids in ammonia, and ^{15}N nuclear magnetic resonance spectra of thiotrithiazyl cations. Lists of 1965 publications are included, and research plans for 1966 are outlined. (J.R.D.)

31219 (UCRL–16658, pp 11-20) CHEMICAL THERMODYNAMICS. (Lawrence Radiation Lab., Univ. of California, Berkeley).

Results of investigations are reported on lifetimes of vibrational levels in gaseous I_2 and gaseous metallic elements, determination of high-temperature molecule ground states, spectra of high-temperature diatomic gases, spectra of high-temperature species in rare gases, transition metal alloy systems, and metal bonding theories. Lists of 1965 publications are included, and research plans for 1966 are outlined. (J.R.D.)

31220 (UCRL–16658, pp 39-72) ELECTROCHEMISTRY. (Lawrence Radiation Lab., Univ. of California, Berkeley).

Results of investigations are presented concerning interfacial phenomena in films, models of single pores in porous electrodes, surface colorimetry, digital data recorders, ionic mass transport in redox systems, current and potential distributions in mass transfer at plane electrodes, anodic metal dissolution, electrolytic gas evolution mechanisms, properties of liquid ammonia solutions of Ca, solvent properties of dimethyl sulfoxide, solubility and diffusivity of gases in liquids, concentration gradients in cathodic depletion, metal-surface adsorption of ions from solutions, electrodialytic sea water desalting, ocean-bottom potentiometers, porous gas electrode operation, reactions in porous metal anodes, droplet evaporation mechanisms, combustion of droplets and particles in hot gases, dynamics and control of complex chemical process systems, flow past obstacles, mass transfer and polarization at rotating-disk electrodes, binary electrolyte polarography, transport properties of electrolytes, heat and mass transfer, falling drop hydrodynamics, and migration effects on currents in electrolytes. Lists of 1965 publications are included, and research plans for 1966 are outlined. (J.R.D.)

31221 (UCRL–16658, pp 73-87) PHYSICAL CHEMISTRY. (Lawrence Radiation Lab., Univ. of California, Berkeley).

Results of investigations are reported concerning ionization of alkali metal vapors, diffusion of Rb and Cs in their vapors, photolysis of nitric oxide, ion-neutral association mechanisms, attachment of gaseous electrons to SF_6 and C_7F_{14}, reactions of $^1\Delta g$ O_2 molecules, mass spectra of ionized gases, neutralization of gaseous ions, hyperfine interactions of ^{17}O in O_2 $^1\Delta g$ state, spin-lattice relaxation times of transition metal ions, electron spin resonance spectra of nitrogen-containing heterocyclics and chromium complexes, microwave spectra of silyl methyl ether, electron spin resonances of metal chlorides at liquid He temperatures, temperature effects on ultraviolet absorption by F_2, XeF_2, and XeF_4, atomic and free-radical intermediates in gas-phase reactions, and the molecular states of nitric and perchloric acids. Lists of 1965 publications are included, and research plans for 1966 are outlined. (J.R.D.)

31222 (ANL-Trans–310) ELECTRON DIFFRACTION STUDY OF THE STRUCTURE OF NEODYMIUM HALIDE MOLECULES. Akishin, P. A.; Naumov, V. A.; Tatevskii, V. M. Translated by Elmar K. Wilip (Argonne National Lab., Ill.), from Nauch. Dokl. Vysshei Shkoly, Khim. Khim. Tekh., 229-32(1959). 7p. Dep. mn. CFSTI $1.00 cy, $0.50 mn. JCL $1.10 fs, $0.80 mf.

Data were collected on the configuration and geometric parameters of gaseous molecules of NdX_3(X = F, Cl, Br, and I). Electron diffraction pictures of the vapors were obtained with electron scattering voltages of 40 and 80 kv. It was established that the molecules of all neodymium halides possess, in the vapor phase, a plane configuration with the neodymium atom in the center of a regular triangle. The interatomic distances were determined and the effective mean square oscillation amplitudes of atoms were estimated. (M.C.G.)

31223 (BNL-tr–78) THE ACTION OF LITHIUM VAPOR ON GRAPHITE. Bagouin, M.; Guerard, D.; Herold, A. Translated by Stephen J. Amoretty (Brookhaven National Lab., Upton, N. Y.), from Compt. Rend., Ser. C, 262: 557-9(Feb. 14, 1966). 5p. Dep. mn. JCL $1.10 fs, $0.80 mf.

The action of lithium vapor on graphite produced the insertion compound of yellow LiC_6 from the first stage; purple LiC_{18} and blue LiC_{28} from the second stage; blue-black LiC_{36} from the fourth stage; and black LiC_{72} from the eighth stage. (auth)

31224 CHARGE TRANSFER AND ATOM TRANSFER IN ION-MOLECULE INTERACTIONS STUDIED BY A TIME-OF-FLIGHT MASS SPECTROMETER. Homer, J. B. (National Research Council, Ottawa); Lehrle, R. S.; Robb, J. C.; Thomas, D. W. Advance. Mass Spectrometry, 3: Proc. Conf. Paris, 1964, 415-32(1966).

A Bendix mass spectrometer, previously modified so that a continuous ion beam replaced the normal electron beam, was further developed so that this primary ion beam may be pulsed. The pulse of ions is created in the primary source at any desired interval prior to the application of the Bendix draw-out pulse, so that the time of arrival of the primary ions in the collision chamber, and hence the residence time of the secondary ions, may be controlled. The translational energy of the primary ions may be varied up to 2 kev. A number of charge-transfer and atom-transfer reactions were studied; in all cases the molecules with which these ions interact have normal thermal velocities. The primary ion beams used in this work were normally rare gas ions and N_2^+, and the principal target gases were Ar, N_2, CH_4, H_2, and D_2. The charge-transfer cross section has a maximum value at a particular relative translational energy of the interacting particles; the value of this energy may be interpreted to a first approximation in terms of the near-adiabatic theory. Some charge-transfer reactions are complicated by the concurrent dissociation of the product ion. The translational energy threshold for such a process can be computed from the conservation laws. In atom-transfer reactions both primary and product ions are collected and mass analyzed by the same method, so that absolute cross sections may be measured. The atom-transfer reactions studied all involved H or D atom transfer. These are observed over only a low energy range (up to approx 60 ev), as expected from the Gioumousis and Stevenson orbiting theory. However, the detailed dependence of cross section on translational energy for these reactions indicates that this simple orbiting theory must be regarded with some reservation. A further modification of the instrument allowed the study of the interaction of translationally energetic neutral molecules with molecules at thermal energies. Both ionization and dissociative ionization was observed in such cases. (auth)

31225 INFLUENCE OF OXYGEN ON THE SURFACE IONIZATION OF SOME RARE EARTH METALS ON TUNGSTEN AND RHENIUM. Weiershausen, W. (Univ., Marburg, Ger.). Advance. Mass Spectrometry, 3: Proc. Conf. Paris, 1964, 755-64(1966).

The influence of oxygen adsorption on W and Re on the surface ionization of Sm and Nd is investigated. On the one hand the work function of the hot metal surface increases due to oxygen adsorption. This was proved by a retarding potential method. On the other hand the rare earth atoms, for instance Nd atoms, impinging on to the surface are oxidized. Thus NdO^+ ions originate. Using a simple statistical model the heats of oxidation for Nd and Sm were evaluated from the temperature dependence of the metal and oxide ion currents and their ratio. The values are (for oxidation by atomic oxygen in the gaseous phase): w = (7.4 ± 0.5) ev and (6.3 ± 0.5) ev for Nd and (5 ± 0.5) ev for Sm. (auth)

31226 THERMAL IONIZATION OF ELEMENTS OF HIGH IONIZATION POTENTIAL. Crouch, E. A. C.; Tuplin, T. A. (Atomic Energy Research Establishment, Harwell, Eng.). Advance. Mass Spectrometry, 3: Proc. Conf. Paris, 1964, 769-73(1966).

The method used previously to produce relatively efficient thermal ionization of Ag was developed for Sn and Pd. Sn ionizes from a tungstic oxide surface if it is bound by means of a fluoborosilicate melt and Pd is best ionized from a silica surface to which it is bound by a boric oxide melt. Ru may be treated in the same way as Pd. Mo was found to give large positive ion beams when it is reduced to metal in hydrogen on Re filaments; Tc and Ru also respond to this treatment. Other methods of improving thermal ionization efficiency, such as carbiding, and the use of aluminum silicate or zirconium silicophosphate melts are discussed. (auth)

31227 THERMODYNAMIC AND KINETIC STUDIES IN HIGH-TEMPERATURE CHEMISTRY. Drowart, J. (Univ. Libre, Brussels); Pattoret, A.; Smoes, S.; Degreve, F.; Detry, D. Advance. Mass Spectrometry, 3: Proc. Conf. Paris, 1964, 931-43(1966). (In French).

A new determination of the vapor pressure of uranium leads to the value $\Delta H^{\circ}_{298} = 125.5 \pm 2.5$ kcal/g atom for the heat of sublimation of uranium and to the values $D^{\circ}_{0}(UO) = 179.6 \pm 5$ and $D^{\circ}_{0}(UO_2) = 344.4 \pm 5$ kcal/mole for the atomization energies of the molecules UO and UO_2. The comparison of the partial pressures in the system U(l) + UO_2(s) with the uranium pressures given in the literature suggests that these are in fact the total pressures in the system U(l) + UO_2(s). The rates of oxidation of tungsten and tantalum were studied in the respective temperature intervals 1450°–2500° and 1900°–2900°K at oxygen pressures between 8×10^{-6} and 7×10^{-5} torr. The apparent partial pressures of the gaseous oxides formed, WO_2, WO_3, TaO, and TaO_2, were determined. The rate of oxidation of tantalum is strongly time-dependent. At the maximum, the amounts of oxides produced represent for W and Ta respectively about $1/92$ and $1/16$ of the incident molecular oxygen. (auth)

31228 SPIN ORIENTATION DETERMINATION BY LINEARLY POLARIZED, RECOIL-FREE γ RAYS. Gonser, U.; Grant, R. W.; Wiedersich, H.; Geller, S. (North American Aviation Science Center, Thousand Oaks, Calif.). Appl. Phys. Lett., 9: 18-21(July 1, 1966).

The use of linearly polarized, recoil-free γ rays to determine the spin directions in a magnetic material was demonstrated by analyzing the line intensities obtained from one single crystal cut in an arbitrary direction. $Ca_2[Fe](Fe)O_5$ was the crystal studied. It was concluded that in $Ca_2[Fe](Fe)O_5$ all spins in the octahedral and tetrahedral sites are oriented in the c direction. The Mössbauer spectrum of a polycrystalline $Ca_2[Fe](Fe)O_5$ absorber at room temperature obtained with a single line source revealed two superimposed Zeeman patterns. Data are presented in tables and graphs. (M.C.G.)

31229 LONGITUDINAL MAGNETO-OPTICAL KERR EFFECT IN EuO AND EuS. Greiner, J. H.; Fan, G. J. (Watson Research Center, Yorktown Heights, N. Y.). Appl. Phys. Lett., 9: 27-9(July 1, 1966).

Kerr magneto-optical measurements were made on single crystals of EuO and EuS in the ferromagnetic state. A very large longitudinal Kerr effect and magneto-optical resonances were observed for EuO and EuS. The observed Kerr resonance is believed to correspond to a $4f \rightarrow 5d$ transition. The Kerr coefficient, the off-diagonal reflectivity tensor element, is a direct measure of the magneto-optic energy conversion from the incident beam to the beam emerging from the analyzer. The Kerr effect was measured by a polarimetric method. (M.C.G.)

31230 SYSTEM URANIUM–NITROGEN. Stoecker, H. J.; Nickel, H.; Imoto, S.; Naoumidis, A. (Kernforschungsanlage, Juelich, Ger.). Ber. Deut. Keram. Ges., 43: 130-1(Feb. 1966). (In German).

The uranium monocarbide UC, uranium mononitride UN, and the mixed crystal U(CN), the carbonitride, possess good thermal conductivity and high melting points. Thermodynamic calculations were made to determine the phase boundaries and the purities theoretically obtainable in the mononitride and the carbonitride. The results are tabulated. The minimum and maximum limiting pressure for N_2 and CO_2 are given as a function of the carbon concentration of the mixed crystals for a temperature of 2000°K. The oxygen concentrations obtained from the interaction of UO_2 with various amounts of carbon were calculated and tabulated. Experimental results agreed satisfactorily with theory. (J.S.R.)

31231 ELECTROCHEMICAL PROPERTIES OF RADIOACTIVE SPECIMENS OF IRON AND STEEL. Spitsyn, V. I.; Balezin, S. A.; Jandushkin, K. N. (Inst. of Physical Chemistry, Moscow). Indian J. Chem., 4: 151-6(Apr. 1966).

The electrode potentials of radioactive specimens of iron and steel-2, with specific activity of 0.5 and 5.5 mC/g have been measured. The intensifying effect of internal beta and gamma radiation on the kinetics of anode and cathode processes and the preferential change of the latter with increase in specific activity of specimens has been investigated making use of the polarization curves. The effect of internal radiation on the anode reaction of metal ionization has also been determined by measuring the electrode potential of radioactive specimens in distilled water and in 10 mM solution of sodium nitrite by periodically alternating natural and intensive aeration. The initial values of the electrode potentials of the active specimens are shifted through 100–200 mv in the negative direction as compared to the potentials of nonactive specimens. The stationary value of the potential is mainly dependent on the value of the specific activity; the greater the specific activity, the more the stationary values of potentials tend to shift in the positive direction. By measuring the electrode potential of the radioactive specimens of iron in distilled water and in 10 mM solution of $NaNO_2$, by periodically alternating natural and intensive aeration, significant effect of internal radiation on the anode reaction has also been determined. Under the above conditions and in the absence of diffusion control of the cathode reaction, the electronic conductivity along with the semiconductive properties of the oxide film is shown to assume considerable importance. (auth)

31232 SYNTHESIS OF NEW EUROPIUM CHELATES. Janardhanarao, V.; Sinha, A. P. B. (National Chemical Lab., Poona). Indian J. Chem., 4: 196-8(Apr. 1966).

A number of new Eu chelates, viz., (a) mixed ligand complexes containing β-diketones and the acetate anion, (b) β-diketonates complexed with nitrogen donors, and (c) β-diketonates complexed with Lewis bases have been prepared for possible application as laser materials. (auth)

31233 MEAN AMPLITUDES OF VIBRATION AND BASTIANSEN-MORINO SHRINKAGE EFFECTS FOR THE DI- AND TRIOXIDES OF MOLYBDENUM, TUNGSTEN, AND URANIUM. Nagarajan, G. (Univ. of Maryland, College Park). Indian J. Pure Appl. Phys., 4: 158-62 (Apr. 1966).

Employing Cyvin's method, the mean-square amplitude quantities, generalized mean-square amplitudes and mean amplitudes of vibration were evaluated for the di-and trioxides of molybdenum, tungsten and uranium, possessing a linear symmetrical structure and a planar symmetrical structure, respectively. The linear and nonlinear Bastiansen-Morino shrinkage effects in these molecules were also calculated. It is observed that the larger the distance between the atoms the greater will be the mean amplitude of vibration, and the addition of an end atom to the molecular system i-j-i not only changes the symmetry of the system but also causes a decrease in the fundamental frequencies and an increase in the mean amplitudes of vibration for the bonded and nonbonded distances. (auth)

31234 PRODUCTION OF CARRIER-FREE ^{131}I-IODATE. Toth, G.; Nagy, Agnes G. (Inst. of Isotopes, Budapest). Int. J. Appl. Radiat. Isotop., 17: 359-60(June 1966).

Production of carrier-free ^{131}I-iodate by adsorption of

iodine ions on Pt surfaces with subsequent electrochemical oxidation of the adsorbed iodine is described. (M.C.G.)

31235 NEPTUNIUM CHLORO-COMPLEXES. Bagnall, K. W.; Laidler, J. B. (Atomic Energy Research Establishment, Harwell, Eng.). J. Chem. Soc., No. 5, 516-20(1966).

The yellow anhydrous neptunium(V) chloro-complexes, M_2NpOCl_5 ($M = Cs^+$ or Ph_4As^+), turquoise $Cs_3NpO_2Cl_4$, and the dark yellow neptunium(VI) complex, $Cs_2NpO_2Cl_4$, were prepared from aqueous hydrochloric acid. Neptunium pentoxide and neptunium(V) hydroxide were chlorinated by acetyl chloride and thionyl chloride, but disproportionation occurred with the former, and reduction to neptunium(IV) with the latter. The attempted preparation of hexachloroneptunates(V) was also unsuccessful. X-ray diffraction, infrared spectra, and magnetic susceptibility results are reported for the oxychloro-complexes, for Cs_2NpCl_6, and for the N,N-dimethylacetamide (DMA) complex, $NpCl_4 \cdot 2.5DMA$. (auth)

31236 THE CHEMISTRY OF URANIUM(IV). II. SOME NEW COMPOUNDS WITH OXYGEN AND NITROGEN DONOR LIGANDS. Selbin, J.; Schober, M.; Ortego, J. D. (Louisiana State Univ., Baton Rouge). J. Inorg. Nucl. Chem., 28: 1385-95(June 1966).

Some compounds of uranium(IV) were synthesized and characterized. Preparations are reported for $U(OCOCH_3)_4$, $U(OH)(OCOCH_3)_3$, $UO(OCOCH_3)_2$, $U(OCOC_2H_5)_4$, $U(OH)_2(OCOC_2H_5)_2$, $UO_{1.5}(OCOC_2H_5)$, $UCl_4 \cdot 8NH_3$, $UCl_4 \cdot 4NH_3$, $UCl_4 \cdot 2NH_3$, UCl_3NH_2, $UCl_4 \cdot 4(n\text{-}C_4H_9NH_2)$, $UCl_3 \cdot (n\text{-}C_4H_9NH)$, $UCl_4 \cdot 2(C_5H_5N)$, $UCl_4 \cdot 4(C_5H_{10}NH)$, $UCl_4 \cdot 4(NH_2CH_2CH_2NH_2)$, $UCl_4 \cdot 4[(CH_3)_2SO]$, $UCl_4 \cdot 3[(C_6H_5)_2SO]$, and $U(C_7H_5O_2)_4$ (salicylaldehydo). The compounds with nitrogen-donor ligands are less stable toward both moisture and oxygen than the compounds with oxygen-donor ligands. Some compounds displayed surprising stability for this oxidation state of uranium. Visible and infrared spectral data are reported, as well as other characterizing data. (auth)

31237 RADIOMETRIC DETERMINATION OF THE SOLUBILITY OF CADMIUM IN MOLTEN CADMIUM CHLORIDE. Moscinski, J. (Inst. of Nuclear Technique, Krakow); Suski, L. J. Phys. Chem., 70: 1727-31(June 1966).

A method for the determination of the solubility of cadmium in molten cadmium chloride by measurement of γ absorption is described. The decrease in the relative intensity of the radiation depending on the concentration of the absorbing solution of cadmium in cadmium chloride obeys the absorption equation. From the discontinuity of this relation the solubility limit can be determined with good accuracy. The data presented are in good agreement with those given in the literature, which were obtained by other methods. (auth)

31238 VAPOR PRESSURE AND HEAT OF SUBLIMATION OF CERIUM(III) FLUORIDE. Lim, Mahnjick; Searcy, Alan W. (Univ. of California, Berkeley). J. Phys. Chem., 70: 1762-6(June 1966). (UCRL-16150(Rev.1)).

The vapor pressure of CeF_3 is found by the torsion-effusion method to be given at 1373 to 1634°K by the expression $\log P = -(2.046 \pm 0.014)(10^4/T) + 9.205 \pm 0.092$, where P is the pressure in atmospheres and the quoted errors are the standard deviation from the least-squares fit. Extrapolations yield a calculated normal boiling point of 2421 ± 120°K and a heat of sublimation at 298.15°K of 99.7 ± 3 kcal/mole by the third-law method and 102.2 ± 3 kcal/mole by a second-law method. Most of the uncertainty in the third-law value arises from uncertainties in estimation of free energy functions for CeF_3 gas. (auth)

31239 THE KINETICS OF THE REACTION BETWEEN VANADIUM(III) AND URANIUM(VI) IN ACID PERCHLORATE SOLUTIONS. EVIDENCE FOR A BINUCLEAR INTERMEDIATE. Newton, T. W.; Baker, F. B. (Los Alamos Scientific Lab., N. Mex.). J. Phys. Chem., 70: 1943-9(June 1966). (LA-DC-7633).

The kinetics of the reaction between V(III) and U(VI) were studied using the catalysis of the V(III)–Fe(III) reaction by U(VI). Without regard to H^+, the mechanism is V(III) + $U(VI) \underset{k_{-1}}{\overset{k_1}{=}} V(IV) + U(V)$ and $U(V) + Fe(III) \overset{k_2}{=} U(VI) + Fe(II)$. The hydrogen ion dependence of k_1 was studied at an ionic strength of 2.0 M from 0.5 to 1.67 M $HClO_4$ and from 0.2 to 34.8°C. The observed ion dependence was not consistent with a single rate-determining step for the first reaction above nor with a set of such steps occurring in parallel. The dependence was consistent with consecutive reactions and a binuclear intermediate. The principal net activation processes are: $V^{3+} + UO_2^{2+} + H_2O = [VOH \cdot UO_2^{4+}]^* + H^+$ and $V^{3+} + UO_2^{2+} + H_2O = [VO \cdot UO_2^{3+}]^* + 2H^+$, for which the heats and entropies of activation are 17.7 and 22.1 kcal/mole and 3.8 and 12.9 cal/mole deg, respectively. Rabideau (1958) found that the analogous reaction between V(III) and Pu(VI) proceeds by a parallel-path mechanism. The difference in mechanism for these two reactions, together with the observed difference in ΔS^* for analogous net activation processes, is consistent with the suggestion that the U(VI) reaction proceeds by inner-sphere activated complexes while the Pu(VI) reaction proceeds by outer-sphere activated complexes. (auth)

31240 ABSORPTION EDGE SPECTRUM OF SCANDIUM OXIDE. Tippins, H. H. (Aerospace Corp., El Segundo, Calif.). Contract AF 04(695)-669. J. Phys. Chem. Solids, 27: 1069-71(June-July 1966).

The ultraviolet absorption spectrum of single crystals of nominally pure Sc_2O_3 was measured at room temperature and at liquid nitrogen temperature. The results were compared with the probable energy level structure of the system. An estimate of the expected position of the absorption threshold based on a simple charge transfer model gives reasonable agreement with the observed absorption edge. (auth)

31241 STUDY OF THE ROTATIONAL BEHAVIOUR OF THE AMMONIUM ION IN SEVERAL SALTS BY NEUTRON SPECTROMETRY. Venkataraman, G.; Deniz, K. Usha; Iyengar, P. K.; Roy, A. P.; Vijayaraghavan, P. R. (Atomic Energy Establishment, Bombay). J. Phys. Chem. Solids, 27: 1103-23(June-July 1966).

The dynamics of the ammonium ion, particularly its rotational behavior, was studied in NH_4Cl, ND_4Cl, NH_4Br, ND_4Br, NH_4I, $(NH_4)_2SnCl_6$ and $(NH_4)_2SnBr_6$ using the techniques of neutron spectrometry. Neutron energy loss data obtained with a modified beryllium detector spectrometer clearly showed that the ammonium ion performs torsional oscillations in all these salts at 100°K, the torsional frequencies being 389, 280, 335, 254, 293, 240 and 193 cm^{-1}, respectively. Using the frequencies, the barrier heights for rotation were derived. Energy-gain data at 300°K was obtained for the undeuterated salts using a rotating crystal spectrometer giving neutrons of incident energy 0.0047 ev and the results confirmed those of the energy-loss experiments. The angular distributions of elastically scattered neutrons from the undeuterated salts were also studied, using a triple axis spectrometer. In NH_4Cl (300°K), NH_4Br (300°K), and NH_4I (220°K) the form factor was found to be Gaussian and the mean square displacements of the proton were consistent with those estimated from the observed frequencies. In NH_4I, $(NH_4)_2SnCl_6$ and $(NH_4)_2SnBr_6$ (all at 300°K), the form factor was in agreement with the inelastic scattering results. The form factor for NH_4I (at 300°K) was compared with the calculations based on free rotation and uniaxial rotation models. (auth)

31242 PHYSISORPTION OF XENON AND KRYPTON ON GLASS AND ON MOLYBDENUM FILMS. Endow, N.; Pasternak, R. A. (Stanford Research Inst., Menlo Park, Calif.). J. Vac. Sci. Technol., 3: 196-201(July-Aug. 1966).

Physisorption of room temperature xenon and krypton at low pressures (10^{-9}–10^{-4} torr) on Pyrex and on molybdenum films at 77 and 87°K was investigated. The initial sticking probabilities are close to unity, and the adsorbate shows high surface mobility. The steady-state data, which can be shown to differ little from equilibrium data, fit the Polyani potential theory and the Dubinin-Radushkevich isotherm. For the films, the isotherm slopes (which are re-

lated to the isosteric heats of adsorption) increase with film age; for old films, they approach the values found for physisorption of xenon and krypton on Pyrex and on zirconium films. Constancy of isotherm slopes for argon on widely different adsorbents has been noted previously. Thus, the physisorption forces in these systems appear to be unrelated to specific properties of the sorbing surfaces, except in the case of highly porous adsorbents. (auth)

31243 STUDIES OF THE ADSORPTION AND ELECTRODEPOSITION OF PROTACTINIUM. Sakanoue, Masanobu; Takagi, Tomoo; Maeda, Mamoru (Kanazawa Univ., Japan). Radiochim. Acta, 5: 79-87(May 1966).

Experiments on the adsorption, sedimentation, and electrodeposition of protactinium solutions were carried out with solutions containing two isotopes of this element (^{231}Pa and ^{233}Pa). Two maxima were found in the adsorption study of the common soda-lime glass from various pH acetate or formate solutions, but a uniform distribution of Pa was ascertained by α-track autoradiography of the glass plate. Various materials were tested with respect to the adsorption of protactinium, and the desorption of this element from adsorbed plates was examined by means of several solvents. The electrodeposition of protactinium on a gold-plated copper plate from ammonium sulfate-formate solutions with various initial pH values was also studied. It was shown that the deposition yield depends greatly on the initial pH value and that a nearly complete electrodeposition can be realized by electrolysis under our conditions from a solution with a pH value of about 3.3. (auth)

31244 TERNARY AND QUATERNARY OXIDES OF TETRA-, HEXA- AND HEPTAVALENT TECHNETIUM WITH ALKALINE EARTHS. Keller, C.; Wassilopulos, M. (Technische Hochschule, Karlsruhe, Ger. Kernforschungszentrum, Karlsruhe, Ger.). Radiochim. Acta, 5: 87-91 (May 1966). (In German).

In the system alkaline earth oxide-technetium oxide-oxygen the following compounds were obtained by solid-state reactions: $Me^{II}(TcO_4)_2 \cdot 2H_2O$ (Me = Sr, Ca), $Me^{II}(TcO_4) \cdot H_2O$ (Me = Sr, Ca), $Me^{II}(TeO_4)_2$ (Me = Ba, Sr, Ca) $Me^{II}_3(TcO_5)_2$ (Me = Ba, Sr), $Me^{II}_5(TcO_6)_2$ (Me = Ba, Sr, Ca) and $Me^{II}(Me^{I}_{0.5}, Tc^{VII}_{0.5})O_3$ (Me^{II} = Ba, Sr, Me^{I} = Li, Na) with heptavalent technetium; $Ba_3Te_2O_9$ with hexavalent technetium; and $Me^{II}TcO_3$(Me = Ba, Sr, Ca) and$Me^{II}_2TcO_4$ (Me = Ba, Sr) with tetravalent technetium. $BaTcO_3$ and $SR(TcO_4)_2$ could be obtained in two modifications. Most of the Tc(VII)- and Tc(VI)- compounds are isotypic with the corresponding ternary oxides of rhenium, but analogous ternary oxides of Re(IV) are not existent. Chemical and structural properties of these compounds are discussed. (auth)

31245 RADIOTRACER STUDY OF MANAGANESE ADSORPTION ON GLASS FROM VERY DILUTE AQUEOUS SOLUTIONS. Benes, P.; Garba, A. (Faculty of Technical and Nuclear Physics, Prague). Radiochim. Acta, 5: 99-104(May 1966).

Adsorption and desorption of traces of manganese were studied as a function of manganese concentration, pH value, and composition of the solution and time using $^{52(54)}$Mn as the tracer. The observations are explained on the basis of Mn^{2+} ion exchange, electrostatic and physical adsorption of Mn(III) hydrolysis products, and electrostatic adsorption of colloidal $Mn(OH)_2$, respectively. The influence of foreign trace impurities on the adsorption and the possible reasons for aging of trace manganese solutions are discussed. On the basis of the adsorption studies some conclusions about the state of traces of manganese in aqueous solutions were drawn. (auth)

31246 PREPARATION OF ^{36}Cl-LABELLED IODINE MONOCHLORIDE BY ISOTOPE EXCHANGE. Elias, H.; Lieser, K. H. (Technische Hochschule, Darmstadt, Ger.). Radiochim. Acta, 5: 119-20(May 1966). (In German).

Preparation of pure ^{36}Cl-labeled ICl by isotopic exchange between ICl and $Li^{36}Cl$ was investigated. Distilled ICl was heated with water-free $Li^{36}Cl$ in an evacuated glass ampule. After 18 hr a degree of exchange of 97% was obtained with about 88% of the chlorine activity in the ICl. (M.C.G.)

31247 FAR INFRARED SPECTRA OF H_2O_2 AND D_2O_2 IN THE SOLID STATES. Giguere, P. A.; Chapados, C. (Laval Univ., Que.). Spectrochim. Acta, 22: 1131-7(June 1966).

The absorption spectra of hydrogen and deuterium peroxides in the crystalline and glassy states were measured in the far infrared down to 50 cm^{-1}. All of the lattice vibrations predicted by group theory on the basis of the known structure of the crystal were observed. Previous assignments of internal torsion and high-frequency libration were revised. The data confirmed that in the crystal the H_2O_2 molecules are caught in a strained configuration. The samples were always obtained first as glasses that showed no definite low-frequency bands. With deuterium peroxide two distinct metastable phases could often be observed. Frozen mixtures containing a few percent of isotopic peroxides were also studied in the middle infrared to identify possible combinations with lattice modes as well as the fundamentals of the hybrid species HDO_2. (auth)

31248 ABSORPTION SPECTRUM OF NEPTUNIUM HEXAFLUORIDE. Steindler, M. J.; Gerding, T. J. (Argonne National Lab., Ill.). Spectrochim. Acta, 22: 1197-1200(June 1966).

The spectrum of gaseous neptunium hexafluoride was recorded in the region of 2000 to 20,000 Å and the principal peaks, together with their molar absorptivities, were tabulated. (M.C.G.)

31249 PURITY OF YTTRIUM ISOLATED FROM THE SEA WATER CARBONATE PRECIPITATES. Patin, S. A.; Popov, N. I. Tr. Inst. Okeanol., Akad. Nauk SSSR, 79: 31-3(1965). (In Russian).

For the separation of ^{90}Y on Y_2O_3 carrier in pure form, the CO_3^{2-} precipitate should contain 2 to 5 g Mg^{2+} per 40 g Ca^{2+}. The $Y(OH)_3$ precipitate should be dissolved and reprecipitated, then transformed into oxalate, which yields on ignition Y_2O_3 of 95% purity. (C.H.)

31250 HIGH-TEMPERATURE TECHNIQUE FOR DETERMINING TERMINAL SOLUBILITIES: NITROGEN IN NIOBIUM (COLUMBIUM). Evans, B.; Pasternak, R. A. (Stanford Research Inst., Menlo Park, Calif.). Trans. Met. Soc. AIME, 236: 942-4(June 1966).

An initially clean sample, maintained at constant high temperature, is exposed to the gas at low pressure; the rate of sorption and the corresponding change in sample resistance are measured continuously. A pronounced decrease in the slope of the resistance concentration curve is observed at the terminal solubility. (W.L.G.)

31251 NMR STUDIES OF SOLUBILITY OF HYDROGEN IN LIQUID NITROGEN AND OF HELIUM IN LIQUID HYDROGEN. Matyash, I. V.; Mank, V. V.; Starkov, M. G. (Inst. of Low Temperature Physics and Technology, Kharkov). Ukr. Fiz. Zh., 11: 497-501(1966). (In Ukrainian).

The solubility of hydrogen in liquid nitrogen was studied at 77°K over a pressure range of 0 to 8 atm, and that of ^{3}He in liquid hydrogen over a temperature range of 17 to 24°K and a pressure range of 0 to 10 atm. The dissolved substance was recorded using the method of nuclear magnetic resonance absorption. The results of this study and of other authors are compared. The solubility of ^{4}He and ^{3}He differs little as was to be expected. (auth)

31252 ADSORPTION OF ^{90}Sr BY AGED HORSE MANURE. Chia, P'an-hsing; T'ao, Tseng-hsin; Liu, Yung-ho; Hsu, Hsing. Yuan Tzu Neng, No. 3, 261-4(1965).

An attempt was made to use aged horse manure to adsorb ^{90}Sr from solutions of strontium chloride in tap water containing 44 mg/l of calcium, with a specific radioactivity of 10^{-6} curie/l, and made up to pH 7.0 with NaOH. The results obtained are compared with the result of decontamination by means of fresh horse manure, activated charcoal, sawdust, and sand. The aged horse manure was found to yield the best results; thus, when the aged horse manure produced 40% decontamination, sawdust and fresh horse manure yielded only 22% and 26%, respectively, and when activated charcoal and sand were 55% and 17% effective, respectively, the aged horse

manure sometimes produced 85% decontamination. The decontaminating effect of the aged horse manure was directly proportional to the quantity used; when the quantity used was held constant, better results were observed when the flow speed was lower, and the best result was observed when the flow rate was 1.2 ml/min. It was also found that the adsorption of ^{90}Sr by aged horse manure is not as effective in the presence of acid as in the presence of alkali. These findings are consistent with the results obtained by Lacy in the adsorption of ^{144}Ce and ^{90}Sr by means of mixed clay. (ATD)

31253 CRYSTAL STRUCTURE OF $Ce_3Ni_6Si_2$ AND RELATED COMPOUNDS. Hladyschewskii, E. I.; Krypiakewytsch, P. I.; Bodak, O. I. (Lvov State Univ.). Z. Anorg. Allg. Chem., 344: 95-101(Apr. 1966). (In German).

The existence of the ternary compounds $R_3Ni_6Si_2$ (R = Ce, Pr, Nd, Sm, Eu, Gd, Tb, Dy, Ho, Er, Tm, Yb, and Lu) with the superstructure of the Ca_3Ag_8 type was established by means of x-ray diffraction analysis. The lattice constants are given. The atoms in the $Ce_3Ni_6Si_2$ structure have the following positions (space group $Im3m-O_h^9$): 12 Ce in 12 (e) x00 with x = 0.280, 24 Ni in 24 (h) 0xx with x = 0.670, and 8 Si in 8 (c) ¼ ¼ ¼. (auth)

31254 NEUTRON-DIFFRACTION STUDY OF $Bi_4Si_3O_{12}$. Segal, D. J.; Santoro, R. P.; Newnham, R. E. (Massachusetts Inst. of Tech., Cambridge). Z. Kristallog., 123: 73-6(Apr. 1966).

Oxygen and silicon positions in the mineral eulytite were determined by neutron-diffraction analysis. The refined structure corresponds to one of the two models proposed by Menzer, in which irregularly coordinated bismuth ions link discrete SiO_4 tetrahedra. (auth)

31255 THE ELECTRICAL CONDUCTIVITY OF SOLID AND MOLTEN $^6Li_2SO_4$ AND $^7Li_2SO_4$. Kvist, Arnold (Chalmers Inst. of Tech., Goteborg). Z. Naturforsch., 21a: 487(Apr. 1966).

The electric conductivity of Li_2SO_4 with different concentrations of ^6Li and ^7Li was measured from 575 to 930°C. The ratio of the specific conductivity of $^6Li_2SO_4$ and $^7Li_2SO_4$ is 1.042 ± 0.002 and within the experimental errors independent of the temperature. A comparison with the mass effect found in electromigration experiments shows that there is a cooperative motion of the cations in $\alpha - Li_2SO_4$. (auth)

31256 H/D SEPARATION FACTORS IN ELECTROLYSIS AND DIFFUSION BY USE OF Pd AND Pd/Ag MEMBRANES. Brodowsky, H.; Gibmeier, H.; Wicke, E. (Univ., Muenster, Ger.). Z. Phys. Chem. (Frankfurt), 49: 222-39(May 1966). (In German).

In the diffusion of hydrogen isotope mixtures H/D = 0.05 to to 0.95 through a Pd membrane (wall of Pd tube) at approximately 775 to 2000 torr total pressure the separation factor $S_D = 1.6 \pm 0.1$ was measured between 0 and 50°C. The enrichment of light hydrogen in the diffusion current depends on its higher solubility in Pd (in the β phase of $PdH_{\underline{n}H}D_{\underline{n}D}$) and not on its higher mobility in diffusion transport. Measurement of the separation factor in the anodic dissolution of an isotope mixture H/D ≈ 1/1 with series diffusion through the wall of Pd/Ag ≈ 75/25 (diffusion anode) gave, with $S_A \mp 1.7 \pm 0.15$, practically the same value, almost independent of the temperature from 20 to 70°C and of the anodic current from 20 to 70 mamp/cm². In the cathodic precipitation from solution of K_2CO_3 in $D_2O/H_2O \approx 0.85/0.15$ with subsequent inserted diffusion through the wall of the Pd/Ag tube (diffusion cathode) separation factors of 8 at 60°C up to 16 at −30°C were obtained. The magnitude of this separation factor can be understood by the combined effect of the precipitation on the metal surface and the diffusion through the metal membrane. From research data on the determination of the diffusion separation factor S_D the concentration and activity profile of H and D along the diffusion gap were calculated. Over a certain deuterium content in the initial mixture (D/H > 0.25 under the given research conditions) the concentration of H increases in the diffusion direction, that is, proceeds in an opposite direction to its activity. (tr-auth)

31257 TERNARY COMPOUNDS IN THE BERYLLIUM–BORON–CARBON SYSTEM. Markovskii, L. Ya.; Vekshina, N. V.; Kondrashev, Yu. D.; Stroganova, I. M. Zh. Prikl. Khim., 39: 13-20(Jan. 1966). (In Russian).

To study the reaction of beryllium with boron and carbon, powdered mixtures of the components were sintered at 1200 to 2000°C, and the products were subjected to x-ray and chemical phase analysis. The data showed the existence of two beryllium borocarbides, BeC_2B_2 and BeC_2B_{12}. The structure of BeC_2B_2, (studied by the single-crystal method) is characterized by a hexagonal system, Laue class (6/m) mm, and lattice constants a = 10.84 and c = 6.18. The structure of BeC_2B_{12}, (studied by the powder method) belongs to the $B_4C(B_{12}C_3)$ structural type. The lattice constants are a = 5.615, c = 12.28 Å, c/a = 2.187. It is shown that in contrast to alkaline earth and rare earth borocarbides, beryllium borocarbides are chemically stable compounds and do not undergo hydrolytic decomposition. Ternary compounds of beryllium with boron and carbon form from the elements and also as a result of the reaction of beryllium borides, beryllium carbide Be_2C, and boron carbide with one another as well as with elemental carbon, boron, and beryllium respectively. (ATD)

31258 INVESTIGATION OF THE RARE EARTH SESQUIOXIDES AT HIGH PRESSURE. Hoekstra, Henry R. 15p. (CONF-650902-30). ORAU. Gmelin, AED-CONF-65-235-63.

From American Chemical Society, 150th National Meeting, Atlantic City.

Rare earth sesquioxides were subjected to pressures of 15 to 60 kbar at temperatures of 550, 1000, and 1450°C. X-ray-diffraction studies showed that the monoclinic (B) form of Ho, Er, Tm, Yb, Lu, and Y sesquioxides were obtained at each of these temperatures. Unit cell parameters were calculated for each of the monoclinic oxides including those formed at ambient pressure and high temperature (Sm_2O_3 through Tb_2O_3). The location of the B ⇌ C (cubic) phase equilibrium line as a function of temperature, pressure, and cation radius was studied. Entropy and enthalpy changes in the cubic-to-monoclinic phase transformations were estimated. (A.G.W.)

Organic Chemistry

Refer also to abstracts 31198, 31221, and 31224.

31259 SIMPLE TECHNIQUE FOR THE HYDROGENATION OF ETHYLENE. Perschke, H. (International Atomic Energy Agency, Niederoesterreich, Austria). Int. J. Appl. Radiat. Isotop., 17: 358-9(June 1966).

A simple, quantitative and rapid procedure for hydrogenation of ethylene for preparation of tritium-labeled ethane is described. A mixture of hydrogen and ethylene is expanded into a vacuum while passing over palladized asbestos. Only 15 min is required for preparation of ethane from 3 liters of ethylene and the nearly equivalent quantity of hydrogen. The reaction efficiency is better than 99% based on hydrogen. (M.C.G.)

31260 ISOTOPIC EXCHANGE OF ACTIVE METHYL HYDROGENS. II. DEUTERATION OF DIPHENYLMETHYLPYRYLIUM AND METHYLTROPYLIUM SALTS. Gard, E.; Bally, I.; Vasilescu, A.; Arsene, A.; Balaban, A. T. (Inst. of Atomic Physics, Bucharest). J. Label. Compounds, 1: 182-8(July-Sept. 1965).

Isotopic analysis, infrared, and nuclear magnetic resonance spectra showed that benzylic hydrogens of alkyl groups in α and γ positions of pyrylium rings are deuterated under mild conditions (in water at 80 to 100°C for 1 to 2 hr with no catalyst added). At pH 5 the isotopic exchange proceeds faster than at pH 1, but even at acidities as high as that, the exchange is fairly rapid. A kinetic study of the dedeuteration of 2,4,6-tri-d_3-methylpyrylium perchlorate gave a composite kinetic curve, which provided evidence for a faster exchange of the α methyl groups than of the γ methyl. A study was undertaken to compare the isotopic exchange of: two pyrylium salts with only one

methyl group able to undergo exchange, namely 2,4-diphenyl-6-methylpyrylium (I) and 2,6-diphenyl-4-methylpyrylium (II); and methyl-substituted pyrylium (I, II) and tropylium salts (III). Methyl groups of I, II, and III were deuterated with deuterium oxide and/or acetic acid. A comparison between the two pyrylium salts I and II was made on the basis of dedeuteration experiments. At 50°C only the 4-d_3-methyl derivative, II, was markedly dedeuterated in 10 min. At 80°C both compounds were dedeuterated relatively rapidly. Under comparable conditions, methyltropylium salts are deuterated much more slowly than diphenylmethylpyrylium salts. The faster dedeuteration of II relatively to I was unexpected and contrary to the analogy with 2,4,6-trimethylpyrylium where methyl groups in positions 2 and 6 were more reactive than the methyl in position 4. An attempt to deuterate 1,2,4,6-tetramethylpyridinium perchlorate by refluxing in deuterium oxide showed that this compound does not react. The experiments showed that methyl groups adjacent to tropylium rings or to 2 or 4 positions of pyrylium rings undergo hydrogen exchange under mild and comparable conditions (temperatures under 100°C and pH range of 1 to 7). (BBB)

31261 PREPARATION OF PLASTIC SCINTILLATORS IN PLATE FORM. Bezuglyi, V. D.; Zaplesnichenko, G. P. (All-Union Scientific-Research Inst. of Monocrystals, Khar'kov). Prib. Tekh. Eksp., No. 1, 186-8(Jan.-Feb. 1966). (In Russian).

A process was developed for obtaining plastic scintillator plates with smooth, polished surfaces and without any defects or bubbles. The process involves polymerization carried out between two polished sheets and performed not directly on the styrene monomer but on the monomer reduced to a given viscous consistency. The polymerization proceeds quickly but without turbulent boiling and emissions. Plates of varying dimensions and thicknesses can be obtained. The effects of temperature on the process are considered. (M.J.T.)

31262 PLASTIC SCINTILLATORS WITH HIGH HEAT RESISTANCE. Chernobai, A. V.; Pimakhov, A. S.; Nagornaya, L. L.; Kolesnikov, L. N. (All-Union Research Inst. of Monocrystals, Khar'kov). Prib. Tekh. Eksp., No. 1, 188-90(Jan.-Feb. 1966). (In Russian).

A method is described for preparing plastic scintillators with increased heat resistance up to 110°C, on the basis of copolymers of styrene and divinylbenzene with phosphors of various classes. A study of the thermal aging of the scintillators showed that the most stable to thermal aging are the cross-linked plastic scintillators with 1,1,4,4-tetraphenyl-1,3-butadiene, 1-α-naphthyl-2-β-naphthylethylene, and 2-(4-biphenylyl)-5-(α-naphthyl)-1,3-oxazole. (tr-auth)

31263 SYNTHESIS OF OXALIC-$^{14}C_1$ ACID FROM ACETIC-$^{14}C_1$ ACID. Peeters, H. L.; Rumbaut, N. A. (State Technical Inst. for Nuclear Industries, Mol, Belg.). Radiochim. Acta, 5: 109-10(May 1966).

A procedure was developed for transformation of acetic-^{14}C, acid into oxalic-$^{14}C_1$ acid. The acetic acid is brominated and the resulting labeled bromoacetic acid can be hydrolyzed to the corresponding glycolate. Reaction with permanganate in an alkaline medium then leads to the formation of the desired oxalate, which can conveniently be separated as the calcium salt. Calcium oxalate-^{14}C, was obtained in yields varying from 78 to 85%. (M.C.G.)

31264 PREPARATION OF RADIOIODINATED SERUM GLOBULINS. Abdel-Wahab, M. F. (Middle Eastern Regional Radioisotope Center for Arab Countries, Dokki, U.A.R.). Ibrahim, M. S.; El-Kinawy, S. A. Radiochim. Acta, 5: 110-11(May 1966).

Serum globulins were labeled with ^{131}I and the α, β, and γ fractions were separated using Sephadex columns. Preliminary results with labeled globulins did not suggest that any denaturing of the administered labeled proteins takes place. (M.C.G.)

31265 PREPARATION OF TECHNETIUM (^{99m}Tc), TYROSINE, THYROXINE, INSULIN AND HUMAN SERUM PROTEINS LABELLED-^{99m}Tc. Abdel-Wahab, M. F.; El-Garhy, M. A.; Megahed, Y. M.; El-Kinawy, S. A. (Middle Eastern Regional Radioisotope Centre for the Arab Countries, Dokki, Cairo). Radiochim. Acta, 5: 111-13 (May 1966).

^{99m}Tc was milked from ^{99}Mo prepared by irradiating MoO_3 in the UAR-R, reactor. Methods of preparing ^{99m}Tc-labeled tyrosine, thyroxine, insulin, and proteins are described. (M.C.G.)

31266 PREPARATION OF TOLUENE DIISOCYANATE-^{14}C. Wilkniss, Peter; Levine, Donald (Naval Propellant Plant, Indian Head, Md.). Radiochim. Acta, 5: 118-19 (May 1966).

Labeled toluene diisocyanate was prepared in a two-step reaction. Toluenediamine, dissolved in methylene chloride, was reacted at 0°C with ^{14}C-labeled phosgene, also dissolved in methylene chloride. The precipitate formed is suspended in high-boiling Aroclor 1248 and reacted with inactive phosgene at 130°C until a clear solution is obtained. The labeled toluene diisocyanate is recovered from this solution by vacuum distillation. (M.C.G.)

Radiation Chemistry

See also BIOLOGY AND MEDICINE — Radiation Effects on Biochemicals Radiation Effects on Tissues

Refer also to abstracts 31003 and 31231.

31267 (BNWL-SA-658) A SURVEY OF THE USE OF PLASTICS AT HANFORD. Kleinpeter, J. H. (Battelle-Northwest, Richland, Wash. Pacific Northwest Lab.). Apr. 22, 1966. Contract AT(45-1)-1830. 14p. Dep. mn. CFSTI $1.00 cy, $0.50 mn.

The role of plastics in the operation of Hanford production and research facilities is reviewed. The use of plastic film for handling and storing waste products is described. Plastic gaskets between pipe flanges, transparent plastic sheet for glove boxes, perforated plates for extraction columns in the chemical separations plants, plastic sheets for wall and floor coverings, plastic pipes, plastic ion exchange resins, protective coatings, and other uses of plastics are discussed. The effect of radiation on plastics are described. The most significant of these are ionization and excitation of molecules, which can cause rupture of chemical bonds. (M.C.G.)

31268 (COO-1088-20) THE RADIATION CHEMISTRY OF HIGH POLYMERS. Technical Report No. 11, April 1, 1965-April 1, 1966. Dole, Malcolm (Northwestern Univ., Evanston, Ill. Dept. of Chemistry). May 1, 1966. Contract AT(11-1)-1088. 15p. Dep. mn. CFSTI $1.00 cy, $0.50 mn.

The use of ultraviolet absorption spectra in identifying transient and reactive species produced during and subsequent to the irradiation of polyethylene is discussed. Oxygen diffusion into and reaction with allyl free radicals in irradiated polyethylene was studied by uv spectroscopy. The temperature coefficients of crosslinking, double bond formation, and hydrogen gas evolution in irradiated polyethylene were determined over the temperature range from 25 to 120°C. Repurification of atactic and isotactic polypropylene oxide is described. (M.C.G.)

31269 (NSJ-tr-56) RECENT PROGRESS IN RADIATION CHEMISTRY ON POLYMERS IN JAPAN. Hayashi, Koichiro. Translated from Nippon Genshiryoku Gakkaishi, 5: 997-1005(1963). 17p. Dep. mn. JCL $1.60 fs, $0.80 mf. JAERI.

Progress in the radiation chemistry of polymers is reviewed with reference to papers presented at the 5th Japanese Conference on Radioisotopes, May 1963, in Tokyo. Topics covered include: radioinduced polymerization, graft polymerization, irradiation of high polymers, and industrialization of the radiation chemistry of high polymers. (M.C.G.)

31270 STUDY OF IONS FROM THE ALPHA-PARTICLE IRRADIATION OF GASES AT HIGH PRESSURES. Kebarle,

P.; Hogg, A. M. (Univ. of Alberta, Edmonton, Can.). Advance. Mass Spectrometry, 3: Proc. Conf. Paris, 1964, 401-13(1966).

An α particle ionization mass spectrometer is described, which was constructed for sampling of ions in gases at 10–200 torr pressure. The ions emerge from the field-free ionization chamber by effusion and are near steady state. The spectra obtained are very sensitive to impurities of low ionization potential. The ionic polymerization of ethylene was studied. The mass spectrum at 40 torr shows the presence of numerous polymeric ions extending without much attenuation beyond the highest mass (215) measured. The major ions are of empirical formula C_nH_{2n-1}. The polymerization pattern can be simplified by a dilution-charge exchange technique. The ethylene spectrum from 0.7 per cent ethylene in xenon at 34 torr total pressure shows the polymerization caused by the $C_2H_4^+$. The $(C_2H_4)_n^+$ chain is the most important. Next come the chains $(C_3H_5^+ + nC_2H_4)$ and $(C_6H_{11}^+ + nC_2H_4)$. The temperature effect on the spectra in the range 20 to 60°C was studied. The ethylene spectrum is changed little. Some gases show large changes because of cluster rearrangements. Heats of solvation might be obtained with the technique. Preliminary experiments indicate that the $H(H_2O)_7^+$ ion is not uniquely stable but that hydrates of n = 5 and 6 have similar stability. (auth)

31271 ISOTOPIC EFFECTS IN THE DISSOCIATION OF TRIATOMIC MOLECULES BY ELECTRON IMPACT. II. FORMATION OF S^+, SH^+, IN H_2S, HDS AND D_2S. Fiquet-Fayard, Florence; Guyon, Paul-Marie (Faculte des Sciences, Orsay, France). Advance Mass Spectrometry, 3: Proc. Conf. Paris, 1964, 489-501(1966).

The ions S^+, SH^+, and SD^+ formed from mixtures of H_2S, HDS, and D_2S were studied by mass spectrometry, and the part played by the two types of isotopic effect, π and γ, was shown. The abundance of the S^+ ions diminishes rapidly and regularly as the molecule is deuterated once and then twice, $A_{H_2S}/A_{D_2S} = 1.3 \pm 0.01$. The abundance of the SH^+ and SD^+ diminishes slightly as the molecule is deuterated—$A'_{H_2S}/A'_{D_2S} = 1.08 \pm 0.01$. In the HDS the breaking of the SH bond is 2.8 times more probable than that of the SD bond: $\pi = SD^+/SH^+ = 2.8 \pm 0.1$. The importance of the π effect indicates that the dissociation brings in a competitive process between the rupture of the two bonds; this result is identical to that previously obtained for water. These effects were studied as a function of the electron energies. (auth)

31272 OPTICAL ABSORPTIONS OF NEUTRON-IRRADIATED ZnS. Yoshida, Toshio; Seiyama, Takeyoshi; Shono, Yoshihiko; Kitagawa, Michiharu (Radiation Center, Osaka). Appl. Phys. Lett., 9: 26-7(July 1, 1966).

Cubic single-crystal samples of 2nS were irradiated in the JRR-1 reactor or the CP-5 reactor. Optical transmission spectra before and after fast neutron irradiation (6.7×10^6 and 8.6×10^{17} nvt) are shown. No significant absorption was observed in the samples before irradiation except the intrinsic absorption around 330 mμ. At least four new kinds of absorption were produced by neutron irradiation: the absorption near the intrinsic absorption edge and three bands with peaks around 540, 430, and 390 mμ. The densities of these 3 bands were increased by illumination with light of shorter wavelengths than ~380 mμ. (M.C.G.)

31273 RADIATION STABILITY OF ADAMANTANE. Hattenbach, K.; vom Baur, E. (Institut fuer Reaktorphysik am Forschungsreaktor, Geesthacht, Ger.). Atomkernenergie, 11: 262(May-June 1966). (In German).

Adamantane was exposed to γ irradiation at 300°C and its radiolysis products were determined. The results showed that the radiation stability of adamantane is comparable with that of the aliphatic hydrocarbons and not with that of the radiation resistant hydrocarbons. (J.S.R.)

31274 EFFECT OF ^{60}Co GAMMA RAYS ON COMMERCIAL POLYPROPYLENE FILMS. Kaushal, P. K.; Thampy, R. T.; Bhardwaj, I. S. Chem. Age India, 16: 291-3(1965).

Commercial polypropylene films were treated with ^{60}Co γ rays for various dosages. The tensile strength of films increase up to 4.28×10^5 rads and then starts showing degradation. When irradiated for a longer period, say 51 hr., the material becomes brittle and breaks to pieces when touched. Irradiation with uv strengthens the polypropylene film. (auth)

31275 PRODUCTION OF RADIOISOTOPES OF HIGH SPECIFIC ACTIVITY FOR MEDICAL USE. Iya, V. K.; Mani, R. S.; Manohar; Pankajakshan, K.; Ballaney, A. K.; Sanjana, S. M. (Atomic Energy Establishment, Trombay, India). Indian J. Chem., 4: 171-3(Apr. 1966).

Simple and rapid methods for the production of Cr-51, Fe-59, and Br-82 of high specific activity for use in medicine are described. Cr-51 has been produced by a Szilard-Chalmers enrichment method from pile irradiated potassium chromate; Fe-59 has been produced by the irradiation of cobalt metal in a reactor, from which it is subsequently separated by ion exchange; and Br-82 has been produced by a Szilard-Chalmers enrichment method from irradiated p-dibromobenzene. Preliminary studies on the production of Cu-64, Zn-65, and As-76 are also reported. (auth)

31276 CARBOXYLATION OF POLYCHLORO COMPOUNDS TO TRICHLOROACETIC ACID BY RADIATION CHEMISTRY. Guetlbauer, F.; Bildstein, H. (Reaktorzentrums Seibersdorf, Vienna). Int. J. Appl. Radiat. Isotop., 17: 313-18(June 1966). (In German).

Trichloroacetic acid is formed as a main product from γ-irradiation of aqueous, Co_2-saturated solutions of CCl_4 or $CHCl_3$. The radioinduced carboxylation process was studied by means of these systems in respect to its dependence on the radiation dose and the pH. The formation of trichloroacetic acid can be explained by reactions of the primary species of the radiolysis of water. (auth)

31277 USE OF ^{14}C IN STUDYING THE REACTION OF OXALIC ACID RE-FORMATION DURING GAMMA RADIOLYSIS OF AQUEOUS OXALATE SOLUTIONS. Draganic, Z. D.; Nenadovic, M. T. (Boris Kidric Inst. of Nuclear Sciences, Vinca, Yugoslavia). Int. J. Appl. Radiat. Isotop., 17: 319-28(June 1966).

^{14}C was used as a radioactive tracer in studying the possibility of oxalic acid re-formation during γ radiolysis of aqueous oxalate solutions with and without O_2. A simple procedure was developed for the quantitative separation of labeled oxalic acid from irradiated samples. The radioactivity measurements showed that re-formation does not take place in solutions in which oxygen is present during irradiation. However, it is easy to observe labeled oxalic acid in the absence of oxygen. If carbon dioxide is a source of labeled carboxyl ion radicals, the amount of radioactive oxalate is proportional to the absorbed dose for the given pH, and it decreases with increasing pH. If labeled formate is present in the irradiated solutions, the radioactivity of the labeled oxalate is proportional to the dose, irrespective of the pH of the solution between 9 and 13. These findings are discussed on the basis of the known radiation chemical reactions. The observed phenomena clarify some results regarding the behavior of the oxalate system and give some information on the synthesis of labeled oxalic acid. (auth)

31278 RADIATION-CHEMICAL CARBOXYLATION OF FORMIC ACID AND METHANOL IN AQUEOUS SOLUTION. Getoff, N.; Guetlbauer, F.; Schenck, G. O. (Max-Planck-Institut fuer Kohlenforschung, Muelheim-Ruhr, Ger.). Int. J. Appl. Radiat. Isotop., 17: 341-9(June 1966). (In German).

The carboxylation of formic acid with CO_2 in H_2O by irradiation using ^{60}Co γ rays yielded oxalic acid, that of methanol, glycolic acid. The formation of oxalic acid was studied with respect to its dependence on the concentration of formic acid (10^{-4} to 10M HCOOH), as well as on the dose rate (50 to 1070 krad/hr) within a pH range from 2.8 to 5.8. A G-value of 5.9 was obtained for the formation of oxalic acid by irradiation of a 5M HCOONa solution saturated with CO_2. The formation of glycolic acid was investigated under the same conditions. The yield of glycolic acid plotted against the methanol concentration passed a maximum at ~5×10^{-1} M CH_3OH. The radioinduced carboxylation could also

be obtained with formate. The reaction mechanisms of these processes are discussed. (auth)

31279 RADIATION PROTECTION STUDIES WITH POLYETHYLENE. Kopp, P. M.; Charlesby, A. (Royal Military Coll. of Science, Shrivenham, Eng.). Int. J. Appl. Radiat. Isotop., 17: 352-5(June 1966).

The yields of products from irradiation of ethylene can be changed by the presence of relatively small amounts of additive, too small to absorb a major fraction of the total energy absorbed. Small concentrations of additives were hot milled into the polymer and solubility measurements were carried out on sample strips of uniform thickness after irradiation in a high vacuum to different doses. The effects of sulfur, selenium, and tellurium were determined. They were found to be very efficient in protecting solid polyethylene against crosslinking. (M.C.G.)

31280 THE EFFECT OF IRRADIATED, LOW-TEMPERATURE, HIGH pH WATER ON NYLON. Whittle, I. (Berkeley Nuclear Labs., Eng.); Hill, S. S. Int. J. Appl. Radiat. Isotop., 17: 362-3(June 1966).

Flexible nylon tubing, which received no direct irradiation, was exposed to irradiated water at a pH of 10.5 at 40 to 45°C. The water rapidly became yellow and the color intensity increased with time. Appreciable quantities of ammonia and carbonate ion accumulated in the water. The concentration of dissolved oxygen in the water became low. It was concluded that the nylon was attacked by oxidizing radiolytic products such as hydrogen peroxide present in the water. (M.C.G.)

31281 ABSORPTION SPECTRA AND TRANSIENT SPECIES FOUND IN THE PULSE RADIOLYSIS OF ALKALINE AQUEOUS BENZOATE SOLUTIONS. Sangster, D. F. (Australian Atomic Energy Commission Research Establishment, Sydney). J. Phys. Chem., 70: 1712-17 (June 1966).

The spectra of the short-lived transient species, which are produced during the pulse radiolysis of degassed aqueous benzoate solutions at pH 12.8 were observed. By adding radical scavengers it was possible to distinguish between the spectra of the transient products of the oxidizing radical–benzoate and electron–benzoate reactions. The spectrum of the oxidizing radical–benzoate adduct has a band with a maximum at 328 mμ, and this is attributed to the hydroxycyclohexadienylcarboxylate radical anion. The product of the electron–benzoate reaction has two absorption bands with maxima at 322 and 444 mμ. This is attributed to the cyclohexadienylcarboxylate radical anion. The electron–benzoate adduct is considered to have undergone rapid protonation by reaction with the water. (auth)

31282 RADIOLYTIC ISOTOPIC EXCHANGE OF GASEOUS NITROGEN. Anbar, M.; Perlstein, P. (Weizmann Inst. of Science, Rehovoth, Israel. Soreq Nuclear Research Center, Rehovoth, Israel). J. Phys. Chem., 70: 2052-3(June 1966).

Results of a previous investigation of the isotopic exchange of nitrogen between $N_2^{14,14}$ and $N_2^{15,15}$ in the gas phase under radiolytic conditions are compared with studies by Dawes and Back (J. Phys. Chem., 69, 2385 (1965)). Certain discrepancies that are not readily resolved indicate the need for further study on the mechanisms leading to the exchange. (J.G.B.)

31283 EFFECT OF IONIZING RADIATION ON GLASSES: THE KINETICS OF RADIOCOLOURATION AND PHOSPHORESCENCE OF BORATE GLASS. Novotny, J. (Faculty of Technical and Nuclear Physics, Prague); Spurny, Z. J. Phys. Chem. Solids, 27: 1031-4(June-July 1966).

The kinetics of x-ray induced coloration and phosphorescence of borate glass was studied. The growth-phosphorescence curves and decay-phosphorescence curves of glass were established and the species corresponding to phosphorescence, thermoluminescence, and color centers were determined. (auth)

31284 SPECIFIC VOLUME STUDIES OF γ-IRRADIATED POLYTETRAFLUOROETHYLENE FROM 40 TO 150°C. Licht, W. R.; Kline, D. E. (Pennsylvania State Univ., University Park). J. Polym. Sci., Pt. A-2, 4: 313-25(June 1966).

The effects of γ radiation and post-irradiation heat treatment on the specific volume versus temperature relations of polytetrafluoroethylene (PTFE) samples (½-in. diameter rods) were studied over the 40–150°C temperature range for radiation doses up to 8.9×10^8 rad. At low doses the specific volume at any temperature decreased with dose, but above about 10^8 rad it increased with dose. Similarly, the rate of volumetric expansion initially decreased with dose, while, at very high doses (8.9×10^8 rad) the rate of expansion at temperatures above 100°C exceeded that of the unirradiated PTFE. Heating at 150°C for 100 hr produced a substantial decrease in the specific volume and a decrease in the rate of expansion for the irradiated samples. Irradiation effects in PTFE are considered to be a result of such factors as radiation-induced chain scission, increased crystallinity, and increased void content. Changes resulting from post-irradiation heat treatment can be attributed to increased crystallinity, decreased void content, and weight loss. (auth)

31285 HYDROGEN REDUCTION OF γ-IRRADIATED NICKEL OXIDE. Yamashina, Toshiro; Nagamatsuya, Takaaki (Hokkaido Univ., Sapporo, Japan). J. Soc. Mater. Sci., Jap., 15: 146-50(Mar. 1966). (In Japanese).

Hydrogen reduction experiments were carried out on the unirradiated and the γ-irradiated nickel oxide (NiO) in order order to interpret their mechanism at the initial stage of reduction, i.e., the induction period. The reduction velocities were found to decrease with the radiation dose, being remarkable over a total dose of 5.8×10^7 R. These phenomena are similar to the increase in the excess oxygen in the nickel oxide by irradiation. From the experimental results of the effect of the preevacuation at various temperatures on the initial reduction kinetics, it was concluded that the reduction kinetics of nickel oxide was associated with the amount of surface excess oxygen by γ-irradiation. It was suggested that the increase of induction period by irradiation was due to the water vapor on the surface of nickel oxide acting as a barrier-layer against the diffusion of hydrogen. (auth)

31286 STUDY OF COMPOSITE SOLID PROPELLANTS CONTAINING IRRADIATED AMMONIUM PERCHLORATE. Flanagan, J. E.; Gray, J. C. (Rocketdyne, Canoga Park, Calif.). J. Spacecraft Rockets, 3: 135(Jan. 1966).

In an attempt to separate binder-oxidizer interactions, composite solid propellants containing preirradiated ammonium perchlorate were formulated and tested. Two polybutadiene propellants, one metallized and one unmetallized, and a polysulfide formation were fired successfully. Burning rates increased and the pressure exponent increased for polybutadiene propellants, but the exponent decreased in the polysulfide formulation. Heats of explosion were reduced in propellants containing irradiated oxidizer. (M.C.G.)

31287 RADIATION-INDUCED SOLID-STATE POLYMERIZATION OF TWO-COMPONENT SYSTEMS. I. SOLID-STATE POLYMERIZATION OF ACRYLIC MONOMERS AND CROTONIC ACID SYSTEMS. Kaetsu, Isao (Sekisui Chemical Co., Osaka); Hayashi, Koichiro. Kobunshi Kagaku, 23: 125-30(Feb. 1966). (In Japanese).

In order to clarify the mechanism of the radiation-induced solid state polymerization of vinyl monomers, the binary systems containing acrylic monomers and crotonic acid were investigated. These systems form a eutectic mixture in the solid state, and the polymerization rate of acrylic monomer is accelerated in the presence of the other component, although the rate in the liquid phase is retarded. The polymerization rates in solid-liquid equilibrium phase show characteristics of both solid and liquid phases and have a maximum peak at a certain monomer composition. The degree of polymerization is decreased, and the gel formation from acrylic polymer is almost inhibited in the solid state polymerization of these systems. The experimental results suggest that certain accelerative effects of polymerization based on the crystal structure do exist, and

chemical interaction such as chain transfer is also effective in the solid state polymerization of the eutectic mixture systems. (auth)

31288 PROPERTIES OF POLYETHYLENE–VINYL CHLORIDE GRAFT COPOLYMERS. Ueda, Kazuo; Kadonaga, Masao (Nippon Telegraph and Telephone Publishing Corp., Japan). Kobunshi Kagaku, 23: 165-71(Mar. 1966). (In Japanese).

Graft copolymers were prepared by irradiating polyethylene films or powder in the atmosphere of vinyl chloride with a ^{60}Co source. Physical and physicochemical properties, such as tensile strength, modulus, dynamic loss, thermal flow, stress cracking, gas permeability, clarity and dielectric loss, of the graft copolymer were measured and compared with those of polyblends. Effects of grafting vinyl chloride to low density polyethylene are as follows: Physical properties of polyethylene are highly reinforced by grafting compared with blending, the maximum temperature of mechanical loss of polyvinyl chloride in graft copolymer is lower than that of polyvinyl chloride itself, whereas that of polyblend scarcely shifts, the gas permeability of graft copolymer decreases with increasing graft percent, the graft copolymer (only 4% grafted) shows more remarkable crack-resistivity than the parent polyethylene, although the clarity of graft copolymer in film shows little change compared with the parent polyethylene, that of film processed by hot press has been markedly improved. Some properties of graft copolymers prepared from high density polyethylene have also been clarified. (auth)

31289 RADIATION-INDUCED SYNTHESIS OF AMMONIA FROM NITROGEN AND WATER. Getoff, Nikola (Institut fuer Radiumforschung und Kernphysik, Vienna). Nature, 210: 940-1(May 28, 1966).

The synthesis of small amounts of ammonia by irradiation of nitrogen and water either with ultraviolet light below 1800 Å or with gamma rays is reported. No ammonia was detected after the irradiation of pure water saturated with nitrogen, but small amounts of ammonia could be found in acidic media. The yield of ammonia was increased by adding ferrous ions. It was found that: a maximum ammonia yield was reached after irradiation with ultraviolet light for 6 hrs; the yield was lower when a 1 : 1 mixture of nitrogen and hydrogen was bubbled through the solution; and the yield was higher when methanol was added as a scavenger for the hydroxyl radicals. (H.G.D.)

31290 USE OF HEXAFLUOROBENZENE AND SOME OF ITS CHLORINE-SUBSTITUTED COMPOUNDS FOR DEVELOPING LIQUID SCINTILLATORS WITH LOW SENSITIVITY FOR NEUTRONS. Protopopov, Kh. V. (Inst. of Nuclear Physics, Novosibirsk, USSR). Prib. Tekh. Eksp., No. 1, 92-4(Jan.-Feb. 1966). (In Russian).

The possibility of using hexafluorobenzene and some of its chlorine-substituted compounds for preparing liquid scintillators with low sensitivity to neutrons was studied. The scintillation efficiencies of a series of solutions of PPO + POPOP in C_6F_6, C_6F_5Cl, $C_6F_4Cl_2$, and $C_6F_3Cl_3$ were measured. It was shown that the optimum concentration of PPO in C_6F_6 is equal to 12 g/l. At this concentration, the scintillation efficiency is 0.36 of that of a solution of 4 g/l PPO in toluene. It was found that solutions of PPO in the enumerated fluorine-chlorine derivatives have a scintillation efficiency of not more than 0.05 on the indicated scale. (tr-auth)

31291 RADIOLYSIS OF AROMATIC COMPOUNDS: TOLUENE. Weiss, J.; Collins, C. H. (Brookhaven National Lab., Upton, N. Y.). Radiat. Res., 28: 1-12(May 1966). (BNL-9550).

The radiolysis of toluene was studied in the presence and in the absence of scavenger. The yields of gaseous, liquid, and solid radiolysis products were measured as a function of dose and temperature, and a mechanism scheme is proposed. (auth)

31292 DETERMINATION OF W_β AND ABSORBED DOSE IN GAMMA-IRRADIATED HCl, HBr, AND SF_6. Davidow, R. S.; Armstrong, D. A. (Univ. of Alberta, Calgary). Radiat. Res., 28: 143-56(May 1966).

A comparative ionization chamber method was employed in the determination of the average energy of electrons in the production of ion pairs W_β for HCl (24.8 ± 0.4 ev), HBr (24.4 ± 0.4 ev), and SF_6 (34.9 ± 0.4 ev). Saturation ionization currents at pressures equivalent in mean stopping power to air at 65 cm and 23°C were measured for these and three standard gases of known W_β in a parallel-plate ionization chamber irradiated with ^{60}Co γ rays. For each of the unknown gases there was at least one standard gas with an excitation potential of similar magnitude: argon for HCl, krypton for HBr, and air and argon for SF_6. Saturation ionization currents in Pyrex cells of the size typically employed in radiation chemical studies were compared with the predictions of the Bragg-Gray theory. For gases of mean excitation potential in the range 85 to 180 ev at pressures equivalent in mean stopping power to air in the range 15 to 65 cm, there was reasonable agreement with the theory. For gases of mean excitation potential in the region of 300 ev and above significant deviations (about 10%) were observed. The importance of using gas pressures that are equivalent in mean stopping power in comparative gas phase dosimetry is stressed. (auth)

31293 MODEL OF TRACKS OF IONIZING RADIATIONS FOR RADICAL REACTION MECHANISMS. Mozumder, A.; Magee, J. L. (Univ. of Notre Dame, Ind.). Radiat. Res., 28: 203-14(June 1966). (COO-38-395).

A track model for electrons was reviewed to establish a better basis for radiation chemical mechanisms, particularly those of diffusion-controlled radical reactions. On the basis of calculated ranges for low-energy electrons (~100 to ~5000 ev), it was concluded that one must consider two more entities on the track other than the spur. These are named blobs and short tracks, and they represent energy losses of ~100 to ~500 ev (for blobs) and ~500 to ~5000 ev (for short tracks). Because of high radical concentration, blobs are expected to behave differently from spurs in reactions in the presence of solute. Short tracks, on the other hand, represent roughly finite cylindrical regions of high LET embedded sporadically in the long track due to an ionizing particle of essentially low LET. A simple algorithm was developed to count the percentage breakup of the energy of the ionizing radiation in the form of isolated spurs, isolated blobs, and short tracks. Result shows that, with increasing primary energy (that is, decreasing over-all LET), the short track fraction goes down, and the isolated spur fraction goes up, but the blob fraction goes through a maximum. It is suggested that a model of a track composed of right ratios of isolated spurs, isolated blobs, and short tracks will provide a better clue to radical reactions and will also offer a physically correct picture of the track itself. (auth)

31294 SIMPLIFIED APPROACH TO DIFFUSION-CONTROLLED RADICAL REACTIONS IN THE TRACKS OF IONIZING RADIATIONS. Mozumder, A.; Magee, J. L. (Univ. of Notre Dame, Ind.). Radiat. Res., 28: 215-31 (June 1966). (COO-38-395).

On the basis of the approximation that the track of an ionizing particle may be supposed to consist of essentially nonoverlapping spurs, blobs, and short tracks, radical reactions are considered in the presence of scavenger over a large range of LET for the primary particle. Results are given in terms of fraction of recombining radicals in the long time limit. In some cases, the evolution of various radical fractions in time is shown. Consideration is made of scavenger depletion in the linear approximation of prescribed depletion, and it is concluded that in the present theory it is not an important effect. Throughout, a sharp boundary model was used. In the scheme and approximation used, consideration of spur (and blob) size distribution is important. This was obtained for a 1-Mev primary with the use of the Monte Carlo technique, and the same relative spectrum was assumed for other energies. Results obtained for a primary are compared with low LET cases (essentially isolated spur and/or blob) and also with a high LET

case (individual short track). Results are also compared with those of other models and with experiment (in respect of lowering of molecular yield with scavenger concentration). (auth)

31295 CHEMICAL STATES OF ^{32}P AND ^{35}S ATOMS IN NEUTRON-IRRADIATED SULPHUR. Cifka, J. (Nuclear Research Inst., Czechoslovak Academy of Sciences, Rez.). Radiochim. Acta, 5: 61-5(May 1966).

The distribution of ^{32}P and ^{35}S atoms between fractions of irradiated sulfur soluble and insoluble in carbon disulfide was studied. Heating increased the percentage of ^{32}P activity separable with the insoluble Sμ fraction while the percentage of ^{35}S activity in the same fraction decreased. The high yield of ^{32}P in the Sμ fraction was due to the oxygen present in sulfur. (auth)

31296 RECOIL BROMINATIONS OF AROMATIC COMPOUNDS. Laser, M.; Merz, E. (Kernforschungsanlage, Juelich, Ger.). Radiochim. Acta, 5: 65-70(May 1966). (In German).

In the neutron irradiation of bromobenzene in a mixture with other halogen benzenes, a nonstatistical distribution for the formation of position isomeric ^{82}Br-labeled dibromo- and bromohalogen benzenes was observed. For elucidation of the reaction mechanism, toluene, which acts as a scavenger for the predominantly formed radical bromine, was added to the irradiation samples. Under the conditions mentioned, brominations occurring in the aromatic nucleus must take place by an electrophilic substitution. The non statistical formation of position isomeric radioactively labeled compounds is due to different activation entropies of the reactive positions in the molecule. They, on the other hand, may be reflected by action of polarization and polarizability effects. (auth)

31297 HOT-ATOM REACTION PRODUCTS IN CRYSTALS OF HEXA- AND TRIVALENT CHROMIUM COMPOUNDS. I. Guetlich, Philipp; Harbottle, Garman (Brookhaven National Lab., Upton, N. Y.). Radiochim. Acta, 5: 70-9(May 1966).

The distribution of ^{51}Cr recoil atoms among the various possible chemical forms in neutron-irradiated chromium compounds was reexamined. Chromous ions were not found in potassium chromate. However, in both potassium and ammonium chromates a large proportion of the reduced fraction is found in the form of a dimer. In irradiated (hydrated) chromic salts, substantial percentages of labeled chromous ions are found, as well as the dimer. The results are interpreted in terms of possible recoil mechanisms. (auth)

31298 BEHAVIOR OF THE RADIO-IODINE RECOILS PRODUCED IN ISOTOPIC AND NONISOTOPIC LATTICES. Dema, I.; Zaitseva, N. G. (Inst. of Atomic Physics, Bucharest). Radiochim. Acta, 5: 113-14(May 1966).

The fate of radioiodine recoils formed by high-energy proton irradiation in iodine-containing lattices was compared to the fate of reduced atoms produced in nonisotopic lattices. The radioiodine was obtained as a product of 660-Mev irradiation of potassium iodate. The irradiated material was dissolved in water containing elementary iodine and the radioiodine produced was divided into two fractions: a reduced one and an oxidized one. The percentage of the activity in the oxidized fraction is considered as retention. The data obtained were compared with data on ^{131}I in cesium chloride and cesium nitrate lattices. The experiments indicated a very essential difference in the behavior of a ^{131}I recoil in isotopic and nonisotopic crystalline lattices. (M.C.G.)

31299 DEAMINATION OF AQUEOUS GLYCINE–Cu(II) SOLUTION BY GAMMA-RAYS. [PART] II. Ikeda, Toshio. Rep. Fac. Sci., Shizuoka Univ., 1: 13-18(Dec. 1965).

Gamma-induced deamination was studied on aqueous solutions of glycine-copper systems at pH = 4.0, keeping the concentration at a constant, 0.02M with regard to the glycine component. The $G(NH_3)$ value was measured on the following solution systems: Gl, $CuGl_2$, $CuGl_2 + CuSO_4$, $CuGl_2 + Gl$, $CuGl_2 + Gl + CuSO_4$, and $Gl + CuSO_4$, where Gl = glycine and $CuGl_2$ = Bis-(glycinato)copper(II). The curve of $G(NH_3)$ vs the constitution of solution was found to be a characteristic of the type of solution. It was found that glycine is deaminated at a higher efficiency in the form of the copper chelate than in the state of free molecule. Copper sulfate was found to be ineffective for the deamination reaction of $CuGl_2$, but seemed to be effective for glycine. $CuGl_2$ was effective for the deamination of glycine, and the degree of deamination from the solution system appeared to be much higher than the sum of those expected by assuming additivity of $G(NH_3)$ values for its two constituents, Gl and $CuGl_2$. These results seemed to provide a possible indication for a certain interaction occurring between radicals inherent in both constituents, Gl and $CuGl_2$, on irradiation. Some qualitative interpretations were given by taking into consideration the role of the hydrated electrons. (auth)

31300 EFFECT OF ULTRAVIOLET RAY IRRADIATION ON ^{124}Sb(III) IN HYDROCHLORIC ACID SOLUTIONS. Kambara, Tomihisa; Kashihira, Nobuyuki; Hagita, Katsuyuki. Rep. Fac. Sci., Shizuoka Univ., 1: 23-7(Dec. 1965).

^{124}Sb(III) in HCl solutions was irradiated by ultraviolet rays to investigate ^{124}Sb(V) formation procedures. Differences between the effects of the gamma-irradiation and those of the ultraviolet-irradiation were found to exist. (auth)

31301 STUDY ON THE EXTINCTION COEFFICIENT FOR TITANIUM IONS. Hasegawa, Kunihiko. Rep. Fac. Sci., Shizuoka Univ., 1: 33-4(Dec. 1965).

The effects of acid concentrations and of temperature on the extinction coefficient of titanium ions in H_2SO_4 were studied. Temperature, acid concentration, and sodium and potassium chlorides had almost no influence on the extinction coefficient. Potassium fluoride and potassium bromide did affect the extinction coefficient values. (M.C.G.)

31302 POLAROGRAPHIC INVESTIGATIONS ON Pu(IV) IN SULPHURIC ACID SOLUTION. Faraone, Giovanni; Trozzi, Marcello; Romeo, Raffaello (Univ., Messina, Italy. Univ., Padua). Ric. Sci. Riv., 36: 271-5 (Apr. 1966). (In Italian).

Data concerning polarographic investigations on Pu(IV) in sulfuric acid solution are reported. The reduction occurs by an irreversible process. The standard redox potential of Pu(III)-Pu(IV) was found to be $+0.750 \pm 0.002$ v referred to the normal hydrogen electrode. Experimental results also indicated a self-oxidation of Pu(III) to Pu(IV) and this was suggested as due to α radiation. Thirty-nine percent of the total energy emitted by disintegrations is used to perform the oxidation. (auth)

31303 RADIATION RESISTANCE OF COMPLEX ORGANOPHOSPHORUS RESINS. Nikolaev, A. V.; Gribanova, I. N.; Yakovleva, N. I.; Khol'kina, I. D. Zh. Fiz. Khim., 40: 848-9(Apr. 1966). (In Russian).

Data on the radiation resistance of resin-sorbents based on diallyl ester of phosphonic acid are reported. After irradiation of the sorbent, a marked decrease in the degree of swelling and in its capacity for uranyl nitrate and the appearance of exchange capacity for sodium are characteristic. It is assumed that after irradiation the sorptive mechanism is changed. (tr-auth)

31304 RADIATION CHEMISTRY OF CARBOHYDRATES. V. FORMATION OF ACID PRODUCTS IN THE RADIOLYSIS OF AQUEOUS SOLUTIONS OF LACTOSE, CELLOBIOSE, AND MALTOSE. Kudryashov, L. I.; Bortsov, E. I.; Yarovaya, S. M.; Kochetkov, N. K. Zh. Obshch. Khim., 36: 229-32(1966). (In Russian).

It was found that under the action of the gamma radiation from ^{60}Co on aqueous solutions of lactose, cellobiose, and maltose in the absence of oxygen, radiation hydrolysis of these carbohydrates to the corresponding monosaccharides is not accompanied by the formation of acid products. The acids formed in radiolysis are secondary products. The process of radiolysis of disaccharides in aqueous solutions in the absence of oxygen may be broken down into two steps. In the first step, below 1.4×10^{19} ev/ml, no formation of acids is observed. At a higher dose, acids are formed in

proportion to the absorbed radiation. Below the indicated dose limit, radiolysis occurs chiefly under the action of H and OH radicals, with the main radiation hydrolysis of the disaccharide; at higher doses the hydrogen peroxide concentration becomes appreciable, which reacts with the H and OH radicals to form the peroxide radical. This undergoes secondary reactions to form acids. (CFSTI)

31305 DEPENDENCE OF LUMINESCENCE SPECTRA OF ORGANIC URANYL SALT SOLUTIONS ON THE EXCITING LIGHT WAVE LENGTH. Volodko, L. V.; Turetskaya, E. A. Zh. Prikl. Spektrosk., Acad. Nauk BSSR, 4: 327-9 (Apr. 1966). (In Russian).

The excitation spectra for different wavelengths of organic uranyl salt solution luminescence and the dependence of emission spectra on the exciting light wavelength are studied. The presence of two absorption and luminescence centers in each solution and a weak interaction between them are shown. (auth)

31306 ESR STUDY OF FREE RADICALS FORMED BY γ-IRRADIATION OF POLYETHYLENE TEREPHTHALATE. Araki, K.; Campbell, D.; Turner, D. T. (Research Triangle Inst., Durham, N. C.). 7p. (CONF-650902-29). ORAU. Gmelin, AED-CONF-65-235-61.

From American Chemical Society. 150th National Meeting, Atlantic City.

Samples of amorphous polyethylene terephthalate (PET), partially crystalline PET (Mylar film), partially deuterated PET, and single crystals of ethylene glycol dibenzoate were exposed at various temperatures to ^{60}Co γ radiation at a dose rate of 0.2 Mrad/hr. Electron spin resonance spectra for the irradiated samples are shown. Possible reactions and free radicals that might account for the spectra are discussed. (A.G.W.)

Radiochemistry

See also Separation Processes and Procedures

31307 PREPARATION OF ^{32}P-LABELED NUCLEOSIDE 5′-MONOPHOSPHATES. Greenlees, A. W.; Symons, R. H. (Univ. of Adelaide). Biochim. Biophys. Acta, 119: 241-8 (May 19, 1966).

A convenient and reliable method is described that was modified from published chemical procedures for the small-scale preparation of ^{32}P-ribonucleoside 5′-monophosphates of high specific activity. The starting materials are 2′,3′-O-isopropylidene nucleoside, 2-cyanoethanol, labeled orthophosphoric acid and dicyclohexylcarbodiimide; the reaction is carried out in a small volume of pyridine and dimethyl sulfoxide. (C.H.)

31308 SYNTHESIS OF 3,3′-DIMESYLOXY-N-METHYL-^{14}C-DIPROPYLAMINE HYDROCHLORIDE. El-Merzabani, Mahmoud M. (Tokyo Univ.). Chem. Pharm. Bull. (Tokyo), 13: 1362-3(Nov. 1963).

The strong carcinostatic activity of 3,3′-dimesyloxy-N-methyldipropylamine hydrochloride (No. 838) is being studied. For experiments on its metabolic fate in vivo, the ^{14}C-labeled compound was prepared, starting from methylamine-^{14}C. Methylamine-^{14}C was treated with ethyl acrylate in triethylamine for 10 days at room temperature. Ether was then added to precipitate triethylamine and the filtrate containing bis(2-carboethoxyethyl)-methyl-^{14}C-amine was evaporated at reduced pressure. The product, in the form of an oily residue, was reduced with $LiAlH_4$ to give 3,3′-dihydroxy-N-methyl-^{14}C-dipropylamine, which was separated on a column of Amberlite IR-120. Elution was performed with 5% NH_4OH-MeOH, which was converted to the desired substance by sulfonation (with methanesulfonic acid anhydride) and conversion to the hydrochloride. The specific activity of the product was equivalent to 1.84×10^6 cpm/mg. (BBB)

31309 SEPARATION OF ^{32}P FROM A ^{32}P-^{35}S MIXTURE BY COPRECIPITATION WITH FERRIC HYDROXIDE USING SEVERAL ORGANIC BASES AS PRECIPITANTS. Koda, Yoshio (Government Industrial Research Inst., Nagoya, Japan); Ito, Masayuki. Nagoya Kogyo Gijutsu Shikensho Hokoku, 15: No. 3, 96-101(Mar. 1966). (In Japanese).

A study is described for the separation of carrier free ^{32}P from a $H_3{}^{32}PO_4$-$H_2{}^{35}SO_4$ mixture by co-precipitation with ferric hydroxide. To maintain a pH value of a test solution in a narrow range without buffer solution, such organic bases as pyridine, α-picoline, benzylamine, ethylamine were used as precipitants, in addition to the ordinary precipitants, ammonia and sodium hydroxide. Carrier-free ^{32}P was co-precipitated with yields of above 80% within the range of pH 4-10; however, yields were decreased above pH 10. Carrier-free ^{35}S was considerably co-precipitated under pH 6, and yields were rapidly decreased above this pH value. Addition of a sulfate ion to a test solution as carrier brought about further decrease in yields of co-precipitation of ^{35}S. Therefore, the suitable condition of separation of carrier free ^{32}P from a ^{32}P-^{35}S mixture by co-precipitation was in the range of pH 8–10, and in this range ^{35}S contents could be decreased under $1/1000$ by a single operation. (auth)

31310 THE MEASUREMENT OF TRITIUM ACTIVITY IN NATURAL WATERS. PART I. TECHNIQUES. Lal, D.; Athavale, R. N. (Tata Inst. of Fundamental Research, Bombay). Proc. Indian Acad. Sci., Sect. A, 63: 166-83 (Mar. 1966).

To exploit natural and artificial activity of tritium, ^3H (half life, 12.3 yr), as a tracer for the study of the large-scale circulation of air in the troposphere, water balance and characteristics of ground water, systematic measurements of its activity in wet precipitations, surface and subsurface waters have been carried out since 1961. The levels of tritium activities in such samples vary over a wide range, factors of 10^4 or more. Because of large dilution with hydrogen of the tropospheric water, the specific activities in surface and subsurface waters are very low, and employment of sensitive detection techniques becomes necessary. The techniques adopted for the measurement of tritium which permit an accurate determination of T/H ratios exceeding 10^{-17}, without carrying out an electrolytic enrichment are reported. A factor of twenty enrichment then suffices to measure natural levels of tritium in ground waters of up to 25 years "age" corresponding to T/H ratios of ca. 5×10^{-19}. (auth)

31311 APPLICATION OF PERTURBED ANGULAR CORRELATION TO HOT-ATOM CHEMISTRY OF RHENIUM. Sato, Jun; Yokoyama, Yuji; Yamazaki, Toshimitsu (Tokyo Univ.). Radiochim. Acta, 5: 115-17(May 1966).

An attempt was made to measure the perturbed angular correlation for ^{188}Re in some chemical states in order to study the effects of initial chemical environments of rhenium on the correlation and to examine the possibility for applications to hot atom chemistry. It was concluded that the influence on the angular correlation is due to the interaction between the ^{188}Os nucleus and its extranuclear field. The extranuclear field around the osmium nuclei is the same in the case where the initial rhenium nuclei are situated in the same chemical environment in these samples. Where a difference in the extranuclear field around the osmium nuclei is found, it must be attributed to the difference of the initial chemical environment in which the ruthenium nuclei are situated. (M.C.G.)

31312 BIOSYNTHESIS OF RADIOACTIVE ESTRIOL-3-GLUCOSIDURONATE BY GUINEA PIG LIVER HOMOGENATE. Goebelsmann, Uwe (Karolinska Sjukhuset, Stockholm); Diczfalusy, Egon; Katz, Joseph; Levitz, Mortimer. Steroids, 6: 859-64(Dec. 1965).

Synthesis of tritiated estriol-3-glucosiduronate was accomplished by incubating ^3H-labeled estriol with homogenate of guinea pig liver. This resulted in the formation of a water-soluble metabolite in high yield, which was isolated and identified as estriol-3-glucosiduronate (E_3-3Gl). Evidence that guinea pig liver homogenate fortified with UDPGA converted E_3-15-^3H into a glucosiduronate and that this glucosiduronate was identical with E_3-15-^3H-3Gl is presented. The distribution of radioactive material agreed with the theoretical distribution values in counter-current distribution in three solvent systems. The data presented showed that ~85% of the radioactive material recovered

following incubation was E_3-15-^{3}H-3Gl. This corresponded to more than 70% of the original radioactive material incubated. It is apparent therefore that E_3-15-^{3}H-3Gl was the predominant product of incubation. Since the principal conjugate formed by incubation of E_3 with human liver homogenate is E_3-16Gl, whereas homogenate of guinea pig liver forms predominantly E_3-3Gl, it is possible to prepare these two glucosiduronates of labeled E_3 for metabolic studies. These two compounds account for more than 90% of the conjugated E_3 excreted in pregnancy urine at midterm. (TCO)

Separation Processes and Procedures

See also Analytical Procedures
ISOTOPE TECHNOLOGY — Separation and Production

Refer also to abstract 31447.

31313 (ANL–6853) ESTIMATED TEMPERATURES OF EBR-II FUEL CYCLE FACILITY SHIELDING WINDOWS AT GAMMA RADIATION LEVEL OF 3.5 x 10^5 RAD PER HOUR. Eckels, T. W.; Coleman, L. F. (Argonne National Lab., Ill.). Feb. 1966. Contract W-31-109-eng-38. 34p. Dep. mn. CFSTI $2.00 cy, $0.50 mn.

Calculations were made of the transient and steady-state temperatures that may be expected to occur in EBR-II Fuel Cycle Facility shielding windows subjected to gamma radiation. The limiting assumptions are stated, and observations were made of the temperature effects of installing a $\frac{1}{4}$-in.-thick glass cover plate over the exposed surface of the heavy glass slab that is at the hot side of each window. The window temperature that will result from a proposed schedule of opening and closing a 6-in.-thick steel shielding shutter is also discussed. (auth)

31314 (ANL–7175, pp 1-41) COMPACT PYROCHEMICAL PROCESSES. (Argonne National Lab., Ill.).

Results of investigations concerning new pyrochemical processes for future fast reactor fuels are reported. EBR-II fuel cycle developments are described, and information from supporting chemical investigations and supporting engineering studies are included. (J.R.D.)

31315 (ANL–7175, pp 42-103) VOLATILITY AND FLUIDIZATION PROCESSES. (Argonne National Lab., Ill.).

Laboratory investigations are reported on fluid-bed oxidation and fluorination of simulated UO_2-PUO_2, reactions of BrF_5, UF_6-PUF_6 equilibria NPF_6 chemistry, and corrosion in fluid-bed reactors. Engineering-scale investigations are reported on recovery of U and Pu in the Alpha facility, processing UO_2 fuels, PuF_6 separation from cell exhaust air, and fluid-bed processing of fuels. Investigations of fluid-beds are related to process operations are also reported. (J.R.D.)

31316 (ANL–7175, pp 104-18) STUDIES AND EVALUATIONS. (Argonne National Lab., Ill.).

Results of investigations concerning cost differentials among processes for fast reactor fuels in conceptual facilities are presented. Discussions of process requirements and technical ground rules, chemical flowsheets, plant designs, and economic ground rules are presented. (J.R.D.)

31317 (BAW–393-3) RECYCLE OF HWOCR THORIUM FUEL. Moncrief, E. C.; Schileo, G. (Babcock and Wilcox Co., Lynchburg, Va. Research and Development Div.). Mar. 1966. Contract AT(38-1)-393. 147p. Dep. mn. CFSTI $5.00 cy, $0.75 mn.

Fuel processing costs were evaluated for two of the more promising HWOCR fuels, thorium oxide–uranium oxide and thorium–uranium alloy. The costs for reprocessing, conversion, fabrication, and waste disposal ranged from $62 to $79 per kilogram for oxide cores at capacities of 2.2 to 2.6 tons per day and from $43 to $78 per kilogram for alloy cores at capacities of 2.2 to 5.7 tons per day. The costs were based on a hypothetical 15,000 Mw(e) HWOCR economy that used both thorium and uranium recycled in a heavily shielded, remotely operated, integrated plant, the TRIP facility. Capital costs for the TRIP facility were estimated to be about $70 million for oxide core fabrication and from $80 to $100 million for alloy fabrication, depending on the fuel design. Annual operating costs were $40 to $50 million for oxide cores and $50 to $65 million for alloy cores. Oxide processing included a single-cycle acid-thorex extraction, feed material conversion by the sol-gel process, and refabrication by vibratory compaction. The alloy processing scheme likewise included the single-cycle extraction operation, but used a calcium reduction flow sheet for thorium metal preparation and a coextrusion flow sheet for alloy refabrication. (auth)

31318 (BMwF-FBK–65-04) BEITRAEGE ZUR DEKONTAMINATION VON RADIOAKTIV VERSEUCHTEM WASSER MIT HILFE CHEMISCHER FAELLUNGEN. (Contributions to the Decontamination of Radioactive Contaminated Water Using Chemical Precipitation Methods). Keese, H. (Technische Hochschule, Brunswick (West Germany). Institut fuer Anorganische Chemie). Dec. 1965. 66p. Dep. mn.

The applicability and the kinetics of various precipitation methods for the decontamination of water, slightly contaminated by radioactive ions, were examined. Precipitations of barium phosphate with sodium sulfate, and potassium aluminum alum with barium chloride gave the best results. About 97% of the isotopes ^{144}Ce, ^{91}Y, ^{89}Sr, ^{90}Sr, and ^{60}Co are removed simultaneously, whereas the removal of ^{137}Cs is small. (auth)

31319 (ISO-SA–10) SOLVENT EXTRACTION OF NEPTUNIUM(VI) FROM AN ACID DEFICIENT NITRATE SYSTEM. Colvin, Curtis A. (Isochem Inc., Richland, Wash.). Apr. 27, 1966. Contract AT(45-1)-1851. 11p. (CONF-660615–1). Dep. mn. CFSTI $1.00 cy, $0.50 mn.

From American Chemical Society, Northwest Regional Meeting, Vancouver, B. C.

Separation of neptunium from fission products by methyl isobutyl ketone extraction was previously limited to positive free acid flowsheets. This limitation was due to the lack of a compatible oxidant with sufficient potential to oxidize neptunium to the extractable (VI) state in acid-deficient solutions. An acid-deficient system is preferable to a free acid system owing to the much lower distribution ratios for fission products. Ceric ammonium nitrate was used as a neptunium oxidant in an acid-deficient nitrate system. Subsequent extraction of neptunium(VI) by methyl isobutyl ketone resulted in arithmetic decontamination factors exceeding 10^4 for zirconium-niobium and 400 for ruthenium across one solvent extraction cycle. (auth)

31320 (UCRL–16108) LIQUID METAL EXTRACTION OF FISSION PRODUCTS FROM URANIUM REACTOR FUELS. Pasternak, Alan David (Lawrence Radiation Lab., Univ. of California, Berkeley). Jan. 1966. Contract W-7405-eng-48. 174p. Dep. mn. CFSTI $5.00 cy, $1.00 mn.

Thesis.

The rate of extraction of a rare earth fission product, ^{140}La, and its precursor and ^{140}Ba from the uranium-5 wt % chromium eutectic by molten magnesium at 1000°C was measured by the falling liquid drop technique. Use of the low melting U–Cr eutectic (MP 859°C) instead of pure uranium (MP 1132°C) permits operation at temperatures well below the boiling point of magnesium. Magnesium and the U–Cr alloy form an essentially immiscible two phase liquid-liquid system. Fission products were introduced in the U–Cr alloy by light neutron irradiation. The relative abundance of ^{140}La was determined by scintillation counting of its 1,6 Mev gamma photopeak. The relative abundance of ^{140}Ba was determined by following the decay of ^{140}La activity after extraction. Measurements were made on U–Cr drops of 2 to 4 mm diameter.

The overall mass transfer coefficient for La, based on the U–Cr phase was determined to be 0.0041 ± 30% cm/sec. Drop velocity was determined by measuring the time interval between the output of collimated scintillation counters placed along the extraction column. The measured velocity was about 70 cm/sec, 13% higher than predicted by the correlation of Hu and Kintner. Equilibrium experiments showed the distribution coefficient for La (on a concentration basis) between U–Cr and Mg to be 0.14 at 1000°C, and that for Ba to be about 0.0035. The results of the kinetic and equilibrium measurements indicated that the mechanism of solute lanthanum transfer is molecular diffusion through a stagnant drop with external resistance. Diffusion coefficients in liquid metal systems were corresponding states theories. (auth)

31321 STUDY OF THE DRY CHEMICAL TREATMENT OF URANIUM-ZIRCONIUM FUELS. Bourgeois, Michel; Nollet, Patrick. Energ. Nucl., 8: 165-74(May 1966). (In French).

A dry process was studied for separating the uranium from the zirconium, either for recovering the enriched uranium from fuel element production waste, or with a view to treating these elements after irradiation. In this process the alloy is treated with hydrochloric acid at 400°C in a fluidized corundum bed which causes the zirconium to volatilize as tetrachloride and the uranium to form the trichloride. This latter is then converted into the hexafluoride by attack with fluorine. After the laboratory tests, a pilot plant with a capacity of 1 kg of alloy was tried out at the Fontenay-aux-Roses Nuclear Research Center; this made it possible to fix the operational conditions for the process. An industrial scale plant was then built and operated until a satisfactory process was developed for treating the waste. This installation treats 3 kg/hr of alloy with a yield for the hydrochloric acid of about 50% and with a uranium loss in the zirconium tetrachloride of about 0.1%. An active pilot plant capable of treating a few kilograms of irradiated alloy is now being studied. (auth)

31322 EXTRACTION OF URANIUM(VI) FROM HYDROCHLORIC ACID SOLUTIONS BY LONG-CHAIN ALIPHATIC AMINES. Sato, Taichi (Louisiana State Univ., New Orleans). J. Appl. Chem., 16: 143-8(May 1966).

The partition of uranium(VI) between hydrochloric acid solutions and organic solutions of long-chain aliphatic amines was investigated at different concentrations of hydrochloric acid, solvent, and aqueous uranium, and at different temperatures. The effects of amine structure and of organic solvent and the mechanism of uranium extraction are discussed on the basis of the results obtained. From infrared spectral measurements it was postulated that a chloro complex of uranium(VI) is formed in the extraction of uranium(VI) from hydrochloric acid solution by tri-n-dodecylamine in benzene. (auth)

31323 APPLICATION OF EXTRACTION CHROMATOGRAPHY IN THE PROCESSING OF IRRADIATED AMERICIUM. Kooi, J (EURATOM, Ispra, Italy). Radiochim. Acta, 5: 91-9(May 1966).

Processing of 2.5 g of highly irradiated americium by extraction chromatography using dilute hydrochloric acid from columns loaded with di-2 ethylhexyl orthophosphoric acid was successfully used for the isolation and purification of weighable amounts of berkelium and californium. The procedures, the separations obtained, and the column performance are discussed. It was also shown that the application of extraction chromatography may lead to very simple flow schemes for the processing of irradiated americium, avoiding the use of lithium chloride columns. (auth)

31324 REMOVAL OF ^{89}Sr AND ^{137}Cs ON CELLULOSE PHOSPHATE. Hasegawa, Kunihiko. Rep. Fac. Sci., Shizuoka Univ., 1: 29-32(Dec. 1965).

Cellulose phosphate as an ion exchanger for separation of radioisotopes was investigated. The exchange adsorption of Sr in the cellulose phosphate was different from that of Cs. The exchange capacities of Sr and Cs were about 3 meq/g (pH 1 to 12) and 6.4 meq/g (pH 9), respectively. ^{137}Cs could be easily eluted with 1N NH_4NO_3, while all the ^{89}Sr remained in the cellulose phosphate column. The ^{89}Sr was later eluted from the column with 3N NH_4NO_3. The strength of cellulose phosphate might be decreased by the radiation, but the exchange capacity was hardly influenced under about 10^7R. (auth)

31325 FRACTIONATION OF COPPER IN NEUTRON-ACTIVATED SOILS. Kline, J. R.; Rust, R. H. Soil Sci. Soc. Amer. Proc., 30: 188-92(Mar.-Apr. 1966).

Copper in surface and subsurface horizons of six soils was fractionated by chemical methods after irradiation of the samples with thermal neutrons. The first fraction was obtained by a process of self diffusion in which soil Cu was allowed to diffuse into dilute $CuSO_4$ solutions. The second was obtained by extracting the soils in hot solutions of dilute $CuSO_4$ which were 0.1M in HCl after removal of the diffusible Cu. The third consisted of the residual Cu after the first two increments had been removed. Determinations were done using a 400 channel gamma ray spectrometer. From 35 to 70% of the total Cu in these soils was found to be freely diffusible. Self diffusion took place as readily in calcareous soils as in noncalcareous soils. Extractions in 0.5M NaOH released amounts of Cu similar to those released by diffusion which suggests that much of the freely diffusible Cu is of organic origin. Copper released by acidic $CuSO_4$ ranged from 20 to 40% of the total and residual Cu ranged from 4 to 40% of the total. (auth)

31326 REPROCESSING METHODS AND COSTS FOR SELECTED THORIUM-BEARING REACTOR FUEL TYPES. Roberts, J. T.; Ferris, L. M.; Nicholson, E. L.; Rainey, R. H.; Watson, C. D. (Oak Ridge National Lab., Tenn.). pp 313-52 of STI-DOC-10/52.

Developments in the USA in the field of chemical reprocessing of thorium-bearing spent fuels from nuclear reactors are reviewed. Consideration is restricted to fuels of the most promising reactor types in the USA advanced converter reactor program. Emphasis is placed on the differences in reprocessing methods and costs between these thorium fuels and standard low-enrichment uranium metal or oxide fuels clad in aluminum, zirconium, or stainless-steel alloys. The relationship between reprocessing and the rest of the fuel cycle for the most important proposed thorium-uranium recycle schemes is discussed. Head-end processes, starting with irradiated fuel elements and ending with a nitrate solution suitable for feed to solvent extraction, are described for the various fuel types. Solvent extraction flowsheets for separating the uranium and thorium from each other and from the fission products are evaluated. The interim and ultimate waste disposal problems associated with the various recycle schemes, head-end processes and solvent extraction flowsheets are presented. Finally, comments are made on the costs of reprocessing thorium fuels, by comparison with standard uranium fuels and with respect to the economic problems associated with sizing and starting a reprocessing plant when the fuel load is small initially but promises to increase substantially with time. (M.O.W.)

ENGINEERING

General

Refer also to abstract 32794.

31327 (K–1671) UCAPP: UNION CARBIDE APT POST PROCESSOR. Program Documentation. Neu, R. E.; Schellinger, W. V. (Oak Ridge Gaseous Diffusion Plant, Tenn.). June 28, 1966. Contract W-7405-eng-26. 158p. Dep. mn. CFSTI $4.00 cy, $1.00 mn.

A study was made to aid the computer-programmer when modifications to or extensions of the UCAPP program become necessary. Program listings, logic flow diagrams, a variable dictionary, and subroutine cross references were compiled and indexed to enable the programmer to find any pertinent information about a particular subroutine or portion of the program. Within the program listings, comment cards were utilized to describe the specific function accomplished by each subroutine. In addition to these descriptions, comments were inserted which define logic branching and logic flow. (M.O.W.)

31328 (KAPL-M–6539) THE VIBRATION RESPONSE OF A CANTILEVERED CYLINDER SURROUNDED BY AN ANNULAR FLUID. Fritz, R. J.; Kiss, E. (Knolls Atomic Power Lab., Schenectady, N. Y.). Feb. 24, 1966. Contract W-31-109-eng-52. 27p. Dep. mn. CFSTI $2.00 cy, $0.50 mn.

A theoretical analysis and test results are presented which describe the response to a forced vibration of a cantilever supported cylinder, surrounded by a fluid annulus. The effects of the fluid annulus on natural frequency and displacement of the vibrating system are considered. (auth)

31329 (KAPL-M–6543) SOME CONSIDERATIONS OF ROTOR DYNAMICS INCLUDING VIRTUAL MASS AND STABILITY EFFECTS. Fritz, R. J. (Knolls Atomic Power Lab., Schenectady, N. Y.). Feb. 24, 1966. Contract W-31-109-eng-52. 23p. Dep. mn. CFSTI $1.00 cy, $0.50 mn.

Bearing equations are derived for small deflections of a noncavitating, long-sleeve bearing, based on continuity and a turbulent form of the Navier-Stokes equation and including inertial terms. This bearing was shown to be inherently unstable. A virtual mass is calculated which agrees with the results of previous work for the case of no rotation and agrees with bearing theory for the case of half-frequency whirl. A dynamic system was considered which is intended to represent a tilted-pad bearing with displacement cross-coupling. The criterion for stability for this system was shown to depend on the degree of cross-coupling. (auth)

31330 (KAPL-M–6546) FRICTION FACTORS FOR USE IN ANALYSIS OF JOURNAL BEARINGS WITH VORTEX-TURBULENT FLOW. Fritz, R. J. (Knolls Atomic Power Lab., Schenectady, N. Y.). Feb. 24, 1966. Contract W-31-109-eng-52. 19p. Dep. mn. CFSTI $1.00 cy, $0.50 mn.

Friction factors were estimated for Couette turbulence occurring in long sleeve bearings. The estimates were based on pipe flow correlations and are shown to agree very well with Robertson's data using the roughness factor $\epsilon/D = 0.0004$. It is predicted that a practical bearing will have significantly greater relative roughness. Friction factors are proposed for combined Reynold's (turbulent) and Taylor's (vortex) correlations assuming a roughness $\epsilon/D = 0.004$ which is considered reasonable for a bearing surface of ASA roughness 10 and a radial bearing clearance of 5 mils. A proposal is made to estimate the friction factor for axial flow combined with rotational flow. These proposals are intended to apply to moderate bearing eccentricities, the range of which must be established by test. (auth)

31331 (UCRL–14616) PROPAGATION OF ELASTIC STRESS DISTURBANCES IN DEFORMABLE SOLIDS. Wasley, R. J. (Lawrence Radiation Lab., Univ. of California, Livermore). Dec. 21, 1965. Contract W-7405-eng-48. 213p. Dep. mn. CFSTI $6.00 cy, $1.25 mn.

Presented are fundamental ideas on propagation of elastic disturbances in extended, semi-extended, and bounded media. The treatment is principally classical, although newer techniques are discussed, especially with respect to experimental work. The presentation is coherent, if not complete in all details, and is intended to serve as a useful aid for self-study or as a basis for organized lectures. (auth)

31332 (URS–651-4) FORMATION OF DEBRIS FROM BUILDINGS AND THEIR CONTENTS BY BLAST AND FIRE EFFECTS OF NUCLEAR WEAPONS. Final Report. Rotz, J.; Edmunds, J.; Kaplan, K. (URS Corp., Burlingame, Calif.). Apr. 1966. 118p.

Debris charts, failure overpressure data, contents-debris criteria, and estimating procedures are presented to facilitate application of the debris prediction model and increase its range of applicability. A description of the debris prediction model and its operation and a detailed worked example are presented illustrating the use of the model to determine debris contours over the entire city of Detroit and debris profiles along a route through the city. In this example, debris depths before and after fire and the percentage contribution by building contents and structural components in each case are given. (J.R.D.)

31333 (Y–1541) SINGLE-TRANSDUCER DIFFERENTIAL MEASURING DEVICE. Whitten, L. G. (Union Carbide Corp., Oak Ridge, Tenn. Y-12 Plant). June 21, 1966. Contract W-7405-eng-26. 7p. Dep. mn. CFSTI $1.00 cy, $0.50 mn.

A review of current practice showed that to keep abreast of present-day machine-tool capabilities, the precision of on-the-machine gaging should be improved by at least an order of magnitude. A simple, easily operated, portable, on-the-machine measuring device utilizing a single-transducer measuring system was designed, built, and tested. Its performance demonstrated an improvement in precision over current practice by one to two orders of magnitude. (auth)

31334 APPROXIMATE METHOD FOR THERMOVISCOELASTIC STRESS ANALYSIS. Taylor, R. L.; Chang, T. Y. (Univ. of California, Berkeley). Nucl. Eng. Design, 4: 21-8(May-June 1966).

An approximate method of analysis for problems in thermoviscoelasticity is discussed. Axisymmetric and point-symmetric boundary value problems are considered. The method employed consists of dividing the body to be analyzed into a set of finite element subregions. Approximate displacements are assumed and the behavior of each element is established through the principle of virtual displacements. Satisfaction of compatibility and continuity conditions between elements leads to a set of simultaneous integral equations (for integral constitutive equations) defining the response of the entire body. A step-forward integration scheme is employed to solve the set of equations. Numerical examples are included to illustrate the method as well as the effect of temperature gradients on the response of viscoelastic cylinders. (auth)

31335 LARGE DEFLECTIONS OF RIGID-PLASTIC CYLINDRICAL SHELLS UNDER AXIAL TENSION AND EXTERNAL PRESSURE. Lepik, U. (Univ. of Tartu). Nucl. Eng. Design, 4: 29-38(May-June 1966).

Using Tresca's yield condition and the associated flow rule, axis-symmetric modes of deformation for sandwich-type cylindrical shells with simply supported ends are studied. The shell under observation is loaded with ex-

ternal pressure and with a prescribed constant tensile end-load. Deflections may be of the same order as the thickness of the shell. Within the limits of the concept of a rigid-plastic body, exact and closed-form solutions are found. The applicability of the solutions obtained depending on the shell length and the end-load value is discussed. The elastic-plastic problem is resolved for shells without an end-load. It turned out that considerable plastic deformations developed in the shell already under a load corresponding to a transition from the pure elastic state to the elastic-plastic one. This fact is compared with some experimental data available. (auth)

Applications of Nuclear Explosions

Refer also to abstract 31393.

31336 NUCLEAR EXCAVATION. Walterscheid, Edward C. (Los Alamos Scientific Lab., N. Mex.). Ind. Res., 54-9(Jan. 1966).

The use of nuclear explosives for excavation of a new sea-level canal in Central America is considered. Of the two routes studied, it was concluded that approximately 294 nuclear devices will be needed to excavate the Panamanian route, with 14 separate detonations over a 2-yr period. Thirteen of the detonations each will have a yield of about 10 megatons; the remaining one will be 35 megatons. The portion of the Columbia route excavated with nuclear explosives requires 262 nuclear devices with a total yield of 270.9 megatons. Twenty-one detonations could take place over a 3-yr period. An empirical scaling law for comparing explosives of different yields was derived. Economic comparisons with conventional methods are included. (M.C.G.)

Facilities and Equipment

31337 NRL HIGH LEVEL RADIATION LABORATORY. PART III. OPERATING EXPERIENCE. Watson, H. E. (Naval Research Lab., Washington, D. C.). Nucl. Eng. Design, 4: 97-107(May-June 1966).

The U. S. Naval Research Laboratory High Level Radiation Laboratory (HLRL) has recently completed its initial eighteen months of operation. The final part of a detailed description of this laboratory is reported and a description of radiation operating procedures, the development and modification of specialized equipment, along with plans for further improving overall laboratory operations are included. (auth)

31338 PHYSICS OF INDUSTRIAL RADIOLOGY. Halmshaw, R. (ed.). New York, American Elsevier Publishing Co., Inc., 1966. 505p.

The physics of ionizing radiations is considered. Topics covered include the fundamental characteristics and properties of x and gamma rays, the generation of x rays, modern x-ray generators, gamma-ray sources, the principles of recording and detecting x rays, absorption and scattering processes, the response of recording and screening media, a radiographic definition, and sensitivity and image-quality indicators. Other topics are factors governing the choice of techniques, general procedures in radiography, fluoroscopic techniques, applications of radiological inspection. Image-intensifier systems, xeroradiography and ionography, and radiology with high-energy x rays. (J.F.P.)

31339 COMPARATIVE MERITS OF RADIOISOTOPE AND MACHINE SOURCES OF X-RADIATION FOR AEROSPACE APPLICATIONS. Carroll, David I.; Cohen, Martin, J.; Wernlund, Roger F. (Franklin GNO Corp., West Palm Beach, Fla.). 8p. (CONF-660207-7). ORAU. Gmelin, AED-CONF-66-011-12.

From Symposium on Radioisotope Applications in Aerospace, Dayton, Ohio.

The results of a study performed to define the relative advantages and limitations of radioisotope and machine sources of radiation for typical aerospace applications are described. The advantages and limitations of representative state-of-the-art gamma and x radiation sources are examined with regard to the aerospace application potential. The several areas of unique difference between radioisotope and machine sources are isolated and described in order to delineate clearly the area of aerospace application particularly suitable to each of these radiation sources. (auth)

Heat Transfer and Fluid Flow

See also PHYSICS — Fluid Physics and Thermodynamics

Refer also to abstracts 32238 and 32349.

31340 (ANL-7093) FLOW-REGIME TRANSITIONS AT ELEVATED PRESSURES IN VERTICAL TWO-PHASE FLOW. Baker, James L. L. (Argonne National Lab., Ill. Associated Midwest Universities, Lemont, Ill.). Sept. 1965. Contract W-31-109-eng-38. 148p. Dep. mn, CFSTI $4.00 cy, $1.00 mn.

Thesis. Submitted to Illinois Univ., Urbana.

Two-phase flow-regime transitions at elevated pressures for a single-component fluid, trichloromonofluoromethane (Refrigerant-11), were investigated for forced-circulation, upward flow in a vertical, rectangular conduit with internal dimensions of 0.380 by 1.050 in. The two-phase mixture was generated by an electrically-heated tube at a constant heat flux. The orthobaric-density ratio ranged from 7 to 60. The mass qualities based upon thermodynamic equilibrium ranged to 90%; however, most of the data encompassed the segment from saturation to 50%. The flow regimes were observed in the unheated rectangular section by employing an x-ray and television monitoring system. Three principal flow regimes were delineated: churn, annular, and wispy-annular flow. The plug-flow regime was not observed at elevated pressures. For comparison of fluids as widely divergent in their physical properties as R-11 and water, identical orthobaric-density ratios were more suitable than reduced temperature or reduced pressure. Expressions were developed to correlate surface tension and liquid dynamic viscosity for refrigerants and water as a function of reduced saturation pressure. Through an examination of these correlations of orthobaric properties, a simplified modeling of the flow-regime transitions was possible. A comparison of the saturation properties of R-11 and water at constant orthobaric-density ratio revealed that the ratios of the various properties were relatively constant over the range of test conditions. An examination of the Taylor-Helmholtz and Kelvin-Helmholtz stability criteria for flow-regime transitions yielded results that closely bounded the result from consideration of a purely inertial system. Local void-fraction distributions were obtained for six orthobaric-density ratios by employing a gamma traversing unit. The average void fractions were compared to available void data for water and a refrigerant, R-22, at identical orthobaric-density ratios. Agreement within the data was found. However, none of the existing correlations predicted the results over the entire range of quality and mass flow rate. An expression for the average void fraction was obtained for mass flow rates below 0.70×10^6 lb/hr-sq ft. (auth)

31341 (BNL-9546) LAMINAR HEAT TRANSFER IN A HEXAGONAL CHANNEL WITH INTERNAL HEAT GENERATION AND UNEQUALLY HEATED SIDES. Hsu, Chia-Jung (Brookhaven National Lab., Upton, N. Y.). Aug. 22, 1965. Contract AT(30-2)-Gen-16. 43p. (CONF-660801-1). Dep. mn, CFSTI $2.00 cy, $0.50 mn.

From 3rd International Heat Transfer Conference, Chicago.

The heat transfer characteristics for the case of laminar flow through a hexagonal channel were determined for the following conditions. The uniform heat flux on any one side of the hexagon is identical to that on the opposite side, and may be equal to or different from those on the two adjacent

sides; both the velocity and temperature profiles are fully established; and the heat transfer from the walls may or may not be accompanied by simultaneous internal heat generation in the flowing fluid. By employing a triangular network, the two-dimensional Poisson's equations which govern the velocity and temperature fields were solved numerically, under the appropriate boundary conditions with the aid of a high-speed digital computer. Fundamental temperature solutions and equations are presented which may be used to predict the temperature field, or to calculate the difference between local wall temperature and the bulk fluid temperature for a variety of cases. Methods of predicting the variation of local wall temperature are illustrated for several typical cases, including the case of uniformly distributed wall heat flux. The circumferential variation of the local Nusselt number and the mean Nusselt number are also reported, with and without internal heat generation. (auth)

31342 (EURAEC–1482) RESEARCH INTO THE CRITICAL HEAT FLUX (BURNOUT) IN BOILING WATER. Quarterly Progress Report No. 16, July 1, 1965–September 30, 1965. Mayinger, F.; Schad, O.; Weiss, E. (Maschinenfabrik Augsburg-Nuernberg A. G., Nuremberg (West Germany)). Nov. 1965. Contract 057-61-RDD. 46p. (EUR–2650). Dep. mn. CFSTI $2.00 cy, $0.50 mn.

Work Performed under United States–Euratom Joint Research and Development Program.

Measurements of the critical heat flux during boiling are reported. The first test series, i.e., measurements in respect of the influence of inlet conditions, were carried out with tubes of 7 mm. inside diameter at pressures of 70 and 100 atm., mass flows of 200 to 400 g./cm^{2}s, L/D ratios of 40 and 80 as well as in a range of 50 deg C sub-cooling up to 20% steam quality at the inlet to the test channel. The inlet conditions were varied by connecting non-heated stabilizing sections and installation of short twisted tapes and orifices at the test channel inlet. From the results of this work the influence of the twisted tapes in the range $0 < x_E < 0.2$ should be given special mention. With a steam quality at the test channel inlet of $x_E = 0.2$ it was possible by installing a twisted tape to increase the critical heat flux by 40% with otherwise constant conditions. In the sub-cooled range the improvement due to twisted tapes is not so marked. For the second object of the tests, the investigation of the influence of the hydraulic diameter on the critical heat flux during boiling, tubes of 7, 11 and 15 mm. inside diameter were used. With 70, 100 and 140 atm. the tests cover a range of $-0.3 < x_E < 0$ and were carried out with mass flows of 100–250 g./cm^{2}s. These measurements confirmed the tendency known from the relevant literature for the critical heat flux to decrease slightly as the tube diameter increases. In both test series the hydrodynamically stable as well as the pulsating burnout were thoroughly investigated. With larger hydraulic diameters of the test channel, compressible volumes upstream of the test section, e.g., the steam cushion of the pressurizer, lead to pulsating burnout in the same manner. With increasing pressure, as this was previously found with tubes of 7 mm. inside diameter, the tendency to pulsations decreases and the differences in the figures of the maximum heat flux during pulsating and during hydrodynamically stable burnout becomes smaller which can be explained by the fact that due to the decreasing density differential of the two phases, water and steam, the intensity of the disturbing impulses is reduced and consequently the stability of the flow improves. (auth)

31343 (GEAP–5056) TWO-PHASE FLOW AND HEAT TRANSFER IN MULTIROD GEOMETRIES. Fourth and Fifth Quarterly Progress Reports, July 26, 1965–January 25, 1966. (General Electric Co., San Jose, Calif. Atomic Power Equipment Dept.). Feb. 1966. Contract AT(04-3)-189. 35p. Dep. mn. CFSTI $2.00 cy, $0.50 mn.

A series of two-phase flow structure tests using vertical upflow of air and water at 85 to 90 psia in a 1-inch i.d. round tube and concentric annulus (1-inch tube with ½-inch center rod) was completed. Local void fraction, local quality, local slip ratio, and linear velocity profiles for both phases were determined by the isokinetic sample-probe technique. Film-flow rates were determined by wall suction through porous walls. The time-dependent nature of the flow structure was investigated with a "continuity probe" and pressure transducers. Typical results are presented. (auth)

31344 (LA–3497) A TWO-DIMENSIONAL TIME-DEPENDENT NUMERICAL STUDY OF ROTATIONAL COUETTE FLOW. Meyer, Kenneth A. (Los Alamos Scientific Lab., Univ. of California, N. Mex.). Feb. 15, 1966. Contract W-7405-eng-36. 174p. Dep. mn. CFSTI $5.00 cy, $1.00 mn.

Thesis. Submitted to Stanford Univ., Calif.

Finite difference techniques were applied to the study of two-dimensional time-dependent rotational Couette flow, developing into Taylor vortices. A set of finite difference equations utilizing the stream-function to satisfy continuity was developed and their accuracy and stability were considered. Investigations included a comparison with a second system of difference equations using velocities rather than the streamfunction and a study of the effect on accuracy of varying both the spatial and time increments. The effect of the form of the difference approximation to the radial boundary conditions was considered and the problem of choosing the wavelength for the periodic axial boundary condition is discussed in detail. The system of difference equations was judged quite adequate for the proposed hydrodynamic study. A series of problems with varying Reynolds numbers was considered for a configuration with a radius ratio of outer to inner cylinder of 1.2, with the outer cylinder stationary. The critical Reynolds number for onset of Taylor vortices ascertained was in good agreement with linear theory. It was found that for the steady secondary flow there is a preferred vortex axial wavelength which depends on Reynolds number. In a second series of problems comparison was made with analytic results of Davey and experimental results of Donnelly and Simon. Davey's analysis assumes that the wavelength is as given in the linear theory; his analysis agrees with the experiments only very close to the critical Reynolds number. It was found that by using this axial wavelength the numerical results agreed with Davey's theory; however, by allowing the wavelength to vary with Reynolds number, good agreement with the experimental torque values was obtained over a wide range of Reynolds numbers. Within the context of numerically obtained "preferred states" the previously conjectured principle of maximum dissipation was shown not to apply. The numerical results provide insight on the possible cause of the second (circumferential) instability. Some results concerning flows between counterrotating cylinders were also obtained. (auth)

31345 (NSJ-tr–47) BOILING HEAT TRANSFER AT THE COEXISTENCE OF NUCLEATE AND FILM REGIONS. Nishikawa, Kaneyasu; Shimomura, Ryutaro. Translated from Nippon Kikai Gakkai Rombunshu, 28: 1381-8(1963). 12p. Dep. mn. JCL $1.60 fs, $0.80 mf. JAERI.

According to the method of E. Zielinski, if a wire that is causing nucleate boiling with heating current adjusted to a rather low heat flux is pulled out of water for a short time, the surface of the wire dries and its temperature rises because of the contact of the wire and air, even when heat flux is kept constant. If the wire is dipped in water later, for a second time, it heats red-hot in a few seconds, followed by the appearance of film boiling. Film boiling is reproduced with comparative ease by temporarily breaking the contact of the heating surface with water. Nucleate boiling and film boiling are made to coexist stably on the same heating surface by heating them with a given heat flux. This is considered to be a kind of transition boiling, and the boiling phenomena at the coexistence of nucleate and film regions in saturated water, subcooled water, and sodium oleate solution are considered as well as their relation with the boiling characteristic curve. In this region the coefficient of heat transfer decreases with increasing temperature difference, while heat flux increases with increasing temperature difference. (auth)

31346 TEMPERATURE OF HEATED TUBES WITH PULSATING FLOW. Dolgov, V. V.; Sudnitsyn, O. A. At. Energ. (USSR), 20: 70-4(Jan. 1966). (In Russian).

Previous experiments indicated that pulsations in tubes containing flowing boiling water occur only under specific hydraulic conditions; they may be eliminated by specific operational steps, such as changing pressure and heating conditions. Further tests were carried out to determine temperature conditions in the outlet section of the tube, under conditions of "degenerate" flow pulsations. It was found that as the water temperature is increased, the tube may be divided into four regions: 1. the pulsations cause changes in the wall temperature; 2. at a certain amplitude, the pulsations cause a worsening of the heat transfer; 3. the pulsations create temperature oscillations at a certain amplitude; 4. worsening of the heat transfer after a certain number of flow oscillations. It was not found possible to establish a quantitative relation between the worsening of the heat transfer and factors, such as vapor content of the steam, pressure drop, heat load, amplitude, and flow pulsation frequency, on the basis of the available experimental data but the qualitative effect of these factors was determined. The flow pulsations usually caused a worsening of the heat transfer in the tubes. In the wall portions cooled with nonboiling water, the wall temperature oscillations were found to be due to changes in the conductive heat transfer. Reduction of the heat transfer in certain portions may result in excessively high wall temperatures. The heat load at which the worsening of the heat transfer starts lies below the critical load and depends on the simultaneous action of the vapor content, flow, pulsation amplitude and pressure. (TTT)

31347 CRITICAL THERMAL FLUXES AND HEAT TRANSFER OF BOILING POTASSIUM IN TUBES. Alad'ev, I. T.; Gorlov, I. G.; Dodonov, L. D.; Koroleva, V. S.; Fedynskii, O. S. Izv. Akad. Nauk SSSR, Energ. Transp., No. 2, 136-44(Mar.-Apr. 1966). (In Russian).

The results of the experimental study of the critical thermal fluxes and heat transfer of boiling potassium in tubes at pressures from 1.1 to 1.3 bars were reported. The calculated recommendations were given. (tr-auth)

31348 FORCED CONVECTIVE BOILING HEAT TRANSFER TO HYDROGEN. Chi, J. W. H. (Westinghouse Electric Corp., Pittsburgh). J. Spacecraft Rockets, 3: 150-2(Jan. 1966).

An annular flow model is postulated for forced convective heat transfer to hydrogen. Comparisons were made of calculated and observed values. (M.C.G.)

31349 TEMPERATURE AND HEAT FLUX DISTRIBUTION IN NUCLEAR FUEL ELEMENT RODS. Nijsing, R. (EURATOM, Ispra, Italy). Nucl. Eng. Design, 4: 1-20 (May-June 1966).

A mathematical study is presented which deals with the effect of nonuniform heat transfer conditions on the temperature and heat flux distribution in the rods of a nuclear fuel element. The analytic method employed yields the temperature and heat flux distribution in both fuel and cladding without the necessity of an iterative procedure. (auth)

31350 VELOCITY OF TURBULENT FLOW OF WATER THROUGH A BUNDLE OF HOLLOW RODS. T'ien, Chi-an; Tsao, Fu-chuen; Fan, Cheng-t'sai; Feng, Kuei-tsu; Ch'iang, Tiao-yuen; Ma, Hsiu-chen. Sci. Sinica (Peking), 15: 730-48(May 1966). (In Russian).

Experiments on the distribution of the velocity of turbulent flow in channels of finite bundles of hollow rods with square dimensions (65 × 65 mm) (under steady conditions) were carried out in horizontal hydraulic loops of narrow dimensions. The curves of local distributions of the velocity of flow in the central unit channels in the middle of the finite bundle of rods were determined for the case when the ratio S/d = 1.63. The channels have a square and right triangular arrangement. The experimental results were compared with calculations by the Deissler-Taylor method. The velocities in the center of each central unit of the channel of finite bundles of rod with three different quadratic arrangements (ratio S/d = 1.28, 1.33, and 1.63 and the distance S'' = 3.1, 1.6, and 3.6 mm) and also the velocity in the space between the wall of the peripheral rod and the cell were measured. For measurement of the local velocity Pitot tubes with stainless steel injection needles with a diameter of 0.5 mm (internal diameter of 0.25), were used. (tr-auth)

31351 PROCEEDINGS OF THE 1966 HEAT TRANSFER AND FLUID MECHANICS INSTITUTE. Held at the University of Santa Clara, Santa Clara, California, June 22, 23, 24, 1966. Saad, Michel A.; Miller, James A. (eds.). Stanford, Calif., Stanford University Press, 1966. 452p. $12.50. (CONF-660618).

The discussion of fluid dynamics and heat transfer includes topics on boundary-layer flows including stability, non-Newtonian flow, and shock-boundary layer interactions; two-phase flows and change of phase, free and forced convective heat and mass transfer, wakes, separated regions, and radiation gas dynamics, and special problems such as vortex flows, fluid motion in modified force fields, fluid dynamics of biological systems, and heat transfer in constricted areas. (J.F.P.)

Materials Testing

31352 (ANL-7042) A TELEVISION SYSTEM FOR ULTRASONIC IMAGING. Berger, Harold (Argonne National Lab., Ill.). Jan. 1966. Contract W-31-109-eng-38. 25p. Dep. mn. CFSTI $2.00 cy, $0.50 mn.

The capabilities of a continuous-wave, ultrasound, television imaging system as applied to several nondestructive testing problems are discussed. Application of the system to flaw detection is stressed, but some discussion and examples concerning the use of the system for other application areas, including liquid-level indication and fluid-flow studies, are also presented. It is concluded that, in the area of flaw detection, the television system offers particular promise for the ultrasonic inspection of thin, flat material. In inspections of objects of this nature, such as flat reactor fuel elements, the television system as normally used in these studies is capable of approximately one-mm resolution, of linear object inspection speeds of 120 cm/min, and of detecting such anomalies as bonding flaws, fuel inhomogeneities, and grain-size variations. The use of the television system in such inspection applications is recommended. (auth)

31353 RAPID AND ACCURATE B.E.T. SURFACE AREA MEASUREMENT USING RADIOACTIVE KRYPTON. Houtman, J. P. W.; Medema, J. (Reactor Instituut, Delft, Netherlands). Ber. Bunsenges. Physik. Chem., 70: 489-93(June 1966).

A method for determination of the surface area of a solid is described. This method is based on the measurement of the reversible part of the gas-adsorption isotherm, with the aid of radioactive ^{85}Kr as adsorbate. The amount adsorbed and the gas-pressure are measured with Geiger-Mueller tubes. The advantages of this method are a simple apparatus and the possibility of rapid and exact measurements. The same instrument can be used to measure areas of 0.003 to 1000 m^2/g. The amounts of ^{85}Kr, necessary for it, are specified. For determining surface areas of high-density materials, a correction for "bremsstrahlung" should be applied. (auth)

31354 NONDESTRUCTIVE TESTING OF MATERIALS IN FUEL ELEMENT PRODUCTION. Becker, E. (Technische Hochschule, Magdeburg, Ger.). Kernenergie, 9: 33-40(Feb. 1966). (In German).

A review is presented of the methods used in the nondestructive testing of fuel element coatings, fuel elements, and the junctions between the fuel element coatings and the fuel element. 47 references are included. (J.S.R.)

31355 SAFEGUARDS METHODS. (International Atomic Energy Agency, Vienna). pp 77-8 of STI-DOC-10/53.

The nondestructive testing of fuel elements by Compton recoil spectrometry is described. Measurements were made of ^{137}Cs. Burnup determinations with an accuracy of about 10% were obtained. (M.C.G.)

Space Propulsion

See also ISOTOPE TECHNOLOGY — Power Application
REACTOR TECHNOLOGY — Propulsion and Space

Refer also to abstract 32650.

31356 (N-66-12435) SUMMARY OF PERFORMANCE OF THREE TYPES OF ARC HEATERS FOR MHD EXPERIMENTS. Technical Memorandum No. 30. Period Covered: 1961–64. Richmond, J. Kenneth; Goldstein, Raymond (Boeing Scientific Research Labs., Seattle, Wash. Flight Sciences Lab.). Mar. 1964. 72p.

A summary is presented of experimental data obtained over a three-year period in testing different types of arc heaters, resulting in the development of a device especially suitable for producing the gas flow desired in plasma accelerators utilizing to the best advantage an available d-c power supply. The only gases considered were argon, helium, nitrogen, and mixtures of these. (M.O.W.)

31357 POWER CONDITIONING SYSTEMS FOR ION ENGINES. Work, G. A.; Herron, B. G. (Hughes Aircraft Co., Malibu, Calif.). Contracts NAS 3-4108; NAS3-2510; NAS 3-3565. J. Spacecraft Rockets, 3: 315-20(Mar. 1966).

The design and performance of the power conditioner for the SERT-I flight test are discussed with emphasis on the design features required by the nature of the ion-engine load. The development and testing of prototype power-conditioning systems for a 3- to 5-kev ion engine are also summarized. (D.C.W.)

31358 FACTORS IN LIFE TESTING ION ENGINES. Anderson, J. R.; Thompson, S. A.; King, H. J. (Hughes Research Labs., Malibu, Calif.). J. Spacecraft Rockets, 3: 321-7(Mar. 1966).

Several key physical processes in determining surface-contact ion engine lifetime, are discussed in the light of recent experimental results. It is found that charge-exchange erosion is the fundamental limitation to engine lifetime. Although experiment and analysis indicate attainable lifetimes of 5000 to 20,000 hr at 10 ma/cm^2 using the best present-day ionizers, shorter lifetimes result when interrelated secondary physical phenomena within the acceleration region of the engine emerge. Cesium ionization on the focus electrodes is considered in detail, since it is a lifetime barrier in those designs which utilize such beam-forming elements. Tolerable charge-exchange erosion of accel electrodes, to assure a given lifetime, is used to provide boundary conditions for ionization efficiency, focus temperature, and focus ion current. The effect of focus electrode roughness on accel erosion patterns is studied in detail. The influence of the ground-based test chamber environment vs a true space vacuum environment is also considered. (auth)

31359 EFFECTS OF RELIABILITY CONSIDERATIONS ON THE DESIGN OF ELECTRIC THRUSTER ARRAYS. Molitor, J. H.; Pinckney, K. R.; Seliger, R. L. (Hughes Research Labs., Malibu, Calif.). J. Spacecraft Rockets, 3: 554-60(Apr. 1966).

A study of the effects of reliability considerations on the design of the power-conditioning equipment and thruster arrays associated with electric propulsion systems is presented. The mathematical model required to compute thruster system reliability is developed. A power conditioning and thruster system reliability optimization study is then performed to determine the degree of redundancy required for power-conditioning circuits and the optimum number of ion engine modules and standbys necessary to obtain the requisite system reliability for least increase in system specific weight. The effects of power conditioner and thruster module size and number are evaluated in terms of reliability. It is shown that, by proper application of redundant circuit and component techniques, the reliability of both the power-conditioning equipment and the thruster array can be raised to the desired levels without prohibitive increases in propulsion system weight. (auth)

31360 POWER CONDITIONING FOR SPACE PROPULSION SYSTEMS USING CONTACT ION THRUSTERS. Erway, D. D.; Eilenberg, S. L. (Electro-Optical Systems, Inc., Pasadena, Calif.). J. Spacecraft Rockets, 3: 561-70(Apr. 1966).

The problems associated with matching the output of a large nuclear-electric power source to the requirements of contact ion thrusters are considered. The factors that influence the design requirements and the technical approach to power conditioning, switching, and control (PCSC) subsystems are discussed. Thruster requirements, power source characteristics, and environmental constraints are analyzed from the standpoint of their relationships to power conditioning. The results of the development of a breadboard PCSC unit at a 30-kw power level are also described. This work gives an insight into the problems and the possible solutions that will result in the realization of power conditioning equipment whose specific weight, efficiency, and reliability are compatible with requirements of large scale nuclear-electric rockets of the future. In particular, one of the most promising experimental results is a 30-kw breadboard whose components exhibit a total weight of 3.2 lb/kw. The results of a design study for a 300-kw system show that it is feasible to build a PCSC system weighing 9.1 lb/kw input power including radiators and shadow shielding with a power efficiency of 93%. (auth)

31361 POTENTIALITIES OF RADIOISOTOPE PROPULSION FOR SPACE PROBES. Romero, Jacob B. (Boeing Co., Seattle, Wash.). J. Spacecraft Rockets, 3: 570-6(Apr. 1966).

The application of radioisotope engines to space probes is investigated, with emphasis on design concepts, operating constraints, and performance. Direct heating engines, which incorporate cooling schemes to reject radioisotope energy during engine-off periods, are considered. The performance of these engines is limited by isotope availability, power density, and half life. Large-scale production of the high-power-density isotopes (^{242}Cm, ^{95}Nb, and ^{210}Po) is necessary to allow engine designs of a few pounds thrust and reasonable performance. Payloads delivered from Earth orbit by radioisotope and radioisotope-augmented chemical stages for various flyby missions are compared with high-performance chemical systems. A radioisotope engine of 10-lb thrust and 800-sec specific impulse, fueled with a high-power-density isotope, outperforms chemical systems for some of the missions studied. Increasing the specific impulse of radioisotope engines by the use of fluidized beds or molten cores results in considerable payload advantage over chemical systems. (auth)

31362 DEVELOPMENT OF ION MICROTHRUSTORS FOR SATELLITE APPLICATIONS. Eilenberg, Stanton L.; Toms, Ronald S. H. (Electro-Optical Systems, Inc., Pasadena, Calif.). New York, American Inst. of Aeronautics and Astronautics, 1966, Preprint No. 66-118, 26p., $1.00. (CONF-660109-1). ORAU.

From AIAA 3rd Aerospace Sciences Meeting, New York.

The first use of electrical propulsion in space will be for the control of satellites. Several types of devices are under immediate consideration for orbital and attitude control of certain satellites within the next three years. The thrust level for these devices lies between one and one-thousand micropounds. The power requirements range from ten to three-hundred watts. In contrast to the main propulsion power needs for electric propulsion which dictate a low specific weight ratio nuclear power source, these control devices will require only a small portion of the satellite power supply. The type of thruster will be determined by the specific needs of the satellite. For example, a gravity-gradient controlled satellite which requires east-west station keeping must use very low station keeping thrust levels to prevent upsetting the gravity-gradient control. The various considerations involved in the specification of the satellite control thrustor system are discussed as well as the design considerations involved in the ulti-

mate development of the device. The state-of-the-art in ion microthruster development is also presented. (auth)

31363 PROPELLANT INJECTION INTO A COAXIAL PLASMA ACCELERATOR. Karras, Thomas W.; Gorowitz, Bernard; Gloersen, Per (General Electric Co., King of Prussia, Pa.). New York, American Inst. of Aeronautics and Astronautics, 1966, Preprint No. 66-241, 22p., $1.50. (CONF-660310-27). ORAU.

From AIAA 5th Electric Propulsion Conference, San Diego, Calif.

The design, operation, and testing of three types of plasma injectors (an electromagnetically actuated valve with an O-ring seal, a piezoelectric valve, and an exploded-liquid-metal injector) for plasma accelerators are discussed. (D.C.W.)

31364 DEVELOPMENT AND TESTING OF A LIGHTWEIGHT FLIGHT PROTOTYPE ION ENGINE SYSTEM. King, H. J. (Hughes Research Labs., Malibu, Calif.); Pinckney, K. R.; Knauer, W.; Molitor, J. H.; Muldoon, W. J.; Kovar, D. G. New York, American Inst. of Aeronautics and Astronautics, 1966, Preprint No. 66-216, 33p., $1.50. (CONF-660310-8). ORAU.

From AIAA 5th Electric Propulsion Conference, San Diego, Calif.

The thrustor, the propellant feed system, the power conditioning modules, the hardware test programs, and the control system of a lightweight flight prototype ion-engine system are described. (G.O.Y.)

31365 STEADY STATE OPERATION OF A TWO-STAGE PULSED COAXIAL PLASMA ENGINE. Gorowitz, Bernard; Gloersen, Per; Karras, Thomas W. (General Electric Co., Philadelphia). New York, American Inst. of Aeronautics and Astronautics, 1966, Preprint No. 66-240, 27p., $1.50. (CONF-660310-28). ORAU.

From AIAA 5th Electric Propulsion Conference, San Diego, Calif.

Some changes in the electrode geometry and capacitor-bank electrical characteristics as well as some refinements of the predischarge propellant distribution are described. The efficiency of the electrically triggered pulsed coaxial plasma engine was improved to 67% by these modifications. Operation of the engine for periods of sufficient length to provide steady-state conditions demonstrated that there is no degradation in the measured performance over time spans as long as ten hours. (G.O.Y.)

31366 DEVELOPMENT AND LONG-LIFE PERFORMANCE OF ION ENGINES FOR SATELLITE CONTROL. Anderson, J. Robert; Thompson, S. A. (Hughes Research Labs., Malibu, Calif.). New York, American Inst. of Aeronautics and Astronautics, 1966, Preprint No. 66-234, 43p., $1.50. (CONF-660310-30). ORAU.

From AIAA 5th Electric Propulsion Conference, San Diego, Calif.

Single-strip cesium-contact ion engines covering the thrust range from 0.1 mlbf to 1.0 mlbf were developed. Extensive life testing with a number of engines has demonstrated that this thrustor design potentially has the long life required for satellite control missions for both station-keeping and attitude-control functions. Several steady-state life tests accumulated over 3000 hours of total thrust time, including a successful 2000-hour test at an average thrust level of 0.56 mlbf. Diagnosis of observed accelerator electrode sputtering gives a projected lifetime of three years as limited by charge exchange erosion. Lifetimes greater than five years are possible with high work function ionizers. Neutralizers were operated without failure during these steady-state tests. Specific emission of the filament-type neutralizers averaged 50 mA/W, and no deterioration was observed. The ability of this ion engine design to operate in a pulse mode is currently being demonstrated by cesium life tests of two thrustors for 50,000 cycles each. Electrostatic beam deflection for thrust vector control is incorporated in a prototype station design in which two single-strip thrustors are supplied with cesium from a common zero-gravity reservoir. (auth)

31367 LIFE TESTING OF ELECTRON-BOMBARDMENT CESIUM ION ENGINES. Sohl, G. (Electro-Optical Systems, Inc., Pasadena, Calif.); Speiser, R. C.; Wolters, J. A. New York, American Inst. of Aeronautics and Astronautics, 1966, Preprint No. 66-233, 22p., $1.50. (CONF-660310-31). ORAU.

From AIAA 5th Electric Propulsion Conference, San Diego, Calif.

A model "DF" engine has been operated at a power-to-thrust ratio of 182 kW/lb at 7000 seconds specific impulse for 2610 hours without failure. Redesign of the engine for operation at a power-to-thrust ratio of 160 kW/lb including neutralization and zero-gravity feed system powers is described. The distributed geometry electrode design, which doubled the overall perveance, and redesign of the highly efficient cesium autocathode for increased reliability are described. Development of the plasma-bridge or discharge neutralizer which has been proven highly efficient and reliable is also discussed. Two complete engine systems, with 20- and 40-pound zero-gravity feed systems and plasma-bridge neutralizers, were fabricated. The power-to-thrust ratio for both systems was 150 kW/lb at 5000 seconds specific impulse at the start of long tests conducted with these systems. When this paper was written, both systems were operating satisfactorily and had accumulated 3000 and 1000 hours respectively. Performance to date and performance projections are presented. (auth)

31368 ELECTRON-BOMBARDMENT THRUSTERS USING LIQUID-MERCURY CATHODES. King, H. J.; Eckhardt, W. O.; Ward, W.; Knechtli, R. C. (Hughes Research Labs., Malibu, Calif.). New York, American Inst. of Aeronautics and Astronautics, 1966, Preprint No. 66-232, 21p., $1.50. (CONF-660310-32). ORAU.

From AIAA 5th Electric Propulsion Conference, San Diego, Calif.

Kaufman-type electron bombardment thrustors equipped with liquid-mercury cathodes were built in 10, 15 and 20 cm diameters. One such 20-cm thrustor has passed the 2700 hour point of a continuing life test with no change in performance, thus permitting the system life to be confidently extrapolated well beyond 10^4 hours. The propellant efficiency is 82% and the power efficiency 90% at a beam current of 600 mA. The thrustor design and the measured performance as a function of thrust and specific impulse are discussed. The propellant feed system for this thrustor is unique in that no vapor phase is required because liquid mercury is fed directly to the cathode. A system was developed for monitoring and controlling small ($\ll 1$ cm^3/hr) liquid flow rates in a zero-gravity environment. Closed-loop operation was achieved in which the beam current was used to stabilize and control the propellant feed rate, thus holding the beam current at a set value. There are upper temperature limits imposed for satisfactory operation of the cathode and permanent magnets. These problems have been considered both for a single thrustor and for a module consisting of an array of several individual thrustors. (auth)

31369 ION BEAM DEFLECTION FOR THRUST VECTOR CONTROL. Anderson, J. Robert; Work, George A. (Hughes Research Labs., Malibu, Calif.). New York, American Inst. of Aeronautics and Astronautics, 1966, Preprint No. 66-204, 36p., $1.50. (CONF-660310-15). ORAU.

From AIAA 5th Electric Propulsion Conference, San Diego, Calif.

By controlling the direction of thrust, ion propulsion systems can be used for the combined functions of attitude control and station keeping of a synchronous satellite. Principal advantages of such a control system are the sharing of power supplies and thrustors, reduction of system weight, and easy inclusion of redundant equipment. Because of the electrostatic acceleration process, the ion engine is uniquely suited to purely electric control of the ion beam thrust vector. Electrostatic deflection of ion beams originating from both linear- and button-type ion sources was studied using an electrolytic tank-analog computer controlled trajectory tracer. Quantitative experiments in both linear and cylindrical ion beams were performed. In one experiment, the deflection control from a neutralized cesium beam obtained from a button-type ion source operated under near typical ion engine conditions

was demonstrated in an ion microscope. It showed that it was possible to deflect the cesium ion beam through any azimuthal angle using electrodes divided into insulated quadrants. The deflection was linear with voltage and in good agreement with results of a trajectory tracer study. The ion beam from a linear strip engine was deflected to an angle of 16 degrees. In vacuum better than 10^{-6} Torr, no significant increase in accel current was measured as the beam deflected. Trajectory tracer studies show that electrostatic deflection of the ion beam to an angle of 30 degrees is practical for both single-strip and button-type ion engines. (auth)

31370 SURFACE IONIZATION ENGINE DEVELOPMENT. James, E. L. (Electro-Optical Systems, Inc., Pasadena, Calif.); Worlock, R. M.; Ernstene, M. P.; Forrester, A. T. New York, American Inst. of Aeronautics and Astronautics, 1966, Preprint No. 66-236, 13p., $1.50. (CONF-660310–29). ORAU.

From AIAA 5th Electric Propulsion Conference, San Diego, Calif.

Recent development in surface ionization engine systems is reported. Lifetime limitations are discussed. Results of life testing of sastrugi thrustors are presented and work on an experimental thrustor is reported. The thrustors that have been tested are characterized by a sastrugi porous emitter three inches in diameter. This thrustor is the logical development of earlier work with sastrugi ionizers. The experimental thrustor departs from the sastrugi concept. In this thrustor, circular sources one-eighth inch in diameter are mounted away from the cesium feed manifold on tubes to allow heat shielding of all high temperature components except the actual emitting surfaces. The beam forming electrode is thus kept relatively cool, reducing ion formation on the beamformer and the associated erosion of the accelerator. By spacing the sources on quarter inch centers, the neutral cesium density in the accelerating gap is lowered, thus reducing the number of charge exchange ions formed in the gap and the accelerator erosion resulting from them. (auth)

31371 MERCURY ELECTRON-BOMBARDMENT ION THRUSTOR SUITABLE FOR SPACECRAFT STATION KEEPING AND ATTITUDE CONTROL. Kerslake, William R.; Wasserbauer, Joseph F.; Margosian, Paul M. (Lewis Research Center, Cleveland). New York, American Inst. of Aeronautics and Astronautics, 1966, Preprint No. 66-247, 36p., $1.50. (CONF-660310–24). ORAU.

From AIAA 5th Electric Propulsion Conference, San Diego, Calif.

An ion thrustor system, including a new type of mercury feed system and a shielded neutralizer, was designed and tested at a thrust level of 0.5 millipound. The use of a radial flow propellant distributor and an oxide-coated brush cathode resulted in discharge power losses one-fourth of those previously encountered at this thrust level. Different lengths and diameters of the discharge chamber were tested to establish a compromise between discharge power losses and propellant utilization. The final design discharge chamber was 5-centimeters in diameter and 7.5-centimeters long. The complete flight-type thrustor system used a permanent magnet field and weighed (without propellant) 1.36 kilograms. The power to thrust ratio, including power to heat the feed system and the neutralizer, was 222 watts per millipound at a thrust of 0.65 millipound and a specific impulse of 3050 seconds. The oxide-coated brush cathode was endurance tested 1553 hours in a thrustor and an identical cathode was heat cycled in a separate test for 418,000 cycles before failure. (auth)

31372 PLASMA INVESTIGATION IN A REVERSED CURRENT ELECTRON BOMBARDMENT ION ENGINE. Masek, Tommy D. (California Inst. of Tech., Pasadena). New York, American Inst. of Aeronautics and Astronautics, 1966, Preprint No. 66-246, 19p., $1.50. (CONF-660310–25). ORAU.

From AIAA 5th Electric Propulsion Conference, San Diego, Calif.

Results are presented of an experimental study of the plasma in a cesium electron bombardment ion engine. The engine configuration used has a center anode and an annular cathode, the inverse of conventional bombardment engines. The engine is approximately 10 cm in diameter and uses a molybdenum surfaced cathode through which the propellant is fed. Measurements of electron temperature, ion density, and plasma potential made with a single movable Langmuir probe are presented for several operating conditions. The effects of propellant utilization, magnetic field, and arc conditions on the plasma properties are graphically presented. The plasma measurements are compared with those made in conventional bombardment engines and indicate that the reversed cathode-anode configuration improves the radial ion distribution uniformity in plasma by about a factor of five over the conventional engines. (auth)

31373 DESIGN OF A SOLAR-ELECTRIC PROPULSION SYSTEM FOR INTERPLANETARY SPACECRAFT. Molitor, J. H.; Berman, D.; Seliger, R. L.; Olson, R. N. (Hughes Research Labs., Malibu, Calif.). New York, American Inst. of Aeronautics and Astronautics, 1966, Preprint No. 66-214, 51p., $1.50. (CONF-660310–9). ORAU.

From AIAA 5th Electric Propulsion Conference, San Diego, Calif.

A design study of a solar powered ion propulsion system for an interplanetary spacecraft was performed. The primary objective of this study was to show the feasibility of solar-electric propulsion to interplanetary missions in general. However, to uncover specific problem areas, Mars Orbiter missions utilizing the Saturn IB/Centaur and the Atlas/Centaur boost vehicles were chosen as mission models. The system design constraints which are evaluated include the requirements of the mission, the interface problems between spacecraft and propulsion system, and the characteristics of state-of-art ion engine subsystems; that is, thrustor, feed system, power conditioning and controls. The design considerations presented include analyses on the the effect of power level on the design and operating characteristics of major subsystems, the effect of reliability on choice of thrustor module size and on system design, power matching between solar panel output and engine load, and thrust vector displacement in redundant thrustor arrays. Based on these considerations as well as on analysis of the thermal, mechanical, and electrical integration problems associated with a modularized ion engine system, conceptual designs of both 10 kw and 48 kw propulsion systems are developed. (auth)

31374 DURABILITY TESTS OF MERCURY ELECTRON-BOMBARDMENT ION THRUSTORS. Reader, Paul D. (Lewis Research Center, Cleveland). New York, American Inst. of Aeronautics and Astronautics, 1966, Preprint No. 66-231, 38p., $1.50. (CONF-660310–33). ORAU.

From AIAA 5th Electric Propulsion Conference, San Diego, Calif.

A program to experimentally determine the lifetime of the oxide-cathode mercury electron-bombardment thrustor is described. Runs of 1250 and 1600 hours have been made with a 20-cm diameter thrustor operating at a beam power of 1200 W. The specific impulse values were 5400 and 4300 seconds, respectively, for the two runs. The total accelerator weight loss (30 g) during 3171 hours of testing represented 3.5 percent of the mass of the accelerator grid within the radius of the anode. The material sputtered from the facility was found to significantly affect the accelerator erosion measurements. Several 15 cm thrustors with a beam power of 750 W at 4300 seconds were tested both in the 5 by 16 ft vacuum facility initially used and in a 25 by 70 ft facility. The wire brush, indirectly heated, and oxide-magazine cathodes used in these tests are detailed. A cathode changer is also described. A thrustor control system with primary propellant-feed control based on both an accelerator impingement current and a current-limited ion chamber discharge was used for most of the duration tests. (auth)

31375 DEVELOPMENT OF POROUS IONIZER MATERIALS. Kirkpatrick, M. E.; Mendelson, R. A. (Thompson Ramo Wooldridge Inc., Redondo Beach, Calif.). New York, American Inst. of Aeronautics and Astronautics, 1966,

Preprint No. 66-221, 27p., $1.50. (CONF-660310-5). ORAU.

From AIAA 5th Electric Propulsion Conference, San Diego, Calif.

Two separate approaches to the preparation and fabrication of porous ionizers have been studied, and experimental data relevant to ionizer evaluation are presented. Closely sized, spherical tungsten powders in six separate size ranges were investigated to determine optimum compaction methods, compaction pressures, and sintering parameters. Laboratory evaluations included density, porosity, permeability, pore parameters, mechanical properties, and ionization properties. Porous structures having surface pore densities to 7.4×10^6 pores per cm^2 were produced and investigated. The concept and preliminary experimental data relating to the preparation of porous ionizer structures for two-phase tungsten–rhenium alloys are presented. Arc-cast alloys in the two-phase, sigma plus tungsten solid solution field of the binary tungsten–rhenium system are investigated. Alloys exhibiting suitable microstructures are prepared and methods developed for the removal of the interconnecting sigma phase alloy component. Experimental data pertaining to alloy microstructures and phase removal techniques are discussed. Tungsten–rhenium alloy microstructures exhibiting equivalent surface pore densities exceeding 10 million pores/cm^2 are investigated. (auth)

31376 ANODE LOSSES IN COAXIAL HALL CURRENT ACCELERATORS. Hassan, H. A.; Garrison, G. W. Jr. (North Carolina State Univ., Raleigh). New York, American Inst. of Aeronautics and Astronautics, 1966, Preprint No. 66-201, 17p., $1.50. (CONF-660310-17). ORAU.

From AIAA 5th Electric Propulsion Conference, San Diego, Calif.

Analysis of anode power losses in a coaxial Hall current accelerator is presented. Both the anode and cathode sheaths are assumed to be less than a mean free path. Outside the sheaths, the governing equations are the conservation equations of a partially ionized gas in the presence of electric and magnetic fields and nonequilibrium ionization. In these equations the loss mechanism is a result of conduction and diffusion of electrons, ions and neutrals. A simple geometry consisting of an inner cathode and an outer ring anode combined with an axial magnetic field is considered. The calculations carried out here show that the anode power loss increases with an increase in magnetic field strength and/or total current. Also, if the viscous dissipation is small compared to the power input, the anode power loss is independent of the mass flow rate. The results also show that for the range considered here, the electron contribution to the anode power loss increases and then decreases with an increase in magnetic field strength. (auth)

31377 GEOMAGNETIC THRUSTOR: A HIGH PERFORMANCE ALFVEN WAVE PROPULSION SYSTEM UTILIZING PLASMA CONTACTS. Moore, R. David (Electro-Optical Systems, Inc., Pasadena, Calif.). New York, American Inst. of Aeronautics and Astronautics, 1966, Preprint No. 66-257, 22p., $1.50. (CONF-660310-20). ORAU.

From AIAA 5th Electric Propulsion Conference, San Diego, Calif.

The geomagnetic thrustor is an advanced version of the Alfven propulsion engine previously described by Drell, Foley, and Ruderman. Like the Alfven propulsion engine, the geomagnetic thrustor is similar to an electric motor, using the $\bar{I} \times \bar{B}$ force of the geomagnetic field on a current carrying conductor to provide thrust. The geomagnetic thrustor differs from the Alfven engine in not requiring large surface areas for the photoemission and collection of electrons. Instead, plasma contacts are used which bridge the electrical path between the conductor ends and the ionospheric plasma. The non-directional characteristics of the plasma contactors allow the use of a flexible system composed of the electrical power source and a very long wire terminated with the plasma contactors and oriented by gravity-gradient forces, as opposed to the rigid construction previously proposed. Compared with electric rockets, the geomagnetic thrustor has a considerably better thrust/mass ratio in the region below 5000 kilometers altitude. This is particularly true in the decelerating mode where the geomagnetic thrustor does not require a power supply and the thrust/mass ratio is 10 to 100 times that of the best electric rockets. (auth)

31378 ACCELERATION OF CESIUM IONS BY MEANS OF A NEGATIVE SPACE CHARGE SHEATH. Meyer, Rudolf X. (Aerospace Corp., Los Angeles). New York, American Inst. of Aeronautics and Astronautics, 1966, Preprint No. 66-256, 19p., $1.50. (CONF-660310-21). ORAU.

From AIAA 5th Electric Propulsion Conference, San Diego, Calif.

Initial results of an experimental investigation of the electrostatic acceleration of cesium ions in the presence of a transverse magnetic field are reported. No accelerating electrodes are employed; their function is assumed by a magnetically confined electron sheath which is produced by thermionic emission from a tungsten filament located outside the ion beam. Cesium ions are accelerated in the small gap between the surface of a porous tungsten ionizer and the magnetic field surface intersecting the filament. The magnetic field strength is such that the electron cyclotron radius is small or at most comparable to the length of the accelerating gap (1 mm or less), whereas the motion of the cesium ions is essentially unaffected by the magnetic field. Measurements have indicated that a well collimated ion beam can be obtained. Potential advantages in applying this new concept to electric propulsion may include high perveance and relative freedom from ion sputtering (since no accelerating electrodes are used). The main difficulty with this approach, however, is a strong possibility that at high current densities an excessive leakage of electrons to the ionizer could take place through Bohm diffusion. The ultimate goal of the investigation is to elucidate this point in detail. A summary of the theoretical considerations basic to the operation of the device and a description of some of the experimental results obtained to date are included. (auth)

31379 SURFACE TENSION STORAGE AND FEED SYSTEMS FOR ION ENGINES. Trump, G. E.; Forrester, A. Theodore; Barcatta, F. A. (Electro-Optical Systems, Inc., Pasadena, Calif.). New York, American Inst. of Aeronautics and Astronautics, 1966, Preprint No. 66-249, 29p., $1.50. (CONF-660310-22). ORAU.

From AIAA 5th Electric Propulsion Conference, San Diego, Calif.

A type of zero-g vapor feed system involving no moving parts was developed. Surface tension forces retain the liquid and pump it to a heated surface where vaporization occurs. An analysis was carried out for both wetting and nonwetting liquids. Some zero gravity experiments with wetting fluids were conducted. These experiments used configurations similar to those used in actual propellant systems and provided verification of the surface energy concepts. Extensive laboratory testing of the feed system was also conducted. One was used in an ion engine lift test which continued for 2160 hours with a propellant use efficiency of 99.33 percent. The feed system is lightweight, easily fabricated, has no moving parts, has excellent response and is easily and accurately controlled. (auth)

31380 EXPERIMENTAL EVALUATION OF A TWO-DIRECTIONAL ELECTRON-BOMBARDMENT ION THRUSTOR. Margosian, Paul M.; Kerslake, William R. (Lewis Research Center, Cleveland). New York, American Inst. of Aeronautics and Astronautics, 1966, Preprint No. 66-248, 29p., $1.50. (CONF-660310-23). ORAU.

From AIAA 5th Electric Propulsion Conference, San Diego, Calif.

The possibility of obtaining an ion beam in either of two directions from an electron-bombardment ion thrustor by means of two accelerator-grid systems are investigated experimentally. Of the two thrustors tested, one produced a beam in either of two directions 180° apart, and the other

was capable of producing two beams which diverged at an angle of 90°. The first of the two thrustors was found to perform acceptably over a thrust range of 0.75 to 3.0 millipounds. Leakage ion current from the unused grid system was monitored by three independent means and found to be less than 10 percent of the primary ion beam in most cases. The neutral propellant leakage through the unused grid system constituted an additional loss that was equivalent to about 15 percent of the primary ion beam. A typical operating point was at a thrust of 1 millipound, a power efficiency of 55 percent, a propellant utilization efficiency of 60 percent, and a total power consumption of 250 watts. The second thrustor (90°) did not perform as well. (auth)

31381 CESIUM TRANSPORT THROUGH A TUNGSTEN CAPILLARY. Bates, T. R. (Electro-Optical Systems, Inc., Pasadena, Calif.); Forrester, A. T. New York, American Inst. of Aeronautics and Astronautics, 1966, Preprint No. 66-207, 40p., $1.50. (CONF-660310-14). ORAU.

From AIAA 5th Electric Propulsion Conference, San Diego, Calif.

The problem of cesium transport through tungsten capillaries is being studied as part of an effort to develop an optimum ionizer structure. The assumed model is that cesium transport takes place by coupled molecular flow and surface diffusion through a tungsten capillary and that evaporation along the capillary wall is determined by the function of surface coverage known as the Langmuir isotherm. Previous treatments have used approximations and these led to serious difficulties near the exhausting orifice. These difficulties are eliminated by means of an exact formulation for the distribution of surface coverage along the capillary which takes the form of an integrodifferential equation of second degree. This is reduced to a pure integral equation. Solutions are obtained by iteration and the procedure of boundary matching the capillary solution to the solutions for the front and rear surfaces is carried out for one case. (auth)

31382 POTENTIALS OF SOLAR POWER ELECTRIC PROPULSION. Ritchie, D. (California Inst. of Tech., Pasadena); Toms, R.; Menetrey, W. New York, American Inst. of Aeronautics and Astronautics, 1966, Preprint No. 66-210, 27p., $1.50. (CONF-660310-12). ORAU.

From AIAA 5th Electric Propulsion Conference, San Diego, Calif.

Recent studies have shown that multikilowatt photovoltaic power systems can be integrated with electric propulsion to perform meaningful interplanetary missions in the mid-1970 era. Spacecraft mission capabilities using advanced solar arrays exhibiting 25 to 50 lb per kw will be discussed along with present and projected state of the art of photovoltaic array systems, associated power conditioning, possible array configurations, and systems integration and operational problems. Recent developments in array structures and photovoltaic devices, solar cell matrix integration to substrates and integrated filter systems are all contributing factors to substantial weight decreases in future systems. Some details of current development contracts will be reviewed. (auth)

31383 ELECTRODE MATERIALS FOR CESIUM CONTACT ION THRUSTORS. Wilson, R. G. (Hughes Aircraft Corp., Malibu, Calif.). New York, American Inst. of Aeronautics and Astronautics, 1966, Preprint No. 66-208, 14p., $1.50. (CONF-660310-13). ORAU.

From AIAA 5th Electric Propulsion Conference, San Diego, Calif.

The experimental and analytical data from an extensive program of research on the electron and ion emitting characteristics of cesiated surfaces of a number of candidate materials for ionizers and focus and accel electrodes in cesium ion engines have been obtained, reduced, and compared. High temperature metals with measured work functions higher than that of tungsten (4.50 ev) are rhenium (4.96 ev), osmium (4.83 ev), iridium (5.27 ev), and platinum (5.78 ev), for the particular surfaces studied. However, because of other practical materials considerations, not all of these metals are superior to tungsten for porous ionizers in ion thrustors. No completely satisfactory metal or semiconductor was found among the materials studied for focus electrode surfaces. High temperature insulators, such as alumina, beryllia, zirconia, and thoria, fabricated as thin layers on conductors or directly on the ionizer surfaces probably offer the best possibilities for surface ionization inhibitors. A generalized axiom has been determined for the choice of the best accel electrode material for combination with any given ionizer material, choose, from the group of metals easily desorbable from hot refractory metal surfaces, the metal whose work function matches most closely that of the ionizer. No material superior to copper has been found for combination with tungsten. (auth)

31384 POWER CONVERSION SYSTEM FOR HIGH PAYLOAD LUNAR AND PLANETARY ELECTROSTATIC PROPULSION MISSIONS. Cox, A. Lucile; McDaniel, M. Lee (Brown Engineering Co., Inc., Huntsville, Ala.). New York, American Inst. of Aeronautics and Astronautics, 1966, Preprint No. 66-211, 44p., $1.50. (CONF-660310-11). ORAU.

From AIAA 5th Electric Propulsion Conference, San Diego, Calif.

A comparative analysis of various electrostatic thrustors confirms the need for power systems with specific masses of 10 lb/kwe for planetary missions. A colloidal ion engine, however, might deliver competitive payloads as a lunar freighter with a power system specific mass of 40 lb/kwe. The low pressure colloidal power converter, proposed to meet these requirements, employs a nozzle to convert thermal energy to directed kinetic energy which pushes growing colloidal ions against a field, producing directly the high voltage required by electrostatic thrustors. Theoretical analyses which consider efficiency of energy transfer in collisions, ion retardation by a field, and the colloid cooling rate dependence on gas collisions, show the importance of kinetic factors in this converter. Maximizing conversion efficiency or power density is illustrated for different working fluids. Results of stepwise calculations of the growth and energy exchange processes are compared with experimental results from a cadmium converter operated at the conditions assumed for the analysis. A one-dimensional treatment is employed, since the high degree of collimation which theoretically results from the energy exchange process was experimentally demonstrated. A propulsion system incorporating a colloid thrustor and a colloidal ion power converter is illustrated. (auth)

31385 CHARACTERISTICS OF MICROPOUND RANGE ION THRUSTORS. Worlock, R. M.; Caplinger, E.; Eilenberg, S. L. (Electro-Optical Systems, Inc., Pasadena, Calif.). New York, American Inst. of Aeronautics and Astronautics, 1966, Preprint No. 66-212, 8p., $1.50. (CONF-660310-1). ORAU.

From AIAA 5th Electric Propulsion Conference, San Diego, Calif.

The need for microthrustors is reviewed and a specific application outlined. It is shown that the station keeping requirements of a nominal 500-pound satellite can be met by electric thrustors in the micropound range. The values for significant parameters of such a thrustor are determined and an early design is described. Data for an operating engine are given and thrust vectoring by electrostatic deflection is demonstrated. (auth)

31386 IMPROVED SURFACE IONIZATION EFFICIENCY BY HIGH WORK FUNCTION REFRACTORY METALS AND METAL ALLOYS. Husmann, Otto K. (Hughes Research Labs., Malibu, Calif.). New York, American Inst. of Aeronautics and Astronautics, 1966, Preprint No. 66-223, 36p., $1.50. (CONF-660310-3). ORAU.

From AIAA 5th Electric Propulsion Conference, San Diego, Calif.

The use of high work function refractory metals and metal alloys to improve the ionization efficiency in long term ion engine performance is discussed. Tungsten,

rhenium, iridium, and tungsten–rhenium alloys are investigated with regards to electron work function and threshold temperature for surface ionization. (B.G.D.)

31387 ADVANCED LOW-THRUST PROPULSION SYSTEMS FOR STATION KEEPING AND STABILITY CONTROL OF THE NASA MANNED ORBITAL RESEARCH LABORATORY (MORL): RESISTOJETS AND RADIOISOTOPE THRUSTORS. Goodman, Milton (Douglas Aircraft Co., Inc., Santa Monica, Calif.). New York, American Inst. of Aeronautics and Astronautics, 1966, Preprint No. 66-226, 31p., $1.50. (CONF-660310–2). ORAU.

From AIAA 5th Electric Propulsion Conference, San Diego, Calif.

Results are presented of a preliminary evaluation of resistojets, arcjets, ion engines, radioisotope thrustors, and catalytic monopropellant engines. Descriptions, specifications, and stabilization and control requirements are given for the zero-g and artificial-g spin modes with two electric power configurations: solar cell and Brayton cycle power system. Propellant resupply occurs every 90 days by use of an Apollo logistics vehicle. Propellants studied included cryogenic hydrogen and space storable ammonia and hydrazine. Also included is an assessment of the propellant potential of carbon dioxide, hydrogen, and water in the biowaste resulting from the environmental control and life support cycle. The stabilization and control studies indicated that the drag makeup and attitude control functions previously performed by 50-lb thrust chemical engines, firing for a few seconds per orbit, can be accomplished with millipound thrust engines. The millipound thrust engines may be used in nearly continuous operation in conjunction with control moment gyros. Liftoff, resupply, and 5-year mission weight comparisons resulted in the selection of resistojets and radioisotope thrustors for further detailed studies. (auth)

31388 SURFACE PHYSICS COMPARISON OF IONIZER MATERIALS. Taylor, Lawnie H. (Electro-Optical Systems, Inc., Pasadana, Calif.). New York, American Inst. of Aeronautics and Astronautics, 1966, Preprint No. 66-222, 29p., $1.50. (CONF-660310–4). ORAU.

From AIAA 5th Electric Propulsion Conference, San Diego, Calif.

Surface physics experiments were conducted which measure coverage, and ion and electron mission when cesium is adsorbed upon surfaces of several polycrystalline-wire materials, notably tungsten, rhenium, alloys of W–Re and Mo–Re, molybdenum, tantalum, and iridium, in that order. The data render ion and atom evaporation times, desorption energy, and transition temperatures associated with hysteresis. Two-dimensional critical point temperature for the adsorbed cesium is shown to exist and found to be related to the clean surface electron work function. The work function of iridium, generally regarded as one of the highest known for a metal, is found to be as low as those of molybdenum and tantalum. The electron work function appearing in the Saha equation is shown experimentally to be in disagreement with the value obtained from electron emission Richardson plots when there is evidence of contamination. A correspondence between the maximum obtainable ion current and the bulk lattice structure of the metal is observed. (auth)

31389 EXPERIMENTAL STUDY OF POROUS METAL IONIZERS. Hall, David F.; Cho, Alfred Y.; Shelton, H. (Thompson Ramo Wooldridge Inc., Redondo Beach, Calif.). New York, American Inst. of Aeronautics and Astronautics, 1966, Preprint No. 66-218, 50p., $1.50. (CONF-660310–7). ORAU.

From AIAA 5th Electric Propulsion Conference, San Diego, Calif.

Extensive tests were conducted on 24 samples of porous metal from five manufacturers to evaluate the suitability of the materials for use in cesium contact thrustors by measurement of ionization characteristics. Data obtained include powder size and shape, pore size and pore density, neutral efflux vs. ionizer temperature at ion current densities between 1 and 50 ma/cm^2, and neutral efflux vs. angle. The experimental configuration, which is discussed in detail allows control of the arrival of contaminants at the surface and does not interpose a grid structure between the neutral detector and the ionizing surface. It was found that the burnished, machined surfaces of the samples had to be opened by electrolytic etching and/or sputtering, or by polishing. The angular distribution of the neutral efflux during nonion production was found to be cosine, whereas it is deficient in atoms at large angles to the normal when the accelerating potentials are applied. This finding requires an ~50% reduction of the conventionally measured values of neutral efflux. Neutral effluxes of 0.15 to 0.5 percent at 20 ma/cm^2 were obtained from four materials, with critical temperatures between 1385 and 1450°K. The following effects of contaminants have been noted; applying Be, Cl, Cu, Fe, and Ni to the ionizer surface at ~1 monolayer/sec had little effect on ionizer performance, Al at much lower arrival rates could be tolerated, trace contamination by B, C, Ir, Re, or Si was either acceptable or desirable, Ca, Cr, Mo, Rh, Ta, Ti, and Zr should be avoided, and O_2 and F_2 at high arrival rates reduced neutral efflux and increased critical temperature. (auth)

Vacuum Engineering

31390 INCREASE OF RESIDUAL BACKGROUND GASES DURING ULTRAHIGH-VACUUM MASS-SPECTROSCOPIC ANALYSIS. Rozgonyi, G. A. (Bell Telephone Labs., Inc., Murray Hill, N. J.). J. Vac. Sci. Technol., 3: 187-91(July-Aug. 1966).

It was observed that anomalously high residual background-gas pressures will occur in an ultrahigh-vacuum mass spectrometer exposed to increasing argon pressure. The gases were identified as hydrogen, helium, neon, carbon monoxide, methane, and ethane. The vacuum system is bakeable, with sputter-ion and cryogenic sorption pumps. Vacua of less than 1×10^{-10} torr are routinely obtained. A mechanism is described to account for the appearance of the above gases based on the vacuum-system components. The gases either evolve from the sputter-ion pump or are inefficiently pumped by it. These gases migrate through the system and are adsorbed on the various internal surfaces when the pressure is below 10^{-9} torr. They are subsequently desorbed by argon bombardment, most likely in the vicinity of the total- and partial-pressure gauges, as the argon pressure is increased. In a static system, the residual gases will increase to as much as 1% of the argon pressure. In a dynamic system, the gases are still observed, but at lower concentrations. (auth)

31391 VACUUM SCIENCE AND ENGINEERING. PROPERTIES OF GASES AT LOW PRESSURE; VACUUM MEASUREMENTS; DESIGN AND OPERATING FEATURES OF VACUUM PUMPS AND SYSTEMS. Van Atta, C. M. New York, McGraw-Hill Book Co., 1965. 470p. $15.00.

The discussion of vacuum technology includes a discussion of the nature and flow of gases, a description of the behavior of gases absorbed on solid surfaces, detailed explanations of the performance of various types of vacuum pumps, vacuum gages, and other accessory devices. Also a discussion of the design of vacuum systems both for conventional applications and ultrahigh vacuum is presented. (J.F.P.)

31392 PUMPING SYSTEM AND SINGLE-WALL CHAMBER FOR 10^{-13} TORR. Henderson, W. G.; Mark, J. T. (Radio Corp. of America, Lancaster, Pa.). 10p. (CONF-651046–4). ORAU. Gmelin, AED-CONF-65-403-1.

From 12th National Symposium of the American Vacuum Society, New York.

A pumping system and work chamber to produce pressures of 10^{-13} torr were designed and demonstrated. The chamber is a vertically oriented stainless-steel cylinder of single-wall construction 16 inches in diameter and 24 inches long. A sputter-ion pumping system is used and the chamber is outgassed by two methods: first, by heating to 250°C for several hours and, second, by electron-beam scrubbing. Liquid helium for cryopumping is generated in a refrigerator within the vacuum enclosure. The system can attain 10^{-13} torr in 30 hours from atmospheric pressure including the outgassing cycle. (A.G.W.)

GEOLOGY, METEOROLOGY, AND MINERALOGY

General

31393 (PNE–711F) CLOSE-IN AIR BLAST FROM A RELATIVELY DEEP LOW-YIELD NUCLEAR DETONATION IN BASALT. Project SULKY. Vortman, L. J. (Sandia Corp., Albuquerque, N. Mex.). May 1965. Contract AT(29-1)-789. 27p. Dep. mn. CFSTI $1.50 cy, $0.50 mn.

Close-in air-blast measurements were made on the Sulky shot (an 85-ton nuclear detonation buried 90 feet below the surface in basalt). The dominant overpressure was that resulting from a ground shock, which transmitted pressure to the air at the epicenter; the pressure wave then propagated away from the epicenter at sonic velocity in air. An earlier wave of 1/7 the amplitude of the ground-shock-induced peak propagated at the velocity of a seismic surface wave. It may have been due to gage sensitivity to ground surface motion, or it may have been measurement of overpressure resulting at the gage from such ground motion. The pulse from venting gases was weak because of the relatively great burial depth. It was superimposed on the negative wave following the ground-shock-induced pulse and gave peak values equal to or less than ambient pressure. In one sense, the gas-venting pressures were in agreement with those of Danny Boy, which also were superimposed on a negative wave but which were strong enough to have positive values because of the relatively shallower burial depth. Ground-shock-induced peaks from both Sulky and Danny Boy are in agreement with those from high-explosive shots at comparable burial depths. (auth)

31394 RADIOISOTOPE APPLICATIONS IN HYDROLOGY. (International Atomic Energy Agency, Vienna). pp 115-20 of STI-DOC–10/53.

The determination of hydrological characteristics of a groundwater system, such as rates of recharge, mixing patterns, origin of water, and turnover times, by correlation of the tritium content of groundwater to that of recharging waters is described. (M.C.G.)

Natural Radioactivity and Fallout

See also HEALTH AND SAFETY

Refer also to abstracts 31191 and 31428.

31395 (CEX–58.4.5) AERORADIOACTIVITY SURVEY AND RELATED SURFACE GEOLOGY OF PARTS OF THE SAN FRANCISCO REGION, CALIFORNIA (ARMS-I). Books, Kenneth G. (Geological Survey, Washington, D. C. Division of Biology and Medicine (AEC), Washington, D. C.). Sept. 1963. 24p. Dep. mn. CFSTI $1.00 cy, $0.50 mn.

An aeroradioactivity survey in the San Francisco region, Calif., showed a moderate range of 0 to 1000 counts per second in the levels of natural radioactivity. The lower levels can be related to unconsolidated sediments with a high water content and the higher levels can be related to igneous rocks or alluvium and soils derived from igneous rocks. The survey was approximately 14,000 square miles in area. Continuous radioactivity profiles were obtained with scintillation counting equipment at approximately 500 ft above the ground on parallel northeast-southwest flight lines spaced 1 mile apart. A map of aeroradioactivity levels was prepared from the profiles. (auth)

31396 (CEX–61.6.2) ALBUQUERQUE–LOS ALAMOS AREA (ARMS-II). Guillou, R. B. (Edgerton, Germeshausen and Grier, Inc., Santa Barbara, Calif.). Apr. 1964. 51p. Dep. mn. CFSTI $1.00 cy, $0.50 mn.

An Aerial Radiological Measuring Survey (ARMS) of the Albuquerque–Los Alamos area was part of a nationwide program to measure the present environmental levels of gamma radiation. Approximately 9500 traverse miles were flown, at an altitude of about 500 ft in an area that consists of two 100-mile squares centered on Albuquerque and Los Alamos, N. Mex. Data are presented as aeroradioactivity units, or areas with similar gamma count rates at 500 ft, at two map scales: generalized at about 1:1,000,000, and detailed at 1:250,000. The maximum aeroradioactivity in about one-half of the area is less than 800 counts/sec, and in most of the remainder, it is less than 1200 counts/sec. Maximum count rates of more than 1200 but less than 4000 counts/sec occur in about one-tenth of the area. Aerial measurements of ground radioactivity in the ARMS-II Albuquerque–Los Alamos area were consistent with what was expected, considering the geology of the area. Pre-Cambrian metamorphic rocks, Tertiary intrusive rocks, and rhyolites were generally more radioactive than basaltic and andesitic rocks and clastic materials. Artificial radionuclides were probably present in only small quantities, for background gamma radioactivity was less than 200 counts/sec in several places. (auth)

31397 (RLO–1776-2) HYDROSPHERE: ATMOSPHERE RADIOCHEMICAL MEASUREMENTS. Progress Report, May 1, 1963–April 1, 1966. Fairhall, A. W. (Washington Univ., Seattle. Dept. of Chemistry). Apr. 28, 1966. Contract AT(45-1)-1776. 101p. Dep. mn. CFSTI $4.00 cy, $0.75 mn.

The possibility of using the ^{14}C produced in the atmosphere by nuclear weapons tests in 1961 and 1962 to study atmospheric circulation and mixing phenomena and to study the rate of exchange between atmospheric CO_2 and CO_2 dissolved in the sea is discussed. The air sampling program is described. Data are presented in tables and graphs. Relatively low values of radioactivity were observed in the anticyclonic stratosphere, compared with the cyclonic side of the jet, even up to distances of 12000 ft above the jet core. These low values indicated an upward transport of tropospheric air on the anticyclonic side of the jet. The distribution of ozone in the vicinity of the jet stream indicated the same upward transport of tropospheric air into the anticyclonic stratosphere. Transport of fission product debris by the jet stream was observed. Lower ^{14}C activities were almost invariably associated with anticyclones and higher activities with cyclones. This suggests a different ^{14}C history for these two types of air masses. Data indicated that excess ^{14}C is transferred to the ocean below the mixed layer at about the same rate ^{14}C is added to the ocean surface. ^{14}C inventories were calculated for 5 one to two month periods. A model of atmospheric mixing and exchange with the sea is presented. (M.C.G.)

31398 (NSJ-tr–49) MEASUREMENT OF TRITIUM AT NATURAL LEVELS. Takahashi, Tan. Translated from Genshiryoku Kogyo, 10: No. 2, 65-8(1964). 10p. Dep. mn. JCL $1.10 fs, $0.80 mf. JAERI.

In order to measure the concentration of tritium in natural waters, the distilled sample and NaOH were put into an electrolytic cell, and, by using electrodes of Ni and stainless steel, electrolysis was carried out at 0.15 amp/cm of current density and 10.5°C. When the volume of sample was condensed to 1/12 of the initial volume, the concentration of T was 8 to 10 times as much as that in the initial sample. The initial concentration of T calculated from the measured value on the basis of the concentration-ratio of heavy water was in agreement with the actual concentration of T. The hydrogen generated by contacting the sample vapor to a Mg chip at 570 to 600°C filled the counting tube. The counting tube was made of copper, and its volume is 2.5 liters. The counting tube is surrounded by 18 anticoincidence tubes. The contents of T in river water and tap water at several places in Japan were measured. In 1962, the content of T in tap water was about 100 T.U. (auth)

31399 PRECISION DETERMINATIONS OF ISOTOPE ABUNDANCES. Hintenberger, H. (Max Planck-Institut

fuer Chemie, Mainz). Advance. Mass Spectrometry, 3: Proc. Conf. Paris, 1964, 517-46(1966).

In a review of measurement of isotopic abundances the following points are discussed: usefulness of isotope abundance measurements, basic principles and experimental apparatus for mass spectroscopic isotope abundance measurements, sources of error, examples of isotope abundance measurements with single-collector sector-field instruments, precision measurements of isotopic abundances using instruments with double detectors by comparison with standards, isotope abundance variations in nature, and special methods of isotope abundance measurements. (174 references) (A.G.W.)

31400 MEASUREMENT OF NATURAL ABUNDANCE OF ^{234}U. Bir, R. (CEA-CEN, Saclay, France). Advance. Mass Spectrometry, 3: Proc. Conf. Paris, 1964, 569-70 (1966). (In French).

Measurements of the natural isotopic abundance of ^{234}U were carried out on four samples. Great care was taken to correct for systematic errors. Results are presented and compared with those of previous measurements. (M.J.T.)

31401 DETERMINATIONS OF ISOTOPIC ABUNDANCES OF IRON. Chenouard, J. (CEA-CEN, Saclay, France). Advance. Mass Spectrometry, 3: Proc. Conf. Paris, 1964, 583-4(1966). (In French).

Natural isotopic abundances of ^{54}Fe, ^{56}Fe, ^{57}Fe, and ^{58}Fe were measured, using an Fe^+ surface ionization source. Results, together with those of four previous measurements, are shown. Calculations of the atomic mass of elemental Fe were carried out, starting from the values for the exact masses of the isotopes. The results are given and compared with those from eight other determinations. (M.J.T.)

31402 RELATION OF STRATOSPHERIC-TROPOSPHERIC MASS EXCHANGE MECHANISMS TO SURFACE RADIOACTIVITY PEAKS. Mahlman, J. D. (Colorado State Univ., Fort Collins). (Contract AT(11-1)-1360. Arch. Meterol., Geophys. Bioklimatol., Ser. A, 15: 1-25 (1966).

The atmospheric origin of the debris which produced a sudden increase of surface radioactivity is studied. Because all the radioactivity measurements show the mean debris ages to be greater than one hundred days for the entire sequence, the air is inferred to have been of recent stratospheric origin in view of an assumed mean tropospheric debris residence time of one month. The trajectories of the layer which caused the sudden increase in debris concentration were traced isentropically backward from the point of the fallout increase. The computed trajectory is seen to originate in the region traditionally considered to be the "jet stream front" and is shown definitely to be stratospheric air through potential vorticity considerations. The sinking is associated with upper air cyclogenesis and takes place to the rear of this high level cyclone. The air appears to cross the jet axis as viewed on an isobaric surface, but viewed isentropically, the trajectory is seen to "slip under" the jet core in such manner that no appreciable lateral shears are observed. (auth)

31403 ^{90}Sr IN THE AUSTRALIAN ENVIRONMENT. Kelly, F. H. C. (Univ. of Tasmania, Australia). Austral. J. Sci., 28: 357-8(Mar. 1966).

A study of published data on ^{90}Sr content in sheep bones from various areas in Australia during 1961, 1962, and 1963 indicates that the proximity of high industrial activity is associated with higher content of ^{90}Sr in sheep bones while heavy rainfall appears to have a secondary influence. It is postulated that the smog associated with industrial activity may catalyze precipitation of atmospheric ^{90}Sr. (C.H.)

31404 VERTICAL DISTRIBUTION OF RADON AND THORON AND OF THEIR SHORT-LIVED DECAY PRODUCTS IN THE ATMOSPHERE UNDER STATIONARY CONDITIONS. Bakulin, V. N. (Kirov State Teachers Coll., USSR). Fiz. Atmos. Okeana, 2: 436-8(Apr. 1966). (In Russian).

The proposed solutions of the differential equation on the vertical diffusion of the radioactive emanations Rn and Tn (^{220}Rn) and their daughters in the atmosphere differ primarily because of the method used for finding the value of the vertical diffusion coefficient D as a function of the altitude. In a simplified case, it may be assumed that D has a constant value. Regardless of the value of the coefficient of turbulence near the ground, mixing in the upper layers of the atmosphere exerts a strong suction effect on Rn, preventing the increase of its concentration near the surface. It is thus justified to use the simplest method for finding the value of D. The calculated data based on observations reported in the literature are presented in graphs. The greatest deviations from the equilibrium between the emanations and their daughter products are noted in the surface layers. The concentration of the daughters becomes larger than that of Rn and Tn — especially in the case of the latter above a certain height. Atmospheric precipitation decreases the concentration of the Rn daughters only by 10 to 15%; if the exhalation is not changed, 2 to 3 hours later the original concentration is reestablished. The ThB concentration is more strongly affected by rainfall and is regenerated more slowly. (TTT)

31405 FALLOUT RADIOACTIVITY DUE TO THE UNDERGROUND NUCLEAR TEST OF USSR, JAN. 15, 1965. Kobayashi, Ugoro; Sasaki, Hideho (Niigata Univ., Nagaoka, Japan). J. Radiat. Res. (Jap.), 6: 64-72(June 1965).

Fallout radioactivity in Japan due to a leakage of the underground nuclear explosion test of USSR (Jan. 15, 1965) was investigated. Abnormal increase of radioactive fallout was observed at first on the early morning of Jan. 20 at Nagaoka, Niigata Pref. In the fallout after Feb. 10, the influence by short lived nuclides could not be found. Gamma-ray spectrum of rain-snow sample of Jan. 20 coincided well with that of $^{140}Ba + ^{140}La$, and the counting rate of gamma-rays decayed to a half in every 13 days through the beginning of March. Most part of gamma-activity was considered to be attributed to $^{140}Ba + ^{140}La$ in the transient equilibrium state. Radioactive product, ^{140}Ba, was used as a checking source and $^{140}Ba + ^{140}La$ content in each fallout sample collected after Jan. 20 was estimated. After subtracting $^{140}Ba + ^{140}La$ activity from the total activity in each sample, the residual decayed almost exponentially, with a half-life of 51 to 53 days, extending for a fairly long period of time. Maximum beta-ray energy was estimated to be 1.5 to 1.6 Mev at the end of March when $^{140}Ba + ^{140}La$ was considered to be practically extinct. Thus a chief component of the residual was thought to be ^{89}Sr. Cumulative deposition of $^{140}Ba + ^{140}La$ and other nuclides during the period from Jan. 19 to Feb. 9 was estimated to be about 110 mC/km^2 and 270 mC/km^2 respectively as compared with values of Feb. 15. (auth)

31406 STRONTIUM ISOTOPES AND TRACE ELEMENTS IN CARBONATITES AND LIMESTONES FROM ICE RIVER, BRITISH COLUMBIA. Deans, T. (Overseas Geological Surveys, London); Snelling, N. J.; Rapson, J. E. Nature, 210: 290-1(Apr. 16, 1966).

Specimens from the alkaline complex of the Ice River, comprised of five carbonatites from Aquilla Ridge, three metamorphosed limestones from the contact of the nepheline syenites and ijolites with the Ottertail Limestone, and four specimens of unaltered Ottertail Limestone, are examined. (B.G.D.)

31407 LOCAL GROUND-LEVEL AIR CONCENTRATIONS OF ^{210}Pb AT WINCHESTER, MASSACHUSETTS. Shleien, B.; Friend, A. G. (Public Health Service, Winchester, Mass.). Nature, 210: 579-80(May 7, 1966).

Lead-210 occurs naturally and, due to its 22-yr half-life, is not restricted to the vicinity of its origin. The mean atmospheric residence time for ^{210}Pb has been estimated to be approximately 4 weeks and it has been estimated that about half of the amount of this isotope present in bones is acquired through inhalation. Measurements of the ^{210}Pb content in ground-level air collected at Winchester, Mass., indicate that maritime air contains lower ^{210}Pb concentrations than does continental air. The contribution of local meteorological parameters is discussed. The data support the hypothesis that lower values of ^{210}Pb in the bones of

island dwellers can be attributed to the lower atmospheric concentration of ^{219}Pb over oceans. (C.H.)

31408 FRESH FALLOUT IN ISRAEL FROM THE SECOND CHINESE NUCLEAR DETONATION. Eisenberg, A. (Ministry of Health, Jerusalem); Donagi, A.; Prulov, Y.; Shalmon, E.; Feige, Y. Nature, 210: 833-4(May 21, 1966).

A nuclear detonation was reported on the Chinese mainland on May 14, 1965. The test was apparently conducted in the atmosphere and involved a ^{235}U fission device. Fallout attributable to this detonation was detected on air filter samples in Israel on May 28, 1965. About three weeks later ^{131}I was detected in milk samples and animal thyroids. Monitoring data collected through Nov. 15, 1965 are summarized. (C.H.)

31409 RADIOCHEMICAL DATA CORRELATIONS FOR SEAWATER AND CORAL-SURFACE BURSTS. Crocker, G. R. (Naval Radiological Defense Lab., San Francisco). Nature, 210: 1028-31(June 4, 1966).

Radiochemical data from 3 high-yield nuclear bursts of Operation Hardtack, one on a coral surface, one on the surface of deep water, and one on the surface of shallow water over a coral bottom, were analyzed for evidence of fractionation in fallout formation. Data are tabulated for ^{45}Ca, ^{89}Sr, ^{90}Sr, ^{91}Y, ^{99}Mo, ^{136}Cs, ^{137}Cs, ^{156}Eu, ^{237}U, ^{24}Na, ^{144}Ce, and ^{239}U. Parameters are compared with data from Operation Redwing. (C.H.)

31410 ^{14}C VARIATIONS IN NATURE. PART 2. INCREASE IN ^{14}C ACTIVITY IN THE ATMOSPHERE OF THE SOUTHERN HEMISPHERE FROM THE TESTING OF NUCLEAR WEAPONS. Rafter, T. A. (Inst. of Nuclear Sciences, Lower Hutt, New Zealand). New Zeal. J. Sci., 8: 472-93(Dec. 1965).

One hundred and thirty measurements of the ^{14}C activity of the atmosphere collected at Makara, New Zealand; Melbourne, Australia; Lauthala Bay, Fiji, and Scott Base, Antarctica are presented. At Makara, New Zealand, a record of the ^{14}C activity of the atmosphere kept since November 1954 showed the build-up in ^{14}C activity in the Southern Hemisphere from the testing of nuclear weapons in the Northern Hemisphere. ^{14}C activity slowly increased to mid-1959, remained essentially constant for 2½ years then, after mid-1962, increased considerably following the 1961–62 bomb test series. The ^{14}C activity of the atmosphere in the Southern Hemisphere is remarkably uniform, showing only small variations with latitude. The ^{14}C activity enters the southern troposphere not only through the mid-latitude stratospheric-tropospheric break but also from across the Equator. The Northern Hemisphere, from 1955 to the end of 1958, remained several percent higher in ^{14}C activity than the Southern Hemisphere. Although large fluctuations in activity at higher latitudes in the Northern Hemisphere in 1959 were reported, only minor fluctuations were recorded at Makara two years later. Following the moratorium on bomb testing the ^{14}C activity in both hemispheres rapidly approached a uniform ^{14}C activity of approximately 22% above the pre-bomb level. A very rapid increase in ^{14}C activity from the USSR tests of September-October 1961 was apparent in the Northern Hemisphere commencing in January 1962. A similar rapid increase was observed at Makara 12 months later. An indication that an influx of ^{14}C reached New Zealand within a few weeks of the 1961 September-October USSR tests was observed but whether this is due to these tests or to inhomogeneities in the ^{14}C activity of the lower stratosphere, was not definitely established. Comparisons were made between Northern and Southern Hemisphere measurements. (auth)

31411 RADIOACTIVE RAIN, SNOW, AND ATMOSPHERIC CONTAMINATION OBSERVED IN NAGAOKA CITY, JAPAN. II. TOTAL INTENSITIES OF THE RADIOACTIVE FALLOUT DURING THE YEAR 1965. Kobayashi, Ugoro; Sasaki, Hideho (Niigata Univ., Japan). Niigata Daigaku Kogakubu Kenkyu Hokoku, No. 15, 1-13(Mar. 1966). (In Japanese).

As a sequel to the research over the last ten years, the artificial radioactivity of rain, snow, and air-borne dusts in Nagaoka City due to nuclear detonations was investigated in 1965. Owing to underground nuclear test of U.S.S.R. Jan. 15, 1965, the radioactive fallout increased rapidly on 20th January, and a high level of contamination continued for several days and diminished gradually until the middle of May. In the latter part of May the radioactive fallout increased again on account of the nuclear test of China on May 14th, but the contamination by this test did not remain so long and diminished not later than the end of June. With the exception of these two periods, the contamination by artificial radioactivity due to nuclear tests has, on the whole, diminished through 1965. (auth)

31412 RADIOACTIVE GIANT PARTICLES CONTAINED IN RADIATION FALLOUT. REPORT V. Kobayashi, Ugoro; Sasaki, Hideho (Niigata Univ., Japan). Niigata Daigaku Kogakubu Kenkyu Hokoku, No. 15, 15-19(Mar. 1966). (In Japanese).

Giant radioactive particles were found on the morning of May 17, three days prior to the arrival of fresh nuclear debris from the Chinese test. The density of distribution of giant particles was not large, but the contamination per unit area was higher than that from radioactive air-borne dusts. Radioactivity per unit volume of giant particles was about 2 $\mu\mu C/\mu^3$ 50 days after the nuclear test and about $1\mu\mu C/\mu^3$ 100 days after the test. Giant particle activity was about 100 times that from the first Chinese test on Oct. 16, 1964. From the decay characteristics, it was concluded that the giant particles were richer in $^{95}Zr-^{95}Nb$ than the radioactive substances normally found in rain water. (auth)

31413 OBSERVATIONS OF THE FALLOUT RADIONUCLIDES AT KANAZAWA. Sakanoue, Masanobu; Osawa, Masumi (Kanazawa Univ., Japan). Sci. Repts. Kanazawa Univ., 10: No. 2, 69-78(Dec. 1965).

From January 1963 to May 1965, four events in regard to the fallout were experienced at Kanazawa, owing to nuclear tests in foreign countries. In these cases, some studies were carried out by the members of the radiochemical laboratory of Kanazawa University and their results are reported. (auth)

31414 ^{90}Sr IN THE WATERS OF THE PACIFIC OCEAN. REPORT 3. ON VERTICAL DISTRIBUTION IN THE CENTRAL REGION, 1961. Popov, N. I.; Patin, S. A.; Polevoi, V. A.; Konnov, V. A. Tr. Inst. Okeanol. Akad. Nauk SSSR, 82: 5-15(1966). (In Russian).

The results of determinations of ^{90}Sr concentration in deep waters of the Central Pacific at the end of 1961 are presented. The vertical distribution of ^{90}Sr along the 162th meridian, East, and 176th, 154th, 140th meridians, West, from 18°S to 15°N was obtained. The horizontal samples included practically all the water strata of the ocean from the surface to the bottom. The common regularities of vertical distribution of ^{90}Sr in the Pacific Ocean were determined. The amount of ^{90}Sr under the surface of the ocean in the limits of the region investigated was estimated. (auth)

31415 ^{90}Sr IN THE WATERS OF THE PACIFIC OCEAN. REPORT 4. THE SURFACE WATERS OF THE SOUTH CHINA SEA, 1962. Popov, N. I.; Orlov, V. M.; Dabizha, V. F. Tr. Inst. Okeanol. Akad. Nauk SSSR, 82: 16-19(1966). (In Russian).

The results of determinations of ^{90}Sr concentration in the surface waters of the South China Sea and in regions adjacent to the Pacific Ocean in November, 1962 are presented. It was determined that the concentration of ^{90}Sr in the surface waters of this region was not changed in comparison with 1961. (auth)

31416 ^{90}Sr CONTENT OF THE WATERS OF THE PACIFIC OCEAN IN 1962 AND IN 1964. Chumichev, V. B. Tr. Inst. Okeanol. Akad. Nauk SSSR, 82: 20-3 (1966). (In Russian).

The results of determinations of ^{90}Sr concentration on the surface and in subsurface layer in the central region of the Pacific Ocean are presented. In July and August, 1962, the concentration of ^{90}Sr was somewhat higher than in January. In January and February, 1964, concentrations of ^{90}Sr were the same as in January, 1962. (auth)

31417 ^{90}Sr IN DEEP WATERS OF THE INDIAN OCEAN. Popov, N. I.; Orlov, V. M.; Patin, S. A. Tr. Inst. Okeanol. Akad. Nauk SSSR, 82: 24-31(1966). (In Russian).

Results of determinations of ^{90}Sr concentration in the deep waters of the Indian Ocean in 1960 and 1961 are presented. The region of the ocean from 40°S to the Arabian Sea and including the Bay of Bengal was investigated. ^{90}Sr was found everywhere within the whole strata of water in the ocean from the surface to the bottom. The amount of ^{90}Sr per square unit of the surface of the ocean was estimated. (auth)

31418 DISTRIBUTION OF ^{90}Sr ON THE SURFACE OF THE ATLANTIC OCEAN DURING THE SECOND PART OF 1961. Patin, S. A.; Aleksandrov, A. V.; Orlov, V. M. Tr. Inst. Okeanol. Akad. Nauk SSSR, 82: 32-4(1966). (In Russian).

Results of the determination of ^{90}Sr concentration in the surface waters of the Atlantic Ocean are presented. The concentration of ^{90}Sr in 1961 was the same as was observed in previous years. ^{90}Sr concentration varied in the surface layer of ocean according to latitude of the region in each hemisphere. (auth)

31419 CONCENTRATIONS OF LONG-LIVED FISSION PRODUCTS FROM NUCLEAR TEST EXPLOSIONS IN THE SURFACE WATERS OF THE WORLD OCEANS DURING MORATORIUM OF 1959-1961. Popov, N. I. Tr. Inst. Okeanol. Akad. Nauk SSSR, 82: 35-41(1966). (In Russian).

Published data on the concentrations of long-lived fission products in the surface waters of the oceans are considered. Average concentrations of ^{137}Cs, ^{90}Sr, ^{147}Pm, ^{106}Ru, ^{144}Ce, ^{14}C and ^{3}H in different regions of the oceans of the world in 1960 and 1961 were estimated. (auth)

31420 THE PRIMARY FEATURES OF GLOBAL DISTRIBUTION OF ^{90}Sr ON THE SURFACE OF WORLD OCEANS (1960-1961). Popov, N. I.; Patin, S. A. Tr. Inst. Okeanol. Akad. Nauk SSSR, 82: 42-55(1966). (In Russian).

The geographical distribution of ^{90}Sr on the surfaces of the Pacific, the Indian, and the Atlantic Oceans and on the surfaces of some seas according to known data on the concentration of ^{90}Sr in their surface waters is considered. The concentration of ^{90}Sr in the surface layers of the oceans and of the seas apparently fluctuates. However, every region may be characterized by an average ^{90}Sr concentration. According to the degree of contamination the oceans are in the following order: Atlantic, Indian, Pacific. The waters of the northern hemisphere are characterized by higher ^{90}Sr concentration than the waters of the southern hemisphere. The seas have higher contamination in comparison with the waters of the open ocean at the same latitudes. An accumulation of ^{90}Sr in the surface layers of oceans is significantly behind the rate of ^{90}Sr deposition from the atmosphere. The ^{90}Sr concentration in the surface layers of oceans remained unchanged during the last few years with the exception of the Pacific Ocean, where exceptionally high concentrations of ^{90}Sr after nuclear tests on the Pacific Islands were observed. (auth)

31421 COMPARATIVE ANALYSIS OF GLOBAL DISTRIBUTION OF NUCLEAR TEST EXPLOSION FALLOUT OVER CONTINENTS AND OCEANS. Karol, I. L.; Krasnopevtsev, Yu. V.; Vilenskii, V. D.; Malahov, S. G. Tr. Inst. Okeanol. Akad. Nauk SSSR, 82: 56-71(1966). (In Russian).

A qualitative and quantitative comparison of intensities of world-wide radioactive fallout on the ocean and on the continents was carried out by means of the estimation of ^{90}Sr accumulated per square unit of the ocean surface and per square unit of the continents' surface at the same latitudes. The results of direct measurements of radioactive fallout intensity on the continents and on the islands and the data on the concentration of radioactive fission products in the air above the sea surface and above the surface of dry land were considered. On the basis of the considered data it is assumed that the intensity of radioactive fallout on the sea surface is higher than it is on the surface of dry land. (auth)

31422 STUDIES OF THE FORMS OF EXISTENCE AND MIGRATION OF ARTIFICIAL RADIOISOTOPES IN SEA WATERS. Patin, S. A. Tr. Inst. Okeanol. Akad. Nauk SSSR, 82: 72-90(1966). (In Russian).

Data on sources and distribution of artificial radioisotopes and their natural carriers within sea water are considered. The characteristic groups of radionuclides are distinguished in accordance with the peculiarities of their physical states and in connection with the regularities of their migration within the ocean. Hydrological factors determine the distribution of ^{90}Sr and of ^{137}Cs within the ocean. The isotopes of rare earths, zirconium, niobium, and ruthenium migrate both as the active forms and the components of the ocean sediments. The isotopes of iron, manganese, and zinc take active part in the process of the biocirculation. (auth)

31423 ON THE RELIABILITY OF THE PRESENT DAY CHEMICAL DETERMINATIONS OF ^{90}Sr IN THE SEA WATER. Popov, N. I.; Patin, S. A. Tr. Inst. Okeanol. Akad. Nauk SSSR, 82: 91-106(1966). (In Russian).

The errors in different stages of the sea water analysis for determination of ^{90}Sr including estimations of chemical yield of ^{90}Sr and of ^{90}Y, measurement of the ^{90}Y activity, and identification of ^{90}Y are considered. The analysis of possible errors indicated that the measurement of ^{90}Y activity is the most unreliable stage of ^{90}Sr determination at present concentrations of ^{90}Sr in the seas and oceans. Sources of error and statistical methods of correction are discussed. (J.G.B.)

31424 RADIONUCLIDE CONCENTRATIONS IN INDIVIDUAL FALLOUT PARTICLES. Benson, Philip A. (TRACERLAB, Richmond, Calif.). 22p. (CONF-650616-26; TLW-1105). ORAU.

From Health Physics Society, Annual Meeting, Los Angeles.

Gross beta activities of isolated fallout particles from high-altitude nuclear explosions are plotted as a function of particle diameter. The decay rate of the particles was determined during the period 3 to 200 days after time zero. Values of the decay constants varied from 0.7 to 1.4 with an average value of 1.10. No correlation was found between the decay slope and particle size or color. The radionuclide distributions in selected particles were analyzed radiochemically and by gamma spectrometry. The ^{95}Zr, ^{140}Ba, ^{141}Ce, and ^{144}Ce contents of single particles as a function of particle diameter are shown. (A.G.W.)

Site Survey and Selection

31425 (PNE-481, pp 1115-19) AERORADIOACTIVITY SURVEY OF THE LISBURNE PENINSULA AND ADJACENT AREAS. Bates, Robert G. (Geological Survey, Washington, D. C.).

A detailed airborne radioactivity survey was made of a 1000-sq-mile area centered at Cape Thompson on the Lisburne Peninsula. An additional 600 miles of single-line traverses were also flown east of the detailed area. Radioactivity levels ranged from 50 to 750 counts/sec and averaged about 300 to 400 counts/sec. Highest values were recorded over exposed river gravels and areas of little or no vegetation cover. Lowest values were associated with areas of thick vegetation cover and with swampy areas, particularly near the Arctic Ocean. (auth)

31426 (PNE-481, pp 1121-39) ADSORPTION EQUILIBRIA BETWEEN EARTH MATERIALS AND RADIONUCLIDES. Baker, J. H.; Beetem, W. A.; Wahlberg, J. S. (Geological Survey, Menlo Park, Calif.).

The concept and the derivation of a distribution coefficient are developed. Ion exchange and the nature of competition among cations are discussed. Distribution coefficients for carrier-free cesium, strontium, and iodine were determined on 17 soil samples collected during July 1961 in the vicinity of Cape Thompson. High percentage uptake of these ions was measured under the test conditions. Cesium adsorption

after 1 day was found to be represented by the mass-action equation. The distribution coefficients for cesium adsorption were so large that in all but a few cases very little of this nuclide would remain long in solution in the natural waters of the area. Strontium adsorption was found to be a function of the calcium-plus-magnesium concentration and independent of the sodium concentration. In most samples strontium equilibrium was reached in less than 1 day. Iodine sorption varied with percent organic matter in the samples. If the iodine were in contact with organic matter for several days, a substantial part of it probably would be removed from solution in the natural waters. (auth)

31427 (PNE-481, pp 1141-9) RADIOLOGICAL ANALYSES OF MARINE ORGANISMS. Seymour, Allyn H. (Washington Univ., Seattle. Lab. of Radiation Biology).

The radionuclide content of Chukchi Sea organisms collected from 1959 to 1962 was determined to establish a reference point for samples that were expected to be collected after the Chariot event. Of the 50 sample types counted for gross-beta activity, only a few individual samples exceeded the counting rate of naturally occurring radionuclides. Cerium-144 and strontium-90 were present in an occasional sample but in amounts that were only slightly greater than the limits of detection. Strontium-90 values in sea water were 21 and 41 disintegrations/min/100 liters in 1959 and 1961, respectively. Fallout nuclides from the autumn 1961 USSR experiments were not present in samples from an under-the-ice collection made at the Chariot site in May 1962. The absence of fallout radionuclides in marine organisms from the Chukchi Sea and their presence in lichens, caribou, and other terrestrial organisms from adjacent areas in the consequence of greater physical and chemical dilution in the sea and holdup of the entry of radionuclides into seawater when fallout occurs during time of ice cover. (auth)

31428 (PNE-481, pp 1165-1200) RADIONUCLIDES IN TERRESTRIAL AND FRESHWATER BIOTA. Watson, D. G.; Hanson, W. C.; Davis, J. J.; Rickard, W. H. (General Electric Co., Richland, Wash. Hanford Atomic Products Operation).

The kinds, amounts, and distribution of radionuclides originating from worldwide fallout were studied in the biota of the Chariot site from 1959 through 1962. Possible routes of uptake and transfer of fallout nuclides are discussed. Foliar adsorption appeared to be the principal route of radionuclide uptake by plants, and plants with persistent aerial parts had highest levels of radionuclides. Levels of ^{137}Cs and ^{90}Sr in caribou were several fold greater than in ruminants from the contiguous United States. (auth)

Techniques and Equipment

31429 ISOTOPE CHRONOLOGY AND RECORDED HISTORY. Libby, Willard F. Int. At. Energy Agency Bull., 8: No. 2, 28-37(June 1966).

Radiocarbon dating is discussed with regard to its relation to recorded history and ascertaining dates that important things in history occurred. Examples are described. (M.C.G.)

31430 SINGLE-WELL METHOD FOR DETERMINING THE DIRECTION OF FLOW OF GROUND WATER USING A NEUTRON SOURCE. Selecki, A.; Filipek, S. (Polytechnic of Warsaw). Int. J. Appl. Radiat. Isotop., 17: 351-2(June 1966).

In the closed neutron source method proposed, the absorption of neutrons by compounds containing lithium, boron, cadmium, etc., is utilized. A solution of these salts is poured into the bore-hole. The probe, containing in its lower part a neutron source of 2 to 3C activity, is introduced. A neutron counter is placed acentrically above the source. By turning the probe around its vertical axis and measuring the intensity of the dispersed neutron stream every $1/8$ or $1/16$ part of the circle showed the direction of lowest neutron stream intensity, which is identical with the direction of the neutron absorbing substances displacement and consequently identical to water flow direction. (M.C.G.)

31431 POTASSIUM–ARGON DATING BY ACTIVATION WITH FAST NEUTRONS. Merrihue, Craig; Turner, Grenville (Univ. of California, Berkeley). J. Geophys. Res., 71: 2852-7(June 1, 1966).

Preliminary data are presented on a new technique of potassium–argon dating, in which neither potassium and argon absolute abundances are required. It is shown how the method may be usefully extended by observing variations in the isotopic ratio with temperature during gas release. (B.G.D.)

31432 'DATING' GROUND WATERS OF AGES YOUNGER THAN 1,000–1,500 YEARS USING NATURAL ^{32}Si. Nijampurkar, V. N.; Amin, B. S.; Kharkar, D. P.; Lal, D. (Tata Inst. of Fundamental Research, Bombay). Nature, 210: 478-80(Apr. 30, 1966).

The possibility of using ^{32}Si, half-life of about 500 yr which is continuously produced in the atmosphere by spallation of argon by the primary and secondary particles of cosmic rays, for the dating of ground waters of ages younger than 1,000 to 1,500 years was investigated. Silicon-32 decays by β emission to ^{32}P, half-life of 14.3 days, and ^{32}Si activity is conveniently determined by milking ^{32}P activity. Results are reported from measurements of ^{32}Si content in surface and ground waters from various locations. Age estimations of some of the samples were compared with age estimations based on tritium activity. It was concluded that ^{32}Si activity can be used to determine upper limits of age within a few hundred years, and possibly for precise dating of ground waters. (C.H.)

31433 ^{14}C VARIATIONS IN NATURE. PART 1. TECHNIQUE OF ^{14}C PREPARATION, COUNTING, AND REPORTING OF RESULTS. Rafter, T. A. (Inst. of Nuclear Sciences, Lower Hutt, New Zealand). New Zeal. J. Sci., 8: 451-71(Dec. 1965).

The chemical procedures, the counting equipment, and methods of reporting ^{14}C ages and ^{14}C enrichments as at present in operation at the Carbon–14 Laboratory of the Institute of Nuclear Sciences, New Zealand, are described. Carbon dioxide is used as the counting gas in an 8-liter proportional counter capable of being operated up to 2 atm pressure. In addition to ^{14}C aging a considerable amount of research was directed into the study of ^{14}C enrichments in the atmosphere, ocean waters, and biological specimens. (auth)

31434 MINERAL EXPLORATION AND SOIL ANALYSIS USING IN SITU NEUTRON ACTIVATION. Senftle, F. E.; Hoyte, A. F. (Geological Survey, Washington, D. C.). Nucl. Instrum. Methods, 42: 93-103(June 1966).

A feasibility study was made to operate by remote control an unshielded portable positive-ion accelerator type neutron source to induce activities in the ground or rock by in situ neutron irradiation. Selective activation techniques make it possible to detect some thirty or more elements by irradiating the ground for periods of a few minutes with either 3-Mev or 14-Mev neutrons. The depth of penetration of neutrons, the effect of water content of the soil on neutron moderation, gamma ray attenuation in the soil and other problems are considered. The analysis shows that, when exploring for most elements of economic interest, the reaction $^{2}H(d,n)^{3}He$ yielding ~3-Mev neutrons is most practical to produce a relatively uniform flux of neutrons of less than 1 kev to a depth of 19–20''. Irradiation with high energy neutrons (~14 Mev) can also be used and may be better suited for certain problems. However, due to higher background and lower sensitivity for the heavy minerals, it is not a recommended neutron source for general exploration use. Preliminary experiments were made which indicate that neutron activation in situ is feasible for a mineral exploration or qualitative soil analysis. (auth)

31435 SOIL-MOISTURE MEASUREMENT BY THE NEUTRON METHOD IN ROCKY WILDLAND SOILS. Koshi, Paul T. (Forest Hydrology Lab., Tempe, Ariz.). Soil Sci. Soc. Amer. Proc., 30: 282-4(Mar.-Apr. 1966).

To accurately interpret moisture readings taken by the neutron-scattering technique in rocky soils, methods of access tube installation, influence of voids and rocks around access tubes, and accuracy of factory calibration curve were evaluated. Because access tubes could not be installed by the hand-auger method where hard rocks were present, power-driven portable drilling rigs were tried. Vacuum evacuation of cuttings in wet soils failed. Water injection worked well except in the presence of loose rocks. Air injection was most satisfactory except in wet clays. Voids around access tubes of $<^3/_8$ inch had little or no influence on slow neutron count rates. Rocks had little influence on soil moisture determination unless they were large. Because readings of soil moisture from factory calibration seemed too high, a laboratory calibration curve was developed. (auth)

Thorium and Uranium Minerals

31436 WORLD RESERVES OF URANIUM AND THORIUM. At. Strom, 12: 34-40(Mar.-Apr. 1966). (In German).

The preliminary results in the evaluation of the world's reserves in uranium and thorium for the price range 5 to 10, 10 to 15, and 15 to 30 dollars/lb were reported. The reliability of the evaluations is discussed. The availability of uranium from sea water is considered. The estimated uranium reserves are reported for the individual countries excluding the Soviet Union, China, and Eastern Europe. (J.S.R.)

31437 URANIUM IN COAL-BEARING BEDS OF MIKAWA AND AKATANI AREAS, NIIGATA PREFECTURE. Takeda, Eizo; Mochizuki, Tsunekazu (Geological Survey of Japan). Chishitsu Chosasho Geppo, 16: No. 9, 1-29 (Sept. 1965).

The uranium contents of 129 samples in Mikawa and Akatani areas ranged from 2 to 450 ppM U_3O_8. It was clearly recognized that uranium is more concentrated in coaly shales or mudstones which have higher ash content than in the good coal. It is considered that the carbonaceous matter has played important roles in uranium enrichment, in the way of not only adsorber but also of preparing and reserving the reducing environments, which enable and accelerate the adsorption of uranium. (auth)

31438 THORIUM RESOURCES IN THE UNITED ARAB REPUBLIC AND THEIR POSSIBLE UTILIZATION. El Shazly, E. M. (United Arab Republic Atomic Energy Establishment, Cairo). pp 186-98 of STI-DOC-10/52.

Thorium resources of the following types are discussed: Th–U mineralizations in the basement rocks, monazite-bearing beach placers on the Mediterranean Sea coast of Sinai, and monazite-bearing beach placers on the Mediterranean Sea coast derived from the Nile and localized between Damietta and Port Said, East Rosetta and West Rosetta. (M.O.W.)

HEALTH AND SAFETY

See *also* BIOLOGY AND MEDICINE — Radiation Hazards and Protection
GEOLOGY, METEOROLOGY, AND MINERALOGY — Natural Radioactivity and Fallout

Refer also to abstracts 31164 and 32855.

31439 (AECL–2540) ANALYSIS OF EXTERNAL RADIATION EXPOSURES IN 1965. Cowper, G.; Knight, G. B.; Rowe, P. C. (Atomic Energy of Canada Ltd., Chalk River (Ontario)). Feb. 1966. 16p. Dep. mn. AECL $0.50.

An analysis of occupational radiation exposures received by workers at AECL sites in 1965 was carried out by machine accounting methods. Results of β and γ radiation as determined from dosimeter films are presented in tables and graphs. (C.H.)

31440 (ANL–7175, pp 159–83) REACTOR SAFETY. (Argonne National Lab., Ill.).

Results of basic studies on metal-water reactions related to water-cooled reactor accidents are reported. Results of investigations are also reported concerning reactions of fuel and cladding materials with liquid Na, transient heat transfer, fuel migration and segregation in mixed U–Pu compounds, properties of fast reactor materials, and reactions of Na with air. (J.R.D.)

31441 (BNWL-SA–40) IDERM: AN ANALOG COMPUTER PROGRAM FOR INTAKE, DISTRIBUTION AND EXCRETION OF RADIONUCLIDES IN MAMMALS. Watson, E. C.; Harvey, R. A.; Bustad, L. K. (Battelle-Northwest, Richland, Wash. Pacific Northwest Lab.); Hauser, H. N. (Columbia Basin Coll., Pasco, Wash.); Panesko, J. V. (General Electric Co., Richland, Wash. [Hanford Atomic Products Operation]). June 3, 1965. Contracts AT(45-1)-1830; AT(45-1)-1350. 17p. (CONF-650616–3). Dep. mn. CFSTI $1.00 cy, $0.50 mn.

From Health Physics Society Annual Meeting, Los Angeles.

The environmental consequences of accidental releases of radionuclides ultimately involve the exposure of people to ionizing radiations. Generally, this exposure consists of two components: One results from exposure to emissive radiations of radionuclides external to the human body. The other and equally important component derives from internally deposited material following ingestion or inhalation of the released radionuclides. An analog computer program was developed to facilitate a realistic appraisal of the internal exposure following an accidental release of radionuclides. The program is generally applicable to mammals provided suitable values of biological parameters are available. Both chronic and short term intakes can be accommodated whether intake is by inhalation, ingestion, percutaneous absorption or injection. Although the program presently computes organ burdens only for the parent radionuclide and first daughter, it could be easily expanded to include a second or more daughter radionuclides. A mathematical model of organ burdens is presented for the ingestion of ^{132}Te which decays to ^{132}I. The contribution to organ dose from ^{132}I is included. (C.H.)

31442 (BNWL-SA–661) RADIOECOLOGICAL CONCENTRATION PROCESSES CHARACTERIZING ARCTIC ECOSYSTEMS. Hanson, W. C. (Battelle-Northwest, Richland, Wash. Pacific Northwest Lab.). Apr. 25, 1966. Contract AT(45-1)-1830. 22p. (CONF-660405–13). Dep. mn. CFSTI $1.00 cy, $0.50 mn.

From Symposium on Radioecological Concentration Processes, Stockholm.

The lichen-reindeer-(caribou)-man food chain has been observed to constitute the most important concentration process for fallout radionuclides in Arctic regions. The higher levels of most radionuclides, especially ^{90}Sr and ^{137}Cs, within this system result from the tendency for lichens to absorb and retain fallout material; the utilization of lichens for food, by reindeer and caribou especially in winter, and the dependence upon reindeer and caribou for food by certain northern populations. Although there are differences in radionuclide concentrations in plants and animals from various locations within the Arctic region, the same general ecological processes have been found to efficiently transfer significant amounts of radionuclides. Differences in radionuclide behavior within Arctic ecosystems in Alaska, Finland, and Sweden have resulted from the important effects of climatic factors, animal behavior, food habits, physiological parameters, and human cultural practices. Cesium-137 has proved to be the most important fallout radionuclide from the standpoint of rates, routes, and amounts cycled within Arctic ecosystems, and a most useful tool for radioecological research. (48 references.) (auth)

31443 (CONF-650673–1) CALIBRATION PROBLEMS IN WHOLE-BODY COUNTING WITH NaI(Tl) DETECTORS. Dudley, R. A.; ben Haim, A. (International Atomic Energy Agency, Vienna (Austria)). [nd]. Contract AT(30-1)-2819. 21p. Dep. mn. CFSTI $1.00 cy, $0.50 mn.

From Meeting on Clinical Uses of Whole-Body Radioactivity Counting, Vienna.

An evaluation of NaI(Tl) detectors was made for whole-body counting. Measurements on people containing known tracer doses of various isotopes, measurements on phantoms of various sorts, and computer calculations both for the conditions of measurement and for other conditions were made. Each measurement was made with a single NaI(Tl) detector suspended inside a steel room and connected to a multichannel analyzer. Three different detectors were tested: 8″ D × 4″, 4″ D × 4″, and 3″ D × 3″ NaI(Tl) crystals. Results are presented. (M.O.W.)

31444 (CONF-660405–15) RESULTS OF PROJECT LAPLAND AT THE BEGINNING OF 1966. Miettinen, Jorma K.; Hasanen, Erkki (Helsinki Univ. (Finland). Dept. of Radiochemistry). [1965]. Contract AT(30-1)-3446. 8p. Dep. mn. CFSTI $1.00 cy, $0.50 mn.

From Symposium on Radioecological Concentration Processes, Stockholm.

Data are presented on the content of ^{137}Cs and K in the body of Finnish Lapps obtained by whole-body counting in March and April, 1966. Data are included on the content of ^{55}Fe in the various tissues and organs of reindeer. (C.H.)

31445 (N–65-12416) RADIOLOGICAL SAFETY HANDBOOK. King, P. V. (National Aeronautics and Space Administration, Cocoa Beach, Fla. John F. Kennedy Space Center). Nov. 1, 1964. 117p. (NASA-TM–X-54859). CFSTI $4.00 cy, $0.75 mn.

This handbook describes the organization, policy, procedures, and safety requirements for a radiological safety program. It is written as a technical supplement to safety regulations and safety plans for users of x rays and radioactive materials. The handbook specifically defines KSC procedures and requirements for the procurement, transfer, and shipment of radioactive materials, for the handling and disposal of radioactive materials, and for personnel monitoring, and emergency procedures. (STAR)

31446 (NP–16015) ENVIRONMENTAL RADIOACTIVITY IN NEW ZEALAND. Quarterly Report, October–December 1965. Annual Summary. (National Radiation Lab., Christchurch (New Zealand)). 34p. (NRL–F19). Dep. mn.

Radioactivity measurements in New Zealand are reported for the fourth quarter of 1965 and data are summarized for

1965. Results of total gamma activity measurements on air filter samples from Aukland and Christchurch were similar to those for the third quarter, but the average deposition of ^{90}Sr at nine collecting stations increased slightly during the same time. In general, average annual fallout deposition was slightly less in 1965 than in 1964. Strontium-90 measurements in milk decreased throughout the latter half of 1965 to a low of 8.7 Sr units in the fourth quarter, but the annual level was higher for 1965. Data for cesium-137 content in milk showed slight increases in annual and quarterly results. Strontium-90 and ^{210}Pb were measured in rainfall samples and ^{210}Po was determined in tobacco. (H.G.D.)

31447 (ORNL–3956) HOT-CELL EVALUATION OF THE RELEASE OF TRITIUM AND ^{85}Kr DURING PROCESSING OF ThO_2–UO_2 FUELS. Goode, J. H. (Oak Ridge National Lab., Tenn.). June 1966. Contract W-7405-eng-26. 20p. Dep. mn. CFSTI $2.00 cy, $0.50 mn.

Hot-cell experiments with prototype ThO_2–UO_2 power reactor fuel specimens irradiated to 24,600 Mwd/metric ton (Th + U) showed that up to 0.2% of the fission-produced tritium and 1% of the ^{85}Kr were released when the fuel was sheared into short lengths. Another 0.2% of the tritium and the balance of the krypton were released to the atmosphere when the fuel was dissolved to make solvent extraction feed. This quantity of tritium was less than 0.5% of the estimated 1200 C of ^{3}H that may be safely discharged to the atmosphere from a 6-ton-per-day processing plant. In the preparation of solvent extraction feed, the acidic dissolver solution, containing about 430 C of tritium per ton of fuel, was evaporated and the excess acid recovered in a rectification column. The solvent extraction feed would contain an estimated 30% of the tritium, the rectifier overhead about 47%, and the concentrated acid about 23%. This rectifier overhead, containing 200 C of tritium per ton of fuel, must be diluted with 18 million gallons of environmental water to permit discharge at concentrations less than $^{1}/_{10}$ the MPC_w for tritium (3×10^{-3} μC/cc). Further dilution to 1×10^{-3} μC/cc would be required at the plant boundary to meet the MPC_w for tritium for the general population. Alternative tritium control measures would be volatilization of the tritiated water to disperse it into the atmosphere or recycle of the water within the plant. (auth)

31448 (RLO–1725-15) PHYSICAL, CHEMICAL, AND BIOLOGICAL DATA FROM THE NORTHEAST PACIFIC OCEAN: COLUMBIA RIVER EFFLUENT AREA, JANUARY–OCTOBER 1962. VOLUME I. BROWN BEAR CRUISE 299: JANUARY 23–FEBRUARY 7. Technical Report No. 119. Love, C. M. (Washington State Univ., Seattle. Dept. of Oceanography). Aug. 1965. Contracts AT(45-1)-1385; AT(45-1)-1725; Nonr-477(10); and Nonr-477(37). 186p. (M65–30). Dep. mn. CFSTI $5.00 cy, $1.00 mn.

Physical, chemical, and biological data collected during Cruise 299 of the Research Vessel Brown Bear during the months of January and February 1962 in an area within 120 miles of the coasts of Washington and Oregon are tabulated. These data were collected as part of a year-round study which has as its objective the determination of the gross features of movement and dispersion of Columbia River effluent water in the northeast Pacific. (27 references.) (auth)

31449 (RLO–1725-16) PHYSICAL, CHEMICAL, AND BIOLOGICAL DATA FROM THE NORTHEAST PACIFIC OCEAN: COLUMBIA RIVER EFFLUENT AREA, JANUARY–OCTOBER 1962. VOLUME II. BROWN BEAR CRUISE 304: MARCH 27–APRIL 12. Technical Report No. 119. Love, C. M. (Washington Univ., Seattle. Dept. of Oceanography). Aug. 1965. Contracts AT(45-1)-1385; AT(45-1)-1725); Nonr-477(10); and Nonr-477(37). 193p. (M65–31). Dep. mn. CFSTI $5.00 cy, $1.00 mn.

Physical, chemical, and biological data collected during Cruise 304 of the Research Vessel Brown Bear during the months of March and April 1962 in an area within 150 miles of the coasts of Washington and Oregon are tabulated. These data were collected as part of a year-round study which has as its objective the determination of the gross features of the movement and dispersion of Columbia River effluent water in the northeast Pacific. (auth)

31450 (RLO–1725-17) PHYSICAL, CHEMICAL, AND BIOLOGICAL DATA FROM THE NORTHEAST PACIFIC OCEAN: COLUMBIA RIVER EFFLUENT AREA, JANUARY–OCTOBER 1962. VOLUME III. BROWN BEAR CRUISE 308: JUNE 7–19; BROWN BEAR CRUISE 310: JULY 10–23; BROWN BEAR CRUISE 311: JULY 24–AUGUST 14. Technical Report No. 119. Love, C. M. (Washington Univ., Seattle. Dept. of Oceanography). Aug. 1965. Contracts AT(45-1)-1385; AT(45-1)-1725; Nonr-477(10); and Nonr-477(37). 272p. (M65–32). Dep. mn. CFSTI $6.00 cy, $1.50 mn.

Physical, chemical, and biological data collected during Cruises 308, 310, and 311 of the Research Vessel Brown Bear during the months of June through August 1962 in an area within 360 miles of the coasts of Washington, Oregon, and northern California are tabulated. These data were collected as part of a year-round study which has as its objective the determination of the gross features of the movement and dispersion of Columbia River effluent water in the northeast Pacific. (auth)

31451 (RLO–1725-18) PHYSICAL, CHEMICAL, AND BIOLOGICAL DATA FROM THE NORTHEAST PACIFIC OCEAN: COLUMBIA RIVER EFFLUENT AREA, JANUARY–OCTOBER 1962. VOLUME IV. BROWN BEAR CRUISE 309: JUNE 20–JULY 9. Technical Report No. 119. Love, C. M. (Washington Univ., Seattle. Dept. of Oceanography). Aug. 1965. Contracts AT(45-1)-1385; AT(45-1)-1725; Nonr-477(10); and Nonr-477(37). 197p. (M65–33). Dep. mn. CFSTI $5.00 cy, $1.00 mn.

Physical, chemical, and biological data collected during Cruise 309 of the Research Vessel Brown Bear during the months of June and July 1962 in an area within 220 miles of the coasts of Washington and Oregon are tabulated. These data were collected as part of a year-round study which has as its objective the determination of the gross features of the movement and dispersion of Columbia River effluent water in the northeast Pacific. (auth)

31452 (RLO–1725-19) PHYSICAL, CHEMICAL, AND BIOLOGICAL DATA FROM THE NORTHEAST PACIFIC OCEAN: COLUMBIA RIVER EFFLUENT AREA, JANUARY–OCTOBER 1962. VOLUME V. BROWN BEAR CRUISE 312: SEPTEMBER 14–OCTOBER 18. Technical Report No. 119. Love, C. M. (Washington Univ., Seattle. Dept. of Oceanography). Aug. 1965. Contracts AT(45-1)-1725; Nonr-477(10); and Nonr-477(37). 272p. (M65–34). Dep. mn. CFSTI $6.00 cy, $1.50 mn.

Physical, chemical, and biological data collected during Cruise 312 of the Research Vessel Brown Bear during the months of September and October 1962 in an area within 300 miles of the coasts of Washington, Oregon, and northern California are tabulated. These data were collected as part of a year-round study which has as its objective the determination of the gross features of the movement and dispersion of Columbia River effluent water in the northeast Pacific. (auth)

31453 (STI-PUB–121) TECHNIQUES FOR CONTROLLING AIR POLLUTION FROM THE OPERATION OF NUCLEAR FACILITIES. Report of a Panel held in Vienna, 4–8 November 1963. Safety Series No. 17. (International Atomic Energy Agency, Vienna (Austria)). Mar. 1966. 124p. IAEA: $2.50; S52.50; 15/-stg; F Fr 10,-; DM 8,-.

Requirements for the design of ventilation and air cleaning systems in nuclear facilities, including research and power reactors and radioisotope and research laboratories, are reviewed. The control and monitoring of ventilation and air cleaning systems and factors affecting the dilution of contaminated air discharged into the atmosphere are discussed. Technical data on air cleaning devices are appended. (115 references.) (C.H.)

31454 (USNRDL-TR–967) RADIOLOGICAL RECLAMATION PERFORMANCE SUMMARY. VOL. I. PERFORMANCE TEST DATA COMPILATION. Owen, W. L.; Kawahara, F. K.; Wiltshire, L. L. (Naval Radiological Defense Lab., San Francisco, Calif.). Oct. 13, 1965. 124p. CFSTI $4.00 cy, $0.75 mn.

A great deal of fallout reclamation-performance data

has been generated over the past decade that is useful to planners of radiological recovery operations. Because it was contained in a variety of reports and documents prepared by different agencies, this material was neither convenient to Civil Defense planners nor was it always available in a comprehensible form. As a first step toward correcting the situation, this current volume presents a tabular data compilation summarizing the performance of land reclamation methods and equipment. The tabled entries were gathered from 18 different experiments and field operations. They include those operational and enviromental factors known to influence reclamation effectiveness. A second volume will be devoted to the evaluation and reorganization of the above compilation into a form compatible with the pre-planning of radiological recovery operations. (25 references.) (auth)

31455 DOSE-EQUATED PHANTOM FOR SPACE RADIATION RESEARCH. Clark, Benton C.; Janni, Joseph F. (Kirtland Air Force Base, N. Mex.). Aerospace Med., 37: 479-84(May 1966).

A rugged dose-equivalent plastic manikin was fabricated that is suitable for use in space flight. This phantom simulates the interaction of all types of radiation with the geometry of the human body allowing precise experimental measurements of the depth-dose, linear-energy transfer spectrum, and dosage to critical organs. Dosimeter insertion holes are located in important organs and other appropriate locations within the body. Extensive environmental testing was done to guarantee the capability of the manikin to withstand the rigors of space flight, launch and recovery. A complete analysis of the dose equivalency was performed. The manikin contains every element that composes at least 0.1% of the human body. The interaction characteristics of the manikin are dose-equated to within 15% for neutrons, and within 10% for photons with energies greater than .04 Mev. The response is within 1.5% for electrons with energy between .05 and 10.0 Mev, less than 1.2% for protons with energy greater than 1.0 Mev, and within 1.2 percent for alpha particles of energy greater than 5 Mev. (auth)

31456 CONTROL OF RADIOACTIVE POLLUTION OF MILK BY ^{131}I. Audren, M. L.; Bertrand, S.; Jeanmaire, L.; Michon, G. (Centre d'Etudes Nucleaires, Fontenay-aux-Roses, France). Bull. Acad. Vet. France, 36: 287-90 (June 1963). (In French).

Milk received at the Section of Sanitary Control at Fontenay-aux-Roses is monitored for ^{131}I; when it appears, national general control is established. Twenty departments of France analyze milk samples every 48 hours during the period necessary, using γ spectrometry, which allows detection of 15 pC/l. Samples were examined from September 1961 to January 1963. Monthly mean data are tabulated for September 1962 to January 1963; values range from 0 to 316 pC/l, although not all data are based on sufficient sampling. The departments in the North and East of France report lower values than values given by the West, South, and Central Plain. It is not certain whether these variations are due to meteorological differences or differences in the feeding of cattle at the end of autumn in different regions of the country. Four-month data are reported for 1961 and 1962; the mean data do not reach or surpass the maximum acceptable value of 150 pC/l. Several departments in the South, West, and Central Plain report means of over 100 pC. (BBB)

31457 CONTROL OF RADIOACTIVE POLLUTION. Laurence, G. C. (Atomic Energy Control Board, Ottawa). Can. J. Public Health, 57: 195-8(May 1966).

The possibility of radioactive pollution from nuclear reactor operation and uranium mining is discussed. The basis for deciding what level is harmful to health and the control measures in effect by local and national authorities are examined briefly. (AECL)

31458 THE BASIS FOR THE LIMIT ON WHOLE-BODY EXPOSURE—EXPERIENCE OF RADIOLOGISTS. Warren, Shields (New England Deaconess Hospital, Boston. Harvard Cancer Commission, Boston). Contract AT(30-1)-901. Health Phys., 12: 737-41(June 1966). (NYO-901-34).

The maximum permissible dose for radiologists and others occupationally exposed to ionizing radiation has been progressively reduced to the present levels, which have stood since 1949. The end points for these observations were life shortening, induction of leukemia, bone tumors, skin cancers, and sterility. Observations of the life spans of radiologists are presented that confirm earlier reports of shortening of life spans in this occupational group. Additional data show that life spans were lengthened by the MPD guides. (H.G.D.)

31459 DEPOSITION OF SOME FISSION PRODUCTS OF STRATOSPHERIC ORIGIN ON TROPOSPHERIC AEROSOLS. Shalmon, Eliahu (Soreq Nuclear Research Center, Yavne, Israel). Health Phys., 12: 751-6(June 1966).

Two parallel systems, each consisting of two standard all-glass impingers in series, followed by a 2-in. diameter membrane filter, were employed to separate the airborne radionuclides according to the size of the particles on which they resided. The samples were counted for gross beta radioactivity and then analyzed by gamma spectral analysis for the radioisotopes $^{144}Ce-^{144}Pr$, $^{106}Ru-^{106}Rh$, ^{137}Cs, and $^{95}Zr-^{95}Nb$. About 90% of the radioactivity in tropospheric aerosols was found on particles larger than 0.7 μ in diameter. It was concluded that the commonly used fallout samplers (i.e., filters) provide a good evaluation of the retention of fallout particles by man. (auth)

31460 RADIONUCLIDE FRACTIONATION IN DEBRIS FROM A LAND SURFACE BURST. Mamuro, Tetsuo; Yoshikawa, Kazuko; Matsunami, Tadao; Fujita, Akira (Radiation Center of Osaka Prefecture). Health Phys., 12: 757-63(June 1966).

Two opposite types of radionuclide fractionation were found in the highly radioactive fallout particles which originated from the first Chinese nuclear test explosion carried out on 16 October 1964. The first type was quite similar to the fractionation that was observed in the highly radioactive fallout particles which originated from the large scale air-bursts carried out by the U.S.S.R. in the autumns of 1961 and 1962. The radiochemical composition of the particles fractionated in this type was always much enriched in $^{95}Zr + ^{95}Nb$ and impoverished in ^{103}Ru, taking a middle position for most of other nuclides. The particles fractionated in the second type were, just contrary to those fractionated in the first type, much enriched in ^{103}Ru and impoverished in $^{95}Zr + ^{95}Nb$. The second type of fractionation was never found in the Russian particles that were examined. The fractionation factors were measured for some fallout samples. It was found that the particles having exceedingly higher activities among the collected 300 particles were all fractionated in the second type and that the others were fractionated in different degrees, some being fractionated in the first type and others in the second type. The difference in fractionation behavior between the Chinese and the Russian particles may be considered to be ascribed to the fact that the former were produced in a small scale land surface burst, while the latter were produced in large scale air-bursts. (auth)

31461 DISTRIBUTION OF RADIOACTIVITY ON A POLYDISPERSE AEROSOL BY THE DIFFUSION METHOD. Thomas, Jess W. (Atomic Energy Commission, New York). Health Phys., 12: 765-8(June 1966).

A mathematical method was developed for obtaining information on the distribution of radioactivity on particles in different size ranges from one or two measurements of the diffusion rate of polydisperse radioactive aerosols. The method is very widely applicable since it makes no assumption regarding the particle size distribution of the radioactive aerosol. Results with the form "at least a certain fraction a of the activity is on particles equal to or less than a certain size" may be obtained from a single measurement. For two measurements, the upper and lower limit on the quantity a may be delineated. For certain combinations of diffusion devices and particle size distribu-

tions, the method will give valuable information. In other cases, the precision of the method is low and worthwhile information cannot be obtained. Further theoretical analysis should establish the most valuable range of applicability of the method. (auth)

31462 NUCLEAR TRACK REGISTRATION IN DOSIMETER GLASSES FOR NEUTRON DOSIMETRY IN MIXED RADIATION FIELDS. Becker, K. (Naval Radiological Defence Lab., San Francisco). Health Phys., 12: 769-85 (June 1966).

The properties of combinations of some dosimeter glasses with several fissionable materials for thermal and fast neutron dosimetry in mixed radiation fields, using an etching technique for the visualization of the fission fragment tracks, were investigated. The registration efficiency, effect of the glass composition, different etching chemicals (NaOH, EDTA, and HF), their concentration and temperature on etching kinetics, and the fading and over-etching stability of the tracks were studied. The neutron sensitivity is given for natural U and Th, ^{235}U, ^{238}U, and ^{237}Np with and without additional thermal neutron absorbers for several neutron energies. For thick foils of fissionable metals, the sensitivity was 1.3×10^{-5} track/neutron/barn ± 10 per cent. For higher neutron energies (2 to >20 Mev), ^{238}U is of particular interest because of its rem-equivalent response. The detection limits are discussed. Different techniques for the automatic optical (microscopic and macroscopic) evaluation of the fission track density in glasses are described. The effects of the foil radioactivity and the neutron induced fission fragments on the glass radiophotoluminescence were studied. The system was superior to nuclear track emulsions (gamma insensitive, no fading or fogging, easier evaluation, extended dose and energy range, no directional dependence, etc.) as well as to activation foils (no radioactive decay, higher sensitivity) in personnel dosimetry and for several special applications. Most of the results given are also valid for ordinary glasses. (auth)

31463 USE OF THERMOLUMINESCENT DOSIMETERS FOR MEASUREMENT OF EXTERNAL RADIATION IN GUARAPARI, BRAZIL. Cullen, Thomas L. (Catholic Univ. of Rio de Janeiro). Health Phys., 12: 970-1 (July 1966).

Thermoluminescent detectors, consisting of 180 mg of Type N phosphor enclosed in a medal hung from the neck, were distributed to residents of Guarapari, Brazil, for long-term (3 mo.) measurements of environmental radiation dose. Guarapari is a city of some 5000 persons in the monazite zone on the Atlantic coast where previous surveys have shown radiation doses of between 0.05 and 0.2 mR/hr at street level, 0.6 mR/hr in homes, and patches of black sand with up to 2.0 mR/hr. The radiation dose rate to the population was shown to average 750 mR/yr with a range of 160 to 2500 mR/yr. Analysis of results and comparison with other data indicated the thermoluminescent dosimeters are practical and reliable for measurement of environmental radiation doses. (C.H.)

31464 PERSONNEL DOSIMETRY IN INDUSTRIAL DEFECTOSCOPY. Khol, Frantisek (State Research Study of Materials, Prague). Jad. Energ., 12: 146-9 (1966). (In Czech).

Both x and gamma (^{192}Ir, ^{137}Cs, ^{60}Co, and ^{228}Ra) sources are used in Czechoslovakian industries for defectoscopy. In order to meet the radiation protection requirements, workers in industries using these procedures use pencil dosimeters, blind ionization chambers, and film dosimeters, the characteristics of which are tabulated. Conclusions reached from an examination of the situation are that film dosimetry is adequate for monthly personnel dose monitoring, while ionization chambers are suitable for daily or weekly determination of dose. Measurements of dose with ±10 to 25% precision are sufficient for safety. Experiments on defectoscopic practices showed that workers are well protected, they observe the basic principles in working with ionizing radiation, and doses obtained in normal work do not exceed permissible levels. (TTT)

31465 ^{137}Cs AND ^{90}Sr IN NORWEGIAN MILK, 1960-1964. Hvinden, T.; Lillegraven, A. (Norwegian Defence Research Establishment, Kjeller). Nature, 210: 580-3 (May 7, 1966).

Measurements of the content of ^{137}Cs and ^{90}Sr in Norwegian milk from 1956 through 1965 revealed seasonal variations and variations from district to district. Data are summarized for measurements made from 1960 through 1964. (C.H.)

31466 ESTIMATION OF BONE MARROW DOSE DUE TO FLUOROSCOPIC RADIATION IN JAPAN. Hashizume, Tadashi (National Inst. of Radiology Sciences, Chiba, Japan); Maruyama, Shizuo. Nippon Igaku Hoshasen Gakkai Zasshi, 25: 1410-18 (Mar. 1966). (In Japanese).

As a part of a program to estimate the population dose in Japan, an estimation was made of the absorbed bone marrow dose from fluoroscopic diagnosis per year per person. To determine the bone marrow dose for each fluoroscopy, 24 to 29 pieces of $8 \times 8 \times 4.5$ mm glass or LiF crystals were placed in phantoms of adults or children at sites corresponding to the bone marrow. The number of exposures in 1960 in Japan was 4.8×10^9. Exposures for 1963 were estimated from the number of films consumed. From these data, it was found that the yearly dose contribution of fluoroscopy was 37.7 mrad for females and 52.7 mrad for males. These values are approximately 20 times the contribution of radiography estimated earlier. (auth)

31467 PROTON DEPTH-DOSE DOSIMETRY. Mitchell, John C.; Dalrymple, Glenn V.; Williams, Gwilym H.; Hall, James D.; Morgan, Ira L. (Brooks Air Force Base, Tex.). Radiat. Res., 28: 390-405 (June 1966).

Glass rod microdosimeters and alanine were irradiated with proton energies ranging from 6.8 to 400 Mev. Exposures were made under conditions of minimal scatter as well as in several phantoms which included stationary blocks and rotated Lucite and Masonite cylinders. In addition to these, two specially constructed primate phantoms (Macaca mulatta) were irradiated in the same manner as the primates used for the biological experiments. The depth-dose measurements are considered in the light of calculations made with a digital computer, and the calculated depth-dose distributions in representative tissue phantoms are presented for 32-, 55-, 138-, 250-, and 400-Mev proton exposures. (auth)

31468 RADIATION AND SUPERSONIC FLIGHT. Wilson, I. J. (Atomic Weapons Research Establishment, Aldermaston, Eng.). Sci. J., 2: No. 5, 31-7 (May 1966).

Upper atmosphere radiation is evaluated as a biological hazard to the passengers and crew of supersonic aircraft. The effects of galactic cosmic ray particles and solar flare particles are discussed in detail. The development of an in-flight warning meter is described. (M.H.R.)

31469 RADIOCHEMICAL SAFETY PROCEDURES AT SMITH KLINE AND FRENCH LABORATORIES. Flanagan, Thomas L.; Intoccia, Alfred P. 13p. (CONF-651141-1). ORAU. Gmelin, AED-CONF-65-398-1.

From 16th Annual Meeting of the Animal Care Panel, Philadelphia.

At Smith Kline and French Laboratories there are three radiochemical areas: the radiochemical synthesis laboratories, the radio-chemical analytical area, and the isotope tracer laboratories including the animal care rooms. The types of work carried on in each area, the isotope facilities, the radiation safety organization, personnel monitoring procedures, the handling and housing of animals that have received radiochemicals, methods for transporting isotopes, and disposal of radioactive wastes are discussed. (A.G.W.)

31470 GUARAPARI: DOSIMETRIC SURVEY OF POPULATION. Cullen, Thomas L. 11p. (CONF-650616-20. ORAU. Gmelin, AED-CONF-65-153-44.

From Health Physics Society, Annual Meeting, Los Angeles.

Attempts to measure lifetime radiation dosages received by inhabitants of Guarapari are described. The main problems encountered were unavailability of human bone and

tissue samples and unreliability of dosimeters. Results are presented from one survey in which 156 lithium fluoride dosimeters were distributed to a sampling of the population in May 1964. (A.G.W.)

31471 DIETARY INTAKE OF RADIONUCLIDES IN CALIFORNIA. **Cornish, Amasa C.; Greenberg, Arnold E. (California State Dept. of Public Health, Berkeley). 15p. (CONF-650616-30). ORAU.**

From Health Physics Society Annual Meeting, Los Angeles.

The house diets of twenty hospitals in all major population and geographic centers of the state were selected as sample sources for a study of dietary intake of radionuclides. Samples were collected from each hospital once every two months for a year. Average amounts of ^{90}Sr, ^{137}Cs, and ^{226}Ra found in each area are shown. It is concluded that these radionuclides are not present in amounts sufficient to warrant a change in diet for health considerations. Fallout nuclides are highest in the northern part of the state and lowest in the south. Naturally occurring radium is present in all diets in California. (A.G.W.)

31472 SAFETY DEVICE. **Cooke, Brian Frederick (to Nuclear Power Plant Co. Ltd. AEI-John Thompson Nuclear Energy Co. Ltd.). British Patent 1,030,543. May 25, 1966. Filed Mar. 13, 1964.**

A safety device is described for ensuring that an enclosed space is evacuated by human beings prior to sealing off the space. The device comprises means for counting the personnel passing through inlet(s) and outlet(s) and for comparing the number who have passed through the inlet(s) with the number who have passed through the outlet(s) and interlocking means responsive to the difference between the number who have entered and the number who have left to prevent sealing off of the space while there is a difference in the two numbers. Additional interlocking means may be provided to prevent material that might be harmful to personnel from entering the space unless the difference between the two numbers is zero. (B.L.M.)

INSTRUMENTATION

General

Refer also to abstracts 30960, 30961, and 31390.

31473 (BNWL–235-4) PACIFIC NORTHWEST LABORATORY ANNUAL REPORT FOR 1965 IN THE PHYSICAL SCIENCES. VOLUME 4: INSTRUMENTATION. Pearce, D. W.; Green, J. K. (eds.) (Battelle-Northwest, Richland, Wash. Pacific Northwest Lab.). May 1966. Contract AT (45-1)-1830. 38p. Dep. mn. CFSTI $2.00 cy, $0.50 mn.

Research and development work on instruments is summarized in eleven sections. Separate abstracts were prepared for each section. (J.R.D.)

For abstracts of individual sections see: 30960, 30961, 31474–31476, and 31500–31505.

31474 (BNWL–235-4, pp 1-4) PHYSIOLOGICAL DATA TELEMETRY SYSTEM. Hoitink, N. C.; Porter, N. S. (Battelle-Northwest, Richland, Wash. Pacific Northwest Lab.).

Telemetry instrumentation, capable of monitoring either temperature or heart function (ECG), was modified to permit high temperature operation, simultaneous transmission of both parameters, and automatic time-shared recording of the information. Solid state circuits were developed and incorporated into the system. The completed system includes two miniature transmitters, ECG electrodes, thermistor temperature probes, two FM receivers, a demodulator unit, and a dual-channel recorder. Satisfactory performance is being achieved over 200-ft ranges in general field operation. (J.R.D.)

31475 (BNWL–235-4, pp 19-20) INSTRUMENTATION TECHNIQUES FOR TOXICITY STUDIES OF INHALED RADIONUCLIDES. Porter, N. S. (Battelle-Northwest, Richland, Wash. Pacific Northwest Lab.).

A respiration register was developed to automatically count total test-animal respirations during biological experiments. Improvements were also made to the valve controller to facilitate the use of direct current devices. (J.R.D.)

31476 (BNWL–235-4, pp 21) RAINDROP CHARGE AND VELOCITY MEASUREMENT TECHNIQUES. Ratcliffe, C. A.; Hoitink, N. C. (Battelle-Northwest, Richland, Wash. Pacific Northwest Lab.).

A solid state instrument designed to measure low electric charges on raindrops traveling at 30 to 1000 cm/sec is described. The raindrops pass through shielded inductor rings connected to charge-sensitive amplifiers. Charge and speed of the raindrops are determined from the outputs of the amplifiers. (J.R.D.)

31477 (CEA-R-2981) MONOCHROMATEUR DE NEUTRONS LENTS. (Slow Neutron Monochromator). Gobert, Gerald (Commissariat a l'Energie Atomique, Saclay (France). Centre d'Etudes Nucleaires). Mar. 1966. 6p. Dep. mn.

A mechanical selector for slow neutrons using the selection for relative trajectory is described. (auth)

31478 (K–1670) UCAPP: UNION CARBIDE APT POST PROCESSOR. First Edition. Fowler, A. H.; Henderson, R. W.; Miskell, R. V.; Neu, R. E.; Schellinger, W. V.; Schenk, W. (Oak Ridge Gaseous Diffusion Plant, Tenn.). June 14, 1966. Contract W-7405-eng-26. 42p. Dep. mn. CFSTI $2.00 cy, $0.50 mn.

UCAPP, the Union Carbide APT Post Processor, is a computer program which processes the output of the APT computer system into control tapes for numerically controlled machines. It is generalized to handle a wide variety of N/C machines. (auth)

31479 (Y–1533) AN AUTOMATIC FILM READER. Arrowood, J. L. (Union Carbide Corp., Oak Ridge, Tenn. Y-12 Plant). June 20, 1966. Contract W-7405-eng-26. 41p. Dep. mn. CFSTI $2.00 cy, $0.50 mn.

Automation techniques were applied to the digitizing of analog data recorded on positive transparent oscillograms. The system provides a rapid and economical method of obtaining accurate data from these oscillograms. (auth)

31480 (Y–1535) THICKNESS MEASUREMENTS BY NONDESTRUCTIVE TESTING METHODS. Cofield, R. E. (Union Carbide Corp., Oak Ridge, Tenn. Y-12 Plant). June 21, 1966. Contract W-7405-eng-26. 15p. Dep. mn. CFSTI $1.00 cy, $0.50 mn.

Dimensional parameters such as thickness can frequently be measured by nondestructive testing methods, which are normally used for the evaluation of internal quality. These methods generally respond to the nature of the test object material rather than merely to the relative location of its surfaces. Thus, many of the techniques can measure thickness when only one surface is accessible or when the thicknesses of several layers of materials are involved. Tangential-projection radiography, narrow-beam radiation absorption gaging, radiation backscatter, electromagnetic induction, microwave interaction, and ultrasonic wave propagation are practical thickness-measurement techniques that are discussed. (auth)

31481 (AERE-Trans–1050) A SIMPLIFIED TYPE OF SPECTROMETER OF HIGH APERTURE RATIO. Vasil'ev, R. F.; Zhuchkova, T. N.; Petukhov, S. M. Translated by J. Stuart (U.K.A.E.A. Atomic Energy Research Establishment, Harwell, Eng.), from Optiko-Mekh. Prom., No. 3, 2–3(1963). 6p. Dep. BIS $0.30. HMSO 1s. 2d.

A spectrometer was designed to investigate the faint chemiluminescence in various chemical reactions. It can also be used in other cases where maximum light-gathering power is essential but high resolving power is not required. The great sensitivity of the apparatus is due to the long slits, the large aperture, and to the choice and cooling of the photomultipliers. The spectrometer is described. (M.O.W.)

31482 MICROWAVE EMISSION FROM SUPERCONDUCTING POINT CONTACTS. Dayem, A. H.; Grimes, C. C. (Bell Telephone Labs., Inc., Murray Hill, N. J.). Appl. Phys. Lett., 9: 47-9(July 1, 1966).

A much tighter coupling between a superconducting diode and an external microwave cavity than was previously reported was achieved. Microwave radiation generated by a bridge, which displays constant voltage steps at voltages corresponding to the resonance frequencies of the microwave cavity, was observed. Radiation was also observed from a bridge in the absence of constant voltage steps. The largest power output obtained was 10^{-10} w. (M.C.G.)

31483 NEW HOT-FILAMENT IONIZATION GAGE WITH LOW RESIDUAL CURRENT. Redhead, P. A. (National Research Council, Ottawa). J. Vac. Sci. Technol., 3: 173-80(July-Aug. 1966).

The design and performance of a new type of hot-filament ionization gauge is described. The ions are extracted from the ionization region, focused through an aperture in a shield electrode, and then collected on a short, fine wire. The sensitivity factor of this gauge is about 13 $torr^{-1}$ for nitrogen. The ratio of the soft x-ray flux reaching the collector of the new gauge to that of a Bayard-Alpert gauge is calculated, and the x-ray limit of the new gauge estimated to be 3×10^{-13} torr. Measurements at low pressures indicate that the x-ray limit cannot be greater than 7×10^{-13} torr and may be considerably less. False pressure indications, caused by the electronic desorption of positive ions from chemisorbed gases on the grid (in particular, oxygen), are at least 500 times smaller in the new gauge than in the Bayard-Alpert gauge. (auth)

31484 CALCULATION OF THE MAGNETIC ANALYZER OF A MASS SEPARATOR. Tarantin, N. I.; Dem'yanov, A. V. (Joint Inst. for Nuclear Research, Dubna, USSR). Prib. Tekh. Eksp., No. 1, 41-5(Jan.-Feb. 1966). (In Russian).

A calculation is presented for the magnetic analyzer of a

mass separator, constructed for the identification according to mass number of radioactive nuclei formed in reactions under the action of heavy accelerated ions. (tr-auth)

31485 FEASIBILITY OF OPERATING ELECTRON MULTIPLIERS AS H-F AMPLIFIERS. Gel'tsel', M. Yu.; Panasyuk, V. S.; Serov, A. F.; Yudin, L. I. (Inst. of Nuclear Physics, Novosibirsk, USSR). Prib. Tekh. Eksp., No. 1, 136-9(Jan.-Feb. 1966). (In Russian).

The possibilities of using electron multipliers for amplification of h-f oscillations are evaluated. Results are presented of experiments on the stability of secondary emission from the dynodes in standard photomultipliers and in an electron multiplier with thermionic cathode and control grid, at a high density of the primary electron current in a long pulse and also at a significant average current in the regime of continuous operation. (tr-auth)

31486 USE OF A PLASMA GUN FOR PRODUCING HIGH ELECTRON-CURRENT PEAKS. Kozhukhov, I. V.; Muratov, Yu. V.; Rashevskii, V. P.; Ryl'tsev, P. I.; Sarantsev, V. P.; Smirnov, E. V. (Joint Inst. for Nuclear Research, Dubna, USSR). Prib. Tekh. Eksp., No. 1, 139-43 (Jan.-Feb. 1966). (In Russian).

A previous design for a plasma gun was used to obtain high peak values of electron current. Studies of the effect of the gun parameters on the magnitude of the electron current were carried out, and the possibilities of plasma guns were determined. (tr-auth)

31487 WIDE-RANGE INTENSITY METER FOR HETEROGENEOUS MAGNETIC FIELDS. Beskrovnyi, I. M.; Gorelinskii, Yu. V.; Pivovarov, L. P.; Chuvashov, R. M.; ((Inst. of Nuclear Physics, Academy of Sciences, Kazakh SSR). Prib. Tekh. Eksp., No. 6, 171-4(Nov.-Dec. 1965). (In Russian).

A device measurement of the absolute size of the magnetic field intensity with the precision of approximately 10^{-3} at gradients reaching 1000% cm^{-1} is described. During measurements of homogeneous fields the precision can reach 2 to 5×10^{-5}. With the meter fields are signals of the electron paramagnetic resonance. The complete device can be constructed from standard radiometric equipment of domestic manufacture. The range of measurement of the intensity of radiometric fields from 7 to 350 oersteds completely overlaps without switching of the instrument. (tr-auth)

31488 ELECTRON BOMBARDMENT MOLECULAR BEAM DETECTOR. Brink, Gilbert O. (Cornell Aeronautical Lab., Inc., Buffalo). Rev. Sci. Instrum., 37: 857-60(July 1966).

A molecular beam electron bombardment detector is described and operational data are presented. The detector makes use of a Paul mass filter to increase its versatility. The detector is calibrated by the use of molecular beams of neon, argon, and krypton. Respective detection efficiencies are 1 atom in 2400, 320, and 80. (auth)

31489 MEGAMPERE PULSE TRANSFORMER FOR COAXIAL LOAD. Clark, William H.; Myrberg, John E. (Utah Research and Development Co., Inc., Salt Lake City). Rev. Sci. Instrum., 37: 883-5(July 1966).

A transformer is described which delivers 2 Mamp into a low impedance load through a coaxial output line of about 6.35 mm inner conductor diameter and 12.7 mm cavity diameter. The transformer primary is connected to a 20 μF, 50 kv capacitor bank by forty-eight flexible coaxial cables. The ringing frequency of the system with the secondary shorted is 70 kc. (auth)

31490 MICROWAVE INTERFEROMETERS WITH AMPLITUDE MODULATION. Grigorenko, V. G.; Dushin, L. A.; Leontovich, K. A. (Physico-Technical Inst., Kharkov). Ukr. Fiz. Zh., 11: 491-6(1966). (In Ukrainian).

Methods of designing microwave interferometers with amplitude modulation are considered. These methods make it possible to transfer phase shift from the microwave band to the radiofrequency band. A description is given of possible interferometer schemes. (auth)

31491 HIGH TEMPERATURE DIFFERENTIAL PRESSURE TRANSDUCER /Q-2756/ (Engineering Materials). (Oak Ridge National Lab., Tenn.). (CAPE-1353).

4 drawings.

An instrument that measures differential pressures at temperatures up to 1500°F is described. (For details, see TID-4100). (G.O.Y.)

31492 ELECTRON BOMBARDMENT MOLECULAR BEAM DETECTOR. Brink, Gilbert O. (Cornell Aeronautical Lab., Inc., Buffalo). 12p. (CONF-651213-2). ORAU. Gmelin, AED-CONF-65-400-15.

From American Physical Society, Winter Meeting in the West, Los Angeles.

A molecular beam electron bombardment detector is described and operational data are presented. The detector makes use of a Paul mass filter to increase its versatility. The detector is calibrated by the use of molecular beams of neon, argon, and krypton. Respective detection efficiencies are 1 atom in 2400, 320 and 80. (auth)

31493 PULSED X-RAY INSTRUMENT FOR ALTITUDE MEASUREMENT AND TERRAIN IDENTIFICATION. Wernlund, Roger F.; Cox, Jerry V.; Carroll, David I.; Cohen, Martin J. (Franklin GNO Corp., West Palm Beach, Fla.). 13p. (CONF-660207-16). ORAU. Gmelin, AED-CONF-66-011-11.

From Symposium on Radioisotope Applications in Aerospace, Dayton, Ohio.

An all-weather instrument for altitude measurement and terrain identification has been designed and is being built using the principle of x-radiation backscattering. The altitude is determined by measuring the time interval between a transmitted pulse of x-radiation and the back-scattered return signal from the ground. Automatic gain characterization is used to maintain a constant return signal amplitude which is independent of height above the terrain. Accuracies of ±6 inches at 50 feet altitude and ±2 feet at 300 feet altitude are expected. The instrument will recognize the type of terrain over which the aircraft is flying, such as concrete, sand, water, steel, by changes in the magnitude of the backscattering. The measurement is affected, to a negligible extent, by barometric pressure, rain, fog, snow, and air density changes encountered in the operational situation. The design details and results of the initial tests of the breadboard model are described. (auth)

31494 SOLID STATE BETA GAUGE FOR MEASURING THE DENSITY OF LIQUID HYDROGEN. James, David T.; Milam, James Kelly (Oak Ridge Technical Enterprises Corp., Tenn.). 32p. (CONF-660207-11). ORAU. Gmelin, AED-CONF-66-011-5.

From Symposium on Radioisotope Applications in Aerospace, Dayton, Ohio.

Silicon surface barrier detectors were used successfully with beta ray sources to determine local densities of cryogenic liquids. A 10-channel system was designed, built, calibrated, and installed in a liquid hydrogen tank facility. Measurement precision of 0.1% in a one-second response time was attained. Results of the calibration and field tests, together with system design and development, are discussed. (auth)

31495 MISSILE LIFT OFF MEASUREMENT SYSTEM. Jernigan, E. D. (Industrial Nucleonics Corp., Columbus, Ohio). 24p. (CONF-660207-12). ORAU. Gmelin, AED-CONF-66-011-14.

From Symposium on Radioisotope Applications in Aerospace, Dayton, Ohio.

A missile lift off measurement system is described and experimental results are presented which verify the claimed accuracy and propagation characteristics. (B.G.D.)

31496 IN-FLIGHT INSTRUMENTATION FOR PROMPT MISS DISTANCE MEASUREMENT USING GAMMA RAY TECHNIQUES. Cohen, Martin J.; Wernlund, Rober F.; Carroll, David I. (Franklin GNO Corp., West Palm Beach, Fla.). 14p. (CONF-660207-8). ORAU. Gmelin, AED-CONF-66-011-10.

From Symposium on Radioisotope Applications in Aerospace, Dayton, Ohio.

Extremely versatile miss distance measurement systems have been produced using missiles tagged with a gamma emitting radioisotope. The technique uses a mea-

surement of the strength of the gamma radiation during the missile flight past a target. Equipment within the target, and at remote locations, converts the measured signal strength into the desired miss distance information. Systems have been designed and tested which are capable of operation at any altitude under the environmental conditions associated with these altitudes and capable of indicating miss distances independent of missile closing velocities. Great versatility results from the small size of the gamma emitting tag and its complete independence of power sources, electromagnetic equipment, and all environmental factors. Use of the tag makes the measurement independent of the size and shape of the missile. By properly designing the target equipment and remote equipment, far more sophisticated systems can be produced which will plot missile trajectory relative to the target. (auth)

31497 NANOSECOND PULSE LIGHT SOURCE. Kerns, Quentin A.; Cox, G. C.; Innes, T. G.; Flood, W. S. (to U. S. Atomic Energy Commission). U. S. Patent 3,252,046. May 17, 1966.

A visible light pulse generator which can respond almost instantaneously to a pulse of trigger current and having practically no afterglow after cessation of the current pulse is considered. Pulses one to two nanoseconds long are obtainable. The light source is enclosed in an envelope containing a readily ionizable gas. A conductive coating is provided on the curved surface of a barium titanate cylinder disposed in the envelope while a conductive probe makes point contact at a central portion on the uncoated end of the cylinder. A current pulse is applied from the conductive coating to the probe to obtain a light pulse. (AEC)

Radiation Detection

Refer also to abstracts 31093, 31290, 31443, 31467, 31832, and 32373.

31498 (AD–632527) DEPENDENCE OF PULSE AMPLITUDE AND POLARITY ON POSITION OF ENTRY IN A SOLID-STATE PARTICLE DETECTOR. Basso, Michael (Army Electronics Command, Fort Monmouth, N. J.). Mar. 1966. 17p. (ECOM–2680). CFSTI $1.00 cy, $0.50 mn.

The dependence of pulse height and polarity on the point of entry by an incident energetic particle on a p-n type silicon solid-state radiation detector was investigated. It is shown that the application of an external bias across the base material (p type) alters the charge carrier collection characteristics of the solid-state radiation detector sufficiently to produce these observed changes in the recorded signal. This effect is attributed to the difference in mobilities between holes and electrons generated by the incident energetic particle and the influence of injected carriers on the space charge region. It is also shown that the collection time of charge carriers within the space charge region is not dependent on position of entry by the incident particle while the collection time of charge carriers outside the space charge region is position dependent. (auth)

31499 (AD–633752) COMPARISON OF CESIUM IODIDE AND SODIUM IODIDE FOR UNDERWATER RADIATION DETECTION SYSTEMS. Wesley, E. J.; Nyberg, R. A. (Naval Radiological Defense Lab., San Francisco, Calif.). Apr. 21, 1966. 16p. (USNRDL-TR–1012). CFSTI $1.00 cy, $0.50 mn.

Comparison is made between NaI and CsI scintillation detectors for application to an ultrasensitive underwater detection system. A series of measurements are reported on the response of each crystal to the gamma rays from ^{40}K distributed in water, the attenuation of the integrated count rate by aluminum and steel absorbers surrounding the detector and the background count rate from contaminants on the crystal-phototube assembly and pressure housing. It is assumed in the discussion that NaI crystals will always have to be protected from thermal and mechanical shock by a pressure vessel and that CsI, which is much less susceptible to these types of shock, can be exposed to the hydrostatic pressures in the ocean without damage. The minimum detectable change in ^{40}K concentration is calculated, based on the measured signal and background counts for a CsI crystal and several NaI assemblies with steel and aluminum pressure vessels. It is concluded that, for deep submergence work with detectors of equivalent size, a CsI system is the most sensitive and when compared in terms of a specific detection capability, the least expensive. To complete the evaluation, the assumption that CsI can be operated to all depths without a pressure vessel must be confirmed. (auth)

31500 (BNWL–235-4, pp 4-10) SOLID-STATE GAMMA SPECTROMETRY DEVELOPMENTS. Dau, Gary J. (Battelle-Northwest, Richland, Wash. Pacific Northwest Lab.).

Fabrication and testing of Li-drifted germanium radiation detectors are described. The detectors were fabricated to determine their characteristics and to explore their potential uses. Data are included on detector efficiency and gamma energy spectra of ^{239}Pu and ^{241}Am. (J.R.D.)

31501 (BNWL–235-4, pp 10-11) FISH ENVIRONMENT DOSE RATE MEASUREMENTS. Porter, N. S. (Battelle-Northwest, Richland, Wash. Pacific Northwest Lab.).

For measurement of the external dose rate of fish reared in reactor effluent waters an existing logarithmic-response area monitor was adapted to measure from 0.1 to 10^3 mR/hr in 4 decades. The detector is a plastic scintillator, having relative accuracy, compared with Ra calibration sources, of ±10 to ±30% depending on the reading range. A strip-chart recorder was incorporated into the system to allow continuous monitoring of any given fish trough in the facility. (J.R.D.)

31502 (BNWL–235-4, pp 11-14) DIGITAL CONTROL FOR WHOLE-BODY SCANNER. Sheen, E. M.; Palmer, H. E.; Stringer, J. L. (Battelle-Northwest, Richland, Wash. Pacific Northwest Lab.).

A method of providing scanner velocity based on analyzer live time is described. A digital stepping motor is used to drive the scanner, and the motor is driven by solid state circuitry using the analyzer live timer frequency divider as a source of pulses. Each pulse causes the motor to advance 1.8°. The described circuitry additions are easily incorporated into the multichannel analyzer. (J.R.D.)

31503 (BNWL–235-4, pp 14-16) MINIATURE DOSE RATE MEASUREMENT INSTRUMENT. Sheen, E. M.; Ratcliffe, C. A. (Battelle-Northwest, Richland, Wash. Pacific Northwest Lab.).

Solid state circuit development was completed on a miniature dose-rate meter featuring selectable signal-alarm points and with both meter and aural indication for use in locations with high levels of acoustic noise. The instrument includes a miniature high voltage supply, G-M tube detector, log count-rate meter, linear count-rate selectable alarm points, and a continuous aural output. Circuits were designed to permit trade-off between acoustic output power and for both 9- and 4-v batteries, where the drain is approximately 2.5 ma (for either battery) for non-alarming conditions. (auth)

31504 (BNWL–235-4, pp 16-18) MEASUREMENT OF RADIONUCLIDE UPTAKE BY ALGAE. Porter, Newell S.; Hoitink, Neil C. (Battelle-Northwest, Richland, Wash. Pacific Northwest Lab.).

Instrumentation was developed for in situ measurements of radionuclide uptake by algae. The system comprises algae and background counting chambers, pulse amplifiers, count-rate circuits, an operational amplifier, a count-rate meter, high and low voltage power supplies, and a scaler. With the exception of the scaler, all circuitry is solid state. Preliminary specifications of a detection limit at least 10^4 times the natural river background levels for ^{65}Zn and ^{32}P were met. (auth)

31505 (BNWL–235-4, pp 30-4) MEASUREMENT OF MIXED-FIELD NEUTRON AND GAMMA DOSE RATES. Philipp, L. D. (Battelle-Northwest, Richland, Wash. Pacific Northwest Lab.).

Mixed neutron and gamma fields at reactor locations and

fuel processing centers create radiation hazards. Two instruments are being developed to measure neutron and gamma dose rates separately. Both instruments feature solid state circuitry, portable rechargeable battery operation, rugged construction, and detectors isolated from the main instruments with appropriate cables. With the detectors separated from the readout instrumentation, data may be taken without unnecessary exposure to operating personnel. (J.R.D.)

31506 (CEA-R-2915) DETECTION DES β DURS DANS L'EAU PAR EFFET CERENKOV. (Detection of Hard β Radiation in Water Using the Cherenkov Effect). Turck, Bernard (Commissariat a l'Energie Atomique, Saclay (France). Centre d'Etudes Nucleaires). 1966. 70p. Dep. mn.

Thesis. Submitted to Paris Univ., France. Faculte des Sciences.

The light emitted from a liquid during the passage of a particle of sufficiently high energy can be used to determine the contamination of water by β-emitters. The detector based on this principle requires no special treatment of the water. Particular attention was paid to the optical yield of the detector. However the excellent sensitivity to which this principle leads can only be attained if the background noise is considerably reduced. The electronics associated with detector make it possible to detect a contamination of 8×10^{-8} $\mu c/cm^3$ of strontium-90 in water in about ten minutes. The apparatus presents the double advantage of having a high sensitivity and of being easy to use. Its characteristics make it possible for it to be used for the continuous control of water. (auth)

31507 (COO-1018-1013) BUBBLE SCAN I PROGRAM. Report No. 167. Narasimhan, R. (Illinois Univ., Urbana. Digital Computer Lab.). Aug. 18, 1964. Contract AT(11-1)-1018. 31p. Dep. mn. CFSTI $2.00 cy, $0.50 mn.

A detailed description is given of the first version of BUBBLE SCAN as it was implemented in the IBM 7094-1401 system at the University of Illinois. The input-output features, the data-structure, and the scanning procedure used are first described with specific reference to this implementation. Detailed descriptions and schematic flow charts are given of MAIN and SEARCH, the two major subprograms which together make up the principal part of BUBBLE SCAN. Several outputs resulting at various stages in the processing carried out by this first version of the scanning program are included as illustrative examples to supplement the descriptions given. (M.O.W.)

31508 (COO-1018-1075) TECHNICAL PROGRESS REPORT [ON ILLIAC III], SEPTEMBER 1, 1964-AUGUST 1, 1965. PART I. (Illinois Univ., Urbana. Dept. of Computer Science). Aug. 15, 1965. Contract AT(11-1)-1018. 74p. Dep. mn. CFSTI $3.00 cy, $0.75 mn.

A bibliography of articles dealing with this project of computer use for analysis of nuclear interactions is presented. Major subdivisions of the ILLIAC III computer system are described. File memoranda on systems programming, automatic scanning of bubble chamber negatives, and theory of visual pattern recognition are listed. (M.O.W.)

31509 (EIR-97) TRANSISTORIZED COUNTING CHANNEL FOR MEASURING BETA-ACTIVITIES WITH PROPORTIONAL COUNTERS. Behringer, K. (Eidgenoessisches Institut fuer Reaktorforschung, Wuerenlingen (Switzerland)). Apr. 1966. 32p. Dep. mn.

A transistorized counting channel specifically developed for measuring β-activities with proportional counters is described. The system is designed for operation with high counting rates and consists of a non-overload current amplifier, a pulse-height discriminator, and a dead-time stage for obtaining a defined resolution time. (auth)

31510 (N-65-33971) AN EXAMINATION OF THE AMES PROTON ANALYZER FOR PHOTON SENSITIVITY. Final Report. (American Machine and Foundry Co., Alexandria, Va.). Apr. 1965. Contract NAS2-2475. 12p. (NASA-CR-67078). CFSTI $1.00 cy, $0.50 mn.

A proton analyzer, designed to determine the energies of positive ions emanating from the sun by cycling energies through 15 channels each sensitive to ions of a portion of the total energy range, was tested for sensitivity by bombarding it with photons of three different wavelengths with fluxes corresponding to those produced by the sun. During the bombardment, the orientation of the analyzer was changed and the output measured as a function of the azimuth and elevation angles, and wavelength. Channels 2 through 14 responded to all sources with from 0.25 to 0.75 volts. A lyman alpha source appeared to saturate channel 15. When the orientation was changed the response of the analyzer dropped off rapidly. With Lyman alpha as the source, the azimuth and elevation angles were changed in 12.5° increments. (STAR)

31511 (N-66-16936) SOFT X-RAY PHOTOIONIZATION DETECTOR. Young, R. M.; Stober, A. K. (National Aeronautics and Space Administration, Greenbelt, Md. Goddard Space Flight Center). Feb. 1966. 13p. (NASA-TN-D-3169). CFSTI $1.00 cy, $0.50 mn.

A direct-current, gas-filled ionization chamber, which is a simple ceramic radiation detector used in solar and astrophysical observations from rockets and satellites, is discussed. The detector consists of a ceramic shell incorporating a beryllium window and containing xenon fill gas. The sensitivity is determined by the ion-pair yield and spectral absorption characteristics of xenon along with the transmission properties of beryllium. The fabrication technique for this detector and some observed operating characteristics are also described. (STAR)

31512 (SGAE-SS-5/1966) METHODEN ZUR ERMITTLUNG DER MINDESTIMPULSRATE UND NACHWEISGRENZE EINES MESSGERAETES BEI DER MESSUNG RADIOAKTIVER STRAHLEN. (Method for Determination of Minimum Pulse Rate and Detection Limit of an Apparatus in the Measurement of Radioactive Rays). Soyberk, Oezdemir A. (Oesterreichische Studiengesellschaft fuer Atomenergie G.m.b.H., Seibersdorf). 1966. 14p. Dep. mn.

In radioprotection practice it is very important to determine radiotoxic nuclides in order to keep them under the tolerance dose. It is therefore vital to determine the detection limits of a device. The most suitable equations and individual methods for the determination of the detection limits and the minimum pulse rate were treated. In the calculation of the equations it was considered that the error is as large as the pulse rate so that the error should be multiplied with confidence factor K so that the deviations remain in a given probability range. (tr-auth)

31513 (UCRL-14561) A FABRICATION TECHNIQUE FOR SIGNIFICANTLY REDUCING THE CAPACITANCE OF LARGE-VOLUME Ge LID DETECTORS. Armantrout, Guy A. (Lawrence Radiation Lab., Univ. of California, Livermore). Feb. 10, 1966. Contract W-7405-eng-48. 17p. (CONF-660304-15). Dep. mn. CFSTI $1.00 cy, $0.50 mn.

From Institute of Electrical and Electronics Engineers, Scintillation and Semiconductor Counter Symposium, Washington, D. C.

Practical drift depths for Ge LID detectors are limited to less than 15 mm so that large-volume detectors have a relatively high capacitance because of their increased junction area. A fabrication technique was developed and evaluated which significantly reduces this capacitance by increasing the effective thickness of the intrinsic material between the junctions and decreasing the junction area. In making a large-volume, low-capacity detector, a conventional Ge diode is first drifted to a depth greater than 1 cm. The original junctions used for the drifting operation are then removed and new junctions are applied to the compensated material in a more favorable geometry. A number of these detectors were fabricated with a contact structure consisting of a gold surface-barrier P-type contact and a diffused-lithium N-type contact. The diodes that were made had an active volume of 4.5 cm^3 and a final capacity of less than 2 pF as compared to their original capacity of 9 pF. The detector performance with a pre-

amplifier and a source confirmed the improvement in resolution that would be expected for this decrease in the diode capacitance without a significant reduction in the active detector volume. This technique may be extended to larger detectors and would make possible the fabrication of a 30-cm^3 Ge LID detector with a capacitance less than 5 pF. (auth)

31514 (UCRL–14881) HAZARDS CONTROL QUARTERLY REPORT NO. 24, JANUARY–MARCH 1966. (Lawrence Radiation Lab., Univ. of California, Livermore). Contract W-7405-eng-48. 14p. Dep. mn. CFSTI $1.00 cy, $0.50 mn.

Brief summaries of research work in the following areas are presented: tissue equivalence of LiF, lithium-drifted Ge gamma detector, response of the Rem neutron dosimeter to intermediate energy neutrons, criticality analysis of LRL shipping container for fissile material, dust removal from high speed printers using wet cyclone scrubbers, and condensation of high expansion foam using a centrifugal separator. (M.O.W.)

31515 MODIFIED VERSION OF THE MIT RUTHERFORD SCATTERING APPARATUS FOR USE IN ADVANCED UNDERGRADUATE LABORATORIES. Earl, James A. (Univ. of Minnesota, Minneapolis). Amer. J. Phys., 34: 483-8(June 1966).

Modifications of the MIT Rutherford Scattering Apparatus (Apparatus Drawings Project No. 16) are described. These include use of a self-contained circuit for amplifying, analyzing, and counting pulses from the scintillation detector and interchangeable foil holders which aid in the determination of background effects and which permit studies of scattering from various foils to be made. A description of the experiment performed by students at the University of Minnesota is given. (auth)

31516 COMPARATIVE STUDY OF SATURATION CHARACTERISTICS OF AIR- AND HYDROGEN-FILLED IONIZATION CHAMBERS. Toivola, Ahti (Inst. of Radiation Physics, Helsinki). Ann. Acad. Sci. Fenn., Ser. A VI, No. 196, 1-12(1966).

A series solution of the differential equations for an ionization chamber shows that the diffusion losses, together with the field of the space charge, govern the behavior of a hydrogen-filled ionization chamber, whereas in an air-filled chamber the recombination of the ions is practically the only type of loss. However, better saturation characteristics are achieved with a hydrogen-filled chamber when high dose rates are to be measured. The theoretical results were compared with measurements carried out in a Triga Mark II reactor at gamma dose rate of 1.6 $(10)^5$ rad/s. (auth)

31517 CONSTRUCTION AND OPERATION AT HIGH TEMPERATURES OF GEIGER-MUELLER COUNTERS FILLED WITH MERCURY VAPOR. Blanc, Daniel; Bourrieau, Jacques. Ann. Fac. Sci. Univ. Toulouse Sci. Math. Sci. Phys., 26: 83-97(1964). (In French).

Glass cylindrical counters with external conducting layers and filled with saturated mercury vapor were studied between 200 and 400°C. They have all the characteristics of self-quenching detectors and their efficiency for the γ photons of ^{60}Co is almost equal to that of counters with a classical filling (argon + organic vapor). From measurement of the recovery time, it is deduced that the mobility of the positive ions is 1.75 $cm^2\ sec^{-1}\ v^{-1}$; Hg_2^+ and Hg_3^+ ions seem to be formed in the discharge. The self-quenching character of the detectors is attributed to a very weak photoelectric emission from the internal wall of the glass cylinder. (tr-auth)

31518 MEASUREMENT OF SOFT β EMITTERS BY MEANS OF LIQUID SCINTILLATORS, USING EXTERNAL STANDARDS. Desi, Sandor; Pethes, Gyoergy (School of Veterinary Medicine, Budapest). Atomtech. Tajek., 9: 15-21(1966). (In Hungarian).

A previously described method for determining ^3H and ^{14}C, using an internal reference standard, required a double measurement of the specimens, and the small amounts of liquids caused relatively large errors. These difficulties were eliminated by irradiating the already measured specimens by an external standard. The second measurement may be carried out more rapidly than was found possible previously, and the errors arising from the inexact determination of the standard are eliminated. A differential discriminator was used with a photomultiplier for the determination. A correlation was established between the counting efficiency and the count rate of the external standard. A 10-μC ± 5% ^{226}Ra source was found to be most suitable for these experiments. The organic liquid scintillator detected the γ radiation through the Compton effect. Calibration of the measurement efficiency by an external standard also presents the advantage that the scintillation pulses due to the soft β emitter are not counted by the system because it is sensitive only toward the external standard; this improves the statistical accuracy of the measurement. (TTT)

31519 RESPONSE OF A LARGE SENSITIVE VOLUME LITHIUM-DRIFTED SILICON DETECTOR TO GAMMA AND BETA RAYS. Nishiu, Sakae (Kyoto Univ.). Bull. Inst. Chem. Res., Kyoto Univ., 44: 74-83(Jan. 1966).

The construction and characteristics of a large sensitive volume lithium-drifted silicon detector are reported. Its spectroscopic response for gamma and beta rays, especially photoelectric absorption peaks and Compton electron distributions are discussed comparing with that of a NaI(Tl) scintillator. In contrast with lithium-drifted germanium detectors, silicon detectors have lower counting efficiency, but have the merit of being able to be stored at room temperature when it is not in use. Using these characteristics combined with its excellent energy resolution and anti-coincidence counting method, there will be new gamma spectroscopic applications in large sensitive volume silicon detectors despite its low counting efficiency. (auth)

31520 PROPERTIES OF QUARTZ THERMOLUMINESCENCE DOSIMETERS. Ichikawa, Yoneta; Morii, Takashi (Nara Gakugei Univ., Japan). Bull. Inst. Chem. Res., Kyoto Univ., 44: 84-8(Jan. 1966).

The use of quartz as a thermoluminescence dosimeter was investigated. The glow curve resulting from natural Brazilian quartz showed three glow peaks at approximately 110, 220, and 310°C. It was found that the second peak of the three is the most desirable one from a viewpoint of dosimetry in the case of an accident. In the case of normal dosimetry the susceptibility of quartz for radiothermoluminescence could be increased by irradiation with ^{60}Co gamma rays on a large scale (1×10^7 R). This dosimeter had the advantage of low fading because of the high peak-temperature (280°C) and of excellent linearity to the absorbed dose to 1×10^4 R at least. (auth)

31521 SIMPLE SCINTILLATION DEVICE FOR MEASURING β ABSORPTION IN LIQUIDS. Dillinger, P.; Toelgyessy, J. (Slovak Polytechnic Inst., Bratislava). Chem. Zvesti, 20: 206-8(1966). (In Czech).

The construction of a simple measurement head for the measurement of the absorption of β radiation in liquid samples was described. One wall of the flow-through curvette is the β scintillator and the second wall consists of a 1-mm thick plexiglass membrane. The measurement device described is suitable for the batch analysis of binary liquid mixtures, for radiometric β absorption titrations, and for continuous measurements. (tr-auth)

31522 STRUCTURE OF PARTICLE TRACKS IN NUCLEAR EMULSIONS: DISTRIBUTION OF THE BUNDLE LENGTH. Dellagi, Mohamed (Univ., Tunis). Compt. Rend., Ser. B, 262: 1091-3(Apr. 18, 1966). (In French).

The bundles are formed in a random process. It is shown on the basis of the Barkas model, that the probability density of the length of bundle $\underline{b}$ in the region $\alpha - 2\alpha$ is expressed by $\exp(-\underline{g}\alpha)\ \delta(\underline{b} - \alpha) + +\underline{g}\exp(-\underline{g}\alpha)$, where δ is the unit pulse function, $\underline{g}$ is the density of the silver grains, and α is the diameter of the silver grains. (tr-auth)

31523 PROPERTIES OF CADMIUM TELLURIDE DIODES AND APPLICATION TO DETECTION OF NUCLEAR PARTICLES. Delcroix, Victor; Knispel, Gerard; Lancon,

Rene; Rodot, Michel (CNRS, Bellevue, France. Centre d'Etudes Nucleaires, Grenoble, France). Compt. Rend., Ser. B, 262: 1223-6(May 2, 1966). (In French).

Cadmium telluride (CdTe) p-n junctions were fabricated that had electrical characteristics that made it possible to use them for α particle detectors. (tr-auth)

31524 A TISSUE-EQUIVALENT IONIZATION CHAMBER FOR IN-PHANTOM DOSIMETRY: COMPARISON OF MEASURED VALUES WITH CALCULATED VALUES. Fairchild, R. G.; Robertson, J. S.; Levine, D. A.; Goodman, L. J. (Brookhaven National Lab., Upton, N. Y.). Health Phys., 12: 787-92(June 1966). (BNL-9256).

A tissue-equivalent chamber designed for in-phantom dosimetry is described. The use of non-tissue-equivalent material was restricted to amounts too small to perturb the radiation field significantly. Various chamber sensitivities were obtained by the use of gas fillings and electrodes of different properties, thus making it possible to distinguish among the absorbed doses from fast neutrons, γ rays, and the $^{14}N(n,p)^{14}C$ reaction. The absorbed dose delivered to a cylinder of tissue by each component of an incompletely thermalized neutron beam was measured. A computer code was developed to calculate the absorbed dose from x rays and the $^{14}N(n,p)^{14}C$ reaction when a cylinder of tissue is irradiated with a beam of thermal neutrons. Measured results were compared with calculated results, and showed good agreement. (auth)

31525 BIOLOGY SPECTROMETER AND ANALYZER. Porter, N. S.; Sheen, E. M. (Battelle-Northwest, Richland, Wash.). Contract AT(45-1)-1830. Health Phys., 12: 801-9(June 1966). (BNWL-SA-208).

The biology spectrometer and analyzer was developed to fill the need for a portable field instrument suitable for use with a variety of radiation detectors. The solid state circuitry comprises a high voltage supply for the detectors, pulse amplifier, single channel analyzer, count-rate-meter, five-decade scaler, timer, power supply, and the required testing and logic circuitry. During operation, data presentation is made either on the count-rate-meter, on the scaler, or both as determined by the operator. All circuitry was designed for efficient, maintenance-free operation for extended periods of time. Provision was made for both battery and 100 v a-c operation. The rechargeable Ni-Cd battery, which can power the unit for 8 hr, is contained in a separate carrying case as a convenience feature. Portability is such that one man can easily handle both units in the laboratory or field. (auth)

31526 THERMOLUMINESCENT DOSIMETERS FOR ENVIRONMENTAL MONITORING. Hall, R. M. (E. I. du Pont de Nemours and Co., Aiken, S. C.); La Rocca, J. P. Contract AT(07-2)-1. Health Phys., 12: 851-2(June 1966). (TID-22413).

The use of thermoluminescent dosimeters for environmental monitoring at the Savannah River Plant is discussed. The dosimeters are composed of LiF crystals prepared from enriched lithium that varied ±30% from the average in response per unit weight due to non-uniform doping of the larger crystals from which they were cleaved. Crystals were matched from response to gamma radiation by reducing the weight of those crystals with responses higher than selected values. Thermoluminescence is viewed by a photomultiplier tube operated at 100 v to obtain the optimum ratio of gain to dark current. Total charge accumulated by the capacitor is measured with a multirange electrometer. No effect on dosimeter response was noted where the dosimeters were exposed to 500 R prior to storage at 0, 100, or an average of 60% relative humidity. A comparison between the average daily exposure rates for two 4-week periods determined by G_m instruments, and the thermoluminescent dosimeters indicated the merit of LiF crystals. (H.G.D.)

31527 MODIFICATION OF THE TOSHIBA FGD-3B GLASS DOSIMETER READER TO IMPROVE ACCURACY AND REPRODUCIBILITY. Menkes, Cirel K. (Naval Radiological Defense Lab., San Francisco). Health Phys., 12: 852-5(June 1966).

Modifications and refinements were made on the FGD-3B model Fluoro Glass Dosimeter reader with a resultant capability of reading 25 mR to 5% with 6 × 6 × 3.3 mm glass squares. From the results it is suggested that the same accuracy could be obtained with the larger squares, having a sensitivity of 2.5 times that of the 6 × 6, at the 10 mR dose level. (P.C.H.)

31528 CALIBRATION OF THE ORNL MODEL Q-2240, CONTINUOUS AIR MONITOR. Ohnesorge, W. F.; Gupton, E. D.; Butler, H. M. (Oak Ridge National Lab., Tenn.). Health Phys., 12: 857-60(June 1966).

A method is given for calculating the approximate radiation hazard in the neighborhood of the air monitor in units of MPCa-hr from information available from the air monitor in counts/min as a function of time. The formula given is for a single radioisotope, but it may be applied to a mixture of radioisotopes by treating each separately in terms of its relative abundance. Values are given for ^{32}P, ^{59}Fe, ^{60}Co, ^{89}Sr, $^{90}Sr + ^{90}Y$, and $^{137}Cs + ^{137m}Ba$. (P.C.H.)

31529 MEASUREMENT, BY GAGING, OF THE LUMINESCENCE PULSE FORMS OF SOME ORGANIC SCINTILLATORS. Perroud, J.-P.; Taqqu, D.; Grin, G.-A. (Univ., Lausanne, Switzerland). Helv. Phys. Acta, 39: 205-7(1966). (In French).

The form of the luminous pulses of several organic noncrystalline scintillators frequently used in nuclear physics was determined by a gaging method. The values of characteristic constants for the scintillators Naton 136, NE 102 A and NE 213 are given. Also the spectra of the measured delay for the scintillator Naton 136 is shown. (J.F.P.)

31530 FAST NEUTRON DOSIMETRY BY ANION EXCHANGE SEPARATION OF ^{137}Cs FROM IRRADIATED THORIUM. Hilton, D. A.; Reed, D. (Berkeley Nuclear Labs., Eng.). Int. J. Appl. Radiat. Isotop., 17: 335-40 (June 1966).

The measurement of fast neutron fluxes is described using the determination of ^{137}Cs formed by the fast neutron fission reaction of thorium. The method involves retention of thorium and fission products on a mixed oxalate hydroxide anion exchange resin while ^{137}Cs is determined in the effluent by γ spectrometry. For samples that were not shielded from thermal neutrons an initial solvent extraction of the ^{233}Pa activation product with tri-n-octyl phosphine oxide is necessary. The method has a coefficient of variation better than 2.5% at specific activities greater than 0.01 μc ^{137}Cs/g thorium, which results from an integrated fast neutron flux of about 10^{17} neutrons/cm^2. (auth)

31531 PERIODS FOR VERIFYING RADIOMEASURING INSTRUMENTS. Kelin, A. V.; Kriksunov, V. M. Izmeritel. Tekh., No. 3, 8-11(Mar. 1966). (In Russian).

The overall reliability of radiation measuring instruments depends on the probability that no time-dependent hidden defects appear during the operation. The meteorological reliability may be estimated on the basis of the probability that the error will not exceed the permissible limits, determined by the technical requirements of the operation. The probability of the appearance of hidden failure factors during a mean testing period depends not only on the physical structure of the instrument and external factors but also on the distribution of the defects after the last checking. This distribution follows the usual laws. During operation, the components undergo wear and tear and other irreversible changes, resulting in an increase of faulty measurements. The situation during and after routine checks is analyzed, concluding that selected tolerances allow an increase of the period between verifications. This period may serve as the time-dependent reliability coefficient of the instrument. (TTT)

31532 FAST NEUTRON SCINTILLATION COUNTER. Muminov, V. A.; Babal'yants, V. F.; Abdurakhmanov, A. Kh. (Inst. of Nuclear Physics, Academy of Sciences, Uzbek SSR). Izv. Akad. Nauk Uz. SSR, Ser. Fiz.,-Mat. Nauk, No. 1, 74-6(Jan.-Feb. 1966). (In Russian).

Many neutron recording devices are based on the recording of recoil protons, extensively employing scintillation counters which are, as a rule, sensitive to a gamma background. It is often difficult to exclude the

effects of the gamma rays. However, it has been found that the effective time of the fluorescence of scintillations for neutrons is approximately twice higher than that for gamma rays, and of a stilbene crystal it is about 26 nanosec for protons and about 13 nanosec for electrons. In view of this, there is an opportunity for a more convenient separation of the pulses of fast neutrons from gamma quanta. A fast neutron sensor described by Doroshenko and Stolyarov (PTE, 1961, No. 3) is used in the design of a neutron counter. The fast neutron scintillation counter consists of a stilbene crystal, an FEU-33 photomultiplier, and a discriminator made of two D2E diodes and two White cathode followers. It is concluded on the basis of operation of the counter that practically a complete cut-off of the gamma background is achieved. The counter is stable during an 8-hr continuous operation. (ATD)

31533 SECONDARY ELECTRON EMISSION-TYPE NEUTRAL PARTICLE DETECTOR. Morita, Kenji; Akimune, Hideo; Suita, Tokuo (Osaka Univ.). Jap. J. Appl. Phys., 5: 511-18(June 1966).

Experimental studies were made on the secondary electron emission yields from metal surfaces bombarded by H_1^0, H_1^+, and H_2^+ with energies ranging by 10 to 40 kev. The yields increase with the incident beam energy. The yield from H_1^0 is smaller than that by H_1^+ and is proportional to the cosecant of the incidence angle. The yield by H_2^+ is larger by a factor of two than that by H_1^0 with the same velocity. The mechanism of the secondary electron emission is discussed by comparing the yield by H_1^0 with that by H_1^+ and by considering the observed angular dependence. The observed difference in the yields by H_1^0 and H_1^+ is considered to originate essentially from the difference between the ionization cross sections of the two particles within the shallow layer below the surface. A neutral particle detector was made on the basis of the angular dependence results. (auth)

31534 CHARACTERISTIC OF A MICROWAVE DISCHARGE CHAMBER. Ohashi, Yozo (Nagoya Univ., Japan). Jap. J. Appl. Phys., 5: 519-33(June 1966).

Some fundamental properties of a discharge chamber operated by a pulsed microwave field were investigated. The discharge chamber was operated at an electric field of about 3 kv/cm, which is as low as in the case of the conventional d-c discharge chamber. Under the optimum operating condition, it gave a three-dimensional track of a particle. The track was reasonably sharp, the average radius of discharge spots being about 0.7 mm and the root-mean-square deviation from the path of a particle being about 0.9 mm. The number of discharge spots per unit track length varied with ionizing intensity of a particle. Delayed triggering was found to improve the ionization density measurement as does delayed expansion of the cloud chamber. The mechanism of spot formation is discussed with particular attention to the relation between the observed spot density and the initial ion pair density. (auth)

31535 CALCULATION AND EVALUATION OF INFORMATION OBTAINABLE FROM PULSE SHAPE DISCRIMINATION. Kiss, Gabor. Magyar Tud. Akad. Kozp. Fiz. Kut. Int. Kozlem., 14: 173-82(1966). (In Hungarian).

The differences between scintillation pulse shapes are evaluated from the properly weighted difference between the charges collected over different time intervals. The amplitude and spread of the difference signal depend on the characteristics of the scintillator, the choice and setting of the sorting circuit. These relations are formulated and some possibilities of their application are shown. (auth)

31536 DETERMINATION OF BETA ACTIVITY IN PREPARATIONS USING CYLINDRICAL COUNTERS. Yagovoi, P. N.; Alfimov, N. N. (Kirov Order of Lenin Military-Medical Academy, Leningrad). Med. Radiol., 11: No. 5, 49-56(May 1966). (In Russian).

To determine the beta activity of thick-layered preparations and of those in the intermediate-layer range by means of cylindrical counters, it is proposed to make use of a cell with a set of cylindrical screens. The employment of cylindrical screens allowed elaborating a procedure for estimating the radioactivity of materials under study with due consideration of corrections for the difference in the beta energy, levels of the reference standard, and the specimen. This method makes it possible to analyze very accurately materials of low activity and to detect any rise thereof from mild radioactive isotope contamination. (auth)

31537 DETECTION OF RADIOACTIVE RADIATION WITH p-i-n TRANSITIONS IN SILICON AND GERMANIUM. Hofker, W. K. (N. V. Philips' Gloeilampenfabrieken, Amsterdam). Ned. Tijdschr. Natuur., 32: 5-11(Jan. 1966). (In Dutch).

The Li ion drift method for the preparation of silicon and germanium detectors is outlined. The performance of silicon and germanium detectors is illustrated. (J.S.R.)

31538 CONSIDERATION ON THE APPLICATION OF A FLUOROGLASS DOSIMETER. Antoku, Shigetoshi (Hiroshima Univ.); Yoshinaga, Haruma. Nippon Igaku Hoshasen Gakkai Zasshi, 25: 1385-9(Mar. 1966). (In Japanese).

The use of fluoroglass dosimeters for dosimetry in diagnostic x-ray examination was studied. A glass plate (FD-P8, 8 × 8 × 4.7 mm) was useful for depth-dose measurements, particularly in a small spaces. The conversion factor for the plate was 3.53 mR per μ amp for 60 to 80 Kvp x rays, 3.00 mR per μ amp for 140 Kvp (1.0 mm Al filter) x rays, and 2.80 mR per μ amp for 140 Kvp (0.2 mm Cu filter) x rays. Directional dependency was not observed for ^{60}Co gamma rays and was ignored for 180 Kvp x rays; but for diagnostic x rays, it was about 10% in a water phantom and about 40% in air. The fluorescence rapidly increased until about one day after exposure and tended to remain at a constant value for 1 to 3 weeks and then gradually decreased. (auth)

31539 CHARGE RELEASE MECHANISM FOR FERROELECTRIC RADIATION DETECTORS. Hester, Donald L. (Sandia Corp., Albuquerque, N. Mex.); Glower, Donald D. Nucl. Appl., 2: 41-3(Feb. 1966).

Previous publications revealed that poled ferroelectrics can be used as detectors of radiation; however, the source of the charge release was speculative. A theoretical derivation using the theory of pyroelectricity was verified by the previously published data and by an especially designed experiment whereby the graph of the normalized charge release as a function of temperature is compared with normalized pyroelectric coefficient data. The experiment verified that the constant of proportionality K in the equation, $i/A = K(d\gamma/dt)$, is equal to p/C, where p is the pyroelectric coefficient and C is the specific heat. The appropriate value for K for ceramic lead zirconate titanate, $Pb(Zr_{0.65}Ti_{0.35})O_3 + 1$ wt % Nb_2O_5 (65 : 35 PZT), is determined to be 0.6 picocoulombs per square centimeter per rad (PZT). (auth)

31540 LOW-BACKGROUND COUNTING OF BETAS AND ALPHAS WITH SILICON DETECTORS. Walter, F. J.; Boshart, R. R. (RIDL, Nuclear-Chicago Corp., Oak Ridge, Tenn.). Nucl. Instrum. Methods, 42: 1-14(June 1966).

A comprehensive study of the use of silicon detectors for low background counting of charged particles is described. A discussion of the effect of electronic noise on the beta detection efficiency and background is included along with experimental measurements of detection efficiency. Detailed measurements of background, with and without shielding and anticoincidence umbrella, are presented. The performance of silicon surface barrier detectors is compared with that of a conventional gas flow counter and it is shown that for sample sizes less than 1'' in dia, silicon detectors have a number of distinct convenience and performance advantages, but are presently handicapped by cost and fragility considerations. (auth)

31541 APPLICATION OF GAMMA-RAY SPECTROMETRY AND COMPUTER TECHNIQUES TO THE DETERMINATION OF THE MINIMUM DETECTABLE CONTENT

OF TRACE ELEMENTS IN NEUTRON-ACTIVATED MATERIALS. Pauly, J.; Guzzi, G.; Girardi, F.; Borella, A. (EURATOM, Ispra, Italy). Nucl. Instrum. Methods, 42: 15-25(June 1966).

A computer method is developed in order to derive from the gamma ray spectrum of a neutron activated material the detection limits for a great number of trace elements. A sensitivity spectrum is calculated from the experimental data. The detection limit for 57 elements is then deduced using library data of specific activities. With this procedure it has been made possible to determine, in a sample of nuclear graphite, detection limits smaller than 1 ppm for about 40 elements. The performances of a 3" × 3" NaI(Tl) scintillator and of a lithium drifted germanium semiconductor detector for this particular application are compared. The computer program is written in FORTRAN-4 for the IBM 7090 computer. (auth)

31542 LOSS OF CHARGED PARTICLES BY NUCLEAR INTERACTIONS IN SCINTILLATORS. Measday, D. F. (Harvard Univ., Cambridge, Mass.); Schneider, R. J. Nucl. Instrum. Methods, 42: 26-8(June 1966).

Some particles, when detected by total energy counters, undergo inelastic collisions. These particles are lost from the full energy peak. This loss has been calculated for deuterons and alpha particles of up to 160 Mev, for NaI and plastic scintillators. (auth)

31543 PROGRAMMED AUTOMATIC CONTROL SYSTEM FOR A TRIPLE-AXIS NEUTRON SPECTROMETER. Bevilacqua, S. (CSN, Casaccia, Italy. CNEN, Rome); De Agostino, E.; Rispoli, B.; Cribier, D. Nucl. Instrum. Methods, 42: 29-37(June 1966).

The programmed automatic control system of the triple axis neutron spectrometer which is fitted to the EL-3 reactor is described. The system includes six measurement units. The instructions can be given by means of two input channels: a Read-Punch cards machine and a typewriter. The results of the measurements are punched on the cards and printed. The facilities and the system organization are described. (auth)

31544 SPECTROMETRY OF SOFT X-RAYS IN PROPORTIONAL COUNTERS. I. CALCULATION OF ENERGY RESOLUTION OF PROPORTIONAL COUNTERS. Siewert, I.; Schmidt, H. (Deutsche Akademie der Wissenschaften, Berlin). Nucl. Instrum. Methods, 42: 45-8(June 1966). (In German).

The optimal energy resolution (full width of peak at half counting rate), which can be obtained with a proportional counter is calculated as a function of the quantum energy of monochromatic X- and of K-radiation. The working conditions of a wall-less proportional counter with anti-coincidence-ring, which was applied in x-ray spectrometry of liquid and solid sources is described. The energy resolution is compared with the calculated values and data from literature. (auth)

31545 SPECTROMETRY OF SOFT X-RAYS IN PROPORTIONAL COUNTERS. II. A WALLLESS PROPORTIONAL COUNTER WITH ANTICOINCIDENCE RING FOR X-RAY SPECTROMETRY. Schmidt, H.; Siewert, I.; Schaefer, H. (Deutsche Akademie der Wissenschaften, Berlin). Nucl. Instrum. Methods, 42: 49-55(June 1966). (In German).

The optimal energy resolution (full width of peak at half counting rate), which can be obtained with a proportional counter was calculated as a function of the quantum energy of monochromatic X- and of K-radiation. The working conditions of a wall-less proportional counter with anti-coincidence ring, which was applied in x-ray spectrometry of liquid and solid sources is described. The energy resolution is compared with the calculated values and data from literature. (auth)

31546 LIGHT ATTENUATION IN SCINTILLATION COUNTERS. Kuijper, P.; Tiesinga, C. J.; Jonker, C. C. (Vrije Univ., Amsterdam). Nucl. Instrum. Methods, 42: 56-60(June 1966).

The light from detection events in scintillation counters will be attenuated before reaching the phototube. This attenuation effect can be already important in rather small scintillators and is caused by absorption and reflection of the photons in the scintillator. The experiment shows that this effect depends on the geometrical and optical properties of the scintillator and can diminish the response and detection efficiency considerably. (auth)

31547 DETERMINATION OF COINCIDENCE-CIRCUIT STATISTICAL PARAMETERS ON THE BASIS OF A SINGLE EMPIRICAL DELAYED-COINCIDENCE CURVE. Kalisz, J. (Inst. of Nuclear Research, Swierk Otwocka, Poland). Nucl. Instrum. Methods, 42: 61-7(June 1966).

A mathematical method is described for determination of the main coincidence-circuit parameters (resolving time, jitter breadth, efficiency) only on the basis of a single empirical delayed-coincidence curve. The method assumes Gaussian jitter distributions and permits this assumption to be verified if required. Exact graphs and an example illustrating the method are given. (auth)

31548 ROUTINE PROCEDURE FOR 4π PROPORTIONAL COUNTING SOFT BETA PARTICLES FROM SOLID SOURCES. Keith, R. L. G.; Watt, D. E. (Atomic Weapons Research Establishment, Aldermaston, Eng.). Nucl. Instrum. Methods, 42: 68-70(June 1966).

Freeze-drying has been used routinely for preparing low energy beta sources. The sources have a better distribution of active material than those prepared by heat or air drying and result in far less self absorption. The inherent self-absorption is estimated by an extrapolation method. Confidence limits of 1, 2, and 4% are placed on determinations of specific activity of ^{60}Co, ^{35}S, and ^{63}Ni, respectively. Extension of the method to alpha sources and to spontaneous fission sources has also given good results. (auth)

31549 MORE ON THE SPHERICAL CONDENSER AS AN ANALYZER. I. NONRELATIVISTIC PART. Sar-El, H. Z. (Soreq Nuclear Research Centre, Yavne, Israel). Nucl. Instrum. Methods, 42: 71-6(June 1966).

The dynamical and optical properties of the spherical condenser for nonrelativistic charged particles were studied for certain arrangements of the source and very interesting features of this analyzer were found. A point source embedded in the hollow inner sphere of the condenser can be imaged, at least theoretically, without any spherical aberration. Very small sources and even weak ones, may be analyzed since the device provides very high transmission for a given resolution in comparison with other devices. In addition, fringing effects are eliminated. The deflecting voltages which have to be used are higher than those needed for the sector field analyzer, but this seems a reasonable price to pay for the other advantages. (auth)

31550 PROJECTOR FOR LARGE-SIZE BUBBLE CHAMBER PICTURES. Heughebaert, J.; Debaisieux, J.; Grard, F. (Laboratoire des Hautes Energies, Brussels). Nucl. Instrum. Methods, 42: 87-92(June 1966).

A low cost projector specially designed to project the pictures produced by the CERN 2 m bubble chamber is described. The projector projects simultaneously up to 4 pictures superposable 2 by 2, of maximum dimensions 240 mm × 50 mm at a linear magnification factor 15. A general description of the machine and a detailed description of the original elements are given. The more attractive characteristics concern the high safety level for the films and the the ease of handling. Moreover the projector is equipped with all the facilities required from a bubble chamber film projector for rapid and efficient work. (auth)

31551 SOME PARTICULAR SOLUTIONS FOR A NUCLEAR COUNTING CHAIN. Colombo, G.; Stanchi, L. (CCR-EURATOM, Ispra, Italy). Nucl. Instrum. Methods, 42: 104-8(June 1966).

A brief description of some new characteristics of the modular chain of Ispra is given. Accent is set on the particular solutions which add something to the classical design of modular chains. Functions are described rather than a list of instruments. Some circuit details are given. The instruments are made according to the rules of the ESONE system. (auth)

31552 TIME RESOLUTION MEASUREMENTS WITH XP 1020 PHOTOMULTIPLIERS. Bertolini, G.; Mandl, V.; Rota, A.; Cocchi, M. (EURATOM, Ispra, Italy). Nucl. Instrum. Methods, 42: 109-17(June 1966).

Time resolution measurements on XP 1020 photomultipliers were performed using a hydrogen discharge lamp and a ^{60}Co source. Fast electronics with tunnel diode discriminators were used. A time resolution of 192 ps fwhm was obtained with ^{60}Co. The time distribution of the light pulses was measured by a sampling technique. The resolution obtained was compared to theoretical data calculated by means of a statistical model of photomultiplier behavior. (auth)

31553 TOTAL AND PHOTOPEAK EFFICIENCIES FOR A WELL-TYPE NaI(Tl) CRYSTAL FOR CYLINDRICAL SOURCES. Tiwari, P. N.; Kondaiah, E. (Tata Inst. of Fundamental Research, Bombay). Nucl. Instrum. Methods, 42: 118-24(June 1966).

The total and photopeak efficiencies for a 6.5 cm × 6.5 cm well type NaI(Tl) crystal with 0.8 cm well dia and 3.2 cm well depth are determined. These efficiencies are determined for cyclindrical monoenergetic sources of 0.5 cm dia and various heights in steps of 0.5 up to 3.0 cm as a function of the gamma-ray energy from 0.14 to 2.75 Mev, using standard gamma sources and various absorbers covering the whole periodic table. Formulas are given to calculate the effective total and photopeak efficiencies in the case of gamma rays in cascade using the monoenergetic gamma ray efficiencies presented. (auth)

31554 MONTE CARLO CALCULATIONS FOR A GAMMA-RAY TELESCOPE. Avni, A. (Brookhaven National Lab., Upton, N. Y.); Sadeh, D. Nucl. Instrum. Methods, 42: 125-7(June 1966).

A gamma ray directional detector using long and narrow plastic scintillators was designed. Its angular resolution and its efficiency were calculated by allotting randomly the components which determine the paths of the electron-positron pair and calculating the amount of energy dissipated in the scintillators. This was done with a fast computer, using Monte Carlo methods. The results show that for a certain configuration of scintillators an angular resolution of 1.5° and an efficiency of 10% can be achieved. An estimation of the counting rates and background is given for certain celestial objects. (auth)

31555 EVALUATION OF PEAKS IN NUCLEAR SPECTROSCOPY. Daddi, L.; D'Angelo, V. (CAMEN, Pisa, Italy). Nucl. Instrum. Methods, 42: 134-6(June 1966).

Assuming that the peaks obtained in gamma-ray scintillation spectrometry and in other cases have an approximately continuous and Gaussian shape, the consequences of the channel width choice and of the statistical fluctuations were studied. (auth)

31556 REACTION CHAMBER WITH SEMICONDUCTOR DETECTORS ADAPTED FOR MEASUREMENT OF PARTICLE CORRELATIONS. Hossenlopp, J.; Haberer, A.; Bilwes, R. (CRN, Strasbourg). Nucl. Instrum. Methods, 42: 137-40(June 1966). (In French).

A brief description is presented of a reaction chamber. Special characteristics of this chamber are three movable detectors with continuously variable solid angle, a target storage box in a vacuum, a short-lived radioactive source lock, and a beam centering system. (B.G.D.)

31557 ANALOG AND DIGITAL READOUT SYSTEM FOR THE CIRCULATING MEMORY. Bonacic, V. (Inst. Ruder Boskovic, Zagreb). Nucl. Instrum. Methods, 42: 154-6(June 1966).

An analog and digital readout system for the circulating memory of a pulse-height analyzer is described and analyzed. Simultaneously one obtains here the spectrum display by the analog system and precise knowledge of the number of pulses in each channel by the digital system. The spectrum display is recorded by a pen recorder, whereas the channel content is printed by the digital system in decimal notation on paper tape. The advantages of the described readout system are the simplicity of its logic and reliability in work. (auth)

31558 DETECTION EFFICIENCY OF SPARK CHAMBERS AND ITS EXACT CALCULATION. Maurel, J.; Segur, P.; Trapp, J. P.; Blanc, D. (Centre de Physique Atomique Nucleaire, Toulouse). Nucl. Instrum. Methods, 42: 173-80(June 1966). (In French).

The efficiency theory of Bella and Franzinetti is adapted to the case of a spark chamber, working with a clearing field. The existence of a plateau in the curves giving the efficiency as a function of the delay time, is justified. It is shown that the length of the plateau may be larger than predicted by the theory of Cranshaw and De Beer. The validity limits of this calculation are discussed and a criterion for the formation of the spark, which might be a start for a more accurate theory, is finally proposed. (auth)

31559 NOTE ON THE IMPROVEMENT OF LUMINOSITY OF A DOUBLE FOCUSSING β SPECTROMETER. Mauron, G.; Schellenberg, L. (Univ., Freiburg i. B.). Nucl. Instrum. Methods, 41: 147-8(Apr. 1966). (In French).

A study was made to determine if, for a given resolution, the luminosity of a double focusing β spectrometer could be increased by increasing the source height. Theoretical considerations show that the image would be enlarged and would curve more with the increase of the source height. Experimental studies using the K line of the 662-kev transition of ^{137}Ba for source heights from 12 to 35 mm show that up to approximately 22 mm the experimental data agrees with theory. The relative augmentations of the source and the luminosity are equal. Above 22 mm the increase of the luminosity is weaker. (J.S.R.)

31560 PRESENT VIEWS OF DOSIMETRY WITH SOLID-STATE DETECTORS. Scarpa, G. (Comitato Nazionale per l'Energia Nucleare, Casaccia, Italy). Nunt. Radiol., 31: 1107-19(Oct. 1965). (In Italian).

Dosimetric systems based on the use of solid indicators are reviewed. Thermoluminescence, radiophotoluminescence, photoelectric effects, photoconductivity, and photochromic effects proved to be phenomena able to supply the investigator with more or less detailed data on the physical magnitudes associated with the radiation fields. A schematic description is presented of the fundamental mechanisms of the functions of the solid indicators and the practical features of these new dosimeters are analyzed with regard to the measurable dose interval and the energy dependence. On the basis of these characteristics possible fields of use are postulated. The development of methods founded on the thermoluminescence of crystals with low atomic weight, such as lithium fluoride, is considered. (auth)

31561 PROBLEM OF PROTECTIVE DOSIMETRY OF NEUTRONS IN PRESENCE OF GAMMA RADIATION. Nikodemova, Denisa. Prac. Lek., 18: 164-7(May 1966). (In Czech).

Attention is paid to the measurement of rapid neutrons, independently from energy within the range 0.1–15 Mev. For this purpose the advantageous properties of the proportional detectors, filled with enriched BF_3 were used: the nonsensitivity to gamma radiation and the high effective cross section for thermal neutrons. The BF_3 serves as detector of rapid neutrons with high efficiency and a low directional dependency; to achieve this low dependency from energy in the whole mentioned area of neutron energy, moderators are used (paraffin, polyethylene) the form and layer of which are determined on the computation base. Such a device was used for measurement of the neutron-flow density and the dose intensity, as well as for determination of the dose-intensity spatial distribution, during work with a shielded as well as with the free Po-Be neutron-source. (auth)

31562 MULTICHANNEL RECORDING DEVICES AND DIGITAL COMPUTERS FOR LOW-ENERGY PHYSICS (REVIEW). Zabiyakin, G. I. (Joint Inst. for Nuclear Research, Dubna, USSR). Prib. Tekh. Eksp., No. 1, 5-31 (Jan.-Feb. 1966). (In Russian).

Trends in the development of recording devices for use in low-energy physics studies are examined in detail. Discussions are given of apparatus for multichannel analysis,

the use of digital computers for automatic analysis of data, multidimensional analysis with a large number of channels, treatment of measurement results, and information flow in measurement centers. 113 references. (M.J.T.)

31563 MAGNETIC ANALYSIS OF RELATIVISTIC PARTICLES. Vovchenko, V. G. (Inst. of Physics and Tech., Leningrad). Prib. Tekh. Eksp., No. 1, 36-40(Jan.-Feb. 1966). (In Russian).

By using linear equations connecting the initial and final characteristics of the particle trajectories in a magnetic spectrometer, expressions are obtained for the average solid angle of the system, and a method is proposed for determining the apparatus distribution of particles according to the momentum deviations from the axis momentum, p_0. The mechanism of formation of the spectrum is examined as an example of the two-particle reactions $a + b \rightarrow c + d$. It is shown that at the spectrometer input the momentum distribution of the particles with respect to p_0 arises because of multiple Coulomb scattering and the finite interval of incidence angles. A comparison is made of the proton spectrum measured using a single-crystal spectrometer with the results of calculations of the spectral shape. (tr-auth)

31564 SENSITIVITY FUNCTION OF CsI(Tl) CRYSTAL SCINTILLATION γ SPECTROMETER TO γ RADIATION AT ENERGIES UP TO 10 Mev. Orlov, Yu. V.; Sevost'yanov, Yu. A. Prib. Tekh. Eksp., No. 1, 45-50(Jan.-Feb. 1966). (In Russian).

A method is described for constructing two matrices with uniform (50th order) and nonuniform (42nd order) energy intervals for treating the apparatus spectra of a single-crystal scintillation gamma spectrometer with energies up to 10 Mev. The matrices are constructed for a cylindrical CsI(Tl) crystal with diameter and height of 80 mm for the case of an incident collimated radiation beam of diameter 15 mm. Treated spectra, obtained in experiments on a reactor, are presented. (tr-auth)

31565 AUTOMATIC DEVICE FOR MEASURING CONVERSION SPECTRA AT WIDE RANGE OF ENERGIES IN A MAGNETIC β SPECTROMETER. Andreev, Yu. A.; Beskrovnyi, I. M.; Gorbatov, E. A. (Inst. of Nuclear Physics, Alma-Ata, USSR). Prib. Tekh. Eksp., No. 1, 50-2(Jan.-Feb.1966). (In Russian).

A device is described for recording conversion spectra by means of a discrete change of the magnetic field with automatic recording of the results of the measurements. Spectra of the gadolinium fraction measured on this device are presented. (tr-auth)

31566 TIME-OF-FLIGHT NEUTRON SPECTROMETER. Anufrienko, V. B.; Devkin, B. V.; Ivanov, A. A.; Kotel'nikova, G. V.; Kulabukhov, Yu. S.; Lovchikova, G. N.; Sal'nikov, O. A.; Timokhin, L. A.; Fetisov, N. I. (Inst. of Physics and Power Engineering, Obninsk, USSR). Prib. Tekh. Eksp., No. 1, 53-61(Jan.-Feb. 1966). (In Russian).

A neutron time-of-flight spectrometer, having a range of measuring energies from 0.1 to 14 Mev, is described. The resolving power of the spectrometer, determined from the gamma peak, is 4 nsec/m. The channel width is 2.12 nsec. The integral nonlinearity is 0.25%. Signals from the output of a time-to-amplitude converter are fed to a 256-channel analyzer. The spectrum of neutrons scattered on Mn, recorded on the spectrometer, is presented. (tr-auth)

31567 PULSED REACTOR COLD-NEUTRON MEASURING DEVICE. Golikov, V. V.; Shapiro, F. L.; Shkatula, A. (Joint Inst. for Nuclear Research, Dubna, USSR). Prib. Tekh. Eksp., No. 1, 62-9(Jan. Feb. 1966). (In Russian).

A device for time-of-flight studies of neutron spectra produced by the scattering of cold neutrons was constructed, based on the JINR fast pulsed reactor. The moderator, placed near the reactor reflector, and the Be filter are kept at liquid nitrogen temperature. The sample, located 60 cm from the moderator, is irradiated by cold neutron bursts, whose duration is determined by the lifetime of the neutrons in the moderator and the spread of the times of flight over the distance 60 cm. The energy of the scattered neutrons is determined from the time of flight over the sample-detector distance, amounting to 10 to 45 m. In the region of elastic and quasielastic scattering of the cold neutrons, the device is characterized by high resolving power and high intensity. (tr-auth)

31568 OPTIMIZATION OF MEASUREMENTS OF ELECTRON ENERGY IN HEAVY-LIQUID BUBBLE CHAMBERS. Budagov, Yu. A.; Volod'ko, A. G.; Flyagin, V. B.; Shlyapnikov, P. V. (Joint Inst. for Nuclear Research, Dubna, USSR). Prib. Tekh. Eksp., No. 1, 70-2 (Jan.-Feb. 1966). (In Russian).

When the measurement errors are included in the error in momentum, the optimum track length grows with increasing electron energy; thus the method of cut-off of the spectrum of radiative losses is extended into the high-energy region. Formulas are obtained for the average value of electron momentum and its accuracy, valid for the whole spectrum of possible values of cut-off threshold. (tr-auth)

31569 IRRADIATION OF COMBINED EMULSION AND SPARK CHAMBER SYSTEM. Basova, E. S.; Vovenko, A. S.; Gulyamov, U. G.; Kolesnik, V. G.; Sanevska, T.; Sil'vestrov, L. V.; Skzhipchak, Z.; Hsu, Yung-chang; Khvastunov, M. S. (Joint Inst. for Nuclear Research, Dubna, USSR). Prib. Tekh. Eksp., No. 1, 73-6(Jan.-Feb. 1966). (In Russian).

A system composed of emulsion and spark chambers permits the point of incidence of a charged particle in the emulsion to be determined from its track in the spark chamber. Results are described of the irradiation of an emulsion in cosmic rays and in an accelerator using this apparatus. The inaccuracy in the indication of the coordinates of particles incidence in the emulsion is on the average ±0.4 mm, and the inaccuracy in indication of the angle of particle incidence is on the average ±0.5°. (tr-auth)

31570 DETERMINATION OF KINEMATIC PROPERTIES OF PARTICLES IN A SPARK CHAMBER ACCORDING TO THE MULTIPLE SCATTERING AND SECONDARY SPARKS. Bayukov, Yu. D.; Vorob'ev, L. S.; Leksin, G. A.; Stolin, V. L.; Fedorov, V. B.; Khovanskii, V. D. (Inst. of Theoretical and Experimental Physics, Moscow). Prib. Tekh. Eksp., No. 1, 77-9(Jan.-Feb. 1966). (In Russian).

The possibility of determining the momenta of particles from scattering in a multilayered spark chamber was shown, using two spark chambers exposed to beams of 50- and 200-Mev protons and 250-Mev pions. The secondary sparks arising near the particle track were analyzed, and the portion of the sparks genetically associated with the track was selected. Apparently these sparks were caused by δ-electrons produced in the electrodes and the gas of the chamber. The number of these sparks increases with increasing energy. (tr-auth)

31571 SERIAL POWER SUPPLY FOR SPARK CHAMBER GAPS. Gus'kov, B. N.; Matyushin, A. T.; Matyushin, V. T. (Joint Inst. for Nuclear Research, Dubna, USSR). Prib. Tekh. Eksp., No. 1, 80-3(Jan.-Feb. 1966). (In Russian).

The operations of spark chambers with series and parallel power supplies are compared. It is shown that the chamber with series power supply reaches the plateau faster and has a greater efficiency and sharper drop-off of the efficiency curve as a function of the delay of the supply pulse. (tr-auth)

31572 CHERENKOV COUNTER WITH CONTROLLED THRESHOLD. Klebanov, Yu. D. (Inst. of Atomic Energy, Moscow). Prib. Tekh. Eksp., No. 1, 84-7(Jan.-Feb. 1966). (In Russian).

The construction of a Cherenkov counter with total internal reflection and controlled threshold is described, and results of tests on the counter are presented. In the range of values of β from 0.89 to 0.97, a resolution $\Delta\beta/\beta = 10^{-2}$ is obtained for a recording efficiency of ~90%. (tr-auth)

31573 HIGH-PRESSURE IONIZATION ^{3}He CHAMBER PERFORMANCE AS SLOW NEUTRON DETECTOR. Dmitriev, A. B.; Istomin, I. V.; Novikov, A. G.; Malyshev,

E. K. Prib. Tekh. Eksp., No. 1, 87-90(Jan.-Feb. 1966). (In Russian).

The construction and parameters of a high-pressure ^{3}He chamber, used as a detector in neutron time-of-flight spectrometry, are described. (tr-auth)

31574 SELECTION OF SCINTILLATORS FOR COUNTERS RECORDING γ RADIATION IN THE PLATEAU REGION. Vedekhin, A. F.; Pavlov, Yu. P.; Chernykh, L. P. Prib. Tekh. Eksp., No. 1, 90-1(Jan.-Feb. 1966). (In Russian).

Results are presented of a study of the counting characteristics of γ-ray counters with various types of scintillators. Scintillators considered include NaI(Tl), CsI(Tl), and KI(Tl) monocrystals and organic phosphors of the type of stilbene, diphenyl acetylene, anthracene, and naphthalene. (M.J.T.)

31575 DETERMINATION OF STABILITY OF RADIOMETRIC INSTRUMENTS. Belle, Yu. S. (Leningrad Research Inst. of Radiation Protection). Prib. Tekh. Eksp., No. 1, 94-7(Jan. Feb. 1966). (In Russian).

A device for the automatic tape recording of successive time intervals of pulses from radiometric instruments, using the self-recording potentiometer EPP-09, is described. The recordings are in the form of diagrams from which the stability of the radiometric instrument and the effects of unstabilizing factors, such as supply voltage and temperature, can be estimated easily. Examples of the use of this device in adjusting the operation of a large liquid scintillation counter are given. (tr-auth)

31576 PRECISION OF RADIOMETRIC MEASUREMENTS IN CASES OF SMALL PREPARATION/BACKGROUND RATIOS. Malykhin, V. M. (Leningrad Scientific-Research Inst. of Radiation Protection). Prib. Tekh. Eksp., No. 1, 98-9(Jan.-Feb. 1966). (In Russian).

Graphs are presented for determining the relative error of radiometric measurements in cases of poor statistics, i.e., at low sample/background ratios and low number of pulses during the measurement. (tr-auth)

31577 PULSE-HEIGHT RECORDING AND LOGARITHMIC CONVERSION OF PULSE HEIGHTS IN THE 10^4 TO 10^5 DYNAMIC RANGE. Grigorov, N. L.; Gadalov, A. N.; Mineev, Yu. V.; Rapoport, I. D.; Savenko, I. A. (Moscow State Univ.). Prib. Tekh. Eksp., No. 1, 100-6(Jan.-Feb. 1966). (In Russian).

A logarithmic pulse-height converter for recording pulses from radiation detectors is described. The dynamic range of 10^4 to 10^5 with error of 10% in the pulse-height measurement over the whole range is achieved by automatic shifting of the conversion scale. Logarithmic pulse-height-to-number conversion is accomplished using an oscillatory circuit, adjustable in resonance to the incident pulse; the range of this circuit is $\sim 10^3$. The apparatus is transistorized and operates stably in a temperature range from –20 to +50°C in the external medium. (tr-auth)

31578 TIME-DIGITAL-CODE CONVERTER FOR NANOSECOND RANGE. Ivanov, A. A. Prib. Tekh. Eksp., No. 1, 111-14(Jan.-Feb. 1966). (In Russian).

A converter of time intervals in the nanosecond range to a binary digital code is described, in which the principle is used of comparing a time interval with the number of pulses, whose repetition period is known. The pulse repetition frequency is 200 Mc, i.e., the time resolution is 5 nsec. The capacity of the counting apparatus is 2^8, i.e., the maximum measurable time interval is 1.28 μsec. The differential nonlinearity of the converter does not exceed ±0.4%. (tr-auth)

31579 PRODUCING STARTING PULSES IN TIME-OF-FLIGHT NANOSECOND TECHNOLOGY. Kononov, V. N.; Stavisskii, Yu. Ya. Prib. Tekh. Eksp., No. 1, 115-17(Jan.-Feb. 1966). (In Russian).

Time-of-flight measurements of secondary particles produced in a target by primary ion beams require the knowledge of the moment of production. Two methods for producing starting pulses — the voltage pulses accompanying the secondary-particle production — are described. The first involves placing a scintillation counter near the target to obtain pulses from the part of the primary beam which is deflected by a grid. The second uses amplification of the current pulses in the target by a broad-band transistorized amplifier with low input impedance. Experiments with these two methods were carried out using a cascade generator operating at proton pulse durations from 10 to 30 μsec, repetition frequency of 1 Mc, proton currents in the target from 100 to 150 μamp pulse, and proton energy of 1.1 Mev. (M.J.T.)

31580 STABLE PULSE AMPLIFIER. Alkhazov, G. D.; Vorob'ev, A. A. (Inst. of Physics and Tech., Leningrad). Prib. Tekh. Eksp., No. 1, 123-4(Jan.-Feb. 1966). (In Russian).

A description is given of an amplifier, intended for operation in an ionization alpha spectrometer, with stability of amplification coefficient better than 0.1%. A diagram of the main circuit of the amplifier and tables of the variation of the output-signal amplitude with time are included. (M.J.T.)

31581 SPECTROMETER FOR STUDYING THE FINE STRUCTURE OF X-RAY SPECTRA (URS-1I). Sadovskii, A. P.; Vainshtein, E. E.; Finogenov, V. M.; Aushtikailis, V. I. (Inst. of Inorganic Chemistry, Novosibirsk, USSR). Prib. Tekh. Eksp., No. 1, 174-7(Jan.-Feb. 1966). (In Russian).

The vacuum focusing x-ray spectrometer URS-1I is described, intended for the study of the fine structure of x-ray spectra of atoms in materials in various aggregate states, in solutions of any acidity, and in alloys. The operating interval of Bragg angles is from 30 to 75°. Ionization recording of the spectra is used. Focusing is by the Kapitsa-Johann method. The radius of curvature of the crystal is 1000 mm. The spectrometer permits spectra to be obtained using secondary as well as primary methods of excitation. The use of standard high-voltage apparatus is assumed. (tr-auth)

31582 MEASUREMENT OF TRACK BRIGHTNESS IN A SPARK CHAMBER. Pavlovskii, F. A. (Inst. of Theoretical and Experimental Physics, Moscow). Prib. Tekh. Eksp., No. 1, 184-5(Jan.-Feb. 1966). (In Russian).

The brightness of tracks in a spark chamber was measured using apparatus consisting of a spectrometric photomultiplier, which transforms light pulses from the track into current pulses, and a ballistic galvanometer, included in the photomultiplier output circuit to measure these pulses. The galvanometer readings are not a linear function of the track brightness, for brightness ratios of about 10^4. The variation of track brightness with the amplitude of the high-voltage pulse is shown for constant pulse length of 100 nsec. The effect of photomultiplier aging on the stability of the amplification coefficient was studied; instability of the amplification coefficient did not exceed 5% during 10 hr operation. (M.J.T.)

31583 MAGNETIC BETA SPECTROMETER WITH SPACE FOCUSING OF ELECTRON BEAMS AT $\pi\sqrt{10}$ ANGLE. Baranov, S. A.; Polevoii, R. M.; Volchkov, Yu. A.; Aliev, I. G.; Belen'kii, S. N. (Inst. of Nuclear Energy, Moscow). Prib. Tekh. Eksp., No. 6, 64-6 (Nov.-Dec. 1965). (In Russian).

A magnetic β spectrometer with space focusing of the electron beam at an angle $\pi\sqrt{10}$ to the surface of the axial-symmetric magnetic field was described. The hit of the electrons in the detector in the first coil was eliminated by a special diaphragm system placed between recorder and detector. The radius of the equilibrium orbit of the device was $\rho_0 = 400$ with a dispersion of D = 20, $\rho_0 = 8000$ mm. The half width of ^{137m}Ba line is 0.038% at source area of 1.5×40 mm^2, detector aperture of 2×50 mm^2, and solid angle of $3 \times 10^{-4} \times 4\pi$. It was shown that the device gives an octuple gain in luminescence with equal resolution and radius of equilibrium orbits ρ_0 in comparison with spectrometers with focusing angle of $\pi\sqrt{2}$. (tr-auth)

31584 INVESTIGATION OF NEUTRON COUNTER EFFICIENCY AT INTERMEDIATE ENERGIES. Baranov,

P. S.; Slovokhvatov, L. I.; Sokol, G. A.; Shtarkov, L. N. (Inst. of Physics, Moscow). Prib. Tekh. Eksp., No. 6, 77-81(Nov.-Dec. 1965). (In Russian).

The energy dependence of the efficiency of scintillation neutron counters in the neutron energy range from 20 to 70 Mev was investigated experimentally. The results obtained were compared with theoretical results. (tr-auth)

31585 MEASUREMENTS USING TWO-AMPLITUDE DIFFERENTIAL ANALYZER CONNECTED TO COINCIDENCE SCHEME. Zavel'skii, F. S. (Geological Inst., Moscow). Prib. Tekh. Eksp., No. 6, 89-93(Nov.-Dec. 1965). (In Russian).

Measurement errors in work with amplitude differential analyzers connected by coincidence wiring were analyzed. It was shown that the distribution and magnitude of the maximum of the differential spectrum depends on the measurement method. Distortions in the vicinity of spectra boundaries were examined and a method for improving the accuracy of the measurements was outlined. (tr-auth)

31586 STUDY ON THE MEDICAL UNIVERSAL HUMAN COUNTER. I. DEVELOPMENT OF MUHC AND FUNDAMENTAL STUDY ON THE WHOLE-BODY COUNTING WITH MUHC. Hiramatsu, Hiroshi; Hisada, Kin-ichi; Matsudaira, Masamichi (Kanazawa Univ., Japan). Radioisotopes (Tokyo), 15: 109-16(1966). (In Japanese).

A whole-body counter is described that has wide clinical use. The Medical Universal Human Counter (MUHC) is composed of four detectors using 3 × 2 NaI(Tl) crystals. In addition to whole-body counting, it can be used for most types of external counting including temporal, linear, and area scanning. (H.G.D.)

31587 FACTORS AFFECTING RESOLUTION OF LEAD SCINTILLATOR SANDWICH SHOWER COUNTERS. Walker, J. K.; Knasel, T. M. (Harvard Univ., Cambridge, Mass.). Rev. Sci. Instrum., 37: 913-16(July 1966).

Recent results by Crawford and Messel on the development of showers in lead by the Monte Carlo method are used to estimate the energy resolution of total energy absorption scintillation shower counters. It is probable that slight improvements in energy resolution over existing counters can be obtained by using 15 radiation lengths in the direction of the incident particle and sampling the shower after every $1/10$ radiation length. (auth)

31588 CONSTANT CURRENT SOURCE FOR INSTRUMENT CALIBRATION. Santoro, R. T.; Gillespie, F. E.; Aebersold, P. M. (Oak Ridge National Lab., Tenn.). Contract W-7405-eng-26. Rev. Sci. Instrum., 37: 919-22 (July 1966). (ORNL-TM-1337).

Two current sources that give a constant current over a wide range of applied voltage were built for use in calibrating electrometers having input resistors in the 10^{+10} to 10^{+12} Ω range. The sources consist of sealed parallel plate ionization chambers having one electrode coated with ^{241}Am. Calibrations using the rate of charge method spaced over a period of 1 year define the respective current output of the sources as $(6.943 \pm 0.003) \times 10^{-11}$ and $(4.263 \pm 0.004) \times 10^{-12}$ amp. (auth)

31589 GAS FLOW PROPORTIONAL COUNTER FOR ELECTRON-PROBE LIGHT-ELEMENT ANALYSIS. Vogel, Raymond S.; Fergason, Lewis A. (Mallinckrodt Chemical Works, Weldon Spring, Mo.). Contract W-14-108-Eng-8. Rev. Sci. Instrum., 37: 934-8(July 1966). (TID-22641).

A gas flow proportional counter designed for use as the detector in a microprobe nondispersive system is described. The counter design incorporates (1) relatively low operating voltage with high multiplication factor, (2) an anode wire support to minimize "end effects" on the pulse height distribution curve, and (3) an over-all design to permit convenient disassembly and replacement of the anode wire or other components. Results of performance studies indicate higher resolving power than similar commercial counters and negligible shift in multiplication factor over a wide range of counting rates. (auth)

31590 IMPROVEMENTS ON ELECTROMAGNETIC VELOCITY DRIVE FOR MOESSBAUER EXPERIMENTS. Cohen, R. L. (Bell Telephone Labs., Inc., Murray Hill, N. J.). Rev. Sci. Instrum., 37: 957-9(July 1966).

A number of improvements to a previously described velocity drive (R. L. Cohen et al., Rev. Sci. Instr., 34: 671 (1963)) are briefly described, which ease construction and enable the drive to be used with parabolic motion even at low velocities. Diagrams are shown of the LVsyn loudspeaker combination, the error signal amplifier, and the revised power amplifier. (L.B.S.)

31591 GAIN SHIFT OF PROPORTIONAL COUNTER WITH COUNTING RATE. Fergason, Lewis (Mallinckrodt Chemical Works, St. Charles, Mo.). Rev. Sci. Instrum., 37: 964-5(July 1966).

Mean pulse height measurements of x rays from pure Ni and Fe specimens were made using a xenon proportional counter and a 400-channel analyzer in order to investigate the nonlinear behavior of proportional counters with respect to counting rate. The detector gain was found to vary exponentially with counting rate. It is pointed out that the peak amplitude shift is often significant when comparing even relatively low counting rates. (L.B.S.)

31592 ANALOG PLOTTING SYSTEM FOR RECORDING ENERGY SPECTRA OF LOW-ENERGY CHARGED PARTICLES. Rudd, M. E. (Univ. of Nebraska, Lincoln). Rev. Sci. Instrum., 37: 971-3(July 1966).

An electrostatic analyzer and plotting system is described for recording energy spectra of electrons emitted from gases under positive ion bombardment. With suitable modification it can also be used for positive ions. A block diagram of the system is shown and a brief discussion is given of its operation. (L.B.S.)

31593 DESIGN AND USE OF SPHERICAL GEIGER COUNTERS. Jacob, A. W. B. Sci. Proc. Roy. Dublin Soc., Ser. A, 2: 43-6(1965).

A 4π gamma detector is described. This was a small Geiger counter with concentric spherical electrodes which had a plateau of more than 100 volts with a slope of 0.15%/volt at the operational voltage of 1300 v. Over an angle of 340° in the vertical section the sensitivity variation for gamma rays was only $\pm 2\frac{1}{2}\%$. One of these counters was used to plot the gamma ray flux inside an irradiator and the agreement with previously predicted flux values was good. (auth)

31594 APPLICATIONS OF LAPLACE TRANSFORMS FOR THE CALCULATION OF COUNTING LOSSES. Weise, Lothar. Z. Instrum., 72: 298-302(1964). (In German).

The formalism of Laplace-transforms has been used previously to clear connections of counter statistics. Expressions for counting losses in a nuclear particle scaler are derived with the help of Laplace-transforms. It appears that the method is very elegant in some cases whereas the treatment of other imaginable examples of counting arrangements in this manner is difficult. The method may be useful for the calculation of other examples, which are not mentioned here. (auth)

31595 APPARATUS FOR THE INVESTIGATION OF DIRECTIONAL CORRELATION OF γ-RAYS EMITTED IN CASCADE. Jatczak, Jerzy; Lipinski, Andrzej; Stepinski, Marian (Univ., Lodz, Poland). Zesz. Nauk Uniw. Lodz., Ser. II, 17: 89-95(1964). (In Polish).

The apparatus for investigation of the directional correlation of γ rays emitted in cascade was described. The special electronic system forming the pulses, which proceeds from the scintillation detectors was elaborated. The use of nanosecond technique allows one to obtain the number of real coincidences comparable to number of chance coincidences. (auth)

31596 PROGRESS IN REACTOR DETECTORS DESIGN AND CONSTRUCTION CARRIED OUT IN THE YEARS 1963-1965. Jablonska, Jadwiga; Janikowski, Andrzej; Topa, Jerzy. 25p. (CONF-651123-9). ORAU.

From Conference on Reactor Physics and Engineering, Budapest.

Some developments in the technology of neutron detectors for reactors are outlined including improved insulating ma-

terials, hydrogen filling for boron chambers, and assembly methods. Some boron-lined ionization chambers and some fission chambers are briefly described. (D.C.W.)

31597 MEASUREMENTS OF THE FREQUENCY RESPONSE OF NEUTRON-SENSITIVE CURRENT ION CHAMBERS. Gasiorowski, L.; Labno, L. 21p. (CONF-651123-8). ORAU.

From Conference on Reactor Physics and Engineering, Budapest.

The frequency-response characteristics of three types of ionization chambers were measured using the neutron-beam-modulation technique. The operating range of each chamber was thus determined. (G.O.Y.)

31598 MINIATURE THERMOLUMINESCENT DOSIMETRY FOR APPLICATION IN MEDICINE AND BIOLOGY. Malsky, S. J.; Roswit, B.; Reid, C.; Amato, C. G.; Spreckels, C. (Veterans Administration Hospital, New York). 19p. (CONF-651113-2). ORAU. Gmelin, AED-CONF-65-322-1.

From 18th Annual Conference on Engineering in Medicine and Biology, Philadelphia.

An operable, in-vivo radiothermoluminescent dosimetry system has been developed for use in therapeutic and diagnostic radiology, nuclear medicine, radiobiological, and environmental health studies. Encapsulated, miniature (1 × 10 mm) out-gassed CaF_2:Mn dosimeters have been used to detect one milliroentgen exposures. The estimated accuracy is ±10 percent at the three sigma confidence level. Encapsulated lithium fluoride (LiF) having the same dimensions and solid LiF crystals (2 × 2 × 10 mm) have also been studied. The fluorimeter reader operates at room temperature and is designed to correlate the peak amplitude of the dosimeters' glow curve with dose over 7 decades of range. Integrated values are also obtained for further intercomparison at the higher dosage levels. Knowledge of the exposure level is necessary, to avoid loss of reading, therefore, several dosimeters are employed for each exposure. (auth)

31599 HIGH INTENSITY RADIATION SURVEY PROBE (Engineering Materials). (Bettis Atomic Power Lab., West Mifflin, Pa.). (CAPE-1339).

8 drawings.

A high-intensity radiation survey probe that uses a double-crystal coincidence Compton recoil spectrometer is described. (For details, see TID-4100.) (G.O.Y.)

31600 REMMETER (Engineering Materials). (Lawrence Radiation Lab., Univ. of California, Livermore). (CAPE-1360).

21 drawings.

A portable survey instrument that measures neutron doses directly in rem/hr and is independent of the neutron energy in the thermal to 15-Mev range is described. The instrument uses a $^{10}BF_3$ tube in conjunction with transistorized circuitry. (For details, see TID-4100.) (G.O.Y.)

31601 RADIOLOGICAL MONITOR (Engineering Materials). (Battelle-Northwest, Richland, Wash. Pacific Northwest Lab.). (CAPE-1361).

1 drawing.

A portable field instrument that is suitable for radiobiological experiments using alpha-, beta-, and gamma-emitting isotopes is described. (For details, see TID-4100.) (D.C.W.)

31602 DETECTION AND MEASUREMENT OF GAMMA RAYS IN THE PRESENCE OF A HIGH INTENSITY NEUTRON FLUX. Richter, J. M. 32p. (CONF-641127-3). ORAU. Gmelin, AED-CONF-64-297-4.

From American Physical Society, Fall Meeting of the Ohio Section, Oxford, Ohio.

A stilbene scintillation crystal was used to detect gamma rays in the presence of a neutron flux by means of pulse shape discrimination. The principal advantages of stilbene are the absence of long-lived neutron activation products in the scintillator and an improved time response for coincidence measurements. The gamma ray energy was determined by finding the Compton edge energy. The position of the Compton edge on the pulse height spectrum was found by using the Klein-Nishina formula in a computer program which constructs the detector response to monoenergetic gamma rays. Measurements of the linearity, efficiency, and resolution of a $1\frac{1}{2}'' \times 1\frac{1}{2}''$ stilbene crystal for gamma rays were made. The feasibility of using pulse shape discrimination to select gamma rays in the presence of a neutron flux was demonstrated by detecting the gamma rays resulting from neutron inelastic scattering. (auth)

31603 LOW-BACKGROUND BETA-RAY SCINTILLATION SPECTROMETER. Tanaka, Eiichi; Hiramoto, Toshiyuki (to Hoshasen Igaku Sogo Kenkyusho). Canadian Patent 735,057. May 24, 1966. Priority date Mar. 6, 1961, Japan.

In measuring very low activity of solid samples, cosmic ray mu-mesons may cause an inaccurate result if their effect is not removed. The scintillation detector uses a solid phosphor and has a hollow portion. The device also incorporates a Geiger-Mueller counter. A discriminator rejects large pulses caused by cosmic rays so that by coincidence counting, a display may be obtained which represents almost the sample activity alone. (F.S.A.)

31604 RADIATION MEASURING APPARATUS. Shombert, Donald James (to Siemens and Halske AG). German Patent 1,213,539. Mar. 31, 1966. Priority date May 12, 1961, United States.

The detector is composed of a plurality of silicon p-type and n-type regions with p-n junctions between them. The diffusion length of the minority carriers is small in each of the regions in relation to the thickness of the region. The detector is suited for the detection of all kinds of energetic particles. (Gmelin Inst.)

31605 NUCLEAR PARTICLE SEMICONDUCTOR DETECTORS FOR AEROSPACE APPLICATIONS. Ziemba, Francis P. (Solid State Radiations Inc., Los Angeles). 19p. (CONF-660207-20). ORAU. Gmelin, AED-CONF-66-011-19.

From Symposium on Radioisotope Applications in Aerospace, Dayton, Ohio.

A review is presented on four types of semiconductor detectors including description, manufacturing techniques, and applications for aerospace research. These detectors are surface-barrier, diffused-junction, lithium-compensated silicon, and lithium compensated germanium. (B.G.D.)

31606 STATE OF THE ART NEUTRON DETECTION. Morgan, J. L. (Texas Nuclear Corp., Austin). 33p. (CONF-660207-18). ORAU. Gmelin, AED-CONF-66-011-29.

From Symposium on Radioisotope Applications in Aerospace, Dayton, Ohio.

The state-of-the-art in neutron detection depends on the neutron intensity, energy, and experimental requirements. A review is presented on neutron detectors and techniques. (B.G.D.)

31607 RADIATION DOSIMETRY IN RELATION TO HIGH-INTENSITY RADIATION SOURCES. Jarrett, Robert D. Sr. (Army Natick Labs., Natick, Mass.). 18p. (CONF-650902-28). ORAU. Gmelin, AED-CONF-65-235-62.

From American Chemical Society, 150th National Meeting, Atlantic City.

Experience in using the ferrous-copper system in measuring large doses of radiation is described. Effects of variation of the following on results obtained with the system are discussed: acid concentration, reagent concentration, storage time, and temperature during reading. It was found that the standard solution of $FeSO_4$, $CuSO_4$, and H_2SO_4 can be stabilized by preirradiating it to ~10^5 rads. Preirradiation reduces the useful range of the dosimeter, but the range can be increased by increasing the concentration of ferrous iron. Experience confirmed that the ferrous-copper dosimeter can be used for routine dose measurements; variations between different solutions prepared did not exceed ±1%. (A.G.W.)

31608 M.B.L.E. THERMOLUMINESCENT DOSIMETRY SYSTEM. DETAILED PRODUCTION PROGRAM OF PERSONAL DOSIMETERS, DOSIMETER READERS, AND RESEARCH EQUIPMENTS. 26p. (CONF-650637-8). ORAU. Gmelin, AED-CONF-65-151-9.

From International Conference on Luminescent Dosimetry, Palo Alto, Calif.

The physical principle of thermoluminescence and the characteristics and advantages of thermoluminescent detectors are reviewed. A general description of the thermoluminescent dosimeter and its sheath is followed by brief descriptions of seven different types of dosimeters produced by Manufacture Belge de Lampes et de Materiel Electronique S. A. The general reader system and five specific readers are also described. (A.G.W.)

31609 NUCLEAR ELECTRONICS FOR AEROSPACE APPLICATIONS. Katzenstein, Henry S. (Solid State Radiations Inc., Los Angeles). 29p. (CONF-660207-17). ORAU. Gmelin, AED-CONF-66-011-20.

From Symposium on Radioisotope Applications in Aerospace, Dayton, Ohio.

The problems encountered in the design of radiation detection systems for space research are outlined. Electronic instrumentation associated with radiation detectors such as preamplifiers, pulse height analyzers, scalers, and power supplies are discussed with regards to high reliability requirements of a space environment. (B.G.D.)

31610 SOME APPLICATIONS OF GAS COUNTERS IN SPACE RESEARCH. Fisher, Philip C. (Lockheed Missiles and Space Co., Palo Alto, Calif.). 21p. (CONF-660207-10). ORAU. Gmelin, AED-CONF-66-011-15.

From Symposium on Radioisotope Applications in Aerospace, Dayton, Ohio.

Geiger counters, proportional counters, and ion chambers have been used extensively for space measurements of electron, proton, and photon fluxes. Several of the physical characteristics affecting the detection efficiency and use of these detectors are reviewed. Some of the advantages and limitations of the various counters are illustrated by brief descriptions of typical space radiation investigations. (auth)

Radiation Effects

31611 (AD-633468) THE EFFECT OF RADIATION-INDUCED CHARGE ON TRANSISTOR SURFACES. Maier, R. J. (Naval Radiological Defense Lab., San Francisco, Calif.). Mar. 21, 1966. 81p. (USNRDL-TR-997). CFSTI $3.00 cy, $0.75 mn.

The deleterious effects of 10^3 to 10^4 rads absorbed dose on transistors are analytically studied to determine the mechanisms. Several mechanisms for producing surface charge at the transistor junctions are important. The effect of the charge on the width and depth of the channel at the collector junction causes an increase of collector leakage current I_{CBO} when the sign of the charge is such as to drive the surface potential toward inversion. Variations of the transistor gain are due to the variations of the surface recombination velocity, which is a function of surface potential. It is suggested that mitigation be achieved by attempting to eliminate the variations of transistor surface potential. This can be accomplished by preventing the charging of the surfaces and surrounding medium. (auth)

31612 (SC-DC-66-1415) ANOMALOUS PHOTOCURRENT GENERATION IN TRANSISTOR STRUCTURES. Habing, Donald H.; Wirth, John L. (Sandia Corp., Albuquerque, N. Mex.). Apr. 1966. Contract AT(29-1)-789. 10p. (CONF-660705-2). Dep. mn. CFSTI $1.00 cy, $0.50 mn.

From IEEE Annual Conference, Palo Alto, Calif.

A common assumption made in the experimental characterization of transient radiation effects in transistors is that primary photocurrent scales linearly with dose or dose rate. Although this assumption is valid for a large variety of devices, there are notable exceptions. Rosenberg and Caldwell, for example, reported that many silicon device types exhibit an anomalous photocurrent response at modest dose rates (~10^8 R/sec.). Additional experimental evidence concerning the anomalous photocurrent problems is presented and a model which explains the observed data in terms of carrier generation and transport processes within the device is developed. (M.O.W.)

31613 (SC-DC-66-1443) TRANSIENT ANNEALING IN SEMICONDUCTOR DEVICES FOLLOWING PULSED NEUTRON IRRADIATION. Sander, H. H.; Gregory, B. L. (Sandia Corp., Albuquerque, N. Mex.). Apr. 1966. Contract AT(29-1)-789. 9p. (CONF-660705-1). Dep. mn. CFSTI $1.00 cy, $0.50 mn.

From IEEE Annual Conference, Palo Alto, Calif.

It was earlier shown that when a Si transistor is exposed at room temperature to a pulse of fast neutrons, the common emitter current gain is initially reduced to a value which is considerably lower than the gain which obtains several seconds or minutes after irradiation. Experiments with transistors and other Si semiconductor devices are reported which demonstrate that transient gain recovery in transistors is due principally to bulk annealing rather than a surface effect. In addition, the results of these and other experiments were compared with the predictions of various annealing models, e.g., the diffusion model, a first order close pair recombination model, etc. A general discussion of these models and the observed correlation is also presented. (M.O.W.)

31614 LITHIUM-DOPED, RADIATION-RESISTANT SILICON SOLAR CELLS. Wysocki, J. J. (RCA Labs., Princeton, N. J.); Rappaport, P.; Davison, E.; Hand, R.; Loferski, J. J. Appl. Phys. Lett., 9: 44-6(July 1, 1966).

It is shown that the use of lithium in silicon devices leads to a significant improvement in their ability to withstand a radiation environment. It was found that when lithium is the dominant impurity in floating-zone N-type silicon, a new center is formed by electron irradiation, which preserves the minority-carrier lifetime. Results are presented in terms of the conversion efficiency N of the cells. Lithium cells irradiated at a high rate degrade in a comparable fashion as cells without lithium, but the lithium cells recover after bombardment. This recovery process is time- and temperature-dependent. (M.C.G.)

31615 MODEL FOR RADIATION DAMAGE IN METAL-OXIDE-SEMICONDUCTOR STRUCTURES. Grove, A. S.; Snow, E. H. (Fairchild Semiconductor, Palo Alto, Calif.). Proc. IEEE (Inst. Elec. Electron. Eng.), 54: 894-5(June 1966).

A model is proposed to describe the effect of ionizing radiation on metal-oxide-silicon structures. A significant feature of this model is that it provides a link between observations made with MOS structures and earlier investigations of the defect structure of the silicas, thereby facilitating the study of both phenomena. (B.G.D.)

31616 LOW-ENERGY PROTON IRRADIATION OF COATED AND UNCOATED THIN-FILM CdS AND SINGLE-CRYSTAL Si SOLAR CELLS. Brucker, G. J.; Hui, W. L. C.; Noel, G. T. (RCA Astro-Electronics Div., Princeton, N. J.). Proc. IEEE (Inst. Elec. Electron. Eng.), 54: 895-6(June 1966).

An investigation of low-energy proton damage in thin film cadmium sulfide and in single-crystal silicon solar cells, which have been shielded over their entire area by the application of a special coating is reported. (B.G.D.)

31617 OPTICAL ABSORPTION IN GALLIUM ARSENIDE WHICH HAS BEEN IRRADIATED BY HIGH INTEGRATED FLUXES OF FAST NEUTRONS. Vodopyanov, L. K.; Kurdiani, N. I. (Lebedev Inst. of Physics, Moscow). Soviet Phys.-Solid State (Engl. Transl.), 8: 204-5(July 1966).

Translated from Fiz. Tverd. Tela, 8: 254-6(Jan. 1966).

The measurements showed that after irradiation by large integrated fluxes of fast neutrons the binary compound GaAs retains its basic semiconductor properties. However, the mobility and carrier concentration decrease by a large amount. Measurements of optical absorption show that after an intense irradiation the periodicity of the lat-

tice is preserved in GaAs, and one can continue to apply the usual band model to the crystal. Such irradiation did not cause any change in the width of the forbidden energy gap. (M.H.R.)

31618 RADIATION HARDENING OF AN ION PROPULSION SYSTEM. Davis, John J.; Burnett, James R. (Electro-Optical Systems, Inc., Pasadena, Calif.). 25p. (CONF-651136–1). ORAU. Gmelin, AED-CONF-65-343-11.

From International Space Electronics Symposium, Miami Beach, Fla.

A radiation tolerant electric propulsion system was developed and built to operate on the SNAPSHOT satellite, permitting the orbital test of ion propulsion and the test of an ion propulsion system with a nuclear power supply (SNAP-10A). The radiation environment in which the ion propulsion system must operate is 1×10^{13} n/cm^2 (fast) and 1×10^{10} ergs/g (carbon), accumulated over a 1-year period. The system described is one of the first complete systems designed entirely for operation in high-radiation fields. All electrical components have undergone both gamma and fast neutron testing at levels far exceeding those associated with the SNAP-10A. (auth)

31619 IDENTIFICATION OF RADIATION-PREFERRED ELECTRONICS. Brown, Richard R. (Boeing Co., Seattle). 13p. (CONF-651136–2). ORAU. Gmelin, AED-CONF-65-343-3.

From International Space Electronics Symposium, Miami Beach, Fla.

The space radiation environment assumed for this study is that anticipated for a typical interplanetary mission. Certain aspects of the radiation vulnerability of critical properties of electronic components were considered and a correlation made between the space environment and laboratory tests. Radiation safety margins for a typical interplanetary mission have been assigned to a large number of reliable electronic components that are desirable for space applications. (auth)

31620 ACTION DES RAYONNEMENTS NUCLEAIRES SUR LES COMPOSANTS ELECTRONIQUES, LYON 22–25 NOVEMBRE 1965. (Effect of Nuclear Radiations on Electronic Components, Lyon, November 22 25, 1965). Villeurbanne, France, Institut de Physique Nucleaire, [1966]. 223p. (CONF-651145–(Vol.1).

Lectures on the effect of nuclear radiations on electronic components are compiled. A rapid review of concepts necessary in the understanding of radiation effects: definition and characteristics of radiation, detection method, and the different types of radiation found in space, around reactors, and around accelerators is given. The properties of semiconductor materials are discussed, and the effect of radiation on the properties of transistors and the methods used to measure radiation effects are also discussed. (J.S.R.)

31621 CIRCUIT HARDENING USING COMPUTER TECHNIQUES. Stevens, G. G.; Dickhaut, R. H.; Caldwell, R. S. (Boeing Co., Seattle). 27p. (CONF-650707–25). ORAU.

From IEEE Annual Conference on Nuclear and Space Radiation Effects, Ann Arbor, Mich.

The degree of usefulness of a radiation network analysis computer program in performing hardened circuit redesign was determined. The general procedure and radiation testing technique are given. Circuits which were hardened and tested using this procedure are described. They are a high-level video amplifier, crystal oscillator, pulse former, pulse adder, and an ultrahigh monostable multivibrator. (J.F.P.)

ISOTOPE TECHNOLOGY

General

31622 RADIOISOTOPES FOR ARMY AIRCRAFT APPLICATIONS. Aldridge, George W. Jr. (Army Combat Developments Command Aviation Agency, Fort Rucker, Ala.). 24p. (CONF-660207-6). ORAU. Gmelin, AED-CONF-66-011-9.

From Symposium on Radioisotope Applications in Aerospace, Dayton, Ohio.

A survey is presented on the problems confronting Army aviation with regards to propulsion, control and alarm systems, navigation, and surveillance systems. (B.G.D.)

Industrial Applications

Refer also to abstract 31109.

31623 (AECD/AG-15) SUSCEPTIBILITY OF ADULT RICE WEEVIL, SITOPHILUS ORYZAE (L.) TO GAMMA RADIATION. Abdul Matin, A. S. M. (Atomic Energy Centre, Dacca (Pakistan). Agriculture Div.). Jan. 1966. 7p. Dep. mn.

An attempt was made to determine the effects of γ radiation on the adult rice weevil. Weevils were exposed to varying doses of radiation from 5 to 100 kR. All doses caused 100% mortality within one month except 5 kR. (auth)

31624 (BNWL-261) IRRADIATED WOOD-PLASTIC MATERIALS COMMERCIALIZATION IN THE PACIFIC NORTHWEST AND GREAT LAKES REGIONS. Rohrmann, C. A. (Battelle-Northwest, Richland, Wash. Pacific Northwest Lab.). June 1, 1966. Contract AT(45-1)-1830. 49p. Dep. mn. CFSTI $2.00 cy, $0.50 mn.

The potential for commercialization of irradiated wood-plastic materials in the Pacific Northwest and Great Lakes areas was studied and it was concluded that the selling price under large-scale production will range from about $2.10 to $2.60 per board foot. The examination of a variety of local wood species showed that Pacific Northwest hardwoods, red alder and big leaf maple, as well as the following softwoods, are most suitable for this treatment process: Douglas fir, western hemlock, ponderosa pine and Engelmann spruce. The problem of monomer loss at surfaces and particularly at the end grain of treated wood sections indicated that only uses involving a minimum of trimming losses are potentially commercial. In view of the high cost of the product a strong case could not be made for a specific site location for a plant. Further research and development work is suggested to solve the surface depletion problem so that the process can be applied to veneers and pre-shaped wood pieces. Work to impart fire retardency and cross linking or grafting of polymer to the cellulose fraction of the wood was also proposed. (auth)

31625 (NYO-3569-1) COMMERCIALIZATION STUDIES ON WOOD-PLASTIC COMBINATIONS PROCESS. Final Report. Evans, James C.; Egan, Douglas M.; McDonald, Philip R.; Collins, Carol H.; Knopp, Jacky (Western New York Nuclear Research Center, Inc., Buffalo). Dec. 17, 1965. Contract AT(30-1)-3569. 151p. (WNY-021). Dep. mn. CFSTI $1.75 cy, $1.00 mn.

The potential for commercialization of wood-plastic combinations in the northeastern United States was investigated. Market and demand analysis, cost and process analysis, technical analysis, and locating the facilities are discussed. (M.C.G.)

31626 MICROBIAL FLORA OF IRRADIATED DUNGENESS CRABMEAT AND PACIFIC OYSTERS. Shiflett, Maureen A.; Lee, J. S.; Sinnhuber, R. O. (Oregon State Univ., Corvallis). Contract AT(04-3)-502. Appl. Microbiol., 14: 411-15(May 1966).

Microorganisms in Dungeness crabmeat and Pacific oysters were identified by the replica-plating and computer analysis method. The initial flora of the shellfish and the flora change during storage at 7°C were determined. The microbial flora shifts in both shellfish were also determined after irradiation at 0.1 and 0.4 Mrad and during subsequent storage at 7°C. The Achromobacter species predominated in the initial flora of crabmeat (77.0%). The predominant position of this group increased to 99.2% after 0.1 Mrad and 100% after 0.4 Mrad. A large percentage of Lactobacillus was detected in oysters (55.0%). The Lactobacillus species were the predominant survivors after 0.1 Mrad (92.4%) but the predominant survivors after 0.4 Mrad were Achromobacter species (99.3%). (auth)

31627 APPLICATION OF MOISTURE MEASUREMENTS BY MEANS OF NEUTRONS. Netz, G. Atoomenergie Haar Toepass., 8: 110-15(May 1966). (In German).

The principles and the possibilities of measuring moisture contents by the recoil of neutrons are considered. As examples of the utility of the method, moisture content measurements of fine sand and coke are described. (tr-auth)

31628 PROGRESS OF FOOD IRRADIATION WORK AND PROGRAMMES IN O.E.C.D. MEMBER COUNTRIES. Food Irradiat., 6: No. 3, 3-27(Jan.-Mar. 1966).

Research on food irradiation in Austria, Belgium, Canada, Denmark, France, Germany, Italy, Netherlands, Spain, Sweden, Switzerland, United Kingdom, and United States is reviewed. Regulations and petitions on radiopreservation of foods in the United States are tabulated. (M.C.G.)

31629 BIOCHEMICAL CHANGES OCCURRING IN APPLE JUICE IRRADIATED FOR STORAGE. Tentcheva-Malinova, S. (Commissariat a l'Energie Atomique, Paris). Food Irradiat., 6: No. 3, 35-8(Jan.-Mar. 1966).

The effects of radiation dose and intensity, of temperature, and of processing method on the development of sugars, organic acids, and nitrogenous substances in stored apple juice were studied. The irradiated apple juice was lighter in color than the control, and there was appreciable though not very great, differences in taste. Doses of 0.6 and 1 Mrad were not enough to inhibit fermentation, while juice given doses of 1.5 and 2.1 Mrad was completely sterile and kept perfectly. (M.C.G.)

31630 TREATMENT OF MEATS WITH IONIZING RADIATIONS. XII. EFFECTS OF IONIZING RADIATION ON THE AMINO ACIDS OF MEAT PROTEIN. Rhodes, D. N. Contract DA91-591-EUC-2900. J. Sci. Food Agr., 17: 180-2(Apr. 1966).

The amino acid composition of meat protein was measured by ion-exchange chromatography after acid hydrolysis. No significant change in the proportion of any ninhydrin-reacting component was found when the meat was exposed at 0° to γ radiation at dose levels of 5 or 20 Mrads, with the exception of ammonia. These results confirm that the nutritional quality of meat protein is not impaired by doses of radiation likely to be used in practice. (auth)

31631 EFFECTS OF GAMMA RADIATION ON FREEZE-DEHYDRATED APPLES (PYRUS MALUS). Lee, C. Y.; Salunkhe, D. K. (Utah State Univ., Logan). Nature, 210: 971-2(May 28, 1966).

Chemical and histological effects of gamma radiation on freeze-dried apple slices are reported. Progressive browning and softening were observed during irradiation as the doses increased beyond 1×10^5 rads. Chemical analyses showed that volatile compounds were reduced by low doses of radiation, but increased at doses of more than 3×10^5 rads. Free reducing sugars were increased almost imperceptibly as doses increased, while ascorbic acid was decreased. Microscopic examination of the cell structure showed that parenchyma cells, cell wall rupture, and co-

agulation of cellular materials were induced by irradiation. It was concluded that freeze-dehydrated fruits are more stable than fresh fruits when both are similarly irradiated. (H.G.D.)

31632 CHANGES IN COMPOSITION AND IN ENZYMATIC ACTIVITIES OF FLAVEDO AND JUICE OF SHAMOUTI ORANGES FOLLOWING GAMMA IRRADIATION. Monselise, S. P.; Kahan, R. S. (Hebrew Univ., Rehovoth, Israel. Soreq Nuclear Research Center, Yavneh, Israel). Radiat. Bot., 6: 265-74(June 1966).

Green and mature Shamouti oranges were treated with 14 to 280 krad of γ radiation, applied at 420 krad/hr. Effects increased with dose (above 56 krad); in some cases they decreased with increasing delay between picking and irradiation. Green fruit was usually more affected than mature fruit. Influences of tissue dehydration and aging on radiation effects are thus shown. Effects obtained included: peel damage (pitting) greater at the stem end; a very marked decrease of the ascorbic acid content in flavedo (external peel layers), but only a small decrease in juice; an increase in peroxidase and a decrease in catalase activities of flavedo; and a decrease in reducing sugars of flavedo but no decrease in total soluble solids and citric acid of juice. Peroxidase, ascorbic acid, and sugars in flavedo showed differences from control within 2 days, but maximum effects were recorded 8 days after irradiation. (auth)

31633 MITOCHONDRIA: INCREASE IN OXIDATIVE CAPACITY AND QUANTITATIVE RECOVERY AFTER MASSIVE DOSES OF IONIZING RADIATION. Romani, R. J.; Ku, Lily Lim; Fisher, L. K.; van Kooy, J. G. (Univ. of California, Davis). Contract AT(11-1)-34). Radiat. Res., 28: 257-65(June 1966).

Two levels of massive γ irradiation, 200 to 250 krads and 600 to 1000 krads, produce divergent responses in fruit tissues. For several days after the higher doses, tissue respiration falls below that of control fruit, mitochondrial yields are reduced, and metabolic activity of isolated mitochondria remains at near control levels. The lower doses produce an elevated tissue respiration, a minor loss followed by a recovery in mitochondrial yield with time post-irradiation, and an increase in mitochondrial capacity for Krebs cycle activity. The possibility of mitochondrial repair of massive radiation damage is discussed. Applications in the radiation processing of pears to extend storage life are discussed. (auth)

31634 CRYOGENICS IN FOOD IRRADIATION. Snyder, Oscar P. Jr.; Shults, Gary (Army Natick Labs., Natick, Mass.). 19p. (CONF-650905-3). ORAU. Gmelin, AED-CONF-65-382-4.

From American Institute of Chemical Engineers Symposia, Minneapolis.

Early efforts toward sterilization of meat by radiation are reviewed. Recently better facilities made possible higher dose rates and irradiation at low temperatures. Experimental results indicated that flesh foods irradiated at low temperatures are superior in color, texture, flavor, and nutritional quality to those irradiated at ambient temperatures. Low temperatures also appear to protect the spores of certain important microorganisms such as C. botulinum 33A. Further study is in progress on microbiological problems, effects of rates of cooling, packaging of products, and irradiation equipment. (A.G.W.)

31635 A LOOK TOWARD COMMERCIAL USE OF RADIATION PRESERVATION. Urbain, Walter M. (Swift and Co., Chicago). 32p. (CONF-650552-5). ORAU. Gmelin, AED-CONF-65-111-5.

From Institute of Food Technologists, 25th Annual Meeting, Kansas City, Mo.

Three general requirements for commercial utilization of radiation preservation of food are discussed: that the process be permitted under the law, that the treated serve a useful purpose that can justify the cost involved, and that the cost of irradiation be competitive with alternate possibilities or be reasonable for the product involved. A table shows the current status of irradiated food petitions submitted to the U.S. Food and Drug Administration. Possible purposes of irradiation are listed. Costs (initial investment and operating costs) of a ^{60}Co facility and an x-ray facility are computed. It is concluded that, at an adequate scale of operation and a 13% rate of return, the additional processing cost will be in the range of 10 to 15 cents/lb. Finally, possible reaction of the consumer to irradiated foods is considered. (A.G.W.)

31636 IMPROVEMENTS IN OR RELATING TO SELF-LUMINOUS SIGNS OR PATTERNS. Hegarty, William (to Saunders Roe and Nuclear Enterprises Ltd.). British Patent 1,030,951. May 25, 1966. Filed Jan. 18, 1964.

A luminous display arrangement is described that consists of a number of self-luminous light sources of the type where a phosphor coating within a transparent envelope is excited to luminescence by a gaseous radionuclide of a quantity to produce the desired light intensity but not to produce health dangers. The light sources are disposed in any required order to form or described by their external profile the characters, symbols, or patterns that make up the luminous display. (B.L.M.)

Power Application

See also ENGINEERING — Space Propulsion

Refer also to abstracts 31361, 31387, and 31965.

Separation and Production

See also CHEMISTRY — Separation Processes and Procedures

Refer also to abstracts 31197 and 32837.

31637 (NYO-755-1) SEPARATION OF ISOTOPES. Annual Progress Report. Taylor, T. I. (Columbia Univ., New York. Dept. of Chemistry). Sept. 1, 1964. Contract AT(30-1)-755. 208p. (CU-17-64-AT(30-1)-755-Chem.). Dep. mn. CFSTI $6.00 cy, $1.25 mn.

Research progress is summarized in four sections. Separate abstracts were prepared for each section. (J.R.D.)

For abstracts of individual sections see: 31638–31641.

31638 (NYO-755-1, pp 12-76) SOLVENT CARRIER SYSTEM FOR CONCENTRATION OF ^{15}N BY CHEMICAL EXCHANGE BETWEEN OXIDES OF NITROGEN. Jeevanandam, M.; Taylor, T. I. (Columbia Univ., New York. Dept. of Chemistry).

Research directed toward developing methods of reducing concentrations of gas-phase NO_2 and N_2O_4 in processes for ^{15}N enrichment by exchange of NO with N_2O_3 is described. Work on the effects of carrier solvents on separation in exchange columns is reported. The effects of variables such as temperature, nitrogen oxides concentration, column packing, and flow rates were investigated. Improved separation was effected by using CCl_4-Freon 112 carrier solvent in columns packed with Helipack 3013 operated at N_2O_4 flows of 10 millimoles per minute. (J.R.D.)

31639 (NYO-755-1, pp 77-129) A STUDY OF THE FACTORS AFFECTING THE EXCHANGE OF ^{15}N BETWEEN NITRIC OXIDE AND NITRIC ACID IN EXCHANGE COLUMNS. Garbazevich, J.; Taylor, T. I. (Columbia Univ., New York. Dept. of Chemistry).

Factors that control the rates of ^{15}N exchange in the NO–HNO_3 system were investigated by testing the effects of additives to the nitric acid. Data are included on the effects of H_2SO_4, HCl, $HClO_4$, H_3PO_4, $CoSO_4$, $Fe_2(SO_4)_3$, $NaNO_3$, and $CuSO_4$ additions on overall separation for the NO–HNO_3 system. (J.R.D.)

31640 (NYO-755-1, pp 130-72) INVESTIGATION OF THE EXCHANGE BETWEEN METHYL ACETYLENE AND WATER FOR CONCENTRATION OF DEUTERIUM. Mahadevan, E. G.; Taylor, T. I. (Columbia Univ., New York. Dept. of Chemistry).

Results of investigations are reported in which data were gathered on deuterium exchange between methyl acetylene and water. Methods of contacting the gas and liquid phase were studied along with effects of catalyst types, catalyst concentrations, and types of solvents. (J.R.D.)

31641 (NYO-755-1, pp 173-208) ENRICHMENT OF ^{18}O AND ^{13}C BY CARBON DIOXIDE EXCHANGE IN SOME AMINE-SOLVENT SYSTEMS. Agrawal, J. P.; Taylor, T. I. (Columbia Univ., New York. Dept. of Chemistry).

Experiments were conducted to obtain data on exchange rates of ^{18}O and ^{13}C between CO_2 and various aqueous solutions. Similar experiments are reported using non-aqueous solvents containing amines. Chromatographic experiments to determine the concentration of water in the solvents and mixtures are described. The experiments were carried out using exchange columns and kinetic apparatuses based on gas-liquid contact in long capillaries. (J.R.D.)

31642 (ORNL-P-2190) THE U. S. ATOMIC ENERGY COMMISSION DEVELOPMENT PROGRAM FOR HIGH-SPECIFIC-ACTIVITY ISOTOPES FOR RESEARCH AND INDUSTRIAL APPLICATIONS. Baker, P. S. (Oak Ridge National Lab., Tenn.). [1966]. Contract W-7405-eng-26. 20p. (CONF-660503-3). Dep. mn. CFSTI $1.00 cy, $0.50 mn.

From 7th Japanese Conference on Radioisotopes, Tokyo.

The development program for high-specific-activity isotopes for research and industrial applications is discussed and the isotopes involved indicated. Properties and production methods of the isotopes considered are discussed. (M.C.G.)

31643 PRODUCTION AND APPLICATION OF RADIOELEMENTS IN BELGIUM. Constant, R. (CEN, Mol, Belg.). Energ. Nucl., 8: 175-84(May 1966). (In French).

The production of radioisotopes in Belgium reached 4048 consignments in 1964 or 31,700 curies distributed. The irradiation is usually carried out in the BR-2 reactor. In addition to short-lived radioelements, ^{60}Co, ^{192}Ir, ^{59}Fe, ^{45}Ca, ^{131}I, and labeled organic molecules, etc., are produced. Uses of the radioisotopes (radiation as well as tracers) are reviewed. (auth)

31644 STOICHIOMETRIC NUMBER AND ELECTROLYTIC SEPARATION FACTOR OF DEUTERIUM ON NICKEL HYDROGEN ELECTRODE. Enyo, Michio (Hokkaido Univ., Sapporo); Yokoyama, Takamitsu; Hoshi, Masamitsu. J. Res. Inst. Catalysis, Hokkaido Univ., 13: 222-37(1965).

A method is described, which determines (without neglecting the isotope effect) the stoichiometric number $\nu(r)$ of the rate-determining step r of the hydrogen electrode reaction from measurements of isotopic exchange reaction rate and reaction resistance. The method was applied to the nickel hydrogen electrode, and $\nu(r)$ determined at unity from the two experimental parameters obtained in the system of light water (0.124N NaOH) and pure deuterium at 25°C. Based on this value, the electrolytic separation factor of deuterium in the hydrogen ionization reaction, S_g, at the rest potential was determined at 1.5 from similar measurements of the two parameters at a deuterium content of 12.5% in gaseous hydrogen. From this S_g, the electrolytic separation factor of deuterium in the hydrogen evolution reaction, S_l, was deduced to be approximately 6 using the relation $S_l/S_g = S$, which holds at low deuterium content when the deuterium-containing hydrogen in contact with water is isotopically in equilibrium S is the partition coefficient of deuterium between aqueous solution and gaseous hydrogen. This S_l-value compares well with data in the literature, which were obtained at considerable cathodic polarizations. The results thus obtained support the theory that the hydrogen electrode reaction on nickel obeys the catalytic mechanism. (auth)

MATHEMATICS AND COMPUTERS

Refer also to abstract 32311.

31645 (AD-627094) PROGRESS REPORT [ON ELECTRONICS], SEPTEMBER–NOVEMBER 1965. (Illinois Univ., Urbana. Coordinated Science Lab.). Jan. 21, 1966. Contract Nonr-3985(08). 118p. CFSTI $4.00 cy, $0.75 mn.

The ionosphere program is now concerned only with rocket data reduction. For the general relativity satellite program, Baker-Nunn thresholds are discussed in relation to the problem of photographic observability, and the effect of micrometeorite cratering on determining the optimal diameter of the gyro satellite is discussed. Improvements in the electron source of the high-resolution electron spectrometer have resulted in a substantial increase in the sensitivity of the instrument. Preliminary measurements are reported that indicate the presence of low-energy loss peaks due to adsorbed gas. Progress on the construction of the apparatus for the measurement of the angular distribution of secondary electrons and on the instrumentation for the adsorption experiment is reported. Operation statistics, new facilities for bubble-chamber data processing, and new display equipment are reported. Several results were obtained in the continuing projects on the parameter-variation problem, stability of nonlinear systems, suboptimal linear time-invariant control, and computer-oriented formulation and solution of the optimal control problem. Several new projects were initiated in the area of optimal control of plants which are subject to parameter variations. PLATO research is described. Additional measurements on the pumping speeds of getter-ion pumps at low pressures were made. These measurements and those on the effects of bakeout and processing of uhv systems in ultimate pressure are discussed. In the studies on beam-plasma interaction, anomalous diffusion was observed during the beam instability together with intense radiation from plasma oscillations. Investigation of electron runaway in the linear plasma betatron has revealed an anomalous resistivity of the conduction current, which appears to stop the runaway current. Qualitative evidence was obtained for a collisionless damping of the Tonks-Dattner modes. Work is reported on a superconducting parametric amplifier (picovoltmeter), a study of the anisotropy of the energy gap in super-conducting niobium and studies of flux flow in type II superconductors. When electrodes are gas-conditioned, the sharp protuberances on the cathode are blunted, thereby increasing the breakdown voltage by a factor of about 5 and the effective emitting area and prebreakdown current by about two and one orders of magnitude, respectively. The permanence or stability of the gas-conditioned surface is being investigated. Continued work is reported on preparations for the size effect and Hall effect experiments. Development of the ionization-gage deposition monitor was continued to provide feedback control of the deposition rate. Several new investigations were started during this quarter. These include computer aided design of structures, dynamic analyses of structures, and the propagation of errors in finite memory encoding-decoding schemes. Further progress is reported on the computer compiler and self-diagnosis studies. In studies of nonlinear networks, new conditions were found such that transients decay to a unique periodic steady-state solution. These conditions permit a larger operating range of the nonlinear device (varactor) than is permitted by other solutions. In communication nets, studies include the overall reliability of nets with unreliable components, conditions for optimal flow in a net in which edge flow is limited, and nets with censors. In graph theory, studies are in progress on properties of biweighted graphs, and the determination of the minimum feedback arc set. (M.O.W.)

31646 (AECL-1744) LIBRARY PROGRAMS FOR THE A.E.C.L. G-20 COMPUTER. PARTS A AND B. Okazaki, E. A.; Fowler, J. K. (Atomic Energy of Canada Ltd., Chalk River (Ontario)). May 1963. 443p. (CRT-1149). Dep. mn. AECL $9.00 per set.

Included are descriptions of library programs that were written at Chalk River for the G-20 computer. Subroutines for use with the SNAP assembler, and library procedures for use with the APEX Compiler are described. Listings of the source code for these programs are found in part B. (M.O.W.)

31647 (AECL-1744(Pt.A)(Add.1)) LIBRARY PROGRAMS FOR THE A.E.C.L. G-20 COMPUTER. Cowley, S. J. (Atomic Energy of Canada Ltd., Chalk River (Ontario)). Jan. 1966. 61p. (CRT-1149(Pt.A)(Add.1)). Dep. mn. AECL $1.50.

Several other computer programs are listed and described which calculate various mathematical functions. (M.O.W.)

31648 (COO-1018-1021) WEB: A LANGUAGE TO DESCRIBE THE INTERCONNECTION AND PACKAGING OF THE LOGICAL UNITS IN A DIGITAL PROCESSOR. PART I: PREPARATION OF INPUT DATA. Hazelhurst, J. H.; McCormick, B. H. (Illinois Univ., Urbana. Dept. of Computer Science). Aug. 17, 1964. Revised Feb. 10, 1965. Contract AT(11-1)-Gen-8. 43p. Dep. mn. CFSTI $2.00 cy, $0.50 mn.

Input data for interim WEB are divided into two parts. First, the Logic Description specifies how the logical elements of the system are to be interconnected. Second, the Packaging Description specifies the circuit modules, card bins, etc., available. The preparation of the input description (both logic and packaging) of the logic processor is discussed. (M.O.W.)

31649 (COO-1018-1030) DETAILS OF TRANSFER MEMORY INPUT/OUTPUT SIGNALS. Ray, S. R. (Illinois Univ., Urbana. Digital Computer Lab.). Nov. 3, 1964. Contract AT(11-1)-1018. 10p. Dep. mn. CFSTI $1.00 cy, $0.50 mn.

A discussion is presented of the details of the TRANSFER MEMORY (TM) input/output signals. The discussion concerns requests, controls, addresses, and information. A table of typical TM operations is presented. (M.O.W.)

31650 (COO-1018-1031) SYNTAX LOADER AND SUBSCANNER FOR A COMPILER-COMPILER. Northcote, Robert S.; Steiner, Albert J. (Illinois Univ., Urbana. Digital Computer Lab.). Dec. 1, 1964. Contract AT(11-1)-1018. 65p. Dep. mn. CFSTI $3.00 cy, $0.75 mn.

The Compiler-compiler described earlier by Feldman was shown to consist of three main parts: A Syntax Loader, a Semantics Loader, and a Basic Compiler—a general purpose table driven compiler which uses the tables generated by the loaders. Included is a detailed description of the use and construction of the Syntax Loader and the Basic Compiler. (M.O.W.)

31651 (COO-1018-1054) GRAMMAR FOR A PATTERN DESCRIPTION LANGUAGE. Report No. 177. Breeding, Kenneth James (Illinois Univ., Urbana. Dept. of Computer Science). May 27, 1965. Contract AT(11-1)-1018. 62p. Dep. mn. CFSTI $3.00 cy, $0.75 mn.

A language is derived which may be used to describe a class of pictures. The language is shown to be applicable to a limited pattern recognition problem. The grammar and some of the simple properties of the language are described. (M.O.W.)

31652 (COO-1018-1057) ILLIAC III: A PROCESSOR OF VISUAL INFORMATION. Report No. 183. McCormick, Bruce H.; Ray, Sylvian R.; Smith, Kenneth C.; Yamada, Shigeharu (Illinois Univ., Urbana. Dept. of Computer Science). June 10, 1965. Contract AT(11-1)-1018. 9p. Dep. mn. CFSTI $1.00 cy, $0.50 mn.

An outline for visual data processing using the ILLIAC III is presented. The input image is digitized by a TV-like scan, then digitally filtered and idealized to a line drawing in the Pattern Articulation Unit. Upon output from this unit the image is described by a string of displacement vectors, appropriate for an incremental plotter with coordinate stack storage. Subsequent recognition consists of programmed syntactic and semantic analysis of the vector string description using an enriched repertoire of list processing instructions. (M.O.W.)

31653 (COO–1018-1061) PRELIMINARY PROGRAMMING MANUAL FOR THE ILLIAC III COMPUTER. Report No. 185. McCormick, Bruce H.; Bond, William D.; Ibuki, Kimio; Wiegel, Roger E.; Wilber, John A. (Illinois Univ., Urbana. Dept. of Computer Science). July 7, 1965. Contract AT(11-1)-1018. 39p. Dep. mn. CFSTI $2.00 cy, $0.50 mn.

Included are discussions on the following areas for operation of the ILLIAC III computer: information formats, operand addressing/imprimitive instructions, primitive instructions and the basic machine language. (M.O.W.)

31654 (COO–1018-1066) QUARTERLY TECHNICAL PROGRESS REPORT, JULY–SEPTEMBER 1965. (Illinois Univ., Urbana. Dept. of Computer Science). Contract AT (11-1)-1018. 208p. (COO–1469-0012). Dep. mn. CFSTI $6.00 cy, $1.25 mn.

Developments in the circuit research program are reported. Efforts in the Paramatrix System were concentrated on the checkout of the interpolator. In the Electro-Optical work a new fast infrared detecting circuit is described. Some modifications were made to the optical differential amplifier and several experiments are proposed for its use. Detailed experimental results of the Random Sequence Coding are presented showing very close agreement with theory. The Film Scanner project is now complete and the entire system is described. Other research developments are reported on the following: hardware systems, software systems, ILLIAC III, numerical methods–computer arithmetic and artificial language, ILLIAC IV, ILLIAC II service and uses, and other associated studies. (M.O.W.)

31655 (COO–1018-1076). QUARTERLY TECHNICAL PROGRESS REPORT, OCTOBER–DECEMBER 1965. (Illinois Univ., Urbana. Dept. of Computer Science). Contract AT(11-1)-1018. 181p. (COO–1469-0017). Dep. mn. CFSTI $5.00 cy, $1.00 mn.

Further research developments are reported for each of the following areas: circuit program, hardware systems, time-sharing systems, ILLIAC III, numerical methods– computer arithmetic and artificial languages, ILLIAC II service and uses, and other associated research areas. (M.O.W.)

31656 (IDO–17175) NUMERICAL TECHNIQUES FOR SOLVING FREDHOLM'S INTEGRAL EQUATIONS OF THE FIRST KIND. Marshall, Neldon H. (Phillips Petroleum Co., Idaho Falls, Idaho. Atomic Energy Div.). May 1966. Contract AT(10-1)-205. 36p. Dep. mn. CFSTI $2.00 cy, $0.50 mn.

Integral equations of the first kind occur where two or more effects are superimposed to produce a measureable result. The solution of these equations is equivalent to separating the undesirable effects from the one which is to be studied. Three general approaches of solution are discussed, i.e., least square methods, iterative techniques, and smoothing techniques. The merits and limitations of each method are also discussed. Results are shown demonstrating the application of these methods to test data. In practice, one or more of these techniques may be applicable to give a satisfactory solution. (auth)

31657 (KAPL-M-6548) LIZARD-IV: A PROGRAM TO SOLVE NONLINEAR, ORDINARY DIFFERENTIAL EQUATIONS. Guillette, Robert W.; Mueller, Gerhard O.; Schmid, Joseph R. (Knolls Atomic Power Lab., Schenectady, N. Y.). Mar. 17, 1966. Contract W-31-109-eng-52. 25p. Dep. mn. CFSTI $1.00 cy, $0.50 mn.

LIZARD-IV is a program that can be used to solve nonlinear, ordinary differential equations. The program is capable of handling up to twenty-five first order equations. Higher order equations must be reduced to first order by the substitution of new dependent variables. Several examples, typical of problems that can be solved with this program, are illustrated. The results may also be plotted using the CALCOMP Plotter. Typical running time for a LIZARD-IV problem is dependent upon the number of equations, number of terms per equation, and the number of time steps required for the solution. Several two-equation LIZARD-IV runs, using 200 time steps, consumed between 55 and 70 seconds of machine time on a Philco 2000-212 computer. The LIZARD-IV program supersedes LIZARD, the original FORTRAN-II version of the program. The LIZARD-IV program is written in FORTRAN-IV language. (auth)

31658 (NAA-SR-Memo–11653) SPENCER: A FORTRAN PROGRAM TO APPROXIMATELY RECONSTITUTE A ONE-DIMENSIONAL FUNCTION FROM A FINITE NUMBER OF ITS MOMENTS. O'Reilly, Bruce D.; Lewis, Richard C. (Atomics International, Canoga Park, Calif.). Nov. 1965. Contract AT(11-1)-Gen-8. 35p. Dep. mn. CFSTI $2.00 cy, $0.50 mn.

The approximate reconstitution of a function G(x), from a finite number of its moments is accomplished using L. V. Spencer's function-fitting method. G(x) is assumed to exist in the region $-\infty < x < \infty$. The even and odd components of G(x) are assumed to be fitted by the forms.

$$G_e(x) = \tfrac{1}{2}[G(x) + G(-x)] \doteq \overline{G}_e(x) = \sum_{j=1}^{J} \frac{a_{ej}}{\sqrt{b_{ej}}} f\left(\frac{x}{\sqrt{b_{ej}}}\right)$$

and

$$G_0(x) = \tfrac{1}{2}[G(x) - G(-x)] \doteq \overline{G}_0(x) = \sum_{j=1}^{J} \frac{a_{0j}}{b_{0j}} f\left(\frac{x}{\sqrt{b_{0j}}}\right)$$

The method extends directly to the reconstitution of functions existing only in the semi-infinite domain $0 \leq x < \infty$. The form of the trial function f is chosen to reflect whatever characteristics of G(x) are known a priori. The use of the FORTRAN II code SPENCER, which implements the application of Spencer's method, is discussed. The preparation of input data is described in detail. The input and output data for a sample problem are given in an appendix. Some emphasis is placed on showing how the code can be used to numerically invert certain types of integral transforms. (auth)

31659 (ORNL-TM–1497) NUMERICAL ANALYSIS OF A PARABOLIC PARTIAL DIFFERENTIAL EQUATION CONTAINING BOTH FLOW AND DIFFUSION TERMS. Pickel, T. W. (Oak Ridge National Lab., Tenn.). June 1966. Contract W-7405-eng-26. 116p. Dep. mn. CFSTI $4.00 cy, $0.75 mn.

Thesis. Submitted to the Univ. of Tennessee, Knoxville.

Two approaches for the numerical solution of a partial differential equation containing both flow and diffusion terms were investigated. In the first approach, explicit difference equations were used to approximate the differential equation. In the second approach, the diffusion and flow effects were calculated separately and then combined to obtain a solution. The stability and convergence requirements for each approach were determined. Numerical examples were calculated on a Control Data Corporation Model 1604 computer to test these approaches, two methods being tested for each approach. The numerical examples indicate that the approach of separating the effects of flow and diffusion gives a better approximation to the partial differential equation. Possible changes in the calculation procedure for this approach that would improve the accuracy for a given computer running time are indicated. (auth)

31660 (RISO–M–385) BERETNING OM ARBEJDET I ELEKTRONIKAFDELINGEN I TIDEN 1 OKTOBER TIL 31 DECEMBER 1965. (Quarterly Report of the Electronics Department for the Period October 1–December 31, 1965. (Danish Atomic Energy Commission, Risoe. Research Establishment). Mar. 1966. 18p. (R–2–66). Dep. mn.

Work is reported on the PDP-8 computer system, apparatus for testing of digital computers, numerical studies on instrumentation, effects of dial instruments, and coupling of PDP-8 to analog computers. (J.S.R.)

31661 (SLAC-PUB-191) CHARACTERISTICS OF SMALL COMPUTER SYSTEMS FOR ON-LINE APPLICATIONS. Brown, Richard M. (Stanford Linear Accelerator Center, Stanford Univ., Calif.). May 1966. Contract AT(04-3)-400. 13p. (CONF-660527-3). Dep. mn. CFSTI $1.00 cy, $0.50 mn.

From Symposium on Use of Computers in Analysis of Experimental Data and Control of Nuclear Facilities, Argonne, Ill.

A summary of the characteristics of 31 domestic computers relevant to on-line applications is presented. Some of the problems specific to on-line use are discussed and the alternatives available in different models are described. For the survey, a small computer is taken as any which might be dedicated to on-line operation, excluding time-sharing systems. (auth)

31662 (TID-23020) ANNUAL REPORT, SEPTEMBER 1, 1965-AUGUST 31, 1966. (Illinois Univ., Urbana. Dept. of Computer Science). May 26, 1966. Contract AT(11-1)-1469. 62p. Dep. mn. CFSTI $3.00 cy, $0.75 mn.

The study and implementation of the central computer software and remote console designs for special and general purpose time-sharing are described. During the year, the operational status of the ILLIAC II software system has changed from a Batch processing system through a Temporary Time-Sharing System to a Provisional Time-Sharing System using three consoles for general purpose time-sharing simultaneously with regular batch processing. An initial version of the final Time-Sharing System is expected to be operational in the fall. Hardware was constructed to interface Teletype consoles to the main frame of the ILLIAC for the Provisional System, and a channel was constructed to interface the PDP-7 Satellite Computer to the ILLIAC. Revisions are being made to the batch processing translators FORTRAN and NICAP for interactive use in the time-sharing system. A number of special purpose time-shared programs were written to handle desk calculator work, interactive debugging of FORTRAN programs and automatic interactive numerical integration of ordinary differential equations. Work has begun on a study of the types of programming languages that should be used at a remote console with graphic capability and some preliminary work was done on the type of remote console that can be constructed for, say, $10,000 in 4 years' time, and what sort of language should be used to communicate between such a console and the main machine. Pattern processing and memory research is described. (M.O.W.)

31663 PHYSICAL STATE VECTOR-SPACE REPRESENTATIONS OF NONCOMPACT GROUPS. Roman, P.; Koh, C. J. (Boston Univ.). Nuovo Cimento (10), 43A: 1162-4 (June 21, 1966).

A method is proposed for constructing physically acceptable representations of noncompact groups and algebras, which avoids the problems connected with question of domains of observables, their self-adjointness, and the nature of their eigenstates in relevance to physical state vectors. Two applications are pointed out. (L.B.S.)

METALS, CERAMICS, AND OTHER MATERIALS

General

Refer also to abstract 32796.

31664 POSSIBLE ROLE OF SUPERCOOLING IN THE SPEARPOINTS OBSERVED DURING THE COMBUSTION OF ZIRCONIUM DROPLETS. Nelson, L. S. (Sandia Lab., Albuquerque, N. Mex.). Nature, 210: 410-11(Apr. 23, 1966).

Experiments on vibrational nucleation of burning zirconium droplets suggest that supercooling may participate significantly in the formation of spearpoints on photographic time exposures. An attempt to distinguish between intensification by solidification after supercooling and an increased emittance on freezing was made by causing the burning droplets to collide with an aluminum plate at various times during free fall. Studies were performed with 525μ droplets of zone-melted zirconium burning in ultrapure oxygen at 625 torr. The burning droplets were photographed simultaneously with both a still camera and a high-speed movie camera. Results suggest that nucleation was induced with high probability by deflecting the burning droplets from an aluminum plate; and that the droplets had cooled to the true freezing point at 152 msec, the earliest time at which solidification could be induced by mechanical shock. (H.G.D.)

31665 REACTOR MATERIALS. Volume 9, Number 1. Dayton, R. W.; Simons, E. M.; Endebrock, R. W. (eds.). Contract W-7405-eng-92. One of the five Quarterly Technical Progress Reviews published for the Division of Technical Information, USAEC. Battelle Memorial Inst., Columbus, Ohio, Spring 1966. 71p. GPO $0.70 Domestic, $0.90 Foreign.

Separate abstracts were prepared for the five sections of the report. (W.L.G.)

For abstracts of individual sections see: 31666–31670.

31666 FUEL AND FERTILE MATERIALS. Reactor Mater., 9: 1-19(Spring 1966).

A summary of recent research developments is presented. (84 references). (W.L.G.)

31667 MODERATOR MATERIALS. Reactor Mater., 9: 20-31(Spring 1966).

A summary of recent research developments is presented. (27 references). (W.L.G.)

31668 NUCLEAR POISONS. Reactor Mater., 9: 32-4 (Spring 1966).

A summary of recent research developments is presented. (6 references). (W.L.G.)

31669 CLADDING AND STRUCTURAL MATERIALS. Reactor Mater., 9: 35-62(Spring 1966).

A summary of recent research developments is presented. (115 references.) (W.L.G.)

31670 SPECIAL FABRICATION TECHNIQUES. Reactor Mater., 9: 63-71(Spring 1966).

A summary of recent research developments is presented. (43 references.) (W.L.G.)

31671 PREFERRED ORIENTATION OF BERYLLIUM SHEET USING SMALL SPHERICAL SPECIMENS. Damiano, V. V. (Franklin Inst. Research Labs., Philadelphia); Herman, M.; Hoover, D. Trans. Met. Soc. AIME, 236: 829-32 (June 1966).

The Jetter and Borie technique of determining textures using a spherical specimen was applied to the study of compression-rolled beryllium sheet. Small spheres the order of 1 mm in dia cut from the beryllium sheet were automatically rotated about two axes using the G. E. single-crystal goniometer. Quantitative pole figures were obtained without the need to apply absorption corrections. Compression-rolled beryllium exhibited peak intensities for (0002) planes of positions tilted 10° to the rolling plane and a near random distribution of $(10\bar{1}0)$ planes about the normal to the rolling plane. (auth)

31672 MECHANISMS OF GRAIN-BOUNDARY GROOVING IN CHROMIUM, MOLYBDENUM, TUNGSTEN, Cr–35Re, Mo–33Re, AND W–25Re. Allen, B. C. (Battelle Memorial Inst., Columbus, Ohio). Trans. Met. Soc. AIME, 236: 915-24(June 1966).

Grain-boundary grooving was studied in Cr, Mo, W, and the solid-solution alloys, Cr–35Re, Mo–33Re, and W–25Re at 0.6 to 0.9 of the absolute liquidus temperature under an inert atmosphere, foreign and metal vapor, and liquid metal. The controlling mechanism of matter transport was deduced from groove size and shape, kinetics of growth, and comparison with theoretical relationships derived by Mullins. Grooves in Cr formed primarily by volume diffusion through He or Ar at 1 atm pressure and by evaporation-condensation in a static vacuum. Grooves in the other metals and alloys formed primarily by surface diffusion, the coefficients of which were calculated. C was found to decrease the activation energy for surface diffusion on Mo. Surface diffusivities were similar for Mo–0.2C and Mo–33Re. The presence of about 1-mm pressure of Ag or Sn vapor did not affect the mechanism of groove formation. In liquid Sn or Ag, grain boundary grooves formed by volume diffusion in the liquid. (auth)

31673 TECHNIQUE FOR REVEALING MICROSTRUCTURES AND VARIATIONS IN {hkl} ORIENTATIONS IN TANTALUM. Dunn, C. G. (General Electric Research and Development Center, Schenectady, N. Y.). Trans. Met. Soc. AIME, 236: 947-8(June 1966).

Three steps are involved. First, an amorphous film of Ta_2O_5 is formed anodically on the surfaces of the Ta. The amount needed depends on the thickness of the substrate tantalum; 1600Å of oxide is generally satisfactory in the $\frac{1}{2}$ to 3-mil thickness range. The film at this point is uniform in color. Second, the anodized specimen is heated to 800°C in vacuo during a period of a few minutes and held at temperature for 5 min. The presence of a residual oxide layer after the heat treatment usually is not apparent; in most instances the surfaces have a metallic appearance. The third step reveals (or produces) a varied colored film of tantalum oxide. Two methods can be used. If the specimen is dipped in 48% HF for a few seconds, the Ta is found to be covered with a multicolored oxide. Moreover the colors correlate with the grain structure of the substrate Ta through an orientation dependence. The alternative third step is to reanodize the specimen. The optical nature of the final anodic film depends on the presence of the crystalline oxide phase; color variations indicate optical thickness variations in the film. As the reanodization voltage is increased from zero, straw and light brown colors appear followed by variations in color from grain to grain depending on {hkl} orientation. Suitable end points, which are determined by voltage and time, are easily established. (W.L.G.)

31674 EFFECT OF STOICHIOMETRY ON THE PROPERTIES OF MIXED OXIDE U–Pu FUEL. Zebroski, E. L.; Lyon, W. L.; Baily, W. E. (General Electric Co., San Jose, Calif.). 40p. (CONF-651009–26). ORAU. Gmelin, AED-CONF-65-307-39.

From Conference on Safety, Fuels, and Core Design in Large Fast Power Reactors, Argonne, Ill.

Some investigations of the preparation, properties, and performance of PuO_2-UO_2 fuel are discussed. The results lead to a tentative preference for a stoichiometry of 1.97 to 1.98 for mixed PuO_2-UO_2 fuel. Some observations on the effect of stoichiometry on the properties of UO_2 are also summarized. (D.C.W.)

31675 ACCOUNT OF SOME WORK ON THE SAFETY ASPECTS OF CARBIDE FAST REACTOR FUELS. Bradbury, B. T.; Russell, L. E.; Waldron, M. B. (Atomic Energy Research Establishment, Harwell, Eng.). 47p.

(CONF-651009-27; FRPC-FEWP-P(65)298). ORAU. Gmelin, AED-CONF-65-307-44.

From Conference on Safety, Fuels, and Core Design in Large Fast Power Reactors, Argonne, Ill.

The experimental results thus far obtained on three aspects of fuel and cladding behavior which are important to the safety of an operating fuel element are described and discussed. These are the compatibility of (UPu)–C and U–C with 316L stainless steel cladding material under both gas bonded and sodium bonded conditions, the compatibility of (UPu)–C with a number of nickel-based alloys, the gas release and swelling behavior of (UPu)–C of varying composition using sintered, arc-cast, and powder fuel, and some initial experiments on plutonium-bearing oxycarbides which give some indication of the stability of these fuels at high temperatures. (J.F.P.)

Corrosion

Refer also to abstract 31959.

31676 (COO–1319-39) A STUDY OF THE MECHANISM OF STRESS CORROSION CRACKING IN THE IRON–NICKEL–CHROMIUM ALLOY SYSTEM. Quarterly Report, December 17, 1965–March 16, 1966. Staehle, R. W. (Ohio State Univ. Research Foundation, Columbus). Apr. 28, 1966. Contract AT(11-1)-1319. 37p. Dep. mn. CFSTI $2.00 cy, $0.50 mn.

Work on installing a source of high-purity water was completed. A preliminary study of the effect of specimen surface preparation on time to breaking suggested that the explanation for the wide range of the data may lie in the nature of the passive film. The effect of boiling $MgCl_2$ on time to breaking of various alloy compositions is being studied for subsequent comparison with results from circulating autoclave studies. Information from boiling $MgCl_2$ studies showed cracking in commercial alloys at nickel contents as high as 55%. Thin foils of iron were exposed to boiling $MgCl_2$ with the result that stressed foils exhibited dissolution patterns that suggest preferential dissolution in regions through which mobile dislocations passed. This finding was similar to the results for pure nickel and various ternary alloys. (auth)

31677 (GEAP–4840) SPECIFIC ZIRCONIUM ALLOY DESIGN PROGRAM. Quarterly Progress Report No. 9, April–June 1965. Klepfer, H. H.; Baroch, C. J.; Blood, R. E.; Jaech, J. L.; Pickett, E. A. (General Electric Co., San Jose, Calif. Atomic Power Equipment Dept.). July 1965. Contract AT(04-3)-189. 55p. (EURAEC–1460). Dep. mn. CFSTI $3.00 cy, $0.75 mn.

Work Performed under United States–Euratom Joint Research and Development Program.

The Specific Zirconium Alloy Design Program was reinstated in November 1964 for the evaluation of a Zr + 2.0 at. % Cr + 0.16 at. % Fe alloy as nuclear fuel cladding. Tubing and bar stock of the alloy was obtained by full-scale vendor fabrication. Alloy-clad fuel rods were fabricated for irradiation in Consumer's Big Rock Reactor to a target exposure of 15,000 MWD/T. Technologically, there were no fabrication difficulties with the alloy. The fuel irradiation was delayed, however, by variable corrosion performance by this first vendor batch of alloy tubing and bar stock. Further tests on laboratory melts run side-by-side with the vendor samples confirmed the potential of the composition for excellent corrosion performance. The difference in performance between material from large, slow-cooling vendor ingots and small, fast-cooling laboratory melts was shown to be related to the size and uniformity of distribution of the intermetallic precipitates in the alloy. Material re-melted from the vendor forging and processed in the laboratory gave excellent performance; purposely slow-cooled laboratory samples gave poor performance in the same test. Experiments to determine the proper fabrication schedule for control of microstructure in full-scale processing are to be made. Another experiment is in progress to establish the effect of nitrogen content in the range of 20 to 500 ppM on the corrosion rate of Zr + 2.0 at. % Cr + 0.16 at. % Fe in high-pressure, refreshed steam at 300, 400, and 500°C. (auth)

31678 (HIT–3583-24) LOW ENRICHED PM REPLACEMENT CORE. CONTROL MATERIALS METALLURGICAL EVALUATION. (Hittman Associates, Inc., Baltimore, Md.). Apr. 26, 1966. Contract AT(30-1)-3583. 17p. Dep. mn. CFSTI $1.00 cy, $0.50 mn.

Europium oxide–titanium oxide compositions of molar ratios ranging from 1:3 to 1:0.6 europium oxide to titanium oxide were prepared and evaluated for corrosion resistance in high-temperature water. It was concluded that all compositions of greater than 50 mole percent TiO_2 content show excellent corrosion resistance in water at 596°F and 1500 psia and the Eu_2O_3–TiO_2 blends are compatible with silicon-bearing stainless steel when sintered as stainless steel cermets at 1250°C. The stainless steel cermets of the europium oxide–titanium oxide compositions also show good corrosion resistance to high-temperature water. Although the resistance of the blends containing less titania than the Eu_2O_3–$2TiO_2$ position shows some decrease in corrosion resistance, all of the cermets containing the Eu_2O_3–TiO_2 are superior to the high-fired europium oxide-stainless steel cermets. (auth)

31679 (LA–3524) QUARTERLY STATUS REPORT ON ADVANCED REACTOR TECHNOLOGY (ART) FOR PERIOD ENDING APRIL 30, 1966. (Los Alamos Scientific Lab., Univ. of California, N. Mex.). May 1966. Contract W-7405-eng-36. 68p. Dep. mn. CFSTI $3.00 cy, $0.75 mn.

Further developments in the various components of the Fast Reactor Core Test Facility are described. Some of the cores of the FRCTF are briefly described. Containers for the molten Pu–Co–Ce fuels were tested. Corrosion tests were made on carburized and uncarburized Ta, Ta–W, Ta–W–Y, Nb–Zr, and Nb–W alloys. The tensile properties of uncarburized and carburized Ta–W alloys are given. Burst tests were made on several of the containers. Other brief discussions of various supporting research are presented. (M.O.W.)

31680 (NAA-SR-Memo-11652) COMPILATION OF DATA AND BIBLIOGRAPHY CONCERNING CORROSION OF STRUCTURAL MATERIALS IN LIQUID ALKALI METALS. Cuffel, R. F. (Atomics International, Canoga Park, Calif.). Oct. 13, 1960. Contract AT-11-1-GEN-8. 131p. Dep. mn. CFSTI $4.00 cy, $1.00 mn.

A bibliography and data compilation on corrosion of various structural material in liquid alkali metals are presented. The search was primarily directed to material published after 1950. The primary sources were the Liquid Metal Abstract Bulletins LM/TAB-1 through 14, the subject card index at Atomics Interantional for AEC reports, and the references given in the material located. Over 300 references are included. (M.C.G.)

31681 (NAA-SR-Memo-11707) BRITTLE FAILURES OF CARBON STEEL TUBES. Winborne, R. A. (Atomics International, Canoga Park, Calif.). Nov. 15, 1965. Contract AT-11-1-GEN-8. 15p. Dep. mn. CFSTI $1.00 cy, $0.50 mn.

Information from case histories is presented pertaining to brittle (thick-edge) failures of low-carbon steel tubes in pressure boilers operating at temperatures of 600 to 1000°F and pressures of 450 to 2700 psi. A theory development is included, which is an extension of Dr. E. P. Partridge's methane theory. Six major factors are believed to be involved in initiation and subsequent progress of a crack advancing through a tube wall: initial tube damage, corrosion, decarburization, methane production, tensile (hoop) stress, and the direct action of tube internal pressure on crack wall surfaces. Tube failure could occur in the manner outlined below. Tube embrittlement starts with corrosion of interior (water side) surfaces producing hydrogen. Methane is produced by reaction of hydrogen with carbon in steel near the corroding surface. Microfissures along grain boundaries, enlarged by methane pressure, propagate to the corroding surface. Crevice

corrosion produces pitting of this surface. Ligaments between fissures are destroyed by corrosion, and embrittlement extends through the tube wall. The weakened tube section eventually is partially cracked by tensile (hoop) stress. Hoop stress and the direct action of tube internal pressure then contribute to fissure rim stress concentration to enlarge fissures ahead of the crack moving through the tube wall. Rupture occurs and the crack extends in an axial direction the length of the embrittled tube section. (auth)

31682 (NP–16003) NOVYI METOD IZUCHENIYA INTENSIVNOSTY KORROZII KONSTRUKTSIONNYKH MATERIALOV REAKTOROV. (A New Method for Studying the Intensity of Corrosion of Reactor Construction Materials). Akol'zina, P. A.; Ivanova, E. N. [nd]. 13p.

An examination of the method showed that it is especially sensitive to local corrosion. A prediction was obtained of the measured growth of the resistance of the sample in comparison with theoretically calculated growth with respect to weight loss. The coefficients of distribution and the velocity of the corrosion penetration into the metal could be calculated. In homogeneous corrosion the growth of the resistance, calculated from the weight loss of the sample, agreed almost completely with results from measurements made at the end of the test. This method required continuous registration of the increase in electric resistance during corrosion of the sample and, in the case of local corrosion in aqueous media, evaluation of the sample's weight loss during the entire test period. During homogeneous corrosion (gaseous and organic thermal conductors) observations on the development of the corrosion process were limited only by the fixation of the growth of the electric resistivity of the sample: weighting it was not necessary. In tests in liquid metal heat conductors the corrosion stability of metals was evaluated only by the primary and final measurement of the electric resistance of the sample in the absence of the contact with the metal. In determination of the corrosion stability of different metals and alloys, in the absence of wire samples, the latter could be measured by narrow foil strips. The method given can be used principally as a corrosion indicator and for corrosion graphs with automatic registration and signalling of corrosion. (tr-auth)

31683 (ORNL–3936, pp 95-121) METALLURGY. (Oak Ridge National Lab., Tenn.).

Thermal convection loops made of Hastelloy N and type 304 stainless steel have circulated molten fuel salt for 33,000 and 22,000 hr, respectively, without incident. A Cb–1% Zr loop circulating lead at 1400°F with a 400°F ΔT was found to produce columbium crystals by mass transfer. Specimens of Hastelloy N and grade CGB graphite showed no detectable changes as a result of 1100 hr exposure to molten fluoride salts in the MSRE core during the precritical, initial critical, and associated zero-power experiments. The reactor control specimen rig, which will establish base-line data by exposing graphite and Hastelloy N surveillance specimens to approximately the operating conditions of the MSRE except for radiation, was loaded with salt and is being calibrated with the computer that monitors the MSRE. Metallographic examination of capsules from in-pile experiment MTR-47-6 showed no evidence of nitriding of the Hastelloy N. No apparent change in wall thickness or evidence of attack was observed, although an unexplained change in the etching characteristics of the grain boundaries at the surface was noted. Development of methods of joining graphite to metal has included: (1) the design of a transition joint to reduce shear stresses arising from thermal expansion differences and (2) screening tests on potential brazing alloys. A small pipe of grade CGB graphite brazed to molybdenum satisfactorily contained molten fluoride salts at 700°C under pressures of 50, 100, and 150 psig for periods of 100, 100, and 500 hr respectively. This is the first of a series of tests of graphite-to-metal joints to determine if such joints are corrosion resistant and mechanically adequate for the requirements of molten-salt breeder reactors. A few samples of needle-coke graphite and isotropic graphite were obtained and are being evaluated to determine their suitability for use in molten-salt breeder reactors. The radiation-damage problems were evaluated for graphite in advanced molten-salt reactors, considering growth rate, creep coefficient, flux gradient, and geometric restraint as important factors. The stress developed by differential growth in an isotropic graphite should not be allowed to exceed the fracture strength of the graphite and thus cause failures. The estimated life of graphite is at least five years before failure from inability to absorb creep deformation. The major uncertainty seems to be the ability of graphite to sustain doses of 2×10^{23} nvt without loss of integrity. Creep-rupture life of Hastelloy N was found to be less affected by irradiation as the stress levels are lowered. The effects of irradiation temperature on the postirradiation creep life of air-melted heats are uncertain. Vacuum-melted heats show a large dependency on irradiation temperature. Pretest heat treatment can improve the ductility of irradiated specimens. The creep-rupture properties of structural material in the MSRE appear to be better than originally predicted on the basis of linear extrapolation of data for stress vs log of rupture time. Experimental welds were made to study methods of improving the weldability of Hastelloy N. (auth)

31684 VOID FORMATION DURING THE OXIDATION OF TANTALUM. Stringer, J. (Battelle Memorial Inst., Columbus, Ohio). J. Less-Common Metals, 11: 111-18 (Aug. 1966).

Lines of small voids are a common feature of scales formed on tantalum at high temperatures. Evidence was found to show that voids originate over suboxide plates. The lines of pores may therefore be regarded as evidence of the existence of the plates at reaction temperature. The tantalum-atom density in the suboxide was estimated, and compared with the values calculated for the various suboxides reported in the literature. (auth)

31685 OXIDATION KINETICS OF SOLID SOLUTIONS OF URANIA–YTTRIA. Aitken, E. A. (General Electric Co., Cincinnati). Contract AT(40-1)-2847. J. Nucl. Mater., 19: 248-66(June 1966).

Solid solutions of UO_2 and Y_2O_3 react with O_2 changing the average valence of the U. The amount and rate of O_2 uptake varies with the Y_2O_3 content. The uptake kinetics are influenced by the type of structure of the solid solution and the degree of anion deficiency in the lattice. A detailed oxidation study of the 50 mole % Y_2O_3 composition from –196°C to 110°C revealed that the chemisorption characteristics were similar to that of UO_2 except the uptake beyond the first layer occurrred at a much lower temperature. Oxidation beyond the first layer occurred readily above –43°C and the kinetics followed a one-fourth power time dependence if the initial O_2 to U ratio was 2.27. If the average O_2 to U ratio was 2.58 initially, then the oxidation kinetics were parabolic with time but the rate was decreased by two orders of magnitude. Possible mechanisms compatible with the data are proposed. (auth)

31686 OXIDATION OF YTTRIUM IN AIR. Vorob'ev, V. V. Ukr. Fiz. Zh., 11: 416-23(Apr. 1966). (In Ukrainian).

The kinetics of yttrium oxidation to various degrees of purity in moist air at atmospheric pressure was investigated as well as the dependence of the rate of oxidation on the moisture of the air. The metals used for the investigation had a purity of 97.2 and 99.8% by weight. The humidity was 34 and 47%. The temperature range was 400 to 660°C. (auth)

31687 PITTING CORROSION OF ZIRCONIUM IN PERCHLORATE SOLUTIONS. Gil'man, V. A.; Kolotyrkin, Ya. M. (Karpov Scientific-Research Inst. of Physics and Chemistry, USSR). Zashchita Metal., 2: 360-1(May-June 1966). (In Russian).

Pitting corrosion of Zr was found to occur in 0.1 and 1.0 N solutions of $NaClO_4$ and $HClO_4$. Zr remained in a passive state until a definite critical potential ϕ_{cr} was attained.

The anodic behavior of Zr in perchlorate solutions is analogous to its behavior in chloride solutions except that the critical pitting potential in chlorate solutions is almost a whole volt more positive than in chloride solutions. Thus, the value of ϕ_{cr} is 1.35 v in 1N $HClO_4$ or 1N $NaClO_4$, and 1.45 v in 0.1 N $HClO_4$ or 0.1 N $NaClO_4$ (the corresponding values of ϕ_{cr} in chloride solutions are +0.40 and +0.47 v). The critical potential was determined by the perchlorate concentration, and did not depend on solution pH and anode current density. (TTT)

Fabrication

Refer also to abstract 31375.

31688 (NASA-CR-507) GRAPHITE–METAL CARBIDE COMPOSITES. Harada, Y. (IIT Research Inst., Chicago, Ill.). June 1966. Contract NASr-65-(09). 67p. CFSTI $3.00 cy, $0.50 mn.

Investigations were conducted to determine the feasibility of fabricating metal–graphite composites by hot pressing at 2800–3000°C. Mixtures of calcined petroleum coke with varying amounts of different metals (or their carbides) were used as the raw materials, and no binders were involved in this simple, one-step process. Ten metal additions were studied in this program: niobium, hafnium, molybdenum, tantalum, zirconium, titanium, boron, beryllium, uranium, and thorium. Evaluation of the resulting bodies included measurements of physical properties and examination of microstructure. The results show that strong, dense bodies can be realized by this method. Liquid phase sintering occurs through formation and diffusion of a carbide–carbon eutectic under the hot pressing conditions, and subsequent recrystallization of this phase yields strong bonding. The strongest bodies to emerge from these studies are in the Nb–C, Hf–C, and Mo–C systems. Compositions containing 50 wt.% metal (or 6 to 11 at.%) exhibited flexural strengths in excess of 10,000 psi, the highest being 16,000 psi for 50 wt.% Nb–C processed at 3000°C. This system and a 50 wt.% Hf–C also pressed at 3000°C have displayed increases in strength at 2000°C. Intermediate (~5000 psi) strengths were shown by most of the other systems incorporating other metal additives. (auth)

31689 (ORNL-P-2159) SOL-GEL PROCESS DEVELOPMENT AND MICROSPHERE PREPARATION. Haas, P. A.; Lloyd, M. H.; Bond, W. D.; McBride, J. P. (Oak Ridge National Lab., Tenn.). [1966]. Contract W-7405-eng-26. 42p. (CONF-660524-4). Dep. mn. CFSTI $2.00 cy, $0.50 mn.

From 2nd International Thorium Fuel Cycle Symposium, Gatlinburg, Tenn.

The development of the sol-gel process at the Oak Ridge National Laboratory is reviewed. Sols of ThO_2, UO_2, PuO_2, and other actinide or rare earth oxides were prepared. These sols can be gelled and fired to give high-strength oxide particles. Most of the sols are prepared from nitrate salts and peptized by nitrate ions. The thoria sol preparation procedure is unique in that the basic colloidal particle is formed by steam denitration at temperatures approaching 500°C. The most completely developed procedure for urania sols is based on precipitation-dispersion starting with U(IV) nitrate solution. Hydrous uranium dioxide is precipitated by $NH_4OH–N_2H_4 \cdot H_2O$ solution, washed to incipient peptization, and then heated to 60°C to form a sol. The addition of formic acid prior to precipitation helps to maintain a high U(IV) content and simplifies the precipitation step. Plutonia sols may be prepared from $Pu(NO_3)_4$ solution by a precipitation-peptization technique; careful control of the temperature and other process conditions is necessary. The plutonia sols are polymers of hydrated Pu(IV) oxide. Mixed sols were prepared by either co-precipitation or by simply mixing of the different sols. Limited amounts of a second component may be adsorbed on the colloidal particles of a sol; for example, up to about 10 mole % of uranyl ion can be adsorbed when UO_3 or uranyl nitrate is added to a thoria sol. A process was developed for converting these sols into strong, dense oxide spheres, 10 to 1000 microns in diameter. The sols were dispersed into droplets in an organic liquid that converted them to gel spheres by extracting water at slow, controlled rates. To suspend the sol drops and avoid coalescence clustering, and deposition on the wall, the use of surfactants in the organic liquid and of apparatus having special configurations was necessary. The spherical gel particles were separated from the organic liquid, then dried and fired to give the oxide product. Microspheres were prepared by using 2-ethyl-1-hexanol as the drying solvent in continuous column systems that included solvent recovery. Capacities were up to about 1200 g of thoria microspheres per hour. Several hundred kg of thoria microspheres, over 15 kg of urania microspheres, and smaller amounts of the other composition were prepared. (auth)

31690 (ORNL-P-2176) THE IMPACT OF KILOROD OPERATIONAL EXPERIENCE ON THE DESIGN OF FABRICATION PLANTS FOR ^{233}U–Th FUELS. Brooksbank, R. E.; Nichols, J. P.; Lotts, A. L. (Oak Ridge National Lab., Tenn.). [1965]. Contract W-7405-eng-26. 34p. (CONF-660524-3). Dep. mn. CFSTI $2.00 cy, $0.50 mn.

From 2nd International Thorium Fuel Cycle Symposium, Gatlinburg, Tenn.

The Kilorod program was aimed at advancing the Th–^{233}U fuel cycle technology by coupling the ORNL and sol-gel process to the vibratory compaction method of fuel fabrication by semi-remote methods on a 10 kg/day scale. Because of the importance of the radiation information on the economics and safety of the fuel cycle, the radiation data obtained during the program are described in detail. (M.O.W.)

31691 PITFALL IN THE PREPARATION OF METAL–HYDROGEN ALLOYS FOR TRANSMISSION ELECTRON MICROSCOPY. Westlake, D. G.; Gray, W. R. (Argonne National Lab., Ill.). Appl. Phys. Lett., 9: 3-4(July 1, 1966).

Samples of vanadium and niobium, each containing 100 ppM hydrogen were electrothinned. During examination in an electron microscope domain walls were observed indicating that the hydrogen concentration increased during electrothinning. It was shown that the electrothinning technique does not introduce hydrogen. Instead, the hydrogen initially present in the alloy must have tended to concentrate in the thinned sample as metal atoms were stripped away. Data were also obtained on tantalum and zirconium with small additions of hydrogen. (M.C.G.)

31692 FUEL ELEMENT FABRICATION DEVELOPMENT IN BELGIUM. Lejeune, J. M. Belgicatom, Ass. Belge Develop. Pac. Energ. At., Bull. Inform., 11: No. 61, 3-6(Apr. 1966). (In French).

The Mol Nuclear Energy Center has reactors of three different types: graphite-moderated, air-cooled, research reactors with fuels of metallic uranium clad in aluminum; material testing reactors with fuels of sandwich plates in coaxial tubular bundles; and PWR power reactors with fuel of uranium oxide tablets clad with stainless steel. The fabrication techniques used for each fuel element type are described. (J.S.R.)

31693 INDUSTRIAL FABRICATION OF FUEL ELEMENTS IN FRANCE. Salesse, M.; Aragou, M.; Julia, M. Belgicatom, Ass. Belge Develop. Pac. Energ. At., Bull. Inform., 11: No. 61, 9-17(Apr. 1966). (In French).

The evolution of the industrial fabrication of fuel elements for gas graphite reactors, heavy water reactors, and fast neutron reactors is traced. The importance of research in this area both on the behavior of existing elements and on the development of new fuel elements is emphasized. (J.S.R.)

31694 DEVELOPMENT AND PREPARATION OF NUCLEAR FUELS IN THE UNITED KINGDOM. Franklin, N. L. Belgicatom, Ass. Belge Develop. Pac. Energ. At., Bull. Inform., 11: No. 61, 19-21(Apr. 1966). (In French).

The procedures and installations for the production of nuclear fuel elements in the United Kingdom are briefly reviewed. (J.S.R.)

31695 EXPERIMENTAL INVESTIGATION OF COMPACTING AND SINTERING BEHAVIOR OF A TUNGSTEN

CARBIDE–COBALT ALLOY. Exner, H. E. (Max-Planck-Institut fuer Metallforschung, Stuttgart). Metall, 20: 448-54(May 1966). (In German).

The compacting behavior of tungsten carbide–cobalt powders is dependent on the particle size and the particle size distribution of the carbides and on the type of cobalt additions. The compacting density can be increased by the use of powder mixtures that show various agglomerate sizes as a result of different milling treatments. The final density of the sintered alloy is independent of the compacting density and increases with the intensity of the milling treatment and the decarbonizing of the initial powder. Isothermal sintering studies are not in agreement with present sintering theories. The initial stages indicate a time-independent sintering velocity and an activation energy of 59 kcal/mol for temperatures over and above the eutectic temperatures. With a continuous temperature increase, the sintering begins at 800°C and proceeds very rapidly up to 1100°C, where before melting of the W–C–Co eutectic occurs a large part of the porosity appears. At temperatures above the eutectic temperatures, densities of 99% of theoretical were obtained in powders milled together. Hand-mixed mixtures were sintered almost as fast, but the final density was under 98%. Decreasing particle size increased the sintering velocity. The effect of the particle size distribution could not be established. (tr-auth)

31696 SELF-SUPPORTING METAL FOILS PREPARED FROM THE OXIDES OF THE SEPARATED ISOTOPES OF RARE EARTH ELEMENTS. Westgaard, L.; Bjoernholm, S. (Univ. of Copenhagen). Nucl. Instrum. Methods, 42: 77-80(June 1966).

Metallic samples of the separated isotopes of Yb, Sm, Dy, Er, Nd, Gd, and Lu are prepared from the oxides in batches of 20-40 mg by reduction in a vacuum with lanthanum or thorium metal powder. Foils 1-4 cm^2 large and down to 0.5 mg/cm^2 thick are made by cold rolling. Over-all yields from 50-60 per cent down to 20-25 per cent (Gd,Lu) are obtained. The foils are used as targets in connection with spectroscopic measurements with a tandem Van de Graaff accelerator. Supported targets are prepared by evaporation of the metal directly onto carbon or metal backings. (auth)

31697 SLIP CASTING OF MOLYBDENUM DISILICIDE. Dobrovolskii, A. G.; Nazarchuk, N. V. Porosh. Met., Akad. Nauk. Ukr. SSR, No. 5, 1-8(May 1966). (In Russian).

A method is described for slip casting of parts made of finely ground molybdenum disilicide powder using distilled water as a suspending medium. The effect of the pH of the slip medium, the solid-liquid ratio and the temperature on the properties of the slip and the castings is shown. It is pointed out that slips have two casting intervals at pH = 4-5 and 9-11, the second of which ensures better casting properties and higher compactness, up to 3.76 g/cm^3. The rate of collection of the composition increases with an increase in casting temperature. The final density of samples sintered in two hours at 1650°C is 5.5 g/cm^3. (auth)

31698 REGULARITIES OF SINTERING ALLOYS OF ZIRCONIUM DIBORIDE WITH MOLYBDENUM. Kislyi, P. S.; Kuzenkova, M. A. Porosh. Met., Akad. Nauk Ukr. SSR, No. 5, 16-23(May 1966). (In Russian).

A description is given of the regularities of shrinkage of samples from mixtures of ZrB_2 and 5, 10, and 15% Mo during formation of solid Mo solutions in ZrB_2 on heating at high temperatures. On the basis of the kinetic dependences of the shrinkage and the changes in porosity it is shown that in the process of slow heating to high temperatures, or during the initial period of sintering with rapid heating, diffusion growth of the samples takes place owing to the difference in the partial diffusion coefficients. The presence of molybdenum activates the shrinkage process. (auth)

31699 HOT-PRESSING OF METALLIC CARBIDES. Ramqvist, Lars (Axel Johnson Inst. for Industrial Research, Nynaeshamn, Sweden). Powder Met., 9, No. 17, 26-46(Spring 1966).

A survey is presented of published work on the hot pressing of metallic carbides. On the basis of a comparison of the apparatus described in the literature, hot-pressing equipment has been built, designed for vacuum sintering using resistance heating, a combination that has many advantages. Nine metallic carbides from Groups IV, V, and VI of the Periodic Table were hot pressed to high densities, as well as mixed carbides and carbides of varying carbon content. Compacting details are summarized, together with data covering lattice parameters and microhardness. The purity of the metallic carbides has great significance as regards the sintering mechanism. This is demonstrated both by theory and experiment. (auth)

31700 SOL-GEL PROCESSES FOR THORIUM FUEL PRODUCTION. Van der Plas, Th.; Slooten, H. S. G. (Euratom–RCN–KEMA, Arnhem, Netherlands). pp 165-8 of STI-DOC-10/52.

Sol-gel processes for the preparation of spherical ThO_2 fuels are briefly described. The first step of the process involves the preparation of a sol of hydrated ThO_2 by peptizing a thoroughly de-ionized $Th(OH)_4$ precipitate in $Th(NO_3)_4$, $UO_2(NO_3)_2$, or HNO_3 solution. Subsequently this sol is dispersed in an organic medium to form an emulsion. (M.O.W.)

31701 REFABRICATION TECHNOLOGY FOR THE THORIUM–^{233}U FUEL CYCLE. Lotts, A. L.; Douglas, D. A. Jr. (Oak Ridge National Lab., Tenn.). pp 212-45 of STI-DOC-10/52.

A number of factors is presented which must be considered if one is to refabricate bred fuel and methods of attacking problems encountered in refabrication technology are suggested. Plans are discussed for pilot-scale demonstration of the refabrication of two types of fuel elements. An analysis is presented of the effect of production rate and isotopic content of fuel on refabrication cost. (M.O.W.)

31702 NUCLEAR FUELS. Dressler, Jacques H.; De Lajarte, Stephane D. (to Compagnie de Saint-Gobain). Canadian Patent 734,864. May 24, 1966. Priority date Nov. 18, 1957, France.

For homogeneous reactors, a fuel incorporated into glass beads of 10-60 micrometers diameter is fabricated. These microbeads contain up to 45% uranium oxide or some other fissile material. They are intended for suspension in water which circulates in the reactor vessels where fission occurs. Methods of manufacturing the beads, which require rather elevated temperatures, are described. (F.S.A.)

31703 FABRICATION OF HIGH-STRENGTH, HEAVY-WALL PRESSURE VESSELS. Davis, M. W.; Lorentz, R. E. (Combustion Engineering, Inc., Chattanooga). 9p. (CONF-660211-1). ORAU. Gmelin, AED-CONF-66-010-1.

From 1st Midwest Symposium on Nondestructive Testing of Welds, Chicago.

It is shown that materials selection, design, fabrication, and testing must be well coordinated to produce the heavy-walled, high-strength pressure vessels for nuclear reactors. (W.L.G.)

31704 METHOD AND APPARATUS FOR VIBRATORY COMPACTION. Ayer, James E.; Soppet, Frederick E. (to U. S. Atomic Energy Commission). U. S. Patent 3,261,378. July 19, 1966.

A method is described for making a uniform close-packed dispersion of masses of different diameters within a container, comprising subjecting masses of a predetermined diameter to axial vibration within the container until a close-packed uniform configuration is attained, and thereafter introducing masses of smaller diameter while holding the configuration last previously attained in position by pressure and subjecting it to combined axial and radial vibration until a uniform, close-packed configuration is attained. (auth)

31705 IMPROVEMENTS IN OR RELATING TO THE PRODUCTION OF SPHEROIDS. Ingleby, Bryan Edward (to United Kingdom Atomic Energy Authority). British Patent 1,031,153. May 25, 1966. Filed Apr. 13, 1962.

The present patent describes some modifications of the Brit. Pat. No. 938,671 for the production of spheroids of

materials suitable for nuclear reactor fuels. The process is particularly applicable to the production of UC fuel. The particles are produced by mixing together substances with or without a binder, grinding the mixture to produce the particles, and reaction-sintering the spheroidal particles to produce a solid compound. The substances to be mixed are selected for their ability to chemically react together at elevated temperatures to produce the solid compound. Prior to the reaction-sintering, the particles may be sieved for the removal of the spheroids which are not within the desired size range. (B.L.M.)

31706 IMPROVEMENTS IN OR RELATING TO NUCLEAR REACTOR FUEL ELEMENTS. Ingleby, Bryan Edward (to United Kingdom Atomic Energy Authority). British Patent 1,031,154. May 25, 1966. Filed Apr. 13, 1962.

A method is described for producing a fission-product retaining nuclear reactor fuel body and for the incorporation of these bodies into fuel elements. Each body consists of a spheroid of sintered UC with a coating of SiC, and the spheroids are dispersed in a matrix of SiC. The spheroids are formed by producing spheroids of mixed UO_2 and C with a suitable amount of binder, reaction-sintering these spheroids to form dense sintered spheroids of UC, coating the spheroids with SiC, dispersing the coated particles in the SiC matrix, and forming the matrix into the desired shape. The element may be formed from a number of the bodies supported or located in a desired configuration, such as cylindrical or hollow cylindrical, which are arranged in clusters or stacks of clusters. (B.L.M.)

31707 IMPROVEMENTS IN OR RELATING TO CERMETS. Gittus, John Henry; Williams, Lewis Rhoslyn; Baily, George Arthur (to United Kingdom Atomic Energy Authority). British Patent 1,031,678. June 2, 1966. Filed Nov. 30, 1962.

A method is described for manufacturing a cermet having particles of a ceramic material dispersed in a continuous metal matrix that is suitable for a reactor fuel material. Alternate layers of ceramic particles, one particle in depth, and layers of metal matrix material are arranged in a die and subsequently pressed to form a compact which is then sintered at an elevated temperature. The metal matrix material may take several other forms, such as powdered metal or powdered metal mixed with a resinous binder. (B.L.M.)

Properties and Structure

See also CHEMISTRY — Inorganic and Physical Chemistry
PHYSICS — Solid State Physics

Refer also to abstracts 31227, 31386, and 31388.

31708 (ANL–7119) A FACILITY FOR STUDYING ELASTIC MODULI AS A FUNCTION OF TEMPERATURE BY AN ULTRASONIC METHOD. MEASUREMENTS ON VANADIUM–20 w/o TITANIUM. Peterson, Ronald G. (Argonne National Lab., Ill.). Feb. 1966. Contract W-31-109-eng-38. 18p. Dep. mn. CFSTI $1.00 cy, $0.50 mn.

A facility used to determine ultrasound velocities in materials at temperatures up to around 1000°C is described. The way to compute the elastic constants of a material from these velocities is shown. Results of measurements made upon V-20 wt % Ti are given. (auth)

31709 (IITRI–B6042-5) VANADIUM ALLOY STUDIES. Final Report, March 1, 1965–May 31, 1966. (IIT Research Inst., Chicago, Ill.). June 29, 1966. Contract NOw65-0427-f. 34p.

Alloys based on V–20 Nb and V–Nb–Ta, enriched in Ti, Si, and C, were fabricated by arc-melting, hammer forging, and cold rolling to sheet or foil; the Si and C additives promoted age hardening. The V–20 Nb–10 Ti base alloys were highly fabricable and had density-corrected strengths up to 1,300,000-in. at –320°F, 800,000-in. at 1200°F, and 250,000-in. at 1800°F. Somewhat reduced fabricability was noted for V–Nb–Ta base alloys which contained from 28 to 54% V. The Ta-containing materials were nearly as strong as the V–Nb–Ti alloys up to 1200°F, and they were much stronger in the 1800 to 2400°F range. Density-corrected strengths were above 400,000-in. at 1800°F, and 160,000-in. at 2200°F. Improved workability but slightly reduced strengths (density-corrected) were noted in V–Nb–Ta alloys as V contents were raised. (auth)

31710 (NASA-CR–54983) DETERMINATION OF ELEVATED-TEMPERATURE FATIGUE DATA ON REFRACTORY ALLOYS IN ULTRA-HIGH VACUUM. Seventh Quarterly Report, January 1, 1966–April 1, 1966. Honeycutt, C. R.; Sawyer, J. C. (TRW Equipment Labs., Thompson Ramo Wooldridge Inc., Cleveland, Ohio). Apr. 15, 1966. Contract NAS3-6010. 41p.

Notched fatigue tests were conducted at 2000°F on TZC alloy. From the results of these tests S/N curves were defined for "A" ratios (ratio of dynamic stress to mean stress) of ∞ and 0.67. Smooth specimens of TZC were tested at an "A" ratio of approximately 0.20 and a static load of 20 Ksi ($1.38 \times 10^9 N/m^2$). Limited creep data were also obtained from these smooth-specimen fatigue tests. Specimens of TZM with various notch configurations are being evaluated under dynamic load conditions. The results obtained to date indicate that the peak stress required for fatigue of smooth specimens is significantly greater than that required for notched specimens. At present the specific reason for this difference is not known but the effect of localized self-heating may be a contributing factor. Further study was undertaken to assess the requirements necessary to cause fatigue of smooth TZC specimens at an "A" ratio of ∞. The results of tests conducted to determine the requirements for producing fatigue in smooth specimens show that with the vibrational drive available at 20 kHz, the magnitude of the dynamic stress delivered to the specimen is limited by the large amount of energy converted to heat through internal damping. (auth)

31711 (NASA-TN–D-3467) STRESS-RUPTURE PROPERTIES OF TUNGSTEN WIRE FROM 1200 DEG TO 2500 DEG F. McDanels, David L.; Signorelli, Robert A. (National Aeronautics and Space Administration, Cleveland, Ohio. Lewis Research Center). July 1966. 21p. CFSTI $1.00 cy, $0.50 mn.

The stress-rupture properties of 5-mil-diameter, type 218 CS tungsten wire were determined for rupture times up to about 200 hours at test temperatures from 1200 to 2500°F. Results showed that the rupture properties were superior to those reported for other forms of tungsten, other refractory metals, and superalloys in this temperature range. The onset of primary recrystallization observed between 1800 and 2000°F was indicated by a decrease in microhardness, a decrease in ductility, and a coarsening of grain size. The strength superiority of the wire over the other materials was maintained beyond the onset of primary recrystallization. (auth)

31712 (UCRL–14227(Rev.1)) CONTACT CONDUCTANCE MEASUREMENTS DURING TRANSIENT HEATING. Schauer, Dale A.; Giedt, Warren H. (Lawrence Radiation Lab., Univ. of California, Livermore). Oct. 20, 1965. Contract W-7405-eng-48. 10p. Dep. mn. CFSTI $1.00 cy, $0.50 mn.

An experimental method is described for determining the interface conductance between two plates during transient heat transfer. The technique is based on heating one plate in about 100 μsec with a capacitor-bank discharge and then recording the contacting-surface temperatures of the two slabs as they come to equilibrium. Results are presented for combinations of: (1) aluminum and stainless steel with contact-surface finishes of 5-5 μin. AA (arithmetic average), 12-30 AA, 15-38 AA, and 50-35 AA; and (2) stainless steel and ceramic with contact-surface finishes of 31-38 AA, and 64-38 AA. The pressure was varied from 100 to 2000 psi. For metallic contacts the

conductance increased about 200% with time. The reverse behavior occurred with the metal-ceramic contacts. (auth)

31713 (UCRL-16658, pp 93-8) CRYSTAL IMPERFECTIONS. (Lawrence Radiation Lab., Univ. of California, Berkeley).

Results of investigations are reported concerning intersection cross slip in metals, stability of work-hardened FCC metals, dislocation dipoles in deformed MgO calculations of dislocation dipole contrasts, and determination of stacking-fault energies in Ag and Ag-In alloys. Lists of 1965 publications are included, and research plans for 1966 are outlined. (J.R.D.)

31714 (UCRL-16658, pp 99-103) KINETICS OF DISLOCATION MECHANISMS. (Lawrence Radiation Lab., Univ. of California, Berkeley).

Results of investigations are presented concerning annealing point defects in high-purity Ta, constricted energy of dissociated dislocations in metals, mechanical properties of Mg_3Cd single crystals, low-temperature deformation dislocations in Mo and Ta, creep of Mg-Li single crystals, vacancy distributions in ordered alloys, high-temperature creep of Fe-4% Si, motion of small-angle tilt boundaries in Mg, basal slip in Zn, and gas-operated high-velocity impact machines. Lists of 1965 publications are included, and research plans for 1966 are outlined. (J.R.D.)

31715 (UCRL-16658, pp 105-20) RELATION OF STRUCTURE TO PROPERTIES IN METALLIC SYSTEMS. (Lawrence Radiation Lab., Univ. of California, Berkeley).

Results of investigations are presented concerning electron-diffraction and dark-field metallographic methods, electron diffraction Kikuchi patterns, properties of dark-field electron images, identification of prismatic dislocation defects, structures of ausformed steels, dislocation climb and stacking-fault energies of Al and Al-Mg alloys, and electric and mechanical properties of Mo-Ta alloy single crystals. Lists of 1965 publications are included, and research plans for 1966 are outlined. (J.R.D.)

31716 (UCRL-16658, pp 121-32) HIGH-STRENGTH MATERIALS. (Lawrence Radiation Lab., Univ. of California, Berkeley).

Results of investigations are presented concerning properties of dynamically strain-aged alloy steels, strain aging of Fe alloys, deformed austenite, solidification effects on Al-Si structures, fracture of Au-Pt alloys, properties of Cr-W alloys, and properties of Nb-H systems. Lists of 1965 publications are included, and research plans for 1966 are outlined. (J.R.D.)

31717 (UCRL-16658, pp 143-9) THERMODYNAMICS OF METAL SYSTEMS. (Lawrence Radiation Lab., Univ. of California, Berkeley).

Results of investigations are presented concerning properties of intermetallic phases, solute interactions in dilute liquid alloys, thermodynamics of Ag-Pb alloys, Pb vapor pressures, thermodynamic properties of binary liquid alloys, thermal stabilities of Nb oxides and Ta oxides, thermal properties of Au-Sn alloys, and preparation of β Mo and β W. Lists of 1965 publications are included, and research plans for 1966 are outlined. (J.R.D.)

31718 (UCRL-16658, pp 149-54) HIGH-TEMPERATURE REACTIONS. (Lawrence Radiation Lab., Univ. of California, Berkeley).

Results of investigations are reported concerning evaporation of BaF_2, vaporization of AlN and Mg_3N_2, vapor pressures of CeF_3, and reactions of W with N_2O. Lists of 1965 publications are included, and research plans for 1966 are outlined. (J.R.D.)

31719 (UCRL-16658, pp 155-69) PHYSICAL CERAMICS. (Lawrence Radiation Lab., Univ. of California, Berkeley).

Results of investigations are presented concerning mechanical properties of composite systems, permeation of gases through alumina, colorimeter development, preparation and deformation of MgO crystals, diffusion of Fe and Ni in single-crystal MgO, diffusion in MgO-CaO systems, anatase-rutile transformations, hydrolysis of MgF_2, dehydration of hydrous aluminum oxides, diffusion of cobalt oxides and iron oxides in silicate glass, and structures at $Al-Al_2O_3$ interfaces. List of 1965 publications are included, and research plans for 1966 are outlined. (J.R.D.)

31720 (AD-629415) MOLTEN METALS AS HIGH-TEMPERATURE LUBRICANTS. Fialko, N. M.; Dintses, A. I. Translated from Khim. Tekhnol. Topliv Masel, 9: No. 3, 54-8(1964). 9p. (FTD-TT-65-1447). CFSTI $1.00 cy, $0.50 mn.

Due to the ease of oxidation of liquid metals and their corrosive effects on construction materials, it is concluded that molten inorganic salts are the better potential lubricants for use at temperatures of 400 to 700°C. (W.L.G.)

31721 (AD-630971) CALIBRATION OF THE VR-5/20 THERMOCOUPLE TO CRITICAL POINTS UP TO 3000 DEG C. DETERMINATION OF THE MELTING POINTS OF VANADIUM AND NIOBIUM OF HIGH PURITY. Kocherzhinskii, Yu. A.; Kobzenko, G. F.; Pan, V. M.; Sviridenko, V. K.; Yunko, L. M. Translated from Sb. Nauch. Tr. Inst. Metallofiz., Akad. Nauk UKR. SSR, No. 17, 209-10(1963). 6p. (FTD-TT-65-1888). CFSTI $1.00 cy, $0.50 mn.

The calibration graph of a W-5% Re/W-20% Re thermocouple constructed from the fusion points of 8 metals is given. The thermocouple was then used to determine the melting points of zone-refined V (1950°C) and Nb (2520°C). (W.L.G.)

31722 (ORNL-tr-1227) THERMAL BEHAVIOR OF CONCRETE: FIRST RESULTS OF STUDIES AND TESTS TOWARDS APPLICATION OF A PRESTRESSED CONCRETE CONTAINMENT IN A NUCLEAR REACTOR. Buvat; Foucault. Translated for Oak Ridge National Lab., Tenn., from Ann. Inst. Tech. Batiment Trav. Publ., 18: 1280-9(1965). 29p. Dep. mn. JCL $2.60 fs, $1.07 mf.

Tests were made of the thermal behavior of concrete in reactor containment vessels of prestressed concrete. It was found that the thermal performance of concrete, particularly its strength, is directly influenced by the dehydration phenomena, which are more pronounced at temperatures of 400 to 500°C than at 150°C. The problem of water formation in the mass of the concrete was considered. Of 30 initial concrete mixes, 27 retained a static elastic modulus above 100,000 bars after the thermal test at 150°C, 19 at 300°C, and only 2 at 500°C. It was concluded that the mixes with slag aggregates had a slightly higher bond limit in the cold than that of the other mixes. This superiority was observed in the hot although the drop of the bond limit was more marked in slag aggregate mixes. New measuring techniques were developed. (M.C.G.)

31723 THE APPLICATION OF HIGH-TEMPERATURE MASS SPECTROMETRY TO THE STUDY OF THE COMPOSITION FUNCTION OF THERMODYNAMIC PROPERTIES IN NON-STOICHIOMETRIC COMPOUNDS. Gingerich, K. A. (Pennsylvania State Univ., University Park). Advance. Mass Spectrometry, 3: Proc. Conf. Paris, 1964, 1009-16(1966).

The Knudsen effusion method combined with mass spectrometric analysis of the effusing vapor was applied to incongruent vaporization processes of transition metal phosphides and praseodymium-group V compounds. The application of this method for the detection of a range of homogeneity of a binary phase and the determination of its boundary compositions is shown for a number of compounds. The method is suitable for the measurement of the width of broad to extremely narrow homogeneity ranges. The application for the determination of the enthalpy-composition function is discussed for the PrP_{1-x} phase. The measurement of the apparent partial free enthalpies of formation, $\Delta G[P_2]$, in kcal per mole P_2, as a function of composition within a solid solution is shown for the same phase. For the measured P_2-partial pressures, isotherms of apparent $\Delta G[P_2]$ values were calculated for temperatures between 1000-1700°K and different P/Pr ratios using the experimental enthalpy-composition relationship. (auth)

31724 NOMOGRAM FOR DETERMINING PRANDTL NUMBER OF SOME LIQUID METALS. Chernyshev, A. K. At. Energ. (USSR), 20: 69-70(Jan. 1966). (In Russian).

Knowledge of the dimensionless Prandtl number, derived from thermophysical properties, such as kinematic viscosity and thermal conductivity, at various temperatures is required for heat-transfer calculations and treatment of certain experimental data. In order to facilitate the determination of this number for a number of liquid metals in a broad temperature range, a relatively simple nomogram was constructed on the basis of data currently available in the literature. Deviation from the true values does not exceed 1%, except for lead, for which the error may reach up to 2%. The following liquid metals and alloys are included: Li; 56.5% Bi + 43.5% Pb; Pb; Bi; 25% Na + 75% K; 50% Na + 50% K; Sn; Hg; Na; and K. Temperatures in the range from near 0 to 700°C are covered in the nomogram. (TTT)

31725 TEMPERATURE AND THERMAL CONDUCTIVITY OF METALLIC BERYLLIUM. Chirkin, V. S. At. Energ. (USSR), 20: 80-2(Jan. 1966). (In Russian).

The thermal properties of hot-pressed beryllium, containing 1.264 wt % impurities (mostly magnesium and aluminum) were determined by means of O. A. Kraev's method, using 36-mm dia and 16-mm high cylindrical specimens. The temperature was measured within the specimen by suitably placed thermocouples. The temperature coefficients at 200°C, measured in directions parallel and perpendicular to the direction of pressing, were found to be 0.111 ± 0.012 and 0.138 ± 0.012, respectively. Annealing in a purified argon atmosphere and in a vacuum resulted in a reduction of these values. The thermal conductivity was not too strongly affected by annealing when the direction of the heat flux coincided with that of pressing. The temperature t and the time dependence τ of the coefficient of thermal conductivity in the temperature range θ from 700 to 1100°C are related to each other through the following expression: $\lambda_{t,\theta,\tau} = (1 - 5.6 \cdot 10^{-4}t)[160 + 25\overline{e}^{1.69\tau 10^{-6}(\theta-700)}]$. Thus, beyond a threshold temperature θ', the thermal conductivity of beryllium used as moderator or reflector at a temperature t, depends on the time τ of soaking. (TTT)

31726 MOLTEN CERAMIC OXIDES AS A POSSIBLE FUEL MATRIX FOR HOMOGENEOUS THERMAL NUCLEAR REACTORS. Johannsen, Klaus (Berlin Technical Univ.). Interceram., No. 3, 219-20(1965).

The conception of a homogeneous thermal nuclear reactor containing ceramic oxides in molten form as a matrix for the uranium dioxide fuel is discussed. The study of high-melting ceramic oxides from the point of view of neutron physics and heat technology suggests that beryllium oxide and zirconium oxide, as well as aluminum and magnesium oxides, might be suitable for this purpose. In order to lower the high melting point of these oxides, it is recommended that ternary systems such as $BeO-ZrO_2-MgO$ and $BeO-Al_2O_3-MgO$ should be used, the lowest melting temperatures of which lie in the neighborhood of 1700°C. (auth)

31727 X-RAY STRUCTURAL ANALYSIS OF SOME Zr–Fe AND Zr–CO ALLOYS. Kuz'ma, Yu. B.; Markiv, V. Ya.; Voroshilov, Yu. V.; Skolozdra, R. V. (Lvov State Univ.). Izv. Akad. Nauk SSSR, Neorg. Mater., 2: 259-63 (1966). (In Russian).

The compound Zr_2Fe with the structural type $CuAl_2$ ($\underline{a}$ = 6.457 ± 0.005 Å, $\underline{c}$ = 5.542 ± 0.004 Å, and c/a = 0.858) existing in equilibrium with $\alpha-Zr$ and $ZrFe_2$ was formed in the Zr–Fe system. Small admixtures of oxygen cause the transition of the structure type $CuAl_2$ to the structure type n-phase Ti_2Ni (a = 12.140 ± 0.005 Å); the parameters of the position of the atoms in the latter structure were determined. The state Zr_6Co_{23} and the structure type Th_6Mn_{23} (a = 11.516 ± 0.005 Å) correspond with the previously known compound $ZrCo_4$. (tr-auth)

31728 CRYSTAL STRUCTURE OF $HoAl_3$ AND $DyAl_3$ COMPOUNDS. Zalutskii, I. L.; Kripyakevich, P. I. (Lvov State Univ.). Izv. Akad. Nauk SSSR, Neorg. Mater., 2: 264-8(1966). (In Russian).

The crystal structure of the compound $HoAl_3$ was determined by the powder method. It was established that $HoAl_3$ belongs to a new structural type [superstructure to the 15-layer close packing ABACBCACBABCBAC; space group $R\bar{3}m-D^5_{3d}$, 3Ho in 3(a) 000, 6Ho in 6(c) 00$\underline{z}$ with $\underline{z}$ = 0.4013, 6Ho in 6(c) 00z with z = 0.1290, 9Al in 9(e) 1/21/20, 18Al in 18(h) $\underline{xxz}$ with x = 0.151 and z = 0.7312, 18Al in 18(h) x = 0.165 and z = 0.1978]: a = 6.040 ± 0.002 Å, $\underline{c}$ = 35.79 ± 0.01 Å, and c/a = 5.925. One of the modifications of $DyAl_3$ has a structure of the $HoAl_3$ type (a = 6.075 ± 0.002 Å, c = 35.89 ± 0.01 Å, c/a = 5.908). The compounds $HoAl_3$ and $DyAl_3$ have a constant composition. Aluminum dissolves neither Ho nor Dy. (tr-auth)

31729 PHASE DIAGRAM OF THE HfC–Mo SYSTEM. Ordan'yan, S. S.; Krasovskaya, A. A.; Avgustinik, A. I. (Lensovet Tech. Inst., Leningrad). Izv. Akad. Nauk SSSR, Neorg. Mater., 2: 299-302(1966). (In Russian).

The alloys along the HfC–Mo profile in the ternary system Hf–C–Mo were investigated by x-ray, metallographic and chemical methods. It was shown that this profile was quasibinary just as the profiles TiC–Mo and ZrC–Mo and the corresponding ternary systems. On the basis of these data and of the results of the determination of the fusion temperature, the constitution diagram of the quasibinary system HfC–Mo of eutectic type with composition of the eutectic $Hf_{0.143}Mo_{0.857}C_{0.143}$ (alloys with 75 wt % Mo) only at 2310°C was constructed. (tr-auth)

31730 DETERMINATION OF THE HEAT OF ADSORPTION OF CESIUM ON FILAMENTARY TUNGSTEN DEPENDING ON THE METHOD OF FILAMENT TREATMENT. Kakharov, O.; Shuppe, G. N. (Tashkent State Univ.). Izv. Akad. Nauk Uz. SSR, Ser. Fiz.-Mat. Nauk, No. 1, 65-8 (Jan.-Feb. 1966). (In Russian).

The problem investigated was the behavior of cesium on tungsten. A study was made in a sealed device placed in a thermostat, in which various vapor pressures of cesium could be created, corresponding to a temperature range from −180 to +100°C. All the basic inputs of the device were fitted into glass tubes, which were heated by small heaters on the outside to prevent the precipitation of layers of cesium near the inputs on the inner surface of the glass and the appearance of conductivity between the inputs. The vacuum in the device with a frozen source of cesium was of the order of 10^{-9} mm Hg. The following conclusions were reached. The absence of a sufficiently satisfactory theory made it impossible to compare the results obtained with the corresponding theoretical calculations. As in the case of thorium, with cesium on tungsten the curves I (θ) (the dependence of the thermoelectron emission current I on the underlayer (θ)) are monotonic at temperatures which assure the formation of the single layer. The work function of the cathodes Th–|W| (3.4 ev) and Cs–|W| (1.8 ev) is no lower at the most optimal covering of the work functions of thorium and cesium. The presence of humps on the I(0) curves is related to the traces of oxygen, either in the space of the device, on the surface of the cathode, or in the source. The average heat of adsorption of cesium on tungsten wires with coverings lower than "optimal" is (2.1 ± 0.1) ev after treatment of the filament with a-c and (2.7 ± 0.1) ev after treatment with d-c. (ATD)

31731 PERMEABILITY OF ZIRCONIA, HAFNIA, AND THORIA TO OXYGEN. Smith, A. W.; Meszaros, F. W.; Amata, C. D. (Union Carbide Corp., Parma, Ohio). Contract AF 33(657)-11253. J. Amer. Ceram. Soc., 49: 240-4 (May 21, 1966).

The permeability to oxygen of 4 wt % lime-stabilized zirconia and hafnia and of pure thoria was determined between 1100 and 2050°C. The permeability constant (permeability multiplied by the thickness) at 25 torr oxygen pressure is given by: $P_{Zr_{0.92}Ca_{0.08}O_{1.92}} \cdot l = 5.4 \times 10^{-2}e^{-55,700/RT}$ cm²/sec, $P_{Hf_{0.86}Ca_{0.14}O_{1.86}} \cdot l = 0.14e^{-58,500/RT}$ cm²/sec, and $P_{ThO_2} \cdot l = 4.0 \times 10^{-3}e^{-46,100/RT}$ cm²/sec. A ¼-power oxygen pressure dependence of the permeability was found for zirconia and

hafnia and a variable power dependence was found for thoria. The diffusivities for zirconia and hafnia were determined from the time dependence of permeation. These are given by: $D_{Zr_{0.86}Ca_{0.14}O_{1.86}} = 185\ e^{-57{,}600/RT}\ cm^2/sec$, and $D_{Hf_{0.86}Ca_{0.14}O_{1.86}} = 22\ e^{-55{,}700/RT}\ cm^2/sec$. A transport mechanism suggested for zirconia and hafnia involves migration of oxygen ion vacancies and electron holes. (auth)

31732 CATIONIC SELF-DIFFUSION IN CALCIA-STABILIZED ZIRCONIA. Rhodes, W. H.; Carter, R. E. (General Electric Research and Development Center, Schenectady, N. Y.). J. Amer. Ceram. Soc., 49: 244-9(May 21, 1966).

Self-diffusion of Zr in 12 and 16 mole % CaO and of Ca in 16 mole % CaO cubic zirconia was measured by the sectioning technique from 1700 to 2150°C. Lattice self-diffusion coefficients are: $D_{Ca} = 0.444 \exp - (100{,}200 \pm 2800)/RT\ cm^2/sec$, and $D_{Zr} = 0.035 \exp - (92{,}500 \pm 2400)/RT\ cm^2/sec$. Autoradiographs show rapid grain boundary diffusion. D_B is estimated as $<10^5\ D_L$ between 1800 and 2150°C. The low cation self-diffusion coefficients are compared with the high anion rate, and their effect on the diffusion-controlled properties of zirconia is discussed. (auth)

31733 PREPARATION AND FARADAY ROTATION OF DIVALENT EUROPIUM GLASSES. Shafer, M. W.; Suits, J. C. (Thomas J. Watson Research Center, Yorktown Heights, N. Y.). Contract AF 49(638)-1230. J. Amer. Ceram. Soc., 49: 261-4(May 21, 1966).

A large glass-forming region was discovered in the system $EuO-Al_2O_3-B_2O_3$ and chemically stable glasses of good optical quality were produced. The concentration range extends from about 3 to 43 mole % EuO. Room-temperature Verdet constants as large as −2.55 min/oe-cm were measured on a glass containing 30.5 mole % Eu^{2+}. This is somewhat higher than those reported for the trivalent rare-earth ions in similar glass matrices. The effective transition wavelength causing the rotation is 380 ± 20 mμ. Compared to Ce^{3+}, Tb^{3+}, and Pr^{3+} the large rotation of Eu^{2+} in the visible region is due primarily to a large J (total angular momentum) value as well as to a large effective transition wavelength. (auth)

31734 PHASE RELATIONS IN THE SYSTEM $CoNb_2O_6$–$CoTa_2O_6$. Felten, E. J.; Sprang, P. G.; Rosen, S. (Pratt and Whitney Aircraft, North Haven, Conn.). J. Amer. Ceram. Soc., 49: 273-6(May 21, 1966).

The pseudobinary system $CoNb_2O_6-CoTa_2O_6$ was investigated. $CoNb_2O_6$ crystallizes in either the columbite or rutile structure, whereas $CoTa_2O_6$ assumes only the trirutile structure. In an argon atmosphere at about 1400°C, $CoNb_2O_6$ undergoes a phase transition from columbite or rutile. Between 1000 and 1400°C the solubility of $CoTa_2O_6$ in $CoNB_2O_6$ is about 10 mole %; in the same temperature region the solubility of $CoNb_2O_6$ in $CoTa_2O_6$ varies from about 40 to 70 mole %. The extensive solubility of $CoNb_2O_6$ in $CoTa_2O_6$ is explained by the ability of niobium to induce some disorder in the trirutile phase. The columbite to rutile transformation is also discussed on this basis. (auth)

31735 CRYSTAL CHEMISTRY AND DIELECTRIC PROPERTIES IN THE SYSTEMS $BaTiO_3$–UO_2 AND $BaTiO_3$–$BaUO_3$. Van Loan, Paul R.; Chakrabarty, M. R. (Ontario Research Foundation, Toronto). J. Amer. Ceram. Soc., 49: 276-80(May 21, 1966).

Polycrystalline barium titanate fired in nitrogen at 1300 to 1400°C accommodates up to 3 mole % UO_2 in solid solution; its structure is then cubic at room temperature. With $BaUO_3$ additions the structure becomes disordered and quasi-cubic. In air, about 1 mole % UO_2 goes into solid solution in $BaTiO_3$ but the structure remains tetragonal. Diffraction peaks of a new phase, possibly a ternary oxide of barium, uranium, and titanium, appear in patterns of specimens containing more than 2 mole % UO_2. The dielectric constant of $BaTiO_3$ ceramics fired in air, steam, or oxygen increases with up to about 0.5 mole % UO_2 but declines rapidly above this level. The dielectric constant of $BaUO_3$ is about two orders of magnitude lower than that of $BaTiO_3$, and additions of $BaUO_3$ invariably lower the dielectric constant of $BaTiO_3$. (auth)

31736 METASTABLE TRANSITIONS OF ZIRCONIUM OXIDE OBTAINED FROM DECOMPOSITION OF ALKOXIDES. Mazdiyasni, K. S.; Lynch, C. T.; Smith, J. S. J. Amer. Ceram. Soc., 49: 286-7(May 21, 1966).

Ultra-high-purity submicron zirconium oxide prepared by alkoxide vapor decomposition was metastable cubic as formed. The transition of metastable cubic to metastable tetragonal zirconia was relatively sharp and occurred at 300 to 305°C in a powder with average particle size of 50 Å. Powders with average particle size of 80 to 100 Å transformed at 250 to 270°C to the metastable tetragonal form. The transformation of the metastable tetragonal to the monoclinic form was more gradual and occurred between 305 and 400°C in a powder with average particle size of 50 Å. (W.L.G.)

31737 NEW CsCl-TYPE INTERMEDIATE PHASES IN BINARY ALLOYS INVOLVING RARE-EARTH ELEMENTS. Chao, C. C.; Duwez, P. (California Inst. of Tech., Pasadena). J. Appl. Phys., 37: 2631-2(June 1966).

To further work on intermediate phases having the CsCl-type structure in binary alloys involving one rare earth, fifteen additional phases in alloys of rare earths with Zn, Cd, Hg, In, and Tl are described. (auth)

31738 GRAIN BOUNDARY PRECIPITATION IN OXIDE SYSTEMS. Stubican, V. S.; Viechnicki, D. (Pennsylvania State Univ., University Park). J. Appl. Phys., 37: 2751-4(June 1966).

The spatial distribution of precipitate in several polycrystalline oxide systems after annealing of the crystalline solutions was investigated by using an electron probe microanalyzer. Preferential grain boundary and intergranular voids precipitation of the minor component was found in the majority of systems with limited crystalline solubility, e.g., $MgO-Al_2O_3$, $MgO-CaO$, UO_2-CaO, $CaO-Yb_2O_3$, as well as with the ZrO_2-MgO system which has an eutectoid. The formation of an intermediate phase during the precipitation may have a varied effect on the contribution of the surface free energy to the activation energy for nucleation. The intermediate phase appears in both $MgAl_2O_4-Al_2O_3$ and $CaO-Yb_2O_3$ systems, although complete phase separation occurs in the former and grain boundary precipitation in the latter. (auth)

31739 COALESCENCE OF TWO SPHERES BY SURFACE DIFFUSION. Nichols, F. A. (Bettis Atomic Power Lab., Pittsburgh). J. Appl. Phys., 37: 2805-8(June 1966). (WAPD-T-1866).

A numerical solution was obtained which gives the morphological changes and kinetics during the coalescence of two spheres by surface diffusion. The solution may be utilized for determining surface diffusion coefficients by observing the coalescence of two gas bubbles within a solid or interfacial diffusivities by observing the same phenomenon involving spherical precipitates in a solid matrix. The former parameters are of great interest in the fission-gas swelling of nuclear fuels whereas the latter figure prominently in various transformations in the solid state. The present analysis provides a theoretical framework by which these parameters may be determined under conditions of minimal absorption difficulties, as well as guidelines for applicability of the results. (auth)

31740 DILANTHANIDE MOLYBDATES AND TUNGSTATES Ln_2MO_6. Blasse, G. (Philips' Gloeilampenfabrieken, Eindhoven, Netherlands). J. Inorg. Nucl. Chem., 28: 1488-9(June 1966).

Dilanthanide molybdates, Ln_2MoO_6 (Ln = La, Pr-Lu, and Y), were prepared by firing mixed oxides at 1000°C. The structures of the molybdates and tungstates are described. X-ray powder data were used. (F.J.H.)

31741 RESEARCH OF NEW METHODS FOR IMPROVING THE DUCTILITY OF MOLYBDENUM. Semchyshen, M.; Barr, R. Q. (Climax Molybdenum Co. of Michigan, Ann Arbor). J. Less-Common Met., 11: 1-13(July 1966).

Vacuum-arc-cast ingots were prepared using powder that had been treated in palladium-diffused hydrogen, then transferred to the melting furnace without exposure to air. Ad-

ditions were made to the ingots so that various deoxidizing agents could be studied. Unnotched Charpy impact specimens prepared from bars which had been deoxidized by thorium or neodymium sustained 30 ft-lb. (41.5×10^3 g-cm) of energy without fracture at temperatures below −80°C; the best carbon-deoxidized bar subjected to similar test condition absorbed 30 ft-lb. without fracturing at a temperature of −60°C. A series of ingots was prepared with small additions of aluminum, chromium, or nickel. Rolled bar stock from an ingot to which chromium had been added yielded unnotched Charpy impact specimens which absorbed 30 ft-lb. of energy without fracturing at a temperature of −129°C. (auth)

31742 RESISTIVITY CHANGES IN NIOBIUM DURING STRAINING AND STRAIN AGING. **Kramer, D. (Atomics International, Canoga Park, Calif.). J. Less-Common Met., 11: 64-7 (July 1966).**

The effect of tensile strain on the resistivity of Nb was measured for Nb samples of varying purity. Resistivity changes during isochronal annealing to 500°C of strained and unstrained samples are also reported. The resistivity failed to increase with strain. This failure is attributed to a rearrangement of interstitial atoms. Assuming that interstitials contribute more to resistivity when they are dispersed, a clustering process must take place as a result of strain. Of the three interstitials present, O_2 diffuses considerably faster than either C or N_2. Therefore it appears that O_2 clustering during strain lowers the resistivity. Annealing at 500°C after each increment of strain serves to disperse the O_2 atoms that have clustered during the strain increment. The small resistivity changes occurring below 500°C are probably due to O_2 diffusion. Changes in resistivity at 500°C are due to C, which become mobile at this temperature. (W.L.G.)

31743 MELTING POINTS OF $REZn_2$ INTERMETALLIC COMPOUNDS. **Michel, D. J.; Ryba, E.; Kejriwal, P. K. (Pennsylvania State Univ., University Park). J. Less-Common Met., 11: 67-9 (July 1966). (NYO-2581-100).**

Two thermal arrests were observed in the differential thermal analysis curves of all but four of the $REZn_2$ compounds. The large thermal arrest at the highest temperature is considered to correspond to the melting point of the compound. These melting points are shown plotted against the atomic numbers of the rare-earth metal. The secondary thermal arrests were generally quite small relative to the thermal arrests observed for melting, and were very sharp. The secondary thermal arrest was investigated more thoroughly in a $YbZn_2$ composition. It was established that the arrest was due to the eutectic reaction that occurs in alloys of higher Zn contents. On this basis, the secondary thermal arrests observed in the other compounds were attributed to eutectic reactions. (W.L.G.)

31744 THE ZIRCONIUM–HAFNIUM SYSTEM. **Domagala, R. F. (Illinois Inst. of Tech., Chicago). J. Less-Common Met., 11: 70-2 (July 1966).**

Eleven Hf–Zr alloys at 10 wt % increments were annealed at and quenched from temperatures between 800 and 1800°C. Metallographic examination revealed that the hcp (α) and bcc (β) phases are continuously soluble in all proportions, with a narrow intervening two-phase $\alpha + \beta$ field. (W.L.G.)

31745 EFFECT OF HYDRIDE ON THE THERMAL EXPANSIVITY OF ZIRCONIUM ALLOYS. **Slattery, G. F. (United Kingdom Atomic Energy Authority, Springfields Works, Eng.). J. Less-Common Metals, 11: 89-98 (Aug. 1966).**

Dilatometric data were determined for hydrided Zircaloy-4, Zircaloy-2, and zirconium–2½ wt % niobium alloys. The thermal expansivity of the hydrided alloys is dependent on the nature and distribution of the hydride phase. At low hydrogen contents up to ~600 ppM by weight, the face-centered tetragonal γ'-hydride phase found at room temperature has a thermal expansivity less than that of the α-Zr phase and when directionally aligned as platelets, it can restrain the thermal dilation of the alloy and lower its thermal expansivity. At higher temperatures, the γ'-hydride phase transforms to the less dense face-centered cubic δ-hydride phase with a thermal expansivity considerably higher than that of the alpha phase, and there is a marked increase in the thermal expansivity of the alloy to values approaching that of the pure δ-hydride phase. The (α + hydride)/hydride boundary is indicated by a marked reduction in expansivity on heating and a corresponding increase on cooling, when the less dense hydride is dissolved or precipitated from the α-Zr matrix. On cooling below the boundary, the initial formation of δ-hydride is followed by a transformation to γ'-hydride. The transition $\gamma' \rightleftharpoons \delta$-hydride may be related to the brittle/ductile transition found in hydrided zirconium alloys. (auth)

31746 NEW MODIFICATION OF NIOBIUM PENTOXIDE. **Gruehn, R. (Univ., Muenster, Ger.). J. Less-Common Metals, 11: 119-26 (Aug. 1966). (In German).**

A new modification of Nb_2O_5, called R-Nb_2O_5, was observed. The formation of R-Nb_2O_5, often together with some of the known Nb_2O_5-modifications, took place at different conditions, particularly in transport experiments with Nb_2O_5. The lattice constants from Guinier-photographs are: a = 3.98, b = 3.83, and c = 12.79 Å; and $\beta = 90.7_5°$. Intensities calculated on the basis of an idealized V_2O_5 structure are in good agreement with observed data from Guinier-photographs. Consequently, R-Nb_2O_5 has a simpler structure than all known Nb_2O_5-modifications. (auth)

31747 ELECTRONIC STRUCTURE OF TRANSITION METAL–INTERSTITIAL ATOM ALLOY SUPERCONDUCTORS. **Ralls, K. M.; Wulff, J. (Massachusetts Inst. of Tech., Cambridge). J. Less-Common Metals, 11: 127-34 (Aug. 1966).**

Simple electronic structures of transition metal alloys are considered through a comparison of superconducting critical temperatures. It was found that hydrogen, nitrogen, and oxygen act as electron donors in group V transition metals. With the exception of hydrogen, the interstitial elements only donate p-electrons. Interstitial elements apparently act as electron acceptors in group VII transition metals. Comparisons of materials with different crystal structures are necessary for an understanding of electronic structures. (auth)

31748 ELASTIC PROPERTIES OF POLYCRYSTALLINE Sc, Re, Ru AND Pt–21Ir. **Brown, H. L.; Armstrong, P. E.; Kempter, C. P. (Los Alamos Scientific Lab., N. Mex.). J. Less-Common Metals, 11: 135-40 (Aug. 1966). (LA-DC-7872).**

The elastic properties of polycrystalline Sc, Re, Ru, and Pt–21 wt % Ir were determined at 23°C. In units of 10^6 kg/cm^2, the Young's moduli are 0.770, 4.63, 4.47, and 2.18; the shear moduli, 0.294, 1.78_6, 1.73, and 0.899; and the bulk moduli, 0.672, 3.78, 3.65, and 1.25, respectively. The Poisson's ratios are 0.31, 0.30, 0.30, and 0.21, respectively. The specific electrical resistivities ($\mu\Omega$-cm at 20°C) are 86.6, 17.4, 7.06, and 29.9, respectively. The deviation of these values for scandium from those previously reported or estimated [Young's ≅ 0.81, shear ≅ 0.32, bulk ≅ 0.44 (units of 10^6 kg/cm^2), and Poisson's ratio ≅ 0.27] is most probably the result of some degree of preferred orientation in the samples used for the measurements. (auth)

31749 SYSTEM SILVER–HOLMIUM. **Gebhardt, E.; von Erdberg, M. (Max-Planck-Institut fuer Metallforschung, Stuttgart). J. Less-Common Metals, 11: 141-7 (Aug. 1966). (In German).**

The system Ag–Ho was investigated by thermal analysis, microscopic examination, and x-ray methods, and the existence of three intermetallic compounds (Ag_7Ho_2, Ag_2Ho, and AgHo) was established. All compounds have congruently melting maxima: Ag_7Ho_2 at 920°C, Ag_2Ho at 990°C, and AgHo at 1165°C. According to x-ray examinations Ag_7Ho_2 is primitive orthorhombic, Ag_2Ho, tetragonal of the $MoSi_2$-type, and AgHo, bcc of the CsCl-type. The system Ag–Ho consists of four eutectic partial systems, each of which lies between two neighboring phases. The eutectic points appear at about 11.5, 26.5, 36.5, and 81 at. % Ho and the respective eutectic temperatures are about 775, 890, 970, and 880°C. The solubility of Ho in solid Ag is temperature dependent; it attains, at the most, 1.6 at. %. The system Ag–Ho showed great similarity with the systems Ag–Y and Ag–Sm described previously. (auth)

31750 MAKING SUPERCONDUCTORS HARD. Livingston, J. D. (General Electric Research and Development Center, Schenectady, N. Y.). J. Metals, 18: 698-704(June 1966).

The effects of metallurgical variables on superconductivity are discussed, with analogies between superconducting and mechanical or ferromagnetic properties. Hard superconducting properties are reviewed, along with standard ways of increasing hardness. The major role of physical metallurgists is to improve understanding of structure-properties relations and thereby provide a basis for improved properties. (auth)

31751 INFLUENCE OF THE ALUMINUM CONTENT AND THE TEMPERATURE ON THE ELASTIC AND PLASTIC PROPERTIES OF A SOLID SOLUTION OF IRON–ALUMINUM. Mouturat, P.; Moinet, J.; Romeggio, M.; Sainfort, G.; Cabane, G. (CEN, Saclay, France). J. Nucl. Mater., 19: 234-47(June 1966). (In French).

In the course of a detailed study of Fe–Al alloys with high Al content, it appeared necessary to examine the influence of atomic order in this solid solution on the mechanical properties. A systematic study over the composition range 0 to 40 at. % Al showed that this large range can be subdivided into several intervals which closely correlate with fields in the equilibrium diagram. With increasing solute content up to 20 at. % Al, the alloys acquire progressively more short range order, which reveals itself by an increase in the flow stress, especially at low temperatures, whereas the work-hardening rate remains slight. The deformation mechanisms in this alloy range appear to be identical with those in pure Fe. Long range order begins to form at higher Al contents and results in straight slip lines, and by an abnormal temperature dependence of the flow stress which, after dropping rapidly with rising temperature up to 200°C again increases to a sharp maximum which appears to correspond to the critical temperature for the transformation from Fe_3Al-type to FeAl-type order. These variations are still observed, in an enhanced form, when the solute content increases beyond 28 at. %. The flow stress decrease up to 200°C does not appear to relate to a change in the degree of order. Several theories have been proposed to explain the maximum at a higher temperature: the observations made during the present study, in particular the variations in work-hardening rate and changes in the appearance of dislocations and antiphase boundaries should assist in deciding between the various models which have been proposed. (auth)

31752 $\delta-U_3O_8$, A HIGH-TEMPERATURE MODIFICATION. PART I. PREPARATION AND CHARACTERIZATION. Karkhanavala, M. D.; George, A. M. (Atomic Energy Establishment, Trombay, India). J. Nucl. Mater., 19: 267-73(June 1966).

By heating α-U_3O_8 to high temperatures (T > 1100°C) and cooling extremely slowly a different modification, now designated $\delta-U_3O_8$, is obtained. The yield of $\delta-U_3O_8$ is dependent on the soaking temperature and time and on the rate of cooling. The optimum conditions are: soak at 1350°C for 15 days and cool at a rate of 100°/day. X-ray investigations on powders give an orthorhombic cell: a = 6.70 Å, b = 12.46 Å and c = 8.51 Å. DTA shows that $\delta-U_3O_8$ transforms endothermically at 120°C to $\alpha-U_3O_8$ with heat of transition of 1050 ± 50 cal/g · mole. The transformation is irreversible. (auth)

31753 EFFECT OF PRESTRAIN ON MECHANICAL RECOVERY IN Pu-1Ga. Hanson, I. G.; Pavlick, J. E. (Dow Chemical Co., Golden, Colo.). J. Nucl. Mater., 19: 274-82(June 1966).

The recovery of yield stress in a Pu–1 wt % Ga alloy was studied as a function of prestrain. The specimens were prestrained by either tension or rolling and the kinetics of recovery were studied at 100 and 160°C. The total amount of recovery and the initial rate of recovery were found to be dependent on prestrain and annealing temperature. (auth)

31754 METALLOGRAPHIC OBSERVATIONS OF PLASTIC DEFORMATION IN THERMALLY CYCLED URANIUM. Somasundaram, R.; Premanand, V. (Atomic Energy Establishment, Trombay, India). J. Nucl. Mater., 19: 283-9(June 1966).

Structural changes in cold-rolled and annealed uranium subjected to varying thermal cycles between room temperature and 550°C were studied by optical and electron microscopy using a dislocation etch pit method. Fine slip is observed to be an important deformation process during thermal cycling. During the heating part of a thermal cycle as well as during cooling, plastic deformation by slip and twinning seems to take place in grains irrespective of their texture. (auth)

31755 ELECTRON MICROSCOPE OBSERVATIONS ON THIN FILMS OF ZIRCONIA OBTAINED BY OXIDATION OF ZIRCONIUM. Beranger, G.; Duffaut, F.; de Gelas, B.; Lacombe, P. (Ecole des Mines, Paris). J. Nucl. Mater., 19: 290-300(June 1966). (In French).

Thin films of zirconium oxide, formed by oxidation of the metal in oxygen for several minutes at temperatures near 600°C, were removed from their metallic substrates and studied in detail by electron and optical metallography. The study covered the epitaxial character of the oxide film, preferential oxidation at grain boundaries, the pronounced influence of metal orientation on the growth of the oxide and on the fine structure of the oxide film. The influence of the oxidation temperature and chemical purity of the metal on the morphology of the oxide film was established and discussed. (auth)

31756 NEUTRON DIFFRACTION INVESTIGATION OF Au_2Mn UNDER PRESSURE. Smith, F. A.; Bradley, C. C.; Bacon, G. E. (National Physical Lab., Teddington, Eng.). J. Phys. Chem. Solids, 27: 925-30(June-July 1966).

Apparatus for examining the elastic scattering of neutrons by solids under hydro-static pressures and at temperatures between 373 and 77°K, is described. The pressure cell consists of a piston-cylinder device with load applied by a hydraulic intensifier. The cylinder, of Al–7% Zn, and pistons, of K9 steel, contain carbon disulfide as the pressure transmitting fluid up to pressures of 10 kb. Preliminary measurements on the effect of pressure on the magnetic structure of Au_2Mn are reported. A change in pressure from zero to 9 kb increased the pitch of the helical structure tending to produce a ferromagnetic alignment. This contrasted with the effect of decreasing temperature when the pitch reached a maximum value at 120°K, and suggests the possible importance of an indirect exchange interaction involving the conduction electrons. (auth)

31757 SUPERCONDUCTING TRANSITION TEMPERATURES OF MERCURY–ALKALINE EARTH METAL COMPOUNDS. Claeson, T.; Luo, H. L. (Univ. of California, San Diego, La Jolla). J. Phys. Chem. Solids, 27: 1081-5(June-July 1966).

The superconducting transition temperatures of several Hg–Mg metallic compounds were determined. The critical temperature decreased monotonically with increasing Mg content, and showed no apparent crystal-structure dependence. An attempt was made to extrapolate to the transition temperature of pure Mg. This procedure yielded an estimate (rather uncertain) of between 1 and 10×10^{-3}°K for the T_c of pure Mg. The transition temperatures of Hg_2Mg, HgMg, Hg_3Mg_5, $HgMg_2$ and $HgMg_3$ fall in the range of 4.0 to 0.16°K. The critical temperatures of a few compounds of Hg with Ba and Ca were measured above 1.25°K. (auth)

31758 ANOMALOUS RESISTANCE OF MAGNESIUM–GADOLINIUM ALLOYS. Das, S. B.; Gerritsen, A. N. (Purdue Univ., Lafayette, Ind.). J. Phys. Chem. Solids, 27: 1167-71(June-July 1966).

Resistance and magnetoresistance measurements with two polycrystalline magnesium samples containing 0.43 and 1.38 at. % gadolinium indicated a solid solution behavior. Anomalies observed at low temperatures in the resistance and in the magnetoresistance were partly similar to those found in alloys of the copper-manganese type. A qualitative comparison between the temperatures where the magnetic transition occurs for different alloys led to the suggestion that a polarization of the d-band of the base

metal is probably of some importance for the magnetic properties of these alloys. (auth)

31759 EFFECTS OF LATTICE DEFECTS ON CRITICAL CURRENT OF HARD SUPERCONDUCTING Nb. **Komata, Toranosuke; Mitsumoto, Seiichi; Kitakaze, Keizo (Mitsubishi Electric Corp., Amagasaki, Japan). Nippon Kinzoku Gakkaishi, 30: 340-5(1966). (In Japanese).**

The effects of lattice defects on the critical current behavior of superconducting Nb in d-c applied fields were studied. The concentrations of lattice defects were varied by a various combination of cold work and heat treatment and the changes of these concentrations were estimated by measurements of the electrical resistivity and Vicker's hardness, and observations by means of electron and optical microscopy. The disappearance of some point defects takes place at about 150°C, but no appreciable change in critical current was observed. The disappearance of dislocations in heavily cold worked Nb begins at about 400°C, and the rate of dislocation disappearance becomes smaller at higher temperatures. It was observed by electron microscopy that during annealing at 900°C grain growth took place and in grown-up grains the dislocation density was very low. Comparison of the change in the density of dislocations and grain boundaries with the critical current behavior shows that the dislocations in Nb increase the critical current. From this result the dislocations are considered as the important pinning center of the magnetic flux in Nb. (auth)

31760 SOME PROPERTIES OF WC–20 PERCENT Co AND WC–5 PERCENT TaC–20 PERCENT Co ALLOYS. **Suzuki, Hisashi; Sugiyama, Masataka; Yamamoto, Takaharu (Tokyo Univ.). Nippon Kinzoku Gakkaishi, 30: 367-71(1966). (In Japanese).**

Properties of WC–20% Co and WC–5% TaC–20% Co alloys were examined as a function of the carbon content and their properties compared with WC–TaC–10% Co alloys. Two series of alloys, viz., WC–20% Co and WC–5% TaC–20% Co with various carbon contents in the two or three-phase (γ + carbides) range, were prepared by vacuum-sintering at 1375°C for 1 hr. The grain size of carbides in all the alloys was controlled to be approximately the same through some treatments before sintering. The main results are as follows: A maximum value of the transverse-rupture strength is obtained at the low carbon alloys in the two or three-phase range. However, in the case of 10% alloys, the maximum value is at the high carbon alloys. The addition of TaC up to 5% does not decrease the transverse-rupture strength, but the 3% TaC addition to 10% Co alloys decreases its value. The width of the two or three-phase range is approximately two times as wide as that of 10% Co alloys. The TaC addition increases the hardness but decreases the density. The γ-phase contains almost no TaC. The aging phenomena accompanied by the Co_3W type precipitation is also ascertained in these alloys, but there is the difference that the hardness and the coercive force of these alloys increase after aging. (auth)

31761 ANISOTROPY OF THE DUCTILE-BRITTLE TRANSITION BEHAVIOR OF BERYLLIUM SHEETS. **Tsuya, Kazuo (National Research Inst. for Metals, Tokyo). Nippon Kinzoku Gakkaishi, 30: 372-6(1966). (In Japanese).**

The relation between the ductile-brittle transition behavior and the specimen direction was investigated with beryllium sheet. Most of the basal planes of beryllium sheets used in this experiment were parallel to the rolling direction, but in the transverse direction there was a concentration of the basal poles at 25° from the normal to the sheet. Two kinds of tensile test pieces, i.e., longitudinal and transverse specimens, were cut from the sheet. The tensile ductility of the longitudinal specimens was compared with that of the transverse specimens in the temperature range of 100 to 400°C. The results obtained are as follows: Beryllium sheets were inferior in tensile ductility in the transverse direction to those in the longitudinal direction in the temperature range of 100 to 400°C. Furthermore, it was found that the shape of transverse tensile test curve was quite different from that of the longitudinal test curve. The effects of precipitation treatment and grain refinement on the tensile ductility were examined. Aging at 700°C for 120 hr increased the transverse ductility at 400°C, though it was not observed below 300°C. On the other hand, the grain refinement from 180 to 40 μ increased the ductility of the transverse specimens at 300 and 400°C. Besides, the anomalous shape of the transverse tensile test curve was remarkably changed by the grain refinement. In the temperature range of 100 to 300°C, the tensile ductility decreased with the increasing rate of loading, while the ductility at 400°C did not vary or increase with the loading rate. (auth)

31762 LOW-TEMPERATURE SPECIFIC HEAT OF DILUTE SILVER–GADOLINIUM ALLOYS. **Pickett, G. R. (Clarendon Lab., Oxford). Phys. Lett., 21: 618 (July 1, 1966).**

Specific heat measurements on two dilute alloys of Ag–Gd in the temperature range 0.4° to 4.5°K are reported. (auth)

31763 MAGNETIC PROPERTIES OF SOLID SOLUTIONS OF THE HEAVY RARE EARTHS WITH EACH OTHER. **Bozorth, R. M.; Gambino, R. J. (Watson Research Center, Yorktown Heights, N. Y.). Phys. Rev., 147: 487-94(July 15, 1966).**

The Curie and Néel points, and other critical points, of alloys of heavy rare earth elements with each other were determined for 14 binary alloy systems. To a good approximation the Néel points of all of the alloys vary linearly with the $^2/_3$ power of the average de Gennes factor, $J(J+1)(g-1)^2$, as previously known. The Curie points, however, are definitely characteristic of the alloy system, each system showing a different dependence on concentration. The properties of each system are discussed, and related when possible to the transformations found in the elements and to atomic processes. Special effects are noted when the average 4f electron concentration lies between 10 (Ho) and 11 (Er), where the Stevens factor changes sign. Magnetization processes in several alloys are interpreted according to the model of Kitano and Nagamiya. (auth)

31764 NON-S-STATE PARAMAGNETIC RESONANCE IN A DILUTE ALLOY. **Griffiths, D.; Coles, B. R. (Imperial Coll. of Science and Tech., London). Phys. Rev. Lett., 16: 1093-5(June 13, 1966).**

The paramagnetic resonance in samples of filed powders prepared from a silver–0.3 at % erbium ingot was measured using a h-f-modulation reflection spectrometers. (G.O.Y.)

31765 DETERMINING THE STRUCTURE OF SINTERED MATERIALS OF THE Me–MeO SYSTEM BY IONIC BOMBARDMENT. **Gladneva, L. I.; Efremenkova, N. I.; Lebedeva, L. S.; Spivak, G. V.; Shelamov, V. A.; Yurasova, V. E. Porosh. Met., Akad. Nauk. Ukr. SSR, No. 5, 67-73 (May 1966). (In Russian).**

A study of the structure of SAP material by the ionic bombardment method showed the practical value of this method for the investigation of materials obtained by means of powder metallurgy. The method should be used for manufacturing samples before electron-microscopy investigation. An analysis of microphotographs shows that the base of SAP is a cellular lattice consisting of oxide particles bounded by aluminum pseudograins. (auth)

31766 RELAXATION EFFECT DUE TO DIFFUSION OF INTERSTITIAL DEUTERIUM IN TANTALUM. **Cannelli, Gaetano; Verdini, Livio (CNR, Rome). Ric. Sci. Riv., 36: 246-52(Apr. 1966). (In Italian).**

The elastic energy dissipation coefficient Q^{-1} was measured as a function of temperature and vibration frequency in tantalum after electrolytic charging with deuterium. A thermally activated relaxation effect was found below room temperature, and it was related to the stress-induced diffusion of interstitial deuterium atoms. From these measurements the characteristic parameters of the diffusion process were calculated. The activation energy was equal

to the one previously obtained for diffusion of hydrogen in tantalum, but the ratio between the diffusion constants was about 80 instead of $\sqrt{2}$ predicted by the classical theory of interstitial diffusion. (auth)

31767 PROPERTIES OF THORIUM, ITS ALLOYS, AND ITS COMPOUNDS. Peterson, S.; Adams, R. E.; Douglas, D. A. Jr. (Oak Ridge National Lab., Tenn.). pp 292-312 of STI-DOC-10/52.

A survey was made of available data on the physical, mechanical, and other properties of thorium alloys and compounds for use in advanced converters and breeder reactors. (M.O.W.)

31768 PHASE EQUILIBRIA IN THE THORIUM–CARBON SYSTEM. Henney, J.; Jones, J. W. S. (Atomic Energy Research Establishment, Harwell, Eng.). Trans. Brit. Ceram. Soc., 65: 207-17(Apr. 1966). (AERE-R-4993).

Metallography, x-ray diffraction and DTA techniques were used to study phase equilibria in the system over the composition range 5-15 wt % C (50-77 at % C). The results show that ThC_2 undergoes two polymorphic transformations, changing from monoclinic to tetragonal at 1410 ± 20°C and from tetragonal to cubic at 1500 ± 20°C. When ThC is present, the temperature of the monoclinic to tetragonal change is lowered to 1290 ± 20°C. A solid solution is formed between ThC and cubic ThC_2 at temperatures higher than about 2100°C. A tentative phase diagram over the composition range 4-11 wt % C is given. (auth)

31769 EQUILIBRIUM PHASE DIAGRAM, NIOBIUM (COLUMBIUM)–ALUMINUM. Lundin, Charles E.; Yamamoto, Albert S. (Univ. of Denver). Contract AT(11-1)-1092. Trans. Met. Soc. AIME, 236: 863-72(June 1966).

The phase equilibria of the binary system, Nb–Al, were established by metallographic, x-ray diffraction, hardness, and thermal-analysis techniques. Three intermediate phases were identified, Nb_3Al, Nb_2Al, and $NbAl_3$. The Nb_3Al and Nb_2Al phases have extensive ranges of solubility. The maximum solubility of Al in Nb is 23.0 ± 0.5 at. % Al at 1960 ± 10°C. The maximum solubility of Nb in Al is less than 0.3 ± 0.1 at. % Nb. The Nb_3Al and Nb_2Al intermediate phases form peritectically at 1960 ± 10°C and 1870 ± 10°C, respectively, whereas the $NbAl_3$ phase forms congruently from the melt at 1605 ± 10°C. A eutectic reaction occurs at 57.8 ± 0.5 at. % Al and 1500 ± 10°C between Nb_2Al and Nb_2Al and $NbAl_3$. The Al-rich region of the system has a peritectic reaction where liquid reacts with $NbAl_3$ to form Al solid solution. Structural and lattice-parameter data for the intermediate phases were determined by x-ray diffraction analysis. An unusual transformation having characteristics of nucleation-growth and martensitic mechanisms occurs on cooling the Nb solid solution in the region from 18 at. % Al to 23 at. % Al. The transformed product on rapid quenching is an acicular Nb_3Al. (auth)

31770 ELEVATED-TEMPERATURE TENSILE PROPERTIES OF TUNGSTEN FIBER COMPOSITES. Petrasek, Donald W. (Lewis Research Center, Cleveland). Trans. Met. Soc. AIME, 236: 887-96(June 1966).

The effects of selected alloying elements on the elevated-temperature tensile properties of copper alloy–tungsten fiber reinforced composites were investigated. A comparison of the elevated-temperature tensile properties of copper alloy–tungsten fiber reinforced composites, representing soluble systems, was made with copper–tungsten fiber reinforced composites, representing a mutually insoluble system. A linear relation between tensile strength and volume percent fiber content existed at elevated temperatures for all the systems investigated. The copper alloy composites were weaker in tension at high volume percent fiber contents than copper composites in which alloying with the fiber did not occur. The tensile strength of the alloyed tungsten fiber decreased with increasing penetration of the alloying element into the tungsten fiber. (auth)

31771 ANISOTROPY OF SELF-DIFFUSION IN ALPHA URANIUM. Rothman, S. J.; Bastar, R.; Hines, J. J.; Rokop, D. (Argonne National Lab., Ill.). Trans. Met. Soc. AIME, 236: 897-9(June 1966).

Self-diffusion was measured along each principal axis of mosaic-structured and relatively perfect α uranium single crystals. The anisotropy reported before, $D_{[100]} \approx D_{[001]} \gg D_{[010]}$, was confirmed, and is shown to represent volume diffusion. Diffusion along the dislocations in the imperfect crystals increases the measured value of D significantly without changing either the shapes of the penetration plots or the anisotropy. (auth)

31772 TITANIUM–BERYLLIUM PHASE DIAGRAM UP TO 10 Be. Hunter, Donald B. (Titanium Metals Corp. of America, Henderson, Nev.). Trans. Met. Soc. AIME, 236: 900-2(June 1966).

The Ti–Be system up to 10 wt % Be with commercially pure Ti was determined using metallographic techniques. Be forms the β eutectoid type of diagram with Ti; the eutectoid occurs at 0.5 wt % Be and 1500°F, while a eutectic is formed at 1887°F containing between 5 and 7.5 wt % Be. The solubility of Be in α Ti does not exceed 0.05 wt % and the maximum solubility of Be in β Ti is 1 wt %. (auth)

31773 EFFECT OF RHENIUM ON THE INTERFACE ENERGIES OF CHROMIUM, MOLYBDENUM, AND TUNGSTEN. Allen, B. C. (Battelle Memorial Inst., Columbus, Ohio). Trans. Met. Soc. AIME, 236: 903-15(June 1966).

The interface energies of Cr, Mo, W, and their solid-solution alloys Cr–35Re, Mo–33Re, and W–25Re were studied at 0.6 to 1.0 of the absolute liquidus temperature using five methods. Liquid surface tension, γ_{LV}, was determined using the pendant-drop and drop-weight methods. Results are, respectively, 1700, 2370, and 2480 ± 100 dynes per cm for the Re-containing alloys and essentially the same as those reported for liquid Cr, Mo, and W. Average solid surface energy, γ_{SV}, was measured using the fiber-extension method. The ratio of γ_{SS}, the average high-angle grain-boundary energy, to γ_{SV} was found from grain-boundary groove angles formed at the surface in an inert atmosphere. Absolute interface energies were determined using multiphase equilibria involving suitable liquids of known surface tension. Interpretation of the experimented results in view of probable temperature, orientation, and purity effects gives the following approximations in ergs per sq cm: γ_{SV} (Mo, Mo–33Re) ~ 2100, γ_{SS} (Mo, Mo–33Re) ~ 800, γ_T (deformation twins in Mo–33Re at 1200°C) ~ 800, γ_{SV} (Cr, Cr–35Re) ~ 2400, γ_{SS} (Cr, Cr–35Re) ~ 1000. Probably $\gamma_{LV} \sim \gamma_{SV} \sim 2500$ for W and W–25Re, giving γ_{SS}(W, W–25Re) ~ 900. The interface energies of solid and liquid Cr, Mo, and W are not greatly affected by Re and therefore are not a major factor in the ductilizing Re effect in Group VI-A metals. (auth)

31774 CLUSTERING OF INTERSTITIALS IN DILUTE NIOBIUM–OXYGEN–NITROGEN SOLID SOLUTIONS. Gibala, R.; Wert, C. (Univ. of Illinois, Urbana). Trans. Met. Soc. AIME, 236: 924-9(June 1966).

Internal-friction and elastic-aftereffect measurements utilized to detect O–O clusters and O–N clusters in Nb. Variation of the anelastic parameters with composition and temperature has aided in identification of these clusters and in calculation of some of the equilibrium and kinetic properties of the clusters. The binding enthalpy of the O–O clusters is deduced to be 0.08 ev and of the O–N clusters 0.11 ev. (auth)

31775 RESISTIVITY ANOMALIES IN THE SYSTEM NICKEL–TANTALUM. Baer, Hans-Guenter (Laboratorium der Vacuumschmelze AG, Hanau, Ger.). Z. Metallk., 57: 392-5(May 1966). (In German).

The solubility of Ta in Ni was investigated. It was found that Ni dissolves up to 12 at. % Ta at 800°C. Measurements of the electrical resistivity show that there are anomalies that can be attributed to the K-state, which is dependent on short range order. (auth)

31776 ION-MICROSCOPE STUDIES OF CESIUM SURFACE IONIZATION ON POROUS REFRACTORY METALS. Jamba, D. M.; Husmann, O. K. (Hughes Research Labs., Malibu, Calif.). New York, American Inst. of Aeronautics and Astronautics, 1966, Preprint No. 66-220, 33p., $1.50. (CONF-660310-6). ORAU.

From AIAA 5th Electric Propulsion Conference, San Diego, Calif.

The Cs ion emission patterns obtained from rear-fed, porous refractory metals were investigated using a thermal emission microscope. Current densities were measured in areas as small as 1μ in diameter. It was found that the areas around the pore exit on clean porous W are the ion emission centers and that the diameter of these centers decreases slightly with increasing emitter temperature at constant alkali flow rate. In the threshold region of surface ionization, the ion emission centers are covered with excessive Cs, which increases the atom evaporation; the region of ion emission encircles this area. A similar pattern was observed on a Mo layer sputtered on the W substrate. (G.O.Y.)

31777 THERMAL CONDUCTIVITY OF COMPACTED POWDER CARBONS AND MIXTURES OF CARBON POWDERS WITH URANIUM CARBIDE PARTICLES. Tye, R. P.; Woodman, Margaret J. (National Physical Lab., Teddington, Eng.). 18p. (CONF-650632-12). ORAU. Gmelin, AED-CONF-65-149-23.

From 7th Biennial Conference on Carbon, Cleveland.

Measurements of thermal conductivity and electrical resistivity were performed over the temperature range 20 to 200°C for a series of compacted graphite powder matrices and a further series of matrix materials mixed with different volumes of coated uranium carbide particles. The temperature range was extended to 1000°C for particular samples. Results indicate that the manufacturing process produces homogeneous materials whose measured transport properties are affected markedly by variations of several parameters including the initial compacting pressure, the volume of added particles, and the amount of pyrolitic carbon deposited in the pores. Large increases in both physical properties are obtained at the lower temperatures for changes in each of these parameters. In the case of the pressure variable, the thermal conductivity is found to change linearly with increase of pressure over the range 6-1000 psi. At higher temperatures the differences are much reduced and the materials behave in a manner consistent with that shown by other carbons and graphites having similar properties at the lower temperatures. (auth)

31778 MECHANICAL PROPERTIES OF TUNGSTEN-25 PERCENT RHENIUM ALLOY SHEET. Barto, R. L. (General Electric Co., Cleveland). 30p. (CONF-651062-6). ORAU. Gmelin, AED-CONF-65-325-14.

From Metallurgical Society Fall Meeting, Detroit.

The mechanical properties of W–25Re alloy sheet prepared by rolling pressed and sintered ingots are reported. Room temperature and elevated temperature short time tensile tests, stress rupture and creep properties to 4000°F along with bend and weld ductility were determined. Structural changes, as they relate to the various test conditions encountered, are correlated with the mechanical properties. The W–25 Re alloy is stronger and more ductile than pure W under all test conditions that were investigated, provided equivalent structural conditions for both materials are compared. (auth)

31779 SOME PROPERTIES OF SUPPORTED SMALL α-Fe_2O_3 PARTICLES DETERMINED WITH THE MOESSBAUER EFFECT. Kuendig, Walter (Univ. of California, Los Angeles); Boemmel, Hans; Constabaris, G.; Lindquist R. H. 27p. (CONF-650927-14). ORAU. Gmelin, AED-CONF-65-222-24.

From American Physical Society, Honolulu, Hawaii.

The Mössbauer spectra of ^{57}Fe in α-Fe_2O_3 were measured as a function of particle size and temperature. The crystalline anisotropy constant in the c-plane was calculated. (G.O.Y.)

31780 ULTRASONIC STUDIES IN NORMAL AND SUPERCONDUCTING THALLIUM. Weil, Raoul B. (Univ. of California, Riverside). 113p. (CONF-651212-1). ORAU. Gmelin, AED-CONF-65-348-2.

Thesis. From Ultrasonics Symposium, Boston.

Ultrasonic attenuation and velocity measurements were made on single crystals of pure Tl using the double-ended pulse-echo technique in the range of 12 to 108 Mc; in this range, the sound wave length is larger than the mean free path of the electrons for the specimens used. The results verified Pippard's phenomenological equation for the attenuation of sound waves by normal electrons. (G.O.Y.)

31781 ALLOYING-ELEMENT/DISPERSED-PHASE INTERACTIONS IN TUNGSTEN-BASE ALLOYS. White, J. E. (Aerospace Corp., El Segundo, Calif.). 27p. (CONF-651062-8). ORAU. Gmelin, AED-CONF-65-325-18.

From Metallurgical Society Fall Meeting, Detroit.

The tendency for alloy additions of Zr, Ta, Nb, Re, Mo, and Hf to interact with ThO_2 particles in tungsten-base alloys during exposure to elevated temperature (>2200°C) was evaluated. The details of this interaction were studied during exposure up to 3000°C. (auth)

Radiation Effects

See also CHEMISTRY — Radiation Chemistry

Refer also to abstract 31690.

31782 (BNWL-SA-67) RADIATION EFFECTS IN GRAPHITE AT HIGH TEMPERATURES. Helm, J. W. (Battelle-Northwest, Richland, Wash. Pacific Northwest Lab.). June 4, 1965. Contract AT(45-1)-1830. 25p. Dep. mn. CFSTI $1.00 cy, $0.50 mn.

Graphite irradiations are being conducted in the temperature range from 800 to 1200°C to determine neutron effects on dimensional stability. Several types of raw-coke and isotropic graphites were also studied at 500 to 1150°C. Data are presented in tables and graphs. The length changes of graphites tested over the temperature range from 450 to 1200°C showed a dependence on the temperature of irradiation, particularly in the parallel direction. The transverse samples irradiated at 1200°C contracted more than those irradiated at 800°C and about the same as samples irradiated at 450°C. Those irradiated at 1000°C contracted at the highest rate. The raw-coke graphites contracted less than the other graphites and in some cases expanded. It appeared that the binder phase has an effect on the amount of physical distortion induced by irradiation. The irradiation expansion was not annealed out by heating above the irradiation temperature, but continued to expand. It was concluded that in an anisotropic graphite containing a large amount of less-graphitic material the expansion of the crystallites in the c direction becomes a controlling factor in physical property changes. (M.C.G.)

31783 (FTI-16(6.1)) RADIATION EFFECTS ON SOLID, URANIUM BASED NUCLEAR FUEL MATERIALS. A Bibliography. Vol. 6, No. 1. Uhlmann, W. (Aktiebolaget Atomenergi, Stockholm (Sweden)). May 1966. 42p. Dep. mn.

Seventy-five abstracts on radiation effects on solid uranium-based nuclear fuel materials are presented. A subject index, coordinate index, publications index, and corporate author index are included. (M.C.G.)

31784 (NASA-CR-54976) EFFECT OF NUCLEAR RADIATION ON MATERIALS AT CRYOGENIC TEMPERATURES. Quarterly Report No. 3, January 21, 1966–April 21, 1966. (Lockheed Nuclear Products, Marietta, Ga.). May 1966. Contract NAS3-7985. 94p. (LAC-ER-8538).

Tensile test results from Titanium 55A, partial in-pile tensile test results from Aluminum 1099 (including annealing) and Ti–5 Al–2.5 Sn (ELI), and out-of-pile tensile test results from Aluminum 1099 and Aluminum 7178 are given. (W.L.G.)

31785 (ORNL-P-2162) IN-REACTOR MECHANICAL PROPERTIES EXPERIMENTS. Woods, J. W. (Oak Ridge National Lab., Tenn.). [nd]. Contract W-7405-eng-26. 45p. (CONF-660511-7). Dep. mn. CFSTI $2.00 cy, $0.50 mn.

From International Symposium on Capsule Irradiation Experiments, Pleasanton, Calif.

The design and development of materials and techniques

used in conducting mechanical properties experiments in the irradiation facilities of the Oak Ridge Research Reactor are discussed and illustrated. Detailed description of fabrication and operation of instrumented capsules used for stress-rupture testing, creep testing, and postirradiation studies are presented. A variety of materials tested include stainless steels, beryllium, Inconel, Hastelloy N, and graphite. Temperatures of the tests described cover a wide range: stress-rupture testing from 300 to 800°C, creep testing from 300 to 650°C, and postirradiation studies from 250 to 900°C. Auxiliary equipment such as heaters, loading systems, access tubes, junction boxes, and instrumentation is discussed. (auth)

31786 (ORO-2891-5) THE EFFECTS OF NEUTRON IRRADIATION ON THE RESISTIVITY OF BINARY ALLOYS. Progress Report. Lewis, A. B. (Mississippi Univ., University. Dept. of Physics and Astronomy). June 1, 1966. Contract AT(40-1)-2891. 32p. Dep. mn. CFSTI $2.00 cy, $0.50 mn.

Radiation effects data obtained during the past nine month period are summarized, and progress made in operation of the Dynamitron accelerator is reported. A spectrum of the neutrons obtained at various operating levels of the accelerator shows that better beam tubes will speed up data acquisition. Energies of 2.3 Mev and beam currents of 1 ma are produced for long periods with no machine breakdown. A new accelerator tube offers sustained operation at 3 Mev and 4 ma beam current. Lower level operation data reveals the improved spectrum obtainable from a small increase in voltage using the new tube. The new beam tube has not been installed in the present machine. A discussion of targets, and ways of building them is included. (J.R.D.)

31787 LIQUID IMMERSION FOR REDUCING DAMAGING EFFECT OF LASER GIANT PULSES TO DIELECTRIC MIRROR COATINGS. Gregg, David W.; Thomas, Scott J. (Univ. of California, Livermore). Appl. Phys. Lett., 8: 316-18(June 15, 1966). (UCRL-14777).

The effects of dielectric mirror coating immersion in nitrobenzene were investigated. It was found that the resistance of the coatings to damage when exposed to the high light intensities obtained in ruby laser giant pulses was greatly increased. Hard and soft coatings were investigated, and both showed a large improvement in the damage threshold as a result of immersion. Giant pulse intensities which caused total destruction of the coatings in 1 to 5 pulses caused little damage to the same coatings immersed, even when exposed to over fifty pulses. Still higher intensities resulted in the destruction of the glass window in front of the immersed coating before serious damage occurred to the coating itself. (J.F.P.)

31788 COMPARISON BETWEEN NEUTRON DAMAGE IN ANNEALED GOLD AND IN QUENCHED GOLD. Cotterill, R. J. J. (Argonne National Lab., Ill.). Appl. Phys. Lett., 9: 29-31(July 1, 1966).

The defects that can be resolved as dislocation loops (with diameters in the range from 100 to 500 Å) in neutron-irradiated gold are completely suppressed if the gold initially contains stacking-fault tetrahedra. It is inferred that these loops are of the interstitial type. (auth)

31789 STUDY, BY MEANS OF LENGTH MEASUREMENTS, OF FAULTS CREATED BY IRRADIATION IN PURE IRON. Bonjour, Emmanuel; Vigier, Pierre; Moser, Pierre (Centre d'Etudes Nucleaires, Grenoble, France). Compt. Rend., Ser. B, 262: 1149-51(Apr. 25, 1966). (In French).

The variations in volume of a sample irradiated with neutrons at 77°K are measured during linear increase of temperature. Very sharp annealing states were observed. They are connected to those observed by measurements of resistivity and magnetic hysteresis. Some arguments are given to attribute the most important state to the annealing of iron interstitials in their parent fault. The volume occupied by an iron interstitial is estimated roughly. It sharply exceeds an atomic volume. (tr-auth)

31790 TRAPPING AND THERMAL RELEASE OF IRRADIATION ELECTRONS FROM POLYETHYLENE TEREPHTHALATE FILMS. Monteith, Larry K. (Research Triangle Inst., Durham, N. C.). J. Appl. Phys., 37: 2633-9(June 1966).

Electron irradiation of capacitor-type structures consisting of polyethylene terephthalate films with thin aluminum electrodes can result in a net charge distribution in the dielectric region. Irradiating with a nonpenetrating beam of electrons (10-20 kev) and a constant beam current density (5×10^{-8} amp/cm^2), the transfer of charge through an external circuit after ceasing the irradiation was correlated with the practical range of the primary electrons. Assuming that the irradiated volume of the polyethylene terephthalate contained a uniformly distributed space charge, the observed values of external charge transfer were used to obtain a minimum value for the trapped irradiation electron density. For the 14-kev irradiation with a practical range approximately one half the thickness of the sample, a value of 1.6×10^{15} electrons/cm^3 was obtained. The corresponding internal electric field near the irradiated electrode was 2×10^5 v/cm. (auth)

31791 MEASUREMENTS OF THE DISTRIBUTION OF DEFECT INTRODUCTION RATE WITH DEPTH IN SILICON IRRADIATED WITH 300-kev ELECTRONS. Hitchcock, A. J. (Atomic Weapons Research Establishment, Aldermaston, Eng.). J. Appl. Phys., 37: 2726-9(June 1966).

The potentialities of a silicon field effect device, having a-c and d-c fields superimposed on the gate terminals, are investigated for determining the distribution of defect introduction rate with depth. In particular this device is designed for examining defect introduction mechanisms near threshold energies. In these preliminary experiments, 300-kev electrons are incident on devices made from 600-Ω·cm float-zone silicon. When correction is applied for the proximity of the Fermi level to the $E_c - 0.4$-ev defect level, a distribution of a form similar to that obtained by Flicker and Loferski for 500-kev electrons is obtained. (auth)

31792 TRANSMISSION ELECTRON MICROSCOPY OF FAST-NEUTRON-IRRADIATED SILICON. Hemment, P. L. F.; Gunnersen, E. M. (Atomic Weapons Research Establishment, Aldermaston, Eng.). J. Appl. Phys., 37: 2912(June 1966).

Specimens of n-type silicon were examined by thin-film transmission electron microscopy in a search for defect clusters produced by fast neutron irradiation. No evidence was found in unannealed specimens. Black spots were observed in the micrographs of specimens annealed at 560°C, but the results are inconclusive. (L.B.S.)

31793 DISLOCATION LOOPS IN OXYGEN-ION-IRRADIATED SAPPHIRE. Gulden, T. D. (Berkeley Nuclear Labs., Eng.). J. Appl. Phys., 37: 2915-16 (June 1966).

Transmission electron microscope observations of damage produced in sapphire platelets by 100-kv oxygen ions are reported. Large discoloration loops were observed in a well-annealed specimen, which lie on the $\{10\bar{1}0\}$ plane, perpendicular to the basal plane. It is believed that the interstitial loops were formed by the condensation of two layers of oxygen ions and the appropriate number of aluminum ions on the $\{10\bar{1}0\}$ plane. (L.B.S.)

31794 EFFECT OF NEUTRON IRRADIATION ON THE MECHANICAL PROPERTIES OF HOT-PRESSED AND EXTRUDED BERYLLIUM. Walters, G. P. (United Kingdom Atomic Energy Authority, Harwell, Eng.). J. Less-Common Metals, 11: 77-88(Aug. 1966).

Hot-pressed and extruded Pechiney and Brush beryllium was examined after irradiation at 100, 350, and 600°C to doses up to 8×10^{20} fast n/cm^2. Density measurements showed no volume changes during irradiation. Tensile tests were carried out at 20, 150, 300, 450, and 600°C. There was an increase in yield stress and a decrease in ductility during irradiation at 100 and 350°C; however, no changes in these properties were observed on irradiating at 600°C. The behavior of irradiated beryllium is discussed in terms of the structure as observed by transmission electron-

microscopy, and it was shown that the increase in yield stress of irradiated material is primarily due to the helium bubble distribution. (auth)

31795 STUDY OF IRRADIATED AND UNIRRADIATED COATED FUEL PARTICLES BY THE ELECTRON MICROPROBE. Quatart, D.; Schleicher, H. W. (EURATOM CCR, Ispra, Italy). J. Nucl. Mater., 19: 221-33(June 1966).

Methods of examination of coated particle nuclear fuel by the electron microprobe are described. The determination of low concentrations of uranium in graphite and the analysis of highly radioactive, fully irradiated particles necessitated special alterations to equipment and procedures which resulted in a remarkable improvement in precision. Examples of the results obtained on different types of particles are presented. (auth)

31796 CONTRIBUTION TO A STUDY OF HARDENING BY IRRADIATION OF LOW ALLOY STEEL FOR REACTOR PRESSURE VESSEL. Milasin, N. (Centre d'Etudes Nucleaires, Saclay, France). J. Nucl. Mater., 19: 301-11(June 1966). (In French).

Tensile specimens of one low alloy steel for a reactor pressure vessel were irradiated in a flux of fast neutrons and the changes in mechanical properties were measured at ambient temperature. The integrated neutron flux was $\sim 2 \times 10^{19}$ n/cm^2 (E > 1 Mev); the irradiation temperature was below 100°C. Irradiation caused an increase in the elastic limit (~20 kg/mm^2) and in the fracture stress (~ 9 kg/mm^2) together with a reduction of the total and uniform elongations. The relation between the hardening obtained for two series of specimens prepared in different ways and the initial elastic limit was explained and found that the relative change in the elastic limit $(\Delta\sigma_{0.2}/\sigma_{0.2}) \times 100$ depends on the original value of $\sigma_{0.02}$ and, at the same time, the influence of other metallurgical factors (microstructure, chemical composition, etc.) becomes obvious. Some irradiated specimens were annealed at different temperatures above the temperature of irradiation and tensile tests were done at ambient temperature. These samples showed an additional hardening which had a maximum value between 150–200°C. When the annealing temperature was raised to 450–500°C, the mechanical properties of the irradiated steel gradually returned to the original (unirradiated) values; the recovery process took place. The contribution of these results to the understanding of irradiation-hardening and thermal hardening in this type of steel are discussed. (auth)

31797 BEHAVIOR OF HELIUM GAS IN IRRADIATED COPPER–BORON ALLOYS. Vela, P.; Russell, B. (Univ. of Queensland, Brisbane). J. Nucl. Mater., 19: 312-26 (June 1966).

The behavior of helium in neutron-irradiated copper–boron alloys was investigated in the temperature range between 300 and 800°C. It was found that bubbles nucleate preferentially upon dislocations which are created by the annealing of displacement damage. After gas precipitation is complete, the bubbles grow by migration and coalescence, at such a rate that the average bubble radius is proportional to $t^{1/4}$, where t is time. Helium causes solution-hardening and the strength of an alloy containing bubbles is inversely proportional to the bubble spacing. One atomic per cent of helium causes a 3 μohm · cm increase in electric resistivity. The changes which occur in the resistance during annealing are complicated and contributions arise from the concentration of helium in solution and the changing distribution of bubbles. An activation energy of 0.98 ± 0.1 ev was obtained for the first stage of annealing during which all of the gas leaves solution to form bubbles. (auth)

31798 SPONTANEOUS GRAIN BOUNDARY SWELLING IN IRRADIATED COPPER–BORON ALLOYS. Vela, P.; Russell, B. (Univ. of Queensland, Brisbane). J. Nucl. Mater., 19: 327-40 (June 1966).

The degeneration of grain boundaries during the annealing of copper–helium alloys was investigated. The grain boundary bubbles are stable at temperatures below 700°C, but at higher temperatures they grow spontaneously by absorbing vacancies generated in the grain boundaries. Resistivity measurements are particularly sensitive to grain boundary degeneration and can be used to investigate the process in its earliest stages. Increasing the temperature after bubbles have reached an equilibrium size causes breakaway growth of grain boundary bubbles at temperatures below those at which it would normally occur. Gas concentrations as low as 46 ppM are sufficient to cause spontaneous grain boundary degeneration at 800°C. The ultimate failure of grain boundaries is caused by the growth of bubbles until they touch and the conditions which contribute to this growth in the absence of an applied stress are examined. (auth)

31799 GAS FORMATION BY TRANSMUTATION OF MgO AND Al_2O_3. Wilks, R. S. (Atomic Energy Research Establishment, Harwell, Eng.). J. Nucl. Mater., 19: 351-3(June 1966). (AERE-R-5143).

The volume of monatomic gas per cm^3 of target material produced by the neutron-induced transmutations in alumina and magnesia was computed and compared with experimental results. Similar calculations have been performed by others, but in the present work it is assumed that the ^{25}Mg $(n,\alpha)^{22}$Ne reaction does not occur with thermal neutrons. The discrepancy between the experimentally determined concentration of ^{4}He and that calculated could be explained by the presence of approximately 1 ppM of B or 8 ppM of Li. (W.L.G.)

31800 STAGE IV RECOVERY OF PLATINUM AFTER ELECTRON IRRADIATION. Bauer, Walter (Atomics International, Canoga Park, Calif.); Sosin, A. Contract AT(11-1)-Gen-8. Phys. Rev., 147: 482-7(July 15, 1966).

The activation energy of the stage IV resistivity recovery after electron irradiation of platinum was measured to be 1.36 ± 0.08 ev. The recovery is due to the migration of single vacancies. A model of diffusion to inexhaustible internal sinks, complicated by a vacancy-impurity trapping interaction, is found to describe the platinum recovery data. In addition, the stage IV recovery of deformed nickel is found to follow the same recovery model. (auth)

31801 HIGH-TEMPERATURE EMBRITTLEMENT OF AUSTENITIC STEELS AND NICKEL ALLOYS BY (n,α) REACTIONS. Boehm, Horst; Dienst, Wolfgang; Hauck, Hansjurgen (Kernforschungszentrum, Karlsruhe, Ger.). Z. Metallk., 57: 352-7(May 1966). (In German).

The dose dependence of embrittlement is evaluated with respect to the average spacing of critical bubbles, based on an estimate of the produced amount of helium and the bubble distribution. It turns out that the dependence of the embrittlement on the bubble spacing can be approximated by one curve for all alloys. The influence of the strength of an alloy on the initiation for embrittlement was derived assuming that a certain bubble spacing is required for it. The experimental results are in accordance with this assumption. (auth)

31802 ENERGY RELEASED AT HIGH TEMPERATURE BY IRRADIATED GRAPHITE. Rappeneau, J.; Taupin, J. L.; Grehier, J. (CEN, Saclay, France). 34p. (In French). (CONF-650632-17). ORAU. Gmelin, AED-CONF-65-149-31.

From 7th Biennial Conference on Carbon, Cleveland.

The energy H stored by graphite due to the effect of neutron radiation can be released by thermal annealing. By differential thermal analysis, it is possible to determine the differential enthalpy $(dH/d\theta)$ (cal/g/°C) as a function of the annealing temperature θ. Integration of the spectrum obtained gives the overall quantity of energy $H(\theta)$. To determine the form of the energy spectrum at high temperature, a differential thermal analysis apparatus operating up to 1800°C was built. The tests were carried out under vacuum in a graphite resistance furnace and the temperatures measured as a function of time by means of thermocouples. A description of the apparatus is followed by an examination of graphites irradiated at doses between 1000 and 4000 MwJ/t and at temperatures between 70 and 250°C. The energy spectra obtained show, for all the samples studied, the presence of a healing peak at temperatures of the order of 1200 to 1500°C. This peak was also found in the case of

thermal healing of other physical properties of irradiated graphites. In addition, the overall quantities of energy measured by differential thermal analysis were compared with those measured by combustion heat on similar samples. (auth)

31803 ANNEALING OF IRRADIATION DAMAGE IN GRAPHITE. Kelly, B. T. (United Kingdom Atomic Energy Authority, Culcheth, Eng.); Martin, W. H.; Price, A. M.; Dolsby, P.; Smith, K. 26p. (CONF-650632-11). ORAU. Gmelin, AED-CONF-65-149-20.

From 7th Biennial Conference on Carbon, Cleveland.

A detailed study was made of the thermal annealing of irradiation damage in graphite after fast-neutron bombardment at temperatures between 150 and 350°C. The study includes two types of material, highly crystalline well-oriented pyrolytic graphite and Pile Grade A polycrystalline reactor graphite. The physical properties measured include dimensional changes, thermal conductivity and thermal expansion coefficients on the pyrolytic graphite, and dimensional changes, thermal expansion coefficients, thermal conductivity, electrical resistivity, and Young's modulus on the reactor graphite. It is shown that analysis of the dimensional changes of the reactor graphite on annealing, using the thermal expansion coefficients together with the theory of Simmons, leads to crystal dimensional changes on annealing in reasonable agreement with those observed in the pyrolytic graphite. It is found that the crystal dimensional changes induced by irradiation above 300°C are essentially nonannealable, although all other physical properties recover their unirradiated values. The results show that there is a transition from recoverable to non recoverable dimensional changes in the temperature range and also that the defects mainly responsible for dimensional changes have little effect on other properties. The results are interpreted in terms of the defect content of graphite irradiated at these temperatures and the annealing stages allocated to specific defect reactions. (auth)

31804 PLUTONIUM AND FISSION PRODUCT REDISTRIBUTION IN MIXED OXIDE FUELS. Novak, P. E.; Lauritzen, T. A.; Protsik, R.; Davies, J. H.; Zebroski, E. L. (General Electric Co., San Jose, Calif.). 19p. (CONF-651009-22). ORAU. Gmelin, AED-CONF-65-307-40.

From Conference on Safety, Fuels, and Core Design in Large Fast Power Reactors, Argonne, Ill.

An in-pile experiment to evaluate the effect of stoichiometry on the Pu and fission-product distributions after irradiation was performed. The variations in microstructure and in distribution were studied. The consequences of various patterns of Pu redistribution on Doppler reactivity were also calculated for a large sodium-cooled fast reactor fueled with mixed oxides. (G.O.Y.)

31805 DAMAGE PRODUCTION IN ELECTRON-IRRADIATED PALLADIUM. Lowe, L. F.; Jimenez, C. M.; Burke, E. A.; Sherman, C. H. (Air Force Cambridge Research Labs., Bedford, Mass.). 17p. (CONF-651015-16). ORAU. Gmelin, AED-CONF-65-312-37.

From American Physical Society, Chicago.

Palladium was irradiated with electrons at 1.6 to 3.0 Mev, and the effective threshold for atomic displacement in Pd (27 ± 2 ev) was determined from the data by applying the Kinchin-Pease cascade model. The damage production by the electrons was also measured. (G.O.Y.)

31806 STRUCTURAL ANALYSIS OF FUEL GROWTH IN FUEL PLATES. Scavuzzo, R. J. (Univ. of Toledo). 21p. (CONF-651101-66). ORAU. Gmelin, AED-CONF-65-332-13.

From 13th Conference on Remote Systems Technology, Washington, D. C.

A method is outlined by which dimensional changes in fuel plates caused by fuel growth can be predicted. (D.C.W.

PHYSICS

General

Refer also to abstract 31562.

31807 (TID-23030) FARADAY EFFECT AT HIGH MAGNETIC FIELDS. Dismukes, Robert Key (Vanderbilt Univ., Nashville, Tenn.). June 1966. Contract AT(40-1)-1087. 50p. Dep. mn. CFSTI $2.00 cy, $0.50 mn.

Thesis.

Experiments were made to determine the extent of the region of measurement of Verdet constants and to investigate the possibility of nonlinearities at high magnetic fields, or of variations in the effect as a result of the field's time dependence. Monochromatic light from a laser was directed down the axis of a high field pulsed magnet and detected by a photomultiplier. This gave light intensity versus time data which were converted to a rotation versus field history for each run. (M.O.W.)

31808 PRECISION MEASUREMENTS OF ATOMIC MASSES AND SOME OF THEIR IMPLICATIONS ON NUCLEAR STRUCTURE AND SYNTHESIS. Mattauch, J. H. E. (Max-Planck-Institut fuer Chemie, Mainz). Advance. Mass Spectrometry, 3: Proc. Conf. Paris, 1964, 1-19(1966).

Developments in the field of mass spectrometry since 1926 are reviewed. The packing fraction curve of F. W. Aston (1927) and its correlation with cosmic abundances, development of focusing techniques and the double-focusing spectrometer, models and formulas for calculation of atomic masses and their comparison with experimental data, the peak matching method, determination of Q values of nuclear reactions, and examples of measurements made by various groups are discussed. (47 references) (A.G.W.)

31809 FOCUSING OF AN ELECTRON BEAM FROM A LOW-NOISE GUN WITH DIFFERENT MAGNET SYSTEMS. PART I. TRAJECTORIES OF THE OUTERMOST ELECTRON IN AN INITIALLY UNPERTURBED BEAM FOCUSED BY A UNIFORM MAGNETIC FIELD. Chen, Tsung-Shan (Radio Corp. of America, Harrison, N. J.). Int. J. Electron., 20: 1-20(Jan. 1966).

The computer solutions on the trajectories of the outermost electron in a beam focused by means of different magnet systems are discussed. The electron beam is produced by a low-noise gun which is immersed in a constant magnetic field. The beam voltage and beam current have the values usually found in X-band, medium-power, low-noise traveling-wave tubes. The boundary of an initially "ideal" beam which is confined by a uniform magnetic field throughout the drift space is determined by linearizing and solving the paraxial-ray differential equation, and by solving the exact equation with use of a computer. Emphasis is laid upon the determination of the size of beam ripples, the wavelength of rippling or the scalloping wavelength, and the lowest constraining magnetic flux density below which the linearization process does not hold valid. (auth)

31810 MOMENTUM TRANSFER PRODUCED BY FOCUSED LASER GIANT PULSES. Gregg, David W.; Thomas, Scott J. (Univ. of California, Livermore). J. Appl. Phys., 37: 2787-9(June 1966). (UCRL-14563).

The momentum transfer caused by focusing a laser "giant pulse" on a surface in a vacuum was studied. A simple pendulum was used for measuring the momentum. Data obtained for Be, C, Al, Zn, Ag, and W show the light intensity which gives maximum momentum transfer per unit of laser energy, and the decrease in momentum transfer as the light intensity is increased. The maximum shock pressures generated in the target materials were estimated to range from 6×10^5 to 10^6 bars, depending on the material. (auth)

31811 SIZABLE PROTON POLARIZATIONS IN FROZEN TOLUENE. Wagner, R. J.; Haddock, R. P. (Univ. of California, Los Angeles). Phys. Rev. Lett., 16: 1116-18(June 13, 1966).

Proton polarizations greater than 30% were obtained using the solid effect in a frozen solution of about 2% diphenyl picrylhydrazyl in polystrene (DPPH) dissolved in toluene. (G.O.Y.)

31812 MOTION OF AN ISOLATED CHARGED PARTICLE IN A SIMPLE FORCE-FREE MAGNETIC FIELD. Willis, D. M. (Radio and Space Research Station, Slough, Bucks, Eng.). Planet. Space Sci., 14: 483-501(June 1966).

The motion of an isolated energetic charged particle in a particularly simple force-free magnetic field with rectilinear lines of force is examined in detail. The equations of particle motion are solved exactly without assuming that the guiding center approximation is valid. One component of the equation of particle motion is shown to be formally identical to the general equation of motion of a pendulum, which implies that three distinct types of particle motion can arise. Criteria are derived for these different types of motion and it is found that under certain conditions a particle travels predominantly across the magnetic lines of force rather than along them. The motion transverse to the magnetic field does not depend upon the existence of a neutral line or plane. It is suggested that some energetic charged particles may be able to escape from force-free magnetic fields by this process. The results are discussed briefly in relation to the trapping of solar cosmic rays in sunspot magnetic fields and the passage of galactic cosmic rays through interstellar space. (auth)

31813 MAGNETIC FIELD STABILIZER WITH A BROADBAND EPR SENSOR. Denisov, Yu. N.; Ivashkevich, S. A.; Kalinichenko, V. V. (Joint Inst. for Nuclear Research, Dubna, USSR). Prib. Tekh. Eksp., No. 1, 158-62 (Jan.-Feb. 1966). (In Russian).

A system is described for stabilizing the magnetic field of an electromagnet using a field sensor based on EPR. The sensor is constructed in the form of a short-circuited segment of a waveguide and does not require exact tuning to the resonance frequency. The range of stabilized fields is from 0.6 to 1.37 tesla. For preliminary stabilization of the electromagnet current with an accuracy of (1 to 5) $\times 10^{-2}$%, the instability of the absolute magnitude of the stabilized field does not exceed (1 to 3) $\times 10^{-3}$%. (tr-auth)

Accelerators

Refer also to abstracts 31786 and 32318.

31814 (AD-634300) NRDL 70'' CYCLOTRON EXTERNAL ION OPTICS SYSTEM. Horen, D. J. (Naval Radiological Defense Lab., San Francisco, Calif.). Apr. 15, 1966. 10p. (USNRDL-TR-1008). CFSTI $1.00 cy, $0.50 mn.

The initial external ion-optics system for the NRDL 70-inch cyclotron is presented. Initially, four experimental target areas will be developed. The magnetic components consist of a homogeneous-field, circular switching magnet, an inhomogeneous field analyzing magnet and two element quadrupole magnets. Focused or defocused, unanalyzed beams will be available for biomedical research and irradiations of nuclear chemistry targets. An unanalyzed but focused beam will be provided for irradiating neutron producing targets for neutron shielding studies, and an analyzed beam for nuclear reaction studies. A schematic diagram of the beam handling system is included. (auth)

31815 (BNL-10144) A SUPERCONDUCTING QUADRUPOLE LENS. Kruger, P. Gerald; Sampson, W. B.; Britton, R. B. (Brookhaven National Lab., Upton, N. Y.). Mar. 30, 1966. Contract AT(30-2)-Gen-16. 20p. Dep. mn. CFSTI $1.00 cy, $0.50 mn.

The general properties of superconducting quadrupole lenses are discussed. Experiments demonstrate that superconductors may be wound into unusual configurations and

that static fields of almost any desired shape can be produced. (M.O.W.)

31816 (CEA-R-2929) LA CONSTRUCTION DE L'ANNEAU DE STOCKAGE ACO D'ORSAY. I. ETAT DES TRAVAUX. II. SYSTEMES DE DETECTION. (Construction of the Orsay ACO Storage Ring. I. Status of Work. II. Detection Systems). (Commissariat a l'Energie Atomique, Saclay (France). Centre d'Etudes Nucleaires). Apr. 1966. 16p. (CONF-650923-30). Dep. mn.

From 5th International Conference on High Energy Accelerators, Frascati, Italy.

A brief progress report is given, with mention of the difficulties solved since the 1963 Dubna Conference and the extra facilities which will be available on the ring (beam observation and measurements). Typical large solid angle detecting systems and equipment for accurate monitoring under construction at Orsay are also presented. Emphasis is put on some peculiar features of ACO as a tool for physics: a long experimental straight section and a short length of bunches. (auth)

31817 (CERN-66-15) PRECISION SERVO: N.M.R. FIELD MEASURING EQUIPMENT FOR THE CERN MUON STORAGE RING. Brown, R. Armstrong (European Organization for Nuclear Research, Geneva (Switzerland)). Mar. 28, 1966. 30p. Dep. mn.

Nuclear magnetic resonance equipment for measuring the muon magnetic moment in the CERN muon storage ring is described. Schematic drawings are included. (M.O.W.)

31818 (ITEF-385) VYBOR NAILUCHSHEI FORMY IZGIBA PRYAMOUGOL'NYKH SVETOVODOV POLNOGO VNUTRENNEGO OTRAZHENIYA. (Selection of Optimum Curve of Rectangular Light Pipes with no Light Losses by Reflection). Blagorodov, A. M.; Radkevich, I. A. (Gosudarstvennyi Komitet po Ispol'zovaniyu Atomnoi Energii SSSR, Moscow. Institut Teoreticheskoi i Eksperimental'noi Fiziki). 1965. 19p. Dep. mn.

The form of the curve of the side edge of a curved light-pipe at which there are no light losses by reflection is calculated. Results of the absorption measurements in the light-pipe curved according to calculations have shown that the absorption is the same as in rectangular lightpipe of the same length. (auth)

31819 (LA-3521) QUARTERLY STATUS REPORT ON THE MEDIUM-ENERGY PHYSICS PROGRAM FOR PERIOD ENDING APRIL 30, 1966. (Los Alamos Scientific Lab., Univ. of California, N. Mex.). May 1966. Contract W-7405-eng-36. 95p. Dep. mn. CFSTI $3.00 cy, $0.75 mn.

During the past quarter, work has continued at a high level on the development of more efficient, more stable, and more easily constructed 805-MHz accelerating structures. In addition, a substantial effort was devoted to the 201.25-MHz drift tube structures, including the focusing quadrupoles. Design and construction of subsystems for the 805-MHz amplifier to be used in the accelerator mockup experiments are progressing satisfactorily on the basis of a mid-summer completion date. The test stand will accommodate either a coaxitron or Amplitron as the final amplifier. Effort was concentrated on equipment for the Mockup Facility which would permit the control of two 805-MHz tanks and associated rf power modules. The purpose is to test the overall concepts involving computer-based control of the accelerator. Specifications for a small (8000, 16-bit word memory) digital computer were developed and a system selected. Installation of this computer and peripheral equipment is scheduled for late this year. In the meantime, interface equipment will be designed and constructed. Particle dynamics calculations on the first tank of the Alvarez linac (0.75–5.027 Mev) and the first few tanks of the waveguide linac were made to study their operation as a function of tank excitation level and particle acceleration rate. The purpose is to improve the matching of the emittance of the Alvarez linac to the acceptance of the waveguide section of the accelerator. The computer program which designs a waveguide linac was modified so that the phase velocity of the rf wave increases in steps from tank to tank rather than continuously along each tank. (M.O.W.)

31820 (LNF-66/14) CALCOLO DELLE SCHERMATURE INTORNO ALLE TARGHETTE DELL'ACCELERATORE LINEARE DI FRASCATI. (Calculation of the Shielding around all Targets of the Frascati Linear Accelerator. Note No. 313). Pelliccioni, M. (Laboratori Nazionali di Frascati, Comitato Nazionale per l'Energia Nucleare (Italy)). Mar. 8, 1966. 14p. Dep. mn.

A calculation is made of the shielding around those points of the Frascati linear accelerator in which the power of the beam is either partially or totally absorbed. The two areas considered are the tungsten target and the collimator at the end of the accelerator with which the electrons collide with an energy of 400 Mev. In the calculations only the contributions of the neutrons are considered. Numerical results are tabulated. (tr-auth)

31821 (ORNL-P-2239) OPERATING CHARACTERISTICS OF THE ORIC BEAM EXTRACTION SYSTEM. Hudson, E. D.; Lord, R. S.; White, W. H. Jr. (Oak Ridge National Lab., Tenn.). [nd]. Contract W-7405-eng-26. 5p. (CONF-660510-7). Dep. mn. CFSTI $1.00 cy, $0.50 mn.

From International Conference on Isochronous Cyclotrons, Gatlinburg, Tenn.

The extraction system for ORIC has proved to be stable, reliable, and easy to operate. The harmonic necessary to achieve the coherent oscillations is not easy to calculate but can be obtained in operation and optimized without difficulty. The operating experience with the beam extraction system is described. (M.O.W.)

31822 (ORNL-P-2260) THE ORIC HIGH-RESOLUTION SPECTROGRAPH FACILITY. Ball, J. B. (Oak Ridge National Lab., Tenn.). [nd]. Contract W-7405-eng-26. 7p. (CONF-660510-8). Dep. mn. CFSTI $1.00 cy, $0.50 mn.

From International Conference on Isochronous Cyclotrons, Gatlinburg, Tenn.

The installation of a broad-range spectrograph system at ORIC has now been completed. The system consists of a beam analyzing magnet, two triplet quadrupole magnets, and the spectrograph magnet. These magnets are operated as a compound system to obtain optimum energy resolution. The quadrupole pair gives the system a unique flexibility in matching the properties of the beam preparation and the spectrograph magnets. Preliminary results of the operation of the system show the importance of this compound operation with obtained resolutions approaching 1 part in 2000. (auth)

31823 (RPP-N-5) THE EXTERNAL PROTON BEAM AT NIMROD. Egginton, A. J.; Gray, D. A.; King, N. M.; Mathews, W. A.; Morgan, R. H. C.; O'Connell, M. J.; Whiteside, D. (National Inst. for Research in Nuclear Science, Chilton (England). Rutherford High Energy Lab.). [1965]. 26p. (CONF-650923-31). Dep. mn.

From 5th International Conference on High Energy Accelerators, Frascati, Italy.

The achromatic extraction system for Nimrod is briefly described. The extraction system equipment and external focusing are discussed. Some of the secondary beam plans are also outlined. (M.O.W.)

31824 (SLAC-62) THE STORY OF STANFORD'S TWO-MILE-LONG ACCELERATOR. Dupen, Douglas Wm. (Stanford Linear Accelerator Center, Stanford Univ., Calif.). May 1966. Contract AT(04-3)-400. 126p. Dep. mn. CFSTI $4.00 cy, $0.75 mn.

Included is the history of this accelerator, the background of the development of machines for high energy physics, the appearance and evolvement of traveling wave electron linear accelerators, the design and engineering of this machine, the construction of the facility with particular attention to geological considerations, calculations and planning for radiation containment, and the use of the machine in elementary particle physics research. (M.O.W.)

31825 (SLAC-PUB-192) HYDROGEN THYRATRON PERFORMANCE IN THE SLAC TWO-MILE ACCELERATOR. Bradford, Robert W. (Stanford Linear Accelerator Center, Stanford Univ., Calif.). May 1966. Contract AT(04-3)-400. 16p. (CONF-660528-2). Dep. mn. CFSTI $1.00 cy, $0.50 mn.

From 9th Modulator Symposium, Fort Monmouth, N. J.

The modulator design and the operating performance of the switch tube are described. (M.O.W.)

31826 (UCD-CNL-47) INITIAL INTERNAL BEAM STUDIES WITH THE DAVIS 76-INCH CYCLOTRON. Jungerman, J. A. (California Univ., Davis. Crocker Nuclear Lab.). Apr. 29, 1966. Contract AT(11-1)-Gen-10. 8p. (CONF-660510-6). Dep. mn. CFSTI $1.00 cy, $0.50 mn.

From International Conference on Isochronous Cyclotrons, Gatlinburg, Tenn.

Initial operation of the Davis 76-inch cyclotron with a beam of H_2^+ ions is described. Preliminary beam measurements are reported. (M.O.W.)

31827 (UCRL-16794) REGENERATIVE BEAM EXTRACTION FOR THE BERKELEY 88-INCH CYCLOTRON. Clark, D. J.; Close, E.; Grunder, H. A.; Kim, Hogil; Pellissier, P.; Smith, B. H. (Lawrence Radiation Lab., Univ. of California, Berkeley). Apr. 1966. Contract W-7405-eng-48. 12p. (CONF-660510-10). Dep. mn. CFSTI $1.00 cy, $0.50 mn.

From International Conference on Isochronous Cyclotrons, Gatlinburg, Tenn.

The electrostatic regenerative beam extraction system for the Berkeley 88'' cyclotron is described. Results of the orbit studies using the modified general orbit code are shown. The design features of the regenerator with a 3 section electrostatic deflector are given. The results obtained from the machine tests are summarized. (auth)

31828 EXTRACTION BY PEALING OF A BEAM OF HEAVY IONS ACCELERATED IN A CYCLOTRON WITH STARRED FIELD. Cabrespine, Andre; Martin, Emile; Sergolle, Henri; Langlois, Denise; Poffe, Nina (Institut de Physique Nucleaire, Orsay, France). Compt. Rend., Ser. B, 262: 1359-62(May 16, 1966). (In French).

A new beam extraction device that makes possible a yield of 100% was studied at the sector focusing cyclotron and heavy ion cyclotron at Orsay. This procedure is applicable to multicharged incompletely ionized heavy ions and makes possible an extraction with energy variable as a function as a pealing radius. (tr-auth)

31829 500-kev COCKCROFT-WALTON TYPE PROTON ACCELERATOR. Goto, Masayuki (Mitsubishi Electric Mfg. Co., Ltd., Tokyo); Imamura, Gen. Mitsubishi Denki Giho, 40: 565-72(Mar. 1966). (In Japanese).

A 500-kev Cockcroft-Walton accelerator is used as an injector for a 5 Mev proton linear accelerator. The beam has a repetition rate of 20 p/sec and a pulse width of 60 μsec. The accelerated beam current is 10 m amp at the crest at the present time, but a 20 p/sec increased output is expected. A PIG ion source has been developed and a beam current of 160 m amp has been successfully extracted. (auth)

31830 IMPROVEMENTS AT THE SYNCHROCYCLOTRON. Nucl. Energy, 134-7(May 1966).

The improvement program established for the CERN 600 Mev synchrocyclotron for research in elementary particle physics, nuclear structure physics, and radiation chemistry is discussed. (B.G.D.)

31831 ESTIMATES OF RESIDUAL RADIATION LEVELS INDUCED BY HIGH-ENERGY NUCLEONS. Toth, K. S. (Oak Ridge National Lab., Tenn.); Fulmer, C. B.; Barbier, M. Nucl. Instrum. Methods, 42: 128-33(June 1966). (ORNL-P-1838).

Previously reported studies of residual radiation levels to be encountered in high intensity accelerators are continued and extended. Normalization factors were obtained by comparing the amount of ^{22}Na activity present in the calculated and the experimental decay curves for the aluminum sample. These factors were then used to convert the available experimental decay curves from count rates to dose rates as a function of cooling time. In this manner, the expected residual radiation levels were estimated for thick samples irradiated with collimated beams equivalent to 1μA under the following conditions: 600-Mev protons; exposure times of 96 h, 3 months and 2 years, spallation neutrons from 600-Mev protons; exposure times of 6 weeks and 8 months and 19-26 Bev protons, 5-month exposure. (auth)

31832 MEASUREMENT OF RADIATION ABSORBED BY PARTICLE ACCELERATOR STRUCTURAL COMPONENTS. Chapman, C. E.; Sheldon, R. (Rutherford High Energy Lab., Chilton, Eng.). Nucl. Instrum. Methods, 42: 141-53(June 1966). (RHEL-R-106).

A description is given of the development of dosimetry techniques for the vacuum envelope of the 7 Bev proton synchrotron Nimrod and the results obtained using these techniques are indicated. The service life of the components is estimated from a knowledge of their radiation stability. (auth)

31833 ELECTRONIC RIPPLE FILTER FOR THE BROOKHAVEN ALTERNATING-GRADIENT SYNCHROTRON. Halama, H. J.; Cassel, R. L. (Brookhaven National Lab., Upton, N. Y.). Nucl. Instrum. Methods, 42: 157-62(June 1966). (BNL-9866).

For high energy experiments requiring a long particle spill at constant energy at the Brookhaven Alternating Gradient Synchrotron, the ripple of the magnet power supply is several times 1000 v. This voltage ripple produces a ripple in the magnetic field which, in turn, causes a radial motion in the orbit of accelerated particles. The design and performance of the apparatus which reduces the total ripple of the magnet voltage to less than 5% of the unfiltered value is described. It is a closed loop system with a carefully controlled transfer function. A large power tube, used as a direct coupled regulator, is driven from an r-f link by low level circuits at ground potential. (auth)

31834 IMPROVEMENT IN STABILITY OF THE POWER SUPPLY SYSTEM FOR THE MAGNETS OF THE CAMBRIDGE ELECTRON ACCELERATOR. Pallottino, G. V. (CNEN-CSN, Rome). Nucl. Instrum. Methods, 42: 163-8 (June 1966).

The origin of the fluctuations of the a-c component of the magnet current was investigated. A feedback system was built around the power supply and the magnets, achieving a reduction of the fluctuations of at least one order of magnitude. (auth)

31835 CONSTRUCTION OF A POLARIZED BEAM WITH BOTH SPIN ORIENTATIONS AT THE CERN SYNCHROCYCLOTRON. Coignet, G. (Institut du Radium, Orsay, France); Cronenberger, D.; Kuroda, K.; Le Guen, Y.; Michalowicz, A.; Olivier, J. C.; Dick, L.; di Lella, L. Nuovo Cimento (10), 43A: 701-7(June 1, 1966).

The construction of a proton beam which can also be vertically polarized in both orientations is described. To reverse the beam polarization, the incident scattering angle was reversed. This polarized beam has a sufficiently high intensity $(2(10)^6$ protons per second) and polarization (near 40%) to be used in experiments. Measurements of the analyzing power of carbon at 600 Mev are also given for four scattering angles. (auth)

31836 NONLINEARITY OF QUADRUPOLE LENS FIELDS DURING FOCUSING OF BEAMS EXTRACTED FROM PROTON SYNCHROTRONS. Plotnikov, V. K. (Inst. of Theoretical and Experimental Physics, State Atomic Energy Commission, USSR). Prib. Tekh. Eksp., No. 1, 32-6(Jan.-Feb. 1966). (In Russian).

Simple approximate formulas are given for calculating the nonlinearity of the field in quadrupole lenses whose pole generatrices in the parts free from windings are hyperbolas. The formulas for lenses with noncircular aperture are especially simple. Also a calculation is presented of the magnitude of the allowable field nonlinearity in lenses of channels for the extraction of beams from a proton synchrotron with hard focusing. (tr-auth)

31837 MULTICHANNEL CURRENT STABILIZER. Voronin, V. S.; Kanunnikov, V. N. (Inst. of Physics. Moscow). Prib. Tekh. Eksp., No. 1, 143-6(Jan.-Feb. 1966). (In Russian).

A device is described for stabilizing a direct current, used for the feeding of the magnet blocks of a ring phasotron during tests before magnetic measurements. The current is stabilized in five different circuits with nominal values from 0.1 to 270 amp. A self-triggering d-c generator is used as a common source, and semiconductor triodes serve as regulating elements. The range of regulating of the current in each channel is from 10 to 120%, and the stabilized power is ~10 kw for a 60-w drain by the stabilizer from the network. The use of silicon triodes and thermal stabilization in the amplifier with direct coupling permits a stability of better than ±0.05% to be achieved. (tr-auth)

31839 DEVICE FOR MEASURING CHARGED PARTICLE BEAM PARAMETERS. Mineev, F. I.; Yashin, V. P.; Kodyakov, V. M. (Inst. of Physics and Tech., Khar'kov). Prib. Tekh. Eksp., No. 1, 181-2(Jan.-Feb. 1966). (In Russian).

A device is described which permits measurements to be made of the current, the current density distribution, and the geometry of an axially symmetric charged-particle beam in its drift region, where external fields, which can affect the transverse displacement of the beam, are absent. (tr-auth)

31838 CORRECTING SYSTEM FOR FORCED OSCILLATIONS IN AN ACCELERATOR WITH A REVERSE COUPLING. Zenkevich, P. R.; Koshkarev, D. G. (Inst. of Theoretical and Experimental Physics, Moscow. Inst. of High Energy Physics, Moscow). Prob. Tekh. Eksp., No. 6, 19-23(Nov.-Dec. 1965). (In Russian).

The system for the suppression of forced oscillations in circular accelerators was described. Questions on the quantity and distribution of transmitters on the effect of inaccuracies, and on the establishment of closed orbits during connection of the systems were examined. Derivative corrections for adjustment of the first revolution and correction of the closed orbit was investigated. (tr-auth)

31840 PROGRAMMING THE OPERATION OF THE JINR SYNCHROPHASOTRON FOR EXPERIMENTAL WORK IN PHYSICS. Issinskii, I. B.; Kazanskii, G. S.; Mikhailov, A. I.; Myznikov, K. P.; Omel'chenko, B. D.; Tzarenkov, A. P. (Joint Inst. for Nuclear Research, Dubna, USSR). Prib. Tekh. Eksp., No. 6, 23-6(Nov.-Dec. 1965). (In Russian).

A system of programming of accelerator operation, adaptable to JINR synchrophasotron is described. The program makes it possible to combine some experiments during one cycle and also to set sequences of experiments in different accelerator cycles. (tr-auth)

31841 COMPUTATION OF PARTICLE DYNAMICS IN WAVEGUIDE SEPARATORS. Val'dner, O. A.; Glazkov, A. A. (Moscow Engineering-Physics Inst.). Prib. Tekh. Eksp., No. 6, 27-37(Nov.-Dec. 1965). (In Russian).

On the basis of equations of the motion of particles in separators with moving waves, their displacement and diffraction was calculated as a function of the beam energy. The principles of the selection of the phase velocity of the wave and other parameters of the separator were considered for optimum separation of particles of a given type from the beam with a single pulse. The longitudinal and transverse type of separator, the effect of sectioning of the wave guide, and the chronic development of the beam were described. The beam requirements and tolerances on the separator parameters were considered. The case of particle separators with super-fast pulses were examined. The report was illustrated with the example of the separation of K mesons and antiprotons with pulse of 5 and 21 Bev/c in a separator with 10-cm wavelengths. (tr-auth)

31842 COMPUTATIONS ON ACCELERATOR TUBES IN OBLIQUE FIELDS. Romanov, V. A.; Serbinov, A. N. (Inst. of Physics and Power Engineering, Obninsk, USSR). Prib. Tekh. Eksp., No. 6, 38-42(Nov.-Dec. 1965). (In Russian).

The motion of charged particles under different combinations of oblique fields which can be used in tubes with oblique fields was examined. One of the variants of the calculation of prismatic fields, that is necessary in the calculation of real tubes, was shown. (tr-auth)

31843 ON ONE CAUSE FOR INCREASED PARTICLE DISPERSION IN PROTON LINEAR ACCELERATORS WITH VARIABLE ACCELERATION PERIODS. Plotnikov, V. K. (Inst. of Theoretical and Experimental Physics, Moscow). Prib. Tekh. Eksp., No. 6, 43-4(Nov.-Dec. 1965). (In Russian).

The systematic error in the measurement of the distribution of fields in the accelerating gap, apparently the cause of increased particle dispersion per pulse, was examined. It was shown that in the case when in different resonators the period of acceleration has different multiples, the dispersion can be increased more than 1.1 times. (tr-auth)

31844 USE OF MAGNETIC QUADRUPOLE LENSES FOR FOCUSING PARTICLES PASSING THROUGH STOPPING FOILS. Teplov, I. B.; Fateeva, L. N. (Moscow State Univ.). Prib. Tekh. Eksp., No. 6, 45-51(Nov.-Dec. 1965). (In Russian).

Relations for systems with two quadrupole lenses connecting the parameters of the lenses, the distance from lens to source and image, and the magnification were given. The expressions, obtained in the first approximation with respect to the parameter 1/f, have a simple form and were used for the calculation of magnetic quadrupole lenses, designed for focusing particles passing through stopping foils. The construction of the lenses was described and the test results were reported. The measured intensity of the particle beam passing through thick stopping foils and with focusing lens was compared with the results obtained by use of the formula. (tr-auth)

31845 PRODUCTION OF METALLIC AND OTHER IONS IN rf ION SOURCE. Hall, R. S.; Poole, D. H.; Stagg, M. S. (Berkeley Nuclear Labs., Eng.). Rev. Sci. Instrum., 37: 956-7(July 1966).

A brief report is given of the production of metallic ions in an r-f ion source using the technique of inserting appropriate materials directly into the ion source bottle. The equipment is based on a Sames 150-kev accelerator with the addition of a crossed electric-magnetic field velocity selector together with the necessary focusing device. The equipment was used to study the nucleation and migration behavior of gas bubbles in UO_2 produced by bombardment with krypton ion beams, as well as the mechanism of irradiation damage in metals. (L.B.S.)

31846 FAST SENSITIVE NONINTERRUPTING MONITOR FOR NANOSECOND PULSED BEAMS. Ebert, P. J.; Lasher, D. R. (Univ. of California, Livermore). Contract W-7405-eng-48. Rev. Sci. Instrum., 37: 964(July 1966). (UCRL-14663).

A brief description is given of a noninterrupting beam monitor for a 175-kv electron accelerator used for radiation detector research. (L.B.S.)

31847 SIMPLE SYSTEM FOR DISPERSIONLESS DEFLECTION OF BEAM OF PARTICLES. Draper, James E. (Univ. of California, Davis). Rev. Sci. Instrum., 37: 969-70(July 1966).

A simple method for overcoming the problem of beam dispersion in deflection systems for accelerators is outlined. (L.B.S.)

31848 USE OF LIQUID NITROGEN-COOLED SHIELD TO PROTECT PROTON ACCELERATOR AGAINST OIL VAPOR CONTAMINATION. Hoenig, Stuart A. (Univ. of Arizona, Tucson). Contracts NsG-458; NsG-161-61. Rev. Sci. Instrum., 37: 977(July 1966).

The installation of a nitrogen-cooled shield for preventing oil vapor contamination of a 5 kv, 3 μ amp proton accelera-

tor operated in an oil pumped vacuum chamber is briefly reported. (L.B.S.)

31849 CHANNEL FOR ELECTRON BEAM INJECTION INTO THE MAGNETIC QUADRANT OF AN ACCUMULATOR AT 100 Mev. Grishaev, I. A.; Rakityanskii, A. A.; Tarasenko, A. S.; Tolstoi, A. E. (Inst. of Physics and Tech., Khar'kov). Ukr. Fiz. Zh., 11: 359-62(Apr. 1966). (In Ukrainian).

Considerations are presented on the selection of a magnetic channel for intake of an electron beam with energy 100 Mev from outside to a point with given coordinates in an inhomogeneous magnetic field. On the basis of calculations of the trajectory of the particles of cylindrical screens of steel a magnetic channel was created for the intake of a monoenergetic electron beam in the quadrant of the accumulator. The final screen, set up in the injection quadrant, was modeled with the aid of a filament under current. (auth)

31850 LINEINYE USKORITELI ELEKTRONOV. (OSNOVY RASCHETA LUZ NA MALYE ENERGII). (Linear Electron Accelerators. (Basic Calculations of Small Energy Linear Electron Accelerators)). Val'dner, O. A. Moscow, Atomizdat, 1966. 168p.

The bases for calculations of linear electron accelerators of the waveguide type at low energies are presented. Methods for calculating capture and electron dynamics in the bunching sections and formulas for calculating bunchers of various types are given. A technique for computing an iris waveguide is described. A large number of graphs is presented, constructed from theoretical and experimental data; this presentation substantially facilitates the calculation of iris waveguides with alternating structure. A 5-Mev electron accelerator is described as an example. (tr-auth)

31851 TRAVELING-FIELD PARTICLE LINEAR ACCELERATOR. Pinel, Jaques; Mangin, Jean-Paul (to CSF Compagnie Generale de Telegraphie sans Fil). German Patent 1,213,546. Mar. 31, 1966. Priority date Oct. 8, 1963, France.

The linear accelerator comprises an iris loaded wave guide, the iris diaphragms being provided with elongated apertures. In order to attain the necessary radial focusing the apertures are symmetrically in relation to two orthogonal mirror lines, and the direction of the mirror lines of successive diaphragms is rotated about a predetermined angle. (Gmelin Inst.)

31852 PHASING OF MULTISECTION LINEAR ACCELERATOR BY ALTERNATELY TURNING ON AND TURNING OFF APPROPRIATE ELECTROMAGNETIC DRIVERS. Loew, Gregory A. (to U. S. Atomic Energy Commission). U. S. Patent 3,257,577. June 21, 1966.

A method of phasing individual klystron tubes which supply driving energy to respective sections of a traveling wave multisection linear accelerator is described. With klystron driving energy removed from a reference section and a section to be tuned, the phase difference between a voltage induced in the reference section and a voltage induced in the section to be tuned solely by a particle beam is determined. Then, with klystron energy applied to the two sections, the phase of the klystron voltage applied to the section being tuned is adjusted so that the applied klystron voltages have the same phase difference as the voltages induced solely by the particle beam. (AEC)

Astrophysics and Cosmology

Refer also to abstracts 32044, 32259, 32285, 32656, and 32670.

31853 IDENTIFICATION OF EXTRAGALACTIC RADIO SOURCES BETWEEN DECLINATIONS 0 DEG AND +20 DEG. Clarke, Margaret E.; Bolton, J. G.; Shimmins, A. J. (CSIRO, Chippendale, N. S. W.). Austral. J. Phys., 19: 375-87(June 1966).

Identifications or suggested identifications are given for 138 extragalactic radio sources in the declination zone 0° to +20°. The identifications are based on a search of the Palomar Sky Survey plates in the positions of sources in the Parkes catalog. Forty-two of the identifications are with quasi-stellar objects or suggested quasi-stellar objects and the remainder with galaxies. The radio luminosity distribution and a possible variation in the identification percentage with galactic latitude are discussed. (auth)

31854 OBSERVABILITY OF INDIGENOUS ORGANIC MATTER ON THE MOON. Gilvarry, J. J. (National Aeronautics and Space Administration, Moffett Field, Calif.). Icarus, 5: 228-36(May 1966).

The theories of Gilvarry and Sagan implying the presence of indigenous organic matter on the moon are reviewed briefly, for comparison. The former postulates the presence in the lunar maria of organic remains derived from a pristine biota in a hydrosphere formed by exudation from the moon's interior and lasting several billion years. The latter assumes the presence of organic matter on the lunar highlands, now covered by meteoritic infall, formed by the action of solar ultraviolet light and other agencies on a reducing protoatmosphere lasting significantly less than a billion years. However, the fact that meteoritic infall on a moon without an atmosphere causes a net loss of mass from that body is determinative for observability in the Surveyor and Apollo missions of the organic vestiges postulated in the two theories. On Gilvarry's model, a loss of mass from the lunar surface of at least 7 meters in depth is found for the effects of meteoritic impact and sputtering action (by the particles of the solar wind and flares) over the period of several billion years since the atmosphere and hydrosphere vanished. As the organic remains producing the dark color of the maria are assumed distributed throughout the bulk of the sediments in the maria floors, the coloration cannot be destroyed by superficial loss of mass by meteoritic impact. It follows that future lunar explorers should find organic fossils below the depth of roughly 3 to 5 meters fixed by the charring action of the most penetrating radiation, the cosmic rays. Self-consistently on Sagan's theory, no over-all gain of mass by meteoritic action on the moon could occur, which is at variance with his conclusion of a depth of burial of organic vestiges amounting to some tens of meters. The actual loss of mass on the model after the lunar atmosphere vanished would be at least 10 meters in depth, and hence the organic remains postulated as superficially distributed at a remote time would be completely unobservable at present. (auth)

31855 APPROXIMATE THEORY OF THE RED SHIFT IN A CONFORMALLY PLANE SPACE. Pugachev, Ya. I. (Krasnodar State Pedagogical Institut, USSR). Izv. Vyssh. Ucheb. Zaved., Fiz., No. 5, 15-18(1965). (In Russian).

An approximate theory of the red shift of spectral lines for a gravitational field described by a conformally plane space is presented. This phenomenon is interpreted as the consequence of different values of the gravitational potential at various points of the field and is not associated with real motion of radiating bodies. (tr-auth)

31856 BISTATIC-RADAR MEASUREMENTS OF INTERPLANETARY PLASMA STREAMS. Gee, Sherman (Stanford Univ., Calif.). J. Geophys. Res., 71: 2353-64 (May 1, 1966).

The use of bistatic-radar transmissions between earth and an interplanetary spacecraft for studying interplanetary plasma streams is suggested. Nonrelativistic stream velocities are considered. A derivation of the propagation characteristics of an electromagnetic wave transmitted through a (collisionless) plasma stream in the presence of a uniform magnetic field is presented. The direction of the magnetic field is assumed to be aligned perpendicular to the direction of the plasma flow. The effect of the stream medium is shown to introduce a second-order correction to the Faraday rotation undergone by a linearly polarized electromagnetic wave transmitted through the medium. The results are employed to arrive at a possible method for measuring the average stream velocity along the propa-

gation path using two-way propagation between the two transmission terminals. This method is shown to be particularly appropriate for plasma stream measurements under conditions of enhanced solar activity. (auth)

31857 EFFECT OF COHERENT DENSITY FLUCTUATIONS ON RADAR DETERMINATION OF TOTAL ELECTRON CONTENT. Scarf, Frederick L. (Thompson-Ramo-Wooldridge Inc., Redondo Beach, Calif.). Contract NASW-1366. J. Geophys. Res., 71: 2709-13(June 1, 1966).

The effect of density fluctuations on the radar determination of total electron content is studied in terms of the recent measurement of average cislunar density. It is shown that a grating effect is possible, and that severe modifications in the propagation constants occur if the incident wave is scattered by coherent plasma oscillations for which the electrostatic wavelength is near half the radio wavelength. Evidence suggesting that such plasma oscillations may be present in the magnetosphere is discussed. (auth)

31858 BISTATIC-RADAR MEASUREMENTS OF PROPAGATING INTERPLANETARY SHOCK WAVES. Gee, Sherman (Stanford Univ., Calif. Sylvania Electric Products, Inc., Mountain View, Calif.). Contract Nonr-225(83). J. Geophys. Res., 71: 2729-37(June 1, 1966).

A method for detecting and measuring collisionless MHD shock waves propagating in interplanetary space using bistatic-radar transmissions from earth to a spacecraft is suggested. The shock wave is represented by a one-dimensional flow model in which the magnetic field is taken to be aligned normal to the plasma flow. The method basically involves performing multichannel phase and group path measurements of the columnar electron density between transmitter and receiver. Detection is accomplished from observation of typical shock signatures on the time response of the measurements. The magnitudes of the time response provide information for establishing a number of magnetoacoustic shock parameters characterizing the shock intensity. In addition, the proposed measurements under suitable conditions can possibly detect shock-density oscillations as well as provide information needed to help resolve certain fundamental questions concerning the structure of collisionless MHD shock waves. (auth)

31859 HEAVY RARE GASES IN SILICATES FROM THE ESTHERVILLE MESOSIDERITE. Pepin, Robert O. (Univ. of Minnesota, Minneapolis). Contract Nonr-710 (58). J. Geophys. Res., 71: 2815-29(June 1, 1966).

Krypton in Estherville silicates is shown to be a mixture of primordial and spallation-produced components, and xenon a mixture of primordial, spallation, and fission components. Small amounts of radiogenic ^{129}Xe may also be present. An average isotopic composition for Estherville spallation xenon is $^{124}Xe:{}^{126}Xe:{}^{128}Xe:{}^{130}Xe:{}^{131}Xe:{}^{132}Xe = .34:.62:1.00:1.05:4.80:3.3$. This composition is compared with theoretical isobaric production rates calculated from a model of cosmic-ray spallation in meteoritic material. The relative abundance of ^{131}Xe is found to be significantly higher than predicted: whether this implies either thermal neutron irradiation or a departure from a simple cosmic irradiation history is at present uncertain. The possible presence of a spallation component in carbonaceous chondrite xenon is considered. Extinct radioactivity chronologies and the question of concordant formation intervals are examined for Estherville and for the Pasamonte achondrite. I–Xe and Pu–Xe formation intervals for Pasamonte are probably concordant at ~220 ± 40 million years. The isotopic composition of Pasamonte fission xenon, after correction for spallation contributions, is estimated as $^{131}Xe:{}^{132}Xe:{}^{134}Xe:{}^{136}Xe = 0.18:0.91:0.97:1.00$. (auth)

31860 VARIATIONS IN THE POLARITY DISTRIBUTION OF THE INTERPLANETARY MAGNETIC FIELD. Coleman, P. J. Jr. (Univ. of California, Los Angeles); Davis, Leverett Jr.; Smith, E. J.; Jones, D. E. Contracts NsG-249(PJC); NsG-426(LD); NASw-7(EJS); NGR-45-001-011(DEJ). J. Geophys. Res., 71: 2831-9(June 1, 1966).

The variations in the interplanetary field observed during the flight of Mariner 2 are reviewed. Evidence that a specific field polarity is associated with each solar wind stream that was detected with the Mariner 2 plasma probe is discussed. The field variations observed during the flight of Mariner 4 are described. The data from the two Mariner flights and the IMP 1 results are compared. The correlation between persistent features of these field variations and persistent features of the K_p index is also discussed. (B.G.D.)

31861 ISOTOPIC COMPOSITION OF SILVER IN THE CANYON DIABLO METEORITE. Dews, Jon R. (Univ. of California, Berkeley). J. Geophys. Res., 71: 3069-81 (June 15, 1966).

Trace quantities of silver in the iron meteorite Canyon Diablo were isolated by chemical procedures with an average yield of 80%. The isotopic composition of 5 samples of silver from the meteorite was measured on a 12-inch radius of curvature, double-focusing, fast-sweep mass spectrometer. The isotopic composition of 18 samples of terrestrial silver was measured for comparison. The meteoritic and terrestrial ratios of $^{107}Ag/^{109}Ag$ were found to be identical to within 1%. The silver content of Canyon Diablo is 58 parts per billion from isotopic dilution analyses of aliquots of the meteorite samples. Blanks were less than 10% of the sample size in the analyses. Thus a previous report of a 4% excess of ^{107}Ag for Canyon Diablo is not confirmed. (auth)

31862 GRAVITATIONAL COLLAPSE IN THE PRESENCE OF A MAGNETIC FIELD. Strittmatter, P. A. (St. Johns Coll., Cambridge, Eng.). Mon. Notic. Roy. Astron. Soc., 132: 359-78(1966).

The effect of a frozen-in magnetic field on the gravitational instability of a primeval gas cloud is examined by means of the scalar and tensor virial theorems. It is shown in particular that the critical mass, below which a cloud is unable to contract indefinitely across the lines of force under its own gravitational field, is reduced by a factor ~0.5 if the cloud becomes highly flattened due to flow of material down the field lines. For a cloud of given mass, it is found that a change by a factor ~4 in magnetic flux will account for the difference between the possibility of complete gravitational collapse and the establishment of an equilibrium position at almost (within 1% of) the original lateral dimensions of the cloud. The possible effects of rotation and thermal energy, in the presence of a magnetic field, are briefly discussed. (auth)

31863 CLASSIFICATION OF GENERAL RELATIVISTIC WORLD MODELS. Stabell, R.; Refsdal, S. (Univ. of Oslo). Mon. Notic. Roy. Astron. Soc., 132: 379-88(1966).

General relativistic world models are classified by means of the deceleration parameter q_0 and the density parameter σ_0. The evolution of the different models is illustrated by "evolution" in the (q,σ) plane. The age of the universe is computed for the exploding models. A discussion of the particle horizon and the event horizon in the different models is given in the last section. (auth)

31864 CONTINUOUS ABSORPTION BY THE CARBON NEGATIVE ION. II. FREE-FREE ABSORPTION. Myerscough, V. P.; McDowell, M. R. C. (Univ. of Durham, Eng.). Mon. Notic. Roy. Astron. Soc., 132: 457-61(1966).

The free-free absorption coefficient of electrons in the field of neutral carbon atoms is calculated per unit electron pressure per carbon atom in the static central field exchange approximation, assuming a Maxwellian distribution of velocities at temperature T°K. The results are presented in a table over a wide range of wavelengths, and for various values of T, together with the contribution to the total absorption coefficient provided by the bound-free transitions. The total absorption coefficient per unit electron pressure per carbon atom, including stimulated emission, is presented, and is seen to be of the same order of magnitude as that for electrons in the field of neutral hydrogen atoms at the same temperature. (auth)

31865 RELATIVE ABUNDANCE OF SILICON, IRON, AND NICKEL IN THE SOLAR CORONA. Jordan, Carole (London Univ.). Mon. Notic. Roy. Astron. Soc., 132: 463-70(1966).

The method of analysis, developed by Pottasch, for determining the relative abundance of elements represented in the far ultra-violet part of the solar spectrum was extended to include recently identified lines of iron and nickel. The calculations of the ionization equilibrium included the process of dielectronic recombination. The results indicate that the abundance of iron relative to nickel is the same in the corona as in the photosphere, but that the abundance of iron relative to silicon is an order of magnitude larger in the corona than in the photosphere. The distribution of $\int_R N_e^2 dh$ with temperature now indicates a general coronal temperature of 1.4×10^6°K and a decrease in the quantity of coronal material for temperatures in excess of this value. (auth)

31866 NOTE ON THE ONSET OF HELIUM BURNING IN DEGENERATE CORES. Eggleton, P. Mon. Notic. Roy. Astron. Soc., 132: 479-84(1966).

Schwarzschild et al., (1962, 1962 and 1964) have considered the onset of helium burning in partially degenerate cores, using the assumption that the degenerate part of the core is isothermal because electron conduction transports heat very efficiently. They therefore find that the helium flash begins at the center, where the density is greatest. It is shown that if electron conduction is included both the temperature and the rate of helium burning may increase outwards from the center in certain stars, depending on their zero-age composition, and some computational results supporting this are presented based on a simplified model. In particular, it is shown how the position of the point at which helium first burns can be estimated. It is suggested that the helium flash may be preceded by an explosion in a shell within the core, and in consequence the reaction products may float very rapidly to the surface. (auth)

31867 ABUNDANCE OF IRON IN THE SOLAR CORONA. Jordan, Carole (London Univ.). Mon. Notic. Roy. Astron. Soc., 132: 515-26(1966).

A comparison of the observed intensities of lines within FeX, XI, XIV, and XV multiplets, in the far ultra-violet solar spectrum, enables the population of the excited level of the ground term (N_u) to be found, relative to that of the ground level (N_g). This factor N_u/N_g is needed in the determination of the abundance from the equivalent widths of forbidden emission lines in the near-visible spectrum. Hence, it was possible to calculate the abundance of iron in the solar corona. The value obtained is $\log N(Fe)/N(H) = -4.30$. This is in accordance with other coronal estimates, but is an order of magnitude greater than the value from photospheric determinations. The values of N_u/N_g were also used in combination with theoretical excitation cross sections, to calculate the electron density, N_e. (auth)

31868 MAGNETIC FIELD WITHIN SOME QUASI-STELLAR RADIO SOURCES. Williams, P. J. S. (Cambridge Univ., Eng.). Nature, 210: 285-6(Apr. 16, 1966).

The energy requirements of powerful quasi-stellar radio sources, which are dependent on the equipartition between the magnetic and particle energies, are discussed. This requirement is established by making reasonable assumptions about the upper and lower limits in the energy spectrum of relativistic electrons responsible for emission and knowing the volume of the source. Six sources are considered. (B.G.D.)

31869 OBSERVATIONS ON THE PROPAGATION OF SOLAR-FLARE ELECTRONS IN INTERPLANETARY SPACE. Anderson, K. A.; Lin, R. P. (Univ. of California, Berkeley). Phys. Rev. Lett., 16: 1121-4(June 13, 1966).

Eight solar-flare electron events were identified and studied. It was shown that the propagation of electrons in the region of the earth is highly anisotropic in two respects. (D.C.W.)

31870 EXCITATION OF CYCLOTRON RADIATION IN THE FORWARD SUBLUMINOUS MODE AND ITS APPLICATION TO JUPITER'S DECAMETRIC EMISSIONS. Fung, P. C. W. (Univ. of Tasmania, Commonwealth of Australia). Planet. Space Sci., 14: 469-81(June 1966).

The growth rate of a forward-subluminous-mode electromagnetic wave excited in a helical stream–plasma system is calculated for general wave-normal angle, with parameters appropriate to the Jovian magnetosphere. The first three harmonics have been included in this investigation. It is found that for the fundamental harmonic, the growth rate maximizes at θ_m which ranges from about 40 to 50° (with respect to the static magnetic field vector) for pitch angles and energies of electron streams considered appropriate for Jupiter. The growth rate of the second and third harmonics maximizes at θ_m ranging from 60 to 80°, and the second harmonic will have significant effect only when the kinetic energy of the electron stream is high. The application of the amplification theory to Jupiter's decametric burst radiation is discussed and found to support the cyclotron theory of Ellis for this radiation. (auth)

31871 EXACT ANALYTIC SOLUTION FOR PROPAGATION OF SHOCK WAVES IN SELF-GRAVITATING GAS SPHERE. Deb Ray, G. (St. Xavier's Coll., Calcutta). Proc. Nat. Inst. Sci. India, Pt. A, 31: 276-86(May 1965).

An exact solution of the equations representing a spherical wave of explosion in a stellar model of polytrope 5 was worked out. The shock moves with constant strength and carries a constant amount of energy. The solution, however, is strictly valid when the ratio of the specific heats, γ, equals $4/3$ and was found to be applicable also for all other values of γ. (auth)

31872 EVOLUTION OF A ROTATING PROTOSTAR. Bird, Joseph F. (Johns Hopkins Univ., Silver Spring, Md.). Contract NOw 62-0604-c. Progr. Theoret. Phys. (Kyoto), 35: 615-21(Apr. 1966).

A theory of a rotating uniform gas cloud that contracts gravitationally due to secular loss of angular momentum is applied to (Pop. I) protostars of hypothetical origin in the interstellar medium. Representative thermal histories are displayed and the influence of various parameters discussed. It appears that some protostars, particularly the more massive ones, are apt to approach the main sequence by a Helmholtz-Kelvin-like expansion from below rather than by the familiar contraction from above. (auth)

31873 PROBLEMS OF STAR FORMATION. I. Mestel, L. Quart. J. Roy. Astron. Soc., 6: 161-98(June 1965).

The formations of subcondensations in diffuse gas clouds with strong magnetic and centrifugal fields is considered. The simplest problem in which gravitation is opposed only by thermal and turbulent pressure is discussed, then angular momentum and magnetic flux are introduced separately, and finally a synthesis is attempted. Gravitational instability in a nonmagnetic nonrotating medium and the effect of rotation are considered. (J.F.P.)

31874 COMETS AND THE SOLAR WIND. Biermann, Ludwig (Max-Planck-Inst. for Physics and Astrophysics, Munich). Sci. J., 2: No. 5, 69-73(May 1966).

The interaction between the solar wind and cometary tails is described and the information gained from the interaction is reviewed. Evidence is given for magnetic fields in comets themselves. The chemical constituents of comets are discussed. The recently discovered magnetic tail of the earth is compared to a comet's tail. A planned experiment to produce an artificial cometary tail in the form of an artificial plasma cloud visible from the earth's surface is mentioned. (M.H.R.)

31875 SPALLATION, FISSION, AND NEUTRON CAPTURE ANOMALIES IN METEORITIC KRYPTON AND XENON. Marti, K.; Eberhardt, P.; Geiss, J. (Univ., Bern). Z. Naturforsch., 21a: 398-413(Apr. 1966).

Measurements of the Kr and Xe concentrations and isotopic compositions in five meteorites are reported. Ex-

perimental techniques and reproducibility are discussed in detail. In the Stannern achondrite 75% of the total Kr and 30% of the total Xe are due to cosmic ray induced spallation reactions. Also Bruderheim and H- Ausson show distinct spallation components. The isotopic composition of pure spallation Kr is derived as $^{78}Kr:{}^{80}Kr:{}^{82}Kr:{}^{83}Kr:{}^{84}Kr = 0.179:0.495:0.765:1.00:0.63$ and of spallation Xe as $^{124}Xe:{}^{126}Xe:{}^{128}Xe:{}^{130}Xe:{}^{131}Xe:{}^{132}Xe = 0.590:1.00:1.45:0.97:3.9:0.9$. It is shown that the spallation components found were produced by the cosmic radiation late in the history of the meteorite during a period given by the radiation age. The observed $^{126}Xe/^{124}Xe$ spallation ratio rules out a substantial contribution of spallation products in the xenon of carbonaceous chondrites. The Xe fission spectrum derived by Rowe and Kuroda from Pasamonte is corrected for spallation and the following composition is obtained for fission Xe: $^{131}Xe:{}^{132}Xe:{}^{134}Xe:{}^{136}Xe = 0.22:1.00:1.02:1.00$. In Mezö-Madaras and Abee ^{80}Kr, ^{82}Kr, and ^{128}Xe excesses are found, due to (n,γ) reactions on Br and I. It is shown that neutrons produced by the cosmic radiation during the radiation age can account for the observed effect in Abee and the evidence so far suggests that this is also true for Mezö-Madaras. (auth)

31876 RARE GAS MEASUREMENTS IN 30 STONE METEORITES. Eberhardt, P.; Eugster, O.; Geiss, J.; Marti, K. (Univ., Bern). Z. Naturforsch., 21a: 414-26 (Apr. 1966).

The concentrations and isotopic composition of He, Ne, and Ar in 29 chondrites and 1 achondrite have been determined. Detailed accounts of the experimental technique used and the reproducibility and accuracy obtained are given. The U, Th–^{4}He, and K–Ar ages derived from these results are in agreement with the already known age distributions of the different chondrite classes. These measurements have revealed a linear correlation between the $(^3He/^{21}Ne)_{spall}$ and the $(^{22}Ne/^{21}Ne)_{spall}$ ratios, following the equation (constants for chondrites): $^3He/^{21}Ne = 2.40 + 23.4\,(^{22}Ne/^{21}Ne - 1)$. The significance of this correlation and its possible application in detecting diffusion losses are discussed. The radiation ages derived confirm the salient features observed in the radiation age distributions of the different chondrite classes. Five new meteorites with trapped gases were found (2 solar type, 3 planetary type). (auth)

31877 SOLAR WIND SIMULATION WITH THE PIONEER SPACECRAFT. Kemp, Robert F.; Sellen, J. M. Jr. (Thompson Ramo Wooldridge Inc., Redondo Beach, Calif.). New York, American Inst. of Aeronautics and Astronautics, 1966, Preprint No. 66-153, 23p., $1.50. (CONF-660315-17). ORAU.

From AIAA Plasmadynamics Conference, Monterey, Calif.

The simulation of the solar-wind environment for the Pioneer vehicle using arc lamps and plasma sources in a vacuum chamber is discussed. The experimental facility is described, and the calibration of the two plasma probes carried by the vehicle is discussed in detail. (D.C.W.)

31878 PHOTON-INDUCED BETA DECAY IN STELLAR INTERIORS. Shaw, P. B.; Clayton, D. D.; Michel, F. C. (Rice Univ., Houston, Tex.). 35p. (CONF-650927-17). ORAU. Gmelin, AED-CONF-65-222-14.

From American Physical Society, Honolulu, Hawaii.

The rate of photon-induced beta decay (photobeta process) is calculated for stellar interiors. An infrared divergence problem for exothermic photobeta decay is discussed along with applications in the driven decay of stable nuclei. The competition between the photobeta process and excited-state beta decay is also discussed. (G.O.Y.)

31879 LONG-RANGE SOLAR FLARE PREDICTION TECHNIQUE. Blizard, Jane B. (Univ. of Denver). 17p. (CONF-650961-8). ORAU. Gmelin, AED-CONF-65-224-15).

From American Geophysical Union, 5th Western National Meeting, Dallas.

A method of forecasting solar proton events far in advance is needed before extended manned missions in space. The procedure described is capable of predicting three-quarters of the proton events at least 6 months ahead of time. A statistical study was made of all proton events during 1956–1961 (NASA TR R-169) and of solar activity during the IQSY period (1962–1965). The proton events correlate with solar perturbations in an instability zone in the subphotosphere. Three-quarters of the proton flares occurred within 10 days after a perturbation, including nearly all of the high-dose, high-energy, and multiple events. The possibility of such a correlation occurring by chance alone is less than five in 10,000. Further refinements could determine the phase lag more accurately by use of active longitudes on the sun. The major difference between the present approach and other prediction methods is that here the causes of flares are studied, whereas other methods merely observe their effects. (auth)

31880 (JPL-TR-32-630) THE SOLAR WIND. Proceedings of a Conference Held at The California Institute of Technology, Pasadena, California, April 1–4, 1964, and Sponsored by the Jet Propulsion Laboratory. Mackin, Robert J. Jr.; Neugebauer, Marcia (eds.) (California Inst. of Tech., Pasadena). 1966. 445p. (CONF-640418).

The conference included 29 papers. Separate abstracts were prepared for each paper. (J.F.P.)

For abstracts of individual papers see: 31881–31900, 31955, and 32275–32282.

31881 MARINER-2 MEASUREMENTS OF THE SOLAR WIND. Neugebauer, Marcia; Snyder, Conway W. (California Inst. of Tech., Pasadena). pp 3-23 of The Solar Wind. Mackin, Robert J. Jr.; Neugebauer, Marcia (eds.), Pasadena, Calif., California Inst. of Tech., 1966.

The analysis of data from the Mariner-2 measurements of solar wind is considered. The method of calculating velocity and temperature; the time dependence of proton velocity, temperature, and density; the effect of change in distance from the sun, correlation with geomagnetic K_p, alpha-particle temperature, the alpha-proton ratio, and the dependence of alpha-particle and proton temperature upon the magnetic field are discussed. It is proven that the temperature of the solar-wind plasma is not simply related to the temperature at the base of the corona and that shock-wave heating may be an important process. (J.F.P.)

31882 RELATION OF MARINER-2 PLASMA DATA TO SOLAR PHENOMENA. Snyder, Conway W.; Neugebauer, Marcia (California Inst. of Tech., Pasadena). pp 25-34 of The Solar Wind. Mackin, Robert J. Jr.; Neugebauer, Marcia (eds.). Pasadena, Calif., California Inst. of Tech., 1966.

The correlation between the velocity of solar wind and solar phenomena is considered. The daily geomagnetic character figures and sunspot numbers for solar rotation numbers 1759 to 1780, and time plots of magnetic storms, solar-wind velocity, extrapolation lines to the sun's surface, counting-rate increases on Mariner G-M counters, and features of the solar map are shown. (J.F.P.)

31883 INTERPLANETARY MAGNETIC MEASUREMENTS. Davis, Leverett Jr. (California Inst. of Tech., Pasadena); Smith, E. J.; Coleman, P. J. Jr.; Sonett, C. P. pp 35-52 of The Solar Wind. Mackin, Robert J. Jr.; Neugebauer, Marcia (eds.). Pasadena, Calif., California Inst. of Tech., 1966.

The analysis of data for the interplanetary magnetic fields from the Mariner-2 magnetometer experiment is discussed. The preliminary results and the correction for spacecraft fields and zero effect are given. The corrected interplanetary magnetic field, solar-wind, and magnetic fluctuations are shown. (J.F.P.)

31884 RELATIONSHIP BETWEEN HIGH-ENERGY PARTICLES IN SPACE AND THE SOLAR PLASMA. Anderson, Hugh R. (California Inst. of Tech., Pasadena). pp 53-67 of The Solar Wind. Mackin, Robert J. Jr.; Neugebauer, Marcia (eds.). Pasadena, Calif., California Inst. of Tech., 1966.

The effect of the magnetic field on radiation measured by the Mariner instruments is discussed. This discussion includes the modulation of galactic cosmic radiation, which

it is supposed implies that the magnetic field allows greater or lesser quantities of the radiation to reach a given position in the solar system, and the determination by the field of the propagation and storage of charged particles injected into the interplanetary medium by the sun. (J.F.P.)

31885 SATELLITE OBSERVATIONS OF Mev PHENOMENA RELATED TO THE SOLAR WIND. [PART I]. EXPLORER-12 OBSERVATIONS. Bryant, D. A.; Cline, T. L.; Desai, U. D.; McDonald, F. B. (Goddard Space Flight Center, Greenbelt, Md.). pp 69-73 of The Solar Wind. Mackin, Robert J. Jr.; Neugebauer, Marcia (eds.). Pasadena, Calif., California Inst. of Tech., 1966.

Periodic solar-proton fluctuations observed by Explorer 12 are discussed. The solar-proton event of September 10, 1961, is discussed. The 27-day variation in the intensity of very low-energy protons is also considered, and data from some observed solar-proton events are illustrated. (J.F.P.)

31886 SATELLITE OBSERVATIONS OF Mev PHENOMENA RELATED TO THE SOLAR WIND. [PART II]. IMP OBSERVATIONS OF PRIMARY 3-Mev ELECTRONS. Cline, T. L.; Ludwig, G. H.; McDonald, F. B. (Goddard Space Flight Center, Greenbelt, Md.). pp 73-81 of The Solar Wind. Mackin, Robert J. Jr.; Neugebauer, Marcia (eds.). Pasadena, Calif., California Inst. of Tech., 1966.

Evidence is presented for the detection of extraterrestrial electrons in interplanetary space by the IMP satellite. These electrons have energies of about 3 Mev. Electron energy distributions and count rates during geomagnetic disturbances are shown. (J.F.P.)

31887 INTERPLANETARY MAGNETIC-FIELD MEASUREMENTS BY THE IMP-1 SATELLITE. Ness, N. F. (Goddard Space Flight Center, Greenbelt, Md.). pp 83-107 of The Solar Wind. Mackin, Robert J. Jr.; Neugebauer, Marcia (eds.). Pasadena, Calif., California Inst. of Tech., 1966.

The discussion of the results of the interplanetary magnetic-field measurements taken by the IMP satellite includes a discussion of the IMP-1 satellite itself, the magnetic field experiment, the IMP-1 orbit, features of the interplanetary magnetic field, and magnetic disturbances. (J.F.P.)

31888 RADIO ASTRONOMY OBSERVATIONS IN RELATION TO THE SOLAR-WIND PROBLEM. Wyndham, J. D. (California Inst. of Tech., Pasadena). pp 109-22 of The Solar Wind. Mackin, Robert J. Jr.; Neugebauer, Marcia (eds.). Pasadena, Calif., California Inst. of Tech., 1966.

The application of the techniques of radio astronomy to the study of the interplanetary medium is considered. The observational procedure, radial variation of scattering, magnetic fields, latitude effects, solar cycle effects, an upper limit to the scale of the irregularities, and a model of the solar corona are discussed. (J.F.P.)

31889 WHAT WE KNOW AND WHAT WE DO NOT KNOW ABOUT THE SOLAR WIND. Bridge, H. S. (Massachusetts Inst. of Tech., Cambridge). pp 123-43 of The Solar Wind. Mackin, Robert J. Jr.; Neugebauer, Marcia (eds.). Pasadena, Calif., California Inst. of Tech., 1966.

The experimental results and theory of solar wind are considered in the framework of Parker's theory. Parker's theory is briefly described, and the various solar wind properties to be investigated are noted. Early experiments, the IMP satellite results, and energetic particle experiments are discussed. It is concluded that there is a continuous gradation in the phenomena which includes everything from a plasma containing trapped protons to essentially free particles. (J.F.P.)

31890 MODELS OF THE INTERPLANETARY FIELDS AND PLASMA FLOW. Davis, Leverett Jr. (California Inst. of Tech., Pasadena). pp 147-64 of The Solar Wind. Mackin, Robert J. Jr.; Neugebauer, Marcia (eds.). Pasadena, Calif., California Inst. of Tech., 1966.

Various models are discussed which are based on experimental data, and some of the important considerations necessary for the construction of a satisfactory model are indicated. The discussion includes the long-lived jets of high-velocity gas ejected from the sun and the interplanetary magnetic-field component perpendicular to the ecliptic which is predominantly directed toward the south. (J.F.P.)

31891 EVIDENCE FOR A COLLISION-FREE HYDROMAGNETIC SHOCK IN INTERPLANETARY SPACE. Sonett, C. P.; Colburn, D. S.; Briggs, B. R. (Ames Research Center, Moffett Field, Calif.). pp 165-75 of The Solar Wind. Mackin, Robert J. Jr.; Neugebauer, Marcia (eds.). Pasadena, Calif., California Inst. of Tech., 1966.

The observations and implications of the collision-free hydromagnetic shock in interplanetary space are considered. The observations of the shock by Mariner-2, properties of the shock, and the problem of temperature are discussed. (J.F.P.)

31892 MAGNETIC FIELDS IN THE SOLAR PHOTOSPHERE. Leighton, R. B. (California Inst. of Tech., Pasadena). pp 177-84 of The Solar Wind. Mackin, Robert J. Jr.; Neugebauer, Marcia (eds.). Pasadena, Calif., California Inst. of Tech., 1966.

The structure of magnetic lines of force in the solar photosphere is discussed. Spectroheliograms and magnetograms are shown and described. It is concluded that the lines of force might be concentrated into narrow channels but with the same polarity over fairly large regions, and at other locations on the sun similar concentrations of the lines of force but oppositely directed would exist. Presumably small loops connecting the parts of a bipolar region could be drawn, but some of the lines might extend outward for a very large distance before they reconnect. However, every time a line of force goes off into space another comes back to a similar kind of region. (J.F.P.)

31893 ORIGIN OF THE SOLAR WIND. Scarf, F. L. (TRW-Space Tech. Labs., Redondo Beach, Calif.). pp 199-214 of The Solar Wind. Mackin, Robert J. Jr.; Neugebauer, Marcia (eds.). Pasadena, Calif., California Inst. of Tech., 1966.

The discussion of the origin of solar wind includes coronal models, coronal heating, effects of viscosity, the region beyond 15 R_S, velocity distributions, field effects, the termination of the solar wind, dynamic pressure balance, and the flow stability. (J.F.P.)

31894 EFFECTS OF DIFFUSION ON THE COMPOSITION OF THE SOLAR CORONA AND THE SOLAR WIND. Jokipii, J. R. (California Inst. of Tech., Pasadena). pp 215-19 of The Solar Wind. Mackin, Robert J. Jr.; Neugebauer, Marcia (eds.). Pasadena, Calif., California Inst. of Tech., 1966.

An investigation of the effects of radial diffusion in the solar corona and the solar wind is summarized. The existence of a solar wind with a flux of 3 $(10)^8$ proton/cm^2 sec at 1 AU was assumed, and a kinematic description of the effects of diffusion is obtained. (J.F.P.)

31895 RECONNECTION AND ANNIHILATION OF MAGNETIC FIELDS. Petschek, H. E. (Avco-Everett Research Lab., Everett, Mass.). pp 221-8 of The Solar Wind. Mackin, Robert J. Jr.; Neugebauer, Marcia (eds.). Pasadena, Calif., California Inst. of Tech., 1966.

An idealized plasma configuration in which two adjacent magnetic-field regions have oppositely directed field lines is discussed. The problem of determining the velocity at which these field lines approach each other and become reconnected is considered. The analysis indicates that the velocity for approaching field lines is roughly equal to the Alfvén speed divided by the logarithm of the magnetic Reynolds number; this velocity is thus about $\frac{1}{10}$ the Alfvén speed. It is proposed that the process for bringing the field lines together is much more rapid, and that the approach velocities are not too different from the expected fluid-flow velocities involved. (J.F.P.)

31896 INTERACTION OF THE SOLAR WIND WITH COMETS (NATURAL AND ARTIFICIAL). Biermann,

Ludwig; Luest, Reimar (Max-Planck-Institut fuer Physik und Astrophysik, Munich). pp 355-63 of The Solar Wind. Mackin, Robert J. Jr.; Neugebauer, Marcia (eds.). Pasadena, Calif., California Inst. of Tech., 1966.

The evidence for solar-wind interaction with comets, the different types of interaction that may occur between the solar wind and comets, theoretical aspects, and some preliminary ion-cloud experiments for the purpose of understanding the physics of comets and their interaction with solar wind are considered. The topics covered include properties of comets, acceleration in ionized comet tails, correlation between geomagnetic and cometary disturbances, the aberration angle, types of interactions, and comets as probes of solar wind. (J.F.P.)

31897 MAGNETOHYDRODYNAMIC ASPECTS OF THE INTERACTION OF THE SOLAR WIND WITH COMETS. Biermann, Ludwig (Max-Planck-Institut fuer Physik und Astrophysik, Munich). pp 365-71 of The Solar Wind. Mackin, Robert J. Jr.; Neugebauer, Marcia (eds.). Pasadena, Calif., California Inst. of Tech., 1966.

Equations of magnetofluiddynamics are used to study some details of the comet-solar wind interaction. From the results it is expected that some analog of the earth's magnetopause and a shock front in the direction of the sun would be found around a comet. Also the mass velocity around a comet is expected to have some observable gradient. (J.F.P.)

31898 THEORY OF TYPE-I COMET TAILS. Beard, David B. (Univ. of California, Davis). pp 373-80 of The Solar Wind. Mackin, Robert J. Jr.; Neugebauer, Marcia (eds.). Pasadena, Calif., California Inst. of Tech., 1966.

Solar wind effects are considered in the theory for type-I comet tails. It is noted that tail rays are formed by energetic electrons in the transition layer that is located on the outer surface of the slowed interplanetary magnetic field lines, and that the acceleration of each unit length of tail ray varies inversely with its mass and directly with the pressure of the solar wind. (J.F.P.)

31899 MAGNETOSPHERE OF THE MOON. Gold, T. (Cornell Univ., Ithaca, N. Y.). pp 381-91 of The Solar Wind. Mackin, Robert J. Jr.; Neugebauer, Marcia (eds.). Pasadena, Calif., California Inst. of Tech., 1966.

Analysis of the solar wind interaction with the moon is presented. Topics considered are the field around a stationary moon, the effect of rotation, an experiment to determine the time history of the sense of the magnetic field component normal to the ecliptic and the time history of the solar wind stagnation pressure, and shock waves, electrons and x rays on the moon. (J.F.P.)

31900 PROBABLE OBSERVATION OF THE WAKE OF THE MOON. Ness, N. F. (Goddard Space Flight Center, Greenbelt, Md.). pp 393-400 of The Solar Wind. Mackin, Robert J. Jr.; Neugebauer, Marcia (eds.). Pasadena, Calif., California Inst. of Tech., 1966.

The discussion of the observation of the wake of the moon includes mainly the relative positions of the moon, the satellite, and the earth. The satellite and lunar positions for detection of the wake, the January and February interceptions, and flow pattern considerations are discussed. (J.F.P.)

Atomic Physics

Refer also to abstract 32525.

31901 (N-65-34224) ELECTRON CAPTURE BY PROTONS IN HYDROGEN IN AN ELECTRIC FIELD. Omidvar, Kazem (National Aeronautics and Space Administration, Greenbelt, Md. Goddard Space Flight Center). July 1965. 28p. (NASA-TM-X-55289; X-641-65-306). CFSTI $2.00 cy, $0.50 mn.

A simple closed formula for the electron capture cross section in parabolic coordinates, appropriate to the charge transfer in an electric field, is derived with the electron initially and finally in two arbitrary sublevels of the atom. It is shown that the cross section, apart from a weighting factor, is independent of the particular sublevel and depends only on the principal quantum numbers involved. In this way the charge transfer cross section in an electric field is obtained. In addition, the solution of the problem in parabolic coordinates leads, through a transformation, to the determination in closed form of the cross section in spherical coordinates. It is found that the momentum distribution of electrons in the Stark levels of the hydrogen has extremely simple form in contrast to the momentum distribution in the optical levels. The averaged momentum distribution over the sublevels of a principal quantum number gives results identical to the results originally obtained. The classical momentum distribution of a bound particle in a Coulomb field is shown to be the same in form as the quantum mechanical distribution. The use of this distribution function in classical calculation of scattering will make the classical and the quantum mechanical calculations more consistent. (STAR)

31902 (N-66-16249) ELECTRONIC CHARGE DENSITY IN HELIUM IN THE FIRST-ORDER SHIELDING APPROXIMATION. Epstein, Jean H.; Epstein, Saul T. (Wisconsin Univ., Madison. Theoretical Chemistry Inst.). Jan. 4, 1966. 15p. (NASA-CR-69849; WIS-TCI-145). CFSTI $1.00 cy, $0.50 mn.

An attempt was made to calculate electronic charge density, $\rho(r)$, as a function of nuclear charge, Z, $\rho(r) = (Z^3/\pi) \exp[-2Zr]$, taking into account the difference between the actual nuclear charge, Z, and an assumed nuclear charge, ξ. The result in terms of singularity, and agreement with exact values, was disappointing. (STAR)

31903 (N-66-16702) WAVELENGTHS OF ELECTRONIC TRANSITIONS IN FOIL-EXCITED BEAMS OF LIGHT ELEMENTS. Fink, David (Arizona Univ., Tucson). [1966]. 68p. (NASA-CR-70036). CFSTI $3.00 cy, $0.75 mn.

Thesis.

Resolved spectral lines from deuterium, carbon, nitrogen, and oxygen were recorded on photographic plates. In each case, the source of the light was a beam of particles which, following acceleration in a Van de Graaff generator, passed through a thin carbon foil. Comparison spectra, from a standard iron-neon lamp, were also recorded on each plate. The plates were used to measure the wavelengths of the spectral lines characteristic of the radiating beams, and to identify the transitions responsible for those lines. The wavelengths of 109 spectral lines were measured, the transitions responsible for 26 spectral lines were identified, and possible transitions for 54 others were specified. (STAR)

31904 (UCRL-16581) HYPERFINE STRUCTURES IN THE ATOMIC 2p SHELL. Judd, B. R. (Lawrence Radiation Lab., Univ. of California, Berkeley). Jan. 1966. Contract W-7405-eng-48. 18p. Dep. mn. CFSTI $1.00 cy, $0.50 mn.

An examination is made of the hyperfine structures of those levels comprising the ground configuration $1s^2 2s^2 2p^N$ of the neutral atoms B, C, N, O, and F. Perturbation theory is used to study the effects of configuration interaction, thereby exhibiting the dependence of these effects on the quantum numbers defining the levels. Relativistic effects are considered. The importance of including the $s \rightarrow d$ excitations as well as those of the type $p \rightarrow p'$ is stressed. (auth)

31905 MASS SPECTROMETRIC STUDIES OF THE SPECIES OF PARTICLES LEAVING A MONOCRYSTALLINE TARGET IN A CHARGED OR UNCHARGED STATE UNDER HIGH-ENERGY ION BOMBARDMENT. Kaminsky, Manfred (Argonne National Lab., Ill.). Advance. Mass Spectrometry, 3: Proc. Conf. Paris, 1964, 69-90 (1966).

A portable mass spectrometer was used in conjunction with a 4.5-Mev Van de Graaff accelerator and a Cockcroft-

Walton generator to determine the species of particles leaving the (110) and (100) planes of monocrystals of copper and silver under the impact of protons, deuterons, and He^+ ions in the energy range from 0.1 to 0.25 Mev and from 0.50 to 4.0 Mev. In these energy regions the collisions between the incident ion and the lattice atom can be treated in terms of the Coulomb repulsion between the nuclei (Rutherford collisions). A typical example of the experimental results in the case of deuterons bombarding a Cu (100) plane; such neutral particles as Cu, Cu_2, and CuO were observed. The intensity of the species was measured relative to the atomic species. In addition, singly and doubly charged Cu ions were observed but no more highly charged ions could be detected. It is observed that incident particles form gas bubbles in the target, and these bubbles in turn explode and re-emit these particles in bursts. Measurements at various incident-ion energies E indicate that the sputtering rates S_0 and S_i for neutral atoms and for singly charged ions, respectively, decrease as E increases. For example, for D^+ normally incident on a Cu (100) plane, the yield varied from $S_0 = 3.1 \times 10^{-3}$ atoms per incident ion at 100 kev to $S_0 = 0.5 \times 10^{-3}$ atoms per incident ion at 1 Mev. The results are compared with theoretical predictions. Preliminary results for the ratio of the number of particles sputtered as positive ions to the number as neutrals are given. A model of charge-changing collisions between energetic recoil atoms and the quasi-stationary lattice atoms is discussed to interpret the results. (auth)

31906 IONIZATION CROSS-SECTION MEASUREMENTS FOR 0.6-TO 20-kev ELECTRONS IN ATOMIC AND MOLECULAR GASES. Schram, B. L.; Boerboom, A. J. H.; van der Wiel, M. J.; de Heer, F. J.; Kistemaker, J. (FOM-Laboratorium voor Massacheiding, Amsterdam). Advance. Mass Spectrometry, 3: Proc. Conf. Paris, 1964, 273-86(1966).

Measurements were made of the absolute ionization cross sections of electrons with energy of 0.6–20 kev impinging on several gases. The gases that were studied include the noble gases, diatomic molecules, and the series of n-alkanes from methane to hexane. With a mass spectrometer an analysis was made of the abundance of singly, doubly, and triply charged ions in argon and krypton. In all cases the cross sections can be represented by $\sigma = (A/E_{el}) \ln BE_{el}$, in agreement with theoretical predictions. This energy dependence holds for the gross ionization cross section as well as for the total ionization cross sections for single, double, and triple ionization in argon and krypton. The values of A and B are given for all cases. A comparison of the magnitude of A with results obtained from photoionization cross-section measurements shows good agreement for helium, neon, and argon. (auth)

31907 STUDIES OF ATOMIC IMPACT PHENOMENA ON METAL SURFACES WITH A PULSED-MOLECULAR-BEAM MASS SPECTROMETER. Kaminsky, Manfred (Argonne National Lab., Ill.). Advance. Mass Spectrometry, 3: Proc. Conf. Paris, 1964, 295-318(1966).

A new technique of combining modulated molecular beams with phase-sensitive mass-spectrometric detection was used to study the kinetics of ion desorption from polycrystalline tungsten surfaces. The experimental arrangement allowed the direct determination of the mean residence time τ_i of an ion on both atomically clean and strongly gas-covered surfaces of polycrystalline tungsten. The dependence of τ_i on the surface temperature T is given by Frenkel's equation $\tau_i = \tau_i^0 \exp E_i/kT$, where E_i is the ion desorption energy. With alkali chloride sources, the values in the table were determined over ranges within the temperature region $900^\circ K < T < 1400^\circ K$. The sensitive mass spectrometric detection technique allowed measurements at very small incident-beam intensities (10^9–10^{12} particles cm^{-2} sec^{-1}) to avoid an influence of surface coverage by the beam material itself. In addition, it was possible to demonstrate more quantitatively that the atomic and molecular composition of the beam significantly affected τ_i. (auth)

31908 ZERO-POINT ENERGY AND THE LAMB SHIFT. Power, Edwin A. (London Univ. National Bureau of Standards, Boulder, Colo.). Amer. J. Phys., 34: 516-18 (June 1966).

A suggestion by Feynman that the Lamb-shift energy can be obtained from the changes in zero-point energy due to the presence of the atoms involved is worked through in detail for the Bethe nonrelativistic contribution to the energy shift. The self energy of a free electron is obtained in the same way and is equivalent to the state independent shift due to the $e^2A^2/2me^2$ term in the normal perturbation methods. (auth)

31909 STUDY OF THE IONIZATION OF SOME GASES BY ACCELERATED H^+ AND H_2^+ IONS. Desesquelles, Jean; Cao, Guy Do; Dufay, Maurice (Faculte des Sciences, Lyon). Compt. Rend., Ser. B, 262: 1329-32(May 16, 1966). (In French).

The total effective cross section for ionization and for charge exchange of H, He, Ne, N_2, O_2, CO, CO_2, CH_4, C_2H_6, C_2H_4, and C_2H_2 for H^+ and H_2^+ ions at 20 to 120 kev were measured. (tr-auth)

31910 UNCERTAINTY PRINCIPLE AND SHORT-LIVED ATOMIC AND SUBATOMIC STATES. Massey, Harrie (Univ. Coll., London). Endeavour, 25: 59-64 (May 1966).

One of the practical results of Heisenberg's uncertainty principle is that the lines of absorption and emission spectra must have a finite width. The application of the principle to optical and impact spectra of atoms, ions, and nuclear particles is described, and it is shown how it can be used to detect and measure the lifetimes of "resonance particles" that exist for only 10^{-23} sec. (auth)

31911 RESONANCE (HERTZ COHERENCE) IN HYPERFINE ATOMIC STRUCTURE. Badan, P.; Geneux, E. (Institut de Physique Experimentale, Geneva). Helv. Phys. Acta, 39: 174-6(1966). (In French).

Dipolar magnetic transitions were induced by alternating magnetic fields between hyperfine levels of the excited $6^2P_{\frac{1}{2}}$ state of rubidium-85. They were detected in the form of coherent resonances. A characteristic of these resonances is a width at constant mid-height independent of the field inducing the transition. This width is determined uniquely by the duration of the life of the atomic state studied. The variation of the square of the width at mid-height as a function of the square of the amplitude of the field is shown for the transition F = 2 to F = 1 of the state $6^2P_{\frac{1}{2}}$ of rubidium-85. (J.F.P.)

31912 ENERGY DISTRIBUTION OF ELECTRONS EMITTED FROM FILMS OF ALKALI HALIDE COMPOUNDS SUBJECTED TO BOMBARDMENT BY He^+ AND Ar^+ IONS. Arifov, U. A.; Gaipov, S.; Ikramova, M.; Rakhimov, R. (Physics Technical Inst., Academy of Sciences, Uzbek SSR). Izv. Akad. Nauk Uz. SSR, Ser. Fiz.-Mat. Nauk, No. 1, 51-6(Jan.-Feb. 1966). (In Russian).

A study of the energy spectrum of emitted electrons is important in understanding the mechanism of ion-electron emission from film emitters. The energy distribution of electrons emitted from NaCl films to Mo during bombardment by He^+ and Ar^+ ions in the 40–2000 ev range is investigated. The experimental results presented show that the adsorption and condensation of molecules of alkali-halide salts on a metal surface leads to substantial variations in the spectrum of the energy of electrons emitted during ion bombardment. An increase in the coefficient of ion-electron emission from a thick film detected previously is determined by the increase in electron yield with the most probable energy. A decrease in the most probable energy, a simultaneous increase in the total yield with an increase in the thickness of the film, and an absence in the influence of the latter on the maximum energy of secondary electrons are all additional evidence in confirmation of the depth character of ion-electron emission in the region of low energies (potential emission) as well as in the region of relatively high energies (kinetic emission). It is extremely interesting that the energy spectrum of secondary electrons emitted from NaCl is very weakly dependent on the nature and the energy of the

bombarding ions. This fact, evidently, is due to the difference in the mechanism of the ion-electron emission from metals and alkali-haloid compound films. (ATD)

31913 COEFFICIENT OF SURFACE IONIZATION OF FAST SECONDARY PARTICLES. Arifov, U. A.; Khadzhimukhamedov, Kh. Kh.; Ayukhanov, A. Kh. (Physics Technical Inst., Academy of Sciences, Uzbek SSR). Izv. Akad. Nauk Uz. SSR, Ser. Fiz.-Mat. Nauk, No. 1, 57-61 (Jan.-Feb. 1966). (In Russian).

The charged state of fast particles emitted from a surface and the application of the law of surface ionization to these particles is discussed. It was shown earlier that there are slow (evaporated and diffused) as well as fast (scattered) ions in the secondary ion emission. Experimental work on the charge state of emitted fast particles was conducted without separating the secondary ions into the individual components. Therefore, the experimental study of the charge state of surface-emitted fast particles depending on the ionization energy and potential of bombarding ions is investigated. On the basis of the experimental data obtained in the present work and by other authors it is concluded that the scattering in the form of positive ions depends not on the charge state of the primary particle, but on the ionization potential of the bombarding particle. This process, however, only qualitatively agrees with the mechanisms of surface ionization. This should have been expected, since secondary scattered ions have an entire energy spectrum, from thermal to limiting, determined by single and multiple elastic collisions of the bombarding particle with the atoms of the metal. A better agreement of the results with the surface ionization mechanism may be obtained, apparently, only for the group of slow ions with energies below 10 ev. (ATD)

31914 SPUTTERING YIELDS OF SEVERAL SEMICONDUCTING COMPOUNDS UNDER ARGON ION BOMBARDMENT. Comas, James; Cooper, C. Burleigh (Univ. of Delaware, Newark). Contract DA-18-001-AMC-748X. J. Appl. Phys., 37: 2820-2(June 1966).

Sputtering yields of single crystals of SiC, InSb, GaAs, GaP, CdS, and PbTe under argon ion bombardment were measured. The energy of the argon ions, obtained from a magnetically confined argon arc, ranged from 75 to 600 ev. The sputtering yields were determined from target weight losses measured by an in situ quartz spring microbalance. Yields at 500-ev argon ion energy ranged from 0.40 for SiC to 1.30 for PbTe. (auth)

31915 TEMPERATURE DEPENDENCE OF SPUTTERING YIELDS OF Ge(100) AND (110) SURFACES. Anderson, G. S. (Litton Systems, Inc., Minneapolis). Contract AT(11-1)-722. J. Appl. Phys., 37: 2838-40(June 1966).

The temperature dependence of sputtering yields of Ge (100) and (110) under low-energy Ne^+ and Ar^+ ion bombardment was investigated. For target temperatures above the annealing temperature T_a where atom ejection patterns are observed, yield differences up to 50% are noted. For target temperatures below T_a the sputtering yield is independent of the crystallographic surface. Furthermore, this yield is less than the high-temperature yield for the (100) surface and higher than the high-temperature yield for the (110) surface. (auth)

31916 ATTENUATION LENGTH FOR SECONDARY ELECTRONS IN BULK-DENSITY KCl AND CsI. Edgecumbe, J.; Garwin, E. L. (Stanford Univ., Calif.). J. Appl. Phys., 37: 2916-17(June 1966). (SLAC-PUB-154).

An experiment was performed to remeasure the attenuation length for secondary electrons in bulk-density KCl and CsI, in order to resolve a contradiction in previously reported data and to aid in understanding the emission process in alkali halide transmission dynodes. The attenuation lengths determined from measured curves of the secondary emission coefficient as a function of film thickness were 325 ± 50 Å for KCl and 500 ± 50 Å for CsI. Sources of error in previous experiments are pointed out. (L.B.S.)

31917 CROSS SECTION FOR IONIZATION OF ALKALI ATOMS BY COLLISION WITH EXCITED NOBLE GAS ATOMS. Sheldon, John W. (Lewis Research Center, Cleveland). J. Appl. Phys., 37: 2928-9(June 1966).

Calculations based on the impact-parameter treatment and the quantum-defect theory of photo-ionization are described for velocity-dependent cross sections for ionization of alkali atoms by collisions with excited noble gas atoms. Ionization cross sections for He, Ne, Ar, Kr, and Xe collisions with Na, K, Rb, and Cs, referenced to a collision velocity of 10^5 cm/sec, are tabulated. (L.B.S.)

31918 SECONDARY ELECTRON PRODUCTION FROM APPROXIMATELY 1-Mev ALPHA PARTICLES EMERGING FROM GOLD. Yarger, L. L.; Anno, J. N. (Battelle Memorial Inst., Columbus, Ohio). J. Appl. Phys., 37: 2929-30(June 1966).

Measurements are reported of the secondary electron production due to relatively low-energy alpha particles emerging from a gold surface. The alpha particles were produced by the reaction of thermal neutrons with boron metal [$^{10}Be(n,\alpha)^7Li$] deposited as a substrate below a gold surface film. The secondary electron yield is compared with earlier measurements with 3.1-Mev alpha particles. (L.B.S.)

31919 SUBCONFIGURATION $f^6(^7F)sp$ IN Sm I. Racah, G. (Hebrew Univ., Jerusalem); Ganiel, U. J. Opt. Soc. Amer., 56: 893-5(July 1966).

A theoretical interpretation for all 70 observed energy levels belonging to the subconfiguration $4f^6(^7F)4s4p$ of Sm I is given. Energy matrices of both electrostatic and spin-orbit interactions were included in the calculation. The interaction parameters were adjusted by least squares to give an average agreement within 1% between the predicted and observed levels. (auth)

31920 SIMPLE NONBINARY SCATTERING MODEL APPLICABLE TO ATOMIC COLLISIONS IN CRYSTALS AT LOW ENERGIES. Andersen, Hans Henrik; Sigmund, Peter. Kongel. Dan. Vidensk. Selsk., Mat.-Fys. Medd., 34: No. 15, 1-50(1966).

The solution of a special scattering problem is presented which may be important in the theory of slowing-down of atomic particles in crystals. A projectile moves along the center axis of a regular ring of n equal atoms which are free and do not interact with each other. The interaction between the projectile and each ring atom is described by a Born-Mayer potential, and the scattering is assumed to be elastic and governed by the classical equations of motion. Because of symmetry, the problem can be reduced to plane motion of a particle in a potential of elliptic symmetry. The elliptic force field is approximated by a spherical one, which is dependent on the initial conditions of the individual scattering problem. For the spherical symmetrical potential, scattering angles and related quantities have been tabulated, but simple analytical approximations can be used too. As a result, one obtains the asymptotic velocities of the ring atoms as well as the energy loss of the projectile. Furthermore, it can be decided whether the projectile is reflected by the ring. Both the feasibility of assumptions specifying the problem and the validity of different approximations made in the transformation from the elliptic to the spherical potential are investigated. Special attention is paid to proper definitions of collision time and collision length which are important in collisions in crystals. Limitations to classical scattering arising from the uncertainty principle prove to be more serious than assumed previously. Inelastic contributions to the energy loss can easily be included. The oscillator forces binding lattice atoms turn out to influence the scattering process only at very small energies. The validity of the so-called momentum approximation and a related perturbation method are also investigated. (auth)

31921 EMISSION SPECTRA OF RAREFIED MOLECULAR GASES EXCITED BY FAST ELECTRONS. Koval', A. G.; Koppe, V. T.; Fogel', Ya. M. Kosm. Issled., 4: 74-88(Jan.-Feb. 1966). (In Russian).

An investigation is made of the emission spectra of nitrogen excited by an electron beam of an energy of 0.1 to 20 kev, and of oxygen and air bombarded by 13-kev electrons. Estimates are obtained of the relative intensities of the various emissions in each spectrum, in the visual range. The relative intensity of the various nitrogen emissions is studied as a function of electron energy in the range between 0.1 and 20 kev. The N_2, O_2, and air spectra excited by electrons are compared with their spectra excited by 37-kev protons and with the spectra of polar auroras. (Int. Aerospace Abstr.)

31922 DYNAMICAL GROUPS OF SIMPLE NON-RELATIVISTIC MODELS. Boehm, A. (International Atomic Energy Agency, Trieste). Nuovo Cimento (10), 43A: 665-83(June 1, 1966).

The construction of the generators of the dynamical group of the nonrelativistic rotator and the hydrogen atom is discussed. (auth)

31923 RELATIVISTIC VERSUS NONRELATIVISTIC SCATTERING OF SLOW ELECTRONS. Spruch, Larry (New York Univ., New York). Phys. Rev. Lett., 16: 1137-9(June 20, 1966).

The calculation for slow electron scattering at 2 to 200 ev by neutral heavy atoms by Browne and Bauer (Phys. Rev. Letters, 16: 495(1966)) is considered. It is argued that relativistic effects are probably not very important. The approach used is more general than a numerical calculation and provides more insight but no explicit estimate of relativistic effects. (J.F.P.)

31924 IMPORTANCE OF CORRELATION EFFECTS IN THE IONIZATION OF HELIUM BY ELECTRON IMPACT. Byron, F. W. Jr.; Joachain, C. J. (Univ. of California, Berkeley). Phys. Rev. Lett., 16: 1139-42 (June 20, 1966).

The double ionization process is considered to proceed via final- (initial-) state interactions between the atomic electrons, following (preceding) a single interaction with the projectile electron. If exact initial- and final-state helium wave functions are used in the Born approximation to first order in the interaction between the projectile and the atom, then the initial- and final-state interactions between the two atomic electrons are included to all orders. The case is considered where the incoming electron, although nonrelativistic, has sufficiently high energy that exchange between the incident and bound electrons may be neglected. (J.F.P.)

31925 REMEASUREMENT OF THE LAMB SHIFT IN H, n = 2. Robiscoe, R. T.; Cosens, B. L. (Yale Univ., New Haven). Phys. Rev. Lett., 17: 69-72(July 11, 1966).

The results are reported of an independent experiment confirming a previous measurement of the Lamb shift δ in the first excited state of atomic hydrogen, based on the level-crossing technique. A consistent systematic difference of 0.28 ± .14 MHz in δ is established between the results of present experiment and those of the Lamb experiments. (L.B.S.)

31926 AMPLIFICATION FACTORS OF A PARTICLE MULTIPLIER FOR MULTIPLY CHARGED NOBLE GAS IONS. Schram, B. L.; Boerboom, A. J. H.; Kleine, W.; Kistemaker, J. (FOM-Laboratorium voor Massacheiding, Amsterdam). Physica, 32: 749-61(Apr. 1966).

Multiplier efficiencies were determined for multiple charged noble gas ions, by a direct comparison of the signals of a particle multiplier and a Faraday cage at the detector side of a mass spectrometer. The energy of the ions was varied between 3 and 90 kev. The ions involved were He^+ and He^{2+}, Ne^+ up to Ne^{3+}, Ar^+ up to Ar^{5+}, Kr^+ up to Kr^{7+} and Xe^+ up to Xe^{9+}. For neon the isotope effect was examined. The secondary emission factors show an almost exact linear dependence on the velocity of the ions, independent of their charges. The extrapolated straight lines all cut the velocity axis at 5.5×10^6 cm/s. The slopes of the lines are proportional to the square roots of the ion masses. (auth)

31927 CORRELATION IN THE ELASTIC AND INELASTIC S-WAVE SCATTERING OF ELECTRONS BY H AND He^+. Burke, P. G.; Taylor, A. Joanna (Atomic Energy Research Establishment, Harwell, Eng.). Proc. Phys. Soc. (London), 88: 549-62(July 1966).

Equations are derived describing the scattering of electrons by hydrogen-like ions when electron–electron correlation terms are added to the close-coupling expansion of the total wave function. The 1s, 2s, and 2p terms are retained in the latter expansion, while up to sixteen correlation terms are retained in the former expansion. Provided the incident electron energy is insufficient to excite the third quantum level of the target the resultant solution satisfies a minimum principle. The numerical solution of the equations is discussed and results are presented for elastic and inelastic S-wave transitions in e^--H and e^--He^+. Above the energy where the minimum principle applies it is possible to obtain physically significant results by varying a nonlinear parameter in the wave function in order to avoid singularities in the solution. (auth)

31928 IONIZATION OF HYDROGEN AND OF HYDROGENIC POSITIVE IONS BY ELECTRON IMPACT. Rudge, M. R. H. (High Altitude Observatory, Boulder, Colo.); Schwartz, S. B. Proc. Phys. Soc. (London), 88: 563-78 (July 1966).

Calculations of the ionization cross section of hydrogen and of hydrogenic positive ions are described in which the initial state is either the ground or the excited 2s state. The first procedures used are the Born and Born-exchange approximations. These results are compared with other theoretical calculations and with experimental data. It is seen that, for the case of ionization of hydrogen from its ground state, none of the theoretical results is in good agreement with the experimental data. A certain defect of the theory is then corrected by adopting a third procedure for this case in which an angle-dependent Coulomb potential is used in the description of the final state for the process. It is then found that, despite the sounder theoretical footing of this latter calculation, no improved agreement with experimental data is obtained. In the near threshold region, however, the third procedure yields a linear behavior, whereas the first two approximations do not. This is in accord with theoretical predictions though there exists some uncertainty in the experimental situation. Convenient formulas are presented which represent the best data for the ionization cross sections, and the associated reaction rates for the case of an initial Maxwellian distribution of velocities. (auth)

31929 EXCITATION OF LITHIUM-LIKE IONS BY ELECTRON IMPACTS. Bely, O. (Joint Inst. for Lab. Astrophysics, Boulder, Colo.). Proc. Phys. Soc. (London), 88: 587-95(July 1966).

The cross sections corresponding to the transitions $Q(2s \rightarrow np)$ and for $2 \leq n \leq 7$ were computed for Be(II), N(V), and Ne(VIII), using the Coulomb-Born approximation. The cross sections $Q(2s \rightarrow 3p)$ and $Q(2s \rightarrow 7p)$ were also computed for a hydrogenic ion with an infinite nuclear charge. The results obtained are compared with the semiclassical and the $\bar{g}$ treatments. Simple analytic forms are fitted to the calculated cross sections. The corresponding parameters are then extrapolated along the quantum number n and the charge Z. Tables and graphs are given which enable one to rapidly obtain any cross sections of the type $Q(2s \rightarrow np)$ in any ion of the lithium isoelectronic series. (auth)

31930 HIGH-ENERGY CROSS SECTIONS FOR ELECTRON EXCITATIONS OF EXCITED HYDROGEN ATOMS IN WHICH THE PRINCIPAL QUANTUM NUMBER IS CHANGED BY 2. Kingston, A. E. (Queen's Univ., Belfast); Lauer, J. E. Proc. Phys. Soc. (London), 88: 597-603(July 1966).

At large energies E the cross section Q for the electron excitation from the n, l state of hydrogen to the n′, l′ state may be written in the form $QE = A \log E + B$. The first Born approximation is used to calculate these A's and B's for all transitions with n = 1, 2, 3, 4, 5, and 6 and n′ = n +

2. The A's and B's associated with the main optically allowed transitions (i.e., $l' = l + 1$) are largest. In calculating the A's for the average cross section from one level to another it is found that only the main optically allowed transitions must be considered, but in calculating B's for the average cross sections the other transitions, besides the main optically allowed transitions, could not be ignored since the sum total effect of these minor transitions is almost as large as that of the main optically allowed transitions. These minor transitions increased the B's for the average cross sections of most of the transitions considered by more than 50%. (auth)

31931 DISSOCIATION OF HYDROGEN MOLECULES BY ELECTRON IMPACT. Khare, S. P.; Moiseiwitsch, B. L. (Queen's Univ., Belfast). Proc. Phys. Soc. (London), 88: 605-10(July 1966).

The first-order exchange approximation, together with a separated-atoms approximation, is used to calculate the cross section for the dissociation of hydrogen molecules by electron impact assuming that the main process causing dissociation is the excitation of the repulsive $1\,^3\Sigma_u$ state. It is found that the cross section obtained with the use of the first-order exchange approximation is considerably smaller than that calculated employing the Born-Oppenheimer approximation. Comparison is made between the experimental data on the efficiency of dissociation of hydrogen molecules by electrons and the theoretical efficiency derived from the first-order exchange approximation to the dissociation cross section. (auth)

31932 ROTATIONAL EXCITATION OF H_2 AND D_2 BY H IMPACT. Dalgarno, A. (Queen's Univ., Belfast); Henry, R. J. W.; Roberts, C. S. Proc. Phys. Soc. (London), 88: 611-15(July 1966).

A complete distorted wave calculation is carried out of the rotational excitation of molecular hydrogen and of molecular deuterium in thermal collisions with atomic hydrogen. Total cross sections, angular distributions, and rate coefficients are presented. (auth)

31933 EXCITATION OF H ATOMS BY FAST PROTONS. Cheshire, I. M.; Kyle, H. L. (Goddard Space Flight Center, Greenbelt, Md.). Proc. Phys. Soc. (London), 88: 785-6(July 1966).

A simple formula for the total Born cross section for the excitation of ground state H atoms to any excited state n is given and a table of cross sections is included for representative n and impact energies. (auth)

31934 AN EXPANSION METHOD FOR CALCULATING ATOMIC PROPERTIES. VI. THE EXTENDED HARTREE–FOCK APPROXIMATION. Cohen, M. (Hebrew Univ., Jerusalem); Parkinson, E. M. Proc. Roy. Soc. (London), Ser. A, 292: 193-202(May 17, 1966).

An expansion method is used to calculate the expectation values of various operators for all states $1s^2 2s^a 2p^b$ SL of all members of the isoelectronic sequences from beryllium to neon. Explicit account is taken of the interaction between the configurations $1s^2 2s^a 2p^b$ SL and $1s^2 2p^{b+2}$ SL and is found to be entirely negligible for these systems. (auth)

31935 AN EXPANSION METHOD FOR CALCULATING ATOMIC PROPERTIES. VII. THE CORRELATION ENERGIES OF THE LITHIUM SEQUENCE. Chisholm, C. D. H.; Dalgarno, A. (Queen's Univ., Belfast). Proc. Roy. Soc. (London), Ser. A, 292: 264-71(May 17, 1966).

If the energy of an atomic system is expanded in inverse powers of the nuclear charge Z, the leading term of the correlation energy after degeneracies have been removed is a constant which can be expressed as a weighted sum of electron pair energies and certain nonadditive terms. The pair energies may be obtained from direct two-electron variational calculations and the nonadditive terms may be evaluated exactly. Calculations are carried out for the lithium ^2S sequence with the result that the nonrelativistic eigenvalues are given by $E(Z) = -1.125Z^2 + 1.02280521Z - 0.40814899 + O(Z^{-1})$. (auth)

31936 ATOMIC FLUORESCENCE YIELDS. Fink, R. W. (Georgia Inst. of Tech., Atlanta); Jopson, R. C.; Mark, Hans; Swift, C. D. Rev. Mod. Phys., 38: 513-40 (July 1966). (UCRL-14327).

The mechanisms of the reorganization of atoms with inner shell vacancies are reviewed. All available experimental values of K-, L-, and M-shell fluorescence yields, together with L-shell Coster-Kronig yields are summarized and compared with available theoretical calculations. Rather good agreement exists in general between theory and experiment for the K shell, but experimental values of the L_2 and L_3 subshell fluorescence yields disagree substantially with the semitheoretical results of Listengarten. Related phenomena in μ-mesic atoms are included. Experimental methods of measurement are summarized and discussed, together with suggestions for future studies with high resolution techniques. Results from the literature are included up to 10 May 1966. (auth)

31937 30-kev ION BOMBARDMENT APPARATUS FOR STUDY OF INTERACTION OF LIGHT IONS WITH SURFACES. McCracken, G. M.; Maple, J. H. C.; Watson, H. H. H. (United Kingdom Atomic Energy Authority, Culham, Abingdon, Eng.). Rev. Sci. Instrum., 37: 860-6 (July 1966).

An ultrahigh vacuum system is described which was designed to study particles emitted from surfaces under bombardment by hydrogen ions. Stress was placed on obtaining pressures $\sim 10^{-9}$ torr in the presence of the ion beam. The beam is mass analyzed and its energy is variable from 5 to 30 kev. A maximum current of 300 μ amp over 0.1 cm^2 is obtainable at the target, so that a beam/neutral gas bombardment ratio of better than 1000/1 can be achieved. A target mounting turntable is described which allows up to six targets to be bombarded in turn. A quadrupole mass filter is incorporated in the target chamber as a residual gas analyzer and as a means of identifying gas species resulting from the bombardment of surfaces. (auth)

31938 ANGULAR DEPENDENCE OF THE SECONDARY EMISSION COEFFICIENTS FOR A KBr SINGLE CRYSTAL BOMBARDED WITH POTASSIUM IONS. Abroyan, I. A.; Lavrov, V. P.; Fedorova, I. G. (Kalinin Polytechnic Inst., Leningrad). Soviet Phys.-Solid State (Engl. Transl.), 7: 2954-5(June 1966).

Translated from Fiz. Tverd. Tela, 7: 3660-2(Dec. 1965).

The angular dependence of the coefficients of ion-electron emission γ and ion-ion emission K for a dielectric single crystal of KBr bombarded with K ions is investigated. (B.G.D.)

31939 ENERGY DISTRIBUTION OF ELECTRONS EJECTED FROM MOLYBDENUM BY 2-, 5-, 10-, AND 15-kev He AND Ar IONS. Wehner, Guenter (Univ., Mainz). Z. Phys., 193: 439-42(1966). (In German).

The energy distribution of electrons ejected from Mo by He and Ar ions of 2, 5, 10, and 15 kev was measured by an electrostatic analyzer of the 127° cylindrical condenser type. The relative number of faster electrons grows with increasing primary energy, but the position of the maximum of the distribution curves (1.9 ev for He and 1.7 ev for Ar) is the same for ion energies of 5, 10, and 15 kev. Only for 2 kev the maximum is shifted slightly towards lower energies. (auth)

31940 LEVEL CROSSING EXPERIMENT IN THE $6^2P_{\frac{1}{2}}$ STATE OF Rb–I SPECTRUM. Bucka, H.; Grosswendt, B.; Schuessler, H. A. (Technische Univ., Berlin). Z. Phys., 194: 193-200(1966). (In German).

Level crossing obeying the selection rule $\Delta m = 2$ were detected in the $6^2P_{\frac{1}{2}}$-state of both ^{85}Rb and ^{87}Rb. Using the measured crossing points, the ratios of the hyperfine structure constants to the g_J-factor are determined from a calculation for intermediate magnetic fields. The ratios are $A_{85}/g_J = 6.119$ (3) Mc/s, $B_{85}/g_J = 6.14$ (2) Mc/s, $A_{87}/g_J = 20.70$ (3) Mc/s, $B_{87}/g_J = 2.93$ (5) Mc/s. From the zero field level crossing of ^{87}Rb the lifetime $\tau = 1.14\ (6) \cdot 10^{-7}$ sec of the $6^2P_{\frac{1}{2}}$-state is obtained. Level crossing signals were also observed in the presence of noble gas admixtures. (auth)

31941 INVERSION OF LEVELS DURING EXCITATION BY A MONOENERGETIC ELECTRON BEAM. Belousova,

I. M.; Znamenskii, V. B.; Mustafin, K. S.; Strieva, A. V. Zh. Prikl. Spektrosk., Acad. Nauk BSSR, 4: 240-4(Mar. 1966). (In Russian).

The energy distribution of electrons in a monoenergetic beam is studied at various gas pressures and the effect of electron gun design on this distribution is considered. The variation in energy homogeneity of the electron beam with gas pressure was evaluated from the change in the half-width of the electron energy distribution. Curves are given showing the current-voltage characteristics and distribution of electrons with respect to energies in neon and helium at various gas pressures. At a pressure of $5(10)^{-6}$ mm Hg, the half-width of the maximum in electron energy distribution is 0.5−0.6 ev and remains constant up to a pressure of $5(10)^{-1}$ mm Hg. This peak becomes shorter as the pressure is increased. This is due to a loss of electrons through inelastic collisions with gas atoms. It is shown that the design of the electron gun may be simplified by using a single control grid without destroying the energy homogeneity of the electron beam to any great extent. It is shown that the ratio of the populations in the $3s_2$ and $2p_4$ levels of neon for the case of excitation by a monoenergetic electron beam is approximately 3 times as high as in a shock tube. These experimental data agree satisfactorily with theoretical predictions of a greater selectivity for population of levels during excitation in an electron beam than in a gas discharge plasma. (ATD)

31942 ATOMIC TRANSITION PROBABILITIES. VOLUME I. HYDROGEN THROUGH NEON. A Critical Data Compilation. Wiese, W. L.; Smith, M. W.; Glennon, B. M. National Standard Reference Data Series, National Bureau of Standards 4. (Category 3: Atomic and Molecular Properties). Washington, D. C., National Bureau of Standards, 1966. 171p. $2.50 GPO.

Atomic transition probabilities for about 4,000 spectral lines of the first ten elements, based on all available literature sources, are compiled. The data are presented in separate tables for each element and stage of ionization. For each ion the transitions are arranged according to multiplets, supermultiplets, transition arrays, and increasing quantum numbers. Allowed and forbidden transitions are listed separately. For each line the transition probability for spontaneous emission, the absorption oscillator strength, and the line strength are given along with the spectroscopic designation, the wavelength, the statistical weights, and the energy levels of the upper and lower states. In addition, the estimated accuracy and the source are indicated. In short introductions, which precede the tables for each ion, the main justifications for the choice of the adopted data and for the accuracy rating are discussed. A general introduction contains a critical review of the major data sources. (auth)

31943 STUDY OF THE RENNER EFFECT IN THE LINEAR XY_2 MOLECULE. Carlone, Cosmo (Univ. of British Columbia, Vancouver). 58p. (CONF-650664–9). ORAU. Gmelin, AED-CONF-65-288-12.

From Canadian Association of Physicists Congress, Vancouver, B. C.

The variational principle is applied to the Schroedinger equation for the XY_2 linear molecule. Trial solutions are synthesized from the nuclear eigenstates, which are assumed to be simple harmonic oscillator eigenstates, and from the unperturbed electronic states, whose azimuthal dependence is known because of the cylindrical symmetry of the field of the nuclei. The secular equation is discussed, and an expression for the Renner splitting of the π state is obtained. (auth)

31944 PERTURBATION THEORY OF BRUECKNER AND GOLDSTONE APPLIED TO ATOMS. Kelly, Hugh P. (Univ. of Virginia, Charlottesville). 33p. (CONF-650834–2). ORAU. Gmelin, AED-CONF-65-230-3.

From Alberta Symposium on Quantum Chemistry, Edmonton, Ont.

The perturbation theory of Brueckner and Goldstone is reviewed and its application to atoms is discussed. The choice of potential for the single-particle states is considered and it is shown how the potential affects the convergence of the perturbation expansion. Numerical results are presented for correlation energies of beryllium and oxygen and for polarizabilities and shielding factors of beryllium. (auth)

31945 ANOMALOUS INTENSITY RATIOS IN MUONIC LEAD AND BISMUTH. Huefner, J. (Univ., Heidelberg). 9p. (CONF-660209–10). ORAU. Gmelin, AED-CONF-66-023-10.

From Conference on Intermediate Energy Physics, Williamsburg, Va.

The intensity ratio for muonic x rays from lead and bismuth is considered. A mechanism, which explains the experimental results is described, and the calculated results are given. (J.F.P.)

31946 SELF-CONSISTENT EQUATIONS INCLUDING EXCHANGE AND CORRELATION EFFECTS. Technical Report No. 31. Kohn, W.; Sham, L. J. (Univ. of California, La Jolla, San Diego). 21p. (CONF-650927–5). ORAU. Gmelin, AED-CONF-65-222-31.

From American Physical Society, Honolulu, Hawaii.

From a theory of Hohenberg and Kohn, approximation methods for treating an inhomogeneous system of interacting electrons are developed. These methods are exact for systems of slowly varying or high density. For the ground state, they lead to self-consistent equations analogous to the Hartree and Hartree-Fock equations, respectively. In these equations the exchange and correlation portions of the chemical potential of a uniform electron gas appear as additional effective potentials. (The exchange portion of our effective potential differs from that due to Slater by a factor of $\frac{2}{3}$.) Electronic systems at finite temperatures and in magnetic fields are also treated by similar methods. An appendix deals with a further correction for systems with short wavelength density oscillations. (auth)

31947 HORNBECK-MOLNAR CROSS-SECTIONS FOR THE n = 3 STATES OF HELIUM. Teter, M. P.; Niles, F. E.; Robertson, W. W. (Univ. of Texas, Austin). 18p. (CONF-651070-4). ORAU. Gmelin, AED-CONF-65-395-4.

From 18th Annual Gaseous Electronics Conference, Minneapolis.

Analysis of the atomic light originating from energy levels of principal quantum number n = 3 in the helium positive column shows that a pressure dependent loss process exists for states other than the S-states. The loss mechanism is identified as the Hornbeck-Molnar process $He^* + He \rightarrow He_2^+ + e^-$ by observing the effects of varying the atomic populations when the positive column is irradiated with intense atomic light. Comparison of the pressure dependent loss rate with the radiation loss rate from a particular state yields the Hornbeck-Molnar cross section. An independent measurement relating the molecular ion concentration to the 3^3D population yields a separate value for the 3^3D cross section which agrees quite well with that measured by the previous method. (auth)

31948 CESIUM ION SPUTTERING OF ALUMINUM, COPPER, AND TITANIUM. Daley, Howard L.; Perel, Julius (Electro-Optical Systems, Inc., Pasadena, Calif.). New York, American Inst. of Aeronautics and Astronautics, 1966, Preprint No. 66-203, 14p., $1.50. (CONF-660310–16). ORAU.

From AIAA 5th Electric Propulsion Conference, San Diego, Calif.

Sputtering measurements were made as part of a program to investigate the properties of selected materials for use as electrodes on cesium ion engines. The sputtering yields of polycrystalline aluminum, copper, and titanium were measured as a function of cesium ion energies ranging from 0.5 kev to 15 kev. The yield of powder metallurgy copper was also measured at cesium ion energies of 2, 5, and 7 kev. The polycrystalline and powder metallurgy copper results are compared with the single crystal copper data of Olson and Smith. The momentum transfer sputtering model of Rol, Fluit, and Kistemaker was ex-

amined and compared with the experimental results. The comparison suggests a relationship between the functional dependence of the ion mean free path in the target lattice and a factor related to the target atom density per unit area. Comparisons with experiment show that for a given lattice structure material, the factor $(\rho/M)^{\frac{1}{3}}$ effectively averages the lattice orientations and can be used to predict yield ratios. (auth)

31949 THE APPLICATION OF SPECTRAL DATA FROM ISOTOPICALLY SUBSTITUTED MOLECULES TO THE DETERMINATION OF ANHARMONIC POTENTIAL ENERGY CONSTANTS. **Hart, Robert R. (Illinois Inst. of Tech., Chicago. Bell Telephone Labs., Inc., Murray Hill, N. J.). 43p. (CONF-650634-5). ORAU. Gmelin, AED-CONF-65-155-12.**

From 16th Annual Mid-America Symposium on Spectroscopy, Chicago.

The feasibility of using data from several isotopically substituted molecules as a way of increasing the amount of data available for characterizing the anharmonicities of their common internuclear force field was studied. A systematic method is described and tested for partially characterizing a molecule's anharmonicities using insufficient data. The general approach of identifying the physically most important constants and using the limited data available to determine these yielded good results in that considerable information about the anharmonicities was obtained. The molecules H_2O, HDO, and D_2O were used to test the method. (A.G.W.)

Cosmic Radiation

See also Elementary Particles and Radiations
Nuclear Properties and Reactions

Refer also to abstract 31884.

31950 (CONF-650120) SEMINARIUM NA TEMAT WIELKICH PEKOW ATMOSFERYCZNYCH PROMIENIOWANIA KOSMICZNEGO, LODZ, 4–8 STYCZNIA 1965 R. (The Seminar on Cosmic-Ray Extensive Air Showers, Lodz, Poland, 4–8 January 1965). (Institute of Nuclear Research, Lodz (Poland)). 1965. 267p. Dep.

Text is in Russian.

A total of 15 papers were presented at a conference on cosmic ray showers (CRS) held at Lodz, Poland on Jan. 4th-8th, 1965, with participants from France, Poland and the USSR. The subjects included the energy spectrum and composition of primary cosmic radiation, a discussion on cosmic ray showers poor in muons, energy losses of relativistic muons due to electromagnetic interactions, factors determining the muon spectrum in ordinary showers, low-energy particles in cosmic ray showers, the variation in muon component with height, a study of high-energy muons, the special distribution of muons near the shower axis, the probable origin of showers poor in muons and a hodoscope made of neon lights. No record, unfortunately, was made of the questions and discussions which were lively. (TTT)

31951 COSMIC-RAY HEAVY NUCLEI AT GEOMAGNETIC LATITUDE 42 DEG NORTH. **Nelson, M. E. (Univ. of Puget Sound, Tacoma, Washington); Kerlee, D. D; Krienke, O. K. Jr. J. Geophys. Res., 71: 2389-94(May 1, 1966).**

The flux of primary cosmic-ray heavy nuclei was measured with a sandwich of C.2 and G.5 emulsions near the coast of Georgia, magnetic latitude 42°N. The emulsions were exposed at about 122,000 feet for 7.5 hours, and the calculated fluxes at the top of the atmosphere in particles/m^2-sec-ster were found to be; Li, Be, B (L nuclei), 1.14 ± 0.3; C, N, O, F (M nuclei), 4.05 ± 0.4 and Z ≥ 10 (H nuclei); 1.32 ± 0.3. This flight took place on May 25, 1960, near sun spot maximum. Evidence of solar modulation of the primary cosmic-ray flux is shown by comparison with neutron monitor data. (auth)

31952 RADIATION MEASUREMENTS IN COMMERCIAL AIRCRAFT USING A SINGLE COUNTER. **Hopper, V. D.; Rawlinson, W. R. (Univ. of Melbourne). Nature, 210: 473-5(Apr. 30, 1966).**

Cosmic radiation, the count rate due to cosmic rays with the unshielded Geiger tube; the cosmic ray count rate with the tube shielded by 2.12 g/cm^2 of lead; and measurements of radiation from transported radioactive sources were made on aircraft during flight. A single thick-walled halogen-quenched Geiger tube connected to a ratemeter unit giving a direct reading in counts per second was used. Results obtained on each section of the trip are plotted against GMT and the altitude record of each flight. The minimum count rate occurred at the geomagnetic equator with a slow increase to 10° and a steep increase between 25 and 40°. Between 40 and 50° there was a sudden drop in the slope of the curve, giving the knee. From 55° upwards the increase was very slow. The maximum radiation dosage observed was much less than the permissible dose. (H.G.D.)

31953 FLUX OF THE COSMIC-RAY HYDROGEN AND HELIUM NUCLEI AT KIRUNA, SWEDEN. **Courtier, G. M.; Linney, A. D. (Imperial Coll. of Science and Tech., London). Planet. Space Sci., 14: 503-18(June 1966).**

The results of measurements made at balloon altitudes at locations with nominal geomagnetic threshold rigidities of 0.5 and 2.5 GV are presented. Data are obtained on the differential energy spectra of primary hydrogen and helium nuclei in 1964 at a time close to solar minimum, using a combined scintillator and scintillator-Cherenkov technique. These data are compared with the results obtained with similar equipment which was flown at the same locations in 1961 and 1962, and also with those of other investigators. The solar modulation of the primary cosmic ray beam is examined as a function of particle velocity and rigidity and the implications of the measurements are briefly discussed in connection with the interaction of galactic cosmic radiation with the interplanetary environment. (auth)

31954 MODEL FOR THE ORIGIN AND PROPERTIES OF THE COSMIC-RAY RIGIDITY SPECTRUM. **Kaplon, M. F.; Skadron, G. (Univ. of Rochester, N. Y.). Rev. Geophys., 4: 177-221(May 1966). (NP-15930).**

A model is proposed to explain a number of features of the differential rigidity spectra of the nuclear component of the primary cosmic radiation. A supernova explosion is assumed to result in the acceleration of nuclei to a pure power law rigidity spectrum and a composition relatively rich in heavy and medium weight nuclei. The supernova remnant into which these particles are injected is characterized as a large-scale trapping region resulting from predominantly closed magnetic field lines that partially isolate the region from the surrounding galactic space. This feature of the supernova region is represented by a dipole-like field. It is assumed that, superimposed on this field, magnetic irregularities produce a certain amount of distortion of the field lines in the interior of the source, and that irregularities along the periphery of the source lead to local distortions of the field and, hence, a mixing of galactic and source field lines in the neighborhood of these irregularities. The observed large-scale regularity of the magnetic field in the Crab leads us to treat the particle motion within the source region in the guiding center approximation (except at very high rigidities), so that these particles are capable of guiding outward to the source boundary and returning inward to the interior along the source's predominantly closed magnetic lines of force. The well defined inward field gradient and field curvature, however, cause the particles to drift longitudinally as they spiral along the periphery of the source region, and accordingly they have a certain probability of drifting into a neighborhood of field mixing and onto a galactic field line which guides them out of the source region. During their confinement within the source region, the particles undergo nuclear interactions and ionization loss, and, therefore, the differential rigidity spectrum of particles escaping from the source boundary into the galaxy is jointly determined by their injection spectrum, their escape probability, and

the extent to which they suffer loss processes. A continuity equation combining these various processes is constructed and then averaged over the entirety of active sources in the galaxy. The solutions of the averaged continuity equation for each charge group then give us the differential rigidity spectra with which the cosmic radiation is injected into the galactic medium. The additional effects of intragalactic motion on the cosmic-ray spectrum are treated in the approximation that the particles escaping from source regions undergo magnetic diffusion in the galactic volume with a rigidity independent scattering mean free path. The differential rigidity spectra of the various charge groups incident on the solar system are thereby obtained. The effects of solar modulation on the galactic cosmic-ray spectrum are treated in accordance with the solar wind theory. The resulting differential rigidity spectra are derived and compared with data taken near solar minimum, and it is found that the calculated spectra, as well as the rigidity dependence of various abundance ratios, are in reasonable agreement with the available data. (auth)

31955 PENETRATION OF GALACTIC COSMIC RAYS INTO THE SOLAR SYSTEM. Parker, E. N. (Univ. of Chicago). pp 185-96 of The Solar Wind. Mackin, Robert J. Jr.; Neugebauer, Marcia (eds.). Pasadena, Calif., California Inst. of Tech., 1966.

The physics of the penetration of interstellar cosmic rays into the solar system is summarized. The discussion includes interplanetary magnetic fields, Forbush decreases, the 11-year, 27-day, and diurnal variations. Outstanding problems for the development of a more quantitative model are noted. (J.F.P.)

31956 DEPENDENCE OF THE π-MESON PRODUCTION SPECTRUM EXPONENT ON THE PRODUCTION LEVEL. Hofmokl, Helena (Univ., Lodz, Poland). Zesz. Nauk Uniw. Lodz., Ser. II, 19: 13-17(1965). (In Polish).

The relation of the meson (π) production spectrum exponent with the production level was computed in the momentum region 0.4 – 1 Bev/c. The approximation is used that the distance traveled by mesons (π) before decay is negligible and the meson (π) production spectrum of the form $N_\pi(p_\pi) = \text{const } p_\pi^{-\gamma_\pi}$ will give rise to a meson (μ) spectrum at sea level $N_\mu(p) = \text{const } P(p,t_0)\ (p + \Delta p_0)$. (auth)

31957 COSMIC BACKGROUND RADIATION AT 3.2 cm.—SUPPORT FOR COSMIC BLACKBODY RADIATION. Roll, P. G.; Wilkinson, David T. (Palmer Physical Lab., Princeton, N. J.). 9p. (CONF-660107-37). ORAU. Gmelin, AED-CONF-66-003-60.

From American Physical Society Meeting, New York.

The result of a measurement of the microwave background at a wavelength of 3.2 cm is reported. This measurement tends to provide a severe test of the cosmic blackbody radiation hypothesis. (B.G.D.)

31958 CERENKOV-SCINTILLATION COUNTER STUDIES OF THE PRIMARY COSMIC RADIATION AT BALLOON ALTITUDES. Jenkins, R. W. (Univ. of Alberta, Calgary). 12p. (CONF-650961-4). ORAU. Gmelin, AED-CONF-65-224-6.

From American Geophysical Union, 5th Western National Meeting, Dallas.

Some preliminary results of measurements of proton rigidity spectra that were performed in a series of balloon flights spanning the recent solar minimum are presented. (D.C.W.)

Direct Energy Conversion

Refer also to abstracts 31164, 31384, and 31614.

31959 (ANL-7175, pp 184-211) ENERGY CONVERSION. (Argonne National Lab., Ill.).

Research on regenerative galvanic systems for energy conversion is described. Results of laboratory and engineering investigations are included on physical-chemical aspects of regenerative emf cells. (J.R.D.)

31960 (N-66-16447) THE DEVELOPMENT OF A CESIUM-VAPOR-FILLED THERMIONIC ENERGY CONVERTER. Final Technical Report. Eastman, G. Y.; Ernst, D. M. (Radio Corp. of America, Lancaster, Pa. Electron Tube Div.). Dec. 1962. Contracts NAS7-100; JPL-950229. 182p. (NASA-CR-69861). CFSTI $4.00 cy, $1.25 mn.

For Jet Propulsion Lab., Calif. Inst. of Tech., Pasadena.

This report covers development, fabrication and test of cesium-vapor-filled thermionic energy converters. The units were designed for use in a solar-heated space application. The geometry was limited by stringent system parameters of size and temperature. The program was directed toward the generation of twenty-five watts of output power at an emitter temperature not exceeding 2000°K. Design objectives included a service life of one year at rated capacity at an efficiency of twenty percent. RCA has delivered five converters designed to these requirements at operating temperature of less than 2000°K. The objectives of life and efficiency have been approached by incorporating materials and fabrication techniques which will obtain the greatest reliability and performance. The report covers the specific techniques, procedures and geometry of the converters shipped under the contract. In addition, details of problems encountered and their solutions are explained. Test data on converters shipped is included. (STAR)

31961 (SC-DC-66-1115) THERMIONIC POWER GENERATION FROM REENTRY VEHICLES. Touryan, K. J.; Sluyter, M. M. (Sandia Corp., Albuquerque, N. Mex.). Jan. 3, 1966. Contract AT(29-1)-789. 53p. Dep. mn. CFSTI $3.00 cy, $0.50 mn.

Theoretical and experimental analyses are presented which describe the operation and characteristics of a hypersonic plasma generator for reentry vehicles. The principle of the generator operation is outlined, previous results are briefly reviewed, and supporting arc tunnel experimental data are included. The ionization enhancement by nose cone cesium seeding of the flow field is analyzed with special attention given to the nonequilibrium chemical reaction between cesium atoms and ionized air species. The results of the previous two sections are extended to reentry applications using several typical ballistic and super-orbital reentry trajectories. (auth)

31962 LOSSES CAUSED BY THE HALL EFFECT AND THEIR INFLUENCE ON THE EFFICIENCY OF THE THERMAL CYCLE IN MHD GENERATORS. Halasz, D.; Szendy, K. Acta Tech. Acad. Sci. Hung., 49: 373-85 (1965).

The losses caused by the Hall effect and their effect on the thermal cycle in MHD generators were investigated. It was found that the Hall losses are not total losses from the viewpoint of the thermodynamic cycle because the generator re-uses the heat being introduced into the working gas. Total loss is caused only by the increase of the entropy of the gas, and the magnitude of this loss is equal to the product of the entropy increase and the mean temperature of heat removal. Since the ratio of the temperature of heat input to that of heat removal is practically 8 to 10, the loss in the cycle amounts to 0.100 to 0.125 of the heat loss. (TCO)

31963 NONEQUILIBRIUM IONIZATION FOR MPD POWER GENERATION. Tipton, Donald L.; Rosebrock, T. L. Allison Res. Eng., 10: 2-19(2nd Quarter 1966).

Analytical studies of nonequilibrium ionization have progressed to the stage where theoretical studies of MPD generator performance may logically be initiated. Results to date appear most promising; however, considerably more research effort will be required before the closed loop MPD generator employing nonequilibrium ionization becomes a competitive method for power generation. Results of this study indicate that magnetically induced ionization will be the primary method of nonequilibrium ionization. Pre-ionization by an auxiliary process may be required to overcome the problem of inlet relaxation. (auth)

31964 PRESENT AND POSSIBLE PERFORMANCES OF THERMO-IONIC CONVERSION. Bliaux, J. (CEN, Saclay, France). Bull. Inform. Sci. Tech. (Paris), No. 104, 3-21(May 1966). (In French).

After a brief description of the principle and of the present performances of thermionic convertors, the research now in progress in the Electronic Physics Service at Saclay on the direct conversion of nuclear-produced heat into electricity is described. The work undertaken includes basic and technological laboratory research, and in-pile experiments in the reactor Triton at the Fontenay-aux-Roses Nuclear Research Center. The relatively rapid improvements of the performances and of the life times of the convertors make it appear likely that both spatial and terrestrial nuclear applications will be found within the next ten years. (auth)

31965 USE OF ACTINIDES ELEMENTS IN ISOTOPIC POWER GENERATORS. Berger, R. Bull. Inform. Sci. Tech. (Paris), No. 104, 23-34(May 1966). (In French).

Some alpha emitter actinide elements can be used as heat source for isotopic power generators. This application depends on their nuclear characteristics and the physical properties of their practical chemical compounds. Because of their high specific power, they are choice fuels for space propulsion and auxiliary electric energy production. But the radiation intensity and toxicity of these radioisotopes impose safety conditions, particularly shielding and containment. An economic study shows that the specific investment in an 8-hour or 24-hour orbit for thermionic generators using ^{227}Ac and ^{244}Cm is in the range of the silicon solar cell generator. That of the thermoelectric-generator using ^{238}Pu is twice to three times as high. (auth)

31966 OSCILLATIONS IN THE THERMAL CESIUM PLASMA DIODE. Cutler, William H.; Burger, Peter (Stanford Univ., Calif.). J. Appl. Phys., 37: 2867-73 (June 1966).

Oscillations with frequencies corresponding to ion transit times are observed in thermal cesium diodes having parallel-plane construction. Electrons and ions are emitted from heated flat tungsten disks immersed in cesium vapor. Measurements are made with one emitter facing a cold collector and also with two emitters facing each other. Large-amplitude oscillations are observed whenever the collector potential is large enough to draw electron saturation current through the diode. Characteristics of these oscillations are well correlated with computer-simulated results and explained by theory developed earlier. High-frequency bursts during some parts of the low-frequency fluctuations are also observed as predicted from current-vs-time curves of the computer-simulated diode. The electron-rich and ion-rich regimes of the two-emitter diode are found and switching between the two regimes is demonstrated by measuring the ion saturation current with a probe at the middle of the diode. (auth)

31967 THERMIONIC CONVERTERS OPERATING IN THE IGNITED MODE. PART I. THEORETICAL OUTPUT-CURRENT CHARACTERISTICS. Wilkins, Daniel R.; Gyftopoulos, Elias P. (Massachusetts Inst. of Tech., Cambridge). J. Appl. Phys., 37: 2888-91(June 1966).

Output current characteristics of thermionic converters are derived without reference to specific elastic and inelastic collision mechanisms, and are expressed in terms of arbitrary plasma electron density and temperature profiles. The general expression for the characteristics indicates that for a given current the output voltage is composed of two parts: (a) a reference output voltage which depends only upon the output current and electrode properties and contains implicitly the effect of electron–electron collisions; and (b) a plasma voltage loss which depends only upon certain average properties of the interelectrode plasma. It is shown that conceptually different models for the interelectrode plasma can lead to similar estimates for the plasma voltage loss and to agreement with experimental output current characteristics. For this reason, it is concluded that the successful correlation of experimental output current–voltage data is necessary but not sufficient to test the validity of a given model for the interelectrode plasma. (auth)

31968 THERMIONIC CONVERTERS OPERATING IN THE IGNITED MODE. PART II. A QUASI-EQUILIBRIUM MODEL FOR THE INTERELECTRODE PLASMA. Wilkins, Daniel R.; Gyftopoulos, Elias P. (Massachusetts Inst. of Tech., Cambridge). J. Appl. Phys., 37: 2892-9(June 1966).

A multistage ionization–recombination model is proposed to describe the formation and loss of atomic ions in low-energy cesium plasmas. Solutions of the ambipolar diffusion equation are investigated with due consideration given to these processes. The solutions indicate the existence of a state of quasi-equilibrium throughout most of a low-energy plasma in which the electron temperature is more than several hundred degrees above a critical ignition temperature. The assumption of quasi-equilibrium in the interelectrode plasma of a thermionic converter operating in the collisional ignited mode is shown to result in a plasma model which correlates a wide variety of experimental data. Included in the successful correlations are electron random current density and temperature profiles as well as output-current characteristics. The experimentally observed state of quasi-equilibrium in thermionic converter plasmas is found to be near the Saha-equilibrium limit. It is therefore concluded that the multistage ionization–recombination processes in these plasmas involve numerous excited states. (auth)

31969 THERMIONIC ENERGY CONVERTER USING FILM-BOILING LIQUID METAL. Ulrich, A. J. (Argonne National Lab., Ill.). Nucl. Appl., 2: 36-40(Feb. 1966).

A thermionic energy-conversion diode that uses a liquid metal as the electron collector was evaluated. Liquids, such as cesium, rubidium, or potassium and their alloys, are separated from the hot emitter by the vapor film produced in film boiling. Such a vapor film would maintain electrical separation if the emitter became warped because of radiation damage, thus greatly improving the reliability of the in-core thermionic diode. An experiment showed that stable film boiling occurs for ranges of emitter temperatures and cesium and potassium vapor pressures that are appropriate for thermionic diodes. The typical thermionic series-connected fuel-element geometry can be used in a film-boiling liquid-metal design to produce power in the zero g field of space. The improved tolerance to radiation damage and to emitter evaporation requires more precise control of collector temperatures, a modified startup and shutdown schedule to avoid nucleate boiling, and further development of a thermal divider to exclude nucleate boiling at the edges of the collector surfaces. (auth)

31970 DIRECT GENERATION OF ELECTRICITY. Spring, K. H. (ed.). New York, Academic Press, 1965. 416p. $16.00.

The thermodynamic and economic principles which determine the likely role of different types of generators for specific large- or small-scale application are discussed. Chapters on the fuel cell, magnetohydrodynamics, thermionic converters, thermoelectricity, and on various miscellaneous processes, (such as solar cells and piezoelectric generators) are included. (M.H.R.)

31971 PLASMA PHYSICS OF THERMIONIC CONVERTERS. Bullis, R. H.; Hansen, L. K.; Houston, J. M.; Koskinen, M. F.; Rasor, N. S.; Warner, C. 21p. (CONF-651049-19). ORAU. Gmelin, AED-CONF-65-324-15.

From IEEE Thermionic Conversion Specialist Conference, San Diego, Calif.

The plasma physics of thermionic converters is discussed in an attempt to develop a single coherent picture of this aspect of the converter in all regions of operation. The usefulness of certain characteristic features of the I-V curve, in determining the physical processes governing converter operation, is pointed out. Nine regions of converter operation are identified by these features of the I-V curve and are discussed. The importance of two parameters of converter operation, the pressure-spacing

product pd and the ion richness ratio β, in controlling converter behavior is emphasized. Which of these nine regions of converter operation appear on any particular I-V curve appears to be controlled by the values of pd and β. (auth)

31972 TRANSPORT PARAMETERS OF CESIUM IONS IN CESIUM VAPOR. Rufeh, F.; Kitrilakis, S. S.; Lieb, D. (Thermo Electron Engineering Corp., Waltham, Mass.). 9p. (CONF-651049–14). ORAU. Gmelin, AED-CONF-65-324-9.

From IEEE Thermionic Conversion Specialist Conference, San Diego, Calif.

The diffusion coefficient of cesium ions in cesium plasma and the reflection coefficient of the ions from the plasma boundaries were measured using a three-collector planar-geometry diode. A source of ions was introduced instantaneously in the center of the diode, and the ion density was monitored as a function of time away from the source. From the time-constant data, the product of diffusion coefficient and pressure was measured to be 230 cm-torr/sec for the pressure range of 0.3 – 3.0 torr. (auth)

31973 GENERATOR DEVELOPMENT FOR FLUID METAL MHD POWER CONVERSION. Prem, L. L. (Atomics International, Canoga Park, Calif.). New York, Inst. of Electrical and Electronics Engineers, 1966, Preprint No. 31 CP 66-45, 11p., $1.00. (CONF-660108–5). ORAU.

From IEEE Winter Power Meeting, New York.

Fluid metal magnetohydrodynamics represents a new approach in direct energy conversion. The concept and some of its applications are discussed, and compared to the plasma concept, but emphasizes the development of an a-c induction generator. A constant fluid velocity generator was fabricated and tested. A liquid metal, NaK, was accelerated through the generator channel. A traveling magnetic field is produced by a 3-phase current. A net power output of 1840 watts was observed. (auth)

31974 THEORY OF THE IGNITED MODE WITH ELECTRON TEMPERATURE VARIATIONS T(x). Warner, Charles (Atomics International, Canoga Park, Calif.). 7p. (CONF-651049–17). ORAU. Gmelin, AED-CONF-65-324-12.

From IEEE Thermionic Conversion Specialist Conference, San Diego, Calif.

The theory of the ignited mode is extended to include electron temperature variations of the form $[ev_i/kT(x)] = (eV_i/kT_0) + (x/\lambda_T)$ where V_i is the cesium ionization potential. This form allows the temperature T(x) to decrease with distance x from the emitter and also allows the plasma equations to be solved for the plasma density n(x). The introduction of the new parameter λ_T necessitates one additional equation which is taken to represent the continuity of electron energy flow at the emitter edge of the plasma. The cesium ions are generated by thermalized electrons in one- and two-step processes. The electrons also lose energy by excitation of the resonance level, this radiation being largely trapped. The model predicts electron temperature T(x), plasma density n(x), the sheath drops, the plasma potential V(x) and finally the volt-ampere curve. (auth)

31975 RESULTS OF A CLOSED LOOP MPD POWER GENERATION EXPERIMENT. Schneider, R. T.; Wilhelm, H. E. (Univ. of Florida, Gainesville). New York, American Inst. of Aeronautics and Astronautics, 1966, Preprint No. 66-168, 38p., $1.50. (CONF-660315–13). ORAU.

From AIAA Plasmadynamics Conference, Monterey, Calif.

Results of a closed loop MPD power generation experiment are reported as is a multicomponent analysis of the nonequilibrium processes in the magnetoactive flow. Objective of the experiment was to investigate whether nonequilibrium ionization exists and whether this effect is of sufficient magnitude to make closed loop MPD power generation feasible at low operation temperatures. It was observed that the generator can be operated in two different modes— the nonsaturated mode and the saturated mode. In the latter, the U-B curves show not only a saturation at medium magnetic fields but also a decrease of the output voltage at higher magnetic fields. An explanation of this "saturation effect" is proposed. Objective of the theory was to predict the plasma fields in the reacting nonisothermal flow with transverse magnetic field. Conclusions obtained show that nonisothermal plasma state develops within a relatively small length and that an ionization equilibrium determined by the electron temperature is not reached within the subsonic flow length. Experiment and theory are compared. (auth)

31976 PERFORMANCE OF A SELF-EXCITED MHD GENERATOR. Research Report 238. Mattsson, Arne C. J.; Ducharme, Edward L.; Govoni, Edward M.; Morrow, Irving B. Jr.; Brogan, Thomas R. (Avco Everett Research Lab., Everett, Mass.). 37p. (CONF-650826–5). ORAU.

From International Conference on Energetics, Rochester, N. Y.

A rocket-driven self-excited MHD generator designed for a net power output of 20,000 kilowatts was successfully operated. The generator was designed to demonstrate the feasibility of using an MHD device to provide power for limited duration at very high levels with relatively simple equipment. The active length of the water-cooled MHD channel is 2.70 meters. The magnet, which is a copper heat sink air core design with a maximum field of 35,000 gauss, has a resistance of 0.032 ohms and inductance of 0.27 henries. It is a single-series circuit matched to the impedance of the first half of the MHD channel where the gas pressure is a maximum. Lower power level (≈200 kw) pre-excitation of the magnet is provided by a battery bank. The net power is extracted from the downstream portion of the MHD channel, which is operated in the segmented electrode mode. The initial test period was devoted primarily to achieving self-excitation. The stress is placed on the importance of establishing the proper excitation rate through control of pre-excitation, burner ignition point, and magnet shunt loading. Further effort was concentrated on the production of net power output. The chief problem encountered during the test program was electrical breakdown between adjacent electrodes with consequent arc damage which usually induced water leaks. It was found necessary to carefully schedule the loading pattern in the generator in order to reach high power level without arcing. The rated net output of the generator was exceeded during the testing program. (auth)

31977 THE PROSPECTS FOR CLOSED-CYCLE MPD POWER GENERATION. Lindley, B. C. (International Research and Development Co. Ltd., Newcastle-upon-Tyne, Eng.). 16p. (CONF-650826–3). ORAU. Gmelin, AED-CONF-65-210-9.

From International Conference on Energetics, Rochester, N. Y.

The development of MPD power generation is considered. Topics discussed include nonequilibrium ionization, characteristics of the working fluid, operating pressure, and specific power. The use of superconducting field coils, the heat source, and recent experiments are also discussed. (J.F.P.)

31978 POWER GENERATOR. Jones, Carmen B. (to U. S. Atomic Energy Commission). U. S. Patent 3,257,571. June 21, 1966.

The production of alternating current in a magnetohydrodynamic generator is considered. The apparatus consists of a container having two parallel fluid output channels with electric output leads therein, a common fluid input channel and a fluid triode interposed between the input and output channels. The apparatus is arranged so that the hot ionized gas in the input channel is deflected automatically by the fluid triode alternately into the two output channels such that alternating current is generated. The fluid triode may have several forms, all of which produce a control jet of fluid to deflect the main stream of fluid. The fluid for the control jet may be provided automatically either from an external source or as regenerative or degenerative feedback from the output channels. (AEC)

31979 IMPROVEMENTS IN AND RELATING TO APPARATUS FOR THE DIRECT GENERATION OF ELECTRICITY. Lindley, Bryan Charles; Crompton, Felix Jeremy Philip (to C. A. Parsons and Co. Ltd.). British Patent 1,031,921. June 2, 1966. Filed May 31, 1962.

A design for a MHD generator for the direct generation of electricity comprises a duct across which is generated a magnetic field and which consists of two opposing walls including elements which serve as electrodes on at least one part of the walls. The electrodes are liquid cooled and electrically insulated from each other by either the gas flowing through the duct or by solid insulation. The ends of the elements nearest the gas in the ducts may be of rectangular, hexagonal, or triangular cross section. Alternatively, each element may have a tapered projection at right angles to its face which is in contact with the gas in the duct, and the projection fits into a tapered recess in the duct wall surrounding the element. (B.L.M.)

31980 ELECTRIC CURRENT GENERATION BY MEANS OF THERMIONIC ENERGY CONVERTERS. Gabor, Dennis; Kretsch, Hans Walter (to National Research Development Corp.). British Patent 1,031,862. June 2, 1966. Filed Nov. 4, 1963.

A device is described for generating an alternating current in which the output current from one or more thermionic energy converters is switchable to flow along two or more alternative paths in cyclic sequence by means of control signals applied to the auxiliary electrodes of thermionic converters of the triode-type included in the paths. Each path also includes transformer windings for enabling the alternating current to be derived by an output winding coupled to the windings. Preferably, the triode-type thermionic converters are connected in series and the converters are used continuously to carry a constant, or almost constant, current. (B.L.M.)

Elementary Particles and Radiations

See also Field Theory, Scattering Theory, and Symmetries

Refer also to abstracts 32305 and 32388.

31981 (AD-634517) LIMITATIONS IN THE ENERGY RESOLUTION OF SLOW ELECTRONS. Friz, Walter (Aerospace Research Labs., Wright-Patterson AFB, Ohio). Apr. 1966. 30p. (ARL-66-0061). CFSTI $2.00 cy, $0.50 mn.

The limiting factors of resolution in electron spectrometry at low energies were investigated. It is shown that monochromatic electron beams with energy spread $\Delta E/E = 10^{-3}$ may be produced well below 1 ev provided the necessary and quite possible technological effort is being made. It appears that in conjunction with standard detection schemes space charge effects and their restrictions on beam intensities pose a lower energy limit for attainable monochromatic beams. However, using coincidence counting detection schemes much lower beam intensities will suffice and then physical-chemical surface effects on the electrodes and their influence on the electron trajectories will be determining this limit. (auth)

31982 (AD-634703) ON THE OFF-DIAGONAL MASS MATRIX ELEMENT OF THE NEUTRAL K SYSTEM. Technical Report No. 521. Woo, Ching-Hung (Maryland Univ., College Park. Dept. of Physics and Astronomy). Nov. 1965. 11p. CFSTI $1.00 cy, $0.50 mn.

A recent interference experiment of Fitch et al. was interpreted as suggesting that the imaginary part of the off-diagonal $K^0-\bar{K}^0$ mass matrix is mainly responsible for the observed CP noninvariance in 2π decay, whereas the imaginary parts of the width matrices are negligible. The consistency of such a proposition was investigated with simple theoretical models. (auth)

31983 (CALT-68-71) PHOTOPRODUCTION OF NEGATIVE PIONS FROM HYDROGEN. Hauser, Michael G.; Walker, Robert L. (California Inst. of Tech., Pasadena). Apr. 1966. Contract AT(11-1)-68. 21p. (CONF-660411-3). Dep. mn. CFSTI $1.00 cy, $0.50 mn.

From American Physical Society Meeting, Washington, D. C.

The reaction $\gamma + p \rightarrow \pi^- + \pi^+ + p$ is being studied by observing negative pions produced in liquid hydrogen by the photon beam from the CalTech synchrotron. The π^- momentum and angle are analyzed using a magnetic spectrometer and counter system, and the photon energy is fixed by performing a synchrotron subtraction. The reaction is studied for photon energies from 0.9 to 1.3 Bev and π^- angles from 7 to 120° c.m. Missing mass spectra at fixed c.m. angles show the reaction is dominated by the pseudo-2-body process $\gamma + p \rightarrow \pi^- + N^*(1238)$, particularly at forward angles. These spectra are fit with a Breit-Wigner shape plus phase space; the integral of the resonance term over missing mass is presented as a differential cross section. The angular distributions are peaked strongly forward, supporting a peripheral model of the interaction. Preliminary data indicate the total cross section decreases smoothly from 75 ± 5 μb at a photon energy of 925 Mev to 43 ± 9 μb at 1275 Mev. The resonant part of the total cross section drops from 63 ± 8 μb to 20 ± 8 μb over the same range. (auth)

31984 (IC-66/54) PHOTOPRODUCTION OF VECTOR MESONS FROM NUCLEONS. ar-Rashid, Harun (International Centre for Theoretical Physics, Trieste (Italy)). May 1966. 27p. Dep. mn.

The photoproduction of rho and omega mesons from nucleons is treated phenomenologically, emphasizing the suitability of choosing a particular set of twelve invariant amplitudes of this process. These are obtained in analogy with Compton scattering from nucleons so that the expressions for the physical observables are closely related in the two cases. Contributions to the amplitudes from nucleon exchange in the direct channel and one-pion exchange in the crossed channel are given and the latter diagram is explicitly compared with the few experimental data available at present. (auth)

31985 (IC-66/57) NON-LEPTONIC DECAYS OF Ω^-. Hara, Y. (International Centre for Theoretical Physics, Trieste (Italy)). May 31, 1966. 10p. Dep. mn.

By making use of the PCAC hypothesis and equal time commutation relations suggested by the quark model, it was found that (i) asymmetries of Ω^- non-leptonic decays ($\Omega \rightarrow \Lambda + K$, $\Xi + \pi$ and $\Xi^* + \pi$) are very small, (ii) the lifetime of Ω, $\tau(\Omega) \approx (0.3 \sim 0.8) \times 10^{-10}$ sec, (iii) $\Gamma(\Omega \rightarrow \Lambda K)/\Gamma(\Omega \rightarrow \Xi\pi) \lesssim 1/30$ for the SU(3)-symmetric $B_{10}\ B_8\ P_8$ coupling and $\sim (1/10 \sim 1/2)$ for the broken SU(3)-symmetric $B_{10}\ B_8\ P_8$ coupling and (iv) $\Gamma(\Omega \rightarrow \Xi^*\pi)/\Gamma(\Omega \rightarrow \Xi\pi) \approx 1/3$. (auth)

31986 (NEVIS-148) ELECTRON PRODUCTION BY HIGH-ENERGY NEUTRINOS. Burns, R. R. (Nevis Labs., Columbia Univ., Irvington-on-Hudson, N. Y.). May 1966. Contract AT(30-1)-1932. 96p. (CU-254; R-548). Dep. mn. CFSTI $3.00 cy, $0.75 mn.

Thesis.

Interactions of high energy electron neutrinos from K_{13} decay were studied using massive aluminum spark chambers at the Brookhaven AGS external proton beam. In particular, three specific and closely related topics were studied: (1) muon-electron universality at high momentum transfer ($\langle q \rangle \approx 6 \times 10^2$ Mev), (2) the question of two neutrinos, and (3) neutrino-flip hypotheses. The results of this study showed that μ-e universality is a valid concept for high energy neutrino interactions within the limited statistics due to the low electron event rate. The two neutrinos were found to be distinct; the upper limit for muon neutrinos giving rise to an electron as the final state lepton is less than 5.5%. Lastly, the experimental results are found to be in disagreement with the predictions of the neutrino-flip hypotheses. (auth)

31987 (NP–16097) A BUBBLE CHAMBER INVESTIGATION OF THE K* RESONANCE. Gelsema, E. S. (Amsterdam Univ. (Netherlands)). May 19, 1965. 79p. Dep. mn.

Thesis.

A bubble chamber experiment in a beam of K^--mesons of 1.455 Bev/c incident momentum is described. A review is presented of the analysis of the pictures through all stages of the experiment in chronological order. The beam properties, the scanning procedure and the computer programs needed to identify the events are discussed. A method is outlined to determine the purity of the beam to a high precision. In particular the computer programs involve many problems. The function of each of these programs is therefore given, without going into any detail concerning their actual structure. The cross sections given agree only very roughly with those from other experiments. This may be due to difficulties in the distribution of the unidentified events. A study of the K* resonance is described. The values found for the mass ($M = 895 \pm 3$ Mev/c^2) and the width ($\Gamma = 50 \pm 5$ Mev/c^2) are in agreement with other experiments. The experiment yields a spin ≥ 1 for the K*. Statistics are not good enough to set an upper limit on the spin of the K*; the method described is shown to yield the value 1 for the spin, when applied to another experiment. At low values of the four-momentum transfer the K* is produced through the exchange of a spinless particle, whereas at high values the one particle exchange-model is no longer appropriate. There are indications that the K* is then produced through an intermediate Y*. The Appendix contains some formulas useful for the calculation of physical quantities in different inertial systems. (auth)

31988 (UCRL–11510) PROPERTIES OF THE NEUTRAL CASCADE HYPERON. Hubbard, John Richard (Lawrence Radiation Lab., Univ. of California, Berkeley). Apr. 25, 1966. Contract W-7405-eng-48. 59p. Dep. mn. CFSTI $3.00 cy, $0.75 mn.

Thesis.

The production of neutral cascade hyperons by incident K^- on hydrogen was studied from threshold at 1.05 Bev/c to 1.7 Bev/c. A sample of 206 Ξ^0 events was obtained. Production cross sections rise to about 120 μb for Ξ^0K^0, 25 μb for $\Xi^0K^0\pi^0$, and 50 μb for $\Xi^0K^-\pi^-$ at 1.7 Bev/c. The mean life is $\tau_{\Xi^0} = 2.53^{+0.38}_{-0.28} \times 10^{-10}$ sec. The decay asymmetry is $\alpha_{\Xi^0} = -0.20 \pm 0.22$. The branching ratios are less than 1% for $\Xi^0 \to \Sigma^+l^-\nu$, $\Xi^0 \to pl^-\nu$, and $\Xi^0 \to p\pi^-$, where l^- signifies e^- or μ^-. (auth)

31989 (UCRL–16275) PROTON-PROTON ELASTIC SCATTERING AT INCIDENCE MOMENTA 3, 5, AND 7 Bev/C. Clyde, Allan Roy (Lawrence Radiation Lab., Univ. of California, Berkeley). May 1966. Contract W-7405-eng-48. 110p. Dep. mn. CFSTI $4.00 cy, $0.75 mn.

Thesis.

Differential cross sections for p-p elastic scattering were measured for incident momenta, 3, 5, and 7 Bev/c. The backward scattered protons were momentum analyzed with magnetic spectrometers and detected with scintillation counters for the missing mass spectrum of $p + p \to p + x$ for x = a proton. A hydrogen gas target was used for recoil momenta from 75 to 600 Mev/c and polyethylene with matched carbon for subtraction was used from 500 to 4000 Mev/c. Statistical errors were approximately 2% at low momentum transfer, and increased to about 5% for 90° scattering in the center-of-mass. The data indicates shrinkage of the diffraction peak with incident energy, a strong energy dependence of $d\sigma/d|t|$ at 90° and is consistent with a logarithmic decrease in the total elastic cross section with the center-of-mass energy. The behavior of the forward scattering indicates the presence of a real scattering amplitude. The values obtained for the ratio of the real to the imaginary scattering amplitudes are 43, 39, and 34% respectively. An assumption of similar angular dependence of the real and imaginary parts of the nucleon scattering amplitude is indicated by these data. (auth)

31990 (UCRL–16648) THE REACTION $K^-p \to \Lambda\omega$ FROM 1.2 TO 2.7 Bev/c: THE ABSORPTION MODEL WITH STRANGE-MESON EXCHANGE. Flatte, Stanley Martin (Lawrence Radiation Lab., Univ. of California, Berkeley). Mar. 9, 1966. Contract W-7405-eng-48. 81p. Dep. mn. CFSTI $3.00 cy, $0.75 mn.

Thesis.

Over 9000 $K^-p \to \Lambda\omega \to (p\pi^-)(\pi^+\pi^-\pi^0)$ events were analyzed in four momentum regions between 1.2 to 2.7 Bev/c. The differential cross section and the eleven independent decay-correlation parameters were determined as a function of production angle for each of the four momentum regions. A striking forward peak in the differential cross section at our highest momentum, 2.6 Bev/c, suggests the appearance of strange-meson exchange. Using a new formalism for the absorption model it is shown that the behavior of the differential cross section and the decay-correlation parameters at 2.6 Bev/c as a function of production angle is qualitatively explained by the absorption model with K and K* exchange. Using available data on $K^-p \to \Lambda\phi$ at 2.6 Bev/c, it is shown that the absorption model also explains the behavior of $K^-p \to \Lambda\phi$, and that the comparison between the couplings of $K^-p \to \Lambda\omega$ and $K^-p \to \Lambda\phi$ is in reasonable agreement with SU(3) predictions. (auth)

31991 (UCRL–16771) LEPTONIC DECAYS OF NEUTRAL K MESONS. Golden, Robert Leon (Lawrence Radiation Lab., Univ. of California, Berkeley). Mar. 28, 1966. Contract W-7405-eng-48. 52p. Dep. mn. CFSTI $3.00 cy, $0.50 mn.

Thesis.

In the Alvarez 72-inch hydrogen bubble chamber, neutral K mesons are obtained from 6544 reactions of the type $\pi^-p \to \Lambda K^0$, with a visible Λ decay, $\Lambda \to p\pi^-$ (the beam was operated at π^- momenta of 1035 and 1170 Mev/c). A sample of 54 neutral K decays of the types $K \to \pi^\pm e^\mp \nu$, $\pi^\pm \mu^\mp \nu$ is examined to test the $\Delta I = 1/2$ and $\Delta S = \Delta Q$ selection rules. An analysis of about one third of the 54-event sample was previously published by Alexander et al. The long-lived K_L leptonic decay rate was measured and found to be $\Gamma_L = (11.3 \pm 1.9) \times 10^6$/sec. This differs by 0.6 standard deviation from the $\Delta I = 1/2$ prediction $\Gamma_L = 2[\Gamma(K^+_{e3}) + \Gamma(K^+_{\mu 3})] = (12.4 \pm 0.7) \times 10^6$/sec. 31 events were used for which the lepton charge is known to construct a likelihood function based on the T-invariant time distribution $1 + \gamma \exp(-\lambda_s t) + 2q\alpha \cos \Delta mt \exp(-\lambda_s t/2)$, where $q = +1$ if the decay involves a positive lepton and $q = -1$, if the decay involves a negative lepton. Using $\Delta m = 0.75 \times 10^{10}$/sec, one measures $\gamma = 1.4^{+1.4}_{-0.9}$, $\alpha = 1.0^{+0.3}_{-0.5}$, consistent with the $\Delta S = +\Delta Q$ predictions $\gamma = 1.0$, $\alpha = 1.0$. An analysis is presented of the time distribution of all 54 events. The time distribution used was $1 + Z \exp(-\lambda_s t) - 2\beta \exp(-\lambda_s t/2)\sin \Delta mt$. Assuming $\Delta m = 0.75 \times 10^{10}$/sec, we find $Z = -0.7^{+1.2}_{-0.8}$, $\beta = -0.8^{+0.5}_{-0.7}$. The $\Delta S = \Delta Q$ rule prediction is $Z = 1 + 0.6$, $\beta = 0$; the 0.6 is a correction for the $K_s \to \pi^+\pi^-\gamma$ process. The likelihood of the $\Delta S = \Delta Q$ prediction is less the maximum by $e^{-0.6}$. T symmetry requires $\beta = 0$. Results are consistent with T symmetry, but one cannot rule out significant T-nonpreserving amplitudes. (auth)

31992 GUIDED SURFACE WAVES AND THE RADIATION FROM CHARGES MOVING IN CURVED PATHS. Lawson, J. D. (National Inst. for Research in Nuclear Science, Chilton, Eng.). Amer. J. Phys., 34: 601-5(July 1966).

The analogy between the radiation from a guiding surface which is bent or curved, and the radiation from an electron which is deflected (bremsstrahlung) or moves in a curved path in a magnetic field (synchrotron radiation) is illustrated. In developing this analogy the significance of the "characteristic radius" associated with a cylindrical or spherical wave system, defined as the radius at which the argument of the radial wavefunction is equal to its order, is examined. A small diversion is made to illustrate the relevance of this concept to atomic radiation, supergain antennas, and wave-mechanical scattering. (auth)

31993 DERIVATION OF COMPTON SCATTERING RELATION IN COVARIANT NOTATION. Farmer, Ger-

ald (Univ. of Wisconsin, Madison). Amer. J. Phys., 34: 614(July 1966).

The Compton scattering relation is derived from the consideration of 4-momentum conservation for the system of electrons and photons. (M.H.R.)

31994 ELASTIC COLLISIONS AS LORENTZ TRANSFORMATIONS WITH APPLICATION TO COMPTON SCATTERING. Siemon, Richard E.; Snider, Dale R. (Univ. of California, La Jolla, San Diego). Amer. J. Phys., 34: 614-15(July 1966).

It is shown that the scalar product of two 4-momenta is unchanged by an elastic collision since such collisions are equivalent to a Lorentz transformation. A simple derivation of the wavelength shift in Compton scattering is given as an example. (M.H.R.)

31995 FORMAL ANALOGY BETWEEN COMPTON SCATTERING AND DOPPLER EFFECT. Nielsen, A.; Olsen, J. (Danish Atomic Energy Commission, Risoe, Denmark). Amer. J. Phys., 34: 621-2(July 1966).

For the case of elastic scattering it is shown that viewed from the scatterer, the energy of the incoming photon or particle is equal to that of the outgoing, and the angle of incidence is equal to the angle of reflection, when the direction of the velocity of the scatterer after the collision is taken as reference. The momentum-energy 4-vector is used. Only the Compton scattering process is considered, but the analogy to the Doppler effect is apparent. (C.E.S.)

31996 PHOTOPION PRODUCTION, DISPERSION RELATIONS, AND $\gamma\rho\pi$ COUPLING. Donnachie, Alexander; Shaw, Graham (Univ. Coll. London). Ann. Phys. (N. Y.), 37: 333-64(Apr. 1, 1966).

Fixed t dispersion relations are used to evaluate the transition amplitudes which lead to final S-, P-, and D-wave scattering states. Knowledge of the pion-nucleon scattering phase shifts up to 700 Mev allows the coupled integral equations for the dominant M_{1+}, E_{0+} transitions to be solved explicitly by an iterative method. The other multipoles are assumed to be given in the (Born + $M_{1+}^{(3)}$) approximation which is valid due to the small values of the scattering phase shifts concerned except in the case of the $M_{1-}^{(0,1)}$ and $E_{1+}^{(3)}$ transitions. These latter are not amenable to calculation and constitute the principal sources of error. Agreement with experiment is excellent in the case of π^0 production, but there are systematic discrepancies in the case of π^+ production due to the approximate nature of the $M_{1-}^{(0,1)}$ and $E_{1+}^{(3)}$ multipoles. The effect of higher transitions is investigated and found to be small except at extreme forward angles. Initially it was assumed that the $\gamma\rho\pi$ coupling constant was zero. After calculation, comparison with low energy experiments yields the value $(\Lambda/e) = 0.05 \pm 0.15$, consistent with the original assumption. (auth)

31997 BREMSSTRAHLUNG PRODUCTION IN 48-Mev p-p COLLISIONS. Warner, Robert E. (Univ. of Manitoba, Winnipeg). Can. J. Phys., 44: 1225-37(June 1966).

Measurements of the cross section $d^2\sigma/d\Omega_1 d\Omega_2$ for the bremsstrahlung reaction $p + p \rightarrow p + p + \gamma$ were made with 48 ± 1 Mev incident protons. Both final protons were detected in coincidence at equal angles on either side of the beam and coplanar with the beam, and bremsstrahlung events were identified kinematically. Cross sections of 2.12 ± 0.36 and 3.04 ± 0.44 μb/sterad^2 were obtained at 30 and 35°, respectively. Both measured cross sections are smaller than the predictions of Signell and Marker by about a factor of 10; this discrepancy is considered to be well established, since various tests show that our detection efficiency is nearly 100%. It is concluded that further theoretical work, especially predictions of cross sections for noncoplanar events, is needed to determine whether the discrepancy results from a strong preference for coplanar events or from some basic defect in the theory. (auth)

31998 EXPERIMENTAL DETERMINATION OF THE EFFICIENCY OF γ-RAY CIRCULAR POLARIZATION ANALYZERS. Michalec, R. (Nuclear Research Inst., Czechoslovak Academy of Sciences, Rez) Czech. J. Phys., 16: 481-4(1966).

Methods are proposed for the direct experimental determination of the efficiency of analyzers of the circular polarization of gamma rays based on the Compton scattering of polarized photons by polarized electrons. (auth)

31999 SUM RULES FOR π-π SCATTERING. Wanders, G. (Univ., Lausanne, Switzerland). Helv. Phys. Acta, 39: 228-46(1966).

Scattering amplitudes T(s, t, u) having simple symmetry properties in s, t, and u can be expressed as functions of suitably chosen homogeneous variables. The assumption of the validity of the Mandelstam representation determines the analyticity properties of the amplitudes as functions of these homogeneous variables. These properties lead to a new type of dispersion relations involving integrals along curves of the (s, t, u)-space. In the case of the $\pi-\pi$-system, these dispersion relations imply a set of sum rules relating S-, P- and D-wave scattering lengthes, S-wave effective ranges and integrals over physical quantities. The present experimental information does not allow a detailed test of these sum rules. (auth)

32000 SCATTERING AND ABSORPTION OF ELECTROMAGNETIC RADIATION BY ELECTRONS IN THE LIGHT OF THE HARMONIC PHENOMENON. Dutt, J.; Bali, L. M. (Univ. of Lucknow, India). Indian J. Pure Appl. Phys., 4: 133-6(Apr. 1966).

A more detailed study is made of higher harmonics in the light scattered by electrons with a view to correlating the earlier observations and explaining certain observed discrepancies in the earlier work by Vachaspati (Phys. Rev., 128: 664(1962); 130: 2598(1963)) and N. C. Rastogi and Vachaspati (Indian J. Pure Appl. Phys., 1: 311(1963)). The first and second harmonic cross sections for the scattering produced by bound electrons are evaluated taking into account the relativistic effects. These cross sections are shown to be consistent with the absorption cross section. Also, the relative importance of the electron's interactions with the electric and magnetic vectors of the impressed field in the phenomenon of second harmonic scattering was determined for both free and bound electrons. It is found that in the production of the harmonic phenomenon the contribution of the electric field is, on the whole, much more than that of the magnetic field. (auth)

32001 HARMONICS IN THE SCATTERING OF ELECTROMAGNETIC RADIATION BY ELECTRON CURRENT. Bali, L. M.; Dutt, J.; Vachaspati (Univ. of Allahabad, India. Univ. of Lucknow, India). Indian J. Pure Appl. Phys., 4: 137-40(Apr. 1966).

The significant characteristics of the harmonics in the electromagnetic radiation scattered by electrons moving with a uniform translational velocity were studied. Cross sections for scattering into the second harmonic are found to depend on the intensity and square of wavelength of the incident beam. For a given incident radiation the second harmonic cross sections for relativistic velocities of the scatterers are found to be exceedingly large compared with those for electrons at rest. Consequently, for relativistic electrons, for obtaining large second harmonic cross sections the intensity of the incident radiation need not be as high nor the frequency as low as in the case of electrons at rest. The results are significant because they point to an easier experimental verification of the harmonic phenomenon over a wider range of frequencies. (auth)

32002 SOME THOUGHTS ON THE ELECTRON. Thomson, J. (Sangamo Weston Ltd., Middlesex, Eng.). Int. J. Electron., 20: 81-5(Jan. 1966).

The anomaly of the charge of the electron being contained in a small effective volume with nothing to hold it together is discussed. Some relationships which exist in electronic physics are pointed out, and it is suggested that these reinforce the idea that the whole of the electron's mass is electromagnetic in origin. The Fitzgerald-Lorentz contraction is derived in a different manner taking account of the gyrational nature of the electronic charge. (M.H.R.)

32003 COMMENT ON "MOTION OF A CHARGED PARTICLE IN A PLANE ELECTROMAGNETIC WAVE." Sanderson, J. J. (English Electric Co. Ltd., Whetstone, Eng.). Int. J. Electron., 20: 87-9(Jan. 1966).

The nonrelativistic approximation was applied consistently to the motion of a charged particle in a plane electromagnetic wave. Explicit solution terms of simple functions were obtained. (M.H.R.)

32004 CALCULATION OF CROSS SECTIONS FOR DEUTERON PHOTODISINTEGRATION AND NEUTRON CAPTURE BY A PROTON FOR THE CASE OF A NONLOCAL POTENTIAL. Dotsenko, B. B.; Salasyuk, V. M. (Kiev State Un.iv.). Izv. Vyssh. Ucheb. Zaved., Fiz., No. 5, 80-5(1965). (In Russian).

The processes of photodisintegration of a deuteron by a gamma quantum and of radiative capture of a neutron by a proton with emission of a gamma quantum are examined. The interaction between the nucleons is described by a nonlocal potential of the Yamaguchi type but with the repulsion caused by the nucleon cores taken into account. The Schrödinger equation for the proposed potential is solved exactly. The values of the parameters of the potential are determined more precisely in comparison with previously obtained values. The effective photodisintegration and radiative-capture cross sections are calculated. The calculations show that the proposed potential allows the processes of photodisintegration at low energies (up to 20 Mev) to be described sufficiently well. The calculated radiative-capture cross section agrees somewhat better with experiment than that determined for other potentials. (tr-auth)

32005 NEUTRINO SCATTERING ON A BOUND ELECTRON. Romanov, Yu. I. (Inst. of Medical Radiology, Academy of Medical Sciences, USSR). Izv. Vyssh. Ucheb. Zaved., Fiz., No. 6, 24-6(1965). (In Russian).

The scattering of a neutrino on an atom with the transition of an electron into the continuous spectrum is studied in the V-A version of weak interactions ($C_A = -C_V = \sqrt{2G}$) Calculations are carried out for transitions from the K shell in the Born approximation. (The electron making the transition is described by a plane wave.) An expression is obtained for the total ν-e scattering cross section, depending on the free-electron scattering cross section and on the ionization energy. Taking the effect of the nuclear Coulomb field into account leads to a negligible additional term in the expression for the cross section. (M.J.T.)

32006 NEW MEASUREMENT TECHNIQUE FOR PAIR PRODUCTION IN PHOTOGRAPHIC EMULSIONS. Bertin, P. Y. (Faculte des Sciences, Clermont-Ferrand, France); Castor, J.; Augerat, J.; Gardes, J.; Avan, L.; Isabelle, D. B. Nucl. Instrum. Methods, 42: 38-44(June 1966). (In French).

A new technique for the measurement of the opening angle of electron-positon pairs produced by γ-rays in nuclear emulsion is described. The photon beam axis is normal to the emulsion plane, while in the classical method it will be parallel to that plane. For the scanning of the plates in this method one follows the two electron tracks in the emulsion by displacing the stage along a direction parallel to the beam axis. It is shown that such a technique eliminates most of the systematic errors found in other methods and that the measurement errors are smaller in this case. Results are given for measurements done on 15460 pairs. (auth)

32007 MEASUREMENT OF THE COMPTON SCATTERING CROSS SECTION. Sahota, H. S.; Anand, S.; Singh, M.; Sood, B. S. (Punjabi Univ., Patiala, India). Nucl. Phys., 83: 508-12(1966).

Absolute differential cross sections of Compton scattering of 0.662 and 1.25 Mev gamma rays from cylindrical scatters of different materials and diameters at scattering angles 40, 60 and 90° were measured in order to confirm the validity of the method of correcting for the absorption of radiation in the scatterer and to contradict the objections raised by Ghose. The results are in good agreement with theory for the value of $\mu r < 0.6$, where μ is the absorption coefficient of scattered radiation and r the radius of the scatterer, and hence present investigations confirm our previous results. (auth)

32008 DISPERSION THEORY CALCULATIONS FOR NUCLEON-NUCLEON SCATTERING. Feldman, K. S.; Hochberg, S. (Imperial Coll. of Science and Tech., London). Nucl. Phys., 83: 645-65(1966).

The nucleon-nucleon interaction is investigated using the dispersion formalism of Goldberger, Grisaru, MacDowell and Wong. The contributions due to the exchange of one and two pions are included. The N/D method is employed and the resulting sets of integral equations are solved to a desired degree of accuracy by digital computer techniques. Scattering phase shifts and coupling parameters are calculated for values of the total angular momentum J = 0, . . ., 5 at laboratory energies up to 400 Mev. Fair agreement with experiment is obtained for $J \geq 3$. A short discussion of the deuteron is incorporated and its binding energy estimated. (auth)

32009 PRODUCTION AND DECAY OF Ξ^* IN THE ONE-PARTICLE EXCHANGE MODEL. Watal, Chitra; Agarwal, Bipin K.; Gupta, Yogendra M. (Univ. of Allahabad, India). Nucl. Phys., 83: 666-72(1966).

The production and decay of Ξ^* is studied on the basis of the one-particle exchange model. (auth)

32010 ANALYSIS OF K AND $\eta \rightarrow 3\pi$ DECAY SPECTRA. Taylor, S.; Huetter, T.; Koller, E. L.; Stamer, P. (Stevens Inst. of Tech., Hoboken, N. J.). Nucl. Phys., 83: 690-4 (1966).

A discussion of the analysis of experimental 3π decay spectra of the K and η mesons is presented. A linearized Brown and Singer resonance model is shown to produce the same results as Weinberg's linear approximation. Provided that the experimental K and $\eta \rightarrow 3\pi$ reduced spectra are statistically indistinguishable from straight lines, as is currently the case, it is further shown that a large correlated range of values for the resonance mass m_0 and width, Γ_0 will give acceptable fits to the data. This leads to the conclusion that the present experimental data, although consistent with the Brown and Singer theory, are insufficient to serve as a strong test of the theory. (auth)

32011 THE ρ-MESON ELECTROMAGNETIC MASS SPLITTING. Beder, D. S. (Univ. of California, Berkeley). Nuovo Cimento (10), 43A: 553-75(June 1, 1966). (UCRL-16465).

Perturbation techniques are applied to the S-matrix dynamical equations specifying the ρ-meson state, thereby calculating the ρ electromagnetic mass splitting. Approximate solutions to the N/D equations (for the $J^\pi = 1^-$ partial wave) are employed in two models; $\pi\pi$ inelastic scattering with ρ exchange and photon exchange "driving" force; SU_3 octet-octet scattering of pseudoscalars. The numerical results are $M_{\rho^0} - M_{\rho^\pm} \approx +13$ Mev. (auth)

32012 EXPERIMENTAL LIMITS ON THE NEUTRINO-SEA DENSITY. Csonka, P. L. (Univ. of California, Livermore); Marx, G. Nuovo Cimento (10), 43A: 591-6(June 1, 1966). (UCRL-14519-T).

Two upper limits for the depth of the degenerate (anti) neutrino sea are discussed. The first one is based on a recent experimental upper limit for the density of antineutrinos with energy between 400 and 12 Mev. The second makes use of the energy dependence of the observed $K_2 \rightarrow 2\pi$ events. (auth)

32013 PCAVC HYPOTHESIS AND THE PION-LAMBDA INTERACTION. Martin, B. R. (Univ. of Copenhagen). Nuovo Cimento (10), 43A: 629-40 (June 1, 1966).

The partially conserved axial-vector current hypothesis (PCAVC) is used to derive a consistency condition on π-Λ scattering, which is then examined quantitatively, using the results of a recent analysis of the low-energy π-Λ interaction. The consistency condition is $A^{\pi-\Lambda}(\nu = 0, \nu_B = 0, k^2 = 0) = 0$, and it is found that $A^{\pi-\Lambda} = 2 \pm 3$. The result is com-

parable with that obtained by Adler for π-A scattering. (auth)

32014 TWO-CHANNEL PROBLEM AND THE INELASTIC UNITARITY CONDITION IN EIGENSTATES OF THE TOTAL ANGULAR MOMENTUM. Amaldi, U. Jr.; Biancastelli, R.; Francaviglia, S. (Istituto Superiore di Sanita, Rome). Nuovo Cimento (10), 43A: 641-53(June 1, 1966).

The relations coming from the unitarity of the S-matrix in the two-elastic-channel problem when also inelastic channels are open are written down. If the inelastic contributions are known, the moduli of the elastic amplitudes are obtained. A careful study is made of the conditions implied by unitarity on the inelastic "absorptions" and on the moduli and the (real) phases of the elastic amplitudes. (auth)

32015 ANTIPROTON ANNIHILATION AT REST IN DEUTERIUM. Chinowsky, W.; Kojoian, G. (Univ. of California, Berkeley). Nuovo Cimento (10), 43A: 684-700(June 1, 1966). (UCRL-16335).

Annihilation of antiprotons at rest in the Lawrence Radiation Laboratory's 15-inch deuterium-filled bubble chamber was studied. Particular emphasis was on investigation of the characteristics of the antiproton-neutron annihilations. With a total of 2071 observed events, the ratio of the number of annihilations on protons to that on neutrons was found to be 1.3 ± 0.07. The observed momentum distribution of proton recoils accompanying the neutron-annihilation products deviates strongly from the deuterium internal-momentum distribution and cannot be explained by final-state pion-proton interactions. Three-body effects are considered. Multiplicity and momentum distributions of the annihilation products are in agreement with predictions of a Lorentz-invariant phase-space model with an interaction volume of radius about 2.2 pion Compton wavelengths. Annihilations yielding mesons (K) accounted for 0.05 ± 0.01 of the neutron annihilations. (auth)

32016 POLARIZATION AND SPIN CORRELATION PARAMETER MEASUREMENTS IN 600-Mev PROTON-PROTON SCATTERING USING A POLARIZED PROTON TARGET. Coignet, G. (Institut du Radium, Orsay, France); Cronenberger, D.; Kuroda, K.; Michalowicz, A.; Olivier, J. C.; Poulet, M.; Teillac, J.; Borghini, M.; Ryter, C. Nuovo Cimento (10), 43A: 708-15(June 1, 1966).

Using a polarized or unpolarized proton beam previously described and a polarized proton target (70%) the parameters $P(\theta)$ and $C_{i,j}(\theta)$ were measured in the angular interval from 23 to 104° in the center-of-mass system at about 600 Mev. The experimental set-up and the way in which the data were carried out are discussed. Results are presented and compared to those already obtained in the same energy region. (auth)

32017 MULTIPLE PION PRODUCTION IN PROTON-PROTON COLLISIONS AT 24 Gev/c. Nilsson, S. (Univ. of Stockholm); Breivik, F.; Buran, T.; Toefte, H. Nuovo Cimento (10), 43A: 716-20(June 1, 1966).

Multiple pion production by 24 Bev/c protons in a hydrogen bubble chamber is studied. Effective-mass plots are shown for 4-prong and 6-prong events for the combinations $p\pi^+$ and $p\pi^-$ against the squared four-momentum transfer to the same systems and for the combination $\pi^+\pi^-$. The results give support to the assumption that the peripheral interaction is the dominant one. (auth)

32018 CALCULATION ON THE PROCESSES $e^-e^+ \rightarrow N\bar{N}^*$ AND $e^-e^+ \rightarrow \bar{N}N^*$ FOR THE FIRST FOUR BARYONIC RESONANCES. Kessler, P. (College de France, Paris). Nuovo Cimento (10), 43A: 731-40(June 1, 1966). (In French).

In view of future electron-positron colliding beam experiments, the differential cross sections of the processes $e^- + e^+ \rightarrow (N + \bar{N}^*) \rightarrow N + \bar{N} + \pi$ and $e^- + e^+ \rightarrow (\bar{N} + N^*) \rightarrow \bar{N} + N + \pi$ were calculated for the first four baryonic resonances (or antiresonances). This is the third type of reactions one can consider in order to determine the electromagnetic form factors of the γNN^* vertices in different physical regions; the two other types (electroproduction of baryonic resonances, and lepton pair production from those resonances) were studied previously. (auth)

32019 NOTE ON BROKEN SU_3 SYMMETRY. Ghose, P. (Indian Association for the Cultivation of Science, Calcutta); Sen, S. Nuovo Cimento (10), 43A: 752-6(June 1, 1966).

On the assumption that the violation of unitary symmetry transforms like the I = 0, Y = 0 member of a unitary octet the coupling constants corresponding to the four observed decay modes $\Lambda'^{*-} \rightarrow n\pi^-$, $Y^{*-} \rightarrow \Lambda\pi^-$, $Y_1^{*-} \rightarrow \Sigma\pi$ and $\Xi'^{*-} \rightarrow \Xi\pi$ of the $J^P = 3/2^+$ baryon decuplet may be expressed in terms of three parameters. The ratio between two of the parameters was estimated from the observed mass splittings by a simple ansatz. It was predicted that $\Gamma(Y_1^{*-} \rightarrow \Lambda\pi) = 46$ Mev and $\Gamma(Y_1^{*-} \rightarrow \Sigma\pi) = 0.002$ Mev in good agreement with experimental data. (auth)

32020 ELECTROMAGNETIC INTERACTIONS AND T VIOLATION. Leonardi, R. (Institut de Physique Nucleaire, Orsay, France); Strocchi, F. Nuovo Cimento (10), 43A: 757-8(June 1, 1966).

The γ-nucleon-$N_{\frac{3}{2}}^*$ vertex is analyzed as an example of T violation in electromagnetic interactions. The effective electromagnetic current of the two hadrons is considered. (J.F.P.)

32021 PARTIALLY CONSERVED CURRENTS AND CP VIOLATION IN K^0-MESON DECAYS. Pestieau, J.; Weyers, J. (Univ., Louvain, Belg.). Nuovo Cimento (10), 43A: 759-61(June 1, 1966).

The model proposed by Gupta (Phys. Rev. Lett. (14), 20: 838(1965)) for CP nonconservation in weak interactions is considered. Some additional predictions of this model when it is combined with the partially conserved axial current hypothesis and the current commutation relations assumed by Gell-Mann are reported. (J.F.P.)

32022 DISPERSION-RELATION APPROACH TO ABSORPTIVE CORRECTION IN THE PERIPHERAL MODEL OF HIGH-ENERGY PHYSICS. Griffiths, D. (Argonne National Lab., Ill.); Saperstein, A. M. Nuovo Cimento (10), 43A: 769-85(June 21, 1966).

A successful formula for absorptive corrections to the peripheral model of high-energy elementary-particle reactions has been given by Jackson and Gottfried. An analysis is made of previous derivations of the formula and some of the implicit difficulties are pointed out. A new derivation, based upon the Omnès equation, is presented in which all assumptions are made explicit and which is free of the difficulties contained in the previous derivations. The $\pi p \rightarrow \rho p$ reaction is used as an illustration and a complete treatment of spin is given for this system. (auth)

32023 A BOUNDARY-CONDITION MODEL FOR THE P_{33} PION-NUCLEON STATE. Huffman, A. H. (Univ. of Washington, Seattle); Lomon, E. L. Nuovo Cimento (10), 43A: 817-33(June 21, 1966).

A singular boundary condition model with potential tail is developed for the P_{33} pion-nucleon resonance. The logarithmic derivative F is given a pole form suggested by theoretical considerations. Both Yukawa and square-well potential tails are treated. It was found that for boundary radii $r_0 = 0.50\ \mu^{-1}$ or $0.35\ \mu^{-1}$ an attractive Yukawa tail of strength -2μ and range $0.5\ \mu^{-1}$ gives an excellent fit to the P_{33} scattering data correcting violations of the Wigner condition, $dF/dE \leq 0$, previously seen at low energies in zero-potential tail models. Only repulsive square-well tails give good fits, and then the improvement seems to depend on the peculiar behavior of relativistic corrections. Below $r_0 = 0.20\ \mu^{-1}$ the single-pole model merges into a constant-F model with $F = -1.95$. Attractive tails agree with theoretical studies of the long-range pion-nucleon force. (auth)

32024 LOW-ENERGY s-WAVE $\bar{K}N$ SCATTERING. Cho, K. S. (Drexel Inst. of Tech., Philadelphia). Nuovo Cimento (10), 43A: 840-58 (June 21, 1966).

A study of the low-energy s-wave $\bar{K}N$ scattering in the I = 0 and I = 1 states was carried out in the multi-channel N/D formulation. In solving the matrix N/D equations, the

Balàzs method was incorporated. The exchange contributions included in this calculation are: vector mesons, $p_{\frac{1}{2}}$ baryons, $p_{\frac{3}{2}}$ baryons and low-lying $d_{\frac{3}{2}}$ baryons. The coupling constants of these exchange particles are calculated either from the experimental parameters or from unitary symmetry. Imposing the condition that Y_0^* (1405) be the resonance below the $\overline{K}N$ threshold, the scattering lengths for the I = zero state and its coupling constants to the $\overline{K}N$ system and the energy dependence of k ctg δ are calculated. Further adjusting the residue of poles, the experimental scattering lengths for the I = 1 state were reproduced. From these results we calculated elastic absorptive cross sections. All these calculated values agree quite well with the experimental values. (auth)

32025 THE $K_1^0 - K_2^0$ MASS DIFFERENCE IN S-MATRIX THEORY. Beder, D. S. (Univ. of California, Berkeley). Nuovo Cimento (10), 43A: 865-74(June 21, 1966). (UCRL-16474).

General considerations are presented on the perturbing effect of weak interactions on S-matrix dynamics specifying the neutral K-meson states. The perturbations due to weak-interaction amplitudes in the N/D dynamical scheme are illustrated for two models of the neutral K's: a) $K \equiv \sigma K$ bound state ($\sigma = \pi\pi$, I = 0, $J^\pi = 0^+$), b) $K \equiv \omega K$ bound state ($\omega = 3\pi$, I = 0, $J^\pi = 1^-$). The main result of examining these perturbations is the relation $m(K_2) > m(K_1)$. Inadequacies of the (current) dynamical models permit only a crude estimate of the magnitude of the mass difference, namely between 10^{-5} and 10^{-6} ev. (auth)

32026 ON THE COMPARISON OF FORWARD PION-NUCLEON DISPERSION RELATIONS WITH EXPERIMENTS. Olesen, P. (Niels Bohr Inst., Copenhagen). Nuovo Cimento (10), 43A: 875-86(June 21, 1966).

It was previously shown that it is possible to construct some tests of forward dispersion relations which are independent of the high-energy behavior of the total cross sections. An investigation is made of the dependence of these tests on the threshold parameters (f^2 and the scattering lengths). It is well known that the threshold parameters are not very well determined experimentally. Therefore, in order that our tests are reliable, it is necessary that they are practically independent of the threshold parameters. It turns out that there exist two tests of the forward dispersion relations which are practically independent of the actual values of the threshold parameters. This result yields the most critical test of forward dispersion relations (i.e., essentially local commutativity. Lorentz invariance and unitarity) proposed up to now. In the spirit of the previous work it is then shown that the two threshold parameters f^2 and $T_s(m)$ can be determined by a method, which is independent of the high-energy behavior of the total cross sections. Finally, it is shown that the existing experimental data indicate that $\sigma_A(E) = \frac{1}{2}(\sigma_-(E) - \sigma_+(E))$ might change its sign somewhere between 20 Bev and 50 Bev. In an Appendix a discussion of the comparison of sum rules of the Khuri-Kinoshita-Martin type with experiments is given. It turns out that the sum rules of this type are much weaker than the tests discussed. (auth)

32027 CURRENT EXPERIMENTAL STATUS OF BARYON EXCHANGE. Lyons, L. (Nuclear Physics Lab., Oxford). Nuovo Cimento (10), 43A: 888-910(June 21, 1966).

The experimental situation on the importance of the baryon exchange (B.E.) process for reactions meson + baryon → meson' + baryon' is investigated. Some general comments are made about the expected absolute cross sections, angular distributions and incident momentum dependence of the B.E. mechanism. It is found that it should be easiest to study the process when the incident momentum is in the few Bev/c region. The simplest reactions in which to search for B.E. are those for which meson exchange (M.E.) is forbidden. Of these, $K^-p \to \Xi^-K^+$, $K^-p \to \Sigma^-\pi^+$ and $\pi^-p \to \Sigma^-K^+$ all show forward baryon peaks of the order of 10 μb/sr. Results are presented in a table. A study of reactions for which B.E. is forbidden ($\overline{K}N \to N\overline{K}$ or $\Delta\overline{K}$) reveals that several of these processes exhibit enhancements in the backward meson hemisphere. These are probably due to mechanisms of the type $\overline{K}N \to Y^* \to N\overline{K}$, and this emphasizes the need for high-energy experiments for investigating B.E. The majority of reactions are allowed both for B.E. and M.E. Of those cases which have been studied in sufficient detail, a large number show backward meson peaks with cross sections similar to those observed in M.E.-forbidden reactions. Results on some of these reactions are presented in a table. Although it seems that B.E. can be regarded as an established process, some details deserve further study, and suggestions are made for experiments which would enable a better understanding to be obtained of the B.E. mechanism. (auth)

32028 ANTIPROTON-PROTON ELASTIC SCATTERING AT HIGH ENERGIES IN THE UNCORRELATED JET MODEL. Kokkedee, J. J. J. (CERN, Geneva). Nuovo Cimento (10), 43A: 919-38(June 21, 1966).

The uncorrelated jet model proposed by Van Hove as a phenomenological description of hadron collisions at high energies is applied to antiproton-proton scattering. An analysis is made of the experimental elastic-scattering data at laboratory momenta above 4 Bev/c. A modification to the model is introduced, made necessary by the presence of $\bar{p}p$-annihilation channels at finite energies. The modified model is shown to reproduce excellently the existing data concerning total cross sections and small-angle diffraction scattering. (auth)

32029 STRANGE-PARTICLE PRODUCTION IN π^-p AND π^+p COLLISIONS AT 4 Gev/c. Bartsch, J. Technische Hochschule, Aachen); Bondar, L.; Speth, R.; (and others). Nuovo Cimento (10), 43A: 1010-27(June 21, 1966).

In photographs taken with the 81-cm hydrogen bubble chamber of Saclay at the proton synchrotron of CERN, the production of strange particles in π^-p collisions (621 events) and π^+p collisions (932 events) was studied. The beam momentum was 4 Bev/c. The cross sections for the various strange-particle reactions are given and compared with the values obtained in other experiments at different pion momenta. The c.m.s. angular distributions of the baryons in reactions of the types $\pi p \to NK\overline{K}$, $NK\overline{K}\pi$, YK, $YK\pi$, and $YK\pi\pi$ are discussed. The K*(891) is observed in the $K\pi$ and $\overline{K}\pi$ effective-mass distributions of the reactions $\pi^-p \to NK\overline{K}\pi$, $YK\pi$, $Y^0K^+\pi^-\pi^0$ and of the reactions $\pi^+p \to \Sigma^+K_1^0\pi_1^0$, $Y^0K\pi\pi$, $\Sigma^+K\pi\pi$. The Y* (1385) shows up only in the $Y^0\pi^+$ mass distributions of the reactions $\pi^+p \to Y^0K^+\pi^+$ and $Y^0K^+\pi^+\pi^0$. For the two reactions $\pi^-p \to Y^0K^{*0}$ and $\pi^+p \to \Sigma^+K^{*+}$ the K* density matrix elements were determined from the decay angular distributions by a Gottfried-Jackson analysis. (auth)

32030 CHARGE-DEPENDENT EFFECTS IN NUCLEON-NUCLEON $^1S_0$ SCATTERING LENGTHS BY THE DASHEN-FRAUTSCHI METHOD. Duck, I.; Khanna, F. (Rice Univ., Houston, Tex.). Nuovo Cimento (10), 43A: 1047-61(June 21, 1966). (TID-22556).

The dispersion relation of Dashen and Frautschi was used in conjunction with the nucleon-nucleon scattering amplitudes of Scotti and Wong, and the nucleon electromagnetic form factors to calculate the charge dependence of the nucleon-nucleon $^1S_0$ scattering lengths due to single-photon exchange and to the charge dependence of the pion mass and coupling constants. The contribution of the one-photon exchange is considerably enhanced over what one would expect from a potential calculation using hard cores. (auth)

32031 SPLITTING OF A PHOTON INTO TWO PHOTONS IN THE COULOMB FIELD OF A NUCLEUS. Boccaletti, D. (Istituto Nazionale di Fisica Nucleare, Bologna); de Sabbata, V.; Gualdi, C. Nuovo Cimento (10), 43A: 1115-20(June 21, 1966).

The cross section for the splitting of a photon into two photons in the Coulomb field of a nucleus is determined with the standard techniques of the quantum electrodynamics for the case in which the energy of the incident photon is smaller than two electron masses. Numerical

evaluations for some values of the variables are made in this energy range. (auth)

32032 CANONICAL COMMUTATION RELATIONS AND ASYMPTOTIC BEHAVIOR OF THE TRANSITION AMPLITUDES. Minguzzi, A. (Univ., Bologna. Istituto Nazionale di Fisica Nucleare, Bologna). Nuovo Cimento (10), 43A: 1131-6(June 21, 1966).

The asymptotic behavior of the π-N and γ-N elastic scattering amplitudes in the boson mass is investigated with the aid of the canonical commutation relations. (auth)

32033 ONE-PARAMENTER FIT TO THE ELECTROMAGNETIC FORM FACTORS OF THE NUCLEON. Massam, T. (CERN, Geneva. Istituto Nazionale di Fisica Nucleare, Bologna); Zichichi, A. Nuovo Cimento (10), 43A: 1137-48(June 21, 1966).

A new fit to the world data on (ep) and (en) elastic scattering, and on ($\bar{p}$p) annihilation into lepton pairs, was obtained by using a model for the isovector and isoscalar nucleon form factors, which is suggested by the use of unitary symmetry and of its breaking. The fit allows for a nonpointlike behavior of one out of the two couplings which enter in the expression for nucleon electromagnetic form factors. The fit is a one-parameter fit and the corresponding values of χ^2 for the proton and neutron data are discussed. The contributions coming from the possible existence of "core-terms" and of "q^2-dependent background" in the expression of the nucleon electromagnetic form factors are found to be lower than a few per cent. The q^2 dependence of the vector-meson-nucleon couplings is also discussed. (auth)

32034 $Y_1^*[Y_1^+]$ (1385) PRODUCTION AND A POSSIBLE I = 0 MEMBER OF AN OCTET AT 1660 Mev. Kwak, N. (Univ. of Kansas, Lawrence). Nuovo Cimento (10), 43A: 1149-53(June 21, 1966).

The behavior of the Y_1^* (1385) production cross section in the region of 1660 Mev in the K^--p system was examined to investigate the possibility of a Y_0^* (1660) resonance in this region with I = 0, using a model analogous to the pole model of isobar production. (L.B.S.)

32035 A CURRENT-ALGEBRA PREDICTION OF THE FIRST-ORDER SU_3 VIOLATIONS IN ρ AND K DECAYS. Renner, B. (Univ. of Cambridge, Eng.). Nuovo Cimento (10), 43A: 1154-7(June 21, 1966).

A relation between the decay widths of $\rho \rightarrow 2\pi$ and $K^* \rightarrow K\pi$ is presented, which follows from the SU_3 algebra and resonance dominance in form factors of vector currents. (L.B.S.)

32036 CROSS-SECTION COMPUTATIONS FOR CHARGE-RETENTION SCATTERING OF HIGH-ENERGY NEUTRINOS. Ahrens, T. (Georgia Inst. of Tech., Atlanta). Nuovo Cimento (10), 43A: 1158-61(June 21, 1966)

The total cross sections for charge-retention and charge-exchange scattering of very-high-energy neutrinos by protons and neutrons are calculated. (L.B.S.)

32037 EQUAL-TIME COMMUTATORS AND $\eta \rightarrow 3\pi$ DECAYS. Bose, S. K.; Zimerman, A. M. (IAEA, Trieste, Italy). Nuovo Cimento (10), 43A: 1165-7(June 21, 1966).

The $\eta = 3\pi$ decay modes were studied by using the equal-time current commutation relations. Partial rates and branching ratios were obtained for the $3\pi^0$, $\pi^+\pi^-\pi^0$, and 2γ decay modes. (L.B.S.)

32038 PRODUCTION OF NEUTRAL PIONS FROM ELECTRON-PROTON COLLISIONS. Kikuchi, R. (Tohoku Univ., Sendai); Baba, K.; Kaneko, S.; Huke, K.; Kobayashi, Y.; Yamakawa, T. Nuovo Cimento (10), 43A: 1178-81 (June 21, 1966).

The results are reported of a preliminary measurement of the reaction $e^- + p \rightarrow e^- + p + \pi^0$ at 593 Mev. The experimental cross section $(1.0 \pm 0.6) \cdot 10^{-34}$ cm^2 Mev^{-1} sr^{-1} was found to be in poor agreement with the calculated value of $3.96 \cdot 10^{-34}$ cm^2 Mev^{-1} sr^{-1} using the theory of Dalitz and Yennie. No definite conclusions are drawn from the comparison, but it is conjectured that the theory of static approximation gives too high a value. (L.B.S.)

32039 RELATION BETWEEN LEPTONIC AND NON-LEPTONIC K-MESON DECAYS AND CURRENT ALGEBRAS. Bose, S. K.; Biswas, S. N. (IAEA, Trieste, Italy). Nuovo Cimento (10), 43A: 1182-4(June 21, 1966).

The $K_1^0 \rightarrow 2\pi$ decay amplitude is related to the $K^+ \rightarrow \mu\nu$, $\pi^+ \rightarrow \mu\nu$ amplitudes by using a model of nonleptonic weak processes developed by Sugawara and Suzaki. The partial rate predicted from the relation was found to be $R(K_1^0 \rightarrow 2\pi^0) = 3.8 \times 10^9$ sec^{-1}, which is in good agreement with the experimental value of 3.6×10^9 sec^{-1}. (L.B.S.)

32040 AN ALTERNATIVE INTERPRETATION OF THE ENHANCEMENT OBSERVED AT $M^*_{pp\pi^+} \simeq 2.52$ Gev/c^2. Duimio, F.; Kidd, J.; Mosca, L.; Ratti, S.; Russo, V.; Zampieri, E. (Univ., Milan. INFN, Milan). Nuovo Cimento (10), 43A: 1210-14(June 21, 1966).

A possible interpretation of the ppπ^+ peak observed at 252 Bev/c^2 in p-p interactions is suggested in terms of interference effects between the production amplitudes of the nucleon isobars as due respectively to double isobar graphs and to Drell graphs. The interpretation seems to explain at least qualitatively the observed distributions. (L.B.S.)

32041 EFFECTS OF D-STATE ADMIXTURE AND HARD-CORE RADIUS ON THE PHOTOPRODUCTION OF NEUTRAL PIONS FROM DEUTERONS. Ananthanarayanan, K.; Rao, K. Srinivasa (Inst. of Mathematical Sciences, Madras). Nuovo Cimento (10), 44A: 31-8(July 1, 1966).

The effects of the inclusion of D-state admixture and the hard-core radius in the ground state of the deuteron on the differential cross section for the elastic photoproduction of neutral pions were studied in the impulse approximation using the amplitudes of Chew et al. The differential cross section is found to be not very sensitive to the variation of the hard-core radius. A D-state admixture of 3% is found to yield a reasonable agreement with experimental results. (auth)

32042 SOME TESTS OF TIME REVERSAL IN ELECTROPRODUCTION PROCESSES. Piketty, C. A. (Laboratoire de Physique Theorique et Hautes Energies, Orsay, France). Nuovo Cimento (10), 44A: 39-46(July 1, 1966).

The C-violating effects for the general electromagnetic inelastic processes lepton + nucleon $\rightarrow$ lepton + all final states were studied. The upper bound for the asymmetry of the recoil lepton near the first inelastic peaks corresponding to the Λ^* ($\frac{3}{2}^+$) and Λ^{**} ($\frac{3}{2}^-$) π-Λ resonances was estimated. (auth)

32043 MEASUREMENT OF THREE K^+-DECAY BRANCHING RATIOS. Callahan, A. C. (Univ. of Wisconsin, Madison). Nuovo Cimento (10), 44A: 90-108 (July 1, 1966). (COO-881-56).

The following three K^+-meson decay branching ratios were measured: $B_{K\mu3} = 0.0277 \pm 0.0018$, $B_{Ke3} = 0.0394 \pm 0.0017$, $B_{K\pi2} = 0.216 \pm 0.009$. Details of the experimental method are given. The form-factor ratio for $K_{\mu3}$ decay, $\xi = f_+/f_-$ is found, using our value of $B_{K\mu3}/B_{Ke3} = 0.70 \pm 0.05$, to have a real part $\mathrm{Re}\,\xi = +0.40 \pm 0.40$. This number depends on μ-e universality and $|\mathrm{Im}\,\xi| < 1$. Recent measurements on the $K_{\mu3}$ mode obtain $\mathrm{Re}\,\xi = 0.34 \pm 0.30$ and $|\mathrm{Im}\,\xi| < 1$. The agreement of the real parts can be said to confirm μ-e universality or put quantitatively $f_+(K_{\mu3})/f_+(K_{e3}) = 1.01 \pm 0.05$. (auth)

32044 COMPOSITION OF A DEGENERATE GAS OF ELEMENTARY PARTICLES. Barker, B. M.; Bhatia, M. S.; Szamosi, G. (Univ. of Windsor, Ont.). Nuovo Cimento (10), 44A: 109-19(July 1, 1966).

An elementary-particle model is considered for investigating the composition of superdense matter. Equations are derived for determining baryon, meson, and lepton densities. Conservation of electric charge and hypercharge is considered for determining the stable components of matter at high and low densities. (L.B.S.)

32045 MESON DECAY OF STRONGLY INTERACTING SYSTEMS. Parkinson, M. (Univ. of California, Los

Angeles); Yellin, J. Nuovo Cimento (10), 44A: 120-30 (July 1, 1966). (BNL-9706).

The decays of strongly interacting systems with the quantum numbers $J^P = 1^-$ and $C = -1$ into pseudoscalar mesons are discussed. The $^3S_1$ $\bar{p}p$ system at rest is within this category and predicted branching ratios for its annihilation are presented. The related processes of $K_N^* \to K\pi\pi$ and $^1S_0$ $\bar{p}p$ annihilation are discussed. Interesting results include the determination of the SU_3 $\bar{B}BV$ D/F ratio to be 2.3 rather than the SU_6 value of $\frac{3}{2}$ and the indication that $f_{\eta^*NN} - 2f_{\pi^*NN}$ where the η^* is the 960 Mev $\eta\pi\pi$ resonance. Such a large negative value for the η^* coupling constant may help to explain the rapid increase with energy of the proton Compton scattering cross section. (auth)

32046 SCATTERING OF MASSIVE PHOTONS WITH VECTOR-SCALAR COUPLING. Bebel, D.; Kaschluhn, F.; Zoellner, W. (Humboldt-Univ., Berlin). Nuovo Cimento (10), 44A: 166-76(July 1, 1966).

The elastic scattering of neutral massive spin-1 particles coupled to scalar nucleons is considered in lowest nonvanishing order of the coupling constant. It is shown that all helicity amplitudes contain terms leading to Kronecker delta singularities in the complex angular-momentum plane. The contribution of these terms to the amplitude in the crossed channel is considered. Some consequences in connection with the Froissart theorem are discussed. (auth)

32047 ANALYSIS OF $p\bar{p} \to \pi K\bar{K}$ AT REST. Razmi, M. S. K. (Tait Inst. of Mathematical Physics, Edinburgh); Roberts, R. G. Nuovo Cimento (10), 44A: 177-84(July 1, 1966).

A method is developed for analyzing the Dalitz plot density for the $\pi\bar{K}K$ final state assuming intermediate production of K^* and A_2. The angular-momentum and SU_3 analysis takes into account the interference between the K^*'s and between each K^* and the A_2. Computation of the expressions shows that the enhancement seen for low KK mass cannot be explained by angular-momentum effects. (auth)

32048 CONSIDERATION OF n-p DIRECT AND CHARGE-EXCHANGE SCATTERING BASED ON TRANSVERSE MOMENTUM DISTRIBUTION AND MANDELSTAM REPRESENTATION. Narayan, D. S. (Tata Inst. of Fundamental Research, Bombay). Nuovo Cimento (10), 44A: 213-17(July 1, 1966).

The n-p direct and charge-exchange scattering was considered according to a recent model of Chavda and Narayan based on transverse-momentum distribution and Mandelstam representation, and the results are compared with the available experimental data. (auth)

32049 POSSIBLE TEST FOR THE $|\Delta I| = 0$ WEAK NUCLEAR FORCE. Ramachandran, G. (Indian Statistical Inst., Calcutta). Nuovo Cimento (10), 44A: 218-21(July 1, 1966).

The longitudinal polarization of electrons or muons scattered elastically on unpolarized deuterons provides a method of detecting possible p-state admixture in the deuteron wave function and consequently of the $|\Delta I| = 0$ weak nuclear force. An explicit calculation taking into account the s, p and d states shows that the percentage helicity not only depends on the extent of p-state admixture but also in a sensitive way on the relative phases between the s, p and d states. (auth)

32050 BROKEN SYMMETRIES AND NONLEPTONIC HYPERON DECAYS. Tadic, D.; Padjen, R. (Inst. Ruder Boskovic, Zagreb). Nuovo Cimento (10), 44A: 222-8 (July 1, 1966).

SU_6 symmetry + CP invariance (or its relativistic generalizations in the zero-momentum-transfer limit) give for the nonleptonic hyperon decay s-wave amplitudes a result which is invariant under RP. If the symmetry is broken in such a way that the same invariance holds for the p-wave amplitudes, the resulting equalities $-P(\Xi^-) = P(\Lambda^0) = (1/\sqrt{3})P(\Sigma^+) = (1/\sqrt{6})[P(\Sigma^+) - P(\Sigma^-)]$ seem to be in reasonably good agreement with the experimental results. (auth)

32051 SINGLE-π^0 PHOTOPRODUCTION FROM HYDROGEN AROUND THE "SECOND RESONANCE". Bellettini, G. (Univ., Pisa. INFN, Pisa); Bemporad, C.; Biggs, P. J.; Braccini, P. L.; del Prete, T.; Foa, L. Nuovo Cimento (10), 44A: 239-52(July 1, 1966).

New results are presented on the differential cross section for the reaction $\gamma + p \to \pi^0 + p$, at energies between 600 and 1000 Mev, and c.m. pion angles $\Theta_\pi^* = 30°$ and $\Theta_\pi^* = 60°$. The present data, together with that at $\Theta_\pi^* = 40°$ already published, show an angle-independent position of the second resonance at about 750 Mev. Rather flat angular distributions in the forward c.m. hemisphere are also favored by these data. On comparing the cross sections obtained when detecting both the neutral pion and the recoil proton, and when detecting only the latter, estimates of the background of "ghost protons" are obtained, in agreement with a proposed empirical curve. (auth)

32052 DECAY ANGULAR CORRELATION FOR Y_1^{*-} IN THE PERIPHERAL MODEL. Gupta, Y. M.; Agarwal, B. K. (Allahabad Univ., India). Nuovo Cimento (10), 44A: 262-4(July 1, 1966).

The decay angular distribution of Y_1^{*-} in the $K^- + p \to Y_1^{*-} + \pi^+ \to \Lambda + \pi^- + \pi^+$ interaction was calculated according to the one-nucleon-exchange model. The results are found to be in good agreement with the experimental histogram of Shafer et. al. A test of the one-fermion-exchange model is proposed. (L.B.S.)

32053 COVARIANT MAGNETIC-MOMENT OPERATOR FOR SU_6. Ryder, L. H. (Univ. of Durham, Eng.). Nuovo Cimento (10), 44A: 272-5(July 1, 1966).

A covariant form of the SU_6 prediction $\mu(p)/\mu(n) = -1.5$ is obtained by using the Pauli-Labanski pseudovector, and is shown to hold at any time-like momentum transfer. (L.B.S.)

32054 HIGH-ENERGY THEOREM BY ALGEBRA OF CURRENTS. Okubo, S. (IAEA, Trieste, Italy). Nuovo Cimento (10), 44A: 276-81(July 1, 1966).

A high-energy theorem is derived using the algebra of currents for the Compton scattering of the nucleon. The theorem may be used, in addition, to distinguish the validity at various models of elementary particles. (L.B.S.)

32055 RELATION BETWEEN $\eta \to 2\pi\gamma$ AND $\eta \to 2\gamma$ FROM CURRENT ALGEBRA. Ademollo, M.; Gatto, R. (Univ., Florence. INFN, Florence). Nuovo Cimento (10) 44A: 282-4(July 1, 1966).

The branching ratio for $\eta \to \pi^+\pi^-\gamma/\eta \to 2\gamma$ was calculated to be 0.14, based on the assumption of partial conservation of axial current and on the commutation relation between the axial charges and the axial currents. (L.B.S.)

32056 EXPERIMENTAL TESTS OF SU_{6W} IN NUCLEON-ANTINUCLEON ANNIHILATION AT REST. Bettini, A. (Univ., Padua. INFN, Padua). Nuovo Cimento (10), 44A: 285-90(July 1, 1966).

Predictions of SU_{6W} symmetry are discussed for $p\bar{p}$ and $n\bar{p}$ annihilations at rest into two pseudoscalar mesons and a pseudoscalar and a vector meson. Poor agreement is found between theory and experiment. (L.B.S.)

32057 SIMPLE MODEL OF THE n-p MASS DIFFERENCE. Muta, T. (Kyoto Univ.). Nuovo Cimento (10), 44A: 306-8(July 1, 1966).

It is shown that the correct sign of the electromagnetic mass difference of nucleons can be derived in the SU_3-symmetric Lee model if the symmetry breaking due to the electromagnetic interaction is treated in a self-consistent manner. (L.B.S.)

32058 A DETERMINATION OF THE $(\omega$-$\varphi)$ MIXING ANGLE USING NUCLEON ELECTROMAGNETIC FORM FACTORS. Massam, T. (CERN, Geneva. INFN, Bologna); Zichichi, A. Nuovo Cimento (10), 44A: 316-17(July 1, 1966).

An analysis is made of electron-nucleon elastic scattering and proton-antiproton annihilation on the basis of a

model previously studied for the electromagnetic form factors of the nucleon. Corrections to previous results (Nuovo Cimento; 43A: 137(1966)) are given. (L.B.S.)

32059 PROTON-PROTON BREMSSTRAHLUNG WITH THE TABAKIN POTENTIALS. Duck, I.; Pearce, W. A. (Rice Univ., Houston, Tex.). Phys. Lett., 21: 669-71 (July 1, 1966). (TID-22804).

p-p-γ cross sections calculated with the Tabakin potentials are found to be in good agreement with experimental results at E_p = 158 Mev. A discrepancy persists at E_p = 50 Mev. (auth)

32060 A POSSIBLE DIRECT TEST OF CP VIOLATION IN THE K_2^0 INTERACTIONS. Arbuzov, B. A.; Filippov, A. T. (Joint Inst. for Nuclear Research, Dubna, USSR). Phys. Lett., 21: 711-13(July 1, 1966).

Experiments are proposed to test CP violation in a direct way. The processes $K_2^0 \rightarrow \pi^0 e^+ e^-$ and $K_2^0 + Z \rightarrow \pi^0(\eta,\eta') + Z$ which are forbidden in the one-photon exchange approximation by CP invariance, are considered. Estimates are given for the probabilities of these processes on the basis of the CP violating mechanism that was proposed earlier. (auth)

32061 PREDICTIONS OF THE STATIC QUARK MODEL ON BOSON DECAYS. Pietschmann, H.; Thirring, W. (Univ. of Vienna). Phys. Lett., 21: 713-15(July 1, 1966).

Some decays of the 36 $\bar{q}q$ mesons are calculated within the static quark model. Introducing as new parameter the radius of the wave function the V-γ vertex, the $P \rightarrow 2\gamma$, the $P \rightarrow \mu + \nu$ and the $\eta \rightarrow 2\pi + \gamma$ decays are calculated. (auth)

32062 PROTON-PROTON BREMSSTAHLUNG AT 204 Mev. Rothe, K. W.; Koehler, P. F. M.; Thorndike, E. H. (Univ. of Rochester, N. Y.). Phys. Rev. Lett., 16: 1118-21(June 13, 1966).

The gamma energy spectra, the angular distributions in the two-nucleon cms and the gamma and p-p asymmetries due to an initially polarized, 204-Mev proton beam are presented. (G.O.Y.)

32063 STRONG COUPLING OF PSEUDOSCALAR-MESON OCTET. Goebel, C. J. (Univ. of Wisconsin, Madison). Phys. Rev. Lett., 16: 1130-4(June 13, 1966).

The SU(3)-symmetric model is considered in which the meson is $\underline{8}$, 0^-, i.e., a pseudoscalar octet (π, k, $\bar{k}$, η), and its only interaction is taken to be a Yukawa coupling of the p-wave part of the meson field with a fixed scatterer. Only the solution in which the scatterer has states (isobars) $\underline{8}$, $\frac{1}{2}$, $\underline{10}$, $\frac{3}{2}$ is presented. (G.O.Y.)

32064 OBSERVATION AND PROPERTIES OF THE NEUTRAL A_2 MESON. Benson, G.; Lovell, L.; Marquit, E.; Roe, B.; Sinclair, D.; Vander Velde, J. (Univ. of Michigan, Ann Arbor). Phys. Rev. Lett., 16: 1177-80 (June 20, 1966).

The production and properties of the neutral meson (A_2) were observed from a 250,000-picture exposure of 3.65-Bev/c mesons (π^+) in a bubble chamber. The three-meson (π) mass spectrum obtained from 2993 events of the type $\pi^+ + d \rightarrow \pi^+ + \pi^- + \pi^0 + p + p$ shows an enhancement at about 1300 Mev which is interpreted as the meson (A_2^0) (1300). Its subsequent decay into $\rho^\pm\pi^\mp$ was also found. The branching ratios of the meson (A_2^0) indicate an I = 1 state which strongly prefers $\rho\pi$ (as opposed to direct 3π) decay. The Dalitz plot density favors a spin-parity assignment of 2^+. (J.F.P.)

32065 SPECULATIONS ON THE REAL PART OF THE FORWARD pp($\bar{p}p$) SCATTERING AMPLITUDE. Sakurai, J. J. (Univ. of Chicago). Phys. Rev. Lett., 16: 1181-4 (June 20, 1966).

A discussion is given of ρ (pp) and its analog in $\bar{p}p$ scattering, ρ ($\bar{p}p$) from the point of view of vector meson exchange. It is noted that the existing data do not favor the conventional Regge-pole picture in which the real part of the forward pp scattering amplitude is visualized as arising from the exchange of Reggeized mesons; that the sign, the order of magnitude, and the energy dependence of ρ (pp) are in agreement with a model based on un-Reggeized ω exchange with absorptive corrections; at infinite energies it is expected that ρ_∞ ($\bar{p}p$) = $-\rho_\infty$ (pp) $\approx$ 0.3; and that the observed persistence of the real part in the forward pp scattering may be not unrelated to the non-Reggeization of a neutral vector meson found theoretically in massive electrodynamics. (J.F.P.)

32066 SEARCH FOR Y = 2, S = 0 RESONANCES. Lamb, R. C. (Argonne National Lab., Ill.); Lundy, R. A.; Novey, T. B.; Yovanovitch, D. D.; Lander, R. Phys. Rev. Lett., 17: 100-2(July 11, 1966).

Dibaryon resonance production in the reaction p + p $\rightarrow$ π + X at 12.5 Bev was studied. The deuteron-production cross section was found to be 3.1 $\pm$ 1.0 μb/sr in the c.m. system. A limit on other dibaryon production was set at $\leq$1.5 μb/sr. (auth)

32067 NEW STRUCTURE IN THE K^+-p AND K^+-d TOTAL CROSS SECTIONS BETWEEN 0.9 AND 2.4 Gev/c. Cool, R. L.; Giacomelli, G.; Kycia, T. F.; Leontic, B. A.; Li, K. K.; Lundby, A.; Teiger, J. (Brookhaven National Lab., Upton, N. Y.). Phys. Rev. Lett., 17: 102-5(July 11, 1966). (BNL-10078R).

Preliminary analysis of data on K^+-p and K^+-d interactions shows two new peaks in the total cross sections, one in isotopic spin zero and one in isotopic spin one. No conclusive interpretation is given for the structure in the K^--p total cross section. The total cross section in the pure isotopic spin states σ_0 and σ_1 shows the structure at approximately the same mass value. (L.B.S.)

32068 Y*'S WITH SPIN 7/2. Wohl, Charles G.; Solmitz, Frank T.; Stevenson, M. Lynn (Univ. of California, Berkeley). Phys. Rev. Lett., 17: 107-13(July 11, 1966). (UCRL-16868).

Cross sections and polarization angular distributions were measured for K^--p interactions at 1.22 to 1.70 Bev/c, and evidence was found for an I = 0, Y*($\approx$ 2100) resonance. In addition, the Y*(2030) and Y_1^*($\approx$ 2100) were determined to have spin and parity of $J^P = \frac{7}{2}^+$ and $J^P = \frac{7}{2}^-$, respectively. (L.B.S.)

32069 REGGE-POLE THEORY AND p-n AND $\bar{p}$-n CHARGE-EXCHANGE SCATTERING AT SMALL ANGLES. Flores-Maldonado, Victor (Univ. of California, Berkeley). Phys. Rev. Lett., 17: 113-15(July 11, 1966). (UCRL-16799).

The sharp forward peak observed in high-energy p-n charge-exchange scattering is explained on the basis of Regge-pole theory with exchange of the ρ and R trajectories. The calculated charge-exchange differential cross sections at 3.0 Bev/c are shown to be in agreement with experiment. (L.B.S.)

32070 LEPTON SCATTERING AND THE ANAPOLE. Sarkar, S. (Indian Association for the Cultivation of Science, Calcutta). Proc. Phys. Soc. (London), 88: 788-90(July 1966).

The polarization of the scattered electron in the collision of electrons with electrons, positrons and protons, and the cross section and μ^- polarization for the reaction $e^- + e^+ \rightarrow \mu^- + \mu^+$ were evaluated in first Born approximation with interactions that include the "anapole" moment for the leptons. (auth)

32071 SUGGESTED EXPERIMENT TO MEASURE PART OF THE TRANSVERSE ELECTROMAGNETIC MASS OF THE ELECTRON. Power, E. A. (National Bureau of Standards, Boulder, Colo. University Coll., London). Proc. Roy. Soc. (London), Ser. A, 292: 424-32(May 31, 1966).

The changes in self energy of a nonrelativistic charged particle are calculated where such changes are due to confinement of the charge within conducting plates. This confinement will alter the mode structure of the virtual photons involved in the transverse self-energy calculation: it will lead to a reduction in the number of modes at the long wavelength limit and, where the modes have a wavelength comparable to the distance, L, between the plates, the normal integrals over virtual momenta are replaced by

sums over the integers describing the modes. It is found that mass changes of 1 part in 10^{10} can be induced by plate separations of the order of 1 mm. It is suggested that such relative mass shifts could be measured by the use of high precision atomic beam techniques, such as those used in "atomic clocks." The atomic beam would be directed between two closely spaced parallel conducting plates (or through long cylindrical tubes) located between the oscillating fields used to excite a transition between the hyperfine structure levels. The mass change will be reflected in frequency shifts of the hfs separation of the same order as the mass change. With a high precision cesium beam apparatus, it should be possible to demonstrate not only that changes do indeed occur but also obtain a quantitative estimate of such effects as a function of the plate separation, L. It is predicted that the frequency shifts will be inversely proportional to L. (auth)

32072 NON-ZERO ELASTIC AMPLITUDE REAL PART EFFECTS AND NUCLEON RECOIL EFFECTS ON RELATIONSHIP BETWEEN ELASTIC DIFFRACTION SCATTERING AND INELASTIC COLLISIONS AT HIGH ENERGIES. Fujimura, Kimio; Kobayashi, Tetsuro; Namiki, Mikio (Waseda Univ., Tokyo). Progr. Theoret. Phys. (Kyoto), 35: 391-407(Mar. 1966).

It is shown that the nonzero elastic amplitude real part effects and the nucleon recoil effects may be reflected in the relation between elastic scattering and inelastic collisions at high energies. The effects are illustrated by some simple models so designed as to express the essential features of high energy collisions. In some cases the results are quite different from those obtained by discarding the real part and/or the nucleon recoil. (auth)

32073 PION-PION CORRELATION EFFECT IN TWO-PION-EXCHANGE CONTRIBUTION FOR NUCLEON-NUCLEON SCATTERING. Furuichi, Susumu (Rikkyo Univ., Tokyo); Watanabe, Keiji. Progr. Theoret. Phys. (Kyoto), 35: 408-15(Mar. 1966).

The pion-pion correlation effect is investigated, starting from the pion-pion scattering phase shifts which show the presence of a ρ meson in the I = L = 1 state and a strong attraction without resonance in the I = L = 0 state. By comparing with the one boson exchange contribution amplitude, the roles of the pion-pion correlation and the normalization $f_+^{(+)0}(0) = C_0$ in nucleon-nucleon scattering are clarified. Comparison with the empirical phase shifts in the isotriplet state shows that $C_0 \sim 0$ and a rather small value of g_ω^2 are probable and not inconsistent with the analysis of pion-nucleon scattering. (auth)

32074 POSSIBLE C AND T VIOLATION IN THE PHOTOPRODUCTION OF NEUTRAL PIONS. Ebata, Takeshi; Hiida, Kichiro (Tokyo Univ.). Progr. Theoret. Phys. (Kyoto), 35: 432-9(Mar. 1966).

To estimate an upper limit of possible C and T violation in the electromagnetic interaction of hadrons, the photoproduction of neutral pion is reanalysed. (auth)

32075 NON-LEPTONIC WEAK INTERACTION IN CURRENT-CURRENT INTERACTION. Hayashi, Takemi; Nakagawa, Masami (Univ. of Nagoya, Japan). Progr. Theoret. Phys. (Kyoto), 35: 515-27(Mar. 1966).

Nonleptonic interactions in the current-current interaction are examined and critized. By using a Born (factorization) approximation, it is concluded that the pure $\Delta I = 3/2$ process, i.e., the $K^+ \to \pi^+ + \pi^0$ decay can be caused with strength about 20 times greater than the observed value and that the $\Delta I = 1/2$ processes are, on the contrary, caused only partially ($1/20 \sim 1/50$) irrespective of the process (hyperonic or mesonic) and of the presence or absence of parity conservation in the transition. It is also pointed out that this universal character of "theoretical" suppression for the $\Delta I = 1/2$ processes is due almost directly to the unwanted factor $\cos^2\theta \sin^2\theta$. A new two-body interaction of leptons and a corresponding nonleptonic interaction with $\Delta I = 1/2$ is discussed. (auth)

32076 SOME REMARKS ON THE FORMULATION OF THE THEORY OF ELEMENTARY PARTICLES. Sato, Shigeo (Rikkyo Univ., Tokyo). Progr. Theoret. Phys. (Kyoto), 35: 540-61(Mar. 1966).

Two important features of the Hamiltonian formalism of the theory of elementary particles are discussed. One is related to the existence of the S operator and the other to the possibility of introducing negative energy particles. The former problem is relevant to the general treatment of the Hamiltonian formalism, and it is pointed out by using a perturbational method that the S operators in Jauch-Kuroda's sense do not exist for most Hamiltonians used in the conventional second quantized theories. This difficulty is overcome by a modification of the Hamiltonian, and a unique recipe for obtaining the effective Hamiltonian, from which we can calculate the S operator, is given. An important outcome of the method is that Dyson's external line correction is automatically involved in our framework without considering the asymptotic state vectors. The motive for considering the latter problem comes from the reformulation of quantum electrodynamics by making use of a negative energy photon instead of an indefinite metric. The utility of the negative energy particles is explained by an example in which the divergences appearing in the φ^3-type interaction are removed by the introduction of these particles. (auth)

32077 POSSIBLE DETERMINATION OF THE $\gamma\pi\omega$ COUPLING CONSTANT. Kawaguchi, Masaaki; Yokomi, Hiroyuki (Osaka Univ.). Progr. Theoret. Phys. (Kyoto), 35: 564-5(Mar. 1966).

A few methods for determining the $\gamma\pi\omega$ coupling constant from the low energy experiments of the pion photoproduction are presented assuming that the $\gamma\pi p$ coupling constant is known. (B.G.D.)

32078 (3,3) RESONANCE IN THE NUCLEUS. Mes, Hans; Ahmad, Ishfaq; Hebert, Jacques (Univ. of Ottawa). Progr. Theoret. Phys. (Kyoto), 35: 566-7(Mar. 1966).

The absorption of pions with energy less than 800 Mev in nuclear matter is studied, in order to ascertain the magnitude of the absorption cross section for pions in the region $0 < E_\pi < 500$ Mev. (B.G.D.)

32079 M(12) AND MESON-BARYON INELASTIC TWO-BODY SCATTERING AT HIGH ENERGY. Hosoda, Masataka; Yamamoto, Kunio (Osaka Univ.). Progr. Theoret. Phys. (Kyoto), 35: 574-6(Mar. 1966).

The present data on the interactions $\pi^- p \to \pi^0 n$, $\pi^- p \to \eta n$, and $K^- p \to K^0 n$ at high energy and small momentum transfer are shown to be consistent with the results of the M(12) symmetry applied to very small t. (B.G.D.)

32080 ON THE EXCITATION OF THE $J^P = 3/2^+$ DECUPLET AND $J^P = 3/2^-$ OCTET IN THE NEUTRINO REACTION ON THE QUARK AND THE CLOUD MODELS. Kawakami, Akira; Minamikawa, Toshiyuki (Tokyo Univ. of Education). Progr. Theoret. Phys. (Kyoto), 35: 638-47 (Apr. 1966).

The 70-56 currents between the $J = 3/2$ baryon resonance and the $J = 1/2$ baryon are calculated on the $SU(12)$ model. The results of Sakita and Wali and the authors are tabulated. The $J = 3/2$ baryon resonance-baryon currents on the cloud effect model were also calculated, namely assuming the Cabibbo currents for the virtual baryon octet and the virtual meson octet in the SU(3) theory. The Goldberger-Treiman relation, was taken into account by assuming the conservation of weak vector and axial vector currents. A comparison of the $SU(12)$ model and the cloud effect model can be made from the experiments on the inelastic one pion production by neutrino-nucleon collision and the electron-neutrino angular correlation in the β decay of Ω^- particles. An investigation of whether the success of SU(6) as to the static properties of the baryon can be extended to our N^* production by neutrino, and also to consider as an extreme opposite model, the pion cloud model which is not taken into account in the SU(6) and to compare both results to clarify the validity of the SU(6) theory. (auth)

32081 SYSTEMATIC ANALYSIS OF THE WEAK γ DECAY OF HYPERONS. Hirooka, Masahiko; Hosoda, Masataka (Osaka Univ.). Progr. Theoret. Phys. (Kyoto), 35: 648-58(Apr. 1966).

The weak γ decays of the hyperons are investigated systematically assuming SU(3) symmetry and the invariance of the weak vertex under the five transformations, U, R, RP, RU, and RPU. Characteristic relations among the decay amplitudes, decay rates, and the asymmetry parameters of various decay modes are obtained. (auth)

32082 STRUCTURE OF HADRONS. Matumoto, Ken-iti (Kanazawa Univ., Japan). Progr. Theoret. Phys. (Kyoto), 35: 659-72(Apr. 1966).

The picture of the structure of hadrons which has been proposed by Matumoto and Nakagawa is developed, based on an analogy to the structure of atoms and molecules. The b-charge is extended and called urbaric charge which corresponds to the electric charge in atoms and molecules. Hadrons are supposed to be urbarically neutral and to be constructed with urbarically charged substances (a single urbaryon triplet + something unknown) by the urbaric force acting between the urbaric charges. The urbaric force is supposed to be superstrong and to have a range of the order of the hadron size a_{hadron} $(\sim 1/(1\sim 2)M_N)$ and therefore to be mediated by a heavy quantum having mass $m\sim 1/a_{hadron}$ $\sim(1\sim 2)M_N$. (The urbaric force does not act between separated (urbarically neutral) hadrons. Therefore, the urbaric force has an essentially different nature from the so-called OBE (one-boson-exchange) force acting between separated hadrons.) Based on Iizuka's results on the characteristic nature of the constructive force of hadron, a heavy quantum theory of the constructive force is developed. It is clarified that only the properties of the heavy quantum expected from the above picture—a (unitary scalar) vector boson coupled with a (unitary scalar) urbaryon vector current—are consistent with Iizuka's results. It is further shown that the urbaryon mass is about 10 Bev which makes the so-called Thomas term also consistent with Iizuka's results. Some remarks are given on the problems which may be connected with the subquantal nature of the heavy quantum and of urbaryon dynamics. The characteristic behavior of the heavy quantum in high energy phenomena is investigated. There it is shown that the heavy quantum has a nature similar to that of the H-quantum, and the H-quantum itself may be just the heavy quantum of the constructive force of hadrons. The characteristic energy E_1 and E_2, from which the heavy quantum radiation and $t-\bar{t}$ pair production begin to take place respectively, are estimated. The stability of urbarically ionized substances is investigated and their possible existence pattern as matter is presented. (auth)

32083 A POSSIBLE SCHEME OF ELEMENTARY PARTICLE STRUCTURE: TRION MODEL WITH INTEGRAL QUANTUM NUMBERS AND ADDITIONAL FORCE-FIELD. Namiki, Mikio (Waseda Univ., Tokyo). Progr. Theoret. Phys. (Kyoto), 35: 673-82(Apr. 1966).

By analogy with the nuclear shell model, a possible scheme for the structure of elementary particles is presented, in which the baryon is a composite system of three fundamental particles bound by a sort of additional force-field like a Hartree field. It is assumed that the fundamental particles, the isodoublet ξ and η and the isosinglet ζ form a unitary triplet t and the additional force-field a unitary scalar U_B, and therefore that the baryon is of the type $\sim(ttt)U_B$. The symmetry properties to be expected in this scheme are just those obtained in the Zweig-Gell Mann scheme. In contrast with the latter scheme, however, it is shown that one can assign integral values of the baryon number, the hypercharge and the electric charge to the above fundamental particles ξ, η and ζ, if the additional force-field is assumed to be responsible for some part of the quantum numbers. There are many ways to assign integral quantum numbers to the triplet and the force-field. Possible schemes of the meson structure are also discussed. As for the lepton structure, it is pointed out that the baryon-lepton symmetry may be interpreted even in this scheme. Finally, some speculative discussion is given on the additional force-field. The present scheme may be called the shell model type of elementary particle structure because of the additional force-field, while the conventional ones may be of the triton type because the baryon is assumed to be bound by some interparticle force. The differences between them may be observed through the electromagnetic form factor of the nucleon and other phenomena. (auth)

32084 DOUBLE OCTET MODEL OF BOSONS. Sugano, Reiji (Osaka City Univ.). Progr. Theoret. Phys. (Kyoto), 35: 683-91(Apr. 1966).

The properties of the eight dimensional representation of a four-body system which are expressed in terms of the tensor $T^{\{\mu\alpha\}}_{\{\nu\alpha\}}$ (or $T^{[\mu\alpha]}_{[\nu\alpha]}$) are investigated. Since these bosons are not self-conjugate for the charge conjugate transformation, they are not eigenstates of G and A parities, but the linear combination states of the two multiplets $T^{\{\mu\alpha\}}_{\{\nu\alpha\}}$ and $T^{[\mu\alpha]}_{[\nu\alpha]}$ are. Hence, there appear two boson octets with opposite G and A parities. The double octet scheme is applied to the vector and axial vector bosons. In the former case, ω, ρ, K* and κ are assumed to belong to the double octets and then it is required that there exist an isoscalar vector boson with positive G parity and an isovector one with negative G parity whose masses are about 850 and 830 Mev respectively. In the latter case, supposing A_1, B, D, $K\pi\pi$ (1175 Mev) and C are members of the double octets, it is predicted that there exists an isoscalar axial vector boson with negative G parity whose mass is about 1140 Mev. In addition it is noticed that vector bosons with abnormal G parity have no local Yukawa interactions and some topics related to this fact are discussed. (auth)

32085 GROUND STATE OF A NON-INTERACTING ELECTRON GAS EXCHANGE-COUPLED TO A LOCALIZED SPIN. Ishikawa, Koji; Mizuno, Yukio (Tokyo Univ.). Progr. Theoret. Phys. (Kyoto), 35: 746-8(Apr. 1966).

It is shown that the calculation of a localized spin exchange-coupled to conduction electrons by the Wigner-Brillouin type perturbation method is successful as compared to the Rayleigh-Schrödinger method, in which difficulties arise from the vanishing of the energy denominator at the Fermi level. (B.G.D.)

32086 LARGE-ANGLE ELASTIC SCATTERING AT HIGH ENERGIES. Kitazoe, Tetsuro; Nakatani, Hiroshi (Osaka Univ.). Progr. Theoret. Phys. (Kyoto), 35: 748-50(Apr. 1966).

An investigation is presented on large angle elastic p-p and π-p scattering at high energies, using the assumptions that the fixed angle dispersion relation is valid and the imaginary scattering amplitude has an exponentially damped diffraction pattern. (B.G.D.)

32087 ON THE POLARIZATION IN ELASTIC PION-NUCLEON SCATTERING IN A FEW-Gev REGION. Hasebe, Katsuya; Hyakawa, Satio; Kanada, Hiroyuki; Otsuki, Shoichiro; Yasuno, Masaru (Nagoya Univ., Japan). Progr. Theoret. Phys. (Kyoto), 35: 755-7(Apr. 1966).

Results of a phenomenological analysis of the π^--p elastic differential cross section and polarization observed by Suwa et al., at 1.7, 1.88, 2.08, 2.27, and 2.5 Bev/c are presented and some of their possible implications are discussed. (B.G.D.)

32088 APPLICATION OF FOLDY-WOUTHUYSEN TRANSFORMATION TO THE STUDY OF THE ELECTRON POLARIZATION. Gabos, Zoltan; Goia, Mihai. Stud. Babes-Bolyai, Ser. Math.-Phys., No. 1, 129-34(1966). (In Rumanian).

The direct relation between the matrix of density $\tilde{\rho}$ and the matrix of polarization $P^{(+)}$ is given. As an application of the obtained results, the expression of matrix for the electron that took part in an interaction between the elementary particles is established. (auth)

32089 BOSON RESONANCES. Samios, N. P. (Brookhaven National Lab., Upton, N. Y.). pp 24-37 of Symmetry Principles at High Energy. Perlmutter, Arnold; Wojtaszek, Joseph; Sudarshan, George; Kursunoglu, Behram (eds.). San Francisco, W. H. Freeman and Co., 1966.

The status of research on boson resonances including known regularities, information not verified, and the possible difficulties to be encountered, is outlined. (B.G.D.)

32090 INELASTIC PROCESSES IN INTERACTIONS OF A NEUTRINO WITH NUCLEONS AND UNITARY SYMMETRY. Rekalo, M. P. (Inst. of Physics and Tech., Khar'kov). Ukr. Fiz. Zh., 11: 351-8(Apr. 1966). (In Ukrainian).

Proceeding from the hypothesis of unitary symmetry of strong interactions, a relation was found between the amplitudes of processes $\bar{\nu} + N \rightarrow \mu^+ + B^{*-} + M + M$ where B^{*-} is the negatively charged baryon belonging to the irreducible representation SU_3 of dimensionality 10, M is the pseudoscalar meson. Relations were found for two possible selection rules for U-spin: $\Delta U = 1/2$ and $\Delta U = 3/2$. Moderately strong interaction is not taken into account. (auth)

32091 SELF-CONSISTENT CALCULATION OF THE 11- AND 33-AMPLITUDE IN LOW-ENERGY π-N SCATTERING. Bender, Iring; Heiss, Dieter (Freie Univ., Berlin). Z. Phys., 193: 479-89(1966).

A self-consistent calculation of the masses of the nucleon and the 33-resonance, the πN-coupling constant and the resonance width is made. By using a simplified version of the N/D-method the consistency equations are reduced to algebraic equations. Therefore self-consistency can be obtained at once for both partial waves. In order to suppress the high energy contributions a second subtraction at threshold is made. The thereby introduced subtraction constants are connected with the 11- and 33-scattering lengths which are known from experiment. (auth)

32092 RADIATIVE CORRECTIONS TO e-p SCATTERING FOR ANGULAR AND ENERGY COINCIDENCE EXPERIMENTS. Kohaupt, R. D. (Physikalische Staatsinstitut, Hamburg). Z. Phys., 194: 18-49(1966). (In German).

Calculations of radiative corrections to e-p-scattering are performed for experiments in which the final particles are detected in coincidence. Both the angles and energies of the outgoing particles are measured. The dependence of radiative corrections on angle and energy resolution parameters is discussed in detail. (auth)

32093 NEUTRAL VECTOR BOSONS IN BHABHA SCATTERING. Karpf, A. D. (Univ., Freiburg i. B.). Z. Phys., 194: 50-60(1966).

The colliding-beam experiments of e^+- and e^--annihilation scattering mediated by a weakly coupled neutral vector boson W^0 as suggested by various authors are recalculated in more detail. It is shown that the height of the resonance, which is to be expected at the mass-shell energies of W^0, can be determined exactly by renormalizing the second-order self-energy diagram of W^0. It is further shown, how the special form of the cross section could serve as a test for the correctness of a V-A ansatz in neutral current interactions. (auth)

32094 TREATMENT OF PAIRING IN SMALL SYSTEMS BY GREEN FUNCTIONS. Zawischa, D. (Univ., Heidelberg). Z. Phys., 194: 61-74(1966).

A finite system of fermions with pairing interaction is treated by the Green function method. It is shown that a finite number of "bound pairs" must be assumed to get the correct properties of the system in that region of the interaction strength where the BCS-solution is incorrect. Also the difference between $E_0(N+2) - E_0(N)$ and $E_0(N) - E_0(N-2)$, $E_0(N)$, being the ground state energy of the N-particle system, has to be considered. The formulas derived give an interpolation between the region where perturbation theory applies and the region of validity of the BCS-equations. (auth)

32095 APPROXIMATE CONSTRUCTION OF THE SCATTERING AMPLITUDE FROM MANDELSTAM REPRESENTATION AND ELASTIC UNITARITY. Klar, H.; Krueger, H. (Univ., Freiburg i. B.). Z. Phys., 194: 89-100(1966).

An approximate expression for the scattering amplitude is derived from the Mandelstam representation and the elastic unitarity. To demonstrate the procedure in the relativistic case $\pi-N$ scattering is considered, omitting spin and isospin for simplicity. Nonrelativistic potential scattering is discussed in detail. (auth)

32096 MEASUREMENT OF THE POLARIZATION OF THE RECOIL PROTON FROM THE PHOTOPRODUCTION OF NEUTRAL PIONS ON HYDROGEN IN THE REGION OF THE FIRST RESONANCE. I. Althoff, K. H.; Kramp, K.; Matthaey, H.; Piel, H. (Univ., Bonn). Z. Phys., 194: 135-43(1966).

The polarization of the recoil proton from the reactor $\gamma + p \rightarrow \pi^0 + p$ was measured using liquid helium as polarization analyzer. The photon energy was varied between 250 and 360 Mev, the pion angle (cm) between 58 and 100°. (auth)

32097 MEASUREMENT OF THE ANGULAR DISTRIBUTION OF THE POLARIZATION OF THE RECOIL PROTON FROM THE PHOTOPRODUCTION OF NEUTRAL PIONS ON HYDROGEN AT A PHOTON ENERGY OF 360 Mev. II. Althoff, K. H.; Kramp, K.; Matthaey, H.; Piel, H. (Univ., Bonn). Z. Phys., 194: 144-55(1966).

The angular distribution of the polarization of the recoil protons from the reaction $\gamma + p \rightarrow \pi^0 + p$ was measured at a photon energy of 360 Mev and at pion cm angles of 58°, 75°, 96° and 105°. The polarization of the protons was determined by the left to right ratio in scattering on a helium gas target. The trajectory of each scattered proton was measured by a system of spark chambers. (auth)

32098 CHERENKOV RADIATION OF ELECTRONS IN A THICK DIELECTRIC. Ulrich, Reinhard (Univ., Freiburg i. B.). Z. Phys., 194: 180-92(1966). (In German).

The Cherenkov radiation of an electron moving parallel to a dielectric boundary is calculated using Toraldo Di Francia's expansion of the electron field in a set of evanescent waves. The radiation field is composed of these waves which are refracted at the boundary. In contrast to a previous treatment of this problem by Linhart it is shown that in addition to the TM-waves TE-waves are produced of comparable energy. The angular and frequency distribution is discussed for both types of waves. (auth)

32099 ANOMALOUS LONG ANNIHILATION MEAN-LIVES OF POSITRONS IN SOME IONIC CRYSTALS. Paulin, Robert; Ambrosino, Georges (Institut National des Sciences et Technique Nucleaires, Saclay, France). 7p. (CONF-650721-18). ORAU. Gmelin, AED-CONF-65-211-18.

From Positron Annihilation Conference, Detroit.

The annihilation lifetime spectrum of positrons in different ionic crystals was measured with the help of classical "fast-slow" experimental device. A long mean-life ($\simeq 5.1 \pm 0.1\ 10^{-8}$s) was found in some oxides (Al_2O_3, BeO, MgO) with 12% intensity and in two fluorides (F_2Mg, F_2Ca) a little shorter but less abundant mean-life ($\simeq 3.3$ and $4.2\ 10^{-8}$s respectively). These results compared with the 3 γ annihilation probabilities measured do not permit however conclusions on the nature of the bound-state created (ortho-positronium or positronium bound with a negative ion). (auth)

32100 COMPARISON OF RESONANCE FORMULAS FOR THE (1236 Mev, 3/2) PION-NUCLEON RESONANCE. Deans, S. R.; Holladay, W. G. (Vanderbilt Univ., Nashville). 15p. (CONF-660209-5). ORAU. Gmelin, AED-CONF-66-023-5.

From Conference on Intermediate Energy Physics, Williamsburg, Va.

To obtain information on the energy dependence of relativistic particle resonances, for which no well-defined theory exists, a comparison among six commonly used expressions for the total cross section in the reaction $\pi^+ + p \rightarrow \pi^+ + p$ was made in the energy region between 38 and 307 Mev (pion lab kinetic energy). The parameters in these expressions were systematically varied until the best fit (minimum chi-square) to fifty points was achieved for each formula. It was found that a significant statistical, difference exists among some of the formulas used. (auth)

32101 THE PHYSICS OF POSITRON ANNIHILATION. DeBenedetti, S. (Carnegie Inst. of Tech., Pittsburgh).

23p. (CONF-650721-14). ORAU. Gmelin, AED-CONF-65-211-14.

From Positron Annihilation Conference, Detroit.

A survey of the development in the physics of positrons is presented. 63 references. (G.O.Y.)

32102 BACKWARD PROTON-DEUTERON ELASTIC SCATTERING FROM 1.0 TO 1.5 Bev. Coleman, E.; Heinz, R. M.; Overseth, O. E.; Pellett, D. E. (Univ. of Michigan, Ann Arbor). 8p. (CONF-660107-2). ORAU. Gmelin, AED-CONF-66-003-7.

From American Physical Society Meeting, New York.

The differential cross sections for backward elastic proton-deuteron scattering at 1.0, 1.3, and 1.5 Bev were measured, together with the differential cross section for forward elastic scattering at 2.0 Bev. (D.C.W.)

32103 EVIDENCE FOR A $\Sigma^- \eta$ ENHANCEMENT NEAR THRESHOLD. Cline, David; Olsson, Martin (Wisconsin Univ., Madison). 15p. (CONF-660107-41). ORAU. Gmelin, AED-CONF-66-003-91.

From American Physical Society Meeting, New York.

The reaction $K^- + n \rightarrow \Sigma^- + \eta,\eta \rightarrow$ neutrals is studied by scanning for K^--deuterium interactions with a spectator proton and a Σ^- in the final state. Preliminary results are presented from the parts of the experiment with K^- momentum at 920 Mev/c and at 1120 Mev/c. (B.G.D.)

32104 RADIATIVE DECAY OF THE MU MESON. Bogart, Elliot; DiCapua, Enrico; Strelzoff, Alan; Nemethy, Peter (Columbia Univ., New York). 41p. (CONF-651015-15). ORAU. Gmelin, AED-CONF-65-312-38.

From American Physical Society, Chicago.

The radiative decay $\mu^+ \rightarrow e^+ + \gamma + \nu_e + \bar{\nu}_\mu$ was investigated. The decay products e^+ and γ were observed at relative angles near 180° using scintillation counters and two 9 in. × 10 in. NaI crystals, which permitted the simultaneous measurement of the positron and gamma energies. The two-dimensional energy spectrum was obtained for approximately 900 events after subtraction of the background. This spectrum and the measured rate were compared with the prediction of a pure V-A theory; good agreement was obtained within the statistical errors. (D.C.W.)

32105 ANNIHILATION OF POSITRONS IN ARGON. Jones, G.; Orth, P. H. R. (Univ. of British Columbia, Vancouver). 12p. (CONF-650721-4). ORAU. Gmelin, AED-CONF-65-211-10.

From Positron Annihilation Conference, Detroit.

Results of calculations of elastic scattering cross sections and annihilation rates as a function of applied electric field are presented for positrons in argon. The scattering of positrons from the Hartree-Fock distribution of electrons in an argon atom is used as a model. An additional induced dipole polarization interaction is included. It is observed that such a model can yield annihilation rates of the same magnitude as the experimental values, but detailed agreement was not obtained. (A.G.W.)

Field Theory, Scattering Theory, and Symmetries

See also Elementary Particles and Radiations

Refer also to abstract 31910.

32106 (AD-634706) HIGH ENERGY BEHAVIOUR OF SCATTERING AMPLITUDES AND CROSS SECTIONS USING CROSSING SYMMETRY AND HOLOMORPHY IN TWO VARIABLES. Technical Report No. 532. Eden, R. J. (Maryland Univ., College Park. Dept. of Physics and Astronomy). Dec. 1965. 7p. CFSTI $1,00 cy, $0.50 mn.

An attempt is made to show how the relation for scattering amplitudes derived using crossing symmetry and hermitean analyticity in E can be combined with holomorphy in the variable t and temperedness in E within the domain of holomorphy. The method is a general one, but it is most spectacular in the neighborhood of the Greenberg-Low bound. (C.E.S.)

32107 (IC-66/48) GENERALIZED NONET REPRESENTATION OF SU(3) × SU(3) AND ITS APPLICATIONS. Bose, S. K. (International Centre for Theoretical Physics, Trieste (Italy)). May 1966. 17p. Dep. mn.

A class of representations of the non-chiral SU(3) ⊗ SU(3), is worked out. These consist of a sequence of self-conjugate representations of SU(3), starting always with a singlet and with each SU(3) representation occurring once. An analog of Gell-Mann-Okubo mass formula, valid for these representations of SU(3) ⊗ SU(3) is obtained. When applied to the lowest non-trivial representation, this formula correctly explains $\omega-\phi$ mixing, thus providing a justification of Okubo's "ansatz." Possible use of the next higher representation is indicated. From the same construction the corresponding unitary irreducible representations of SL(3,C) and T_8 × SU(3) are simultaneously obtained. (auth)

32108 (IC-66/59) CABIBBO ANGLE AND THE NINTH BARYON. Pradhan, T. (International Centre for Theoretical Physics, Trieste (Italy)). May 1966. 7p. Dep. mn.

Using Fubini-Furlan-Adler-Weisberger type sum rules it was shown by many workers that the renormalized $\Delta S = 0$ and $\Delta S = 1$ axial vector coupling constants are approximately equal if one uses the SU(3) ⊗ SU(3) algebra of integrated time components of vector and axial vector currents with the baryons belonging, in the exact symmetry limit, to the (8,1) + (1,8) representation. The Cabibbo cos θ and sin θ factors appearing in the matrix elements of the hadronic weak current cannot therefore be interpreted as renormalization effects due to strong interactions; these have to be taken as phenomenological factors in the hadronic weak current. It is shown that the situation is somewhat different if the baryons are taken to belong to the $(\bar{3},3) + (\bar{3},3)$ representation so that there is a nonet of them instead of an octet. The renormalized $\Delta S = 1$ axial vector coupling constant is then found to be appreciably smaller than the $\Delta S = 0$ axial vector coupling constant showing thereby that a substantial part of the Cabibbo factors can arise from strong interaction effects. It is shown that this result has much more general validity, can be obtained without any assumptions about D currents and without the necessity of using experimental d/f ratio. (M.O.W.)

32109 TWO-DIMENSIONAL SPINOR FIELDS IN RIEMANNIAN SPACE. Kramer, D.; Stephani, H. (Univ., Jena, Ger.). Acta Phys. Pol., 29: 379-86(Mar. 1966). (In German).

The bispinor formalism represented is covariant with respect to the random similarity transformations. With the Dirac matrices γ_μ as basic magnitudes the metric field equations were derived from a variational principle. From the invariance of the Lagrange function with respect to the similarity transformations there is no conservation law except the continuity equation; there is an identity between the Lagrange expressions so that the metric field equation can be reduced to the Einstein equations. (tr-auth)

32110 DERIVATION OF CONSERVED QUANTITIES FROM SYMMETRIES OF THE LAGRANGIAN IN FIELD THEORY. Boyer, Timothy H. (Harvard Univ., Cambridge, Mass.). Amer. J. Phys., 34: 475-8(June 1966).

A derivation of the conserved quantities arising from symmetries of the lagrangian density under continuous transformations is reviewed with an eye to brevity and clarity. The derivation is sufficiently general to include virtually all cases of interest in field theory. Also covered is a separate and very short derivation which is valid only in the special case, frequent in quantum field theory, of internal symmetries where the transformations are independent of space–time. Some sources of confusion and error in the published accounts of the problem are noted. (auth)

32111 OPERATOR GAUGE TRANSFORMATIONS AND GAUGE TRANSFORMATIONS OF THE THIRD KIND.

Gaisser, T. K. (Brown Univ., Providence). Amer. J. Phys., 34: 597-601(July 1966). (NYO–2262-110).

A connection between gauge transformations of the third kind and operator gauge transformations of the first and second kinds is shown to hold for the electron propagator and for the vertex function of quantum electrodynamics as well as for the photon propagator. A method for calculating the gauge change of any time ordered n-point function is indicated. (auth)

32112 CAUSALITY IN S-MATRIX THEORY. Peres, Asher (Israel Inst. of Tech., Haifa). Ann. Phys. (N.Y.), 37: 179-208(Apr. 1, 1966).

A few common sense requirements which any decent S-matrix must satisfy is discussed. First, it is required that if the initial state consists of wave packets colliding at time t', and the final state of wave packets colliding (when produced backwards) at time t", then the transition amplitude should be vanishingly small if t" < t'. Moreover, if there is an appreciable time delay (t" > t'), the latter should be interpretable as arising from the propagation of an unstable intermediate particle. The above requirements, which are readily generalized to multiple scattering processes, are sufficient to derive the pole structure of the S-matrix and the existence of antiparticles. However, maximal analyticity and crossing symmetry cannot be proved from these assumptions—they can only be postulated separately. (auth)

32113 THREE-PARTICLE PARTIAL WAVE AMPLITUDES AND UNITARITY CONDITIONS AT COMPLEX VALUES OF ANGULAR MOMENTUM. Anselm, A. A.; Azimov, Ya. I.; Danilov, G. S.; Dyatlov, I. T.; Gribov, V. N. (Ioffe Physico-Technical Inst., Leningrad). Ann. Phys., (N.Y.), 37: 227-63(Apr. 1, 1966).

An analytic continuation of three-particle production partial wave amplitudes f_{jm} in complex values of total angular momentum j is studied. In contrast to the two-particle case, there is no continuation of f_{jm} which decreases in the whole right half-plane of j. Nevertheless, at fixed values of pair energies of three particles it is possible to construct a unique continuation increasing slowly enough in the right half j-plane. If the amplitudes f_{jm} are studied in the whole three-particle physical region, it is necessary to consider at least six different analytic functions of j. This fact is a generalization of signature for the case of amplitudes f_{jm}. Each of the six continuations satisfies a simple unitarity condition in one of the pair energies at complex j. The integration domain in these unitarity conditions includes, generally speaking, the integration over nonphysical values of angles. These properties were obtained while investigating the simplest Feynman diagrams. However, as it follows from the derivation they are to be of a general character. The three-particle contribution to the unitarity condition for elastic scattering amplitude at complex j is also considered. This enables the study of the origin of Mandelstam branch points. However, the exact expression for the three-particle contribution can be written into the unitarity condition only in the case of some simplest diagrams. (auth)

32114 MASS SPLITTING AS A COVARIANT CONCEPT IN THE GENERALIZED POINCARE GROUP. Fulton, T.; Wess, J. (Univ. of Vienna). Ann. Phys. (N.Y.), 37: 271-302(Apr. 1, 1966).

Various consequences of the two thirty-six component momentum operators occurring in the generalized inhomogeneous Poincaré group ISL(6,C) are examined and discussed, in an effort to understand their physical significance and to discover whether they can be consistently dealt with. After a brief comparison of various properties and consequences of the recently proposed $\tilde{U}(12)$ group and ISL(6,C), the properties of the multicomponent momentum operator are examined in more detail. It is shown that coordinate frames exist in which the covariant and contragredient momenta have the same values, if certain subsidiary conditions (expressible as polynomial equations for the momenta covariant in ISL(6,C)) are imposed. Hypercharge, charge, total isotopic spin, and three four-momenta can be simultaneous observables with nonzero eigenvalues. The remaining six four-momenta have zero eigenvalues. The little group, corresponding to the situation where two four-momenta are not zero, is also obtained. As an illustration of this case, new covariant free quark equations are next obtained. Their solutions are shown to give unitary representations in Hilbert space and, in the physical world, to reduce to Dirac equations with different masses for the quarks of different strangeness. Equations are also postulated for the meson representation. They lead to the prediction of four scalar K mesons, in addition to the octet of pseudoscalar and nonet of vector mesons. It is next shown that the so-called "kinematic" mass operator, proposed earlier by the authors, is naturally arrived at from the discussion of free particle equations. A typical dynamical mass term responsible for the spin split of the masses is briefly discussed. The general form of the S matrix for quark-singlet scattering, its unitarity and electromagnetic form factors are also considered. Symmetry breaking is an essential concomitant of almost all groups which are relativistic extensions of SU(6). However, it is shown that it can be carried out at such a late stage of the analysis that the symmetry properties are reflected in various features of the results, such as number of particles in a multiplet, and the number and structure of invariants. Symmetry breaking is required to discuss the case of multiplets with nondegenerate mass in exactly the same sense as for those with degenerate masses. Surprisingly, the subsidiary conditions in the former are less stringent than those in the latter case. (auth)

32115 A RELATIVISTIC EXTENSION OF SU(6) SYMMETRY. Zimmermann, W. (New York Univ., N. Y.). Ann. Phys. (N.Y.), 37: 303-14(Apr. 1, 1966).

A new formulation of relativistic SU(6) symmetry is proposed which applies to the full lagrangian (including kinetic energy terms) and is consistent with the principles of quantum field theory. This symmetry requires the classification of particles according to SU(6) multiplets and yields the characteristic relations among bare coupling constants which are known from the phenomenological theories. While the bare masses within an SU(6) supermultiplet must be equal, the physical masses of different SU(3) multiplets are expected to split for interacting systems. In the formulation proposed the S-matrix is unitary. However, relativistic SU(6) symmetry of the lagrangian does not imply corresponding symmetry properties of the S-matrix. As examples the free sextet field and the sextet-sextet interactions are discussed. A lagrange formulation for free spin $\frac{3}{2}$ fields is given and generalized to an invariant description of the 56-component baryon field. (auth)

32116 INVARIANT MESON-SEXTET INTERACTIONS IN A RELATIVISTIC FORMULATION OF SU(6) SYMMETRY. Zimmermann, W. (New York Univ., N. Y.). Ann. Phys. (N.Y.)., 37: 315-32(Apr. 1, 1966).

In the framework of relativistic SU(6) symmetry the Yang-Mills method is applied to the gauge group of a sextet field. It is shown that invariance under coordinate dependent gauge transformations requires the introduction of meson fields with the correct spin, unitary spin, and parity assignments of the observed mesons. Moreover, a meson mass term may be introduced which is gauge invariant provided the gauge functions are restricted to solutions of a generalized Klein-Gordon equation. The general form of the meson-sextet interaction is discussed in detail. For simplicity the case of a sextet field is considered only; however, the extension to the case of meson-baryon interaction is possible. (auth)

32117 COMPLETE CONTINUITY OF KERNEL IN GENERALIZED POTENTIAL SCATTERING. I. SHORT-RANGE INTERACTION WITHOUT STRONG SINGULARITY. Tani, S. (New York Univ., N. Y.). Ann. Phys. (N.Y.), 37: 411-50(May 1966).

It is shown that the iteration of the kernel in the Lippmann-Schwinger equation is the basic manipulation by which a meaningful result is obtained for any finite strength of the potential, no matter whether the Born series converges or not. In order that this statement may be true the potential must be free from a long range tail and a strong

singularity. The conditions for a generalized potential, which can be nonlocal and/or energy-dependent, to have these properties when transformed into the configuration space are discussed directly in terms of its matrix element in momentum space. These conditions are interpreted as equivalent to the restriction that the potential decreases faster than $1/r^3$ at a large distance and is less singular than $1/r^2$ at the origin. It follows from these conditions that all the individual terms of the Born series as well as the traces of the kernel and its iteration to an arbitrarily higher order are bounded. (auth)

32118 COMPLETE CONTINUITY OF KERNEL IN GENERALIZED POTENTIAL SCATTERING. II. GENERALIZED FOURIER SERIES EXPANSION. Tani, S. (New York Univ., N. Y.). Ann. Phys. (N.Y.), 37: 451-86(May 1966).

The complete continuity of the kernel, which allows the approximation of a given potential by a sum of separable potentials, is established by a simple method, when the potential is free from a long range tail and a strong singularity as defined in Part I of this paper. Through the eigenfunction expansion, this completes the analytic continuation of the Born series required when the potential is strong. The use of the Padé approximant which was proposed recently is discussed in detail concerning its theoretical basis and a solid base for its validity was found, if its rank is suitably large; the relation of such an approximation with the Fredholm method is discussed. The possibility of unambiguous identification of the passage of the phase shift through $\frac{1}{2}\pi$ (modulo π) with a particular form factor (which causes a "resonance") is pointed out using the standing wave solution; and the analytic properties of the partial wave amplitude, derived by Weinberg for a local potential, are rederived for a generalized potential. (auth)

32119 GENERALIZED DIRAC THEORY. Krori, K. D. (Cotton Coll., Gauhati, India). Indian J. Pure Appl. Phys., 4: 212-13(May 1966).

The Dirac equation was generalized on the basis of a generalized affine connection proposed. This generalization introduces fields as a natural consequence into the equation. (auth)

32120 POLARIZATION PROPERTIES OF BOSON RADIATION. Bagrov, V. G. (Moscow State Univ.). Izv. Vyssh. Ucheb. Zaved., Fiz., No. 5, 121-7(1965). (In Russian).

A study is carried out of the polarization properties of the radiation of a boson in a magnetic field, and expressions are found for the integral intensity of the radiation of a boson and a fermion in a magnetic field, valid at arbitrary energies. (tr-auth)

32121 MASS OF A FUNDAMENTAL FERMION AND DEGENERACY OF THE VACUUM. Naumov, A. I. (Moscow State Univ.). Izv. Vyssh. Ucheb. Zaved., Fiz., No. 5, 137-44(1965). (In Russian).

An attempt is made to calculate the mass of a fundamental fermion ("nucleon") in the framework of the Heisenberg version of the unified nonlinear spinor theory of elementary particles. The guiding idea is of the existence of a connection between the helicity properties of the particles and their masses. It turns out that, for this hypothesis, it is necessary to take into account the possibility of the degeneracy of the vacuum of a system of interacting fields with respect to certain quantum numbers. A program is presented for constructing a realistic scheme of elementary particles, including their isotopic and strange properties. The possibility is briefly evaluated of eliminating from the nonlinear theory the divergences, while retaining the applicability, of a somewhat modified perturbation theory. (tr-auth)

32122 ELECTROMAGNETIC STRUCTURE OF ELEMENTARY PARTICLES. Didyk, Yu. K. (All-Union Correspondence Polytechnic Inst., USSR). Izv. Vyssh. Ucheb. Zaved., Fiz., No. 6, 9-15(1965). (In Russian).

Similarity criteria found on the basis of similarity and dimensionality methods are used as transformations with which the transition from one natural system of units to another is accomplished; this process determines the exclusion principles which serve for obtaining the order of similarity criteria in quantitative relations. Systems of units of the fermion and boson type are used for a very simple identification of the parameters of the corresponding elementary particles. The obtained set of electric and magnetic physical constants with length, area, and volume dimensionality are successfully unified in the framework of a vortical torus, the maximum dimensions of which are determined by the Compton wavelength and the minimum, by the classical radius of the particle. The vortical torus model is in agreement with the latest experimental data and permits particle-shell and particle-target phenomena in the scattering process to be predicted. (tr-auth)

32123 FOUR-DIMENSIONAL SYMMETRIC CANONICAL FORMALISM OF FIELD THEORY. Mitskevich, N. V. (Patrice Lanumba Univ., Moscow). Izv. Vyssh. Ucheb. Zaved., Fiz., No. 6, 87-92(1965).

A heuristic scheme is presented for transforming from classical mechanics into field theory. The basic role in this transformation is played by the division of time—exchanging the independent variable t with four independent variables x^μ. Instead of the coordinates of material points, the canonical coordinates of the continuous system are taken: instead of the field, the potentials of the fields being considered. Correspondingly, the time integrals are changed into four-dimensional integrals, the number of components of the canonical momentum is quadrupled in comparison with the number of canonical coordinates, etc. Integral values, e.g., energy, momentum, and angular momentum, are determined as integrals with respect to spatially similar hypersurfaces. Transformation of the Euler-Lagrange equations to the analogous four-dimensional symmetric hamiltonian equations in field theory is carried out. Results provide a single-values connection between classical and quantum entities such as energy-momentum and spin. (M.J.T.)

32124 THE U(n) ⊃ R(n) PROBLEM. [PART] I. Resnikoff, M. (Univ. of Maryland, College Park). Contract AFOSR 500-64. Nucl. Phys., 83: 632-8(1966).

The number of operators required to label the rows of an irreducible representation of U(n), in addition to those of the proper rotation group R(n), is calculated, both for the case of n non-zero rows of a Young tableau of U(n), and $m \leqq n$ non-zero rows. For the physical case of m = 3, these additional operators are constructed. (auth)

32125 CURRENTS AND SUM RULES IN VECTOR-MESON THEORY. Pocsik, G. (Roland Eoetvoes Univ., Budapest). Nuovo Cimento (10), 43A: 541-52(June 1, 1966).

A set of massive vector fields interacting with nonconserved currents is considered and from the positivity it is proved that: (1) The spectral functions are the coefficients of positive definite quadratic forms. (2) The nonvanishing of the equal-time charge-current density commutator is a general feature of the currents coupled to vector fields. (3) Mass-squared and inverse-mass-squared sum rules cannot be simultaneously valid. For the first possibility a simple model with particle mixing is presented. The results (2) and (3) lead to the conclusion that a large class of currents, e.g., the usual weak currents contradict the positivity provided than canonical quantization is used. A rough estimation shows that a strong self-interaction of the W-meson could explain the large W mass, as it was recently raised by Feinberg. Finally, various theories, in particular the vector mixing approximation, are examined from the point of view of the result (1) and in each case several mass inequalities are found. (auth)

32126 THOMAS-WIGNER PRECESSION OF POLARIZATION. Chakrabarti, A. (Ecole Polytechnique, Paris). Nuovo Cimento (10), 43A: 576-90(June 1, 1966).

A very simple derivation of the Thomas equation is given which makes explicit its relation to the canonical representation of the Poincaré group. The equations of motion of the longitudinal and total transverse polarizations are

derived. The equations are solved explicitly for some simple but important cases. Comparisons are made throughout with the BMT formalism. The possible precessional effects of an extra force term proposed by Liebowitz are examined. Care is taken to explain the canonical definition of polarization adopted and its consequences. The relation with the Michel-Wightman definition also is discussed. (auth)

32127 FIELD-THEORETICAL FORMULATION OF LEVINSON'S THEOREM. Hagen, C. R. (Univ. of Rochester, N. Y.). Nuovo Cimento (10), 43A: 597-614 (June 1, 1966). (UR-875-109).

A field-theoretical proof is given of a relativistic generalization of Levinson's theorem. Though the final form of this relation is in disagreement with an earlier attempt in this direction by Charap, a complete correspondence is shown to exist between the result obtained and that derived by Warnock on the basis of dispersion theory. It is demonstrated that the discrepancy between Charap's approach and that presented originates both in the technique used for the treatment of bound states as well as in the method of counting constraint equations and CDD poles. As a test of this work it is shown that there is complete consistency in the case of the Zachariasen model, independent of whether the bound state is elementary or composite. As an auxiliary result a useful representation for the reciprocal of the usual denomination function of dispersion theory is derived which includes the effect of inelastic channels. (auth)

32128 BREAKING OF SU_3 SYMMETRY IN A STRONG-COUPLING THEORY. von der Linden, F. J. M.; Dullemond, C. (Univ. van Nijmegen, Netherlands). Nuovo Cimento (10), 43A: 615-28 (June 1, 1966).

With the help of SU_3 symmetry and strong coupling of an octet of baryons and an octet of scalar mesons the mass breakings of the physical baryon octet and decuplet are computed. The bare baryon masses are assumed not to be broken, but the symmetry breaking is assumed to appear due to a breaking of the masses within the meson octet. In this way the mass breaking due to the medium strong SU_3-breaking interactions and due to the electromagnetic interaction are calculated. If it is required that the mass breakings in the octet due to the medium strong interactions agree with reality, then the ratio $\alpha = F/(F + D)$ is fixed and turns out to be about 0.3. (auth)

32129 SPONTANEOUS BREAKDOWN OF THE SU_3 SYMMETRY IN A FIELD-THEORETICAL APPROACH. Nagy, T. (Roland Eoetvoes Univ., Budapest). Nuovo Cimento (10), 43A: 654-64 (June 1, 1966).

Starting with an SU_3-symmetric lagrangian and assuming that SU_3-symmetry is not represented in the physical Hilbert space, mass formulas are obtained for baryons and pseudoscalar mesons in pole approximation. (auth)

32130 MODEL OF STRONGLY INTERACTING PARTICLES. Ram, B. (Univ. of North Carolina, Chapel Hill). Nuovo Cimento (10), 43A: 721-4 (June 1, 1966).

An oscillator (or noncompact group) model of strongly interacting particles is given. Mass formulas for baryons, baryon resonances, and vector mesons are derived. Possible existence of new pseudoscalar mesons is discussed. (auth)

32131 COLLINEAR PROCESSES IN $U_3 \times U_3$. Mahanta, P. (Imperial Coll. of Science and Tech., London). Nuovo Cimento (10), 43A: 725-30 (June 1, 1966).

The group $U_3 \times U_3$ which commutes with the Lorentz translation along a given direction is used to calculate the amplitudes for baryon-meson scattering in forward and backward directions and also in collinear processes involving production of members of the decuplet. Comparison with similar results obtained by using the SU_{6w} group was also made. (auth)

32132 MASS FORMULA WITHOUT SYMMETRY BREAKING. Formanek, J. (Faculty of Technical and Nuclear Physics, Prague). Nuovo Cimento (10), 43A: 741-51 (June 1, 1966).

An infinite-dimensional Lie algebra G containing the Poincaré algebra and SU_3 algebra as subalgebras is constructed. Particles with different masses can belong to the same irreducible representation of G. A nontrivial mass formula for an octet is obtained without breaking down G. The existence of the algebra G proves that the O'Raifeartaigh's theorem cannot be generalized to denumerable infinite-dimensional Lie algebras. (auth)

32133 RIGOROUS VERSION OF AN ARGUMENT BY COLEMAN. Pohlmeyer, K. (Univ., Hamburg). Nuovo Cimento (10), 43A: 762-6 (June 1, 1966).

It was shown by Coleman that if particles moving along the 3-axis are assumed to fall into representations of the hybrid U(6) algebra suggested by Dashen and Gell-Mann for describing collinear processes, this actually implies that the entire group $U(6) \times U(6)$ is an exact symmetry. These intuitive arguments are sharpened by using exact field-theoretical cluster properties, and hence a rigorous proof is found in the framework of general quantum field theory. (J.F.P.)

32134 LIMITING PROCEDURES FOR SINGULAR POTENTIALS. III. Cornille, H. (CERN, Geneva). Nuovo Cimento (10), 43A: 786-816 (June 21, 1966).

In previous works, for singular potentials, the validity of the use of the cut-off $\theta(r - \epsilon)$ has been established. It is shown that, in potential scattering, a sufficient condition for the use of nonsingular cut-off potentials $V(\lambda,r,\epsilon)$ is: i) $V(\lambda,r,\epsilon)$ for $r > 0$ and $0 \leq \epsilon \leq \epsilon_0$ is continuous in (r,ϵ) (or even weaker conditions), and V is well behaved when $r \to \infty$. ii) $V(\lambda,r,\epsilon) > 0$ for $0 \leq r \leq R_0$, $0 \leq \epsilon \leq \epsilon_0$ (R_0 independent of ϵ). If instead of ii) $V(\lambda,r,\epsilon)$ is attractive near the origin, the situation is more delicate but it turns out that the study of the roots of the cut-off-dependent wave function is the key in order to establish the validity of the procedure. There are two cases following whether the number of roots does not increase or increases when the cut-off decreases. In the first case the limit of the cut-off going to zero gives a solution (the regular physical solution or a singular solution) and in the second case the limit does not exist. In previous works the properties of the Fredholm formulation of cut-off-dependent solutions have been studied in the case $\lambda V(r)\theta(r - \epsilon)$. Here the possibility to extend these properties to other types of $V(\lambda,r,\epsilon)$ is studied. (auth)

32135 APPLICATION OF A MODIFIED DETERMINANTAL METHOD TO YUKAWA POTENTIAL SCATTERING. Smith, J. (Univ. of Copenhagen). Nuovo Cimento (10), 43A: 834-9 (June 21, 1966).

Using the modified determinantal method of Nath and Srivastava, the S, P and D wave effective-range values are calculated for the Yukawa potential. The results are then compared with the effective-range values predicted by the usual determinantal method and are found to be superior. (auth)

32136 EXACT SOLUTIONS FOR SOME SU_n-INVARIANT AMPLITUDES IN THE STATIC APPROXIMATION. Fairlie, B. D. (Univ. of Durham, Eng.). Nuovo Cimento (10), 43A: 857-64 (June 21, 1966).

Some new exact solutions are obtained for the elastic scattering of a particle transforming as a totally symmetric tensor with λ indices off a quark in SU_n in the approximations of a fixed quark target and two-particle unitarity. These solutions take a simple closed form in the case when λ is an integral multiple of n, and agree with known results for SU_2. This extension to SU_n is nontrivial, however, and involves a new technique. (auth)

32137 FREE PARAMETERS AND THE COMPOSITENESS CONDITIONS IN A PARTIAL-WAVE SCATTERING AMPLITUDE. Akiba, T. (Tohoku Univ., Sendai). Nuovo Cimento (10), 43A: 939-60 (June 21, 1966).

If only the unitarity and the analyticity in energy, but not the analyticity in angular momentum, are used from the principles of the S-matrix theory, a partial-wave amplitude may in general involve free parameters which represent the mass or the coupling constant of an elementary particle, or the Castillejo-Dalitz-Dyson ambiguity. The precise form in which these parameters appear is investigated, assuming a

suitable convergence at infinity of the generalized potentials and the existence of just one stable-particle pole. Discussion is given on the compositeness conditions that eliminate all free parameters and reduce scattering amplitudes to the one obeying the analyticity requirement in angular momentum. (auth)

32138 THE DASHEN-FRAUTSCHI METHOD AND PARITY-CONSERVING BARYON-MESON COUPLINGS. Diu, B. (CERN, Geneva); Rubinstein, H. R.; Van Royen, R. P. Nuovo Cimento (10), 43A: 961-94(June 21, 1966).

The Dashen-Frautschi method, which was successfully applied in particular to the mass differences among the baryon octet and decuplet, is used to treat parity-conserving SU_3-noninvariant baryon-meson couplings (the method being "universal," the same arguments hold for medium-strong SU_3 breaking and for parity-conserving weak interactions). The results are not very gratifying: 1) Both octet and 27-like coupling shifts are enhanced by comparable factors, which means in particular that the $\Delta I = 1/2$ rule for P-wave nonleptonic hyperon decays does not come out as a consequence of a dynamical enhancement, as it did in the S-wave (parity-violating) case. 2) Furthermore, if one nevertheless tries the hypothesis of octet dominance, the model investigated is incapable of fitting the experimental results concerning the relevant hyperon decays. As for medium-strong interactions, the situation is better: the calculated widths for the $3/2^+$ resonances are reasonable; however, the overall magnitude of the SU_3-breaking constants needed is so large as to make the use of first-order perturbation theory quite questionable. (auth)

32139 ON THE GELL-MANN–OKUBO RULE AS A CONSEQUENCE OF EIGHTFOLDEDNESS. Neville, D. E. (Univ. of California, Livermore). Nuovo Cimento (10), 43A: 995-1009(June 21, 1966). (UCRL-14533-T).

A qualitative explanation is given for the tendency of SU_3 symmetry-breaking calculations to favor symmetry-breaking terms transforming as an SU_3 representation of relatively low dimension N. Upper bounds falling off as $N^{-1/2}$ are derived for the norms of the factors containing the N-dependence in such calculations. Since small factors correlate with small symmetry violation, terms with N = 8 are favored. Octuplet dominance is only favored, not guaranteed by this result, because it is only an upper bound. A general discussion is given of methods for putting upper bounds on invariant sums over products of Clebsch-Gordan coefficients (i.e., on the analogs for higher groups of the 3n-J symbols for SU_2). (auth)

32140 S MATRIX WITH THE GENERALIZED POTENTIAL AND ITS ASYMPTOTIC BEHAVIOR. Igi, K.; Kawai, T. (Tokyo Univ. of Education). Nuovo Cimento (10), 43A: 1028-46(June 21, 1966).

Starting from the Mandelstam representation with the strip approximation, an integral equation is obtained for the signature of partial-wave amplitudes. In addition to a long-range generalized potential, a short-range generalized potential is introduced here in order to express the effects from distant singularities. High-energy effects at low momentum transfers can be automatically taken into account, if one solves the integral equation by employing the above potentials in a finite strip. A method is proposed to express the short-range potential in terms of low-energy resonances in the direct channel. This method may simplify a complete bootstrap to calculate both the low-energy resonances and the asymptotic behavior. As a preliminary application quantities like $\sigma(\infty)$, $\alpha_\rho'(0)$ and $\alpha_\rho(0)$ are calculated, by imposing the conditions $\alpha_\rho(0) = 1$ and using the low-energy resonance parameters as inputs. Both $\sigma(\infty)$ and $\alpha_\rho'(0)$ are calculated without assuming one of them and are in qualitative agreement with high-energy experiments. (auth)

32141 BEHAVIOR OF PARTIAL-WAVE AMPLITUDES FOR LARGE ANGULAR MOMENTA IN THE PRESENCE OF COULOMB FORCES. Klarsfeld, S. (Institut de Physique Nucleaire, Orsay, France). Nuovo Cimento (10), 43A: 1077-94(June 21, 1966).

A rigorous method due to Martin for proving the validity of the Born approximation at large (real) values of l is extended in order to account for an additional Coulomb interaction (attractive or repulsive). (auth)

32142 STRONGER FORM OF THE EDGE OF THE WEDGE THEOREM. Minguzzi, A. (Univ., Bologna. Istituto Nazionale di Fisica Nucleare, Bologna). Nuovo Cimento (10), 43A: 1126-30(June 21, 1966).

The theorem "Edge of the Wedge" is proved under conditions which are weaker than the microcausality and spectrum conditions. (auth)

32143 SU_3 SYMMETRY AS A BROKEN SU_8 SYMMETRY. Goldberg, H. (Univ. of Rochester, N. Y.). Nuovo Cimento (10), 43A: 1168-70(June 21, 1966).

The existence of weak interactions imposing $\Delta Q = \Delta S$ transitions is considered in the formalism of SU_8. The charged currents which induce $\Delta S = \Delta Q$ and $\Delta S = 2\Delta Q$ transitions are tabulated together with the generators of the corresponding rotations. It is concluded that a dynamics for the symmetry breaking may be suggested, and that the break may be considered to occur in two steps, according to the chain $SU_8 \supset R_8 \supset SU_3/Z_3$. Also, the nonexistence of quarks is implied by SU_8. (L.B.S.)

32144 EQUIVALENCE OF QUARK MODELS AND UNIVERSALITY PREDICTIONS FOR HIGH-ENERGY SCATTERING. Freund, P. G. O. (Univ. of Chicago). Contract AT(11-1)-264. Nuovo Cimento (10), 43A: 1171-4 (June 21, 1966).

It is shown that the predictions of quark models and universality for high-energy scattering are equivalent. In addition, it is shown that the additivity of quark-quark amplitudes within hadrons follows from the principle of universality of strong interactions. (L.B.S.)

32145 COMMENTS ON A PAPER BY R. A. BERG ON GENERAL SPIN EQUATIONS. Sachs, M. (Boston Univ.). Nuovo Cimento (10), 43A: 1175-7(June 21, 1966).

The one-to-one correspondence between the conservation equations and invariants of vector formalism and those of the spinor formalism was demonstrated. It is noted that this point was missed in a recent discussion by Berg (Nuovo Cimento, 42A: 148 (1966)) on the construction of representations of Lorentz-covariant fields with arbitrary spin, and that, in view of this correspondence, the form invariance in terms of E and B was not required in order to describe the electromagnetic phenomena. (L.B.S.)

32146 RELATIVISTIC FIELDS WITH SPACELIKE MOMENTUM SPECTRA. Hellman, W. S.; Rosen, J.; Roman, P. (Boston Univ.). Nuovo Cimento (10), 43A: 1188-90(June 21, 1966).

It is shown that a relativistic theory whose spectrum admits spacelike momenta contains conditions incompatible with canonical quantization. (L.B.S.)

32147 BOUND STATES OF A QUARK-ANTIQUARK SYSTEM. Hendry, A. W. (Rutherford High-Energy Lab., Chilton, Eng.). Nuovo Cimento (10), 43A: 1191-4 (June 21, 1966).

It was previously pointed out that if the ratio of the vecton mass to the quark mass is reasonably small the quarks may be considered as moving nonrelativistically in the potential well produced by the exchange of the vecton. This idea is examined in greater detail for the case of the mesons, which are regarded as the bound states of a potential due to the exchange of a vecton between a quark and an antiquark. The model is extended to consider the effect of exchanging an octet of vector mesons, as well as the unitary singlet vecton. (L.B.S.)

32148 CLASSIFICATION OF THE POSITIVE-PARITY MESONS IN SU_6. Montvay, I.; Nagy, T. (Roland Eoetvoes Univ., Budapest). Nuovo Cimento (10), 43A: 1195-1200 (June 21, 1966).

A single analysis was made of higher meson resonances of the $J^{PC} = 2^{++}$ nonet using SU_6 mass formulas which are well obeyed in the usual 35 multiplet of mesons and 56 multiplet of baryons. Mass relations are obtained for both 189 and 405 representations. The states with definite SU_4 properties are tabulated. (L.B.S.)

32149 ON AN ANALYSIS OF A PROPOSED ANALYTICITY TEST. **Albino, E. (Univ., Genoa); Bertero, M.; Viano, G. A. Nuovo Cimento (10), 43A: 1201-2(June 21, 1966).**

Remarks are given to comments on a previous paper (Campbell, Nuovo Cimento, 42A: 126 (1966)) concerning the computational procedure applied to the determination of analyticity properties of scattering amplitudes. (L.B.S.)

32150 A LAGRANGE FORMALISM AND THE RELATIVISTIC QUANTIZATION OF THE BARGMANN-WIGNER FIELDS. **Kamefuchi, S. (Tokyo Univ. of Education); Takahashi, Y. Nuovo Cimento (10), 44A: 1-16(July 1, 1966).**

A Lagrangian formalism of the Bargmann-Wigner fields with spin $\frac{1}{2}$, 1, and $\frac{3}{2}$ is proposed and the relativistic quantization of the above fields is performed. It is pointed out that the Umezawa-Visconti formula for the highest derivative in the Green function fails to be true in the case of a field with spin $\frac{3}{2}$. The electromagnetic interaction with the Bargmann-Wigner fields is also briefly discussed. (auth)

32151 BOOTSTRAP POSSIBILITIES OF A 70-PLET OF SU_6. **Mani, H. S.; Mohan, G.; Pande, L. K. (National Physical Lab., New Delhi). Nuovo Cimento (10), 44A: 47-56(July 1, 1966).**

The scattering of the 35-plet meson on a 70-plet baryon is considered in the static limit. The crossing matrix depends on a parameter v which is the ratio between the two types of coupling of 70 to 35 $\otimes$ 70. The best value for the parameter v, which indicates the possibility of bootstrap of 70-plet, is found to be -1. (auth)

32152 ON THE INVERSION PROBLEM IN THE λ PLANE. II. **Burdet, G.; Giffon, M.; Goldberg, J. (Univ., Lyon). Nuovo Cimento (10), 44A: 138-46(July 1, 1966).**

The inversion problem in the complex angular-momentum plane is treated for a class of potentials behaving near the origin more singularly than the centrifugal term. Equations of the Gel'fand and Levitan type are established which allow the potential to be constructed from the knowledge of the discrete spectrum in the complex angular-momentum plane for any k (linear momentum) such that Im $k \geq 0$. (auth)

32153 BOOTSTRAP CONDITIONS IN FIELD THEORY. **Deshpande, N. G. (Imperial Coll. of Science and Tech., London). Nuovo Cimento (10), 44A: 147-65(July 1, 1966).**

The behavior of field theory is studied in the limit of vanishing renormalization constants and the possibility that field theory admits solutions which are equivalent to the usual bootstrap solutions is shown based on the N/D method. The recent work of Gerstein and Deshpande on spin-zero mesons is extended, and it is shown that a consistent application of $Z_3 = 0$ and $Z_3\delta\mu^2 = 0$ conditions lead to a bootstrap behavior, and that these are necessary and sufficient conditions. The spinor field was further studied and it is found that if a further condition is imposed, the bootstrap behavior again follows. It is also suggested that vector mesons may show a similar behavior. In all three cases it is shown that the conditions imposed lead to zeros of the propagator and vertex poles. These vertex poles move to the elementary-particle mass in the limit, and replace it. This behavior is suggested as the condition for field theory bootstrap, and the correspondence of this to the usual definition is given. (auth)

32154 ON THE USE OF THE IMAGINARY-MASS REPRESENTATIONS OF THE POINCARE GROUP IN SCATTERING AMPLITUDES. **Hadjioannou, F. T. (CERN, Geneva). Nuovo Cimento (10), 44A: 185-212(July 1, 1966).**

The imaginary mass representations of the Poincaré group are used in the S-matrix theory in order to describe two-particle elastic-scattering amplitudes F(s,t) for fixed momentum transfer $t < 0$. In this first Part, I, the definitions of the various group-theoretical quantities are given in terms of scattering kinematics. At this stage a phase-shift analysis in the t-channel can be formulated in a precise covariant language using the imaginary-mass representations of the Poincaré group. This is the natural starting formula for further theoretical investigations. An expression is given for the fixed-t dispersion relations in the group-theoretical language. Analyticity of the scattering amplitude is stated in a simple and transparent manner, as a relation between real and imaginary parts. The asymptotic behavior at high energies is very simple and Regge-pole like. (auth)

32155 ALGEBRA OF CURRENTS BASED UPON THE SU_{W6} GROUP. **Khanna, M. P.; Okubo, S. (Univ. of Rochester, N. Y.). Nuovo Cimento (10), 44A: 229-38(July 1, 1966).**

Some consequences based upon the algebra of currents of the SU_{W6} group were investigated by a method originally due to Lee. In this way, almost all of the conventional SU_6 results can be reproduced without explicitly assuming its validity. (auth)

32156 COUPLING CONSTANTS AND MASS SHIFTS IN THE BROKEN SU_3 SYMMETRY. **Eberle, E. (Univ., Genoa. INFN, Genoa). Nuovo Cimento (10), 44A: 253-61(July 1, 1966).**

The terms violating the SU_3 symmetry in the coupling constants between elementary particles are written in terms of a particular set of invariants. The procedure which is described has the advantage of separating the contribution of each multiplet to the SU_3 violating part of the coupling constants. Moreover it suggests a possible simple connection between the mass- and coupling-shifts due to the SU_3 breaking; this can be checked in the case of the DBP coupling ($\frac{3}{2}^+$-baryon decay) and reasonable results are obtained. (auth)

32157 AXIAL-VECTOR COUPLING CONSTANT RENORMALIZATION IN β DECAY. **Mani, H. S.; Mohan, G.; Pande, L. K. (National Physical Lab., New Delhi). Nuovo Cimento (10), 44A: 265-9(July 1, 1966).**

An expression is presented for the renormalized axial-vector coupling constant in beta decay, which involves only the off-mass-shell pion-nucleon vertex. Numerical results are obtained using experimental data on $S_{\frac{1}{2}}$ and $P_{\frac{1}{2}}$ π-N phase shifts. (L.B.S.)

32158 ON THE STRUCTURE OF THE CLEBSCH-GORDAN SERIES FOR SEMI-SIMPLE LIE GROUPS. **Vitale, B. (Univ. of Wisconsin, Madison. Univ., Naples. INFN, Naples). Nuovo Cimento (10), 44A: 291-4(July 1, 1966).**

Conditions are defined for irreducible representations of semisimple Lie groups of rank two in order to satisfy certain requirements for the Clebsch-Gordan series. It is also shown how these conditions can be generalized to rank-three groups. The possibility of defining conditions for any semi-simple Lie group independently of any rank is briefly considered. (L.B.S.)

32159 APPROXIMATE SATURATION OF THE ALGEBRA OF MOMENTS. **Veneziano, G. (Univ., Florence). Nuovo Cimento (10), 44A: 295-8(July 1, 1966).**

A theorem on the approximate saturation of the dipole algebra within any finite set of states is proved, which prevents good electromagnetic predictions from current algebra. It is concluded that the difficulties arising from the theorem leave essentially two possibilities for moments of the time components: contributions from Schwinger terms symmetric in the unitary indices; and nonsaturability of commutation relations within a finite set of particles. (L.B.S.)

32160 DE SITTER MODEL FOR ELEMENTARY PARTICLES. **Prasad, R. (Institut Henri Poincare, Paris). Nuovo Cimento (10), 44A: 299-305(July 1, 1966).**

The embedding of isometric groups of motion which apply to elementary particles in curved Riemannian manifolds is investigated, considering the simplest possibility of embedding in space-time of constant curvature. $SO_{4,1}$,

called D^+, is adopted as the external event space and $SO_{3,2}$, called D^-, as the internal space, both embedded in $V_4(+++-)$. A parallel analysis is made for both de Sitter groups, by examining the Laplace-Beltrami operator acting on a Riemann manifold. (L.B.S.)

32161 LOCAL REPRESENTATIONS AND MASS SPECTRUM. Flato, M.; Sternheimer, D. (Institut Henri Poincare, Paris). Phys. Rev. Lett., 16: 1185-6(June 20, 1966).

The negative result by O'Raifeartaigh (Phys. Rev. 139: B1052 (1965)) which states that given any real Lie algebra containing the Poincaré Lie algebra and an irreducible representation of it in an Hilbert space so that $P_\mu P^\mu$ is self-adjoint, then if there exists one eigenvalue m of $P_\mu P^\mu$, it is all the spectrum, is discussed. A counter example is presented which might be of physical interest to the conjecture, and thereby clarify the situation. (J.F.P.)

32162 ANALYTICITY AS A USEFUL COMPUTATION TOOL. Schlessinger, L.; Schwartz, C. (Univ. of California, Berkeley). Phys. Rev. Lett., 16: 1173-4(June 20, 1966).

The solution of a potential scattering problem for negative (unphysical) values of the energy, E, and the analytic continuation of the numerical results to $E > 0$, which yields the actual phase shifts, are reported. Although this method has some advantages over the usual methods for solving the Schroedinger equation, it is anticipated that the real value of the approach will be realized in the study of three-body scattering and in relativistic (Bethe-Salpeter) equations. (J.F.P.)

32163 CURRENT-COMMUTATOR CONSTRAINTS ON THREE- AND FOUR-POINT FUNCTIONS. Cornwall, John M. (Univ. of California, Los Angeles). Phys. Rev. Lett., 16: 1174-7(June 20, 1966).

The general theory of current-commutator constraints on forward-scattering amplitudes is briefly discussed, and the constraints are given in the form of sum rules in the vertex function VVP, where V is a vector particle and P is a pseudoscalar particle. (J.F.P.)

32164 CONSISTENCY QUESTIONS RAISED BY SIMULTANEOUS MANDELSTAM AND ANGULAR-MOMENTUM ANALYTICITY. Goldberger, Marvin L.; Jones, C. Edward (Princeton Univ., N. J.). Contract AF49(638)-1545. Phys. Rev. Lett., 17: 105-7(July 11, 1966).

The consistency requirement imposed by simultaneous l-plane and Mandelstam analyticity of the elastic scattering amplitude for unequal-mass particles is considered. (L.B.S.)

32165 SYMMETRY OF THE STRESS TENSOR. McLennan, J. A. (Los Alamos Scientific Lab., N. Mex.). Physica, 32: 689-92(Apr. 1966).

The stress tensor for a medium with internal angular momentum is considered, and it is shown how a symmetric stress tensor can be formed. Construction of the symmetric tensor requires that the contribution to the linear momentum of a distribution of internal angular momentum be taken into account. (auth)

32166 THE OPERATOR METHOD FOR ANGULAR MOMENTUM AND SU_3. Van Eekelen, H. A. M.; Ruijgrok, Th. W. (Rijksuniversiteit, Utrecht). Physica, 32: 765-78(Apr. 1966).

It is well known how Schwinger's operator method can be used to construct all representations of the angular momentum operators. A brief account of this method is presented and it is shown to be very convenient for a short derivation of the general Clebsch-Gordan coefficients. The method is then applied to SU_3 and all representations are constructed. Only for a few special cases have we been able to find the Clebsch-Gordan coefficients of SU_3. (auth)

32167 MATRICES AND PROJECTION OPERATORS IN ABBREVIATED THEORIES FOR PARTICLES WITHOUT MASS. Beckers, J. (Univ., Liege). Physica, 32: 785-92(Apr. 1966).

It is shown that the matrix Γ_5, previously obtained in the abbreviated theory of spin one particles with zero mass, is intimately connected with the matrix β_5 of the Kemmer algebra. In the case of spin 1, this matrix plays a role similar to the matrix γ_5 for spin $\frac{1}{2}$ and is convenient to define the projection operators which achieve the abbreviation of the theory for $m = 0$. The case of an arbitrary spin s is also considered. (auth)

32168 IDENTIFICATION OF S-MATRIX ELEMENTS IN NEUTRAL PSEUDOSCALAR-PSEUDOVECTOR AND EXPONENTIAL THEORIES. Dixon, G. M. (Univ. of Exeter, Eng.). Proc. Phys. Soc. (London), 88: 629-39 (July 1966).

Chisholm has shown that a particular change of nucleon field variable in neutral pseudoscalar-pseudovector theory yields an interaction which is exponential in the meson field. The S-matrix elements for neutral pseudoscalar-pseudovector and exponential theories are written down with the help of Feynman graphs and are shown to be identical. This result provides an example of the general theorem stated by Chisholm that the S matrix is invariant under any change of variables which preserves the free field part of the lagrangian. It also emphasizes that the "equivalence" between pseudovector and pseudoscalar couplings is to first order only. (auth)

32169 COUPLING OF NON-COMPACT GROUP REPRESENTATIONS. Salam, A.; Strathdee, J. (Imperial Coll. of Science and Tech., London. International Centre for Theoretical Physics, Trieste, Italy). Proc. Roy. Soc. (London), Ser. A, 292: 314-21(May 31, 1966).

The problem of coupling three "most-degenerate" representations of an $SL(\nu,C)$ group is solved. It is shown that if $GL(\nu,C)$ represents a collinear subgroup of a noncompact rest-symmetry group $U(\nu,\nu)$, the number of amplitudes to be expected for a vertex function on the basis of collinear symmetry is infinite. (auth)

32170 DIBARYON STATES AND F/D RATIO. Kohmura, Toshitake (Tokyo Univ.). Progr. Theoret. Phys. (Kyoto), 35: 416-22(Mar. 1966).

Dibaryon states are investigated in the framework of the SU(3) symmetry. Probable bound states are shown to exist in triplet states of pn(deuteron), $\Sigma^+\Xi^0$ and $\Sigma^-\Xi^-$. A nucleon does not interact so strongly with a hyperon. The ratio F/D for which deuteron is most strongly bound is 2.16/3 which agrees well with its value established in the meson-baryon coupling. (auth)

32171 FOUR-PARTICLE SCATTERING IN NONRELATIVISTIC THEORY. II. Mishima, Nobuhiko (Tokai Univ., Hiratsuka, Japan); Takahashi, Yasutaro. Progr. Theoret. Phys. (Kyoto), 35: 440-51(Mar. 1966).

A reconstruction of the four-particle scattering theory so as to be useful in practical applications is presented. From this point of view, the integral equation for the four-particle scattering matrix, given in a previous paper is extended to a more useful one, in which the kernel is separated into two parts; one refers to the scattering matrix between an arbitrary three-particle subsystem and a free particle, and the other to the scattering matrix between two two-particle subsystems. By using these equations, as will be shown, the treatment of practical problems becomes quite convenient. As a case of special interest, a composite-composite particle scattering in the four-particle system is discussed by approximating the two two-particle subsystems by bound-state and/or resonance poles. (auth)

32172 VERTEX ZEROS AND LEVINSON'S THEOREM. Hayashi, Koichi (Tokyo Univ.). Progr. Theoret. Phys. (Kyoto), 35: 452-62(Mar. 1966).

Vertex zeros on the second Riemann sheet are investigated. It is shown that these zeros correspond to redundant poles or elementary particle poles of the total amplitude. The relations between these zeros and Levinson's theorem are discussed. (auth)

32173 IMPACT PARAMETER FORMALISM. II. HIGH-ENERGY ELASTIC SCATTERING. Adachi, Toshimi (Tokyo Metropolitan Technical Coll.). Progr. Theoret. Phys. (Kyoto), 35: 463-84(Mar. 1966).

The mathematical structure of the impact parameter formalism proposed by Kotani and Adachi is discussed. The formalism is regarded as a counterpart of the partial wave expansion of the scattering amplitude. An impact parameter amplitude is defined as a function of impact parameter and total energy. This amplitude has two characteristic features, corresponding to particle-like and wave-like pictures. The latter nature has not been taken into account in previous impact parameter formalisms. In order to investigate the character of the impact parameter amplitude, this formalism is applied to high energy elastic scattering. A phenomenological analysis of the diffraction scattering is characterized by two parameters. Various expressions for the impact parameter amplitudes which are connected with the large angle proton-proton scattering are derived. The absorption coefficients for each partial wave are obtained. The Lommel function of two variables is widely used in the diffraction scattering, just as it has been employed in the diffraction theory of classical light waves. (auth)

32174 IMPACT PARAMETER FORMALISM. III. STRONG ABSORPTION MODEL. Adachi, Toshimi (Tokyo Metropolitan Technical Coll.); Kotani, Tsuneyuki. Progr. Theoret. Phys. (Kyoto), 35: 485-507(Mar. 1966).

In order to understand the physical meaning of an impact parameter amplitude, the formalism proposed is applied to various strong absorption models. A simple black disc model with a sharp boundary is not self-consistent; that is, the total elastic cross section derived from the angular distribution is not equal to what is calculated from the impact parameter amplitude. This inconsistency is expressed as the violation of the unitarity relation. It disappears in the high energy limit, where the semiclassical particle picture is applicable. A general rule is given for getting consistent results even in the finite energy region. It is observed that the model proposed by Fernbach, Serber and Taylor contains the same inconsistency. On the other hand, a sharp cutoff-model with a sharp cutoff angular momentum involves no such difficulty. The strong interaction region expressed by this model has a diffuse edge with respect to the impact parameter. Thus, the concept of a radius of this region is introduced. It is pointed out that the so-called high energy approximation to the familiar partial-wave expansion of the scattering amplitude for large angular momenta does not include any limitation on the scattering angle. (auth)

32175 BARYON DECAYS AND UNITARY SYMMETRY. Yokoo, Yoshimatsu (Osaka Univ.). Progr. Theoret. Phys. (Kyoto), 35: 508-14(Mar. 1966).

Nonleptonic and leptonic decays of the baryons are quantitatively discussed on the basis of the current-current picture by introducing the axial vector current belonging to the 27-dimensional representation of SU(3) instead of the F-type one used in Cabibbo's theory. It is shown that the decay $\Sigma^+ \to n\pi^+$ proceeds through a pure P wave and that the P wave is larger than the S wave for the decay $\Sigma^+ \to p\pi^0$. The interaction types of the decays $\Lambda \to p + l^- + \bar{\nu}$ and $\Xi^- \to \Lambda + l^- + \bar{\nu}$ are predicted to be V−1.1A and V + 1.1A, respectively. Another interesting result is the predominance of the 27-dimensional representation part for the axial vector current. It is concluded that Cabibbo's currents are not the only ones possible to explain the semileptonic processes. (auth)

32176 INNER SYMMETRY IN BARYON STRUCTURES AND LEPTONIC DECAYS. Kobayashi, Tsunehiro (Waseda Univ., Tokyo); Machida, Shigeru; Nakagawa, Masami; Namiki, Mikio; Ohba, Ichiro. Progr. Theoret. Phys. (Kyoto), 35: 528-39(Mar. 1966).

Under the assumption that the baryon is composed of three subnuclear particles in a nonrelativistic bound state analogous to the nuclear structure, the possible inner symmetries of the baryon structure are discussed by comparing with some characteristic features of the leptonic decays, such as $n \to p$ and $\Lambda \to p$. First, under the charge independence, the characteristic parameters of the neutron β decay are expressed in terms of the nucleon structure constants. By comparing the parameters with experiments, it is concluded that the totally symmetric spin-unitary spin part is dominant in the nucleon structure. This is true in the baryon structures in the SU_3 symmetric case. Under the SU_3 invariance, the following relation between the β decays of neutron and Λ particle is also derived: $(G_A/G_V)_{\Lambda\to p} = (1/2) \times (G_A/G_V)_{n\to p} - 1/6 \simeq -0.76$, where $(G_A/G_V)_{n\to p} \simeq -1.185$ is used. The broken SU_3 symmetry is estimated by making use of the existing experiments on the β decay of Λ particle. Finally the decay rates for various leptonic decays are obtained from the theoretical values, $F \simeq 0.55$ and $D \simeq 0.65$, determined by the experimental value of $(G_A/G_V)_{n\to p}$ in the SU_3 symmetry case of the present theory. The results are consistent with the experiments. (auth)

32177 STRONG INTERACTION OF INTERMEDIATE VECTOR MESONS AND EXTREMELY HIGH-ENERGY PHENOMENA. Fujii, Kanji; Iwata, Kenzo; Tanaka, Hajime (Hokkaido Univ., Sapporo). Progr. Theoret. Phys. (Kyoto), 35: 562-3(Mar. 1966).

The possibility that the intermediate meson W mediating the weak interaction also participates in strong interactions and further that the W meson can be identified with the H quantum suggested in high energy physics by Hasegawa is discussed. (B.G.D.)

32178 A REMARK ON THE BARYON MAGNETIC MOMENTS. Yellin, Joel (Brookhaven National Lab., Upton, N. Y.). Progr. Theoret. Phys. (Kyoto), 35: 565(Mar. 1966). (BNL–9712).

A set of relations for the baryon magnetic moments, which arise purely from symmetry properties, is presented. (B.G.D.)

32179 REAL AND IMAGINARY AMPLITUDES IN HIGH-ENERGY ELASTIC SCATTERING. Sumi, Yoshio (Osaka Univ.). Progr. Theoret. Phys. (Kyoto), 35: 573-4 (Mar. 1966).

The assumptions on the origins of the first and second terms in the formula $(d\sigma/d\Omega) = (\sigma_T/4\pi)^2 p^2 e^{At} + (B/s)e^{-ap}\sin\theta$ for the angular dependence of high energy elastic cross sections presented by Orear (Phys. Letters 13, 190(1964)) are pointed out as contradictory with unitarity. (B.G.D.)

32180 ANALYTIC PROPERTY OF IMPACT PARAMETER AMPLITUDE. Adachi, Toshimi (Tokyo Metropolitan Technical Coll.); Kotani, Tsuneyuki. Progr. Theoret. Phys. (Kyoto), 35: 576-8(Mar. 1966).

An analytical property of the impact parameter amplitude is discussed, when the scattering amplitude is assumed to be in the Mandelstam form. (B.G.D.)

32181 N/D METHODS FOR MULTICHANNEL SCATTERING. Ida, Masakuni (Tokyo Univ.). Progr. Theoret. Phys. (Kyoto), 35: 692-704(Apr. 1966).

Two-particle multichannel scattering is investigated in a state which has a one-particle intermediate state. The elementarity or compositeness of this particle is reflected on the asymptotic behavior of various functions. The discussion is based on the decomposition of the partial wave scattering amplitude into its one-particle reducible and irreducible parts. The present approach, which applies a matrix N/D method to the latter part, is shown to be equivalent to Bjorken's N/D method for the full amplitude. Compositeness conditions for multichannel scattering are obtained by considering transitions from an elementary or intermediate type of solution to a composite one. Also given are some remarks on generalizing this work so as to include three-particle states. (auth)

32182 HOMOLOGICAL STUDY OF THE GENERALIZED SINGULAR FUNCTIONS. I. PRELIMINARY FORMULATION BASED MAINLY UPON THE THREE-POINT CASE. Minami, Masatsugu (Kyoto Univ.). Progr. Theoret. Phys. (Kyoto), 35: 705-37(Apr. 1966).

Källén's generalized singular functions $\Delta_n^+(x_1, x_2, \ldots x_n; a)$ is regarded as the inner products of suitably defined fundamental differential form and certain cocycles, hoping that various properties of $\Delta_n^+(x_1, x_2, \ldots x_n; a)$ may be reduced to those of the cocycles. Some elementary considerations are given for the three- and four-point cases. This viewpoint prompts us to consider other distributions than Δ_n^+ through

appropriate choices of cycles, and to study a duality between the position space and the momentum space. (auth)

32183 A REFORMULATION OF THE QUARK MODEL IN TERMS OF GEMISCH. Hara, Osamu (Nihon Univ., Tokyo). Progr. Theoret. Phys. (Kyoto), 35: 738-44(Apr. 1966).

It is shown that if we use the concept of Gemisch, it is possible to reformulate the quark model into a more consistent form which is free from difficulties such as the fractional baryonic number or the fractional electric charge, which are inherent to the quark model in its present form. (auth)

32184 $\Delta S = \Delta Q$ SEMI-LEPTONIC DECAYS AND CP VIOLATION. Tsai, S. Y. (Osaka Univ.). Progr. Theoret. Phys. (Kyoto), 35: 745-6(Apr. 1966).

An investigation of the leptonic decay of baryons and mesons is presented using Lee's model and unitary symmetry for strong interactions. (B.G.D.)

32185 PRESENT PHENOMENOLOGICAL STATUS OF THE REGGE POLE THEORY. Leader, E. (Univ. of California, Berkeley). Rev. Mod. Phys., 38: 476-82 (July 1966). (UCRL-16361).

An attempt is made to give an objective survey of the present status of the Regge-pole theory in relation to experiment. The analysis is restricted to elastic and charge-exchange scattering processes in the region of high energies and small momentum transfers. A strong distinction is made between strictly forward ($t = 0$) and nonforward ($t \lesssim 0$) processes. In discussing the latter, an attempt is made to examine the phenomenological validity of the so-called "factorization theorem," the proof of which depends critically upon the assumption of the Regge poles being simple poles. (auth)

32186 REGGE POLES IN THE POTENTIAL THEORY. I. ANALYTICAL PROPERTIES OF THE S MATRIX IN THE K PLANE. Stihi, M.; Velculescu, V. G. A. Studii Cercet. Fiz., 17: 71-100(1965).

A survey of potential theory is presented with emphasis on the bases for the introduction of the concepts of Regge pole and Regge trajectory in the complex plane of the orbital kinetic momentum. Various aspects of scattering on a spherically symmetric potential; Jost functions and solutions for s-waves; the analytic properties of the Jost function; the study of amplitude singularities by Martin's method; the connection between the discontinuity of the s-matrix along the cut, the s-matrix, and the potential; and the generalization for higher-order waves are considered. (TCO)

32187 EXPLICIT RELATION BETWEEN THE NONRELATIVISTIC PARTIAL WAVE AMPLITUDE AND THE TRAJECTORIES OF ITS POLES IN THE λ PLANE. Lomsadze, Yu. M.; Tokar, S. S. (Uzhgorod State Univ., Ukrainian SSR). Ukr. Fiz. Zh., 11: 465-70(1966). (In Ukrainian).

The nonrelativistic partial wave amplitude $f_\lambda(l,s)$ for scattering by the arbitrary twice continuously differentiable "physical" potentials $\lambda V(r)$ is considered. By means of a generalization of the Fubini method it is possible to find the asymptotic of the amplitude $f_\lambda(l,s)$ as $|\lambda| \to \infty$ along an arbitrary direction. Use of this asymptotic makes it possible to introduce Fourier's transformation of the function $F_\lambda(l,s)$ with respect to λ and after some manipulations to obtain an explicit expression for $f_\lambda(l,s)$ in terms of the trajectories of its poles $\lambda_n(l,s)$ and the residues $r_n(l,s)$ at these poles only. It follows in particular that the asymptotic of the amplitude $f_\lambda(l,s)$ as $s \to \infty$ is determined by the Born term completely. (auth)

32188 STRUCTURE OF THE λ PLANE OF PARTIAL AMPLITUDE IN THE NONRELATIVISTIC PROBLEM WITH NONLOCAL POTENTIAL. Khimich, I. V. (Uzhgorod State Univ., Ukrainian SSR). Ukr. Fiz. Zh., 11: 478-81(1966). (In Ukrainian).

It is shown that the partial amplitude $f_\lambda(l,p)$, determined from Schroedinger's equation with an arbitrary nonlocal spherically symmetrical potential satisfying certain conditions, is a meromorphic function in λ throughout the finite λ-plane. The position of all poles $\lambda_0(l,p)$ depends on the pulse modulus p. The localization of these poles with change in the energy E along the real axis from $-\infty$ to $+\infty$ is ascertained. (auth)

32189 MOTION OF SINGULARITIES OF A THEORETICAL FIELD PARTIAL AMPLITUDE IN A COMPLEX λ PLANE. Khimich, I. V. (Uzhgorod State Univ., Ukrainian SSR). Ukr. Fiz. Zh., 11: 482-90(1966). (In Ukrainian).

On the basis of an analysis of the multiparticle terms of the unitarity conditions, a detailed investigation was made of the motion of singularities of the three-particle partial wave amplitude $f_\lambda(j,t)$ in the complex λ-plane. (L.B.S.)

32190 ANALYTIC PROPERTIES OF CERTAIN VERTEX AMPLITUDES IN THE PERTURBATION THEORY. Fushchich, V. I. Ukr. Mat. Zh., 17: No. 3, 137-41(1965). (In Russian).

On the basis of the field theory, Kunio Yamamoto showed that the vertex amplitude, as a square function of external impulses $p_1^2 \equiv \bar{s}$ and $p_3^2 \equiv \bar{t}$, does not possess complex singularities if the square of the third external impulse is negative ($p_2^2 \equiv \bar{u} < 0$); he also derived the Mandelstam representation with respect to these variables for the case of $p_3^2 < 0$. Knowledge of the analytic properties of the vertex amplitudes of Feynman graphs allows a study of the dispersion structure and originating amplitudes in any arbitrary order of the perturbation theory for the desired class of graphs. The amplitude of the relatively simple graphs considered presented no Mandelstam representation if $\bar{u} > 0$. It is shown that the amplitudes corresponding to the graphs do not have complex singularities with respect to the variables $\bar{s}$ and $\bar{t}$ under certain limiting conditions concerning the mass of virtual particles and the square of the impulse p_2^2. (TTT)

32191 SPECTRAL REPRESENTATION FOR SINGLET AND TRIPLET GREEN'S FUNCTIONS. Wiegel, M. (Univ., Frankfurt am Main). Z. Phys., 193: 389-93(1966).

Spectral representations of special Green functions are given explicitly. The density correlation function $G_2(x_1\eta_1x_2\eta_2,\ x_1^+\eta_1'x_2^+\eta_2')$ and the function $G_2(x_1\eta_1x_2^-\eta_2,\ x_2\eta_1'x_2^-\eta_2')$ are considered. Coupling the field operators $\Psi^\tau(x,\eta)$, $\Psi(x,\eta)$ to singlet and triplet operators $A_{SM_sTT_3}(x)$, spectral representations for these G-functions are obtained. The formulas derived may be of use when studying the system of equations for the Green functions, which describe many particle systems from a microscopic point of view. (auth)

32192 RESONANT AND NONRESONANT CONTRIBUTIONS FROM UNPHYSICAL REGIONS IN DISPERSION RELATIONS. Sommer, G. (Freie Univ., Berlin). Z. Phys., 193: 426-38(1966).

Unphysical regions on the right hand cut in partial wave dispersion relations for a two-particle process $A + B \to A' + B'$ are expressed by measurable quantities, under the assumption that there is only one important 2-particle channel in the unphysical region. The solution is unique, if the phase shift δ_1 for the elastic scattering in the channel responsible for the appearance of the unphysical region takes a value between 0 and π at the physical threshold for $A + B \to A' + B'$. The difference between nonresonant ($\delta_1 \neq \pi/2$ in the unphysical region) and resonant contributions is briefly discussed. (auth)

32193 CONNECTION BETWEEN THE PHASE SHIFTS AND THE COEFFICIENTS OF THE M-MATRIX FOR THE ELASTIC SCATTERING OF SPIN 1 BY SPIN 0 PARTICLES. Fick, D. (Univ., Erlangen-Nuernberg, Ger.). Z. Phys., 194: 156-62(1966).

Explicit formulas for the M-matrix in terms of phase shifts and mixing parameters are derived for the case of spin 1 spin 0 elastic scattering. The formulas are applied to the case $l, l' \leqq 2$. (auth)

32194 PHENOMENOLOGICAL TREATMENT OF ELASTIC SCATTERING OF SPIN-1 PARTICLES ON SPIN-0 PARTICLES. Hofmann, H. M.; Fick, D. (Univ., Erlangen-Nuernberg, Ger.). Z. Phys., 194: 163-79(1966). (In German).

The elastic scattering of spin 1 particles by spin 0 particles is treated in terms of the Wolfenstein M-matrix. The purpose of these calculations is to find a method that allows vector and tensor polarization of a spin 1 particle beam scattered by a spin 0 target to be measured and to find out experiments that determine all parameters of the M-matrix. The scattering cross section for double and triple scattering was calculated. The discussion shows, that the use of a polarized ion source is much more favorable than the conventional double and triple scattering technique. (auth)

32195 CORAL GABLES CONFERENCES ON SYMMETRY PRINCIPLES AT HIGH ENERGY. Third Conference, January 19–21, 1966, Center For Theoretical Studies, University of Miami. Perlmutter, Arnold; Wojtaszek, Joseph; Sudarshan, George; Kursunoglu, Behram (eds.). A Series of Books in Physics. San Francisco, W. H. Freeman and Company, 1966. 288p. $6.50. (CONF-660105).

Separate abstracts are prepared for 17 of the 18 papers presented. One paper was previously included in NSA as 20:19541. (B.G.D.)

For abstracts of individual papers see: 32089, and 32196–32211.

32196 NONLEPTONIC DECAYS OF HADRONS. Nambu, Yoichiro (Univ.of Chicago). pp 2-11 of Symmetry Principles at High Energy. Perlmutter, Arnold; Wojtaszek, Joseph; Sudarshan, George; Kursunoglu, Behram (eds.). San Francisco, W. H. Freeman and Co., 1966.

The application of the partially conserved axial vector-current hypothesis to the nonleptonic decay of hyperons which leads not only to sum rules for both s and p wave amplitudes, but also determines their relative magnitudes is discussed. (B.G.D.)

32197 SYMMETRY AND WEAK INTERACTIONS. Cabibbo, N. (CERN, Geneva). pp 12-23 of Symmetry Principles at High Energy. Perlmutter, Arnold; Wojtaszek, Joseph; Sudarshan, George; Kursunoglu, Behram (eds.). San Francisco, W. H. Freeman and Co., 1966.

The application of symmetry theory to the understanding of the weak interactions of leptons is discussed. The structure of leptonic decays is investigated by analysis based on approximate SU(3) symmetry, the use of chiral SU(3) ⊗ SU(3) to obtain sum rules for axial coupling constants, and the use of zero energy theorems to connect axial and vector transitions. (B.G.D.)

32198 REMARKS ON THE QUARK MODEL AS A MAXIMAL PROBE OF CHIRAL SYMMETRIES. Marshak, R. E. (Univ. of Rochester, N. Y.). pp 38-47 of Symmetry Principles at High Energy. Perlmutter, Arnold; Wojtaszek, Joseph; Sudarshan, George; Kursunoglu, Behram (eds.). San Francisco, W. H. Freeman and Co., 1966.

Results obtained with approximate symmetry groups based on the quark model with chiral decomposition are reported. (B.G.D.)

32199 APPLICATIONS OF UNITARY REPRESENTATIONS OF SL(6,C) TO ELEMENTARY PARTICLES. Fronsdal, Christian (International Centre for Theoretical Physics, Trieste). pp 48-59 of Symmetry Principles at High Energy. Perlmutter, Arnold; Wojtaszek, Joseph; Sudarshan, George; Kursunoglu, Behram (eds.). San Francisco, W. H. Freeman and Co., 1966.

A brief discussion is presented on the physical basis for the relativistic extension of SU(6) and mathematical treatment of SL(6,C). The applications of SL(6,C) to elementary particles is emphasized. (B.G.D.)

32200 SPACE-TIME SYMMETRIES, SPACE-TIME U(3,3) AND MAGNETIC CHARGE. Kursunoglu, Behram (Univ. of Miami, Coral Gables, Fla.). pp 60-74 of Symmetry Principles at High Energy. Perlmutter, Arnold; Wojtaszek, Joseph; Sudarshan, George; Kursunoglu, Behram (eds.). San Francisco, W. H. Freeman and Co., 1966.

A new approach to particle physics using the proposal that all symmetry groups originate from the Lorentz transformation properties of dynamical variables is developed. The close relation between the photon and electric charge on one hand, and the dependence of the latter on the quantum numbers of strongly interacting particles on the other, is utilized as a starting point for the space-time origin of all symmetries. (B.G.D.)

32201 EXPERIMENTAL STATUS OF ELECTROMAGNETIC INTERACTIONS. Frisch, David (Massachusetts Inst. of Tech., Cambridge). pp 75-96 of Symmetry Principles at High Energy. Perlmutter, Arnold; Wojtaszek, Joseph; Sudarshan, George; Kursunoglu, Behram (eds.). San Francisco, W. H. Freeman and Co., 1966.

A review of the experimental status of electromagnetism, plus a discussion of a few of many new prospects are presented. (B.G.D.)

32202 QUARKS, SYMMETRIES, SYMMETRY BREAKING, AND THE JOHNSON-TREIMAN RELATIONS. Lipkin, Harry J. (Weizmann Inst. of Science, Rehovoth, Israel). pp 97-117 of Symmetry Principles at High Energy. Perlmutter, Arnold; Wojtaszek, Joseph; Sudarshan, George; Kursunoglu, Behram (eds.). San Francisco, W. H. Freeman and Co., 1966.

Two apparently different types of assumptions which lead to the same results not only for the magnetic moment and the Johnson-Treiman relations but also give the M1 dominance of N* photoproduction, the Stodolsky-Sakurai model for vector meson exchange, and many predictions for collinear two-body scattering processes are discussed. These assumptions were the SU(6) treatments and derivations based on the quark model. (B.G.D.)

32203 MESON SPECTRUM AND INTERNAL DYNAMICS. Sinanoglu, Oktay (Univ. of Miami, Coral Gables, Fla.). pp 118-36 of Symmetry Principles at High Energy. Perlmutter, Arnold; Wojtaszek, Joseph; Sudarshan, George; Kursunoglu, Behram (eds.). San Francisco, W. H. Freeman and Co., 1966.

The rest frame problem of the quantum numbers and mass spectrum of static mesons is investigated. In particular: the quantum number assignments of mesons, comparison with data and prediction of missing ones; the general features of an effective quark-antiquark ($q\bar{q}$) interaction indicated by the spectrum; mesons as ($q\bar{q}$) Regge recurrences; and the derivation of a mass formula applicable to higher mesons are discussed. (B.G.D.)

32204 SOME ALGEBRAIC COMMENTS ON REGGE RECURRENCES. Gotsman, E.; Ne'eman, Y. (Tel-Aviv Univ., Israel). pp 137-49 of Symmetry Principles at High Energy. Perlmutter, Arnold; Wojtaszek, Joseph; Sudarshan, George; Kursunoglu, Behram (eds.). San Francisco, W. H. Freeman and Co., 1966.

The analytical Regge poles structure of the Coulomb potential, the 3-dimensional oscillator, and the signature appearing in exchange potentials are reviewed. The system of spectrum generating algebras (SGA) corresponding to the examples mentioned above is discussed. The various Regge noncompact subalgebras whose unitary representations provide the sequence of recurring bound states are identified. Finally, the connections with the hadron approximate symmetry algebras and SGA's are discussed. (B.G.D.)

32205 ASSIGNMENT OF SPIN 2^+ MESONS AND THE NATURE OF QUARK-QUARK INTERACTIONS. Meshkov, Sydney (National Bureau of Standards, Washington, D. C.). pp 150-67 of Symmetry Principles at High Energy. Perlmutter, Arnold; Wojtaszek, Joseph; Sudarshan, George; Kursunoglu, Behram (eds.). San Francisco, W. H. Freeman and Co., 1966.

An attempt is made to distinguish between two schemes of meson quark models by looking at the decay widths of the various mesons. (B.G.D.)

32206 ALGEBRA OF CURRENT COMPONENTS AT INFINITE MOMENTUM. Dashen, Roger F.; Gell-Mann,

Murray (California Inst. of Tech., Pasadena). pp 168-89 of Symmetry Principles at High Energy. Perlmutter, Arnold; Wojtaszek, Joseph; Sudarshan, George; Kursunoglu, Behram (eds.). San Francisco, W. H. Freeman and Co., 1966.

A progress report on some incomplete investigations of sum rules and broken symmetry is presented. A description of hadrons is also presented. (B.G.D.)

32207 SYMMETRY OF THE STRONG COUPLING THEORY. Goebel, C. J. (Univ. of Wisconsin, Madison); Cook, T.; Sakita, B. pp 190-202 of Symmetry Principles at High Energy. Perlmutter, Arnold; Wojtaszek, Joseph; Sudarshan, George; Kursunoglu, Behram (eds.). San Francisco, W. H. Freeman and Co., 1966.

It is shown that the origin of the strong coupling symmetry is closely tied with the structure of the dynamical system (meson-baryon system in the static limit) and with the dynamical conditions (crossing symmetry, unitarity relation, and analyticity), so that the symmetry would not hold otherwise. The symmetry of the strong coupling theory is discussed and some preliminary results are presented. (B.G.D.)

32208 BOOTSTRAP INTERPRETATION OF SU(6). Capps, Richard H. (Northwestern Univ., Evanston, Ill.). pp 220-32 of Symmetry Principles at High Energy. Perlmutter, Arnold; Wojtaszek, Joseph; Sudarshan, George; Kursunoglu, Behram (eds.). San Francisco, W. H. Freeman and Co., 1966.

A few facts are presented which illustrate the interpretation of SU(6) that is natural in bootstrap models. Only the baryon states are discussed. (B.G.D.)

32209 MAGNETIC CHARGE AND QUANTUM FIELD THEORY. Schwinger, Julian (Harvard Univ., Cambridge, Mass.). pp 233-48 of Symmetry Principles at High Energy. Perlmutter, Arnold; Wojtaszek, Joseph; Sudarshan, George; Kursunoglu, Behram (eds.). San Francisco, W. H. Freeman and Co., 1966.

A review of Dirac's original treatment of magnetic charge and the charge quantization condition is presented. The compatibility of the magnetic charge concept with the principles of relativistic quantum field theory is discussed. (B.G.D.)

32210 NONCOMPACT GROUPS IN PARTICLE PHYSICS. Sudarshan, E. C. G. (Syracuse Univ., N. Y.). pp 249-62 of Symmetry Principles at High Energy. Perlmutter, Arnold; Wojtaszek, Joseph; Sudarshan, George; Kursunoglu, Behram (eds.). San Francisco, W. H. Freeman and Co., 1966.

The formulation of particle physics in terms of its characteristic noninvariance groups is discussed. (B.G.D.)

32211 HADRON MATRIX MECHANICS. Ne'eman, Yuval (Tel-Aviv Univ., Israel). pp 263-74 of Symmetry Principles at High Energy. Perlmutter, Arnold; Wojtaszek, Joseph; Sudarshan, George; Kursunoglu, Behram (eds.). San Francisco, W. H. Freeman and Co., 1966.

A brief outline is presented on the general development of elementary particle physics. Topics included are hadron matrix mechanics, status of the approximate symmetry algebras, sum rules due to transition operator algebras, and the hadron spectrum generating algebra. (B.G.D.)

32212 FOUNDATIONS OF THE BOOTSTRAP THEORY. Brout, R.; Englert, F.; Stern, H. (Univ. Libre, Brussels). 15p. (CONF-660107-44). ORAU. Gmelin, AED-CONF-66-003-103.

From American Physical Society Meeting, New York.

The bootstrap equations are presented as a sum of generalized ladder graphs. Beginning with an initial small attractive interaction v, one opens up each interaction into a ladder of interactions in an infinite iterative procedure. Equations are produced which allow the limit $v \to 0$. The resulting self-consistent equations are examined for bound-state solutions and a procedure for the solution is discussed. All integrals converge through the presence of self-consistent form factors. It is shown how to reduce the system to the N/D pole approximation and hence how one loses convergence. The results are discussed in terms of vacuum instability, possible additional ghosts in a Yukawa theory with bound states, the vanishing of Z_1 and Z_3. (auth)

32213 ISOTOPIC SPACE, COMPLEX CONJUGATION, AND U_3 SYMMETRY FOR PARTICLES. Teitler, S. (Naval Research Lab., Washington, D. C.). 15p. (CONF-650653-21). ORAU.

From American Physical Society, Summer Meeting, New York.

The inherent U_4 symmetry over spinor spaces of the regular decomposition indicated previously is discussed from the viewpoint of a single spinor space. It is noted that this symmetry does not yet include isotopic spin. Isotopic space is introduced by considering that the space-time vectors and its vector Clifford algebra are imbedded in the algebra of a six dimensional Euclidean space. Three of the latter's dimensions are identified with ordinary space, and three are identified with isotopic space. The time vector corresponds to the pseudoscalar element in isospace and the imaginary unit is expressed as a linear combination of the bivectors in isospace. The relation among complex conjugation, time inversion and space inversion is thereby clarified. Some comments on the application of these ideas to particle symmetry discussions are made. In particular one obtains as the first extension of the SU_2 symmetry of isotopic spin, a U_3 symmetry for particles. (auth)

32214 LORENTZ EQUIVALENCE, UNITARY SYMMETRY, AND SPIN UNITARY SYMMETRY. Teitler, S. (Naval Research Lab., Washington, D. C.). 14p. (CONF-650653-20). ORAU.

From American Physical Society, Summer Meeting, New York.

The enumeration and classification of the minimal ideals (spinor spaces) of the vector Clifford algebra generated from the vector basis of Lorentz space time obtained previously are used in a discussion of equivalence mappings among these minimal ideals. Lorentz equivalence is defined as an equivalence mapping which possesses Lorentz symmetry. The concept of regular decomposition is introduced by which any element of the complete algebra is expressed in terms of a complete set of minimal ideals or spinor spaces. A regular current density which is invariant under unitary symmetry U(4) among the spinor spaces of the regular decomposition is defined. The spin unitary symmetry within a spinor space under which the spinor current density is invariant is discussed. (auth)

32215 BARYONS, LEPTONS, AND ISOTOPIC SPINOR MODULATION. Teitler, S. (Naval Research Lab., Washington, D. C.). 20p. (CONF-650653-22). ORAU.

From American Physical Society, Summer Meeting, New York.

The space-time structure of ordinary spinors expressed in terms of the minimal ideals of the vector Clifford algebra C_{16} generated with the basis vectors of Lorentz space-time is reviewed. The model of isospace and ordinary space used previously in the imbedding of C_{16} in a higher algebra is considered further. Isotopic spinors are introduced and it is specified that they further entwine isospace and space-time so as to emphasize that isospace is not to be considered as an ad hoc space independent of space-time. The isospinors are used to modulate various principal fields. In particular the baryons are assigned as principally standard-type minimal ideal spinors whereas the leptons are assigned as principally of the Weyl-type. The significance of these assignments in the understanding of the two neutrino problem is indicated. (auth)

32216 STRUCTURE OF 4-SPINORS. Teitler, S. (Naval Research Lab., Washington, D. C.). 28p. (CONF-650653-23). ORAU.

From American Physical Society, Summer Meeting, New York.

The possible underlying spinor spaces used in the description of Dirac 4-spinors are enumerated and classified within the framework of vector Clifford algebra. The relation with the usual matrix formulation is reviewed. Proper Lorentz transformation, space and time inversions

are described in the Clifford algebra formalism. A representation independent definition of charge conjugation is given. (auth)

Fluid Physics and Thermodynamics

See also Plasma Physics and Thermonuclear Processes

Refer also to abstracts 31724 and 32740.

32217 (N-65-33713) EXPERIMENTS WITH MAGNETOHYDRODYNAMICALLY SUPPORTED SHOCK LAYERS. Locke, E.; Petschek, H. E.; Rose, P. H. (Avco-Everett Research Lab., Everett, Mass.). July 1964. Contract NASw-748. 36p. (NASA-CR-58153). CFSTI $2.00 cy, $0.50 mn.

Shock tube experiments were performed to quantitatively determine the interaction of a hypersonic flow with the magnetic field of a straight current-carrying wire oriented perpendicular to the flow direction. The interaction which takes place in a thin layer behind a detached shock wave is subject to the following restrictions: (1) negligible conductivity upstream of the shock; (2) low magnetic Reynolds number and scaler-conductivity in the shock layer. The straight wire geometry under these restrictions has been analyzed theoretically by Levy and Petschek. The analysis, which is briefly reviewed, predicts the location of a thin shock layer which is concentric with the wire. Most of the experimental work was performed in a 50--50 mixture of argon and oxygen, at an initial pressure of 1 mm Hg, and in a range of shock velocities between 4.3 and 6 mm/μsec. Data were obtained by observing the flow luminosity, using an image converter and mirror camera looking both perpendicular to and along the wire. A circular shock front was observed to stand up to $5\frac{1}{2}$ cm in front of a 1 cm radius cylinder producing the magnetic field. (STAR)

32218 (NYO-1480-29) MAGNETOHYDRODYNAMIC SHOCK RELATIONS IN NONALIGNED FLOWS. Lynn, Y. M. (Courant Inst. of Mathematical Sciences, New York Univ., N. Y.). Sept. 1, 1965. Contract AT(30-1)-1480. 101p. (MF-47). Dep. mn. CFSTI $4.00 cy, $0.75 mn.

The transition solution across a plane magnetohydrodynamic shock of finite strength in nonaligned flows in a perfect gas is investigated. A unified point of view is taken to analyze shocks in both unsteady one-dimensional flows and steady two-dimensional flows. Sets of conversion formulas connecting pertinent parameters in these two cases are given. A convenient parametric representation is presented of the shock solution from which an analytical solution expressed in terms of any desirable shock strength parameter can be readily obtained by performing a straightforward calculation. Major emphasis is then placed on the analytical and numerical solutions in terms of the flow deflection angle across the shock, the parameter most often prescribed in steady two-dimensional flows; entire ranges of upstream parameters are covered. Limiting solutions for several special cases are derived. Analytical solutions in terms of the magnetic field deflection angle across the shock are also given. The connection of the present general solution with several other major results in the literature is shown. Dynamical stability criteria associated with general magnetohydrodynamic shocks are discussed. (auth)

32219 (SCL-DC-66-2) SHOCK PULSE COMPUTER. Jacobson, R. S. (Sandia Corp., Livermore, Calif.). Apr. 1966. Contract AT(29-1)-789. 20p. CFSTI $1.95.

A Shock Pulse Computer was designed which enables easy determination of a number of mechanical-shock test parameters. The computer may be used for square, half-sine, triangular, haversine, and parabolic-cusp pulses. Pulses involving no rebound may be symmetrical or skewed; those involving rebound must be symmetrical. (auth)

32220 (UCRL-14912-T) A GENERAL THEORY FOR THE NUMERICAL SOLUTION OF THE EQUATIONS OF HYDRODYNAMICS. Noh, William F. (Lawrence Radiation Lab., Univ. of California, Livermore). May 6, 1966. Contract W-7405-eng-48. 35p. Dep. mn. CFSTI $2.00 cy, $0.50 mn.

A numerical procedure is presented (which is adaptable to most difference methods) in which the difference equations which are valid in the neighborhood of the contact discontinuity and which are completely consistent with the difference equations used away from the contact surface are derived. In addition, the method determines the position of the contact by explicitly invoking the conditions of continuity of pressure and continuity of the normal component of velocity. (auth)

32221 STEADY HYDROMAGNETIC FLOW IN A CHANNEL WITH POROUS WALLS IN THE PRESENCE OF A TRANSVERSE MAGNETIC FIELD. Agrawal, K. M.; Agrawal, J. C. Agra Univ. J. Res., 13: No. 1, 57-63(1964).

The problem of steady flow of an electrically conducting, incompressible, viscous fluid of constant electric and magnetic properties in the space between two parallel, porous, infinite plane walls in the presence of a transverse magnetic field was studied. The general magnetohydrodynamic equations are simplified by the conditions of the problem to mainly three equations. Two of these equations are coupled for the velocity and the magnetic field and are capable of an exact solution. The third gives the variation of pressure. (auth)

32222 NOTE ON THE STEADY MHD FLOW IN AN ANNULAR CHANNEL. Ray, M.; Agrawal, J. C. (Agra Coll., India). Agra Univ. J. Res., 13: No. 2, 1-3(1964).

The radial and axial pressure variations are studied in the case of a steady hydromagnetic flow of an incompressible fluid in an annular channel bounded by two infinitely long coaxial cylinders whose walls are porous and are capable of injecting or sucking in the fluid. It was concluded that the radial pressure variation, unlike that in the absence of magnetic field as reported by Berman depends on the direction of the cross flow. (Indian Science Abstr.)

32223 USE OF A RADIOISOTOPE TO DEMONSTRATE THE FIXATION OF ELECTRONS ON AN ELECTRONEGATIVE GAS. Debiesse, Jean; von Engel, A.; Klein, Siegfried (Institut National des Sciences Nucleaires, Saclay, France). Compt. Rend., Ser. B, 262: 1121-4(Apr. 25, 1966). (In French).

The mean probability of the attachment of the electrons of a flame on an electronegative gas was determined with a radioactive tracer in the medium. This new technique permits measurements and is rich in possibilities for the study of ionized gases and plasmas. (tr-auth)

32224 SPATIO-TEMPORAL DISTRIBUTION OF THE INITIAL BRILLIANCE OF A LASER DISCHARGE IN AIR. Capet, Maurice; Chalmeton, Vincent; Papoular, Renaud (EURATOM-CEA, Fontenay-aux-Roses, France). Compt. Rend., Ser. B, 262: 1125-8(Apr. 25, 1966). (In French).

With the use of a photomultiplier preceded by a movable shutter, an initial impulse and a pulse attributed to the passage of a shock wave was distinguished in the luminescence emission of a laser discharge. The detailed study of the initial pulse makes it possible to define the geometric distribution of the brilliance of the discharge during the primary phase of its evolution. (tr-auth)

32225 NOTE ON RELATIVISTIC THERMODYNAMICS. Penney, R. (Ford Motor Co., Dearborn, Mich.). Nuovo Cimento (10), 43A: 911-18(June 21, 1966).

It is shown by detailed calculation that the usual Lorentz-transformation formula for thermodynamic work is not incorrect as recently claimed by Arzeliès. The defects of Arzeliès' calculations are corrected and explained. (auth)

32226 MAGNETOHYDRODYNAMIC CHANNEL ENTRANCE FLOW WITH PARABOLIC VELOCITY AT THE ENTRY. Hwang, C. L.; Li, K. C.; Fan, L. T. (Kansas

State Univ., Manhattan). Phys. Fluids, 9: 1134-40 (June 1966).

A finite difference analysis is employed to investigate the laminar magnetohydrodynamic flow in the entrance region of a flat channel. The velocity is assumed to be parabolic (nonmagnetohydrodynamic fully developed) at the entry and develops to Hartmann velocity in this magnetohydrodynamic entrance region. Velocity profiles, entrance lengths, and pressure drops are numerically computed at values of the Hartmann number of 2.5, 4, 10, and 50. Values of the entrance length computed are compared with the only available results by Maciulaitis and Loeffler. The comparison shows a substantial difference. (auth)

32227 HAMILTON'S PRINCIPLE FOR FLUIDS. Penfield, Paul Jr. (Massachusetts Inst. of Tech., Cambridge). Phys. Fluids, 9: 1184-94(June 1966).

Hamilton's principle is used to derive the force equation for both nonrelativistic and relativistic flow of a compressible, one-species, inviscid fluid. Rotational flow is predicted by use of Lin's constraint. Lin's constraint is given a physical interpretation and found to be considerably simplified by use of four-dimensional notation. (auth)

32228 HAMILTON'S PRINCIPLE FOR ELECTROMAGNETIC FLUIDS. Penfield, Paul Jr.; Haus, Hermann A. (Massachusetts Inst. of Tech., Cambridge). Phys. Fluids, 9: 1195-1204(June 1966).

Hamilton's principle is used to derive the force equation for both nonrelativistic and relativistic flow of a compressible, inviscid fluid with polarization and magnetization. The resulting expression is used to settle the long-standing controversy concerning the electromagnetic momentum. The derivation is based on the formulation of Hamilton's principle for ordinary fluids. (auth)

32229 CARTESIAN TENSOR FORM OF THE MAGNETOHYDRODYNAMIC WAVE EQUATION. Kraut, Edgar A. (Univ. of California, Los Angeles). Phys. Fluids, 9: 1256-7(June 1966).

The magnetohydrodynamic wave equation for a compressible infinitely conducting fluid is formulated in Cartesian tensor form. It is shown that the resulting fourth rank Cartesian tensor is singular and thus has no inverse. (auth)

32230 APPLICATION OF THE FADDEEV EQUATIONS TO THE CALCULATION OF THE QUANTUM-MECHANICAL THIRD VIRIAL COEFFICIENT. Gibson, W. G. (Univ. of New South Wales, Kensington). Phys. Lett., 21: 619-21(July 1, 1966).

An expression for the quantum-mechanical third virial coefficient of a Bose-Einstein gas is obtained in terms of the $T^{(\alpha)}$ operators introduced by Faddeev. A possible method of solution, based on a variational principle, is suggested. (auth)

32231 NONSTATIONARY AXISYMMETRIC FLOWS IN MAGNETOGASDYNAMICS. Apanasewicz, Stanislaw. Prace Inst. Maszyn Przeplywowych, No. 26, 3-46(1965). (In Polish).

An analysis of unsteady two-dimensional axisymmetric plasma flows is given. Only isentropic or incompressible flows are considered. Flows without a circular velocity component are classified into four groups according to the magnetic field configurations in which such flows can occur. A general form of the solutions of the general system of differential equations is derived for two groups of flows. For the remaining two groups (corresponding to circular magnetic or electric fields), it is shown that the general system of equations reduces to a closed system of four equations with four unknowns. Some transforms are proposed by the use of which the general equations can be written in a simple form. The properties of potential flows and the plane shock waves are examined. (Int. Aerospace Abstr.)

32232 APPLICATION OF THE MAGNETOGASDYNAMIC EQUATIONS TO THE INVESTIGATION OF ELECTRIC-ARC CHARACTERISTICS. Apanasewicz, Stanislaw. Prace Inst. Maszyn Przeplywowych, No. 27, 51-8(1966). (In Polish).

A derivation of ordinary differential equations that describe the relations between the electric resistance, voltage, and intensity of the current in an electric arc is given. The equations are obtained on the basis of the system of equations for radial flows in magnetogasdynamics. Solutions of the equations derived are obtained for several special cases. (Int. Aerospace Abstr.)

32233 VISCOUS EFFECTS IN THE LIQUID CONDUCTOR MODEL OF HARD-CORE PINCH. Murty, G. S. (Tata Inst. of Fundamental Research, Bombay). Proc. Indian Acad. Sci., Sect. A, 63: 145-65(Mar. 1966).

The influence of viscous forces on the instability of liquid conductor model of hard-core pinch is investigated theoretically. It is shown that these forces decrease considerably the growth rate of instability in the experiments of Lehnert and Sjögren. An order of magnitude of the reduction is obtained for the experimental conditions. It is suggested that as a result of viscous forces, the time scale of instability, if any, is so large that instabilities cannot be observed in these experiments when the inner and outer currents are parallel. (auth)

32234 CONTINUED FRACTION EXPANSION OF TIME CORRELATION FUNCTIONS. Dupuis, Marc (Tokyo Univ.). Progr. Theoret. Phys. (Kyoto), 35: 752-3(Apr. 1966).

Results are presented concerning the relation of the continued fraction expansion for the Laplace transforms of the time correlation functions of dynamical variables with the moment expansion and its convergence. (B.G.D.)

32235 CALCULATION OF THE AVERAGE LORENTZ FIELD STRENGTH $\overline{v \times B}$ FOR AN ELECTRICALLY CONDUCTING MEDIUM IN TURBULENT MOTION INFLUENCED BY CORIOLIS FORCES. Steenbeck, M.; Krause, F.; Raedler, K.-H. (Deutsche Akademie der Wissenschaften, Berlin). Z. Naturforsch., 21a: 369-76(Apr. 1966). (In German).

A turbulent, electrically conducting fluid containing a magnetic field with nonvanishing mean-value is investigated. The magnetic field strength and the conductivity may be so small that the turbulence is not influenced by the action of the Lorentz force. The average of the crossproduct of velocity and magnetic field is calculated in a second approximation. It contains the averages of the products of two components of the velocity field, i.e., the components of the correlation tensor. Here the structure of the correlation tensor is determined for a medium with gradients of density and/or turbulence intensity, furthermore the turbulent motion is influenced by Coriolis forces. As the main result is shown that in those turbulent velocity fields the average crossproduct of velocity and magnetic field generally has a nonvanishing component parallel to the average magnetic field. Such a turbulence may be present in rotating stars. (auth)

32236 ELECTRON CYCLOTRON HARMONIC RESONANCE PHENOMENA IN AN RF-EXCITED DISCHARGE. Tetenbaum, S. J. (Lockheed Research Labs., Palo Alto, Calif.). 11p. (CONF-651126-9). ORAU. Gmelin, AED-CONF-65-353-8.

From American Physical Society, 7th Annual Meeting of the Division of Plasma Physics, San Francisco.

The phenomenon of electron cyclotron harmonic resonance has been observed in the ionosphere, in cold and hot-cathode d-c discharges and in electron beam generated plasmas. Some results of an experimental study of an rf-excited, electrodeless, low pressure helium discharge which simulates a plasma slab are presented. The experimental arrangement is shown. The plasma is created by a 21.7 MHz pulsed or CW transmitter capacitively coupled to a rectangular Pyrex vessel. Its walls were ground to a thickness of a half-wavelength at 9.15 GHz, the frequency of the incident wave P_{in} and of the detected noise emission. The discharge vessel is located in a magnetic field which can be automatically swept from 0 to 4000 gauss. The magnet is specially shimmed to provide a uniformity within

0.3% over the effective volume of the plasma. The measured magnetic field positions of the resonances are estimated to be accurate to 0.1%. A 36.0 GHz interferometer measures the electron density. Electron density measurements were also made with a K-band interferometer at frequencies of 18.2 and 22.0 GHz and gave results which agreed with the K_a-band results to within 5%. (auth)

32237 EXACT STATISTICAL THERMODYNAMICS OF NON-EXTENSIVE SYSTEMS. Salzberg, Allan M. 6p. (CONF-651213-11). ORAU. Gmelin, AED-CONF-65-400-24.

From American Physical Society, Winter Meeting in the West, Los Angeles.

The thermodynamics of a gas of N identical particles each of which possess charge q and mass m was obtained through the use of the constant pressure partition function. In the region where the electrostatic repulsions are dominant, the system is characterized both by non-extensive thermodynamics and by the fact that a large external pressure is needed to ensure stability of the ensemble. If $P < P_c \alpha N^2$, the system becomes unstable, and the interparticle separation becomes infinite. The region in which the electrostatic forces is not dominant is shown to be equivalent to the previously analyzed case of one dimensional masses. In addition the equation of state of the analogous two dimensional system was determined as a special case of a generalized equation of state which can be obtained for any system in which the potential is both pairwise additive and proportional to the logarithm of the interparticle distance. (auth)

32238 RADIATION GAS DYNAMICS. Pai, Shih-I. New York, Springer-Verlag, Inc., 1966. 236p.

The discussion of radiation transfer and gasdynamics includes the fundamentals of radiative transfer, gasdynamics with emphasis on the coupling terms between the radiation terms and the gasdynamics, and important parameters of radiation gasdynamics. Flow problems of radiative gasdynamics based on the continuum point of view and emphasizing wave motion, shock waves, and heat transfer; the kinetic theory of radiating gas, relativistic mechanics, problems of rarefied radiating gas, and the radiative properties of high-temperature gases are considered. (J.F.P.)

32239 KINETIC EQUATION FOR THE ELECTRON-PHONON GAS. Chappell, Willard R. (Smithsonian Astrophysical Observatory, Cambridge, Mass. Harvard Univ., Cambridge, Mass.). 21p. (CONF-660107-26). ORAU. Gmelin, AED-CONF-66-003-55.

From American Physical Society Meeting, New York.

The random-phase approximation equations of motion for the electron-phonon system are solved to obtain long-time expressions for the basic operators that appear in the calculation of correlation functions. These operator expressions are used to obtain a kinetic equation for the electrons and an expression for the phonon spectral function. The kinetic equation has the same form as the Balescu-Lenard equation. Expressions for the density autocorrelation function and the two-particle correlation function are also obtained. The latter is shown to have the same form as the test-particle result for a classical plasma. (auth)

32240 RADIATION OF OXYGEN AND NITROGEN AND THERMAL CONDUCTIVITY OF NITROGEN UP TO 15,000 DEG K. Morris, J. C.; Knopp, C. F.; Krey, R. U.; Liebermann, R. W.; Garrison, R. L. (Avco Corp., Wilmington, Mass.). New York, American Inst. of Aeronautics and Astronautics, 1966, Preprint No. 66-182, 39p., $1.50. (CONF-660315-4). ORAU.

From AIAA Plasmadynamics Conference, Monterey, Calif.

The transport of energy by radiation and thermal conduction was investigated as a function of temperature and pressure using a wall stabilized arc. The radiation studies included the contribution to the total radiation from positive ion and neutral atom collisions with electrons as well as atomic line radiation. These data were obtained from an optically thin gas at wavelengths greater than 2000 Å using standard spectroscopic techniques. Based upon comparison with published experimental and theoretical data, the theories in best agreement with experiment were used to predict the radiation in the vacuum ultraviolet. Progress in measuring ultraviolet radiation is described. Thermal conductivity measurements have been made at 0.5, 1, and 2 atmospheres using the Elenbaas-Heller equation assuming no radiative losses. Under this assumption it was found that, contrary to theoretical predictions, the measured conductivity decreased approximately as the particle density over the factor of 4 change in ambient pressure. The 1-atmosphere data were in agreement with published data, being an order of magnitude larger than theoretical predictions at 14,000°K. It was demonstrated that inclusion of ultraviolet radiation as a mechanism for energy transfer produced satisfactory agreement between experiment and theory. (auth)

32241 RADIATIVE HYDROGENIC SHOCK STRUCTURE. Nakagawa, Y.; Wu, S. T. (High Altitude Observatory, Boulder, Colo.). 25p. (CONF-660217-2). ORAU. Gmelin, AED-CONF-66-013-4.

From Symposium on Interdisciplinary Aspects of Radiative Energy Transfer, Philadelphia.

An improved Navier-Stokes Equation for the study of a radiative flow under nonlocal thermodynamic equilibrium conditions was obtained on the basis of the kinetic theory of gases. A multi-fluids model, namely the fluid consisting of electrons, ions, and neutral atoms, is adopted and a systematic estimate is made which includes the radiation, i.e., the photon gas, of various interactions between constituents of the gas. Utilizing such a set of equations, a radiative shock structure is numerically evaluated for a hydrogenic gas. (auth)

32242 LIQUID-VAPOR PHASE EQUILIBRIA OF THE NEON-NORMAL HYDROGEN SYSTEM. Heck, C. K.; Barrick, P. L. (Univ. of Colorado, Boulder). 14p. (CONF-650802-11). ORAU. Gmelin, AED-CONF-65-193-22.

From Cryogenic Engineering Conference, Houston, Tex.

Isotherms for the normal H–Ne system were measured at seven temperatures between 24.54 and 44.40°K for pressures up to 26 atm. The data were compared with some other experimental data for temperatures from 24.59 to 33.73°K. (D.C.W.)

Geophysics

Refer also to abstracts 31402 and 32669.

32243 (AD-634704) ORIGIN AND LOSS OF INNER ZONE PROTONS. Technical Report No. 524. Lenchek, A. M. (Maryland Univ., College Park, Dept. of Physics and Astronomy). Aug. 1965. 23p. CFSTI $1.00 cy, $0.50 mn.

A survey was made of earlier work on the origin and loss of inner zone protons. The survey topics include: injection from fast neutron decay, loss mechanisms, and the trapped protons. (M.O.W.)

32244 (N-66-13126) AN ENVIRONMENTAL MODEL FOR VAN ALLEN BELT PROTONS. Roberts, William T. (National Aeronautics and Space Administration, Huntsville, Ala. George C. Marshall Space Flight Center). Oct. 21, 1965. 31p. (NASA-TM-X-53351). CFSTI $2.00 cy, $0.50 mn.

The radiation environment for earth orbiting vehicles consists primarily of (1) Van Allen particles, (2) solar flare particles, and (3) galactic cosmic particles. Of these three, the Van Allen belt particles present the greatest hazard. The knowledge of the energy spectrum and distribution of the Van Allen proton belt as it is known today is summarized. A computer program was developed for calculating Van Allen particles incident upon vehicles in earth orbits. Based upon the 1963 FLUX program of

McIlwain, it is found that a vehicle in a highly elliptic orbit may encounter as many as 1.1×10^8 protons/cm^2/orbit with 40 Mev $\leq F \leq$ 110 Mev. In the magnetic equatorial plane, the flux of protons with $E \geq .5$ Mev may be as high as 2.2×10^7 protons/cm^2/sec. (STAR)

32245 (NSJ-tr-48) ON THE GEOCHEMICAL STUDIES OF STABLE ISOTOPES. III. ON THE ESTIMATION OF THE ISOTOPE RATIO IN THE MANTLE. Shima, Makoto. Translated from Shitsuryo Bunseki, 12: No. 25, 17-20 (1964). 6p. Dep. mn. JCL $1.10 fs, $0.80 mf. JAERI.

The chemical composition of the interior of the earth and of the isotopic ratios in those parts are considered. For any theories concerning the model composition of the interior, it might be concluded that elements such as Li, Na, K, Ca, Al, and halogens are concentrated toward the earth's surface, while S, Mg, Fe, and Ni are enriched in the deeper layer. In order to estimate the isotope ratio in the mantle, the following cases are discussed: that the isotope ratio in the mantle might have a composition similar to the meteoritic value; that the isotope ratio in the mantle might have a composition similar to the terrestrial value; and that the isotope ratio in the mantle is different from that of the meteoritic composition or of the terrestrial composition. (auth)

32246 EXCITATION AND IONIZATION BY AURORAL PROTONS. Eather, R. H.; Burrows, K. M. (Univ. of New South Wales, Kensington). Austral. J. Phys., 19: 309-22(June 1966).

Height distributions are presented for the atmospheric ionization rate and Balmer radiation resulting from precipitation of auroral protons. These results were computed assuming proton fluxes with several different energy spectra and pitch-angle distributions about the magnetic field, the total proton energy range being restricted to 1–1000 kev. The ionization results are used to obtain height distributions of radio absorption at a frequency of 27.6 MHz. It is concluded that proton impact ionization could contribute significantly to observed auroral absorption of cosmic radio noise. Computed Ha line profiles for observation in the magnetic zenith and horizon directions are compared with observed profiles, and proton flux parameters giving best agreement are deduced. (auth)

32247 ALOUETTE II SATELLITE. Nelms, G. L. (Defence Research Telecommunications Establishment, Ottawa); Barrington, R. E.; Belrose, J. S.; Hartz, T. R.; McDiarmid, I. B.; Brace, L. H. Can. J. Phys., 44: 1419-30(July 1966).

The successful launch of the Alouette II satellite is announced. A brief description is given of the experiments on board and some early indications of the results obtained are presented. (auth)

32248 MICROPULSATIONS AND THE OUTER RADIATION ZONE. Cornwall, John M. (Aerospace Corp., El Segundo, Calif.). J. Geophys. Res., 71: 2185-99 (May 1, 1966).

Recently the present author and others have suggested that Pc 1 micropulsations (hydromagnetic waves of frequency 0.1-5 cps) are generated in the outer radiation zone ($L > 4$) by low-energy protons via a cyclotron instability. Several points are discussed in the present paper; the first concerns the interpretation of ground-based experimental data in the light of the above model. A simple formula is given for the highest emitted frequency on a given field line, which formula is in good agreement with the data. Secondly, it is observed that the combined processes of cyclotron instabilities and pitch-angle scattering give rise to upper limits on both the energy density of trapped particles and of Pc 1 wave fields. This saturation effect may account for the remarkable stability of the low-energy proton population against fluctuations associated with the source mechanism. Finally, it is pointed out that the wave periods are in quasi-resonance with the bounce periods of moderately energetic electrons, and this leads to radial diffusion of such electrons. (auth)

32249 OBSERVATION OF THE LOW-ALTITUDE ACCELERATION OF AURORAL PROTONS. Mozer, F. S.; Bruston, P. (Service d'Aeronomie, Essonne, France). J. Geophys. Res., 71: 2201-6(May 1, 1966).

Proton data obtained from a rocket flight into the breakup phase of an IBC I aurora are presented. It is shown that over a period of 10 seconds the 140-kev to 250-kev protons were moving predominantly up the magnetic field line away from the atmosphere at an altitude of 320 km; that some of these protons came from apparent mirror points well within the atmosphere; and that the ratio of downward- to upward-moving 250-kev to 450-kev protons outside of the loss cone probably varied during this period. Several natural effects are investigated and found inadequate for the explanation of these results. In the absence of other possibilities it is concluded that the data offer direct evidence of the acceleration of auroral protons by at least tens of kilovolts at altitudes below about 300 km. (auth)

32250 LOW-ENERGY PROTON RADIATION BELTS. Mihalov, J. D.; White, R. Stephen (Aerospace Corp., El Segundo, Calif.). J. Geophys. Res., 71: 2207-16 (May 1, 1966).

B-L flux plots and differential energy distributions for low-energy protons in nine energy intervals from 0.17 to 3.4 Mev are presented. The data were obtained from a directional low-energy proton spectrometer on the satellite 1964-45A. The satellite was launched on August 14, 1964, into a near-polar orbit with a 3765-km apogee and 270-km perigee. The data presented here were taken during August 15–22, 1964. The results show that protons of different energies are concentrated on concentric L shells about the earth. The lowest energy protons of 0.19 Mev peak at $L = 4.4$, while the highest measured ones of 2.8 Mev peak at $L = 2.40$. For energies $\leq$0.75 Mev the quantity L^3E for the proton maxima is constant to within 20%, indicating that the first adiabatic invariant is conserved. At higher energies, however, L^3E increases. The fluxes at the maxima and at constant B are approximately constant up to 0.5 Mev (in to $L = 3.0$) but fall rapidly at higher energies and lower L values. The flux, $j_\perp$, at B = 0.10 gauss has a maximum peak value of 4×10^6 protons/cm^2-sec-ster-Mev for 0.48-Mev protons at $L = 3.0$. The differential energy distributions are soft at high L values. Quite narrow peaks in the energy distributions first appear at 0.26 Mev for $L = 4.0$. At $L = 3.0$ the peak moves to 0.42 Mev and remains at this energy until it is no longer measurable at $L = 2.1$. Here the fluxes are lower, but the spectra are harder. Beyond the peak the flux decreases as a power of the energy with the exponent varying from -4.1 at $L = 4.0$ to -2.0 at $L = 2.1$. The data give support to the theory that the protons' source is inward diffusion while conserving the magnetic moment but not the third adiabatic invariant. However, there are disagreements in detailed comparisons of the theory with the results, particularly for $L < 3.0$. (auth)

32251 ENERGETIC ELECTRON SPECTRA IN THE RADIATION BELTS. Mihalov, J. D.; White, R. Stephen (Aerospace Corp., El Segundo, Calif.). J. Geophys. Res., 71: 2217-26(May 1, 1966).

Differential electron spectra in the radiation belts in 10 energy intervals from 0.17 to 4.5 Mev were obtained from a directional electron spectrometer on satellite 1964-45A. The satellite was launched on August 14, 1964, into a near polar orbit with a 3765-km apogee and a 270-km perigee. Typical quiet-time data of August 15, 1964, are presented. A soft and a hard component both are clearly present in the electron spectra for $1.7 < L < 2.2$. For $L < 1.7$, on the other hand, only the hard component is seen. Both the soft and hard components, for $1.2 < L < 2.2$ and minimum mirror altitudes >400 km, are fit by exponential energy distributions with characteristic energies of 0.9 ± 0.5 Mev for the hard component and 0.2 to 0.07 Mev for the soft component. The hard component is the remnant of fission electrons injected by the July 9, 1962, high-altitude nuclear test. The soft component becomes softer as L increases, and may largely be due to cosmic-ray albedo neutron decay. For $3.5 < L < 8$ the portions of the differential spectra above

0.5 Mev are fit by single exponential distributions with characteristic energies of 0.6 to 0.2 Mev, becoming generally softer as L increases. The quiet-time outer zone electrons peak at lower L for higher energies. The magnetic moments of the electrons at the peaks change along computed inward drift trajectories, which conserve the first two adiabatic invariants. Consequently, this diffusion is a dominant source of these electrons only if a comparable loss process is present. Generally, there are no pronounced changes in quiet-time electron spectra with altitude along a field line in either the outer or inner zones. However, in the outer zone the flux of 0.2-Mev electrons increases by up to a factor of 2 as B changes from 0.24 to 0.1 gauss. (auth)

32252 ELECTRON AND PROTON FLUXES IN THE TAIL OF THE MAGNETOSPHERE. Konradi, Andrei (Goddard Space Flight Center, Greenbelt, Md.). J. Geophys. Res., 71: 2317-25(May 1, 1966).

Observation and energy spectra of electrons and protons in islands at the back of the magnetosphere are presented. It is shown that typically for electrons J(>20 kev) $\lesssim 8 \times 10^6$/cm^2-sec-ster and for protons J(>125 kev) $\lesssim 10^4$/cm^2-sec-ster. The electron spectra for particles with 20 kev $\lesssim$ E $\lesssim$ 70 kev can be characterized by e-folding energies ranging from 15 to 5 kev or by γ from 2.6 to 4.3 for differential power law spectra. For protons with energies E >125 kev, the spectra display e-folding energies in the range from 20 to 40 kev and γ between 7.8 and 4.9 for differential power law spectra. The electron spectrum in the islands shows a characteristic softening with time. A comparison is made with electron fluxes observed with the Alouette, IMP 1, and Vela satellites. The similarity between particles in the islands and those observed in the aurora is discussed. (auth)

32253 MAGNETIC STORMS IN THE EARTH'S MAGNETIC TAIL. Behannon, K. W.; Ness, N. F. (Goddard Space Flight Center, Greenbelt, Md.). J. Geophys. Res., 71: 2327-51(May 1, 1966).

Detailed measurements of the earth's magnetic field at distances between 7 and 31.4 R_E were obtained by the IMP 1 satellite between November 27, 1963, and May 30, 1964. The interaction of the solar wind with the geomagnetic field compresses it on the sunlit hemisphere but extends the field to form a magnetic tail in the antisolar direction with a median magnitude of 16 gammas. From March 15 to June 3, 1964, the satellite was imbedded well within the magnetic tail and for 19+ orbits (29–48) it measured principally the temporal variation and spatial structure of this tail field. The experimental data reveal the development of a magnetically neutral sheet in the tail separating fields of opposite direction that are aligned parallel to the earth-sun line. A total of 5 magnetic storms were observed terrestrially that are correlated with satellite data and discussed in this paper. Three storms of an M-region sequence, presumed to be associated with the sector structure within the co-rotating interplanetary medium are presented and discussed in detail, as well as two other magnetic storms. Both positive and negative correlations with world wide H-component terrestrial data are observed. The former is interpreted to be due to large-scale compression of the entire magnetosphere and tail. Anticorrelation of the H component with the tail field magnitude is shown to be due to an increased number of lines of force being carried into the tail by the enhanced solar plasma flow. This occurs simultaneously with the main phase decrease and thus supports geomagnetic storm theories invoking such a tail field mechanism. Positive correlations of an increased tail field magnitude with the planetary magnetic index K_p are also obtained. (auth)

32254 VALIDITY OF THE HYDROMAGNETIC APPROACH IN DISCUSSING INSTABILITY OF THE MAGNETOSPHERIC BOUNDARY. Lerche, I. (Univ. of Chicago). J. Geophys. Res., 71: 2365-71(May 1, 1966).

A simplified magnetohydrodynamic model of the interface between the solar wind and the geomagnetic field on the tail side of the earth is described. Using linearized MHD theory it is shown that unstable waves can exist that grow exponentially with time. It is also shown that the dominant waves are those with the shortest wavelengths, and consequently a fluid analysis is inadequate since it does not describe the main physical process. Thus, the calculation should be repeated taking into account the finite thickness of the boundary layer and also the finite radii of gyration of the particles involved. The acceleration of particles trapped on the magnetic field lines by unstable waves is discussed in a qualitative manner. (auth)

32255 MATHEMATICAL MODEL OF THE GEOMAGNETIC FIELD FOR 1965. Hurwitz, L.; Knapp, D. G.; Nelson, J. H.; Watson, D. E. (Environmental Science Services Administration, Rockville, Md.). J. Geophys. Res., 71: 2373-83(May 1, 1966).

A mathematical model of the geomagnetic field for 1965.0 is presented. The field is given by internal and external spherical harmonic coefficients to degree and order 12. This model was derived from approximately 425,000 measurements made since 1900. An important step in the derivation was the analytic smoothing of data, which produced the regularly spaced grid values used as input to the two-stage spherical harmonic analysis. Consequently it has been possible to construct the 1965 world magnetic charts (published by the United States Naval Oceanographic Office) from the model, instead of the reverse. On the whole, the smoothed surface field defined by the model (and by the charts exactly drawn from the model) is believed to be at least as faithful to nature as that defined by any previously published model or set of charts. Plans for future analyses include the use of a modified truncation of the series expression for the potential and an allowance for the earth's oblateness. (auth)

32256 ASSOCIATION BETWEEN VLF EMISSIONS AND FLICKERING AURORA. Ungstrup, Eigil (Stanford Univ., Calif.). J. Geophys. Res., 71: 2395-6(May 1, 1966).

An experiment is described in which v-l-f signals were recorded and correlated to active periods in the aurora. (B.G.D.)

32257 SEMIANNUAL WAVE IN THE RECURRENCE TENDENCY OF GEOMAGNETIC ACTIVITY. Meyer, Joachim (Univ., Goettingen, Ger.). J. Geophys. Res., 71: 2397-2400(May 1, 1966).

A harmonic analysis of the equivalent recurrence numbers is presented, which yields a significant semiannual wave in the recurrence tendency of geomagnetic activity, with maxima at the equinoxes and a varying amplitude during the sunspot cycle. (B.G.D.)

32258 FURTHER REMARKS ON THE ABSENCE OF A VERY EXTENDED MAGNETOSPHERIC TAIL. Van Allen, J. A. (Univ. of Iowa, Iowa City). J. Geophys. Res., 71: 2406-7(May 1, 1966).

Evidence is presented to substantiate the absence of the magnetospheric tail at large distances ($\sim 10^6$ R_E). (B.G.D.)

32259 GEOMAGNETIC AND SOLAR DATA. Lincoln, J. Virginia (ed.) (Inst. for Telecommunication Sciences and Aeronomy, Boulder, Colo.). J. Geophys. Res., 71: 2411-17(May 1, 1966).

Data are presented for geomagnetic and solar activity in December, 1965. Range indices and sunspot numbers are given. Sudden commencements and solar-flare effects are given for the fourth quarter, 1965. Final sunspot numbers for the whole disk of the sun 1965 are included. (B.G.D.)

32260 CORRELATION OF OUTER RADIATION ZONE ELECTRONS ($E_e \sim 1$ Mev) WITH THE SOLAR ACTIVITY CYCLE. Frank, L. A.; Van Allen, J. A. (Univ. of Iowa, Iowa City). Contract Nonr-1509(06). J. Geophys. Res., 71: 2697-2700(June 1, 1966).

A comparison of observations with several earth satellites reveals that the inner edge of the outer radiation zone of electron $E_e > 1.6$ Mev intensities has moved outward from L $\simeq$ 2.2 in mid 1958 to L = 3.0 in late 1964. This

outward motion in the outer radiation zone occurs during the declining phase of solar activity cycle 19 and strongly suggests a systematic change of the average value of one or more of the solar wind parameters over this time period. (auth)

32261 PROTON TRAJECTORIES IN THE RADIATION BELTS. Mozer, F. S. (Service d'Aeronomie, Verrieres-Le-Buisson, France). J. Geophys. Res., 71: 2701-8 (June 1, 1966).

Trajectories of charged particles in a static dipole magnetic field are considered for the case of small equatorial pitch angles under the assumption of the conservation of the adiabatic invariants. By physical reasoning, higher order correction terms to the conventional first invariant $\sin^2\alpha/B$, are deduced. These terms, being functions of particle mass, velocity, and gyration angle around the field line, produce the following effects in the radiation belts; near the equatorial plane at large L, the oscillation of the proton pitch angle at the cyclotron frequency is significant. For example, at L = 10, the 150-kev proton pitch angle oscillates by as much as 10°. At low altitudes the pitch angular distribution of protons accelerated near the equatorial plane is limited to certain general forms. Results of detailed calculations are presented. (auth)

32262 ROLE OF ELECTROSTATIC PLASMA OSCILLATIONS IN ELECTRON SCATTERING IN THE EARTH'S OUTER MAGNETOSPHERE. Eviatar, Aharon (Univ. of Maryland, College Park). J. Geophys. Res., 71: 2715-27 (June 1, 1966).

The scattering of electrons in a spatially homogeneous magnetic field-free stable plasma by ion and electron plasma waves excited by suprathermal particles is considered using a test-particle approach. A previously derived theory is modified and extended to the case of ion-waves propagating in a current bearing plasma. The results are applied to electrons in the earth's magnetosphere and in the transition zone between the magnetosphere and the interplanetary medium, where the geomagnetic field is weak in the sense that $\Omega^2 \ll \omega_{pe}^2$ ($\Omega = eB/mc$; $\omega_{pe}^2 = 4\pi ne^2/m$). It is found that interaction with electron plasma oscillations is competitive with whistlers in scattering suprathermal electrons, and that ion waves are the dominant mechanism for the diffusion of subthermal electrons across the magnetopause and the shock wave. (auth)

32263 THE 4-SECOND SUMMERTIME MICROPULSATION BAND AT COLLEGE. Heacock, R. R. (Univ. of Alaska, College). Contract AF 19(628)-1695. J. Geophys. Res., 71: 2763-75(June 1, 1966).

A significant summertime micropulsation band at ~4-sec period is revealed in the several years of continuous micropulsation recording. The band contains mainly Pc-type activity, but is also seen in certain weak Pi 1 bursts. The intensity of the band is greatest in afternoon and has a positive correlation with K_p in afternoon. A small diurnal variation in band midperiod was observed, with periods near 4 sec in day and near 3 sec at night. The 4-sec events are usually less well structured than higher frequency pearl-type events, and the frequency-time elements are often irregularly spaced. The possibility exists that the 4-sec band is due to the principal exospheric resonance. (auth)

32264 THE NATURE OF WORLDWIDE GEOMAGNETIC DISTURBANCES GENERATED BY THE STARFISH EXPLOSION OF JULY 9, 1962. Bomke, Hans A.; Harris, Arthur K.; Walker, John W.; Ramm, Wolfgang J. (Army Electronics Command, Fort Monmouth, N. J.). J. Geophys. Res., 71: 2777-89(June 1, 1966).

A new approach was used to study the worldwide effects recorded by standard magnetometers a few minutes after the Starfish detonation. The magnitudes of the total disturbance were plotted on a world map and, by the use of standard contouring techniques, global lines of equal signal strength were obtained. In this system of isopleths, an outstanding feature is a pair of clearly defined maximums located near the geomagnetic meridian of the source and centered at geomagnetic latitudes of about 45° North and South, whereas there is a relatively low value near the shot location. Another innovation was the introduction of a coordinate system based upon the geomagnetic field direction at each station; one axis (called a) is along the dipole field line and the other two orthogonal axes lie in the plane (called p) perpendicular to the dipole field. The close resemblance between the isopleths of the p component and those of the total disturbance (at 3 min postshot) indicates that the major portion of the signal was in the p plane at that time. The a pattern, while more complicated than the p, clearly exhibits certain symmetries that are described and tentatively identified. To account for the two p maximums a possible mechanism was advanced, namely, that the pattern is the result of coupling of energy from the isotropic, modifed Alfvén mode into transverse, pure Alfvén waves in regions where favorable coupling conditions exist. (auth)

32265 EFFECTIVE ATMOSPHERIC LOSSES FOR 125-Mev PROTONS IN SOUTH ATLANTIC ANOMALY. Heckman, Harry H.; Brady, Victor O. (Univ. of California, Berkeley). Contract W-7405-eng-48. J. Geophys. Res., 71: 2791-8(June 1, 1966). (UCRL-16592).

Orbit calculations are carried out to evaluate the effective atmospheric densities for geomagnetically trapped 125-Mev protons whose guiding centers mirror between 200- and 560-km altitude in the South Atlantic anomaly. Such orbits are limited to the region of B-L space L = 1.38 and $0.2043 < B_m < 0.2355$ gauss. Calculated are the effective atmospheric densities and scale heights experienced by the particle and its guiding center. Rates of energy loss by ionization are also calculated, taking into account atmospheric composition and the ionization energies for each constituent. Atmospheres used in the computations are the Harris and Priester S = 100 and S = 200 models, each diurnally averaged, and the Johnson model for solar minimum. The geomagnetic field is described by the 48-term spherical harmonic expansion of Jensen and Cain. The numerical results show that for the trajectories considered, the effective atmospheric density averaged over the particle's motion is about twice the density averaged over the guiding center's trajectory. Also, the effective atmospheric scale heights can be three to four times the scale height of the model atmosphere, depending upon altitude and time in the solar cycle. (auth)

32266 SPATIAL DISTRIBUTION OF PROTONS FROM NEUTRON DECAY TRAPPED BY THE GEOMAGNETIC FIELD. Hess, W. N. (Goddard Space Flight Center, Greenbelt, Md.); Killeen, John. J. Geophys. Res., 71: 2799-2810(June 1, 1966).

The neutron sources at the earth due to galactic cosmic rays and solar protons interacting with the terrestrial atmosphere and also due to solar neutrons are examined quantitatively to see if the observed radiation belt protons can be produced by these neutrons. It is shown that solar protons and solar neutrons do not play any important part in producing the trapped protons. It seems that galactic cosmic rays may be able to make the observed high energy inner-belt proton flux near the equator, but it is difficult to see how the fluxes off-equator can be produced without some other mechanism being involved. Also for $E \leq 10$ Mev the galactic cosmic-ray source is inadequate to produce the observed fluxes even for the center of the inner belt. (auth)

32267 SOLAR FLARE EFFECTS AND THE RELAXATION TIME OF THE IONOSPHERE. Baker, Donald M.; Davies, Kenneth (Inst. for Telecommunication Sciences and Aeronomy, Boulder, Colo.). J. Geophys. Res., 71: 2840-2(June 1, 1966).

Evidence is presented to show that the daytime relaxation time of the e-f_1 region of the ionosphere is probably less than one minute. The data are based on observations of solar radio noise and the ionospheric phenomenon of sudden deviation, which is a sudden change in frequency of the carrier of an ionospherically propagated h-f radio wave caused by a solar flare. (B.G.D.)

32268 IONOSPHERIC PHENOMENON ASSOCIATED WITH EXPLOSIVE SOLAR FLARES. Davies, Kenneth;

Donnelly, Richard F. (Inst. for Telecommunication Sciences and Aeronomy, Boulder, Colo.). Contract GP-3092. J. Geophys. Res., 71: 2843-5(June 1, 1966).

The relation between the occurrences of the ionospheric phenomenon f sudden frequency deviations and the explosive phases of visible Hα flares is discussed. A sudden frequency deviation being a sudden change in frequency of a h-f radio signal reflected from the ionosphere. (B.G.D.)

32269 HIGHER-MODE SEISMIC SURFACE WAVES FROM ATMOSPHERIC NUCLEAR EXPLOSIONS OVER NOVAYA ZEMLYA. Crampin, Stuart (Seismological Inst., Uppsala). J. Geophys. Res., 71: 2951-8(June 15, 1966).

The second Rayleigh mode and the second and third Love modes were observed at Uppsala from atmospheric nuclear explosions over Novaya Zemlya. The group velocity dispersion, the energy, and the initial phase of the higher modes are calculated. The Rayleigh modes are generated by the action of the shock wave on the ground, and the energy is most effectively coupled when the apparent velocity of the shock wave is equal to the phase velocity of the surface wave. The Love modes are generated by some form of coupling with the second Rayleigh mode. (auth)

32270 INVESTIGATION OF THE SOFTEST PARTICLES BY MEANS OF THE COSMOS 3 AND COSMOS 5 SATELLITES. Muliarchik, T. M. Kosm. Issled., 4: 95-104(Jan.-Feb. 1966). (In Russian).

An evaluation of the energy spectrum of the electrons recorded by fluorescent-screen indicators with different foil thicknesses on board Cosmos 3 and Cosmos 5 is given. It is shown that the contribution of electrons with $E < 40$ kev to the recorded signal is not a constant value. The ratio of electron intensities $E < 40$ kev to $E > 40$ kev varies approximately from 10^{-2} to 5. In the $E < 40$ kev group, the principal contribution comes from electrons with energies from 10 to 20 kev. Soft electrons ($E \sim$ 10 to 20 kev) are recorded mainly at small invariant heights h_{min} (minimum height of a given trajectory of mirror points above the earth's surface) in the case where the corresponding real heights are large (500 to 1000 km), as above Central and South Asia, the Indian Ocean, Indonesia, and the West Pacific. The intensity of soft electrons at heights of ~1000 km above the South Atlantic was appreciably less than at the same heights in the eastern hemisphere. The maximum intensity of soft electrons measured at ~1500 km was up to 10^3 particles/cm^2-sec-ster, for an instrument sensitivity threshold corresponding to ~5×10^5 particles/cm^2-sec-ster. (Int. Aerospace Abstr.)

32271 RADIOACTIVITY OF THE SATELLITE "COSMOS 3" AFTER THE EXPLOSION OF JULY 9, 1962. Boliunova, A. D. Kosm. Issled., 4: 167-9(Jan.-Feb. 1966). (In Russian).

A discussion is given of radiation data gathered by the Soviet satellite Cosmos 3 (1962 Nu 1) shortly after the detonation of a U. S. thermonuclear device on July 9, 1962, over Johnston Island. The Geiger counter on board Cosmos 3 was not turned on at the time of the detonation. The day after the detonation, the counting rate was 2.7 times as high as normal for the altitude (~320 km). The decrease in the counting rate to the normal background level was slower than expected. It is considered possible that this effect is due to radioactive particles collected by the satellite during its passage ~550 km from the detonation point ~6 hr after the explosion. (Int. Aerospace Abstr.)

32272 UNUSUAL AURORA OF SEPTEMBER 22-3, 1963. Feibelman, W. A. (Univ. of Pittsburgh). Planet. Space Sci., 14: 524-5(June 1966).

Observation of an unusual aurora which contained a number of lobes extending for considerable distances from the main arc towards the southwest and south and shorter spikes extending to the north is reported. (B.G.D.)

32273 SPREAD F AND IONOSPHERIC F-REGION IRREGULARITIES. Herman, John R. (Avco Corp., Wilmington, Mass.). Rev. Geophys., 4: 255-99(May 1966).

The results of ionospheric observations by means of a variety of techniques are summarized to show that magnetic field-aligned irregularities exist in the ionosphere. The irregularities appear in patches having horizontal dimensions up to 1000 km in the east-west direction and several hundred kilometers in the north-south direction. Size of the irregularities is typically about 1 km transverse to the magnetic field and elongated along the field line. Irregularities associated with spread F occur in the altitude range from 250 km up to the height of F_{max}. Correlations between ionogram spread F and other ionospheric observations indicate that spread echoes are closely related to the field-aligned irregularities. A critique of theories explaining why the irregularities cause spread echoes is given. Statistical studies of the geographic and temporal variations in spread-F occurrence are summarized. The fundamental question of how irregularities causing spread F are produced in the ionosphere is discussed. (auth)

32274 VAN ALLEN RADIATION BELTS. Penselin, Siegfried (Univ., Bonn). Sterne Weltraum, 5: 33-5(Feb. 1966). (In German).

The discovery of the Van Allen belts is briefly recounted and current knowledge about their composition is summarized. The fundamentals of the motion of a charged particle in a dipolar magnetic field are given. The possible origin of the particles in the Van Allen belts is discussed. (Int. Aerospace Abstr.)

32275 SOLAR-WIND INTERACTION WITH THE MAGNETOSPHERE: FLUID DYNAMIC ASPECTS. Axford, W. I. (Cornell Univ., Ithaca, N. Y.). pp 231-41 of The Solar Wind. Mackin, Robert J. Jr.; Neugebauer, Marcia (eds.). Pasadena, Calif., California Inst. of Tech., 1966.

The discussion of fluid dynamic aspects of the solar-wind interaction with the magnetosphere includes solar-wind fluid flow past the magnetosphere, supersonic flow and shock waves, the shape of the magnetosphere, magnetospheric interchange motions, and electric field and energy dissipation in the magnetosphere during magnetic storms. (J.F.P.)

32276 SOLAR-WIND INTERACTION WITH THE MAGNETOSPHERE: PARTICLE ASPECTS. Dungey, J. W. (Imperial Coll. of Science and Tech., London). pp 243-55 of The Solar Wind. Mackin, Robert J. Jr.; Neugebauer, Marcia (eds.). Pasadena, Calif., California Inst. of Tech., 1966.

The open or connected model is used in the discussion of the solar-wind interaction with the magnetosphere. The motion of individual particles is considered rather than fluid flow. The topics discussed are the topology of the geomagnetic field, the electric field in the magnetosphere, the motion of the plasma particles, and time-dependent effects. (J.F.P.)

32277 MECHANISM FOR RECONNECTION OF GEOMAGNETIC AND INTERPLANETARY FIELD LINES. Petschek, H. E. (Avco-Everett Research Lab., Everett, Mass.). pp 257-73 of The Solar Wind. Mackin, Robert J. Jr.; Neugebauer, Marcia (eds.). Pasadena, Calif., California Inst. of Tech., 1966.

The magnetospheric boundary with its structure of shock wave, Alfvén wave, and slow expansion wave is shown. The reconnection of the field lines at the boundary is discussed and shown. Also parameters describing the connection of the dipole field to the interplanetary field, the cross section of the magnetosphere perpendicular to the earth-sun line, and parameters involved in estimating the DS-current driving potential are shown. (J.F.P.)

32278 OCCURRENCE OF TOPOLOGICAL CHANGES OF THE MAGNETOSPHERE. Sonnerup, B. U. O. (Royal Inst. of Tech., Stockholm). pp 275-80 of The Solar Wind. Mackin, Robert J. Jr.; Neugebauer, Marcia (eds.). Pasadena, Calif., California Inst. of Tech., 1966.

The topology of the magnetosphere is described. The linear stability of the closed configuration was investigated under the assumption of a stationary interplanetary

plasma. Also the main phase of the geomagnetic storm is considered as the result of a transition from the closed to the open magnetosphere. (J.F.P.)

32279 MOTION OF PARTICLES TRAPPED IN THE MAGNETOSPHERE. Hones, E. W. Jr. (Inst. for Defense Analysis, Washington, D. C.). pp 281-94 of The Solar Wind. Mackin, Robert J. Jr.; Neugebauer, Marcia (eds.). Pasadena, Calif., California Inst. of Tech., 1966.

A computer study was made of the motions of particles assumed to be injected and initially mirroring near the magnetic neutral lines at the front of the magnetosphere. This study was made in an attempt to understand the morning spiral patterns of magnetic activity and radio absorption and to discover whether these spiral patterns might signify the entry of solar-wind plasma through the front of the magnetosphere and the ultimate precipitation of the plasma along a path determined by the electromagnetic fields within the magnetosphere. The results of these calculations are discussed for the motion of protons initially mirroring at positions along the 13 and 8° lines. (J.F.P.)

32280 EXPLORER-18 PLASMA MEASUREMENTS. Lyon, E. F. (Massachusetts Inst. of Tech., Cambridge). pp 295-314 of The Solar Wind. Mackin, Robert J. Jr.; Neugebauer, Marcia (eds.). Pasadena, Calif., California Inst. of Tech., 1966.

Some of the specific data obtained from the Explorer-18 plasma-measurement experiment are described, and conclusions drawn from these data are presented. The detector is described, and the sequence and timing of the measurements are explained. A map and spectrum of the transition zone obtained from the satellites passage through the shock front and through the magnetopause and typical interplanetary spectra are shown. The dependence on the sun-earth-satellite angle is described, and a comparison with data from Explorer-10 is given. Other topics are summary plots through the transition zone, low-altitude electron flux, and a transition-zone anomaly. (J.F.P.)

32281 OBSERVATIONS OF THE MAGNETIC FIELD AT THE MAGNETOPAUSE AND INTERACTION REGION BY IMP 1. Ness, N. F. (Goddard Space Flight Center, Greenbelt, Md.). pp 315-35 of The Solar Wind. Mackin, Robert J. Jr.; Neugebauer, Marcia (eds.). Pasadena, Calif., California Inst. of Tech., 1966.

Data from the first 19 orbits of the IMP-1 satellite are discussed. This discussion includes examples of the magnetic-field data at the extremity of the geomagnetic field, the determination of the positions and shapes of the boundaries, a comparison of observed and theoretical results, and a correlation of plasma and magnetic-field data. It is concluded that there is a shock wave associated with the solar plasma flow around the earth and its magnetic field, that this shock wave can be understood on the basis of an aerodynamic analogy, and also that beyond the shock the flow around the earth has the properties of plasma flow. (J.F.P.)

32282 SHAPE OF THE MAGNETOSPHERE AND DISTORTION OF THE GEOMAGNETIC FIELD. Mead, Gilbert D. (Goddard Space Flight Center, Greenbelt, Md.). pp 337-52 of The Solar Wind. Mackin, Robert J. Jr.; Neugebauer, Marcia (eds.). Pasadena, Calif., California Inst. of Tech., 1966.

The assumptions on which the Newtonian theory for the magnetosphere is based are reviewed, and an attempt is made to determine the validity of the results based on these assumptions. The topics covered include the basic assumptions, the shape of the magnetosphere, and the field within the magnetosphere. (J.F.P.)

32283 MEASUREMENT OF THE SECONDARY GAMMA SPECTRUM FROM 0.2 TO 2 Gev IN THE UPPER ATMOSPHERE. Koehn, Diederich; Pinkau, Klaus; Wibberenz, Gerd (Christian-Albrechts-Univ., Kiel). Z. Phys., 193: 443-58(1966). (In German).

A balloon experiment was carried out to measure the energy spectrum of photons between about 100 and 2000 Mev, using a lead-scintillator-sandwich spectrometer. The energy calibration of this instrument was performed theoretically utilizing Nagel's Monte-Carlo calculations. The results of a test flight carried out from Meppen (cutoff 2.5 Gv) on October 19, 1963, were: The attenuation length of atmospheric photons of several hundred Mev energy increases with depth beyond the transition maximum. The integral intensity of photons at an average altitude of 355 g/cm^2 is I ($\geq$200 Mev) = $3.6 \cdot 10^{-2}$ cm^{-2} sec^{-1} sterad^{-1}. The shape of the energy spectrum was obtained. It may be approximated by a power law $E^{-1.3 \pm 0.2}$ between 500 and 2000 Mev. A comparison of these results is made with previous measurements. It is possible to construct a differential gamma spectrum at a depth of 7 g/cm^2 indicating a possible minimum at about 20 Mev followed by a maximum at about 70 Mev. (auth)

32284 LABORATORY SCALED SOLAR PLASMA PHENOMENA. Osborne, F. J. F.; Bachynski, M. P. (RCA Victor Co., Ltd., Montreal). New York, American Inst. of Aeronautics and Astronautics, 1966, Preprint No. 66-154, 19p., $1.50. (CONF-660315-16). ORAU.

From AIAA Plasmadynamics Conference, Monterey, Calif.

Using simulation techniques, a series of experiments is being conducted to determine the influence of selected parameters on the form of the solar-wind magnetosphere interaction. Using various diagnostic techniques, the formation of the magnetospheric cavity has been observed including the Cahill discontinuity at the equilibrium boundary. This boundary occurs at the position dictated by the equating of the streaming plasma pressure with that of the terrella magnetic field. The thickness of the magnetic boundary is generally compatible with a Ferraro-Rosenbluth sheath. The cavity, when viewed from above the polar axis shows pronounced asymmetry in both the visual and magnetic data. The interior of the cavity shows a phenomenon resembling the Van Allen belts in that a plasma is trapped and circulated on a constant L shell. The generation mechanism of the model belts has associated magnetic and electric field fluctuations at frequencies which suggest the presence of a magnetohydrodynamic wave. This MHD wave is probably launched by the plasma front moving against the terrella field. At specific times in the interaction there is a precipitation of plasma onto the terrella surface in a form reminiscent of aurora zones. (auth)

32285 PARTICLES IN THE ATMOSPHERE AND SPACE. Cadle, Richard D. New York, Reinhold Publishing Corp., 1966. 234p. $10.00.

Various aspects of the nature and sources of particles in the troposphere are discussed (including volcanoes, biological material, air pollution, and rain formation), and in the stratosphere and mesosphere. All aspects of radioactive fallout are covered: mechanisms of fallout formation (air, surface, and underground bursts, crater formation, airborne particles from nuclear reactors and separation plants, and fallout from accidents); close-in fallout (base surge, and combined effects of meteorology and particle size); worldwide fallout (troposphere and stratosphere delayed fallout, and fallout from the high atmosphere); and the fate of deposited fallout. Interplanetary dust, dust on the lunar surface, and particles in the atmosphere of the major planets are dealt with. (M.H.R.)

32286 PRELIMINARY RESULTS FROM THE AMES RESEARCH CENTER PLASMA PROBE OBSERVATIONS OF THE SOLAR WIND-GEOMAGNETIC FIELD INTERACTION REGION ON IMP-II AND OGO-I. Wolfe, J. H.; Silva, R. W.; Myers, M. A. (Ames Research Center, Moffett Field, Calif.). 38p. (CONF-650422-20). ORAU. Gmelin, AED-CONF-65-118-60.

From American Geophysical Union Program for Section of Seismology Annual Meeting, Washington, D. C.

Some recent data on the plasma characteristics in the transition region and near interplanetary space are presented. The data reveal that there is, in general, less

than a factor of two decrease in the convective velocity of the plasma as it passes from interplanetary space into the transition region and an accompanying increase of almost an order of magnitude. Evidence is presented for significant plasma acceleration in the transition region. The validity of interpreting the interaction of solar plasma with the earth's field in terms of an aerodynamic analogy is questioned. A possible mechanism for the injection of high-energy particles into the magnetosphere is also presented. (G.O.Y.)

32287 THE GEOELECTRIC FIELD: ITS EXISTENCE, CAUSE, AND EFFECT. Ling, S. C. (Catholic Univ. of America, Washington, D. C.). 57p. (CONF-650422-22). ORAU. Gmelin, AED-CONF-65-118-62.

From American Geophysical Union, Program for Section of Seismology Annual Meeting, Washington, D. C.

The existence of a geoelectric field closely associated with the Van Allen radiation belt is postulated using the hypothesis that plasma is generated continuously inside the magnetosphere and that the trapped plasma can have a finite rate of diffusion. (G.O.Y.)

32288 ELECTRON LOSS FROM THE VAN ALLEN ZONES DUE TO PITCH ANGLE SCATTERING BY ELECTROMAGNETIC DISTURBANCES. Roberts, Charles S. (Bell Telephone Labs., Inc., Murray Hill, N. J.). 44p. (CONF-650653-26). ORAU. Gmelin, AED-CONF-65-170-52.

From American Physical Society, Summer Meeting, New York.

Experimental observations indicate that relativisitic electrons in the Van Allen zones are perturbed by physical processes that violate one or more adiabatic invariants of the electron's motion. One such possible process is discussed, that of pitch angle or mirror point diffusion. A qualitative explanation of pitch angle diffusion and how this process can lead to loss of trapped particles is presented, and then a Fokker-Planck type diffusion equation is introduced to describe the process mathematically. This diffusion equation is used to treat the loss of electrons from trapped orbits due to pitch angle diffusion that results from cyclotron resonant scattering of electrons by whistlers. Predictions are compared with satellite data on the loss from the Van Allen zones of electrons artificially injected by a nuclear explosion. It is found that the data indicate that pitch angle diffusion does indeed play an important role in the loss process, but the dominant mechanism producing the pitch angle scattering must be something other than cyclotron resonant scattering by whistlers since this mechanism leads to several predictions that are in disagreement with the data. These include prediction of the electron pitch angle distribution, the variation of the pitch angle distribution with L-shell and energy, the variation of the loss rate with energy, and the magnitude of the loss rate. Further investigation reveals that a process that, unlike whistlers, scatters electrons more or less uniformly along their spiral path would produce a pitch angle diffusion mechanism in much better accord with observation. Interaction with some type of wide band electromagnetic noise is suggested as such a process which might be of importance. (auth)

32289 ATOMIC HYDROGEN AND HELIUM IN THE AIRGLOW. Krassovskii, V. I.; Shefov, N. N.; Vaisberg, O. L. (Inst. of Physics of the Atmosphere, Moscow). 32p. (CONF-650835-1). ORAU. Gmelin, AED-CONF-65-234-3.

From Aeronomy Symposium, Boston.

A survey of data on the atomic hydrogen and helium emissions in the upper atmosphere is given. (auth)

32290 DETERMINATION OF THE ELECTRON DISTRIBUTION IN THE MAGNETOSPHERE USING HYDROMAGNETIC WHISTLERS. Watanabe, Tomiya (Univ. of British Columbia, Vancouver). 36p. (CONF-650961-5). ORAU. Gmelin, AED-CONF-65-224-2.

From American Geophysical Union, 5th Western National Meeting, Dallas.

Two methods are investigated for determining the electron density distribution in the magnetosphere from the dispersion characteristics of a hydromagnetic wave propagating between hemispheres along a line of force of the earth's magnetic field. (G.O.Y.)

32291 STEADY STATE FLUID MODEL OF THE IONEXOSPHERE. Gliddon, J. E. C.; Yeh, K. C. (Univ. of Illinois, Urbana). 34p. (CONF-650961-3). ORAU. Gmelin, AED-CONF-65-224-9.

From American Geophysical Union, 5th Western National Meeting, Dallas.

The equations of the double adiabatic theory are solved in the dipole coordinate system by assuming that at the base of the ion-exosphere the collisions are sufficiently frequent to make the pressure isotropic. Analytic expressions for the density, the elements of the pressure tensor, and the temperature of the fluid are also derived; and a formula for the ring current is obtained. (G.O.Y.)

32292 MODEL FOR THE PROTONS TRAPPED IN THE MAGNETIC FIELD OF THE EARTH. Galbraith, Thomas L. (General Electric Co., Philadelphia). 22p. (CONF-650961-2). ORAU. Gmelin, AED-CONF-65-224-1.

From American Geophysical Union, 5th Western National Meeting, Dallas.

A model was developed for the protons trapped in the geomagnetic field over an energy range of 100 kev to 680 Mev and extending from h minimum to a magnetic shell of 8 Earth radii. The data used for this model were obtained from published and unpublished reports presenting satellite measurements from Explorer IV (1958) to Relay I (1963). (G.O.Y.)

Gravitation, Quantum Mechanics, and Relativity Theory

Refer also to abstract 32548.

32293 (N-66-17084) QUANTUM THEORY OF TIME-DEPENDENT PHENOMENA TREATED BY THE EVOLUTION OPERATOR TECHNIQUE. Loewdin, Per-Olov (Florida Univ., Gainesville). June 15, 1965. 83p. (NASA-CR-70301; TN-100). CFSTI $3.00 cy, $0.50 mn.

A brief discussion is presented of the treatment of time dependent phenomena in the nonrelativistic quantum theory. Consideration is given to such areas as the coordinate and momentum space, the Schrödinger equation, the Schrödinger equation for particles in an electromagnetic field, the evolution operator, the reformulation of quantum theory, transition probabilities, and the time-dependent perturbation theory. Included are discussions of specific applications and agreement with experimental results for such equations as the complex wave function, and the evolution and differential operators. (STAR)

32294 RELATIVISTIC ROCKET. Pomeranz, Kalman B. (New York Univ.). Amer. J. Phys., 34: 565-6 (July 1966).

The equation of motion for a relativistic rocket or for any particle with a variable rest mass may be derived by applying the relativistic impulse-momentum and work-energy principles in the instantaneous rest frame. The equation of motion in this frame is in the classical non-relativistic form. The equation of motion in the observer's rest frame may then be deduced by applying the relativistic transformation equations for velocity, force, and time. (auth)

32295 WKB TREATMENT OF BOUND STATES IN AN ELECTRIC-DIPOLE POTENTIAL. Fox, Kenneth (Univ. of Tennessee, Knoxville); Turner, J. E. Amer. J. Phys., 34: 606-10(July 1966). (ORNL-P-1746).

The WKB method is applied to the problem of bound states of an electron in the field of a finite dipole. A necessary condition for binding is derived which suggests that bound states may exist only if the dipole moment is larger than a certain minimum value. It is also shown that the number of bound states given by the WKB method is comparable to the

exact number for the one- and three-dimensional square-well potentials. (auth)

32296 RELATIVISTIC TRANSPORT THEORY. Lindquist, Richard W. (Univ. of Texas, Austin). Ann. Phys. (N.Y.), 37: 487-518(May 1966).

A general-relativistic form of the Boltzmann transport equation is developed for particles or radiation interacting with an external medium. Thus generalized, the equations can be used to study radiative transfer in strong, time-varying gravitational fields. In particular, they are supplied to the problem of neutrino transport in a massive spherically symmetric star undergoing gravitational collapse. The mathematical basis of relativistic transport theory is clarified, in terms of intrinsic geometric structures in the tangent bundle over the space-time manifold. (auth)

32297 EMBEDDING PROPERTIES OF GENERAL RELATIVISTIC MANIFOLDS. Szekeres, P. (Cornell Univ., Ithaca, N. Y.). Nuovo Cimento (10), 43A: 1062-76 (June 21, 1966).

Integrability conditions for embedding a Riemannian manifold in a pseudo-Euclidean space of higher dimensions are derived. They are used to show that essentially the only physically significant solutions of the Einstein field equations which can be embedded in five dimensions are the Friedmann universes. The relation between symmetry properties and embedding properties of a manifold is discussed, setting upper bounds to the embedding class in certain cases. (auth)

32298 ENERGY MECHANICS OF SEMISTATIC SPACE-TIMES. Edelen, D. G. B. (Rand Corp., Santa Monica, Calif.). Nuovo Cimento (10), 43A: 1095-1114(June 21, 1966).

Let E be a 4-dimensional, hyperbolic normal metric space and let K denote a time-oriented normal congruence in E. If the Lie derivative of the metric tensor vanishes when projected onto the hypersurfaces normal to K, then E is termed semistatic. A unique characterization of such spaces is given in terms of the admissible forms of the metric tensor. If the Einstein field equations are assumed to hold in E, the most general form of the momentum-energy tensor that supports a semistatic energy mechanics is obtained. It is shown that all cosmological line elements previously considered are conformally equivalent to a semistatic space in which the metric tensor on the hypersurfaces orthogonal to K is Euclidean. This provides a simple and straightforward means of analyzing cosmological line elements in which there are small inhomogeneities and anisotropies. It turns out that all physical quantities can be determined in terms of the metric and curvature of the hypersurfaces orthogonal to K and one additional function of all four coordinates. These determinations are exhibited and provide a means whereby the hypersurface geometry is uniquely determinable in terms of the projection of the momentum-energy tensor onto the hypersurface. The treatment concludes with the study of a semistatic perfect fluid. (auth)

32299 INCONSISTENCY OF NORDSTROEM-TYPE THEORIES OF GRAVITATION WITH THE PRINCIPLE OF EQUIVALENCE. Harvey, A. L. (Queens Coll. of the City Univ. of New York, Flushing). Nuovo Cimento (10), 43A: 1121-5(June 21, 1966).

An unpublished argument due to Einstein was previously reconstructed showing the first Nordström theory of gravitation to be in violation of the principle of equivalence because a rotating object would fall with lesser acceleration than a nonrotating object in a static, homogeneous, gravitational field. It has been suggested that this effect is that found by Papapetrou in his study of the motion of spinning particles in the general theory of Einstein. It is shown here that the effect is (1) present in any theory of the Nordström type and (2) not dependent on rotation as such but on the essential dependence of acceleration in one direction on the velocity in the transverse direction. (auth)

32300 SCALAR PRODUCTS OF PAULI SPIN MATRICES. Chisholm, J. S. R. (Univ. of Kent, Eng. Texas A and M Univ., College Station). Nuovo Cimento (10), 43A: 1185-7(June 21, 1966).

Reduction formulas are established for nonrelativistic scalar products of Pauli spin matrices. (L.B.S.)

32301 DYNAMICAL GROUP OF THE ANISOTROPIC HARMONIC OSCILLATOR. Duimio, F. (Univ., Milan, INFN, Milan); Zambotti, G. Nuovo Cimento (10), 43A: 1203-7(June 21, 1966).

It is shown that the group $Sp_{n,r}$ can be taken as the dynamical group of an n-dimensional isotropic harmonic oscillator with an indefinite metric. It is also shown that $Sp_{n,r}$ can be taken as the dynamical groups of the anisotropic oscillator. (L.B.S.)

32302 ON CORSON'S UNIFIED VARIATIONAL PRINCIPLE. Arthurs, A. M. (Univ. of Wisconsin, Madison). Nuovo Cimento (10), 43A: 1208-9(June 21, 1966).

It is shown that the fundamental equation of dynamics, $\delta \Sigma_h \exp [iS_h] = 0$, postulated by Corson (Journ. Math. Phys., 4: 42(1963)) leads to Lagrange's equations for the classical case for summation over a definite path, but an additional postulate involving the notion of state is required for the many-path case in order to formulate quantum dynamics from classical action expressions. (L.B.S.)

32303 GROUND-STATE WAVE FUNCTION IN THE RANDOM-PHASE APPROXIMATION. Providencia, J. Da (Univ., Coimbra). Phys. Lett., 21: 668(July 1, 1966).

An equation for some parameters specifying the ground-state wave function in the random phase approximation was solved. (auth)

32304 CONDITIONS FOR EXISTENCE OF A DIAGONAL REPRESENTATION FOR QUANTUM MECHANICAL OPERATORS. Bonifacio, R. (Univ., Milan); Narducci, L. M.; Montaldi, E. Phys. Rev. Lett., 16: 1125-7(June 13, 1966).

The necessary and sufficient conditions to insure that a given operator possesses a diagonal representation in the space of rapidly decreasing tempered distributions are outlined. (G.O.Y.)

32305 TEST OF QUANTUM ELECTRODYNAMICS BY ELECTRON-ELECTRON SCATTERING. Barber, W. C. (Stanford Univ., Calif.); Gittelman, B.; O'Neill, G. K.; Richter, B. Phys. Rev. Lett., 16: 1127-30(June 13, 1966).

The differential cross section for electron-electron scattering at a total energy of 600 Mev cms was measured using a colliding-beam technique. The final analysis of the data is summarized. (D.C.W.)

32306 GRAVITATIONAL COLLAPSE IN A COSMOLOGICAL BACKGROUND. Raychaudhuri, A. K. (Presidency Coll., Calcutta). Proc. Phys. Soc. (London), 88: 545-7(July 1966).

A solution representing a model of gravitational collapse in the background of an expanding universe is presented, there being no discontinuity in the density distribution anywhere and the outside universe being of negative curvature. It is found that the phenomenon of collapse would not be observable from the expanding region. (auth)

32307 PROBLEM OF HIDDEN VARIABLES IN QUANTUM MECHANICS. Bell, John S. (Stanford Univ., Calif.). Rev. Mod. Phys., 38: 447-52(July 1966).

The demonstrations of von Neumann and others, that quantum mechanics does not permit a hidden variable interpretation, are reconsidered. It is shown that their essential axioms are unreasonable. It is urged that in further examination of this problem an interesting axiom would be that distant systems are independent of one another. (auth)

32308 PROPOSED SOLUTION OF THE MEASUREMENT PROBLEM IN QUANTUM MECHANICS BY A HIDDEN VARIABLE THEORY. Bohm, D.; Bub, J.

(London Univ.). Rev. Mod. Phys., 38: 453-69(July 1966).

The measurement problem in quantum mechanics is re-examined and it is shown that it cannot really be solved in a satisfactory way, within the framework of the usual interpretation of the theory. Von Neumann's attempts to prove that quantum mechanics is incompatible with the introduction of hidden variables are discussed, a more detailed form of Bell's argument is developed, showing that von Neumann's analysis is invalid. Using certain ideas that are implicit in the "differential-space" theory of Wiener and Siegel, a new deterministic equation of motion, is given, describing a kind of coupling of the measuring instrument to the observed system that explains in detail how the wave packet is "reduced" during a measurement in a continuous and causally determined way. By averaging over the hidden parameters, the usual statistical results of quantum mechanics are recovered as a special case. However, a more detailed analysis of the theory shows that new experimental and theoretical questions can now be raised, which go outside the framework of the quantum theory as it is now formulated. These questions are examined briefly. (auth)

32309 REFUTATION OF THE PROOF BY JAUCH AND PIRON THAT HIDDEN VARIABLES CAN BE EXCLUDED IN QUANTUM MECHANICS. Bohm, D.; Bub, J. (London Univ.). Rev. Mod. Phys., 38: 470-5(July 1966).

An argument of Jauch and Piron, which aims to prove the impossibility of hidden variables underlying the quantum theory is examined on the basis of certain assumptions that are weaker than those used by von Neumann for the same purpose. It is shown that, while the assumptions of Jauch and Piron are in fact weaker than those of von Neumann, the net result is that they actually prove nothing new at all. The conclusions of Jauch and Piron concerning the non-existence of hidden variables are indeed seen to follow from a false assumption; i.e., that the impossibility of propositions that describe simultaneously the results of measurements of two noncommuting observables is an "empirical fact." Actually, it is shown that this assumption follows if and only if one first assumes that the current linguistic structure of quantum mechanics is the only one that can be used correctly to describe the empirical facts underlying the theory. (auth)

32310 HAMILTONIAN PATH-INTEGRAL METHOD. Garrod, Claude (Univ. of California, Davis). Rev. Mod. Phys., 38: 483-94(July 1966).

A path-integral formulation of quantum mechanics is investigated which is closely related to that of Feynman. It differs from Feynman's formulation in that it involves the hamiltonian function of the canonically conjugate coordinates and momenta. The classical limit yields the variational principle: $\delta \int f(p\ddagger - N)\,dt = 0$. A path-integral formula is also obtained for the energy eigenstate projection operator associated with the time-independent Schroedinger equation. The classical limit of the projection operator formula yields a modified form of the well-known variational principle for the phase-space orbit of given energy. Relativistically covariant hamiltonian variational principles are analyzed and lead naturally to a relativistic scalar wave equation which involves a proper time variable which is canonically conjugate to the mass in the same manner as the ordinary time variable is conjugate to the energy in nonrelativistic quantum theory. (auth)

Low Temperature Physics

Refer also to abstracts 31482, 31634, 31780, 32242, and 32702.

32311 (ORO-2430-27) SUPERCONDUCTIVE THRESHOLD LOGIC CIRCUITRY. Jones II, Leonidas John (Duke Univ., Durham, N. C. Dept. of Electrical Engineering). Mar. 1966. Contract AT(40-1)-2430. 139p. Dep. mn. CFSTI $4.00 cy, $1.00 mn.

An investigation of threshold logic elements utilizing thin-film superconductive devices was made. Both fixed and adjustable logic elements were developed. The analysis of these circuits and the results of experimental verification of their performance are treated. The superconductive devices used in the logic circuits are inductors, cryotrons, and cryotron storage loops. The characteristics of these devices are formulated on the basis of the London equations and an experimental determination of penetration depth and critical field. The nature and application of both fixed and adjustable threshold logic elements are discussed. Weight values and tolerances enumerated by other investigators are used as design requirements here. (M.O.W.)

32312 (UCRL-16658, pp 133-43) HIGH-FIELD SUPERCONDUCTIVITY. (Lawrence Radiation Lab., Univ. of California, Berkeley).

Results of investigations are presented concerning aging effects on superconducting Zr-Nb alloys, niobium carbonitrides, carbides with β-Mu structure, and pulsed magnetic fields. Lists of 1965 publications are included, and research plans for 1966 are outlined. (J.R.D.)

32313 FLUX PINNING BY SUPERCONDUCTING PRECIPITATES. Livingston, J. D. (General Electric Co., Schenectady, N. Y.). Appl. Phys. Lett., 8: 319-20 (June 15, 1966).

The precipitation of Sn in Pb-Sn and Pb-In-Sn was previously shown to produce flux pinning at 4.2°K. Magnetization measurements on these alloys are extended to lower temperatures. It was found that Sn precipitates in a Pb-In matrix produce magnetic hysteresis (hence, a critical current density) that increases with increasing field and temperature. Magnetization curves at 2.0 and 4.2°K are shown. The underlying concept provides a general model for explaining the peak effect and suggests a means of producing thermally stable superconductors that may be relatively immune to flux jumping. (J.F.P.)

32314 LIQUID HELIUM AS AN ENGINEERING FLUID. Keller, W. E.; Hammel, E. F. (Los Alamos Scientific Lab., N. Mex.). Cyrog. Eng. News, 1: No. 8, 32-6(June 1966). (LA-DC-7785).

The current cryogenic applications of liquid helium are considered briefly. Some of the fluid properties that might be capitalized upon in the future are described. (M.H.R.)

32315 METHODS AND COSTS OF TESTING AT LIQUID HELIUM TEMPERATURES. PART I. Bernert, R. E. Cryog. Eng. News, 1: No. 8, 60; 62(June 1966).

Several methods of cooldown and operation using bulk cryogenic liquids are compared. To show the effect of facility costs on the selection of a method for a given set of conditions, facility cost estimates are presented for a typical example. (M.H.R.)

32316 TEMPERATURE DEPENDENCE OF MAGNETIC FIELDS TRAPPED IN Nb_3Sn HOLLOW CYLINDERS. Lange, F. (Deutsche Akademie der Wissenschaften, Dresden). Cryogenics, 6: 141-3(June 1966).

The temperature dependence of the magnetic field trapped in Nb_3Sn hollow cylinders was investigated in order to find relations to the Anderson-Kim theory. The maximum field was trapped at a temperature as low as possible, and then the entire measuring arrangement was slowly heated. The resulting temperature dependence, and the magnetic field and temperature curves are shown. (J.F.P.)

32317 CRITICAL CURRENTS AND i/v RELATIONS IN SUPERCONDUCTING ALLOY FILMS. Burton, R. (Oxford Univ.). Cryogenics, 6: 144-9(June 1966).

An attempt was made to evaluate the performance of the current in alloy films where Joule heating is avoided and current distribution in the strips is considered. The alloys used were dilute solutions of bismuth in tin and indium. Curves are given showing the critical currents obtained. Measurements of the critical currents of the films when the magnetic field was applied in the plane of the film and at right angles to it were also made, and the results are

shown for the field dependence of the critical current. (J.F.P.)

32318 SOME CRYOGENIC DEVELOPMENTS AT THE JOINT INSTITUTE FOR NUCLEAR STUDIES. Balandiko, N. I.; Belushkin, V. A.; Golovanov, L. B.; Dyachkov, E. I.; Zeldovich, A. G.; Pilipenko, Yu. K. (Joint Inst. for Nuclear Studies, Dubna, USSR). Cryogenics, 6: 158-64(June 1966).

The cryogenic engineering research laboratory of the Joint Institute for Nuclear Studies, which is concerned with the development of cryogenic equipment used in experiments in conjunction with charged particle accelerators, is described. A technical description of the laboratory equipment, the 100-cm liquid hydrogen bubble chamber, a medium-capacity expansion engine hydrogen liquefier, and a plane thin-walled liquid hydrogen target are discussed. (J.F.P.)

32319 LOW-TEMPERATURE ELECTRON IRRADIATION OF METALS: EXPERIMENTAL TECHNIQUE. Lucasson, P.; Lucasson, A.; Lelogeais, G. (Faculte des Sciences, Orsay, France). Cryogenics, 6: 169-74(June 1966).

A cryostat for electron irradiation of metals at liquid helium temperatures is described. Also experiments performed using this cryostat are discussed, and typical isochronal annealing temperature-time curves recorded during such an experiment are shown. (J.F.P.)

32320 CRITERION FOR STABILITY AGAINST FLUX JUMPING IN HIGH-FIELD HIGH-CURRENT SUPERCONDUCTORS. Lange, F. (Deutsche Akademie der Wissenschaften, Dresden). Cryogenics, 6: 176-7(June 1966).

To obtain a criterion for the stability against flux jumps the energy in the superconductor is considered. This involves the internal energy and magnetic energy. The system is stable if $dE/dT > 0$, that is if heat must be added to warm up the superconductor. But if $dE/dT < 0$, heat will be developed during warming of the superconductor. The criterion found is valid only for the case of an infinitely slow change of the exciting field. Values are obtained for porous sintered Nb_3Sn. (J.F.P.)

32321 MAGNETIC MOMENT OF A SUPERCONDUCTING ELLIPSOID IN A MIXED STATE. Kulik, I. O. (Physico-Technical Inst. of Low Temperatures, Academy of Sciences, Ukrainian SSR). JETP Lett., (USSR) (Engl. Transl.), 3: 259-61(May 15, 1966).

Translated from Zh. Eksp. Teor. Fiz., Pis'ma Redakt, 3: 398-401(May 15, 1966).

The manner in which the superconductivity is destroyed by a magnetic field in bulky specimens of type II superconductors with a nonzero demagnetizing factor is investigated. (M.H.R.)

32322 EFFECT OF PRECIPITATES ON THE CRITICAL CURRENT OF A Ti–32Nb SUPERCONDUCTOR. Sutton, J.; Baker, C. Phys. Lett., 21: 601-2(July 1, 1966).

The effects of martensitic structure and precipitates on the critical current density, J_c, are reported. Peaks in the I_c versus H curves are attributed to pinning of fluxons by the precipitate. (auth)

32323 RELATION BETWEEN THE SUPERFLUID DENSITY AND ORDER PARAMETER FOR SUPERFLUID He NEAR T_c. Josephson, B. D. (Univ. of Illinois, Urbana). Contract DA-31-124-ARO(D)-114. Phys. Lett., 21: 608-9(July 1, 1966).

Relations are derived between the superfluid density, the order parameter, and the specific heat singularity for superfluid helium near the lambda point. (auth)

32324 MACROSCOPIC QUANTIZATION IN SUPERCONDUCTING FILMS. Wolfram, T.; Lehman, G. W. (North American Aviation Science Center, Thousand Oaks, Calif.). Phys. Lett., 21: 631-2(July 1, 1966).

It is shown that the imposition of boundary conditions on the solutions of Grokov's equations can result in mixing of the degenerate hole-like and electron-like states. An example is discussed in which this mixing leads to a "macroscopic" quantization condition. (auth)

32325 SUPERCONDUCTORS AND GRAVITATIONAL DRAG. DeWitt, Bryce S. (Univ. of North Carolina, Chapel Hill). Phys. Rev. Lett., 16: 1092-3(June 13, 1966).

It is shown that a current arises from an induced motion of electrons on the surface of superconductors. This motion rotates in the same direction as the motion of the rotating mass and represents another instance of the drag effect produced by the Lense-Thirring field. (G.O.Y.)

32326 MAGNETIC FIELD-INDUCED ANISOTROPY OF THE SUPERCONDUCTING ENERGY GAP DETERMINED BY MICROWAVE ABSORPTION. Budzinski, W. V.; Garfunkel, M. P. (Univ. of Pittsburgh). Phys. Rev. Lett., 16: 1100-2(June 13, 1966).

The absorption of microwaves by a single-crystal Al disk having a thickness-to-diameter ratio of about 0.05 was measured for frequencies between 15 and 100 Gc per sec. The results for a static magnetic field that is parallel to the microwave field showed a large anisotropy in the energy gap. (G.O.Y.)

32327 THERMAL CONDUCTIVITY OF THE SUPERCONDUCTING SURFACE SHEATH. Mochel, J. M.; Parks, R. D. (Univ. of Rochester, N. Y.). Phys. Rev. Lett., 16: 1156-9(June 20, 1966).

Quantitative measurements were obtained for the temperature dependence of the variation in the thermal conductivity with magnetic field of the superconducting surface sheath near the upper critical field. Also the thickness of the surface sheath near the upper critical fields was determined from the thermal-conductivity measurements. Measurements were made on three thick In– Pb alloy films on substrates of H-Film. (J.F.P.)

32328 MICROWAVE-ENHANCED CRITICAL SUPERCURRENTS IN CONSTRICTED TIN FILMS. Wyatt, A. F. G.; Dmitriev, V. M.; Moore, W. S.; Sheard, F. W. (Nottingham Univ., Eng.). Phys. Rev. Lett., 16: 1166-9 (June 20, 1966).

It was found that the value of the maximum supercurrent at zero voltage that can flow through a constriction in a tin film depends on both the temperature and the incident microwave power at the constriction, and that under certain conditions the critical current is larger than its value without microwaves at the same temperature. The critical current through the constriction is shown as a function of microwave power at different temperatures, and the threshold microwave power as a function of temperature and the critical current without microwaves as a function of temperature are also shown. (J.F.P.)

32329 PROPAGATION OF ZERO SOUND IN LIQUID ^{3}He AT LOW TEMPERATURES. Abel, W. R.; Anderson, A. C.; Wheatley, J. C. (Univ. of Illinois, Urbana). Contract AT(11-1)-1198. Phys. Rev. Lett., 17: 74-8(July 11, 1966). (COO–1198-375).

Measurements were made of the propagation of sound in liquid ^{3}He at 0.32 atm. and at frequencies of 15.4 and 45.5 MHe down to a temperature of 2 m deg K on the CMN scale. The results show quantitative agreement with theory on velocity changes and semiquantitative agreement on attenuation, which demonstrate clearly the phenomena of the propagation of zero sound. (L.B.S.)

32330 EFFECT OF SPIN-ORBIT SCATTERING ON THE UPPER CRITICAL FIELD OF HIGH-FIELD SUPERCONDUCTORS. Neuringer, L. J.; Shapira, Y. (Massachusetts Inst. of Tech., Cambridge). Phys. Rev. Lett., 17: 81-4(July 11, 1966).

Evidence in support of the recent theoretical conjecture that spin-orbit scattering counteracts the effect of Pauli spin paramagnetism on H_{c2} was found from measurement of the temperature variation of H_{c2} for three concentrated titanium alloys, viz. Ti-58 at. % V, Ti-44 at. % Nb, and Ti-52 at. % Ta. (L.B.S.)

32331 SUPERHEATING AND SUPERCOOLING IN THE SUPERCONDUCTING TRANSITION OF SMALL INDIUM SPHERES. Feder, J.; Kiser, S. R.; Rothwarf, F. (Faculte des Sciences, Orsay, France). Phys. Rev. Lett., 17: 87-9(July 11, 1966).

The supercooling and superheating fields in the superconducting transition of small indium spheres were determined from measurements of the oscillator frequency as a function of applied field at various temperatures. The values for the Ginzburg-Landau parameter obtained from the supercooling and superheating fields were found to be equal within experimental error at all temperatures. (L.B.S.)

32332 ISOTHERMAL FLOW OF LIQUID He II THROUGH NARROW CHANNELS. Keller, W. E.; Hammel, E. P. (Los Alamos Scientific Lab., N. Mex.). Physics, 2: 221-45(May 1966).

Isothermal flow of liquid He II through narrow slits of width 0.3, 2.3 and 3.4 μ was examined using two different types of experimental arrangements, one in which the liquid flows under its own gravitational head, the other in which the liquid is pushed by a plunger through the slit. In these experiments to a good approximation only the superfluid flows. Values of the superfluid critical velocity, $v_s = v_{s,c}$, are found to be 18.0, 5.85, and 2.73 cm/sec for the three slits respectively, independent of temperature for the range $1.1 < T < 2.0°K$. At the λ point $v_{s,c}$ becomes zero. At temperatures, the critical velocities as obtained in these flows are the same as found in heat flow measurements using the same slits; but above 1.6°K results from the latter show that $v_{s,c}$ increases. Possible reasons for this behavior are discussed in terms of the vortex line model, the principal conclusion being that for both isothermal flow and heat flow in narrow channels the breakdown of superfluidity occurs because of interactions between the superfluid and the wall. At supercritical velocities ($v_s > v_{s,c}$) the dissipation effects observed in isothermal flow can be described entirely in terms of a force F_s associated with the superfluid alone, whereas in the case of heat flow the mutual force F_{sn} is dominant. The experiments show that the pressure gradient is proportional to F_s, and F_s is independent of the slit width, has a temperature variation below 1.9°K much like that of the superfluid density squared, and depends upon the velocity as $(v_s - v_{s,c})^n$. For low supercritical velocities n = 1 and for $(v_s - v_{s,c})$ greater than about 1.5 cm/sec n = 1.75. These results are also considered from the viewpoint of the vortex line model. (auth)

32333 CRYOTRON RELAXATION OSCILLATOR WITH CONTROLLED FREQUENCY. Kan, Ya. S.; Rakhubovskii, V. A. (Inst. of Physics and Tech., Khar'kov). Prib. Tekh. Eksp., No. 1, 221-2(Jan.-Feb. 1966). (In Russian).

An apparatus constructed on the basis of a cryotron generator of relaxation oscillations is described, in which it is possible to control the frequency independently from the supply current by means of auxiliary windings. The basic characteristics of this apparatus are presented. Since the circuit for the control of the cryotron relaxation oscillator can be completely superconducting, the apparatus can serve as an ammeter in superconducting circuits. (tr-auth)

32334 CRYOSTATS FOR SUPERCONDUCTING SOLENOIDS WITH THERMAL WORKING VOLUME. Fradkov, A. B.(Inst. of Physics, Moscow). Prib. Tekh. Eksp., No. 6, 215-16(Nov.-Dec. 1965). (In Russian).

The results of a test of metallic cryostats for superconducting solenoids are reported. The effects observed during sudden transition of the solenoid from superconducting to normal state are described. (tr-auth)

32335 ULTRASONIC ATTENUATION IN SUPERCONDUCTORS. Kadanoff, L. P.; Pippard, A. B. (Cambridge Univ., Eng.). Proc. Roy. Soc. (London), Ser. A, 292: 299-313(May 31, 1966).

The theory of ultrasonic attenuation in a superconductor, particularly its relation to the attenuation in the normal state of the same metal, is developed for rather general conditions, by means of a Boltzmann-equation approach. In principle no special assumptions are made about the shape of the Fermi surface or the scattering function, but in order to obtain simple results it is found necessary to assume the energy gap to take the same value at all points on the Fermi surface, and to consider elastic scattering only. It is then found that for all values of ql the attenuation of longitudinal waves follows the original BCS law, $\alpha_s/\alpha_n = 2f(\Delta)$, f being the Fermi function, while for other than purely longitudinal waves there should be a discontinuity in α_s/α_n at the transition temperature, with the residual attenuation below the discontinuity also varying as $f(\Delta)$. Considerable attention is paid to the special case $ql \ll 1$, since here the behavior is particularly sensitive to violations of the conditions assumed; variations of Δ especially can lead in principle to quite different forms of α_s/α_n. (auth)

32336 TECHNIQUES FOR USING LIQUID HELIUM IN VERY LOW-TEMPERATURE APPARATUS. Vilches, O. E.; Wheatley, J. C. (Univ. of Illinois, Urbana). Contract AT(11-1)-1198. Rev. Sci. Instrum., 37: 819-31(July 1966). (COO-1198-324).

A discussion of what is known experimentally about the thermal contact problem at very low temperatures is given. Liquid ^{4}He is a particularly promising contact agent. Methods of using liquid ^{4}He, thermometry using cerium magnesium nitrate, and solutions to the filling and isolation problems using an open capillary are discussed. The techniques are applied to an apparatus suitable for heat capacity measurements to below 0.02°K and to an apparatus for measurement of superconductive properties at temperatures substantially below 0.01°K. The performance of the apparatus for heat capacity and superconductivity measurements is discussed. (auth)

32337 ULTRAHIGH MAGNETIC FIELDS. Parkinson, D. H. (Royal Radar Establishment, Malvern, Eng.). Sci. J., 2: No. 5, 51-5(May 1966).

The contributions to basic physics and to technology which the ultrahigh magnetic fields are making are discussed. The use of high-powered water cooled solenoids and superconducting solenoids are described. The future limits in this field are estimated. (M.H.R.)

32338 SUPERCONDUCTIVITY PHENOMENA IN THIN SEMICONDUCTOR FILMS. Demikhovskii, V. Ya. (Lobachevskii State Univ., Gor'kii, USSR). Soviet Phys.-Solid State (Engl. Transl.), 7: 2903-7(June 1966).

Translated from Fiz. Tverd. Tela, 7: 3600-6(Dec. 1965).

The appearance of superconductivity is examined in thin films in which, as a consequence of linking the dimensions in one direction, the electron energy is quantized, $E(k_x,k_y,n)$. It is shown that in a film, in contrast to a massive specimen, the Cooper pairs are formed by electrons possessing opposite two-dimensional momenta and identical n. Generally speaking, the value of the parameter Δ_n differs for different two-dimensional subsystems. The dependence of the parameters Δ_n and T_{cr} on the film thickness L is determined and the effect of certain specific characteristics of the electron energy spectrum on the $\Delta_n(L)$ and $T_{cr}(L)$ dependences is investigated. (auth)

32339 SUPERCONDUCTIVE MATERIAL. Kvasil, B. Vestn. Cesk. Akad. Ved., 73: 566-70(1964). (In Czech).

Superconductors are discussed. The properties of superconductors, uses of superconductivity in technology and research, and the status of basic and applied research on superconductivity in the world and in Czechoslovakia are considered. (J.F.P.)

32340 EFFECT OF THE SPATIAL VARIATION OF THE ORDER PARAMETER ON THE TUNNELING DENSITY OF STATES OF SUPERCONDUCTING ALLOYS. Juranek, H. J.; Neumann, L.; Tewordt, L. (Univ., Hamburg). Z. Phys., 193: 459-70(1966).

Expressions of the Ginzburg-Landau (GL) type for the local tunneling density of states of superconducting alloys are derived. These expressions are quite generally applicable at high excitation energies. One can see immediately that the density of states, $N(r,\omega)$, at any position r and high energies ω is always larger than the local BCS density of states if the space dependence of the order parameter is governed by the GL-equation. This effect is largest for long mean free paths l. The spatial average of the

density of states, $\bar{N}$, at all energies ω for a lattice of vortex lines in a magnetic field slightly below the upper critical field is calculated. The resulting curve of $[\bar{N} - N(0)]/N(0)$ versus ω shows no gap and has a zero at about the gap value in zero field. Its value at $\omega = 0$ depends on l like $\ln(\xi_0/l)$ for $l \gg \xi_0$ [$N(0)$ denotes the normal density of states, and ξ_0 is the BCS coherence length]. (auth)

32341 SUPERCONDUCTING TRANSITIONS OF AMORPHOUS BISMUTH ALLOYS. Shier, J. S.; Ginsberg, D. M. (Univ. of Illinois, Urbana). 28p. (CONF-651015-22). ORAU. Gmelin, AED-CONF-65-312-47.

From American Physical Society Meeting, Chicago.

Measurements were made of the critical temperatures T_c of binary alloy films composed of amorphous bismuth with lead, thallium, or antimony in concentrations up to 13 at. %. The curves showing T_c as a function of impurity concentration are nearly linear, as expected for a superconductor with no crystalline anisotropy. The slopes of the curves are not simply related to the valence or atomic size of the impurity atoms. It is suggested that this may be explainable by extending Faber and Ziman's theory of the breakdown of Linde's rule for liquid alloys. The transitions of the films into the superconducting state are extremely sharp (~5 millidegrees wide). This indicates strongly that the electromagnetic coherence length does not limit the sharpness of the transition. (auth)

32342 TUNNEL EFFECT MEASUREMENTS ON SUPERIMPOSED LAYERS OF LEAD AND ALUMINUM. Frerichs, R.; Wilson, J. P. (Northwestern Univ., Evanston, Ill.). 14p. (CONF-660107-4). ORAU. Gmelin, AED-CONF-66-003-14.

From American Physical Society Meeting, New York.

Superimposed Al and Pb films are studied using the tunnel effect as an indication of the influence of a normal metal (Al) on a superconductor (Pb). The structures are composed of four layers, $Al/Al_2O_3/Pb/Al$. The Pb and top Al layers were vacuum evaporated onto 77°K substrates to eliminate diffusion problems. Curves are presented which show the effect of an overlayer on the tunnel junction I-V characteristic and density of states function. The film thicknesses are varied over a wide range. The variation in energy gap with Pb thickness is plotted for a constant Al overlayer of 3100 Å. In addition there are three samples made to determine the critical temperature by resistive measurements with the same structure as a check on the reliability of the tunnel junction results. The energy gap transition occurs between 300 Å and 4500 Å of Pb. Comparison with Hauser and Theuerer's results on superimposed Al and Pb films is included in the discussion. (auth)

32343 APPARATUS FOR RADIO FREQUENCY SURFACE MEASUREMENTS ON SINGLE CRYSTAL SUPERCONDUCTORS. Bryson III, C. E.; Whitmore, Frank C. (Southwest Research Inst., San Antonio). 10p. (CONF-651213-8). ORAU. Gmelin, AED-CONF-65-400-8.

From American Physical Society, Winter Meeting in the West, Los Angeles.

In an effort to take full advantage of the method of measurement of flux penetration into a superconductor used by Schawlow and Devlin (Phys. Rev., 113: 120(1959)), the external oscillator was replaced by an extremely stable tunnel diode oscillator circuit operated entirely within the liquid helium bath. When the oscillator is operated in the near sinusoidal mode, inductance changes due to flux penetration into the superconducting core are reflected as changes in frequency of the oscillator. Examples of the critical curves for mercury single crystals are shown to illustrate the application of the method. (auth)

32344 MACROSCOPIC QUANTUM INTERFERENCE IN SUPERCONDUCTORS. Jaklevic, R. C.; Lambe, J.; Mercereau, J. E.; Silver, A. H. (Ford Motor Co., Dearborn, Mich.). 45p. (CONF-641210-22). ORAU. Gmelin, AED-CONF-64-236-44.

From American Physical Society Meeting, Berkeley, Calif.

An experimental study of interference phenomena in multiply connected superconductors utilizing Josephson tunneling is reported. The results are a striking confirmation of the extensive phase coherence of the superconducting state. London's theory is used in conjunction with Josephson's prediction to explain the observations. Modulation of the maximum supercurrent flow through junction pair devices was measured in an applied magnetic field and showed periodicities resulting from quantum wave interference. These interference "fringes" were found to occur even when the magnetic flux is confined to a region not accessible to the superconductor. Another experiment allows the measurement of an interference directly attributable to phase modulation by the superconducting electron drift velocity. These results offer a direct verification of long range quantum behavior in the superconducting state and further demonstrate the validity and usefulness of Josephson tunneling methods. (auth)

32345 POSITRON ANNIHILATION IN LIQUEFIED GASES. Briscoe, C. V.; Stewart, A. T. (Univ. of North Carolina, Chapel Hill). 7p. (CONF-650721-3). ORAU. Gmelin, AED-CONF-65-211-11.

From Positron Annihilation Conference, Detroit.

Data are presented on the angular distribution of photons from positrons annihilating in the liquids hydrogen, oxygen, nitrogen, neon, and argon. Except for oxygen the results show a distribution that appears to be the sum of two separate distributions, a narrow one that shows up as a central peak and a much broader one. The angular distribution for oxygen shows no narrow component at all. The intensity of the narrow component in the other gases is compared with existing data on positronium formation. The width of the narrow component is discussed in terms of the bubble picture of positronium in certain liquids. (A.G.W.)

32346 POSITRON ANNIHILATION IN LIQUID HELIUM. Stewart, A. T.; Briscoe, C. V. (Univ. of North Carolina, Chapel Hill). 7p. (CONF-650721-5). ORAU. Gmelin, AED-CONF-65-211-12.

From Positron Annihilation Conference, Detroit.

Measurements of the angular correlation between photons from positrons annihilating in liquid helium show a narrow peak of intensity about 5%. If this narrow component is interpreted as being due to singlet positronium, this supports the conclusion that about 20% of positrons in helium form positronium. The results are discussed in relation to the bubble picture of positronium in certain liquids. (A.G.W.)

32347 CRYOGENIC QUALITY METER. Kendall, Perry E. (Industrial Nucleonics Corp., Columbus, Ohio). 29p. (CONF-660207-13). ORAU. Gmelin, AED-CONF-66-011-16.

From Symposium on Radioisotope Applications in Aerospace, Dayton, Ohio.

A discussion of the problems encountered in the design and development of a cryogenic quality meter is presented. The basic requirement is to monitor the fluid passing through the hydrogen vent line on the Saturn S-IVB stage under orbital conditions. A detailed study, performed earlier showed that the best method for such a measurement was a backscatter technique using low energy gamma photons. Quality is a term normally used to define the steam in a heating system; however, it is equally applicable to cryogenic fluid in the vent line of the vehicle. Ideally, the quality should always be near 100%; however, under zero operating conditions, it is quite possible for liquid hydrogen to creep along the vent line. Such creepage is, of course, undesirable and should be detected if possible. This meter will measure such creepage and indicate the actual percentage of vaporous fluid in the vent line. Application of radioisotope techniques eliminates the need for contacting the fluid other than indirectly. Hence, there is no possible chance of fuel contamination. A summary of the performance obtained under simulated test conditions is included. (auth)

32348 ELECTRICALLY PUMPED LIQUID HELIUM TRANSFER SYSTEM. Darrel, B.; Schoch, K. (General

Electric Co., Schenectady, N. Y.). 12p. (CONF-650802-10). ORAU. Gmelin, AED-CONF-65-193-24.

From Cryogenic Engineering Conference, Houston, Tex.

A liquid-He transfer system, which can maintain continuous flow at rates as low as one liter per hour for periods of up to several days, is described. A superconducting liquid-He pump and a liquid level sensing system, which automatically maintain a fixed He level in the cryostat, are also described. (G.O.Y.)

32349 BOILING HEAT TRANSFER FROM CYLINDERS IN A SATURATED LIQUID HELIUM II BATH. Holdredge, R. M.; McFadden, P. W. (Purdue Univ., West Lafayette, Ind.). Paper No. H-2, 20p. (CONF-650802-12). ORAU. Gmelin, AED-CONF-65-193-22.

From Cyrogenic Engineering Conference, Houston, Tex.

The boiling heat transfer characteristics were determined for two cylindrical test sections of 0.145- and 0.245-cm diameter. The saturated helium bath was maintained at constant temperatures of 2.10, 1.96, and 1.80°K. Three distinct heat transfer regions were observed—for the smallest heat fluxes, the Kapitza resistance region; for intermediate heat fluxes, a departure from the Kapitza resistance region; and at the largest heat fluxes, film boiling. The transition to film boiling occurred with a temperature jump as occurs with other liquids. The effect of depth was investigated and was found to be a significant parameter in the two regions of highest fluxes. (auth)

Neutron Physics

See also REACTOR TECHNOLOGY — Criticality Studies

Refer also to abstract 31567.

32350 (KAPL-M-6536) DOUBLE DIFFERENTIAL SCATTERING CROSS SECTIONS AND SCATTERING LAW FOR H_2O AT 302 DEG K. Kirouac, G. J.; Moore, W. E.; Seemann, K. W. (Knolls Atomic Power Lab., Schenectady, N. Y.). Jan. 1966. Contract W-31-109-eng-52. 30p. Dep. mn. CFSTI $2.00 cy, $0.50 mn.

Inelastic neutron scattering cross sections for H_2O at 302°K were obtained with a linear accelerator-phased chopper time-of-flight spectrometer. Data were accumulated for nine incident neutron energies from 0.15 to 1.8 ev and at three scattering angles: 25, 60, and 90°. The measured double differential neutron scattering cross section, and the scattering law obtained from it, are presented in tabular form. The scattering law, $S(\alpha,\beta)$, obtained by interpolating the experimental data, is tabulated for twenty integer values of β, the dimensionless energy transfer parameter. (auth)

32351 CONSTRUCTION AND PERFORMANCE OF A COLD NEUTRON SOURCE. Tunkelo, Eino (Inst. of Tech., Otaniemi, Finland). Acta Polytech. Scand., Phys. Nucl. Ser., No. 38, 1-48(1966).

The description is presented of a cold neutron source installed in a tangentially piercing beam tube of the FiR 1 reactor of Institute of Technology, Otaniemi. The moderator chamber is given a "black body radiator"-like geometry in order to enhance the moderation of neutrons. The coolant is separated from the moderator to enable use of different liquids as moderator and coolant. The influence of the moderating material and temperature as well as of the shape and size of moderator is discussed. Cryogenic and safety considerations are also presented. The performance of the cold neutron source is given in terms of the intensities and spectra of emerging neutrons. Methane (at 78°K) and liquid hydrogen (at 20°K) are used as moderators giving an intensity of 6.7×10 neutrons/sec and 1.3×10^{7} neutrons/sec for the beryllium filtered beam 3×4 cm^2. (auth)

32352 TIME DEPENDENCE OF NEUTRON YIELDS FROM (Ra + MsTh)-Be SOURCE. Khovanovich, A. I.; Kokovikhin, V. F. At. Energ. (USSR), 20: 59-60(Jan. 1966). (In Russian).

As a result of the relatively short half-life of mesothorium, the neutron yield of the (Ra + MsTh)-Be sources changes with time. The neutrons are generated in the source by the $^{9}Be(\alpha,n)^{12}C$ reaction; the α particles are emitted by the Ra and the Ra + MsTh daughters. The neutrons emitted by Ra are practically independent of time. Decay of the non-α-emitting mesothorium results in the accumulation of Th and its daughters which are α emitters. Designating by A and B the MsTh and Ra concentrations of a freshly prepared source, expressed in mg equiv of Ra and assuming that $A/B = 2/3$, as is often the case, the relation $N_t = N_0(1 + 2.02\ \eta_t)$ is obtained, whereby N_0 and N_t represent the neutron yields immediately after preparation of the source and after a time, t, respectively. The term η_t is a function of the decay constants of MsTh and Ra; its time dependence was calculated for the time period from 0 to 25 years. The curve obtained was verified during the past six years with a source containing 40% MsTh and 60% Ra. The experimental data and the calculated values agreed within a maximum error of 3%. (TTT)

32353 THEORY OF COLD NEUTRON SCATTERING BY HOMONUCLEAR DIATOMIC LIQUIDS. I. FREE ROTATION. Sears, V. F. (Atomic Energy of Canada Ltd., Chalk River, Ont.). Can. J. Phys., 44: 1279-97(June 1966). (AECL-2427).

The cold neutron scattering cross section for a system of homonuclear diatomic molecules with arbitrary nuclear spin and an arbitrary ortho-para ratio is calculated in the first Born approximation, assuming that the molecular rotation is unhindered. The cross section is expressed in the form of an expansion in terms of the angular momentum transfer. This expansion is shown to be rapidly convergent for all the permanent homonuclear diatomic liquids. To the extent that the intermolecular forces are described by an isotropic Lennard-Jones potential, the terms in the expansion can be calculated with the help of the law of corresponding states and the observed scattering functions for the condensed inert gases. The problem of neutron diffraction by homonuclear diatomic liquids is also investigated. (auth)

32354 THEORY OF COLD NEUTRON SCATTERING BY HOMONUCLEAR DIATOMIC LIQUIDS. II. HINDERED ROTATION. Sears, V. F. (Atomic Energy of Canada Ltd., Chalk River, Ont.). Can. J. Phys., 44: 1299-1311 (June 1966). (AECL-2423).

The partial wave expansion of the cold neutron scattering cross section for a homonuclear diatomic liquid in terms of the angular momentum transfer, which was previously introduced for the case of free rotation, is generalized to include hindered rotation. The cross section is expressed in terms of an orientational distribution function that is the rotational analog of the Van Hove self-correlation function. The rotational scattering function for the lth partial wave is shown to be the Fourier transform of a rotational relaxation function, $F_l(t)$, which is also the lth coefficient of the expansion of the orientational distribution function in terms of spherical harmonics. The functions $F_l(t)$ are calculated for the limiting cases of free rotation and rotational diffusion. The problem of neutron diffraction by homonuclear diatomic liquids is also investigated, and it is shown that the small angle scattering is determined by the isothermal compressibility. This is the generalization of the well-known result for monatomic liquids. (auth)

32355 NEUTRON DOSE CONVERSION FACTORS FOR RADIOACTIVE NEUTRON SOURCES. Fry, R. M. (Australian Atomic Energy Commission, Sutherland, New South Wales). Health Phys., 12: 855-6(June 1966).

The results of calculations made of the factors converting neutron fluence to kerma in soft tissue for PuBe sources are given. In the calculations only elastic collisions, with isotropic scattering in the center of mass system, were considered. The asymmetry of emission from commercial PuBe neutron sources was also measured for the case of the source axis normal to the detector-source axis. Data are tabulated. (P.C.H.)

32356 NEUTRON DOSE CONVERSION FACTORS FOR AmBe AND AmB SOURCES. Johnson, D. R. (Oak Ridge National Lab., Tenn.). Health Phys., 12: 856-7(June 1966). (ORNL-P-1780).

Neutron dose conversion factors for AmBe and AmB neutron sources are reported. The measured output of the 5 C AmBe source was $1.22 \pm 0.04 \times 10^7$ neutrons/sec and the average first collision tissue dose per neutron was $4.05 \pm 0.30 \times 10^{-9}$ rad/neutron per cm^2. Corresponding values for the 10 C AmB source were $5.55 \pm 0.17 \times 10^6$ neutrons/sec and $3.51 \pm 0.26 \times 10^{-9}$ rad/neutron per cm^2. These dose per neutron values correspond to mean neutron energies of 4.4 and 3.0 Mev, respectively. The dose conversion factor recommended for both sources and also for PuBe is $4.0 \pm 0.30 \times 10^{-9}$ rad/neutron per cm^2. (P.C.H.)

32357 ON THE PROBLEM OF DETERMINING NEUTRON FIELDS IN TIME-DEPENDENT MEDIA. [PART] II. Barz, H.-U. (Zentralinstitut fuer Kernforschung, Rossendorf, Ger.). Kernenergie, 9: 40-9(Feb. 1966). (In German).

The derivation of the theory of determining neutron fields in time-dependent media is concluded by a formal solution of the basic kinetic equations by iteration and a determination of the properties of the base system. (J.S.R.)

32358 PULSED NEUTRON GENERATOR. Serbinov, A. N.; Yakushev, V. P.; Rezvykh, K. A.; Marin, N. I.; Povsten, V. A.; Lutikov, V. K.; Doktorova, T. V. (Inst. of Physics and Power Engineering, Obninsk, USSR). Prib. Tekh. Eksp., No. 6, 51-7(Nov.–Dec. 1965). (In Russian).

A pulsed neutron generator with pulse length of 1 μsec, frequency range of 3 to 1000 hertz, and intensity of neutron yield on dT reactions of approximately 10^{12} neutrons/sec was described. (tr-auth)

32359 POLARIZATION OF NEUTRONS FROM $^7Li(p,n)^7Be$ REACTION AND FROM THE ELASTIC SCATTERING ON ^{12}C. Minzatu, I. Studii Cercet. Fiz., 17: 13-69(1965).

A survey of the general theory of polarization is presented; a polarization expression that gives a reasonable fit to experimental results is derived. An investigation of the polarization of neutrons from the reaction $^7Li(p,n)^7Be$ at 4.3 and 4.5 Mev and in elastic scattering of the neutrons by ^{12}C is summarized. (TCO)

32360 PULSED NEUTRON SOURCES APPLIED TO NUCLEAR ENGINEERING. Garlid, K. L.; Opstad, M. T. Trend Eng. Univ. Wash., 18: No. 2, 12-15(Apr. 1966).

Dynamic analysis of nuclear-engineering properties of materials and systems can be carried out quickly and easily with small, portable accelerators used as pulsed neutron generators. Some of the uses and analyses made at the University of Washington are briefly described. Further applications are anticipated. (auth)

32361 SLOWING DOWN AND THERMALIZATION OF NEUTRONS. Williams, M. M. R. New York, Interscience Publishers, 1966. 593p.

Neutrons whose motions are influenced by the temperature and physical state of the moderator are considered. The various physical models employed to describe the scattering of neutrons by gases, liquids, and solids are discussed, taking into account the different types of chemical binding and the effects of thermal motion of the target nuclei. The Boltzmann equation for neutrons is solved for situations of increasing degrees of complexity, both in scattering model and geometric configuration. Many details of the eigenvalue spectrum of the Boltzmann equation are discussed from a physical point of view and applied to an understanding of the results of the pulsed neutron and diffusion length experiments. Some of the methods used to treat the Boltzmann equation in small highly absorbing regions are described and some idea of the sensitivity of reactor physics parameters to the solid or liquid state of the moderator is given. Synthetic scattering kernels are discussed. The slowing down to energies of about one electron volt is treated including the problem of the energy spectrum of neutrons from a pulsed source, the method of synthetic kernels, and some treatments of the deep penetration problem and the resonance absorption of neutrons. The systematic derivation of the scattering kernel for an arbitrary moderator and a derivation of the classical Boltzmann equation, with particular reference to the validity of using quantum mechanical cross sections in classical equations, are included. (M.H.R.)

32362 PULSE PROPAGATION EXPERIMENTS USING A REACTOR SOURCE. Miley, G. H.; Tsoulfanidis, N.; Doshi, P. K. (Univ. of Illinois, Urbana). 29p. (CONF-660206-10). ORAU. Gmelin, AED-CONF-66-014-8.

From Symposium on Neutron Noise, Waves, and Pulse Propagation, Gainesville, Fla.

Thermal neutron pulse propagation experiments using the Illinois TRIGA Reactor as a source are briefly reviewed. An analysis which treats the problem of a pulse generated by a distributed or slowing down source in the sample is developed in detail. The solution, found in the ω-piane (corresponding to the Fourier transform with respect to time), is shown to be consistent with wave propagation theory. An initial test of the method is presented where calculations using a 2-energy mode model are directly compared to the transform of experimental data obtained using the Oak Ridge Fast Burst Reactor (HPRR). A reasonable agreement is noted and the development of this technique is continuing. (auth)

32363 ANALYSIS OF NEUTRON WAVE-TYPE EXPERIMENTS. Brehm, R. L. (Univ. of Arizona, Tucson). 21p. (CONF-660206-6). ORAU. Gmelin, AED-CONF-66-014-2.

From Symposium on Neutron Noise, Waves, and Pulse Propagation, Gainesville, Fla.

Theoretical concepts used in the analysis of neutron wave-type experiments are considered. Two aspects important only at high frequencies are discussed. These are a general investigation of the adequacy of diffusion theory both in the usual sense and in the consistent or P_1 approximation, and analysis limitations introduced by considering the slowing down of neutrons. The discussion refers to the wave experiment in which the temporal portion of the neutron flux is spatially attenuated as a single mode. That is, one measures the complex relaxation length of the temporal flux component as a function of the modulation frequency and from these measurements obtains information concerning the parameters characterizing the medium. (J.F.P.)

32364 REGULAR EIGENFUNCTIONS OF TIME DEPENDENT TRANSPORT EQUATION FOR THERMAL NEUTRONS. Copic, M. (Kansas State Univ., Manhattan). 17p. (CONF-651101-77). ORAU. Gmelin, AED-CONF-65-332-45.

From 13th Conference on Remote Systems Technology, Washington, D. C.

The regular eigensolutions of the neutron transport equation are found for finite bodies by the superposition of elementary eigensolutions for infinite medium in the form of plane waves and the transition function which is required by the boundary conditions. The orthogonality relation between the adjoint function and the neutron current at the boundary is used to determine the value of the laplacian for the infinite medium solution. The same orthogonality relation and the symmetry properties of the body determine the distribution function of elementary eigensolutions in each mode. The transition function for outgoing neutrons, needed in the orthogonality relation, is expressed by the generalized albedo operator acting on the infinite medium solution for ingoing neutrons at the boundary. The resulting integral equation for the distribution function of elementary eigensolutions can be a convenient starting point for development of suitable approximations. (auth)

32365 PULSED NEUTRON SOURCES AND APPLICATIONS. Morgan, I. L. (Texas Nuclear Corp., Austin). 29p. (CONF-660207-19). ORAU. Gmelin, AED-CONF-66-011-28.

From Symposium on Radioisotope Applications in Aerospace, Dayton, Ohio.

A discussion of fixed voltage and energy, variable voltage and energy, pulsed neutron devices and some of their applications in the aerospace industry is presented. (B.G.D.)

32366 NEW DEVELOPMENTS IN REACTOR THEORY AND NEUTRON TRANSPORT. Zelazny, R. 44p. (CONF-651123-15). ORAU.

From Conference on Reactor Physics and Engineering, Budapest.

Some generalization and application of the eigenfunctions expansion method to the solution of neutron transport problems are reviewed. The time-dependent problems encountered in the neutron transport theory are discussed from the viewpoint of the spectral properties of the Boltzmann operator. (G.O.Y.)

32367 RECENT NUMERICAL METHODS IN NEUTRON THERMALIZATION IN THE REACTOR ELEMENTARY CELL. Weiss, Z. 23p. (CONF-651123-14). ORAU.

From Conference on Reactor Physics and Engineering, Budapest.

The thermalization codes that are used at Kjelles, (Norway) and Swierk are discussed with emphasis on the numerical methods involved. The Boltzmann equation for thermal neutrons, the transport kernel for a heterogeneous medium, and the energy-transfer kernel are considered. (D.C.W.)

32368 SUPPRESSION OF NEUTRON REFLECTION BY SURFACE COATINGS. Jones, Ian R. (to U. S. Atomic Energy Commission). U. S. Patent 3,257,560. June 21, 1966.

Instruments for defining neutron passages, such as monochromators and collimators are considered. The interior instrument surfaces contacting the neutron flux are coated with an organic compound having an "Na" product between 0 and -5×10^8 barns/cc, the "Na" product being defined as $\Sigma_j N_j a_j$ where N_j is the total number of atoms of the jth species of said organic compound and a_j is the bound coherent scattering amplitude of the jth atomic species of the compound. The total reflection of neutrons from the collimator walls is thereby totally eliminated and the partial reflection of neutrons nearly completely suppressed. (AEC)

Nuclear Properties and Reactions

Refer also to abstracts 31164, 31205, 31565, 31566, 31831, 31878, 31910, 31945, and 32839.

32369 (AECL-2535) METHODS OF APPLYING COMPTON SCATTERED NEUTRON CAPTURE RADIATION TO NUCLEAR PHOTO-EXCITATION. Knowles, J. W.; Ahmed, N. M. (Atomic Energy of Canada Ltd., Chalk River (Ontario)). Mar. 14, 1966. 90p. Dep. mn. AECL $3.00.

Two facilities are described which use Compton scattered (n,γ) radiation as a source of radiation of continuous energy distribution suitable for nuclear photo-excitation experiments. In the first facility, thermal neutrons are captured in a thin plate of cadmium and the subsequent (n,γ) radiation is scattered from surrounding graphite. The intensity of the scattered radiation incident on the target, 10 meters from the source, is ≈ 1 quantum $ev^{-1}cm^{-2}sec^{-1}$ and includes all energies from 0.1 to 8.0 Mev. In the second facility, neutrons are captured in a composite plate of titanium and nickel. Characteristic radiations from this source, the 1.37- and 6.75-Mev γ-rays of ^{49}Ti and the 8.99-Mev γ-ray of ^{59}Ni, are Compton scattered from a curved aluminum plate. The relative positions of source, scatterer and target are such that scattered radiation of one energy converges to a line at the target position. The energy of the incident radiation is varied by moving the target to a different angular position with respect to the scatterer. The energy range is 0.5 to 8.5 Mev and the energy selection is 1-3%. The intensity of γ-radiation, of 7 Mev, incident on the target is ~1 quantum $ev^{-1}cm^{-2}sec^{-1}$. Radiation from a target, scattered between 90° and 135°, is detected by NaI (Tl) scintillators. Using the first facility, nuclear resonance scattering of γ-radiation was observed, between 0.8 and 6 Mev, from targets of LiF, Au and Al. Using the second facility, scattering and self-absorption measurements were made, between 5.5 and 8.0 Mev, on targets of natural and radio-lead. (auth)

32370 (ANL-7175, pp 212-16) DETERMINATION OF NUCLEAR CONSTANTS. (Argonne National Lab., Ill.).

Investigations of capture cross sections of reactor structural materials are reported. Data are included on radiative capture cross sections of ^{98}Mo, ^{89}Y, ^{139}La, ^{141}Pr, ^{176}Yb, and ^{175}Lu. (J.R.D.)

32371 (CEA-R-2832) ETUDE DE LA REACTION $^{51}V(p,n)^{51}Cr$ ET CONTRIBUTION A LA SPECTROSCOPIE DE ^{51}Cr. (Study of the $^{51}V(p,n)^{51}Cr$ Reaction and Contribution to the Spectroscopy of ^{51}Cr). Cassagnou, Yves (Commissariat a l'Energie Atomique, Saclay (France). Centre d'Etudes Nucleaires). 1966. 82p. Dep. mn.

Thesis. Submitted to Paris Univ., France. Faculte des Sciences.

Neutrons and gamma rays from the reaction $^{51}V(p,n)^{51}Cr$ were studied between 2.3 and 5.1-Mev. Energy levels of ^{51}Cr at 0.75, 1.15, 1.35, 1.47 and 1.56 Mev and unresolved levels at 1.94, 2.4, 2.75 and 2.9 Mev are observed. The gamma ray cascades of the low-lying states of ^{51}Cr up to 2.5-Mev excitation energy were completely determined through coincidence measurements. From the cascade ratios and gamma ray yields, excitation functions for the $^{51}V(p,n)^{51}Cr$ reactions, leading to the five lowest levels of ^{51}Cr were obtained from reaction threshold to 4.6 Mev. The analysis of cross section fluctuations with good resolution shows they are due to the excitation of unresolved compound nucleus isolated resonances. From the decay scheme and an Hauser-Feshbach calculation of the $^{51}V(p,n)$ excitation functions, spin assignments of $3/2^-$, or $5/2^-$ (0.75 Mev), $7/2^-$ (1.15 Mev), $3/2^-$ (1.35 Mev), $5/2^-$ (1.47 Mev) are proposed. (auth)

32372 (COO-1120-43) SPIN ASSIGNMENTS FROM TRIPLE CORRELATION UTILIZING AXIAL SYMMETRY. Prosser, F. W. Jr. (Kansas Univ., Lawrence. Nuclear Physics Lab.). [1966]. Contract AT(11-1)-1120. 44p. (CONF-660417-1). Dep. mn. CFSTI $2.00 cy, $0.50 mn.

From International Symposium on the Structure of Low-Medium Mass Nuclei, Wright-Patterson AFB, Ohio.

An analysis of the following situation is presented. Consider an initial gamma emitting state of interest a_0 which is prepared by bombardment of an unpolarized target with and incident, unpolarized radiation L_1, whose direction is the z-axis, and the subsequent emission of a radiation L_2. The only property of L_2 of immediate interest is that its detection be such as to preserve the axial symmetry of the system. The general angular correlation is given in terms of the statistical and efficiency tensors of state a_0. However, the conditions of axial symmetry, unpolarized target and beam, and sharp spin and parity for a_0 cause the density matrix to be diagonal with equal values for positive and negative substates. Several examples are described. (M.O.W.)

32373 (COO-1530-1) LOW-ENERGY NUCLEAR REACTIONS AND NUCLEAR SPECTROSCOPY. Technical Progress Report, September 15, 1965-June 15, 1966. Sarantites, D. G. (Washington Univ., St. Louis, Mo.). June 15, 1966. Contract AT(11-1)-1530. 38p. Dep. mn. CFSTI $2.00 cy, $0.50 mn.

Good progress was made on the research program proposed last year concerning low-energy reactions and nuclear spectroscopy. The level of effort and the accomplishments were about as planned in the theoretical calculations on nuclear reactions, and in the instrumentation for nuclear spectroscopy until the cyclotron became operative (February, 1966) for external irradiations with unmonitored beam. Extensive calculations on the excitation functions of alpha induced reactions on ^{107}Ag and on isomer ratios produced in the same reactions were made using the Monte-Carlo method and the statistical theory of nuclear reactions. Cross section measurements for

radiative capture of charged particles have begun. Silicon and germanium detectors were made and systems for mounting and cooling were developed. Apparatus for measurement of angular correlations of the type γ-γ, e^--γ and β^--γ were constructed and used. Decay scheme studies on a number of nuclides have begun. Instrumentation for measurement of charged particle evaporation spectra was assembled and measurements will be undertaken in the near future. (auth)

32374 (IITRI-578P25-15) EFFECT OF HIGH SPIN ON ELECTROMAGNETIC DECAY OF NUCLEI. Third Annual Report. Sperber, Daniel (IIT Research Inst., Chicago, Ill.). June 9, 1966. Contract AT(11-1)-578. 24p. Dep. mn. CFSTI $1.00 cy, $0.50 mn.

A new method was developed for calculating isomeric cross sections. The method is very general and does not depend on the spin value of the compound nucleus. It can be applied equally well both to heavy-ion reactions, in which the compound nucleus has a high spin value, and to (n,γ) reactions, in which the compound nucleus has a low spin value. A method based on the collective model was developed for calculating angular distribution. The method enables evaluation of the angular distribution due to transitions between high spin states in highly deformed nuclei. A method was developed for calculating effects of competition between M1 and E2 transitions involving high spin states. The method showed that this competition influences the angular distribution of gamma rays from high spin states and that the energy dependence of the angular distribution is due to this competition. Parametric studies showed that comparison between the described theory and experiment allows determination of the multipolarity of radiation between high spin states and better determination of the nuclear density of levels. Combination of all the above information leads to more complete understanding of the approximate model for high spin states. (auth)

32375 (ITEF-351) KONVERSIONNYE ELEKTRONYI SOPROVOZHDAYUSHCHIE α-RASPAD ^{241}Am I SKHEMA UROVNEI ^{237}Np. (Conversion Electrons Associated with α Decay of ^{241}Am and Level Scheme of ^{237}Np). Kondrat'ev, L. N.; Tret'yakov, E. F. (Gosudarstvennyi Komitet po Ispol'zovaniyu Atomnoi Energii SSSR, Moscow. Institut Teoreticheskoi i Eksperimental'noi Fiziki). 1965. 17p. Dep. mn.

Spectra of the α-e coincidences of ^{241}Am were measured by means of the ITEF double thoroidal β-spectrometer. Transitions from some high-energy levels of ^{237}Np were found; the transition from the 723-kev level was found for the first time. Energies and intensities of some weak transitions were remeasured more precisely. The level scheme of ^{237}Np was discussed. (auth)

32376 (KAPL-3090) A PROPOSAL FOR THE MEASUREMENT OF THE TOTAL NEUTRON CROSS SECTIONS OF ^{147}Pm, ^{148}Pm, AND ^{148m}Pm. Hickman, G. D.; Walker, F. W. (Knolls Atomic Power Lab., Schenectady, N. Y.). May 16, 1966. Contract W-31-109-eng-52. 38p. Dep. mn. CFSTI $2.00 cy, $0.50 mn.

A proposal is made to measure the total cross section of ^{147}Pm, ^{148}Pm, and ^{148m}Pm. Details on the formation and destruction of these and other secondary isotopes which are formed during irradiation for various flux levels are described. In addition, the "hot" chemistry which will be required for isotope separation is described. (auth)

32377 (KFK-117) DIE MATHEMATISCHE BEHANDLUNG DER ZERFALLS- UND BILDUNGSGESETZE DER RADIOAKTIVITAET MIT GRAFISCH GELOESTEN BEISPIELEN. (The Mathematical Treatment of the Decay and Formation Laws of Radioactivity with Graphically Solved Examples). Auflage, Zweite; Seelmann-Eggebert, W.; Flegenheimer, J.; Pfennig, G. (Kernforschungszentrum, Karlsruhe (West Germany). Institut fuer Radiochemie). July 1965. 33p. Dep. mn.

Lectures on decay laws and the formation of radioisotopes by nuclear reactions, that were given in connection with radiochemical laboratory courses in Buenos Aires, Mainz, and Karlsruhe, are presented. (J.S.R.)

32378 (NASA-TR-R-239) MONTE CARLO INTERPRETATION OF SPHERE TRANSMISSION EXPERIMENTS FOR AVERAGE CAPTURE CROSS SECTIONS AT 24 kev. Bogart, Donald; Semler, Thor T. (National Aeronautics and Space Administration, Cleveland, Ohio. Lewis Research Center). June 1966. 26p. (CONF-660303-33). CFSTI $1.00 cy, $0.50 mn.

From American Physical Society, Conference on Neutron Cross Section Technology, Washington, D. C.

Monte Carlo analyses of sphere transmission experiments at 24 kev are made by using statistical results from slow neutron resonance spectroscopy as input data. An average capture cross section $\bar{\sigma}_C$ for gold of 700 ± 50 millibarns is obtained compared with a reported value of 532 ± 60 millibarns evaluated by a widely used multiple scattering analysis. A small p-wave contribution is required for gold. For iodine s-wave and p-wave contributions of 442 ± 50 and 358 ± 60 millibarns, respectively, provide a $\bar{\sigma}_C$ of 800 ± 80 millibarns. This value is in substantial agreement with a reported value of 768 ± 90 millibarns. For nuclei with large s-wave scattering, such as gold, the usual multiple scattering analysis is shown to encounter difficulties because of ambiguity as to the effective scattering cross section to be used. (auth)

32379 (ORNL-TM-1208) CDC-160A PROGRAMS FOR PROCESSING DATA FROM A NEUTRON TIME-OF-FLIGHT CROSS-SECTION EXPERIMENT. Kinney, W. E.; Biggerstaff, J. A. (Oak Ridge National Lab., Tenn.). Apr. 1966. Contract W-7405-eng-26. 21p. Dep. mn. CFSTI $1.00 cy, $0.50 mn.

Codes were written for processing the data from experiments which measure neutron elastic- and inelastic-scattering cross sections by the time-of-flight technique. The data are accumulated in an ND-160 4096-channel pulse-height analyzer and are extracted from it by means of punched paper tape or sent directly to a CDC-160A computer over a data-link cable. The codes enable the data to be printed, the background to be normalized and subtracted, the walk in the circuitry to be corrected, and the corrected results to be printed. (auth)

32380 (SC-RR-66-229) TABULATION OF CROSS SECTIONS, Q-VALUES, AND SENSITIVITIES FOR NUCLEAR REACTIONS OF NUCLIDES WITH 14-Mev NEUTRONS. Kenna, B. T.; Conrad, F. J. (Sandia Corp., Albuquerque, N. Mex.). June 1966. Contract AT(29-1)-789. 42p. Dep. mn. CFSTI $2.00 cy, $0.50 mn.

This compilation is divided into two parts. The first tabulates target and product isotopes by chemical symbol and mass number, percentage abundance, reaction cross section, half life, decay characteristics, and an indication of sensitivity for (n,γ), (n,α), (n,p) and (n,2n) reactions of nuclides with 14-Mev neutrons. The second part lists the target isotope by chemical symbol and mass number, the mass in ama based on ^{12}C, and the Q-values in Mev for (n,2n), (n,p), and (n,α) reactions of nuclides with 14-Mev neutrons. (auth)

32381 (SGAE-PH-37/1966) ^{210}Pb, SCHALENMODELL-RECHNUNGEN MIT HARMONISCHEN OSZILLATORWELLENFUNKTIONEN. (^{210}Pb, Shell Model Calculations with Harmonic Oscillator Wave Functions). Hertenberger, Gerhard; Steinbach, Gerda; Geramb, Heinrich V. (Oesterreichische Studiengesellschaft fuer Atomenergie G.m.b.H., Seibersdorf). 1966. 8p. Dep. mn.

The dependence of the energy level splitting for 0+, 2+, 4+, and 6+ were shown from the range of the configuration mixing the potential form, and the potential parameter for singlet and triplet potential depths. (tr-auth)

32382 (UCRL-14582-T(Rev.1)) GENERAL NON-DYNAMICAL FORMALISM FOR REACTIONS WITH PARTICLES OF ARBITRARY SPIN. NUMBER OF FORM FACTORS. PARITY CONSERVATION. Csonka, Paul L.; Moravcsik, Michael J.; Scadron, Michael D. (Lawrence Radiation Lab., Univ. of California, Livermore). Dec. 1965. Contract W-7405-eng-48. 93p. Dep. mn. CFSTI $3.00 cy, $0.75 mn.

The general non-dynamical formalism for reactions in-

volving particles of arbitrary spins is further developed. The number of form factors in the M-matrix is determined under parity conservation as well as other conservation laws, and from this it is derived that many conservation laws have no non-dynamical tests of validity in reactions involving spin-zero particles only. The factorization of the M-matrix into irreducible constituents is developed for parity conserving reactions and it is shown how the compound observable can be written down in terms of observables and so-called pseudo-observables of the constituent reactions. It is then demonstrated that for parity conserving reactions, an unpolarized and uncorrelated particle is in general equivalent to a fictitious spin-zero particle possessing both positive and negative parity (dual particle). The structure of observables in terms of the type of traces they contain is studied. The number of terms in a compound observable is derived. It is shown that the number of observables in a parity conserving reaction is always larger than the number of independent bilinear combinations of form factors. Thus, there are always linear relations among the observables. The number and character of these relations are explored and it is shown that they also lead to the complete list of parity experiments, i.e., experiments from which one can determine the intrinsic parity of one of the particles in the reaction, knowing the intrinsic parities of the other participating reactions but knowing nothing about the dynamics of the reaction. It is shown that the observables can be divided into subclasses, a given subclass containing observables which are different linear combinations of the same bilinear combinations of form factors. Each such bilinear combination appears in one and only one subclass. (auth)

32383 MATRIX ELEMENTS FOR INELASTIC SCATTERING OF HEAVY PARTICLES. [PART] I. Kalinkin, B. N.; Grabovskii, Ya. (Joint Inst. for Nuclear Research, Dubna, USSR). Acta Phys. Pol., 29: 283-95(Mar. 1966). (In Russian).

An analysis was made of the structure of the matrix elements of the inelastic scattering of heavy particles at $E > V_V$. It is shown that the use of quasiclassical approximations can greatly simplify its calculation. The role of the deformations introduced by the nuclear forces is described and evaluated. (tr-auth)

32384 MATRIX ELEMENTS FOR INELASTIC SCATTERING OF HEAVY PARTICLES. [PART] II. Grabovskii, Ya.; Kalinkin, B. N. (Joint Inst. for Nuclear Research, Dubna, USSR). Acta Phys. Pol., 29: 297-302(Mar. 1966). (In Russian).

The orbital representation of the matrix elements for inelastic scattering of heavy particles ($E < V_B$) is presented. The results of part one were generalized to the case of the calculation of the energy loss and of the projection of the momentum transfer different from 0. (tr-auth)

32385 PRELIMINARY REPORT ON THE HALF LIFE OF ^{130}Te DOUBLE β DECAY. Ogata, K.; Okano, J.; Takaoka, N. (Osaka Univ.). Advance. Mass Spectrometry, 3: Proc. Conf. Paris, 1964, 603-14(1966).

The half life of ^{130}Te double β decay was determined by the isotope dilution method with a high-sensitivity mass spectrometer. The samples used were old tellurium ores obtained from Oya gold mine, Teine mine, and Kawazu mine in Japan. The ores were crushed in fine grains and ^{130}Xe, product of ^{130}Te double β decay, was extracted from the ores by heating them in an electric furnace. The spike ^{128}Xe used for the dilution method was prepared by neutron bombardment of KI in a nuclear reactor. The positive results were obtained for two samples from Oya mine; the amounts of sample used were 17.5 g and 10.9 g and the content of Te in them was 33.8 per cent and 13.2 per cent respectively. The determined amount of ^{130}Xe, the daughter of ^{130}Te, was $(2.09 \pm 0.27) \times 10^{-11}$ ccSTP and $(1.01 \pm 0.18) \times 10^{-11}$ ccSTP. From these results, the half lives of ^{130}Te double β decay calculated for each case above were $(1.07 \pm 0.21) \times 10^{21}$ years and $(5.38 \pm 0.95) \times 10^{20}$ years. On the calculation, the Xe age of the ore was determined from the age of porphyrite, of which the age is expected to be about the same as that of the Te ore. The age of the poryphyrite was determined by K–Ar method with the same mass spectrometer as used for ^{130}Xe measurement. (auth)

32386 STUDY BY MASS SPECTROMETRY OF La(p,3pxn)Cs REACTIONS. Nguyen-Long-Den (Laboratoire Joliot-Curie de Physique Nucleaire, Orsay, France). Advance. Mass Spectrometry, 3: Proc. Conf. Paris, 1964, 615-17(1966). (In French).

A preliminary study was made of the determination of cross sections for production of cesium isotopes in the spallation reactions, La(p,3pxn)Cs induced by 30- to 155-Mev protons. The cesium is extracted from the target by vacuum distillation and is directly deposited on the filament of the mass spectrometer. Production of the stable isotope mass 133 was determined by measurement of the quantities of ^{133}Cs produced in samples irradiated for various times. The amount of natural cesium contamination in the lanthanum target material was determined to be 10^{-10} g/g. (auth)

32387 INTERACTION RADIUS INDEPENDENT THEORY OF RESONANCE AND DIRECT NUCLEAR REACTIONS. Saperstein, Alvin M. (Wayne State Univ., Detroit). Ann. Phys. (N.Y.), 37: 209-23(Apr. 1, 1966).

A general theory of nuclear reactions is formulated which is valid for arbitrary short-range interactions between identical nucleons and which is independent of any assumptions about the existence of a nuclear radius. Assumptions are made, instead, about the analytic character of the reduced transition matrix. Both resonance and direct reactions, as well as the relation between them, follow directly from the formalism. (auth)

32388 COUPLED EQUATIONS FOR REARRANGEMENT COLLISIONS. II. Chen, J. C. Y. (Brookhaven National Lab., Upton, N. Y.); Mittleman, M. H. Ann. Phys. (N.Y), 37: 264-70(Apr. 1, 1966). (BNL-9451).

A projection operator which projects out direct and rearranged scattering from the total wave function is derived. It is much simpler than one previously presented; however, this new method has certain limitations, the most important one being that the recoil of the target must be neglected. (auth)

32389 s- AND p-WAVE NEUTRON SPECTROSCOPY. PART XIa. LEVEL SPACINGS IN EVEN INTERMEDIATE ELEMENTS. Farrell, J. A.; Bilpuch, E. G.; Newson, H. W. (Duke Univ., Durham, N. C.). Ann. Phys. (N.Y.), 37: 367-410(May 1966).

High resolution neutron total cross sections of separated isotopes of ^{42}Ca, ^{44}Ca, ^{50}Cr, ^{54}Cr, ^{58}Ni, ^{60}Ni, ^{62}Ni, ^{64}Ni, ^{46}Ti, ^{48}Ti, and ^{50}Ti were measured using the ^{7}Li(p,n)^{7}Be reaction as the source of neutrons. The data were fitted with a multilevel formula derived from the R Matrix Theory. Widths have been obtained for all recognizable s-wave resonances and for most of the p-wave resonances. The distributions of the reduced widths and local spacings of the s-wave resonances were found to be in good agreement with the combined Porter-Thomas and Wigner distributions. The average s-wave level spacings were corrected to an excitation energy of 6 Mev and combined with data for Part VIII in this region in order to compare the behavior of the average level spacings with the predictions of various shell models. We obtain reasonably good agreement with both the Rosenzweig model and the model of Newson and Duncan if we assume that, at the excitation energies involved, a major shell is closed at 16 nucleons instead of 20. The data indicate that a dependence of the average level spacing on neutron excess exists but that it probably is not a simple exponential. Attempts to find triple and quadruple coincidences of the resonances due to the Ni, Cr, and Ca isotopes were unsuccessful. (auth)

32390 DYNAMIC ORIENTATION OF SPIN-1 NUCLEI. II. Bhatia, K. L.; Narchal, M. L. (Kurukshetra Univ., India). Appl. Opt., 5: 1075-82(June 1966).

The Jeffries-Abragam effect in an electron-nuclear coupled spin system ($S = \frac{1}{2}$, $I = 1$) is studied in detail. From a population-distribution analysis of the system,

the nuclear orientation parameters are computed and their temperature dependence discussed. Conditions for obtaining stimulated emission are examined in detail. The results are compared with those of an earlier paper. (auth)

32391 GAMMA SPECTROMETER MEASUREMENTS OF ^{238}U CAPTURE-TO-FISSION RATIO. Yurova, L. N.; Bushuev, A. V. At. Energ. (USSR), 20: 60-1(Jan. 1966). (In Russian).

The capture-to-fission cross section ratio of ^{238}U may be measured by determining the relative intensities of two lines of the γ spectrum of a neutron-irradiated specimen; one of these lines belongs to an isotope formed by capture, such as ^{239}U or ^{239}Np, the other to the fission product ^{140}La. Evaluation of these data requires knowledge of the absolute yields of these lines, of the probability of formation of ^{140}La, and of the efficiency of the γ spectroscope which depends largely on the properties of the detector. Even though all these factors are not known with the desired precision, valuable data were obtained. The ratio may be determined more conveniently by calibrating the specimen before the actual measurement in a thermal flux, assuming that the ^{140}La is formed only by the fission of ^{235}U. This method was used in experiments carried out on the BR-1 reactor; an accuracy of 0.5% was reached. The method is considered suitable for determining other reactor parameters, such as the initial breeding ratio, fast-neutron multiplication factor, etc; it may be used for systems ranging from fast assemblies to thermal reactors. (TTT)

32392 INFLUENCE OF CHEMICAL BINDING ON NEUTRON CROSS SECTIONS AT HIGH ENERGY. Drittler, K. Atomkernenergie, 11: 262(May-June 1966). (In German).

Experiments have indicated that chemical binding effects the total cross section of copper in its irradiation with neutrons with energies above 10 ev. An equation expressing the total cross section, that takes into consideration the chemical binding, is presented. It is in agreement with the experimental results. (J.S.R.)

32393 THE EXPERIMENTAL DETERMINATION OF THE MATRIX ELEMENTS IN THE FIRST-FORBIDDEN β-TRANSITIONS. Subotowicz, M. ATOMKI (Atommag Kut. Intez.) Kozlem., 7: 237-53(Dec. 1965). (In Hungarian).

Discovery of the nonconservation of parity led to an increase of the possible experiments concerning the first-order forbidden β transitions and made it possible to interpret better the data that became available. The information available on this area is summarized, outlining the material needed for the determination of matrix elements. The order of the individual matrix elements in specific β transitions must satisfy the following correlation: $I J_1 - J_2 I = \Delta J \leq \lambda \leq J_1 + J_2$, where J_1 and J_2 represent the angular momentum of the nucleus before and after β decay. In not unequivocally forbidden transitions, the determinable values depend on the second, first, and zero power of the ξ (xi) parameter. The following factors, which depend on ξ^2, are most important: the form factor, the β circular polarization of the γ-angular correlation and the γ longitudinal polarization of the β angular correlation. The measured values allow a determination of the linear combination ratio V/Y of the matrix elements in the ξ correlation. Valuable experimental data are available on nuclei, such as ^{124}Sb, ^{154}Eu, and ^{140}La for further studies in the approximation. The error is still too high; its reduction below 1% would make it possible to determine the limits of applicability of the approximation. The experiments require sources with high activity, reduced thickness and small diameter; the decay must be a first-order forbidden one, without branching, with a half life of the order of a few days, with relatively low successive γ quantum energies. This limits the number of possible experiments. (Review article, 54 references). (TTT)

32394 ENERGY SPECTRA OF PHOTOPROTONS FROM ALUMINIUM, SULFUR, AND SILICON. Lichtblau, H.; Spicer, B. M. (Univ. of Melbourne). Austral. J. Phys., 19: 297-307(June 1966).

Energy distributions of photoprotons emitted at 90° to the bombarding x-ray beam of the Melbourne 35-Mev betatron from thin targets of natural aluminum, sulfur, and silicon, measured with a scintillation spectrometer incorporating pulse-shape discrimination (PSD), are presented. The ^{27}Al proton spectrum, whose shape is found to be inconsistent with predominant evaporation of particles from a compound nucleus, exhibits a "hump" at 8.6 Mev, which is attributed to transitions between known levels in target and residual nuclei. Comparisons of the photoproton spectra from silicon and sulfur with simple particle-hole model calculations indicate that simultaneous agreement of the theory with observed locations of giant resonances and decay modes is not obtainable. (auth)

32395 EXCITED STATES OF ^{11}C FROM n-γ ANGULAR CORRELATIONS AND GAMMA BRANCHING RATIOS. Rupaal, A. S.; White, B. L.; Prescott, J. R. (Univ. of British Columbia, Vancouver). Can. J. Phys., 44: 1213-23(June 1966).

An experimental study of excited states of ^{11}C below 6.5 Mev has been made using the ^{10}B (d,nγ)^{11}C reaction at a deuteron bombarding energy of 0.8 Mev. Measurements were made of the n-γ angular correlations of the ground-state gamma transitions from the 6.49- and 4.32-Mev levels, and of the gamma-ray branching ratios from the 6.49-, 4.81-, and 4.32-Mev levels. Theoretical analysis of the n-γ angular correlations suggests that the J values of the 6.49- and 4.32-Mev levels are ($^3/_2$), ($^5/_2$), or ($^7/_2$). The parities of all the states observed in this experiment are already known to be negative from high-energy stripping data. A comparison of the experimental branching ratios with theoretical branching ratios predicted by the intermediate coupling shell model is consistent with the following spin and parity assignments in ^{11}C: ground state ($^3/_2$)$^-$, 2.00 Mev ($^1/_2$)$^-$, 4.32 Mev ($^5/_2$)$^-$, 4.81 Mev ($^3/_2$)$^-$, and 6.49 Mev ($^7/_2$)$^-$. (auth)

32396 DIRECTIONAL CORRELATIONS IN ^{127}I. Neeson, J. F.; Roalsvig, J. P.; Arns, R. G. (State Univ. of New York, Buffalo). Can. J. Phys., 44: 1313-20(June 1966).

Gamma-gamma coincidence measurements on the decay of 9.3-hour ^{127}Te to ^{127}I form the basis of the decay scheme presented, which confirms the accepted decay sequence. Directional correlation measurements were made on the 215-203 kev and 360-58 kev cascades. The respective correlation functions are: $W(\theta) = 1 + (0.22 \pm 0.02)P_2(\cos\theta)$, and $W(\theta) = 1 + (0.35 \pm 0.02)P_2(\cos\theta)$. The directional correlation results were interpreted in terms of the accepted spin sequence, and limits of multipole mixtures are presented. A short discussion of the collective properties of the levels is presented. (auth)

32397 SUPERCONDUCTIVITY FOR THE NUCLEAR-PAIRING INTERACTION. Goodfellow, J. F.; Nogami, Y. McMaster Univ., Hamilton, Ont.). Can. J. Phys., 44: 1321-7(June 1966).

An alternative formulation of the method developed by Nogami to eliminate the effect of the number fluctuation in the superconductivity approximation for the nuclear pairing interaction is given. The excited states of nonzero seniority are also discussed, where the effects of blocking and number fluctuation should be taken into account simultaneously. This can be done readily by this method. The excitation energies are obtained with good accuracy, as it is shown by comparing these results with exact ones for the model of Ni isotopes obtained by Kerman, Lawson, and Macfarlane. (auth)

32398 LOW-LYING NEGATIVE PARITY STATES IN THE A = 17 NUCLEI. Margolis, B.; De Takacsy, N. (McGill Univ., Montreal). Can. J. Phys., 44: 1431-47 (July 1966).

The low-lying negative parity states of the A = 17 nuclei are calculated assuming a two-particle-one-hole structure. The level structure and the electromagnetic and β-decay transition rates are calculated and compared with experiment. (auth)

32399 NEW ALPHA-DECAY BARRIER PENETRABILITIES WITH IGO POTENTIAL: EVEN-MASS NUCLEI. Kohlmann, L.; Voeroes, T. (Hungarian Academy of Sciences, Budapest). Can. J. Phys., 44: 1479-84(July 1966).

The Igo potential is used for the calculation of barrier penetrabilities for ground-state and excited-state transitions of even-even nuclei and for transitions of odd-odd nuclei, measured after 1959. The barrier penetration factors were calculated by numerical integration in the WKB approximation, taking into consideration centrifugal barrier effects for even-even nuclei, but ignoring noncentral interactions. Using the calculated penetration factors and the experimental alpha half-lives, the reduced level widths were calculated in each case. The barrier penetration factors and the reduced level widths are given for total decay energy (alpha-particle energy plus electron-screening correction plus recoil energy). (auth)

32400 ^{35}Cl AND THE UNIFIED MODEL. Taras, P. (Univ. of Montreal). Can. J. Phys., 44: 1563-72(July 1966).

The experimental results obtained for ^{35}Cl are interpreted in terms of the unified model. Members of five rotational bands can be identified. The band based on the ground state can be assigned $K = 3/2$ and positive parity. Of the three excited-state bands, two have positive parity and $K = 1/2$, while the third one has negative parity and $K = 3/2$. (auth)

32401 HALF LIFE OF THE 570-kev EXCITED LEVEL OF ^{207}Pb. Gorodetzky, Serge; Schulz, Norbert; Knipper, Albert (Institut de Recherches Nucleaires, Strasbourg). Compt. Rend., Ser. B, 262: 1158-61(Apr. 25, 1966). (In French).

A direct measurement of the half life of the excited level at 570 kev gives a value $T_{1/2} = 1.28 \pm 0.05 \times 10^{-10}$ sec. This result is compared with values published previously. (tr-auth)

32402 REACTION ^{11}B(p,$\alpha\alpha$)^{4}He AT 163 kev. Longequeue, Jean-Pierre; Engelhardt, Dieter; Giorni, Alain; Perrin, Claude; Bouchez, Robert (CEA, Grenoble, France). Compt. Rend., Ser. B, 262: 1162-5(Apr. 25, 1966). (In French).

The angular and energy correlations between the 3 α particles show the energy level structure of ^{8}Be. However at approximately 60° of the recoil direction, the emission of 3 α particles without correlation does not appear to be completely excluded. (tr-auth)

32403 METHOD FOR THE SIMULTANEOUS MEASUREMENT OF THE BEAM ENERGY IN ANGULAR DISTRIBUTION STUDIES. Hulubei, Horia; Indreas, Grigore; Scintei, Neculai; Berinde, Alexandru; Martalogu, Nicolae; Neamu, Ionel; Teodorescu, Crina (Institut de Physique Atomique, Bucharest). Compt. Rend., Ser. B, 262: 1351-4(May 16, 1966). (In French).

A kinematic variant for the measurement of the energy of accelerated particles is proposed in which the inelastic scattering spectra are used. (tr-auth)

32404 DETERMINATION OF INTRINSIC QUADRUPOLE MOMENTS OF BARIUM BY MEASUREMENTS OF ISOTOPIC DISPLACEMENTS. Comaniciu, Nicolae; Draganescu, Vasile; Ionescu-Pallas, Nicolae; Tatu, Vasile (Institut de Physique Atomique, Bucharest). Compt. Rend., Ser. B, 262: 1355-8(May 16, 1966). (In French).

The nuclear deformation parameters α and the intrinsic quadrupoles Q_0 were measured by using the values of the isotopic displacements of Ba(II) rays, λ4,934 Å, and λ4,554 Å, measured on samples enriched in ^{134}Ba, ^{135}Ba, ^{136}Ba, ^{137}Ba, and ^{138}Ba. (tr-auth)

32405 NUCLEAR MICROSCOPY. Bishop, G. R. (Univ of Glasgow). Endeavour, 25: 89-94(May 1966).

The nucleus of the atom is usually regarded as a dense central mass occupying only about 2 parts in 10^{14} of the atom. This value is derived from Rutherford's observations of the anomalous scattering of a stream of α particles. For a number of reasons, electrons are more suitable probes than α particles; experiments using electron probes, and the results obtained from them, which include the discovery that many nuclei are ellipsoidal are described. (auth)

32406 HALF-LIFE OF ^{125}I. Richmond, C. R.; Findlay, J. S. (Los Alamos Scientific Lab., N. Mex.). Health Phys., 12: 865(June 1966). (LA-DC-7479).

During long-term metabolic studies, a new value for the half life of ^{125}I was obtained. In one sample a value of 58.72×0.10 days was obtained and in another sample a value of 58.80 ± 0.08 days was found. The arithmetic average value of 58.76 days with a standard deviation of 0.13 lies between the previously reported values of 57.4 ± 0.2 and 60 days. (P.C.H.)

32407 ON THE DECAY OF ^{140}Ba. Kern, J.; Mauron, G.; Huber, O. (Univ., Fribourg, Switzerland). Helv. Phys. Acta, 39: 212-13(1966). (In French).

The intensities of gamma rays from the disintegration of barium-140 were determined. The intensities relative to five transitions, 163, 304, 424, 438, and 537 kev, were measured and are indicated in the ^{140}Ba – ^{140}La spectra shown. (J.F.P.)

32408 EXCITATION OF LEVELS AT 7.66, 9.63, 10.1, 10.84, AND 11.82 Mev OF ^{12}C NUCLEUS BY INELASTIC SCATTERING OF 14.1-Mev NEUTRONS. Grin, G.-A.; Joseph, C.; Alder, J. C.; Vaucher, B.; Loude, J.-F. (Univ., Lausanne, Switzerland). Helv. Phys. Acta, 39: 214-16 (1966). (In French).

Angular distributions (absolute value of the differential cross sections) for the reactions induced by 14.1-Mev neutrons on carbon-12 nuclei from which a neutron is emitted were deduced from measurements made by the analysis of time-of-flight in coincidence with the detection of events associated with scintillation scattering. The differential cross sections for elastic and inelastic scattering by carbon-12 are shown, including new levels at 10.84 and 11.82 Mev and the excitation of a broad level. (J.F.P.)

32409 TRANSFER THEOREM FOR MULTICHANNEL SCATTERING. Amrein, W. (Univ., Geneva). Helv. Phys. Acta, 39: 226(1966).

A theorem expressing the transfer of a measureable quantity averaged over the scattering cross section for all possible outgoing states of a multichannel reaction is derived in terms of a certain integral over the ingoing state. This theorem is valid for operators that commute with all channel hamiltonians. If the identity operator is chosen as the operator, the optical theorem is obtained as a special case for multichannel processes. (J.F.P.)

32410 NOTE ON THE DECAY OF ^{51}Cr. Ribordy, C. (Univ., Fribourg, Switzerland); Huber, O.; Siffert, P.; Stab, L. Helv. Phys. Acta, 39: 262-6(1966). (In French).

The γ spectrum following the decay of ^{51}Cr is investigated with a germanium-lithium drifted detector. Beside the well-known transition of 320 kev, the weak 470- and 645-kev transitions did not appear. A maximum intensity ratio is given for them. The pile-up spectra of germanium diodes and NaI(Tl) scintillation counters are compared. (auth)

32411 THE ^{6}Li(d,n)^{7}Be* REACTION WITH POLARIZED DEUTERONS. Michel, G.; Benenson, R. E.; Buergisser, H.; Huber, P.; Schier, W. A.; Striebel, H. R. (Univ., Basel). Helv. Phys. Acta, 39: 267-80(1966). (In German).

The ^{6}Li(d,n)^{7}Be* -reaction (429 kev) was studied with incident polarized deuterons from the Basel source over an energy range from 270 to 600 kev. The neutrons corresponding to the first excited state of ^{7}Be were detected in coincidence with the de-excitation γ rays using a fast tunnel diode circuit of about 5×10^{-9} s time resolution. The γ radiation and the neutrons were detected with NaI- and Ne 102 plastic scintillators respectively. In a preceding experiment, angular distributions of ^{6}Li(d,n)^{7}Be* -neutrons were measured with unpolarized

deuterons at energies between 200 and 800 kev. The results clearly exhibit stripping patterns for an angular momentum transfer of $l_p = 1$. The angular distributions obtained with tensor polarized (aligned) deuterons indicate that the reaction is within statistical errors (2%) not sensitive to any component of the deuteron tensor polarization. However, measurements of right-left asymmetries of the neutrons showed vector polarization effects of up to 40% corresponding to a maximum analyzing power of $P_2^2 = 0.35 \pm 0.03$. Over the whole energy range the measured angular distributions of P_2^2 remain positive and do not change appreciably with incident energy. (auth)

32412 POSSIBLE EXAMPLE OF A $^{12}_{\Lambda}$B HYPERFRAGMENT. Pathak, K. M. (Cotton Coll., Gauhati, India). Indian J. Phys., 39: 600-1(Dec. 1965).

An event is described which was observed in a systematic study of hyperfragments produced as a result of the interactions of 3 Bev π^- mesons with the G5 emulsion nuclei. The event was interpreted as due to a $^{12}_{\Lambda}$B hypernucleus emitted from a parent star of the type $(9 + 2)\ \pi^-$. A microphotograph of this event is given. The most plausible decay scheme is given. (M.H.R.)

32413 THE GAMMA RADIATION OF ^{83}Br. Gobrecht, H.; Tausend, A.; Braetter, P.; Willers, G. (Technische Univ., Berlin). Int. J. Appl. Radiat. Isotop., 17: 365-6 (June 1966).

The gamma spectrum of ^{83}Br was investigated. After irradiation of pure selenium in a reactor and a chemical procedure for separation of halogens, ^{83}Br was measured as silver bromide. One peak for ^{83}Br was found at an energy of $E = 0.522 \pm 0.001$ Mev. (M.C.G.)

32414 MEASUREMENT OF THE DECAY SCHEME CORRECTION IN THE ABSOLUTE STANDARDIZATION OF ^{57}Co. Williams, A.; Birdseye, Rosemary A. (National Physical Lab., Teddington, Eng.). Int. J. Appl. Radiat. Isotop., 17: 366-7(June 1966).

The decay scheme of ^{57}Co is shown. The relation between the disintegration rate number and the observed β, γ, and $\beta\gamma$ coincidence rates, corrected for background and accidental coincidences, is presented. (M.C.G.)

32415 INVESTIGATION OF CONVERSION ELECTRON SPECTRA OF THE ISOTOPES ^{166}Tm, ^{164}Yb, ^{164}Tm, AND ^{162}Tm. Abdumalikov, A. A.; Abdurazakov, A. A.; Gnatovich, V.; Gromov, K. Ya.; Dzhelepov, B. S. (Tashkent Polytechnic Inst.). Izv. Akad. Nauk Uz. SSR, Ser. Fiz.-Mat. Nauk, No. 6, 56-63(Nov.-Dec. 1965). (In Russian).

The conversion electron spectra of thulium and ytterbium isotopes were investigated with a beta spectrograph and a constant magnetic field. The samples were obtained by irradiating a tantalum target for 1–2 hours with 660 Mev protons in the synchrocyclotron of the Joint Institute of Nuclear Research. Film exposure usually began about 3 hours after irradiation. The electron conversion lines for ^{166}Tm, ^{164}Yb, ^{164}Tm, and ^{162}Tm are reliably identified and the results tabulated. Accuracy of gamma-transition energy determinations was about 0.1%, and that of intensity determinations was about 20% for strong lines and about 40% for weak lines. Previously unknown gamma transitions were found having the energies 112.8, 215.9, 228.1, 238.4, 293.2, 389.3, 496.8, 543.9, and 703.0 kev. Results of the study are discussed in detail, analyzed and compared with other published data. The decay schemes of ^{166}Tm and ^{164}Yb are diagrammed. The following gamma-transitions, arising during decay of ^{164}Yb between the odd-odd levels of the ^{164}Tm nucleus, were discovered for the first time: 37.5 (MI), 149.3, 164.5 (MI), 187.7 (MI), 190.3, 324.2, 327.3, 362.9, and 390.4 kev. The intensities of these lines are discussed in detail, and conclusions reached are compared with those of other authors. (CFSTI)

32416 MOMENTS OF INERTIA OF STRONGLY DEFORMED NUCLEI. Alkhimov, V. I. (Inst. of Physics and Tech., Moscow). Izv. Vyssh. Ucheb. Zaved., Fiz., No. 5, 55-61(1965). (In Russian).

The moments of inertia of nuclei whose deformation significantly exceeds equilibrium are calculated. This deformation is possessed by fissioning nuclei in the process of fission or by fission fragments at the moment of their formation. The method developed by Migdal for finite dimensional systems having the property of superconductivity is used. (M.J.T.)

32417 INFLUENCE OF SURFACE INHIBITORS ON THE RELAXATION TIME OF ORIENTED ATOMS. Preobrazhenskii, N. G.; Senina, S. V. (Kuznetsov Inst. of Physicotechnical, Siberian SSR). Izv. Vyssh. Ucheb. Zaved., Fiz., No. 5, 73-6(1965).

Previous work on developing a theory which takes into account the effects of both a buffer gas and a surface inhibitor on the relaxation time is reviewed. The diffusion of oriented atoms in a cell with cylindrical or spherical configuration and the probability of the occurrence of disorientation during a collision of the atom with a cell wall coated with an inhibitor are calculated. (M.J.T.)

32418 RATIONAL TABLE OF THE RADIOACTIVE DECAY FUNCTION. Gavrik, V. Ya. (Mozhaiskii Military Academy, Leningrad). Izv. Vyssh. Ucheb. Zaved., Fiz., No. 5, 158-61(1965). (In Russian).

Determinations of the change of activities with time can be carried out by a simple method over an unlimited range, if, together with the half life $T_{0.5}$, the time corresponding to a decrease of the initial activity by one order, i.e., $T_{0.1} = T_{0.5}/\ln 2 = 3.322\ T_{0.5}$, is considered. Then the total part of the relative decay time $t/T_{0.1}$ indicates the order of the tenfold decrease of the portion of the remaining activity determined from the table (or a nomogram) according to its fractional part. Because of the simplicity of extrapolating the data, the table of fractional parts of $t/T_{0.1}$, supplemented by the rule for its use, can find a wide application in reference and educational literature on physics, replacing the cumbersome tables with limited range of relative decay time and proportion of remaining activity. (tr-auth)

32419 ORIENTATION OF ^{111}Cd NUCLEI BY 3261 Å RESONANT RADIATION. Aleksandrov, E. B.; Sokolov, A. P. JETP Lett. (USSR) (Engl. Transl.), 3: 273-5 (May 15, 1966).

Translated from Zh. Eksp. Teor. Fiz., Pis'ma Redakt., 3: 419-22(May 15, 1966).

Appreciable orientation of ^{111}Cd nuclei was obtained in vapor at a density on the order of 10^{14} cm^{-3}, with the aid of circularly polarized 3261-Å light. The experimental setup is diagrammed. A distinct resonance signal with half-width of several cps was observed in a field of 5.2 Oe, which approximately corresponds to the published value of the nuclear moment of ^{111}Cd. (M.H.R.)

32420 COLLECTIVE M1 TRANSITIONS OF EVEN NUCLEI. Grechukhin, D. P. JETP Lett. (USSR) (Engl. Transl.), 3: 275-7(May 15, 1966).

Translated from Zh. Eksp. Teor. Fiz., Pis'ma Redakt., 3: 422-4(May 15, 1966).

It is shown that Lipas' criticism (Phys. Letters, 8: 279 (1964)) of the results of Davydov (Nucl. Phys., 8: 237(1958)) and Grechukhin (Nucl. Phys., 40: 422(1963)) is incorrect, since not all the relations between the classical quantities are valid for quantum operators. The correction for an error found in those results has no significance for the problem, and in addition the uncertainty of the coefficient g_1 is of the same order. (M.H.R.)

32421 RECOMMENDATION OF THE USE OF UNIFORM HALF LIVES OF SOME IMPORTANT RADIONUCLIDES. Sucker, K.-H.; Ringel, V.; Landrock, K. (VEB Vakutronik, Dresden). Kernenergie, 9: 63-4(Feb. 1966). (In German).

The necessity for the use of uniform half lives by different institutes and research installations is emphasized. The most accurate half lives obtained from a literature evaluation are tabulated for 27 isotopes. These are ^{3}H, ^{14}C, ^{24}Na, ^{32}P, ^{40}K, ^{41}Ar, ^{45}Ca, ^{55}Fe, ^{56}Mn, ^{60}Co, ^{65}Zn, ^{85}Kr, ^{90}Sr, ^{124}Sb, ^{125}I, ^{131}I, ^{137}Cs, ^{141}Ce, ^{147}Pm, ^{170}Tm, ^{185}W, ^{192}Ir, ^{198}Au, ^{203}Hg, ^{204}Tl, ^{210}Po, and ^{226}Ra. (J.S.R.)

32422 STUDY OF THE $^{127}I(n,\gamma)^{128}I$ AND $^{133}Cs(n,\gamma)^{134}Cs$ REACTIONS. Archer, N. P.; Hughes, L. B.; Kenneth, T. J.; Prestwich, W. V. (McMaster Univ., Hamilton, Ont.). Nucl. Phys., 83: 241-58(1966).

The capture γ-ray spectra of the $^{127}I(n,\gamma)^{128}I$ and $^{133}Cs(n,\gamma)^{134}Cs$ reactions are investigated using a Ge(Li) spectrometer. A total of 184 high- and low-energy γ rays were observed for the $^{127}I(n,\gamma)^{128}I$ reaction. A neutron separation energy of 6826 ± 3 kev was deduced by means of coincidence experiments. For the $^{133}Cs(n,\gamma)^{134}Cs$ reaction 86 γ rays were observed. Both spectra show an enhancement of high energy intensity which appears to be related to a high level density at low excitation energy. (auth)

32423 PARABOLIC POTENTIAL BARRIER MODEL AS AN APPROXIMATION TO OPTICAL MODEL CALCULATIONS. Rawitscher, G. H. (Yale Univ., New Haven). Nucl. Phys., 83: 259-73(1966). (YALE-1807-30).

In some of the optical-model calculations of nucleus-nucleus interactions, the repulsive hump formed by the Coulomb, centrifugal and nuclear potentials at the larger interaction distances plays a dominant role in the determination of nuclear phase shifts. The potentials in this barrier region are approximated for each partial wave by a combination of two parabolas, as a development of a similar procedure employed in 1953 by Hill and Wheeler. The solution of the Schroedinger equation is given exactly in terms of Weber's parabolic cylinder functions. A combination of two such functions, chosen such as to satisfy an ingoing wave boundary condition at small distances, is taken for the wave function and the real and imaginary parts of the nuclear phase shifts are calculated analytically. The formulas are evaluated for two numerical examples and the results compared with an optical-model calculation. Agreement between the reflection coefficients as a function of the angular momentum quantum number L is satisfactory. The main error arises at the transition of the potentials from the parabolic to the Coulomb region, the real part of the nuclear phase shift being most strongly affected. (auth)

32424 AVERAGE LEVEL WIDTH OF THE COMPOUND NUCLEUS. Tsukada, K.; Lee, T. J. (Japan Atomic Energy Research Inst., Tokyo). Nucl. Phys., 83: 274-88 (1966).

The ratio of average level width to average level spacing of the compound nucleus in a strongly overlapping-resonance region is obtained by the self-indication measurement of the fluctuations in the neutron total cross sections. The observed ratios for Al, Si, and S with the excitation energy of 11-13 Mev are explained in terms of the strong-interaction model of the compound-formation process, though the observed values for Mn, Fe, Co, Ni, Cu, and Zn are systematically smaller than the calculated ones. The fluctuation in the excitation function of the nuclear reaction is analyzed under the condition that the energy resolution or the energy step of the measurement is much larger than the average total width and spacing of the compound states. An apparent period of the fluctuation and a width of the energy-correlation function of the cross section are obtained as functions of the resolution or the energy step. As a result of the present analyses, it is pointed out that the average level width of the compound nucleus is not necessarily larger than the one predicted by the above-mentioned simple model of the compound process. (auth)

32425 ENERGY LEVELS OF ^{106}Pd FED IN THE ^{106m}Rh DECAY. De Aisenberg, E. Y.; Suarez, J. F. (Comision Nacional de Energia Atomica, Buenos Aires). Nucl. Phys., 83: 289-302(1966).

The electron spectrum of ^{106m}Rh was analyzed with an orange type magnetic spectrometer. Four components of the continuum spectrum were observed with end-point energies (in kev) and relative intensities: 1700 ± 50 (0.7 ± 0.2); 1310 ± 20 (3.1 ± 0.6); 920 ± 10 (66 ± 13) and 700 ± 50 (30 ± 13). The conversion electrons of 15 transitions were observed. Their energies, with a relative error of about 1%, and relative intensities are: 221 (525 ± 75); 387 (125 ± 50); 406 (275 ± 125); 426 (300 ± 140); 450 (160 ± 60); 512 (1000); 616 (140 ± 24); 717 (107 ± 38); 1050 (50 ± 10); 1124 (17 ± 5); 1200 (19 ± 6); 1255 (12 ± 3); 1376 (5 ± 2); 1530 (14 ± 4) and 1566 (6 ± 2). The energy of the 616 kev transition was more precisely determined with a double-focussing iron-yoke magnetic spectrometer as 616.0 ± 0.4 kev. Levels in ^{106}Pd are established at energies in kev of: 0, 511.8, 1127.8, 1228.9, 1557.4, 1931.8, 2039.6, 2076.4, 2084.1, 2305.6, 2350.3, 2365.5, 2756.4 and 2951.3 with spins and parities 0^+, 2^+, 2^+, 4^+, $(3,4)^+$, $(4)^+$, 4^+, $(3-6)^+$, 3^+, $(3,4,5)^+$, $(4)^+$, $(3,4,5)^+$, 5^+, $(5,6)^+$, respectively. The total decay energy of ^{106m}Rh was determined to be 3675 ± 10 kev. Spin and parity 6^+ is inferred for ^{106m}Rh. Several features of the decay are explained by the asymmetric rotor theory of Mallmann. (auth)

32426 ELECTROMAGNETIC TRANSITION PROBABILITIES IN SINGLE CLOSED SHELL NUCLEI. Lombard, R. J.; Campi-Benet, X. Nucl. Phys., 83: 303-20(1966).

The description of the lowest 2^+ and 3^- levels of single closed shell nuclei is made in the quasi particle model, using the superposition of the pairing force and of a multipole force. In addition to the extra-core nucleons, the particles of the core are taken into account. The $E2^+$ and $E3^-$ energies are in good agreement with experiment. The B(E2) and B(E3) values, calculated without introducing any effective charge, agree with experimental data for neutron closed shell nuclei, whereas they are systematically too small for proton closed shells. The B(E1) and B(M2) of the $3^- \rightarrow 2^+$ transitions are estimated for the few measured cases. (auth)

32427 LEVELS IN ^{21}Ne USING THE $^{18}O(\alpha,n\gamma)^{21}Ne$ REACTION. Pronko, J. G.; Olsen, W. C.; Sample, J. T. (Univ. of Alberta, Edmonton). Nucl. Phys., 83: 321-31 (1966).

The $^{18}O(\alpha,n\gamma)^{21}Ne$ reaction and the method of triple angular correlations were used to determine the spins of the 0.35, 1.75, and 2.87 Mev levels of ^{21}Ne and the multipole mixing ratios of the gamma rays emitted from these states. The angular correlations of the gamma rays from the 0.35 and 1.75 Mev levels were measured at a bombarding energy of 4.43 Mev with the neutron counter located at zero degrees with respect to the beam direction. The results, when analysed in terms of previously measured lifetimes, yielded spin assignments of $J = 5/2$ and $J = 7/2$ for the 0.35 and 1.75 Mev levels, respectively, and multipole mixing ratios $\delta_{0.35} = +0.08 \pm 0.03$, $\delta_{1.40} = +0.18 \pm 0.03$ and $\delta_{1.75} = +0.03 \pm 0.04$. The 1.75 Mev level was found to decay 4.6% ± 2.0% to the ground state. At a bombarding energy of 5.50 Mev the neutron-gamma-ray correlations yielded a spin of $9/2$ as most probable for the 2.87 Mev level with $\delta_{1.12} = +0.12 \pm 0.06$ and $\delta_{2.52} = +0.03 \pm 0.04$. This level was found to decay 63% ± 4% to the 1.75 Mev level. (auth)

32428 THEORY OF NUCLEAR REACTIONS. II. THE JOST FUNCTION, SUM RULES, INTERACTING CONTINUA. Weidenmueller, H. A.; Dietrich, K. (Univ., Heidelberg). Nucl. Phys., 83: 332-52(1966).

Results obtained in a previous paper are extended and simplified. For the case of many non-interacting continua, the connection between the elements of the S-matrix and what might be called the determinant of the Jost matrix is established. This connection has the same form as that known from the theory of many-channel scattering. The formula thus established allows a simpler and more general derivation of the sum rules obtained previously. They may also be useful for numerical calculations in that the elements of the S-matrix can all be calculated from one function. These results are further generalized to the case that the continua do have a non-vanishing interaction. It is necessary to consider this case not only to obtain the direct interaction matrix elements, but also to obtain the threshold energies for the various channels. The application to photon channels is discussed. The formalism is generalized further to include channels containing fragments other than nucleons, e.g., deuterons or α particles. This generalization, although possibly useful for numerical calculations, is intended to demonstrate the assumptions underlying the present approach and to illustrate the role played by the residual interactions. (auth)

32429 ANGULAR DISTRIBUTIONS OF ^{18}F FROM THE REACTION $^{16}O(^{14}N,^{18}F)^{12}C$. Gaedke, R. M.; Toth, K. S. (Oak Ridge National Lab., Tenn.). Nucl. Phys., 83: 353-63 (1966). (ORNL-P-1995).

The reaction $^{16}O(^{14}N,^{18}F)^{12}C$ was investigated at incident energies of 20, 27, and 33 Mev by bombarding thin nickel oxide targets with ^{14}N ions accelerated in the Oak Ridge Tandem Van de Graaff. Angular distributions were obtained by stopping the radioactive ^{18}F particles in aluminum foil annuli which encompassed known angular increments. After bombardment these annuli were counted under shielded, calibrated Geiger-Mueller counters. The ^{18}F differential cross sections were found to be peaked in the forward direction and to exhibit some structure at larger angles. From the experimental data it was concluded that the production of ^{18}F by the evaporation of three alpha particles from the compound nucleus ^{30}P was negligible. A distorted-wave Born approximation calculation was used in an attempt to fit the data. A good fit to the experimental results at 33 Mev was found when it was assumed that alpha-particle transfer from ^{16}O occurred, with the residual ^{12}C nucleus left in its 4.43 Mev state. Calculations at 20 and 27 Mev, however, did not yield satisfactory fits to the data. (auth)

32430 CROSS SECTIONS AND ISOMER RATIOS FOR THE $^{88}Sr(^{3}He,p)^{90m,90g}Y$ REACTION. Riley, Clyde; Ueno, Kaoru; Linder, Bruno (Florida State Univ., Tallahassee). Contract AT(40-1)-2628. Nucl. Phys., 83: 364-8(1966).

The absolute cross sections for ^{90m}Y and ^{90g}Y produced by the $^{88}Sr(^{3}He,p)$ reaction are determined at 1 Mev intervals from 14 to 19 Mev. The total excitation function peaks at ≈17.5 Mev with a peak value of 9.3 mb. The isomer ratio function shows no apparent variation with energy, maintaining a constant value of $\sigma_m/(\sigma_m + \sigma_g) \simeq 0.25$ over the energy range studied. The constant value of the isomer ratios is attributed to a direct type interaction. (auth)

32431 NEUTRON-INDUCED REACTIONS ON SILICON: PROTON AND α-PARTICLE ENERGY AND ANGULAR DISTRIBUTIONS. Morgenstern, H.; Hilscher, D.; Scheer, J. (Hahn-Meitner-Institut fuer Kernforschung, Berlin). Nucl. Phys., 83: 369-79(1966).

Energy and angular distributions of protons and alpha particles emitted in the reactions $^{28}Si(n,p)^{28}Al$ and $^{28}Si(n,\alpha)^{25}Mg$ were measured at neutron energies of 13.95 and 14.6 Mev by irradiating two Si detectors facing each other and accepting only pulses from charged particles leaving one detector and hitting the other. Particle identification and discrimination between forward and backward angles were achieved by a time-of-flight method. (auth)

32432 SOME FEATURES OF THE CALCULATED NUCLEAR LEVEL DENSITY. Kanestroem, I. (Univ. of Oslo). Nucl. Phys., 83: 380-400(1966).

Formulas for the nuclear level density as a function of the angular momentum, the SU_3 quantum numbers and the nuclear deformation parameter are derived. The calculated level densities as function of the angular momentum are compared with an experimental result for ^{28}Al. The agreement is not good for high spin values. The need for further measurements is stressed. (auth)

32433 ELASTIC SCATTERING OF POLARIZED 4.4 Mev NEUTRONS FROM ^{6}Li AND ^{7}Li. Steuer, M. F.; Kelsey, C. A. (Univ. of Wisconsin, Madison). Nucl. Phys., 83: 401-6(1966). (COO-7-0392).

The polarization of 4.4-Mev neutrons scattered from ^{6}Li and ^{7}Li are measured for center-of-mass scattering angles between 46 and 126°. The angular dependence of polarization observed with both isotopes exhibits a dominant sin 2θ dependence. (auth)

32434 ANGULAR DISTRIBUTION OF THE $^{19}F(n,\alpha)^{16}N$ REACTION AT $E_n = 4.7$ Mev. Bharathi, S. M.; Raheja, U. T.; Kondaiah, E. (Tata Inst. of Fundamental Research, Bombay). Nucl. Phys., 83: 407-12(1966).

The energy and angular distribution of alpha particles arising from the $^{19}F(n,\alpha)^{16}N$ reaction at $E_n = 4.7 \pm 0.05$ Mev were studied using a gas proportional counter telescope. The angular distribution fits well with a Legendre polynomial $a_0 + a_1P_1(\cos\theta)$, with $a_0 = 1.0 \pm 0.1$ and $a_1 = 0.4 \pm 0.1$, showing interference between resonances occurring in the neighborhood of $E_n = 4.7$ Mev used in this study. The cross section for this reaction is obtained as 175 ± 18 mb by comparing the yield of this reaction at 0° with the yield of recoil protons from an alkathene target. (auth)

32435 DETERMINATION OF THE PARTIAL α-HALF-LIFE OF ^{241}Pu. Bertolini, G.; Mannone, F.; Ostidich, A.; Restelli, G. (CCR-EURATOM, Ispra, Italy). Nucl. Phys., 83: 413-17(1966).

The partial α half life of ^{241}Pu is determined evaluating the ^{241}Am and ^{237}U growth from ^{241}Pu by high resolution γ spectrometry with Ge-Li drifted detectors. A value of $5.8 \pm 0.1 \times 10^5$ y is obtained, assuming the half life of ^{241}Am to be equal to 458 y and the half life of ^{237}U to be equal to 6.75 d. (auth)

32436 INTERMEDIATE COUPLING SHELL-MODEL CALCULATIONS FOR LIGHT NUCLEI. Barker, F. C. (California Inst. of Tech., Pasadena. Australian National Univ., Canberra). Nucl. Phys., 83: 418-48(1966).

Intermediate coupling shell-model calculations with a simple effective interaction between nucleons are used to fit observed properties of the nuclei with mass numbers A = 6-9. Only states of the lowest configuration are considered. For each A-value, the exchange mixture and other parameters of the effective interaction are obtained by fitting level energies, M1 matrix elements, log ft values and reduced widths. The exchange mixtures obtained appear to vary with A. Some predictions which may be tested experimentally are given. Evidence for isobaric spin mixing in the ^{8}Be levels in the 16-19 Mev region is discussed; there is difficulty in attributing all the observed mixing to the Coulomb interaction. There is some evidence of the need for configuration mixing and for a more complicated interaction. (auth)

32437 GRAPHICAL METHODS OF SUMMATION AND INTEGRATION OF SPHERICAL HARMONICS. Massot, J. N.; El-Baz, E.; Lafoucriere, J. (Institut de Physique Nucleaire, Lyon). Nucl. Phys., 83: 449-59(1966). (In French).

A graphical method for summation and integration of spherical harmonics, keeping the nomenclature, notations and rules of Yutsis et al. is presented. Essential diagrams and a rule of integration for spherical harmonics, are also presented and the method is then applied to general cases. (auth)

32438 ANGULAR CORRELATIONS FOR $^{12}C(p,p'\gamma)^{12}C$. II. OVERLAPPING RESONANCES AND THE MISSING $\frac{1}{2}^-$ LEVEL IN ^{13}N. Shute, G. G.; Baxter, A. M. (Univ. of Melbourne). Nucl. Phys., 83: 460-80(1966).

A technique is established for the handling of many overlapping resonances in angular correlations of the $0^+ \rightarrow 2^+ \rightarrow 0^+$ kind and this is applied to the 7 Mev region in ^{13}N excitation in an effort to establish the usefulness of angular correlations in deciding the assignment of the 7.4 Mev state in ^{13}N. An in-plane correlation experiment is performed and the results are compared to this theory. The $\frac{5}{2}^-$ assignment appears to be favored. (auth)

32439 POLARIZATION OF 17.8 Mev PROTONS ELASTICALLY SCATTERED BY NUCLEI. Baugh, D. J.; Griffith, J. A. R.; Roman, S. (Univ. of Birmingham, Eng.). Nucl. Phys., 83: 481-92(1966).

Angular distributions are presented for the polarization of 17.8 Mev protons elastically scattered by Be, S, Fe, Co, Cu, Zn, Ga, Ag and In at angles between 25 and 120° (lab). Targets of natural isotopic abundance were used and the experimental technique involved the single scattering of a totally polarized proton beam obtained by bombarding gaseous hydrogen with 40 Mev alpha particles. These results, together with the differential cross-section data and previous results for Si, Ca, ^{58}Ni ^{60}Ni and Mo, were analyzed using an optical model automatic search program. The geometrical parameters were fixed and systematic trends in

the real central, imaginary central and spin-orbit potentials were investigated. Improved fits were obtained by reducing the radius of the spin-orbit potential with respect to the radius of the central potential. (auth)

32440 ASYMMETRIES IN THE ELASTIC AND INELASTIC SCATTERING OF POLARIZED PROTONS FROM C AND Si. **Craig, R. M.; Dore, J. C.; Greenlees, G. W.; Lowe, J.; Watson, D. L. (Univ. of Birmingham, Eng.). Nucl. Phys., 83: 493-507(1966).**

Measurements are presented for the asymmetry produced in the scattering of 29 and 49 Mev polarized protons from carbon and silicon. Results cover the angular range 20° – 120° (lab) for elastic scattering and for inelastic scattering to the first excited state. The angular distributions for inelastic scattering have an oscillatory pattern similar to that for elastic scattering but displaced to higher scattering angles. Differential cross section data are also determined and a coupled-channels analysis of the results has been made. (auth)

32441 ELECTROMAGNETIC DECAY OF THE 1.7 AND 2.43 Mev LEVELS IN ^{9}Be. **Purdom, Paul Jr.; Seeger, P. A.; Kavanagh, R. W. (California Inst. of Tech., Pasadena). Nucl. Phys., 83: 513-27(1966).**

The 1.7 and 2.43 Mev levels in ^{9}Be were populated with the reaction ^{11}B(d,α)^{9}Be* by bombarding thin boron on carbon foils with 1.7 Mev deuterons. The alpha particles were analyzed in energy with a surface-barrier counter set at the kinematically determined angle corresponding to recoiling ^{9}Be nuclei at $\theta_{rad} = 90°$. The latter were analyzed in rigidity with a magnetic spectrometer, in energy by a surface-barrier counter at the spectrometer focus and in velocity by the time delay between an alpha and a ^{9}Be count. When a pulse from the spectrometer counter was in the appropriate delayed coincidence with a pulse from the alpha counter, the two pulses were recorded in a two-dimensional pulse-height analyzer. Most of the ^{9}Be* decay by particle breakup. Only those that gamma decay are detected by the spectrometer counter. Thus the experiment provides a direct measurement of Γ_{rad}/Γ. Analysis of 384 observed events gives $\Gamma_{rad}/\Gamma = (1.16 \pm 0.14) \times 10^{-4}$ for the 2.43 Mev level. Combining this ratio with the value of $\Gamma_{rad} = 0.122 \pm 0.015$ ev found from inelastic electron scattering gives $\Gamma = 1.05 \pm 0.18$ kev. For the 1.7 Mev level, an upper limit $\Gamma_{rad}/\Gamma \leq 2.4 \times 10^{-5}$ was determined. (auth)

32442 HIGH-ENERGY INELASTIC ELECTRON SCATTERING BY ^{16}O. **Gruenbaum, Leon (Max-Planck-Institut fuer Physik und Astrophysik, Munich. Technische Hochschule, Munich). Nucl. Phys., 83: 528-44(1966).**

The experimental form factors for inelastic scattering of electrons from ^{16}O are compared with the theoretical form factors in order to obtain direct information about the nuclear wave functions with particle-hole configuration mixing. Ground state correlations are included. The levels of odd parity agree well with the experimental results. In most cases the inelastic form factors depend little on the average nuclear potential, but strongly on the configuration amplitude. It is possible to distinguish between collective excitations and single-particle excitations from the different behavior of longitudinal and transverse form factors. For levels with isobaric spin T = 0 the form factors are always larger with ground state correlations than without. Levels with isobaric spin T = 1 show the opposite behavior. The most remarkable difference between the evaluation with and without ground state correlations one finds for the octupole levels with T = 0, which are very collective ones. (auth)

32443 MEASUREMENTS OF CONVERSION COEFFICIENTS FOR TRANSITIONS IN ^{154}Gd, ^{160}Dy, ^{170}Yb, ^{171}Yb, AND ^{141}Pr. **Dingus, R. S.; Talbert, W. L. Jr.; Stewart, M. G. (Ames Lab., Ames, Iowa). Nucl. Phys., 83: 545-74(1966). (IS-1273).**

Internal conversion coefficients were measured by observing with a well-type NaI(Tl) crystal the photon spectra emitted during the de-excitation from the first excited state to the ground state of ^{154}Gd, ^{160}Dy, ^{170}Yb, ^{171}Yb and ^{141}Pr. The results were obtained by analysis of either the singles spectra, or spectra obtained by coincidence-sum techniques, or both. For the coincidence work gating was done either with high-energy gamma rays or with beta particles. The spectra from the Yb isotopes were analyzed on a computer using a least-squares, curvefitting program. The photon detection efficiencies were calculated with a computer by performing numerical integrations. The K-shell internal conversion coefficients directly measured were 0.632 ± 0.016 for ^{154}Gd, 1.47 ± 0.05 for ^{170}Yb, 6.9 ± 1.0 for ^{171}Yb and 0.375 ± 0.009 for ^{141}Pr. The total internal conversion coefficients directly measured were 1.20 ± 0.02 for ^{154}Gd and 4.52 ± 0.11 for ^{160}Dy, which yield respective K-shell internal conversion coefficients of 0.637 ± 0.016 and 1.54 ± 0.06 when multiplied by K to total ratios. In order to eliminate interpolation errors from the internal conversion coefficient tables, theoretical values were obtained with computer calculations (point nucleus, no screening) normalized, by use of an effective nuclear charge, to the tables of Rose and Sliv and Band. The results for the transitions in ^{154}Gd, ^{160}Dy and ^{141}Pr are in good agreement with theory The ratio of the experimental result to the theoretical value is 1.60 ± 0.05 for the transition in ^{170}Yb. The result for the transition in ^{171}Yb implies a mixing ratio of E2/M1 = 0.45 ± 0.08, assuming the theoretical internal conversion coefficients are correct. (auth)

32444 HEAVY PARTICLE STRIPPING. **Banerjee, Manoj K.; Pal, Dipti (Saha Inst. of Nuclear Physics, Calcutta). Nucl. Phys., 83: 575-83(1966).**

In the direct reaction treatment of the inelastic scattering of a nucleon by a nucleus, the full wave function is described as the antisymmetric part of a linear combination of products of the target and the projectile wave functions. This configuration description is necessary for the introduction of the Born approximation. The projectile wave functions appearing in this expansion are not the same as the overlaps of the target wave functions with the full wave function because of the exchange effects. The elastic and the inelastic scattering amplitudes are determined in terms of the latter type of functions. The need to take this difference into account is stressed in order to estimate the exchange effect. The difficulties in doing this are pointed out and it is indicated with simple examples how it can be done. (auth)

32445 PHOTODISINTEGRATION OF CALCIUM TO 62 Mev. **Anderson, D. W.; Cook, B. C.; Kadlecek, J. A. (Ames Lab., Ames, Iowa). Nucl. Phys., 83: 584-92(1966). (IS-1253).**

The photoneutron cross section of calcium has been measured from threshold to 62 Mev using least structure analysis of the photon activation curve. The yield from the one second activities, mainly due to the reactions ^{40}Ca(γ,n)^{39}Ca, ^{40}Ca(γ,pn)^{38}K* and ^{40}Ca(γ,2n)^{38}Ca, was separated from the yield due to longer-lived activities. Six maxima in the cross section were evident above 26 Mev. The energies of the peaks were 28.3 ± 0.3 Mev, 34.7 ± 0.4 Mev, 43.1 ± 0.6 Mev, 48.2 ± 0.3 Mev, 54.6 ± 0.4 Mev and 60.0 ± 0.6 Mev. The cross section integrated to 62 Mev was 114 ± 15 Mev · mb with a contribution of 12 ± 7 Mev · mb due to the ^{40}Ca (γ,2n)^{38}Ca reaction. (auth)

32446 ^{52}Cr(p,γ)^{53}Mn REACTION. **Vuister, P. H. (Rijksuniversiteit, Utrecht). Nucl. Phys., 83: 593-618 (1966).**

The ^{52}Cr(p,γ)^{52}Mn reaction was investigated in the energy region $E_p = 1.36 - 2.26$ Mev. The resonance energies, the corresponding ^{53}Mn excitation energies and the resonance strengths of 199 resonances, assigned to this reaction, are reported. The excitation energies and gamma-ray branchings of 13 bound states were determined from the measurement of single and coincidence gamma-ray spectra at 20 resonances. The excitation energies are in excellent agreement with values recently obtained with the ^{56}Fe(p,α)^{53}Mn reaction. (auth)

32447 TRANSVERSE SPIN POLARIZATION IN ODD-MASS DEFORMED NUCLEI. **Bochnacki, Z. (Joint Inst. for Nuclear Research, Dubna, USSR); Ogaza, S. Nucl. Phys., 83: 619-24(1966).**

The spin polarization effect on the value of the magnetic parameter b_0 for the $K = \frac{1}{2}$ rotational bands and on M1 transitions between low-lying states of odd-mass deformed nuclei is considered. The results of numerical calculations for the ground state rotational band of the ^{169}Tm nucleus are presented. (auth)

32448 MACROSCOPIC AND MICROSCOPIC DESCRIPTIONS OF DIPOLE STATES OF ATOMIC NUCLEI. Muenchow, L. (Zentral Inst. fuer Kernphysik, Rossendorf, Ger.). Nucl. Phys., 83: 625-31(1966). (In German).

Two possible descriptions of the dipole state in nuclei are compared. In a macroscopic model one can consider small oscillations of the center-of-mass distance between protons and neutrons and identify the dipole state with the first excitation of such collective oscillations. In the microscopic model the dipole state is formed by a superposition of particles and holes. It is shown that one gets very similar results in both models for the energy of the dipole state, for the wave functions of the ground and first excited states, if in the latter model ground state and correlations are taken into account. (auth)

32449 DETERMINATION OF THE Λ-NUCLEAR POTENTIAL WELL DEPTH. Goyal, D. P. (Dyal Singh Coll., New Delhi). Nucl. Phys., 83: 639-44(1966).

An appraisal was made of the available world data on the Λ binding energy B_Λ in heavy hypernuclei ($30 \lessapprox A \lessapprox 100$). The well depth D_Λ seen by a Λ particle in nuclear matter is then determined from the estimated B_Λ values using the calculations of Bodmer and Murphy and of Dalitz. The value of D_Λ is found to be $\lesssim 32 \pm 2$ Mev. (auth)

32450 ALPHA-DEUTERON-LAMBDA MODEL OF THE HYPERNUCLEUS $^{7}_{\Lambda}$Li. Murphy, J. W. (Univ of Manchester, Eng.); Bodmer, A. R. Nucl. Phys., 83: 673-89(1966).

The hypernucleus $^{7}_{\Lambda}$Li is studied with a three-body model consisting of the Λ and an undistorted α-particle and deuteron. The interactions between the constituents are obtained by making use of the basic α-N and Λ-N interactions. However, the strengths of these are adjusted to give the observed binding energies of the two isolated pairs α-d (i.e., ^{6}Li) and α-Λ(i.e., $^{5}_{\Lambda}$He). The strength of the d-Λ interaction is not fixed but is determined as a function of the binding energy of $^{7}_{\Lambda}$Li by our calculations for $^{7}_{\Lambda}$Li. For ^{6}Li a 2s relative α-d wave function is used. The 1s α-d component ψ_{1s} is assumed to be entirely spurious both for ^{6}Li and ^{7}Li. Variational calculations for $^{7}_{\Lambda}$Li are made with flexible trial wave functions and with particular effort given to reducing the amplitude of ψ_{1s} as much as possible. In achieving this, some interesting new features arise in variational calculation. Results confirm the indications of a previous two-body model study that there is a strong α-Λ correlation together with only a slight distortion of the ^{6}Li core by the Λ. They also indicate that comparing (as a function of the range of the Λ-N interaction) the strength of the Λ-d interaction obtained from $^{3}_{\Lambda}$H with that from $^{7}_{\Lambda}$Li could give information about the range of the Λ-N interaction. However, no conclusive results could be obtained in this respect since although the major part of the binding energy of $^{7}_{\Lambda}$Li is obtained there is nevertheless a sufficient discrepancy to indicate that our model is not completely adequate. In particular, the probable need to consider correlations of the Λ with the individual nucleons of the deuteron suggests the use of a four-body, α-n-p-d-Λ model for further studies of $^{7}_{\Lambda}$Li. (auth)

32451 GAMMA-RAY ANGULAR CORRELATION AND POLARIZATION MEASUREMENTS IN THE REACTION ^{35}Cl(p,γ)^{36}Ar. Erne, F. C. (Rijksuniversiteit, Utrecht). Nucl. Phys., 84: 241-89(1966).

Triple angular correlation measurements were performed at eight resonances in the reaction ^{35}Cl(p,γ)^{36}Ar, with protons in the energy range $E_p = 733-2595$ kev. A number of multiple cascades, from the decay of high-spin levels, were investigated. Appropriate methods of analysis of triple correlation measurements are discussed. Polarization measurements were performed at three of the resonances. The main results of spin and parity determinations of ^{36}Ar levels are tabulated. The 4.34 and 5.21 Mev levels are suggested to have $J^\pi = 0^+$. In addition a number of multipole mixing ratios for proton capture and gamma-ray emission were determined. Isospin selection rules appear to work effectively in this nucleus. This results in the emission of E2 and E3 radiation in several cases. The main configurations of several levels in ^{36}Ar and of some levels in ^{35}Cl, excited by proton emission from the capture state, are discussed. (auth)

32452 POLARIZATION OF NEUTRONS ELASTICALLY SCATTERED FROM ^{3}He AT 3.33 AND 7.90 Mev. Behof, A. F.; Hevezi, J. M.; Spalek, G. (Univ. of Notre Dame, Ind.). Nucl. Phys., 84: 290-301(1966).

The angular distribution of the polarization produced in the scattering of neutrons by ^{3}He was measured for neutron bombarding energies of 3.33 and 7.90 Mev. Measurements at 3.33 Mev were performed for lab scattering angles between 90 and 160° in 10° intervals. At 7.90 Mev, the measurements were carried out between 50 and 150°, also in 10° intervals. The measurements were performed by scattering partially polarized neutrons from ^{3}He in the form of a gas scintillator, and the polarization was determined from the observed asymmetry in scattered intensities. The largest polarization measured at a bombarding energy of 3.33 Mev was 0.29 ± 0.07 at a lab scattering angle of 130°. At 7.90 Mev, the largest value measured was 0.43 ± 0.07 at a lab scattering angle of 100°. The angular dependence of the differential polarization at each energy is dominated by a $\sin 2\theta$ dependence and suggests that this term may contain a substantial contribution from p-wave, p-wave interference. (auth)

32453 NEW WEAK BETA TRANSITION FROM ^{88}Y. Sakai, Mitsuo; Yamazaki, Toshimitsu; Hollander, J. M. (Univ. of California, Berkeley). Nucl. Phys., 84: 302-4 (1966). (UCRL-16548).

By means of a germanium pair spectrometer, a weak 3.24 Mev gamma-ray was found in the photon spectrum of ^{88}Y, indicating the presence of an electron capture branch to the 3.24 Mev level of ^{88}Sr. The log f_1t was found to be 8.2 ± 0.2, which is consistent with a $\Delta I = 2$ yes beta transition and with the spin-parity assignment 2^+ for this level. (auth)

32454 OPTICAL MODEL ANALYSIS OF ELASTIC SCATTERING ON DEUTERONS ON ^{12}C IN THE ENERGY REGION OF 10.6 TO 13.9 Mev. Baldeweg, F.; Bredel, V.; Guratzsch, H.; Klabes, R.; Kuehn, B.; Stiller, G. (Zentralinstitut fuer Kernforschung, Rossendorf, Ger.). Nucl. Phys., 84: 305-15(1966). (In German).

Optical-model analyses on ^{12}C(d,d) elastic scattering data at eight energies from 10.6 to 13.9 Mev were performed using a potential without spin-orbit interaction but including volume and surface absorption. The computing program varies two parameters, the real and imaginary potential depths. At each deuteron energy more than one set of parameters was obtained, leading to minimum values of the error function χ^2, one of them being reasonable according to energy-dependence and magnitude of the parameter values. Using only this set as initial values in the fitting procedure and fixing the other input parameters to optimum but constant values, the best fits were obtained with equal strength of volume and surface absorption. Theoretical and experimental angular distributions are in satisfactory agreement in the angular range up to 120°. At greater angles they disagree due to a deep minimum of the theoretical cross section at 150°, which is responsible for the magnitude of the χ^2 values. This minimum may, perhaps, be filled by use of the spin-orbit interaction in the optical potential. Optimum potentials do not strongly depend on energy. The energy dependence of the real potential can be expressed with an interpolation formula similar to that given by Zeidman, Yntema and Satchler. (auth)

32455 CALCULATION OF NUCLEON-ALPHA CASCADES. Cohen, J. P. (Institut de Physique Nucleaire, Orsay, France). Nucl. Phys., 84: 316-36(1966). (In French).

A Monte-Carlo calculation of nuclear cascades was undertaken, based on the hypothesis that α-substructure

probability is a function of nuclear density which is assumed to have a Hofstadter form. The mode of calculation was first tested with experimental results on compound nucleus formation and inelastic total cross sections. The effect of different α-substructure radial probabilities on α-emission cross sections was then investigated. A good fit was obtained with some experiments by using the value 5-7 for the number of α-substructure in ^{197}Au. It was examined how α-correlations in the diffused edge of the nucleus might affect the (p,pn) reaction. Finally, an attempt was made to explain spallation reactions involving α-emission on the basis of these calculations. (auth)

32456 NUCLEAR STRUCTURE EFFECTS IN BREMSSTRAHLUNG. Hubbard, D. F.; Rose, M. E. (Univ. of Virginia, Charlottesville). Nucl. Phys., 84: 337-79 (1966).

The cross section for bremsstrahlung is calculated in the Born approximation, taking into account the emission by the nucleus of the bremsstrahlung photon, as well as the emission of the bremsstrahlung photon by the electron. The formal results, which are expressed in terms of various form factors, are applicable to an arbitrary nucleus. Nuclear matrix elements for the specific case of ^{16}O are evaluated in the long wavelength limit, using the j-j coupling particle-hole model. Excited states included in evaluating the summaries over intermediate nuclear states are limited to one-particle, one-hole configurations coupled by electric dipole transitions to the ground state. Effects in the bremsstrahlung spectrum due to the intrinsic structure of the ^{16}O nucleus are found to be strikingly apparent, at least in the coincidence arrangement in which scattered electron and photon are observed simultaneously, in the form of peaks superimposed on the background from electron bremsstrahlung. The relative magnitude of the nuclear effects depends strongly on the scattering angles and on the photon energy, essentially a resonance effect, and varies over a wide range from one nuclear level to another. (auth)

32457 BETA-GAMMA CIRCULAR POLARIZATION IN THE DECAY OF ^{48}Sc. van Nooijen, B.; van Krugten, H.; Lourens, W.; van der Kraan, A. M. (Technische Hogeschool, Delft, Netherlands). Nucl. Phys., 84: 380-4 (1966).

The beta-gamma circular polarization correlation in ^{48}Sc between the 654 kev allowed beta transition and the 1040, 1314 and 983 kev E2 gamma rays was measured by means of forward Compton scattering. The result $A = +(0.11 \pm 0.06)$ is in agreement only with a spin of 6^+ for the ^{48}Sc ground state. A value of $x^2 > 32$ is derived for the ratio of Gamow-Teller to Fermi intensities if it is assumed that the beta transition is pure or almost pure Gamow-Teller. The experimental result is in agreement with our earlier measurements. (auth)

32458 ALPHA-ACTIVE PLATINUM ISOTOPES. Slivola, Antti (Univ. of California, Livermore). Nucl. Phys., 84: 385-97 (1966). (UCRL-16673).

Nine new alpha-active platinum isotopes were identified among reaction products in heavy ion bombardments of various rare-earth targets. Earlier results on the decay of ^{182}Pt, ^{183}Pt and ^{184}Pt were verified. The measurements were performed by using a fast recoil collection apparatus, and the isotopes were identified by cross bombardments and excitation function measurements. The decay characteristics of the nuclei studied are presented. (auth)

32459 ^{52}Cr(d,p)^{53}Cr, A TEST OF DISTORTED-WAVE STRIPPING THEORY. Legg, J. C.; Scott, H. D.; Mehta, M. K. (Rice Univ., Houston, Tex.). Nucl. Phys., 84: 398-410 (1966). (TID-21416).

An extensive study of the ^{52}Cr(d,p)^{53}Cr reaction was made between $E_d = 4.3$ Mev and $E_d = 6.3$ Mev. Eight angular distributions were obtained for the (d,p) reaction and the elastic deuteron scattering from ^{52}Cr within this energy range. Eight angular distributions for the elastic scattering of protons from ^{53}Cr were obtained at $E_p(c.m.) = E_d(c.m.) + 5.72$ Mev. The elastic scatterings were fitted using an optical model code. The optical model potentials determined by the elastic scattering were then used in a distorted wave calculation for the stripping reaction. Two different deuteron potentials were considered. For the $l = 1$ stripping patterns, it was found that the potential with a deeper well or a cutoff calculation using either deuteron potential was reasonably successful in fitting the data. For the $l = 3$ stripping pattern, it was found that no DW calculation using reasonable well depth or cutoff radius succeeded in fitting the data. (auth)

32460 THE 67 min ISOMERIC STATE IN ^{240}Np. Qaim, S. M. (Univ. of Birmingham, Eng.). Nucl. Phys., 84: 411-16 (1966).

Evidence favorable to the existence of the controversial 67 min isomeric state in ^{240}Np was adduced by studying the shapes of relative excitation functions of some neptunium activities formed in the interactions of ^{238}U with ^{3}He particles. (auth)

32461 A GENERAL TWO-BODY MATRIX ELEMENT FOR A GAUSSIAN INTERACTION USING CYLINDRICAL HARMONIC OSCILLATOR FUNCTIONS. Copley, L. A.; Volkov, A. B. (McMaster Univ., Hamilton, Ont.). Nucl. Phys., 84: 417-23 (1966).

The two-body matrix element for a Gaussian force is obtained in closed form using cylindrical harmonic oscillator wave functions. The result is completely general allowing all possible cylindrical states and allowing different oscillator constants for each state. These include matrix elements that cannot be determined by the usual methods of separation into relative and center-of-mass coordinates. (auth)

32462 DECAY OF ^{162}Tb AND ^{163}Tb. Funke, L. (Zentralinstitut fuer Kernforschung, Rossendorf, Ger.); Graber, H.; Kaun, K.-H.; Sodan, H.; Geske, G.; Frana, J. Nucl. Phys., 84: 424-42 (1966). (In German).

The decay of ^{162}Tb and ^{163}Tb was investigated with a Ge(Li) detector and a two-dimensional scintillation coincidence spectrometer. The half lives of these isotopes are 8.0 ± 0.5 min and 19.5 ± 0.5 min, respectively. The activities were produced by (γ,p) reactions using the bremsstrahlung of a betatron. A decay scheme of ^{162}Tb is proposed which contains a 2^- level in ^{162}Dy at 1148 kev interpreted as a two-quasi-particle state K,K + 1 of the proton system with the quantum numbers [411 ↑ + 523 ↑]. The ground state of ^{162}Tb has the spin and parity $J^\pi = 1^-$. In the decay of ^{163}Tb about 30 gamma lines were observed. A proposal for the decay scheme is given and the characteristics of the levels in ^{163}Dy are discussed in the framework of the unified model. (auth)

32463 GAMMA TRANSITIONS AND ENERGY LEVELS IN ^{161}Dy. Funke, L. (Zentralinstitut fuer Kernforschung, Rossendorf, Ger.); Graber, H.; Kaun, K.-H.; Roemer, J.; Sodan, H.; Frana, J. Nucl. Phys., 84: 443-8 (1966). (In German).

The γ-spectrum from the decay of ^{161}Tb was measured with a Ge(Li)-detector. Ten γ-transitions with energies between 237 and 551 kev were found. The results confirm the existence of three levels in ^{161}Dy at 368, 419 and 551 kev. Furthermore a new level at 452 kev is proposed. It is suggested that the levels 368, 419 and 452 kev are members of a rotational band based on the one-particle state $1/2$-[521]. (auth)

32464 LEVELS IN ^{157}Tb. Funke, L. (Zentralinstitut fuer Kernforschung, Rossendorf, Ger.); Graber, H.; Kaun, K.-H.; Sodan, H.; Werner, L.; Frana, J. Nucl. Phys., 84: 449-60 (1966). (In German).

The decay of ^{157}Dy was investigated with a magnetic Siegbahn-Slätis spectrometer, Ge(Li)-detector and a two-dimensional scintillation coincidence spectrometer. In addition to the known transitions in ^{157}Tb, new γ-transitions with energies of 296, 404, 498, 897, 932, 992, 1043 and 1104 kev are observed. From the relative K-electron and γ-ray intensities the K-conversion coefficients are deduced and the possible multipolarities of the transitions are given. The 992 kev transition has a value $\alpha_K = (3.9 \pm 1.5) \cdot 10^{-2}$, from which one obtained a mixing ratio 95% E2 + 5% EO. Based on the present observations, levels at

992, 1043, 1095 and 1104 kev were introduced in the level scheme of ^{157}Tb. The 992 kev level may be interpreted as the β-vibrational level based on the ground state $^{3}/_{2}^{+}$[411] of ^{157}Tb. The possible character of the other levels is discussed. (auth)

32465 DECAY ^{157}Eu(β^-)^{157}Gd. Funke, L.; Graber, H.; Kaun, K.-H.; Ross, R.; Sodan, H.; Werner, L.; Frana, J. (Zentralinstitut fuer Kernforschung, Rossendorf, Ger.). Nucl. Phys., 84: 461-70(1966). (In German).

The decay ^{157}Eu(β^-)^{157}Gd was studied with a Ge(Li) detector, a magnetic beta spectrometer and two-dimensional scintillation-coincidence technique. In addition to the known transitions in ^{157}Gd, 15 new γ-transitions were observed. From the electron and γ-ray intensities the conversion coefficients and multipolarities of the transitions 320, 373 and 413 kev are obtained. In the level scheme of ^{157}Gd new levels were introduced. The characteristics of the levels are discussed in the framework of the unified model. (auth)

32466 DECAY OF ^{163}Er. Funke, L.; Graber, H.; Kaun, K.-H.; Sodan, H. (Zentralinstitut fuer Kernforschung, Rossendorf, Ger.). Nucl. Phys., 84: 471-80(1966). (In German).

The γ-spectra from the decay of ^{163}Er produced by the reactions ^{164}Er(γ,n) and ^{162}Er(n,γ) were investigated with a Ge(Li) detector and a $\gamma\gamma$-scintillation-coincidence spectrometer. As a result of these measurements the level scheme of ^{163}Ho is given containing levels up to 1110 kev. The characteristics of the levels are discussed on the basis of the unified model. (auth)

32467 ANTIPROTON-NUCLEI SCATTERING AT 3 Gev/c. Bernheim, A. (Faculte des Sciences, Paris); Fayolle, J. C.; Kesler, G.; Van Hollebeke, M.; Morand, M.; Faucher, G. Nuovo Cimento (10), 44A: 17-30(July 1, 1966). (In French).

In order to eliminate the scanner's bias, the well-known $P(\alpha) = G(\alpha) + S(\alpha)$ probability distribution for small deflections of a particle in nuclear emulsion is used to select events outside the Gaussian limit of multiple scattering. The aim was to find the value of the real part of the nuclear scattering amplitude in elastic interactions of 3 Bev/c antiprotons with nuclei in nuclear emulsion. The experimental results obtained between 0.5 and 7° agree with the optical-model calculations using $R_0 = 1.57$ fermi, W = 22.4 Mev, $V_0 = 2$ Mev. (auth)

32468 FINAL-STATE COULOMB INTERACTION IN QUASI-ELASTIC NEUTRINO SCATTERING ON NUCLEI. Piketty, C. A. (Laboratoire de Physique Theorique et Hautes Energies, Orsay, France). Nuovo Cimento (10), 44A: 57-89(July 1, 1966).

The transverse muon polarization due to the final-state Coulomb interaction was estimated for the quasi-elastic process: ν (or $\bar{\nu}$) + nuclei $\rightarrow \mu$ + N + residual nucleus, using a single-particle model for the nucleus. Maximum effects of few percents are obtained for small muon energy and far from the quasi-elastic peak. So the final-state Coulomb interaction can be neglected and the measurement of transverse muon polarization is a valid test of time reversal invariance. (auth)

32469 ^{8}Li EMISSION IN 5.0-Gev/c K$^-$-MESON INTERACTIONS IN NUCLEAR EMULSION. Bechdolff, A. (Centre de Recherches Nucleaires, Strasbourg); Baumann, G.; Braun, H.; Lonchamp, J.-P.; Cueer, P.; Harmsen, D. M. Nuovo Cimento (10), 44A: 131-7(July 1, 1966).

The results of the emission of ^{8}Li fragments are compared with the theory of the nuclear evaporation in the 5 Bev/c K$^-$-muon interactions. The production rate rises with the incident energy from 0.8 Bev/c up to 5.0 Bev/c whereas the forward to backward ratios decrease. (auth)

32470 SURFACE TENSION OF NUCLEI ACCORDING TO THE FERMI-GAS MODEL. Hilf, E.; Suessmann, G. (Univ., Frankfurt am. Main). Phys. Lett., 21: 654-6 (July 1, 1966).

Within the Fermi-gas model it is established by numerical test-calculations that the expression for the surface energy of nuclei, well known for a square well potential, holds for any shape of the external potential and is not superseded by "residual terms." (auth)

32471 LEVEL STRUCTURE OF ^{92}Mo. Dickens, J. K.; Eichler, E.; Silva, R. J.; Williams, I. R. (Oak Ridge National Lab., Tenn.). Phys. Lett., 21: 657-9(July 1, 1966).

Energies for 34 excited states in ^{92}Mo were determined by analyzing data from inelastic scattering of 10 Mev protons and from the associated gamma-ray spectrum. (auth)

32472 INTERNAL MAGNETIC FIELD OF LUTETIUM IN IRON AND g FACTOR IN ^{175}Lu. Deutch, B. I. (Univ. of Aarhus, Denmark); Hornshoej, P.; Nielsen, K. Bonde; Boehm, F. Phys. Lett., 21: 659-61(July 1, 1966).

Applying γ-γ correlation techniques, the effective magnetic field at room temperature on ^{175}Lu in magnetized iron was determined to be -338 ± 42 kG. With this value, the g factor of the 251 kev state in ^{175}Lu is measured to be $g = 0.37 \pm 0.12$. (auth)

32473 THE MASSES AND EXCITED STATES OF ^{24}Al AND ^{28}P. Mangelson, N.; Reed, M.; Lu, C. C.; Ajzenberg-Selove, F. (Univ. of California, Berkeley). Phys. Lett., 21: 661-3(July 1, 1966).

The ^{24}Mg(^{3}He,t)^{24}Al and ^{28}Si(^{3}He,t)^{28}P reactions were studied at ^{3}He energies in the range 37.8 to 40.1 Mev. The mass excesses of ^{24}Al and ^{28}P are, respectively, -0.07 ± 0.06 and -7.12 ± 0.06 Mev. Eighteen excited states of ^{24}Al and twelve excited states of ^{28}P were observed. (auth)

32474 THE 2.8-Mev DOUBLET IN ^{21}Ne. Smulders, P. J. M.; Alexander, T. K. (Chalk River Nuclear Labs., Ont.). Phys. Lett., 21: 664-5(July 1, 1966).

Gamma ray spectra from the ^{18}O(α,nγ)^{21}Ne reaction were measured using a 25 cm^3 Ge(Li) detector. A doublet of levels in ^{21}Ne was found with energies 2790 ± 5 and 2797 ± 5 kev and lifetimes of >1.0 ps and <0.05 ps, respectively. (auth)

32475 POLARIZATION AND ASYMMETRY IN THE ^{3}He(d,p)^{4}He REACTION. DeFacio, D.; Umerjee, R. K.; Gammel, J. L. (Texas A and M Univ., College Station). Phys. Lett., 21: 666-7(July 1, 1966).

An excellent fit is obtained for the reaction polarization $P(\theta)$ for the protons from the reaction ^{3}He(d,p)^{4}He. The proton asymmetry $A(\theta)$ is also calculated and agreement to experimental values is found to be good only at large angles. (auth)

32476 TWO STATES IN ^{21}Ne AT 2.80-Mev EXCITATION ENERGY. Koempf, R. (Univ., Freiburg i. B.). Phys. Lett., 21: 671-3(July 1, 1966).

The energies of two closely spaced states at 2792 ± 2 kev and 2797 ± 2 kev in ^{21}Ne were measured. The existence of three closely spaced states at 2.80 Mev excitation energy in ^{21}Ne, reported recently, is in disagreement with this experiment. (auth)

32477 FINAL-STATE INTERACTIONS IN THE MESONIC DECAY OF MASS-4 HYPERNUCLEI. Gajewski, W. (Univ. Libre, Brussels); Sacton, J.; Vilain, P.; (and others). Phys. Lett., 21: 673-6(July 1, 1966).

The results of a search for the presence of sharp resonances in systems of four nucleons produced as a result of various π^- mesonic decay modes of the hypernuclei $_{\Lambda}H^{4}$ and $_{\Lambda}He^{4}$ are presented. (auth)

32478 ISOBARIC ANALOG STATES OF DOUBLY MAGIC ^{208}Pb. Bredin, D. J.; Hansen, O.; Lenz, G.; Temmer, G. M. (Rutgers Univ., New Brunswick, N. J.). Phys. Lett., 21: 677-80(July 1, 1966).

The isobaric analog states (T = 22) of the first few states of ^{208}Pb occurring in ^{208}Bi displaced by 18.98 Mev Coulomb energy are studied by examining both elastic and inelastic scattering of protons on ^{207}Pb (enriched). Questions of reduced-width extraction are discussed. Some Coulomb excitation is observed between isobaric analog resonant inelastic scattering. (auth)

32479 INDUCED TERMS AND THE PARTIAL CONSERVATION OF THE AXIAL VECTOR CURRENT IN β-

DECAY. Krmpotic, F.; Tadic, D. (Univ. of Zagreb). Phys. Lett., 21: 680-2(July 1, 1966).

New measurements of $0^- \rightarrow 0^+$ nuclear β decay seen to indicate the existence of the induced term of the second class in the matrix element of the axial vector current if PCAC is valid. (auth)

32480 PHENOMENOLOGICAL DESCRIPTION OF ANHARMONIC VIBRATIONS. Soerensen, B. (NORDITA, Copenhagen). Phys. Lett., 21: 683-5(July 1, 1966).

Quadrupole-type anharmonic terms of third and fourth order are introduced in the phenomenological vibrational hamiltonian and a truncation method is used for solving the eigenvalue equations. For ^{114}Cd a comparison is made with experiments. (auth)

32481 A STUDY OF THE MIRROR REACTIONS ^{10}B(d,t)^{9}B AND ^{10}B(d,^{3}He)^{9}Be AT 11.8 Mev. Baehr, K.; Fitz, W.; Jahr, R.; Santo, R. (Max-Planck-Institut fuer Kernphysik, Heidelberg). Phys. Lett., 21: 686-7(July 1, 1966).

Angular distributions were measured of the mirror reactions ^{10}B(d,t)^{9}B (E_x = 0, 2.34 Mev) and ^{10}B(d,^{3}He)^{9}Be (E_x = 0, 2.43 Mev). The results are in agreement with charge independence of the reactions and suggest similar isospin configurations in the states of the final nuclei. (auth)

32482 ADDITIONAL EVIDENCE OF STABILITY OF THE SUPERHEAVY ELEMENT ^{310}126 ACCORDING TO THE SHELL MODEL. Wong, C. Y. (Oak Ridge National Lab., Tenn.). Phys. Lett., 21: 688-90(July 1, 1966).

The binding energies of the last neutron and the last proton of the superheavy nucleus ^{310}126 are calculated using a shell model potential. Half lives against spontaneous fission, α decay, and β decay are estimated. (auth)

32483 EXCITED STATES OF ^{31}P AND THE NILSSON MODEL. Ramavataram, K. Phys. Lett., 21: 690-3 (July 1, 1966).

A Nilsson model calculation taking into account the three nucleons outside a closed ^{28}Si subshell was made for ^{31}P. Comparison with experimental results shows the validity of a rotational model description for ^{31}P. (auth)

32484 EFFECT OF THE COULOMB INTERACTION ON ISOSPIN SELECTION RULES IN NUCLEAR REACTIONS. Griffy, T. A. (Univ. of Texas, Austin). Phys. Lett., 21: 693-4(July 1, 1966).

The effect of the Coulomb interaction on the $\Delta T = 0$ selection rules for (α,d) and (α,α') reactions is investigated using the electric dipole sum rule to estimate the amount of $T = 1$ admixtures caused by the Coulomb interaction of the target and projectile. (auth)

32485 EXPERIMENTAL TEST OF THE TRITON FORM FACTOR BY COULOMB PICKUP ON ^{208}Pb. Hering, W. R.; Dost, M.; Lynen, U. (Max-Planck-Institut fuer Kernphysik, Heidelberg). Phys. Lett., 21: 695-6(July 1, 1966).

The reaction ^{208}Pb(d,t)^{207}Pb leading to the ground state and the first and second excited states was measured at $\theta = 135°$ and E_d = 8.0, 8.5 and 9.0 Mev. From this a normalization factor N = 3.25 ± 0.50 for zero-range DWBA calculations of (d,t) reactions is determined. (auth)

32486 EXPERIMENTAL STUDY OF THE REACTION D(p,γ)^{3}He AT 156 Mev. Bachelier, D.; Bernas, M.; Brissaud, I.; Detraz, C.; Didelez, J. P.; Langevin-Joliot, H.; Lee, J.; Radvanyi, P. (Institut de Physique Nucleaire, Orsay, France). Phys. Lett., 21: 697-9(July 1, 1966). (In French).

The D(p,γ)^{3}He reaction was studied at 156 Mev in view of obtaining information on the wave function of ^{3}He. The differential cross section was measured from θ_γ(lab) = 30 to 120°. (auth)

32487 MOESSBAUER SCATTERING IN ^{195}Pt. Atac, M.; Debrunner, P.; Frauenfelder, H. (Univ. of Illinois, Urbana). Phys. Lett., 21: 699-702(July 1, 1966).

The Mössbauer effect of the 99 kev transition in ^{195}Pt was studied in a backscattering geometry with platinum in iron, cobalt and nickel. The g-factor of the excited state, $g_{3/2}$ = −0.43 ± 0.10, and the internal fields were determined. (auth)

32488 BINDING ENERGY OF THE DEUTERON DETERMINED FROM MEASUREMENT OF THE HYDROGEN NEUTRON-CAPTURE GAMMA-RAY ENERGY. Greenwood, R. C.; Black, W. W. (Phillips Petroleum Co., Idaho Falls, Idaho). Phys. Lett., 21: 702-4(July 1, 1966).

The energy of the hydrogen neutron capture gamma ray was measured, using a lithium-drifted germanium detector, to be 2223.29 ± 0.07 kev. Based upon this result the binding energy of the deuteron was determined to be 2224.61 ± 0.07 kev. (auth)

32489 J DEPENDENCE IN THE (p,α) REACTION. Nolen, J. A. Jr. (Princeton Univ., N. J.); Glashausser, C. M.; Rickey, M. E. Phys. Lett., 21: 705-8(July 1, 1966).

A strong J-dependence was observed in (p,α) angular distributions with an orbital angular momentum transfer L = 1. This effect was measured in ^{66}Zn and ^{68}Zn targets at 17.5 Mev and ^{66}Zn and ^{92}Zr targets at 28 Mev. (auth)

32490 LEVELS IN ^{60}Ni AND ^{62}Ni AT HIGH EXCITATION ENERGIES. Ballini, R.; Cindro, N.; Delaunay, J.; Fouan, J.; Loret, M.; Passerieux, J. P. (Centre d'Etudes Nucleaires, Saclay, France). Phys. Lett., 21: 708-10 (July 1, 1966).

High-lying 3^- states in Ni isotopes were investigated and their interpretation in terms of core excitation is discussed. (auth)

32491 MESIC DECAY OF HYPERFRAGMENTS PRODUCED BY K^- MESONS OF 1.5 Gev/c. Adamovic, O.; Juric, M.; Popov, S.; Siminovic, J. (Inst. of Physics, Belgrade). Phys. Lett., 21: 716-19(July 1, 1966).

From an examination of 17,000 beam stars collected by area scanning in a stack of Ilford K5 emulsion, 600μ thick and exposed at CERN to K^- mesons of 1.5 Bev/c, a total of 37^{+8}_{-6} π^- mesic hyperfragments were found. It was estimated that among the remaining double stars at least 10^{+4}_{-3} hyperfragments decayed by emission of π^0 mesons. (auth)

32492 NONADIABATIC EFFECTS OF NUCLEAR ROTATIONAL SPECTRA. Udagawa, Takeshi; Sheline, Raymond K. (Florida State Univ., Tallahassee). Phys. Rev., 147: 671-84(July 22, 1966).

Based on the cranking and the pairing-plus-quadrupole force models, a description of the centrifugal stretching and the Coriolis-force antipairing effects is derived by using the number-conserved wave function in treating the pairing correlations Detailed numerical calculations are performed to obtain the lowest order nonadiabatic parameter. The observed deviations of the rotational spectra from the I(I + 1) formula are approximately accounted for in terms of the centrifugal stretching and the Coriolis-force antipairing (CAP) effects. In general, the CAP effects are more important than the centrifugal stretching effects except for nuclei in the beginning of the deformed region. Their centrifugal stretching effects become comparable with the CAP effects. The dependence of both of these effects on the parametric values involved in the theory is discussed. (auth)

32493 THREE-ALPHA MODEL FOR ^{12}C. Harrington, David R. (Rutgers Univ., New Brunswick, N. J.). Phys. Rev., 147: 685-8(July 22, 1966).

A model is proposed in which the ^{12}C nucleus is composed of three rigid alpha particles. Using separable alpha-alpha interactions the homogeneous Faddeev equations for the bound states reduce to a set of coupled nonsingular integral equations in one variable. Specialized to the case of only S-wave interactions, this set reduces to a single equation which is solved numerically. A ground-state solution is found, with a reasonable value for the binding energy, but no excited states. Further calculations are suggested, and an appendix containing the general angular-momentum analysis is included. (auth)

32494 NUMBER-CONSERVING APPROXIMATIONS FOR THE THEORY OF THE PAIRING INTERACTION IN

NUCLEI. II. Dang, Giu Do (Service de Physique Theorique, Orsay, France); Klein, Abraham. Phys. Rev., 147: 689-97(July 22, 1966).

A previous study of the pairing interaction hamiltonian by means of the equations of motion is extended. In the prior note, ground-state and single-quasiparticle properties were treated by an approximation method which was strictly particle conserving. According to the general theory, further improvement of the ground-state energies and single-particle occupation probabilities requires information about excited states of seniority zero and unity. A nonlinear, number-conserving random-phase approximation is developed for this purpose. Numerical calculations are carried out in a linearized version which is almost equivalent to the usual quasi-boson approximation. As part of the approximation, the conservation-of-particles condition is relaxed for the excited states. Results of the numerical study establish the consistency of the assumptions made and yield improved ground-state and single-particle properties. By comparison with the few models for which exact numerical results are available, the results are seen to be comparable with or superior to those of other improved approximation methods so far reported, especially so as the number of particles increases. The results can be extended for more elaborate approximations, which are proposed. (auth)

32495 ANGULAR CORRELATIONS IN THE $^{13}C(^3He,p\gamma)$ ^{15}N REACTION: LEVELS OF ^{15}N. Warburton, E. K.; Olness, J. W. (Brookhaven National Lab., Upton, N.Y.). Phys. Rev., 147: 698-709(July 22, 1966). (BNL-9874)

The particle-gamma angular-correlation method of Litherland and Ferguson was used to gain information on the decay modes and spin assignments of those ^{15}N levels with excitation energies between 8 and 11 Mev. The levels were populated by the $^{13}C(^3He,p)^{15}N^*$ reaction with a ^3He energy of 3.0 Mev. Protons were detected in an annular counter at 180° to the beam and gamma rays were detected at several angles between 0° and 90° to the beam. Decay modes are given for 6 levels. Definite spin assignments of $\frac{3}{2}$, $\frac{5}{2}$, $\frac{7}{2}$, $\frac{3}{2}$, and $\frac{3}{2}$ are obtained for the levels at excitation energies of 8.570, 9.762, 9.832, 10.074, and 10.800 Mev, while further restrictions are placed on the spins of some other levels. The present results combined with previous work lead to assignments of $\frac{5}{2}^-$ and $\frac{3}{2}^+$ for the 9.762- and 10.074-Mev levels. Additional information was obtained concerning the dipole-quadrupole or quadrupole-octupole mixing ratios of some of the gamma-ray transitions. (auth)

32496 HARTREE-FOCK CALCULATION FOR FINITE NUCLEI WITH A NONLOCAL TWO-BODY POTENTIAL. Kerman, A. K.; Svenne, J. P.; Villars, F. M. H. (Massachusetts Inst. of Tech., Cambridge). Phys. Rev., 147: 710-14(July 22, 1966). (MIT-2098-225).

An application of the Hartree-Fock (HF) method to calculation of the structure of finite nuclei is presented. The nonlocal, separable potential of Tabakin is used as the two-body interaction. The calculation is carried out by writing the HF equations in an oscillator basis and applying the Moshinsky transformation to relative coordinates. The closed-shell nuclei ^{16}O and ^{40}Ca are considered. Under the assumption that they are spherical, their binding energy per particle is found to be −2.41 and −3.74 Mev for ^{16}O and ^{40}Ca, respectively. Possible reasons for the large discrepancy with the experimental binding are discussed. The single-particle energies show better agreement with data, but have too much spin-orbit splitting, namely, 10.2 Mev for 1p states in ^{16}O, and 11.13 and 14.59 Mev, respectively, for the 1p and 1d states in ^{40}Ca. The rms radii for ^{16}O and ^{40}Ca were found to be 2.38 and 2.96 F, compared with experimental values of 2.64 and 3.52 F, respectively. Corrections for Coulomb force and center-of-mass motion were also calculated. (auth)

32497 TARGET-EXCITATION EFFECTS IN STRIPPING REACTIONS. Levin, F. S. (Brookhaven National Lab., Upton, N. Y.). Phys. Rev., 147: 715-30(July 22, 1966). (BNL-9807).

Target-excitation effects are studied in (d,p) and (d,n) reactions using simple microscopic models. These effects occur when the outgoing nucleon excites the target nucleus, the stripped nucleon then couples with this excited state to form the final nuclear state. By choosing the optical potential for elastic scattering of the outgoing nucleon by the target nucleus in its ground state as the generator of the final-state distorted waves, and making the usual assumptions of the distorted-wave model, the distorted-wave amplitude separates into the standard distorted-wave Born-approximation amplitude plus one involving target excitation alone. Assuming a shell-model description of the target and residual nuclei and using two-body forces to describe the interaction between the outgoing nucleon and target nucleus, an angular-momentum decomposition of the target-excitation amplitude is made. Numerical estimates of the effect of target excitation are obtained using the following assumptions for the $^{40}Ca(d,p)^{41}Ca$ reaction: the deuteron is a point particle; the two-body force has a Gaussian shape; the target nucleus is doubly magic; the final nucleus is doubly magic plus one open shell; the single-particle states are harmonic-oscillator states; both the real and imaginary parts of the deuteron and proton optical potentials have a Saxon-Woods form factor (volume absorption). Results are obtained for various oscillator strengths and well parameters. Except for certain cases, the effects of target excitation are found to be small. Angular-correlation measurements are discussed as a possible means for detecting the presence of nonnegligible target-excitation effects. (auth)

32498 DIRECT NUMERICAL SOLUTION OF THE THREE-BODY PROBLEM. Rosati, S. (Univ., Pisa, Italy. Istituto Nazionale di Fisica Nucleare, Pisa, Italy); Barbi, M. Phys. Rev., 147: 730-4(July 22, 1966).

A numerical method to determine the binding energy and the wave function for a three-body system is discussed. Radial wave functions of the form $g_1(r_1)g_2(r_2)g_3(r_3)$ are used, r_1, r_2, and r_3 being the interparticle distances. The method is applied to ^3He with central forces and hard core to show the accuracy and the speed of the calculation. (auth)

32499 VECTOR AND TENSOR COULOMB ENERGIES. Jaenecke, Joachim (Univ. of Michigan, Ann Arbor). Phys. Rev., 147: 735-42(July 22, 1966).

Vector and tensor Coulomb energies were extracted from the known experimental Coulomb energy differences between isobaric doublets and triplets in light nuclei. The vector Coulomb energy essentially depends linearly on A within a given shell and shows discontinuities at major shell closures and superimposed weak oscillations. The tensor Coulomb energy exhibits a pronounced oscillatory structure. The characteristic A dependence of both Coulomb energies is discussed and the oscillations in particular are related to Coulomb pairing effects. (auth)

32500 ISOSPIN SELECTION RULE IN THE $^{12}C(d,\alpha)^{10}B$ REACTION. Meyer-Schuetzmeister, L.; von Ehrenstein, D.; Allas, R. G. (Argonne National Lab., Ill.). Phys. Rev., 147: 743-52(July 22, 1966).

The violation of the isospin selection rule was studied in the reaction $^{12}C(d,\alpha)^{10}B$ with deuteron energies between 9 and 12.5 Mev. The differential and total cross sections of the isospin-forbidden transition to the first T = 1 state in ^{10}B (the $J^\pi = 0^+$ state at 1.74-Mev excitation) were compared with the cross sections of the isospin-allowed transitions to the ground state ($J^\pi = 3^+$, T = 0), the first excited state ($J^\pi = 1^+$, T = 0 at 0.72 Mev), and the third excited state ($J^\pi = 1^+$, T = 0 at 2.14 Mev). Mostly the intensity of the T = 1 alpha group is less than 1% of the yield of the α groups leading to the neighboring T = 0 states. This reduction is due not only to isospin forbiddenness but also to angular-momentum and parity selection rules which apply in this particular (d,α) reaction for which both the initial and the final state have $J^\pi = 0^+$. These weighting factors were calculated by use of the statistical theory of nuclear reactions. After these factors have been applied, the T = 1 alpha group has an intensity of about 10% relative to the other three T = 0 transitions at a deuteron energy of 9 Mev and 1 – 2% at an energy of 11 Mev. The small yield is ascribed to the isospin selection rules that to some extent govern this T = 1 transi-

tion. In the energy range from 9 to 11 Mev, the angular distribution of the T = 1 state stays fairly constant and is nearly symmetric around 90°. The yield decreases steadily. At deuteron energies higher than 11.5 Mev, the angular distribution changes drastically and becomes strongly forward peaked and asymmetric around 90°, and the total yield increases slightly. It is assumed that this behavior indicates a direct-interaction mechanism in which the process of mixing the isospins takes place at the surface of the nucleus. Coulomb excitation during the process of d capture or α emission might be responsible for the isospin violation at these higher deuteron energies. (auth)

32501 STUDY OF EXCITED STATES IN ^{15}N AND ^{16}N. Gallmann, A.; Fintz, P.; Nelson, J. B.; Alburger, D. E. (Institut de Recherches Nucleaires, Strasbourg). Phys. Rev., 147: 753-9(July 22, 1966).

A Buechner-type magnetic spectrograph was used to study the following reactions: $^{14}N(d,p)^{15}N$ at 90 and 120° with respect to an incident deuteron beam of E_d = 4 Mev; $^{13}O(^3He,p)^{15}N$ at 60°, 90°, and 120°, with $E_{^3He}$ = 4.0 Mev; and $^{14}C(^3He,p)^{16}N$ at 60°, 90°, and 120° and at bombarding energies of 4.0 and 4.5 Mev. Thirteen proton groups were observed corresponding to levels in ^{15}N between 8 and 11 Mev. Recently reported ^{15}N levels at 9.226, 9.763, and 9.929 Mev are confirmed, but no evidence is found for the ^{15}N levels tentatively reported at 8.643, 8.739, and 9.598 Mev. In the reaction $^{14}C(^3He,p)^{16}N$, 13 proton groups were observed corresponding to the ground state and excited states of ^{16}N up to 5.3 Mev. All of the ^{16}N levels are in agreement with those reported previously by means of other reactions. However, no evidence is found for levels tentatively identified at 1.29, 1.737, and 2.150 Mev. (auth)

32502 NATURAL PARITY STATES OF ^{16}O AT 11.09 AND 12.05 Mev. Larson, J; D.; Tombrello, T. A. (California Inst. of Tech., Pasadena). Phys. Rev., 147: 760-2 (July 22, 1966).

The elastic scattering of alpha particles from ^{12}C was used to measure the spins, parities, and widths of two previously unassigned states of ^{16}O. These levels at excitation energies of 11.094 ± 0.006 and 12.050 ± 0.008 Mev were found to have $J^\pi = 4^+$ and 0^+, respectively, and center-of-mass widths of 0.3 ± 0.1 and 1.5 ± 0.5 kev, corresponding to values of the dimensionless reduced width $\theta_\alpha^2 = 10^{-3}$ and 4×10^{-4}. (auth)

32503 NUCLEAR SPECTROSCOPY IN THE α PARTICLE. de-Shalit, A.; Walecka J. D. (Stanford Univ., Calif.). Contract AF49(638)-1389. Phys. Rev., 147: 763-73(July 22, 1966). (SLAC-PUB-160)

The properties of the 15-dimensional SU(4) supermultiplet of negative-parity excited states of the A = 4 system are discussed. This multiplet consists of the electric-dipole resonance and its spin-isospin analogs. The position of the "center of gravity" of this supermultiplet is determined by the Wigner and Majorana components of the nucleon-nucleon force, while the splittings within the supermultiplet are due to the spin-dependent parts of the force. The energies and state vectors of these levels are calculated within the framework of the shell model after isolating the center-of-mass motion and dealing with proper intrinsic excitations of the system. The position of the "center of gravity" of the supermultiplet and the splittings within it are computed, using both a Kurath force and a force taken from low-energy nucleon-nucleon scattering. The results are compared with some recent experimental findings concerning these levels. (auth)

32504 LIFETIMES OF THE FIRST EXCITED STATES OF ^7Li AND ^7Be. Paul, P.; Thomas, J. B.; Hanna, S. S. (Stanford Univ., Calif.). Phys. Rev., 147: 774-81(July 22, 1966).

The lifetimes of the first excited states of ^7Li and ^7Be were remeasured with the Doppler-shift attenuation method and a lithuim-drifted germanium detector. The value of the mean life obtained for $^7Li^*$, $(1.06 \pm 0.14) \times 10^{-13}$ sec, is in better agreement with earlier measurements from resonance fluorescence than with previous determinations by the Doppler-shift method. The value obtained for $^7Be^*$, $(1.92 \pm 0.25) \times 10^{-3}$ sec, agrees with but is appreciably lower and more precise than an earlier Doppler-shift measurement. The value of 1.82 ± 0.20 obtained for the ratio of the lifetimes, and the lifetimes themselves, are in excellent agreement with the range of values expected for intermediate coupling with L-S coupling predominating (a/K < 3.6). They agree as well with specific theoretical predictions based on studies of p-shell nuclei. (auth)

32505 BETA-DELAYED PROTONS FROM ^{25}Si. Reeder, P. L.; Poskanzer, A. M.; Esterlund, R. A.; McPherson, R. (Brookhaven National Lab., Upton, N. Y.). Phys. Rev., 147: 781-8(July 22, 1966). (BNL-10015).

Silicon-25 was produced by the $^{24}Mg(^3He,2n)^{25}Si$ reaction with a 32-Mev ^3He beam. The beta-delayed proton spectrum was measured from 0.7 to 6.0 Mev, with a resolution of 85 kev full width at half-maximum above 1.7 Mev. Eighteen proton peaks are identified and assigned to transitions from virtual levels of ^{25}Al. Three new levels of ^{25}Al at 6.92 ± 0.04, 7.25 ± 0.03, and 8.20 ± 0.03-Mev excitation energy are proposed in addition to the T = 3/2 analog state at 7.90 ± 0.02 Mev and a state at 8.97 ± 0.04 Mev, which had been seen in previous delayed-proton work. The ^{25}Si half life was determined to be 218 ± 4 msec. (auth)

32506 FERMI AND COULOMB MATRIX ELEMENTS FROM β-γ (CIRCULARLY POLARIZED) CORRELATION MEASUREMENTS ON ^{48}V AND ^{52m}Mn. Bloom, S. D.; Mann, L. G. (Univ. of California, Livermore). Phys. Rev., 147: 789-92(July 22, 1966). (UCRL-14708)

β-γ (circularly polarized) correlation measurements were made for the T = 1 to T = 2 beta decays of ^{48}V and ^{52m}Mn. The spin sequences permit both Gamow-Teller and Fermi contributions in the transitions: $^{48}V[4^+(\beta^+)4^+(\gamma_1)2^+(\gamma_2)0^+]$ and $^{52m}Mn[2^+(\beta^+)2^+(\gamma)0^+]$. The Fermi matrix elements $|M_F|$, impurity coefficients $|\alpha_2(1)|$, and Coulomb matrix elements $|\langle H_C \rangle|$, all of which must be zero for pure $\Delta T = 1$ β transitions, were deduced from the observed asymmetry parameter A, using the well-established V – A beta interaction form. An average of three earlier measurements on ^{48}V is consistent with the results, but has 5.5 times the error. The consistency of the results with each other, and with the over-all behavior of the same quantities characterizing the twenty or so other cases investigated to date, supports the suggestion that isospin conservation for particle-stable nuclear states has a validity which is qualitatively independent of atomic weight or excitation. (auth)

32507 ANGULAR-MOMENTUM EFFECTS IN THE $^{24}Mg(\alpha,^7Be)$ AND $^{27}Al(p,^7Be)$ REACTIONS AT 35-65 Mev. Lindsay, Richard H. (Western Washington State Coll., Bellingham, Wash.). Phys. Rev., 147: 792-6(July 22, 1966).

The reaction $^{24}Mg(\alpha,^7Be)^{21}Ne$ is investigated with alpha particles in the energy range 35-63 Mev. The measured cross sections are compared with the cross sections for $^{27}Al(p,^7Be)^{21}Ne$, a reaction which proceeds through the same compound nucleus, ^{28}Sr. At fixed excitation energy of the compound nucleus (C.N.), the alpha-induced reaction has a higher cross section for $E_{C.N.}$ > 40 Mev. The cross-section ratio $\sigma(\alpha)/\sigma(p)$ increases from 4.4 ± 1.0 at $E_{C.N.}$ = 50 Mev to 6.3 ± 1.4 at $E_{C.N.}$ = 60 Mev. Part of this significant difference is shown to be due to angular-momentum effects in compound-nuclear processes. The balance is attributed to the multinucleon pickup by the He ion. A similar effect is observed in the reactions $^{27}Al(p,\alpha pn)$ and $^{24}Mg(\alpha,\alpha pn)$. (auth)

32508 J DEPENDENCE IN THE $(^3He,\alpha)$ REACTION. Lee, L. L. Jr.; Mayer-Boericke, C.; Siemssen, R. H. (Argonne National Lab., Ill.). Phys. Rev., 147: 797-9 (July 22, 1966).

The reactions $^{56}Fe(^3He,\alpha)^{55}Fe$ and $^{60}Ni(^3He,\alpha)^{59}Ni$ were studied with particular attention to the dependence of the angular distribution on the total angular-momentum transfer. Distinct differences in phase were observed in the angular distributions corresponding to l = 3 neutron pickup to states of different spins. Less pronounced differences were observed for l = 1 transitions. All angular distribu-

tions showed oscillations about an exponential decrease in cross section with increasing angle. This lack of distinct character in the angular distributions may limit the usefulness of the $(^3He,\alpha)$ reaction as a spectroscopic tool. (auth)

32509 INVESTIGATION OF THE LEVELS IN ^{23}Na BELOW 3 Mev BY THE $^{26}Mg(p,\alpha\gamma)^{23}Na$ REACTION. Poletti, A. R. (Brookhaven National Lab., Upton, N. Y.); Start, D. F. H. Phys. Rev., 147: 800-11(July 22, 1966).

The particle-gamma angular correlation method of Litherland and Ferguson was used to gain information on the decay modes and spin assignments of the levels in ^{23}Na below 3 Mev as well as the mixing ratios of the transitions from these levels. The $^{26}Mg(p,\alpha)^{23}Na$ reaction was used at proton energies between 9.3 and 10.5 Mev. The spin of the first excited state was verified as $5/2$. Rigorous limitations are given for the spins of the other five levels, the most probable assignment being 2.08 Mev $(7/2^{(+)})$, 2.39 $(1/2^{(+)})$, 2.64$(1/2)$, 2.71$(3/2)$, 2.98$(3/2)$. The results are discussed in terms of the Nilsson model for the N or Z = 11 nuclei. In particular the phases of the mixing ratios for the transitions from the first two excited states of these nuclei are compared. The problem of the comparison of the signs of the experimentally determined mixing ratios quoted by different authors is also treated. (auth)

32510 POLARIZATIONS AND DIFFERENTIAL CROSS SECTIONS FOR THE ELASTIC SCATTERING OF 40-Mev PROTONS FROM ^{12}C, ^{40}Ca, ^{58}Ni, ^{90}Zr, AND ^{208}Pb. Blumberg, L. N.; Gross, E. E.; van der Woude, A.; Zucker, A.; Bassel, R. H. (Oak Ridge National Lab., Tenn.). Phys. Rev., 147: 812-25(July 22, 1966). (ORNL-P-2055).

The differential cross section and the polarization from the elastic scattering of 40-Mev protons were measured for ^{12}C, ^{40}Ca, ^{58}Ni, ^{90}Zr, and ^{208}Pb. The polarized proton beam was obtained in two ways: (a) by scattering hydrogen from 80-Mev α particles, which gave (89 ± 7)% polarization at an intensity of 2×10^7 p/sec; and (b) by elastic scattering of protons from Ca, resulting in (35 ± 3)% polarization and an intensity of 1.5×10^8 p/sec. A 32-NaI(Tl)-detector array was used to measure the scattering at 10° intervals simultaneously. In addition to the elastic-scattering and polarization measurements given above, the differential cross section and polarization for inelastic scattering from the 4.43-Mev state in ^{12}C, and the differential cross sections alone for the 7.66- and 9.63-Mev states were obtained. Optical-model calculations were made in such a way that simultaneous fits to the polarization and the differential cross section were obtained. An 11-parameter "best fit" search was made on each target, as well as an "average geometry" search where the geometric parameters were fixed and only the depths of the potentials allowed to vary. From the optical-model calculations it is concluded that (1) the radius of the spin-orbit potential is smaller than that for the real potential, (2) for nuclei heavier than Ca, surface absorption alone gives a poorer fit than a combination of volume and surface absorption, and (3) the increase in well depth with A indicates the presence of a nuclear symmetry term in the real potential. (auth)

32511 ENERGY LEVELS OF ^{48}Ca AND ^{40}Ca AS OBSERVED WITH INELASTIC SCATTERING OF 11.5-Mev PROTONS. Marinov, A.; Erskine, J. R. (Argonne National Lab., Ill.). Phys. Rev., 147: 826-8(July 22, 1966).

The $^{48}Ca(p,p')^{48}Ca$ reaction was investigated with a broad-range magnetic spectrograph and an 11.5-Mev beam from a tandem Van de Graaff. Inelastically scattered proton groups were recorded at four angles with an over-all energy resolution width of about 15 kev. Excited states in ^{48}Ca were found at 3833 ± 4, 4284 ± 6, 4506 ± 4, 4613 ± 4, 5146 ± 5, 5368 ± 5, 5728 ± 8, 6106 ± 7, and 6338 ± 10 kev. Proton groups from the $^{40}Ca(p,p')^{40}Ca$ reaction were also observed in these data. Excitation energies of levels in ^{40}Ca were measured to be 3353 ± 4, 3738 ± 4, 3907 ± 4, 4492 ± 5, 5280 ± 8, 5612 ± 8, 5625 ± 8, and 6025 ± 8 kev. (auth)

32512 DEPENDENCE OF THE ANGULAR DISTRIBUTION OF THE (d,p) REACTION ON THE TOTAL ANGULAR-MOMENTUM TRANSFER. II. Schiffer, J. P.; Lee, L. L. Jr.; Marinov, A.; Mayer-Boericke, C. (Argonne National Lab., Ill.). Phys. Rev., 147: 829-35(July 22, 1966).

The (d,p) reaction was studied with targets of ^{12}C, ^{16}O, ^{19}F, ^{28}Si, ^{32}S, ^{34}S, and ^{90}Zr, ^{92}Zr, ^{94}Zr. New evidence on the J dependence of the (d,p) angular distribution was obtained in 1p and 2d transitions. Additional evidence for 1d transitions was also obtained. (auth)

32513 EVIDENCE OF DEFORMATION IN ^{51}V. Scholz, W.; Malik, F. B. (Yale Univ., New Haven). Contract AT(30-1)-3223. Phys. Rev., 147: 836-44(July 22, 1966).

The energy levels, static moments, and transition rates of ^{51}V were investigated using the strong-coupling symmetric-rotator model. Nilsson's energy levels and wave functions in the 1f-2p shell are re-computed for a well depth corresponding to $\hbar\omega_0 = 41/A^{\frac{1}{3}}$ Mev and for a spin-orbit strength $C = -0.26\ \hbar\omega_0$ appropriate to the 1f-2p shell. The shell-model level ordering at zero deformation requires a well-flattening parameter $D = -0.035\ \hbar\omega_0$. Band-head energies are not adjusted, but determined strictly from the appropriate summation over the occupied states. The final spectrum is obtained by diagonalizing the Coriolis coupling term with the rotational wave function based on the ten available single-particle or single-hole states in the 1f-2p shell. The same moment of inertia was used for all bands and is determined from a least-squares fit to the experimental level scheme. Both for a deformation parameter $\beta = -0.32$ and for $\beta = 0.20$, the calculated spectrum is in reasonable agreement with the experiment. The rotational bands are mixed to a high degree. As a consequence the band structure is destroyed and the lowest eigenvalue of the spectrum becomes $7/2$. The wave functions corresponding to the optimal deformation are used in predicting (a) the magnetic moment of the ground and the first excited state, (b) the ground-state quadrupole moment, and (c) the magnetic dipole and the electric quadrupole transition probabilities. The agreement with the experiment, especially for the oblate deformation, is good and is achieved without using an effective charge and an effective gyromagnetic ratio. (auth)

32514 DECAY OF ^{157}Eu, ^{158}Eu, AND ^{159}Eu. Daniels, W. R.; Hoffman, D. C. (Los Alamos Scientific Lab., N. Mex.). Phys. Rev., 147: 845-52(July 22, 1966). (LA-DC-7638).

The radiations of ^{157}Eu, ^{158}Eu, and ^{159}Eu were studied with β- and γ-scintillation spectrometers and a lithium-drifted germanium detector. The energies and intensities of the major β groups and γ rays were determined. On the basis of γ-γ coincidence measurements, the radiations of ^{157}Eu and ^{158}Eu were fitted to partial decay schemes. The total β-decay energies are 1.40 ± 0.15 Mev for ^{157}Eu, $3.40^{+0.20}_{-0.10}$ Mev for ^{158}Eu, and $2.40^{+0.20}_{-0.10}$ Mev for ^{159}Eu. The mass assignments for 15.15-h ^{157}Eu, 45.7-min ^{158}Eu, and 17.9-min ^{159}Eu were confirmed. (auth)

32515 RATIO OF SYMMETRIC TO ASYMMETRIC FISSION IN THE PROTON BOMBARDMENT OF ^{226}Ra. Bowles, B. J.; Beckett, N. (Atomic Energy Research Establishment, Harwell, Eng.). Phys. Rev., 147: 852-7 (July 22, 1966).

The ratio of the symmetric to the asymmetric mode of fission of ^{226}Ra produced by protons is studied over the energy range 10–100 Mev. Discontinuities are observed superimposed upon the over-all rise of this ratio with energy, and this is explained by the periodic emission of neutrons prior to the act of fission when such a mechanism becomes energetically possible. A rough estimation is made of the relative cross sections of successive fission reactions after neutron evaporation, and the relative excitation function for the fission of ^{226}Ra by protons is presented for the energy range studied. (auth)

32516 L-SUBSHELL RATIOS OF SOME LOW-ENERGY E2 TRANSITIONS. Erman, Peter (Research Inst. for Physics, Stockholm. Brookhaven National Lab., Upton, N. Y.); Emery, G. T.; Perlman, M. L. Phys. Rev., 147: 858-60(July 22, 1966). (BNL-9994).

L-subshell internal conversion ratios were measured for low-energy E2 transitions in several deformed nuclei: ^{160}Dy (86.74 kev), ^{166}Er (80.57 kev), ^{169}Tm (130.53 kev), ^{170}Yb (84.23 kev), ^{186}Os (137.15 kev), and ^{188}Os (155.03 kev) The measurements were made with 50-cm radius, double focusing spectrometers at momentum resolutions better than 0.1%, and the ratios were determined with an accuracy of about 2%. In all but one of the six cases the L_2/L_3 ratios agree with theoretical values; however, the L_1/L_3 ratios in all cases are larger than theoretical values, with an average deviation of 6%. There is no immediately available explanation for this discrepancy. (auth)

32517 ISOTOPE SHIFTS OF NEUTRON-DEFICIENT MERCURY ISOTOPES. Davis, Sumner P.; Aung, Tin; Kleiman, Herbert (Univ. of California, Berkeley). Phys. Rev., 147: 861-6(July 22, 1966).

Measurements on the isotope shift and optical hyperfine structure were extended to the neutron-deficient mercury isotopes 193, 193^m, and 192. The shifts are -275 ± 15, -251 ± 8, and -284 ± 5 mK, respectively, referred to the isotope 196 as 0. An explanation of these shifts is given in terms of nuclear deformations. The spins of 193 and 193^m are $\frac{3}{2}$ and $\frac{13}{2}$, as given earlier in preliminary reports. The quadrupole moment of 193 is calculated to be -2.0 ± 1.0 b. (auth)

32518 DECAY OF ^{94}Nb AND ^{94m}Nb. Snyder, R. E.; Beard, G. B. (Wayne State Univ., Detroit). Phys. Rev., 147: 867-70(July 22, 1966).

The beta decay of 2.0×10^4-yr ^{94}Nb was investigated by means of a scintillation spectrometer. The beta spectrum has an end-point energy of 470 ± 6 kev and yields a linear Fermi-Curie plot when a shape factor of $p^2 + \lambda q^2$ ($\lambda = 1.75 \pm 0.15$) is applied. The shape factor indicates the transition is second-forbidden non-unique, in accord with its log ft value of 12. Additional measurements were made of electromagnetic radiations from both ^{94}Nb decay and that of 6.6-min ^{94m}Nb. No new transitions were observed, but more precise energy determinations of the gamma rays emitted in the decay of ^{94}Nb were obtained. The results of this study further support previously proposed spin and parity assignments. (auth)

32519 DIFFERENTIAL SCATTERING OF NEUTRONS FROM ^{208}Pb AT RESONANT ENERGIES. Fowler, J. L. (Oak Ridge National Lab., Tenn.). Phys. Rev., 147: 870-80(July 22, 1966). (ORNL-P-2012).

Measurements are reported on differential elastic scattering of neutrons of a few kev energy spread from 99.75% ^{208}Pb in the energy region 0.715 to 1.761 Mev. The results include absolute differential cross sections at 20 resonant and 9 nonresonant energies. A least-squares phase-shift analysis provides the resonance parameters and reduced widths of 21 resonances. The observed $s_{\frac{1}{2}}$ potential-scattering phase shifts are in agreement with those expected from a type of phenomenological potential which reproduces the single-particle bound states of ^{209}Pb. Parity assignments and widths of the $J = \frac{1}{2}$ resonances are in disagreement with the prediction for 5 intermediate states arising from two-particle one-hole neutron excitations. There are, however, a number of resonances with widths corresponding to several percent of the single-particle limits which are likely candidates for some sort of intermediate states. (auth)

32520 ENERGIES AND HALF-LIVES OF ISOMERIC TRANSITIONS IN ^{115}Sn AND ^{109}Cd. McCarthy, A. L.; Conlon, T. W. (Princeton Univ., N. J.). Phys. Rev., 147: 881-3(July 22, 1966). (PUR-937-177).

The energies and half lives of isomeric transitions in ^{115}Sn and ^{109}Cd measured in pulsed proton beam bombardments of natural In and Ag at 17.5 Mev. The isomeric gamma rays were detected with a lithium-drifted germanium detector; time and energy information were obtained with the use of a 4096-channel two-dimensional analyzer. The values obtained were: ^{115}Sn: 115.9 ± 1 kev, 100.7 ± 2 kev, 498.0 ± 1 kev; 166.4 ± 10 μsec; and ^{109}Cd: 263 ± 5 kev, 206 ± 5 kev; 10.4 ± 1 μsec. The gamma rays are quoted in their probable order of emission. (auth)

32521 DECAY CONSTANT AND MASS-YIELD CURVE FOR THE SPONTANEOUS FISSION OF ^{238}U. Rao, M. N.; Kuroda, P. K. (Univ. of Arkansas, Fayetteville). Phys. Rev., 147: 884-6(July 22, 1966).

The equilibrium ratio of ^{132}Te/^{238}U in nonirradiated natural and depleted uranium was measured to be $(2.2 \pm 0.2) \times 10^{-4}$ disintegrations per second per gram of uranium. This value was used to normalize the mass-spectrometric data for the relative yields of krypton and xenon isotopes from the ^{238}U spontaneous fission. Combining the mass-spectrometric and radiochemical data obtained by previous investigators, a "mass-yield" curve for the spontaneous fission of ^{238}U was constructed in which the equilibrium ratios of the fission products in nonirradiated uranium were plotted against the mass numbers. By summing the area under the curve, a value of $(7.8 \pm 0.9) \times 10^{-17}$ yr^{-1} was obtained for the ^{238}U spontaneous fission decay constant. This value is intermediate between the values reported by Fleischer and Price and by Segrè. (auth)

32522 SYSTEMATICS OF LOW-LYING 0^+ STATES IN LIGHT NUCLEI. Meyerhof, W. E. (Stanford Univ., Calif.). Phys. Rev. Lett., 16: 1114-15(June 13, 1966).

Certain systematics of 0^+ excited states in light even-even nuclei (particularly closed-shell nuclei) are discussed, which show that a breathing-mode liquid-drop description of these states is probably not successful. A description in terms of multipair excitations, a pair consisting of a particle and a hole, is considered. (G.O.Y.)

32523 ANOMALIES IN THE SPIN-ORBIT TERM OF THE OPTICAL MODEL POTENTIAL. Boschitz, Edmund T. (Lewis Research Center, Cleveland). Phys. Rev. Lett., 17: 97-9(July 11, 1966).

An analysis was made of polarization data on elastic scattering of 18.5- and 20.5-Mev polarized protons from complex nuclei in terms of the optical model, in order to investigate the spin-orbit potential dependence on proton energy and to target mass, and to find an interpretation for the large polarization difference observed in the scattering of 18.5-Mev protons from ^{40}Ar and ^{40}Ca. (L.B.S.)

32524 TWO-PARTICLE-TWO-HOLE STATES IN ^{16}O. Boeker, E. (Vrije Univ., Amsterdam). Physica, 32: 669-88(Apr. 1966).

The influence of the residual interaction on 2p2h and 1p1h configurations with an unperturbed energy of 3 $\hbar\omega$ is investigated. A selection of 25 configurations with $J, \pi = 1^-, T = 0$ is made and the major part of the spurious states is projected out. A zero range residual interaction with a Soper exchange mixture is diagonalized on the basis of 23 states, consisting of the 19 practically nonspurious 3 $\hbar\omega$ states in LS coupling and 4 nonspurious 1 $\hbar\omega$ states in jj coupling. Most parameters as the zero order energies and the strength of the interaction have been taken from other authors, 2 parameters have been guessed. The results show 2 more 1^- $T = 0$ states between 20 and 30 Mev than the simple calculations with 1 $\hbar\omega$ configurations only. These may mix with the 1^-, $T = 1$ states in this energy region by the Coulomb interaction, thus giving rise to some fine structure in the giant dipole resonance. Results show that the residual interaction may bring 2p2h states with an unperturbed energy of 3 $\hbar\omega$ and 1 $\hbar\omega$ states in the same energy region. (auth)

32525 DOUBLE NUCLEAR-ELECTRON RESONANCE SPECTROMETER. Stepanov, A. P.; Stotskii, V. M.; Filatov, A. I. (Ural Polytechnic Inst., Sverdlovsk, USSR). Prib. Tekh. Eksp., No. 1, 128-32(Jan.-Feb. 1966). (In Russian).

A device for observing the dynamic polarization of nuclei in solutions of paramagnetic materials is described. With this device, the coefficient of enhancement of polarization of the nuclei and the nuclear and electron time relaxation can be measured, and the hyperfine structure of EPR spectra in a weak magnetic field (8 to 50 Oe) at temperatures from 0 to 80°C can be studied. (tr-auth)

32526 INSTALLATION FOR STUDYING THE ENERGY AND ANGULAR DISTRIBUTION OF RECOIL NUCLEI.

Denisov, F. P.; Duisebaev, A.; Milovanov, V. P. (Inst. of Physics, Moscow). Prib. Tekh. Eksp., No. 1, 183-4(Jan.-Feb. 1966). (In Russian).

A device is described for studying the angular and energy distributions of recoil nuclei, on which the energy distributions can be measured with resolution ~1% and the angular distributions, with resolution of 7°. The device is based on the use of a gaseous absorber as a retarding medium and the presence of a special lock for exchanging the films on which the recoil nuclei are collected. (M.J.T.)

32527 STATES OF ^{13}N IN THE 20 TO 30 Mev REGION. Patterson, J. R.; Poate, J. M.; Titterton, E. W. (Australian National Univ., Canberra). Proc. Phys. Soc. (London), 88: 641-8(July 1966).

Proton transitions to the ground, 4.43, 7.66, and 9.64 Mev states of ^{12}C arising from the ^{10}B(^{3}He,p) reaction were investigated at bombarding energies between 1.2 and 12 Mev. Excitation functions for the four particle groups were taken at 150°. Angular distributions of the p_0 and p_1 groups were measured at twelve energies and total cross sections were obtained. In addition angular distributions were obtained for the p_2 and p_3 groups at a bombarding energy of 5.4 Mev. The experiment provides evidence for excited states of ^{13}N at energies of 22, 24.5, 26, and 28 Mev. (auth)

32528 DETERMINATION OF THE CROSS SECTIONS FOR THE REACTIONS ^{27}Al(n,α) AND ^{56}Fe(n,p) FOR 14-Mev NEUTRONS BY AN ABSOLUTE METHOD. Hemingway, J. D.; James, R. H.; Martin, E. B. M., Martin, G. R. (Univ. of Durham, Eng.). Proc. Roy. Soc. (London), Ser. A, 292: 180-92(May 17, 1966).

Measurements of the cross sections for the reactions ^{27}Al(n,α)^{24}Na and ^{56}Fe(n,p)^{56}Mn for neutrons of energy 13.5 ± 0.1 Mev are made by a radioactivation method. The neutron flux was determined by a variant of the associated particle method, in which the α-particles produced concurrently with the neutrons from the D + T reaction were estimated in terms of the volume of helium which accumulated when they were brought to rest in an aluminum foil. Cross section values obtained at 13.5 Mev were for ^{27}Al(n,α) 118.1 ± 6.0 mb; and for ^{56}Fe(n,p) 106.7 ± 4.7 mb. The errors quoted include both the standard error on the mean of the experimental values and an estimate of possible residual systematic errors. The excitation functions for both reactions in the energy region 13.5 to 14.8 are also investigated, in order to provide secondary cross section values over this range of energies. At 14.8 Mev the values found were ^{27}Al(n,α) 103.6 ± 5.5 mb and ^{56}Fe(n,p) 96.7 = 4.5 mb. (auth)

32529 MOMENTUM DISTRIBUTION OF THE RECOIL NUCLEUS IN THE ^{12}C(p,2p)^{11}B REACTION. Nguyen-Trung, Chi; Sakamoto, Yoshiyuki (Kyoto Univ.). Progr. Theoret. Phys. (Kyoto), 35: 423-31(Mar. 1966).

The momentum distribution of the recoil nucleus in the ^{12}C(p,2p)^{11}B reaction is calculated in the general noncoplanar and nonsymmetric case. Results are reported and an attempt to explain the experimental data obtained by Yuasa et al. with a propane bubble chamber is presented. (auth)

32530 NFC REACTION ($\gamma\pi^-$p) WITH COMPLEX NUCLEI. Nagata, Sinobu (Kyoto Univ.); Kanada, Hiroyuki; Sakai, Kenji. Progr. Theoret. Phys. (Kyoto), 35: 568-9(Mar. 1966).

The ($\gamma\pi^-$p) reaction with complex nuclei is investigated in order to obtain information on the knockout process of deep lying nucleons. The advantages and disadvantages of this method are presented. This method is applied to the reaction ^{12}C(γ,π^-p)^{11}C where structure is revealed by the (p,2p) reaction. (B.G.D.)

32531 OPTICAL POTENTIAL FOR HIGH-ENERGY α-α SCATTERING. Abe, Yasuhisa; Tamagaki, Ryozo (Hokkaido Univ., Sapporo). Progr. Theoret. Phys. (Kyoto), 35: 569-71(Mar. 1966).

An investigation is presented on how the α-α repulsive core at low energies turns to the absorptive core at high energies, where a number of channels are open. An α-α optical potential at E_{lab} = 915 Mev is derived. (B.G.D.)

32532 HIGH-ENERGY α-α SCATTERING. Endo, Osamu (Hokkaido Univ., Sapporo). Progr. Theoret. Phys. (Kyoto), 35: 571-2(Mar. 1966).

An investigation is presented on how the α-α repulsive core at low energies turns to the absorptive core at high energies. The differential cross section at E_{lab} = 915 Mev is analyzed in the diffraction model. (B.G.D.)

32533 PRACTICAL METHOD USING THE ISOSPIN PROJECTION OPERATOR IN NUCLEAR PHYSICS. Fujita, Jun-Ichi; Ikeda, Kiyomi (Tokyo Univ.). Progr. Theoret. Phys. (Kyoto), 35: 622-37(Apr. 1966).

The projection operator projecting a state with a definite value of isospin out of an isospin mixture can be expressed as a power series in the raising and lowering operators for isospin z-components. It is pointed out that such a series representation of the isospin projection operator is especially useful in studying the isospin properties of heavier nuclei. (auth)

32534 NUCLEAR CHARGE DISTRIBUTION OF CALCIUM ISOTOPES. Konishi, Teruaki; Narumi, Hajime (Hiroshima Univ.). Progr. Theoret. Phys. (Kyoto), 35: 750-2(Apr. 1966).

Using a phenomenological approach, attention is called to the charge distribution of the calcium nuclides as a preliminary study of isotopic behavior and in particular to a characteristic feature of nuclei with extra neutrons. (B.G.D.)

32535 SURVEY OF FAST-NEUTRON REACTIONS. Cindro, N. (Inst. Ruder Boskovic, Zagreb). Rev. Mod. Phys., 38: 391-446(July 1966).

A survey of recent experimental and theoretical results (January 1963–July 1965) on fast-neutron-induced reactions is presented. The first part gives an outline of present reaction mechanism theories that may be useful for an experimentalist. A semiclassical and more exact description of both direct and equilibrium processes is given and a brief discussion of intermediate processes included. The second part gives the experimental results relevant to the understanding of the mechanism of the interaction of neutrons with nuclei: energy spectra, angular distributions, and total cross sections. Finally, a survey is presented of the results and possibilities of utilizing fast neutrons for nuclear structure investigations. (auth)

32536 INELASTIC SCATTERING OF ELECTRONS BY LIGHT NUCLEI. Simenog, I. V. (Inst. of Physics, Kiev). Ukr. Fiz. Zh., 11: 471-7(1966). (In Ukrainian).

The inelastic scattering of fast electrons by nuclei of ^{12}C and ^{16}O is considered on the basis of a shell model (potential of a harmonic oscillator with spin-orbit coupling). The calculated excitation cross section of the ^{16}O nucleus is compared with the experimental results. The degree of agreement of the theoretical calculation with the experimental results is discussed. Sum rules for the ^{16}O nucleus are determined, and their analysis is given. (auth)

32537 NUCLEAR CONDITIONS OF INTEGRAL OPERATORS AND THE EXISTENCE OF AN S MATRIX IN THE SCALAR DISPERSION PROBLEM AT THE INFINITE BOUNDARY AND AT LOCAL POTENTIAL. Ramm, A. G. Ukr. Mat. Zh., 17: No. 3, 84-90(1965). (In Russian).

In a three-dimensional system, the operator $Kf = \int K(x,y) f(y)dy$ was determined. On this basis, a theorem was derived, giving the conditions required for establishing the nuclear character of the operator K. The completely continuous operator is designated as being nuclear, if $\sum_{n=1}^{\infty} \lambda_n < \infty$, where λ_n is the eigenvalue of the operator $Q = (K^*K)^{\frac{1}{2}}$. Additional theorems were presented concerning the nuclear nature of the operator, determining the conditions of existence of the wave operators from which the S-matrix may be obtained. The value of the wave operators in the spectral theory is defined by the fact that they allow the unitary equivalence of the absolutely continuous portions of certain operators A and B to be established. (TTT)

32538 YADERNAYA FIZIKA. MEKHANIZM YADERNYKH REAKTSII. (Nuclear Physics. Mechanism of Nuclear Reactions). Moscow, Akademiya Nauk SSSR, Institut Nauchnoi Informatsii, Itoginauki, 1965. 91p.

An abstract is presented for the second section of the book. The first section "Application of Dispersion Theory to Direct Nuclear Reactions" was previously abstracted in NSA 20: 19990. (C.E.S.)

For an abstract of the individual paper see: 32539.

32539 PHOTOABSORPTION OF NUCLEI IN THE THEORY OF FERMI-LIQUIDS. Zaretskii, D. F.; Lushnikov, A. A. pp 35-89 of Yadernaya Fizika. Mekhanizm Yadernykh Reaktsii. Moscow, Akademiya Nauk SSSR, Institut Nauchnoi Informatsii, Itoginauki, 1965. (In Russian).

The giant resonances, relatively narrow peaks in the γ-quantum absorption cross section of nuclei, have been widely studied in order to correlate them to general properties, but all proposed models exhibit some shortcoming. Application of the mathematical methodology of the quantum field theory to the multibody problem resulted in the Fermi liquid theory that allows one to investigate quantitatively the lower excited states of strongly interacting Fermi systems. The nuclear photoabsorption was studied on the basis of such considerations, attempting to interpret giant resonances from the viewpoint of the Fermi liquid theory for finite systems. Determination of the dipole photoabsorption cross section as a function of incident γ quanta includes about a 20% error; the quasiclassical accuracy ($\sim A^{-1/3}$) is sufficient to correlate the experimental data with the calculations. It was shown by the Fermi liquid theory that the interaction of quasiparticles in the case of the giant dipole resonance may be sufficiently determined by a single constant which controls the photoabsorption curve and width. The probability of decay of the nuclei according to alternate schemes was not considered. (Review article, 36 references). (TTT)

32540 STUDY OF NEUTRON REACTIONS WITH α-PARTICLE EMISSION ON ^{23}Na IN THE ENERGY REGION 12.6 TO 18.7 Mev. Woelfer, G.; Bormann, M. (Univ., Hamburg). Z. Phys., 194: 75-88(1966). (In German).

Neutron reactions with alpha particle emission induced in ^{23}Na were investigated in the neutron energy region 12.6 to 18.7 Mev. Alpha particles are emitted mainly in the reactions (n,α), $(n,\alpha n')$, and $(n,n'\alpha)$. The total alpha particle spectra were measured with a NaI crystal, which served as both a target and a detector. Pulse-shape-discrimination was employed for distinguishing alpha particles from other radiations. From the yield of the total spectra the cross sections for the sum of the three reactions were obtained. The spectra show the characteristic evaporation form and from their analysis according to the statistical theory the cross sections for the reaction $(n,n'\alpha)$ were deduced. In a further experiment using the activation method the cross sections only for the reaction (n,α) were measured. Finally, combination of all these results led also to the cross sections for the reaction $(n,\alpha n')$. The excitation functions for the three reactions are given and compared with the predictions of the statistical model. (auth)

32541 DETERMINATION OF ABSOLUTE K-INTERNAL CONVERSION COEFFICIENTS OF SOME TRANSITIONS IN ^{140}Ce BY THE INTERNAL-EXTERNAL CONVERSION METHOD. El-Nesr, M. S.; El-Sayad, G. M. (Atomic Energy Establishment, Cairo). Z. Phys., 194: 125-34 (1966).

The internal K-conversion coefficients of the 331-, 431-, 815-, and 933-kev transitions following the decay of ^{140}La were determined absolutely by the method of comparing internal and external conversion lines measured in a double-focusing beta-ray spectrometer. The K-internal conversion coefficients of the 4+ → 2+ 487-kev transition in ^{140}Ce was used to normalize relative K-electron and gamma-ray intensities for these transitions. Multipolarity assignments based on the results are suggested. The 815-kev transition is found to be pure magnetic dipole character in good agreement with the theoretical values calculated by Sliv and Band. The 331- and 933-kev transitions are proved to have magnetic dipole character with E2/M1 = 0.2852 ± 0.0143 and 0.1750 = 0.0088 respectively. The 431 kev transition was found to have magnetic octupole character. The results obtained are most consistent with the assignment 2+, 4+, 2+, 3+ and 1+ for the 1597-, 2084-, 2184-, 2410, and 2515-kev levels respectively. (auth)

32542 THEORY OF α MATTER. Clark, John W.; Wang, Tso-pin (Washington Univ., St. Louis). 53p. (CONF-651213-9). ORAU. Gmelin, AED-CONF-65-400-16.

The usual concept of nuclear matter is discussed, and a generalization of this concept which allows a qualitative understanding of the effects of clustering phenomena is proposed. As an example of "generalized nuclear matter," the properties of the ground state of a uniform extended system of structureless α particles is studied by means of the method developed by Wu and Feenberg for liquid ^{4}He. The Wu-Feenberg method requires the use of a Bijl-Dingle-Jastrow wave function and the Kirkwood superposition approximation. The assumed α-α interactions fit the S-wave phase shifts up to a C. M. energy of ~10 Mev. The results, in comparison with results from theoretical nuclear-matter calculations which entertain no clustering (both expressed in terms of the energy per nucleon as a function of the radius of the (average) volume per nucleon) are of value in making crude estimates of the percentage of the surface matter of a heavy nucleus which prefers to form into α clusters and in interpreting empirical values for the compressibility of nuclear matter. (auth)

32543 POLARIZATION OF PROTONS SCATTERED FROM ^{3}He. Sanders, Richard Lenoir (Univ. of North Carolina, Chapel Hill). 33p. (CONF-651135-3). ORAU. Gmelin, AED-CONF-65-402-4.

From American Physical Society, Southeastern Section, Charlottesville, Va.

The polarization and differential cross section of an initially unpolarized beam of protons scattered from a ^{3}He target were calculated in terms of a Coulomb scattering amplitude and some nuclear phase shifts. The calculation included only the singlet and triplet S-waves and P-waves corresponding to J = 0, 1, and 2, and was thus restricted in validity to an energy region below about 8 Mev, where the D-wave phase shifts had been shown to be small. Coupling between singlet and triplet states was also neglected. The values of the phase shifts proposed by Tombrello in 1964 were used to verify fits to the existing data. The phase shifts were found to represent the data accurately up to an energy of about 6 Mev where apparently D-waves, and perhaps the mixing of the singlet and triplet P states, are beginning to play a significant role. (auth)

32544 ANALYSIS OF INELASTIC ALPHA-PARTICLE SCATTERING DATA USING THE IBM 1620 COMPUTER. Marr, G. (Miami Univ., Oxford, Ohio). 22p. (CONF-641127-5). ORAU. Gmelin, AED-CONF-64-297-5.

From American Physical Society, Fall Meeting of the Ohio Section, Oxford, Ohio.

A FORTRAN program for the reduction of elastic alpha-particle scattering data was altered to include the analysis of inelastic alpha-particle scattering data. The computer plots the counts versus channel histograms, calculates the differential cross sections, plots an experimental angular distribution, and fits a theoretical curve to the experimental data. Butler's direct interaction theory is the basis for the theoretical calculation. The operation of the program and the results obtained for several alpha-particle scattering experiments are discussed. (auth)

32545 ANALYTICAL AND EXPERIMENTAL INVESTIGATION OF NONADIABATIC PARTICLE LOSSES IN AXISYMMETRIC AND MULTIPOLAR MAGNETIC FIELDS. Roth, J. Reece (Lewis Research Center, Cleveland). 34p. (CONF-651126-3). ORAU. Gmelin, AED-CONF-65-353-2.

From American Physical Society, 7th Annual Meeting of the Division of Plasma Physics, San Francisco.

An investigation of the nonadiabatic behavior of a single

nonrelativistic charged particle is presented in two magnetic field geometries; an axisymmetric magnetic mirror, which was investigated by both analytical and experimental means, and a minimum-B configuration formed by the superposition of a multipolar (Ioffe) magnetic field on an axisymmetric magnetic mirror, which was studied only by analytical means. The nonlinear equations of motion for a charged particle in these magnetic field configurations were solved for 10^5 sets of initial conditions on a high-speed computer. A particle was considered to be nonadiabatic if its "adiabatic invariant" $M_4 \sim v_\perp^2/B$ varied by more than 5 percent during a single interaction with the magnetic mirror in question. By defining suitable dimensionless similarity parameters, it was found possible to summarize the computer results in a single analytical expression, which predicts the conditions under which nonadiabatic behavior will be observed as a function of the particle initial conditions. This similarity relation is a useful substitute for a closed-form solution to the nonlinear and nonholonomic mathematical problem and may be used as a basis for correlating experimental data. An experimental technique was devised to detect the enhanced particle losses resulting from nonadiabatic particle motion in an axisymmetric magnetic mirror. The results from a wide range of experimental conditions were plotted in terms of the similarity parameters that were useful in correlating the analytical results and were found to obey the same similarity relation. This experimentally determined similarity relation gives the conditions for the onset of nonadiabatic losses in terms of the mirror ratio, particle energy, distance between mirrors, etc. This relation may be used as a design criterion to assure adiabatic confinement in all axisymmetric magnetic mirrors of practical interest. (auth)

32546 THREE-BODY PHOTODISINTEGRATION OF ^{3}He. Gerstenberg, H. M.; O'Connell, J. S. (National Bureau of Standards, Washington, D. C.). 18p. (CONF-660107–14). ORAU. Gmelin, AED-CONF-65-003-30.

From American Physical Society Meeting, New York.

The ^{3}He(γ,n)2p cross section was measured in 1 Mev steps from threshold to 30 Mev using the NBS betatron and a ^{4}He cryostat to produce a 40 cm^3 liquid ^{3}He target. The measured cross section shows a broad peak between 14 and 20 Mev with a maximum cross section at about 0.90 mb. The cross section and bremsstrahlung-weighted cross section integrated up to 28 Mev gives 12.1 ± 10% Mev-mb and 0.68 ± 10% mb, respectively. Theoretical calculations of the three-body photodisintegration cross section overestimate the experimental cross section by factors of 3 to 10. (auth)

32547 COMPARISON OF MANY-NUCLEON TRANSFER REACTIONS WITH DWBA CALCULATIONS. Daehnick, W. W.; Denes, L. J. 8p. (CONF-660107–3). ORAU. Gmelin, AED-CONF-66-003-13.

From American Physical Society Meeting, New York.

The results of an investigation of many-nucleon transfers in deuteron reactions are summarized. Experimental results on the cross sections for (d,Be-7), (d,Be-9), (d,Li-6), and (d,Li-7) reactions and for deuteron scattering on some isotopes with A = 12–19 are compared with the results of DWBA calculations. (D.C.W.)

32548 ELECTROMAGNETIC MASS OBSERVATIONS AND THE NATURE OF SPACE-TIME. Phipps, T. E. Jr. 8p. (CONF-660107–8). ORAU. Gmelin, AED-CONF-66-003-12.

From American Physical Society Meeting, New York.

The experiment proposed by Sherwin and Rawcliffe and carried out in 1960 by Johnson and Damerow with the object of observing the classically predicted tensor character of the electromagnetic mass of a nonspherical nucleus led to the result that to within observational accuracy the mass is a true scalar in disagreement with classical electrodynamics. After briefly reviewing the experiment, the far-reaching nature of its implications is indicated which include the first evidence of a possible breakdown of retarded-potential electrodynamics on the comparatively huge scale of 10^{-12} cm, indication of possible illegitimacy (operational meaninglessness) of assigning different proper-time parameters to the description of different portions of a nucleus, and consequent possibility of achieving a significant simplification in the formulation of the quantum mechanical relativistic many-body problem, gained through substituting for Minkowski space in pure-state description a 4-space continuum in which the communal proper time plays a role within the collective somewhat analogous to that of absolute time in Newtonian physics. (auth)

32549 INDUCED RADIOACTIVITY DATA COMPUTED FOR VARIOUS MATERIALS AND COMPARED WITH THAT OF IRRADIATED SAMPLES. Barbier, M. (CERN, Geneva). 15p. (CONF-651101–74). ORAU. Gmelin, AED-CONF-65-332-100.

From 13th Conference on Remote Systems Technology, Washington, D. C.

An empirical formula based on a large number of experimental results has recently been established by G. Rudstam for spallation cross sections by nucleons for bombarding energies above 50 Mev. It permits calculation of the cross section for producing any particular isotope from a given target element. This formula is used to calculate the total activity induced by high energy particles for a number of target elements. The results are compared with some experimental decay curves taken at the CERN Synchrocyclotron. (auth)

32550 SPIN ASSIGNMENTS IN ^{35}Cl AND ^{37}Cl VIA (n,n'γ) REACTIONS. Nichols, D. B.; Kern, B. D.; McEllistrem, M. T. (Univ. of Kentucky, Lexington). 13p. (CONF-651118-16). ORAU. Gmelin, AED-CONF-65-329-20.

From American Physical Society, Gatlinburg, Tenn.

Differential cross sections for the (n,n'γ) reactions in chlorine were measured using time-of-flight techniques. The spectra obtained are shown, and the cross sections, spins, and parities for the various levels are listed. (J.F.P.)

32551 RESONANCE PROPERTIES OF THE MAIN FERTILE AND FISSIONABLE NUCLEI. Schmidt, J. J. (Kernforschungszentrum, Karlsruhe, Ger.). 46p. (CONF-660204–11). ORAU. Gmelin, AED-CONF-66-017-10.

From American Nuclear Society Meeting, San Diego, Calif.

A brief review is given of some important recent changes in resolved and statistical resonance parameters of the main fertile and fissionable nuclei uranium-235, -238, and plutonium-239 in comparison with the expectations of nuclear theory. The review is based on Breit-Wigner single level evaluation of published analysis results of many recent s- and p-wave resonance experiments. (J.F.P.)

32552 NEUTRON SINGLE-PARTICLE LEVELS OF ^{91}Zr. Koshel, R. D. (Ohio Univ., Athens). 7p. (CONF-650451–1). ORAU. Gmelin, AED-CONF-65-408-2.

From American Physical Society, Spring Meeting of the Ohio Section, Athens.

The single particle levels of zirconium-91 were investigated using the nonlocal potential model for the scattering of neutrons by nuclei developed by Perey and Buck. The local and nonlocal binding energies and the equivalent local potentials are listed for the various levels of zirconium-91. It was found that there is agreement between scattering and bound state parameters, that the model used does not affect the characteristic level ordering, and that values of the equivalent local potential depth, which are needed to give observed values of the binding energy per nucleon, are given by the model. (J.F.P.)

32553 THE HYPERFINE-STRUCTURE ANOMALIES OF ^{198}Au AND ^{199}Au. Vanden Bout, Paul A.; Ehlers, Vernon J.; Nierenberg, William A. 5p. (CONF-650927–19). ORAU. Gmelin, AED-CONF-65-222-15.

From American Physical Society, Honolulu, Hawaii.

The hyperfine-structure anomalies of ^{198}Au and ^{199}Au were measured. The values obtained are much larger than the values previously obtained for any isotope. (G.O.Y.)

32554 INELASTIC SCATTERING OF 39.5 AND 31.8 Mev ALPHA-PARTICLES BY ^{16}O. Priest, J. R. (Miami Univ. Lewis Research Center, Cleveland); Vincent, J. S.; Boschitz, E. T.; Bercaw, R. W. 10p. (CONF-641127-2). ORAU. Gmelin, AED-CONF-64-297-1.

From American Physical Society, Fall Meeting of the Ohio Section, Oxford Ohio.

Angular distribution data for inelastic scattering of 39.5- and 31.8-Mev alpha particles by ^{16}O are presented and compared with theoretical predictions. Results are discussed in relation to the level structure of ^{16}O and the processes involved in the reaction. The experimental data are consistent with the excitation of a 2^- unnatural parity state by either the exchange process or multiple phonon process. The data also confirm preferential excitation of the 2^+ and 3^- states as predicted by theory. (A.G.W.)

32555 REACTION STUDY OF $^{19}F(d,n)^{20}Ne$. Warshaw, S. I.; Goldberg, D. A.; Keaton, P. W. Jr.; Owen, G. E. (Johns Hopkins Univ., Baltimore). 19p. (CONF-651015-17). ORAU. Gmelin, AED-CONF-65-312-34.

From American Physical Society, Chicago.

The angular distributions of neutrons from the reaction $^{19}F(d,n)^{20}Ne$ were measured at five energies between 2.0 and 2.5 Mev at angles between 0 and 165°. The differential cross section for this reaction was also measured at laboratory angles of 0 to 120° as a function of energy from 0.9 to 2.7 Mev. (G.O.Y.)

32556 SPIN AND PARITY ASSIGNMENTS IN ^{24}Mg. Ollerhead, R. W.; Kuehner, J. A.; Levesque, R. J. A.; Blackmore, E. W. (Chalk River Nuclear Labs., Ontario, Can.). 15p. (CONF-660107-34). ORAU. Gmelin, AED-CONF-66-003-57.

From American Physical Society Meeting, New York.

Twelve levels in ^{24}Mg were studied by measuring angular correlations between alpha particles detected at 0° and coincident gamma rays from the reaction $^{12}C(^{16}O,\alpha)^{24}Mg$. Detection of alpha particles at 0° from this reaction requires natural parity $(-)^J$ for the level concerned. Levels at 7.56, 7.62, 8.44, 9.00, and 9.15 Mev have ground state transitions with distinctive angular correlations from which unambiguous spin and parity assignments of 1–, 3–, 1–, 2+, and 1–, respectively, were made. The energies and decay modes of levels at 8.12 and 13.2 Mev suggest that these levels may be the 6+ and 8+ members of the ground state rotational band. The angular correlation data are consistent with this interpretation, although the spins were not uniquely determined. The same comments apply to a level at 9.52 Mev, tentatively identified as the 6+ member of a K = 2 band. Doublets at 8.44 and 9.52 Mev each have one member populated in beta decay of ^{24}Al, implying spin and parity, 3+, 4+ or 5+, from which the requirement of natural parity in this experiment indicates 4+ assignments for these two levels. Angular correlation data are consistent with, but do not uniquely determine, spin 4. Tentative spin assignments have also been made to levels at 8.65 (2+) and 10.1 (0+) Mev. (auth)

32557 PROTON SPIN FLIP IN THE REACTION $^{60}Ni(p,p')^{60*}Ni$ (1.33) AT 10.5 AND 14.0 Mev. Kolasinski, W. A.; Schmidt, F. H.; Cramer, J. G. 7p. (CONF-660107-45). ORAU. Gmelin, AED-CONF-66-003-93.

From American Physical Society Meeting, New York.

The results of spin flip measurements in the reaction $^{60}Ni(p,p')^{60}Ni^*$ at 10.5 and 14.0 Mev are presented. (B.G.D.)

32558 THREE-ALPHA MODEL FOR ^{12}C. Harrington, David R. (Rutgers–The State Univ. of New Jersey, New Brunswick). 16p. (CONF-660107-32). ORAU. Gmelin, AED-CONF-66-003-64.

From American Physical Society Meeting, New York.

A model is proposed in which the ^{12}C nucleus is composed of three rigid alpha particles. Using separable alpha-alpha interactions the homogeneous Faddeev equations for the bound states reduce to a set of coupled nonsingular integral equations in one variable. Specializing to the case of only S-wave interactions this set reduces to a single equation which is solved numerically. A ground state solution is found, with a reasonable value for the binding energy, but no excited states. Further calculations are suggested, and an appendix containing the general angular momentum analysis is included. (auth)

32559 BINDING ENERGY OF THE NUCLEUS. Manuel, O. K. (Univ. of Missouri, Rolla). 21p. (CONF-660107-42). ORAU. Gmelin, AED-CONF-66-003-85.

From American Physical Society Meeting, New York.

Nuclear binding energy is based on a particular nuclear model where the bound neutrons and protons are assumed to retain the same 1.29 Mev difference in total energy which these unbound particles exhibit. The binding energy per nucleon therefore has a different ground state for each neutron, (proton ratio predicted by this model). The terms in the Weizsäcker equation cannot logically be equated to this binding energy. It is proposed to replace this awkward and misleading concept by an absolute binding energy similar to that proposed by Harkins and Wilson in 1915 and later by Aston in 1927. (auth)

32560 MONTE CARLO CALCULATIONS OF RADIONUCLIDE PRODUCTION IN IRON TARGETS BOMBARDED WITH 400-Mev PROTONS. Ebeoglu, D. B.; Wainio, K. M.; More, K.; Tiffany, O. L. (Bendix Systems Div., Ann Arbor, Mich.). 21p. (CONF-650961-1). ORAU. Gmelin, AED-CONF-65-224-5.

From American Geophysical Union, 5th Western National Meeting, Dallas.

The effective production rate of a number of radionuclides in iron targets bombarded with a monoenergetic, collimated beam of 400-Mev protons was calculated. The buildup of low-energy products, ^{56}Co, ^{54}Mn, ^{51}Cr, ^{52}Mn, and ^{48}V was followed in a ^{56}Fe target, and the results were compared with previous experimental proton irradiations of identical targets. The results show good agreement for the integral production rates of nuclides and predict the same maxima as a function of depth. (G.O.Y.)

32561 STRUCTURE EFFECTS IN THE CHARGE RADIUS OF SPHERICAL NUCLEI. Technical Report No. 22. Uher, Richard A.; Sorensen, Raymond A. (Carnegie Inst. of Tech., Pittsburgh). 100p. (CONF-651015-24). ORAU. Gmelin, AED-CONF-65-312-54.

From American Physical Society, Chicago.

Isotope and isomer shifts of the nuclear charge radius are calculated using the pairing plus quadrupole model. To accomplish this, the nuclear system is divided into a core plus a few valence particles. Monopole polarization of the core by the particles is taken into account in a phenomenological manner by assuming that the particles interact independently with the core. Quadrupole polarization of the core by the particles is estimated with the help of an effective quadrupole charge determined by fitting BE2 transition rates of even-A nuclei. The independent particle configuration of the valence nucleons is admixed by the pairing plus quadrupole interaction and the resulting wave functions are used to calculate isotope and isomer shifts of the charge radius. The results of even-A to even-A isotope shifts show good agreement with experiment, while the odd-even staggering effects observed in the isotope shifts cannot be obtained. Good agreement is obtained for the few isomer shifts which were measured. (auth)

32562 PRESENT STATUS OF DOUBLE BETA DECAY. Shapiro, Mark H. (Univ. of Pennsylvania, Philadelphia). 29p. (CONF-650653-24). ORAU. Gmelin, AED-CONF-65-170-50.

From American Physical Society, Summer Meeting, New York.

The historical development of the theory for double beta decay is reviewed, and the present theoretical status is summarized. Various experiments for observing such decay are also described, and recent results are given. A lower limit was found, and only two orders of magnitude remain between the theoretical half life predictions for the two-neutrino mode and experiment. However, there was no direct observation of the double beta decay. (J.F.P.)

32563 SPIN ASSIGNMENTS TO LEVELS IN ^{131}I. Devare, S. H.; Devare, H. G. (Tata Inst. of Fundamental

Research, Bombay). 4p. (CONF-651118-10). ORAU. Gmelin, AED-CONF-65-329-9.

From American Physical Society, Gatlinburg, Tenn.

Direction correlation measurements were made with the 30-hr activity of ^{131m}Te in order to make definite spin assignments to some of the well established levels of ^{131}I. The assigned spins for these energy levels are listed, and an energy level diagram showing the spins, parities, and half lives is given. (J.F.P.)

32564 γ-RAY SPECTROSCOPY OF SHORT HALF-LIFE ISOTOPES WITH A LITHIUM-DRIFTED GERMANIUM DETECTOR. Fettweis, P.; Vervier, J. (CEN-SCK, Mol, Belg.). 10p. (CONF-650653-13). ORAU. Gmelin, AED-CONF-65-170-46.

From American Physical Society, Summer Meeting, New York.

The decay spectra of tantalum-182, isomeric indium-116, and vanadium-52 are found using a lithium-drifted germanium detector. The performance of this detector is described. Also the decay spectra of the three isotopes studied and the energy levels of isomeric tantalum-182, tin-116, and chromium-52 are given. (J.F.P.)

32565 STUDY OF LOW-LYING STATES OF ^{33}S. Becker, J. A.; Chase, L. F. Jr.; Fossan, D. B.; McDonald, R. E. (Lockheed Palo Alto Research Labs., Palo Alto, Calif.). 57p. (CONF-650927-27). ORAU. Gmelin, AED-CONF-65-222-58.

From American Physical Society, Honolulu, Hawaii.

The low-lying states of ^{33}S at 0.84-, 1.97-, 2.31-, 2.94- and 3.22-Mev were studied using the charged particle-gamma ray angular correlation method of Litherland and Ferguson. The ^{32}S(d,p)^{33}S reaction was used to populate the levels of ^{33}S, with an incident deuteron energy of 3.20 Mev. Charged particles were detected near 180° with respect to the incident beam direction using a solid-state annulus counter, and gamma radiation was detected in a 10.2 cm × 10.2 cm NaI(Tl) crystal at angles between 0 and 90° relative to the beam direction. Coincident data were stored in a 64- × 64-channel 2-parameter pulse-height analyzer. Gamma branching ratios are presented for the levels mentioned above, and also the 2.87-Mev level of ^{33}S. Spin assignments of $\frac{5}{2}$, $\frac{3}{2}$, $\frac{1}{2}$, and $(\frac{3}{2})$ were established for the levels of ^{33}S at 1.97-, 2.31-, 2.94- and 3.22-Mev, respectively, as well as a most probable assignment of positive parity for the 1.97-Mev level. Some gamma-ray mixing ratios are also presented. These results, combined with the results of previous investigations, lead to spin-parity assignments of $\frac{3}{2}^+$, $\frac{1}{2}^+$, $\frac{5}{2}^{(+)}$, $\frac{3}{2}^+$, and $\frac{7}{2}^-$ for the ^{33}S levels at 0-, 0.84-, 1.97-, 2.31-, and 2.94-Mev, and support the $J = \frac{3}{2}$ assignment to the 3.22-Mev level. (auth)

32566 NUCLEON ENERGY LEVELS IN A NONLOCAL POTENTIAL. Koshel, Richard D. (Ohio Univ., Athens). 11p. (CONF-641127-1). ORAU. Gmelin, AED-CONF-64-297-2.

From American Physical Society, Fall Meeting of the Ohio Section, Oxford, Ohio.

Percy and Buck have recently suggested a nonlocal potential model for the scattering of nucleons by nuclei. Their model has been very successful in the explanation of scattering data. This model is now extended to the bound state problem. A program was written for the IBM-1620 computer at Ohio University to calculate single particle energy levels for both nonlocal and local potentials. The results obtained for these two types of calculations are compared and discussed. In the calculations the potential form factor used is that of the Woods-Saxon form. A spin-orbit interaction of the usual Thomas type was used. (auth)

32567 STUDY OF THE LOW-LYING STATES OF ^{23}Na BY MEANS OF THE ^{26}Mg(p,αγ)^{23}Na REACTION. Poletti, A. R.; Start, D. F. H. (Oxford Univ.). 8p. (CONF-651118-17; BNL-10013). ORAU. Gmelin, AED-CONF-65-329-21.

From American Physical Society, Gatlinburg, Tenn.

The angular correlations between the α particles emitted at 180° in the ^{26}Mg(p,α)^{23}Na reaction and the coincident γ rays were used to study level spins and gamma multipole mixing ratios (x) in the nucleus ^{23}Na. The $J = \frac{5}{2}$ assignment to the first excited state was verified ($J = \frac{3}{2}$ was ruled out with a very high degree of probability). The mixing ratio for the 0.44-Mev ground state transition was measured as $x = (0.08 \pm 0.02)$. The 2.98-Mev level was shown to be $J = \frac{3}{2}$ with $x = 0.10 \pm 0.04$ or 2.70 ± 0.40 for the ground state transition. The 2.08-Mev level was found to be $J = \frac{7}{2}$, $x = 0.20 \pm 0.03$ although $J = \frac{3}{2}$ could not be rigorously eliminated. Isotropic distributions were obtained for all gamma rays from the 2.39-Mev level as well as for the ground-state decay of the 2.64-Mev level. The 2.71-Mev level was found to decay $(70 \pm 10)\%$ to the 0.44-Mev state and $(30 \pm 10)\%$ to the 2.08-Mev level. (auth)

32568 PROTON SPECTRA FROM d + d BREAKUP AT 25.3 Mev. van Oers, W. T. H.; Brockman, K. W. Jr. (Instituut voor Kernphysisch Onderzoek, Amsterdam). 17p. (CONF-641005-3). ORAU. Gmelin, AED-CONF-64-296-3.

From Correlation of Particles Emitted in Nuclear Reactions, Gatlinburg, Tenn.

Continuous proton spectra produced by deuteron bombardment of deuterium have been studied at an incident deuteron energy of 25.3 Mev. Proton spectra were obtained at 37 different laboratory angles in the range of 7–50 degrees. A (dE/dx)-E counter telescope in conjunction with a particle identification system provided the necessary separation between the pulses resulting from the various reaction products. The final results obtained after several background corrections are represented in the center of mass system as energy spectra for a chosen set of angles between 15 and 80 degrees. The small angle spectra show a behavior similar to the zero degree neutron spectrum measured recently at an energy of 18.6 Mev. The spectra give evidence for the formation of pairs of particles in the final state having nonzero relative angular momenta. For increasing angle the spectra become more and more flat. The angular distribution obtained by integrating the energy spectra shows strong forward peaking. Subsequent integration of the angular distribution results in a proton yield of 340 ± 40 mb. (auth)

32569 EXCITATION OF THE SPIN-ISOSPIN GIANT RESONANCE BY 180 DEG INELASTIC ELECTRON SCATTERING. Lewis, Francis H. Jr. (Univ. of Washington, Seattle). 16p. (CONF-650653-14). ORAU. Gmelin, AED-CONF-65-170-47.

From American Physical Society, Summer Meeting, New York.

A very simple Goldhaber-Teller type of collective model is formulated to describe the spin-isospin giant resonance in nuclear matter. The model is used to calculate 180° electron scattering form factors and the results are compared with experiment for ^{12}C and ^{16}O. These results account qualitatively for the observed behavior of the giant resonance form factors as functions of q, although quantitative agreement with experiment is not completely obtained. Some consequences of these results are discussed. (auth)

Plasma Physics and Thermonuclear Processes

See *also* Fluid Physics and Thermodynamics

32570 (D-1-82-0522) THE EFFICIENT UTILIZATION OF AN RF POWER OSCILLATOR FOR PRODUCING LOW-PRESSURE PLASMAS. Kofoid, Melvin J. (Boeing Scientific Research Labs., Seattle, Wash. Plasma Physics Lab.). Apr. 1966. 22p.

In an ordinary arrangement for high-frequency plasma heating a discharge tube is placed inside an r-f coil, as in the analogous case of the induction heating of metals, and the coil is simply connected to a standard power oscillator. If a low-pressure plasma is to be produced, i.e., in gas at 0.1–500 microns pressure, the energy transferred to the plasma then will be only a small fraction of the genera-

tor capacity, because of the low power factor of the load. Simple expedients are described which result in the attainment of a much increased r-f magnetic flux density in the discharge tube. The resulting increase in the plasma conductivity, hence in the load power factor, is sufficient to effect high and efficient loading. The discussion centers around the use of a 15 kW 450 kc/sec oscillator for plasma research studies. The usefulness of the generator is considerably increased by electronic control which allows times of operation as brief as 0.05 sec. Short-time operation and low average loading permit the exceeding of normal oscillator current limits to obtain high r-f fields for starting and maintaining low pressure plasmas — extending the possible range of operation. Comprehensive performance data are presented. (auth)

32571 (IPP-1/2) INDUKTIONSSPULEN ALS MESSELEMENTE AN SCHNELLEN, STROMSTARKEN GASENTLADUNGEN. (Induction Coil as a Measuring Element in Fast Current Intensity Gas Discharge). Koeppendoerfer, W. (Institut fuer Plasmaphysik, G.m.b.H., Garching (West Germany)). Nov. 1, 1961. 24p. Dep. mn.

The equations describing the dimensions and characteristics of an induction coil used as a measuring element in fast high current gas discharges are derived. The Rogovski coil is considered and the magnetic field probe is given. The characteristics of the measurement circuit are derived. The shielding necessary and the calibration of a measurement coil are considered. (tr-auth)

32572 (IPP-6/49) MIKROSKOPISCHE PLASMABESCHREIBUNG UND NICHTLINEARE INKOHAERENTE LICHTSTREUUNG. (Microscopic Description of Plasma and Nonlinear Incoherent Light Scattering). Salat, A. (Institut fuer Plasmaphysik, G.m.b.H., Garching (West Germany)). Mar. 1966. 76p. Dep. mn.

The plasma density is given as a sum of delta functions in 6-dimensional configuration space. From the division of the density into an ensemble average and fluctuations about it, and the equations of motion there results an exact system of equations for these quantities. The equations are expanded up to the first order in the plasma parameter and are suitable for calculations of fluctuations and correlations in plasmas. The equivalence to a generalized dressed particle model is shown without explicit calculations. The relations between the distribution about a test particle, which can be found by the Vlasov equation, and the two-particle correlation function found by Rostoker are generalized to arbitrary initial correlations. It is shown that for stable plasmas the influence of physically reasonable initial conditions on the two-particle correlations vanishes for large times. The equations derived are used to calculate the nonlinear incoherent scattered light produced by two electromagnetic waves on thermal fluctuations. The plasma may have different electron and ion temperatures. The spectrum of the scattered light consists of the linear combinations of the incident frequencies broadened by Doppler effects, generally according to thermal electron density fluctuations. When the difference frequency approaches the plasma frequency the intensity of the scattered light increases and the spectrum is given by the ion density fluctuations. (auth)

32573 (N-65-12780) HALL CURRENT PLASMA ACCELERATOR WITH COUPLED NON-EQUILIBRIUM IONIZATION AT ELEVATED ELECTRON TEMPERATURES. PART I. THEORY AND GOVERNING EQUATIONS. Hoffert, Martin I. (Polytechnic Inst. of Brooklyn, N. Y. Dept. of Aerospace Engineering and Applied Mechanics). Oct. 1964. 26p. (PIBAL-860).

An analytical framework is summarized for the investigation of MGD acceleration by induced Hall currents. Numerical results are given in subsequent reports and utilized to design the experimental phase of this research. Since the mechanism of $j_\theta B_r$ accelerating forces was established experimentally using high temperature arcjets as the plasma source, emphasis is placed on relatively cool working fluids where nonequilibrium ionization due to elevated electron temperatures may be a factor. The analytical model of Kerrebrock for this process is incorporated in the analysis. (auth)

32574 (N-65-32035) THE DESIGN AND DEVELOPMENT OF ROGOWSKI COIL PROBES FOR MEASUREMENT OF CURRENT DENSITY DISTRIBUTION IN A PLASMA PINCH. Wright, Edward S. (Princeton Univ., N. J. Guggenheim Labs. for the Aerospace Propulsion Sciences). June 1965. 36p. (NASA-CR-64582). CFSTI $2.00 cy, $0.50 mn.

Small toroidal Rogowski coil probes were constructed to measure directly the current density distributions in a large-radius plasma pinch discharge. When properly constructed, the emf induced in these coils is proportional to the current passing through the center hole of the toroid, irrespective of the details of its distribution. Current density distributions determined by these probes in discharges at various pressures in two different pinch chambers are found to coincide well with the results of detailed magnetic probe mapping over the major portions of the profiles. In particular, current rise and position of current maxima are practically identical, whereas greater variance is noted in current sheet widths, and in measurements close to the chamber wall. On the basis of these results, further use of the Rogowski coil probe for plasma diagnostics seems indicated. (STAR)

32575 (NASA-TN-D-3372) LIMITS OF VALIDITY OF RADIATIONLESS DECAY OF HIGH-DENSITY PLASMAS. Stankiewicz, Norbert (National Aeronautics and Space Administration, Cleveland, Ohio. Lewis Research Center). June 1966. 25p. CFSTI $0.35 cy, $0.50 mn.

The recombinative decay of collision-dominated plasma is investigated theoretically, and the limit of validity of such radiationless models is determined. The density range considered conforms to those plasma densities usually encountered in the analysis of a magnetohydrodynamic generator. The results indicate that neglecting radiative processes may not always be justified at these densities. It is concluded that the radiationless model is valid for argon when the electron density is greater than 6.8×10^{15} per cubic centimeter and for cesium when it is greater than 1.1×10^{15} per cubic centimeter. (auth)

32576 (NYO-1480-50) THE GUIDING CENTER PLASMA. Grad, Harold (Courant Inst. of Mathematical Sciences, New York Univ., N. Y.). Mar. 15, 1966. Contract AT(30-1)-1480. 159p. (MF-48; CONF-650440-4). Dep. mn. CFSTI $5.00 cy, $1.00 mn.

From American Mathematical Society, 622nd Meeting, New York.

A survey is given of the theory of equilibrium, motion, and stability of a plasma in the guiding center limit. (auth)

32577 (NYO-1480-54) STEADY NONLINEAR WAVES IN A WARM COLLISION-FREE PLASMA. Kever, H.; Morikawa, G. K. (Courant Inst. of Mathematical Sciences, New York Univ., N. Y.). Apr. 1, 1966. Contract AT(30-1)-1480. 37p. (MF-50). Dep. mn. CFSTI $2.00 cy, $0.50 mn.

The speed and structure of steady nonlinear waves moving with uniform velocity in an oblique direction across a magnetic field in a collision-free plasma with temperature are described. This is a self-consistent formulation in which the plasma motion is governed by the Vlasov equations for ions and electrons coupled to the Poisson-Maxwell equations. This difficult problem can be solved in the limiting case of small-amplitude nonlinear waves if one assumes that the same scaling laws hold for the warm plasma as those for a cold plasma. (auth)

32578 (TID-23025) REPORT ON BAGEL II PROGRESS. Status Report No. 14, August 1, 1965-April 30, 1966. Buneman, O. (Stanford Univ., Calif. Inst. for Plasma Research). Apr. 1966. Contract AT(04-3)-326. 17p. Dep. mn. CFSTI $1.00 cy, $0.50 mn.

In a pulsed-toroidal discharge the observed drift and diffusion rates in a uniform magnetic field of several hundred gauss and densities ~10^{13} were reduced using the

bumpy torus principle. Further, by examining the discharge during continuous operation (but at a density ~10^{10} – 10^{11}) a flute instability with k = 0 was found and suppressed in the bumpy field. The suppression of the instability is believed to cause the lowered diffusion rate. The role of the flute instability in the particle loss mechanism, described qualitatively, should be put on a firmer experimental basis by extensive quantitative analysis. (auth)

32579 SUB-THRESHOLD STUDY OF THE AZIMUTHAL MODES OF THE KADOMTSEV PLASMA INSTABILITY. Huchital, D. A.; Holt, E. H. (Rensselaer Polytechnic Inst., Troy, N. Y.). Appl. Phys. Lett., 8: 321-2(June 15, 1966).

A sub-threshold experiment was performed on a helium positive column in a longitudinal magnetic field at a pressure of 0.38 torr in order to study the helical modes of the Kadomtsev instability. The sub-threshold response spectra of a helium positive column are shown at a pressure of 0.38 torr, and as a function of the applied transverse magnetic field. Experimental confirmation was found for the theoretical prediction that a switch from the m = 1 to the m = 2 mode will occur when a suitable increase is made in the strength of the transverse magnetic field applied to a positive-column plasma immersed in a strong longitudinal magnetic field. (J.F.P.)

32580 DIFFRACTION BY A CONDUCTING HALF-PLANE IN PLASMA. Chambers, Ll. G. (Univ. Coll. of North Wales, Bangor, Eng.). Can. J. Phys., 44: 1207-12 (June 1966).

The problem considered is that of a plane electromagnetic wave approaching from an arbitrary direction a perfectly conducting half-plane in an anisotropic plasma, characterized by a permittivity tensor. The system is such that the wave has a single magnetic field component, which is parallel both to the magnetostatic field and the diffracting edge. The work is a simplification of previous work by Jull, involving the use of methods previously developed by the author. (auth)

32581 MEASUREMENTS OF ANISOTROPIC PLASMAS USING A TURNSTILE MULTIPLE-PROBE POLARIMETER. Bachynski, M. P.; Osborne, F. J. F.; Gibbs, B. W. (RCA Victor Research Labs., Montreal). Can. J. Phys., 44: 1649-62(July 1966).

A turnstile multiple-probe polarimeter has been designed for plasma diagnostics at microwave frequencies. With the polarimeter, it is possible to measure simultaneously the amplitude and phase of the space quadrature components of an electromagnetic wave of arbitrary polarization. This technique is thus well suited for determining the properties of time-varying or steady-state anisotropic plasma. Measurements have been conducted at a frequency of 9.2 Gc on a helium afterglow in a magnetic field, using both linearly polarized and circularly polarized incident plane waves. The agreement of these experiments with theory indicates that the multiple-probe polarimeter can be a reliable tool for plasma measurements. (auth)

32582 TEMPORARY CAPTURE OF CHARGED PARTICLES IN A STATIC MAGNETIC BOTTLE. Hubert, Pierre; Touche, Jacques (EURATOM-CEA, Fontenay-aux-Roses, France). Compt. Rend., Ser. B, 262: 1069-71(Apr. 18, 1966). (In French).

Theoretical arguments and experimental results are presented in favor of a temporary capture which associates the properties of resonant perturbations with the properties of a Stormer potential neck. The efficiency of the procedure appears superior to that of the resonant method alone and also to that of the stochastic capture. The experiments made it possible to attain a capture corresponding to 360 transitions on an average for the totality of an electron beam. (tr-auth)

32583 CALCULATION OF THE STATISTICAL ENTROPY OF A PLASMA DURING EQUILIBRIUM. Laval, Guy; Pellat, Rene; Vuillemin, Michel (EURATOM-CEA, Fontenay-aux-Roses, France). Compt. Rend., Ser. B, 262: 1129-32(Apr. 25, 1966). (In French).

The statistical entropy of a plasma during equilibrium was calculated by assuming that the binary correlations remain small and by neglecting the correlations of higher order. At the lowest order an expression is obtained that is an approximate first integral of the two primary equations of the Born-Bogoliubov-Green-Kirkwood-Yvon recurrence. If the plasma is spatially homogeneous, an H theorem can be deduced that makes it possible to study the irreversible evolution of the simple density in situations where the Balescu-Lenard equation is not valid. (tr-auth)

32584 NONLINEAR EFFECTS IN A HOMOGENEOUS LORENTZ PLASMA: CALCULATION OF THE ANISOTROPIES AS A FUNCTION OF THE ELECTRON DISTRIBUTION. Jancel, Raymond (Institut Henri Poincare, Paris). Compt. Rend., Ser. B, 262: 1192-4(May 2, 1966). (In French).

The system of coupled differential equations obtained by developing the electron distribution functions of a Lorentz plasma in an irreducible tensor was considered. This system is decoupled by developing according to the powers of a small parameter characterizing the nonlinearity of the plasma, and the method is applied to the case of a plasma in the presence of a static field. (tr-auth)

32585 DETERMINATION OF THE DENSITY AND DIAMETER OF A PLASMA COLUMN BY THE DIFFRACTION OF AN ELECTROMAGNETIC WAVE. Faugeras, Paul-Etienne (EURATOM-CEA, Fontenau-aux-Roses, France). Compt. Rend., Ser. B, 262: 1195-8(May 2, 1966). (In French).

The electromagnetic wave diffracted by a cylinder of inhomogeneous plasma lighted by a plane wave with normal incidence was calculated numerically. The field diffracted in the direction of the incident field is given for two electron density profiles. It is then shown the fashion in which this diffracted field can be measured and how the density and diameter of the plasma column can be deduced. (tr-auth)

32586 DEUTERIUM–TRITIUM REACTIONS IN A MIXED-PLASMA ACCELERATOR. Bardet, Rene, Consoli, Terenzio; Consolino, Jean; Geller, Richard; Gormezano, Claude; Jacquot, Bernard (Centre d'Etudes Nucleaires, Saclay, France). Compt. Rend., Ser. B, 262: 1325-8 (May 16, 1966).

The reaction of a mixed plasma, composed of electrons and D^+ ions, with a tritiated titanium target was investigated for deuteron energies above 30 kev. The accelerator device consisted of mixed static-magnetic and h-f fields. The alpha particles, resulting from the nuclear reactions of the plasma with the target, were studied as a function of the ion current and of the D^+ ion energy. (G.O.Y)

32587 PLASMA PHYSICS AND ITS APPLICATIONS. Hoyaux, Max F. (Carnegie Inst. of Tech., Pittsburgh). Contemp. Phys., 7: 241-60(Apr. 1966).

The nature of plasma (which is becoming more and more to be considered as a fourth state of matter) is dealt with, its methods of generation, the sometimes paradoxical motion of the charge carriers in a vacuum and in a gas, the conditions in which a strongly or fully ionized plasma can be confined by magnetic fields (the so-called "magnetic bottle"). The main types of plasma waves are described, and some major applications, both industrial and astrophysical are described. (auth)

32588 INCIDENCE OF ELECTROMAGNETIC WAVES ON A PLASMA-VACUUM BOUNDARY. Kopecky, V.; Petrzilka, V. A. (Inst. of Plasma Physics, Prague). Czech. J. Phys., 16: 463-7(1966).

An electromagnetic wave polarized in a plane normal to the magnetostatic field, parallel to the plasma boundary, falls from a vacuum on a half-space filled with magnetoactive plasma and bounded by a wall. The coefficient of wave reflection is computed for plasmas with $\omega_0^2/\omega_H^2 \ll 1$. (auth)

32589 DENSITY WAKE OF A CHARGED PARTICLE MOVING THROUGH A PLASMA. Majumdar, Saroj K. (Saha Inst. of Nuclear Physics, Calcutta). Indian J. Phys., 39: 562-8(Dec. 1965).

A method developed previously was applied to investigate

the density wake created by a moving test particle in the plasma. These wakes are analyzed separately for different harmonics of the cyclotron frequency, and for small velocity perpendicular to the applied magnetic field. It is shown that only the first few harmonics are important to develop the wake in the plasma. (auth)

32590 ELECTRO-ACOUSTIC LATERAL WAVES IN A HOT PLASMA. Samaddar, S. N. (Raytheon Co., Sudbury, Mass.). Int. J. Electron., 20: 93-107(Feb. 1966).

The possibility of excitation of lateral waves in a compressible plasma in contact with conducting boundaries is considered. The investigation demonstrates the existence of a peculiar type of lateral wave which travels a certain distance along the conducting surface with the phase velocity of light in a cold plasma and is then reflected back at the critical angle into the compressible plasma in which the wave propagates with the phase velocity of acoustic waves. These electro-acoustic lateral waves are the contribution to the pressure-field integral from the integration around the branch cut which depends on both the velocity of light and the adiabatic sound velocity in plasma-electrons. (auth)

32591 SOME ASPECTS OF WAVE PROPAGATION AND THE EFFECT OF THE BOUNDARIES AND EXCITATIONS ON THE ELECTRO-ACOUSTIC SPECTRUM IN AN ISOTROPIC COMPRESSIBLE PLASMA. Yildiz, Musa (Stevens Inst. of Tech., Hoboken, N. J.). Int. J. Electron., 20: 157-85(Feb. 1966).

Wave phenomena, due to various types of excitations involving cylindrically stratified regions, are examined by using scalar Green's function formulation. The general expressions for monochromatic electromagnetic field and density deviations from equilibrium ($\eta_{e,i}$ possesses an anisotropy which disappears when the effect of ion motion is neglected), due to an electric dipole immersed in a two-fluid compressible plasma cylinder in the absence of magnetostatic field, are derived. The optical and radar observables during re-entry and the effect of the ionized local environment upon communication with a re-entering vehicle are examples of the prescribed various excitations. The appropriate Debye shielding, the dielectric fluctuations, and the scattering cross section of an unbounded fluctuating, and thermally non-equilibrium plasma are investigated. The spectra, due to the oscillating static electric dipole and moving electron in the radially bounded one-fluid compressible plasma, are discussed explicitly pertaining to the two types of characteristic dampings. (auth)

32592 INVESTIGATION OF A PLASMATRON WITH AN INTERELECTRODE INSERT. Dautov, G. Yu.; Dudnikov, Yu. S.; Sazonov, M. I. (Inst. of Theoretical and Applied Mechanics, Novosibirsk, USSR). Izv. Sibirsk. Otd. Akad. Nauk SSSR, No. 10, Ser. Tekh. Nauk, No. 3, 56-62(1965). (In Russian).

Results are reported of an experimental investigation of a plasmatron (plasma jet) in which cold air pumped into the gap between the insert and the output electrode was used as an insulator; as the effect of a single insert was found to be inadequate, a multiple insert was tried with mica insulation. The arc current-voltage characteristics and the air-enthalpy increase curve are presented, as well as a current-voltage characteristic of the nonselfmaintaining discharge between the positive column and the 4th insert. It is found that: The interelectrode insert permits considerable increase in the arc length, arc voltage drop, and gas temperature; it provides a method for obtaining an ascending characteristic and for eliminating arc shunting; The inserts connected to the power supply through isolating switches provide an additional possibility of adjusting the arc operation "on the run," with no adjustable power supply needed; Gas supply distributed along the channel may provide an additional opportunity for improving arc characteristics. (ATD)

32593 SOME CHARACTERISTICS OF VAPORIZATION OF A MATERIAL FROM THE SURFACE OF A PROBE IN AN ARC. Turko, M. N.; Korshakevich, I. I. (Inst. of Physics, Krasnoyarsk, USSR). Izv. Sibirsk. Otd. Akad. Nauk SSSR, No. 10, Ser. Tekh. Nauk, No. 3, 63-70(1965). (In Russian).

Atoms are introduced into the plasma of an arc by vaporizing a material from the surface of a probe in an attempt to find methods for converting atoms from the solid to the gaseous phase while controlling the quantity of evaporated material without changing the conditions for excitation of the atoms and in this way to determine the basic characteristics of the vaporization process. A half-wave a-c arc was generated with a current amplitude of 7 a in 5-msec intervals with a prf of 12.5 cps. The copper electrodes were held 3 mm apart. The spectra were photographed on high-speed film and the intensity of the spectral lines was measured by ordinary photometric methods. The probe was a wire 0.2-0.4 mm in diameter. Two types of probes were used: cylindrical probes which intersected the arc throughout its entire cross section, and point probes in which the working surface was an area of approximately 0.3 mm^2, the remaining portion of the wire being protected by an insulating covering of molybdenum glass. The material to be evaporated was either coated on the surface of the probe by electrolysis (iron, cadmium, tin, and zinc) or was the material of the probe itself (nichrome, platinum, rhodium, palladium). A schematic diagram of the electric circuit for the experimental setup is given. The evaporation of the material from the surface of the probe was determined by the potential of the probe with respect to the electrode. Curves are given showing the intensity of spectral lines for various substances as a function of probe current density. These curves are parabolic for the lines of nickel, rhodium, platinum, and palladium with a slight distortion at high current densities. The relation is considerably less pronounced for lines of iron, cadmium and tin. A formula is derived for the energy liberated at the probe by the stream of electrons in terms of the time for the current pulse. Calculations show that this energy varies from 0.7 to 95 joules/cm^2. For most of the materials studied, this energy was 4.6 ± 0.7 joules/cm^2 at a capacitance of 58 μf and a voltage of 50 v. The intensity of the lines either increases at a slower rate than the energy (Cd, Sn, Fe, Ni), or surpasses the energy (Pd, Rh, Pt). The proposed method for controlled vaporization of a material from the surface of a probe expands the possibilities for studying processes which take place on electrodes in an arc plasma and may be used in theory for other forms of discharges. (ATD)

32594 CALCULATION OF THE SOURCE FUNCTION FOR AN OPTICALLY DENSE PLASMA LAYER. Preobrazhenskii, N. G.; Senina, A. V.; Senina, S. V. (Kuznetsov Physicotechnical Inst., Siberian SSR). Izv. Vyssh. Ucheb. Zaved., Fiz., No. 6, 67-74(1965). (In Russian).

The problem of finding the source function of an inhomogeneous optically dense plasma is examined using the Ritz method. The dependence of the source function on the frequency and optical thickness of the layer and the accuracy of the variational procedure are analyzed. (M.J.T.)

32595 CONTRIBUTION TO THE THEORY OF A POSITIVE COLUMN OF A GLOW DISCHARGE IN THE PRESENCE OF A SMALL IMPURITY. Pekar, Yu. A. (Tula Polytechnic Inst., USSR). Izv. Vyssh. Ucheb. Zaved., Fiz., No. 6, 167-8(1965). (In Russian).

The influence of nonlinearities in the number of electrons produced by impurities in a positive column on the behavior of the electron temperature, the longitudinal field, and other parameters of discharge in the diffusion mode is investigated. The Schottky boundary-value condition, the equation of electric conductivity, the equation for the power balance of the electrons, and the equation for the conservation of the number of impurity particles are used to derive a system of parametric equations for determining the field, electron temperature, particle densities, and average current density. The results show that the electron temperature and the longitudinal field increase monotonically with the current density and that the number of neutral particles decreases monotonically. It is concluded that the effect of the impurity decreases with increasing current density, when the discharge parameters approach values characteristic of those of the main gas. At relatively low

currents, the composition plays a more important role, and the volt-ampere characteristic can be either positive, negative, or possess a maximum. (ATD)

32596 COMPUTATION OF ELECTROSTATIC AND RAPIDLY PULSED MAGNETIC FIELDS. Lewis, H. R. Jr. (Los Alamos Scientific Lab., N. Mex.). J. Appl. Phys., 37: 2541-50(June 1966). (LA-DC-7460).

It is often required, for example, in the design of some pulsed controlled-thermonuclear-fusion experiments, to calculate electrostatic fields and to calculate magnetic fields in the approximation that flux does not penetrate metal boundaries of the experimental volume. Computation of such magnetic and electric fields by means of the standard relaxation methods is often difficult and very costly, even with high-speed computers. This is because the boundaries of the region of experimental interest are rather arbitrary and because there are generally current- or charge-carrying conductors within the region that make it nonsimply connected. An alternative method of solving the boundary value problems that determine these electric and magnetic fields, which does not involve a difference approximation to the differential equations, was developed. With this method, an exact analytic solution of the appropriate differential equation is obtained in the region of interest, and this solution is made to approximate the boundary conditions. The method and its application are described in detail. Examples of the application of the method to some controlled-thermonuclear-fusion experiments are given. (auth)

32597 PROBE MEASUREMENTS IN A PULSED PLASMA: EXPERIMENTAL VERIFICATION OF THE BBM ANALYSIS FOR ION SATURATION CURRENT. Hosea, J. C. (Stanford Univ., Calif.). J. Appl. Phys., 37: 2695-2702(June 1966).

A technique of probe measurement is given which allows an easy determination of Langmuir probe curves in a reproducible pulsed plasma. The technique is then used to study a pulsed P.I.G. reflex discharge. Experimental probe curves are analyzed with a theory based on the BBM formula for ion saturation current. Comparison of probe measurements of electron density with the measurements of an 8.5-mm interferometer shows that the probe behavior is properly described by the Langmuir–BBM (Bohm, Burhop, Massey) theory. Also as predicted theoretically, the experimental ratio of floating potential to electron temperature is shown to be reasonably constant over wide variations in plasma parameters. (auth)

32598 PLASMA DIAGNOSTICS USING LASERS: RELATIONS BETWEEN SCATTERED SPECTRUM AND ELECTRON-VELOCITY DISTRIBUTION. Brown, Terrence S.; Rose, D. J. (Massachusetts Inst. of Tech., Cambridge). J. Appl. Phys., 37: 2709-14(June 1966).

Laser light scattered from plasma electrons can be used to determine the electron density and velocity distribution. The process is classical Thomson scattering, and the scattered spectum is constructed of the Doppler shifts of the electrons. The spectrum I(k), which appears at all angles and over a range of wave-numbers, is uniquely related to the electron velocity distribution f(v). Either can be obtained from the other, and the expressions $I(k) = Lf(v)$ and $f(v) = L^{-1}(k)$ are derived relativistically correctly. The amount of information about f(v) obtainable from a simple measurement of the scattered spectrum is also discussed. The electron density and mean speed can be measured easily; more subtle features depend upon accurate observation of the low-intensity wings of the spectrum. (auth)

32599 PLASMA DIAGNOSTICS BY THOMSON SCATTERING OF A LASER BEAM. Gerry, Edward T.; Rose, D. J. (Massachusetts Inst. of Tech., Cambridge). Contract AT(30-1)-3285. J. Appl. Phys., 37: 2715-24(June 1966).

The use of Thomson scattering of a laser beam as a diagnostic technique for laboratory plasmas is discussed. Several potential sources of difficulty in the use of this technique are investigated. Included are simple signal-to-noise considerations based upon photon counting statistics and noise due to plasma radiation, Rayleigh or Raman scattering from neutral particles in the plasma, and scattering from walls, apertures, etc., in the apparatus. Also discussed are other effects which may affect the state of the plasma being measured, namely, free–free absorption which leads to electron heating and free–bound absorption or photo-ionization which can produce additional electrons. Experimental determinations of electron density and temperature in a steady-state hollow-cathode arc plasma, by Thomson scattering of a ruby laser beam, are reported and discussed. These measurements refer primarily to argon plasmas over an electron density range $10^{13}-10^{14}$ cm^{-3} and electron temperature range 3–8 ev. Essential agreement of these measurements with measurements of the same quantities by Langmuir probes is obtained, except for some interesting explainable differences. (auth)

32600 COMBINED ANODE-CATHODE FEED OF A HOLLOW-CATHODE ARC. Gerry, E. T.; Rose, D. J. (Massachusetts Inst. of Tech., Cambridge). Contract AT(30-1)-3285. J. Appl. Phys., 37: 2725-6(June 1966).

A simple method is given for separating the anode and cathode regions of a hollow-cathode-arc plasma by a baffle and introducing a small gas feed through the hollow anode. By this stratagem, the anode-region plasma can be tailored within wide limits for ion species and density, and degree of ionization. For example, a 95% pure hydrogen plasma with ion density $10^{13}-10^{14}$ cm^{-3}, 90% ionized, can be produced at low voltage, with the cathode running under ideal conditions in argon. (auth)

32601 PROPAGATION OF LOW-FREQUENCY WAVES IN AN INHOMOGENEOUS PLASMA COLUMN. Tanaka, Masatoshi (Japan Atomic Energy Research Inst., Tokyo). Jap. J. Appl. Phys., 5: 547-53(June 1966).

Propagation of low-frequency waves in a magnetized inhomogeneous plasma cylinder surrounded by a vacuum or a metallic surface is investigated. An orthogonality relation between the modes of a uniform plasma column provides a basis for the derivation of a normal mode expansion. By making use of this expansion a perturbation method is applied to estimate the effect of inhomogeneities of the system. Perturbed dispersion curves of a waveguide filled plasma of a parabolic density distribution are given. It is shown that inhomogeneities of the plasma have little effect on the shear mode propagation. (auth)

32602 DIFFUSION OF METASTABLE HELIUM ATOMS IN A CRYOGENIC PLASMA. Fugol', I. Ya.; Pakhomov, P. L. (Physico-Technical Inst. of Low Temperatures, Academy of Sciences, Ukrainian SSR). JETP Lett. (USSR) (Engl. Transl.), 3: 254-6(May 15, 1966).

Translated from Zh. Eksp. Teor. Fiz., Pis'ma Redakt., 3: 389-94(May 15, 1966).

The rate of diffusion disintegration of metastable helium atoms in a decaying helium plasma at a temperature lower than 6°K was investigated. The helium plasma was excited in a quartz cylindrical cuvette immersed in liquid helium at 4.2 and 1.8°K. The excitation was by an electrodeless method with pulses from a high-frequency discharge of 0.08 msec duration reported every 40 msec. The concentration of the metastable helium atoms in the state 2^3S_1 was determined from the resonance absorption of the 3889 Å line from an external source. (M.H.R.)

32603 WAVE PROPAGATION IN RAREFIED PLASMA UNDER THE ACTION OF THE CORIOLIS FORCE. Tandon, J. N. (Univ. of Delhi); Bajaj, N. K. Mon. Notic. Roy. Astron. Soc., 132: 285-304(1966).

The propagation of waves in a rarefied plasma under the action of Coriolis force, Hall current, and self-gravitation was studied. For propagation along the external magnetic field and rotation (both acting along the same direction) the plane Alfvén wave splits up into two circularly polarized waves, both magnetic field and the rotation contributing to the polarization. In addition there exists a gravitational mode of propagation, independent of magnetic field and rotation. An analog of Jeans's (1929) condition for the fragmentation of interstellar cloud was obtained. Trans-

verse to external magnetic field and rotation there are three modes (electromagnetic, electron-sound and ion-sound modes) for wave propagation which are coupled with each other at low frequencies, the strength of their coupling being dependent on the magnitude of Coriolis force and the magnetic field. Further, rotation restricts the propagation of these modes below a certain critical frequency. In the high frequency limit the three modes are pure and their phase velocities are independent of rotation as well as magnetic field. (auth)

32604 HIGH-FIELD STEADY-STATE SHOCK WAVE IN A PLASMA. Frisch, H. L.; Morrison, J. A. (Bell Telephone Labs., Murray Hill, N. J.). Phys. Fluids, 9: 1053-64(June 1966).

The high magnetic field limit, of a shock wave in a steady-state model plasma moving along the x axis, is studied transverse to the magnetic field, in which the only spatial dependence is that on the x coordinate. The collisions of the model plasma are described by (Krook-type) modified Boltzmann collision terms with constant relaxation times. What occurs is that drift velocity of both electrons and ions behind the transition is converted to an increase in temperature of both species ahead of the transition through ion momentum exchange resulting in Joule heating. First formulation of the equations describing this phenomenon is presented, and then an exact asymptotic development of the integrodifferential transport equations, together with the Maxwell equations and subsidiary conditions. It is shown analytically, in the case for which the relaxation times of the ions and electrons are equal, that a shock wave is possible, provided the plasma is sufficiently dense, which means that the shock is bounded away from the low-temperature plasma limit. The case in which the relaxation times are unequal reduces to the investigation of a nonlinear ordinary differential equation which is not carried out here, but it is conjectured that a shock wave is still possible. (auth)

32605 PREKINETIC EQUATIONS FOR A PLASMA. Oezizmir, Ercuement; Imre, Kaya (Cekmece Nuclear Research and Training Center, Istanbul). Phys. Fluids, 9: 1065-72(June 1966).

Bogoliubov theory for a multicomponent plasma is generalized through relaxation of his assumptions regarding the functional dependence and the initial condition to obtain a theory within which the approach to the kinetic regime can be studied. It is assumed that the correlations $G_l (l > s)$ are functionals of $G_1, \ldots, G_s$ and $e^{\tau\mathcal{H}}G_1(e^{-\tau\mathcal{H}}G_1, \ldots, e^{-\tau\mathcal{H}}G_s) \to 0$ as $\tau \to \infty$, where $\mathcal{H}$ is the Poisson bracket operator corresponding to the kinetic energy and $s(\geq 1)$ is a fixed but otherwise arbitrary integer. It is shown that the analytic solution of the resulting functional chain with respect to the parameters $\alpha = n\lambda^{1/s}$, $\beta = \lambda^{1/s}$ (where n is the density and λ is the interaction strength) is of order β^{l-s} provided $G_1, \ldots, G_s$ are of order β^0. This property enables one to break the hierarchy in the expansion with respect to β only. The time and length scales for which the treatment is valid for a given s are discussed. The case s = 2 which leads to the prekinetic equations is considered in some detail. The closed coupled set of equations for G_1 and G_2 obtained in this case differ from those studied in the literature through appearance of the double pair correlations in the equation for G_2, which makes the latter equation nonlinear. (auth)

32606 TRANSVERSE WAVES IN A RELATIVISTIC PLASMA. Lerche, I. (Univ. of Chicago). Phys. Fluids, 9: 1073-80(June 1966).

Linearized equations are set up to describe transverse waves in a relativistic plasma embedded in a magnetic field and in the presence of a nonrelativistic plasma. The waves are taken to propagate at right angles to the unperturbed field. Unstable waves are found to exist when the momentum distribution is taken to be of the cosmic ray type, but anisotropic. The instability exists only when relativistic particles are present and is a consequence of the mass of a fast particle being different from its rest mass. The maximum amplification rate is found for this case and is illustrated numerically by assuming physical values appropriate to the case of galactic cosmic ray electrons. It is shown that any anisotropy is rapidly destroyed and for cosmic ray electrons which are more than about a million years old isotropy is to be expected. (auth)

32607 NONEXISTENCE OF LOOPING TRAJECTORIES IN HYDROMAGNETIC WAVES OF FINITE AMPLITUDE. Yeh, Tyan (California Inst. of Tech., Pasadena). Phys. Fluids, 9: 1081-3(June 1966).

It is shown that looping trajectories cannot exist in finite amplitude hydromagnetic waves propagating across a magnetic field in a quasi neutral cold collision-free plasma. (auth)

32608 STABILITY LIMITS FOR LONGITUDINAL WAVES IN ION BEAM-PLASMA INTERACTION. Fried, Burton D.; Wong, A. Y. (Univ. of California, Los Angeles. TRW Systems, Inc., Redondo Beach, Calif.). Phys. Fluids, 9: 1084-9(June 1966).

The two-stream instability is examined for the case of an ion beam traversing a plasma. The dispersion equation for linearized, longitudinal waves in a plasma where collisions are negligible is used to find the restrictions on beam velocity, temperature, and density which will lead to growing waves. (auth)

32609 ELECTRIC FIELD PARALLEL TO THE MAGNETIC FIELD IN A LOW-DENSITY PLASMA. Persson, Hans (Royal Inst. of Tech., Stockholm). Phys. Fluids, 9: 1090-8(June 1966).

Stationary states of a collisionless plasma in a one-dimensional magnetic mirror field are considered. Reflection and loss of particles in the presence of a parallel electric field are studied. In many cases the density can be expressed by Abelian integral transforms of monoenergetic distributions. The problem of determining the parallel electric field, necessary to maintain quasi neutrality, is solved for a class of such distributions, and a couple of illustrating examples are presented. A few existence and uniqueness theorems for distributions and fields are proved. (auth)

32610 COMPUTER STUDY OF THE DYNAMIC PHASE OF A SMALL θ PINCH. Dueches, D.; Griem, H. R. (Institut fuer Plasmaphysik, Garching, Ger.). Phys. Fluids, 9: 1099-1109(June 1966).

A three-fluid hydromagnetic computer accounting for hydrogen or deuterium atoms, ions, and electrons is modified to include ionization and excitation of carbon and oxygen impurity ions. Results are presented for energy losses from impurity radiation and are compared with macroscopic and thermal kinetic energies of ions and electrons and with magnetic field energies. Although radiation losses exceed kinetic plasma energies at typical impurity concentrations, electron temperatures are only slightly reduced up to first maximum compression. (auth)

32611 INCLINED END-PLATE EFFECTS IN THE Q DEVICES. Dimock, D. (Princeton Univ., N. J.). Phys. Fluids, 9: 1110-14(June 1966). (MATT-423).

A magnetically confined plasma is considered which is terminated on a conducting end plate having an electron sheath which reflects the ions. It is shown that inclining this plate to the magnetic field results in an ion drift and in an enhanced ion diffusion. The drift is evaluated from elementary plasma theory, and the diffusion is calculated in the limits of ion gyroradii large and small compared to the Debye length. Mechanisms which could eliminate the effects of the drift are discussed. The diffusion is shown to be generally much less than Bohm diffusion and, for typical alkali plasmas, to be of the order of classical diffusion at densities $\sim 10^{11}$ cm^{-3}. (auth)

32612 ANOMALOUS ELECTRON DIFFUSION AND ION ACCELERATION IN A LOW-DENSITY PLASMA. Janes, G. S.; Lowder, R. S. (Avco Everett Research Lab., Everett, Mass.). Phys. Fluids, 9: 1115-23(June 1966).

Ion and electron transport properties are measured in a steady state, weakly turbulent plasma that was subjected to cross E and B fields. The geometry permits quantitative measurements of electron and ion currents. The ion gyro radius is large compared to the apparatus dimensions. Measurements of the potential gradients, Hall currents, and ion velocity show that the ions are freely accelerated through the plasma by electrostatic forces. However, an anomalous diffusion of electrons is observed since the electron current across the magnetic field is much too large to be due to collisional diffusion. The plasma is weakly turbulent, consisting of a slowly rotating density concentration on which higher frequency fluctuations are superimposed. Electric field fluctuations are found that are correlated with the density variations so as to produce the anomalous diffusion via adiabatic E × B drifts. The magnitudes of these electric field and density variations are used to predict a net electron current that agrees with the direct measurements of this current. Reasonable agreement with the turbulent diffusion theory of Yoshikawa and Rose is obtained. (auth)

32613 FLUCTUATION SCATTERING AND ABSORPTION CROSS SECTION IN A SPACE DISPERSIVE PLASMA. **Macrakis, Michael S. (Harvard Univ., Cambridge, Mass.). Phys. Fluids, 9: 1124-33(June 1966).**

The fluctuation scattering and absorption cross section are derived for a space and time dispersive plasma. Fluctuations are introduced in Maxwell's equation describing a space–time dispersive plasma by considering the Boltzmann–Vlasov equations with an external field, and the cross sections are derived by evaluating the imaginary part of the correction to the transverse dielectric coefficient due to fluctuation scattering. The scattering cross section describes the total incoherent scattering from density fluctuations in the plasma while the absorption cross section describes the parametric interaction of an external propagating field with the internal excitations of the plasma. It is shown that when a collisionless plasma is pumped at twice the plasma frequency, the absorption cross section becomes very large. This suggests the possibility of increasing the energy content of the electron fluctuations near the plasma frequency. The pump acts to decrease the interaction between the free electrons and the collective plasma mode, a mechanism considered to account for Landau damping. (auth)

32614 STABILITY OF THE POISEUILLE PLASMA ARC IN AN AXIAL MAGNETIC FIELD. **Yuen, Man Chuen (Harvard Univ., Cambridge, Mass.). Phys. Fluids, 9: 1140-50(June 1966).**

The instability of the positive column of an atmospheric argon Poiseuille plasma arc in an axial magnetic field of the order of 100 G was studied both experimentally and theoretically. The instability was manifest as a helical oscillation of the conducting core. The neutral stability curves of frequency versus applied magnetic field for various arc currents and flow rates were obtained by studying the growth or decay of artificially created helical disturbances. The wavelengths of the helix at neutral stability were measured. The critical magnetic fields for the naturally excited oscillation were measured and found to be higher than that at neutral stability. A linearized stability analysis was developed. The theoretical results predict well the frequency and the shape of the neutral stability curves. From both the experiment and the theory, it was found that the destabilizing force is the J × B force and the stabilizing mechanisms are the viscous and the thermal effects. (auth)

32615 EXPERIMENTS IN A MAGNETICALLY DRIVEN SHOCK TUBE WITH AN AXIAL MAGNETIC FIELD. **Heywood, John B. (Massachusetts Inst. of Tech., Cambridge). Phys. Fluids, 9: 1150-7(June 1966).**

Experiments in a magnetically driven annular shock tube with hydrogen as test gas, with an axial magnetic field are reported. The initial pressure (50–500 μ), axial field (0–0.45 Wb/m^2), and drive field (0.8–1.0 Wb/m^2) were chosen to produce shock speeds and test times such that separation between shock front and current sheet was predicted. Measurements of magnetic and electric fields and intensity of continuum radiation showed that shock front and current sheet coincided both in the regimes where a gas-dynamic shock and a magnetohydrodynamic switch-on shock were predicted. Shock Alfvén Mach numbers covered the range 1.2 to 7.2. Axial and azimuthal momentum balances indicated that snowplow-type models adequately predict the shock tube performance. A radial electric field was measured upstream of the front when the Alfvén Mach number was in the switch-on regime, indicating that a model based on ionizing shock waves is more appropriate for predicting the flow pattern. (auth)

32616 LANDAU DAMPING IN INHOMOGENEOUS PLASMAS. **Jackson, E. A.; Raether, M. (Univ. of Illinois, Urbana). Phys. Fluids, 9: 1257-9(June 1966).**

Solutions of the Vlasov equation for a bounded, one-dimensional, inhomogeneous plasma are presented. The results indicate that the high-frequency modes of oscillation (Tonks–Dattner resonances) can exhibit a very large Landau damping even in the long-wavelength regime. (auth)

32617 ENERGY CHANGE OF A CHARGED PARTICLE MOVING IN A PLASMA. **Itikawa, Yukikazu; Aono, Osamu (Tokyo Univ.). Phys. Fluids, 9: 1259-61(June 1966).**

The energy loss rate of a charged particle moving in a plasma is calculated without any cutoff procedure. The result is applicable to any velocity of the test particle. (auth)

32618 PROPAGATION OF ION ACOUSTIC WAVES ALONG CYLINDRICAL PLASMA COLUMNS. **Wong, A. Y. (Univ. of California, Los Angeles). Phys. Fluids, 9: 1261-2(June 1966).**

A theoretical analysis shows the boundary effects on ion acoustic waves propagating along the magnetic field to be unimportant if the ion Larmor radius is much smaller than the plasma radius. Results are supported by experiments. (auth)

32619 PLASMA WAVES AT SINGULAR TURNING POINTS. **Gorman, D. (Oak Ridge National Lab., Tenn.). Phys. Fluids, 9: 1262-3(June 1966).**

Connection formulas at a singular turning point are presented for the WKB solutions to a biquadratic differential equation governing wave propagation in an inhomogeneous plasma. (auth)

32620 ION SURFACE WAVES. **Emeleus, K. G. (Queen's Univ., Belfast). Phys. Lett., 21: 633(July 1, 1966).**

Attention is called to a possible example of ion surface waves and to the likelihood that these contribute to the complex sub-megacycle noise spectrum of bounded low-pressure discharges in general. (auth)

32621 MEASUREMENTS OF THE ION AND ELECTRON TEMPERATURE IN A THETA-PINCH PLASMA BY FORWARD SCATTERING. **Kronast, B.; Roehr, H.; Glock, E.; Zwicker, H.; Fuenfer, E. (Institut fuer Plasmaphysik, Munich). Phys. Rev. Lett., 16: 1082-5(June 13, 1966).**

Spectrally resolved measurements of the electron and ion temperatures in a deuterium plasma produced by a theta pinch were performed using the forward scattering of a ruby laser beam. (D.C.W.)

32622 INCOHERENT SCATTERING OF MICROWAVES BY UNSTABLE ELECTRON PLASMA OSCILLATIONS. **Boehmer, H.; Raether, M. (Univ. of Illinois, Urbana). Phys. Rev. Lett., 16: 1145-7(June 20, 1966).**

The observation of incoherent scattering of microwaves by h-f oscillations resulting from a beam-plasma instability is reported. The received power versus the electron density is given, and an example of scattered power is shown as a function of the wave number of unstable waves in the direction of the electron beam. (J.F.P.)

32623 MINIMUM B AS A PLASMA STABILITY CRITERION. Grad, Harold (New York Univ., New York). Phys. Rev. Lett., 16: 1147-50(June 20, 1966).

A class of toroidal plasma equilibria with concentric flux surfaces in which a magnetic-field minimum can be continuously varied from the interior to the exterior of the plasma with no apparent alteration of its stability is described. (J.F.P.)

32624 APPARENT HIGH-FREQUENCY STABILITY OF A HIGHLY ANISOTROPIC PLASMA. Bell, P. R.; Dory, R. A.; Guest, G. E.; Kelley, G. G.; Lazar, N. H.; Lyon, J. F.; Stratton, R. F. (Oak Ridge National Lab., Tenn.). Phys. Rev. Lett., 16: 1152-3(June 20, 1966). (ORNL-P-2144).

The plasma produced in the DCX-2 by injecting 540-kev molecular protons and accumulating the dissociated 270-kev protons between magnetic mirror coils is studied. The distribution of charge-exchange particles is shown as a function of the pitch angle of the trapped proton in its helical trajectory, and the energy spectrum of the trapped protons is also shown. These particles form a highly anisotropic plasma which, after the injected beam is off, is stable against microinstabilities at ion cyclotron harmonics. (J.F.P.)

32625 WAVE PROPAGATION THROUGH AN EPSTEIN DENSITY PROFILE ACROSS AN INHOMOGENEOUS MAGNETIC FIELD. Sluijter, F. W.; Weenink, M. P. H. (FOM-Instituut voor Plasmafysica, Rijnhuizen, Netherlands). Physica, 32: 741-8(Apr. 1966).

The propagation of a plane monochromatic electromagnetic wave normally incident on a stratified plasma is considered. The stratification is of the transitional Epstein type, i.e., the density varies in space as a hyperbolic tangent. The static or slowly varying magnetic field is perpendicular to the density gradient. Only the extraordinary wave mode is considered here. The spatial dependence of the magnetic field is of the same type as that of the density, but the magnetic field is maximum where the density is zero and vice versa. The motion of the electrons is described by the ideal fluid equations. The ions are assumed to be infinitely heavy. The problem then leads to Heun's equation. In a special case it reduces to the hypergeometric equation. For this case the reflection and transmission coefficients are given explicitly. (auth)

32626 SELECTIVE RECEIVER OF ELECTROMAGNETIC RADIATION OF THE MILLIMETER AND SUBMILLIMETER RANGES. Gorokhov, N. A.; Dolgov-Savel'ev, G. G. (Moscow Inst. of Engineering and Physics). Prib. Tekh. Eksp., No. 1, 126-7(Jan.-Feb. 1966). (In Russian).

A device is described, intended for the study of microwave signals in the millimeter- and submillimeter-wavelength range. The device consists of a cooled receiver of radiations in this range and a Fabry-Perot-type frequency selector. The selector can be adjusted over a wide frequency range. (tr-auth)

32627 EXPONENTIALLY VARYING ELECTROMAGNETIC FIELDS IN A STRATIFIED MAGNETOPLASMA. Burman, R. (Victoria Univ., Wellington, New Zealand). Proc. IEEE (Inst. Elec. Electron. Eng.), 54: 888-9(June 1966).

The reflection of vertically polarized electromagnetic waves by a horizontally stratified magnetoplasma half-space is discussed. A certain choice is made of the profiles of the magnetoplasma for which the fields can be expressed in terms of simple exponential functions. (B.G.D.)

32628 IONIZATION IN HYDROGEN PLASMAS; COMPARISON OF TWO METHODS OF CALCULATION. Bruce, R. E.; Todd, F. C. (Oklahoma State Univ., Stillwater). Contract NASr-7. Proc. Okla. Acad. Sci., 45: 116-25 (1965).

An outline of the results obtained by methods for calculating the density of ionization in hydrogen plasmas is presented. Three methods are given for calculating the ionization density, and their relative merits are compared and discussed. The variation of the ionization with density is investigated for isotherm curves with energies of the particles of 2 and 5 ev, the results from the three methods are plotted, and the pressure-density relation for constant temperature is calculated. (Int. Aerospace Abstr.)

32629 STABILITY OF A UNIFORM PLASMA COMPOSED OF STREAMS IN THE ABSENCE OF AN EXTERNAL FIELD. Momota, Hiromu (Univ. of Nagoya, Japan). Progr. Theoret. Phys. (Kyoto), 35: 380-90(Mar. 1966).

By means of the collisionless Boltzmann equation and the Maxwell equations with no external field, it is shown that a plasma composed of streams is necessarily unstable for a transverse oscillation propagating perpendicularly to the streams. The instability is attributed to the bunching of the electric current density, corresponding to the bunching of the charge density in the usual two-stream instability which is accompanied by the excitation of a longitudinal oscillation. When the thermal motion of the particles in a stream is taken into account, the instability can be suppressed due to the thermal diffusion of the bunched current. For a transverse oscillation, the criterion of stability is obtained. (auth)

32630 EXCITATIONS OF CYCLOTRON HARMONIC WAVES PROPAGATING PERPENDICULAR TO AN EXTERNAL MAGNETIC FIELD. Momota, Hiromu; Terashima, Yoshinosuke (Nagoya Univ., Japan). Progr. Theoret. Phys. (Kyoto), 35: 754-5(Apr. 1966).

It is shown that the propagation of some waves exactly perpendicular to an external magnetic field exhibit instabilities at frequencies near the cyclotron harmonics. (B.G.D.)

32631 MEASUREMENT OF CURRENTS FLOWING THROUGH ELECTRODE IN CONTACT WITH PLASMA. Haegi, M. (EURATOM-CNEN, Rome). Rev. Sci. Instrum., 37: 850-1(July 1966).

Currents flowing through an electrode, in contact with a plasma, can be measured by inserting Rogowsky coils in the electrode itself. In order to avoid uncontrollable shunting of the current and damage of the coil owing to the plasma, a thin metallic foil is inserted between the coil and the plasma. The effects of such a screen on the measurements are calculated and compared with experimental results. (auth)

32632 WIDE BAND ELECTROSTATIC PROBES FOR USE IN TENUOUS PLASMAS. Sprott, J. C. (Univ. of Wisconsin, Madison). Rev. Sci. Instrum., 37: 897-900 (July 1966). (COO-1233-26).

A derivation is given for the resistance of the sheath surrounding a floating probe and the corresponding limitation to the frequency response. The bandwidth is increased by using probes with built-in attenuators which measure fluctuations in floating potential, electric field, and ion saturation current at frequencies up to 40 MHz with plasma densities as low as 10^9 cm^{-3}. (auth)

32633 CNR MHD PLANT AT THE ISTITUTO DI AERODINAMICA, NAPLES. Monti, Rodolfo; Murino, Pasquale; Barca, Lorenzo (Univ., Naples). Ric. Sci. Riv., 36: 301-6(Apr. 1966). (In Italian).

The MHD plant for plasma generation and control and the devices designed at the Istituto di Aerodinamica di Napoli for MHD energy conversion and plasma diagnostics are described. The results of some of the experiments performed and the program for future work are summarized. (auth)

32634 HIGH-FREQUENCY PLASMA IN A MAGNETIC FIELD. Gheorghe, Victor (Dept. of Physics, Bucharest). Studii Cercet. Fiz., 18: 243-52(1966). (In Rumanian).

While discharges under d-c conditions require hundreds of volts, high-frequency, a-c discharges may be initiated and kept in operation at voltages of the order of a few tens of volts. The presence of a constant, parallel or transversal field changes the discharge characteristics. This problem was investigated in high-frequency discharges in a constant magnetic field, applied in a direction parallel with the electric field. The equipment used in the experiments included

a condenser formed by 2 parallel circular plates and a 5.5-cm long and 3-cm diameter cylindrical discharge tube, placed between the poles of an electromagnet; it also included a wire serving as a probe. The resonant circuit was coupled inductively with an oscillator which could be operated between 20 and 60 Mc. The tube was filled with air at various pressures. The results indicated that the magnetic field intensity, the frequency of the electric field and the pressure affected the aspect of the discharge and the number of charge carriers in the plasma. At magnetic field intensities exceeding 1000 gauss, the number of positive and negative charge carriers was found to be about equal. Formation of coaxial cylindrical shapes in the discharge tube indicates that a double or triple annular discharge is involved. Under certain conditions, a columnar plasma was obtained. The shape of the discharge is also controlled by the radius of rotation of the electrons and positive ions. (TTT)

32635 VIRIAL EXPANSIONS FOR PLASMA IN THE COLLECTIVE VARIABLE METHOD. Yukhnovskii, I. R.; Nekrot, A. A. (Lvov State Univ.). Ukr. Fiz. Zh., 11: 363-71(Apr. 1966). (In Ukrainian).

A general expression was obtained for the free energy with precision to the fifth virial coefficient. Group integrals constructed of exponential functions from screened potentials and short force potentials naturally contain plasma parameters (Debye, Bjerrum and short force radii). An electric expression is considered for the second virial coefficient. There is a connection between the structure of the transfer functions and the structure of the free energy. (auth)

32636 IONIZATION EQUATION FOR OPTICALLY THIN PLASMA. Bohn, W. L. (Institut fuer Plasmadynamik, Stuttgart). Z. Naturforsch., 21a: 377-83(Apr. 1966). (In German).

An ionization formula for optically thin plasmas is proposed taking into account collisional ionization and both collisional and radiative recombination. This rather simple formula allows the calculation of the plasma components over the whole range of electron densities and temperatures. In cases of extremely low or extremely high electron densities it approaches the well known corona, and Saha-equation (for electron temperature), respectively. Furthermore it is shown that the Saha-equation is not valid in a high temperature plasma having a great ionic charge even at high electron densities, and that the proposed ionization formula should be used. Results at constant pressure or constant electron density are given in numerous diagrams. (auth)

32637 INVESTIGATION OF THE CYCLOTRON HARMONIC RADIATION FROM A PLASMA IN A MAGNETIC FIELD. Raeuchle, Eberhard; Hess, Walther (Technische Hochschule, Stuttgart). Z. Naturforsch., 21a: 383-90 (Apr. 1966).

The microwave emission of the positive column of a low pressure discharge in a magnetic field is investigated by means of a 10,000 Mc/sec radiometer. The radiation intensity as a function of the longitudinal magnetic field shows a number of peaks near the electron cyclotron harmonic frequencies. The measurements are performed for noble gases in the pressure range from 10 to 10^{-2} torr at electron densities varying from 10^{9} to 10^{13} cm^{-3}. In order to compare the experimental results with a previous theoretical investigation, the emission of harmonics was observed in dependence on the electron density. A satisfactory agreement between theory and experiment is shown. (auth)

32638 MEASUREMENT OF THE PRESSURE ELEVATION IN A HYDROGEN ARC DISCHARGE IN SUPERIMPOSED AXIAL MAGNETIC FIELD. Doebele, H. F.; Wienecke, R.; Witkowski, S. (Institut fuer Plasmaphysik, Munich). Z. Naturforsch., 21a: 390-8(Apr. 1966). (In German).

In a cylindrically symmetric hydrogen arc discharge located in an axial magnetic field, pressure is increased in the inner region, where ionization occurs. Measurements were made with initial pressures of 7.5 and 15 torr, with temperatures between 8000 and 12,000°K, and the magnetic inductions of 8.5 and 12.5 kGauss. A mercury gauge was connected to a small opening in the anode to measure the radial pressure distribution in the plasma. Temperatures and electron densities were determined spectroscopically. The Saha equation was found to be applicable in this case. Therefore, experimental results can be compared with theory based on the Saha equation. (auth)

32639 UNIPOLAR PULSED PLASMA GENERATOR COMBINED WITH A LASER AS A SOURCE FOR OBTAINING PLASMA JETS. Grechikhin, L. I.; Min'ko, L. Ya. Zh. Prikl. Spektrosk., Acad. Nauk BSSR, 4: 293-7(Apr. 1966). (In Russian).

A pulsed plasma generator started by the plasma formed by the radiation of a laser was described. This plasma generator gives a plasma jet of a comparatively high velocity and of a definite chemical composition. Main parameters of the plasma jet, the stream velocity, the density of charged particles and the temperature were measured. The dependence of plasma jet properties on the ring electrode polarity of the pulsed plasma generator was shown. (auth)

32640 DIFFERENTIAL EQUATION WITH TWO SMALL PARAMETERS. Pukhnachev, V. V. Zh. Vychisl. Mat. Mat. Fiz., 6: No. 1, 178-83(Jan.-Feb. 1966). (In Russian).

Uniform, with respect to x for $x \geq 0$ ($x < 0$), asymptotic representations of four linearly independent solutions of $\epsilon^4\varphi^{(IV)} - 2\epsilon^2 x\varphi'' + \varphi = 0$ as $\epsilon \to 0$ are constructed, which is related to an equation in plasma stability theory. The particular goal is to obtain representations in neighborhoods of branch points. The representation also yields the derivatives up to fourth order. (auth)

32641 PHYSICS OF HIGH TEMPERATURE PLASMAS. An Introduction. Schmidt, George. New York, Academic Press, 1966. 348p. $12.95.

An introduction to the physics of fully ionized, high-temperature plasmas is presented with emphasis on the relation of the physical systems to the corresponding models. Nonadiabatic particle dynamics, minimum-β geometries, finite gyroradius stabilization, and radiation by plasma oscillations are among the topics covered. (D.C.W.)

32642 METHOD FOR TRAPPING CHARGED PARTICLES IN A MAGNETIC FIELD ARRANGEMENT. Kerst, Donald William (to General Dynamics Corp.). German Patent 1,213,543. Mar. 31, 1966. Priority date Feb. 16, 1960, United States.

The method of providing charged particles in an evacuated gastight chamber having a static magnetic confining field established therein and having no varying electric field applied thereto, comprises organizing a beam of particles into discrete bunches of particles and injecting the bunches of particles into the chamber at an angle to the confining field, whereby the bunches become disorganized within the chamber thereby trapping particles in the field. (Gmelin Inst.)

32643 EXPANSION THEOREM FOR THE LINEARIZED FOKKER-PLANCK EQUATIONS. Lewis, Jordan D. (Univ. of Michigan, Ann Arbor). 27p. (CONF-651015-20). ORAU.

From American Physical Society Meeting, Chicago.

The linearized Fokker-Planck kinetic equation for each component of a homogeneous, nondegenerate, fully ionized plasma is separated by means of a spherical harmonic expansion into an infinite set of singular integrodifferential equations. Each equation is shown to generate a continuous set of eigenfunctions, for which asymptotic high-speed forms are found. By extending the theory of singular differential equations an expansion formula is developed, which is shown to be complete with respect to functions square integrable in velocity space. (auth)

32644 MEASUREMENT OF ROTATIONAL-VELOCITY AND ION-DENSITY PROFILES IN PLASMA VORTICES. Bostick, W. H.; Emmert, G.; Farber, E.; Grunberger, L.; Jermakian, A.; Prior, W.; Zorskie, J.; Casale, P.; Desh-

mukh, A. (Stevens Inst.of Tech., Hoboken, N. J.). 18p. (CONF-651126-5). ORAU. Gmelin, AED-CONF-65-353-13.

From American Physical Society, 7th Annual Meeting of the Division of Plasma Physics, San Francisco.

Floating double-probe measurements of the radial electric field E of a plasma eddy or vortex which rotates around d-c magnetic field B gives the rotational velocity profile v, since $E = -vxB$. Measurements on vortices produced by the plasma coaxial accelerator and also by firing a small plasma gun across B, show that the radial electric field is proportional to the radial distance from the rotational center of the eddy. Thus, the eddies rotate as rigid bodies without shear. (auth)

32645 PLASMA MOTION IN A WEAKLY IONIZED GAS WITH A STRONG MAGNETIC FIELD. Barthel, James R. (Univ. of California, San Diego). 22p. (CONF-651126-2). ORAU. Gmelin, AED-CONF-65-353-19).

From American Physical Society, 7th Annual Meeting of the Division of Plasma Physics, San Francisco.

Flows are considered in which the degree of ionization and the magnetic field strength B are low enough to allow treatment of the neutral gas velocity $\vec{V}_N$ as a known forcing function acting on the plasma, but in which B is large enough that the ion collision frequency ν_i is much smaller than the ion Larmor frequency ω_i. From consideration of the linearized axially symmetric case it is concluded that there is a dimensionless parameter $\alpha = \nu_i L/c_A$ (L = characteristic flow dimension, c_A = Alfven speed) such that when $\alpha^2 \gg 1$ the velocity of the plasma closely approximates the velocity of the neutrals for a time of the order of $\alpha^2/4\nu_i$, decaying thereafter as $t^{-\frac{1}{2}}$; for $\alpha \ll 1$, it is concluded that the plasma velocity perpendicular to $\vec{B}$ is much smaller than the neutral velocity, through frequently much larger than the value obtained if induced electric fields are neglected. (auth)

32646 ELECTRON-ATOM COLLISION CROSS-SECTION MEASUREMENTS IN THE AFTERGLOW OF A PULSED CESIUM PLASMA. Ingraham, John Charles (Massachusetts Inst. of Tech., Cambridge). 16p. (CONF-651070-1). ORAU. Gmelin, AED-CONF-65-395-3.

From 18th Annual Gaseous Electronics Conference, Minneapolis.

A gated microwave detector is used to determine the electron-atom collision cross section in the afterglow of a repetitively pulsed d-c discharge in cesium as a function of electron temperature. The detector measures the electron cyclotron absorption resonance and the electron temperature. The width and shape of the resonance are related to the electron-atom collision cross section. Data are presented for a range of electron temperatures from 550 to 3100°K and at a temperature of 6200°K. The measured cross section is 3×10^{-11} cm^2 at 3100°K and is higher for all lower temperatures studied, showing no Ramsauer minimum. (auth)

32647 INVESTIGATION OF TRANSVERSE PLASMA DIFFUSION BY MEANS OF THE DECAY ALONG A MAGNETIC FIELD. Polman, J. (Rijksuniversiteit, Groningen, Netherlands). 9p. (CONF-650806-16). ORAU.

From 7th International Conference on Ionization Phenomena in Gases, Belgrade, Yugoslavia.

The diffusion of the charged particles of a plasma across a magnetic field was studied by a method involving the continuous creation of a weakly ionized plasma at one end of a long discharge tube and its diffusion in axial and radial directions. A homogeneous magnetic field is directed parallel to the tube axis. In this geometry the axial decay length, determined from the axial decrease of the plasma density, is related to the magnitude of the transverse diffusion coefficient. Consequently the magnetic field dependence of this diffusion coefficient can be deduced from the change of the decay length with the magnetic field. (A.G.W.)

32648 ARC SPOT AS A DENSE PLASMA MAINTAINED BY MICRO ANALOGS OF MACRO BEAMS. Rothstein, J. (Lab. for Electronics, Inc., Boston). 28p. (CONF-651070-3). ORAU. Gmelin, AED-CONF-65-395-1.

From 18th Annual Gaseous Electronics Conference, Minneapolis.

Focused electron, ion, and light beams can generate high density plasma conditions in the region of concentrated energy input. In this case plasma generation is generally incompatible with maintenance of beam-concentrating field configurations, and can culminate in destructive arcs. Steady state arc spots (e.g., on mercury) are known, in which energy concentration mechanisms maintain a local dense plasma condition despite its explosive nature. A mechanism is proposed for arc spot maintenance, which can be viewed as a microscopic limit of both the ion and electron beams. The energy input mechanism is viewed as a combination of focused beams of ions and electrons, the former impinging on the cathode surface from outside, the latter being essentially a stream-line flow of electrons from the bulk cathode into the sink provided by the cathode spot. An important role of space charge is then the maintenance of beam-focusing optics for both electrons and ions on a microscopic scale. It is shown that plasma containment results in the spot region, which is rather efficient. Analyses are given of this hot plasma theory of arc spot emission, and comparison is made with other theories. An explanation of important arc spot properties including its retrograde motion, is given in terms of the dense plasma model. Brief mention is made of the transition between conventional beams and destructive arcs, and the possibility of designing beam apparatus in which arcing can be useful rather than destructive. (auth)

32649 NOTE ON THE C.C.L. APPROXIMATION FOR TREATING A COLLISIONLESS PLASMA FLOW. Hida, Kinzo.; Tajiri, Masayoshi (Univ. of Osaka Prefecture). 8p. (CONF-650927-22). ORAU. Gmelin, AED-CONF-65-222-44).

From American Physical Society, Honolulu, Hawaii.

In 1956, Chew, Goldberger, and Low showed that the flow of a collisionless plasma could be treated by a system of hydrodynamical equations with an anisotropic pressure, provided that the heat flow is negligible. For a steady flow subject to an aligned magnetic field, the fundamental equations can be reduced to the conventional ones without a magnetic field by making use of a suitable transformation. A hodograph method previously used by the author for treating the flow of a perfectly conducting fluid with aligned magnetic field, except for the modification of conceptions of both Alfvén and sonic waves, is used for the analysis. (A.G.W.)

32650 DIAGNOSTIC OBSERVATIONS OF A REPETITIVELY PULSED COAXIAL ACCELERATOR. Gloersen, P.; Karras, T. W.; Gorowitz, B. (General Electric Co., Philadelphia). New York, American Inst. of Aeronautics and Astronautics, 1966, Preprint No. 66-197, 20p., $1.50. (CONF-660310-19). ORAU.

From AIAA 5th Electric Propulsion Conference, San Diego, Calif.

A gridded probe that measures the energies of ions in a plasma is described. Some measurements of the ion energy spectra for xenon and carbon are discussed as examples, and the theoretical interpretation of the data is considered. (G.O.Y.)

32651 EXCITATION AND DETECTION OF MAGNETO-ACOUSTIC WAVES IN A ROTATING PLASMA ACCELERATOR. Wilson, G. L.; Woodson, H. H. (Massachusetts Inst. of Tech., Cambridge). New York, American Inst. of Aeronautics and Astronautics, 1966, Preprint No. 66-172, 46p., $1.50. (CONF-660315-11). ORAU.

From AIAA Plasmadynamics Conference, Monterey, Calif.

The results of experiments in which magnetoacoustic waves were observed in a flowing He plasma are presented. The device used to heat and accelerate the gas is described along with the two-dimensional Hartmann flow model used to predict the accelerator characteristics as functions of input power to the accelerator. Some measurements of the

gas-flow properties are described and are compared with the theory. The theory for magnetoacoustic waves in a flowing medium with finite electric conductivity is discussed. Solutions for standing wave resonances in a system closed on itself are found and are compared with eigenfrequencies measured on the accelerator system. (G.O.Y.)

32652 COLLISIONLESS SHOCK WAVE IN A PLASMA. Niu, Keishiro; Hung, Ru-jane (Univ., Osaka). 17p. (CONF-650927-15). ORAU. Gmelin, AED-CONF-65-222-22.

From American Physical Society, Honolulu, Hawaii.

The shock structure in a collisionless plasma is investigated. It is shown that the existence of the collisionless shock can be explained in terms of the motion of the ions, coupled with the field quantities. (D.C.W.)

32653 OPTIMIZATION AND THEORY OF THE LINEAR INDUCTION OR TRAVELING WAVE ELECTROMAGNETIC PLASMA ACCELERATOR. Rashad, A. R. M. (Memphis State Univ.). New York, American Inst. of Aeronautics and Astronautics, 1966, Preprint No. 66-243, 23p., $1.50. (CONF-660310-26). ORAU.

From AIAA 5th Electric Propulsion Conference, San Diego, Calif.

The performance of a cylindrical traveling magnetic wave plasma accelerator is investigated in detail in terms of the finite and infinite conductivity theories. The results are presented in terms of an equivalent induction machine model. Optimization of the accelerator's performance results in the necessary relations between the slip, the plasma conductivity and the Alfven speed. Possible mechanisms of energy transfer from the magnetic field system to the plasma are also discussed briefly. (auth)

32654 NON-LINEAR MOTION OF TWO ION STREAMS IN A BACKGROUND OF HIGH TEMPERATURE ELECTRONS. Taniuti, Tosiya; Yajima, Nobuo; Outi, Akizi (Nagoya Univ., Japan). 35p. (CONF-650927-18). ORAU. Gmelin, AED-CONF-65-222-9.

From American Physical Society, Honolulu, Hawaii.

The propagation of nonlinear ion-acoustic waves in a plasma of warm electrons and streams of cold ions is investigated. A hydrodynamical model that employs ion fluid streams interacting among themselves through the electron pressure gradient is used, and isothermal electrons are assumed. The case of two ion streams with different velocities is considered in detail. (D.C.W.)

32655 PROBE MEASUREMENTS IN AN ELECTRODELESS DISCHARGE. Keefer, D. R.; Clarkson, M. H.; Mathews, B. E. (Univ. of Florida, Gainesville). New York, American Inst. of Aeronautics and Astronautics, 1966, Preprint No. 66-194, 17p., $1.50. (CONF-660315-1). ORAU.

From AIAA Plasmadynamics Conference, Monterey, Calif.

Radial distributions of number density, electron temperature and plasma potential have been measured in an electrodeless discharge using both a symmetric double probe and a highly asymmetric double probe. The symmetric probe shows less consistency in radial distribution of saturation current than the asymmetric probe and also indicates electron temperatures which are lower by 20% to 43%. The discharge was formed in argon at pressures in the micron to millimeter range in a Pyrex tube two inches in diameter. It was excited by a four-turn coil carrying current at a 4.5 MHz. Two Faraday shields were used to isolate the discharge from axial electric fields with the inner shield also serving as the large probe electrode. Radial distributions of number density, electron temperature and plasma potential are presented graphically for several values of pressure and coil current. (auth)

32656 EXPERIMENTAL STUDY OF NEUTRAL POINT IN A PLASMA. Bratenahl, A.; Hirsch, W. (California Inst. of Tech., Pasadena). New York, American Inst. of Aeronautics and Astronautics, 1966, Preprint No. 66-152, 22p., $1.50. (CONF-660315-18). ORAU.

From AIAA Plasmadynamics Conference, Monterey, Calif.

Topological changes of magnetic flux can only occur at neutral points. In a conducting medium (plasma), such changes are generally controlled by the ohmic field which can be severely limiting if the conductivity is large. It has often been said that such processes are very slow on that account. However, Dungey pointed out that neutral points are unstable, collapsing to form a sheet pinch. On the other hand, Furth, et al., have shown that the sheet pinch is unstable to form a neutral point, and Petscheck has shown that a modification of Furth's process can lead to rapid flux changes. In the experiment conducted a neutral point is produced between two parallel line currents in a highly conducting plasma. There is a strong driving force to compel topological flux changes at this point. A remarkable process is observed in which, alternately, a sheet pinch is formed, then a fast flux change takes place with its break-up. This alternating flip flop of instabilities can be described in quite simple terms and reveals an ingenious method by which nature thrusts aside the embarrassment of high conductivity when she wants to sever and reconnect lines of force. This result is related to solar flares, and a new model of solar prominences is suggested. (auth)

32657 RELAXATION TO THE STEADY STATE IN A CONDUCTING NONEQUILIBRIUM PLASMA STREAM. Curry, Bill P. (ARO, Inc., Arnold Air Force Station, Tenn.). New York, American Inst. of Aeronautics and Astronautics, 1966, Preprint No. 66-193, 38p., $1.50. (CONF-660315-2). ORAU.

From AIAA Plasmadynamics Conference, Monterey, Calif.

The relaxation of a seeded plasma subjected to a constant electric field is considered within the formalism of the two temperature theory. Numerical solutions are obtained for stream-wise conductivity profiles in both argon and nitrogen plasmas seeded with potassium. Reaction rates used here are analytical formulas based on the Byron model for collision-induced recombination. Extensive analysis of the computed results and comparison with Zukoski's experiments in argon establishes the validity of the basic treatment and suggests the existence of energy losses resulting from excitation of argon transitions originating at the first excited state, in addition to the usual elastic collision and potassium excitation energy losses. Refined agreement between theory and experiment requires consideration of corrections to the species-averaged momentum transfer cross section, after the manner of Frost, however, present theories are shown to overestimate this correction for argon. Details of the Byron model are validated by comparison of theoretical and experimental time-resolved potassium emission lines. Possible nonequilibrium effects in nitrogen are investigated with various assumed molecular excitation losses. Relaxation times for both types of plasmas are correlated by use of Zukoski's characteristic time parameter. (auth)

32658 CRITERION FOR ELECTRON-HEAVY PARTICLE NONEQUILIBRIUM IN A PARTLY-IONIZED GAS. Jacobs, Paul F.; Grey, Jerry (Princeton Univ., N. J.). New York, American Inst. of Aeronautics and Astronautics, 1966, Preprint No. 66-192, 21p., $1.50. (CONF-660315-3). ORAU.

From AIAA Plasmadynamics Conference, Monterey, Calif.

A study of the degree of electron-heavy particle thermal nonequilibrium typically encountered in a subsonic argon arcjet plasma at a pressure of one atmosphere is presented. The results are extended to other gases at different pressures and flow velocities. An energy equation is written for the electrons which results in an expression for the degree of thermal nonequilibrium in terms of thermal and electrostatic potential gradients, electron and atom particle densities, the flow velocity, and relevant electron-heavy particle collision cross sections.

The governing nonlinear rate equation is similar to the type studied by Blythe. Examination of this equation leads to a simple criterion for impending electron freezing. The values of the critical conditions for electron freezing, as well as the degree of nonequilibrium, are plotted for a physically interesting range of the parameters in both argon and hydrogen plasmas. Four important trends are observed. First, for conditions appropriate to subsonic, atmospheric-pressure arcjets, the initial relaxation phenomena near the jet exit plane are so rapid that this region may be considered to be in thermal equilibrium, to a very close approximation. Second, for these jets the axial temperature decay is sufficiently rapid that, in general, a rather sharply defined point is reached at which nonequilibrium effects begin to become significant. This results primarily from the reduced electron-heavy particle collision frequency as the ion density drops. Third, beyond this critical position the electron temperature decays less rapidly than does the heavy particle temperature (i.e., the electrons tend to freeze). This regime may be characterized by significant electron-heavy particle temperature differences. Finally, at the reduced pressures and higher velocities appropriate to many of the high-specific-impulse arcjet studies (e.g., hydrogen at $P < 10^{-4}$ atm and $U > 10^6$ cm/sec) it is found that nonequilibrium effects are important throughout most of the flow field. These trends appear to be in good agreement with experiment. (auth)

32659 VELOCITY MEASUREMENT BY DOPPLER EFFECT. Ahlborn, Boye; Barnard, A. Johannes (Univ. of British Columbia, Vancouver). New York, American Inst. of Aeronautics and Astronautics, 1966, Preprint No. 66-177, 9p., $1.50. (CONF-660315-7). ORAU.

From AIAA Plasmadynamics Conference, Monterey, Calif.

A discriminating technique is proposed for measuring small Doppler shifts with a low resolution monochromator (about 10 Å/mm). Two neutral density filters with linearly changing transmissions are placed in the focal plane of a monochromator, so that a shift in wavelength produces a change in the transmitted intensities. The shift can be measured independently of line shape and of intensity changes in the source. A test experiment is described and the limits of sensitivity are discussed. (auth)

32660 MEANS FOR THE STUDY OF THE STAGNATION PRESSURE DISTRIBUTION IN A CURRENT-CARRYING PLASMA. Barkan, P.; Whitman, A. M. (General Electric Co., Philadelphia). New York, American Inst. of Aeronautics and Astronautics, 1966, Preprint No. 66-179, 30p., $1.50. (CONF-660315-6). ORAU.

From AIAA Plasmadynamics Conference, Monterey, Calif.

A method is described for measuring stagnation pressures in high temperature, high current plasmas. The device employs a small (<0.060 in. OD) uncooled pitot tube designed for minimum response time (≈0.001 sec) which is rapidly swept through the plasma flow field (≈0.015 sec). Optimum probe dimensions are determined from analysis of a two-degree of freedom discrete model. A test technique for evaluating the transient response of the probe is described. Because the probe tip is inexpensive and expendable, a moderate amount of molten phase ablation is tolerable in the stagnation zone. Consequently, it appears possible to obtain meaningful results at heat flux rates exceeding 10^4 cal/cm^2-sec, which is one to two orders of magnitude greater than have thus far been tolerable with water-cooled probes. In preliminary tests a single probe was successfully employed for eight successive measurements of total pressure in an atmospheric pressure, air-arc plasma at currents ranging from 200 to 1000 amperes at Mach numbers close to unity. The principal merits of the probe described are its small size, rapid response and its inexpensive, expendable probe tip. The principal source of measurement error is related to the inherently low Reynolds numbers associated with plasma flow past the small probe. (auth)

32661 PROBE MEASUREMENTS OF PLASMA INJECTED INTO A B_z GUIDE FIELD FROM A CONICAL THETA-INCH ACCELERATOR. Small, R. L. (Grumman Aircraft Engineering Corp., Bethpage, N. Y.); Valsamakis, E. A.; Bostick, W. H. New York, American Inst. of Aeronautics and Astronautics, 1966, Preprint No. 66-155, 29p., $1.50. (CONF-660315-15). ORAU.

From AIAA Plasmadynamics Conference, Monterey, Calif.

Experimental measurements of the local magnetic field, ion density flow, and electric field in the plasma were made downstream of a theta-pinch accelerator in the presence of a uniform guide field. From data obtained with small three-directional probes, certain gross features of the plasma structure, as a function of its downstream position, are inferred. A conically shaped, theta-pinch coil, ringing at approximately 40 kilo Hertz with a maximum magnetic field strength of 3.5 Tesla, injects preionized argon into a 0.26 Tesla axial guide field. The geometries of and electronics involved with the probes are discussed. The gross features of the radial and axial magnetic probe data and the biased double probe (ion density flow) data imply the existence of at least three separate plasma rings. These rings have a unidirectional j_θ current and move downstream at approximately 10^4 meters/second. Probe data at several downstream points indicate a tendency for these rings to coalesce. (auth)

32662 RADIAL DENSITY AND TEMPERATURE PROFILES AT THE ION CYCLOTRON WAVE RESONANCE POINT. Krawec, Roman (Lewis Research Center, Cleveland). New York, American Inst. of Aeronautics and Astronautics, 1966, Preprint No. 66-158, 22p., $1.50. (CONF-660315-14). ORAU.

From AIAA Plasmadynamics Conference, Monterey, Calif.

A simplified theory for an electrostatic probe in a magnetically confined plasma is presented. Interpretation of probe results using the model are compared with those calculated from Langmuir probe theory. The model presented provides an expression for calculating ion temperature from the probe data. Radial profiles of electron density, radial electric field, electron temperature, and ion temperature are presented for two experiments; a d-c hot-cathode low-pressure (2μ) discharge confined by a steady magnetic field, and a plasma heating experiment where ion cyclotron waves propagate along the plasma column. The radial electron density profiles show that the maximum density does not occur on axis but at radii of 0.5 to 1.0 cm (the plasma radius was approximately 2.5 cm). The average densities are found to be in agreement with microwave interferometer measurements and consistent with the location of maximum power transfer. The ion and electron temperatures are found to reach a maximum near the plasma boundary. The addition of r-f power is found to heat both the ions and electrons but has little effect on the density. (auth)

32663 SURVEY OF NONLINEAR ELECTROMAGNETIC WAVE PROPAGATION IN PLASMAS. Papa, Robert T. (Air Force Cambridge Research Labs., Bedford, Mass.). New York, American Inst. of Aeronautics and Astronautics, 1966. Preprint No. 66-170, 38p., $1.50. (CONF-660315-12). ORAU.

From AIAA Plasmadynamics Conference, Monterey, Calif.

A detailed review of the current literature pertaining to high power r-f field-plasma interactions is presented. In this particular survey, the nonlinear interaction is restricted to that class of problems where the effective dielectric constant of the plasma is a function of the local electric field intensity. Since the propagation characteristics of an em wave depend upon the effective dielectric constant, the presence of an intense r-f field can modify the propagation characteristics of an electromagnetic wave. The assumptions and basic theoretical approach of each author are discussed and the most significant results are summarized. The approaches used by dif-

ferent authors are compared. A critique is made of the various approaches and the advantages and limitations are pointed out. (auth)

32664 COMPARISON OF NUMERICAL CALCULATIONS AND MEASURED SPACE-TIME RESOLVED PLASMA PROPERTIES OF A DYNAMICAL THETA PINCH. Friedrich, Otto M. Jr.; Dougal, Arwin A. (Univ. of Texas, Austin). New York, American Inst. of Aeronautics and Astronautics, 1966, Preprint No. 66-151, 30p., $1.50. (CONF-660315-19). ORAU.

From AIAA Plasmadynamics Conference, Monterey, Calif.

A relatively dense, high temperature, and very dynamic plasma column is produced in a 30 kilojoule theta pinch. The two-fluid hydromagnetic model programmed in Lagrangian coordinates is used to numerically calculate the electron density, magnetic field, electron temperature, and ion temperature as functions of radial position and time. For an initial density of 5×10^{15} cm^{-3}, computations show that a plasma annulus forms near the cylindrical tube wall, implodes at 10^7 cm/sec, and then oscillates at 10–20 Mc/sec. The frequency of these radial oscillations increases and they are damped as the compression field builds up. With forward bias, maximum ion temperatures are only 300–500 ev and electron temperatures are 300–600 ev. Maximum ion temperatures as large as 3 kev and electron temperatures of 1.5 kev result when reverse bias is employed. As the initial density is decreased from 1×10^{16} to 2×10^{15} cm^{-3}, the maximum ion and electron temperatures during the first quarter cycle of compression increase. Experimental space-time resolved electron densities obtained employing an infrared maser excited coupled resonator system and magnetic fields determined from the Faraday rotation of the maser beam compare favorably with calculated values. (auth)

32665 EXPERIMENTAL STUDY OF BREAKDOWN PHENOMENA IN ARGON GAS BY A LASER BEAM AT LOW PRESSURE. Chen, Che Jen (California Inst. of Tech., Pasadena). New York, American Inst. of Aeronautics and Astronautics, 1966, Preprint No. 66-176, 23p., $1.50. (CONF-660315-8). ORAU.

From AIAA Plasmadynamics Conference, Monterey, Calif.

A Q-switched giant pulse laser is focused in an argon gas of pressure less than one atmosphere. The gas breakdown at the focal point is observed by both an electrostatic probe and a phototube. The number density of the charged particles produced as a function of time at different pressures is obtained by measuring the conductivity of the plasma drop produced at the focal point of the laser beam. The energy of the electrons in the plasma drop is obtained from the measurement of the time rate of growth of the size of the plasma drop. The rate of ionization and electron energy of the plasma drop are also calculated by assuming that some pre-existing electrons gain energy from photons through the inverse bremsstrahlung process, and lose their energy to atoms mainly through inelastic ionizing collisions. Because of the agreement between theoretical and experimental data, it is thought that associated inverse bremsstrahlung is the main mechanism responsible for the breakdown of the gas by the laser beam. The plasma drop can be used as a tracer to measure the velocity of flow (both un-ionized and ionized gases) by using the drum camera and probe techniques. Velocity profiles measured using the tracer technique are presented. (auth)

32666 LASER PLASMA PRODUCTION: A NEW AREA OF PLASMADYNAMICS RESEARCH. Meyerand, R. G. Jr. (United Aircraft Corp., East Hartford, Conn.). New York, American Inst. of Aeronautics and Astronautics, 1966, Preprint No. 66-174, 22p., $1.50. (CONF-660315-9). ORAU.

From AIAA Plasmadynamics Conference, Monterey, Calif.

The interaction of extremely high intensity optical frequency electromagnetic radiation with gases and solids is a research area accessible to experimental investigation only with the recent development of high powered lasers. Such studies are important to aerospace activities since they provide a new source of extremely high-density, high-temperature uncontaminated plasma for a variety of studies. Plasma density as high as 10^{20} electrons/cm^3 at gas pressures of 1000–2000 psi can readily be produced by this technique. In addition, solid particles suspended in high vacuum can be irradiated with a laser to produce a fully ionized plasma without surrounding gas. The basic theory of gas breakdown produced by optical radiation will be discussed and the absorption of laser energy in the resultant plasma described. Theories of the dependence of gas breakdown and energy absorption on gas pressure, gas species and optical field strength are discussed. (auth)

32667 MICROWAVE TRANSMISSION IN A PURE AIR PLASMA. Bein, G. P.; Boyer, D. W. (Cornell Aeronautical Lab., Inc., Buffalo). New York, American Inst. of Aeronautics and Astronautics, 1966, Preprint No. 66-173, 46p., $1.50. (CONF-660315-10). ORAU.

From AIAA Plasmadynamics Conference, Monterey, Calif.

An analytical and experimental program performed in preparation for the conduct of microwave transmission tests in a hypersonic shock tunnel (15,000 ft/sec, 125,000 ft altitude) is described. Exact nonequilibrium calculations provided electron density and collision frequency profiles at chosen body stations for selected model configurations. The associated propagation path signal loss and antenna radiation pattern distortion were then predicted. A new computer program was used to determine complex transmission and reflection coefficients of the inhomogeneous plasma assumed to be irradiated by plane waves at arbitrary angles of incidence. Computations were made at frequencies of 1.7, 2.6, and 4 Gc for both polarizations. For example, a blunt, 20° wedge of 1.0 in. nose radius provides for a signal loss from −11 to −14 db. The analytical model for determining radiation pattern distortion was validated by comparing theoretical predictions and experimental measurements of patterns when the antenna was covered with a dielectric of known properties. Microwave instrumentation for the shock tunnel, 35 db dynamic range compression receivers, and the low-reflection-coefficient dielectric test section are described. It appears that the techniques utilized in this study provide for meaningful shock tunnel measurements. (auth)

32668 MEASUREMENT OF THE ELECTRICAL CONDUCTIVITY OF PLASMAS. Stubbe, E. J. (National Research Council, Ottawa). New York, American Inst. of Aeronautics and Astronautics, 1966, Preprint No. 66-181, 22p., $1.50. (CONF-660315-5). ORAU.

From AIAA Plasmadynamics Conference, Monterey, Calif.

The problem of measuring the spatial distribution of the electric conductivity of a sample of plasma generated in a plasma jet has been worked out by using a miniature coil immersed in the plasma. The idea is based upon the interaction of a conducting sample of gas or liquid with a radiofrequency magnetic field. The interaction can be detected either as a reactive or a resistive change of the coil impedance. Some arguments are presented to select the suitable type of detection method, which in general depend upon the parameter $s = \sigma\mu\omega a^2$. A conductivity probe of the resistive type, originally devised by Olson and Lary, is used together with a kind of grid dip meter to detect the amount of joule dissipation arising from the eddy currents around the probe. An absolute calibration of the probe was performed on a $1\frac{1}{2}''$ shock tube which generates a slug of highly ionized plasma behind the reflected shock, having a conductivity very close to the theoretical calculated values by the Shkarofsky method. Experimental results are shown together with the predicted values for the electric conductivity in a nonseeded plasma jet. (auth)

32669 FIRST ORDER CORRECTION TO THE FIRST ADIABATIC INVARIANT. Siambis, John G. (Massachusetts Inst. of Tech., Cambridge). 6p. (CONF-651126-16). ORAU. Gmelin, AED-CONF-65-353-39.

From American Physical Society, 7th Annual Meeting of the Division of Plasma Physics, San Francisco.

An expression for the first order correction to the magnetic moment of a charged particle gyrating in a static magnetic field is presented. The expression is given in terms of the curvature, torsion, and shear coefficients of a local coordinate system natural to the field lines of the magnetic field. (J.F.P.)

32670 RADIATIVE SHOCK STRUCTURE: THEORY AND OBSERVATIONS. Skalafuris, Angelo J. (Goddard Space Flight Center, New York). 36p. (CONF-660217-1). ORAU. Gmelin, AED-CONF-66-013-3.

From Symposium on Interdisciplinary Aspects of Radiative Energy Transfer, Philadelphia.

Radiative shock wave structure is considered. Stellar observations of shock structure are discussed, and the mechanisms for this structure are considered. Criteria for data evaluation are also given. (J.F.P.)

Shielding

32671 (AD-633216) SECONDARY GAMMA RAY TRANSMISSION THROUGH PLANE SLABS OF CONCRETE. Budka, Alfred J.; Dolce, Thomas J. (Ballistic Research Labs., Aberdeen Proving Ground, Md.). Sept. 1965. 127p. (BRL-R-1307). CFSTI $4.00 cy, $0.75 mn.

Secondary gamma ray transmission data are presented for monoenergetic secondary gamma ray sources in concrete slabs of various thicknesses. The data presented were computed using the Monte Carlo method. These secondary gamma ray transmission data along with an appropriate weighting scheme allow one to determine the secondary gamma ray transmission information for any depth distribution of secondary gamma rays in plane concrete slabs. (auth)

32672 (NAA-SR-Memo-11786) EXPERIMENTS ON URANIUM-LITHIUM HYDRIDE SHIELDS AT THE STIR FACILITY. Randen, K. (Atomics International, Canoga Park, Calif.). Dec. 16, 1965. Contract AT-11-1-GEN-8. 24p. Dep. mn. CFSTI $1.00 cy, $0.50 mn.

A series of gamma attenuation measurements in depleted uranium-lithium hydride shields were performed at the STIR facility using the fission plate as a source. The detector (graphite wall, CO_2-filled, ionization chamber) was shielded from contributions due to scattering from the walls of the room and located at a fixed distance from the source. Attenuation curves were obtained for lithium hydride, uranium, and lead and for various combinations of lithium hydride and uranium. The secondary gamma dose produced in the uranium due to neutron capture and fast fission is equal to the direct gamma dose rate from the fission plate at a shield thickness of 4 cm. The corresponding distance for lead is 8.5 cm. Placing lithium hydride between the fission plate and the uranium reduces the secondary gamma production with a relaxation length in the lithium hydride of 4.8 cm. In addition to the gamma dose measurements neutron fluxes inside a uranium and lithium hydride uranium combination shield were measured with sulfur pellets and gold foils. (auth)

32673 (NAA-SR-Memo-11872) APPLICATION OF THE P_3 METHOD TO THE CALCULATION OF PARTICLE FLUXES IN SHIELDS. Green, W. B. (Atomics International, Canoga Park, Calif.). Mar. 17, 1966. Contract AT-11-1-GEN-8. 17p. Dep. mn. CFSTI $1.00 cy, $0.50 mn.

The P_L method for solving the Boltzmann Transport Equation is described and the derivation of the P_3 equations for a one dimensional, source-free, semi-infinite slab medium is summarized. Appropriate boundary conditions for use in a multiregion shield, with a source at the left face and a vacuum at the right face, are introduced. The solutions to the P_3 equations are shown to be analytic within each energy group and a method is outlined in detail for solving the general multigroup problem. The method is applicable to problems in both neutron and gamma ray transport. (auth)

32674 (NP-15697(Vol.3)) DATA COMPILATION AND EVALUATION OF SPACE SHIELDING PROBLEMS. VOLUME III. RADIATION HAZARDS IN SPACE. Hill, C. W.; Ritchie, W. B.; Simpson, K. M. Jr. (Lockheed Nuclear Products, Marietta, Ga.). Apr. 1966. Contract NAS 8-11164. 160p. (ER-7777(Vol.3)).

The results are presented of parametric studies investigating the hazards of space radiations in relation to various local and interplanetary missions. The radiation types include proton and alpha particles emitted in solar flux events and proton and electron particles trapped in the magnetosphere of the Earth. The missions are three Mars expeditions, three 14-day Lunar expeditions, and 29 orbital studies. Detectors are located in the eye and abdomen of a man model placed in a cylindrical vehicle composed of either aluminum or polyethylene. The vehicle wall thickness ranges from 1 to 30 gm/cm^2. Descriptions of the principal computer programs employed in these studies are given. (auth)

32675 (ORNL-TM-1160) FORTRAN LISTINGS AND FLOW CHARTS FOR ZAP31: A PROGRAM TO CALCULATE β-γ RADIATION DOSE RATES FROM A SPHERICAL OR SLAB SOURCE. Thompson, P. A.; Clark, I. G. (Oak Ridge National Lab., Tenn.). May 23, 1966. Contract W-7405-eng-26. 61p. Dep. mn. CFSTI $3.00 cy, $0.75 mn.

A FORTRAN-63 and CODAP2 program, ZAP31 was written for the CDC 1604A computer for the calculation of β-γ radiation depth dose in matter from spherical or slab sources. Listings and flow charts for the ZAP31 program are given. (auth)

32676 OPTIMUM RATIO OF NEUTRON AND GAMMA DOSE BEHIND REACTOR SHIELDING. Veselovskii, L. N.; Kuznetsov, V. G.; Sakovich, V. A. At. Energ. (USSR), 20: 75-6(Jan. 1966). (In Russian).

Calculations were carried out previously for determining the contribution of various types of radiation sources to the optimal radiation dose beyond a lead-water reactor shield; it was assumed thereby that the heavy and light components of the shield possessed identical surfaces. However, the reactor is a point source and the heavy component of the shield is usually closer to the reactor than the light one and therefore has a smaller surface. It is shown that relatively small changes in the surface of the shield surface affect strongly the ratio of the γ and neutron doses when the shield thicknesses are chosen to be optimum. Calculations were made to determine the dose, using a neutron attenuation length in water of 10 g/cm^2 and in lead 104 g/cm^2; the corresponding values for γ attenuations were 39 and 22.20 g/cm^2. The densities of water and lead were taken as 1 and 11, respectively. The optimal doses were obtained by changing the radii of the spherical shields; Lagrange multipliers were used for determining the extremal values. It was concluded that there is no generalized expression which includes the criterion of optimal conditions. However, the optimal condition may be verified, using, as far as it is possible, identical radii for the layers of the various materials. (TTT)

32677 SHIELDING PROPERTIES OF IRON-SERPENTINE CONCRETE. Veselkin, A. P.; Egorov, Ya. A.; Kucheryaev, V. A. At. Energ. (USSR), 20: 76-7(Jan. 1966). (In Russian).

Serpentine filler added to concrete used for shielding presents the advantage that it retains 12 to 14% of water at temperatures up to 450°C; thus, its shielding properties do not change even when it is exposed to relatively high temperatures. In order to further improve the shielding properties of this type of concrete, heavy elements, such as iron, and boron were added to it. The presence of H, Si, and Mg, in addition to water renders this concrete similar to

the composite iron–water shield. The shielding properties of a concrete mixture, containing serpentine gravel (766 kg/m^3 of concrete), metallic iron powder (1900 kg/m^3) and finely ground serpentine additive (248 kg/m^3) were examined; the mixture was worked up to Portland cement, adding 115 kg/m^3 of boron carbide to it. The chemically bound water was assumed to amount to 20% of the total weight. After prolonged heating, the water content decreased to 0.4%. Considering the water in the serpentine, the Fe/H_2O ratio was close to the optimal value of 18.3%, or about 70 volume % of iron. The fast neutron attenuation was found to follow the exponential law; the relaxation lengths varied from 9.95 to 8.95 cm for indicator threshold energies ranging from about 7 to 0.8 Mev. The thermal and epithermal neutrons were sharply attenuated in the concrete layers near the source by the large amount of boron in the system. The shielding properties of the mixture may be further improved by increasing the iron contents to 73 to 74%. (TTT)

32678 SHIELDING CALCULATIONS FOR CYLINDRICAL SOURCES. Kovalev, E. E.; Osanov, D. P. At. Energ. (USSR), 20: 78-80(Jan. 1966). (In Russian).

In shielding calculations, the radiation dose is usually derived as a function of the thickness of the source and the parameters of the source, solving a transcendent equation. Occasionally, it may be desired to determine the thickness which yields a dose close to a given value. In order to achieve this, a method was developed, allowing the shield thickness for radiation emitted by an extended cylindrical source to be obtained directly. In order to simplify the nomograms used for the calculation, it was shown that the effect of self-absorption within the source on the attenuation of the radiation in the shield may be safely neglected. The nomograms take into account the various geometric factors; special graphs were developed for materials, such as concrete, water, iron and lead and for specific radiations, such as 0.5, 1, 2, and 3-Mev γ rays. The graphically obtained values agree with results of more complex calculations. (TTT)

32679 CONCRETE AS A RADIATION SHIELD. Vinkeloe, R. Betonstein Zt., 30: 642-6(1964). (In German).

The shielding properties of concrete in absorbing γ rays and neutrons are reviewed. Bulk density can be widely varied by choice of suitable aggregates, and hydrogen content can also be varied at will. The admixture of small amounts of boron compounds increases the capacity of absorbing thermal neutrons. Detailed consideration is given to suitable composition of the concrete. (auth)

32680 LEAD FOR RADIATION SHIELDING. London, Lead Development Association, 1965. 35p.

Subjects discussed include the following: factors affecting the choice of a shielding material, composition and forms of lead used as shielding, properties of lead and lead alloys, types and design requirements of lead-shielded containers, safety regulations for transport containers, design and application techniques for room shielding, local movable lead shields, individual brick shielding systems, and lead plastic composites. Practical examples of lead shields are shown. (A.G.W.)

Solid State Physics

See also CHEMISTRY — Inorganic and Physical Chemistry
METALS, CERAMICS, AND OTHER MATERIALS — Properties and Structure

Refer also to abstracts 31946, 32085, and 32099.

32681 (BNL–10238) AUTOMATIC ACQUISITION OF NEUTRON SPECTROMETER DATA. Hamilton, Walter C. (Brookhaven National Lab., Upton, N. Y.). [1966]. Contract AT-30-2-GEN-16. 3p. (CONF-660527–2). Dep. mn. CFSTI $1.00 cy, $0.50 mn.

From Symposium on Use of Computers in Analysis of Experimental Data and Control of Nuclear Facilities, Argonne, Ill.

The use of the modern digital computer in the determination of the structure of crystals by diffraction methods is described. Particular reference was made in the area of data acquisition. (M.O.W.)

32682 (ORNL–P–2193) METHODS FOR CALCULATION OF THE ELECTRONIC STRUCTURE OF DEFECTS IN INSULATORS. Oepik, U.; Wood, R. F. (Oak Ridge National Lab., Tenn.). Apr. 1966. Contract W-7405-eng-26. 11p. (CONF-660529–1). Dep. mn. CFSTI $1.00 cy, $0.50 mn.

From Conference on the Calculation of the Properties of Vacancies and Interstitials, Skyland, Va.

Calculational techniques for determining the electronic structure of the F center in alkali halides are described. (M.O.W.)

32683 (ORNL–P–2194) A CALCULATION OF FORCE-CONSTANT CHANGES FOR THE U CENTER. Wood, R. F.; Gilbert, R. L. (Oak Ridge National Lab., Tenn.). Apr. 1966. Contract W-7405-eng-26. 11p. (CONF-660529–2). Dep. mn. CFSTI $1.00 cy, $0.50 mn.

From Conference on the Calculation of the Properties of Vacancies and Interstitials, Skyland, Va.

Calculations were made of both the optical and infrared properties of U centers in KCl, KBr, and KI. The preliminary results are discussed. (M.O.W.)

32684 (UCRL–16658, pp 21-38) SOLID-STATE CHEMISTRY AND PHYSICS. (Lawrence Radiation Lab., Univ. of California, Berkeley).

Results of investigations are presented concerning superconductivity of U, equipment for low-temperature colorimetry, heat capacities of Cu alloys, heat capacities of ferromagnetic $CrBr_3$, heat capacities of AUMn, heat capacities of single-crystal Nb, Ta, and V, heat capacities of Ar and Kr, heat capacity of solid ^{4}He, diffusion in Ar, relaxations about divacancies in Ar, pressure effects on specific heats of metals, Mössbauer spectra of ^{57}Fe in stainless steel vaporization of solids, Cu diffusion in CdS monocrystals, and surface properties of metal monocrystals. Lists of 1965 publications are included, and research plans for 1966 are outlined. (J.R.D.)

32685 ELECTRON PARAMAGNETIC RESONANCE STUDIES ON γ-RAY IRRADIATED $CdCl_2$:Ag AND $CdCl_2$:Cu CRYSTALS. Matsumoto, Hiroaki; Miyanaga, Takeshi (Kyoto Univ.). Bull. Inst. Chem. Res., Kyoto Univ., 44: 1-10(Jan. 1966).

The electron paramagnetic resonance spectrum of γ irradiated $CdCl_2$ doped with AgCl or CuCl was studied. γ Radiation was made with ^{60}Co at room temperature. Irradiation dose was about 15×10^6R. Two paramagnetic centers were found in irradiated $CdCl_2$:Ag. One is substitutional Ag^{2+} ion associated with Cl^- ion vacancy. The values of g tensors for this center are $g_{ww}^2 + g_{uw}^2 = 4.4184$, $g_{uu}^2 = 4.2929$, $g_{vv}^2 = 4.2860$, and $g_{uw}(g_{ww} + g_{uu}) = 0.3459$, values of hyperfine constants are $(|A_c^{Ag}|/g\beta) = (|A_c^{Cl}|/g\beta) = 30$ gauss. The other may be an electron trapped by tetrahedral aggregate of Ag^+ ions or Cd^{2+} ions. ERP pattern was observed at $g = 2.014$ and consisted of five lines with an intensity ratio of 1:5:10:5:1. In irradiated $CdCl_2$:Cu, it was found that substitutional cupric ion was responsible for the ERP patterns and the values of g tensors. The hyperfine constants are $g_{ww}^2 + g_{uw}^2 = 4.783$, $g_{uu}^2 + g_{uw}^2 = 4.987$, $g_{vv} = 2.362$, $g_{uw}(g_{ww} + g_{uu}) = 0.759$, and $(|A|/g\beta) = 110$ gauss. Elongated tetragonal deformation on octahedral environment was concluded. (auth)

32686 ABSORPTION SPECTRA OF POTASSIUM CHLORATE IRRADIATED WITH X RAYS AND ULTRAVIOLET AT ROOM TEMPERATURE. Fayet, Jean-Claude; Thieblemont, Bernard (Univ., Paris, Orsay, France). Compt. Rend., Ser. B, 262: 1084-6(Apr. 18, 1966). (In French).

The study of the optical absorption of potassium chlorate yields results that agree with those obtained by electron paramagnetic resonance. The mechanism by which the Cl_2^- grouping appears can be defined. (tr-auth)

32687 NEUTRON SPECTROSCOPY OF SOLIDS. PART I. Lomer, W. M. (Atomic Energy Research Establishment, Harwell, Eng.). Contemp. Phys., 7: 278-93(Apr. 1966).

Neutrons are scattered weakly by all nuclei, and by any atomic magnetic moment associated with the valence electrons. Isotopic and nuclear spin disorder causes some uniformly diffuse scattering; the coherent average component of scattering leads to structural information. Energy changes of the neutron are easily measured and depend on the dynamics of nuclear or magnetic motion. The experimental techniques are simple in principle and are briefly outlined. Interatomic forces in insulators and metals are related to atomic polarizability and electrostatic screening. Magnetic interactions are analyzed in terms of spin waves for Heisenberg "atomic-like" models and for band theories of metals. The time-dependence of thermodynamic fluctuations is explored, with special reference to phase transformations. The spatial dependence of magnetization round impurity atoms in magnetic materials can be measured and interpreted in terms of electron-band theory. Structural defects and impurities in non-magnetic materials give smaller effects, which can also be studied. The measurement of the transfer of electron spin from a magnetic atom to a nominally non-magnetic chemical partner gives a new look to the theory of chemical covalency. (auth)

32688 INFLUENCE OF THE SUBSTRATE ON THE DEBYE-WALLER FACTOR OF VERY THIN FILMS. Dlouha, J. (Charles Univ., Prague). Czech. J. Phys., 16: 495-505(1966).

The temperature dependence of the Debye-Waller factor of very thin undisturbed films is studied. It is found that if interaction between the substrate and the film does not exist the Debye-Waller factor diverges, with the exception of the case of zero absolute temperature, so that under these conditions resonance recoilless absorption and emission of x- and γ-rays or neutrons by the nucleus of the film cannot occur. In the presence of interaction between the film and substrate the Debye-Waller factor is finite; its temperature dependence was determined. (auth)

32689 PHONON-INDUCED DIPOLE NUCLEAR SPIN TRANSITIONS. Brun, E.; Mahon, H. (Univ., Zurich). Helv. Phys. Acta, 39: 203-4(1966).

The acoustic excitation of nuclear spin transitions via the dipole-dipole transition is calculated for lithium fluoride. It is concluded that although the dipolar transition probability is small, conditions appear favorable for the study of these dipolar transitions for irradiation times of the order of $t_p = 10^4$ sec. (J.F.P.)

32690 TEMPERATURE DEPENDENCE OF FLUORESCENCE DECAY OF URANYL SALTS. Pant, D. D.; Pande, D. N.; Pant, H. C. (D.S.B. Government Coll., Naini Tal, India). Indian J. Pure Appl. Phys., 4: 171-3 (Apr. 1966).

The lifetimes (τ_f) of various uranyl salts were measured at different temperatures (T) in the range 80°K to 350-360°K. Activation energies and pre-exponential factors for nonradiative processes were obtained on the basis of the approach suggested by N. F. Mott (Proc. Roy. Soc., A167: 384(1938)) and F. Sietz (Trans. Faraday Soc., 35: 74(1939)) and it is shown that this approach gives results in agreement with the observations. Two frequencies (≈87 cm^{-1} and 2784 cm^{-1}) are shown to take part in nonradiative dissipation. Individual characteristics of the variation of the rate constant kf with T are pointed out. The disparity between the values of kf observed in the investigation and those reported in literature is found out to be due to the presence of uranyl impurities. (auth)

32691 INVESTIGATION OF PROCESSES INVOLVING THE CREATION AND DESTRUCTION OF COLOR CENTERS IN ALKALI-HALIDE CRYSTALS BY MICROSCOPIC METHODS. Sidlyarenko, V. I.; Zaitov, F. N.; Lukantsever, Yu. L. (Osha State Pedagogical Inst., USSR). Izv. Vyssh. Ucheb. Zaved., Fiz., No. 5, 97-101(1965). (In Russian).

A new microscopic method is presented for experimentally investigating the process of creation of color centers in alkali-halide monocrystals. The processes of creation and destruction of F and M color centers in NaCl monocrystals and also in filamentary NaCl crystals on topographically different microsections of samples were studied. (tr-auth)

32692 ELECTRIC DISCHARGE IN PLASTIC IN A UNIFORM FIELD. Lisetskaya, M. N. (Kirov Polytechnic Inst., Tomsk, USSR). Izv. Vyssh. Ucheb. Zaved., Fiz., No. 5, 108-10(1965). (In Russian).

Experiments were performed to trace the development of an electric discharge in plastic in a uniform electric field and to determine the delay time and the average discharge rate. Square-wave voltage pulses with amplitude from 20 to 60 kv were used. The variation of dielectric strength with breakdown probability, the discharge delay time at various fixed values of field intensity, and the degree of destruction of the plastic were measured. It was found that the discharge develops by means of a cascade propagating from the cathode to the anode and leaving a negative electron charge on its path. After the cascade, a powerful positive streamer flows from the anode to the cathode and induced the principal destruction of the dielectric. (M.J.T.)

32693 INVESTIGATION OF THE MECHANISM OF DESTRUCTION OF COLOR CENTERS AND OF NONSTATIONARY RECOMBINATION LUMINESCENCE OF THE CRYSTAL PHOSPHOR NaCl–Ag. I. Chernenko, V. P.; Lukantsever, Yu. L.; Zaitov, F. N. (Osha Pedagogical Inst., USSR). Izv. Vyssh. Ucheb. Zaved., Fiz., No. 5, 145-52(1965). (In Russian).

The processes of the destruction of the 355-, 465-, and 720-mμ color centers in NaCl–Ag phosphors at temperatures from 100 to 550°K were studied by a composite method. In addition, the luminosity spectra of thermo- and photo-stimulated recombination luminescence of NaCl–Ag, excited at various temperatures by x rays, were studied. The possibility of ion-electron and ion-hole mechanisms for destruction of the color centers in crystalline phosphors at temperatures was examined. (tr-auth)

32694 INVESTIGATION OF THE MECHANISM OF DESTRUCTION OF COLOR CENTERS AND RECOMBINATION LUMINESCENCE OF NaCl–Ag:Ca CRYSTAL PHOSPHOR. II. Chernenko, V. P.; Zaitov, F. N.; Lukantsever, Yu. L. (Osha State Pedagogical Inst., USSR). Izv. Vyssh. Ucheb. Zaved., Fiz., No. 6, 43-7(1965). (In Russian).

A study of relaxation processes in alkali-halide crystalline phosphors excited by x rays was continued. The mechanism of destruction of color centers, the origin of thermoluminescence peaks, and the spectra of thermo- and photo-stimulated luminescence in the NaCl–Ag : Ca crystalline phosphor were studied. (tr-auth)

32695 DEFECTS IN NATURAL QUARTZ. Spencer, W. J.; Smith, W. L. (Bell Telephone Labs., Allentown, Pa.). J. Appl. Phys., 37: 2557-63(June 1966).

X-ray-diffraction topographs show at least two types of defects in natural quartz, planar defects which are parallel to the natural quartz faces and needle-like defects. The planar defects color when exposed to γ irradiation, indicating these are sheets of substitutional aluminum, with an interstitial alkali ion nearby for charge compensation. The linear defects are similar to macroscopic needles of TiO_2 sometimes found in quartz and have previously been associated with dislocations by Lang. Both types of defects show diffraction contrast when observed from different Bragg planes. There does not seem to be a simple relation between either type of defect density and acoustic loss at 300°K in natural quartz. (auth)

32696 DISLOCATION MOBILITY AND STEADY-STATE CREEP OF CRYSTALS WITH SPECIAL REFERENCE TO ALPHA ZIRCONIUM. Ardell, A. J. (Cambridge Univ.). J. Appl. Phys., 37: 2910-11(June 1966).

The results of creep experiments on α zirconium are

reported and are examined in terms of Gilman's concepts on dislocation mobility. The application of these concepts to the description of creep behavior in general is also discussed. (L.B.S.)

32697 MOLYBDENUM DIOXIDE SINGLE CRYSTALS. Vickery, R. C.; Hipp, J. C. (Globe-Union Inc., Milwaukee). J. Appl. Phys., 37: 2926(June 1966).

The single-crystal growth of molybdenum dioxide on the surface of molybdenum furnace elements exposed to limited amounts of oxygen are reported. Properties of the crystals obtained are given. (L.B.S.)

32698 NEUTRON-DIFFRACTION STUDY OF THE STRUCTURES OF FERROELECTRIC AND PARAELECTRIC AMMONIUM SULFATE. Schlemper, Elmer O.; Hamilton, Walter C. (Brookhaven National Lab., Upton, N. Y.). J. Chem. Phys., 44: 4498-4509(June 15, 1966). (BNL–9875).

Three-dimensional neutron-diffraction data were collected for both the room-temperature (paraelectric) and the low-temperature (ferroelectric) phases of ammonium sulfate. Both phases are ordered. The transition, occurring at 223°K and involving a change from Space Group Pnam at room temperature to Space Group $Pna2_1$ in the ferroelectric phase, results in somewhat stronger hydrogen bonds in the ferroelectric phase, although there is no dramatic change in the barrier to rotation of the ammonium ions as a result of the transition. In both phases the two crystallographically independent ammonium ions have quite similar rotational barriers and hydrogen-bond strengths. The transition also results in less distorted ammonium ions in the ferroelectric phase. At room temperature, there are only two hydrogen bonds with O···H distances less than 2.0 Å. In the ferroelectric phase there are six. The mean distance is decreased by 0.1 Å in the ferroelectric phase, although the range of distances remains the same. The principal effect is thus a strengthening of the hydrogen bonds of intermediate length; this is accomplished by a reorientation of the ammonium groups. The shortest bonds at room temperature are not necessarily the shortest at low temperature. (auth)

32699 MAGNETIC CHARACTERISTICS OF $ZrNi_5$ AND $HfNi_5$ AND SOME LANTHANIDE–NICKEL COMPOUNDS HAVING THE Th_7Ni_3 STRUCTURE. Kissell, F.; Tsuchida, T.; Wallace, W. E. (Univ. of Pittsburgh). J. Chem. Phys., 44: 4651-2(June 15, 1966). (NYO–3454-2).

The magnetic characteristics of ZrH_5, $HfNi_5$, $LaNi_3$, $CeNi_3$, and $PrNi_3$ are determined. (B.G.D.)

32700 COMPUTATION OF MAGNETIC REYNOLD'S NUMBERS. Yantovskii, E. I. Magnit. Gidrodin., No. 4, 153-4(1965). (In Russian).

The magnetic Reynolds number is given by the expression $R_m = \mu\sigma vl$. Here μ is the electric conductivity, σ is the magnetic penetrability; v is the characteristic velocity, and l is the characteristic linear dimension. The value of R_m varies with v. It is proposed that the difference between the velocity of the medium and the velocity of the field be used as the characteristic velocity in the magnetic Reynolds number. Then, $R_m = \mu\sigma (v_s - v)l$. Here v_s is the drift velocity. This modification gives a correct estimate of the ratio of forces without the introduction of any other parameters. (TTT)

32701 INTENSITY AND RESOLUTION IN THE TIME-OF-FLIGHT METHOD FOR NEUTRON DIFFRACTION. Schwartz, L. H. (Northwestern Univ., Evanston, Ill. Argonne National Lab., Ill.). Nucl. Instrum. Methods, 42: 81-6(June 1966).

Expressions are derived for the integrated intensities of reflections from powders and single crystals in the time-of-flight method for neutron diffraction. The effect of collimator divergence angle on the intensity and resolution is discussed and it is shown that a fixed Bragg angle of $2\theta = 90°$ is favored for general applications with powders. Experimental and theoretical values of resolution are compared and contrasted with the resolution obtainable from the double axis spectrometer. It is shown that for comparable measuring times the time-of-flight method gives superior resolution for reflections from large interplanar spacings. (auth)

32702 SPECIFIC HEAT, ANTIFERROMAGNETISM, AND SUPERCONDUCTIVITY IN THE Cr–Re SYSTEM. Muheim, J.; Mueller, J. (Technische Hochschule, Zurich). Phys. Kondens. Mater., 2: 377-96(1964). (In German).

The investigation of the specific heat at low temperatures, superconductivity and electric resistivity in the Cr-Re system within the cubic phase shows a relatively sharp transition from an antiferromagnetic to a superconducting region. The results can fully be accounted for by the Overhauser spin-density wave theory. On the other hand, the superconducting transition temperature varies in the manner predicted by the theory of Bardeen, Cooper and Schrieffer. Both phenomena show an evident d-character. A detailed analysis gives strong indication that, although possible, a coexistence of antiferromagnetism and superconductivity in Cr-Re is rather improbable. (auth)

32703 POLARIZED POSITRON ANNIHILATION IN FERROMAGNETIC NICKEL. Mihalisin, T. W.; Parks, R. D. (Univ. of Rochester, N. Y.). Phys. Lett., 21: 610-11(July 1, 1966).

Angular correlation studies of polarized positron annihilation in ferromagnetic nickel are reported. Structure observed in the angular correlation curve is qualitatively understood in terms of recent band structure models of nickel. (auth)

32704 LIFETIMES OF POSITRONIUM IN POLYSTYRENE IRRADIATED BY THERMAL NEUTRONS. Thosar, B. V.; Kulkarni, V. G.; Lagu, R. G.; Chandra, G. (Tata Inst. of Fundamental Research, Bombay). Phys. Lett., 21: 647-8(July 1, 1966).

The intensity of the slow component in the decay of positronium in neutron irradiated polystyrene is studied as a function of the irradiation dose. The results indicate that the positronium forms and annihilates mainly in the benzene rings in polystyrene. (auth)

32705 MAGNETIC STRUCTURE OF $FeSb_2O_4$. Gonzalo, J. A. (Puerto Rico Nuclear Center, Mayaguez); Cox, D. E.; Shirane, G. Contract AT(30-2)-Gen-16. Phys. Rev., 147: 415-18(July 15, 1966). (BNL–10004).

The magnetic structure of $FeSb_2O_4$ at 4.2°K was investigated by powder neutron-diffraction techniques. The spin arrangement is noncollinear, consisting of a combination of three different antiferromagnetic modes. The principal mode (A) is one in which the Fe^{2+} moments are parallel within a given (001) layer, with adjacent layers coupled antiparallel, the moments being directed perpendicular to the tetragonal c axis. However, from the data it is not possible to specify the relative directions of the secondary modes (G and C). The value of the resultant moment is approximately 3.8 μ_B per Fe^{2+} ion. (auth)

32706 APPLICATION OF THE INVERTED-NEUTRON-FILTER TECHNIQUE TO THE STUDY OF INELASTIC SCATTERING BY PARAMAGNETIC SUBSTANCES. Friedman, E. A.; Goland, A. N. (Brookhaven National Lab., Upton, N. Y.). Contract AT(30-2)-Gen-16. Phys. Rev., 147: 457-62(July 15, 1966). (BNL–9792).

Using the filter-cutoff method the quasielastic scattering of slow neutrons from several paramagnetic compounds was measured. The results for MnF_2 at large scattering angles are in reasonable agreement with time-of-flight measurements by Cribier and Jacrot. For small scattering angles the Lorentz-like form of the energy distribution of scattered neutrons predicted by de Gennes was confirmed. Similar measurements at large and small scattering angles on a partially inverted sample of $MnAl_2O_4$ did not exhibit the predicted angular dependence. This suggests that the assumption of A-A interactions only is inappropriate for this compound. From the temperature dependence of the intensity of the (200) magnetic reflection, a Néel temperature of 18°K was deduced for the $MnAl_2O_4$. The results den-

onstrate that with an adequate flux of long-wavelength neutrons the inverted-filter technique can be employed successfully in studies of paramagnetic scattering. (auth)

32707 THEORY OF EXTENDED FINE STRUCTURE IN ABSORPTION OF POLARIZED X RAYS: APPLICATION TO GALLIUM. Perel, Joseph (Cornell Univ., Ithaca, N. Y.). Phys. Rev., 147: 463-6(July 15, 1966).

The "short-range order" method proposed by Shiraiwa et al. for calculating the extended fine structure (EFS) of the K absorption edges in polycrystalline absorbers is generalized to include the case of a crystal of arbitrary symmetry with plane-polarized incident x rays. The generalized theory is then applied to a single crystal of gallium, and the relative EFS is computed for the x-ray electric vector parallel with each of the three principal axes of the crystal. Agreement with existing experimental EFS curves with polarized x rays supports the short-range-order theory. (auth)

32708 RADIATION FROM THICK SILVER FOILS BOMBARDED BY GRAZING-INCIDENCE ELECTRONS. Jones, G. E.; Cram, L. S.; Arakawa, E. T. (Oak Ridge National Lab., Tenn.). Contract W-7405-eng-26. Phys. Rev., 147: 515-17(July 15, 1966). (ORNL-P-1997).

Silver foils several thousand angstroms in thickness were bombarded by electrons by grazing incidence. A peak was observed at approximately 3550 Å in the optical emission spectrum. For an angle of incidence of 89° from the foil normal, the peak intensity was approximately ten times as great as that of previously observed intensities of transition radiation at 3300 Å from silver foils bombarded with normally incident electrons. The intensity was found to be directly proportional to the electron energy from 40 to 80 kev, and showed a marked dependence on the quality of the foil surface. The results are in agreement with the findings of Boersch et al. (auth)

32709 COUPLING BETWEEN H^- LOCALIZED MODES AND RARE-EARTH ION ELECTRONIC STATES IN RARE-EARTH TRIFLUORIDES. Jones, G. D.; Satten, R. A. (Univ. of California, Los Angeles). Phys. Rev., 147: 566-76(July 15, 1966).

Crystals of LaF_3, CeF_3, PrF_3, and NdF_3 doped with hydrogen and deuterium were studied spectroscopically. Two strong polarized fundamentals and their combinations were observed in the infrared for both H^- and D^-. The fundamentals appear also polarized in the vibronic spectrum of doped NdF_3 coupled to several electronic transitions. Extra electronic lines appearing only in the doped crystals occur on the long-wavelength side of the usual rare-earth electronic transitions. From frequency differences, these extra levels are the parent states for the local mode vibronic transitions. The displacement of the extra electronic lines from the usual electronic transitions is mainly due to a changed crystalline field and covalency arising from the replacement of F by H, and is greater at higher levels. In addition the extra electronic levels have slightly different frequencies for hydrogenated and deuterated crystals. This isotope shift depends in both magnitude and sign on the particular electronic level and ranges from 0.5 cm^{-1} (for transitions to $^4F_{\frac{3}{2}}$) to −2.0 cm^{-1} (for transitions to $^4F_{\frac{5}{2}}$). This effect is accounted for by a large difference in zero-point amplitude for H^- and D^- localized modes which, through the electron-vibration interaction, perturbs each electronic level to a different extent. (auth)

32710 NORMAL VIBRATIONS OF POTASSIUM IODIDE. Dolling, G.; Cowley, R. A.; Schittenhelm, C.; Thorson, I. M. (Atomic Energy of Canada Ltd., Chalk River, Ont.). Phys. Rev., 147: 577-82(July 15, 1966).

The frequency/wave vector dispersion relation $\nu_i(q)$ for the normal modes of vibration of pure potassium iodide at 90°K was measured by inelastic neutron scattering techniques. The experiments were performed with both a time-of-flight machine and a triple-axis crystal spectrometer. The results obtained from the latter spectrometer were analyzed in terms of various interionic-force models. A satisfactory fit to the results is provided by an eleven-parameter dipole approximation model, which allows for the polarizability of both ions. Comparison of normal-mode frequencies calculated from this model with those observed in the time-of-flight experiments shows generally good agreement. The frequency distribution function for the normal modes, computed from the best-fit model, displays a well-defined energy gap, from 8.65 to 11.85 mev, separating the acoustic and optic modes. The moments of this function are in excellent agreement with values derived from heat-capacity data. By assuming an exponential form for the nearest-neighbor shortrange force constants, the temperature variation of the thermal expansion, and the frequency shift and inverse lifetime of the transverse optic mode of very long wavelength, were calculated and compared with the available experimental results. The occurrence of localized impurity modes in the energy gap in the frequency distribution for potassium iodide doped with potassium nitrite is briefly discussed. (auth)

32711 NUCLEAR MAGNETIC RESONANCE STUDIES OF SOLIDIFIED H_2–D_2 MIXTURES. II. PULSED TECHNIQUES. Metzger, D. S.; Gaines, J. R. (Ohio State Univ., Columbus). Phys. Rev., 147: 644-57(July 15, 1966).

Standard NMR pulse techniques are applied to the study of the H_2 resonance at 9.3 Mc/sec in solid nH_2-nD_2 mixtures at 4.2 and 1.1°K. At 4.2°K the Bloch decay for nH_2 exhibits an oxcillatory behavior that resembles the beat structure in CaF_2 observed by Lowe and Norberg. This beat structure is not observed for nH_2 concentration below 0.25. At 1.1°K the splitting of the resonance line associated with the λ anomaly is seen as a distinct beat pattern of the Bloch decay. In addition to these Bloch decays, spin echoes that persist for times long compared to the time required for the Bloch decay to vanish are observed to follow a $90° - \tau - \beta$ pulse sequence, τ being the time between pulses and β the rotation produced by the second pulse. The decay of the echoes as a function of 2τ is very nearly exponential and the associated time constant T_E, depends on the rotation β in such a way that T_E increases as β decreases. It is shown that as a result of the latter effect the echoes have maximum amplitude for $\beta = \frac{1}{2}\pi$ when τ is short but $\beta < \frac{1}{2}\pi$ when τ is long. The essential features of the Bloch decays and echoes are adequately accounted for by a single-particle model similar to the one used by Solomon to explain the multiple quadrupole echoes in KI. The hamiltonian describing the energy-level spacing of a given ortho H_2 molecule (in the rotating frame) is taken as $\hat{H}' = -\Delta\omega\hbar\hat{I}_z + \alpha\hbar\hat{I}_z^2$, where the protons of the molecule are considered to be constituents of a particle with spin unity. The parameters $\Delta\omega$ and α represent, respectively, the static intermolecular line broadening and the secular intramolecular dipole-dipole interaction. The spin-lattice relaxation time T_1 was measured using repetitive $\pi/2$ pulses. It is shown that T_1 decreases as α increases. (auth)

32712 SCHOTTKY DISORDER AND LATTICE RELAXATION IN SINGLE CRYSTALS OF NaCl DUE TO X IRRADIATION AT ROOM TEMPERATURE. Crowe, G. J.; Fuchs, W.; Wiegand, D. A. (Carnegie Inst. of Tech., Pittsburgh). Phys. Rev. Lett., 16: 1154-5(June 20, 1966).

Samples of single-crystal NaCl were x irradiated at room temperature at 250 to 300 kv peak and 20 m amp for varying periods of time. The fractional density of the negative-ion vacancies and fractional volume change due to lattice relaxation versus the fractional mass-density change are shown. It is concluded that Schottky disorder is produced by ionizing radiation. Also the results indicate that there is a mechanism by which Frenkel disorder is produced which causes expansion solely by lattice relaxation. (J.F.P.)

32713 TIME INDEPENDENCE OF CHARGE STATES PRODUCED FOLLOWING ELECTRON CAPTURE IN ^{57}Co. Triftshaeuser, Werner (Technische Hochschule, Munich); Craig, Paul P. Phys. Rev. Lett., 16: 1161-4(June 20, 1966).

The measurement of Mössbauer effect spectra at various delay times following the formation of the resonant level in ^{57}Co as an impurity in Cu, CoO, and NiO are reported. These spectra are shown. The measurements show no evidence for time effects, which would result from metastable ^{57}Fe electronic charge states. (J.F.P.)

32714 "s-d" EXCHANGE MODEL OF ZERO-BIAS TUNNELING ANOMALIES. Appelbaum, J. (Univ. of Chicago). Phys. Rev. Lett., 17: 91-5(July 11, 1966).

An analysis is made of the anomalous variations of the tunneling conductance observed near zero-bias voltage in terms of exchange interactions between tunneling electrons and magnetic states in, or near, the insulating layer of the tunnel junction. (L.B.S.)

32715 LOCALIZED MAGNETIC STATES AND FERMI-SURFACE ANOMALIES IN TUNNELING. Anderson, P. W. (Bell Telephone Labs., Murray Hill, N. J.). Phys. Rev. Lett., 17: 95-7(July 11, 1966).

A physical model is presented for the exchange interactions proposed by Appelbaum to explain Fermi-surface anomalies in tunneling. The interactions are evaluated and it is shown why the anomalous conductance need not be small compared to the direct tunneling. (auth)

32716 MICROWAVE RESONANCE OBSERVATIONS IN GADOLINIUM SOLID SOLUTIONS. Harris, A. M.; Popplewell, J.; Tebble, R. S. (Univ. of Sheffield, Eng.). Proc. Phys. Soc. (London), 88: 679-83(July 1966).

Microwave resonance measurements were made on a number of paramagnetic, ferromagnetic, and antiferromagnetic Gd–Lu, Gd–Y, Gd–Sc and Gd–La alloys. A paramagnetic value for $g = 1.998 \pm 0.005$ was obtained for those Gd–Y alloys containing small concentrations of gadolinium and close to the free-ion value; $g = 1.995 \pm 0.010$ for dilute alloys of gadolinium in scandium or lanthanum. These values compare with a value for $g = 2.010 \pm 0.010$ reported by Harris et al., in 1965 for Gd–Lu alloys of similar gadolinium content. In all alloys examined the g factor increases as the gadolinium content of the alloy decreases. The resonance line intensity of the Gd–Y and Gd–Lu alloys falls rapidly on cooling below the Néel temperature and observations were made well into the spiral-spin region. As with ferromagnetic observations there is some uncertainty as to the factors influencing the absorption and no interpretation of these lines is made. (auth)

32717 SYMMETRY OF A COLOR CENTER IN MAGNESIUM OXIDE. Ludlow, I. K. (Atomic Energy Research Establishment, Harwell, Eng.). Proc. Phys. Soc. (London), 88: 763-70(July 1966).

The symmetry of the center responsible for the 9570 cm^{-1} (10,450 Å) line, which appears in the absorption spectrum of neutron-irradiated magnesium oxide, was investigated at 77°K by analysis of the polarization spectra of the line under uniaxial stress. The line is associated with a [110] linear electric dipole oscillator in a center which has orthorhombic symmetry and [110] orientation. The peaks in the phonon-assisted spectrum of the line can be explained by taking 280 cm^{-1} and 380 cm^{-1} as the energies of the fundamental phonon modes. There is some evidence for a second zero-phonon line at 10,070 cm^{-1} having phonon energies of 380 cm^{-1} and 490 cm^{-1}. (auth)

32718 SOLID STATE PHYSICS. ADVANCES IN RESEARCH AND APPLICATIONS. VOLUME 18. Seitz, Frederick; Turnbull, David (eds.). Solid State Phys., 18: 1-435(1966).

The theory for the interaction of high energy atoms with solids and the interpretation of the experimental results in terms of the theory are described. A survey of the theory and experience on optical properties of solids is presented. The application of group theory in conjunction with crystal symmetry in band structure calculations is shown. The effect that point defects and other crystal disorders has on lattice vibrations is reviewed. (M.H.R.)

32719 PARAMAGNETIC RESONANCE OF HYDROGEN ATOMS FORMED IN FROZEN ACIDS IRRADIATED AT 77 DEG K. Zhitnikov, R. A.; Orbeli, A. L. (Ioffe Inst. of Physics and Tech., Leningrad). Soviet Phys.-Solid State (Engl. Transl.), 7: 2843-8(June 1966).

Translated from Fiz. Tverd. Tela, 7: 3522-9(Dec. 1965).

X and ultraviolet irradiation of frozen HF and HCl acids at 77°K were used to produce stabilized hydrogen atoms in these acids; the atoms were detected and investigated by paramagnetic resonance. An investigation of hydrogen atoms, stabilized in aqueous solutions of various acids frozen at 77°K, showed that the hyperfine structure splitting of these atoms depended on the acid concentration. (auth)

32720 X-RAY SPECTROSCOPIC INVESTIGATION OF THE VALENCE STATE OF SAMARIUM IN THE METAL AND IN ITS MONOSULFIDE. Blokhin, S. M.; Vainshtein, E. E.; Bertenev, V. M. (Inst. of Inorganic Chemistry, Novosibirsk, USSR). Soviet Phys.-Solid State (Engl. Transl.), 7: 2870-3(June 1966).

Translated from Fiz. Tverd. Tela, 7: 3558-61(Dec. 1965).

In view of the characteristic features of the electronic structure of the samarium atom, the L_{III} x-ray absorption spectrum of this element was investigated experimentally in the metal and in its monosulfide. It is shown that in both cases the atoms of the rare-earth element are present simultaneously in the divalent and trivalent states. In the monosulfide, the concentration of the trivalent ions increases with temperature which is explained by the thermal excitation of the $4f$-electrons to the conduction band. (auth)

32721 ELECTRICAL CONDUCTIVITY OF X-RAY-IRRADIATED FLUORITE CRYSTALS. Vladimirskii, Yu. B.; Nikitinskaya, T. I. (Kalinin Polytechnical Inst., Leningrad). Soviet Phys.-Solid State (Engl. Transl.), 7: 2912-15 (June 1966).

Translated from Fiz. Tverd. Tela, 7: 3612-16(Dec. 1965).

Measurements were made of the temperature dependence of the conductivity of synthetic CaF_2 (both pure and oxygen-bearing), irradiated with x rays, in the temperature range 80–450°C. It was found that the conductivity of pure fluorite did not change after irradiation but the conductivity of the impure crystal decreased by a factor of 100–1000 (depending on the dose). The initial electrical conductivity of the crystals was reestablished completely by heating to 300°C. It is concluded that there are two processes (fast and slow) in the reestablishment of the conductivity. The activation energy of the fast process is calculated. (auth)

32722 CHARACTERISTICS OF THE SCATTERING OF NEUTRONS BY FERROMAGNETS IN THE REGION OF FERROACOUSTIC RESONANCE. Klochikhin, A. A.; Korenblit, I. Ya. (Ioffe Inst. of Physics and Tech., Leningrad). Soviet Phys.-Solid State (Engl. Transl.), 7: 2916-22(June 1966).

Translated from Fiz. Tverd. Tela, 7: 3617-26(Dec. 1965).

The characteristics of the cross section for inelastic scattering of slow neutrons (polarized and unpolarized) are investigated in the case where the transmitted energy lies within the region of magnon resonances with longitudinal and transverse phonons. It is shown that the cross sections for incoherent scattering by single crystals and coherent scattering by polycrystalline aggregates have extrema when the transmitted energy is close to each of these resonances. In coherent scattering by single crystals, two peaks must be observed in both of these regions corresponding to the absorption and emission of a quasi-particle, independently of the relationship between the magnetic and nuclear scattering cross sections. The intensity of the peaks differs by a certain interference term, the magnitude and sign of which depend on the conditions of observation. The experimental investigation of neutron scattering in the region of ferroacoustic resonance should provide additional opportunities for determining such characteristics of ferromagnets as the exchange interaction constant and dependence of the magnetostriction constant on the frequency. (auth)

32723 ELECTRON PARAMAGNETIC RESONANCE OF TERBIUM IN CeO_2. Greznev, Yu. S.; Zaripov, M. M.; Stepanov, V. G. (Ul'yanov-Lenin State Univ., Kazan). Soviet Phys.-Solid State (Engl. Transl.), 7: 2937-8(June 1966).

Translated from Fiz. Tverd. Tela, 7: 3644-5(Dec. 1965).

The paramagnetic resonance of the Tb^{3+} and Tb^{4+} ions were detected in terbium-doped CeO_2 single crystals at 4.2°K and ~36 Gc. (B.G.D.)

32724 ROLE OF HOLE PROCESSES IN THE FORMATION OF F CENTERS IN IONIC CRYSTALS DURING THE INITIAL STAGE OF RADIATION-INDUCED COLORATION. Vilu, R. O.; Elango, M. A. (Inst. of Physics and Astronomy, Tartu). Soviet Phys.-Solid State (Engl. Transl.), 7: 2967-8(June 1966).

Translated from Fiz. Tverd. Tela, 7: 3673-6(Dec. 1965).

The temperature dependence of the efficiency of F-center formation by x rays in NaCl, KCl, KBr, and KI crystals during the first stage of the radioinduced coloration, in the temperature range from 80 to 450°K, covering the regions of the self localization of holes and intense ionic processes. (B.G.D.)

32725 IONIZATION CURRENTS IN DIAMONDS DURING IRRADIATION WITH 500 TO 1000-kev ELECTRONS. Konorova, E. A.; Kozlov, S. F.; Vavilov, V. S. (Lebedev Inst. of Physics, Moscow). Soviet Phys.-Solid State (Engl. Transl.), 8: 1-5(July 1966).

Translated from Fiz. Tverd. Tela, 8: 3-8(Jan. 1966).

It is shown that in fields exceeding 10^3 v/cm there is a deviation from the linear dependence of the product of the drift velocity and the carrier lifetime on the electric field intensity, and that in fields exceeding 10^4 v/cm this product exhibits saturation. The results obtained are interpreted on the basis of theories predicting a field dependence of the carrier mobility; quantitative estimates are in satisfactory agreement with the theory. It is shown that the electron lifetime in natural diamonds lies within the limits 10^{-11}-10^{-8} sec and, at nitrogen concentrations higher than 10^{19} cm^{-3}, the lifetime is governed by the nitrogen content. (auth)

32726 CONCENTRATION AND ENERGY OF FORMATION OF VACANCIES IN NIOBIUM, MEASURED BY THE METHOD OF MIXTURES. Chekhovskoi, V. Ya.; Zhukova, I. A. (Scientific Research Inst. for High Temperatures, Moscow). Soviet Phys.-Solid State (Engl. Transl.), 8: 6-8(July 1966).

Translated from Fiz. Tverd. Tela, 8: 9-12(Jan. 1966).

On the basis of experimental data on the enthalpy of niobium, obtained in the 600 to 2600°K temperature range, a determination is made of the concentration and energy of formation of vacancies in niobium at high temperatures. For the first time, the method of mixtures is used for measurement of these quantities. (auth)

32727 COLLECTIVE ENERGY LOSSES IN AN ELECTRON AVALANCHE. Yurkov, B. Ya. (Lebedev Inst. of Physics, Moscow). Soviet Phys.-Solid State (Engl. Transl.), 8: 59-63(July 1966).

Translated from Fiz. Tverd. Tela, 8: 77-82(Jan. 1966).

The process of electron avalanche formation in a solid is discussed. The generation of "secondary" electrons is calculated with disregard for the correlation energy, and the energy losses suffered in propagation through the substance are regarded as continuous. Summation of the collective energy losses of all avalanche electrons for the specific case of the transmission of electrons with an initial energy of 50 kev shows that about 60% of the total energy losses pass through a stage of plasma oscillations. This lends promise to the notion of creating a source of ultraviolet light using partial conversion of the energy of plasma oscillations into electromagnetic radiation. (auth)

32728 EPR OF Gd^{3+} IN YTTRIUM AND LANTHANUM DOUBLE MOLYBDATES. Zaripov, M. M.; Livanova, L. D.; Stepanov, V. G.; Falin, M. L. (Ulyanov-Lenin Kazan State Univ.). Soviet Phys.-Solid State (Engl. Transl.), 8: 188-9(July 1966).

Translated from Fiz. Tverd. Tela, 8: 238-9(Jan. 1966).

An EPR study was made on single crystals of $M^+Y(MoO_4)_2$ and $M^+La(MoO_4)_2$, where M^+ = Na, Li, K with 0.1 at. % of gadolinium impurity. The crystal growth is described. With the exception of $KY(MoO_4)_2$, all the crystals turned out to be transparent octahedra of diameters 1–2 mm. The $KY(MoO_4)_2$ crystals grew in the form of transparent plates with flat cleavage planes and exhibited the spectrum of trivalent gadolinium. The other crystals exhibited exceptionally wide absorption lines. The analysis of the data is discussed. (M.H.R.)

32729 VACANCY FORMATION IN ZIRCONIUM. Kanel, O. M.; Kraftmakher, Ya. A. Soviet Phys.-Solid State (Engl. Transl.), 8: 232-3(July 1966).

Translated from Fiz. Tverd. Tela, 8: 283-4(Jan. 1966).

In order to determine the energy of formation and concentration of vacancies in zirconium, measurements of its heat capacity at high temperature were made. The experimental method is described and errors are analyzed. (M.H.R.)

32730 ELECTRON-BOMBARDMENT-INDUCED STIMULATED EMISSION FROM CADMIUM SELENIDE. Nolle, E. L.; Vavilov, V. S.; Golubev, G. P.; Mashtakov, V. S. (Lebedev Inst. of Physics, Moscow). Soviet Phys.-Solid State (Engl. Transl.), 8: 236-7(July 1966).

Translated from Fiz. Tverd. Tela, 8: 286-7(Jan. 1966).

In order to observe the stimulated emission, the sample was cut into a rectangular parallelepiped of dimensions $600 \times 400 \times 50$ μ. The electron beam was incident on the large surface of the sample and the emission from the side faces of the sample was measured at 80°K. (M.H.R.)

32731 DEFECT FORMATION IN UV-IRRADIATED SILVER CHLORIDE. von der Osten, Wolf; Peisl, Hans; Waidelich, Wilhelm (Technische Hochschule, Darmstadt, Ger.). Z. Phys., 193: 400-11(1966). (In German).

The formation of defects in AgCl single crystals under uv and x-ray exposure and their thermal annealing are studied by measuring the optical density, the lattice parameter change, the x-ray Ag reflection and by electron microscopical observations. Specks of crystalline silver are found to be produced at the surface of the crystals as well as in the interior. According to surface and volume darkening the isochronal annealing curves exhibit two stages. The activation energy for stage I, (0.59 ± 0.08) ev, is suggested to be the energy for the thermal formation of electrons and Ag_0^+ ions from Ag aggregates. Stage II appears when the crystal is annealed in chlorine at above 523°K. It is due to the regeneration of silver at the surface, where chlorine was able to leave the crystal during exposure. (auth)

32732 ENERGY LOSS OF 50-kev ELECTRONS IN Ge AND Si. Zeppenfeld, K.; Raether, H. (Univ., Hamburg). Z. Phys., 193: 471-8(1966). (In German).

Electron-energy loss spectra of Ge and Si (amorphous, polycrystalline and monocrystalline) are measured in the low energy region of the band-band transitions and in the energy region of the plasma losses. These spectra are compared with the loss curve calculated from optical data: Discrepancies in the absolute values of the height and in the width of the plasma losses are found; the structures of the region of the band-band excitations show an agreement in the positions of the maxima, but not in their height. Additional electron energy loss maxima are observed. (auth)

32733 ABSORPTION CENTERS IN SOME GLASSES OF SIMPLE COMPOSITIONS FORMED AT LOW TEMPERATURE. Orlov, N. F.; Leko, N. A. Zh. Prikl. Spektrosk., Acad. Nauk BSSR, 4: 323-6(Apr. 1966). (In Russian).

Alkali-silicate and borosilicate glasses were exposed to γ rays of ^{60}Co at the temperature of liquid nitrogen; at the same temperature their induced absorption spectra were measured. The form and intensity of these spectra differ considerably from the spectra observed at the room temperature. (auth)

32734 OPERATOR METHODS IN LIGAND FIELD THEORY. Watanabe, Hiroshi. Prentice-Hall International Series in Chemistry. Englewood Cliffs, New Jersey, Prentice-Hall, Inc., 1966. 202p.

An introduction to operator techniques of spectral analy-

sis for the iron-group ions in crystal lattices and in complexes is presented. Particular attention is given to various types of symmetries, especially the point group symmetry, time inversion, and the concept of seniority and complementarity. Seniority theory is developed to give matrix relations to many-electron systems. A simple and direct treatment of the elements of the theory of angular momentum and of the theory of finite groups that have direct applications to ligand field theory is provided. (M.H.R.)

32735 INTERACTION BETWEEN LIGHT WAVES AND SPIN WAVES. Shen, Y. R.; Bloembergen, N. (Univ. of California, Berkeley). 49p. (CONF-650638-7). ORAU. Gmelin, AED-CONF-65-156-12.

From Physics of Quantum Electronics Conference, San Juan, Puerto Rico.

The coupling of photons and magnons can be treated by the same methods developed for the coupling between photons and phonons. The coupled wave equations are derived directly from the Hamiltonian density for the quantized fields with the density matrix formalism. The similarity between the spin-Raman effect and the vibrational raman effect is emphasized and it is shown that the spin-Raman effect will usually be one or two orders of magnitude smaller than the vibrational effect in Raman liquids. The possibility of exciting spin wave modes by light in ferro-, ferri-, and antiferromagnetic materials is discussed. The combined coupling of magnetic, vibrational and light waves is also analyzed and a magnon excitation may be induced by the stimulated Brillouin effect on a magneto-elastic mode. (auth)

32736 PHOTOCONDUCTIVE PROPERTIES OF CdS AND CdSe INDUCED BY THERMAL NEUTRON IRRADIATION. Oswald, R. B. Jr. (Harry Diamond Labs., Washington, D. C.). 23p. (CONF-650927-26). ORAU. Gmelin, AED-CONF-65-222-51.

From American Physical Society, Honolulu, Hawaii.

Experimental results show that thermal neutron induced defects alter the conductive properties of initially insulating and conducting crystals of CdS and CdSe. The production of defects by thermal neutrons results from the recoil of an energetic ^{114}Cd nucleus. The recoil energy is produced by the capture of a thermal neutron by ^{113}Cd and the prompt emission of 9 Mev of gamma energy through the nuclear reaction $^{113}Cd + n_{th} \rightarrow {}^{114}Cd + \gamma$. Thermal neutron irradiation was accomplished by reactor irradiation at a position having a gold cadmium ratio of 20 to 1. The effects produced by thermal neutrons are interpreted to be the difference in the physical properties of crystals irradiated with and without thermal neutron shields. The results indicate that thermal neutron induced defects change the photosensitivity and extend the spectral response to lower energies. A dominant effect is the introduction of electron trapping levels as measured by increases in the photoconductive decay times. (auth)

32737 TEMPERATURE DEPENDENCE OF VIBRONIC TRANSITIONS IN CRYSTALS AND SPECTROSCOPIC OBSERVATION OF A PHASE TRANSITION. Satten, Robert A.; Wong, Eugene Y. (Univ. of California, Los Angeles). 23p. (CONF-650927-16). ORAU. Gmelin, AED-CONF-65-222-10.

From American Physical Society, Honolulu, Hawaii.

The temperature dependence of vibronic absorption bands, corresponding to either one phonon absorbed or emitted simultaneously with an electron transition in a crystal having an octahedral UCl_6^{2-} complex was measured and was found to agree with the theoretically predicted results. A phase transition was observed by the weak appearance of the pure electronic transition above a transition temperature. (auth)

32738 MAGNETISM AND MAGNETIC MATERIALS: 1965 DIGEST. A SURVEY OF THE TECHNICAL LITERATURE OF THE PRECEDING YEAR. White, R. L.; Wickersheim, K. A. (eds.). New York, Academic Press, 1965. 270p.

A survey of papers which appeared during 1965, with limited supplementing by papers from other years, is presented. Topics include general theoretical problems, neutron diffraction, spin configurations, magnetic transitions, transition metals and their alloys, rare earth metals and their alloys, magnetically dilute alloys, nonmetals, properties of soft magnetic materials, and magnetically hard materials. Other topics are thin films, magnetic domains, chemistry, structure, and crystal growth of magnetic materials; nuclear magnetism, resonance and relaxation, magneto-elastic phenomena, optical effects, thermal and transport phenomena, superconductivity, and laboratory techniques and instrumentation. (J.F.P.)

32739 LOCALIZED MOMENTS. Geballe, T. H.; Matthias, B. T.; Clogston, A. M.; Williams, H. J.; Sherwood, R. C.; Maita, J. P. (Bell Telephone Labs., Murray Hill, N. J.). 28p. (CONF-650653-27). ORAU. Gmelin, AED-CONF-65-170-61.

From American Physical Society, Summer Meeting, New York.

The magnetic properties of dilute solutions of Fe in face-centered-cubic alloys made from the elements Os, Ir and Pt bear a strong resemblance to the behavior of Fe in solutions of corresponding 4d-shell elements. The localized state associated with the Fe atom shows no magnetism until the 5d-band of the matrix is fuller than Ir. The occurrence of superconductivity in the host matrix is found to correlate with the occurrence of the nonmagnetic state of Fe. In pure Ir, the isolated Fe state is at most weakly magnetic, although it contributes a very large density of states at the Fermi level. Solutions containing 5% Fe show definite magnetic properties. In Pt and Pt-rich alloys the magnetic Fe state develops a "giant moment" which is a function of the host lattice susceptibility. (auth)

32740 APPLICATION OF NUCLEAR RADIATION TO THE PUMPING OF LASERS. Derr, V. E.; McNice, G. T.; Rushworth, P. M. (Martin Co., Orlando, Fla.). 51p. (CONF-660207-21). ORAU.

From Radioisotope Applications in Aerospace Symposium, Dayton, Ohio.

One of the major limitations in the use of lasers for tactical and space applications is the availability of power supplies sufficiently portable, long-lived and powerful. A discussion is given of the possible uses of nuclear radiation either from fission or from radioisotopes in providing the primary power for pumping lasers. The employment of all forms of nuclear radiation including α, β, γ and n radiation is considered from the point of view of efficiency and availability. The characteristics of sources necessary to supply this radiation are discussed. The amount of power necessary for the threshold of oscillation is calculated for several types of lasers, gaseous and solid, and compared with the amount of nuclear pumping power available. Spectroscopic studies to establish the parameters of solid state materials favorable to nuclear pumping are described. The mechanism of energy transfer which produces optical fluorescence from the absorption of high energy radiation is discussed. The laser cut-off phenomenon is described, and its potential cures discussed. (auth)

32741 INELASTIC ELECTRON SCATTERING (EXCITATION OF PLASMA LOSSES). Raether, H. (Univ., Hamburg). 3p. (CONF-650840-1). ORAU. Gmelin, AED-CONF-65-316-1.

From International Conference on Electron Diffraction and the Nature of Defects in Crystals, Melbourne.

Electrons traversing a crystal can excite the electron plasma of a solid. Volume- and surface-plasma waves are produced. Calculations concerning energy losses in several materials are compared with observed values. The absolute probability of volume excitation is discussed. (A.G.W.)

32742 RECENT APPLICATIONS OF FIELD ELECTRON MICROSCOPY TO SURFACE PHYSICS PROBLEMS. Swanson, Lynwood W. (Field Emission Corp., McMinnville, Ore.). 35p. (CONF-650571-1). ORAU. Gmelin, AED-CONF-65-223-1.

From 3rd Annual Surface Physics Symposium, Pullman, Wash.

In recent years field electron microscopy has become established as a powerful tool for elucidating phenomena at metal and semiconductor surfaces. The undesirable perturbation of surface events by the high electric field required for field electron microscopy can be relaxed by utilization of pulsed techniques. Where it is of interest to intentionally study the effect of high electric fields on surface absorption or related phenomena, the field electron microscope can be used to great advantage. In addition to kinetical studies of surface adsorption involving single adsorbates, field electron microscopy also lends itself to investigation of co-adsorption. The present trend in surface physics toward confining work function and adsorption measurements to single well-defined crystal plane surfaces is easily accomplished with field electron microscopy by probe techniques. In recent months field electron microscopy has also been employed as a sensitive tool for the investigation of sputtering thresholds and yields for suitable combinations of substrate and impinging ions. Various methods and techniques of adapting field electron microscopy to the above measurements and typical data obtained from such measurements are discussed. (auth)

REACTOR TECHNOLOGY

General

32743 (ORNL–3944) A PROCEDURE AND A COMPUTER CODE (POWERCO) FOR CALCULATING THE COST OF ELECTRICITY PRODUCED BY NUCLEAR POWER STATIONS. Salmon, Royes (Oak Ridge National Lab., Tenn.). June 1966. Contract W-7405-eng-26. 86p. Dep. mn. CFSTI $3.00 cy, $0.75 mn.

A procedure is presented for determining the cost of power produced by a nuclear power station, assuming that all the cash expenses of the project are known, both in amount and in timing. A computer code using this procedure is described. The power cost computed by the code is levelized, that is, held constant over the life of the project. Input data that must be known in advance include the capital investments, desired rates of return on bonds and equity, fraction of investment in equity, income tax rate, project life, annual power production, and a complete schedule of cash expenditures over the life of the project. This includes operating costs, maintenance costs, and fuel-cycle expenditures. Non-cash expenditures, such as carrying charges on capital, are accounted for internally, but are not required as input. Transmission and distribution costs are excluded. The cost calculation is based on the fundamental economic requirement that the incomes received must provide for the recovery of investment, return on investment, and all operating expenses. The method used does not depend on the fixed-charge-rate concept, nor on the fuel-working-capital and carrying-charge concepts. These are part of a conventional alternative procedure for cost calculation, referred to here as the fixed-charge-rate method. This method, although widely used in the power industry, is not well adapted to engineering economic studies, because of a lack of clarity regarding the way in which fixed charge rates, interest rates, and working capital are determined. This lack of clarity has arisen because of a failure to establish a clear relationship between the fixed-charge-rate method and the more fundamental payout-of-investment method. Equations are developed here that clarify this relationship; this makes it possible to calculate true fixed charge rates and true average fuel working capital. The output of the code displays these quantities. The output also includes a tabulation showing the payout of the investment, that is, the gradual decline of the outstanding investments in bonds and equity over the life of the project. Example problems are used to demonstrate that the code provides a practical tool for use in reactor evaluation studies. These examples also demonstrate the validity of the calculated true fixed charge rates. (auth)

32744 (SRIA–1) CONTAINMENT OF FRAGMENTS FROM RUNAWAY REACTOR. Technical Report No. 1. Zabel, N. R. (Stanford Research Inst., Menlo Park, Calif.). Apr. 2, 1958. Contract (04-3)-115. 93p. Dep. mn. CFSTI $3.00 cy, $0.75 mn.

Primary emphasis was placed upon studies of penetration of steel plate by projectiles in the form of long rods. The principal result obtained from experiments is that mild steel of thickness T is penetrated if $e = 16{,}000\ T^2 + 1500\ T$, where e is kinetic energy per unit diameter of rod in foot-pounds per inch and T is in inches. This formula applies specifically when the plate is supported by a rigid backing with 4-inch opening, plate thickness lies between 0.030 and 0.25 inch; the projectile is drill rod steel with a mass between 1 and 10 ounces, a diameter of from $^3/_{16}$ to $^1/_2$ inch, and velocities are from 0 to 400 ft/sec. The range of application was extended to other values of the parameters by supplementary experiments, so that, with these corrections, this formula is expected to apply to conditions met in reactor container design. The problem of deformation of thin plates was formulated theoretically and the static case is ready for numerical computation. A theory of deformation energy for large deformation is presented. (M.O.W.)

32745 NUCLEAR CODES: WHAT ARE THEY USED FOR? WHAT FUTURE DO THEY HAVE? Tamagnini, Carla Mongini. Euratom Bull., 5: 44-8(June 1966).

The use of computer programs for solution of a set of equations describing a problem in reactor physics is discussed. The computations involved in reactor design are outlined. The computer programs are classified in the following categories: thermal spectra and data, fast spectra and data, solution of diffusion equation, solution of transport equation, burnup, kinetics, control, shielding, and heat exchangers. The problem of testing the programs is considered. The development of new and more advanced techniques of numerical computation for the various types of reactor design calculation and the possibility of carrying out series of nuclear computer programs in sequence are discussed. (M.C.G.)

32746 EXPERIMENTAL STUDY OF FUEL ASSEMBLY VIBRATIONS INDUCED BY COOLANT FLOW. Pavlica, R. T.; Marshall, R. C. (Combustion Engineering, Inc., Windsor, Conn.). Nucl. Eng. Design, 4: 54-60(May-June 1966).

Description of experiments which were run to determine the flow-induced vibrations of an assembly of fuel rods having intermediate spacer grids. The results are compared with predictions on the basis of semi-empirical formula developed by Paidoussis and Burgreen. Deviations are discussed. (auth)

32747 DECONTAMINATION SOLUTION AND METHOD. Weed, Ronald D. (to U. S. Atomic Energy Commission). U. S. Patent 3,258,429. June 28, 1966.

An aqueous decontaminating solution was developed for flushing the liquid coolant or moderator circulation systems of nuclear reactors. It consists of five components: oxalic acid, sodium oxalate, hydrogen peroxide, 8-quinolinol, and peracetic acid or a mixture of sodium gluconate and gluconic acid. (AEC)

Auxiliaries and Components

Refer also to abstract 32876.

32748 (BNWL–233) CONTAINMENT SYSTEMS EXPERIMENT. PART III. MATHEMATICAL MODELS OF PRESSURE-TEMPERATURE TRANSIENTS. Johnson, B. M. (Battelle-Northwest, Richland, Wash. Pacific Northwest Lab.). May 1966. Contract AT(45-1)-1830, 154p. Dep. mn. CFSTI $5.00 cy, $1.00 mn.

The current status of theoretical models depicting loss of coolant accidents is described. Critical two-phase flow, system blowdown models, and containment models are discussed. Further theoretical development is reported on the energy balance equations, blowdown flow rates, core pressure drop, heat transfer, and dry well downcomer flow. An evaluation of the primary system model, dry well model, wet wall model, and dry containment model was made. (M.O.W.)

32749 ELECTRONICS IN THE CONTROL OF NUCLEAR REACTORS. Di Giacomo, C. Belgicatom, Ass. Belge Develop. Pac. Energ. At., Bull. Inform., 11: No. 61, 23-9(Apr. 1966). (In French).

Typical transistorized electronic circuits for neutron flux measurements and for the control and monitoring of the reactivity are described. (J.S.R.)

32750 PRESTRESSED CONCRETE IN REACTOR TECHNOLOGY. Gibb, Michel. Euratom Bull., 5: 56-61(June 1966).

Use of prestressed concrete for reactor pressure vessels is reviewed. Adoption of prestressed concrete for gas-graphite reactor vessels is discussed. Fundamental research on prestressed concrete, design of insulation devices, and design of the vessel are described. (M.C.G.)

32751 THREE-DIMENSIONAL PHOTOELASTIC INVESTIGATION OF STRESSES IN NUCLEAR REACTOR PRESSURE VESSELS. Kono, Keisuke; Iki, Tetsuo (Mitsubishi Heavy Industries, Ltd., Tokyo). Mitsubishi Heavy Ind. Tech. Rev., 3: 115-23(Mar. 1966). (In Japanese).

Results are given from a photoelastic investigation of stresses in the closure head, flange, and nozzle of nuclear reactor pressure vessels. The tests were carried out on three model vessels made of epoxy resin: internal pressure was applied to the vessels and external force was applied to the nozzles around them. From the tests, the following can be clarified: (1) Design data for nozzles of the flush and through types, (2) Stress distribution in closure head and flange, and (3) Stress concentration factor for discontinuous parts in vessels. (auth)

32752 BLOWOUT OF THE FLAT END OF A HYDRAULICALLY PRESSURIZED CYLINDRICAL PRESSURE VESSEL. Horvay, G. (General Electric Research and Development Center, Schenectady, N. Y.). Nucl. Eng. Design, 4: 61-82(May-June 1966).

Steady-state two-dimensional incompressible potential flow analysis provides a sequence of free streamlines for the jet emerging from a ruptured pressure vessel and impacting on the blown-out fragment; these are adapted to three-dimensional flow. Thus the force acting on the blown-out end can be determined, the equation of motion solved, and the maximum rise of the fragment calculated. For the proposed design, the fragment, with the canopy on top, acquires a velocity of 22.6 ft/sec and rises 0.1 ft while the pressure in the vessel declines (in 6 msec) from 10^5 psi to atmospheric value; it rises perhaps $\frac{1}{2}$ ft while the honeycomb structure supporting the canopy collapses, and it rises less than another $\frac{1}{2}$ ft in the subsequent free travel. Thus the proposed design may be regarded as safe when the end of the container is blown out upward. The case when, during rupture, the fragment hinges, and then is propelled out sidewise, at a large angle to the vertical, requires special attention. (auth)

32753 FUEL ELEMENT MEASUREMENT SYSTEM. Merckx, K. R. (Battelle-Northwest, Richland, Wash.). Contract AT(45-1)-1830. Nucl. Eng. Design, 4: 83-9(May-June 1966).

An operational measurement system is developed which collects, analyzes, and stores the measurement data for tubular fuel elements. The measurement system is used on both unirradiated and irradiated fuel elements. The description of the measurement concept, measuring equipment, and record system are given. (auth)

32754 MINIATURE DIAMOND ULTRAHIGH PRESSURE CELL ADAPTED FOR IN-REACTOR IRRADIATION STUDIES. Kulcinski, Gerald L.; Maynard, Charles W.; Walsh, Robert C. (Univ. of Wisconsin, Madison). Rev. Sci. Instrum., 37: 871-3(July 1966).

A special Bridgman opposed diamond anvil apparatus was constructed to generate useful static-pressure to 50 kbar at ambient temperatures. It was designed to function in the environment of a nuclear reactor and to occupy 65 cc. A method of bombarding materials under pressure with fission fragments is described. (auth)

32755 MACHINES FOR LOADING AND UNLOADING THE CHANNELS OF A NUCLEAR REACTOR. Peuchmaur, Alphonse; Gilleron, Claude; Canet, Pierre (to Commissariat a l'Energie Atomique). Canadian Patent 735,588. May 31, 1966. Priority date Aug. 16, 1961, France.

A fueling machine is described which is capable of handling slugs for a horizontal reactor while the latter is at power. False slugs and protective slugs (against radiation) may be accommodated at the ends which are of larger diameter than the channel portion containing the active fuel. The means for aligning the machine with any desired channel are described. (F.S.A.)

32756 NUCLEAR REACTORS HAVING FUEL ELEMENT CHANNEL RETAINING PAWL ASSEMBLY. Coates, Didier; Laurent, Noel; Peuchmaur, Alphonse (to Commissariat a l'Energie Atomique). Canadian Patent 735,587. May 31, 1966. Priority date May 27, 1961, France.

The device is intended to prevent the return of a fuel element, once it has been inserted into a channel of the reactor. It is particularly suited to reactors with horizontal channels or for those fueled from the bottom. A thimble or tube of light metal has one end cut into a number of resilient arms or strips. A fuel element spreads these strips on insertion but once passed the ring of strips contracts to a smaller diameter thus preventing backward movement of the fuel member. The thimble is kept in position by a shoulder or by lugs in the fuel channel which articulate with holes in the thimble. (F.S.A.)

32757 MODERATOR-COOLING CIRCUIT OF A NUCLEAR REACTOR WITH SEPARATE PRIMARY CIRCUITS. Costes, Didier (to Commissariat a l'Energie Atomique). German Patent 1,213,544. Mar. 31, 1966. Priority date June 17, 1960 and May 23, 1961, France.

The heat-carrying fluid circulates in pressure tubes which are located in a moderator tank and contain fissile material, said fluid removing the greater part of the heat generated by the fissile material. The cooling circuit comprises a condenser, at least one channel connecting the moderator tank to the condenser for admission of vapor from the moderator tank into the condenser, and a second channel connecting the condenser to the moderator tank for gravity flow of the condensate obtained in the condenser to the tank. (Gmelin Inst.)

32758 NUCLEAR REACTOR PRESSURE VESSEL COVER. Tollet, Louis H. J. (to Societe Anglo-Belge Vulcain Societe Anonyme). Canadian Patent 733,608. May 3, 1966. Priority date Mar. 9, 1961, Belgium.

This cover for the reactor vessel consists of a metallic cap and a plug formed as an integral part of the cap. The plug extends into the reactor vessel and it is pierced by a number of holes of such size and shape as to accommodate the inner elements. It is claimed that this plug arrangement reduces the heavy water inventory. The effect of this additional metal within the reactor on the neutron economy is not stated. (F.S.A.)

32759 LIQUID MODERATOR NUCLEAR REACTORS. Costes, Didier; Lemaitre, Rene (to Commissariat a l'Energie Atomique). Canadian Patent 733,609. May 3, 1966. Priority date July 27, 1961, France.

To prevent damage by the failure of pressure tubes within the vessel of a liquid-moderated reactor, a variety of shock absorbing devices are placed within the rigid containing wall. These may be membranes, an annular array of closed gas-filled tubes oriented vertically, absorbent cushions and springs, or means to cause a liquid to flow into a free space, all deformable under the extra pressure of a ruptured fuel channel. (F.S.A.)

32760 NUCLEAR REACTOR CONTROL SYSTEM. Hitchcock, J. M. (to U. S. Atomic Energy Commission). U. S. Patent 3,255,086. June 7, 1966.

This invention relates to nuclear reactor control rods that have graduated form so that movement of the control rod can take place without creating significant zones of stepwise change of reactivity in the nuclear reactor core structure. The term "graduated form" refers to the reactivity effect of the control rod. In its simplest form the control rod can be made tapered or the amount of neutron absorbing material within the control rod can be varied along the length of the rod. (AEC)

32761 IMPROVEMENTS RELATING TO PHASE OR POSITION RESPONSIVE APPARATUS. McAllister, Lawrence Edward; Mackenzie, Donald (to Associated Electrical Industries Ltd.). British Patent 1,026,694. Apr. 20, 1966. Filed Jan. 26, 1962.

A phase or position responsive apparatus is described for controlling the position of a movable body and has an important application in apparatus for positioning the control rods of a nuclear reactor. Means are provided for generating recurrent electrical impulses in accordance

with the position of the body or phase of the cyclically varying quantity. At least two electrical gating circuits are provided that are periodically opened in succession during respective gating periods which are separated by a time interval. Means are included for applying the impulses to both of the gating circuits so that if the phasing is within permissive limits the impulses will reach the gating circuits during the time interval between the gating periods and will not be passed by the gating circuits; but if the limits of variation in position or phase are exceeded, the impulses will be passed by one or the other of the gating circuits depending on the direction of the error to actuate apparatus tending to correct the error in phase or displacement. Provision is also made for controlling the length of time interval between the gating periods. (B.L.M.)

32762 IMPROVEMENTS IN OR RELATING TO VALVES FOR FLUID FLOW. Jerkins, Ernest Edward (to United Kingdom Atomic Energy Authority). British Patent 1,031,515. June 2, 1966. Filed June 4, 1962.

A fluid flow valve for particular application to the control of coolant flow in the fuel channels of a reactor comprises a valve closure member movable by a hollow stem, electrically conductive temperature sensitive means carried on the valve closure member in a region exposed to fluid flow through the valve, means for allowing the fluid in the valve to pass into the hollow stem, a cable for conducting electrical signals connecting with the temperature sensitive means extending along the hollow stem and passing out from the hollow stem via a gland, a closure member for the stem at its end remote from the valve closure member, and a sampling pipe connecting with the hollow stem. When the valve is used with a reactor, the hollow stem is arranged inside a liner tube which penetrates the concrete reactor vessel wall and is sealed into the vessel wall. The closure member moves inside the tube which accepts coolant from the reactor core and discharges it through ports in the walls of the tube into a collecting chamber. The valve closure member moves to restrict or open the ports. (B.L.M.)

Criticality Studies

Refer also to abstracts 32366 and 32367.

32763 (AECL–2543) EXAMPLES OF CALCULATION OF NEUTRON DIFFUSION PARAMETERS OF A PARALLEL-PLATE LATTICE. Stewart, J. D. (Atomic Energy of Canada Ltd., Chalk River (Ontario)). Feb. 1966. 37p. (CRRP–1233). Dep. mn. AECL $1.00.

For the purpose of illustrating definitions given by the author, formulas are derived for the following cell-average and cell-surface diffusion parameters of a simple parallel-plate lattice: thermal-neutron parameters for thermal relaxation mode (source-free) and for mode produced by a cos Bz thermal source distribution, fast-neutron parameters for a cos Bz (discrete) distribution of fast neutron sources, thermal-neutron parameters for thermal distribution produced by slowing-down of these fast neutrons. (auth)

32764 (CEA-Bib–17(Pt.2)) LISTE DES CODES NUCLEAIRES UTILISES AVEC LES CALCULATEURS ARITHMETIQUES IBM 704, 709 et 7090. (Listing of Nuclear Codes for IBM-704, -709, and -7090). Bornand, Bernard (Commissariat a l'Energie Atomique, Saclay (France). Centre d'Etudes Nucleaires). Jan. 1966. 143p. Dep. mn.

The digital computer codes listed in this bibligraphy were selected on the basis of the most useful codes for reactor computations. In the listing, the reactor codes are arranged chronologically in eight different categories: burn-up, engineering, group diffusion, kinetics, transport, physics, Monte-Carlo, miscellaneous. Only burnup, engineering, and group diffusion are issued in the first section. Machine, fast memory and language are indicated. The number of the report that gives the details of the code is listed. By category an index of code names, by section an index of authors, and whole sections of an index of quoted reports are given. This bibliography was reviewed from 1957 to March 1964, for section I, from 1957 to March 1966 for section II. (auth)

32765 (IAE–957) ISSLEDOVANIE VLIYANIYA SKVAZHNOSTI BERILLIEVOGO OTRAZHATELYA NA POTOK TEPLOVYKH NEITRONOV V GORIZONTAL'NYKH PUCHKAKH. (Investigation of the Effect of Beryllium-Reflector Duty Factor on the Thermal Neutron Flux in Horizontal Beams). Aleksandrov, Yu. V.; Aleksenko, Yu. N.; Batalov, A. A.; Buinitskaya, V. I.; Kochenkov, A. S.; Sarychev, M. A. (Institut Atomnoi Energii, Gosudarstvennyi Komitet po Ispol'zovaniyu Atomnoi Energii SSSR, Moscow). 1965. 32p. Dep. mn.

The core of a square array of fuel elements on a 16 mm pitch was made up of 325 to 337 fuel elements placed in an aluminum tank with a beryllium reflector shield having dimensions of 680 × 780 mm in area by 780 mm high. A cadmium sheet 0.5 mm thick was placed between the Be reflector and the core in order to absorb thermal neutrons and thus imitate actual operating conditions. The thermal neutron distributions in the channels and in the beryllium and graphite reflectors were measured via indium foils. The epithermal flux was estimated by covering the indium foil with cadmium. The results showed that the presence of a single radial channel 13 cm from the core decreased the thermal neutron flux by 28 ± 3% in comparison with an unperturbed reflector. The position of the channels in the reflector could be varied without having a significant effect on the neutron flux. The interference of two radial channels with a 3.4 cm layer of beryllium between them decreased the thermal neutron flux by 23 ± 3%. The presence of 4 to 5 vol. % water in the beryllium had practically no effect on the flux compared to a pure beryllium reflector. The results can be used to obtain a quantitative estimate of the neutron flux in channels up to 30 cm in diameter. (TTT)

32766 (KAPL-M–6550) KINETICS OF LOW SOURCE REACTOR STARTUPS: ADDITIONAL NUMERICAL RESULTS. MacMillan, D. B. (Knolls Atomic Power Lab., Schenectady, N. Y.). Mar. 4, 1966. Contract W-31-109-eng-52. 12p. Dep. mn. CFSTI $1.00 cy, $0.50 mn.

In a 1963 paper, Hurwitz, MacMillan, Smith, and Storm discussed statistical fluctuations of neutron populations in reactors during startup with a low source. They gave numerical results of theoretical calculations of probability distributions for such startups, and a prescription for the application of these results to safeguards analysis of reactor startup. Numerical results are presented for ramp reactivity insertion rates somewhat higher than those considered above. It is shown how the results should be modified when the delayed neutron fraction, β, is 0.007 (β = 0.008 was assumed in calculating the earlier results). (auth)

32767 (UCRL–14720) POST-SHUTDOWN GENERATION OF PHOTONEUTRONS IN BERYLLIUM-MODERATED SYSTEMS. Varljen, Thomas C. (Lawrence Radiation Lab., Univ. of California, Livermore). May 15, 1966. Contract W-7405-eng-48. 51p. Dep. mn. CFSTI $3.00 cy, $0.50 mn.

Thesis. Submitted to Univ. of California, Berkeley.

A calculational method was developed for the prediction of delayed photoneutron yields in infinite, homogeneous media containing beryllium and any given fissionable species and moderating material, over any desired time interval after shutdown. The results are shown to agree with existing experimental data for pure beryllium systems, and yield predictions are made for beryllium-oxide and $BeO-OyO_2$ systems. The build-up and decay of the delayed gamma activity of individual hard-gamma-emitting product nuclides during arbitrary irradiation programs is computed. A multigroup description of the resulting photon source spectrum is then utilized. Use is made of the fact that in an infinite medium the energy history of each source photon is determined strictly by interaction

probabilities which are functions of energy only. The source photon number-energy distribution is modified to account for photon energy transfer by Compton scattering. The number of photoneutrons generated by the effective photon spectrum is then computed. A digital computer program was written to perform the calculations and produce graphical displays of the results. A series of problems was run to predict the photoneutron yield in systems using the delayed gamma activity from the products produced by the thermal fission of ^{235}U. The yield in photoneutrons per fission was computed for constant power irradiation programs of 15 minutes, 6 hours, and 74 hours, for infinite media of pure beryllium, beryllium-oxide, and 90% BeO–10% OyO_2 by weight, over time spans of 100 to 10^9 seconds after shutdown. (auth)

32768 (UNC–5148) ATHENA: A SYSTEM OF FORTRAN PROGRAMS FOR RADIATION TRANSPORT AND HEATING CALCULATIONS IN COMPLEX REACTOR GEOMETRIES. Final Report. Spielberg, D. (United Nuclear Corp., Elmsford, N. Y.). Mar. 1966. Contract NAS3-6200. 187p. (NASA-CR–54905).

ATHENA is a system of 11 coordinated programs, in FORTRAN IV for IBM-7094 and FORTRAN 63 for CDC-1604-A, for the solution of radiation transport and heating problems in complex three-dimensional geometries. Its geometry routines permit especially efficient representation of a reactor core possessing a vertical axis and hexagonal symmetry, such that any two adjacent 30-degree sectors are reflectionally symmetric with respect to the vertical plane separating them. The logic, functions, and interrelations of the component programs are described; in addition, operating instructions and details of the input and output for each program are given. (auth)

32769 STARTING OF CRITICAL ASSEMBLY IN THE NUCLEAR POWER ENGINEERING INSTITUTE OF THE BELORUSSIAN ACADEMY OF SCIENCES. Krasin, A. K.; Yaroshevich, O. I. At. Energ. (USSR), 20: 61-3(Jan. 1966). (In Russian).

The uranium-water critical assembly, called ROZA, was started up in April 1965; it was designed to carry out so-called "clean" core experiments, eliminating flux perturbations caused by beamholes or control channels. During the first series of experiments, fuel elements containing UO_2 with a 10-% enrichment were used in the assembly for the purpose of collecting data on the IRT-type cores. A 1.6 m high and 1.5 m diameter Al cylinder was used as the vessel; its design made it possible to vary the thickness of the lower reflector. The scram rod had the same diameter (10 mm) as the EK-type fuel elements; its lower portion consisted of a movable EK-type fuel element, while the upper portion contained boron carbide. Fine adjustments were made by slowly moving the movable container; the criticality increase rate cannot exceed 1×10^{-3}%. The assembly will be used for the determination of the critical mass, flux density distribution of thermal and epithermal neutrons, ratio of delayed neutrons, effect of voids on neutron leakage, etc. (TTT)

32770 PHYSICAL STAND FOR CRITICAL ASSEMBLY OF THE INSTITUTE OF PHYSICS AT THE UKRAINIAN ACADEMY OF SCIENCES. Klimentov, V. B.; Nechiporuk, V. A.; Konchinskii, G. A.; Yaroshevich, V. F.; Strutsinskii, V. A.; Popov, V. D.; Nikonov, A. V. At. Energ. (USSR), 20: 63-5(Jan. 1966). (In Russian).

The critical assembly of the Institute of Physics, installed in a separate building, was started up at the end of 1964. Fuel elements of the VVR-M reactor were used in the assembly, together with water as moderator and beryllium as reflector. A special loop was installed to add water at a controlled rate to the system. The same instrumentation, remote control systems and emergency shutdown devices were used as in the SUZ-type research reactors. Stability of the instruments is checked while the system is still at a subcritical level. When the power exceeds 0.03 watt, corresponding to an average thermal neutron flux of about 0.4×10^6 n/cm^2, the process becomes automatically controlled by a special system including two ionization chambers, a potentiometric controller, a steel absorbing rod and amplifying systems. In addition to the steel rod, three remotely operated boron rods are used to control the chain reaction. Criticality is reached by remotely filling the core region with water, after completing the "dry" assembly. The unit is suitable for carrying a wide variety of experiments in the fields of reactor physics and engineering. (TTT)

32771 XENON STABILITY IN ABSORBING-LAYER SLAB REACTOR. Stakh, V. At. Energ. (USSR), 20: 65-7(Jan. 1966). (In Russian).

An infinite-slab reactor, with a thickness H and an absorbing layer placed at a distance x_0 from one of its boundaries was examined, in order to determine the effect of the absorber on the xenon stability on the basis of the criteria developed by D. Randall and D. St. John. The perturbation equations related to the xenon and iodine concentrations were analyzed, making use of the orthogonal eigenfunctions of the neutron flux, taking into account the layer and the material parameter of the reactor in the absence of perturbation. Equations were derived and graphs plotted also for the case involving the presence of two absorbing layers in the system. The method does not take into consideration the effect of individual harmonics, which means that only the first members of the perturbation function were used. (TTT)

32772 BURNUP IN PLANE LAYER. Artamkin, V. N.; Voronkov, A. V. At. Energ. (USSR), 20: 67-8(Jan. 1966). (In Russian).

The burnup of absorbers presents complex calculation problems for the reactor designers; currently available methods, such as Monte-Carlo calculations, the S_n method give only a partial solution. This problem was more closely examined in the case of a plane, nonscattering layer with an arbitrary, although symmetrical position of the absorber in the slowing-down medium. Using approximation methods, the usual first-order differential equations were obtained; their solution allowed to determine the spatial distribution of the absorber nuclei at any given time. The burnup in the layer is given by the expression $\delta\Sigma(x,t)/\delta t = -\lambda\Sigma(x,t)$, in which $\Sigma(x,t)$ is the macroscopic absorption cross section in a point x at a time t; $\lambda = \sigma_a\phi(x,t)$, the coefficient concerning the direct or inverse time dimension, and $\phi(x,t)$ the neutron flux in a point x at a time t. The method presented makes it possible to find a graphic solution to the problem. The same method may be also in the case of the P_n approximation, (whereby $n > 1$) but in that case boundary conditions must be set for the upper limit of the reactor or the cell. (TTT)

32773 NUCLEAR MEASUREMENTS WITH A LOW POWER CRITICAL ASSEMBLY. Shaw, J. Nucl. Energy, 129-33(May 1966).

The general performance of the critical assembly at Queen Mary College (University of London) is outlined. Nuclear parameter measurements of this facility including that of critical mass, fuel coefficient of reactivity, control rod calibration, thermal coefficient of reactivity, flux distribution, power calibration and the effect of dumping the moderator are discussed. (B.G.D.)

32774 PHYSICS CALCULATIONS OF THORIUM-FUELLED HEAVY-WATER LATTICES. Gopalan, R.; Nakra, A. N.; Srinivasan, K. R.; Subramanian, T. A.; Rastogi, B. P. (Atomic Energy Establishment, Trombay, India). pp 97-105 of STI-DOC–10/52.

A simple recipe to calculate the lattice parameters of heavy-water-moderated lattices was used to compare the experimental results of ^{235}U-enriched thorium lattices. As expected, the agreement is not very good, although it is not bad. The results have shown that the recipe has to be improved especially in the calculation of the neutron spectrum. More experiments using thorium fuel are also needed to improve the calculational methods. The preliminary studies using plutonium-enriched thorium as fuel show that the discharge irradiation obtained in PHWR-type and CANDU-type reactors is comparable for the same

type of fueling, although the CANDU type seems to be slightly better. (auth)

32775 PHYSICS ASPECTS OF LARGE THORIUM-FUELLED FAST REACTORS. Singh, R. S. (Atomic Energy Establishment, Trombay, India). pp 118-26 of STI-DOC-10/52.

A parametric study was made of reactivity losses in sodium-cooled fast reactors. Doppler coefficients and sodium void effects were calculated for $^{233}U-Th$ and $^{239}Pu-Th$ fueled fast reactors. (M.O.W.)

32776 STUDIES INVOLVING REACTORS. (International Atomic Energy Agency, Vienna). pp 79-85 of STI-DOC-10/53.

Properties of moderating and multiplying media were studied by pulsed neutron techniques. Methods for absolute measurements of neutron fluxes inside reactor cores are described. (M.C.G.)

32777 EFFECTS OF HIGHER HARMONICS ON THE BEHAVIOR OF A SUBCRITICAL REACTOR. Shishkin, G. V.; Sapozhnikov, V. V. (Inst. of Nuclear Power, Academy of Sciences, Belorussian SSR). Vestsi Akad. Navuk BSSR, Ser. Fiz. Tekh. Navuk, No. 2, 5-11(1966). (In Russian).

An attempt is made to estimate the effect of higher harmonics on the behavior of a subcritical reactor by using a two-group diffusion approximation with the delayed neutrons being taken into account by combining into one group with average parametric values. The neutron balance equation in a subcritical reactor is written with an external pulse neutron source. This equation is solved in series form with particular functions of the wave equations. A relation is established between the effective multiplication coefficients for various harmonics. Values of reactivities (negative) for each of the first eight harmonics in terms of the reactivity of the main harmonic are tabulated for rectangular and cylindrical reactors. These data indicate that the higher harmonics dampen out faster than the main harmonic. The damping coefficients do not vary with time, and are determined by the decay constant of the delayed neutrons $\lambda = 0.08\ sec^{-1}$. The contribution of the higher harmonics becomes noticeable at high negative reactivities. (TTT)

32778 COMPUTATIONS OF CRITICAL SYSTEMS BY THE MONTE CARLO METHOD. Mikhailov, G. A. Zh. Vychisl. Mat. Mat. Fiz., 6: No. 1, 71-80(Jan.-Feb. 1966). (In Russian).

Various aspects of calculations of k_{eff}, the coefficient of fission of neutrons on a single generation, by the Monte Carlo method are studied. The proposed technique of computing is termed the method of generations with a constant number of points and is based on the fact that a constant quantity of division points in generations can be retained with the aid of a special algorithm. The chain of fission thus can be viewed as a uniform Markov chain defined in a special finite-dimensional space, which provides convenient properties for computer solutions of k_{eff}. The formulation of the computational method is presented wherein k_{eff} is given in approximation form. The basis of probabilistic convergence of the Markov chain is proved. An analysis of the mean square error of the proposed method is also given. (auth)

32779 UNIFICATION OF THEORY OF NEUTRON MULTIPLYING SYSTEMS. Murray, Raymond L. (North Carolina State Univ., Raleigh). 10p. (CONF-650663-1). ORAU. Gmelin, AED-CONF-65-209-5.

From 73rd Annual Meeting and World Congress on Engineering Education, Chicago.

A description is given of a program to consolidate the theory of neutron multiplying systems. A generalized treatment is based on an examination of fundamental processes and a study of the analogies and common basis of the various special methods applied to specific situations. The benefits sought include improved pedagogical approaches for courses in reactor theory, and a deeper understanding of the relation of mathematical and physical models of multiplying systems. An illustrative example is presented, demonstrating that the analyses of neutron slowing, capture, thermalization and Doppler effect can be formulated in a single analytical approach. The reaction rate for neutron interaction with a Maxwellian distribution of nuclear speeds is developed, with applicability to 1/v absorption, constant scattering and resonance absorption. (auth)

32780 CALCULATING SPACE DEPENDENT REACTOR TRANSFER FUNCTIONS USING STATICS TECHNIQUES. Macdonald, R. N.; Johnson, R. J. (Georgia Inst. of Tech., Atlanta). 15p. (CONF-651101-70). ORAU. Gmelin, AED-CONF-65-332-21.

From 13th Conference on Remote Systems Technology, Washington, D. C.

A method for calculating the space-dependent transfer function for any system that can be analyzed by static technique is outlined. (G.O.Y.)

32781 PROGRESS IN REACTOR KINETICS AT SWIERK. Bouzyk, J.; Bukowski, K.; Ciechanowicz, W.; Kubowski, J.; Latek, S.; Rafalska, J.; Suwalski, W.; Szczechla, B.; Topa, J. 56p. (CONF-651123-3). ORAU.

From Conference on Reactor Physics and Engineering, Budapest.

Some research on reactivity measurements, transfer-function measurements, and resonance-integral measurements using absorption techniques is summarized. (D.C.W.)

32782 THE APPLICATION OF THE EIGENFUNCTION EXPANSION METHOD TO NEUTRON TRANSPORT IN A MULTIPLYING SLAB SURROUNDED BY AN INFINITE REFLECTOR. Kowalska, Krystyna. 23p. (CONF-651123-12). ORAU.

From Conference on Reactor Physics and Engineering, Budapest.

The eigenfunction expansion method is used to test various approximations of the exact solution and to prepare tables of the characteristic functions appearing in the solution of plane-geometry neutron-transport problems. The expressions and numerical results obtained in these approximations are compared with those for a bare slab. The application of the same method to a problem of the time-dependent neutron distribution in a slab with a finite side reflector into which a neutron pulse was initially injected is also considered. (G.O.Y.)

32783 METHODS OF MATERIAL BUCKLING DETERMINATION IN THE HELENA SUBCRITICAL ASSEMBLIES. Dabrowski, Cyryl; Mikulski, Andrzej T. 33p. (CONF-651123-7). ORAU.

From Conference on Reactor Physics and Engineering, Budapest.

A detailed analysis of the material buckling determination in the graphite-moderated natural-uranium-fueled HELENA subcritical assemblies was carried out using neutron-flux measurements along the vertical axis and in one or more horizontal planes. (G.O.Y.)

32784 GENERAL THEORY OF EXCITATION EXPERIMENTS IN SPACE-DEPENDENT KINETICS. Moore, M. N. (San Fernando Valley State Coll., Northridge, Calif.). 45p. (CONF-660206-13). ORAU. Gmelin, AED-CONF-66-014-13.

From Symposium on Neutron Noise, Waves, and Pulse Propagation, Gainesville, Fla.

The response $\psi(\vec{q},t,E)$ of an arbitrary, linear neutronic system to a source $F(\vec{q},t,E)$, where the source is either (a) located at the base of a semi-infinite prism or (b) located within a system of arbitrary geometry is considered. It is shown that source configuration (a) results in a propagation of a signal, whose asymptotic behavior is determined by an isolated pole of the space-time transformed, energy dependent Green's function of the system. It is also shown that source configuration (b) results in excitation of spatial modes of the system, whose amplitudes are, in general, related to singularities of the transformed Green's function. In the particular case that the excitation is periodic, the modal amplitudes are directly related to

the transformed Green's function, evaluated at the excitation frequencies. Hence, in the event that a system has no isolated singularities in its transformed Green's function, the experiment (a) is excluded whereas excitation (b) becomes of interest. Two illustrative examples are then considered. (auth)

32785 RESONANCE ABSORPTION IN HEAVY WATER LATTICES DEVELOPMENT WORK AT ISPRA. Amyot, L.; Beonio-Brocchieri, F.; Boeuf, A.; Casini, G.; de Haan, W.; Diana, E.; Tassan, S. (EURATOM, Ispra, Italy). 54p. (CONF-660204-9). ORAU. Gmelin, AED-CONF-66-017-7.

From American Nuclear Society Meeting, San Diego, Calif.

The work underway at the Euratom CCR Ispra for the study of the neutron resonance absorption in natural or slightly enriched U, heavy water moderated, organic cooled reactor lattices is described. The resonance absorption in ^{238}U is discussed, and the main features of the SKAOL and the SHOCK-II code are presented as well as simplified formulas for the evaluation of effective resonance integrals. Several measurements of the effective resonance integral for ^{238}U capture of UC single-rods and U and UC clustered fuel elements of various geometries, performed at CCR Ispra are described. The results of these measurements and of similar experiments performed in Sweden are compared to the corresponding theoretical predictions. A theoretical study is made of the neutron resonance absorption in ^{240}Pu. This is basically a comparison between various theoretical methods of calculation for homogeneous and heterogeneous systems, and a check is made against the results of experiments performed at Hanford. Finally, a brief outline of the program for the future activity in this field, both theoretical and experimental, is given. (auth)

32786 NOISE ANALYSIS OF THE NUCLEAR REACTORS USING GAMMA RADIATION. Kenney, Edward S. (Pennsylvania State Univ., University Park). 22p. (CONF-660206-9). ORAU. Gmelin, AED-CONF-66-014-6.

From Symposium on Neutron Noise, Waves, and Pulse Propagation, Gainesville, Fla.

The possibility of using gamma radiation in nuclear reactor noise analysis was investigated. Moreover, the delayed gamma rays were found to have a readily understandable effect on the measurements providing the possibility of studying their time behavior by using reactor oscillator techniques. Above one cycle per second, neutron and gamma ray detected noise was similar with the gamma ray method suffering principally from long-lived fission product background problems. The effects of the separation of detector and core appeared to be less severe for the gamma ray detection method. With both detection systems, at high power, the noise spectrum was markedly different than expected with a breakpoint in the region of 4 cycles per second. The known β/l^* breakpoint at 26 cycles per second was obscured in all high power noise measurements but obvious in the oscillator work and low power neutron noise measurements. (auth)

32787 STUDIES OF SUBCRITICAL LATTICES WITH DISTRIBUTED NEUTRON ABSORBER BY MEANS OF THE PULSED NEUTRON SOURCE TECHNIQUE. Bliss, H. E. 10p. (CONF-651101-76). ORAU. Gmelin, AED-CONF-65-332-106.

From 13th Conference on Remote Systems Technology, Washington, D. C.

The theoretical base for pulsed-neutron measurements of the multiplying properties of subcritical lattices, using the addition of a distributed neutron absorber, are outlined; and results are presented for two clean lattice configurations. The results of steady-state measurements in the same lattices and in modified lattices are also presented. (D.C.W.)

Design and Feasibility

32788 HELIUM AT WORK: PEACH BOTTOM ATOMIC POWER STATION. Cryog. Eng. News, 1: No. 8, 56-8 (June 1966).

The helium coolant is traced through a cycle from reactor core to steam generator to helium compressor and back to the reactor. The purge stream with its purification and refrigeration means is discussed at length. (M.H.R.)

32789 HETEROGENEOUS THERMAL NUCLEAR REACTOR AND METHOD OF OPERATION. Knecht, Othmar (to Interatom). German Patent 1,213,545. Mar. 31, 1966. Filed Mar. 5, 1960.

The nuclear reactor comprises tubes situated within the core and containing liquid fuel, which is supplied from a reservoir outside the core by means of a pump. The shim and control of the reactor is attained by varying the level in the tubes. (Gmelin Inst.)

Fuels

Refer also to abstract 31706.

32790 (ANL-6930) PARAMETRIC STUDIES OF THE REACTIVITY COEFFICIENTS FOR LARGE ^{233}U-Th-FUELED FAST REACTORS. Singh, R. S.; Hummel, H. H. (Argonne National Lab., Ill.). Jan. 1966. Contract W-31-109-eng-38. 28p. Dep. mn. CFSTI $2.00 cy, $0.50 mn.

The feasibility of using $^{233}U-Th$ as a fuel in a large fast breeder reactor was studied from the point of view of the Doppler and sodium-void coefficients. The composition and temperature-dependent cross sections for thorium were evaluated by using the latest resonance parameters available. The sodium-void coefficient was studied in detail over a range of compositions and sizes of core for metal and oxide fuels, and the effect of the addition of ^{234}U and fission products on the coefficient is also investigated. The reactivity coefficients due to the Doppler effect are calculated for metal- and oxide-fueled systems of interest. The results indicate that, even with present cross-section uncertainties, the reactivity changes due to both the sodium loss and the Doppler effect are encouraging for the development of fast breeder reactors with very large single cores if ^{233}U and thorium are used as the fuel. (auth)

32791 (NAA-SR-Memo-11731) TEMPERATURE DISTRIBUTIONS FOR VARIOUS FUELS WITH NONUNIFORM HEATING. Noyes, R. C. (Atomics International, Canoga Park, Calif.). Nov. 19, 1965. Contract AT-11-1-GEN-8. 29p. Dep. mn. CFSTI $2.00 cy, $0.50 mn.

Comparative fuel temperature calculations were made for U-Pu carbide, oxide, and cermet fast reactor fuels in $\frac{1}{4}$ in. O.D. clad fuel pins at 20 kw/ft. Representative heat distributions were for irradiation in SRE thermal fluxes in 7-rod clusters and for enrichment between 10 and 20% Pu. The effect of nonuniform heating as compared to uniform heating at 20% enrichment was found to be a reduction in peak fuel temperature of 4-6% of ($T_{max}-T_{Na}$) and an off-center displacement of the point of maximum fuel temperature of 10-20% rod radius. Calculations assumed a constant fuel conductivity, heat transfer coefficient, and local coolant temperature. An exact solution of the conduction equation for these conditions was used. This solution and the digital program used for the calculations are described. (auth)

32792 BUSINESS PATTERN OF THE NUCLEAR FUEL INDUSTRY. Turk, Roland. Euratom Bull., 5: 48-54 (June 1966).

The problem of long-term uranium supplies in the Euratom Community is considered under three headings: requirements, industrial resources for satisfying the requirements, and commercial relations between producer and consumer. (M.C.G.)

32793 NUCLEAR REACTOR FUEL ELEMENT. Koutz, Stanley Lee; Turner, Richard Franklin; Fortescue, Peter (to General Dynamics Corp.). German Patent 1,213,542. Mar. 31, 1966. Priority date July 31, 1961, United States.

The fuel element comprises an annular outer container fabricated of neutron moderating material having a low

permeability to fission products, preferably low permeability graphite, within which are disposed a plurality of generally cylindrical fuel compacts. The fuel compacts are annular and are stacked upon an elongated, vertically disposed central spine of neutron moderating material. An adsorber unit is disposed below the fuel compacts which adsorbs the issuing fission products. A purifying gas is passed downward through the container. (Gmelin Inst.)

32794 POST BUCKLING BEHAVIOR OF HYDRAULICALLY COLLAPSED ASSEMBLY FUEL PLATES. Scavuzzo, R. J. (Univ. of Toledo). 19p. (CONF-651101–67). ORAU. Gmelin, AED-CONF-65-332-14.

From 13th Conference on Remote Systems Technology, Washington, D. C.

An analytical investigation of the post-buckling behavior of flat fuel plate assemblies is summarized. The results show that a sinusoidal deflection shape can be expected and that the wavelength of the buckled plate depends on the fluid velocity. (D.C.W.)

Power and Power-Breeder Reactors

32795 (ACNP–66538) LA CROSSE BOILING WATER REACTOR RADIO AND WATER CHEMISTRY MANUAL. Mueller, James J. (Allis-Chalmers Mfg. Co., Bethesda, Md. Atomic Energy Div.). June 1, 1966. Contract AT (11-1)-1357. 233p. Dep. mn. CFSTI $6.00 cy, $1.25 mn.

The preparation of carrier solutions and standardization procedures to conform with the carrier requirements of the radiochemical procedure included are described. The counting techniques and data handling procedures are described. Water chemistry procedures for determining constituents in reactor steam and water are outlined. A collection is also presented of radiochemical procedures for determining the activity of selected radionuclides. Dissolution procedures for quantitative removal of sorbed activity from ion exchange resin and dissolution of insoluble corrosion products are given. The analyses used during reactor operation are described. (M.O.W.)

32796 (AI-CE–3) HEAVY WATER ORGANIC-COOLED REACTOR. Quarterly Technical Progress Report, January 8, 1965–June 30, 1965. (Combustion Engineering, Inc., Windsor, Conn. Nuclear Div. Atomics International, Canoga Park, Calif.). Aug. 15, 1965. Contracts AT(38-1)-383; AT(38-1)-386. 543p. Dep. mn. CFSTI $8.43 cy, $2.25 mn.

A study was undertaken to develop an advanced converter reactor. Separate detailed investigations on the reactor development are presented as follows: fuel channel assembly development, fuel element assembly development, materials development, coolant technology, reactor physics, reactivity control, on-power refueling, 1000 Mw(e) plant engineering, and 300 Mw(e) plant engineering. (M.O.W.)

32797 (LA-DC–7748) FAST TRANSIENTS IN LIQUID PLUTONIUM. Carmichael, B. M. (Los Alamos Scientific Lab., Univ. of California, N. Mex.). [1966]. Contract W-7405-eng-36. 9p. Dep. mn. CFSTI $1.00 cy, $0.50 mn.

Fast transients in clean fuel were studied using a code, TRN, which is being developed specifically for applications to molten Pu capsules. The code calculates distributed values for the power, temperature, pressure, and motion of the fuel in capsules for given reactivity input functions. Calculations are presented. (M.O.W.)

32798 (LA-DC–7550) FAST REACTOR DEVELOPMENT IN THE UNITED STATES: LOS ALAMOS MOLTEN PLUTONIUM PROGRAM. Hannum, William H. (Los Alamos Scientific Lab., Univ. of California, N. Mex.). [1965]. Contract W-7405-eng-36. 9p. (CONF-660502–1). Dep. mn. CFSTI $1.00 cy, $0.50 mn.

From British Nuclear Energy Society Conference on Fast Breeder Reactors, London.

A core fueled with molten plutonium (LAMPRE I) was operated successfully for over two years. A versatile ternary fuel was selected which appears adequate for use in a well-designed central-station fast breeder core. The reliable containment of this fuel appears to be feasible, and the MPBE will demonstrate this capability. In the present concepts, a tantalum container is used. The associated parasitic neutron losses are tolerable in a hard spectrum, if the plutonium content of the fuel is properly selected as a compromise between heat transfer and breeding potential. The major potential advantages for molten plutonium in a near-term application (e.g., second generation, central-station fast breeders) lie in safety and fuel element lifetime and performance. The main incentive for the program, however, lies less in its near-term capabilities, which are significant, than in the fact that such a near-term use would constitute a base for realistic and potentially spectacular further advances. (auth)

32799 (LA-DC–7752) EVALUATION OF EXISTING REACTORS FOR THE IRRADIATION OF LIQUID PLUTONIUM FAST REACTOR FUELS. Ragan, G. L. (Los Alamos Scientific Lab., Univ. of California, N. Mex.). [1966]. Contract W-7405-eng-36. 4p. Dep. mn. CFSTI $1.00 cy, $0.50 mn.

A brief discussion of the LAMPRE-I, FRCTF, and OWR reactors for irradiation testing of molten Pu fuels is presented. (M.O.W.)

32800 (ORNL–3936) MOLTEN-SALT REACTOR PROGRAM SEMIANNUAL PROGRESS REPORT FOR PERIOD ENDING FEBRUARY 28, 1966. (Oak Ridge National Lab., Tenn.). June 1966. Contract W-7405-eng-26. 224p. Dep. mn. CFSTI $6.00 cy, $1.25 mn.

Separate abstracts were prepared for the 7 included sections. (M.O.W.)

For abstracts of individual sections see: 31683, and 32801–32806.

32801 (ORNL–3936, pp 7-52) MSRE OPERATIONS. (Oak Ridge National Lab., Tenn.).

Operations concerning the MSRE during this period are reported for the following: analysis of experiments, dynamic tests, systems performance, component performance, and instrumentation and control. (M.O.W.)

32802 (ORNL–3936, pp 53-81) COMPONENT DEVELOPMENT. (Oak Ridge National Lab., Tenn.).

Some changes were made in several of the MSRE components. Brief discussions on component development are presented for the following: freeze valves, control rods, control rod drive units, radiator doors, radiator heater electrical insulation failure, sampler-enricher, coolant salt sampler, off-gas system, fuel processing system sampler, off-gas sampler, remote maintenance, pump development, and instrument development. (M.O.W.)

32803 (ORNL–3936, pp 82-92) MSRE REACTOR ANALYSIS. (Oak Ridge National Lab., Tenn.).

For the purpose of on-line computation of control rod reactivity with the TRW-340 data logger, a mathematical formula was fitted to the rod-worth vs position curves obtained from calibration experiments. The form of the expression used was obtained by applying a perturbation technique to evaluate the integral expression for the rod reactivity. A linear least-squares curve-fitting procedure was then used to evaluate the unknown coefficients in the resulting functional expression. Close agreement between calculated and experimental curves was obtained for those configurations of shim and regulating rods of interest in monitoring the control rod reactivity during operation. Theoretical calculations were made to estimate the influence of the overall spatial distribution of ^{135}Xe absorbed in pores near the graphite surfaces in the reactor core. The purpose was to determine spatial correction factors for use in the on-line calculation of ^{135}Xe reactivity with the TRW-340. Based on an approximate model of the reactor core, these calculations indicated that the equilibrium

^{135}Xe reactivity at 10 Mw is reduced by a factor of about 0.76 relative to the value obtained from a "point" calculation. In addition, this correction was found to depend on the time history of the power level. Results of calculations are presented for step changes in power level, increasing to and decreasing from 10 Mw. (auth)

32804 (ORNL–3936, pp 122-71) CHEMISTRY. (Oak Ridge National Lab., Tenn.).

Three innovations were introduced in the chemical analysis of MSRE salts: a new end point for uranium titrations, a new method for determining structural-metal ions, and a new method for oxide analyses. Together they have given increased assurance that fuel conforms to the inventory composition and that the chemical purity of the salt was maintained. Examination of deposits believed to be responsible for the plugging of off-gas lines in the MSRE revealed the presence of oil and polymer products presumed to have formed from oil. A negligible amount of salt was found. In a study of the physical chemistry of fluoride melts, vapor-pressure measurements were made for three compositions in the $LiF-BeF_2$ system. Because of vapor-phase association, the apparent volatility of LiF increases with decreasing concentration of LiF in the melt. Methods were developed for predicting density, specific heat, and thermal conductivity in molten fluorides. The solubility of oxide in MSRE-related fluoride melts was reevaluated with improved experiments. When increasing amounts of ZrF_4, as present in the MSRE fuel, are added to flush salts, the capacity for oxide first decreases, then increases. Interest in reprocessing methods for MSBR fluorides has led to continuing studies of distillation and of chemical reduction as a means of separating rare earths from fuels or protactinium from blankets. The composition that yields MSRE barren solvent as distillate was found; this product distills, leaving the rare earths behind. Alloys of bismuth containing a small amount of lithium have proved very effective for reducing and extracting rare earths into a liquid-metal phase. Thorium was found effective as a reducing agent for removing protactinium from blanket melts. Protactinium can also be removed on ZrO_2. The in-pile molten-salt loop experiment and associated auxiliary equipment are being fabricated and assembled so that modifications to beam hole HN-1 in the ORR and installation of equipment can begin in April. The precision and accuracy of the hydrofluorination method for determining oxide in MSRE salts were established. The method was applied to the analysis of nonradioactive samples taken during the startup of the MSR; the results were in reasonable agreement with those obtained by the $KBrF_4$ method. The hydrofluorination apparatus for the determination of oxide in radioactive samples was fabricated and tested and is now being installed in a hot cell. Ionic iron and nickel were determined voltammetrically on a sample of molten fuel withdrawn from the MSR. These measurements indicate that the major fraction of iron and of nickel in the fuel is present in an un-ionized state, presumably as finely divided metal. Also, a well-defined voltammetric wave for the reduction U(IV) → U (III) was observed. Efforts were continued on the development and evaluation of equipment and procedures for analyzing radioactive MSRE salt samples. The coulometric uranium procedure was modified to eliminate a negative bias. Both flush- and fuel-salt samples were analyzed for U, Zr, Cr, Be, F, Fe, Ni, and Mo. The analyses were routinely performed in the hot cells of the High-Radiation-Level Analytical Laboratory. The quality control program was continued during the past period. The results obtained on synthetic solutions established more realistic limits of error for the methods employed. (auth)

32805 (ORNL–3936, pp 172-92) MOLTEN-SALT BREEDER REACTOR DESIGN STUDIES. (Oak Ridge National Lab., Tenn.).

Design and evaluation studies were made of thermal molten-salt breeder reactors (MSBR) in order to assess their economic and nuclear potential and to identify important design and development problems. The MSBR reference design concept is a two-region, two-fluid system with fuel salt separated from the blanket salt by graphite tubes. The energy produced in the reactor fluid is transferred to a secondary coolant-salt circuit which couples the reactor to a supercritical steam cycle. On-site fluoride volatility processing is employed, which leads to low unit processing costs and economic reactor operation as a thermal breeder. The resulting power cost is estimated to be 2.7 mills/kwhr for investor-owned utilities; the associated fuel cycle cost is 0.45 mill/kwhr (electrical); the specific fissile inventory is 0.8 kg/Mw (electrical); and the fuel doubling time is 21 years. Development of a protactinium removal scheme for the blanket region of the MSBR could lead to power costs of 2.6 mills/kwhr (electrical), a fuel cycle cost of 0.33 mill/kwhr (electrical), a specific fissile inventory of 0.7 kg/Mw (electrical), and a fuel doubling time of 13 years. (auth)

32806 (ORNL–3936, pp 193-211) MOLTEN-SALT REACTOR PROCESSING STUDIES. (Oak Ridge National Lab., Tenn.).

A close-coupled facility for processing the fuel and fertile streams will be an integral part of a molten-salt breeder reactor system. The fuel salt will be processed on a 40-day cycle. The uranium will be removed from the carrier salt and fission products by fluorination, and the carrier salt will be recovered from the fission products by a semicontinuous vacuum distillation. Relative volatilities between lithium and the rare earths were measured to be 0.01 to 0.04 at 900 to 1050°C. The reconstitution of the fuel salt, by combining the purified carrier salt with the purified UF_6, can be done by direct absorption of the UF_6 in fuel salt which already contains some UF_4 and subsequent reduction of the intermediate uranium fluoride to UF_4 with hydrogen. Experimental tests showed rapid and complete absorption. The primary problems in continuous fluorination of the fuel salt to remove the uranium are corrosion and getting adequate mass transfer and countercurrent flow to assure good recovery. Corrosion can probably be eliminated by the use of a layer of frozen salt on the wall of the vessel. Experimental work with a small countercurrent continuous fluorinator gave recoveries of 90 to 96% of the uranium. Fluorination during the processing of the fuel from the MSRE produces volatile chromium fluorides. These can be effectively trapped, with negligible uranium losses, by use of sodium fluoride beds. A preliminary design study was made on a conceptual processing plant incorporating the above concepts. Among the problems which this study illuminated were the complications from the handling of high-heat-generating materials. The fixed capital cost for the conceptual plant was $5.3 million; the salt inventory cost was $0.196 million, and the direct operating cost was $787,790.00 per year. (auth)

32807 (STI-DOC-10/52) UTILIZATION OF THORIUM IN POWER REACTORS. Report of a Panel held in Vienna, 14–18 June 1965. Technical Reports Series No. 52. (International Atomic Energy Agency, Vienna (Austria)). Apr. 1966. 382p. IAEA: $8.00; S168,-; Pound 2.8.0; F Fr 32,-; DM 28,-.

Separate abstracts were prepared for the 23 included papers. (M.O.W.)

For abstracts of individual papers see: 31326, 31438, 31700, 31701, 31767, 32774, 32775, and 32819–32834.

32808 (TID–22973) THE GROWTH OF FOREIGN NUCLEAR POWER. Benedict, Manson; Gols, George A.; Hogerton, John F.; Hopper, Wilbert H.; Jensen, James T.; Stephan, Richard A.; Smith, Don W.; Turner, F. Cort; Old, Bruce S.; (and others) (Little (Arthur D.) Inc., Cambridge, Mass.). Apr. 1966. Contract AT(30-1)-3604. 98p. Dep. mn. CFSTI $4.00 cy, $0.75 mn.

A review was made of published projections on electric energy demand and nuclear power growth. Typical sources were the United Nations, the World Bank, the Agency for International Development, Euratom, the World Power Conference, the International Atomic Energy Agency, Organization for Economic Cooperation and Development, and Edison Electric Institute. On the basis of these projections, estimates were made of electric energy demands and nuclear power growth by nation. A study was made of

the competitive position of fossile fuels and hydroelectric power generation in selected countries. A preliminary study was also made of the capital and operating cost projections for the types of nuclear reactors most likely to be utilized in the period through 1980. (M.O.W.)

32809 (TID-23101) CARBON IN THE PRIMARY SODIUM SYSTEM OF THE ENRICO FERMI ATOMIC POWER PLANT. Technical Memorandum No. 35. Chase, W. L.; Huebotter, P. R.; Kovacic, E. C.; MacLeod, R. A.; Moore, C. R.; Shoudy, A. A. (Atomic Power Development Associates, Inc., Detroit, Mich.). Aug. 1, 1963. Contract AT (11-1)-476. 40p. Dep. mn. CFSTI $2.00 cy, $0.50 mn.

When APDA conducted the 1000 F high temperature tests on the primary system of the Enrico Fermi Atomic Power Plant, carbonaceous gases and vapors were evolved from the graphite in the reactor plug. The efforts that were expended to determine the amount of carbon evolved, the methods suitable for removing the carbon from the sodium, the possible problems that could be caused by the carbon, and methods of operational control of the carbon are outlined. Based upon the study conducted, there should be no further outgassing from the plug due to temperature. Some gas may be evolved each year due to radiation. However, these gases should be mostly hydrogen. Any carbonaceous gas that should be evolved can be readily dissolved into the sodium and removed in the carbon removal system thereby forming no crust. To date, the experiments on methods of removing carbon from sodium are not complete. However, sufficient data are in to indicate that of the possible problems that could be postulated as being caused by the off-gases none appear to be serious. Additional experimental work is under way to provide high-power operating criteria for Fermi. The plugging indicator orifice plate at Fermi was redesigned to provide orifices of 0.030 inches in diameter to indicate particle sizes that would be of the order of the pore size of the screens in the reactor subassemblies. (auth)

32810 GUNDREMMINGEN NUCLEAR POWER PLANT. Jaerschky, Rudolf; Leistner, Bernhard. A E G Mitt., 56: 65-74(1966). (In German).

The essential characteristics of the dual circuit boiling water reactor at Gundremmingen, the arrangement of the most important installation constituents, and the individual buildings are described. The mode of operation of the reactor is discussed. The construction characteristics of the turbine, the condenser, and the generators and some peculiarities of the conventional heat circuits are treated. The control behavior, the operation and monitoring of the installation, and the electrical circuits are briefly described. (tr-auth)

32811 EMERGENCY POWER SUPPLY IN THE GUNDREMMINGEN POWER PLANT. Zwoenitzer, Dieter. A E G Mitt., 56: 75(1966). (In German).

In order to guarantee that the most important electrical installations in a nuclear power plant remain operational in the case of power failure, an independent emergency current installation is necessary. In the Gundremmingen power plant a completely automatic diesel emergency power supply was installed. It consists of two units of 1350 kva each. Their construction and its adaptation to the total installation of the nuclear power plant were described. The automatic circuitry was especially considered. (tr-auth)

32812 BOILING WATER REACTOR CONSTRUCTION OUTLINE OF THE AEG. Bruechner, Hans-Joachim; Taurit, Rudolf. A E G Mitt., 56: 76-81(1966). (In German).

The boiling water reactor projects of the AEG are incorporated by the Kahl, Gundremmingen, and Lingen nuclear power plants and the Grosswelzheim super heated steam reactor installation. The project of 600-Mw(e) boiling water reactor should form the continuation of the construction outline to economically competitive large nuclear power plants capable of construction at the present. In a parallel aim the additional development of the boiling water reactor to integrated boiling superheated reactors and finally to vapor-cooled fast breeders should be carried on. (tr-auth)

32813 EFFICIENCY OF ENERGY TRANSFORMATION IN POWER REACTORS. Kriese, Siegfried. At. Strom, 12: 25-31(Mar.-Apr. 1966). (In German).

The energy transformation process beginning with the energy released through nuclear fission up to the output of the working stream from the steam generator represents the greatest source of losses by irreversibilities in a power plant. The work lost modifies significantly the thermal output of the nuclear reactor and therefore its installation cost. Because of the specific heat loss it also modifies significantly the fuel element cost of the power plant. Therefore a special significance is attached to the energy transformation efficiency of the steam producing reactors. The relations for the efficiency of these energy transformations are given and the question of the effect of various factors on the efficiency of the energy transformation is discussed. (tr-auth)

32814 TECHNICAL-ECONOMIC CALCULATION METHOD FOR DETERMINING THE OPTIMUM TYPE OF ATOMIC POWER STATION AND THE COMPETITION BETWEEN ATOMIC AND CLASSICAL POWER STATIONS. Dinculescu, C.; Danila, N.; Wlezek, C. Bull. Inst. Politeh. Bucuresti, 27: No. 6, 57-80(Nov.-Dec. 1965). (In Rumanian).

A new method of technical economic calculation for determining the optimum type of atomic power station is established based on the criterion of the calculation of the minimum yearly expenses a problem of theoretical and practical interest, both in Rumania and abroad. The proposed method may also determine the relative economic merits of atomic and classical power stations. The way to perform the technical-economic calculations of the method by means of electronic computers and the results obtained are shown. (auth)

32815 PROBLEMS OF CORROSION IN NUCLEAR REACTORS. III. TREATMENT AND DISPOSAL OF LIQUID WASTES IN A NUCLEAR POWER PLANT: A YEARS EXPERIENCE AT THE GARIGLIANO POWER PLANT. Della Rocca, C. Calore, No. 10, 520-9(1965). (In Italian).

The Garigliano BWR (150 MWe) has produced more than one billion of kwh in 18 months of full power operation. The direct operating experience of the liquid radioactive waste system during the above period is considered. The various sources of waste water during full power operation are discussed, together with detailed information on the nature of the isotopes present in the mixture, their mode of formation and transport to the waste system, and their concentrations before and after processing. The liquid waste treatment plant is described, and reasons for design and operating criteria are given. Operating data concerning volumes, activity, chemical quality, concentration and total values of the activity in the batches discharged to the environment, are also presented in detail. (auth)

32816 NUCLEAR POWER PROGRAMME IN INDIA. Magal, B. S. Elec. India, 5: No. 2, 23-9(1965).

Tarapur Atomic Power Station and Rana Pratap Sagar Atomic Power Plant were described. (auth)

32817 DEVELOPMENT OF ATOMIC ENERGY IN INDIA. Ghaswala, S. K. Energ. Nucl., 8: 160-4(May 1966).

The activities of the Tata Institute of Fundamental Research in Bombay and the Atomic Energy Establishment in Trombay are described, with emphasis on the installations at the Trombay station, which has three reactors. The work done by the Trombay research groups is also discussed. The characteristics of two nuclear power stations (at Tarapur and at Rajasthan) that are being constructed, as well as those of a third being planned in the state of Madras, are described. (auth)

32818 FAST REACTORS. Smith, R. D. (Atomic Energy Establishment, Winfrith, Eng.). Sci. J., 2: No. 5, 62-6(May 1966).

The long range advantages in fuel economy of the fast

reactors are described. The history of the fast reactor development in various countries and the engineering problems involved are outlined. Some schemes for solving these problems are mentioned. (M.H.R.)

32819 SUMMARY REPORT AND RECOMMENDATIONS. (International Atomic Energy Agency, Vienna). pp 1-32 of STI-DOC-10/52.

The existing programs for thorium utilization in the various countries represented at the conference are briefly summarized. Thorium reserves in Africa, Asia, Austria, and North America are described. The technical status of research and future work is described. (M.O.W.)

32820 PHYSICS ASPECTS OF DISPERSED FUEL REACTORS CONTAINING THORIA. Gemmell, W. (Australian Atomic Energy Commission Research Establishment, Lucas Heights). pp 33-45 of STI-DOC-10/52.

Neutron buckling and fission ratios for $^{235}U-Th-BeO$, $^{233}U-Th-BeO$, $Pu-Th-BeO$, and $Pu-^{233}U-Th-BeO$ subcritical assemblies were measured. The reactivity worth of cubes of BeO containing dispersed ThO_2 particles was measured in a well-thermalized spectrum with 1/E tail for five particle sizes and for two moderator ratios. (M.O.W.)

32821 THORIUM-CYCLE POSSIBILITIES IN THE BRAZILIAN NUCLEAR POWER PROGRAMME. Santos, J. C. (Comissao Nacional de Energia Nuclear, Rio de Janeiro); Brito, S. S.; Mello, J. C.; Urban, C. W. pp 46-54 of STI-DOC-10/52.

Preliminary results are presented on possible advantages of thorium reactors in a nuclear program for South Central Brazil. (M.O.W.)

32822 PRELIMINARY ASSESSMENT OF THORIUM AS A FUEL FOR THERMAL REACTORS. Duret, M. F.; Halsall, M. J. (Atomic Energy of Canada Ltd., Chalk River, Ontario). pp 55-76 of STI-DOC-10/52.

A comparison was made of various combinations of the fissile materials ^{233}U, ^{235}U, Pu, and the two fertile materials ^{238}U and ^{232}Th in thermal reactors having a neutron economy similar to that of CANDU. The basis for this comparison is the fuel cost such as the manufacturing cost, interest on fuel inventory, and processing costs. The operating fuel cost depends on manufacturing cost and the fuel rating. A single once-through fuel cycle followed by processing was considered. The effect of further recycling is taken into account by ascribing a value to the irradiated fuel. (M.O.W.)

32823 SOME ASPECTS OF THE THORIUM CYCLE IN HEAVY WATER REACTORS. Naudet, R. (Commissariat a l'Energie Atomique, Centre d'Etudes Nucleaires, Saclay, France). pp 77-89 of STI-DOC-10/52. (In French).

Properties of the thorium cycle are clarified by means of simplified calculations, and some general remarks on the neutron economy of the cycle are deduced. The study is limited to the cycles primed and maintained using ^{235}U and concerns especially heavy-water reactors. The primary passage of the ^{232}Th in the reactor is considered, and the variation of burn-up as a function of the initial conditions is studied. Then recyclings are examined. (M.J.T.)

32824 THORIUM FUEL PROGRAMMES IN THE FEDERAL REPUBLIC OF GERMANY. Boettcher, A. (Kernforschungsanlage, Juelich, Ger.). pp 90-2 of STI-DOC-10/52.

A brief summary of thorium utilization in German reactors is presented. The thorium fuels and fuel elements and reprocessing are briefly described. (M.O.W.)

32825 THORIUM IN PEBBLE-BED REACTORS. Schulten, R. (Kernforschungsanlage, Juelich, Ger.). pp 93-6 of STI-DOC-10/52.

Typical design data for a pebble bed reactor using thorium fuel are given. The fuel element types and fuel management schemes are outlined. Advantages and disadvantages are outlined. (M.O.W.)

32826 ROLE OF THORIUM IN A NUCLEAR POWER PROGRAMME. Paranjpe, S. R. (Atomic Energy Establishment, Trombay, India). pp 106-14 of STI-DOC-10/52.

The role of thorium in a nuclear power program is discussed with respect to conservation of fossil and nuclear fuel resources. (M.O.W.)

32827 THORIUM–URANIUM FUEL CYCLE IN ITALY. Orsenigo, G. (Comitato Nazionale per l'Energia Nucleare, Rome). pp 127-37 of STI-DOC-10/52.

The construction status of the PCUT (Programme Ciclo Uranio Thorio) facility is briefly described. Uranium–thorium fuel cycle costs for the PCUT are presented. (M.O.W.)

32828 THORIUM FUEL UTILIZATION RESEARCH IN JAPAN. Tomoda, C. (Atomic Energy Bureau, Science and Technology Agency, Tokyo); Sawai, S. pp 138-45 of STI-DOC-10/52.

The use of thorium in the Japanese semi-homogeneous and aqueous homogeneous reactors is briefly discussed. (M.O.W.)

32829 THORIUM CYCLE AND THE HOMOGENEOUS SUSPENSION REACTOR PROJECT. Hermans, M. E. A.; Kersten, J. A. H.; Warschauer, K. A.; Went, J. J. (Euratom–RCN–KEMA, Arnhem, Netherlands). pp 146-64 of STI-DOC-10/52.

The use of a thorium fuel cycle in homogeneous liquid fuel reactors is discussed. A general outline of the fuel test facility for developing a liquid suspension that will be acceptable fuel for a power breeder or near breeder reactor is presented. Some hydrodynamic problems associated with the transport of five suspension heavy particles in a circulating liquid are briefly described. (M.O.W.)

32830 SWEDISH WORK ON THE ^{232}Th–^{233}U FUEL CYCLE. Almgren, B. (AB Atomenergi, Stockholm). pp 169-71 of STI-DOC-10/52.

A brief description of Swedish research on the $^{232}Th-^{233}U$ fuel cycle is presented. (M.O.W.)

32831 FUEL BREEDING IN INTERMEDIATE ENERGY URANIUM–THORIUM WATER MODERATED REACTOR. Levin, I. K. (USSR State Atomic Energy Commission. I. V. Kurchatov Inst. of Nuclear Energy, Moscow). pp 172-85 of STI-DOC-10/52. (In Russian).

Computer calculations were carried out on a dual-purpose uranium-thorium breeder reactor having a cylindrical shape with a central active zone containing $^{233}UO_2$, H_2O, and the construction materials Ni, Fe, and Cr and a ring breeding zone containing ThO_2, H_2O, Fe, Ni, and Cr. A 12-group program of calculation of a homogeneous reactor with hydrogeneous moderator was used, and for the reactor equations the P_1-approximation of the kinetic equation and the single-velocity equation of thermal-neutron diffusion were employed. Variations with different concentrations of water and construction materials in the active and breeding zones were explored. The dependence of the breeding coefficient on spectral hardness, quantity of poisoning absorbers, reactor dimensions, and choice of nuclear-physics constants used in the calculations was studied, and the change of breeding coefficient during reactor operation was considered. (M.J.T.)

32832 ECONOMIC INCENTIVE FOR THORIUM REACTOR DEVELOPMENT. Lane, J. A. (Oak Ridge National Lab., Tenn.). pp 199-211 of STI-DOC-10/52.

The use of breeder reactors and the role of thorium for conservation of our natural uranium resources are discussed. An economic point of view is considered. (M.O.W.)

32833 IRRADIATION BEHAVIOR OF THORIUM–URANIUM ALLOYS AND COMPOUNDS. Olsen, A. R.; Trauger, D. B.; Harms, W. O.; Adams, R. E.; Douglas, D. A. (Oak Ridge National Lab., Tenn.). pp 246-91 of STI-DOC-10/52.

A review is presented of data obtained from different irradiation test programs on sol-gel and conventionally pro-

cessed thorium-base fuels, as metal-clad bulk oxides and as-coated particles. Finally, the available data on the irradiation characteristics of thorium-base metallic fuels are presented. (M.O.W.)

32834 TECHNICAL AND ECONOMIC CHARACTERISTICS OF THORIUM REACTORS. Rosenthal, M. W.; Bauman, H. F.; Bennett, L. L.; Carlsmith, R. S.; Vondy, D. R. (Oak Ridge National Lab., Tenn.). pp 353-72 of STI-DOC-10/52.

An investigation was made to estimate the performance and power costs that will be achieved with various proposed thorium reactors if they are built in the 1970's. The design information was taken from conceptual designs of 1000 Mw(e) reactors provided by developers of the concepts. A set of economic factors that represent the average conditions over the life of reactors built during that period was defined and physics performance, capital, operating, and fuel cycle costs for all of the reactors were estimated on a consistent basis. For comparison with the Th reactors, similar estimates were made for a 1000 Mw(e) light-water moderator, pressurized water reactor. (M.O.W.)

32835 SAFETY SYSTEMS FOR GAS-COOLED GRAPHITE-MODERATED REACTORS. Vojinovic, Mirko; Carapic, Miodrag (Boris Kidric Inst. for Nuclear Science, Belgrade). Tehnika (Belgrade), No. 3, 507-12(1964).

Basic requirements for safety circuits and systems are analyzed. Descriptions are provided of parameters and channels which control and are part of the safety systems. A system having a majority logic "2 of 3" suitable for a powerplant with a gas-cooled graphite-moderated reactor is described. (auth)

32836 BURNUP ANALYSIS IN LUMPY FUEL. Robkin, M. A. 33p. (CONF-651101-71). ORAU. Gmelin, AED-CONF-65-332-58.

From 13th Conference on Remote Systems Technology, Washington, D. C.

The irradiation of a fuel pin of UO_2–1.5% PuO_2 fuel containing 17% ^{240}Pu was performed in a boiling-water reactor. A model was developed by which the radial variation of the isotopic evolution could be calculated, and the results obtained from this model were compared with the experimental results. (G.O.Y.)

32837 A PRACTICAL PROCESS FOR PRODUCING LARGE QUANTITIES OF ^{237}Np AND ^{238}Pu IN COMMERCIAL POWER REACTORS. Ransohoff, J. A.; Defelice, Joseph A. 14p. (CONF-651101-65). ORAU. Gmelin, AED-CONF-65-332-15.

From 13th Conference on Remote Systems Technology, Washington, D. C.

A hard-spectrum fuel cycle which would be economically practical for increasing substantially the production of ^{237}Np and of ^{238}Pu in existing power reactors is described. (G.O.Y.)

32838 CURRENT BURN-UP PROCEDURE AND FUTURE REQUIREMENTS FOR H.T.G.C.R. EXPERIMENTAL FUELS AT A.A.E.C. RESEARCH ESTABLISHMENT. Smythe, L. E.; Thackray, M. (Australian Atomic Energy Commission Research Establishment, Lucas Heights). 7p. (CONF-650602-83). ORAU. Gmelin, AED-CONF-65-125-111.

From American Nuclear Society 11th Annual Meeting, Gatlinburg, Tenn.

The research carried on at the Research Establishment of the Australian Atomic Energy Commission is discussed. The techniques used for fuel burnup determinations are described including dissolution procedures, cesium decontamination, mass spectrometry of uranium isotopes, and burnup measurements using beryllium-10 accumulation. (J.F.P.)

32839 FUTURE CROSS SECTION NEEDS OF THE NUCLEAR POWER INDUSTRY. Snyder, Thoma M. 16p. (CONF-660303-32). ORAU. Gmelin, AED-CONF-66-034-3.

From American Physical Society, Conference on Neutron Cross Section Technology, Washington, D. C.

As the nuclear power industry grows to a position of dominance in the generation of electric power, the industry needs for neutron cross section data will swing towards the goals of efficient utilization of the enormous by-product isotope production capacity, accurate measurement of nuclear fuel burn-up performance using fission product isotope concentrations, meaningful monitoring of the radiation damage potential of fast neutron fluxes with convenient neutron threshold reactions and a broad grasp of the nuclear properties of the actinides relevant to criticality and nuclear safety. These data needs are discussed in detail. (auth)

32840 DOPPLER COEFFICIENT MEASUREMENTS IN ZEBRA CORE 5. Baker, A. R.; Wheeler, R. C. (Atomic Energy Establishment, Winfrith, Eng.). 29p. (CONF-651009-24). ORAU. Gmelin, AED-CONF-65-307-41.

From Conference on Safety, Fuels, and Core Design in Large Fast Power Reactors, Argonne, Ill.

The Doppler coefficient was measured for various assemblies of fissile and non-fissile pins within the loop of the Zebra core 5. The temperature coefficients were also measured in the range of 300 to 600°K. The results indicate that the Doppler effect varies roughly with the inverse temperature.

Process Heat Reactors

32841 (ORNL-3882) AN ECONOMIC STUDY OF THE PRODUCTION OF AMMONIA USING ELECTRICITY FROM A NUCLEAR DESALINATION REACTOR COMPLEX. Blanco, R. E.; Holmes, J. M.; Salmon, R.; Ullmann, J. W. (Oak Ridge National Lab., Tenn.). June 1966. Contract W-7405-eng-26. 54p. Dep. mn. CFSTI $3.00 cy, $0.50 mn.

One example of the use of large blocks of low-cost nuclear power predicted for the foreseeable future would be production of hydrogen and ammonia fertilizer by the electrolysis of water. The cost of ammonia production at a nuclear desalination site via electrolysis was compared with the cost using the conventional steam-methane reforming process. Factors studied included power cost, natural gas cost, production rate, return on investment, type of electrolytic cell, by-product oxygen credit, and transportation cost. Using electrolytic cells that operate at very high current densities, ammonia can be produced for $39/ton with power at 2.5 to 3.0 mills/kwhr. Such power costs are obtainable on an incremental basis from commercial light-water reactors. Large advanced reactors producing power at 1.6 mills/kwhr appear to be capable of producing ammonia competitive in the United States (assuming a credit for by-product oxygen) with steam-methane reforming using natural gas at 29 to 33¢ million Btu's. The average U. S. industrial natural gas price in 1963 was 34¢ per million Btu's. The production of hydrogen and ammonia fertilizer at a nuclear desalination site is considered sufficiently attractive to justify further study. (auth)

32842 (STI-DOC-10/51) NUCLEAR ENERGY FOR WATER DESALINATION. Report of a Panel held in Vienna, 5-9 April 1965. Technical Reports Series No. 51. (International Atomic Energy Agency, Vienna (Austria)). Mar. 1966. 136p. (CONF-650420). IAEA: $3.00; S63,-; 18/-stg; F Fr 12,-; DM 10,50.

Separate abstracts were prepared for 7 of the 18 included articles. Ten of the remaining articles appear only as abstracts. The remaining article appeared previously in NSA as 19: 29647. (M.O.W.)

For abstracts of individual papers see: 31192–31194, and 32845–32848.

32843 THE HEATING OF SOILS USING THE COOLING CYCLE OF A POWER REACTOR. Grauby, A. (Centre d'Etudes Nucleaires, Cadarache, France). Energ. Nucl., 8: 193-4(May 1966). (In French).

The problems connected with the building of a nuclear power station in an agricultural area led to the establishment of a relation between the disposal of hot water from

the power station and the local agricultural needs, especially for obtaining crops outside of full production periods. Soil heating is a technique in general use in agriculture and which can be carried out by using the cooling cycle of power station condensors. This use of hot water allows the modification of production periods by creating a micro-climate. This technique can be extended, it seems to large areas (several thousands of hectares) and it may have a good effect on the local economy and on the cost of the nuclear kilowatt. (auth)

32844 NUCLEAR REACTORS: A POSSIBILITY OF SUPPLYING HEAT NEEDS. Schwarz, K. (Zentralinstitut fuer Kernforschung, Dresden). Energietechnik, 15: 342-50(Aug. 1965). (In German).

The raw energy situation in the DDR was summarized. The necessary uranium needs for the years 1965 to 1985 were determined assuming the use of tested nuclear energy installations. The application of nuclear energy to electricity production and heat supply was considered. In the investigation of the economy of nuclear energy it was shown that in mining areas heat producing nuclear installations are more costly than nuclear power plants when the installations are compared with conventional power plants. It is assumed that sufficiently large heat centers with high utilization time could become competitive. (tr-auth)

32845 SUMMARY REPORT AND RECOMMENDATIONS. (International Atomic Energy Agency, Vienna). pp 1-15 of STI-DOC-10/51.

A summary of highlights of the latest developments pertaining to nuclear desalination and related topics is presented. Recommendations of the conference panel on the Agency's role and future activities in nuclear desalination are discussed. (M.O.W.)

32846 TECHNICAL AND ECONOMIC ASPECTS OF THE USE OF NUCLEAR REACTORS FOR DESALINATION OF WATER AND ELECTRIC POWER GENERATION. Loginov, A. A.; Koryakin, Yu. I. (State Committee on the Utilization of Atomic Energy, USSR). pp 60-73 of STI-DOC-10/51.

The general properties of dual-purpose plants are briefly discussed. Methods for determining the cost of fresh water and electric power are briefly described. An analysis was made of the prime cost of fresh water and electric power. The results are presented. (M.O.W.)

32847 SOME CONSIDERATIONS ON UTILIZING A CANADIAN HEAVY-WATER REACTOR IN A DUAL-PURPOSE POWER-DESALINATION PLANT. Williams, N. L. (Civilian Atomic Power Dept., Canadian General Electric Co, Ltd., Peterborough, Ont.). pp 91-101 of STI-DOC-10/51.

An analysis was made of a Canadian heavy water reactor for the purpose of evaluating its performance for electric power generation and sea water desalination. Results are discussed. (M.O.W.)

32848 THE DEVELOPMENT OF THE ELECTRICAL ENERGY DEMAND IN GREECE AND OF THE WATER SUPPLY OF THE ATHENS AREA. Delyannis, A. (International Atomic Energy Agency, Vienna). pp 105-9 of STI-DOC-10/51.

The power production and demands in Greece are briefly discussed. The use of a dual-purpose reactor is discussed. (M.O.W.)

32849 BOILING WATER REACTOR. White, G. (General Electric Co., San Jose, Calif.). 20p. (CONF-660311-3). ORAU. Gmelin, AED-CONF-66-037-2.

From Symposium on Water Production Using Nuclear Energy, Tucson, Ariz.

The boiling water reactor, as one of the lowest cost sources of thermal or electric energy available for desalting projects, has been the subject of numerous evaluations over the past few years. The energy cost, which can constitute 30–50% of the total cost of desalted water and can also directly influence the capital investment in the desalter, continues to show a downward trend. Boiling water reactors are now competitive with other energy sources using less than 20¢/MBtu fuel. In consequence, these BWRs can supply heat at ~200°F from the turbine exhaust for less than 10¢ per 1000 pounds of steam. During the past year or so, the rate of BWR commitments has built up to a level of over 2,500 MWe per annum. The design of BWRs required for desalting plants differs very little from these commitments for central station applications. It is concluded that the past few years of encouraging development of the various desalting plant concepts have been paralleled by a comparable gain in BWR operating experience and performance capability, thus further helping maximize the overall promise of current desalting program efforts. (auth)

Propulsion and Space

See also ENGINEERING — Space Propulsion

Refer also to abstract 31618.

32850 (LA-DC-7689) PROJECT ROVER LIQUID HYDROGEN SAFETY: A FIVE YEAR LOOK. Ehrenkranz, T. E. (Los Alamos Scientific Lab., Univ. of California, N. Mex.). [1965]. Contract W-7405-eng-36. 15p. (CONF-660605-2). Dep. mn. CFSTI $1.00 cy, $0.50 mn.

From Cryogenic Engineering Conference, Boulder, Colo.

Large scale use of liquid hydrogen has been associated with Project Rover at Jackass Flats, Nevada, since 1959. There were misadventures; these, together with the advice of specialists led to continuing improvements in procedures and equipment. Main components of the liquid hydrogen system are described; incidents and the lessons learned are related and the gradual refinement of safety devices and procedures are traced. It is felt today that standing operating procedures, control over incompatible operations, room inerting, remote control of high hydrogen flow rates and proven equipment reliability make the main contributions to carrying out large scale liquid hydrogen operations with confidence. (auth)

32851 (N-65-30544) CONTROL OF ABSORPTION CROSS SECTION FOR A NUCLEAR ROCKET. Shen, C. N.; Liu, T. C. (Rensselaer Polytechnic Inst., Troy, N. Y. Dept. of Mechanical Engineering). Apr. 1, 1965. 33p. (NASA-CR-64248; AC-3). CFSTI $2.00 cy, $0.50 mn.

The two energy and one delayed-neutron group kinetics equations with approximations are employed for the nuclear rocket. The perturbation equations for kinetics are derived with the assumption that the deviation from the reference flux are small in comparison with the reference values. The temperature effect due to the change of the Fermi age may be compensated by a feedback loop. The absorption cross section is changed accordingly so that the system will be made independent of the effect of temperature variation. The spatial distribution of the Flux and precursor are assumed to be sinusoidal in the axial direction of the nuclear rocket. The reduced kinetics equations are obtained from the perturbed equation by introducing exponential weighting function. The index of performance is chosen to be the integral of the square errors on perturbed neutron flux and the control effort. Maximum principle is used to derive the control laws which in turn determines the absorption cross section, using the measured flux as feedback with a variable gain. The response of the flux and precursor having optimum control under different starting conditions is determined and plotted. (STAR)

32852 (NAA-SR-Memo-11454) SNAP-10A ELECTRICALLY ACTUATED BAND RELEASE DEVICE (EABRD) DEVELOPMENT. Summary Report. Kranz, I. H.; Adams, R. J.; Prowett, R. H. (Atomics International, Canoga Park, Calif.). Nov. 24, 1965. Contract AT-11-1-GEN-8. 67p. Dep. mn. CFSTI $3.00 cy, $0.75 mn.

The EABRD development program has resulted in the selection of the single tube René 41 housing with the one-piece heater bobbin and the U-bolt cable restraint as the

reference design. The high strength housing consists of a thin-walled tubular section with attachment fittings at either end for connection to the reflector retainer band lugs. The heater consists of a tungsten wire element wound on a ceramic bobbin. Electrical current is delivered to the heater element by a high temperature shielded cable. Actuation occurs when the internal heater is energized and raises the temperature of the tubular section to its fusion temperature. The configuration studies and materials evaluations which lead to the final design selection are described. Design verification tests were performed to establish confidence that the reference design EABRD would successfully meet the SNAP 10A Qualification Test requirements. These tests include the following: (1) firing tests, (2) tensile tests, (3) dynamic load tests, (4) thermal-vacuum endurance tests, (5) maximum no-fire current tests, and (6) irradiation tests. Based on the results of these tests, the reference design EABRD appears to satisfy the SNAP 10A system requirements. (auth)

32853 (NAA-SR-Memo-11925) OPTIMUM POWER TRANSMISSION CABLE WEIGHT. Sobo, D. J. (Atomics International, Canoga Park, Calif.). Apr. 20, 1966. Contract AT-11-1-GEN-8. 28p. Dep. mn. CFSTI $2.00 cy, $0.50 mn.

The optimum specific weight for an Aluminum conductor circular cross section power transmission cable delivering 5 and 15 Kw of d-c power at 28 volts was determined as a function of system incremental specific power. Weighting factors for the optimum specific weight of the transmission cable as a function of temperature are also developed, as are curves for the specific cable power loss and voltage drop. A discussion of design difficulties which may be encountered for the cable unreeling mechanism, cable meteoroid protection, and cable temperature control is also included. Since optimum specific weight can be reduced by transmitting power at a higher voltage, recommendations are made concerning future work for cable design. (auth)

32854 CONSTRUCTION OF SHIP REACTORS. Bogaardt, M. Atoomenergie Haar Toepass., 8: 97-110(May 1966). (In German).

A review is given of the ship reactor projects in various lands. A description is then given of the construction of ship reactors and the cost distribution for a nuclear propulsion installation. (tr-auth)

32855 SAFETY CONSIDERATIONS IN THE USE OF NUCLEAR DEVICES IN SPACE. Lieberman, Joseph A.; Connor, Gerald B. (Atomic Energy Commission, Washington, D. C.). Health Phys., 12: 743-9(June 1966).

The primary safety objective in the design and use of nuclear devices in space is a low probability of introducing the radioisotope or fission product inventories of the devices into the biosphere. The secondary objective is the control of those inventories that might be introduced into the biosphere to ensure that contamination or radiation uptake levels are well below acceptable general population radiation protection guides. Within the design characteristics of space missions presently conceived for nuclear devices, no hazard is presented to the world's population from a space reactor or radioisotope generator. The fission product inventory of a space reactor seen in the biosphere at some distant time can be reduced to almost zero through the employment of various combinations of reactor startup in orbit, positive and reliable ground commanded or on-board fail-safe reactor shutdown systems, aerodynamic burnup of the reactor, and dispersal of fuel particulates at high altitudes on reentry, and long-lived orbital lifetimes. The safe situation with the radioisotope generators can be achieved through some combination of missile trajectory shaping, orbital lifetime that is commensurate with the isotope half life, and a positive means of post-operation disposal, possibly by reentry burnup. The radiologic considerations and mode of safety analysis of nuclear devices are summarized, and approval for space use of nuclear devices, and the aerospace nuclear safety research and development and test programs underway in relation to the factory-flight-reentry sequence are reviewed. (auth)

32856 DEVELOPMENT OF A TITANIUM PRESSURE VESSEL FOR NERVA. Snyder, C. R. (Aerojet-General Corp., Sacramento, Calif.). J. Spacecraft Rockets, 3: 437-9(Mar. 1966).

The development of a titanium pressure vessel for NERVA reactors is briefly discussed with emphasis on the materials studies and fabrication studies that were performed. The bases for the selection of the Al–Sn–Ti alloy that was used are summarized. (D.C.W.)

32857 SNAP 50/SPUR BOILER DEVELOPMENT. Van Hagan, T. H. (AiResearch Manufacturing Co., Los Angeles). 27p. (CONF-651101-72). ORAU. Gmelin, AED-CONF-65-332-22.

From 13th Conference on Remote Systems Technology, Washington, D. C.

The design and status of the SNAP 50/SPUR K boiler are discussed. The steps leading to the fabrication and successful testing of the first conventional-alloy multitube K boiler are outlined. (G.O.Y.)

Research and Test Reactors

Refer also to abstract 31964.

32858 (ANL-7166) SAFETY ANALYSIS FOR THE ZPR-9 FACILITY. Cohn, C. E.; Rosenberg, G. S.; Dates, L. R.; Loewenstein, W. B.; Golden, G. H. (Argonne National Lab., Ill.). Feb. 1966. Contract W-31-109-eng-38. 14p. Dep. mn. CFSTI $1.00 cy, $0.50 mn.

An Addendum to ANL-6271, Safety Analysis Report, Argonne Fast Critical Facility (ZPR-6).

The safety aspects of ZPR-9 were examined for the same class of experiments that were earlier approved for ZPR-6, as a basis for approval of ZPR-9 operation. This class comprises unmoderated systems ranging from small, highly enriched cores to large, dilute configurations having core volumes up to about 1500 liters. The physics of metal, oxide, and carbide cores, the effects of heterogeneity, and the reactivity of hypothetical core-meltdown configurations are some of the investigations made. The experimental program on ZPR-9 involves tungsten-based cores, fueled with ^{235}U and diluted with aluminum and/or graphite. The reflector material will be aluminum, low-carbon steel, or depleted uranium. (M.O.W.)

32859 (DP-991) OPERATIONAL SUMMARY OF THE HEAVY WATER COMPONENTS TEST REACTOR, OCTOBER 1961–DECEMBER 1964. Kiger, Eugene O. (Du Pont de Nemours (E. I.) and Co., Aiken, S. C. Savannah River Lab.). Apr. 1966. Contract AT(07-2)-1. 78p. Dep. mn. CFSTI $3.00 cy, $0.75 mn.

The Heavy Water Components Test Reactor (HWCTR) is a pressurized reactor that is cooled and moderated with heavy water. The reactor is located at the Savannah River Plant, Aiken, South Carolina, and was operated for the Atomic Energy Commission by the Du Pont Company. It was designed for the purpose of testing, at actual operating conditions of flow, temperature, and pressure, candidate fuel assemblies and other reactor components for a heavy water power reactor fueled with natural or slightly enriched uranium. The startup and operating history of the HWCTR from October 1961 to December 1964 is described. The reactor facility was shut down in December 1964. (auth)

32860 (GEAP-5108) SOUTHWEST EXPERIMENTAL FAST OXIDE REACTOR DEVELOPMENT PROGRAM. Quarterly Report No. 7, November 1965–January 1966. Horst, K. M. (comp.) (General Electric Co., San Jose, Calif. Advanced Products Operation). Feb. 1966. Contract AT(04-3)-540. 94p. Dep. mn. CFSTI $3.00 cy, $0.75 mn.

Further research developments in the SEFOR program are reported on the following: the experimental program in ZPR-III, fuel development, special instrumentation,

steady-state and transient characteristics of the core assembly, reactivity controls required for experimentation, fuel handling, and core design. (M.O.W.)

32861 (N-66-12348) MODIFICATION AND MAJOR OVERHAUL OF CRYOGENIC IRRADIATION FACILITY AT PLUMBROOK REACTOR FACILITY. (Lockheed Nuclear Products, Marietta, Ga.). [1964]. Contract NAS3-6210. 165p. (NASA-CR-54770; ER-8207). CFSTI $5.00 cy, $1.00 mn.

Implementation is discussed for the overhaul, modification, repair, and instrument calibration of the equipment used in combined nuclear-cryogenic material studies. The equipment includes a gaseous phase helium refrigerator system, the test loops with their transfer system, and associated instrumentation and appurtenances. The report includes a reliability evaluation of the equipment and a projected maintenance schedule predicated on the results. (STAR)

32862 (ORNL-P-2160) IRRADIATION FACILITIES IN THE OAK RIDGE NATIONAL LABORATORY BULK SHIELDING REACTOR. Kelley, B. C.; Klabunde, C. E. (Oak Ridge National Lab., Tenn.). Apr. 1966. Contract W-7405-eng-26. 28p. (CONF-660511-5). Dep. mn. CFSTI $2.00 cy, $0.50 mn.

From International Symposium on Capsule Irradiation Experiments, Pleasanton, Calif.

Five unique irradiation facilities for materials testing and solid state research are described. These are: the Thermal Neutron Irradiation Facility, the Liquid Helium Cryostat, the Position Five Facility, the Liquid-Nitrogen Cooled Cryostat, and the Fast-Flux Irradiation Facility. (M.O.W.)

32863 (TID-23037) KINETICS PARAMETERS OF A HIGHLY ENRICHED HEAVY-WATER REACTOR. Final Report, February 26, 1965-February 25, 1966. Graham III, W. W.; Cohn, C. E.; Harmer, D. S.; Clement, J. D.; Johnson, R. J.; Macdonald, R. N.; Patrick, R. E.; Reynolds, J. M. (Georgia Inst. of Tech., Atlanta. School of Nuclear Engineering). Apr. 1, 1966. Contract AT(38-1)-403. 74p. (NE-5). Dep. mn. CFSTI $3.00 cy, $0.75 mn.

A method of accounting for the effect of the previous power history of the reactor was developed and used in the evaluation of the reactor kinetics parameters. The detailed results of the measurements of the neutron flux decay following a rod drop in the Georgia Tech Research Reactor and a compilation of effective delayed neutron and photoneutron relative abundances and decay constants were reported. The kinetic parameters, required for precise calculations of the kinetics behavior and reactivity of a reactor, were not previously determined for a reactor of this specific type. A counting system with resolution of better than 200 nanoseconds was developed utilizing newly-devised fast electronics fission chambers, resulting in greatly improved counting statistics. A value of 9.8 sec^{-1} for the ratio of the effective delayed neutron fraction to the prompt neutron lifetime was measured using the pile oscillator technique. The space dependence of the oscillator-detector reactor transfer function was demonstrated by pile oscillator measurements. Presently, the effective delayed neutron fraction of the GTRR is being measured. This work involves the calibration of the reactor power by a method of measuring the coolant flow rate and temperature rise across the core, coupled with corrections for small heat losses in auxiliary systems. These results, together with a technique for extrapolating the power calibration to low power levels (of the order of 100 to 1000 watts), will be combined with results of a noise analysis experiment to yield a measured value for the effective delayed neutron fraction. (auth)

32864 ON DETERMINATION OF NEGATIVE REACTIVITY BY SHOT SOURCE METHOD. Drozdov, F. S.; Rychev, A. S. At. Energ. (USSR), 20: 74-5(Jan. 1966). (In Russian).

For reasons of radiation safety, the subcritical state of the IGR reactor, designed for large excess reactivity was determined during the installation period by the so-called "shot-through" source method. The method involved instantaneous or periodic excitation of activity by sending a source rapidly through the reactor by means of a pneumatic tube, recording the neutron flux ϕ_1 when the source was in the system and the flux ϕ_2 after the "shot-through" period. The reactivity was determined on the basis of these flux data and from the portion of the effective delayed neutrons. The accuracy of the measurements is increased by using shot-through periods which are much smaller than the time of life of prompt neutrons. The method is quite simple, requiring only a suitable pneumatic tube and a Po-Be source. A 5×10^7 n/sec. source was sent through the core within a period of 0.07 to 0.1 second, using an ionization chamber to record the flux. The method was found suitable for ensuing the subcritical state of the reactor. (TTT)

32865 LOOP DOSE TRANSFORMER. Starodubtsev, S. V.; Abdukadyrova, I. Kh.; Generalova, V. V. (Inst. of Nuclear Physics, Academy of Sciences, Uzbek SSR). Izv. Akad. Nauk Uz. SSR, Ser. Fiz.-Mat. Nauk, No. 1, 62-4(Jan.-Feb. 1966). (In Russian).

The operating principle of a loop dose-meter is based on the recording of physiochemical changes in aqueous glucose solutions circulating through the active zone of a reactor. The use of such a system allows the remote and continuous measurement of an absorbed dose of mixed radiation in one of the vertical channels of a VVR-S reactor without substantial disturbance of the dose field of the active zone. The working part of the loop to be placed in the active zone will be U shaped, spiral, or cylindrical, depending on the experimental requirements. An SA-2 photoelectric saccharimeter is used as the recording device. A comparison of the dosimetric characteristics for a loop with a spiral irradiator and one with a U-shaped irradiator showed that the change to a U-shaped irradiator results in an increase in the transformation coefficient. The transformation coefficient can also be increased by maintaining the level of dosimetric liquid or by adding to the device special expanders which increase the total volume of the dosimetric system. (CFSTI)

32866 BORAX-V NUCLEAR SUPERHEAT OPERATING EXPERIENCE. Cerchione, J. D.; Wallin, W. R.; Rice, R. E. (Argonne National Lab., Idaho Falls, Idaho). Nucl. Appl., 2: 11-20(Feb. 1966).

BORAX-V was the fifth in a series of boiling-water reactors operated by Argonne National Laboratory at the National Reactor Testing Station in Idaho. Superheated steam was produced, in different experiments, in both the central and peripheral regions of the core. The nominal design maximum power of 20 MW(t) and 850°F exit steam temperature were both exceeded. Operational procedures and results of experiments are discussed. Areas of particular interest and investigation include: comparison of a centrally versus a peripherally located superheater core; superheater startup and shutdown cooling problems; superheater flooding reactivity worth and inadvertent flooding hazard; control of power split between the boiler and superheater zones of the reactor core; superheater fuel-cladding-material integrity; plant radioactivity levels; results of operation with defective fuel in both the boiler and superheater areas of the core; in-core instrumentation and data collection; transfer-function and physics experiments; and the water-chemistry program. (auth)

32867 COMPUTER CONTROL OF RESEARCH REACTOR TTR-1. Takahashi, Yoshizo (Tokyo Shibaura Electric Co., Ltd.); Takamatsu, Shigeyuki; Monta, Kazuo. Toshiba Rev., Int. Ed., No. 25, 37-43(Spring 1966).

A description of the digital computer control system for the research reactor TTR-1 is presented. This system has enabled automatic operation of all operations from prestartup check, startup, and constant power control to shutdown. (B.G.D.)

32868 REACTIVITY MEASUREMENTS BY NEUTRON NOISE ANALYSIS USING TWO-DETECTOR CORRELATION METHOD AND SUPERCRITICAL REACTOR NOISE ANAL-

YSIS. Nomura, Tsutomu; Gotoh, Seiichiro; Yamaki, Kozo (Nippon Atomic Industry Group Co., Ltd., Tokyo). 37p. (CONF-660206-14). ORAU. Gmelin, AED-CONF-66-014-12.

From Symposium on Neutron Noise, Waves, and Pulse Propagation, Gainesville, Fla.

Experiments were performed on the TTR-1 (Toshiba Training Reactor; Swimming Pool Type) to measure the prompt neutron decay constants by natural neutron noise analysis at subcritical, critical and supercritical states. A two-detector correlation method with band pass filters to eliminate the chamber noise component was developed. Relations between the cross-correlation function and reactor parameters were investigated and the two-detector correlation method using an analog correlator was applied to get neutron generation time and reactivities which could not be easily obtained by the calculation of the auto correlation function using a single-detector experiment due to the large uncorrelated noise particularly at subcritical state. Finally, relations between the reactor parameters and the reactor transfer function of the supercritical state were investigated and positive reactivities were obtained by analyzing the supercritical reactor noise. This experiment corresponds to the Rossi-α experiment between delayed and prompt critical state by Orndoff in his first Rossi-α experiment, where the stationary state was assumed in very short time region concerned with prompt neutron behavior. (auth)

32869 INTERPRETATION OF DOPPLER AND SODIUM REACTIVITY WORTH MEASUREMENTS IN ZERO POWER REACTORS, WITH PARTICULAR REFERENCE TO THE ZEBRA DOPPLER LOOP MEASUREMENTS. Rowlands, J. L.; Wardleworth, D. (Atomic Energy Establishment, Winfrith, Eng.). 47p. (CONF-651009-28). ORAU. Gmelin, AED-CONF-65-307-46.

From Conference on Safety, Fuels, and Core Design in Large Fast Power Reactors, Argonne, Ill.

A study is made of the effect on the Doppler coefficient from plutonium-239 and of the present uncertainties in the data from 0.1 to 10 kev and, in particular, in the resonance parameter data in the unresolved resonance region. Also some of the approximations involved in the methods for comparing calculations with experimental data on the sodium coefficient are examined. (J.F.P.)

32870 DETERMINATION OF THE EWA REACTOR POWER BY ^{16}N ACTIVITY MONITORING. Czerniewski, M.; Szuta, M.; Krzycki, A. 18p. (CONF-651123-5). ORAU.

From Conference on Reactor Physics and Engineering, Budapest.

A method for measuring the power of the EWA reactor by using the ^{16}N activity of the cooling water is described. The experimental results show that the method is generally free from errors caused by changes in the neutron flux distribution. The application of this method to power control in WWR-S-type reactors is discussed. (G.O.Y.)

32871 USE OF HEAVY WATER IN THE RADIAL REFLECTOR OF THE POLISH HIGH-FLUX RESEARCH REACTOR. Dabrowski, Cyryl. 23p. (CONF-651123-6). ORAU.

From Conference on Reactor Physics and Engineering, Budapest.

The use of beryllium, graphite, graphite-water, and heavy-water reflectors in the R2-D reactor was investigated. On the basis of the results, the use of a heavy-water reflector is proposed. (D.C.W.)

32872 ANNA ZERO POWER REACTOR. STARTUP, TWO AND ONE-HALF YEARS OPERATION, AND ITS MAIN CHARACTERISTICS. Dabek, W.; Kubowski, J. 33p. (CONF-651123-17). ORAU.

From Conference on Reactor Physics and Engineering, Budapest.

A short description of the assembly start up, of critical experiments in various core configurations, and of the measurement of various operational characteristics is presented. The data obtained during the operating period are summarized, and some safety aspects are considered. (G.O.Y.)

32873 RECONSTRUCTION OF THE LOW POWER "MARYLA" REACTOR. Baidor, Z. 16p. (In Russian). (CONF-651123-16). ORAU.

From Conference on Reactor Physics and Engineering, Budapest.

The MARYLA-2 reactor which is designed to investigate water-cooled and water-moderated critical assemblies, is described. The characteristics of the pile that allow modifications of the lattice without disturbing the shim rods or the channel are discussed. The method of achieving criticality by changing the water level and the double safety system of the facility are also considered. (G.O.Y.)

32874 ANALYSIS OF REACTOR NOISE MEASURED IN A ZERO-POWER REACTOR AND CALCULATIONS ON ITS ACCURACY. Dragt, J. B. (Reactor Centrum Nederland, Petten). 38p. (CONF-660206-7; RCN-INT-66-013). ORAU. Gmelin, AED-CONF-66-014-1.

From Symposium on Neutron Noise, Waves, and Pulse Propagation, Gainesville, Fla.

Noise experiments performed in the LFR are described, and results are presented. Calculations on the accuracy that can be obtained theoretically for reactor parameters estimated from the noise are also given. (J.F.P.)

32875 METHODS AND RESULTS OF SOME STATIC MEASUREMENTS IN THE ZERO POWER REACTOR ANNA. Adamski, L.; Jozefowicz, E. T.; Jozefowicz, K.; Szechter, A. 30p. (CONF-651123-2). ORAU.

From Conference on Reactor Physics and Engineering, Budapest.

The results of static measurements performed in the zero-power reactor ANNA using core variants with 14.0- and 19.8-cm lattice pitch are presented. Some of the parameters measured are macroscopic and intracell neutron density distributions are measured as well as spectral parameters and the neutron density in the primary cell. The methods used in these measurements are described. (G.O.Y.)

32876 NEW SIMPLIFIED SOLID-STATE INSTRUMENTATION FOR THE CONTROL AND SAFETY OF EXPERIMENTAL NUCLEAR REACTORS. Kaniewski, Jacek; Grzybinski, Ryszard; Szulc, Przemyslaw. 35p. (CONF-651123-10). ORAU.

From Conference on Reactor Physics and Engineering, Budapest.

Some solid-state instrumentation for the control and safety of experimental nuclear reactors is described. The general concepts of the system and its behavior in different states of operation as well as some of the main instruments of the measuring channel are considered. Special dynamic problems are discussed, and the results of the dynamical experiments performed on the system model with an analog reactor simulator are presented. (G.O.Y.)

32877 SELECTED PROBLEMS OF RADIATION PROTECTION AT THE WWRS-TYPE REACTOR "EWA". Filipyak, B.; Sivitski, R.; Zel'chinski, M.; Zharnovetskii, K. 21p. (In Russian). (CONF-651123-18). ORAU.

From Conference on Reactor Physics and Engineering, Budapest.

An analysis and estimates of radiation hazard conditions are presented for a number of arrangements and locations at the WWRS-type reactor EWA. (D.C.W.)

32878 CALCULATIONS OF THE TOP SHIELD OF THE CRITICAL ASSEMBLY MARYLA. Szymendera, Lech. 11p. (CONF-651123-13). ORAU.

From Conference on Reactor Physics and Engineering, Budapest.

The results of calculations for the top shield of the critical assembly MARYLA, which has a thermal power of 15.7 w, are presented. (G.O.Y.)

32879 INCREASING THE POWER OF THE POLISH VVR-S REACTOR UP TO 10 Mwt. Aleksandrovich,

E. A.; Byshevski, V.; Kosmal, V. 31p. (In Russian). (CONF-651123-1). ORAU.

From Conference on Reactor Physics and Engineering, Budapest.

The operating experience of the Polish VVR-S reactor at 4 Mwt is discussed, and modifications to increase its power to 10 Mwt are proposed. (G.O.Y.)

32880 NUCLEAR CALCULATIONS FOR THE 10-Mw EWA REACTOR WITH WWRM-TYPE TUBULAR FUEL. Kowalska, Krystyna. 20p. (CONF-651123-11). ORAU.

From Conference on Reactor Physics and Engineering, Budapest.

The results of some calculations of flux distributions, thermal utilization, and critical size for an EWA reactor using WWRM-type fuel are presented. (D.C.W.)

WASTE DISPOSAL AND PROCESSING

See also **BIOLOGY AND MEDICINE — Ecology**
CHEMISTRY — Radiochemistry
CHEMISTRY — Separation Processes and Procedures
HEALTH AND SAFETY

Refer also to abstract 32815.

32881 TREATMENT OF WASTE WATER AT THE KARLSRUHE ATOMIC RESEARCH CENTER. PART I. Krawczynski, Stefan. Effluent Water Treat. J., 5: 574-6 (Nov. 1965).

The Karlsruhe Nuclear Research Center has waste water from rain; domestic and chemical wastes; showers, laundry, and chemical wastes that may be contaminated with radioactivity; chemical wastes that always are contaminated; reactor wastes; and radioactive liquid concentrates. The source of these wastes and the manner in which they are collected are described. (Public Health Abstr.)

32882 TREATMENT OF WASTE WATER AT THE KARLSRUHE ATOMIC RESEARCH CENTER. PART II. Krawczynski, Stefan. Effluent Water Treat. J., 5: 611-13; 615(Dec. 1965).

The deactivation of contaminated waste water at Karlsruhe Atomic Research Center is discussed. The following methods are used singly or in combination: chemical precipitation (after decarbonization and electroionic deposition); ion exchange (optionally after chemical pretreatment by means of decarbonization, electroionic deposition, partial phosphate precipitation, or similar processes); and evaporation (evaporation of concentrates as well as of the regeneration waste waters of the ion exchange plant). These methods deactivate waste water below the acceptable concentration. (Public Health Abstr.)

32883 RADIOACTIVE WASTE MANAGEMENT AND ENVIRONMENTAL RESEARCH. (International Atomic Energy Agency, Vienna). pp 1-24 of STI-DOC-10/53.

Studies of radionuclides sorbed by marine sediments, hydrodynamics of the disposal of low-level liquid radioactive wastes in soils, the physico-chemico-biological processes affecting the dispersion of radionuclides, ion absorption characteristics of soils, classification of the properties of pyroclastic rocks for uptake of fission products, and evaporation of radioactive liquid wastes by solar energy are reviewed. (M.C.G.)

32884 ^{129}I IN EFFLUENTS TO UNRESTRICTED AREAS. Alexander, R. E. (Atomics International, Canoga Park, Calif.). 16p. (CONF-650616-19). ORAU. Gmelin, AED-CONF-65-153-43.

From Health Physics Society, Annual Meeting, Los Angeles.

As a result of new AEC standards for concentration of ^{129}I in effluents to unrestricted areas, a study was performed to define the locus of reactor operating conditions under which the nonpresence (concentration <10% of its permitted limit) of ^{129}I in fission products can be verified without physical measurement. The quantity of ^{129}I in a reactor during and following formation is shown for operating periods of 100 days, 1 year, and three years. Single bursts, excursions, infinite operation, and daily bursts for periods up to 7 years are also considered. Comparison of these quantities with limiting ratios to effluents indicates that the nonpresence of ^{129}I can be demonstrated without physical measurements and that analyses of this nature may be applicable to other radionuclides. (A.G.W.)

GENERAL AND MISCELLANEOUS

For abstracts of individual sections see: 31425–31428.

32885 (PNE–481) ENVIRONMENT OF THE CAPE THOMPSON REGION, ALASKA. Wilimovsky, Norman J.; Wolfe, John N. (eds.) (Committee on Environmental Studies for Project Chariot). 1966. 1265p. CFSTI $9.25 cy.

In 1957 the U. S. Atomic Energy Commission established the Plowshare Project to investigate and develop peaceful uses for nuclear explosives. In 1958 planning studies were begun for an experimental harbor excavation (Project Chariot) near Cape Thompson on the northwest coast of Alaska. Results of environmental studies are reported. Separate abstracts were prepared on four papers that report levels of natural and artificial radioactivity in the environment. One paper was abstracted previously and appeared in NSA as 18: 20231. (C.H.)

32886 (STI-DOC–10/53) IAEA RESEARCH CONTRACTS. Sixth Annual Report. Technical Reports Series No. 53. (International Atomic Energy Agency, Vienna (Austria)). Apr. 1966. 134p. IAEA: $1.00; S21,–; 6/-stg; F Fr 4,–; DM 3,20.

Summaries of IAEA research contract final reports received during 1965 are presented under 9 general topics. Separate abstracts were prepared for each of these topics. (M.C.G.)

For abstracts of individual sections see: 30965, 31108, 31109, 31142, 31195, 31355, 31394, 32776, and 32883.

32887 (TID–3735) BIBLIOGRAPHIES OF ATOMIC ENERGY LITERATURE. Issued or in Progress During the Period, April–May 1966. (Division of Technical Information Extension (AEC), Oak Ridge, Tenn.). 15p. Dep. DTI Extension Free.

A listing of bibliographies either sponsored by the AEC or received by DTI Extension, Oak Ridge, is presented. An author and subject index is included. (M.O.W.)

32888 (UCRL–16658) INORGANIC MATERIALS RESEARCH DIVISION ANNUAL REPORT, 1965. (Lawrence Radiation Lab., Univ. of California, Berkeley). Feb. 1966. Contract W-7405-eng-48. 183p. Dep. mn. CFSTI $5.00 cy, $1.00 mn.

Research progress is summarized in fourteen sections. Separate abstracts were prepared for each section. (J.R.D.)

For abstracts of individual sections see: 31166, 31218–31221, 31713–31719, 32312, and 32684.

32889 USE OF ATOMIC ENERGY IN INTERCONNECTED NETWORKS. Energ. Nucl., 8: 185-92(May 1966). (In French).

The future of the development of electric energy consumption in France and the demands in primary energy are discussed. Economic aspects are considered. Structure and growth of costs are reviewed. The exploiting of nuclear power stations is discussed. (auth)

32890 NUCLEAR ENERGY IN BELGIUM. Lamarche, Reginald; Vaes, Aime (Belgian Atomic Energy Commission). Euratom Bull., 5: 36-43(June 1966).

The development of nuclear energy in Belgium is reviewed. Resources, programs, fundamental research, applied research, research in the public interest, international cooperation, and nuclear power plants are discussed. (M.C.G.)

32891 CATALOGUE D: PRODUCTS AND SERVICES OFFERED BY THE COMMERCIAL PRODUCTS DIVISION OF ATOMIC ENERGY OF CANADA LIMITED. Ottawa, Atomic Energy of Canada Limited, [nd]. 79p.

Introductory information on the standard products and services offered by the Commercial Products Division of the Atomic Energy of Canada Limited is provided. Products include kilocurie ^{60}Co sources, other gamma sources, neutron sources, alpha and beta sources, pure radioisotopes, unprocessed radioisotopes, labeled compounds, and stable isotopes. Services include irradiation facilities at the NRX and NRU reactors, neutron and gamma service irradiations, gamma irradiation equipment, and shipping containers. Medical products include teletherapy sources, medical sources other than teletherapy, and medical appliances. (A.G.W.)

CORPORATE AUTHOR INDEX

This index contains entries for this period for all report literature and, in addition, for certain published literature items for which it is felt that a corporate approach is especially desirable, e.g., symposia, conference proceedings, and meetings.

Each entry under a corporate author is a shortened version of the title of the publication, followed by the *NSA* volume and abstract number. Report numbers are given in parentheses.

The phrase "Progress report" is abbreviated as "Prog. rpt.," permitting a more rapid and complete alphabetical arrangement of the titles without changing the location of the progress report titles in relation to the other titles.

A

AEROSPACE RESEARCH LABS., WRIGHT-PATTERSON AFB, OHIO.
Limitations in energy resolution of slow electrons, 20: 31981 (AD-634517)

AKTIEBOLAGET ATOMENERGI, STOCKHOLM (SWEDEN).
Bibliography on radiation effects on solid, U based nuclear fuel materials, Vol. 6, No. 1, 20: 31783 (FTI-16(6.1))

ALLIS-CHALMERS MFG. CO., BETHESDA, MD. ATOMIC ENERGY DIV.
La Crosse Boiling Water Reactor radio and water chemistry manual, 20: 32795 (ACNP-66538)

AMERICAN MACHINE AND FOUNDRY CO., ALEXANDRIA, VA.
Examination of Ames proton analyzer for photon sensitivity, 20: 31510 (N-65-33971)

AMSTERDAM UNIV. (NETHERLANDS).
Bubble chamber investigation of K* resonance, 20: 31987 (NP-16097)

ARGONNE NATIONAL LAB., ILL.
Analytical research and development, 20: 31167 (ANL-7175, pp 217-25)
Compact pyrochemical processes, 20: 31314 (ANL-7175, pp 1-41)
Determination of nuclear constants, 20: 32370 (ANL-7175, pp 212-16)
Energy conversion, 20: 31959 (ANL-7175, pp 184-211)
Estimated temperatures of EBR-II fuel cycle facility shielding windows, 20: 31313 (ANL-6853)
Facility for studying elastic moduli as function of temperature, 20: 31708 (ANL-7119)
Flow-regime transitions at elevated pressures in vertical two-phase flow, 20: 31340 (ANL-7093)
Materials chemistry and thermodynamics, 20: 31213 (ANL-7175, pp 119-58)
Parametric studies of reactivity coefficients for large ^{233}U–Th-fueled fast reactors, 20: 32790 (ANL-6930)
Prog. rpt. on chemical engineering, 5/65–4/66, 20: 31164 (ANL-7175)
Reactor safety, 20: 31440 (ANL-7175, pp 159-83)
Safety analysis for ZPR-9 facility, 20: 32858 (ANL-7166)
Studies and evaluations, 20: 31316 (ANL-7175, pp 104-18)
Television system for ultrasonic imaging, 20: 31352 (ANL-7042)
Volatility and fluidization processes, 20: 31315 (ANL-7175, pp 42-103)

ARIZONA UNIV., TUCSON.
Wavelengths of electronic transitions in foil-excited beams of light elements, 20: 31903 (N-66-16702)

ARMY ELECTRONICS COMMAND, FORT MONMOUTH, N. J.
Dependence of pulse amplitude and polarity on position of entry in particle detector, 20: 31498 (AD-632527)

ASSOCIATED MIDWEST UNIVERSITIES, LEMONT, ILL.
Flow-regime transitions at elevated pressures in vertical two-phase flow, 20: 31340 (ANL-7093)

ATOMIC ENERGY CENTRE, DACCA (PAKISTAN). AGRICULTURE DIV.
Mutation types in irradiated population of Jute, 20: 31027 (AECD/AG-14)
Susceptibility of adult rice weevil to gamma radiation, 20: 31623 (AECD/AG-15)

ATOMIC ENERGY COMMISSION, WASHINGTON, D. C.
Adsorption equilibria between earth materials and radionuclides, 20: 31426 (PNE-481, pp 1121-39)
Aeroradioactivity survey of Lisburne Peninsula, 20: 31425 (PNE-481, pp 1115-19)
Environment of Cape Thompson region, Alaska, 20: 32885 (PNE-481)
Radiological analyses of marine organisms, 20: 31427 (PNE-481, pp 1141-9)
Radionuclides in terrestrial and freshwater biota, 20: 31428 (PNE-481, pp 1165-1200)

ATOMIC ENERGY OF CANADA LTD., CHALK RIVER (ONTARIO).
Analysis of external radiation exposures in 1965, 20: 31439 (AECL-2540)
Calculation of neutron diffusion parameters of parallel-plate lattice, 20: 32763 (AECL-2543)
Effects of radionuclides on thermal tolerance of fish, 20: 31028 (AECL-2409)
Library programs for AECL G-20 computer, 20: 31646 (AECL-1744)
Library programs for AECL G-20 computer, 20: 31647 (AECL-1744 (Pt.A)(Add.1))
Methods of applying compton scattered neutron capture radiation to nuclear photo-excitation, 20: 32369 (AECL-2535)

ATOMIC POWER DEVELOPMENT ASSOCIATES, INC., DETROIT, MICH.
Carbon in primary Na system of Enrico Fermi Atomic Power Plant, 20: 32809 (TID-23101)

ATOMICS INTERNATIONAL, CANOGA PARK, CALIF.
Application of P_3 method to calculation of particle fluxes in shields, 20: 32673 (NAA-SR-Memo-11872)
Brittle failures of carbon steel tubes, 20: 31681 (NAA-SR-Memo-11707)
Data and bibliography on corrosion of structural materials in liquid alkali metals, 20: 31680 (NAA-SR-Memo-11652)
Experiments on uranium–lithium hydride shields at STIR facility, 20: 32672 (NAA-SR-Memo-11786)
Optimum power transmission cable weight, 20: 32853 (NAA-SR-Memo-11925)
Prog. rpt. on heavy water organic-cooled reactor, 1–6/65, 20: 32796 (AI-CE-3)
SNAP-10A electrically actuated band release device development, 20: 32852 (NAA-SR-Memo-11454)
SPENCER: FORTRAN program to approximately reconstitute a one-dimensional function from finite number of its moments, 20: 31658 (NAA-SR-Memo-11653)
Temperature distributions for various fuels with nonuniform heating, 20: 32791 (NAA-SR-Memo-11731)

AVCO-EVERETT RESEARCH LAB., EVERETT, MASS.
Experiments with magnetohydrodynamically supported shock layers, 20: 32217 (N-65-33713)

B

BABCOCK AND WILCOX CO., LYNCHBURG, VA. RESEARCH AND DEVELOPMENT DIV.
Recycle of HWOCR thorium fuel, 20: 31317 (BAW-393-3)

BALLISTIC RESEARCH LABS., ABERDEEN PROVING GROUND, MD.
Secondary gamma ray transmission through plane slabs of concrete, 20: 32671 (AD-633216)

BATTELLE-NORTHWEST, RICHLAND, WASH. PACIFIC NORTHWEST LAB.
Animal activity monitor development, 20: 30960 (BNWL-235-4, pp 22-5)
Animal physiological function telemetry developments, 20: 30961 (BNWL-235-4, pp 25-9)

Containment systems experiment. III., 20: 32748 (BNWL-233)
Digital control for whole-body scanner, 20: 31502 (BNWL-235-4, pp 11-14)
Fish environment dose rate measurements, 20: 31501 (BNWL-235-4, pp 10-11)
Hematopoietic tissue neoplasms in animals administered ^{90}Sr, 20: 31031 (BNWL-SA-201)
IDERM: program for intake, distribution and excretion of radionuclides in mammals, 20: 31441 (BNWL-SA-40)
Instrumentation techniques for toxicity studies of inhaled radionuclides, 20: 31475 (BNWL-235-4, pp 19-20)
Irradiated wood-plastic materials commercialization, 20: 31624 (BNWL-261)
Long-term study of inhaled Pu in dogs, 20: 31025 (AD-631690)
Measurement of mixed-field neutron and gamma dose rates, 20: 31505 (BNWL-235-4, pp 30-4)
Measurement of radionuclide uptake by algae, 20: 31504 (BNWL-235-4, pp 16-18)
Miniature dose rate measurement instrument, 20: 31503 (BNWL-235-4, pp 14-16)
Physiological data telemetry system, 20: 31474 (BNWL-235-4, pp 1-4)
Prog. rpt. on physical sciences, annual, 1965. IV. Instrumentation, 20: 31473 (BNWL-235-4)
Radiation chemistry of agarose jellies, 20: 30998 (BNWL-SA-709)
Radiation effects in graphite at high temperatures, 20: 31782 (BNWL-SA-67)
Radioecological concentration processes characterizing arctic ecosystems, 20: 31442 (BNWL-SA-661)
Raindrop charge and velocity measurement techniques, 20: 31476 (BNWL-235-4, pp 21)
Solid-state gamma spectrometry developments, 20: 31500 (BNWL-235-4, pp 4-10)
Treatment and evaluation of internal deposition from Pu wound, 20: 31030 (BNWL-SA-39)
Uptake and retention of ^{32}P and ^{65}Zn from consumption of Columbia River fish, 20: 30969 (BNWL-SA-45)
Use of plastics at Hanford, 20: 31267 (BNWL-SA-658)
Whole-body counting of Pu in dogs, 20: 30968 (BNWL-SA-11)

BETTIS ATOMIC POWER LAB., WEST MIFFLIN, PA.
Enriched uranium scrap assay gage, 20: 31174 (WAPD-T-1905)

BOEING SCIENTIFIC RESEARCH LABS., SEATTLE, WASH. FLIGHT SCIENCES LAB.
Performance of arc heaters for MHD experiments, 20: 31356 (N-66-12435)

BOEING SCIENTIFIC RESEARCH LABS., SEATTLE, WASH. GEOASTROPHYSICS LAB.
New type of low-resolution mass spectrometer, 20: 31169 (D-1-82-0508)

BOEING SCIENTIFIC RESEARCH LABS., SEATTLE, WASH. PLASMA PHYSICS LAB.
Efficient utilization of an r-f power oscillator for producing low-pressure plasmas, 20: 32570 (D-1-82-0522)

BROOKHAVEN NATIONAL LAB., UPTON, N. Y.
Automatic acquisition of neutron spectrometer data, 20: 32681 (BNL-10238)
Hematological effects of space radiation, 20: 31029 (BNL-10221)
Laminar heat transfer in hexagonal channel, 20: 31341 (BNL-9546)
Superconducting quadrupole lens, 20: 31815 (BNL-10144)

C

CALIFORNIA INST. OF TECH., PASADENA.
Conference on the solar wind, Pasadena, 4/64, 20: 31880 (JPL-TR-32-630)
Photoproduction of negative pions from hydrogen, 20: 31983 (CALT-68-71)

CALIFORNIA UNIV., BERKELEY.
Prog. rpt. on radiation of heme proteins, 10/64–9/65, 20: 30999 (UCB-34P95-7)

CALIFORNIA UNIV., DAVIS. CROCKER NUCLEAR LAB.
Initial internal beam studies with Davis 76-inch cyclotron, 20: 31826 (UCD-CNL-47)

CALIFORNIA UNIV., DAVIS. SCHOOL OF VETERINARY MEDICINE.
Strontium-90 in beagle hair, 20: 30972 (TID-22027)

COLUMBIA BASIN COLL., PASCO, WASH.
IDERM: program for intake, distribution and excretion of radionuclides in mammals, 20: 31441 (BNWL-SA-40)

COLUMBIA UNIV., NEW YORK. DEPT. OF CHEMISTRY.
Enrichment of ^{18}O and ^{13}C by carbon dioxide exchange in amine-solvent systems, 20: 31641 (NYO-755-1, pp 173-208)
Exchange between methyl acetylene and water for concentration of deuterium, 20: 31640 (NYO-755-1, pp 130-72)
Factors affecting the exchange of ^{15}N between nitric oxide and nitric acid in exchange columns, 20: 31639 (NYO-755-1, pp 77-129)
Prog. rpt. on separation of isotopes, annual, 1964, 20: 31637 (NYO-755-1)
Solvent carrier system for concentration of ^{15}N by chemical exchange between oxides of N, 20: 31638 (NYO-755-1, pp 12-76)

COMBUSTION ENGINEERING, INC., WINDSOR, CONN. NUCLEAR DIV.
Prog. rpt. on heavy water organic-cooled reactor, 1–6/65, 20: 32796 (AI-CE-3)

COMISION NACIONAL DE ENERGIA ATOMICA, BUENOS AIRES (ARGENTINA).
New colloid of ^{99}Tc in scintillation scanning of the liver, 20: 31147 (CNEA-168)
Scintillation scanning in kidneys, 20: 31148 (CNEA-170)

COMMISSARIAT A L'ENERGIE ATOMIQUE, FONTENAY-AUX-ROSES (FRANCE). CENTRE D'ETUDES NUCLEAIRES.
Kinetic study of fluorination by F of U and Pu compounds, 20: 31214 (CEA-R-2859)

COMMISSARIAT A L'ENERGIE ATOMIQUE, GRENOBLE (FRANCE). CENTRE D'ETUDES NUCLEAIRES.
Effects of x rays on platelet environment, 20: 31032 (CEA-R-2953)

COMMISSARIAT A L'ENERGIE ATOMIQUE, SACLAY (FRANCE). CENTRE D'ETUDES NUCLEAIRES.
Construction of Orsay ACO storage ring. I and II, 20: 31816 (CEA-R-2929)
Detection of hard β radiation in water using the Cherenkov effect, 20: 31506 (CEA-R-2915)
Nuclear codes for IBM-704, -709, and -7090, 20: 32764 (CEA-Bib-17(Pt.2))
Reaction $^{51}V(p,n)^{51}Cr$ and contribution to spectroscopy of ^{51}Cr, 20: 32371 (CEA-R-2832)
Slow neutron monochromator, 20: 31477 (CEA-R-2981)

COMMITTEE ON ENVIRONMENTAL STUDIES FOR PROJECT CHARIOT.
Adsorption equilibria between earth materials and radionuclides, 20: 31426 (PNE-481, pp 1121-39)
Aeroradioactivity survey of Lisburne Peninsula, 20: 31425 (PNE-481, pp 1115-19)
Environment of Cape Thompson region, Alaska, 20: 32885 (PNE-481)
Radiological analyses of marine organisms, 20: 31427 (PNE-481, pp 1141-9)
Radionuclides in terrestrial and freshwater biota, 20: 31428 (PNE-481, pp 1165-1200)

COURANT INST. OF MATHEMATICAL SCIENCES, NEW YORK UNIV., N. Y.
Guiding center plasma, 20: 32576 (NYO-1480-50)
Magnetohydrodynamic shock relations in nonaligned flows, 20: 32218 (NYO-1480-29)
Steady nonlinear waves in warm collision-free plasma, 20: 32577 (NYO-1480-54)

D

DANISH ATOMIC ENERGY COMMISSION, RISOE. RESEARCH ESTABLISHMENT.
Prog. rpt. on electronics, 10–12/65, 20: 31660 (RISO-M-385)

DIVISION OF BIOLOGY AND MEDICINE (AEC), WASHINGTON, D. C.
Aeroradioactivity survey and geology of San Francisco, 20: 31395 (CEX-58.4.5)
Bibliography on terrestrial and freshwater radioecology, 20: 30967 (TID-3910(Suppl.4))

DIVISION OF TECHNICAL INFORMATION (AEC), WASHINGTON, D. C.
Bibliographies of atomic energy literature issued or in progress during 4–5/66, 20: 32887 (TID-3735)

DU PONT DE NEMOURS (E. I.) & CO., AIKEN, S. C. SAVANNAH RIVER LAB.
Operational summary of HWCTR, 10/61–12/64, 20: 32859 (DP-991)

DUKE UNIV., DURHAM, N. C.
Superconductive threshold logic circuitry, 20: 32311 (ORO-2430-27)

E

EDGERTON, GERMESHAUSEN AND GRIER, INC., SANTA BARBARA, CALIF.
Albuquerque–Los Alamos area (ARMS-II), 20: 31396 (CEX-61.6.2)

EIDGENOESSISCHES INSTITUT FUER REAKTORFORSCHUNG, WUERENLINGEN (SWITZERLAND).
Transistorized counting channel for measuring beta-activities with proportional counters, 20: 31509 (EIR-97)

EUROPEAN ATOMIC ENERGY COMMUNITY.
Prog. rpt. on computer science, annual, 9/65–8/66, 20: 31662 (TID-23020)

EUROPEAN ORGANIZATION FOR NUCLEAR RESEARCH, GENEVA (SWITZERLAND).
NMR field measuring equipment for CERN muon storage ring, 20: 31817 (CERN-66-15)

F

FLORIDA UNIV., GAINESVILLE.
Quantum theory of time-dependent phenomena treated by evolution operator technique, 20: 32293 (N-66-17084)

G

GENERAL ELECTRIC CO., RICHLAND, WASH. HANFORD ATOMIC PRODUCTS OPERATION.
IDERM: program for intake, distribution and excretion of radionuclides in mammals, 20: 31441 (BNWL-SA-40)
Radionuclides in terrestrial and freshwater biota, 20: 31428 (PNE-481, pp 1165-1200)

GENERAL ELECTRIC CO., SAN JOSE, CALIF. ADVANCED PRODUCTS OPERATION.
Prog. rpt. on SEFOR development, 11/65–1/66, 20: 32860 (GEAP-5108)

GENERAL ELECTRIC CO., SAN JOSE, CALIF. ATOMIC POWER EQUIPMENT DEPT.
Prog. rpt. on two-phase flow and heat transfer in multirod geometries, 7/65–1/66, 20: 31343 (GEAP-5056)
Prog. rpt. on Zr alloy, 4–6/65, 20: 31677 (GEAP-4840)

GEOLOGICAL SURVEY, MENLO PARK, CALIF.
Adsorption equilibria between earth materials and radionuclides, 20: 31426 (PNE-481, pp 1121-39)

GEOLOGICAL SURVEY, WASHINGTON, D. C.
Aeroradioactivity survey and geology of San Francisco, 20: 31395 (CEX-58.4.5)
Aeroradioactivity survey of Lisburne Peninsula, 20: 31425 (PNE-481, pp 1115-19)

GEORGIA INST. OF TECH., ATLANTA. SCHOOL OF NUCLEAR ENGINEERING.
Prog. rpt. on kinetics parameters of highly enriched D_2O reactor, final, 12/65–12/66, 20: 32863 (TID-23037)

GOSUDARSTVENNYI KOMITET PO ISPOL'ZOVANIYU ATOMNOI ENERGII SSSR, MOSCOW. INSTITUT TEORETICHESKOI I EKSPERIMENTAL'NOI FIZIKI.
Conversion electrons associated with alpha decay of ^{241}Am and level scheme of ^{237}Np, 20: 32375 (ITEF-351)
Selection of optimum curve of rectangular light pipes with no light losses by reflection, 20: 31818 (ITEF-385)

H

HAHN-MEITNER-INSTITUT FUER KERNFORSCHUNG, BERLIN (WEST GERMANY).
Prog. rpt., annual, 1965, 20: 31165 (HMI-B-46)

HELSINKI UNIV. (FINLAND). DEPT. OF RADIOCHEMISTRY.
Results of Project Lapland at beginning of 1966, 20: 31444 (CONF-660405-15)

HITTMAN ASSOCIATES, INC., BALTIMORE, MD.
Low enriched PM replacement core control materials metallurgical evaluation, 20: 31678 (HIT-3583-24)

I

IIT RESEARCH INST., CHICAGO, ILL.
Graphite-metal carbide composites, 20: 31688 (NASA-CR-507)
Prog. rpt. on effect of high spin on electromagnetic decay of nuclei, annual, 5/65–5/66, 20: 32374 (IITRI-578P25-15)
Prog. rpt. on V alloy studies, final, 3/65–5/66, 20: 31709 (IITRI-B6042-5)

ILLINOIS UNIV., URBANA.
Flow-regime transitions at elevated pressures in vertical two-phase flow, 20: 31340 (ANL-7093)

ILLINOIS UNIV., URBANA. COORDINATED SCIENCE LAB.
Prog. rpt. on electronics, 9–11/65, 20: 31645 (AD-627094)

ILLINOIS UNIV., URBANA. DEPT. OF COMPUTER SCIENCE.
Grammar for a pattern description language, 20: 31651 (COO-1018-1054)
ILLIAC III: processor of visual information, 20: 31652 (COO-1018-1057)
Prog. rpt. on computer science, 7–9/65, 20: 31654 (COO-1018-1066)
Prog. rpt. [on ILLIAC III], 9/64–8/65. I., 20: 31508 (COO-1018-1075)
Prog. rpt., 10–12/65, 20: 31655 (COO-1018-1076)
Programming manual for ILLIAC III computer, 20: 31653 (COO-1018-1061)
WEB: language to describe interconnection and packaging of logical units in digital processor. I., 20: 31648 (COO-1018-1021)

ILLINOIS UNIV., URBANA. DIGITAL COMPUTER LAB.
BUBBLE SCAN I program, 20: 31507 (COO-1018-1013)
Details of transfer memory input/output signals, 20: 31649 (COO-1018-1030)
Syntax loader and subscanner for compiler-compiler, 20: 31650 (COO-1018-1031)

INSTITUT ATOMNOI ENERGII, GOSUDARSTVENNYI KOMITET PO ISPOL'ZOVANIYU ATOMNOI ENERGII SSSR, MOSCOW.
Investigation of effect of Be-reflector duty factor on thermal neutron flux in horizontal beams, 20: 32765 (IAE-957)

INSTITUT FUER PLASMAPHYSIK, G.M.B.H. GARCHING (WEST GERMANY).
Induction coil as measuring element in fast current intensity gas discharge, 20: 32571 (IPP-1/2)
Microscopic description of plasma and nonlinear incoherent light scattering, 20: 32572 (IPP-6/49)

INSTITUTE OF NUCLEAR RESEARCH, LODZ (POLAND).
Conference on cosmic-ray extensive air showers, Lodz, Poland, 1/65, 20: 31950 (CONF-650120)

INTERNATIONAL ATOMIC ENERGY AGENCY, VIENNA (AUSTRIA).
Calibration problems in whole-body counting with NaI(Tl) detectors, 20: 31443 (CONF-650673-1)
IAEA research contracts, sixth annual report, 20: 32886 (STI-DOC-10/53)
Panel on nuclear energy for water desalination, Vienna, 4/65, 20: 32842 (STI-DOC-10/51)
Panel on utilization of Th in power reactors, Vienna, 6/65, 20: 32807 (STI-DOC-10/52)
Techniques for controlling air pollution from operation of nuclear facilities, 20: 31453 (STI-PUB-121)

INTERNATIONAL CENTRE FOR THEORETICAL PHYSICS, TRIESTE (ITALY).
Cabibbo angle and the ninth baryon, 20: 32108 (IC-66/59)
Generalized nonet representation of SU(3) × SU(3) and its applications, 20: 32107 (IC-66/48)
Non-leptonic decays of Ω^-, 20: 31985 (IC-66/57)
Photoproduction of vector mesons from nucleons, 20: 31984 (IC-66/54)

IOWA STATE UNIV. OF SCIENCE AND TECHNOLOGY, AMES. VETERINARY MEDICAL RESEARCH INST.
Comparative toxicity of stable rare earth compounds, 20: 30970 (COO-1170-5)

IOWA UNIV., IOWA CITY.
Differential spectrophotometric determination of Pu(III), 20: 31170 (ISO-SA-16)

ISOCHEM INC., RICHLAND, WASH.
Solvent extraction of Np(VI) from acid deficient nitrate system, 20: 31319 (ISO-SA-10)

J

JET PROPULSION LAB., CALIF. INST. OF TECH., PASADENA.
Conference on the solar wind, Pasadena, 4/64, 20: 31880 (JPL-TR-32-630)
Development of Cs-vapor-filled thermionic energy converter, 20: 31960 (N-66-16447)

K

KANSAS UNIV., LAWRENCE. NUCLEAR PHYSICS LAB.
Spin assignments from triple correlation utilizing axial symmetry, 20: 32372 (COO-1120-43)

KERNFORSCHUNGSZENTRUM, KARLSRUHE (WEST GERMANY). INSTITUT FUER RADIOCHEMIE.
Mathematical treatment of decay and formation laws of radioactivity with graphically solved examples, 20: 32377 (KFK-117)

KNOLLS ATOMIC POWER LAB., SCHENECTADY, N. Y.
Application of sputtering ion source to mass analysis of nanogram solid samples, 20: 31168 (CONF-660611-1)
Considerations of rotor dynamics including virtual mass and stability effects, 20: 31329 (KAPL-M-6543)
Double differential scattering cross sections and scattering law for H_2O at 302°K, 20: 32350 (KAPL-M-6536)
Friction factors for use in analysis of journal bearings with vortex-turbulent flow, 20: 31330 (KAPL-M-6546)
Kinetics of low source reactor startups, 20: 32766 (KAPL-M-6550)
LIZARD-IV: program to solve nonlinear, ordinary differential equations, 20: 31657 (KAPL-M-6548)
Measurement of total neutron cross sections of ^{147}Pm, ^{148}Pm, and ^{148m}Pm, 20: 32376 (KAPL-3090)
Vibration response of cantilevered cylinder surrounded by annular fluid, 20: 31328 (KAPL-M-6539)

L

LABORATORI NAZIONALI DI FRASCATI, COMITATO NAZIONALE PER L'ENERGIA NUCLEARE (ITALY).
Calculation of shielding around all targets of Frascati linear accelerator, 20: 31820 (LNF-66/14)

LAWRENCE RADIATION LAB., UNIV. OF CALIFORNIA, BERKELEY.

Chemical thermodynamics, 20: 31219 (UCRL-16658, pp 11-20)
Crystal imperfections, 20: 31713 (UCRL-16658, pp 93-8)
Electrochemistry, 20: 31220 (UCRL-16658, pp 39-72)
High-field superconductivity, 20: 32312 (UCRL-16658, pp 133-43)
High-strength materials, 20: 31716 (UCRL-16658, pp 121-32)
High-temperature reactions, 20: 31718 (UCRL-16658, pp 149-54)
Hyperfine structures in atomic 2p shell, 20: 31904 (UCRL-16581)
Inorganic chemistry, 20: 31218 (UCRL-16658, pp 1-9)
Kinetics of dislocation mechanisms, 20: 31714 (UCRL-16658, pp 99-103)
Leptonic decays of neutral K mesons, 20: 31991 (UCRL-16771)
Liquid metal extraction of fission products from uranium fuels, 20: 31320 (UCRL-16108)
Nuclear science, 20: 31166 (UCRL-16658, pp 89-92)
Physical ceramics, 20: 31719 (UCRL-16658, pp 155-69)
Physical chemistry, 20: 31221 (UCRL-16658, pp 73-87)
Post-shutdown generation of photoneutrons in beryllium-moderated systems, 20: 32767 (UCRL-14720)
Prog. rpt. on inorganic materials research, annual, 1965, 20: 32888 (UCRL-16658)
Properties of neutral cascade hyperon, 20: 31988 (UCRL-11510)
Proton-proton elastic scattering at incidence momenta 3, 5, and 7 Bev/c, 20: 31989 (UCRL-16275)
Reaction $K^- p \rightarrow \Lambda \omega$ from 1.2 to 2.7 Bev/c: absorption model with strange-meson exchange, 20: 31990 (UCRL-16648)
Regenerative beam extraction for Berkeley 88-inch cyclotron, 20: 31827 (UCRL-16794)
Relation of structure to properties in metallic systems, 20: 31715 (UCRL-16658, pp 105-20)
Scintillation photography of intravascular clots in vivo, 20: 31150 (UCRL-16691)
Solid-state chemistry and physics, 20: 32684 (UCRL-16658, pp 21-38)
Thermodynamics of metal systems, 20: 31717 (UCRL-16658, pp 143-9)

LAWRENCE RADIATION LAB., UNIV. OF CALIFORNIA, LIVERMORE.
Contact conductance measurements during transient heating, 20: 31712 (UCRL-14227(Rev.1))
Fabrication technique for significantly reducing capacitance of Ge LID detectors, 20: 31513 (UCRL-14561)
General non-dynamical formalism for reactions with particles of arbitrary spin, 20: 32382 (UCRL-14582-T(Rev.1))
General theory for numerical solution of equations of hydrodynamics, 20: 32220 (UCRL-14912-T)
Post-shutdown generation of photoneutrons in beryllium-moderated systems, 20: 32767 (UCRL-14720)
Prog. rpt. on hazards control, 1–3/66, 20: 31514 (UCRL-14881)
Propagation of elastic stress disturbances in deformable solids, 20: 31331 (UCRL-14616)

LITTLE (ARTHUR D.) INC., CAMBRIDGE, MASS.
Growth of foreign nuclear power, 20: 32808 (TID-22973)

LOCKHEED NUCLEAR PRODUCTS, MARIETTA, GA.
Data compilation and evaluation of space shielding problems, 20: 32674 (NP-15697(Vol.3))
Modification and overhaul of cryogenic irradiation facility at Plumbrook Reactor Facility, 20: 32861 (N-66-12348)
Prog. rpt. on effect of radiation on materials at cryogenic temperatures, 1–4/66, 20: 31784 (NASA-CR-54976)

LOS ALAMOS SCIENTIFIC LAB., UNIV. OF CALIFORNIA, N. MEX.
Bibliography on kinetics of oxidation-reduction reactions of U, Np, Pu, and Am in aqueous solutions, 20: 31215 (LA-3507)
Evaluation of reactors for irradiation of liquid Pu fast reactor fuels, 20: 32799 (LA-DC-7752)
Fast reactor development in United States, 20: 32798 (LA-DC-7550)
Fast transients in liquid Pu, 20: 32797 (LA-DC-7748)
Post-induction kinetics in shock initiated H_2–O_2 reactions, 20: 31217 (LA-DC-7661)
Prog. rpt. on advanced reactor technology, 4/30/66, 20: 31679 (LA-3524)
Prog. rpt. on medium-energy physics, 1–4/66, 20: 31819 (LA-3521)
Project Rover liquid H safety, 20: 32850 (LA-DC-7689)
Shock wave study of recombination in near-stoichiometric H–O mixtures, 20: 31216 (LA-DC-7659)
Two-dimensional time-dependent numerical study of rotational Couette flow, 20: 31344 (LA-3497)

M

MARYLAND UNIV., COLLEGE PARK. DEPT. OF PHYSICS AND ASTRONOMY.
Behavior of scattering amplitudes and cross sections using crossing symmetry and holomorphy in two variables, 20: 32106 (AD-634706)
On off-diagonal mass matrix element of neutral K system, 20: 31982 (AD-634703)
Origin and loss of inner zone protons, 20: 32243 (AD-634704)

MASCHINENFABRIK AUGSBURG-NUERNBERG A. G., NUREMBERG (WEST GERMANY).
Prog. rpt. on critical heat flux (burnout) in boiling water, 7–9/65, 20: 31342 (EURAEC-1482)

MISSISSIPPI UNIV., UNIVERSITY. DEPT. OF PHYSICS AND ASTRONOMY.
Prog. rpt. on effects of neutron irradiation on resistivity of binary alloys, 6/66, 20: 31786 (ORO-2891-5)

N

NATIONAL AERONAUTICS AND SPACE ADMINISTRATION, CLEVELAND, OHIO. LEWIS RESEARCH CENTER.
Limits of validity of radiationless decay of high-density plasmas, 20: 32575 (NASA-TN-D-3372)
Monte Carlo interpretation of sphere transmission experiments for average capture cross sections at 24 kev, 20: 32378 (NASA-TR-R-239)
Stress-rupture properties of tungsten wire from 1200° to 2500°F, 20: 31711 (NASA-TN-D-3467)

NATIONAL AERONAUTICS AND SPACE ADMINISTRATION, COCOA BEACH, FLA. JOHN F. KENNEDY SPACE CENTER.
Radiological safety handbook, 20: 31445 (N-65-12416)

NATIONAL AERONAUTICS AND SPACE ADMINISTRATION, GREENBELT, MD. GODDARD SPACE FLIGHT CENTER.
Electron capture by protons in H in electric field, 20: 31901 (N-65-34224)
Soft x-ray photoionization detector, 20: 31511 (N-66-16936)

NATIONAL AERONAUTICS AND SPACE ADMINISTRATION, HUNTSVILLE, ALA. GEORGE C. MARSHALL SPACE FLIGHT CENTER.
Environmental model for Van Allen belt protons, 20: 32244 (N-66-13126)

NATIONAL INST. FOR RESEARCH IN NUCLEAR SCIENCE, CHILTON (ENGLAND). RUTHERFORD HIGH ENERGY LAB.
External proton beam at Nimrod, 20: 31823 (RPP-N-5)

NATIONAL RADIATION LAB., CHRISTCHURCH (NEW ZEALAND).
Prog. rpt. on environmental radioactivity in New Zealand, 10–12/65, and annual summary, 1965, 20: 31446 (NP-16015)

NAVAL RADIOLOGICAL DEFENSE LAB., SAN FRANCISCO, CALIF.
Comparison of cesium iodide and sodium iodide for underwater radiation detection systems, 20: 31499 (AD-633752)
Effect of radiation-induced charge on transistor surfaces, 20: 31611 (AD-633468)
Injury accumulation in sheep during protracted gamma radiation, 20: 31026 (AD-633606)
NRDL 70″ cyclotron external ion optics system, 20: 31814 (AD-634300)
Radiological reclamation performance summary. I., 20: 31454 (USNRDL-TR-967)

NEVIS LABS., COLUMBIA UNIV., IRVINGTON-ON-HUDSON, N. Y.
Electron production by high-energy neutrinos, 20: 31986 (NEVIS-148)

NORTHWESTERN UNIV., EVANSTON, ILL. DEPT. OF CHEMISTRY.
Prog. rpt. on radiation chemistry of high polymers, annual, 4/65–4/66, 20: 31268 (COO-1088-20)

O

OAK RIDGE GASEOUS DIFFUSION PLANT, TENN.
UCAPP: Union Carbide APT Post Processor, 20: 31327 (K-1671)
UCAPP: Union Carbide APT Post Processor, first edition, 20: 31478 (K-1670)

OAK RIDGE INST. OF NUCLEAR STUDIES, INC., TENN.
Labeling of myeloma cells and leukemic leukocytes, 20: 30971 (ORINS-45)

OAK RIDGE NATIONAL LAB., TENN.
Analysis of parabolic partial differential equation containing both flow and diffusion terms, 20: 31659 (ORNL-TM-1497)
Calculation of electronic structure of defects in insulators, 20: 32682 (ORNL-P-2193)
Calculation of force-constant changes for U center, 20: 32683 (ORNL-P-2194)
CDC-160A programs for processing data from a neutron time-of-flight cross-section experiment, 20: 32379 (ORNL-TM-1208)
Chemistry, 20: 32804 (ORNL-3936, pp 122-71)
Component development, 20: 32802 (ORNL-3936, pp 53-81)
FORTRAN listings and flow charts for ZAP31: program to calculate $\beta\gamma$ radiation dose rates, 20: 32675 (ORNL-TM-1160)
Impact of Kilorod operational experience on design of fabrication plants for ^{233}U–Th fuels, 20: 31690 (ORNL-P-2176)
In-reactor mechanical properties experiments, 20: 31785 (ORNL-P-2162)
Irradiation facilities in ORNL bulk shielding reactor, 20: 32862 (ORNL-P-2160)
Metallurgy, 20: 31683 (ORNL-3936, pp 95-121)
Molten-salt breeder reactor design studies, 20: 32805 (ORNL-3936, pp 172-92)

Molten-salt reactor processing studies, 20: 32806 (ORNL-3936, pp 193-211)
MSRE operations, 20: 32801 (ORNL-3936, pp 7-52)
MSRE reactor analysis, 20: 32803 (ORNL-3936, pp 82-92)
Operating characteristics of ORIC beam extraction system, 20: 31821 (ORNL-P-2239)
ORIC high-resolution spectrograph facility, 20: 31822 (ORNL-P-2260)
Procedure and code for calculating cost of electricity produced by nuclear power stations, 20: 32743 (ORNL-3944)
Production of ammonia using electricity from nuclear desalination reactor complex, 20: 32841 (ORNL-3882)
Prog. rpt. on molten-salt reactor, semiannual, 2/28/66, 20: 32800 (ORNL-3936)
Release of tritium and ^{85}Kr during processing of ThO_2–UO_2 fuels, 20: 31447 (ORNL-3956)
Sol-gel process development and microsphere preparation, 20: 31689 (ORNL-P-2159)
U.S.A.E.C. development program for high-specific-activity isotopes for research and industrial applications, 20: 31642 (ORNL-P-2190)

OESTERREICHISCHE STUDIENGESELLSCHAFT FUER ATOMENERGIE G.M.B.H., SEIBERSDORF.
Determination of I in whole serum and in blood protein with neutron activation analysis, 20: 31173 (SGAE-BL-18/1966)
Lead-210, shell model calculations with harmonic oscillator wave functions, 20: 32381 (SGAE-PH-37/1966)
Minimum pulse rate and detection limit of apparatus in measurement of radioactive rays, 20: 31512 (SGAE-SS-5/1966)
Neutron activation analysis determination of radiosensitizers, 20: 31172 (SGAE-BL-17/1966)

OHIO STATE UNIV. RESEARCH FOUNDATION, COLUMBUS.
Prog. rpt. on stress corrosion cracking in Fe–Ni–Cr alloy system, 12/17/65–3/16/66, 20: 31676 (COO-1319-39)

OREGON UNIV., PORTLAND. MEDICAL SCHOOL.
Prog. rpt. on intracellular pickup of ^{32}P by prostatic epithelial cells and absorption of ^{32}P from canine urinary bladder, final, 1965, 20: 31149 (TID-22969)

P

PACIFIC NORTHWEST RESEARCH FOUNDATION, SEATTLE, WASH.
Prog. rpt. on effects of radiation on testicular function of man, 6/63–5/64, 20: 31034 (RLO-1780-7)
Prog. rpt. on effects of radiation on testicular function of man, annual, 6/64–5/65, 20: 31035 (RLO-1780-8)

PARIS UNIV. (FRANCE). FACULTE DES SCIENCES.
Detection of hard β radiation in water using the Cherenkov effect, 20: 31506 (CEA-R-2915)
Kinetic study of fluorination by F of U and Pu compounds, 20: 31214 (CEA-R-2859)
Reaction $^{51}V(p,n)^{51}Cr$ and contribution to spectroscopy of ^{51}Cr, 20: 32371 (CEA-R-2832)

PENNSYLVANIA STATE UNIV., UNIVERSITY PARK. DEPT. OF BIOPHYSICS.
Prog. rpt. on cellular biophysics, 7/64, 20: 31033 (NASA-CR-59196)

PHILLIPS PETROLEUM CO. IDAHO FALLS, IDAHO., ATOMIC ENERGY DIV.
Numerical techniques for solving Fredholm's integral equations of first kind, 20: 31656 (IDO-17175)

POLYTECHNIC INST. OF BROOKLYN, N. Y. DEPT. OF AEROSPACE ENGINEERING AND APPLIED MECHANICS.
Hall current plasma accelerator. I., 20: 32573 (N-65-12780)

PRINCETON UNIV., N. J. GUGGENHEIM LABS. FOR THE AEROSPACE PROPULSION SCIENCES.
Rogowski coil probes for current density distribution in a plasma pinch, 20: 32574 (N-65-32035)

R

RADIO CORP. OF AMERICA, LANCASTER, PA. ELECTRON TUBE DIV.
Development of Cs-vapor-filled thermionic energy converter, 20: 31960 (N-66-16447)

RENSSELAER POLYTECHNIC INST., TROY, N. Y. DEPT. OF MECHANICAL ENGINEERING.
Control of absorption cross section for nuclear rocket, 20: 32851 (N-65-30544)

RESEARCH TRIANGLE INST., DURHAM, N. C. MEASUREMENT AND CONTROLS LAB.
Dissolved-oxygen analyzer for oceanographic use, 20: 31171 (ORO-596)

S

SAN DIEGO STATE COLL., CALIF.
Prog. rpt. on sensitivity of Drosophila to radiation, three year summary, 1966, 20: 31036 (SAN-529-3)

SANDIA CORP., ALBUQUERQUE, N. MEX.
Anomalous photocurrent generation in transistor structures, 20: 31612 (SC-DC-66-1415)
Close-in air blast from relatively deep low-yield nuclear detonation in basalt, 20: 31393 (PNE-711F)
Tabulation of cross sections, Q-values, and sensitivities for nuclear reactions of nuclides with 14-Mev neutrons, 20: 32380 (SC-RR-66-229)
Thermionic power generation from reentry vehicles, 20: 31961 (SC-DC-66-1115)
Transient annealing in semiconductor devices following pulsed neutron irradiation, 20: 31613 (SC-DC-66-1443)

SANDIA CORP., LIVERMORE, CALIF.
Shock pulse computer, 20: 32219 (SCL-DC-66-2)

STANFORD LINEAR ACCELERATOR CENTER, STANFORD UNIV., CALIF.
Characteristics of small computer systems for on-line applications, 20: 31661 (SLAC-PUB-191)
Hydrogen thyratron performance in SLAC two-mile accelerator, 20: 31825 (SLAC-PUB-192)
Story of Stanford's two-mile-long accelerator, 20: 31824 (SLAC-62)

STANFORD RESEARCH INST., MENLO PARK, CALIF.
Containment of fragments from runaway reactor, 20: 32744 (SRIA-1)

STANFORD UNIV., CALIF.
Two-dimensional time-dependent numerical study of rotational Couette flow, 20: 31344 (LA-3497)

STANFORD UNIV., CALIF. INST. FOR PLASMA RESEARCH.
Prog. rpt. on Bagel II, 8/65–4/66, 20: 32578 (TID-23025)

T

TECHNISCHE HOCHSCHULE, BRUNSWICK (WEST GERMANY). INSTITUT FUER ANORGANISCHE CHEMIE.
Decontamination of radioactive contaminated water, 20: 31318 (BMwF-FBK-65-04)

TENNESSEE UNIV., KNOXVILLE.
Analysis of parabolic partial differential equation containing both flow and diffusion terms, 20: 31659 (ORNL-TM-1497)

TRW EQUIPMENT LABS., THOMPSON RAMO WOOLDRIDGE INC., CLEVELAND, OHIO.
Prog. rpt. on determination of elevated-temperature fatigue data on refractory alloys, 1–4/66, 20: 31710 (NASA-CR-54983)

U

UNION CARBIDE CORP., OAK RIDGE, TENN. Y-12 PLANT.
Automatic film reader, 20: 31479 (Y-1533)
Single-transducer differential measuring device, 20: 31333 (Y-1541)
Thickness measurements by nondestructive testing methods, 20: 31480 (Y-1535)

UNITED NUCLEAR CORP., ELMSFORD, N. Y.
ATHENA: system of FORTRAN programs for radiation transport and heating calculations in complex reactor geometries, 20: 32768 (UNC-5148)

UNITED STATES–EURATOM JOINT RESEARCH AND DEVELOPMENT PROGRAM.
Prog. rpt. on critical heat flux (burnout) in boiling water, 7–9/65, 20: 31342 (EURAEC-1482)
Prog. rpt. on Zr alloy, 4–6/65, 20: 31677 (GEAP-4840)

URS CORP., BURLINGAME, CALIF.
Formation of debris from buildings by blast and fire effects of nuclear weapons, 20: 31332 (URS-651-4)

V

VANDERBILT UNIV., NASHVILLE, TENN.
Faraday effect at high magnetic fields, 20: 31807 (TID-23030)

W

WASHINGTON UNIV., ST. LOUIS, MO.
Prog. rpt. on low-energy nuclear reactions and nuclear spectroscopy, 20: 32373 (COO-1530-1)

WASHINGTON UNIV., SEATTLE. DEPT. OF MICROBIOLOGY.
Prog. rpt. on atmosphere radiochemical measurements, 5/63–4/66, 20: 31397 (RLO-1776-2)

WASHINGTON UNIV., SEATTLE. DEPT. OF OCEANOGRAPHY.
Physical, chemical and biological data from northeast Pacific Ocean: Columbia River effluent area, 1–10/62. Vol. I., 20: 31448 (RLO-1725-15)
Physical, chemical, and biological data from northeast Pacific Ocean: Columbia River effluent area, 1–10/62. Vol. II., 20: 31449 (RLO-

1725-16)
Physical, chemical, and biological data from northeast Pacific Ocean: Columbia River effluent area, 1–10/62. Vol. III., 20: 31450 (RLO-1725-17)
Physical, chemical, and biological data from northeast Pacific Ocean: Columbia River effluent area, 1–10/62. Vol. IV., 20: 31451 (RLO-1725-18)
Physical, chemical, and biological data from northeast Pacific Ocean: Columbia River effluent area, 1–10/62. Vol. V., 20: 31452 (RLO-1725-19)

WASHINGTON UNIV., SEATTLE. LAB. OF RADIATION BIOLOGY.
Radiological analyses of marine organisms, 20: 31427 (PNE-481, pp 1141-9)

WESTERN NEW YORK NUCLEAR RESEARCH CENTER, INC., BUFFALO.
Commercialization studies on wood-plastic combinations process, 20: 31625 (NYO-3569-1)

WISCONSIN UNIV., MADISON. THEORETICAL CHEMISTRY INST.
Electronic charge density in He in first-order shielding approximation, 20: 31902 (N-66-16249)

PERSONAL AUTHOR INDEX

Each entry after an author's name is a shortened version of the title of the report or article, followed by the *NSA* volume and abstract number. Report numbers are given in parentheses.

The phrase "Progress report" is abbreviated as "Prog. rpt.," permitting a more rapid and complete alphabetical arrangement of the titles without changing the location of the progress report titles in relation to the other titles.

Because of problems involving the mechanical preparation of this index, all accent marks are omitted. The following changes in spelling have been introduced to reduce some of the confusion which might result from omitting the accents:

ä	becomes	ae
ö		oe
ø		oe
ü		ue (except in transliterated Chinese names)

A

ABDEL-WAHAB, M. F., Preparation of radioiodinated serum Globulins, 20: 31264

ABDEL-WAHAB, M. F., Preparation of Tc, tyrosine, thyroxine, insulin and human serum proteins labeled-^{99m}Tc, 20: 31265

ABDUKADYROVA, I. Kh., Loop dose transformer, 20: 32865

ABDUL MATIN, A. S. M., Susceptibility of adult rice weevil to gamma radiation, 20: 31623 (AECD/AG-15)

ABDUMALIKOV, A. A., Conversion electron spectra of isotopes ^{166}Tm, ^{164}Yb, ^{164}Tm, and ^{162}Tm, 20: 32415

ABDURAKHMANOV, A. Kh., Fast neutron scintillation counter, 20: 31532

ABDURAZAKOV, A. A., Conversion electron spectra of isotopes ^{166}Tm, ^{164}Yb, ^{164}Tm, and ^{162}Tm, 20: 32415

ABE, Yasuhisa, Optical potential for high-energy α-α scattering, 20: 32531

ABEL, W. R., Propagation of zero sound in liquid ^{3}He at low temperatures, 20: 32329

ABRAMOV, V. I., Improved dosimetric technique in alpha therapy, 20: 31157

ABROYAN, I. A., Secondary emission coefficients for KBr single crystal bombarded with K ions, 20: 31938

ADACHI, Toshimi, Analytic property of impact parameter amplitude, 20: 32180

ADACHI, Toshimi, Impact parameter formalism. II., 20: 32173

ADACHI, Toshimi, Impact parameter formalism. III., 20: 32174

ADAMIKER, D., Neutron activation analysis determination of radiosensitizers, 20: 31172 (SGAE-BL-17/1966)

ADAMOVIC, O., Mesic decay of hyperfragments produced by K$^-$ mesons of 1.5 Bev/c, 20: 32491

ADAMS, R. E., Irradiation behavior of Th–U alloys and compounds, 20: 32833

ADAMS, R. E., Properties of Th, its alloys, and its compounds, 20: 31767

ADAMS, R. J., SNAP-10A electrically actuated band release device development, 20: 32852 (NAA-SR-Memo-11454)

ADAMSKI, L., Methods and results of static measurements in zero power reactor ANNA, 20: 32875

ADEMOLLO, M., Relation between $\eta \to 2\pi\gamma$ and $\eta \to 2\gamma$ from current algebra, 20: 32055

ADLER, Howard I., Genetic control of radiation sensitivity in microorganisms, 20: 31041

AEBERSOLD, P. M., Constant current source for instrument calibration, 20: 31588

AGARWAL, B. K., Decay angular correlation for Y_1^{1-} in the peripheral model, 20: 32052

AGARWAL, Bipin K., Production and decay of Ξ^* in one-particle exchange model, 20: 32009

AGRAWAL, J. C., Steady hydromagnetic flow in channel with porous walls in presence of transverse magnetic field, 20: 32221

AGRAWAL, J. C., Steady MHD flow in an annular channel, 20: 32222

AGRAWAL, J. P., Enrichment of ^{18}O and ^{13}C by carbon dioxide exchange in amine-solvent systems, 20: 31641 (NYO-755-1, pp 173-208)

AGRAWAL, K. M., Steady hydromagnetic flow in channel with porous walls in presence of transverse magnetic field, 20: 32221

AHLBORN, Boye, Velocity measurement by Doppler effect, 20: 32659

AHMAD, Ishfaq, Resonance (3,3) in nucleus, 20: 32078

AHMED, Hafiz, Control of fruit flies by gamma rays, 20: 31046

AHMED, N. M., Methods of applying Compton scattered neutron capture radiation to nuclear photo-excitation, 20: 32369 (AECL-2535)

AHRENS, T., Cross-section computations for charge-retention scattering of high-energy neutrinos, 20: 32036

AINSWORTH, E. J., Injury accumulation in sheep during protracted gamma radiation, 20: 31026

AITKEN, E. A., Oxidation kinetics of solid solutions of urania–yttria, 20: 31685

AJZENBERG-SELOVE, F., Masses and excited states of ^{24}Al and ^{28}P, 20: 32473

AKIBA, T., Free parameters and compositeness conditions in partial-wave scattering amplitude, 20: 32137

AKIMUNE, Hideo, Secondary electron emission-type neutral particle detector, 20: 31533

AKISHIN, P. A., Electron diffraction study of structure of neodymium halide molecules, 20: 31222 (ANL-Trans-310)

AKOL'ZINA, P. A., New method for studying the intensity of corrosion of reactor construction materials, 20: 31682 (NP-16003)

ALADAR, U., Polonium-210 determination in human urine samples, 20: 31187

ALAD'EV, I. T., Critical thermal fluxes and heat transfer of boiling K in tubes, 20: 31347

ALBINO, E., Analysis of a proposed analyticity test, 20: 32149

ALBURGER, D. E., Study of excited states in ^{15}N and ^{16}N, 20: 32501

ALDER, J. C., Excitation of levels of ^{12}C by inelastic scattering of 14.1-Mev neutrons, 20: 32408

ALDRIDGE, George W. Jr., Radioisotopes for Army aircraft applications, 20: 31622

ALEKSANDROV, A. V., Distribution of ^{90}Sr on surface of Atlantic during second part of 1961, 20: 31418

ALEKSANDROV, E. B., Orientation of ^{111}Cd nuclei by 3261 A resonant radiation, 20: 32419

ALEKSANDROV, Yu. V., Effect of Be-reflector duty factor on thermal neutron flux in horizontal beams, 20: 32765 (IAE-957)

ALEKSANDROVICH, E., Increasing power of Polish VVR-S reactor up to 10 Mwt, 20: 32879

ALEKSENKO, Yu. N., Effect of Be-reflector duty factor on thermal neutron flux in horizontal beams, 20: 32765 (IAE-957)

ALESHINA, L. V., Biosynthesis of corticosteroids in adrenal tissue of irradiated hypophysectomized rats, 20: 31011

ALEXANDER, R. E., Iodine-129 in effluents to unrestricted areas, 20: 32884

ALEXANDER, T. K., Doublet (2.8-Mev) in ^{21}Ne, 20: 32474

ALFIMOV, N. N., Determination of beta activity in preparation using cylindrical counters, 20: 31536

ALI, S. M., Mutation types in irradiated population of Jute, 20: 31027 (AECD/AG-14)

ALIEV, I. G., Magnetic beta spectrometer with space focusing of electron beams at $\pi\sqrt{10}$ angle, 20: 31583

ALKHAZOV, G. D., Stable pulse amplifier, 20: 31580

ALKHIMOV, V. I., Moments of inertia of strongly deformed nuclei, 20: 32416
ALLAS, R. G., Isospin selection rule in the $^{12}C(d,\alpha)^{10}B$ reaction, 20: 32500
ALLEN, B. C., Effect of Re on interface energies of Cr, Mo, and W, 20: 31773
ALLEN, B. C., Mechanisms of grain-boundary grooving in Cr, Mo, W, Cr–35Re, Mo–33Re, and W–25Re, 20: 31672
ALLEN, L. S., Combination neutron experiment for remote analysis, 20: 31211
ALMGREN, B., Swedish work on ^{232}Th–^{233}U fuel cycle, 20: 32830
ALTHOFF, K. H., Angular distribution of polarization of recoil proton from photoproduction of neutral pions on H at photon energy of 360 Mev. II., 20: 32097
ALTHOFF, K. H., Polarization of recoil proton from photoproduction of neutral pions on H in region of first resonance. I., 20: 32096
ALTMANN, H., Determination of I in whole serum and in blood protein with neutron activation analysis, 20: 31173 (SGAE-BL-18/1966)
ALTMANN, H., Neutron activation analysis determination of radiosensitizers, 20: 31172 (SGAE-BL-17/1966)
AMALDI, U. Jr., Two-channel problem and inelastic unitarity condition in eigenstates of total angular momentum, 20: 32014
AMATA, C. D., Permeability of zirconia, hafnia, and thoria to O, 20: 31731
AMATO, C. G., Miniature thermoluminescent dosimetry for application in medicine and biology, 20: 31598
AMBLER, J. E., Retention of foliar applications of ^{85}Sr by several plant species, 20: 30996
AMBROSINO, Georges, Anomalous long annihilation mean-lives of positrons in some ionic crystals, 20: 32099
AMIN, B. S., "Dating" ground waters of ages younger than 1,000–1,500 years using natural ^{32}Si, 20: 31432
AMORETTY, Stephen J., Action of Li vapor on graphite, 20: 31223 (BNL-tr-78)
AMREIN, W., Transfer theorem for multichannel scattering, 20: 32409
AMYOT, L., Resonance absorption in heavy water lattices development work at Ispra, 20: 32785
ANAND, S., Measurement of Compton scattering cross section, 20: 32007
ANANTHANARAYANAN, K., Effects of D-state admixture and hard-core radius on photoproduction of neutral pions from deuterons, 20: 32041
ANBAR, M., Radiolytic isotopic exchange of gaseous nitrogen, 20: 31282
ANDERSEN, Hans Henrick, Simple nonbinary scattering model applicable to atomic collisions in crystals, 20: 31920
ANDERSON, A. C., Propagation of zero sound in liquid ^3He at low temperatures, 20: 32329
ANDERSON, D. W., Photodisintegration of Ca to 62 Mev, 20: 32445
ANDERSON, G. S., Temperature dependence of sputtering yields of Ge(100) and (110) surfaces, 20: 31915
ANDERSON, Hugh R., Relationship between high-energy particles in space and solar plasma, 20: 31884
ANDERSON, J. R., Factors in life testing ion engines, 20: 31358
ANDERSON, J. Robert, Ion beam deflection for thrust vector control, 20: 31369
ANDERSON, J. Robert, Ion engines for satellite control, 20: 31366
ANDERSON, K. A., Observations on propagation of solar-flare electrons in interplanetary space, 20: 31869
ANDERSON, Norman G., Radiation-induced division delay in Astasia longa, 20: 31085
ANDERSON, P.W., Localized magnetic states and Fermi-surface anomalies in tunneling, 20: 32715
ANDREEV, S. V., Improved dosimetric technique in alpha therapy, 20: 31157
ANDREEV, Yu. A., Measuring conversion spectra at wide range of energies, 20: 31565
ANDREOLI, M., Conference on thyroid research, Rome, 1965, 20: 31162
ANNO, J. N., Secondary electron production from 1-Mev alpha particles from Au, 20: 31918
ANSELM, A. A., Three-particle partial wave amplitudes and unitarity conditions at complex values of angular momentum, 20: 32113
ANTOKU, Shigetoshi, Application of a fluoroglass dosimeter, 20: 31538
ANTOKU, Shigetoshi, Estimation of exposure dose to fetus from fetal radiography, 20: 31146
ANUFRIENKO, V. B., Time-of-flight neutron spectrometer, 20: 31566
AOKI, Susan, Sensitization of E. coli to radiation by bromouracil, 20: 31062
AONO, Osamu, Energy change of charged particle moving in plasma, 20: 32617
AOYAMA, Hideo, Determination of Ra in river waters, 20: 31191
APANASEWICZ, Stanislaw, Application of magnetogasdynamic equations to investigation of electric-arc characteristics, 20: 32232
APANASEWICZ, Stanislaw, Nonstationary axisymmetric flows in magnetogasdynamics, 20: 32231
APPELBAUM, J., Model of zero-bias tunneling anomalies, 20: 32714
ARAGOU, M., Industrial fabrication of fuel elements in France, 20: 31093
ARAKAWA, E. T., Radiation from thick silver foils bombarded by grazing-incidence electrons, 20: 32708
ARAKI, K., ESR study of free radicals formed by γ-irradiation of polyethylene terephthalate, 20: 31306
ARBUZOV, B. A., Possible direct test of CP violation in the K^0_2 interactions, 20: 32060
ARCHAMBEAU, John, Effects of 250-kv x rays on dog's pancreas, 20: 31089
ARCHER, N. P., Study of the $^{127}I(n,\gamma)^{128}I$ and $^{133}Cs(n,\gamma)^{134}Cs$ reactions, 20: 32422
ARDELL, A. J., Dislocation mobility and steady-state creep of crystals with reference to alpha Zr, 20: 32696
ARIFOV, U. A., Coefficient of surface ionization of fast secondary particles, 20: 31913
ARIFOV, U. A., Energy distribution of electrons from alkali halide compounds bombarded by He^+ and Ar^+ ions, 20: 31912
ARMANTROUT, Guy A., Fabrication technique for significantly reducing capacitance of Ge LID detectors, 20: 31513 (UCRL-14561)
ARMSTRONG, D. A., Determination of W_R and absorbed dose in gamma-irradiated HCl, HBr, and SF_6, 20: 31292
ARMSTRONG, P. E., Elastic properties of polycrystalline Sc, Re, Ru and Pt-21Ir, 20: 31748
ARNS, R. G., Directional correlations in ^{127}I, 20: 32396
ARPAD, T., Polonium-210 determination in human urine samples, 20: 31187
AR-RASHID, Harun, Photoproduction of vector mesons from nucleons, 20: 31984 (IC-66/54)
ARROWOOD, J. L., Automatic film reader, 20: 31479 (Y-1533)
ARSENE, A., Isotopic exchange of active methyl hydrogens. II., 20: 31261
ARTAMKIN, V. N., Burnup in plane layer, 20: 32772
ARTHURS, A. M., Croson's variational principle, 20: 32302
ASAI, Takuo, ESR of human black hair, 20: 31075
ASHER, Peres, Causality in S-matrix theory, 20: 32112
ATAC, M., Moessbauer scattering in ^{195}Pt, 20: 32487
ATHAVALE, R. N., Measurement of tritium activity in natural waters. I., 20: 31310
ATKINS, Harold L., Extracorporeal irradiation of blood in humans, 20: 31000
AUDREN, M. L., Control of radioactive pollution of milk by ^{131}I, 20: 31456
AUFLAGE, Zweite, Mathematical treatment of decay and formation laws of radioactivity with graphically solved examples, 20: 32377 (KFK-117)
AUGENSTEIN, Elizabeth, Effects of added agar on radiation sensitivity of trypsin in solution, 20: 31017
AUGENSTEIN, Leroy G., Advances in radiation biology. II., 20: 31038
AUGENSTEIN, Leroy, Effects of added agar on radiation sensitivity of trypsin in solution, 20: 31017
AUGERAT, J., Measurement technique for pair production in photographic emulsions, 20: 32006
AUNG, Tin, Isotope shifts of neutron-deficient mercury isotopes, 20: 32517
AUSHTIKAILIS, V. I., Spectrometer for studying fine structure of x-ray spectra (URS-11) 20: 31581
AVAN, L., Measurement technique for pair production in photographic emulsions, 20: 32006
AVGUSTINIK, A. I., Phase diagram of the HfC–Mo system, 20: 31729
AVNI, A., Monte Carlo calculations for a gamma-ray telescope, 20: 31554
AXFORD, W. I., Solar-wind interaction with magnetosphere: fluid dynamic aspects, 20: 32275
AYALA, Francisco Jose, Evolution of fitness. I., 20: 31049
AYER, James E., Method and apparatus for vibratory compaction, 20: 31704
AYUKHANOV, A. Kh., Coefficient of surface ionization of fast secondary particles, 20: 31913
AZIMOV, Ya. I., Three-particle partial wave amplitudes and unitarity conditions at complex values of angular momentum, 20: 32113

B

BABA, K., Production of neutral pions from electron-proton collisions, 20: 32038
BABAL'YANTS, V. F., Fast neutron scintillation counter, 20: 31532
BABINI, Lucio, Biological efficiency of 200 kv x rays, ^{60}Co rays and 14-Mev neutrons in Escherichia coli inactivation, 20: 31107
BACHELIER, D., Experimental study of reaction $D(p,\gamma)^3He$ at 156 Mev, 20: 32486
BACHYNSKI, M. P., Laboratory scaled solar plasma phenomena, 20: 32284
BACHYNSKI, M. P., Measurements of anisotropic plasmas using turnstile multiple-probe polarimeter, 20: 32581
BACON, G. E., Neutron diffraction investigation of Au_3Mn under pressure, 20: 31756
BADEN, P., Resonance (Hertz coherence) in hyperfine atomic structure, 20: 31911
BAEHR, K., Mirror reactions $^{10}B(d,t)^9B$ and $^{10}B(d,^3He)^9B$ at 11.8 Mev,

20: 32481
BAER, Hans-Guenter, Resistivity anomalies in system Ni–Ta, 20: 31775
BAGNALL, K. W., Neptunium chloro-complexes, 20: 31235
BAGOUIN, M., Action of Li vapor on graphite, 20: 31223 (BNL-tr-78)
BAGRAMYAN, E. R., Biosynthesis of corticosteroids in adrenal tissue of irradiated hypophysectomized rats, 20: 31011
BAGROV, V. G., Polarization properties of boson radiation, 20: 32120
BAIDOR, Z., Reconstruction of low power "MARYLA" reactor, 20: 32873
BAILY, George Arthur, Improvements in or relating to cermets, 20: 31707
BAILY, W. E., Effect of stoichiometry on properties of mixed oxide U–Pu fuel, 20: 31674
BAIR, William J., Long-term study of inhaled Pu in dogs, 20: 31025 (AD-631690)
BAJAJ, N. K., Wave propagation in rarefied plasma under action of Coriolis force, 20: 32603
BAKER, A. R., Doppler coefficient measurement in Zebra core 5, 20: 32840
BAKER, C., Effect of precipitates on critical current of Ti-32Nb superconductor, 20: 32322
BAKER, Donald M., Solar flare effects and relaxation time of ionosphere, 20: 32267
BAKER, F. B., Kinetics of reaction between V(III) and U(VI) in acid perchlorate solutions, 20: 31239
BAKER, J. H., Adsorption equilibria between earth materials and radionuclides, 20: 31426 (PNE-481, pp 1121-39)
BAKER, James L. L., Flow-regime transitions at elevated pressures in vertical two-phase flow, 20: 31340 (ANL-7093)
BAKER, P. S., U.S.A.E.C. development program for high-specific-activity isotopes for research and industrial applications, 20: 31642 (ORNL-P-2190)
BAKULIN, V. N., Vertical distribution of Rn and Tn and of their decay products in atmosphere, 20: 31404
BALABAN, A. T., Isotopic exchange of active methyl hydrogens. II., 20: 31260
BALANDIKO, N. I., Cryogenic developments at Joint Institute for Nuclear Studies, 20: 32318
BALDEWEG, F., Optical model analysis of elastic scattering on deuterons on ^{12}C, 20: 32454
BALDOCK, Russell, Determination of isotopic abundances for neutron cross-section measurements, 20: 31207
BALEZIN, S. A., Electrochemical properties of radioactive specimens of iron and steel, 20: 31231
BALI, L. M., Harmonics in scattering of electromagnetic radiation by electron current, 20: 32001
BALI, L. M., Scattering and absorption of electromagnetic radiation by electrons in light of harmonic phenomenon, 20: 32000
BALL, J. B., ORIC high-resolution spectrograph facility, 20: 31822 (ORNL-P-2260)
BALLANEY, A. K., Production of radioisotopes of high specific activity for medical use, 20: 31275
BALLINI, R., Levels in ^{60}Ni and ^{62}Ni at high excitation energies, 20: 32490
BALLY, I., Isotopic exchange of active methyl hydrogens. II., 20: 31260
BANERJEE, Manoj K., Heavy particle stripping, 20: 32444
BARANOV, P. S., Investigation of neutron counter efficiency at intermediate energies, 20: 31584
BARANOV, S. A., Magnetic beta spectrometer with space focusing of electron beams at $\pi\sqrt{10}$ angle, 20: 31583
BARBER, W. C., Test of quantum electrodynamics by electron-electron scattering, 20: 32305
BARBI, M., Direct numerical solution of three-body problem, 20: 32498
BARBIER, M., Estimates of residual radiation levels induced by high-energy nucleons, 20: 31831
BARBIER, M., Induced radioactivity data computed for various materials and compared with that of irradiated samples, 20: 32549
BARCA, Lorenzo, CNR MHD plant at the Istituto di Aerodinamica, Naples, 20: 32633
BARCATTA, F. A., Surface tension storage and feed systems for ion engines, 20: 31379
BARDET, Rene, Deuterium–tritium reactions in mixed-plasma accelerator, 20: 32586
BARENDSEN, G. W., Effect of O on impairment of proliferative capacity of human cells by radiations LET, 20: 31123
BARKAN, P., Stagnation pressure distribution in current-carrying plasma, 20: 32660
BARKER, B. M., Composition of degenerate gas of elementary particles, 20: 32044
BARKER, F. C., Intermediate coupling shell-model calculations for light nuclei, 20: 32436
BARNARD, A. Johannes, Velocity measurement by Doppler effect, 20: 32659
BAROCH, C. J., Prog. rpt. on Zr alloy, 4–6/65, 20: 31677 (GEAP-4840)
BARR, R. Q., Improving ductility of Mo, 20: 31741
BARRICK, P. L., Liquid-vapor phase equilibria of neon-normal hydrogen system, 20: 32242
BARRINGTON, R. E., Alouette II satellite, 20: 32247
BARTHEL, James R., Plasma motion in weakly ionized gas with strong magnetic field, 20: 32645
BARTO, R. L., Mechanical properties of W-25% Re alloy sheet, 20: 31778
BARTSCH, J., Strange-particle production in π^-p and π^+p collisions at 4 Bev/c, 20: 32029
BARZ, H.-U., Problem of determining neutron fields in time-dependent media. II., 20: 32357
BASOVA, E. S., Irradiation of combined emulsion and spark chamber system, 20: 31569
BASSEL, R. H., Polarizations and differential cross sections for the elastic scattering of 40-Mev protons from ^{12}C, ^{40}Ca, ^{58}Ni, ^{90}Zr, and ^{208}Pb, 20: 32510
BASSO, Michael, Dependence of pulse amplitude and polarity on position of entry in particle detector, 20: 31498 (AD-632527)
BASTAR, R., Anisotropy of self-diffusion in alpha uranium, 20: 31771
BATALOV, A. A., Effect of Be-reflector duty factor on thermal neutron flux in horizontal beams, 20: 32765 (IAE-957)
BATES, Robert G., Aeroradioactivity survey of Lisburne Peninsula, 20: 31425 (PNE-481, pp 1115-19)
BATES, T. R., Cesium transport through a tungsten capillary, 20: 31381
BAUER, Walter, Stage IV recovery of Pt after electron irradiation, 20: 31800
BAUGH, D. J., Polarization of 17.8 Mev protons elastically scattered by nuclei, 20: 32439
BAUMAN, H. F., Technical and economic characteristics of Th reactors, 20: 32834
BAUMANN, G., Lithium-8 emission in 5.0-Bev/c K$^-$-meson interactions in nuclear emulsion, 20: 32469
BAUMGARTNER, W. V., Treatment and evaluation of internal deposition from Pu wound, 20: 31030 (BNWL-SA-39)
BAXTER, A. M., Angular correlations for $^{12}C(p,p'\gamma)^{12}C$. II., 20: 32438
BAYUKOV, Yu. D., Determination of kinematic properties of particles in spark chamber sparks, 20: 31570
BEARD, David B., Theory of type-I comet tails, 20: 31898
BEARD, G. B., Decay of ^{94}Nb and ^{94m}Nb, 20: 32518
BEBEL, D., Scattering of massive photons with vector-scalar coupling, 20: 32046
BECHDOLFF, A., Lithium-8 emission in 5.0-Bev/c K$^-$-meson interactions in nuclear emulsion, 20: 32469
BECHER, H., Fine structural studies on effect of x rays on retina of guinea pigs, 20: 31118
BECKER, Bernard, Rubidium-86 accumulation in lenses of galactose-fed rats, 20: 30978
BECKER, E., Nondestructive testing of materials in fuel element production, 20: 31354
BECKER, J. A., Study of low-lying states of ^{33}S, 20: 32565
BECKER, K., Nuclear track registration in dosimeter glasses for neutron dosimetry in mixed radiation fields, 20: 31462
BECKERS, J., Matrices and projection operators in abbreviated theories for particles without mass, 20: 32167
BECKETT, N., Ratio of symmetric to asymmetric fission in proton bombardment of ^{226}Ra, 20: 32515
BECKEY, H. D., experimental techniques, applications, and theory of field ion mass spectrometry, 20: 31199
BEDER, D. S., Mass difference ($K_1^0 - K_2^0$) in S-matrix theory, 20: 32025
BEDER, D. S., Rho-meson electromagnetic mass splitting, 20: 32011
BEECHER, Jean, Internal hydrogen ion concentration of Thiobacillus thiooxidans and survival after irradiation, 20: 31139
BEETEM, W. A., Adsorption equilibria between earth materials and radionuclides, 20: 31426 (PNE-481, pp 1121-39)
BEHANNON, K. W., Magnetic storms in earth's magnetic tail, 20: 32253
BEHOF, A. F., Polarization of neutrons elastically scattered from ^3He at 3.33 and 7.90 Mev, 20: 32452
BEHRINGER, K., Transistorized counting channel for measuring beta-activities with proportional counters, 20: 31509 (EIR-97)
BEIN, G. P., Microwave transmission in pure air plasma, 20: 32667
BELEN'KII, S. N., Magnetic beta spectrometer with space focusing of electron beams at $\pi\sqrt{10}$ angle, 20: 31583
BELL, John S., Problem of hidden variables in quantum mechanics, 20: 32307
BELL, P. R., Apparent high-frequency stability of highly anisotropic plasma, 20: 32624
BELL, P. R., Combination neutron experiment for remote analysis, 20: 31211
BELLE, Yu. S., Determination of stability of radiometric instruments, 20: 31575
BELLETTINI, G., Single-π^0 photoproduction from hydrogen around the second resonance, 20: 32051
BELOUSOVA, I. M., Inversion of levels during excitation by a mono-

energetic electron beam, 20: 31941
BELROSE, J. S., Alouette II satellite, 20: 32247
BELUSHKIN, V. A., Cryogenic developments at Joint Institute for Nuclear Studies, 20: 32318
BELY, O., Excitation of lithium-like ions by electron impacts, 20: 31929
BEMPORAD, C., Single-π^0 photoproduction from hydrogen around the second resonance, 20: 32051
BENDER, Iring, Self-consistent calculation of the 11- and 33-amplitude in low-energy π-N scattering, 20: 32091
BENEDICT, Manson, Growth of foreign nuclear power, 20: 32808 (TID-22973)
BENENSON, R. E., Reaction ^{6}Li(d,n)^{7}Be* with polarized deuterons, 20: 32411
BENES, P., Radiotracer study of manganese adsorption on glass from aqueous solutions, 20: 31245
BEN HAIM, A., Calibration problems in whole-body counting with NaI(Tl) detectors, 20: 31443 (CONF-650675-1)
BENNETT, L. L., Technical and economic characteristics of Th reactors, 20: 32834
BENSON, G., Observation and properties of neutral A_2 meson, 20: 32064
BENSON, Philip A., Radionuclide concentrations in individual fallout particles, 20: 31424
BEONIO-BROCCHIERI, F., Resonance absorption in heavy water lattices development work at Ispra, 20: 32785
BERANGER, G., Electron microscope observations on thin films of zirconia obtained by oxidation of Zr, 20: 31755
BERCAW, R. W., Inelastic scattering of 39.5 and 31.8 Mev alpha-particles by ^{16}O, 20: 32554
BERGER, H. J., Mechanism of strontium deposition in bone tissue, 20: 30973
BERGER, Harold, Television system for ultrasonic imaging, 20: 31352 (ANL-7042)
BERGER, R., Use of actinides elements in isotopic power generators, 20: 31965
BERGER, William C., Scintillation photography of intravascular clots in vivo, 20: 31150 (UCRL-16691)
BERGNER, K. G., Rapid estimation of important radionuclides ^{89}Sr, ^{90}Sr, ^{131}I, and ^{137}Cs in food and water. II., 20: 31180
BERINDE, Alexandru, Simultaneous measurement of beam energy in angular distribution studies, 20: 32403
BERMAN, D., Solar-electric propulsion system for interplanetary spacecraft, 20: 31373
BERNARDI, Zena, Biological efficiency of 200 kv x rays, ^{60}Co rays and 14-Mev neutrons in Escherichia coli inactivation, 20: 31107
BERNAS, M., Experimental study of reaction D(p,γ)^{3}He at 156 Mev, 20: 32486
BERNAS, R., Relative abundance and production cross sections of lithium isotopes, 20: 31205
BERNERT, R. E., Methods and costs of testing at liquid He temperatures. I., 20: 32315
BERNHEIM, A., Antiproton-nuclei scattering at 3 Bev/c, 20: 32467
BERTENEV, V. M., Valence state of Sm in metal and in its monosulfide, 20: 32720
BERTERO, M., Analysis of a proposed analyticity test, 20: 32149
BERTIN, P. Y., Measurement technique for pair production in photographic emulsions, 20: 32006
BERTOLINI, G., Determination of partial α-half-life of ^{241}Pu, 20: 32435
BERTOLINI, G., Time resolution measurements with XP 1020 photomultipliers, 20: 31552
BERTRAND, S., Control of radioactive pollution of milk by ^{131}I, 20: 31456
BESKROVNYI, I. M., Measuring conversion spectra at wide range of energies, 20: 31565
BESKROVNYI, I. M., Wide-range intensity meter for heterogeneous magnetic fields, 20: 31487
BETTINI, A., Experimental tests on SU_{6W} in nucleon-antinucleon annihilation at rest, 20: 32056
BEVILACQUA, S., Control system for triple-axis neutron spectrometer, 20: 31543
BEWLEY, D. K., Effect of O on impairment of proliferative capacity of human cells by radiations LET, 20: 31123
BEZUGLYI, V. D., Preparation of plastic scintillators in plate form, 20: 31261
BHARATHI, S. M., Angular distribution of ^{19}F(n,α)^{16}N reaction at E_n = 4.7 Mev, 20: 32434
BHARDWAJ, I. S., Effect of ^{60}Co gamma rays on commercial polypropylene films, 20: 31274
BHATIA, K. L., Dynamic orientation of spin-1 nuclei. II., 20: 32390
BHATIA, M. S., Composition of degenerate gas of elementary particles, 20: 32044
BIANCASTELLI, R., Two-channel problem and inelastic unitarity condition in eigenstates of total angular momentum, 20: 32014
BIEBL, R., Diurnal and annual period of radiation resistance of plant cells, 20: 31079
BIERMANN, Ludwig, Comets and the solar wind, 20: 31874
BIERMANN, Ludwig, Interaction of solar wind with comets, 20: 31896
BIERMANN, Ludwig, Magnetohydrodynamic aspects of interaction of solar wind with comets, 20: 31897
BIGGERSTAFF, J. A., CDC-160A programs for processing data from a neutron time-of-flight cross-section experiment, 20: 32379 (ORNL-TM-1208)
BIGGS, P. J., Single-π^0 photoproduction from hydrogen around the second resonance, 20: 32051
BILDSTEIN, H., Carboxylation of polychloro compounds to trichloroacetic acid by radiation chemistry, 20: 31276
BILLEN, D., Degradation of DNA in polyauxotrophic bacterium, 20: 31015
BILPUCH, E. G., s- and p-Wave neutron spectroscopy. XIa., 20: 32389
BILWES, R., Reaction chamber with semiconductor detectors adapted for measurements of particle correlations, 20: 31556
BIR, R., Measurement of natural abundance of ^{234}U, 20: 31400
BIRD, Joseph F., Evolution of a rotating protostar, 20: 31872
BIRDSEYE, Rosemary A., Measurement of decay scheme correction in absolute standardization of ^{57}Co, 20: 32414
BISHOP, G. R., Nuclear microscopy, 20: 32405
BISWAS, S. N., Relation between leptonic and nonleptonic K-meson decays and current algebras, 20: 32039
BJOERNHOLM, S., Self-supporting metal foils prepared from oxides of separated isotopes of rare earth elements, 20: 31696
BLACK, W. W., Binding energy of deuteron determined from measurement of hydrogen neutron-capture gamma-ray energy, 20: 32488
BLACKMORE, E. W., Spin and parity assignments in ^{24}Mg, 20: 32556
BLAGORODOV, A. M., Selection of optimum curve of rectangular light pipes with no light losses by reflection, 20: 31818 (ITEF-385)
BLAIR, William H., Effect of gamma and proton irradiation on lactic dehydrogenase isoenzymes, 20: 31105
BLANC, D., Detection efficiency of spark chambers and its exact calculation, 20: 31558
BLANC, Daniel, Geiger-Mueller counters filled with Hg vapor, 20: 31517
BLANCO, R. E., Production of ammonia using electricity from nuclear desalination reactor complex, 20: 32841 (ORNL-3882)
BLASSE, G., Dilanthanide molybdates and tungstates Ln_2MO_6, 20: 31749
BLIAUX, J., Present and possible performances of thermo-ionic conversion, 20: 31964
BLISS, H. E., Studies of subcritical lattices with distributed neutron absorber, 20: 32787
BLIZARD, Jane B., Long-range solar flare prediction technique, 20: 31879
BLOEMBERGEN, N., Interaction between light waves and spin waves, 20: 32735
BLOKHIN, S. M., Valence state of Sm in metal and in its monosulfide, 20: 32720
BLOOD, R. E., Prog. rpt. on Zr alloy, 4–6/65, 20: 31677 (GEAP-4840)
BLOOM, S. D., Fermi and Coulomb matrix elements from β-γ correlation measurements on ^{48}V and ^{52m}Mn, 20: 32506
BLUMBERG, L. N., Polarizations and differential cross sections for the elastic scattering of 40-Mev protons from ^{12}C, ^{40}Ca, ^{58}Ni, ^{90}Zr, and ^{208}Pb, 20: 32510
BOCCALETTI, D., Splitting of a photon into two photons in Coulomb field of nucleus, 20: 32031
BOCHNACKI, Z., Transverse spin polarization in odd-mass deformed nuclei, 20: 32447
BODAK, O. I., Crystal structure of $Ce_3Ni_6Si_2$ and related compounds, 20: 31253
BODMER, A. R., Alpha-deuteron-lambda model of the hypernucleus $_{\Lambda}Li^7$, 20: 32450
BOEHM, A., Dynamical groups of simple nonrelativistic models, 20: 31827
BOEHM, F., Internal magnetic field of lutetium in iron and g factor in ^{175}Lu, 20: 32472
BOEHM, Horst, High-temperature embrittlement of austenitic steels and Ni alloys by (n,α) reactions, 20: 31801
BOEHMER, H., Incoherent scattering of microwaves by unstable electron plasma oscillations, 20: 32622
BOEKER, E., Two-particle-two-hole states in ^{16}O, 20: 32524
BOEMMEL, Hans, Properties of supported small α-Fe_2O_3 particles determined with Moessbauer effect, 20: 31779
BOERBOOM, A. J. H., Amplification factors of particle multiplier for multiply charged noble gas ions, 20: 31926
BOERBOOM, A. J. H., Ionization cross-section measurements for 0.6- to 20-kev electrons in atomic and molecular gases, 20: 31906
BOETTCHER, A., Thorium fuel programs in Federal Republic of Germany, 20: 32824
BOEUF, A., Resonance absorption in heavy water lattices development work at Ispra, 20: 32785
BOGAARDT, M., Construction of ship reactors, 20: 32854
BOGART, Donald, Monte Carlo interpretation of sphere transmission experiments for average capture cross sections at 24 kev, 20: 32378 (NASA-TR-R-239)
BOGART, Elliot, Radiative decay of the μ meson, 20: 32104

BOHM, D., Proposed solution of measurement problem in quantum mechanics by hidden variable theory, 20: 32308
BOHM, D., Refutation of proof by Jauch and Piron that hidden variables can be excluded in quantum mechanics, 20: 32309
BOHN, W. L., Ionization equation for optically thin plasma, 20: 32636
BOLIUNOVA, A. D., Radioactivity of satellite Cosmos 3 after explosion of July 9, 1962, 20: 32271
BOLLINGER, J. N., Incorporation of dietary linoleic acid into triglycerides of irradiated bone marrow, 20: 31016
BOLLINI, Vincenzo, Biological efficiency of 200 kv x rays, ^{60}Co rays and 14-Mev neutrons in Escherichia coli inactivation, 20: 31107
BOLTON, J. G., Identification of extragalactic radio sources between declinations 0° and +20°, 20: 31853
BOMKE, Hans A., Worldwide geomagnetic disturbances generated by Starfish explosion, 1962, 20: 32264
BONACIC, V., Analog and digital readout system for the circulating memory, 20: 31557
BOND, V. P., Autoradiographic studies of lymphoid cells in blood and bone marrow of irradiated dogs, 20: 31086
BOND, W. D., Sol-gel process development and microsphere preparation, 20: 31689 (ORNL-P-2159)
BOND, William D., Programming manual for ILLIAC III computer, 20: 31653 (COO-1018-1061)
BONDAR, L., Strange-particle production in π^-p and π^+p collisions at 4 Bev/c, 20: 32029
BONIFACIO, R., Conditions for existence of a diagonal representation for quantum mechanical operators, 20: 32304
BONJOUR, Emmanuel, Faults created by irradiation in pure Fe, 20: 31789
BOOKS, Kenneth G., Aeroradioactivity survey and geology of San Francisco, 20: 31395 (CEX-58.4.5)
BORELLA, A., Determination of minimum detectable content of trace elements in neutron-activated materials, 20: 31541
BORG, Donald, Stable bromine and activation analysis in protein tracer studies, 20: 30990
BORGERS, M., Lysosomal modifications after administration of radioprotective drugs, 20: 30964
BORGERS, M., Ultrastructural aspects of duodenal crypts in x-irradiated mice after chemical protection, 20: 31128
BORGHINI, M., Polarization and spin correlation parameter measurements in 600-Mev proton-proton scattering, 20: 32016
BORMANN, M., Study of neutron reactions with α-particle emission on ^{23}Na in energy region 12.6 to 18.7 Mev, 20: 32540
BORNAND, Bernard, Nuclear codes for IBM-704, -709, and -7090, 20: 32764 (CEA-Bib-17(Pt.2))
BORTSOV, E. I., Radiation chemistry of carbohydrates. V., 20: 31304
BOSCHITZ, E. T., Inelastic scattering of 39.5 and 31.8 Mev alpha-particles by ^{16}O, 20: 32554
BOSCHITZ, Edmund T., Anomalies in spin-orbit term of optical model potential, 20: 32523
BOSE, S. K., Equal-time commutators and $\eta \to 3\pi$ decays, 20: 32037
BOSE, S. K., Generalized nonet representation of SU(3) × SU(3) and its applications, 20: 32107 (IC-66/48)
BOSE, S. K., Relation between leptonic and nonleptonic K-meson decays and current algebras, 20: 32039
BOSHART, R. R., Low-background counting of betas and alphas with silicon detectors, 20: 31540
BOSTICK, W. H., Plasma injected into B_z guide field from conical theta-pinch accelerator, 20: 32661
BOSTICK, W. H., Rotational-velocity and ion-density profiles in plasma vortices, 20: 32644
BOUCHEZ, Robert, Reaction ^{11}B(p,$\alpha\alpha$)^{4}He at 163 kev, 20: 32402
BOURGEOIS, Michel, Dry chemical treatment of uranium–zirconium fuels, 20: 31321
BOURRIEAU, Jacques, Geiger-Mueller counters filled with Hg vapor, 20: 31517
BOUZYK, J., Progress in reactor kinetics at Swierk, 20: 32781
BOWLES, B. J., Ratio of symmetric to asymmetric fission in proton bombardment of ^{226}Ra, 20: 32515
BOYCE, Richard P., Sensitization of E. coli to radiation by bromouracil, 20: 31062
BOYER, D. W., Microwave transmission inpure air plasma, 20: 32667
BOYER, Timothy H., Derivation of conserved quantities from symmetries of Lagrangian in field theory, 20: 32110
BOZORTH, R. M., Magnetic properties of solid solutions of heavy rare earths with each other, 20: 31763
BRACCINI, P. L., Single-π^0 photoproduction from hydrogen around the second resonance, 20: 32051
BRACE, L. H., Alouette II satellite, 20: 32247
BRADBURY, B. T., Safety aspects of carbide fast reactor fuels, 20: 31675
BRADFORD, Robert W., Hydrogen thyratron performance in SLAC two-mile accelerator, 20: 31825 (SLAC-PUB-192)
BRADLEY, C. C., Neutron diffraction investigation of Au_2Mn under pressure, 20: 31756
BRADY, David N., Uptake and retention of ^{32}P and ^{65}Zn from consumption of Columbia River fish, 20: 30969 (BNWL-SA-45)
BRADY, Victor O., Effective atmospheric losses for 125-Mev protons in South Atlantic anomaly, 20: 32265
BRAETTER, P., Gamma radiation of ^{83}Br, 20: 32413
BRATENAHL, A., Study of neutral point in plasma, 20: 32656
BRAUN, H., Lithium-8 emission in 5.0-Bev/c K$^-$-meson interactions in nuclear emulsion, 20: 32469
BREDEL, V., Optical model analysis of elastic scattering on deuterons on ^{12}C, 20: 32454
BREDIN, D. J., Isobaric analog states of doubly magic ^{208}Pb, 20: 32478
BREEDING, Kenneth James, Grammar for a pattern description language, 20: 31651 (COO-1018-1054)
BREHM, R. L., Analysis of neutron wave-type experiments, 20: 32363
BREIVIK, F., Multiple pion production in proton-proton collisions at 24 Bev/c, 20: 32017
BRENT, T. P., Irradiation effects on synthesis of DNA and mitosis in HeLa cells, 20: 31008
BRIDGE, H. S., What we know and what we do not know about solar wind, 20: 31889
BRIDGES, B. A., Site of lethal damage by ionizing radiation in E. coli, 20: 31068
BRIGGS, B. R., Evidence for collision-free hydromagnetic shock in interplanetary space, 20: 31891
BRINK, Gilbert O., Electron bombardment molecular beam detector, 20: 31488
BRINK, Gilbert O., Electron bombardment molecular beam detector, 20: 31492
BRISCOE, C. V., Positron annihilation in liquid He, 20: 32346
BRISCOE, C. V., Positron annihilation in liquefied gases, 20: 32345
BRISSAUD, I., Experimental study of reaction D(p,γ)^{3}He at 156 Mev, 20: 32486
BRITO, S. S., Thorium-cycle possibilities in Brazilian nuclear power program, 20: 32821
BRITTON, R. B., Superconducting quadrupole lens, 20: 31815 (BNL-10144)
BROCKMAN, K. W. Jr., Proton spectra from d+d breakup at 25.3 Mev, 20: 32568
BRODOWSKY, H., H/D separation factors in electrolysis and diffusion by use of Pd and Pd/Ag membranes, 20: 31256
BROGAN, Thomas R., Performance of self-excited MHD generator, 20: 31976
BROOKSBANK, R. E., Impact of Kilorod operational experience on design of fabrication plants for ^{233}U–Th fuels, 20: 31690 (ORNL-P-2176)
BROUT, R., Foundations of the Bootstrap theory, 20: 32212
BROWN, H. L., Elastic properties of polycrystalline Sc, Re, Ru and Pt-21Ir, 20: 31748
BROWN, R. Armstrong, NMR field measuring equipment for CERN muon storage ring, 20: 31817 (CERN-66-15)
BROWN, Richard M., Characteristics of small computer systems for on-line applications, 20: 31661 (SLAC-PUB-191)
BROWN, Richard R., Identification of radiation-preferred electronics, 20: 31619
BROWN, Terrence S., Plasma diagnostics using lasers, 20: 32598
BROWN, W. D., Prog. rpt. on radiation of heme proteins, 10/64–9/65, 20: 30999 (UCB-34P95-7)
BRUCE, R. E., Ionization in hydrogen plasmas, 20: 32628
BRUCKER, G. J., Proton irradiation of thin-film CdS and single-crystal Si solar cells, 20: 31616
BRUECHNER, Hans-Joachim, Boiling water reactor construction outline of AEG, 20: 32812
BRUN, E., Phonon-induced dipole nuclear spin transitions, 20: 32689
BRUSTON, P., Observation of low-altitude acceleration of auroral protons, 20: 32249
BRYANT, B. J., Autoradiographic studies of lymphoid cells in blood and bone marrow of irradiated dogs, 20: 31086
BRYANT, D. A., Mev phenomena related to solar wind. I., 20: 31885
BRYSON III, C. E., Apparatus for radiofrequency surface measurements on single crystal superconductors, 20: 32343
BUCKA, H., Level crossing experiment in the $6^2P_{3/2}$ state of Rb–I spectrum, 20: 31940
BUD, J., Proposed solution of measurement problem in quantum mechanics by hidden variable theory, 20: 32308
BUD, J., Refutation of proof by Jauch and Piron that hidden variables can be excluded in quantum mechanics, 20: 32309
BUDAGOV, Yu. A., Optimization of measurements of electron energy in heavy-liquid bubble chambers, 20: 31568
BUDKA, Alfred J., Secondary gamma ray transmission through plane slabs of concrete, 20: 32671 (AD-633216)
BUDZINSKI, W. V., Magnetic field-induced anisotropy of superconducting energy gap determined by microwave absorption, 20: 32326
BUERGISSER, H., Reaction ^{6}Li(d,n)^{7}Be* with polarized deuterons, 20: 32411
BUINITSKAYA, V. I., Effect of Be-reflector duty factor on thermal neutron

flux in horizontal beams, 20: 32765 (IAE-957)
BUKHONOVA, A. I., Action of hormones on the reparative processes in skin exposed to gamma irradiation, 20: 31061
BUKOWSKI, K., Progress in reactor kinetics at Swierk, 20: 32781
BULLIS, R. H., Plasma physics of thermionic converters, 20: 31971
BUNCE, L. J., Estimation of total hydrogen content of human body, 20: 30993
BUNEMAN, O., Prog. rpt. on Bagel II, 8/65–4/66, 20: 32578 (TID-23025)
BURAN, T., Multiple pion production in proton-proton collisions at 24 Bev/c, 20: 32017
BURDET, G., Inversion problem in the λ plane. II., 20: 32152
BURGER, Peter, Oscillations in thermal cesium plasma diode, 20: 31966
BURKE, E. A., Damage production in electron-irradiated palladium, 20: 31805
BURKE, P. G., Correlation in the elastic and inelastic S-wave scattering of electrons by H and He+, 20: 31927
BURMAN, R., Exponentially varying electromagnetic fields in stratified magnetoplasma, 20: 32627
BURNETT, James R., Radiation hardening of an ion propulsion system, 20: 31618
BURNS, R. R., Electron production by high-energy neutrinos, 20: 31986 (NEVIS-148)
BURROWS, K. M., Excitation and ionization by auroral protons, 20: 32246
BURTON, R., Critical currents and i/v relations in superconducting alloy films, 20: 32317
BUSCHBECK, F., New electrostatic time-of-flight mass spectrometer, 20: 31209
BUSH, Karen J., Pancreatic lipase activity in deuterium oxide, 20: 30995
BUSHUEV, A. V., Gamma spectrometer measurements of ^{238}U capture-to-fission ratio, 20: 32391
BUSTAD, L. K., IDERM: program for intake, distribution and excretion of radionuclides in mammals, 20: 31441 (BNWL-SA-40)
BUTLER, H. M., Calibration of the ORNL model Q-2240, continuous air monitor, 20: 31528
BUTLER, J. A. V., Irradiation effects on synthesis of DNA and mitosis in HeLa cells, 20: 31008
BUTOMO, N. V., Use of cadaver bone marrow in treatment of radiation injuries, 20: 31135
BUTOVETSKII, L. D., Effects of x rays on orchitis development in rabbits and antigen property for reaction of Treponema pallidum immobilization, 20: 31119
BUVAT, Foucault, Thermal behavior of concrete, 20: 31722 (ORNL-tr-1227)
BYRON, F. W. Jr., Importance of correlation effects in ionization of He by electron impact, 20: 31924
BYSHEVSKI, V., Increasing power of Polish VVR-S reactor up to 10 Mwt, 20: 32879

C

CABANE, G., Influence of Al content and temperature on elastic and plastic properties of solid solution of Fe–Al, 20: 31751
CABIBBO, N., Symmetry and weak interactions, 20: 32197
CABRESPINE, Andre, Extraction by pealing of beam of heavy ions accelerated in cyclotron with starred field, 20: 31828
CADLE, Richard D., Particles in atmosphere and space, 20: 32285
CALDWELL, R. L., Combination neutron experiment for remote analysis, 20: 31211
CALDWELL, R. S., Circuit hardening using computer techniques, 20: 31621
CALLAHAN, A. C., Measurement of three K+-decay branching ratios, 20: 32043
CAMPBELL, D., ESR study of free radicals formed by γ-irradiation of polyethylene terephthalate, 20: 31306
CAMPI-BENET, X., Electromagnetic transition probabilities in single closed shell nuclei, 20: 32426
CANET, Pierre, Machines for loading and unloading channels of nuclear reactor, 20: 32755
CANNELLI, Gaetano, Relaxation effect due to diffusion of interstitial deuterium in tantalum, 20: 31766
CAO, Guy De, Ionization of some gases by accelerated H+ and He ions, 20: 31909
CAPET, Maurice, Spatio-temporal distribution of initial brilliance of laser discharge in air, 20: 32224
CAPLINGER, E., Characteristics of micropound range ion thrustors, 20: 31385
CAPPS, Richard H., Bootstrap interpretation of SU(6), 20: 32208
CARAPIC, Miodrag, Safety systems for gas-cooled graphite-moderated reactors, 20: 32835
CARLONE, Cosmo, Renner effect in the linear XY_2 molecule, 20: 31943
CARLSMITH, R. S., Technical and economic characteristics of Th reactors, 20: 32834
CARMICHAEL, B. M., Fast transients in liquid Pu, 20: 32797 (LA-DC-7748)
CARROLL, David I., In-flight instrumentation for prompt miss distance measurement using gamma ray techniques, 20: 31496
CARROLL, David I., Pulsed x-ray instrument for altitude measurement and terrain identification, 20: 31493
CARROLL, David I., Radioisotope and machine sources of x radiation for aerospace applications, 20: 31339
CARTER, R. E., Cationic self-diffusion in calcia-stabilized zirconia, 20: 31732
CASALE, P., Rotational-velocity and ion-density profiles in plasma vortices, 20: 32644
CASINI, G., Resonance absorption in heavy water lattices development work at Ispra, 20: 32785
CASSAGNOU, Yves, Reaction $^{51}V(p,n)^{51}Cr$ and contribution to spectroscopy of ^{51}Cr, 20: 32371 (CEA-R-2832)
CASSANO, C., Conference on thyroid research, Rome, 65, 20: 31162
CASSEL, R. L., Electronic ripple filter for the Brookhaven Alternating-Gradient Synchrotron, 20: 31833
CASTAING, Raymond, Microanalysis by secondary ion emission, 20: 31201
CASTOR, J., Measurement technique for pair production in photographic emulsions, 20: 32006
CECCHETTI, Ervedo, Biological efficiency of 200 kv x rays, ^{60}Co rays and 14-Mev neutrons in Escherichia coli inactivation, 20: 31107
CERCHIONE, J. D., BORAX-V nuclear superheat operating experience, 20: 32866
CHAFFEE, R. R. J., Heritable radiation effects on mouse, 20: 31048
CHAKRABARTI, A., Thomas-Wigner precession of polarization, 20: 32126
CHAKRABARTY, M. R., Crystal chemistry and dielectric properties in systems $BaTiO_3$–UO_2 and $BaTiO_3$–$BaUO_3$, 20: 31735
CHALMETON, Vincent, Spatio-temporal distribution of initial brilliance of laser discharge in air, 20: 32224
CHAMBERS, Ll. G., Diffraction by conducting half-plane in plasma, 20: 32580
CHANANA, Arjun D., Extracorporeal irradiation of blood in humans, 20: 31000
CHANDRA, G., Lifetimes of positronium in polystyrene irradiated by thermal neutrons, 20: 32704
CHANG, T. Y., Approximate method for thermoviscoelastic stress analysis, 20: 31334
CHAO, C. C., New CsCl-type intermediate phases in binary alloys involving rare-earth elements, 20: 31737
CHAO, Juang, Effect of gamma radiation on seeds in second generation, 20: 31113
CHAO, Kuang, Biological variations in agricultural seeds during storage after gamma irradiation, 20: 31024
CHAPADOS, C., Far infrared spectra of H_2O_2 and D_2O_2 in solid states, 20: 31247
CHAPMAN, C. E., Radiation absorbed by particle accelerator structural components, 20: 31832
CHAPPELL, Willard R., Kinetic equation for electron-phonon gas, 20: 32239
CHARLESBY, A., Radiation protection studies with polyethylene, 20: 31279
CHASE, L. F. Jr., Study of low-lying states of ^{33}S, 20: 32565
CHASE, W. L., Carbon in primary Na system of Enrico Fermi Atomic Power Plant, 20: 32809 (TID-23101)
CHAVIN, Walter, Effects of whole-body irradiation on adrenal of Carassius auratus, 20: 31094
CHEKHOVSKOI, V. Ya., Concentration and energy of formation of vacancies in Nb, 20: 32726
CHEN, Che Jen, Breakdown phenomena in Ar gas by laser beam at low pressure, 20: 32665
CHEN, J. C. Y., Coupled equations for rearrangement collisions. II., 20: 32388
CHEN, Tsung-Shan, Focusing of electron beam from low-noise gun with different magnet systems. I., 20: 31809
CHENOUARD, J., Determinations of isotopic abundances of iron, 20: 31401
CHERNENKO, V. P., Destruction of color centers and recombination luminescence of crystal phosphor NaCl–Ag. I., 20: 32693
CHERNENKO, V. P., Destruction of color centers and recombination luminescence of NaCl–Ag : Ca crystal phosphor. II., 20: 32694
CHERNOBAI, A. V., High-heat-resistance plastic scintillators, 20: 31282
CHERNYKH, L. P., Selection of scintillators for counters recording γ radiation, 20: 31574
CHERNYSHEV, A. K., Nomogram for determining Prandtl number of some liquid metals, 20: 31724
CHERRY, R. D., Alpha radioactivity of human blood, 20: 31145
CHESHIRE, I. M., Excitation of H atoms by fast protons, 20: 31933
CHI, J. W. H., Forced convective boiling heat transfer to hydrogen, 20: 31348
CHIA, P'an-hsing, Adsorption of ^{90}Sr by aged horse manure, 20: 31252
CH'IANG, Tiao-yuan, Velocity of turbulent flow of water through a bundle of hollow rods, 20: 31350
CHINOWSKY, W., Antiproton annihilation at rest in deuterium, 20: 32015

CHIRKIN, V. S., Temperature and thermal conductivity of metallic beryllium, 20: 31725

CHISHOLM, C. D. H., Expansion method for calculating atomic properties. VII., 20: 31935

CHISHOLM, J. S. R., Scalar products of Pauli spin matrices, 20: 32300

CHO, Alfred Y., Experimental study of porous metal ionizers, 20: 31389

CHO, K. S., Low-energy s-wave $\bar{K}N$ scattering, 20: 32024

CHOU, To-ch'ing, Effect of x-irradiation on Escherichia coli B. I., 20: 31023

CHOU, To-ch'ing, Effect of x-irradiation on E. coli B. II., 20: 31144

CHUDINOVSKIKH, A. V., Amino acid composition of serum α_3-protein of irradiated and nonirradiated dogs, 20: 31021

CHUMICHEV, V. B., Strontium-90 content of Pacific Ocean in 1962 and in 1964, 20: 31416

CHUVASHOV, R. M., Wide-range intensity meter for heterogeneous magnetic fields, 20: 31487

CHYOJNIK, A., Scintillation scanning in kidneys, 20: 31148 (CNEA-170)

CHYOJNIK, Abraham, New colloid of ^{99}Tc in scintillation scanning of the liver, 20: 31147 (CNEA-168)

CIECHANOWICZ, W., Progress in reactor kinetics at Swierk, 20: 32781

CIFKA, J., Chemical states of ^{32}P and ^{35}S atoms in neutron-irradiated sulphur, 20: 31295

CINDRO, N., Levels in ^{60}Ni and ^{62}Ni at high excitation energies, 20: 32490

CINDRO, N., Survey of fast-neutron reactions, 20: 32535

CLAESON, T., Superconducting transition temperatures of Hg–alkaline earth metal compounds, 20: 31757

CLARK, Benton C., Dose-equated phantom for space radiation research, 20: 31455

CLARK, D. J., Regenerative beam extraction for Berkeley 88-inch cyclotron, 20: 31827 (UCRL-16794)

CLARK, I. G., FORTRAN listings and flow charts for ZAP31: program to calculate β-γ radiation dose rates, 20: 32675 (ORNL-TM-1160)

CLARK, John W., Theory of α matter, 20: 32542

CLARK, William H., Megampere pulse transformer for coaxial load, 20: 31489

CLARKE, Margaret E., Identification of extragalactic radio sources between declinations 0° and +20°, 20: 31853

CLARKE, William J., Long-term study of inhaled Pu in dogs, 20: 31025 (AD-631690)

CLARKSON, M. H., Probe measurements in electrodeless discharge, 20: 32655

CLAYTON, D. D., Photon-induced beta decay in stellar interiors, 20: 31878

CLEARY, J. J., Estimation of stable sulphur in human tissue, 20: 30982

CLEMENT, J. D., Prog. rpt. on kinetics parameters of highly enriched D_2O reactor, final, 12/65–12/66, 20: 32863 (TID-23037)

CLINE, David, Evidence for a Σ^- η enhancement near threshold, 20: 32103

CLINE, T. L., Mev phenomena related to solar wind. I., 20: 31885

CLINE, T. L., Mev phenomena related to solar wind. II., 20: 31886

CLOGSTON, A. M., Localized moments, 20: 32739

CLOSE, E., Regenerative beam extraction for Berkeley 88-inch cyclotron, 20: 31827 (UCRL-16794)

CLYDE, Allan Roy, Proton-proton elastic scattering at incidence momenta 3, 5, and 7 Bev/c, 20: 31989 (UCRL-16275)

COATES, Didier, Nuclear reactors having fuel element channel retaining pawl assembly, 20: 32756

COBIC, B., New mass spectrometer ion source for solids, 20: 31204

COCCHI, M., Time resolution measurements with XP 1020 photomultipliers, 20: 31552

COENEGRACHT, J. M., Treatment of patients with metastasized mammary carcinomas by radioactive Y, 20: 31153

COFIELD, R. E., Thickness measurements by nondestructive testing methods, 20: 31480 (Y-1535)

COHEN, J. P., Calculation of nucleon-alpha cascades, 20: 32455

COHEN, M., Expansion method for calculating atomic properties. VI., 20: 31934

COHEN, Martin J., In-flight instrumentation for prompt miss distance measurement using gamma ray techniques, 20: 31496

COHEN, Martin J., Pulsed x-ray instrument for altitude measurement and terrain identification, 20: 31493

COHEN, Martin, J., Radioisotope and machine sources of x radiation for aerospace applications, 20: 31339

COHEN, R. L., Improvements on electromagnetic velocity drive for Moessbauer experiments, 20: 31590

COHN, C. E., Prog. rpt. on kinetics parameters of highly enriched D_2O reactor, final, 12/65–12/66, 20: 32863 (TID-23037)

COHN, C. E., Safety analysis for ZPR-9 facility, 20: 32858 (ANL-7166)

COIGNET, G., Construction of a polarized beam with both spin orientations at the CERN synchrocyclotron, 20: 31835

COIGNET, G., Polarization and spin correlation parameter measurements in 600-Mev proton-proton scattering, 20: 32016

COLBURN, D. S., Evidence for collision-free hydromagnetic shock in interplanetary space, 20: 31891

COLEMAN, E., Backward proton-deuteron elastic scattering from 1.0 to 1.5 Bev, 20: 32102

COLEMAN, L. F., Estimated temperatures of EBR-II fuel cycle facility shielding windows, 20: 31313 (ANL-6853)

COLEMAN, P. J. Jr., Interplanetary magnetic measurements, 20: 31883

COLEMAN, P. J. Jr., Variations in polarity distribution of interplanetary magnetic field, 20: 31860

COLES, B. R., Non-S-state paramagnetic resonance in dilute alloy, 20: 31764

COLLINS, C. H., Radiolysis of aromatic compounds: toluene, 20: 31291

COLLINS, Carol H., Commercialization studies on wood-plastic combinations process, 20: 31625 (NYO-3569-1)

COLOMBO, G., Solutions for a nuclear counting chain, 20: 31551

COLVIN, Curtis A., Solvent extraction of Np(VI) from acid deficient nitrate system, 20: 31319 (ISO-SA-10)

COLVIN, M., Effect of ^{131}I on aberration rate of chromosomes from Chinese hamster thyroids, 20: 31053

COMANICIU, Nicolae, Determination of quadrupole moments of Ba by measurements of isotopic displacements, 20: 32404

COMAS, James, Sputtering yields of several semiconducting compounds under argon ion bombardment, 20: 31914

CONARD, Robert A., Hematological effects of space radiation, 20: 31029 (BNL-10221)

CONLON, T. W., Energies and half-lives of isomeric transitions in ^{115}Sn and ^{109}Cd, 20: 32520

CONNOR, Gerald B., Safety considerations in use of nuclear devices in space, 20: 32855

CONRAD, F. J., Tabulation of cross sections, Q-values, and sensitivities for nuclear reactions of nuclides with 14-Mev neutrons, 20: 32380 (SC-RR-66-229)

CONSOLI, Terenzio, Deuterium–tritium reactions in mixed-plasma accelerator, 20: 32586

CONSOLINO, Jean, Deuterium–tritium reactions in mixed-plasma accelerator, 20: 32586

CONSTABARIS, G., Properties of supported small α-Fe_2O_3 particles determined with Moessbauer effect, 20: 31779

CONSTANT, R., Production and application of radioelements in Belgium, 20: 31643

COOK, B. C., Photodisintegration of Ca to 62 Mev, 20: 32445

COOK, J. B., Electron spin resonance study of thermal effects in irradiated deoxyribonucleic acid, 20: 31009

COOK, T., Symmetry of the strong coupling theory, 20: 32207

COOKE, Brian Frederick, Safety device, 20: 31472

COOL, R. L., New structure in the K^+-p and K^+-d total cross sections between 0.9 and 2.4 Bev/c, 20: 32067

COOPER, C. Berleigh, Sputtering yields of several semiconducting compounds under argon ion bombardment, 20: 31914

COPIC, M., Regular eigenfunctions of time dependent transport equation for thermal neutrons, 20: 32364

COPLEY, L. A., General two-body matrix element for Gaussian interaction using cylindrical harmonic oscillator functions, 20: 32461

CORINALDESI, Alberto, Biological efficiency of 200 kv x rays, ^{60}Co rays and 14-Mev neutrons in Escherichia coli inactivation, 20: 31107

CORNILLE, H., Limiting procedures for singular potentials. III., 20: 32134

CORNISH, Amasa C., Dietary intake of radionuclides in California, 20: 31471

CORNWALL, John M., Current-commutator constraints on three- and four-point functions, 20: 32163

CORNWALL, John M., Micropulsations and outer radiation zone, 20: 32248

COSENS, B. L., Remeasurement of the Lamb shift in $H_2n = 2$, 20: 31925

COSTES, Didier, Liquid moderator nuclear reactors, 20: 32759

COSTES, Didier, Moderator-cooling circuit of nuclear reactor with separate primary circuits, 20: 32757

COTLIER, Edward, Rubidium-86 accumulation in lenses of galactose-fed rats, 20: 30978

COTTERILL, R. J. J., Comparison between neutron damage in annealed Au and in quenched Au, 20: 31788

COURTIER, G. M., Flux of the cosmic-ray hydrogen and helium nuclei at Kiruna, Sweden, 20: 31953

COWLEY, R. A., Normal vibrations of potassium iodide, 20: 32710

COWLEY, S. J., Library programs for the AECL G-20 computer, 20: 31647 (AECL-1744(Pt.A)(Add.1))

COWPER, G., Analysis of external radiation exposures in 1965, 20: 31439 (AECL-2540)

COX, A. Lucile, Power conversion system for lunar and planetary electrostatic propulsion missions, 20: 31384

COX, D. E., Magnetic structure of $FeSb_2O_4$, 20: 32705

COX, G. C., Nanosecond pulse light source, 20: 31497

COX, Jerry V., Pulsed x-ray instrument for altitude measurement and terrain identification, 20: 31493

CRAIG, Paul P., Time independence of charge states produced following

electron capture in ^{57}Co, 20: 32713
CRAIG, R. M., Asymmetries in elastic and inelastic scattering of polarized protons from C and Si, 20: 32440
CRAM, L. S., Radiation from thick silver foils bombarded by grazing-incidence electrons, 20: 32708
CRAMER, J. G., Proton spin flip in the reaction ^{60}Ni(p,p')^{60*}Ni (1.33) at 10.5 and 14.0 Mev, 20: 32557
CRAMPIN, Stuart, Higher-mode seismic surface waves from atmospheric nuclear explosions over Novaya Zemlya, 20: 32269
CRATHORN, A. R., Irradiation effects on synthesis of DNA and mitosis in HeLa cells, 20: 31008
CRIBIER, D., Control system for triple-axis neutron spectrometer, 20: 31543
CROCKER, G. R., Radiochemical data correlations for seawater and coral-surface bursts, 20: 31409
CROMPTON, Felix Jeremy Philip, Improvements in apparatus for direct generation of electricity, 20: 31979
CRONENBERGER, D., Construction of a polarized beam with both spin orientations at the CERN synchrocyclotron, 20: 31835
CRONENBERGER, D., Polarization and spin correlation parameter measurements in 600-Mev proton-proton scattering, 20: 32016
CRONKITE, Eugene P., Extracorporeal irradiation of blood in humans, 20: 31000
CROOK, G. H., Treatment and evaluation of internal deposition from Pu wound, 20: 31030 (BNWL-SA-39)
CROUCH, E. A. C., Thermal ionization of elements of high ionization potential, 20: 31226
CROWE, G. J., Schottky disorder and lattice relaxation in single crystals of NaCl due to x irradiation, 20: 32712
CSONKA, P. L., Experimental limits on neutrino-sea density, 20: 32012
CSONKA, Paul L., General non-dynamical formalism for reactions with particles of arbitrary spin, 20: 32382 (UCRL-14582-T(Rev.1))
CUEER, P., Lithium-8 emission in 5.0-Bev/c K$^-$-meson interactions in nuclear emulsion, 20: 32469
CUFFEL, R. F., Data and bibliography on corrosion of structural materials in liquid alkali metals, 20: 31680 (NAA-SR-Memo-11652)
CULLEN, Thomas L., Guarapari: dosimetric survey of population, 20: 31470
CULLEN, Thomas L., Use of thermoluminescent dosimeters for measurement of external radiation in Guarapari, Brazil, 20: 31463
CURRY, Bill P., Relaxation to steady state in conducting nonequilibrium plasma stream, 20: 32657
CUTLER, William H., Oscillations in thermal cesium plasma diode, 20: 31966
CZERNIEWSKI, M., EWA reactor power ^{16}N activity monitoring, 20: 32870

D

DABEK, W., ANNA startup, operation, and characteristics, 20: 32872
DABIZHA, V. F., Strontium-90 in waters of Pacific Ocean. IV., 20: 31415
DABROWSKI, Cyryl, Buckling determination in HELENA subcritical assemblies, 20: 32783
DABROWSKI, Cyryl, Use of heavy water in reflector of Polish high-flux research reactor, 20: 32871
DADDI, L., Evaluation of peaks in nuclear spectroscopy, 20: 31555
DAEHNICK, W. W., Comparison of many-nucleon transfer reactions with DWBA calculations, 20: 32547
DALEY, Howard L., Cesium ion sputtering of Al, Cu, and Ti, 20: 31948
DALGARNO, A., Expansion method for calculating atomic properties. VII., 20: 31935
DALGARNO, A., Rotational excitation of H_2 and D_2 by H impact, 20: 31932
DALRYMPLE, Glenn V., Edema: delayed complication of total-body 32-Mev proton irradiation, 20: 31098
DALRYMPLE, Glenn V., Effects of whole-body 32-Mev proton irradiations on primates, 20: 31097
DALRYMPLE, Glenn V., Effects of 55-Mev protons on primates, 20: 31099
DALRYMPLE, Glenn V., Effects of 138-Mev protons on primates, 20: 31101
DALRYMPLE, Glenn V., Effects of 400-Mev protons on primates, 20: 31103
DALRYMPLE, Glenn V., Estimate of biological effects of space proton environment, 20: 31106
DALRYMPLE, Glenn V., Kinetics of recuperation following 55-Mev proton irradiation, 20: 31100
DALRYMPLE, Glenn V., Protons and space travel, 20: 31095
DALRYMPLE, Glenn V., Proton depth-dose dosimetry, 20: 31467
DALRYMPLE, Glenn V., RBE of 138-Mev protons as compared to ^{60}Co gamma radiation, 20: 31102
DAMIANO, V. V., Preferred orientation of beryllium sheet using small spherical specimens, 20: 31671
DANG, Giu Do, Number-conserving approximations for theory of pairing interaction in nuclei. II., 20: 32494
D'ANGELO, V., Evaluation of peaks in nuclear spectroscopy, 20: 31555
DANIELS, W. R., Decay of ^{157}Eu, ^{158}Eu, and ^{159}Eu, 20: 32514
DANILA, N., Method for determining optimum type of atomic power station and competition between atomic and classical stations, 20: 32814
DANILOV, G. S., Three-particle partial wave amplitudes and unitarity conditions at complex values of angular momentum, 20: 32113
DARNAULT, Jean, Effects of x rays on platelet environment, 20: 31032 (CEA-R-2953)
DARREL, B., Electrically pumped liquid helium transfer system, 20: 32348
DAS, S. B., Anomalous resistance of Mg--Gd alloys, 20: 31758
DASHEN, Roger F., Algebra of current components at infinite momentum, 20: 32206
DATES, L. R., Safety analysis for ZPR-9 facility, 20: 32858 (ANL-7166)
DAU, Gary J., Solid-state gamma spectrometry developments, 20: 31500 (BNWL-235-4, pp 4-10)
DAUTOV, G. Yu., Plasmatron with interelectrode insert, 20: 32592
DAVIDOW, R. S., Determination of W_B and absorbed dose in gamma-irradiated HCl, HBr, and SF_6, 20: 31292
DAVIES, A. J. S., Inhibition of radiation-induced leukemia by injection of haematopoietic tissue, 20: 31127
DAVIES, D. R., Role of genetic damage in radiation-induced cell lethality, 20: 31042
DAVIES, J. H., Plutonium and fission product redistribution in mixed oxide fuels, 20: 31804
DAVIES, Kenneth, Ionospheric phenomenon associated with explosive solar flares, 20: 32268
DAVIES, Kenneth, Solar flare effects and relaxation time of ionosphere, 20: 32267
DAVIS, Elizabeth M., Effect of radioprotective compounds on incorporation of tritiated thymidine into mammalian cells, 20: 31125
DAVIS, J. J., Radionuclides in terrestrial and freshwater biota, 20: 31420 (PNE-481, pp 1165-1200)
DAVIS, John J., Radiation hardening of an ion propulsion system, 20: 31611
DAVIS, Leverett Jr., Interplanetary magnetic measurements, 20: 31883
DAVIS, Leverett Jr., Models of interplanetary fields and plasma flow, 20: 31890
DAVIS, Leverett Jr., Variations in polarity distribution of interplanetary magnetic field, 20: 31860
DAVIS, M. W., Fabrication of high strength, heavy-wall pressure vessels, 20: 31703
DAVIS, Sumner P., Isotope shifts of neutron-deficient mercury isotopes, 20: 32517
DAVISON, E., Li-doped, radiation-resistant silicon solar cells, 20: 31614
DAVYDOVA, S. A., Isolating radiation protection agents on basis of Diche-positive compounds in urine, 20: 31140
DAYEM, A. H., Microwave emission from superconducting point contacts, 20: 31482
DAYTON, I. E., New type of low-resolution mass spectrometer, 20: 31169 (D-1-82-0508)
DAYTON, R. W., Reactor materials, Vol. 9, No. 1, 20: 31665
DE AGOSTINO, E., Control system for triple-axis neutron spectrometer, 20: 31543
DE AISENBERG, E. Y., Energy levels of ^{106}Pd fed in the ^{106m}Rh decay, 20: 32425
DEANS, S. R., Comparison of resonance formulas for (1236 Mev, 3/2) pion-nucleon resonance, 20: 32100
DEANS, T., Strontium isotopes and trace elements in carbonatites and limestones from Ice River, British Columbia, 20: 31406
DEBAISIEUX, J., Projector for large-size bubble chamber pictures, 20: 31550
DE BENEDETTI, S., Physics of positron annihilation, 20: 32101
DEBIESSE, Jean, Use of radioisotope to demonstrate fixation of electrons on electronegative gas, 20: 32223
DEB RAY, G., Exact analytic solution for propagation of shock waves in self-gravitating gas sphere, 20: 31871
DEBRUNNER, P., Moessbauer scattering in ^{195}Pt, 20: 32487
DE FACIO, D., Polarization and asymmetry in the ^{3}He(d,p)^{4}He reaction, 20: 32475
DE FELICE, Joseph A., Producing large quantities of ^{237}Np and ^{238}Pu in commercial power reactors, 20: 32837
DE GELAS, B., Electron microscope observations on thin films of zircon obtained by oxidation of Zr, 20: 31755
DE GOEIJ, J. J. M., Errors in activation analysis due to variations in isotopic ratio, 20: 31190
DEGREVE, F., Thermodynamic and kinetic studies in high-temperature chemistry, 20: 31227
DEGROSSI, Osvaldo, New colloid of ^{99}Tc in scintillation scanning of the liver, 20: 31146 (CNEA-168)
DE HAAN, W., Resonance absorption in heavy water lattices development work at Ispra, 20: 32785
DE HEER, F. J., Ionization cross-section measurements for 0.6- to 20-kev

electrons in atomic and molecular gases, 20: 31906
DE LAJARTE, Stephane D., Nuclear fuels, 20: 31702
DE LANGE, S. A., Treatment of patients with metastasized mammary carcinomas by radioactive Y, 20: 31153
DELAUNAY, J., Levels in ^{60}Ni and ^{62}Ni at high excitation energies, 20: 32490
DELCROIX, Victor, Properties of cadmium telluride diodes and application to detection of nuclear particles, 20: 31523
DELLAGI, Mohamed, Structure of particle tracks in nuclear emulsions: Distribution of the bundle length, 20: 31522
DELLA ROCCA, C., Problems of corrosion in nuclear reactors. III, 20: 32815
DELLA ROSA, R. J., Strontium-90 in beagle hair, 20: 30972 (TID-22027)
DEL PRETE, T., Single-π^0 photoproduction from hydrogen around the second resonance, 20: 32051
DELYANNIS, A., Development of electrical energy demand in Greece and of water supply of Athens area, 20: 32848
DEMA, I., Behavior of radio-iodine recoils produced in isotopic and non-isotopic lattices, 20: 31298
DEMIKHOVSKII, V. Ya., Superconductivity phenomena in thin semiconductor films, 20: 32338
DEM'YANOV, A. V., Calculation of magnetic analyzer of mass separator, 20: 31484
DENES, L. J., Comparison of many-nucleon transfer reactions with DWBA calculations, 20: 32547
DENISON, J. G., Liquid scintillation counting, 20: 30997
DENISOV, F. P., Installation for studying energy and angular distribution of recoil nuclei, 20: 32526
DENISOV, Yu. N., Magnetic field stabilizer with broadband EPR sensor, 20: 31813
DENIZ, K. Usha, Rotational behavior of ammonium ion in salts, 20: 31241
DERR, V. E., Application of nuclear radiation to pumping of lasers, 20: 32740
DE SABBATA, V., Splitting of a photon into two photons in Coulomb field of nucleus, 20: 32031
DESAI, U. D., Mev phenomena related to solar wind. I., 20: 31885
DESESQUELLES, Jean, Ionization of some gases by accelerated H^+ and H_2^+ ions, 20: 31909
DE-SHALIT, A., Nuclear spectroscopy in α particle, 20: 32503
DESHMUKH, A., Rotational-velocity and ion-density profiles in plasma vortices, 20: 32644
DESHPANDE, N. G., Bootstrap conditions in field theory, 20: 32153
DESI, Sandor, Measurement of soft β emitters by means of liquid scintillators, 20: 31518
DE TAKACSY, N., Low-lying negative parity states in A = 17 nuclei, 20: 32398
DETRAZ, C., Experimental study of reaction D(p,γ)^{3}He at 156 Mev, 20: 32486
DETRY, D., Thermodynamic and kinetic studies in high-temperature chemistry, 20: 31227
DEUTCH, B. I., Internal magnetic field of lutetium in iron and g factor in ^{175}Lu, 20: 32472
DEVARE, H. G., Spin assignments to levels in ^{131}I, 20: 32563
DEVARE, S. H., Spin assignments to levels in ^{131}I, 20: 32563
DEVKIN, B. V., Time-of-flight neutron spectrometer, 20: 31566
DEWEY, D. L., Internal hydrogen ion concentration of Thiobacillus thiooxidans and survival after irradiation, 20: 31138
DE WITT, Bryce S., Superconductors and gravitational drag, 20: 32325
DEWS, Jon R., Isotopic composition of Ag in Canyon Diablo meteorite, 20: 31861
DIANA, E., Resonance absorption in heavy water lattices development work at Ispra, 20: 32785
DI CAPUA, Enrico, Radiative decay of the μ meson, 20: 32104
DICK, L., Construction of a polarized beam with both spin orientations at the CERN synchrocyclotron, 20: 31835
DICKENS, J. K., Level structure of ^{92}Mo, 20: 32471
DICKHAUT, R. H., Circuit hardening using computer techniques, 20: 31621
DICZFALUSY, Egon, Biosynthesis of radioactive estriol-3-glucosiduronate by guinea pig liver homogenate, 20: 31312
DIDELEZ, J. P., Experimental study of reaction D(p,γ)^{3}He at 156 Mev, 20: 32486
DIDYK, Yu. K., Electromagnetic structure of elementary particles, 20: 32122
DIENES, G. J., Kinetic model of biological radiation response, 20: 31087
DIENST, Wolfgang, High-temperature embrittlement of austenitic steels and Ni alloys by (n,α) reactions, 20: 31801
DIETRICH, K., Theory of nuclear reactions. II., 20: 32428
DI GIACOMO, C., Electronics in control of nuclear reactors, 20: 32749
DI LELLA, L., Construction of a polarized beam with both spin orientations at the CERN synchrocyclotron, 20: 31835
DILLINGER, P., Simple scintillation device for measuring β absorption in liquids, 20: 31521
DIMOCK, D., Inclined end-plate effects in Q devices, 20: 32611
DINCULESCU, C., Method for determining optimum type of atomic power station and competition between atomic and classical stations, 20: 32814
DINGUS, R. S., Measurements of conversion coefficients for transitions in ^{154}Gd, ^{160}Dy, ^{170}Yb, ^{171}Yb, and ^{141}Pr, 20: 32443
DINTSES, A. I., Molten metals as high-temperature lubricants, 20: 31720 (AD-629415)
DISMUKES, Robert Key, Faraday effect at high magnetic fields, 20: 31807 (TID-23030)
DIU, B., Dashen-Frautschi method and parity-conserving baryon-meson couplings, 20: 32138
DIXON, G. M., Identification of S-matrix elements in neutral pseudoscalar-pseudovector and exponential theories, 20: 32168
DLOUHA, J., Influence of the substrate on the Debye-Waller factor of very thin films, 20: 32688
DMITRIEV, A. B., High-pressure ionization ^{3}He chamber performance as slow neutron detector, 20: 31573
DMITRIEV, V. M., Microwave-enhanced critical supercurrents in constricted tin films, 20: 32328
DOBBS, H. E., New O flask apparatus for assay of ^{3}H and ^{14}C, 20: 31185
DOBROVOLSKII, A. G., Slip casting of molybdenum disilicide, 20: 31697
DODONOV, L. D., Critical thermal fluxes and heat transfer of boiling K in tubes, 20: 31347
DOEBELE, H. F., Pressure elevation in H arc discharge in axial magnetic field, 20: 32638
DOKTOROVA, T. V., Pulsed neutron generator, 20: 32358
DOLCE, Thomas J., Secondary gamma ray transmission through plane slabs of concrete, 20: 32671 (AD-633216)
DOLE, Malcolm, Prog. rpt. on radiation chemistry of high polymers, annual, 4/65–4/66, 20: 31268 (COO-1088-20)
DOLGOV, V. V., Temperature of heated tubes with pulsating flow, 20: 31346
DOLGOV-SAVEL'EV, G. G., Selective receiver of electromagnetic radiation of millimeter and submillimeter ranges, 20: 32626
DOLLING, G., Normal vibrations of potassium iodide, 20: 32710
DOMAGALA, R. F., Zirconium–hafnium system, 20: 31744
DONAGI, A., Fresh fallout in Israel from the second Chinese nuclear detonation, 20: 31408
DONNACHIE, Alexander, Photopion production, dispersion relations, and $\gamma\rho\pi$ coupling, 20: 31996
DONNELLY, Richard F., Ionospheric phenomenon associated with explosive solar flares, 20: 32268
DORE, J. C., Asymmetries in elastic and inelastic scattering of polarized protons from C and Si, 20: 32440
DOROFEEV, V. M., Isolating radiation protection agents on basis of Diche-positive compounds in urine, 20: 31140
DORY, R. A., Apparent high-frequency stability of highly anisotropic plasma, 20: 32624
DOSHI, P. K., Pulse propagation experiments using reactor source, 20: 32362
DOST, M., Experimental test of triton form factor by Coulomb pickup on ^{208}Pb, 20: 32485
DOTSENKO, B. B., Calculation of cross sections for deuteron photodisintegration and neutron capture in case of nonlocal potential, 20: 32004
DOUGAL, Arwin A., Space-time resolved plasma properties of dynamical theta pinch, 20: 32664
DOUGLAS, D. A., Irradiation behavior of Th–U alloys and compounds, 20: 32833
DOUGLAS, D. A. Jr., Properties of Th, its alloys, and its compounds, 20: 31767
DOUGLAS, D. A. Jr., Refabrication technology for Th–^{233}U fuel cycle, 20: 31701
DRAGANESCU, Vasile, Determination of quadrupole moments of Ba by measurements of isotopic displacements, 20: 32404
DRAGANIC, Z. D., Reaction of oxalic acid re-formation during gamma radiolysis of aqueous oxalate solutions, 20: 31277
DRAGT, J. B., Analysis of reactor noise measured in zero-power reactor, 20: 32874
DRAPER, James E., Simple system for dispersionless deflection of beam particles, 20: 31847
DRESSLER, Jacques H., Nuclear fuels, 20: 31702
DRITTLER, K., Influence of chemical binding on neutron cross sections at high energy, 20: 32392
DROWART, J., Thermodynamic and kinetic studies in high-temperature chemistry, 20: 31227
DROZDOV, F. S., Determination of negative reactivity by shot source method, 20: 32864
DUBININ, N. P., Chemical protection against genetic effect of small doses of radiation, 20: 31121
DUBININA, L. G., Chemical protection against genetic effect of small doses of radiation, 20: 31121
DUCHARME, Edward L., Performance of self-excited MHD generator,

20: 31976
DUCK, I., Charge-dependent effects in nucleon-nucleon $^1S_0$ scattering lengths by Dashen-Frautschi method, 20: 32030
DUCK, I., Proton-proton bremsstrahlung with the Tabakin potentials, 20: 32059
DUDLEY, R. A., Calibration problems in whole-body counting with NaI(Tl) detectors, 20: 31443 (CONF-650673-1)
DUDNIKOV, Yu. S., Plasmatron with interelectrode insert, 20: 32592
DUECHES, D., Computer study of dynamic phase of small θ pinch, 20: 32610
DUFAY, Maurice, Ionization of some gases by accelerated H^+ and H_2^+ ions, 20: 31909
DUFFAUT, F., Electron microscope observations on thin films of zirconia obtained by oxidation of Zr, 20: 31755
DUIMIO, F., Alternative interpretation of the enhancement observed at $M^*_{pp\pi^+}$ 2.52 Bev/c^2, 20: 32040
DUIMIO, F., Dynamical group of anisotropic harmonic oscillator, 20: 32301
DUISEBAEV, A., Installation for studying energy and angular distribution of recoil nuclei, 20: 32626
DULLEMOND, C., Breaking of Su_3 symmetry in strong-coupling theory, 20: 32128
DUNGEY, J. W., Solar-wind interaction with magnetosphere: particle aspects, 20: 32276
DUNN, C. G., Microstructures and variations in [hkl] orientations in Ta, 20: 31673
DUPEN, Douglas Wm., Story of Stanford's two-mile-long accelerator, 20: 31824 (SLAC-62)
DUPUIS, Marc, Continued fraction expansion of time correlation functions, 20: 32234
DURET, M. F., Preliminary assessment of Th as fuel for thermal reactors, 20: 32822
DUSHIN, L. A., Microwave interferometers with amplitude modulation, 20: 31490
DUTT, J., Harmonics in scattering of electromagnetic radiation by electron current, 20: 32001
DUTT, J., Scattering and absorption of electromagnetic radiation by electrons in light of harmonic phenomenon, 20: 32000
DUWEZ, P., New CsCl-type intermediate phases in binary alloys involving rare-earth elements, 20: 31737
DYACHKOV, E. I., Cryogenic developments at Joint Institute for Nuclear Studies, 20: 32318
DYATLOV, I. T., Three-particle partial wave amplitudes and unitarity conditions at complex values of angular momentum, 20: 32113
DZHELEPOV, B. S., Conversion electron spectra of isotopes ^{166}Tm, ^{164}Yb, ^{164}Tm, and ^{162}Tm, 20: 32415

E

EARL, James A., Modified version of the MIT Rutherford scattering apparatus, 20: 31515
EASTMAN, G. Y., Development of Cs-vapor-filled thermionic energy converter, 20: 31960 (N-66-16447)
EATHER, R. H., Excitation and ionization by auroral protons, 20: 32246
EBATA, Takeshi, Possible C and T violation in the photoproduction of neutral pions, 20: 32074
EBEOGLU, D. B., Radionuclide production in Fe targets bombarded with 400-Mev protons, 20: 32560
EBERHARDT, P., Rare gas measurements in 30 stone meteorites, 20: 31876
EBERHARDT, P., Spallation, fission, and neutron capture anomalies in meteoritic Kr and Xe, 20: 31875
EBERLE, E., Coupling constants and mass shifts in the broken SU_3 symmetry, 20: 32156
EBERT, P. J., Fast sensitive noninterrupting monitor for nanosecond pulsed beams, 20: 31846
ECKELS, T. W., Estimated temperatures of EBR-II fuel cycle facility shielding windows, 20: 31313 (ANL-6853)
ECKHARDT, W. O., Electron-bombardment thrusters using liquid-mercury cathodes, 20: 31368
EDELEN, D. G. B., Energy mechanics of semistatic space-times, 20: 32298
EDEN, R. J., Behavior of scattering amplitudes and cross sections using crossing symmetry and holomorphy in two variables, 20: 32106 (AD-634706)
EDGECUMBE, J., Attenuation length for secondary electrons in bulk-density KCl and CsI, 20: 31916
EDMUNDS, J., Formation of debris from buildings by blast and fire effects of nuclear weapons, 20: 31332 (URS-651-4)
EFREMENKOVA, N. I., Determining structure of sintered materials by ionic bombardment, 20: 31765
EGAN, Douglas M., Commercialization studies on wood-plastic combinations process, 20: 31625 (NYO-3569-1)
EGER, W., Mechanism of strontium deposition in bone tissue, 20: 30973
EGGINTON, A. J., External proton beam at Nimrod, 20: 31823 (RPP-N-5)
EGGLETON, P., Onset of helium burning in degenerate cores, 20: 31866
EGOROV, Yu. A., Shielding properties of iron–serpentine concrete, 20: 32677
EHLERS, Vernon J., Hyperfine-structure anomalies of ^{196}Au and ^{199}Au, 20: 32553
EHRENBERG, L., Post-irradiation modification of biological effects of neutrons. I., 20: 31136
EHRENKRANZ, T. E., Project Rover liquid H safety, 20: 32850 (LA-DC-7689)
EICHLER, E., Level structure of ^{92}Mo, 20: 32471
EILENBERG, S. L., Characteristics of micropound range ion thrustors, 20: 31385
EILENBERG, S. L., Power conditioning for space propulsion systems using contact ion thrusters, 20: 31360
EILENBERG, Stanton L., Development of ion microthrustors for satellite applications, 20: 31362
EINHORN, J., Thyroid antibodies in euthyroid subjects after ^{131}I therapy, 20: 31161
EISENBERG, A., Fresh fallout in Israel from the second Chinese nuclear detonation, 20: 31408
ELANGO, M. A., Role of hole processes in formation of F centers during radiation-induced coloration, 20: 32724
EL-BAZ, E., Graphical methods of summation and integration of spherical harmonics, 20: 32437
EL-GARHY, M. A., Preparation of Tc, tyrosine, thyroxine, insulin and human serum proteins labeled-^{99m}Tc, 20: 31265
ELIAS, H., Preparation of ^{36}Cl-labelled iodine monochloride by isotope exchange, 20: 31246
ELKHALIFA, M. D., Protection by α-aminothioacetamide, cysteine, and anoxia against γ rays on Allium cepa, 20: 31137
EL-KINAWY, S. A., Preparation of radioiodinated serum Globulines, 20: 31264
EL-KINAWY, S. A., Preparation of Tc, tyrosine, thyroxine, insulin and human serum proteins labeled-^{99m}Tc, 20: 31265
EL-MERZABANI, Mahmoud M., Synthesis of 3,3′-dimesyloxy-*N*-methyl-^{14}C-dipropylamine hydrochloride, 20: 31308
EL-NESR, M. S., Determination of absolute K-internal conversion coefficients of transitions in ^{140}Ce by internal-external conversion method, 20: 32541
ELRICK, R. H., Assay of β-emitting radioisotopes using Cherenkov counting, 20: 31184
EL-SAYAD, G. M., Determination of absolute K-internal conversion coefficients of transitions in ^{140}Ce by internal-external conversion method, 20: 32541
EL SHAZLY, E. M., Thorium resources in United Arab Republic and their possible utilization, 20: 31438
EMELEUS, K. G., Ion surface waves, 20: 32620
EMERY, G. T., L-subshell ratios of some low-energy E2 transitions, 20: 32516
EMMERT, G., Rotational-velocity and ion-density profiles in plasma vortex, 20: 32644
ENDEBROCK, R. W., Reactor materials, Vol. 9, No. 1, 20: 31665
ENDO, Osamu, High-energy α-α scattering, 20: 32532
ENDOW, N., Physisorption of Xe and Kr on glass and on Mo films, 20: 31242
ENGELHARDT, Dieter, Reaction ^{11}B(p,$\alpha\alpha$)^{4}He at 163 kev, 20: 32402
ENGLERT, F., Foundations of the Bootstrap theory, 20: 32212
ENYO, Michio, Stoichiometric number and electrolytic separation factor of deuterium on nickel hydrogen electrode, 20: 31644
EPHERRE, M., Relative abundance and production cross sections of lithium isotopes, 20: 31205
EPSTEIN, Jean H., Electronic charge density in He in first-order shielding approximation, 20: 31902 (N-66-16249)
EPSTEIN, Samuel S., Inhibition of selected photosensitizers by agents of varying antioxidant activity, 20: 31018
EPSTEIN, Saul T., Electronic charge density in He in first-order shielding approximation, 20: 31902 (N-66-16249)
ERMAN, Peter, L-subshell ratios of some low-energy E2 transitions, 20: 32516
ERNE, F. C., Gamma-ray angular correlation and polarization measurements in reaction ^{35}Cl(p,γ)^{36}Ar, 20: 32451
ERNST, D. M., Development of Cs-vapor-filled thermionic energy converter, 20: 31960 (N-66-16447)
ERNSTENE, M. P., Surface ionization engine development, 20: 31370
ERSKINE, J. R., Energy levels of ^{48}Ca and ^{40}Ca as observed with inelastic scattering of 11.5-Mev protons, 20: 32511
ERWAY, D. D., Power conditioning for space propulsion systems using contact ion thrusters, 20: 31360
ESTERLUND, R. A., Beta-delayed protons from ^{28}Si, 20: 32505
EUGSTER, O., Rare gas measurements in 30 stone meteorites, 20: 31876
EVANS, B., High-temperature technique for determining terminal solubilities

20: 31250
EVANS, H. J., Role of genetic damage in radiation-induced cell lethality, 20: 31042
EVANS, James C., Commercialization studies on wood-plastic combinations process, 20: 31625 (NYO-3569-1)
EVIATAR, Aharon, Role of electrostatic plasma oscillations in electron scattering in earth's outer magnetosphere, 20: 32262
EXNER, H. E., Compacting and sintering behavior of tungsten carbide–cobalt alloy, 20: 31695

F

FAGRAEUS, Astrid, Thyroid antibodies in euthyroid subjects after ^{131}I therapy, 20: 31161
FAIRCHILD, R. G., Tissue-equivalent ionization chamber for in-phantom dosimetry, 20: 31524
FAIRHALL, A. W., Prog. rpt. on atmosphere radiochemical measurements, 5/63–4/66, 20: 31397 (RLO-1776-2)
FAIRLIE, B. D., Exact solutions for some SU_6-invariant amplitudes in the static approximation, 20: 32136
FALIN, M. L., EPR of Gd^{3+} in Y and La double molybdates, 20: 32728
FAN, Cheng-ts'ai, Velocity of turbulent flow of water through a bundle of hollow rods, 20: 31350
FAN, G. J., Longitudinal magneto-optical Kerr effect in EuO and EuS, 20: 31229
FAN, L. T., Magnetohydrodynamic channel entrance flow with parabolic velocity at entry, 20: 32226
FARAONE, Giovanni, Polarographic investigation on Pu(IV) in sulfuric acid solution, 20: 31302
FARBER, E., Rotational-velocity and ion-density profiles in plasma vortices, 20: 32644
FARMER, Gerald, Derivation of Compton scattering relation in covariant notation, 20: 31993
FARRELL, J. A., s- and p-Wave neutron spectroscopy. XIa., 20: 32389
FATEEVA, L. N., Use of magnetic quadrupole lenses for focusing particles passing through stopping foils, 20: 31844
FAUCHER, G., Antiproton-nuclei scattering at 3 Bev/c, 20: 32467
FAUGERAS, Paul-Etienne, Determination of density and diameter of plasma column by diffraction of electromagnetic wave, 20: 32585
FAYET, Jean-Claude, Absorption spectra of irradiated $KClO_3$, 20: 32686
FAYOLLE, J. C., Antiproton-nuclei scattering at 3 Bev/c, 20: 32467
FEDER, J., Superheating and supercooling in superconducting transition of small In spheres, 20: 32331
FEDOROV, V. B., Determination of kinematic properties of particles in spark chamber sparks, 20: 31570
FEDOROVA, I. G., Secondary emission coefficients for KBr single crystal bombarded with K ions, 20: 31938
FEDYNSKII, O. S., Critical thermal fluxes and heat transfer of boiling K in tubes, 20: 31347
FEIBELMAN, W. A., Unusual aurora of September 22–3, 1963, 20: 32272
FEIGE, Y., Fresh fallout in Israel from the second Chinese nuclear detonation, 20: 31408
FELDMAN, K. S., Dispersion theory calculations for nucleon-nucleon scattering, 20: 32008
FELTEN, E. J., Phase relations in the system $CoNb_2O_6$–$CoTa_2O_6$, 20: 31734
FENG, Kwei-tsu, Velocity of turbulent flow of water through a bundle of hollow rods, 20: 31350
FERGASON, Lewis, Grain shift of proportional counter with counting rate, 20: 31591
FERGASON, Lewis A., Gas flow proportional counter for electron-probe light-element analysis, 20: 31589
FERRIS, L. M., Reprocessing methods and costs for selected thorium-bearing fuel types, 20: 31326
FETISOV, N. I., Time-of-flight neutron spectrometer, 20: 31566
FETTWEIS, P., Gamma-ray spectroscopy of short half-life isotopes with a Li-drifted Ge detector, 20: 32564
FIALKO, N. M., Molten metals as high-temperature lubricants, 20: 31720 (AD-629415)
FICK, D., Connection between phase shifts and coefficients of M-matrix for the elastic scattering of spin 1 by spin 0 particles, 20: 32193
FICK, D., Phenomenological treatment of elastic scattering of spin-1 particles on spin-0 particles, 20: 32194
FIELD, S. B., Effect of O on impairment of proliferative capacity of human cells by radiation LET, 20: 31123
FILATOV, A. I., Double nuclear-electron resonance spectrometer, 20: 32525
FILATOV, P. P., Immunopathology in chronic exposure to ^{65}Zn, 20: 31112
FILIPEK, S., Single-well method for determining direction of flow of ground water using a neutron source, 20: 31430
FILIPPOV, A. T., Possible direct test of CP violation in the K_1^0 interactions, 20: 32060
FILIPYAK, B., Radiation protection at WWRS-type reactor "EWA", 20: 32877
FINDLAY, J. S., Half-life of ^{125}I, 20: 32406
FINK, David, Wavelengths of electronic transitions in foil-excited beams of light elements, 20: 31903 (N-66-16702)
FINK, R. W., Atomic fluorescence yields, 20: 31936
FINOGENOV, V. M., Spectrometer for studying fine structure of x-ray spectra (URS-1I), 20: 31581
FINTZ, P., Study of excited states in ^{15}N and ^{16}N, 20: 32501
FIQUET-FAYARD, Florence, Isotopic effects in dissociation of triatomic molecules by electron impact. II., 20: 31271
FIREMAN, Philip, Stable bromine and activation analysis in protein tracer studies, 20: 30990
FIRKET, H., Effect of cystamine on respiration, oxidative phosphorylation, and ultrastructure of rat mitochondria, 20: 30984
FISHER, L. K., Mitochondria: increase in oxidative capacity and quantitative recovery after massive doses of radiation, 20: 31633
FISHER, Philip C., Applications of gas counters in space research, 20: 31610
FITZ, W., Mirror reactions $^{10}B(d,t)^{9}B$ and $^{10}B(d,^{3}He)^{9}B$ at 11.8 Mev, 20: 32481
FLANAGAN, J. E., Composite solid propellants containing irradiated ammonium perchlorate, 20: 31286
FLANAGAN, Thomas L., Radiochemical safety procedures at Smith Kline and French Laboratories, 20: 31469
FLATO, M., Local representations and mass spectrum, 20: 32161
FLATTE, Stanley Martin, Reaction $K^- \rightarrow \Lambda\omega$ from 1.2 to 2.7 Bev/c: absorption model with strange-meson exchange, 20: 31990 (UCRL-16648)
FLEGENHEIMER, J., Mathematical treatment of decay and formation laws of radioactivity with graphically solved examples, 20: 32377 (KFK-117)
FLOOD, W. S., Nanosecond pulse light source, 20: 31497
FLORES-MALDONADO, Victor, Regge-pole theory and p-n and $\bar{p}$-n charge-exchange scattering at small angles, 20: 32069
FLUKE, Donald J., Dry T_1 bacteriophage in measurement of large doses of ionizing radiation, 20: 31093
FLYAGIN, V. B., Optimization of measurements of electron energy in heavy-liquid bubble chambers, 20: 31568
FOA, L., Single-π^0 photoproduction from hydrogen around the second resonance, 20: 32051
FOGEL', Yo. M., Emission spectra of rarefied molecular gases excited by fast electrons, 20: 31921
FORMANEK, J., Mass formula without symmetry breaking, 20: 32132
FORRESTER, A. T., Cesium transport through a tungsten capillary, 20: 31381
FORRESTER, A. T., Surface ionization engine development, 20: 31370
FORRESTER, A. Theodore, Surface tension storage and feed systems for ion engines, 20: 31379
FORSSMANN, W. G., Effects of x rays on function and ultrastructure of isolated sympathetic ganglion, 20: 31055
FORSYTH, Jeannette, Inhibition of selected photosensitizers by agents of varying antioxidant activity, 20: 31018
FORTESCUE, Peter, Nuclear reactor fuel element, 20: 32793
FOSSAN, D. B., Study of low-lying states of ^{33}S, 20: 32565
FOUAN, J., Levels in ^{60}Ni and ^{62}Ni at high excitation energies, 20: 32490
FOWLER, A. H., UCAPP: Union Carbide APT Post Processor, first edition, 20: 31478 (K-1670)
FOWLER, J. K., Library programs for AECL G-20 computer, 20: 31646 (AECL-1744)
FOWLER, J. L., Differential scattering of neutrons from ^{208}Pb at resonant energies, 20: 32519
FOX, Kenneth, WKB treatment of bound states in an electric-dipole potential, 20: 32295
FRADKOV, A. B., Cryostats for superconducting solenoids with thermal working volume, 20: 32334
FRAMPTON, E. W., Degradation of DNA in polyauxotrophic bacterium, 20: 31015
FRANA, J., Decay of ^{162}Tb and ^{163}Tb, 20: 32462
FRANA, J., Decay $^{157}Eu(\beta^-)^{157}Gd$, 20: 32465
FRANA, J., Gamma transitions and energy levels in ^{161}Dy, 20: 32463
FRANA, J., Levels in ^{157}Tb, 20: 32464
FRANCAVIGLIA, S., Two-channel problem and inelastic unitarity condition in eigenstates of total angular momentum, 20: 32014
FRANK, L. A., Correlation of outer radiation zone electrons with the solar activity cycle, 20: 32260
FRANKLIN, N. L., Development and preparation of nuclear fuels in the United Kingdom, 20: 31694
FRAUENFELDER, H., Moessbauer scattering in ^{195}Pt, 20: 32487
FRENKEL, M., Treatment of patients with metastasized mammary carcinomas by radioactive Y, 20: 31153
FRERICHS, R., Tunnel effect measurements on superimposed layers of Pb and Al, 20: 32342

FREUND, P. G. O., Equivalence of quark models and universality predictions for high-energy scattering, 20: 32144
FRIED, Burton D., Stability limits for longitudinal waves in ion beam-plasma interaction, 20: 32608
FRIEDMAN, E. A., Application of inverted-neutron-filter technique to study of inelastic scattering, 20: 32706
FRIEDRICH, Otto M. Jr., Space-time resolved plasma properties of dynamical theta pinch, 20: 32564
FRIEND, A. G., Local ground-level air concentrations of ^{210}Pb at Winchester, Massachusetts, 20: 31407
FRISCH, David, Experimental status of electromagnetic interactions, 20: 32201
FRISCH, H. L., High-field steady-state shock wave in plasma, 20: 32604
FRISCHAUF, H., Determination of I in whole serum and in blood protein with neutron activation analysis, 20: 31173 (SGAE-BL-18/1966)
FRISCHAUF, H., Neutron activation analysis determination of radiosensitizers, 20: 31172 (SGAE-BL-17/1966)
FRITZ, R. J., Considerations of rotor dynamics including virtual mass and stability effects, 20: 31329 (KAPL-M-6543)
FRITZ, R. J., Friction factors for use in analysis of journal bearings with vortex-turbulent flow, 20: 31330 (KAPL-M-6546)
FRITZ, R. J., Vibration response of cantilevered cylinder surrounded by annular fluid, 20: 31328 (KAPL-M-6539)
FRIZ, Walter, Limitations in energy resolution of slow electrons, 20: 31981 (AD-634517)
FROESE, Gerd, Division delay in HeLa cells and Chinese hamster cells, 20: 31051
FRONSDAL, Christian, Applications of unitary representations of SL(6,C) to elementary particles, 20: 32199
FRY, R. M., Neutron dose conversion factors for radioactive neutron sources, 20: 32355
FUCHS, A., Complexometric microdetermination of heavy metals with ^{60}Co as indicator, 20: 31181
FUCHS, W., Schottky disorder and lattice relaxation in single crystals of NaCl due to x irradiation, 20: 32712
FUENFER, E., Measurements of ion and electron temperature in theta-pinch plasma, 20: 32621
FUGOL', I. Ya., Diffusion of metastable helium atoms in cryogenic plasma, 20: 32602
FUJII, Kanji, Strong interaction of intermediate vector mesons and extremely high-energy phenomena, 20: 32177
FUJIMURA, Kimio, Non-zero elastic amplitude real part effects and nucleon recoil effects on relationship between elastic diffraction scattering and inelastic collisions, 20: 32072
FUJINO, Moriji, Biological effectiveness of 15-Mev betatron x rays and 200 kv x rays for lethality in mice, 20: 31072
FUJITA, Akira, Radionuclide fractionation in debris from land surface burst, 20: 31460
FUJITA, Jun-ichi, Practical method using isospin projection operator in nuclear physics, 20: 32533
FUKUSHI, Kazue, Effects of x radiation on HeLa cells, 20: 31056
FULMER, C. B., Estimates of residual radiation levels induced by high-energy nucleons, 20: 31831
FULTON, T., Mass splitting as covariant concept in generalized Poincare group, 20: 32114
FUNG, P. C. W., Excitation of cyclotron radiation and application to Jupiter's decametric emissions, 20: 31870
FUNKE, L., Decay of ^{162}Tb and ^{163}Tb, 20: 32462
FUNKE, L., Decay of $^{157}Eu(\beta-)^{157}Gd$, 20: 32465
FUNKE, L., Decay of ^{163}Er, 20: 32466
FUNKE, L., Gamma transitions and energy levels in ^{161}Dy, 20: 32463
FUNKE, L., Levels in ^{157}Tb, 20: 32464
FURUICHI, Susumu, Pion-pion correlation effect in two-pion-exchange contribution for nucleon-nucleon scattering, 20: 32073
FUSHCHICH, V. I., Analytic properties of certain vertex amplitudes in perturbation theory, 20: 32190

G

GABELOV, A. A., Treatment of radiation leukopenia by bone marrow autotransplantation, 20: 31134
GABOR, Dennis, Electric current generation by means of thermionic energy converters, 20: 31980
GABOS, Zoltan, Application of Foldy-Wouthuysen transformation to study of electron polarization, 20: 32088
GADALOV, A. N., Pulse-height recording and logarithmic conversion of pulse heights in the 10^4 to 10^5 dynamic range, 20: 31577
GAEDKE, R. M., Angular distributions of ^{18}F from the reaction $^{16}O(^{14}N,^{18}F)^{12}C$, 20: 32429
GAIDOVA, E. S., Immunopathology in chronic exposure to ^{65}Zn, 20: 31112
GAINES, J. R., Nuclear magnetic resonance studies of solidified H_2-D_2 mixtures. II, 20: 32711
GAIPOV, S., Energy distribution of electrons from alkali halide compounds bombarded by He^+ and Ar^+ ions, 20: 31912
GAISSER, T. K., Operator gauge transformations and gauge transformations of third kind, 20: 32111
GAJEWSKI, W., Final-state interactions in mesonic decay of mass-4 hypernuclei, 20: 32477
GALBRAITH, Thomas L., Model for protons trapped in magnetic field of earth, 20: 32292
GALLMANN, A., Study of excited states in ^{15}N and ^{16}N, 20: 32501
GAMBINO, R. J., Magnetic properties of solid solutions of heavy rare earths with each other, 20: 31763
GAMMEL, J. L., Polarization and asymmetry in the $^3He(d,p)^4He$ reaction, 20: 32475
GANIEL, U., Subconfiguration $f^6(^7F)sp$ in Sm I, 20: 31919
GARBA, A., Radiotracer study of manganese adsorption on glass from aqueous solutions, 20: 31245
GARBAZEVICH, J., Factors affecting the exchange of ^{15}N between nitric oxide and nitric acid in exchange columns, 20: 31639 (NYO-755-1, pp 77-129)
GARCIA DEL RIO, H., Scintillation scanning in kidneys, 20: 31148 (CNEA-170)
GARD, E., Isotopic exchange of active methyl hydrogens. II., 20: 31260
GARDES, J., Measurement technique for pair production in photographic emulsions, 20: 32006
GARFUNKEL, M. P., Magnetic field-induced anisotropy of superconducting energy gap determined by microwave absorption, 20: 32326
GARLID, K. L., Pulsed neutron sources applied to nuclear engineering, 20: 32360
GARRISON, G. W. Jr., Anode losses in coaxial Hall current accelerators, 20: 31376
GARRISON, R. L., Radiation of O and N and thermal conductivity of N up to 15,000°K, 20: 32240
GARROD, Claude, Hamiltonian path-integral method, 20: 32310
GARWIN, E. L., Attenuation length for secondary electrons in bulk-density KCl and CsI, 20: 31916
GASIOROWSKI, L., Measurements of frequency response of neutron-sensitive current ion chambers, 20: 31597
GATTO, R., Relation between $\eta \to 2\pi\gamma$ and $\eta \to 2\gamma$ from current algebra, 20: 32055
GAVELLI, Gian Paolo, Biological efficiency of 200 kv x rays, ^{60}Co rays and 14-Mev neutrons in Escherichia coli inactivation, 20: 31107
GAVRIK, V. Ya., Rational table or the radioactive decay function, 20: 32418
GEBALLE, T. H., Localized moments, 20: 32739
GEBHARDT, E., System silver–holmium, 20: 31749
GEE, Shermon, Bistatic-radar measurements on interplanetary plasma streams, 20: 31856
GEE, Shermon, Bistatic-radar measurements of propagating interplanetary shock waves, 20: 31858
GEISS, J., Rare gas measurements in 30 stone meteorites, 20: 31876
GEISS, J., Spallation, fission, and neutron capture anomalies in meteoritic Kr and Xe, 20: 31875
GELLER, Richard, Deuterium–tritium reactions in mixed-plasma accelerator, 20: 32586
GELLER, S., Spin orientation determination by linearly polarized, recoil-free γ rays, 20: 31228
GELL-MANN, Murray, Algebra of current components at infinite momentum, 20: 32206
GELSEMA, E. S., Bubble chamber investigation of K^* resonance, 20: 31987 (NP-16097)
GEL'TSEL, M. Yu., Feasibility of operating electron multipliers as h-f amplifiers, 20: 31485
GEMMELL, W., Physics aspects of dispersed fuel reactors containing thoria, 20: 32820
GENERALOVA, V. V., Loop dose transformer, 20: 32865
GENEUX, E., Resonance (Hertz coherence) in hyperfine atomic structure, 20: 31911
GEORGE, A. M., $\delta-U_3O_8$, a high-temperature modification. I., 20: 31752
GERAMB, Heinrich V., Lead-210, shell model calculations with harmonic oscillator wave functions, 20: 32381 (SGAE-PH-37/1966)
GERDING, T. J., Absorption spectrum of neptunium hexafluoride, 20: 31248
GERRITSEN, A. N., Anomalous resistance of Mg–Gd alloys, 20: 31758
GERRY, E. T., Combined anode-cathode feed of hollow-cathode arc, 20: 32600
GERRY, Edward T., Plasma diagnostics by Thomson scattering of laser beam, 20: 32599
GERSTENBERG, H. M., Three-body photodisintegration of ^3He, 20: 32546
GESKE, G., Decay of ^{162}Tb and ^{163}Tb, 20: 32462
GETOFF, N., Radiation-chemical carboxylation of formic acid and methanol in aqueous solution, 20: 31278
GETOFF, Nikola, Radiation-induced synthesis of ammonia from nitrogen and water, 20: 31289
GETZINGER, Richard W., Shock wave study of recombination in near-stoichiometric H–O mixtures, 20: 31216 (LA-DC-7659)

GHASWALA, S. K., Development of atomic energy in India, 20: 32817
GHEORGHE, Victor, High-frequency plasma in magnetic field, 20: 32634
GHIDONI, John J., Edema: delayed complication of total-body 32-Mev proton irradiation, 20: 31098
GHIDONI, John J., Effects of whole-body 32-Mev proton irradiations on primates, 20: 31097
GHIDONI, John J., Effects of 55-Mev protons on primates, 20: 31099
GHIDONI, John J., Effects of 138-Mev protons on primates, 20: 31101
GHIDONI, John J., Effects of 400-Mev protons on primates, 20: 31103
GHIDONI, John J., Estimate of biological effects of space proton environment, 20: 31106
GHIDONI, John J., RBE of 138-Mev protons as compared to ^{60}Co gamma radiation, 20: 31102
GHOSE, P., Note on broken SU_3 symmetry, 20: 32019
GIACOMELLI, G., New structure in the K^+-p and K^+-d total cross sections between 0.9 and 2.4 Bev/c, 20: 32067
GIBALA, R., Clustering of interstitials in dilute Nb–O–N solid solutions, 20: 31774
GIBB, Michel, Prestressed concrete in reactor technology, 20: 32750
GIBBS, B. W., Measurements of anisotropic plasmas using turnstile multiple-probe polarimeter, 20: 32581
GIBMEIER, H., H/D separation factors in electrolysis and diffusion by use of Pd and Pd/Ag membranes, 20: 31256
GIBSON, W. G., Application of Faddeev equations to calculation of quantum-mechanical third virial coefficient, 20: 32230
GIEDT, Warren H., Contact conductance measurements during transient heating, 20: 31712 (UCRL-14227(Rev.1))
GIELOW, F., Strontium-90 in beagle hair, 20: 30972 (TID-22027)
GIFFON, M., Inversion problem in the λ plane. II., 20: 32152
GIGUERE, P. A., Far infrared spectra of H_2O_2 and D_2O_2 in solid states, 20: 31247
GILBERT, R. L., Calculation of force-constant changes for U center, 20: 32683 (ORNL-P-2194)
GILLERON, Claude, Machines for loading and unloading channels of nuclear reactor, 20: 32755
GILLESPIE, Arthur S. Jr., Dissolved-oxygen analyzer for oceanographic use, 20: 31171 (ORO-596)
GILLESPIE, F. E., Constant current source for instrument calibration, 20: 31588
GIL'MAN, V. A., Pitting corrosion of zirconium in perchlorate solutions, 20: 31687
GILVARRY, J. J., Observability of indigenous organic matter of the moon, 20: 31854
GINGERICH, K. A., Composition function of thermodynamic properties in non-stoichiometric compounds, 20: 31723
GINSBERG, D. M., Superconducting transitions of amorphous bismuth alloys, 20: 32341
GIORNI, Alain, Reaction $^{11}B(p,\alpha\alpha)^4He$ at 163 kev, 20: 32402
GIRARDI, F., Determination of minimum detectable content of trace elements in neutron-activated materials, 20: 31541
GITLIN, David, Stable bromine and activation analysis in protein tracer studies, 20: 30990
GITTELMAN, B., Test of quantum electrodynamics by electron-electron scattering, 20: 32305
GITTUS, John Henry, Improvements in or relating to cermets, 20: 31707
GLADNEVA, L. I., Determining structure of sintered materials by ionic bombardment, 20: 31765
GLASHAUSSER, C. M., J dependence in the (p,α) reaction, 20: 32489
GLAZKOV, A. A., Computation of particle dynamics in waveguide separators, 20: 31841
GLENNON, B. M., Atomic transition probabilities. I., 20: 31942
GLICKSMAN, Arvin S., Effect of L-triiodothyronine on radiation-induced pulmonary fibrosis in dogs, 20: 31138
GLIDDON, J. E. C., Steady state fluid model of ion-exosphere, 20: 32291
GLOCK, E., Measurements of ion and electron temperature in theta-pinch plasma, 20: 32621
GLOERSEN, P., Diagnostic observations of repetitively pulsed coaxial accelerator, 20: 32650
GLOERSEN, Per, Propellant injection into a coaxial plasma accelerator, 20: 31363
GLOERSEN, Per, Steady state operation of a two-stage pulsed coaxial plasma engine, 20: 31365
GLOWER, Donald D., Charge release mechanism for ferroelectric radiation detectors, 20: 31539
GNATOVICH, V., Conversion electron spectra of isotopes ^{166}Tm, ^{164}Yb, ^{164}Tm, and ^{162}Tm, 20: 32415
GOBERT, Gerald, Slow neutron monochromator, 20: 31477 (CEA-R-2981)
GOBRECHT, H., Gamma radiation of ^{83}Br, 20: 32413
GODNEV, T., Effect of uv radiation on pigments in cucumber and tomato plants, 20: 31059
GOEBEL, C. J., Strong coupling of pseudoscalar-meson octet, 20: 32063
GOEBEL, C. J., Symmetry of the strong coupling theory, 20: 32207
GOEBELSMANN, Uwe, Biosynthesis of radioactive estriol-3-glucosiduronate by guinea pig liver homogenate, 20: 31312
GOIA, Mihai, Application of Foldy-Wouthuysen transformation to study of electron polarization, 20: 32088
GOLAND, A. N., Application of inverted-neutron-filter technique to study of inelastic scattering, 20: 32706
GOLD, T., Magnetosphere of the moon, 20: 31899
GOLDBERG, D. A., Reaction study of $^{19}F(d,n)^{20}Ne$, 20: 32555
GOLDBERG, H., SU_3 symmetry as a broken SU_8 symmetry, 20: 32143
GOLDBERG, J., Inversion problem in the λ plane. II., 20: 32152
GOLDBERGER, Marvin L., Consistency questions raised by simultaneous Mandelstam and angular-momentum analyticity, 20: 32164
GOLDEN, G. H., Safety analysis for ZPR-9 facility, 20: 32858 (ANL-7166)
GOLDEN, Robert Leon, Leptonic decays of neutral K mesons, 20: 31991 (UCRL-16771)
GOLDSTEIN, Raymond, Performance of arc heaters for MHD experiments, 20: 31356 (N-66-12435)
GOLIKOV, V. V., Pulsed reactor cold-neutron measuring device, 20: 31567
GOLOVANOV, L. B., Cryogenic developments at Joint Institute for Nuclear Studies, 20: 32318
GOLS, George A., Growth of foreign nuclear power, 20: 32808 (TID-22973)
GOLUBEV, G. P., Electron-bombardment-induced stimulated emission from cadmium selenide, 20: 32730
GONSER, U., Spin orientation determination by linearly polarized, recoil-free γ rays, 20: 31228
GONZALO, J. A., Magnetic structure of $FeSb_2O_4$, 20: 32705
GOODE, J. H., Release of tritium and ^{85}Kr during processing of $ThO–UO_2$ fuels, 20: 31447 (ORNL-3956)
GOODFELLOW, J. F., Superconductivity for nuclear-pairing interaction, 20: 32397
GOODMAN, L. J., Tissue-equivalent ionization chamber for in-phantom dosimetry, 20: 31524
GOODMAN, Milton, Advanced low-thrust propulsion systems for MORL, 20: 31387
GOPALAN, R., Physics calculations of thorium-fuelled heavy-water lattices, 20: 32774
GORBATOV, E. A., Measuring conversion spectra at wide range of energies, 20: 31565
GORELINSKII, Yu. V., Wide-range intensity meter for heterogeneous magnetic fields, 20: 31487
GORLOV, I. G., Critical thermal fluxes and heat transfer of boiling K in tubes, 20: 31347
GORMAN, D., Plasma waves at singular turning points, 20: 32619
GORMEZANO, Claude, Deuterium–tritium reactions in mixed-plasma accelerator, 20: 32586
GORODETZKY, Serge, Half life of the 570-kev excited level of ^{207}Pb, 20: 32401
GOROKHOV, N. A., Selective receiver of electromagnetic radiation of millimeter and submillimeter ranges, 20: 32626
GOROWITZ, B., Diagnostic observations of repetitively pulsed coaxial accelerator, 20: 32650
GOROWITZ, Bernard, Propellant injection into a coaxial plasma accelerator, 20: 31363
GOROWITZ, Bernard, Steady state operation of a two-stage pulsed coaxial plasma engine, 20: 31365
GOTO, Masayuki, Cockcroft-Walton type proton accelerator, 20: 31829
GOTO, Masayuki, INS mass spectrometer, 20: 31208
GOTOH, Seiichiro, Reactivity measurements by neutron noise analysis, 20: 32868
GOTOH, Shiroh, Relation between excretion of radiostrontium and intake of Na phytate, 20: 30977
GOTSMAN, E., Algebraic comments on Regge recurrences, 20: 32204
GOVONI, Edward M., Performance of self-excited MHD generator, 20: 31976
GOYAL, D. P., Determination of the Λ-nuclear potential well depth, 20: 32449
GRABER, H., Decay of ^{162}Tb and ^{163}Tb, 20: 32462
GRABER, H., Decay of $^{157}Eu(\beta^-)^{157}Gd$, 20: 32465
GRABER, H., Decay of ^{163}Er, 20: 32466
GRABER, H., Gamma transitions and energy levels in ^{161}Dy, 20: 32463
GRABER, H., Levels in ^{157}Tb, 20: 32464
GRABOVSKII, Ya., Matrix elements for inelastic scattering of heavy particles. I., 20: 32383
GRABOVSKII, Ya., Matrix elements for inelastic scattering of heavy particles. II., 20: 32384
GRAD, Harold, Guiding center plasma, 20: 32576 (NYO-1480-50)
GRAD, Harold, Minimum B as a plasma stability criterion, 20: 32623
GRADSZTAJN, E., Relative abundance and production cross sections of lithium isotopes, 20: 31205
GRAHAM, III, W. W., Prog. rpt. on kinetics parameters of highly enriched D_2O reactor, final, 12/65–12/66, 20: 32863 (TID-23037)
GRANT, R. W., Spin orientation determination by linearly polarized, recoil-

free γ rays, 20: 31228
GRARD, F., Projector for large-size bubble chamber pictures, 20: 31550
GRAUBY, A., Heating of soils using cooling cycle of power reactor, 20: 32843
GRAY, D. A., External proton beam at Nimrod, 20: 31823 (RPP-N-5)
GRAY, J. C., Composite solid propellants containing irradiated ammonium perchlorate, 20: 31286
GRAY, W. R., Pitfall in preparation of metal–H alloys for transmission electron microscopy, 20: 31691
GRECHIKHIN, L. I., Unipolar pulsed plasma generator combined with laser as source for obtaining plasma jets, 20: 32639
GRECHUKHIN, D. P., Collective M1 transitions of even nuclei, 20: 32420
GREEN, J. K., Prog. rpt. on physical sciences, annual, 1965. IV. Instrumentation, 20: 31473 (BNWL-235-4)
GREEN, W. B., Application of P_3 method to calculation of particle fluxes in shields, 20: 32673 (NAA-SR-Memo-11872)
GREENBERG, Arnold E., Dietary intake of radionuclides in California, 20: 31471
GREENBERG, Michael L., Extracorporeal irradiation of blood in humans, 20: 31000
GREENLEES, A. W., Preparation of ^{32}P-labeled nucleoside 5′-monophosphates, 20: 31307
GREENLEES, G. W., Asymmetries in elastic and inelastic scattering of polarized protons from C and Si, 20: 32440
GREENWOOD, R. C., Binding energy of deuteron determined from measurement of hydrogen neutron-capture gamma-ray energy, 20: 32488
GREGG, David W., Liquid immersion for reducing damaging effect of laser giant pulses to dielectric mirror coatings, 20: 31787
GREGG, David W., Momentum transfer produced by focused laser giant pulses, 20: 31810
GREGORY, B. L., Transient annealing in semiconductor devices following pulsed neutron irradiation, 20: 31613 (SC-DC-66-1443)
GREMIER, J., Energy released at high temperature by irradiated graphite, 20: 31802
GREINER, J. H., Longitudinal magneto-optical Kerr effect in EuO and EuS, 20: 31229
GREY, Jerry, Criterion for electron-heavy particle nonequilibrium in partly-ionized gas, 20: 32658
GREZNEV, Yu. S., EPR of Tb in CeO_2, 20: 32723
GRIBANOVA, I. N., Radiation resistance of complex organophosphorus resins, 20: 31303
GRIBOV, V. N., Three-particle partial wave amplitudes and unitarity conditions at complex values of angular momentum, 20: 32113
GRIEM, H. R., Computer study of dynamic phase of small θ pinch, 20: 32610
GRIEM, Melvin, Effects of 250-kv x rays on dog's pancreas, 20: 31089
GRIFFIN, B. I., Whole-body counting of Pu in dogs, 20: 30968 (BNWL-SA-11)
GRIFFITH, J. A. R., Polarization of 17.8 Mev protons elastically scattered by nuclei, 20: 32439
GRIFFITHS, D., Dispersion-relation approach to absorptive correction in peripheral model of high-energy physics, 20: 32022
GRIFFITHS, D., Non-S-state paramagnetic resonance in dilute alloy, 20: 31764
GRIFFY, T. A., Effect of Coulomb interaction on isospin selection rules in nuclear reactions, 20: 32484
GRIGORENKO, V. G., Microwave interferometers with amplitude modulation, 20: 31490
GRIGOROV, N. L., Pulse-height recording and logarithmic conversion of pulse heights in the 10^4 to 10^5 dynamic range, 20: 31577
GRIMES, C. C., Microwave emission from superconducting point contacts, 20: 31482
GRIN, G.-A., Excitation of levels of ^{12}C by inelastic scattering of 14.1-Mev neutrons, 20: 32408
GRIN, G.-A., Measurement, by gaging, of luminescence pulse forms of organic scintillators, 20: 31529
GRISHAEV, I. A., Electron beam injection into magnetic quadrant of an accumulator at 100 Mev, 20: 31849
GRODZENSKII, D. E., Biosynthesis of corticosteroids in adrenal tissue of irradiated hypophysectomized rats, 20: 31011
GROMOV, K. Ye., Conversion electron spectra of isotopes ^{168}Tm, ^{164}Yb, ^{164}Tm, and ^{162}Tm, 20: 32415
GROSS, E. E., Polarizations and differential cross sections for the elastic scattering of 40-Mev protons from ^{12}C, ^{40}Ca, ^{58}Ni, ^{90}Zr, and ^{208}Pb, 20: 32510
GROSSWEINER, Leonard I., Labile states of biological molecules with flash photolysis, 20: 30974
GROSSWENDT, B., Level crossing experiment in the $6^2P_{3/2}$ state of Rb–I spectrum, 20: 31940
GROVE, A. S., Model for radiation damage in metal-oxide-semiconductor structures, 20: 31615
GRUEHN, R., New modification of niobium pentoxide, 20: 31746
GRUENBAUM, Leon, High-energy inelastic electron scattering by ^{16}O, 20: 32442
GRUNBERGER, L., Rotational-velocity and ion-density profiles in plasma vortices, 20: 32644
GRUNDER, H. A., Regenerative beam extraction for Berkeley 88-inch cyclotron, 20: 31827 (UCRL-16794)
GRZYBINSKI, Ryszard, Solid-state instrumentation for control and safety of experimental reactors, 20: 32876
GUALDI, C., Splitting of a photon into two photons in Coulomb field of nucleus, 20: 32031
GUERARD, D., Action of Li vapor on graphite, 20: 31223 (BNL-tr-78)
GUEST, G. E., Apparent high-frequency stability of highly anisotropic plasma, 20: 32624
GUETLBAUER, F., Carboxylation of polychloro compounds to trichloroacetic acid by radiation chemistry, 20: 31276
GUETLBAUER, F., Radiation-chemical carboxylation of formic acid and methanol in aqueous solution, 20: 31278
GUETLICH, Philipp, Hot-atom reaction products in crystals of hexa- and trivalent Cr compounds. I., 20: 31297
GUILLETTE, Robert W., LIZARD-IV: program to solve nonlinear, ordinary differential equations, 20: 31657 (KAPL-M-6548)
GUILLOU, R. B., Albuquerque-Los Alamos area (ARMS-II), 20: 31396 (CEX-61.6.2)
GULDEN, T. D., Dislocation loops in O-ion-irradiated sapphire, 20: 31798
GULYAKIN, I. V., Effects of soil fractions on uptake of ^{90}Sr into plants, 20: 30985
GULYAMOV, U. G., Irradiation of combined emulsion and spark chamber system, 20: 31569
GUNNERSEN, E. M., Transmission electron microscopy of fast-neutron-irradiated Si, 20: 31792
GUPTA, Y. M., Decay angular correlation for Y_1^{+-} in the peripheral model, 20: 32052
GUPTA, Yogendra M., Production and decay of Ξ^* in one-particle exchange model, 20: 32009
GUPTON, E. D., Calibration of the ORNL model Q-2240, continuous air monitor, 20: 31528
GURATZSCH, H., Optical model analysis of elastic scattering on deuterons on ^{12}C, 20: 32454
GUS'KOV, B. N., Serial power supply for spark chamber gaps, 20: 31571
GUYON, Paul-Marie, Isotopic effects in dissociation of triatomic molecules by electron impact. II., 20: 31271
GUZZI, G., Determination of minimum detectable content of trace elements in neutron-activated materials, 20: 31541
GYFTOPOULOS, Elias P., Thermionic converters operating in ignited mode. I., 20: 31967
GYFTOPOULOS, Elias P., Thermionic converters operating in ignited mode. II., 20: 31968

H

HAAS, P. A., Sol-gel process development and microsphere preparation, 20: 31689 (ORNL-P-2159)
HABERER, A., Reaction chamber with semiconductor detectors adapted for measurements of particle correlations, 20: 31556
HABING, Donald H., Anomalous photocurrent generation in transistor structures, 20: 31612 (SC-DC-66-1415)
HADDOCK, R. P., Sizable proton polarizations in frozen toluene, 20: 31811
HADJIOANNOU, F. T., Use of imaginary-mass representations of Poincare group in scattering amplitudes, 20: 32154
HAEGI, M., Measurement of currents flowing through electrode in contact with plasma, 20: 32631
HAGEN, C. R., Field-theoretical formulation of Levinson's theorem, 20: 32127
HAGITA, Katsuyuki, Effect of uv irradiation on ^{124}Sb(III) in HCl solutions, 20: 31300
HALAMA, H. J., Electronic ripple filter for the Brookhaven Alternating-Gradient Synchrotron, 20: 31833
HALASZ, D., Losses caused by Hall effect and their influence on efficiency of thermal cycle in MHD generators, 20: 31962
HALL, David F., Experimental study of porous metal ionizers, 20: 31389
HALL, James D., Effects of 138-Mev protons on primates, 20: 31101
HALL, James D., Kinetics of recuperation following 55-Mev proton irradiation, 20: 31100
HALL, James D., Proton depth-dose dosimetry, 20: 31467
HALL, James D., RBE of 138-Mev protons as compared to ^{60}Co gamma radiation, 20: 31102
HALL, James D., Whole-body irradiation of primates with protons of energies to 400 Mev, 20: 31096
HALL, R. M., Thermoluminescent dosimeters for environmental monitoring, 20: 31526
HALL, R. S., Production of metallic and other ions in r-f ion source, 20: 31845
HALLIDAY, J. S., Quantitative analysis by spark source mass spectrometry, 20: 31202

HALMSHAW, R., Physics of industrial radiology, 20: 31338
HALSALL, M. J., Preliminary assessment of Th as fuel for thermal reactors, 20: 32822
HAMADA, Tatsumi, Effect of radiation and antitumor agents measured by mouse splenic and thymic weight, 20: 31131
HAMILTON, Charles W., Post-induction kinetics in shock initiated H_2–O_2 reactions, 20: 31217 (LA-DC-7661)
HAMILTON, Walter C., Automatic acquisition of neutron spectrometer data, 20: 32681 (BNL-10238)
HAMILTON, Walter C., Neutron-diffraction study of structures of ferroelectric and paraelectric ammonium sulfate, 20: 32698
HAMMEL, E. F., Liquid helium as engineering fluid, 20: 32314
HAMMEL, E. P., Isothermal flow of liquid He II through narrow channels, 20: 32332
HAMPTON, James C., Comparison of effects of x irradiation and colchicine on intestinal mucosa of mouse, 20: 31082
HAMPTON, James C., Effects of radiation on fine structure of Paneth cells of mouse, 20: 31083
HAND, R., Li-doped, radiation-resistant silicon solar cells, 20: 31614
HANKS, G. E., Injury accumulation in sheep during protracted gamma radiation, 20: 31026 (AD-633606)
HANNA, S. S., Lifetimes of first excited states of ^{7}Li and ^{7}Be, 20: 32504
HANNUM, William H., Fast reactor development in United States, 20: 32798 (LA-DC-7550)
HANSEN, L. K., Plasma physics of thermionic converters, 20: 31971
HANSEN, O., Isobaric analog states of doubly magic ^{208}Pb, 20: 32478
HANSON, I. G., Effect of prestrain on mechanical recovery in Pu-1Ga, 20: 31753
HANSON, W. C., Radionuclides in terrestrial and freshwater biota, 20: 31428 (PNE-481, pp 1165-1200)
HANSON, W. C., Radioecological concentration processes characterizing Arctic ecosystems, 20: 31442 (BNWL-SA-661)
HARA, Osamu, Reformulation of quark model in terms of Gemisch, 20: 32183
HARA, Y., Non-leptonic decays of Ω^-, 20: 31985 (IC-66/57)
HARADA, Y., Graphite–metal carbide composites, 20: 31688 (NASA-CR-507)
HARBOTTLE, Garman, Hot-atom reaction products in crystals of hexa- and trivalent Cr compounds. I., 20: 31297
HARDY, R. W. D., Tandem mass spectrometer for isotopic analysis, 20: 31206
HARM, Walter, Reactivation after photobiological damage, 20: 31039
HARMER, D. S., Prog. rpt. on kinetics parameters of highly enriched D_2O reactor, final, 12/65–12/66, 20: 32863 (TID-23037)
HARMS, W. O., Irradiation behavior of Th–U alloys and compounds, 20: 32833
HARNSEN, D. M., Lithium-8 emission in 5.0-Bev/c K$^-$-meson interactions in nuclear emulsion, 20: 32469
HARPER, Paul, Effects of 250-kv x rays on dog's pancreas, 20: 31089
HARRINGTON, David R., Three-alpha model for ^{12}C, 20: 32558
HARRINGTON, David R., Three-alpha model for ^{12}C, 20: 32493
HARRIS, A. M., Microwave resonance observations in gadolinium solid solutions, 20: 32716
HARRIS, Arthur K., Worldwide geomagnetic disturbances generated by Starfish explosion, 1962, 20: 32264
HARRIS, P. F., Fractionation of bone marrow suspensions and their use to protect against irradiation, 20: 31126
HART, Robert R., Determination of anharmonic potential energy constants, 20: 31949
HARTZ, T. R., Alouette II satellite, 20: 32247
HARVEY, A. L., Inconsistency of Nordstroem-type theories of gravitation with principle of equivalence, 20: 32299
HARVEY, R. A., IDERM: program for intake, distribution and excretion of radionuclides in mammals, 20: 31441 (BNWL-SA-40)
HASANEN, Erkki, Results of Project Lapland at beginning of 1966, 20: 31444 (CONF-660405-15)
HASEBE, Katsuya, Polarization in elastic pion-nucleon scattering in few-Bev region, 20: 32087
HASEGAWA, Kunihiko, Extinction coefficient for Ti ions, 20: 31301
HASEGAWA, Kunihiko, Removal of ^{89}Sr and ^{137}Cs on cellulose phosphate, 20: 31324
HASHIZUME, Tadashi, Estimation of bone marrow dose due to fluoroscopic radiation in Japan, 20: 31466
HASSAN, H. A., Anode losses in coaxial Hall current accelerators, 20: 31376
HASSON, V., Alpha radioactivity of human blood, 20: 31145
HATAYE, Itsuhachiro, Determination of Ra in river waters, 20: 31191
HATTENBACH, K., Radiation stability of adamantane, 20: 31273
HAUCK, Hansjorgen, High-temperature embrittlement of austenitic steels and Ni alloys by (n,α) reactions, 20: 31801
HAUS, Hermann A., Hamilton's principle for electromagnetic fluids, 20: 32228
HAUSER, H. N., IDERM: program for intake, distribution, and excretion of radionuclides in mammals, 20: 31441 (BNWL-SA-40)
HAUSER, Michael G., Photoproduction of negative pions from hydrogen, 20: 31983 (CALT-68-71)
HAWRYLEWICZ, Ervin J., Effect of gamma and proton irradiation on lactic dehydrogenase isoenzymes, 20: 31105
HAYAKAWA, Junichiro, Effects of continuous low-dose irradiation on mice. I., 20: 31074
HAYAMI, Hiroshi, Relation between excretion of radiostrontium and intake of Na phytate, 20: 30977
HAYASHI, Eiichi, Effect of green tea and related substances on G-I absorption of ^{90}Sr, 20: 30987
HAYASHI, Koichi, Vertex zeros and Levinson's theorem, 20: 32172
HAYASHI, Koichiro, Radiation-induced solid-state polymerization of two-component systems. I., 20: 31287
HAYASHI, Koichiro, Recent progress in radiation chemistry on polymers in Japan, 20: 31269 (NSJ-tr-56)
HAYASHI, Takemi, Non-leptonic weak interaction in current-current interaction, 20: 32075
HAYDOCK, Irene C., Radiation-induced changes in properdin system of dog, 20: 31013
HAYES, R., Tandem mass spectrometer for isotopic analysis, 20: 31206
HAZELHURST, J. H., WEB: language to describe interconnection and packaging of logical units in digital processor. I., 20: 31648 (COO-1018-1021)
HEACOCK, R. R., The 4-second summertime micropulsation band at College, 20: 32263
HEATH, R. L., Combination neutron experiment for remote analysis, 20: 31211
HEBERT, Jacques, Resonance (3,3) in nucleus, 20: 32078
HECK, C. K., Liquid-vapor phase equilibria of neon-normal hydrogen system, 20: 32242
HECKMAN, Harry H., Effective atmospheric losses for 125-Mev protons in South Atlantic anomaly, 20: 32265
HEGARTY, William, Improvements in or relating to self-luminous signs or patterns, 20: 31636
HEINZ, R. M., Backward proton-deuteron elastic scattering from 1.0 to 1.5 Bev, 20: 32102
HEISS, Dieter, Self-consistent calculation of the 11- and 33-amplitude in low-energy π-N scattering, 20: 32091
HELLER, Carl G., Prog. rpt. on effects of radiation on testicular function of man, 6/63–5/64, 20: 31034 (RLO-1780-7)
HELLER, Carl G., Prog. rpt. on effects of radiation on testicular function of man, annual, 6/64–5/65, 20: 31035 (RLO-1780-8)
HELLMAN, W. S., Relativistic fields with spacelike momentum spectra, 20: 32146
HELM, J. W., Radiation effects in graphite at high temperatures, 20: 31782 (BNWL-SA-67)
HEMINGWAY, J. D., Cross sections for reactions ^{27}Al(n,α) and ^{56}Fe(n,p) for 14-Mev neutrons, 20: 32528
HEMMENT, P. L. F., Transmission electron microscopy of fast-neutron-irradiated Si, 20: 31792
HENDERSON, R. W., UCAPP: Union Carbide APT Post Processor, first edition, 20: 31478 (K-1670)
HENDERSON, W. G., Pumping system and single-wall chamber for 10^{-13} torr, 20: 31392
HENDRY, A. W., Bound states of quark-antiquark system, 20: 32147
HENNEY, J., Phase equilibria in the Th–C system, 20: 31768
HENRY, R. J. W., Rotational excitation of H_2 and D_2 by H impact, 20: 31932
HENSLEY, J. C., Heritable radiation effects on mouse, 20: 31048
HERING, W. R., Experimental test of triton form factor by Coulomb pickup on ^{208}Pb, 20: 32485
HERMAN, John R., Spread F and ionospheric F-region irregularities, 20: 32273
HERMANS, M. E. A., Thorium cycle and homogeneous suspension reactor project, 20: 32829
HEROLD, A., Action of Li vapor on graphite, 20: 31223 (BNL-tr-78)
HERRON, B. G., Power conditioning systems for ion engines, 20: 31357
HERTENBERGER, Gerhard, Lead-210, shell model calculations with harmonic oscillator wave functions, 20: 32381 (SGAE-PH-37/1966)
HESS, W. H., Spatial distribution of protons from neutron decay trapped by geomagnetic field, 20: 32266
HESS, Walther, Cyclotron harmonic radiation from plasma in magnetic field, 20: 32637
HESTER, Donald L., Charge release mechanism for ferroelectric radiation detectors, 20: 31539
HEUGHEBAERT, J., Projector for large-size bubble chamber pictures, 20: 31550
HEVEZI, J. M., Polarization of neutrons elastically scattered from ^{3}He at 3.33 and 7.90 Mev, 20: 32452
HEYWOOD, John B., Experiments in magnetically driven shock tube with axial magnetic field, 20: 32615
HICKMAN, G. D., Measurement of total neutron cross sections of ^{147}Pm,

^{148}Pm, and ^{148m}Pm, 20: 32376 (KAPL-3090)
HIDA, Kinzo, C.C.L. approximation for treating collisionless plasma flow, 20: 32649
HIGATSBERGER, M. J., New electrostatic time-of-flight mass spectrometer, 20: 31209
HIIDA, Kichiro, Possible C and T violation in the photoproduction of neutral pions, 20: 32074
HILF, E., Surface tension of nuclei according to Fermi-gas model, 20: 32470
HILL, C. W., Data compilation and evaluation of space shielding problems, 20: 32674 (NP-15697(Vol.3))
HILL, S. S., Effect of irradiated, low-temperature, high pH water on nylon, 20: 31280
HILSCHER, D., Neutron-induced reactions on silicon, 20: 32431
HILTON, D. A., Fast neutron dosimetry by anion exchange separation of ^{137}Cs from irradiated Th, 20: 31530
HINES, J. J., Anisotropy of self-diffusion in alpha uranium, 20: 31771
HINTENBERGER, H., Precision determinations of isotope abundances, 20: 31399
HIPP, J. C., Molybdenum dioxide single crystals, 20: 32697
HIRAMATSU, Hiroshi, Study on the medical universal human counter. I., 20: 31586
HIRAMOTO, Toshiyuki, Low-background beta-ray scintillation spectrometer, 20: 31603
HIRAMOTO, Yukio, Cell division: pressure-induced reversal of anti-meiotic effects of heavy water in oocytes of the starfish, 20: 30986
HIROOKA, Masahiko, Systematic analysis of weak γ decay of hyperons, 20: 32081
HIRSCH, W., Study of neutral point in plasma, 20: 32656
HISADA, Kin-ichi, Study on the medical universal human counter. I., 20: 31586
HITCHCOCK, A. J., Distribution of defect introduction rate with depth in Si irradiated with 300-kev electrons, 20: 31791
HITCHCOCK, J. M., Nuclear reactor control system, 20: 32760
HLADYSCHEWSKII, E. I., Crystal structure of $Ce_3Ni_6Si_2$ and related compounds, 20: 31253
HOCHBERG, S., Dispersion theory calculations for nucleon-nucleon scattering, 20: 32008
HOEKSTRA, Henry R., Investigation of rare earth sesquioxides at high pressure, 20: 31258
HOENIG, Stuart A., Liquid nitrogen-cooled shield to protect proton accelerator against oil vapor contamination, 20: 31848
HOFER, K., Diurnal and annual period of radiation resistance of plant cells, 20: 31079
HOFFERT, Martin I., Hall current plasma accelerator. I., 20: 32573 (N-65-12780)
HOFFMAN, D. C., Decay of ^{157}Eu, ^{158}Eu, and ^{159}Eu, 20: 32514
HOFFMEISTER, W., Determination of copper in quartz by neutron activation analysis, 20: 31183
HOFKER, W. K., Detection of radioactive radiation with p-i-n transitions in Si and Ge, 20: 31537
HOFMANN, H. M., Phenomenological treatment of elastic scattering of spin-1 particles on spin-0 particles, 20: 32194
HOFMOKL, Helena, Dependence of the π-meson production spectrum exponent on production level, 20: 31956
HOGERTON, John F., Growth of foreign nuclear power, 20: 32808 (TID-22973)
HOGG, A. M., Ions from alpha-particle irradiation of gases at high pressures, 20: 31270
HOITINK, N. C., Animal physiological function telemetry developments, 20: 30961 (BNWL-235-4, pp 25-9)
HOITINK, N. C., Physiological data telemetry system, 20: 31474 (BNWL-235-4, pp 1-4)
HOITINK, N. C., Raindrop charge and velocity measurement techniques, 20: 31476 (BNWL-235-4, pp 21)
HOITINK, Nell C., Measurement of radionuclide uptake by algae, 20: 31504 (BNWL-235-4, pp 16-18)
HOLDREDGE, R. M., Boiling heat transfer from cylinders in saturated liquid He-II bath, 20: 32349
HOLLADAY, W. G., Comparison of resonance formulas for (1236 Mev, 3/2) pion-nucleon resonance, 20: 32100
HOLLADAY, Wendell, Effects of added agar on radiation sensitivity of trypsin in solution, 20: 31017
HOLLANDER, J. M., New weak beta transition from ^{88}Y, 20: 32453
HOLLARD, Daniel, Effects of x rays on platelet environment, 20: 31032 (CEA-R-2953)
HOLMES, J. M., Production of ammonia using electricity from nuclear desalination reactor complex, 20: 32841 (ORNL-3882)
HOLT, E. H., Sub-threshold study of azimuthal modes of Kadomtsev plasma instability, 20: 32579
HOMER, J. B., Charge transfer and atom transfer in ion-molecule interactions studied by time-of-flight mass spectrometer, 20: 31224
HONES, E. W. Jr., Motion of particles trapped in magnetosphere, 20: 32270
HONEYCUTT, C. R., Prog. rpt. on determination of elevated-temperature fatigue data non refractory alloys, 1–4/66, 20: 31710 (NASA-CR-54983)
HONIG, Richard E., Analysis of solids by mass spectrometry, 20: 31201
HONSTEAD, John F., Uptake and retention of ^{32}P and ^{65}Zn from consumption of Columbia River fish, 20: 30969 (BNWL-SA-45)
HOPE, C. S., Cellular control systems and radiosensitivity, 20: 31064
HOPPER, V. D., Radiation measurements in commercial aircraft using a single counter, 20: 31952
HOPPER, Wilbert H., Growth of foreign nuclear power, 20: 32808 (TID-22973)
HOREN, D. J., NRDL 70-in. cyclotron external ion optics system, 20: 31814 (AD-634300)
HORNSHOEJ, P., Internal magnetic field of lutetium in iron and g factor in ^{175}Lu, 20: 32472
HORST, K. M., Prog. rpt. on SEFOR development, 11/65–1/66, 20: 32860 (GEAP-5108)
HORVAY, G., Blowout of flat end of hydraulically pressurized cylindrical pressure vessel, 20: 32752
HOSEA, J. C., Probe measurements in pulsed plasma, 20: 32597
HOSHI, Masamitsu, Stoichiometric number and electrolytic separation factor of deuterium on nickel hydrogen electrode, 20: 31644
HOSODA, Masataka, N(12) and meson-baryon inelastic two-body scattering at high energy, 20: 32079
HOSODA, Masataka, Systematic analysis of weak γ decay of hyperons, 20: 32081
HOSSENLOPP, J., Reaction chamber with semiconductor detectors adapted for measurements of particle correlations, 20: 31556
HOUSTON, J. M., Plasma physics of thermionic converters, 20: 31971
HOUTMAN, J. P. W., Errors in activation analysis due to variations in isotopic ratio, 20: 31190
HOUTMAN, J. P. W., Rapid and accurate B.E.T. surface area measurement using radioactive Kr, 20: 31353
HOWARD-FLANDERS, Paul, Sensitization of E. coli to radiation by bromouracil, 20: 31062
HOWARD, John M., Direct irradiation of lymph nodes with ^{131}I tagged ethiodol, 20: 31044
HOYAUX, Max F., Plasma physics and its applications, 20: 32587
HOYTE, A. F., Mineral exploration and soil analysis using in situ neutron activation, 20: 31434
HSU, Chao-mei, Effect of gamma radiation on seeds in second generation, 20: 31113
HSU, Chia-Jung, Laminar heat transfer in hexagonal channel, 20: 31341 (BNL-9546)
HSU, Feng-tsao, Damage and recovery of spermatocytes of monkeys following x and gamma radiation, 20: 31117
HSU, Hsing, Adsorption of ^{90}Sr by aged horse manure, 20: 31252
HSU, Mei-ch'i, Biological variations in agricultural seeds during storage after gamma irradiation, 20: 31024
HSU, Yung-chang, Irradiation of combined emulsion and spark chamber system, 20: 31569
HUBBARD, D. F., Nuclear structure effects in bremsstrahlung, 20: 32456
HUBBARD, John Richard, Properties of neutral cascade hyperon, 20: 31988 (UCRL-11510)
HUBER, O., Decay of ^{140}Ba, 20: 32407
HUBER, O., Decay of ^{51}Cr, 20: 32410
HUBER, P., Reaction ^{6}Li(d,n)^{7}Be* with polarized deuterons, 20: 32411
HUBERT, Pierre, Temporary capture of charged particles in static magnetic bottle, 20: 32582
HUCHITAL, D. A., Sub-threshold study of azimuthal modes of Kadomtsev plasma instability, 20: 32579
HUDSON, E. D., Operating characteristics of ORIC beam extraction system, 20: 31821 (ORNL-P-2239)
HUEBOTTER, P. R., Carbon in primary Na system of Enrico Fermi Atomic Power Plant, 20: 32809 (TID-23101)
HUEFNER, J., Anomalous intensity ratios in muonic Pb and Bi, 20: 31965
HUETTER, T., Analysis of K and $\eta \to 3\pi$ decay spectra, 20: 32010
HUFFMAN, A. H., Boundary-condition model for P_{33} pion-nucleon state, 20: 32023
HUGHES, L. B., Study of the ^{127}I(n,γ)^{128}I and ^{133}Cs(n,γ)^{134}Cs reactions, 20: 32422
HUGON, J., Lysosomal modifications after administration of radioprotective drugs, 20: 30964
HUGON, J., Ultrastructural aspects of duodenal crypts in x-irradiated mice after chemical protection, 20: 31128
HUI, W. L. C., Proton irradiation of thin-film CdS and single-crystal Si solar cells, 20: 31616
HUKE, K., Production of neutral pions from electron-proton collisions, 20: 32038
HULUBEI, Horia, Simultaneous measurement of beam energy in angular distribution studies, 20: 32403
HUMMEL, H. H., Parametric studies of reactivity coefficients for large ^{233}U–Th-fueled fast reactors, 20: 32790 (ANL-6930)
HUNG, Ru-jane, Collisionless shock wave in plasma, 20: 32652

HUNT, Dale E., Amino-acid protection of uv-irradiated Bacillus subtilis, 20: 31129
HUNTER, Donald B., Titanium–beryllium phase diagram up to 10 Be, 20: 31772
HUNTER, J., Water problem and desalination, 20: 31192
HUQUE, Hoshamul, Control of fruit flies by gamma rays, 20: 31046
HURWITZ, L., Mathematical model of geomagnetic field for 1965, 20: 32255
HUSMANN, O. K., Ion-microscope studies of Cs surface ionization on porous refractory metals, 20: 31776
HUSMANN, Otto K., Improved surface ionization efficiency by high work function refractory metals, 20: 31386
HYINDEN, T., Cesium-137 and ^{90}Sr in Norwegian milk, 1960-1964, 20: 31465
HWANG, C. L., Magnetohydrodynamic channel entrance flow with parabolic velocity at entry, 20: 32226
HYAKAWA, Satio, Polarization in elastic pion-nucleon scattering in few-Bev region, 20: 32087

I

IBRAGIMOV, A. P., Effects of γ-irradiation of cottonseeds on change of DNA in succeeding generations, 20: 31019
IBRAHIM, M. S., Preparation of radioiodinated serum Globulines, 20: 31264
IBUKI, Kimio, Programming manual for ILLIAC III computer, 20: 31653 (COO-1018-1061)
ICHIKAWA, Sadao, Radiobiological studies in plants. XI., 20: 31078
ICHIKAWA, Yonato, Properties of quartz thermoluminescence dosimeters, 20: 31520
IDA, Masakoni, N/D methods for multichannel scattering, 20: 32181
IGI, K., S matrix with generalized potential and its asymptotic behavior, 20: 32140
IHUMA, Takeshi, Cesium turnover in man following single administration of ^{132}Cs. I., 20: 30988
IKEDA, Kiyomi, Practical method using isospin projection operator in nuclear physics, 20: 32533
IKEDA, Toshio, Deamination of aqueous glycine–Cu(II) solution by gamma-rays. II., 20: 31299
IKI, Tetsuo, Three-dimensional photoelastic investigation of stresses in reactor pressure vessels, 20: 32751
IKRAMOVA, M., Energy distribution of electrons from alkali halide compounds bombarded by He^+ and Ar^+ ions, 20: 31912
IKUSHIMA, Takeji, Radiobiological studies in plants. XI., 20: 31078
IL'INA, G. V., Effect of physiologically active compounds and radiation on metabolism in wheat, 20: 31002
IL'INA, G. V., Effects of spaceflight factors on wheat seeds, 20: 31058
IMAMURA, Gen., Cockcroft-Walton type proton accelerator, 20: 31829
IMOTO, S., System U–N, 20: 31230
IMRE, Kaye, Prekinetic equations for a plasma, 20: 32605
INDREAS, Grigore, Simultaneous measurement of beam energy in angular distribution studies, 20: 32403
INGLEBY, Bryan Edward, Improvements in or relating to production of spheroids, 20: 31705
INGLEBY, Bryan Edward, Improvements in or relating to nuclear reactor fuel elements, 20: 31706
INGRAHAM, John Charles, Electron-atom collision cross-section measurements in afterglow of pulsed Cs plasma, 20: 32646
INNES, T. G., Nanosecond pulse light source, 20: 31497
INOHARA, Sumiko, Effect of green tea and related substances on G-I absorption of ^{90}Sr, 20: 30987
INTOCCIA, Alfred P., Radiochemical safety procedures at Smith Kline and French Laboratories, 20: 31469
IONESCU-PALLAS, Nicolae, Determination of quadrupole moments of Ba by measurements of isotopic displacements, 20: 32404
ISABELLE, D. B., Measurement technique for pair production in photographic emulsions, 20: 32006
ISHIHARA, Tomio, Cesium turnover in man following single administration of ^{132}Cs. I., 20: 30988
ISHIKAWA, Koji, Ground state of a non-interacting electron gas exchange-coupled to localized spin, 20: 32085
ISSINSKII, I. B., Programming operation of JINR synchrophasotron, 20: 31840
ISTOMIN, I. V., High-pressure ionization ^3He chamber performance as slow neutron detector, 20: 31573
ITIKAWA, Yukikazu, Energy change of charged particle moving in plasma, 20: 32617
ITO, Masayuki, Separation of ^{32}P from a ^{32}P–^{36}S mixture, 20: 31309
ITO, Misoru, Histochemical observations of oxidative enzymes in irradiated testis and epididymis, 20: 31090
ITO, Yasuhiko, Effects of x radiation on HeLa cells, 20: 31056
IVANENKO, T. I., Biosynthesis of corticosteroids in adrenal tissue of irradiated hypophysectomized rats, 20: 31011
IVANITSKII, A. M., Primary potentials in animals irradiated during antenatal period, 20: 31037 (JPRS-35315, pp 65-75)
IVANOV, A. A., Time-of-flight neutron spectrometer, 20: 31566
IVANOV, A. A., Time-digital-code converter for nanosecond range, 20: 31578
IVANOVA, E. N., New method for studying the intensity of corrosion of reactor construction materials, 20: 31682 (NP-16003)
IVASHKEVICH, S. A., Magnetic field stabilizer with broadband EPR sensor, 20: 31813
IWATA, Kenzo, Strong interaction of intermediate vector mesons and extremely high-energy phenomena, 20: 32177
IYA, V. K., Production of radioisotopes of high specific activity for medical use, 20: 31275
IYENGAR, P. K., Rotational behavior of ammonium ion in salts, 20: 31241
IZAWA, Masami, Cesium turnover in man following single administration of ^{132}Cs. I., 20: 30988

J

JABLONSKA, Jadwiga, Progress in reactor detectors design and construction, 20: 31596
JACKSON, E. A., Landau damping in inhomogeneous plasmas, 20: 32616
JACKSON, S., Creatinine in urine as index of urinary excretion rate, 20: 30983
JACKSON, W. A., Effect of Ca and Sr on preferential formation of adenosine triphosphatase in wheat roots, 20: 30992
JACOB, A. W. B., Design and use of spherical Geiger counters, 20: 31593
JACOBS, Paul F., Criterion for electron-heavy particle nonequilibrium in partly-ionized gas, 20: 32658
JACOBS, Robert, Effects of whole-body 32-Mev proton irradiations on primates, 20: 31097
JACOBSON, R. S., Shock pulse computer, 20: 32219 (SCL-DC-66-2)
JACQUOT, Bernard, Deuterium–tritium reactions in mixed-plasma accelerator, 20: 32586
JAECH, J. L., Prog. rpt. on Zr alloy, 4–6/65, 20: 31677 (GEAP-4840)
JAENECKE, Joachim, Vector and tensor Coulomb energies, 20: 32499
JAERSCHKY, Rudolf, Gundremmingen nuclear power plant, 20: 32810
JAGERHUBER, P., Rapid estimation of important radionuclides ^{89}Sr, ^{90}Sr, ^{131}I, and ^{137}Cs in food and water. II., 20: 31180
JAHR, R., Mirror reactions $^{10}B(d,t)^9B$ and $^{10}B(d,^3He)^9B$ at 11.8 Mev, 20: 32481
JAKLEVIC, R. C., Macroscopic quantum interference in superconductors, 20: 32344
JAMBA, D. M., Ion-microscope studies of Cs surface ionization on porous refractory metals, 20: 31776
JAMES, David T., Solid state beta gauge for measuring density of liquid H, 20: 31494
JAMES, E. L., Surface ionization engine development, 20: 31370
JAMES, R. H., Cross sections for reactions $^{27}Al(n,\alpha)$ and $^{56}Fe(n,p)$ for 14-Mev neutrons, 20: 32528
JAMIESON, Dana, Mechanisms of chemical radiation protection in vivo. III., 20: 31122
JANARDHANARAO, V., Synthesis of new europium chelates, 20: 31232
JANCEL, Raymond, Nonlinear effects in homogeneous Lorentz plasma, 20: 32584
JANDUSHKIN, K. N., Electrochemical properties of radioactive specimens of iron and steel, 20: 31231
JANES, G. S., Anomalous electron diffusion and ion acceleration in low-density plasma, 20: 32612
JANIKOWSKI, Andrzej, Progress in reactor detectors design and construction, 20: 31596
JANNI, Joseph F., Dose-equated phantom for space radiation research, 20: 31455
JARRETT, Robert D. Sr., Radiation dosimetry in relation to high-intensity radiation sources, 20: 31607
JASELSKIS, Bruno, Titrimetric determination of organic acids by xenon trioxide oxidation, 20: 31196
JATCZAK, Jerzy, Apparatus for investigation of directional correlation of γ-rays emitted in cascade, 20: 31595
JEANMAIRE, L., Control of radioactive pollution of milk by ^{131}I, 20: 31456
JEEVANANDAM, M., Solvent carrier system for concentration of ^{15}N by chemical exchange between oxides of N, 20: 31638 (NYO-755-1, pp 12-76)
JEFFS, A. T., Distribution of Pu dioxide in U dioxide by autoradiography, 20: 31212
JENKINS, R. W., Cherenkov-scintillation counter studies of primary cosmic radiation at balloon altitudes, 20: 31958
JENSEN, James T., Growth of foreign nuclear power, 20: 32808 (TID-22973)
JERKINS, Ernest Edward, Improvements in or relating to valves for fluid flow, 20: 32762
JERMAKIAN, A., Rotational-velocity and ion-density profiles in plasma vortices, 20: 32644
JERNIGAN, E. D., Missile lift off measurement system, 20: 31495
JERVIS, E. L., Effects of whole-body irradiation on transfer capacity of

rat small intestine, 20: 31081
JIMENEZ, C. M., Damage production in electron-irradiated palladium, 20: 31805
JOACHAIN, C. J., Importance of correlation effects in ionization of He by electron impact, 20: 31924
JOHANNSEN, Klaus, Molten ceramic oxides as possible fuel matrix for homogeneous thermal nuclear reactors, 20: 31726
JOHNSON, B. M., Containment systems experiment. III, 20: 32748 (BNWL-233)
JOHNSON, D. R., Neutron dose conversion factors for AmBe and AmB sources, 20: 32356
JOHNSON, Horton A., Extracorporeal irradiation of blood in humans, 20: 31000
JOHNSON, R. J., Calculating space dependent reactor transfer functions using statics techniques, 20: 32780
JOHNSON, R. J., Prog. rpt. on kinetics parameters of highly enriched D_2O reactor, final, 12/65–12/66, 20: 32863 (TID-23037)
JOHNSON, Ray E., Effect of Ca and Sr on preferential formation of adenosine triphosphatase in wheat roots, 20: 30992
JOKIPII, J. R., Effects of diffusion on composition of solar corona and solar wind, 20: 31894
JONES, C. Edward, Consistency questions raised by simultaneous Mandelstam and angular-momentum analyticity, 20: 32164
JONES, Carmen B., Power generator, 20: 31978
JONES, D. E., Variations in polarity distribution of interplanetary magnetic field, 20: 31860
JONES, G., Annihilation of positrons in Ar, 20: 32105
JONES, G. D., Coupling between H⁻ localized modes and rare-earth ion electronic states in rare-earth trifluorides, 20: 32709
JONES, G. E., Radiation from thick silver foils bombarded by grazing-incidence electrons, 20: 32708
JONES, Ian R., Suppression of neutron reflection by surface coatings, 20: 32368
JONES, J. W. S., Phase equilibria in the Tb–C system, 20: 31768
JONES II, Leonidas John, Superconductive threshold logic circuitry, 20: 32311 (ORO-2430-27)
JONKER, C. C., Light attenuation in scintillation counters, 20: 31546
JONSSON, J., Thyroid antibodies in euthyroid subjects after ^{131}I therapy, 20: 31161
JOPSON, R. C., Atomic fluorescence yields, 20: 31936
JORDAN, Carole, Abundance of iron in the solar corona, 20: 31867
JORDAN, Carole, Relative abundance of Si, Fe, and Ni in solar corona, 20: 31865
JOSEFOWICZ, K., Methods and results of static measurements in zero power reactor ANNA, 20: 32875
JOSEPH, C., Excitation of levels of ^{12}C by inelastic scattering of 14.1-Mev neutrons, 20: 32408
JOSEPH, S., Fractionation of bone marrow suspensions and their use to protect against irradiation, 20: 31126
JOSEPHSON, B. D., Relation between superfluid density and order parameter for superfluid He near T_c, 20: 32323
JOZEFOWICZ, E. T., Methods and results of static measurements in zero power reactor ANNA, 20: 32875
JUDD, B. R., Hyperfine structures in atomic 2p shell, 20: 31904 (UCRL-16581)
JUDD, J. M., Effects of radionuclides on thermal tolerance of fish, 20: 31028 (AECL-2409)
JULIA, M., Industrial fabrication of fuel elements in France, 20: 31693
JUNGERMAN, J. A., Initial internal beam studies with Davis 76-inch cyclotron, 20: 31826 (UCD-CNL-47)
JURANEK, H. J., Effect of spatial variation of order parameter on tunneling density of states of superconducting alloys, 20: 32340
JURIC, M., Mesic decay of hyperfragments produced by K⁻ mesons of 1.5 Bev/c, 20: 32491

K

KADANOFF, L. P., Ultrasonic attenuation in superconductors, 20: 32335
KADLECEK, J. A., Photodisintegration of Ca to 62 Mev, 20: 32445
KADONAGA, Masao, Properties of polyethylene–vinyl chloride graft copolymers, 20: 31288
KAETSU, Isao, Radiation-induced solid-state polymerization of two-component systems. I., 20: 31287
KAHAN, R. S., Changes in flavedo and juice of Shamouti oranges following γ irradiation, 20: 31632
KAINDL, K., Neutron activation analysis determination of radiosensitizers, 20: 31172 (SGAE-BL-17/1966)
KAKHAROV, O., Heat of absorption of Cs on filamentary W, 20: 31730
KALINICHENKO, V. V., Magnetic field stabilizer with broadband EPR sensor, 20: 31813
KALINKIN, B. N., Matrix elements for inelastic scattering of heavy particles. I., 20: 32383
KALINKIN, B. N., Matrix elements for inelastic scattering of heavy particles. II., 20: 32384
KALISZ, J., Determination of coincidence-circuit statistical parameters, 20: 31547
KALKWARF, D. R., Radiation chemistry of Agarose jellies, 20: 30998 (BNWL-SA-709)
KAMBARA, Tomihiso, Effect of uv irradiation on ^{124}Sb(III) in HCl solutions, 20: 31300
KAMEFUCHI, S., Lagrange formalism and relativistic quantization of Bargmann-Wigner fields, 20: 32150
KAMINSKY, Manfred, Atomic impact phenomena on metal surfaces with pulsed-molecular-beam mass spectrometer, 20: 31907
KAMINSKY, Manfred, Mass spectrometric studies of particles leaving monocrystalline target in charged or uncharged state, 20: 31905
KAMPP, M., Washout of intraarterially injected ^{85}Kr from intestine of cat, 20: 30979
KAN, Ya. S., Cryotron relaxation oscillator with controlled frequency, 20: 32333
KANADA, Hiroyuki, Polarization in elastic pion-nucleon scattering in few-Bev region, 20: 32087
KANADA, Hiroyuki, Reaction ($\gamma\pi^-$p) with complex nuclei, 20: 32530
KANEKO, S., Production of neutral pions from electron-proton collisions, 20: 32038
KANEL, O. M., Vacancy formation in zirconium, 20: 32729
KANESTROEM, I., Some features of calculated nuclear level density, 20: 32432
KANIEWSKI, Jacek, Solid-state instrumentation for control and safety of experimental reactors, 20: 32876
KANIJ, J. B. W., Errors in activation analysis due to variations in isotopic ratio, 20: 31190
KANNO, Iwao, Effects of x radiation on HeLa cells, 20: 31056
KANUNNIKOV, V. N., Multichannel current stabilizer, 20: 31837
KAPLAN, Henry S., Evidence for tumoricidal dose level in radiotherapy of Hodgkin's disease, 20: 31151
KAPLAN, K., Formation of debris from buildings by blast and fire effects of nuclear weapons, 20: 31332 (URS-651-4)
KAPLON, M. F., Model for origin and properties of cosmic-ray rigidity spectrum, 20: 31954
KARKHANAVALA, M. D., δ–U_3O_8, a high-temperature modification. I., 20: 31752
KAROL, I. L., Distribution of nuclear test explosion fallout over continents and oceans, 20: 31421
KARPF, A. D., Neutral vector bosons in Bhabha scattering, 20: 32093
KARRAS, T. W., Diagnostic observations of repetitively pulsed coaxial accelerator, 20: 32650
KARRAS, Thomas W., Propellant injection into a coaxial plasma accelerator, 20: 31363
KARRAS, Thomas W., Steady state operation of a two-stage pulsed coaxial plasma engine, 20: 31365
KASCHLUHN, F., Scattering of massive photons with vector-scalar coupling, 20: 32046
KASHIHIRA, Nobuyuki, Effect of uv irradiation on ^{124}Sb(III) in HCl solutions, 20: 31300
KATZ, Joseph, Biosynthesis of radioactive estriol-3-glucosiduronate by guinea pig liver homogenate, 20: 31312
KATZENSTEIN, Henry S., Nuclear electronics for aerospace applications, 20: 31609
KAUN, K.-H., Decay of ^{162}Tb and ^{163}Tb, 20: 32462
KAUN, K.-H., Decay $^{157}Eu(\beta^-)^{157}Gd$, 20: 32465
KAUN, K.-H., Decay of ^{163}Er, 20: 32466
KAUN, K.-H., Gamma transitions and energy levels in ^{161}Dy, 20: 32463
KAUN, K.-H., Levels in ^{157}Tb, 20: 32464
KAUSHAL, P. K., Effect of ^{60}Co gamma rays on commercial polypropylene films, 20: 31274
KAVANAGH, R. W., Electromagnetic decay of 1.7 and 2.43 Mev levels in ^9Be, 20: 32441
KAWAGUCHI, Masaaki, Possible determination of $\gamma\pi\omega$ coupling constant, 20: 32077
KAWAHARA, F. K., Radiological reclamation performance summary. I., 20: 31454 (USNRDL-TR-967)
KAWAI, T., S matrix with generalized potential and its asymptotic behavior, 20: 32140
KAWAKAMI, Akira, Excitation of the $J^P = 3/2^+$ decuplet and $J^P = 3/2^-$ octet in the neutrino reaction on the quark and the cloud models, 20: 32080
KAZANSKII, G. S., Programming operation of JINR synchrophasotron, 20: 31840
KEATING, F. Raymond Jr., Hyperfunctioning solitary thyroid nodule, 20: 31154
KEATON, P. W. Jr., Reaction study of $^{19}F(d,n)^{20}Ne$, 20: 32555
KEBARLE, P., Ions from alpha-particle irradiation of gases at high pressures, 20: 31270
KEEFER, D. R., Probe measurements in electrodeless discharge, 20: 32655
KEESE, H., Decontamination of radioactive contaminated water, 20: 31318

(BMwF-FBK-65-04)
KEISER, G., Autoradiographic studies of lymphoid cells in blood and bone marrow of irradiated dogs, 20: 31086
KEITH, R. L. G., Proportional counting soft beta particles from solid sources, 20: 31548
KEJRIWAL, P. K., Melting points of $REZn_2$ intermetallic compounds, 20: 31743
KELIN, A. V., Periods for verifying radiomeasuring instruments, 20: 31531
KELLER, C., Ternary and quaternary oxides of four, six, and seven valent Tc with alkali earths, 20: 31244
KELLER, W. E., Isothermal flow of liquid He II through narrow channels, 20: 32332
KELLER, W. E., Liquid helium as engineering fluid, 20: 32314
KELLEY, B. C., Irradiation facilities in ORNL bulk shielding reactor, 20: 32862 (ORNL-P-2160)
KELLEY, G. G., Apparent high-frequency stability of highly anisotropic plasma, 20: 32624
KELLY, B. T., Annealing of irradiation damage in graphite, 20: 31803
KELLY, F. H. C., Strontium-90 in the Australian environment, 20: 31403
KELLY, Hugh P., Perturbation theory of Brueckner and Goldstone applied to atoms, 20: 31944
KELSEY, C. A., Elastic scattering of polarized 4.4 Mev neutrons from ^{6}Li and ^{7}Li, 20: 32433
KEMP, Robert F., Solar wind simulation with the Pioneer spacecraft, 20: 31877
KEMPTER, C. P., Elastic properties of polycrystalline Sc, Re, Ru and Pt-21Ir, 20: 31748
KENDALL, Perry E., Cryogenic quality meter, 20: 32347
KENNA, B. T., Tabulation of cross sections, Q-values, and sensitivities for nuclear reactions of nuclides with 14-Mev neutrons, 20: 32380 (SC-RR-66-229)
KENNETT, T. J., Study of the $^{127}I(n,\gamma)^{128}I$ and $^{133}Cs(n,\gamma)^{134}Cs$ reactions, 20: 32422
KENNEY, Edward S., Noise analysis of nuclear reactors using gamma radiation, 20: 32786
KERLEE, D. D., Cosmic-ray heavy nuclei at geomagnetic latitude 42° north, 20: 31951
KERMAN, A. K., Hartree-Fock calculation for finite nuclei with nonlocal two-body potential, 20: 32496
KERN, B. D., Spin assignments in ^{35}Cl and ^{37}Cl via $(n,n'\gamma)$ reactions, 20: 32550
KERN, J., Decay of ^{140}Ba, 20: 32407
KERNS, Quentin A., Nanosecond pulse light source, 20: 31497
KERSLAKE, William R., Ion thrustor suitable for spacecraft station keeping and attitude control, 20: 31371
KERSLAKE, William R., Two-directional electron-bombardment ion thrustor, 20: 31380
KERST, Donald William, Method for trapping charged particles in magnetic field arrangement, 20: 32642
KERSTEN, J. A. H., Thorium cycle and homogeneous suspension reactor project, 20: 32829
KESLER, G., Antiproton-nuclei scattering at 3 Bev/c, 20: 32467
KESSLER, P., Calculation on the processes $e^-e^+ \to N\bar{N}^*$ and $e^-e^+ \to \bar{N}N^*$ for first four baryonic resonances, 20: 32018
KEVER, H., Steady nonlinear waves in warm collision-free plasma, 20: 32577 (NYO-1480-54)
KHACHKUZOVA, E. S., Treatment of radiation leukopenia by bone marrow autotransplantation, 20: 31134
KHADZHIMUKHAMEDOV, Kh. Kh., Coefficient of surface ionization of fast secondary particles, 20: 31913
KHALIKOV, D. R., Effects of γ-irradiation of cottonseeds on change of DNA in succeeding generations, 20: 31019
KHANNA, F., Charge-dependent effects in nucleon-nucleon $^{1}S_0$ scattering lengths by Dashen-Frautschi method, 20: 32030
KHANNA, M. P., Algebra of currents based upon the SU_{ws} group, 20: 32155
KHARE, S. P., Dissociation of hydrogen molecules by electron impact, 20: 31931
KHARKAR, D. P., "Dating" ground waters of ages younger than 1,000–1,500 years using natural ^{32}Si, 20: 31432
KHIMICH, I. V., Motion of singularities of theoretical field partial amplitude in complex λ plane, 20: 32189
KHIMICH, I. V., Structure of λ plane of partial amplitude in nonrelativistic problem with nonlocal potential, 20: 32188
KHOL, Frantisek, Personnel dosimetry in industrial defectoscopy, 20: 31464
KHOL'KINA, I. D., Radiation resistance of complex organophosphorus resins, 20: 31303
KHOVANOVICH, A. I., Time dependence of neutron yields from (Ra + MsTh)–Be source, 20: 32352
KHOVANSKII, V. D., Determination of kinematic properties of particles in spark chamber sparks, 20: 31570
KHRUSHCHOV, M. M., Dosage in gonad region in short-range x-ray therapy of angiomas in children, 20: 31156
KHVASTUNOV, M. S., Irradiation of combined emulsion and spark chamber system, 20: 31569
KIDD, J., Alternative interpretation of the enhancement observed at $M^{+}_{pp\pi^0}$ + 2.52 Bev/c^2, 20: 32040
KIEFER, Juergen, X-ray effects on barley roots. I., 20: 31052
KIGER, Eugene O., Operational summary of HWCTR, 10/61-12/64, 20: 32859 (DP-991)
KIKUCHI, R., Production of neutral pions from electron-proton collisions, 20: 32038
KILLEEN, John, Spatial distribution of protons from neutron decay trapped by geomagnetic field, 20: 32266
KIM, Hogil, Regenerative beam extraction for Berkeley 88-inch cyclotron, 20: 31827 (UCRL-16794)
KIMBALL, R. F., Repair of premutational damage, 20: 31040
KING, H. J., Electron-bombardment thrusters using liquid-mercury cathodes, 20: 31368
KING, H. J., Factors in life testing ion engines, 20: 31358
KING, H. J., Light-weight flight prototype ion engine system, 20: 31364
KING, N. M., External proton beam at Nimrod, 20: 31823 (RPP-N-5)
KING, P. V., Radiological safety handbook, 20: 31445 (N-65-12416)
KINGSTON, A. E., High-energy cross sections for electron excitations of excited hydrogen atoms changed by 2, 20: 31930
KINNEY, W. E., CDC-160A programs for processing data from a neutron time-of-flight cross-section experiment, 20: 32379 (ORNL-TM-1208)
KIRKPATRICK, M. E., Development of porous ionizer materials, 20: 31375
KIROUAC, G. J., Double differential scattering cross sections and scattering law for H_2O at 302°K, 20: 32350 (KAPL-M-6536)
KISER, S. R., Superheating and supercooling in superconducting transition of small In spheres, 20: 32331
KISLYI, P. S., Regularities of sintering alloys of zirconium diboride with molybdenum, 20: 31698
KISS, E., Vibration response of cantilevered cylinder surrounded by annular fluid, 20: 31328 (KAPL-M-6539)
KISS, Gabor, Calculation and evaluation of information obtainable from pulse shape discrimination, 20: 31535
KISSELL, F., Magnetic characteristics of $ZrNi_5$ and $HfNi_5$ and lanthanide–Ni compounds having Th_7Ni_3 structure, 20: 32699
KISTEMAKER, J., Amplification factors of particle multiplier for multiply charged noble gas ions, 20: 31926
KISTEMAKER, J., Ionization cross-section measurements for 0.6- to 20-kev electrons in atomic and molecular gases, 20: 31906
KITAGAWA, Michiharu, Optical absorptions of neutron-irradiated ZnS, 20: 31272
KITAKAZE, Keizo, Effect of lattice defects on critical current of hard superconducting Nb, 20: 31759
KITAZOE, Tetsuro, Large-angle elastic scattering at high energies, 20: 32086
KITRILAKIS, S. S., Transport parameters of Cs ions in Cs vapor, 20: 31972
KJELBERG, A., Radiochemical determination of ^{235}U abundances by activation analysis, 20: 31189
KLABES, R., Optical model analysis of elastic scattering on deuterons on ^{12}C, 20: 32454
KLABUNDE, C. E., Irradiation facilities in ORNL bulk shielding reactor, 20: 32862 (ORNL-P-2160)
KLAPISCH, R., Relative abundance and production cross sections of lithium isotopes, 20: 31205
KLAR, H., Approximate construction of scattering amplitude from Mandelstam representation and elastic unitarity, 20: 32095
KLARSFELD, S., Behavior of partial-wave amplitudes for large angular momenta in presence of Coulomb forces, 20: 32141
KLEBANOV, Yu. D., Cherenkov counter with controlled threshold, 20: 31572
KLEIMAN, Herbert, Isotope shifts of neutron-deficient mercury isotopes, 20: 32517
KLEIN, Abraham, Number-conserving approximations for theory of pairing interaction in nuclei. II., 20: 32494
KLEIN, Siegfried, Use of radioisotope to demonstrate fixation of electrons on electronegative gas, 20: 32223
KLEINE, W., Amplification factors of particle multiplier for multiply charged noble gas ions, 20: 31926
KLEINPETER, J. H., Use of plastics at Hanford, 20: 31267 (BNWL-SA-658)
KLEMENT, Alfred W. Jr., Bibliography on terrestrial and freshwater radioecology, 20: 30967 (TID-3910(Suppl.4))
KLEPFER, H. H., Prog. rpt. on Zr alloy, 4–6/65, 20: 31677 (GEAP-4840)
KLEPPER, L. Ya., Computers and programming in choice of conditions for radiation teletherapy, 20: 31155
KLIMEK, M., Radiosensitization of tumor cells by N-ethylmaleinimide, 20: 31130
KLIMENTOV, V. B., Physical stand for critical assembly of Institute of Physics at Ukrainian Academy of Sciences, 20: 32770

KLINE, D. E., Specific volume studies of γ-irradiated polytetrafluoroethylene from 50 to 150°C, 20: 31284
KLINE, J. R., Fractionation of copper in neutron-activated soils, 20: 31325
KLOCHIKHIN, A. A., Scattering of neutrons by ferromagnets in region of ferroacoustic resonance, 20: 32722
KNAPP, D. G., Mathematical model of geomagnetic field for 1965, 20: 32255
KNASEL, T. M., Factors affecting resolution of lead scintillator sandwich shower counters, 20: 31587
KNAUER, W., Light-weight flight prototype ion engine system, 20: 31364
KNECHT, Othmar, Heterogeneous thermal nuclear reactor and method of operation, 20: 32789
KNECHTLI, R. C., Electron-bombardment thrusters using liquid-mercury cathodes, 20: 31368
KNIGHT, G. B., Analysis of external radiation exposures in 1965, 20: 31439 (AECL-2540)
KNIPPER, Albert, Half life of the 570-kev excited level of ^{207}Pb, 20: 32401
KNISPEL, Gerard, Properties of cadmium telluride diodes and application to detection of nuclear particles, 20: 31523
KNOEPPEL, H., Experimental techniques, applications, and theory of field ion mass spectrometry, 20: 31199
KNOPP, C. F., Radiation of O and N and thermal conductivity of N up to 15,000°K, 20: 32240
KNOPP, Jacky, Commercialization studies on wood-plastic combinations process, 20: 31625 (NYO-3569-1)
KNOWLES, J. W., Methods of applying Compton scattered neutron capture radiation to nuclear photo-excitation, 20: 32369 (AECL-2535)
KOBAYASHI, Tetsuro, Non-zero elastic amplitude real part effects and nucleon recoil effects on relationship between elastic diffraction scattering and inelastic collisions, 20: 32072
KOBAYASHI, Tsunehiro, Inner symmetry in baryon structures and leptonic decays, 20: 32176
KOBAYASHI, Ugoro, Fallout radioactivity due to underground nuclear test of USSR, Jan. 15, 1965, 20: 31405
KOBAYASHI, Ugoro, Giant particles contained in fallout. V., 20: 31412
KOBAYASHI, Ugoro, Radioactive rain, snow, and atmospheric contamination observed in Nagaoka City, Japan. II., 20: 31411
KOBAYASHI, Y., Production of neutral pions from electron-proton collisions, 20: 32038
KOBZENKO, G. F., Melting points of V and Nb of high purity, 20: 31721 (AD-630971)
KOCHENKOV, A. S., Effect of Be-reflector duty factor on thermal neutron flux in horizontal beams, 20: 32765 (IAE-957)
KOCHERZHINSKII, Yu. A., Melting points of V and Nb of high purity, 20: 31721 (AD-630971)
KOCHETKOV, N. K., Radiation chemistry of carbohydrates. V., 20: 31304
KODA, Yoshio, Separation of ^{32}P from a ^{32}P–^{35}S mixture, 20: 31309
KODYAKOV, V. M., Device for measuring charged particle beam parameters, 20: 31838
KOEHLER, P. F. M., Proton-proton bremsstrahlung at 204 Mev, 20: 32062
KOEHN, Diederich, Measurement of secondary gamma spectrum from 0.2 to 2 Bev in upper atmosphere, 20: 32283
KOEMPF, R., Two states in ^{21}Ne at 2.80-Mev excitation energy, 20: 32476
KOEPPENDOERFER, W., Induction coil as measuring element in fast current intensity gas discharge, 20: 32571 (IPP-1/2)
KOFOID, Melvin J., Efficient utilization of an r-f power oscillator for producing low-pressure plasmas, 20: 32570 (D-1-82-0522)
KOH, C. J., Physical state vector-space representations of noncompact groups, 20: 31663
KOHAUPT, R. D., Radiative corrections to e-p scattering for angular and energy coincidence experiments, 20: 32092
KOHLMANN, L., New alpha-decay barrier penetrabilities with Igo potential: even-mass nuclei, 20: 32399
KOHMURA, Toshitoke, Dibaryon states and F/D ratio, 20: 32170
KOHN, W., Self-consistent equations including exchange and correlation effects, 20: 31946
KOIRO, M. A., Treatment of radiation leukopenia by bone marrow autotransplantation, 20: 31134
KOJOIAN, G., Antiproton annihilation at rest in deuterium, 20: 32015
KOKKEDEE, J. J. J., Antiproton-proton elastic scattering at high energies in uncorrelated jet model, 20: 32028
KOKOVIKHIN, V. F., Time dependence dof neutron yields from (Ra + MsTh)–Be source, 20: 32352
KOLASINSKI, W. A., Proton spin flip in the reaction ^{60}Ni(p,p')^{60*}Ni (1.33) at 10.5 and 14.0 Mev, 20: 32557
KOLESNIK, V. G., Irradiation of combined emulsion and spark chamber system, 20: 31569
KOLESNIKOV, L. N., High-heat-resistance plastic scintillators, 20: 31262
KOLLER, E. L., Analysis of K and $\eta \to 3\pi$ decay spectra, 20: 32010
KOLLER, P. C., Inhibition of radiation-induced leukemia by injection of haematopoietic tissue, 20: 31127
KOLOTYRKIN, Yu. M., Pitting corrosion of zirconium in perchlorate solutions, 20: 31687
KOMATA, Toronosuke, Effect of lattice defects on critical current of hard superconducting Nb, 20: 31759
KONCHINSKII, G. A., Physical stand for critical assembly of Institute of Physics at Ukrainian Academy of Sciences, 20: 32770
KONDAIAH, E., Angular distribution of ^{19}F(n,α)^{16}N reaction at E_n = 4.7 Mev, 20: 32434
KONDAIAH, E., Efficiencies for well-type NaI(Tl) crystal for cylindrical sources, 20: 31553
KONDRASHEV, Yu. D., Ternary compounds in Be–B–C system, 20: 31257
KONDRAT'EV, L. N., Conversion electrons associated with alpha decay of ^{241}Am and level scheme of ^{237}Np, 20: 32375 (ITEF-351)
KONISHI, Teruaki, Nuclear charge distribution of calcium isotopes, 20: 32534
KONNOV, V. A., Strontium-90 in waters of Pacific Ocean. III., 20: 31414
KONO, Keisuke, Three-dimensional photoelastic investigation of stresses in reactor pressure vessels, 20: 32751
KONONOV, V. N., Producing starting pulses in time-of-flight nanosecond, 20: 31579
KONOROVA, E. A., Ionization currents in diamonds during irradiation with 500 to 1000-kev electrons, 20: 32725
KONRADI, Andrei, Electron and proton fluxes in tail of the magnetosphere, 20: 32252
KOOI, J., Application of extraction chromatography in processing of irradiated americium, 20: 31323
KOOT, C. J., Effect of O on impairment of proliferative capacity of human cells by radiations LET, 20: 31123
KOPECKY, V., Incidence of electromagnetic waves on plasma-vacuum boundary, 20: 32588
KOPP, P. M., Radiation protection studies with polyethylene, 20: 31279
KOPPE, V. T., Emission spectra of rarefied molecular gases excited by fast electrons, 20: 31921
KORENBLIT, I. Ya., Scattering of neutrons by ferromagnets in region of ferroacoustic resonance, 20: 32722
KORKISCH, J., Ion exchange separation of U, Th, and lanthanides in mixed and non-aqueous solvents, 20: 31195
KOROLEV, G. K., Kinetics of accumulation and elimination of radioactive Cs from respiratory organs, 20: 31111
KOROLEVA, V. S., Critical thermal fluxes and heat transfer of boiling K in tubes, 20: 31347
KOROVKINA, A. V., Effects of soil fractions on uptake of ^{90}Sr into plants, 20: 30985
KORSHAKEVICH, I. I., Vaporization of material from surface of probe in an arc, 20: 32593
KORYAKIN, Yu. I., Technical and economic aspects of reactors for desalination of water and electric power generation, 20: 32846
KOSHEL, R. D., Neutron single-particle levels of ^{91}Zr, 20: 32552
KOSHEL, Richard D., Nucleon energy levels in nonlocal potential, 20: 32566
KOSHI, Paul T., Soil-moisture measurement by the neutron method in rocky wildland soils, 20: 31435
KOSMKAREV, D. G., Correcting system for forced oscillations in accelerator with reverse coupling, 20: 31839
KOSKINEN, M. F., Plasma physics of thermionic converters, 20: 31971
KOSMAL, V., Increasing power of Polish VVR-S reactor up to 10 Mwt, 20: 32879
KOTANI, Tsuneyuki, Analytic property of impact parameter amplitude, 20: 32180
KOTANI, Tsuneyuki, Impact parameter formalism. III., 20: 32174
KOTEL'NIKOVA, G. V., Time-of-flight neutron spectrometer, 20: 31566
KOUTZ, Stanley Lee, Nuclear reactor fuel element, 20: 32793
KOVACIC, E. C., Carbon in primary Na system of Enrico Fermi Atomic Power Plant, 20: 32809 (TID-23101)
KOVAL', A. G., Emission spectra of rarefied molecular gases excited by fast electrons, 20: 31921
KOVALEV, E. E., Shielding calculations for cylindrical sources, 20: 32678
KOVAR, D. G., Light-weight flight prototype ion engine system, 20: 31364
KOWALSKA, Krystyna, Calculations for 10-Mw EWA reactor with WWRM-type tubular fuel, 20: 32880
KOWALSKA, Krystyna, Neutron transport in multiplying slab surrounded by an infinite reflector, 20: 32782
KOZHUKHOV, I. V., Plasma gun for producing high electron-current peaks, 20: 31486
KOZLOV, S. F., Ionization currents in diamonds during irradiation with 500 to 1000-kev electrons, 20: 32725
KRAFTMAKHER, Yu. A., Vacancy formation in Zirconium, 20: 32729
KRAMER, D., Resistivity changes in niobium during straining and strain aging, 20: 31742
KRAMER, D., Two-dimensional spinor fields in Riemannian space, 20: 32109
KRAMP, K., Angular distribution of polarization of recoil proton from photoproduction of neutral pions on H at photon energy of 360 Mev. II., 20: 32097

KRAMP, K., Polarization of recoil proton from photoproduction of neutral pions on H in region of first resonance. I., 20: 32096
KRANZ, I. H., SNAP-10A electrically actuated band release device development, 20: 32852 (NAA-SR-Memo-11454)
KRASIN, A. K., Starting of critical assembly in Nuclear Power Engineering Institute of Belorussian Academy of Sciences, 20: 32769
KRASNOPEVTSEV, Yu. V., Distribution of nuclear test explosion fallout over continents and oceans, 20: 31421
KRASOVSKAYA, A. A., Phase diagram of the HfC–Mo system, 20: 31729
KRASSOVSKII, V. I., Atomic hydrogen and helium in airglow, 20: 32289
KRAUSE, F., Calculation of average Lorentz field strength vxB for electrically conducting medium in turbulent motion influenced by Coriolis forces, 20: 32235
KRAUT, Edgar A., Cartesian tensor form of magnetohydrodynamic wave equation, 20: 32229
KRAWCZYNSKI, Stefan, Treatment of waste water at the Karlsruhe Atomic Research Center. I, 20: 32881
KRAWCZYNSKI, Stefan, Treatment of waste water at the Karlsruhe Atomic Research Center. II, 20: 32882
KRAVEC, Roman, Radial density and temperature profiles at ion cyclotron wave resonance point, 20: 32662
KRETSCH, Hans Walter, Electric current generation by means of thermionic energy converters, 20: 31980
KREY, R. U., Radiation of O and N and thermal conductivity of N up to 15,000°K, 20: 32240
KRIENKE, O. K. Jr., Cosmic-ray heavy nuclei at geomagnetic latitude 42° north, 20: 31951
KRIESE, Siegfried, Efficiency of energy transformation in power reactors, 20: 32813
KRIKSUNOV, V. M., Periods for verifying radiomeasuring instruments, 20: 31531
KRIPYAKEVICH, P. I., Crystal structure of $HoAl_3$ and $DyAl_3$ compounds, 20: 31728
KRMPOTIC, F., Induced terms and partial conservation of axial vector current in β decay, 20: 32479
KRONAST, B., Measurements of ion and electron temperature in theta-pinch plasma, 20: 32621
KRORI, K. D., Generalized Dirac theory, 20: 32119
KRUEGER, H., Approximate construction of scattering amplitude from Mandelstam representation and elastic unitarity, 20: 32095
KRUEGER, R. H., Titrimetric determination of organic acids by xenon trioxide oxidation, 20: 31196
KRUGER, P. Gerald, Superconducting quadrupole lens, 20: 31815 (BNL-10144)
KRYPIAKEWYTSCH, P. I., Crystal structure of $Ce_3Ni_6Si_2$ and related compounds, 20: 31253
KRZYCKI, A., EWA reactor power ^{16}N activity monitoring, 20: 32870
KU, Lily Lim, Mitochondria: increase in oxidative capacity and quantitative recovery after massive doses of radiation, 20: 31633
KUBOWSKI, J., ANNA startup, operation, and characteristics, 20: 32872
KUBOWSKI, J., Progress in reactor kinetics at Swierk, 20: 32781
KUCHERYAEV, V. A., Shielding properties of iron–serpentine concrete, 20: 32677
KUDRYASHOV, L. I., Radiation chemistry of carbohydrates. V., 20: 31304
KUEHN, B., Optical model analysis of elastic scattering on deuterons on ^{12}C, 20: 32454
KUEHNER, J. A., Spin and parity assignments in ^{24}Mg, 20: 32556
KUENDIG, Walter, Properties of supported small α-Fe_2O_3 particles determined with Moessbauer effect, 20: 31779
KUIPER, P., Light attenuation in scintillation counters, 20: 31546
KULABUKHOV, Yu. S., Time-of-flight neutron spectrometer, 20: 31566
KULCINSKI, Gerald L., Miniature diamond ultrahigh pressure cell adapted for in-reactor irradiation studies, 20: 32754
KULIK, I. O., Magnetic moment of superconducting ellipsoid in mixed state, 20: 32321
KULKARNI, V. G., Lifetimes of positronium in polystyrene irradiated by thermal neutrons, 20: 32704
KUNDEL, Harold L., Edema: delayed complication of total-body 32-Mev proton irradiation, 20: 31098
KUNDEL, Harold L., Effects of whole-body 32-Mev proton irradiations on primates, 20: 31097
KUNDEL, Harold L., Effects of 138-Mev protons on primates, 20: 31101
KUNDEL, Harold L., Effect of high-energy proton irradiation on cardiovascular system of Rhesus monkey, 20: 31104
KUNDEL, Harold L., RBE of 138-Mev protons as compared to ^{60}Co gamma radiation, 20: 31102
KUO, An-hsi, Effect of gamma radiation on seeds in second generation, 20: 31113
KUO, Chieh-yen, Effect of x-irradiation on Escherichia coli B. I., 20: 31023
KUO, Chieh-yen, Effect of x-irradiation on E. coli B. II., 20: 31144
KURDIANI, N. I., Optical absorption in irradiated gallium arsenide, 20: 31617
KURODA, K., Construction of a polarized beam with both spin orientations at the CERN synchrocyclotron, 20: 31835
KURODA, K., Polarization and spin correlation parameter measurements in 600-Mev proton-proton scattering, 20: 32016
KURODA, P. K., Decay constant and mass-yield curve for spontaneous fission of ^{238}U, 20: 32521
KURSUNOGLU, Behram, Boson resonances, 20: 32089
KURSUNOGLU, Behram, Conferences on symmetry principles at high energy, 3rd Coral Gables, 1/66, 20: 32195
KURSUNOGLU, Behram, Space-time symmetries, space-time U(3,3) and magnetic charge, 20: 32200
KUZENKOVA, M. A., Regularities of sintering alloys of zirconium diboride with molybdenum, 20: 31698
KUZIN, A. M., Quantitative regularities of quinone formation in gamma-irradiated plant tissue, 20: 31001
KUZ'MA, Yu. B., X-ray structural analysis of some Zr–Fe and Zr–Co alloys, 20: 31727
KUZNETSOV, V. G., Optimum ratio of neutron and gamma dose behind reactor shielding, 20: 32676
KUZNETSOVA, N. N., Effect of physiologically active compounds and radiation on metabolism in wheat, 20: 31002
KUZNETSOVA, N. N., Effects of spaceflight factors on wheat seeds, 20: 31058
KVASIL, B., Superconductive material, 20: 32339
KVIST, Arnold, Electrical conductivity of solid and molten $^6Li_2SO_4$ and $^7Li_2SO_4$, 20: 31255
KWAK, N., Production of $Y_1^\dagger$ (1385) and a possible I = 0 member of an octet at 1660 Mev, 20: 32034
KYCIA, T. F., New structure in the K^+-p and K^+-d total cross sections between 0.9 and 2.4 Bev/c, 20: 32067
KYLE, H. L., Excitation of H atoms by fast protons, 20: 31933
KYLIN, Anders, Uptake and loss of Na^+, Rb^+, and Cs^+ in relation to active mechanism for extrusion of Na^+ in Scenedesmus, 20: 30994

L

LABNO, L., Measurements of frequency response of neutron-sensitive current ion chambers, 20: 31597
LACOMBE, P., Electron microscope observations on thin films of zirconia obtained by oxidation of Zr, 20: 31755
LAFOUCRIERE, J., Graphical methods of summation and integration of spherical harmonics, 20: 32437
LAGERSTEDT, H. B., Determination of radioactivity in agar blocks by liquid scintillation techniques, 20: 31179
LAGU, R. G., Lifetimes of positronium in polystyrene irradiated by thermal neutrons, 20: 32704
LAIDLER, J. B., Neptunium chloro-complexes, 20: 31235
LAL, D., "Dating" ground waters of ages younger than 1,000–1,500 years using natural ^{32}Si, 20: 31432
LAL, D., Measurement of tritium activity in natural waters. I., 20: 31310
LAMARCHE, Reginald, Nuclear energy in Belgium, 20: 32890
LAMB, R. C., Search for Y = 2, S = 0 resonances, 20: 32066
LAMBE, J., Macroscopic quantum interference in superconductors, 20: 32344
LANCON, Rene, Properties of cadmium telluride diodes and application to detection of nuclear particles, 20: 31523
LANDER, R., Search for Y = 2, S = 0 resonances, 20: 32066
LANDROCK, K., Use of uniform half lives of important radionuclides, 20: 32421
LANE, J. A., Economic incentive for Th reactor development, 20: 32832
LANGE, F., Criterion for stability against flux jumping in high-field high-current superconductors, 20: 32320
LANGE, F., Temperature dependence of magnetic fields trapped in Nb_3Sn hollow cylinders, 20: 32316
LANGEVIN-JOLIOT, H., Experimental study of reaction $D(p,\gamma)^3He$ at 156 Mev, 20: 32486
LANGLOIS, Denise, Extraction by pealing of beam of heavy ions accelerated in cyclotron with starred field, 20: 31828
LANGSTON, R., Determination of radioactivity in agar blocks by liquid scintillation techniques, 20: 31179
LANKESTER, J., Treatment of patients with metastasized mammary carcinomas by radioactive Y, 20: 31153
LA ROCCA, J. P., Thermoluminescent dosimeters for environmental monitoring, 20: 31526
LARSON, H. V., Treatment and evaluation of internal deposition from Pu wound, 20: 31030 (BNWL-SA-39)
LARSON, J. D., Natural parity states of ^{16}O at 11.09 and 12.05 Mev, 20: 32502
LASER, M., Recoil brominations of aromatic compounds, 20: 31296
LASHER, D. R., Fast sensitive noninterrupting monitor for nanosecond pulsed beams, 20: 31846
LATEK, S., Progress in reactor kinetics at Swierk, 20: 32781

LAUER, J. E., High-energy cross sections for electron excitations of excited hydrogen atoms changed by 2, 20: 31930

LAURENCE, G. C., Control of radioactive pollution, 20: 31457

LAURENT, Noel, Nuclear reactors having fuel element channel retaining pawl assembly, 20: 32756

LAURIE, Jean, Cellular control systems and radiosensitivity, 20: 31064

LAURITZEN, T. A., Plutonium and fission product redistribution in mixed oxide fuels, 20: 31084

LAVAL, Guy, Calculation of statistical entropy of plasma during equilibrium, 20: 32583

LAVROV, V. P., Secondary emission coefficients for KBr single crystal bombarded with K ions, 20: 31938

LAWSON, J. D., Guided surface waves and radiation from charges moving in curved paths, 20: 31992

LAZANYI, Andrei, Effect of sulphoguanidine and p-nitrobenzoic acid on chromosome breakage-reunion process by irradiation, 20: 31124

LAZAR, N. H., Apparent high-frequency stability of highly anisotropic plasma, 20: 32624

LEADER, E., Present phenomenological status of the Regge pole theory, 20: 32185

LEBEDEVA, L. S., Determining structure of sintered materials by ionic bombardment, 20: 31765

LEE, C. Y., Effects of gamma radiation on freeze-dehydrated apples (Pyrus malus), 20: 31631

LEE, J., Experimental study of reaction $D(p,\gamma)^3He$ at 156 Mev, 20: 32486

LEE, J. S., Microbial flora of irradiated Dungeness crabmeat and Pacific oysters, 20: 31626

LEE, L. L. Jr., Dependence of angular distribution of the (d,p) reaction on total angular-momentum transfer. II., 20: 32512

LEE, L. L. Jr., J dependence in the $(^3He,\alpha)$ reaction, 20: 32508

LEE, Robert E., Hyperfunctioning solitary thyroid nodule, 20: 31154

LEE, T. J., Average level width of compound nucleus, 20: 32424

LEGG, J. C., Test of distorted-wave stripping theory by $^{52}Cr(d,p)^{53}Cr$, 20: 32459

LE GUEN, Y., Construction of a polarized beam with both spin orientations at the CERN synchrocyclotron, 20: 31835

LEHMAN, G. W., Macroscopic quantization in superconducting films, 20: 32324

LEHRLE, R. S., Charge transfer and atom transfer in ion-molecule interactions studied by time-of-flight mass spectrometer, 20: 31224

LEIGHTON, R. B., Magnetic fields in solar photosphere, 20: 31892

LEISTNER, Bernhard, Gundremmingen nuclear power plant, 20: 32810

LEJEUNE, J. M., Fuel element fabrication development in Belgium, 20: 31692

LEKO, N. A., Absorption centers in glasses of simple compositions formed at low temperature, 20: 32733

LEKSIN, G. A., Determination of kinematic properties of particles in spark chamber sparks, 20: 31570

LELIEVRE, P., Effect of cystamine on respiration, oxidative phosphorylation, and ultrastructure of rat mitochondria, 20: 30984

LELOGEAIS, G., Low-temperature electron irradiation of metals, 20: 32319

LEMAITRE, Rene, Liquid moderator nuclear reactors, 20: 32759

LENCHEK, A. M., Origin and loss of inner zone protons, 20: 32243 (AD-634704)

LENGEMANN, F. W., Predicting total projected intake of radioiodine from milk by man. I., 20: 30980

LENGEMANN, F. W., Predicting total projected intake of radioiodine from milk by man. II., 20: 30981

LENZ, G., Isobaric analog states of doubly magic ^{208}Pb, 20: 32478

LEONARDI, R., Electromagnetic interactions and T violation, 20: 32020

LEONG, G. F., Injury accumulation in sheep during protracted gamma radiation, 20: 31026 (AD-633606)

LEONTIC, B. A., New structure in the K^+-p and K^+-d total cross sections between 0.9 and 2.4 Bev/c, 20: 32067

LEONTOVICH, K. A., Microwave interferometers with amplitude modulation, 20: 31490

LEPIK, U., Deflections of cylindrical shells under axial tension and external pressure, 20: 31335

LERCHE, I., Transverse waves in a relativistic plasma, 20: 32606

LERCHE, I., Validity of hydromagnetic approach in discussing instability of magnetospheric boundary, 20: 32254

LERTORA, M., Experimental observations on behavior of serum cholesterol after irradiation, 20: 31006

LEUNISSEN, R. L. A., Determination of ^{14}C-lactate adapted to liquid scintillation counting, 20: 31178

LEVESQUE, R. J. A., Spin and parity assignments in ^{24}Mg, 20: 32556

LEVIN, F. S., Target-excitation effects in stripping reactions, 20: 32497

LEVIN, I. K., Fuel breeding intermediate energy U-Th water moderated reactor, 20: 32831

LEVINE, D. A., Tissue-equivalent ionization chamber for in-phantom dosimetry, 20: 31524

LEVINE, Donald, Preparation of toluene diisocyanate-^{14}C, 20: 31266

LEVITZ, Mortimer, Biosynthesis of radioactive estriol-3-glucosiduronate by guinea pig liver homogenate, 20: 31312

LEWIS, A. B., Prog. rpt. on effects of neutron irradiation on resistivity of binary alloys, 6/66, 20: 31786 (ORO-2891-5)

LEWIS, Francis H. Jr., Excitation of the spin-isospin giant resonance by 180 deg inelastic electron scattering, 20: 32569

LEWIS, H. R. Jr., Computation of electrostatic and rapidly pulsed magnetic fields, 20: 32596

LEWIS, Jordan D., Expansion theorem for linearized Fokker-Planck equations, 20: 32643

LEWIS, Richard C., SPENCER: FORTRAN program to approximately reconstitute a one-dimensional function from finite number of its moments, 20: 31658 (NAA-SR-Memo-11653)

LI, Chun-ying, Effect of x-irradiation on Escherichia coli B. I., 20: 31023

LI, Chun-ying, Effect of x-irradiation on E. coli B. II., 20: 31144

LI, K. C., Magnetohydrodynamic channel entrance flow with parabolic velocity at entry, 20: 32226

LI, K. K., New structure in the K^+-p and K^+-d total cross sections between 0.9 and 2.4 Bev/c, 20: 32067

LI, Yu, Effect of radiation on metabolism and respiration of seedlings, 20: 31115

LIBBY, Willard F., Isotope chronology and recorded history, 20: 31429

LIBIKOVA, N. I., Effect of cystamine and S-β-aminoethylisothiuronium on activity of DNase II in spleen and thymus of irradiated rats, 20: 31143

LICHT, W. R., Specific volume studies of γ-irradiated polytetrafluoroethylene from 50 to 150°C, 20: 31284

LICHTBLAU, H., Energy spectra of photoprotons from Al, S, and Si, 20: 32394

LIEB, D., Transport parameters of Cs ions in Cs vapor, 20: 31972

LIEBERMAN, Joseph A., Safety considerations in use of nuclear devices in space, 20: 32855

LIEBERMANN, R. W., Radiation of O and N and thermal conductivity of N up to 15,000°K, 20: 32240

LIESER, K. H., Preparation of ^{36}Cl-labelled iodine monochloride by isotope exchange, 20: 31246

LILLEGRAVEN, A., Cesium-137 and ^{90}Sr in Norwegian milk, 1960-1964, 20: 31465

LIM, Mahajick, Vapor pressure and heat of sublimation of CeF_3, 20: 31238

LIN, R. P., Observations on propagation of solar-flare electrons in interplanetary space, 20: 31869

LINCOLN, J. Virginia, Geomagnetic and solar data, 20: 32259

LINDER, Bruno, Cross sections and isomer ratios for $^{88}Sr(^3He,p)/^{90m,90g}Y$ reaction, 20: 32430

LINDLEY, B. C., Prospects for closed-cycle MPD power generation, 20: 31977

LINDLEY, Bryan Charles, Improvements in apparatus for direct generation of electricity, 20: 31979

LINDQUIST, R. H., Properties of supported small α-Fe_2O_3 particles determined with Moessbauer effect, 20: 31779

LINDQUIST, Richard W., Relativistic transport theory, 20: 32296

LINDSAY, Ian R., Edema: delayed complication of total-body 32-Mev proton irradiation, 20: 31098

LINDSAY, Ian R., Effects of whole-body 32-Mev proton irradiations on primates, 20: 31097

LINDSAY, Ian R., Effects of 55-Mev protons on primates, 20: 31099

LINDSAY, Ian R., Effects of 138-Mev protons on primates, 20: 31101

LINDSAY, Ian R., Effects of 400-Mev protons on primates, 20: 31103

LINDSAY, Ian R., Estimate of biological effects of space proton environment, 20: 31106

LINDSAY, Ian R., Kinetics of recuperation following 55-Mev proton irradiation, 20: 31100

LINDSAY, Ian R., Protons and space travel, 20: 31095

LINDSAY, Ian R., RBE of 138-Mev protons as compared to ^{60}Co gamma radiation, 20: 31102

LINDSAY, Richard H., Angular-momentum effects in the $^{24}Mg(\alpha,^7Be)$ and $^{27}Al(p,^7Be)$ reactions at 35–65 Mev, 20: 32507

LING, S. C., Geoelectric field: its existence, cause, and effect, 20: 32287

LINNEY, A. D., Flux of the cosmic-ray hydrogen and helium nuclei at Kiruna, Sweden, 20: 31953

LIPINSKI, Andrzej, Apparatus for investigation of directional correlation of γ-rays emitted in cascade, 20: 31595

LIPKIN, Harry J., Quarks, symmetries, symmetry breaking, and the Johnson-Treiman relations, 20: 32202

LISETAKAYA, M. N., Electric discharge in plastic in uniform field, 20: 32692

LIU, Chao, Biological variations in agricultural seeds during storage after gamma irradiation, 20: 31024

LIU, Chao, Effect of gamma radiation on seeds in second generation, 20: 31113

LIU, Ching-hsiang, Effect of gamma radiation on seeds in second generation, 20: 31113

LIU, Chin-t'ao, Biological variations in agricultural seeds during storage after gamma irradiation, 20: 31024

LIU, Chin-t'ao, Effect of gamma radiation on seeds in second generation,

20: 31113
LIU, T. C., Control of absorption cross section for nuclear rocket, 20: 32851 (N-65-30544)
LIU, Ts'un-te, Effect of radiation on metabolism and respiration of seedlings, 20: 31115
LIU, Yung-ho, Adsorption of ^{90}Sr by aged horse manure, 20: 31252
LIVANOVA, L. D., EPR of Gd^{3+} in Y and La double molybdates, 20: 32728
LIVINGSTON, J. D., Flux pinning by superconducting precipitates, 20: 32313
LIVINGSTON, J. D., Making superconductors hard, 20: 31750
LLOYD, M. H., Sol-gel process development and microsphere preparation, 20: 31689 (ORNL-P-2159)
LOCKE, E., Experiments with magnetohydrodynamically supported shock layers, 20: 32217 (N-65-33713)
LOEW, Gregory A., Phasing of multisection linear accelerator, 20: 31852
LOEWDIN, Per-Olov, Quantum theory of time-dependent phenomena treated by evolution operator technique, 20: 32293 (N-66-17084)
LOEWENSTEIN, W. B., Safety analysis for ZPR-9 facility, 20: 32858 (ANL-7166)
LOFERSKI, J. J., Li-doped, radiation, resistant silicon solar cells, 20: 31614
LOGINOV, A. A., Technical and economic aspects of reactors for desalination of water and electric power generation, 20: 32846
LOMBARD, R. J., Electromagnetic transition probabilities in single closed shell nuclei, 20: 32426
LOMER, W. M., Neutron spectroscopy of solids. I., 20: 32687
LOMON, E. L., Boundary-condition model for P_{33} pion-nucleon state, 20: 32023
LOMSADZE, Yu. M., Relation between nonrelativistic partial wave amplitude and trajectories of its poles in λ plane, 20: 32187
LONCHAMP, J.-P., Lithium-8 emission in 5.0-Bev/c K^--meson interactions in nuclear emulsion, 20: 32469
LONGEQUEUE, Jean-Pierre, Reaction $^{11}B(p,\alpha\alpha)^4He$ at 163 kev, 20: 32402
LORD, R. S., Operating characteristics of ORIC beam extraction system, 20: 31821 (ORNL-P-2239)
LORENTZ, R. E., Fabrication of high strength, heavy-wall pressure vessels, 20: 31703
LORET, M., Levels in ^{60}Ni and ^{62}Ni at high excitation energies, 20: 32490
LOTTS, A. L., Impact of Kilorod operational experience on design of fabrication plants for ^{233}U–Th fuels, 20: 31690 (ORNL-P-2176)
LOTTS, A. L., Refabrication technology for Th–^{233}U fuel cycle, 20: 31701
LOUDE, J.-F., Excitation of levels of ^{12}C by inelastic scattering of 14.1-Mev neutrons, 20: 32408
LOURENS, W., Beta-gamma circular polarization in decay of ^{48}Sc, 20: 32457
LOUTIT, John F., Tissue grafting and radiation, 20: 31120
LOVCHIKOVA, G. N., Time-of-flight neutron spectrometer, 20: 31566
LOVE, C. M., Physical, chemical and biological data from northeast Pacific Ocean: Columbia River effluent area, 1–10/62. Vol. I., 20: 31448 (RLO-1725-15)
LOVE, C. M., Physical, chemical, and biological data from northeast Pacific Ocean: Columbia River effluent area, 1–10/62. Vol. II., 20: 31449 (RLO-1725-16)
LOVE, C. M., Physical, chemical, and biological data from northeast Pacific Ocean: Columbia River effluent area, 1–10/62. Vol. III., 20: 31450 (RLO-1725-17)
LOVE, C. M., Physical, chemical, and biological data from northeast Pacific Oceans: Columbia River effluent area, 1–10/62. Vol. IV., 20: 31451 (RLO-1725-18)
LOVE, C. M., Physical, chemical, and biological data from northeast Pacific Ocean: Columbia River effluent area, 1–10/62. Vol. V., 20: 31452 (RLO-1725-19)
LOVELL, L., Observation and properties of neutral A_2 meson, 20: 32064
LOWDER, R. S., Anomalous electron diffusion and ion acceleration in low-density plasma, 20: 32612
LOWE, J., Asymmetries in elastic and inelastic scattering of polarized protons from C and Si, 20: 32440
LOWE, L. F., Damage production in electron-irradiated palladium, 20: 31805
LU, C. C., Masses and excited states of ^{24}Al and ^{28}P, 20: 32473
LUCASSON, A., Low-temperature electron irradiation of metals, 20: 32319
LUCASSON, P., Low-temperature electron irradiation of metals, 20: 32319
LUDLOW, I. K., Symmetry of color center in magnesium oxide, 20: 32717
LUDWIG, G. H., Mev phenomena related to solar wind. II., 20: 31886
LUEST, Reimer, Interaction of solar wind with comets, 20: 31896
LUKANTSEVER, Yu. L., Creation and destruction of color centers in alkali-halide crystals, 20: 32691
LUKANTSEVER, Yu. L., Destruction of color centers and recombination luminescence of crystal phosphor NaCl–Ag. I., 20: 32693
LUKANTSEVER, Yu. L., Destruction of color centers and recombination luminescence of NaCl–Ag: Ca crystal phosphor. II., 20: 32694
LUNDBY, A., New structure in the K^+-p and K^+-d total cross sections between 0.9 and 2.4 Bev/c, 20: 32067
LUNDGREN, O., Washout of intraarterially injected ^{85}Kr from intestine of cat, 20: 30979
LUNDIN, Charles E., Equilibrium phase diagram, Nb(Cb)–Al, 20: 31769
LUNDY, R. A., Search for Y = 2, S = 0 resonances, 20: 32066
LUO, H. L., Superconducting transition temperatures of Hg–alkaline earth metal compounds, 20: 31757
LUSHNIKOV, A. A., Photoabsorption of nuclei in theory of Fermi-liquids, 20: 32539
LUTIKOV, V. K., Pulsed neutron generator, 20: 32358
LYNCH, C. T., Metastable transitions of zirconium oxide obtained from decomposition of alkoxides, 20: 31736
LYNEN, U., Experimental test of triton form factor by Coulomb pickup on ^{208}Pb, 20: 32485
LYNN, Y. M., Magnetohydrodynamic shock relations in nonaligned flows, 20: 32218 (NYO-1480-29)
LYON, E. F., Explorer-18 plasma measurements, 20: 32280
LYON, J. F., Apparent high-frequency stability of highly anisotropic plasma, 20: 32624
LYON, W. L., Effect of stoichiometry on properties of mixed oxide U–Pu fuel, 20: 31674
LYONS, L., Current experimental status of baryon exchange, 20: 32027

M

MA, Hsiu-chen, Velocity of turbulent flow of water through a bundle of hollow rods, 20: 31350
MACDONALD, R. N., Calculating space dependent reactor transfer functions using statics techniques, 20: 32780
MACDONALD, R. N., Prog. rpt. on kinetics parameters of highly enriched D_2O reactor, final, 12/65–12/66, 20: 32863 (TID-23037)
MACHIDA, Shigeru, Inner symmetry in baryon structures and leptonic decays, 20: 32176
MACKENZIE, Donald, Improvements relating to phase or position responsive apparatus, 20: 32761
MACKIN, Robert J. Jr., Conference on the solar wind, Pasadena, 4/64, 20: 31880
MACKIN, Robert J. Jr., Effects of diffusion on composition of solar corona and solar wind, 20: 31894
MACKIN, Robert J. Jr., Evidence for collision-free hydromagnetic shock in interplanetary space, 20: 31891
MACKIN, Robert J. Jr., Interplanetary magnetic measurements, 20: 31883
MACKIN, Robert J. Jr., Interplanetary magnetic-field measurements by IMP-1 satellite, 20: 31887
MACKIN, Robert J. Jr., Interaction of solar wind with comets, 20: 31896
MACKIN, Robert J. Jr., Magnetic fields in solar photosphere, 20: 31892
MACKIN, Robert J. Jr., Magnetohydrodynamic aspects of interaction of solar wind with comets, 20: 31897
MACKIN, Robert J. Jr., Magnetosphere of the moon, 20: 31899
MACKIN, Robert J. Jr., Mariner-2 measurements of solar wind, 20: 31881
MACKIN, Robert J. Jr., Mev phenomena related to solar wind. I., 20: 31885
MACKIN, Robert J. Jr., Mev phenomena related to solar wind. II., 20: 31886
MACKIN, Robert J. Jr., Models of interplanetary fields and plasma flow, 20: 31890
MACKIN, Robert J. Jr., Origin of solar wind, 20: 31893
MACKIN, Robert J. Jr., Penetration of galactic cosmic rays into solar system, 20: 31955
MACKIN, Robert J. Jr., Probable observation of wake of moon, 20: 31900
MACKIN, Robert J. Jr., Radio astronomy observations in relation to solar-wind problem, 20: 31888
MACKIN, Robert J. Jr., Reconnection and annihilation of magnetic fields, 20: 31895
MACKIN, Robert J. Jr., Relation of Mariner-2 plasma data to solar phenomena, 20: 31882
MACKIN, Robert J. Jr., Relationship between high-energy particles in space and solar plasma, 20: 31884
MACKIN, Robert J. Jr., Theory of type-I comet tails, 20: 31898
MACKIN, Robert J. Jr., What we know and what we do not know about solar wind, 20: 31889
MAC LEOD, R. A., Carbon in primary Na system of Enrico Fermi Atomic Power Plant, 20: 32809 (TID-23101)
MAC MILLAN, D. B., Kinetics of low source reactor startups, 20: 32766 (KAPL-M-6550)
MACRAKIS, Michael S., Fluctuation scattering and absorption cross section in space dispersive plasma, 20: 32613
MAEDA, Mamoru, Adsorption and electrodeposition of protactinium, 20: 31243
MAGAL, B. S., Nuclear power programme in India, 20: 32816

MAGEE, J. L., Model of tracks of ionizing radiations for radical reaction mechanisms, 20: 31293
MAGEE, J. L., Simplified approach to diffusion-controlled radical reactions in tracks of radiations, 20: 31294
MAHADEVAN, E. G., Exchange between methyl acetylene and water for concentration of deuterium, 20: 31640 (NYO-755-1, pp 130-72)
MAHANTA, P., Collinear processes in $U_3 \times U_3$, 20: 32131
MAHLMAN, J. D., Relation of stratospheric-tropospheric mass exchange mechanisms to surface radioactivity peaks, 20: 31402
MAHON, H., Phonon-induced dipole nuclear spin transitions, 20: 32689
MAI, H., Contribution to investigation of background effects in spark source mass spectrography, 20: 31203
MAIER, R. J., Effect of radiation-induced charge on transistor surfaces, 20: 31611 (AD-633468)
MAISIN, J. R., Lysosomal modifications after administration of radioprotective drugs, 20: 30964
MAISIN, J. R., Ultrastructural aspects of duodenal crypts in x-irradiated mice after chemical protection, 20: 31128
MAITA, J. P., Localized moments, 20: 32739
MAJUMDAR, Saroj K., Density wake of charged particle moving through plasma, 20: 32589
MAKSIMENKO, A. S., Transplantation of homologous bone marrow and intravenous injection of whole blood to irradiated dogs, 20: 31132
MALAHOV, S. G., Distribution of nuclear test explosion fallout over continents and oceans, 20: 31421
MALIK, F. B., Evidence of deformation in ^{51}V, 20: 32513
MALLEVAIS, Jean-Pierre, Factors acting on incorporation of radiophosphoric acid in RNA of rat hepatocytes, 20: 30976
MALSKY, S. J., Miniature thermoluminescent dosimetry for application in medicine and biology, 20: 31598
MALYKHIN, V. M., Precision of radiometric measurements in cases of small preparation/background ratios, 20: 31576
MALYSHEV, E. K., High-pressure ionization ^{3}He chamber performance as slow neutron detector, 20: 31573
MAMURO, Tetsuo, Radionuclide fractionation in debris from land surface burst, 20: 31460
MANDL, V., Time resolution measurements with XP 1020 photomultipliers, 20: 31552
MANGELSON, N., Masses and excited states of ^{24}Al and ^{28}P, 20: 32473
MANGIN, Jean-Paul, Traveling-field particle linear accelerator, 20: 31851
MANI, H. S., Axial-vector coupling constant renormalization in β decay, 20: 32157
MANI, H. S., Bootstrap possibilities of a 70-plet of SU_6, 20: 32151
MANI, R. S., Production of radioisotopes of high specific activity for medical use, 20: 31275
MANK, V. V., NMR studies of solubility H in liquid N and He in liquid H, 20: 31251
MANN, L. G., Fermi and Coulomb matrix elements from β-γ correlation measurements on ^{48}V and ^{52m}Mn, 20: 32506
MANNONE, F., Determination of partial α-half-life of ^{241}Pu, 20: 32435
MANOHAR, Production of radioisotopes of high specific activity for medical use, 20: 31275
MANTEL, Nathan, Inhibition of selected photosensitizers by agents of varying antioxidant activity, 20: 31018
MANUEL, O. K., Binding energy of the nucleus, 20: 32559
MAPLE, J. H. C., Ion bombardment apparatus for study of interaction of light ions with surfaces, 20: 31937
MARCILLE, Genevieve, Effects of x rays on platelet environment, 20: 31032 (CEA-R-2953)
MARGOLIS, B., Low-lying negative parity states in A = 17 nuclei, 20: 32398
MARGOSIAN, Paul M., Ion thrustor suitable for spacecraft station keeping and attitude control, 20: 31371
MARGOSIAN, Paul M., Two-directional electron-bombardment ion thrustor, 20: 31380
MARIN, N. I., Pulsed neutron generator, 20: 32358
MARINOV, A., Dependence of angular distribution of the (d,p) reaction on total angular-momentum transfer. II., 20: 32512
MARINOV, A., Energy levels of ^{48}Ca and ^{40}Ca as observed with inelastic scattering of 11.5-Mev protons, 20: 32511
MARK, Hans, Atomic fluorescence yields, 20: 31936
MARK, J. T., Pumping system and single-wall chamber for 10^{-13} torr, 20: 31392
MARKIV, V. Ya., X-ray structural analysis of some Zr–Fe and Zr–Co alloys, 20: 31727
MARKOVSKII, L. Ya., Ternary compounds in Be–B–C system, 20: 31257
MARQUIT, E., Observation and properties of neutral A_2 meson, 20: 32064
MARR, G., Analysis of inelastic alpha-particle scattering data, 20: 32544
MARSHAK, R. E., Remarks on quark model as maximal probe of chiral symmetries, 20: 32198
MARSHALL, Neldon H., Numerical techniques for solving Fredholm's integral equations of first kind, 20: 31656 (IDO-17175)
MARSHALL, R. C., Study of fuel assembly vibrations induced by coolant flow, 20: 32746
MARSLAND, Douglas, Cell division: pressure-induced reversal of antimeiotic effects of heavy water in oocytes of the starfish, 20: 30986
MARTALOGU, Nicolae, Simultaneous measurement of beam energy in angular distribution studies, 20: 32403
MARTI, K., Rare gas measurements in 30 stone meteorites, 20: 31876
MARTI, K., Spallation, fission, and neutron capture anomalies in meteoritic Kr and Xe, 20: 31875
MARTIN, B. R., PCAVC hypothesis and pion-lambda interaction, 20: 32013
MARTIN, E. B. M., Cross sections for reactions $^{27}Al(n,\alpha)$ and $^{56}Fe(n,p)$ for 14-Mev neutrons, 20: 32528
MARTIN, Emile, Extraction by pealing of beam of heavy ions accelerated in cyclotron with starred field, 20: 31828
MARTIN, G. R., Cross sections for reactions $^{27}Al(n,\alpha)$ and $^{56}Fe(n,p)$ for 14-Mev neutrons, 20: 32528
MARTIN, W. H., Annealing of irradiation damage in graphite, 20: 31803
MARX, G., Experimental limits on neutrino-sea density, 20: 32012
MASEK, Tommy D., Plasma investigation in reversed current electron bombardment ion engine, 20: 31372
MASHTAKOV, V. S., Electron-bombardment-induced stimulated emission from cadmium selenide, 20: 32730
MASON, Ronald, Advances in radiation biology. II., 20: 31038
MASSAM, T., Determination of the $(\omega$-$\phi)$ mixing angle using nucleon electromagnetic form factors, 20: 32058
MASSAM, T., One-parameter fit to electromagnetic form factors of nucleon, 20: 32033
MASSEY, Harrie, Uncertainty principle and short-lived atomic and subatomic states, 20: 31910
MASSOT, J. M., Graphical methods of summation and integration of spherical harmonics, 20: 32437
MATHEWS, B. E., Probe measurements in electrodeless discharge, 20: 32655
MATHEWS, W. A., External proton beam at Nimrod, 20: 31823 (RPP-N-5)
Matin, A. S. M. Abdul
see Abdul Matin, A. S. M.
MATSUDAIRA, Masamichi, Study on the medical universal human counter. I., 20: 31586
MATSUMOTO, Hiroaki, EPR studies on gamma-irradiated $CdCl_2$: Ag and $CdCl_2$: Cu crystals, 20: 32685
MATSUMURA, Seiji, Radiation genetics in wheat. IX., 20: 31080
MATSUNAMI, Tadao, Radionuclide fractionation in debris from land surface burst, 20: 31460
MATTAUGH, J. H. E., Precision measurements of atomic masses and some of their implications on nuclear structure and synthesis, 20: 31808
MATTHAEY, H., Angular distribution of polarization of recoil proton from photoproduction of neutral pions on H at photon energy of 360 Mev. II., 20: 32097
MATTHAEY, H., Polarization of recoil proton from photoproduction of neutral pions on H in region of first resonance. I., 20: 32096
MATTHIAS, B. T., Localized moments, 20: 32739
MATTHIJSSEN, Charles, Program for calculation of liquid scintillation spectrometry data from duel-labeled samples, 20: 31177
MATTSSON, Arne C. J., Performance of self-excited MHD generator, 20: 31976
MATUMOTO, Ken-iti, Structure of hadrons, 20: 32082
MATYASH, I. V., NMR studies of solubility H in liquid N and He in liquid H, 20: 31251
MATYUSHIN, A. T., Serial power supply for spark chamber gaps, 20: 31571
MATYUSHIN, V. T., Serial power supply for spark chamber gaps, 20: 31571
MAUREL, J., Detection efficiency of spark chambers and its exact calculation, 20: 31558
MAURON, G., Decay of ^{140}Ba, 20: 32407
MAURON, G., Improvement of luminosity of double focussing β spectrometer, 20: 31559
MAYER-BOERICKE, C., Dependence of angular distribution of the (d,p) reaction on total angular-momentum transfer. II., 20: 32512
MAYER-BOERICKE, C., J dependence in the $(^{3}He,\alpha)$ reaction, 20: 32508
MAYINGER, F., Prog. rpt. on critical heat flux (burnout) in boiling water, 7–9/65, 20: 31342 (EURAEC-1482)
MAYNARD, Charles W., Miniature diamond ultrahigh pressure cell adapted for in-reactor irradiation studies, 20: 32754
MAZDIYASNI, K. S., Metastable transitions of zirconium oxide obtained from decomposition of alkoxides, 20: 31736
MC ALLISTER, Lawrence Edward, Improvements relating to phase or position responsive apparatus, 20: 32761
MC BRIDE, J. P., Sol-gel process development and microsphere preparation, 20: 31689 (ORNL-P-2159)
MC CARTHY, A. L., Energies and half-lives of isomeric transitions in ^{115}Sn and ^{109}Cd, 20: 32520
MC CLELLAN, R. O., Hematopoietic tissue neoplasms in animals administered ^{90}Sr, 20: 31031
MC CORMICK, B. H., WEB: language to describe interconnection and

packaging of logical units in digital processor. I., 20: 31648 (COO-1018-1021)
MC CORMICK, Bruce H., ILLIAC III: processor of visual information, 20: 31652 (COO-1018-1057)
MC CORMICK, Bruce H., Programming manual for ILLIAC III computer, 20: 31653 (COO-1018-1061)
MC CRACKEN, G. M., Ion bombardment apparatus for study of interaction of light ions with surfaces, 20: 31937
MC DANELS, David L., Stress-rupture properties of tungsten wire from 1200° to 2500°F, 20: 31711 (NASA-TN-D-3467)
MC DANIEL, M. Lee, Power conversion system for lunar and planetary electrostatic propulsion missions, 20: 31384
MC DIARMID, I. B., Alouette II satellite, 20: 32247
MC DONALD, F. B., Mev phenomena related to solar wind. I., 20: 31885
MC DONALD, F. B., Mev phenomena related to solar wind. II., 20: 31886
MC DONALD, Philip R., Commercialization studies on wood-plastic combinations process, 20: 31625 (NYO-3569-1)
MC DONALD, R. E., Study of low-lying states of ^{33}S, 20: 32565
MC DOWELL, M. R. C., Continuous absorption by C negative ion. II., 20: 31864
MC ELLISTREM, M. T., Spin assignments in ^{35}Cl and ^{37}Cl via (n,n'γ) reactions, 20: 32550
MC FADDEN, P. W., Boiling heat transfer from cylinders in saturated liquid He-II bath, 20: 32349
MC HUGH, James A., Application of sputtering ion source to mass analysis of nanogram solid samples, 20: 31168 (CONF-660611-1)
MC KAY, Donald G., Ultrastructural alterations in deuterium intoxication, 20: 30975
MC LENNAN, J. A., Symmetry of stress tensor, 20: 32165
MC NAMARA, W. G., Enriched uranium scrap assay gage, 20: 31174 (WAPD-T-1905)
MC NICE, G. T., Application of nuclear radiation to pumping of lasers, 20: 32740
MC PHERSON, R., Beta-delayed protons from ^{25}Si, 20: 32505
MEAD, Gilbert D., Shape of magnetosphere and distortion of geomagnetic field, 20: 32282
MEAD, W. L., Advances in mass spectrometry. Vol. 3, 9/64, 20: 31197
MEASDAY, D. F., Loss of charged particles by nuclear interactions in scintillators, 20: 31542
MEDEMA, J., Rapid and accurate B.E.T. surface area measurement using radioactive Kr, 20: 31353
MEGAHED, Y. M., Preparation of Tc, tyrosine, thyroxine, insulin and human serum proteins labeled-^{99m}Tc, 20: 31265
MEHTA, M. K., Test of distorted-wave stripping theory by $^{52}Cr(d,p)^{53}Cr$, 20: 32459
MELLO, J. C., Thorium-cycle possibilities in Brazilian nuclear power program, 20: 32821
MENDELSON, R. A., Development of porous ionizer materials, 20: 31375
MENETREY, W., Potentials of solar power electric propulsion, 20: 31382
MENKES, Ciro I K., Modification of the Toshiba FGD-3B glass dosimeter reader, 20: 31527
MENZEL, R. G., Retention of foliar applications of ^{85}Sr by several plant species, 20: 30996
MERCEREAU, J. E., Macroscopic quantum interference in superconductors, 20: 32344
MERCKX, K. R., Fuel element measurement system, 20: 32753
MERGEN, Francois, Effects of chronic exposures to ^{60}Co radiation on Pinus rigida seedlings, 20: 31077
MERRIHUE, Craig, Potassium–Ar dating by activation with fast neutrons, 20: 31431
MERZ, E., Recoil brominations of aromatic compounds, 20: 31296
MES, Hans, Resonance (3,3) in nucleus, 20: 32078
MESHKOV, Sydney, Assignment of spin 2+ mesons and the nature of quark-quark interactions, 20: 32205
MESTEL, L., Problems of star formation. I., 20: 31873
MESZAROS, F. W., Permeability of zirconia, hafnia, and thoria to O, 20: 31731
METZGER, D. S., Nuclear magnetic resonance studies of solidified H_2–D_2 mixtures. II, 20: 32711
METZINGER, G., Experimental techniques, applications, and theory of field ion mass spectrometry, 20: 31199
MEYER, Joachim, Semiannual wave in recurrence tendency of geomagnetic activity, 20: 32257
MEYER, Kenneth A., Two-dimensional time-dependent numerical study of rotational Couette flow, 20: 31344 (LA-3497)
MEYER, Rudolf X., Acceleration of cesium ions by negative space charge sheath, 20: 31378
MEYERAND, R. G. Jr., Laser plasma production. New area of plasma-dynamics research, 20: 32666
MEYERHOF, W. E., Systematics of low-lying 0+ states in light nuclei, 20: 32522
MEYER-SCHUETZMEISTER, L., Isospin selection rule in the $^{12}C(d,\alpha)^{10}B$ reaction, 20: 32500
MIA, M. M., Mutation types in irradiated population of Jute, 20: 31027
(AECD/AG-14)
MICHAELSON, Sol M., Radiation-induced changes in properdin system of dog, 20: 31013
MICHALEC, R., Experimental determination of efficiency of γ-ray circular polarization analyzers, 20: 31998
MICHALOWICZ, A., Construction of a polarized beam with both spin orientations at the CERN synchrocyclotron, 20: 31835
MICHALOWICZ, A., Polarization and spin correlation parameter measurements in 600-Mev proton-proton scattering, 20: 32016
MICHEL, D. J., Melting points of $REZn_2$ intermetallic compounds, 20: 31743
MICHEL, F. C., Photon-induced beta decay in stellar interiors, 20: 31878
MICHEL, G., Reaction $^6Li(d,n)^7Be^*$ with polarized deuterons, 20: 32411
MICHON, G., Control of radioactive pollution of milk by ^{131}I, 20: 31456
MICKLEM, H. S., Tissue grafting and radiation, 20: 31120
MIETTINEN, Jorma K., Results of Project Lapland at beginning of 1966, 20: 31444 (CONF-660405-15)
MIGLIORINI, M., Experimental observations on behavior of serum cholesterol after irradiation, 20: 31006
MIHALISIN, T. W., Polarized positron annihilation in ferromagnetic nickel, 20: 32703
MIHALOV, J. D., Energetic electron spectra in radiation belts, 20: 32251
MIHALOV, J. D., Low-energy proton radiation belts, 20: 32250
MIKHAILOV, A. I., Programming operation of JINR synchrophasotron, 20: 31840
MIKHAILOV, G. A., Computations of critical systems by Monte Carlo method, 20: 32778
MIKHAILOV, V. P., Reparative regeneration of tissues under effect of radiation, 20: 31045
MIKULSKI, Andrzej T., Buckling determination in HELENA subcritical assemblies, 20: 32783
MILAM, James Kelly, Solid state beta gauge for measuring density of liquid H, 20: 31494
MILASIN, N., Hardening by irradiation of low alloy steel for reactor pressure vessel, 20: 31796
MILEY, G. H., Pulse propagation experiments using reactor source, 20: 32362
MILLER, James A., Conference on heat transfer and fluid mechanics, Santa Clara, 6/66, 20: 31351
MILLER, Morton W., Extrapolation number and apical cell number in gemmae of Marchantia polymorpha L., 20: 31065
MILLER, T. A., Effect of age of dog on immunogenic efficiency of double vaccination with x-irradiated Ancylostoma caninum larvae, 20: 31043
MILLS, W. R., Combination neutron experiment for remote analysis, 20: 31211
MILOVANOV, V. P., Installation for studying energy and angular distribution of recoil nuclei, 20: 32526
MINAMI, Masatsugu, Homological study of generalized singular functions. I., 20: 32182
MINAMIKAWA, Toshiyuki, Excitation of the $J^P = 3/2^+$ decuplet and $J^P = 3/2^-$ octet in the neutrino reaction on the quark and the cloud models, 20: 32080
MINEEV, F. I., Device for measuring charged particle beam parameters, 20: 31838
MINEEV, Yu. V., Pulse-height recording and logarithmic conversion of pulse heights in the 10^4 to 10^5 dynamic range, 20: 31577
MINGUZZI, A., Canonical commutation relations and asymptotic behavior of transition amplitudes, 20: 32032
MINGUZZI, A., Stronger form of edge of wedge theorem, 20: 32142
MINKEN, J. W., Experience with electrodialysis, 20: 31194
MIN'KO, L. Yu., Unipolar pulsed plasma generator combined with laser as source for obtaining plasma jets, 20: 32639
MINSKI, Margaret, Estimation of stable sulphur in human tissue, 20: 30982
MINZATU, I., Polarization of neutrons from $^7Li(p,n)^7Be$ reaction, 20: 32359
MISHIMA, Nobuhiko, Four-particle scattering in nonrelativistic theory. II., 20: 32171
MISKELL, R. V., UCAPP: Union Carbide APT Post Processor, first edition, 20: 31478 (K-1670)
MITCHELL, John C., Effects of 55-Mev protons on primates, 20: 31099
MITCHELL, John C., Effects of 138-Mev protons on primates, 20: 31101
MITCHELL, John C., Effects of 400-Mev protons on primates, 20: 31103
MITCHELL, John C., Estimate of biological effects of space proton environment, 20: 31106
MITCHELL, John C., Kinetics of recuperation following 55-Mev proton irradiation, 20: 31100
MITCHELL, John C., Proton depth-dose dosimetry, 20: 31467
MITCHELL, John C., RBE of 138-Mev protons as compared to ^{60}Co gamma radiation, 20: 31102
MITSKEVICH, N. V., Four-dimensional symmetric canonical formalism of field theory, 20: 32123
MITSUMOTO, Seiichi, Effect of lattice defects on critical current of hard

superconducting Nb, 20: 31759
MITTLEMAN, M. H., Coupled equations for rearrangement collisions. II., 20: 32388
MIURA, Takashi, Effect of radiation and antitumor agents measured by mouse splenic and thymic weight, 20: 31131
MIYANAGA, Takeshi, EPR studies on gamma-irradiated $CdCl_2$: Ag and $CdCl_2$: Cu crystals, 20: 32685
MIZUNO, Yukio, Ground state of a non-interacting electron gas exchange-coupled to localized spin, 20: 32085
MOCHEL, J. M., Thermal conductivity of superconducting surface sheath, 20: 32327
MOCHIZUKI, Tsunekazu, Uranium in coal-bearing beds of Mikawa and Akatani areas, Niigata Prefecture, 20: 31437
MOHAN, G., Axial-vector coupling constant renormalization in β decay, 20: 32157
MOHAN, G., Bootstrap possibilities of a 70-plet of SU_6, 20: 32151
MOINET, J., Influence of Al content and temperature on elastic and plastic properties of solid solution of Fe–Al, 20: 31751
MOISEIWITSCH, B. L., Dissociation of hydrogen molecules by electron impact, 20: 31931
MOLITOR, J. H., Effects of reliability considerations on design of electric thruster arrays, 20: 31359
MOLITOR, J. H., Light-weight flight protype ion engine system, 20: 31364
MOLITOR, J. H., Solar-electric propulsion system for interplanetary spacecraft, 20: 31373
MOLNAR, George D., Hyperfunctioning solitary thyroid nodule, 20: 31154
MOMOTA, Hiromu, Excitations of cyclotron harmonic waves propagating perpendicular to external magnetic field, 20: 32630
MOMOTA, Hiromu, Stability of uniform plasma composed of streams in absence of external field, 20: 32629
MONCRIEF, E. C., Recycle of HWOCR thorium fuel, 20: 31317 (BAW-393-3)
MONSELISE, S. P., Changes in flavedo and juice of Shamouti oranges following γ irradiation, 20: 31632
MONTA, Kazuo, Computer control of research reactor TTR-1, 20: 32867
MONTALDI, E., Conditions for existence of a diagonal representation for quantum mechanical operators, 20: 32304
MONTEITH, Larry K., Trapping and thermal release of irradiation electrons from polyethylene terephthalate films, 20: 31790
MONTI, Rodolfo, CNR MHD plant at the Istituto di Aerodinamica, Naples, 20: 32633
MONTREUIL, Jean, Factors acting on incorporation of radiophosphoric acid in RNA of rat hepatocytes, 20: 30976
MONTVAY, I., Classification of positive-parity mesons in SU_6, 20: 32148
MOORE, C. R., Carbon in primary Na system of Enrico Fermi Atomic Power Plant, 20: 32809 (TID-23101)
MOORE, J. L., Induced enzyme in x-irradiated E. coli, 20: 31004
MOORE, M. N., General theory of excitation experiments in space-dependent kinetics, 20: 32784
MOORE, R. David, Geomagnetic thrustor—Alfven wave propulsion system utilizing plasma contacts, 20: 31377
MOORE, W. E., Double differential scattering cross sections and scattering law for H_2O at 302°K, 20: 32350 (KAPL-M-6536)
MOORE, W. Jr., Effect of ^{131}I on aberration rate of chromosomes from Chinese hamster thyroids, 20: 31053
MOORE, W. S., Microwave-enhanced critical supercurrents in constricted tin films, 20: 32328
MORAND, M., Antiproton-nuclei scattering at 3 Bev/c, 20: 32467
MORAVCSIK, Michael J., General non-dynamical formalism for reactions with particles of arbitrary spin, 20: 32382 (UCRL-14582-T(Rev.1))
MORE, K., Radionuclide production in Fe targets bombarded with 400-Mev protons, 20: 32560
MORGAN, I. L., Pulsed neutron sources and applications, 20: 32365
MORGAN, I. L., State of the art neutron detection, 20: 31606
MORGAN, Ira L., Effects of whole-body 32-Mev proton irradiations on primates, 20: 31097
MORGAN, Ira L., Effects of 55-Mev protons on primates, 20: 31099
MORGAN, Ira L., Effects of 138-Mev protons on primates, 20: 31101
MORGAN, Ira L., Effects of 400-Mev protons on primates, 20: 31103
MORGAN, Ira L., Estimate of biological effects of space proton environment, 20: 31106
MORGAN, Ira L., Kinetics of recuperation following 55-Mev proton irradiation, 20: 31100
MORGAN, Ira L., Proton depth-dose dosimetry, 20: 31467
MORGAN, Ira L., RBE of 138-Mev protons as compared to ^{60}Co gamma radiation, 20: 31102
MORGAN, Ira L., Whole-body irradiation of primates with protons of energies to 400 Mev, 20: 31096
MORGAN, R. H. C., External proton beam at Nimrod, 20: 31823 (RPP-N-5)
MORGENSTERN, H., Neutron-induced reactions on silicon, 20: 32431
MORI, Tomoyuki, Measurement of radioisotopes in human body by linear scanning, 20: 31158
MORII, Takashi, Properties of quartz thermoluminescence dosimeters, 20: 31520
MORIKAWA, G. K., Steady nonlinear waves in warm collision-free plasma, 20: 32577 (NYO-1480-54)
MORITA, Kenji, Secondary electron emission-type neutral particle detector, 20: 31533
MORITA, Kozo, Radiation therapy of maxillary sinus, 20: 31159
MORRIS, J. C., Radiation of O and N and thermal conductivity of N up to 15,000°K, 20: 32240
MORRISON, J. A., High-field steady-state shock wave in plasma, 20: 32604
MORROW, Irving B. Jr., Performance of self-excited MHD generator, 20: 31976
MOSCA, L., Alternative interpretation of the enhancement observed at $M^*_{pp\pi^+}$ 2.52 Bev/c², 20: 32040
MOSCINSKI, J., Radiometric determination of solubility of cadmium in molten cadmium chloride, 20: 31237
MOSER, Pierre, Faults created by irradiation in pure Fe, 20: 31789
MOSS, H. D., Enriched uranium scrap assay gage, 20: 31174 (WAPD-T-1905)
MOUTSCHEN, J., Post-irradiation modification of biological effects of neutrons. I., 20: 31136
MOUTSCHEN-DAHMEN, M., Post-irradiation modification of biological effects of neutrons. I., 20: 31136
MOUTURAT, P., Influence of Al content and temperature on elastic and plastic properties of solid solution of Fe–Al, 20: 31751
MOZER, F. S., Observation of low-altitude acceleration of auroral protons, 20: 32249
MOZER, F. S., Proton trajectories in radiation belts, 20: 32261
MOZUMDER, A., Model of tracks of ionizing radiations for radical reaction mechanisms, 20: 31293
MOZUMDER, A., Simplified approach to diffusion-controlled radical reactions in tracks of radiations, 20: 31294
MUELLER, Gerhard O., LIZARD-IV: program to solve nonlinear, ordinary differential equations, 20: 31657 (KAPL-M-6548)
MUELLER, J., Specific heat, antiferromagnetism, and superconductivity in Cr–Re system, 20: 32702
MUELLER, James J., La Crosse Boiling Water Reactor radio and water chemistry manual, 20: 32795 (ACNP-66538)
MUENCHOW, L., Macroscopic and microscopic descriptions of dipole states of atomic nuclei, 20: 32448
MUHEIM, J., Specific heat, antiferromagnetism, and superconductivity in Cr–Re system, 20: 32702
MULDOON, W. J., Light-weight flight prototype ion engine system, 20: 31364
MULIARCHIK, T. M., Investigation of softest particles by means of Cosmos 3 and Cosmos 5 satellites, 20: 32270
MUMINOV, V. A., Fast neutron scintillation counter, 20: 31532
MUNKRES, K. D., Genetics of enzyme locational specificity, 20: 31012
MUNRO, R., Tandem mass spectrometer for isotopic analysis, 20: 31206
MUNSON, R. J., Site of lethal damage by ionizing radiation in E. coli, 20: 31068
MURAMATSU, Susumu, Effects of continuous low-dose irradiation on mice. I., 20: 31074
MURATOV, Yu. V., Plasma gun for producing high electron-current peaks, 20: 31486
MURINO, Pasquale, CNR MHD plant at the Istituto di Aerodinamica, Naples, 20: 32633
MURPHY, J. W., Alpha-deuteron-lambda model of the hypernucleus $_{\Lambda}Li^7$, 20: 32450
MURRAY, Raymond L., Unification of theory of neutron multiplying systems, 20: 32779
MURTY, G. S., Viscous effects in liquid conductor model of hard-core pinch, 20: 32233
MUSTAFIN, K. S., Inversion of levels during excitation by a monoenergetic electron beam, 20: 31941
MUTA, T., Simple model of the n-p mass difference, 20: 32057
MYERS, M. A., Probe observations of solar wind-geomagnetic field interaction region, 20: 32286
MYERSCOUGH, V. P., Continuous absorption by C negative ion. II., 20: 31864
MYRBERG, John E., Megampere pulse transformer for coaxial load, 20: 31489
MYZNIKOV, K. P., Programming operation of JINR synchrophasotron, 20: 31840

N

NAGAI, Teruo, Cesium turnover in man following single administration of ^{132}Cs. I., 20: 30988
NAGAI, Teruo, Labeling of myeloma cells and leukemic leukocytes, 20: 30971 (ORINS-45)
NAGAMATSUYA, Takaaki, Hydrogen reduction of γ-irradiated NiO, 20: 31285

NAGARAJAN, G., Mean amplitudes of vibration and Bastiansen-Morino shrinkage effects for di- and trioxides of Mo, W, and U, 20: 31233
NAGATA, Sinobu, Reaction ($\gamma\pi^-$p) with complex nuclei, 20: 32530
NAGORNAYA, L. L., High-heat-resistance plastic scintillators, 20: 31262
NAGY, Agnes G., Production of carrier-free ^{131}I-iodate, 20: 31234
NAGY, T., Classification of positive-parity mesons in SU_6, 20: 32148
NAGY, T., Spontaneous breakdown of the SU_3 symmetry in field-theoretical approach, 20: 32129
NAIR, V., Regional changes in brain serotonin after head x-irradiation, 20: 31007
NAKAGAWA, Masami, Inner symmetry in baryon structures and leptonic decays, 20: 32176
NAKAGAWA, Masami, Non-leptonic weak interaction in current-current interaction, 20: 32075
NAKAGAWA, Y., Radiative hydrogenic shock structure, 20: 32241
NAKATANI, Hiroshi, Large-angle elastic scattering at high energies, 20: 32086
NAKATSUKA, Haruo, Biological effectiveness of 15-Mev betatron x rays and 200 kv x rays for lethality in mice, 20: 31072
NAKRA, A. N., Physics calculations of thorium-fuelled heavy-water lattices, 20: 32774
NAMBU, Yoichiro, Nonleptonic decays of hadrons, 20: 32196
NAMIKI, Mikio, Inner symmetry in baryon structures and leptonic decays, 20: 32176
NAMIKI, Mikio, Non-zero elastic amplitude real part effects and nucleon recoil effects on relationship between elastic diffraction scattering and inelastic collisions, 20: 32072
NAMIKI, Mikio, Possible scheme of elementary particle structure, 20: 32083
NANCE, Sharron L., Pancreatic lipase activity in deuterium oxide, 20: 30995
NAOUMIDIS, A., System U–N, 20: 31230
NARASIMHAN, R., BUBBLE SCAN I program, 20: 31507 (COO-1018-1013)
NARAYAN, D. S., Direct and charge-exchange scattering (n-p) based on transverse momentum distribution and Mandelstam representation, 20: 32048
NARBAEV, N., Quantitative regularities of quinone formation in gamma-irradiated plant tissue, 20: 31001
NARCHAL, M. L., Dynamic orientation of spin-1 nuclei. II., 20: 32390
NARDUCCI, L. M., Conditions for existence of a diagonal representation for quantum mechanical operators, 20: 32304
NARUMI, Hajime, Nuclear charge distribution of calcium isotopes, 20: 32534
NAUDET, R., Aspects of Th cycle in heavy water reactors, 20: 32823
NAUMOV, A. I., Mass of a fundamental fermion and degeneracy of the vacuum, 20: 32121
NAUMOV, V. A., Electron diffraction study of structure of neodymium halide molecules, 20: 31222 (ANL-Trans-310)
NAZARCHUK, N. V., Slip casting of molybdenum disilicide, 20: 31697
NEAMU, Ionel, Simultaneous measurement of beam energy in angular distribution studies, 20: 32403
NECHIPORUK, V. A., Physical stand for critical assembly of Institute of Physics at Ukrainian Academy of Sciences, 20: 32770
NE'EMAN, Y., Algebraic comments on Regge recurrences, 20: 32204
NE'EMAN, Yuval, Hadron matrix mechanics, 20: 32211
NEESON, J. F., Directional correlations in ^{127}I, 20: 32396
NEKROT, A. A., Virial expansions for plasma in collective variable method, 20: 32625
NELMS, G. L., Alouette II satellite, 20: 32247
NELSON, J. B., Study of excited states in ^{15}N and ^{16}N, 20: 32501
NELSON, J. H., Mathematical model of geomagnetic field for 1965, 20: 32255
NELSON, L. S., Possible role of supercooling in spearpoints observed during combustion of Zr droplets, 20: 31664
NELSON, M. E., Cosmic-ray heavy nuclei at geomagnetic latitude 42° north, 20: 31951
NEMETHY, Peter, Radiative decay of the μ meson, 20: 32104
NENADOVIC, M. T., Reaction of oxalic acid re-formation during gamma radiolysis of aqueous oxalate solutions, 20: 31277
NESS, N. F., Interplanetary magnetic-field measurements by IMP-1 satellite, 20: 31887
NESS, N. F., Magnetic storms in earth's magnetic tail, 20: 32253
NESS, N. F., Observations of magnetic field at magnetopause and interaction region by IMP 1, 20: 32281
NESS, N. F., Probable observation of wake of moon, 20: 31900
NETZ, G., Application of moisture measurements by means of neutrons, 20: 31627
NEU, R. E., UCAPP: Union Carbide APT post processor, 20: 31327 (K-1671)
NEU, R. E., UCAPP: Union Carbide APT post processor, first edition, 20: 31478 (K-1670)
NEUGEBAUER, Marcia, Conference on the solar wind, Pasadena, 4/64, 20: 31880
NEUGEBAUER, Marcia, Effects of diffusion on composition of solar corona and solar wind, 20: 31894
NEUGEBAUER, Marcia, Evidence for collision-free hydromagnetic shock in interplanetary space, 20: 31891
NEUGEBAUER, Marcia, Interplanetary magnetic measurements, 20: 31883
NEUGEBAUER, Marcia, Interplanetary magnetic-field measurements by IMP-1 satellite, 20: 31887
NEUGEBAUER, Marcia, Interaction of solar wind with comets, 20: 31896
NEUGEBAUER, Marcia, Magnetic fields in solar photosphere, 20: 31892
NEUGEBAUER, Marcia, Magnetohydrodynamic aspects of interaction of solar sind with comets, 20: 31897
NEUGEBAUER, Marcia, Magnetosphere of the moon, 20: 31899
NEUGEBAUER, Marcia, Mariner-2 measurements of solar wind, 20: 31881
NEUGEBAUER, Marcia, Mev phenomena related to solar wind. I., 20: 31885
NEUGEBAUER, Marcia, Mev phenomena related to solar wind. II., 20: 31886
NEUGEBAUER, Marcia, Models of interplanetary fields and plasma flow, 20: 31890
NEUGEBAUER, Marcia, Origin of solar wind, 20: 31893
NEUGEBAUER, Marcia, Penetration of galactic cosmic rays into solar system, 20: 31955
NEUGEBAUER, Marcia, Probable observation of wake of moon, 20: 31900
NEUGEBAUER, Marcia, Radio astronomy observations in relation to solar-wind problem, 20: 31888
NEUGEBAUER, Marcia, Reconnection and annihilation of magnetic fields, 20: 31895
NEUGEBAUER, Marcia, Relation of Mariner-2 plasma data to solar phenomena, 20: 31882
NEUGEBAUER, Marcia, Relationship between high-energy particles in space and solar plasma, 20: 31884
NEUGEBAUER, Marcia, Theory of type-I comet tails, 20: 31898
NEUGEBAUER, Marcia, What we know and what we do not know about solar wind, 20: 31889
NEUMANN, L., Effect of spatial variation of order parameter on tunneling density of states of superconducting alloys, 20: 32340
NEURINGER, L. J., Effect of spin-orbit scattering on upper critical field of high-field superconductors, 20: 32330
NEVILLE, D. E., Gell-Mann-Okubo rule as consequence of eightfoldedness, 20: 32139
NEWNHAM, R. E., Neutron-diffraction study of $Bi_4Si_3O_{12}$, 20: 31254
NEWSON, H. W., s- and p-Wave neutron spectroscopy. XIa., 20: 32389
NEWTON, C. E. Jr., Treatment and evaluation of internal deposition from Pu wound, 20: 31030 (BNWL-SA-39)
NEWTON, T. W., Kinetics of reaction between V(III) and U(VI) in acid perchlorate solutions, 20: 31239
NGUYEN-LONG-DEN, Study by mass spectrometry of La(p,3pxn)Cs reactions, 20: 32386
NGUYEN-TRUNG, Chi, Momentum distribution of recoil nucleus in the ^{12}C(p,2p)^{11}B reaction, 20: 32529
NICHOLS, D. B., Spin assignments in ^{35}Cl and ^{37}Cl via (n,n'γ) reactions, 20: 32550
NICHOLS, F. A., Coalescence of two spheres by surface diffusion, 20: 31739
NICHOLS, J. P., Impact of Kilorod operational experience on design of fabrication plants for ^{233}U–Th fuels, 20: 31690 (ORNL-P-2176)
NICHOLSON, E. L., Reprocessing methods and costs for selected thorium-bearing fuel types, 20: 31326
NICKEL, H., System U–N, 20: 31230
NICKSON, James J., Effect of L-triiodothyronine on radiation-induced pulmonary fibrosis in dogs, 20: 31138
NIELSEN, A., Formal analogy between Compton scattering and Doppler effect, 20: 31995
NIELSEN, K. Bonde, Internal magnetic field of lutetium in iron and g factor in ^{175}Lu, 20: 32472
NIERENBERG, William A., Hyperfine-structure anomalies of ^{198}Au and ^{199}Au, 20: 32553
NIJAMPURKAR, V. N., "Dating" ground waters of ages younger than 1,000–1,500 years using natural ^{32}Si, 20: 31432
NIJSING, R., Temperature and heat flux distribution in nuclear fuel element rods, 20: 31349
NIKITINSKAYA, T. I., Electrical conductivity of x-ray irradiated fluorite crystals, 20: 32721
NIKODEMOVA, Denisa, Problem of protective dosimetry of neutrons in presence of gamma radiation, 20: 31561
NIKOLAEV, A. V., Radiation resistance of complex organophosphorus resins, 20: 31303
NIKONOV, A. V., Physical stand for critical assembly of Institute of Physics at Ukrainian Academy of Sciences, 20: 32770
NILES, F. E., Hornbeck-Molnar cross-sections for the n = 3 states of He, 20: 31947
NILSSON, S., Multiple pion production in proton-proton collisions at 24 Bev/c, 20: 32017

NINOMIYA, R., Programmed analysis for counting aqueous samples containing two radioactive isotopes, 20: 31182
NISHIKAWA, Kaneyasu, Boiling heat transfer at coexistence of nucleate and film regions, 20: 31345 (NSJ-tr-47)
NISHIU, Sakae, Response of a large sensitive volume lithium-drifted silicon detector to gamma and beta rays, 20: 31519
NISHIYAMA, Ichizo, Radiobiological studies in plants. XI., 20: 31078
NIU, Keishiro, Collisionless shock wave in plasma, 20: 32652
NOEL, G. T., Proton irradiation of thin-film CdS and single-crystal Si solar cells, 20: 31616
NOGAMI, Y., Superconductivity for nuclear-pairing interaction, 20: 32397
NOH, William F., General theory for numerical solution of equations of hydrodynamics, 20: 32220 (UCRL-14912-T)
NOLEN, J. A. Jr., J dependence in the (p,α) reaction, 20: 32489
NOLLE, E. L., Electron-bombardment-induced stimulated emission from cadmium selenide, 20: 32730
NOLLET, Patrick, Dry chemical treatment of uranium–zirconium fuels, 20: 31321
NOMURA, Tsutomu, Reactivity measurements by neutron noise analysis, 20: 32868
NORMAN, Amos, Proliferation of human lymphocytes in culture, 20: 31067
NORTHCOTE, Robert S., Syntax loader and subcanner for compiler-compiler, 20: 31650 (COO-1018-1031)
NOVAK, P. E., Plutonium and fission product redistribution in mixed oxide fuels, 20: 31804
NOVEY, T. B., Search for Y = 2, S = 0 resonances, 20: 32066
NOVIKOV, A. G., High-pressure ionization ^{3}He chamber performance as slow neutron detector, 20: 31573
NOVOTNY, J., Effect of ionizing radiation on glasses, 20: 31283
NOYES, R. C., Temperature distributions for various fuels with nonuniform heating, 20: 32791 (NAA-SR-Memo-11731)
NYBERG, R. A., Comparison of cesium iodide and sodium iodide for underwater radiation detection systems, 20: 31499 (AD-633752)

O

O'CONNELL, J. S., Three-body photodisintegration of ^{3}He, 20: 32546
O'CONNELL, M. J., External proton beam at Nimrod, 20: 31823 (RPP-N-5)
OEPIK, U., Calculation of electronic structure of defects in insulators, 20: 32682 (ORNL-P-2193)
OEZIZMIR, Ercument, Prekinetic equations for a plasma, 20: 32605
OGATA, K., Half life of ^{130}Te double β decay, 20: 32385
OGAZA, S., Transverse spin polarization in odd-mass deformed nuclei, 20: 32447
OHASHI, Yoko, Characteristic of a microwave discharge chamber, 20: 31534
OHBA, Ichiro, Inner symmetry in baryon structures and leptonic decays, 20: 32176
OHNESORGE, W. F., Calibration of the ORNL model Q-2240, continuous air monitor, 20: 31528
OJAK, Maria, Nucleic acids and phosphatase activity in cerebral nerve cells in rats in course of postradiation disease, 20: 31010
OKADA, Shoji, Effect of green tea and related substances on G-I absorption of ^{90}Sr, 20: 30987
OKANO, J., Half life of ^{130}Te double β decay, 20: 32385
OKAZAKI, E. A., Library programs for AECL G-20 computer, 20: 31646 (AECL-1744)
OKIMURA, Tetsuro, Various problems in stomach scanning, 20: 31160
OKUBO, S., Algebra of currents based upon the SU_{W6} group, 20: 32155
OKUBO, S., High-energy theorem by algebra of currents, 20: 32054
OLD, Bruce S., Growth of foreign nuclear power, 20: 32808 (TID-22973)
OLESEN, P., Comparison of forward pion-nucleon dispersion relations with experiments, 20: 32026
OLIVARI, A. J., Scintillation scanning in kidneys, 20: 31148 (CNEA-170)
OLIVARI, Americo, New colloid of ^{99}Tc in scintillation scanning of the liver, 20: 31147 (CNEA-168)
OLIVER, J. C., Construction of a polarized beam with both spin orientations at the CERN synchrocyclotron, 20: 31835
OLIVIER, J. C., Polarization and spin correlation parameter measurements in 600-Mev proton-proton scattering, 20: 32016
OLLERHEAD, R. W., Spin and parity assignments in ^{24}Mg, 20: 32556
OLNESS, J. W., Angular correlations in the ^{13}C(^{3}He,γ)^{15}N reaction, 20: 32495
OLSEN, A. R., Irradiation behavior of Th–U alloys and compounds, 20: 32833
OLSEN, J., Formal analogy between Compton scattering and Doppler effect, 20: 31995
OLSEN, W. C., Levels in ^{21}Ne using the ^{18}O(α,nγ)^{21}Ne reaction, 20: 32427
OLSON, R. N., Solar-electric propulsion system for interplanetary spacecraft, 20: 31373
OLSSON, Martin, Evidence for a Σ^- η enhancement near threshold, 20: 32103
OMEL'CHENKO, B. D., Programming operation of JINR synchrophasotron, 20: 31840
OMIDVAR, Kazem, Electron capture by protons in H in electric field, 20: 31901 (N-65-34224)
O'NEILL, G. K., Test of quantum electrodynamics by electron-electron scattering, 20: 32305
OOCHO, Emiko, Determination of Ra in river waters, 20: 31191
OPHEL, I. L., Effects of radionuclides on thermal tolerance of fish, 20: 31028 (AECL-2409)
OPSTAD, M. T., Pulsed neutron sources applied to nuclear engineering, 20: 32360
ORBELI, A. L., PMR of H atoms formed in frozen acids irradiated at 77 deg K, 20: 32719
ORDAN'YAN, S. S., Phase diagram of the HfC–Mo system, 20: 31729
O'REILLY, Bruce D., SPENCER: FORTRAN program to approximately reconstitute a one-dimensional function from finite number of its moments, 20: 31658 (NAA-SR-Memo-11653)
ORLOV, N. F., Absorption centers in glasses of simple compositions formed at low temperature, 20: 32733
ORLOV, V. M., Distribution of ^{90}Sr on surface of Atlantic during second part of 1961, 20: 31418
ORLOV, V. M., Strontium-90 in waters of Pacific Ocean. IV., 20: 31415
ORLOV, V. M., Strontium-90 in deep waters of Indian Ocean, 20: 31417
ORLOV, Yu. V., Calculations of CsI(Tl) scintillation γ spectrometer sensitivity, 20: 31564
ORMEROD, M. G., Effect of metal ions on free radical formation and reactions in irradiated proteins, 20: 31003
ORR, J. S., Cellular control systems and radiosensitivity, 20: 31064
ORSENIGO, G., Thorium-uranium fuel cycle in Italy, 20: 32827
ORTEGO, J. D., Chemistry of U(IV). II., 20: 31236
ORTH, P. H. R., Annihilation of positrons in Ar, 20: 32105
OSANOV, D. P., Shielding calculations for cylindrical sources, 20: 32670
OSAWA, Masumi, Observations of the fallout radionuclides at Kanazawa, 20: 31413
OSBORNE, F. J. F., Laboratory scaled solar plasma phenomena, 20: 32284
OSBORNE, F. J. F., Measurements of anisotropic plasmas using turnstile multiple-probe polarimeter, 20: 32581
OSTIDICH, A., Determination of partial α-half-life of ^{241}Pu, 20: 32435
OSWALD, R. B. Jr., Photoconductive properties of CdS and CdSe induced by thermal neutron irradiation, 20: 32736
OTSUKI, Shoichiro, Polarization in elastic pion-nucleon scattering in few-Bev region, 20: 32087
OUTI, Akizi, Non-linear motion of two ion streams in background of high temperature electrons, 20: 32654
OVERSETH, O. E., Backward proton-deuteron elastic scattering from 1.0 to 1.5 Bev, 20: 32102
OWEN, G. E., Reaction study of ^{19}F(d,n)^{20}Ne, 20: 32555
OWEN, W. L., Radiological reclamation performance summary. I., 20: 31454 (USNRDL-TR-967)

P

PADILLA, George M., Radiation-induced division delay in Astasia longa, 20: 31085
PADJEN, R., Broken symmetries and nonleptonic hyperon decays, 20: 32050
PAGE, N. P., Injury accumulation in sheep during protracted gamma radiation, 20: 31026
PAI, Shih-I., Radiation gas dynamics, 20: 32238
PAKHOMOV, P. L., Diffusion of metastable helium atoms in cryogenic plasma, 20: 32602
PAL, Dipti, Heavy particle stripping, 20: 32444
PALAIC, Djuro, Liberation of 5-hydroxytryptamine in brain stem of adrenalectomized rats after x-irradiation, 20: 31069
PALLOTTINO, G. V., Stability of power supply for magnets of the Cambridge Electron Accelerator, 20: 31834
PALMER, H. E., Digital control for whole-body scanner, 20: 31502 (BNWL-235-4, pp 11-14)
PAN, V. M., Melting points of V and Nb of high purity, 20: 31721 (AD-630971)
PANASYUK, V. S., Feasibility of operating electron multipliers as h-f amplifiers, 20: 31485
PANDE, D. N., Temperature dependence of fluorescence decay of uranyl salts, 20: 32690
PANDE, L. K., Axial-vector coupling constant renormalization in β decay, 20: 32157
PANDE, L. K., Bootstrap possibilities of a 70-plet of SU_6, 20: 32151
PANESKO, J. V., IDERM; program for intake, distribution and excretion of radionuclides in mammals, 20: 31441 (BNWL-SA-40)
PANKAJAKSHAN, K., Production of radioisotopes of high specific activity for medical use, 20: 31275
PANT, D. D., Temperature dependence of fluorescence decay of uranyl

salts, 20: 32690
PANT, H. C., Temperature dependence of fluorescence decay of uranyl salts, 20: 32690
PAPA, Robert T., Nonlinear electromagnetic wave propagation in plasmas, 20: 32663
PAPOULAR, Renoud, Spatio-temporal distribution of initial brilliance of laser discharge in air, 20: 32224
PAPPAS, A. C., Radiochemical determination of ^{235}U abundances by activation analysis, 20: 31189
PAPWORTH, D. G., Site distribution parameter for radiation-induced chromosome exchanges, 20: 31057
PARANJPE, S. R., Role of Th in nuclear power program, 20: 32826
PARK, J. F., Whole-body counting of Pu in dogs, 20: 30968 (BNWL-SA-11)
PARK, James F., Long-term study of inhaled Pu in dogs, 20: 31025 (AD-631690)
PARKER, E. N., Penetration of galactic cosmic rays into solar system, 20: 31955
PARKER, R. P., Assay of β-emitting radioisotopes using Cherenkov counting, 20: 31184
PARKINSON, D. H., Ultrahigh magnetic fields, 20: 32337
PARKINSON, E. M., Expansion method for calculating atomic properties. VI., 20: 31934
PARKINSON, M., Meson decay of strongly interacting systems, 20: 32045
PARKS, R. D., Polarized positron annihilation in ferromagnetic nickel, 20: 32703
PARKS, R. D., Thermal conductivity of superconducting surface sheath, 20: 32327
PARNELL, C. J., Effect of O on impairment of proliferative capacity of human cells by radiations LET, 20: 31123
PASSERIEUX, J. P., Levels in ^{60}Ni and ^{62}Ni at high excitation energies, 20: 32490
PASTERNAK, Alan David, Liquid metal extraction of fission products from uranium fuels, 20: 31320 (UCRL-16108)
PASTERNAK, R. A., High-temperature technique for determining terminal solubilities, 20: 31250
PASTERNAK, R. A., Physisorption of Xe and Kr on glass and on Mo films, 20: 31242
PATHAK, K. M., Possible example of a $_{\Lambda}B^{12}$ hyperfragment, 20: 32412
PATIN, S. A., Distribution of ^{90}Sr on surface of Atlantic during second part of 1961, 20: 31418
PATIN, S. A., Forms of existence and migration of artificial radioisotopes in sea waters, 20: 31422
PATIN, S. A., Global distribution of ^{90}Sr on surface of world oceans (1960-1961), 20: 31420
PATIN, S. A., Purity of yttrium isolated from seawater carbonate precipitates, 20: 31249
PATIN, S. A., Reliability of present day chemical determinations of ^{90}Sr in sea water, 20: 31423
PATIN, S. A., Strontium-90 in waters of Pacific Ocean. III., 20: 31414
PATIN, S. A., Strontium-90 in deep waters of Indian Ocean, 20: 31417
PATRICK, R. E., Prog. rpt. on kinetics parameters of highly enriched D_2O reactor, final, 12/65–12/66, 20: 32863 (TID-23037)
PATTERSON, J. R., States of ^{13}N in 20 to 30 Mev region, 20: 32527
PATTORET, A., Thermodynamic and kinetic studies in high-temperature chemistry, 20: 31227
PAUL, P., Lifetimes of first excited states of ^{7}Li and ^{7}Be, 20: 32504
PAULIN, Robert, Anomalous long annihilation mean-lives of positrons in some ionic crystals, 20: 32099
PAULY, J., Determination of minimum detectable content of trace elements in neutron-activated materials, 20: 31541
PAVLICA, R. T., Study of fuel assembly vibrations induced by coolant flow, 20: 32746
PAVLICK, J. E., Effect of prestrain on mechanical recovery in Pu-1Ga, 20: 31753
PAVLOV, Yu. P., Selection of scintillators for counters recording γ radiation, 20: 31574
PAVLOVA, I. B., Ultrafine structure of radioresistant Flexner bacilli, 20: 30966
PAVLOVSKAYA, N. A., Natural content and distribution of thorium in human organism, 20: 30989
PAVLOVSKII, F. A., Measurement of track brightness in spark chamber, 20: 31582
PEARCE, D. W., Prog. rpt. on physical sciences, annual, 1965. IV. Instrumentation, 20: 31473 (BNWL-235-4)
PEARCE, W. A., Proton-proton bremsstrahlung with the Tabakin potentials, 20: 32059
PECORINI, V., Scintillation scanning in kidneys, 20: 31148 (CNEA-170)
PECORINI, Victorio, New colloid of ^{99}Tc in scintillation scanning of the liver, 20: 31147 (CNEA-168)
PEETERS, H. L., Synthesis of oxalic-$^{14}C_1$ acid from acetic-$^{14}C_1$ acid, 20: 31263
PEISL, Hans, Defect formation in uv-irradiated silver chloride, 20: 32731
PEKAR, Yu. A., Theory of positive column of glow discharge in presence of small impurity, 20: 32595
PELLAT, Rene, Calculation of statistical entropy of plasma during equilibrium, 20: 32583
PELLETT, D. E., Backward proton-deuteron elastic scattering from 1.0 to 1.5 Bev, 20: 32102
PELLICCIONI, M., Calculation of shielding around all targets of Frascati linear accelerator, 20: 31820 (LNF-66/14)
PELLISSIER, P., Regenerative beam extraction for Berkeley 88-inch cyclotron, 20: 31827 (UCRL-16794)
PENFIELD, Paul Jr., Hamilton's principle for fluids, 20: 32227
PENFIELD, Paul Jr., Hamilton's principle for electromagnetic fluids, 20: 32228
PENNEY, R., Note on relativistic thermodynamics, 20: 32225
PENSELIN, Siegfried, Van Allen radiation belts, 20: 32274
PEPIN, Robert O., Heavy rare gases in silicates from the Estherville mesosiderite, 20: 31859
PEREL, Joseph, Theory of extended fine structure in absorption of polarized x rays: Application to Ga, 20: 32707
PEREL, Julius, Cesium ion sputtering of Al, Cu, and Ti, 20: 31948
PERLMAN, M. L., L-subshell ratios of some low-energy E2 transitions, 20: 32516
PERLMUTTER, Arnold, Boson resonances, 20: 32089
PERLMUTTER, Arnold, Conferences on symmetry principles at high energy, 3rd Coral Gables, 1/66, 20: 32195
PERLSTEIN, P., Radiolytic isotopic exchange of gaseous nitrogen, 20: 31282
PEROVIC, B., New mass spectrometer ion source for solids, 20: 31204
PERRIN, Claude, Reaction $^{11}B(p,\alpha\alpha)^{8}He$ at 163 kev, 20: 32402
PERRIS, A. D., Effects of whole-body irradiation on transfer capacity of rat small intestine, 20: 31081
PERROTTA, Cornie A., Effect of x irradiation on DNA synthesis in uterine epithelium, 20: 31088
PERROUD, J.-P., Measurement, by gaging, of luminescence pulse forms of organic scintillators, 20: 31529
PERSCHKE, H., Simple technique for hydrogenation of ethylene, 20: 31259
PERSHINA, Z. G., Ultrafine structure of radioresistant Flexner bacilli, 20: 30966
PERSSON, Hans, Electric field parallel to magnetic field in a low-density plasma, 20: 32609
PESTIEAU, J., Partially conserved currents and CP violation in K^0-meson decays, 20: 32021
PETERSON, G., Strontium-90 in beagle hair, 20: 30972 (TID-22027)
PETERSON, Ronald G., Facility for studying elastic moduli as function of temperature, 20: 31708 (ANL-7119)
PETERSON, S., Properties of Th, its alloys, and its compounds, 20: 31767
PETHES, Gyoergy, Measurement of soft β emitters by means of liquid scintillators, 20: 31518
PETRALIA, Stefano, Biological efficiency of 200 kv x rays, ^{60}Co rays and 14-Mev neutrons in Escherichia coli inactivation, 20: 31107
PETRASEK, Donald W., Elevated-temperature tensile properties of tungsten fiber composites, 20: 31770
PETRZILKA, V. A., Incidence of electromagnetic waves on plasma-vacuum boundary, 20: 32588
PETSCHEK, H. E., Experiments with magnetohydrodynamically supported shock layers, 20: 32217 (N-65-33713)
PETSCHEK, H. E., Mechanism for reconnection of geomagnetic and interplanetary field lines, 20: 32277
PETSCHEK, H. E., Reconnection and annihilation of magnetic fields, 20: 31895
PETUKHOV, S. M., Spectrometer of high aperture ratio, 20: 31481 (AERE-Trans-1050)
PEUCHMAUR, Alphonse, Machines for loading and unloading channels of nuclear reactor, 20: 32755
PEUCHMAUR, Alphonse, Nuclear reactors having fuel element channel retaining pawl assembly, 20: 32756
PFENNIG, G., Mathematical treatment of decay and formation laws of radioactivity with graphically solved examples, 20: 32377 (KFK-117)
PHILIPP, L. D., Measurement of mixed-field neutron and gamma dose rates, 20: 31505 (BNWL-235-4, pp 30-4)
PHIPPS, T. E. Jr., Electromagnetic mass observations and nature of space-time, 20: 32548
PIATNEK-LEUNISSEN, D. A., Determination of ^{14}C-lactate adapted to liquid scintillation counting, 20: 31178
PICKEL, T. W., Analysis of parabolic partial differential equation containing both flow and diffusion terms, 20: 31659 (ORNL-TM-1497)
PICKETT, E. A., Prog. rpt. on Zr alloy, 4–6/65, 20: 31677 (GEAP-4840)
PICKETT, G. R., Low-temperature specific heat of dilute Ag–Gd alloys, 20: 31762
PIEL, H., Angular distribution of polarization of recoil proton from photoproduction of neutral pions on H at photon energy of 360 Mev. II., 20: 32097
PIEL, H., Polarization of recoil proton from photoproduction of neutral

pions on H in region of first resonance. I., 20: 32096
PIETSCHMANN, H., Predictions of static quark model on boson decays, 20: 32061
PIHL, Alexander, Radiation sensitivity of cells and base composition of DNA, 20: 31014
PIKETTY, C. A., Final-state Coulomb interaction in quasi-elastic neutrino scattering on nuclei, 20: 32468
PIKETTY, C. A., Time reversal in electroproduction processes, 20: 32042
PILIPENKO, Yu. K., Cryogenic developments at Joint Institute for Nuclear Studies, 20: 32318
PIMAKHOV, A. S., High-heat-resistance plastic scintillators, 20: 31262
PINCKNEY, K. R., Effects of reliability considerations on design of electric thruster arrays, 20: 31359
PINCKNEY, K. R., Light-weight flight prototype ion engine system, 20: 31364
PINEL, Jeques, Traveling-field particle linear accelerator, 20: 31851
PINKAU, Klaus, Measurement of secondary gamma spectrum from 0.2 to 2 Bev in upper atmosphere, 20: 32283
PIPPARD, A. B., Ultrasonic attenuation in superconductors, 20: 32335
PIVOVAROV, L. P., Wide-range intensity meter for heterogeneous magnetic fields, 20: 31487
PLOTNIKOV, V. K., Increased particle momentum dispersion in proton linear accelerators, 20: 31843
PLOTNIKOV, V. K., Nonlinearity of quadrupole lens fields, 20: 31836
POATE, J. M., States of ^{13}N in 20 to 30 Mev region, 20: 32527
POCSIK, G., Currents and sum rules in vector-meson theory, 20: 32125
PODLYASHUK, E. L., Dosage in gonad region in short-range x-ray therapy of angiomas in children, 20: 31156
POFFE, Nino, Extraction by pealing of beam of heavy ions accelerated in cyclotron with starred field, 20: 31828
POHLMEYER, K., Rigorous version of an argument by Coleman, 20: 32133
POLETTI, A. R., Investigation of levels in ^{23}Na below 3 Mev by $^{26}Mg(p,\alpha\gamma)^{23}Na$ reaction, 20: 32509
POLETTI, A. R., Study of the low-lying states of ^{23}Na by $^{26}Mg(p,\alpha\gamma)^{23}Na$ reaction, 20: 32567
POLEVOI, V. A., Strontium-90 in waters of Pacific Ocean. III., 20: 31414
POLEVOII, R. M., Magnetic beta spectrometer with space focusing of electron beams at $\pi\sqrt{10}$ angle, 20: 31583
POLMAN, J., Investigation of transverse plasma diffusion by decay along magnetic field, 20: 32647
POMERANZ, Kalman B., Relativistic rocket, 20: 32294
POOLE, D. H., Production of metallic and other ions in r-f ion source, 20: 31845
POPOV, N. I., Fission products from nuclear test explosions in surface waters of oceans during 1959–1961, 20: 31419
POPOV, N. I., Global distribution of ^{90}Sr on surface of world oceans (1960-1961), 20: 31420
POPOV, N. I., Purity of yttrium isolated from seawater carbonate precipitates, 20: 31249
POPOV, N. I., Reliability of present day chemical determinations of ^{90}Sr in sea water, 20: 31423
POPOV, N. I., Strontium-90 in waters of Pacific Ocean. III., 20: 31414
POPOV, N. I., Strontium-90 in waters of Pacific Ocean. IV., 20: 31415
POPOV, N. I., Strontium-90 in deep waters of Indian Ocean, 20: 31417
POPOV, S., Mesic decay of hyperfragments produced by K⁻ mesons of 1.5 Bev/c, 20: 32491
POPOV, V. D., Physical stand for critical assembly of Institute of Physics at Ukrainian Academy of Sciences, 20: 32770
POPPLEWELL, J., Microwave resonance observations in gadolinium solid solutions, 20: 32716
PORTER, N. S., Animal physiological function telemetry developments, 20: 30961 (BNWL-235-4, pp 25-9)
PORTER, N. S., Biology spectrometer and analyzer, 20: 31525
PORTER, N. S., Fish environment dose rate measurements, 20: 31501 (BNWL-235-4, pp 10-11)
PORTER, N. S., Instrumentation techniques for toxicity studies of inhaled radionuclides, 20: 31475 (BNWL-235-4, pp 19-20)
PORTER, N. S., Physiological data telemetry system, 20: 31474
PORTER, Newell S., Measurement of radionuclide uptake by algae, 20: 31504 (BNWL-235-4, pp 16-18)
POSKANZER, A. M., Beta-delayed protons from ^{28}Si, 20: 32505
POSTERNAK, J. M., Effects of x rays on function and ultrastructure of isolated sympathetic ganglion, 20: 31055
POULET, M., Polarization and spin correlation parameter measurements in 600-Mev proton-proton scattering, 20: 32016
POVSTEN, V. A., Pulsed neutron generator, 20: 32358
POWER, E. A., Suggested experiment to measure part of transverse electromagnetic mass of electron, 20: 32071
POWER, Edwin A., Zero-point energy and the Lamb shift, 20: 31908
PRADHAN, T., Cabibbo angle and the ninth baryon, 20: 32108 (IC-66/59)
PRASAD, R., de Sitter model for elementary particles, 20: 32160
PREM, L. L., Generator development for fluid metal MHD power conversion, 20: 31973
PREMANAND, V., Metallographic observations of plastic deformation in thermally cycled uranium, 20: 31754
PREOBRAZHENSKII, N. G., Calculation of source function for optically dense plasma layer, 20: 32594
PREOBRAZHENSKII, N. G., Influence of surface inhibitors on relaxation time of oriented atoms, 20: 32417
PRESCOTT, J. R., Excited states of ^{11}C from n-γ angular correlations and gamma branching ratios, 20: 32395
PRESTWICH, W. V., Study of the $^{127}I(n,\gamma)^{128}I$ and $^{133}Cs(n,\gamma)^{134}Cs$ reactions, 20: 32422
PRICE, A. M., Annealing of irradiation damage in graphite, 20: 31803
PRIEST, J. R., Inelastic scattering of 39.5 and 31.8 Mev alpha-particles by ^{16}O, 20: 32554
PRILIPKO, L. G., Treatment of radiation leukopenia by bone marrow autotransplantation, 20: 31134
PRIOR, W., Rotational-velocity and ion-density profiles in plasma vortices, 20: 32644
PRONKO, J. G., Levels in ^{21}Ne using the $^{18}O(\alpha,n\gamma)^{21}Ne$ reaction, 20: 32427
PROSSER, F. W. Jr., Spin assignments from triple correlation utilizing axial symmetry, 20: 32372 (COO-1120-43)
PROTOPOPOV, Kh. V., Use of hexafluorobenzene for developing liquid scintillators, 20: 31290
PROTSIK, R., Plutonium and fission product redistribution in mixed oxide fuels, 20: 31804
PROVIDENCIA, J. Da, Ground-state wave function in random-phase approximation, 20: 32303
PROWETT, R. H., SNAP-10A electrically actuated band release device development, 20: 32852 (NAA-SR-Memo-11454)
PRULOV, Y., Fresh fallout in Israel from the second Chinese nuclear detonation, 20: 31408
PUGACHEV, Ya. I., Approsimate theory of red shift in conformally plane space, 20: 31855
PUKHNACHEV, V. V., Differential equation with two small parameters, 20: 32640
PURDOM, Paul Jr., Electromagnetic decay of 1.7 and 2.43 Mev levels in ^{9}Be, 20: 32441
PUSHNITSINA, A. D., Treatment of radiation leukopenia by bone marrow autotransplantation, 20: 31134

Q

QAIM, S. M., Isomeric state (67 min) in ^{240}Np, 20: 32460
QUATART, D., Study of irradiated and unirradiated coated fuel particles by the electron microprobe, 20: 31795
QUIMBY, G. H., Liquid scintillation counting, 20: 30997

R

RACAH, G., Subconfiguration $f^6(^7F)sp$ in Sm I, 20: 31919
RADKEVICH, I. A., Selection of optimum curve of rectangular light pipes with no light losses by reflection, 20: 31818 (ITEF-385)
RADVANYI, P., Experimental study of reaction $D(p,\gamma)^3He$ at 156 Mev, 20: 32486
RAEDLER, K.-H., Calculation of average Lorentz field strength $\overline{v \times B}$ for electrically conducting medium in turbulent motion influenced by Coriolis forces, 20: 32235
RAETHER, H., Energy loss of 50-kev electrons in Ge and Si, 20: 32732
RAETHER, H., Inelastic electron scattering (excitation of plasma losses), 20: 32741
RAETHER, M., Incoherent scattering of microwaves by unstable electron plasma oscillations, 20: 32622
RAETHER, M., Landau damping in inhomogeneous plasmas, 20: 32616
RAEUCHLE, Eberhard, Cyclotron harmonic radiation from plasma in magnetic field, 20: 32637
RAFALSKA, J., Progress in reactor kinetics at Swierk, 20: 32781
RAFTER, T. A., Carbon-14 variations in nature. I., 20: 31433
RAFTER, T. A., Carbon-14 variations in nature. II., 20: 31410
RAGAN, G. L., Evaluation of reactors for irradiation of liquid Pu fast reactor fuels, 20: 32799 (LA-DC-7752)
RAHEJA, U. T., Angular distribution of $^{19}F(n,\alpha)^{16}N$ reaction at E_n = 4.7 Mev, 20: 32434
RAINEY, R. H., Reprocessing methods and costs for selected thorium-bearing fuel types, 20: 31326
RAKHIMOV, R., Energy distribution of electrons from alkali halide compounds bombarded by He^+ and Ar^+ ions, 20: 31912
RAKHUBOVSKII, V. A., Cryotron relaxation oscillator with controlled frequency, 20: 32333
RAKITYANSKII, A. A., Electron beam injection into magnetic quadrant of an accumulator at 100 Mev, 20: 31849
RALLS, K. M., Electronic structure of transition metal-interstitial atom alloy superconductors, 20: 31747
RAM, B., Model of strongly interacting particles, 20: 32130

RAMACHANDRAN, G., Possible test for the $|\Delta I|$ absolute value = 0 weak nuclear force, 20: 32049
RAMAVATARAM, K., Excited states of ^{31}P and the Nilsson model, 20: 32483
RAMBAUD, Francoise, Effects of x rays on platelet environment, 20: 31032 (CEA-R-2953)
RAMM, A. G., Nuclear conditions of integral operators and existence of S matrix in scalar dispersion problem, 20: 32537
RAMM, Wolfgang J., Worldwide geomagnetic disturbances generated by Starfish explosion, 1962, 20: 32264
RAMQVIST, Lars, Hot-pressing of metallic carbides, 20: 31699
RANDEN, K., Experiments on uranium–lithium hydride shields at STIR facility, 20: 32672 (NAA-SR-Memo-11786)
RANSOHOFF, J. A., Producing large quantities of ^{237}Np and ^{238}Pu in commercial power reactors, 20: 32837
RAO, K. Srinivasa, Effects of D-state admixture and hard-core radius on photoproduction of neutral pions from deuterons, 20: 32041
RAO, M. N., Decay constant and mass-yield curve for spontaneous fission of ^{238}U, 20: 32521
RAPOPORT, I. D., Pulse-height recording and logarithmic conversion of pulse heights in the 10^4 to 10^5 dynamic range, 20: 31577
RAPPAPORT, P., Li-doped, radiation-resistant silicon solar cells, 20: 31614
RAPPENEAU, J., Energy released at high temperature by irradiated graphite, 20: 31802
RAPSON, J. E., Strontium isotopes and trace elements in carbonatites and limestones from Ice River, British Columbia, 20: 31406
RASHAD, A. R. M., Theory of linear induction or traveling wave electromagnetic plasma accelerator, 20: 32653
RASHEVSKII, V. P., Plasma gun for producing high electron-current peaks, 20: 31486
RASOR, N. S., Plasma physics of thermionic converters, 20: 31971
RASTOGI, B. P., Physics calculations of thorium-fuelled heavy-water lattices, 20: 32774
RATCLIFFE, C. A., Animal physiological function telemetry developments, 20: 30961 (BNWL-235-4, pp 25-9)
RATCLIFFE, C. A., Miniature dose rate measurement instrument, 20: 31503 (BNWL-235-4, pp 14-16)
RATCLIFFE, C. A., Raindrop charge and velocity measurement techniques, 20: 31476 (BNWL-235-4, pp 21)
RATTI, S., Alternative interpretation of the enhancement observed at $M^0p\pi^+$ 2.52 Bev/c^2, 20: 32040
RATTY, F. J., Prog. rpt. on sensitivity of Drosophila to radiation, three year summary, 1966, 20: 31036 (SAN-529-3)
RAUTH, A. M., Survival of synchronized L cells after uv irradiation, 20: 31084
RAWITSCHER, G. H., Parabolic potential barrier model as an approximation to optical model calculations, 20: 32423
RAWLINSON, W. R., Radiation measurements in commercial aircraft using a single counter, 20: 31952
RAY, M., Steady MHD flow in an annular channel, 20: 32222
RAY, S. R., Details of transfer memory input/output signals, 20: 31649 (COO-1018-1030)
RAY, Sylvian R., ILLIAC III: processor of visual information, 20: 31652 (COO-1018-1057)
RAYCHAUDHURI, A. K., Gravitational collapse in a cosmological background, 20: 32306
RAZMI, M. S. K., Analysis of $p\bar{p} \rightarrow \pi K\bar{K}$ at rest, 20: 32047
READER, Paul D., Durability tests of mercury electron-bombardment ion thrustors, 20: 31374
REDHEAD, P. A., New hot-filament ionization gage with low residual current, 20: 31483
REED, D., Fast neutron dosimetry by anion exchange separation of ^{137}Cs from irradiated Th, 20: 31530
REED, M., Masses and excited states of ^{24}Al and ^{28}P, 20: 32473
REEDER, P. L., Beta-delayed protons from ^{25}Si, 20: 32505
REFSDAL, S., Classification of general relativistic world models, 20: 31863
REID, C., Miniature thermoluminescent dosimetry for application in medicine and biology, 20: 31598
REKALO, M. P., Inelastic processes in interactions of neutrino with nucleons and unitary symmetry, 20: 32090
REMMELG, H., Radiosensitivity of two varieties of Vicia faba L. and of their hybrid, 20: 31054
RENNER, B., Current-algebra prediction of first-order SU_3 violations in ρ and K^* decays, 20: 32035
RESHETNIKOV, A. E., Effect of irradiation of seeds by ^{60}Co γ-rays on forms of water in corn and wheat leaves, 20: 31110
RESNIKOFF, M., The $U(n) \supset R(n)$ problem. I., 20: 32124
RESTELLI, G., Determination of partial α-half-life of ^{241}Pu, 20: 32435
REYNOLDS, J. M., Prog. rpt. on kinetics parameters of highly enriched D_2O reactor, final, 12/65–12/66, 20: 32863 (TID-23037)
REZVYKH, K. A., Pulsed neutron generator, 20: 32358
RHODES, D. N., Treatment of meats with ionizing radiations. XII., 20: 31630
RHODES, W. H., Cationic self-diffusion in calcia-stabilized zirconia, 20: 31732
RIBORDY, C., Decay of ^{51}Cr, 20: 32410
RICE, R. E., BORAX-V nuclear superheat operating experience, 20: 32866
RICHARDSON, Robert D., Process gas chromatograph for measurement of impurities in He, 20: 31210
RICHMOND, C. R., Half-life of ^{128}I, 20: 32406
RICHMOND, J. Kenneth, Performance of arc heaters for MHD experiments, 20: 31356 (N-66-12435)
RICHTER, B., Test of quantum electrodynamics by electron-electron scattering, 20: 32305
RICHTER, J. M., Detection and measurement of gamma rays in presence of high intensity neutron flux, 20: 31602
RICKARD, W. H., Radionuclides in terrestrial and freshwater biota, 20: 31428 (PNE-481, pp 1165-1200)
RICKEY, M. E., J dependence in the (p,α) reaction, 20: 32489
RIDLEY, R. G., Tandem mass spectrometer for isotopic analysis, 20: 31206
RILEY, Clyde, Cross sections and isomer ratios for $^{88}Sr(^3He,p)^{90m,90g}Y$ reaction, 20: 32430
RINGEL, V., Use of uniform half lives of important radionuclides, 20: 32421
RISPOLI, B., Control system for triple-axis neutron spectrometer, 20: 31543
RITCHIE, D., Potentials of solar power electric propulsion, 20: 31382
RITCHIE, W. B., Data compilation and evaluation of space shielding problems, 20: 32674 (NP-15697(Vol.3))
ROALSVIG, J. P., Directional correlations in ^{127}I, 20: 32396
ROBB, J. C., Charge transfer and atom transfer in ion-molecule interactions studied by time-of-flight mass spectrometer, 20: 31224
ROBERTS, C. S., Rotational excitation of H_2 and D_2 by H impact, 20: 31932
ROBERTS, Charles S., Electron loss from the Van Allen zones due to pitch angle scattering by electromagnetic disturbances, 20: 32288
ROBERTS, J. T., Reprocessing methods and costs for selected thorium-bearing fuel types, 20: 31326
ROBERTS, Kenneth F., Dissolved-oxygen analyzer for oceanographic use, 20: 31171 (ORO-596)
ROBERTS, Paul A., Frequency of x-ray induced crossover-suppressing aberrations recovered from oocytes and sperm of Drosophila, 20: 31047
ROBERTS, R. G., Analysis of $p\bar{p} \rightarrow \pi K\bar{K}$ at rest, 20: 32047
ROBERTS, William T., Environmental model for Van Allen belt protons, 20: 32244 (N-66-13126)
ROBERTSON, A. J. B., Production of field ionization mass spectra with sharp edge, 20: 31198
ROBERTSON, J. S., Tissue-equivalent ionization chamber for in-phantom dosimetry, 20: 31524
ROBERTSON, James S., Extracorporeal irradiation of blood in humans, 20: 31000
ROBERTSON, W. W., Hornbeck-Molnar cross-sections for the n = 3 states of He, 20: 31947
ROBISCOE, R. T., Remeasurement of the Lamb shift in H,n = 2, 20: 31925
ROBKIN, M. A., Burnup analysis in lumpy fuel, 20: 32836
RODOT, Michel, Properties of cadmium telluride diodes and application to detection of nuclear particles, 20: 31523
ROE, B., Observation and properties of neutral A_2 meson, 20: 32064
ROEHR, H., Measurements of ion and electron temperature in theta-pinch plasma, 20: 32621
ROEMER, J., Gamma transitions and energy levels in ^{161}Dy, 20: 32463
ROHRMANN, C. A., Irradiated wood-plastic materials commercialization, 20: 31624 (BNWL-261)
ROKOP, D., Anisotropy of self-diffusion in alpha uranium, 20: 31771
ROLL, P. G., Cosmic background radiation at 3.2 cm—support for cosmic blackbody radiation, 20: 31957
ROMAN, P., Physical state vector-space representations of noncompact groups, 20: 31663
ROMAN, P., Relativistic fields with spacelike momentum spectra, 20: 32146
ROMAN, S., Polarization of 17.8 Mev protons elastically scattered by nuclei, 20: 32439
ROMANI, R. J., Mitochondria: increase in oxidative capacity and quantitative recovery after massive doses of radiation, 20: 31633
ROMANOV, V. A., Computations on accelerator tubes in oblique fields, 20: 31842
ROMANOV, Yu. I., Neutrino scattering on bound electron, 20: 32005
ROMEGGIO, M., Influence of Al content and temperature on elastic and plastic properties of solid solution of Fe–Al, 20: 31751
ROMEO, Raffaello, Polarographic investigation on Pu(IV) in sulfuric acid solution, 20: 31302
ROMERO, Jacob B., Potentialities of radioisotope propulsion for space probes, 20: 31361

ROSATI, S., Direct numerical solution of three-body problem, 20: 32498
ROSE, D. J., Combined anode-cathode feed of hollow-cathode arc, 20: 32600
ROSE, D. J., Plasma diagnostics using lasers, 20: 32598
ROSE, D. J., Plasma diagnostics by Thomson scattering of laser beam, 20: 32599
ROSE, M. E., Nuclear structure effects in bremsstrahlung, 20: 32456
ROSE, P. H., Experiments with magnetohydrodynamically supported shock layers, 20: 32217 (N-65-33713)
ROSEBROCK, T. L., Nonequilibrium ionization for MPD power generation, 20: 31963
ROSEN, J., Relativistic fields with spacelike momentum spectra, 20: 32146
ROSEN, S., Phase relations in the system $CoNb_2O_6$–$CoTa_2O_6$, 20: 31734
ROSENBERG, Barnett, Physical approach to visual receptor process, 20: 30963
ROSENBERG, G. S., Safety analysis for ZPR-9 facility, 20: 32858 (ANL-7166)
ROSENTHAL, M. W., Technical and economic characteristics of Th reactors, 20: 32834
ROSS, R., Decay $^{157}Eu(\beta^-)^{157}Gd$, 20: 32465
ROSSI, Harold H., Energy requirements and RBE cytogenetic phenomenon in maize by irradiating seeds, 20: 31092
ROSWIT, B., Miniature thermoluminescent dosimetry for application in medicine and biology, 20: 31598
ROTA, A., Time resolution measurements with XP 1020 photomultipliers, 20: 31552
ROTH, J. Reece, Nonadiabatic particle losses in axisymmetric and multipolar magnetic fields, 20: 32545
ROTHE, K. W., Proton-proton bremsstrahlung at 204 Mev, 20: 32062
ROTHMAN, S. J., Anisotropy of self-diffusion in alpha uranium, 20: 31771
ROTHSTEIN, J., Arc spot as dense plasma maintained by micro analogs of macro beams, 20: 32648
ROTHWARF, F., Superheating and supercooling in superconducting transition of small In spheres, 20: 32331
ROTZ, J., Formation of debris from buildings by blast and fire effects of nuclear weapons, 20: 31332 (URS-651-4)
ROWE, P. C., Analysis of external radiation exposures in 1965, 20: 31439 (AECL-2540)
ROWLANDS, J. L., Interpretation of Doppler and Na reactivity worth measurements in zero power reactors, 20: 32869
ROY, A. P., Rotational behavior of ammonium ion in salts, 20: 31241
ROZGONYI, G. A., Increase of residual background gases during ultrahigh-vacuum mass-spectroscopic analysis, 20: 31390
RUBINSTEIN, H. R., Dashen-Frautschi method and parity-conserving baryon-meson couplings, 20: 32138
RUDD, M. E., Analog plotting system for recording energy spectra of low-energy charged particles, 20: 31592
RUDGE, M. R. H., Ionization of hydrogen and of hydrogenic positive ions by electron impact, 20: 31928
RUEDENAUER, F., New electrostatic time-of-flight mass spectrometer, 20: 31209
RUFEH, F., Transport parameters of Cs ions in Cs vapor, 20: 31972
RUGH, Roberts, Previous reproductive history and susceptibility to x-ray-induced congenital anomalies, 20: 31066
RUIJGROK, Th. W., Operator method for angular momentum and SU_3, 20: 32166
RUMBAUT, N. A., Synthesis of oxalic-$^{14}C_1$ acid from acetic-$^{14}C_1$ acid, 20: 31263
RUNDO, J., Estimation of total hydrogen content of human body, 20: 30993
RUPAAL, A. S., Excited states of ^{11}C from n-γ angular correlations and gamma branching ratios, 20: 32395
RUPERT, Claud S., Reactivation after photobiological damage, 20: 31039
RUSHWORTH, P. M., Application of nuclear radiation to pumping of lasers, 20: 32740
RUSSELL, B., Behavior of He gas in irradiated Cu–B alloys, 20: 31797
RUSSELL, B., Spontaneous grain boundary swelling in irradiated Cu–B alloys, 20: 31798
RUSSELL, L. E., Safety aspects of carbide fast reactor fuels, 20: 31675
RUSSO, V., Alternative interpretation of the enhancement observed at $M^2_{p\pi^+}$ 2.52 Bev/c^2, 20: 32040
RUST, R. H., Fractionation of copper in neutron-activated soils, 20: 31325
RYBA, E., Melting points of $REZn_2$ intermetallic compounds, 20: 31743
RYCHEV, A. S., Determination of negative reactivity by shot source method, 20: 32864
RYDER, L. H., Covariant magnetic-moment operator for SU_6, 20: 32053
RYDKII, S. G., Effect of physiologically active compounds and radiation on metabolism in wheat, 20: 31002
RYDKII, S. G., Effects of spaceflight factors on wheat seeds, 20: 31058
RYL'TSEV, P. I., Plasma gun for producing high electron-current peaks, 20: 31486
RYTER, C., Polarization and spin correlation parameter measurements in 600-Mev proton-proton scattering, 20: 32016

S

SAAD, Michel A., Conference on heat transfer and fluid mechanics, Santa Clara, 6/66, 20: 31351
SAARI, J. M., New type of low-resolution mass spectrometer, 20: 31169 (D-1-82-0508)
SACHS, M., Comments on a paper by R. A. Berg on general spin equations, 20: 32145
SACTON, J., Final-state interactions in mesonic decay of mass-4 hypernuclei, 20: 32477
SADEH, D., Monte Carlo calculations for a gamma-ray telescope, 20: 31554
SADOVSKII, A. P., Spectrometer for studying fine structure of x-ray spectra (URS-11), 20: 31581
SAHOTA, H. S., Measurement of Compton scattering cross section, 20: 32007
SAINFORT, G., Influence of Al content and temperature on elastic and plastic properties of solid solution of Fe–Al, 20: 31751
SAITO, Hiroshi, Labeling of myeloma cells and leukemic leukocytes, 20: 30971 (ORINS-45)
SAITO, Shigeko, Effect of green tea and related substances on G-I absorption of ^{90}Sr, 20: 30987
SAKAI, Kenji, Reaction $(\gamma\pi^-p)$ with complex nuclei, 20: 32530
SAKAI, Mitsuo, INS mass spectrometer, 20: 31208
SAKAI, Mitsuo, New weak beta transition from ^{88}Y, 20: 32453
SAKAMOTO, Yoshiyuki, Momentum distribution of recoil nucleus in the $^{12}C(p,2p)^{11}B$ reaction, 20: 32529
SAKANOUE, Masanobu, Adsorption and electrodeposition of protactinium, 20: 31243
SAKANOUE, Masanobu, Observations of the fallout radionuclides at Kanazawa, 20: 31413
SAKITA, B., Symmetry of the strong coupling theory, 20: 32207
SAKOVICH, V. A., Optimum ratio of neutron and gamma dose behind reactor shielding, 20: 32676
SAKURAI, J. J., Speculations on real part of forward $pp(\bar{p}p)$ scattering amplitude, 20: 32065
SALAK, W. W., Direct irradiation of lymph nodes with ^{131} tagged ethiodol, 20: 31044
SALAM, A., Coupling of noncompact group representations, 20: 32169
SALASYUK, V. M., Calculation of cross sections for deuteron photodisintegration and neutron capture in case of nonlocal potential, 20: 32004
SALAT, A., Microscopic description of plasma and nonlinear incoherent light scattering, 20: 32572 (IPP-6/49)
SALESSE, M., Industrial fabrication of fuel elements in France, 20: 31693
SALMON, R., Production of ammonia using electricity from nuclear desalination reactor complex, 20: 32841 (ORNL-3882)
SALMON, Royes, Procedure and code for calculating cost of electricity produced by nuclear power stations, 20: 32743 (ORNL-3944)
SAL'NIKOV, O. A., Time-of-flight neutron spectrometer, 20: 31566
SALUNKHE, D. K., Effects of gamma radiation on freeze-dehydrated apples (Pyrus malus), 20: 31631
SALZBERG, Allen M., Exact statistical thermodynamics of non-extensive systems, 20: 32237
SAMADDAR, S. N., Electro-acoustic lateral waves in hot plasma, 20: 32590
SAMIOS, N. P., Boson resonances, 20: 32089
SAMPLE, J. T., Levels in ^{21}Ne using the $^{18}O(\alpha,n\gamma)^{21}Ne$ reaction, 20: 32427
SAMPSON, W. B., Superconducting quadrupole lens, 20: 31815 (BNL-10144)
SAMUELS, L. D., Depletion of mouse spermatogonia following exposure to ^{210}Po, 20: 31063
SANDER, H. H., Transient annealing in semiconductor devices following pulsed neutron irradiation, 20: 31613 (SC-DC-66-1443)
SANDERS, Richard Lenoir, Polarization of protons scattered from ^3He, 20: 32543
SANDERSON, J. J., Motion of charged particle in plane electromagnetic wave, 20: 32003
SANEVSKA, T., Irradiation of combined emulsion and spark chamber system, 20: 31569
SANGSTER, D. F., Absorption spectra and transient species found in pulse radiolysis of alkaline aqueous benzoate solutions, 20: 31281
SANJANA, S. M., Production of radioisotopes of high specific activity for medical use, 20: 31275
SANNER, Tore, Radiation sensitivity of cells and base composition of DNA, 20: 31014
SANTHOLZER, Vilem, Quantitative determination of radionuclides using gamma spectra, 20: 31186
SANTO, R., Mirror reactions $^{10}B(d,t)^9B$ and $^{10}B(d,^3He)^9B$ at 11.8 Mev, 20: 32481
SANTORO, R. P., Neutron-diffraction study of $Bi_4Si_3O_{12}$, 20: 31254
SANTORO, R. T., Constant current source for instrument calibration,

20: 31588
SANTOS, J. C., Thorium-cycle possibilities in Brazilian nuclear power program, 20: 32821
SAPERSTEIN, A. M., Dispersion-relation approach to absorptive correction in peripheral model of high-energy physics, 20: 32022
SAPERSTEIN, Alvin M., Interaction radius independent theory of resonance and direct nuclear reactions, 20: 32387
SAPOROSCHETZ, Inno B., Inhibition of selected photosensitizers by agents of varying antioxidant activity, 20: 31018
SAPOZHNIKOV, V. V., Effects of higher harmonics on behavior of sub-critical reactor, 20: 32777
SARANTITES, D. G., Prog. rpt. on low-energy nuclear reactions and nuclear spectroscopy, 9/65–6/66, 20: 32373 (COO-1530-1)
SAR-EL, H. Z., Spherical condenser as an analyzer. I., 20: 31549
SARKAR, S., Lepton scattering and the anapole, 20: 32070
SARYCHEV, M. A., Effect of Be-reflector duty factor on thermal neutron flux in horizontal beams, 20: 32765 (IAE-957)
SASAKI, Hideho, Fallout radioactivity due to underground nuclear test of USSR, Jan. 15, 1965, 20: 31405
SASAKI, Hideho, Giant particles contained in fallout. V., 20: 31412
SASAKI, Hideho, Radioactive rain, snow, and atmospheric contamination observed in Nagaoka City, Japan. II., 20: 31411
SASAKI, M. S., Proliferation of human lymphocytes in culture, 20: 31067
SATHYANESAN, A. G., Effects of whole-body irradiation on adrenal of Carassius auratus, 20: 31094
SATO, Jun, Application of perturbed angular correlation to hot-atom chemistry of Re, 20: 31311
SATO, Kazuo, Effects of x radiation on HeLa cells, 20: 31056
SATO, Shigeo, Formulation of theory of elementary particles, 20: 32076
SATO, Taichi, Extraction of U(VI) from HCl solutions by aliphatic amines, 20: 31322
SATTEN, R. A., Coupling between H^- localized modes and rare-earth ion electronic states in rare-earth trifluorides, 20: 32709
SATTEN, Robert A., Temperature dependence of vibronic transitions in crystals and spectroscopic observation of phase transition, 20: 32737
SAVAGE, John R. K., Site distribution parameter for radiation-induced chromosome exchanges, 20: 31057
SAVENKO, I. A., Pulse-height recording and logarithmic conversion of pulse heights in the 10^4 to 10^5 dynamic range, 20: 31577
SAWAI, S., Thorium fuel utilization research in Japan, 20: 32828
SAWYER, J. C., Prog. rpt. on determination of elevated-temperature fatigue data non refractory alloys, 1–4/66, 20: 31710 (NASA-CR-54983)
SAZONOV, M. I., Plasmatron with interelectrode insert, 20: 32592
SCADRON, Michael D., General non-dynamical formalism for reactions with particles of arbitrary spin, 20: 32382 (UCRL-14582-T(Rev.1))
SCARF, F. L., Origin of solar wind, 20: 31893
SCARF, Frederick L., Effect of coherent density fluctuations on radar determination of total electron content, 20: 31857
SCARPA, G., Present views of dosimetry with solid-state detectors, 20: 31560
SCAVUZZO, R. J., Post buckling behavior of hydraulically collapsed assembly fuel plates, 20: 32794
SCAVUZZO, R. J., Structural analysis of fuel growth in fuel plates, 20: 31806
SCHAD, O., Prog. rpt. on critical heat flux (burnout) in boiling water, 7-9/65, 20: 31342 (EURAEC-1482)
SCHAEFER, H., Spectrometry of soft x-rays in proportional counters. II., 20: 31545
SCHAUER, Dale A., Contact conductance measurements during transient heating, 20: 31712 (UCRL-14227(Rev.1))
SCHEER, J., Neutron-induced reactions on silicon, 20: 32431
SCHELLENBERG, L., Improvement of luminosity of double focussing β spectrometer, 20: 31559
SCHELLINGER, W. V., UCAPP: union carbide apt post processor, 20: 31327 (K-1671)
SCHELLINGER, W. V., UCAPP: Union Carbide APT Post Processor, first edition, 20: 31478 (K-1670)
SCHENCK, G. O., Radiation-chemical carboxylation of formic acid and methanol in aqueous solution, 20: 31278
SCHENK, W., UCAPP: Union Carbide APT Post Processor, first edition, 20: 31478 (K-1670)
SCHER, W. A., Reaction $^6Li(d,n)^7Be^*$ with polarized deuterons, 20: 32411
SCHIFFER, J. P., Dependence of angular distribution of the (d,p) reaction on total angular-momentum transfer. II., 20: 32512
SCHIFFER, Lewis M., Extracorporeal irradiation of blood in humans, 20: 31000
SCHILEO, G., Recycle of HWOCR thorium fuel, 20: 31317 (BAW-393-3)
SCHITTENHELM, C., Normal vibrations of potassium iodide, 20: 32710
SCHLEICHER, H. W., Study of irradiated and unirradiated coated fuel particles by the electron microprobe, 20: 31795
SCHLEMPER, Elmer O., Neutron-diffraction study of structures of ferro-electric and paraelectric ammonium sulfate, 20: 32698
SCHLESSINGER, L., Analyticity as a useful computation tool, 20: 32162
SCHMID, Joseph R., LIZARD-IV: program to solve nonlinear, ordinary differential equations, 20: 31657 (KAPL-M-6548)
SCHMIDT, F. H., Proton spin flip in the reaction $^{60}Ni(p,p')^{60*}Ni$ (1.33) at 10.5 and 14.0 Mev, 20: 32557
SCHMIDT, George, Physics of high temperature plasmas, 20: 32641
SCHMIDT, H., Spectrometry of soft x-rays in proportional counters. I., 20: 31544
SCHMIDT, H., Spectrometry of soft x-rays in proportional counters. II., 20: 31545
SCHMIDT, J. J., Resonance properties of main fertile and fissionable nuclei, 20: 32551
SCHNEIDER, R. J., Loss of charged particles by nuclear interactions in scintillators, 20: 31542
SCHNEIDER, R. T., Closed loop MPD power generation experiment, 20: 31975
SCHOBER, M., Chemistry of U(IV). II., 20: 31236
SCHOCH, K., Electrically pumped liquid helium transfer system, 20: 32348
SCHOEN, R. I., New type of low-resolution mass spectrometer, 20: 31169 (D-1-82-0508)
SCHOLZ, W., Evidence of deformation in ^{51}V, 20: 32513
SCHOTT, Garry L., Post-induction kinetics in shock initiated H_2–O_2 reactions, 20: 31217 (LA-DC-7661)
SCHRAM, B. L., Amplification factors of particle multiplier for multiply charged noble gas ions, 20: 31926
SCHRAM, B. L., Ionization cross-section measurements for 0.6- to 20-kev electrons in atomic and molecular gases, 20: 31906
SCHUESSLER, H. A., Level crossing experiment in the $6^2P_{3/2}$ state of Rb–I spectrum, 20: 31940
SCHULTEN, R., Thorium in pebble-bed reactors, 20: 32825
SCHULTZ, Vincent, Bibliography on terrestrial and freshwater radio-ecology, 20: 30967 (TID-3910(Suppl.4))
SCHULZ, Norbert, Half life of the 570-kev excited level of ^{207}Pb, 20: 32401
SCHULZE, P., Experimental techniques, applications, and theory of field ion mass spectrometry, 20: 31199
SCHWARTZ, C., Analyticity as a useful computation tool, 20: 32162
SCHWARTZ, L. H., Intensity and resolution in time-of-flight method for neutron diffraction, 20: 32701
SCHWARTZ, S. B., Ionization of hydrogen and of hydrogenic positive ions by electron impact, 20: 31928
SCHWARZ, K., Nuclear reactors: possibility of supplying heat needs, 20: 32844
SCHWINGER, Julian, Magnetic charge and quantum field theory, 20: 32209
SCINTEI, Neculai, Simultaneous measurement of beam energy in angular distribution studies, 20: 32403
SCOTT, H. D., Test of distorted-wave stripping theory by $^{52}Cr(d,p)^{53}Cr$, 20: 32459
SEARCY, Alan W., Vapor pressure and heat of sublimation of CeF_3, 20: 31238
SEARS, V. F., Theory of cold neutron scattering by homonuclear diatomic liquids. I., 20: 32353
SEARS, V. F., Theory of cold neutron scattering by homonuclear diatomic liquids. II., 20: 32354
SEEBER, Jose Martinez, New colloid of ^{99}Tc in scintillation scanning of the liver, 20: 31147 (CNEA-168)
SEEGER, P. A., Electromagnetic decay of 1.7 and 2.43 Mev levels in ^9Be, 20: 32441
SEELMANN-EGGEBERT, W., Mathematical treatment of decay and formation laws of radioactivity with graphically solved examples, 20: 32377 (KFK-117)
SEEMANN, K. W., Double differential scattering cross sections and scattering law for H_2O at 302°K, 20: 32350 (KAPL-M-6536)
SEGAL, D. J., Neutron-diffraction study of $Bi_4Si_3O_{12}$, 20: 31254
SEGARD, Emile, Factors acting on incorporation of radiophosphoric acid in RNA of rat hepatocytes, 20: 30976
SEGUR, P., Detection efficiency of spark chambers and its exact calculation, 20: 31558
SEIGEL, Daniel G., Frequency of live births among survivors of Hiroshima and Nagasaki atomic bombings, 20: 31091
SEITZ, Frederick, Solid state physics. Vol. 18, 20: 32718
SEIYAMA, Takeyoshi, Optical absorptions of neutron-irradiated ZnS, 20: 31272
SEKI, Hiromaro, Relation between excretion of radiostrontium and intake of Na phytate, 20: 30977
SEKI, Takakazu, Determination of radiation effect of the body. I., 20: 31141
SELBIN, J., Chemistry of U(IV). II., 20: 31236
SELECKI, A., Single-well method for determining direction of flow of ground water using a neutron source, 20: 31430
SELGA, M., Effect of uv radiation on pigments in cucumber and tomato plants, 20: 31059
SELIGER, R. L., Effects of reliability considerations on design of electric thruster arrays, 20: 31359

SELIGER, R. L., Solar-electric propulsion system for interplanetary spacecraft, 20: 31373
SELLEN, J. M. Jr., Solar wind simulation with the Pioneer spacecraft, 20: 31877
SEMCHYSHEN, M., Improving ductility of Mo, 20: 31741
SEMLER, Thor T., Monte Carlo interpretation of sphere transmission experiments for average capture cross sections at 24 kev, 20: 32378 (NASA-TR-R-239)
SEN, S., Note on broken SU_3 symmetry, 20: 32019
SENFTLE, F. E., Mineral exploration and soil analysis using in situ neutron activation, 20: 31434
SENINA, A. V., Calculation of source function for optically dense plasma layer, 20: 32594
SENINA, S. V., Calculation of source function for optically dense plasma layer, 20: 32594
SENINA, S. V., Influence of surface inhibitors on relaxation time of oriented atoms, 20: 32417
SERBINOV, A. N., Computations on accelerator tubes in oblique fields, 20: 31842
SERBINOV, A. N., Pulsed neutron generator, 20: 32358
SERGOLLE, Henri, Extraction by pealing of beam of heavy ions accelerated in cyclotron with starred field, 20: 31828
SEROV, A. F., Feasibility of operating electron multipliers as h-f amplifiers, 20: 31485
SEVOST'YANOV, Yu. A., Calculations of CsI(Tl) scintillation γ spectrometer sensitivity, 20: 31564
SEYMOUR, Allyn H., Radiological analyses of marine organisms, 20: 31427 (PNE-481, pp 1141-9)
SHAFER, M. W., Preparation and Faraday rotation of divalent europium glasses, 20: 31733
SHAIKH, A. Q., Mutation types in irradiated population of Jute, 20: 31027 (AECD/AG-14)
SHALMON, E., Fresh fallout in Israel from the second Chinese nuclear detonation, 20: 31408
SHALMON, Eliahu, Deposition of fission products of stratospheric origin on tropospheric aerosols, 20: 31459
SHAM, L. J., Self-consistent equations including exchange and correlation effects, 20: 31946
SHAPIRA, Y., Effect of spin-orbit scattering on upper critical field of high-field superconductors, 20: 32330
SHAPIRO, F. L., Pulsed reactor cold-neutron measuring device, 20: 31567
SHAPIRO, Mark H., Present status of double beta decay, 20: 32562
SHAW, Graham, Photopion production, dispersion relations, and ypn coupling, 20: 31996
SHAW, J., Nuclear measurements with a low power critical assembly, 20: 32773
SHAW, P. B., Photon-induced beta decay in stellar interiors, 20: 31878
SHEARD, F. W., Microwave-enhanced critical supercurrents in constricted tin films, 20: 32328
SHEEN, E. M., Biology spectrometer and analyzer, 20: 31525
SHEEN, E. M., Digital control for whole-body scanner, 20: 31502 (BNWL-235-4, pp 11-14)
SHEEN, E. M., Miniature dose rate measurement instrument, 20: 31503 (BNWL-235-4, pp 14-16)
SHEFOV, N. N., Atomic hydrogen and helium in airglow, 20: 32289
SHELAMOV, V. A., Determining structure of sintered materials by ionic bombardment, 20: 31765
SHELDON, John W., Cross section for ionization of alkali atoms by collision with excited noble gas atoms, 20: 31917
SHELDON, R., Radiation absorbed by particle accelerator structural components, 20: 31832
SHELINE, Raymond K., Nonadiabatic effects of nuclear rotational spectra, 20: 32492
SHELTON, H., Experimental study of porous metal ionizers, 20: 31389
SHEN, C. N., Control of absorption cross section for nuclear rocket, 20: 32851 (N-65-30544)
SHEN, Y. R., Interaction between light waves and spin waves, 20: 32735
SHERMAN, C. H., Damage production in electron-irradiated palladium, 20: 31805
SHERWOOD, R. C., Localized moments, 20: 32739
SHIER, J. S., Superconducting transitions of amorphous bismuth alloys, 20: 32341
SHIFLETT, Maureen A., Microbial flora of irradiated Dungeness crabmeat and Pacific oysters, 20: 31626
SHIMA, Makoto, Geochemical studies of stable isotopes. III., 20: 32245 (NSJ-tr-48)
SHIMMINS, A. J., Identification of extragalactic radio sources between declinations 0° and +20°, 20: 31853
SHIMOMURA, Ryutaro, Boiling heat transfer at coexistence of nucleate and film regions, 20: 31345 (NSJ-tr-47)
SHIRANE, G., Magnetic structure of $FeSb_2O_4$, 20: 32705
SHISHKIN, G. V., Effects of higher harmonics on behavior of subcritical reactor, 20: 32777
SHIVELY, James N., Radiation-induced changes in properdin system of dog, 20: 31013
SHKATULA, A., Pulsed reactor cold-neutron measuring device, 20: 31567
SHLEIEN, B., Local ground-level air concentrations of ^{210}Pb at Winchester, Massachusetts, 20: 31407
SHLYAPNIKOV, P. V., Optimization of measurements of electron energy in heavy-liquid bubble chambers, 20: 31568
SHMIDT, N. K., Possibility of therapeutic application of bone marrow autotransplantation in uneven irradiation, 20: 31133
SHMIDT, N. K., Treatment of radiation leukopenia by bone marrow autotransplantation, 20: 31134
SHOMBERT, Donald James, Radiation measuring apparatus, 20: 31604
SHONO, Yoshihiko, ESR of human black hair, 20: 31075
SHONO, Yoshihiko, Optical absorptions of neutron-irradiated ZnS, 20: 31272
SHOUDY, A. A., Carbon in primary Na system of Enrico Fermi Atomic Power Plant, 20: 32809 (TID-23101)
SHTARKOV, L. N., Investigation of neutron counter efficiency at intermediate energies, 20: 31584
SHULTS, Gary, Cryogenics in food irradiation, 20: 31634
SHUPPE, G. N., Heat of adsorption of Cs on filamentary W, 20: 31730
SHUTE, G. G., Angular correlations for $^{12}C(p,p'\gamma)^{12}C$. II., 20: 32438
SIAMBIS, John G., First order correction to first adiabatic invariant, 20: 32669
SIDLYARENKO, V. I., Creation and destruction of color centers in alkali-halide crystals, 20: 32691
SIEMON, Richard E., Elastic collisions as Lorentz transformations with application to Compton scattering, 20: 31994
SIEMSSEN, R. H., J dependence in the $(^3He,\alpha)$ reaction, 20: 32508
SIEWERT, I., Spectrometry of soft x-rays in proportional counters. I., 20: 31544
SIEWERT, I., Spectrometry of soft x-rays in proportional counters. II., 20: 31545
SIFFERT, P., Decay of ^{51}Cr, 20: 32410
SIGMUND, Peter, Simple nonbinary scattering model applicable to atomic collisions in crystals, 20: 31920
SIGNORELLI, Robert A., Stress-rupture properties of tungsten wire from 1200° to 2500°F, 20: 31711 (NASA-TN-D-3467)
SIIVOLA, Antti, Alpha-active platinum isotopes, 20: 32458
SIL'CHENKO, N. N., Possibility of therapeutic application of bone marrow autotransplantation in uneven irradiation, 20: 31133
SILVA, R. J., Level structure of ^{92}Mo, 20: 32471
SILVA, R. W., Probe observations of solar wind-geomagnetic field interaction region, 20: 32286
SILVER, A. H., Macroscopic quantum interference in superconductors, 20: 32344
SILVER, R. S., Fresh water from sea, 20: 31193
SIL'VESTROV, L. V., Irradiation of combined emulsion and spark chamber system, 20: 31569
SIMENOG, I. V., Inelastic scattering of electrons by light nuclei, 20: 32536
SIMINOVIC, J., Mesic decay of hyperfragments produced by K- mesons of 1.5 Bev/c, 20: 32491
SIMONS, E. M., Reactor materials, Vol. 9, No. 1, 20: 31665
SIMONS, H. A. B., Effect of radioprotective compounds on incorporation of tritiated thymidine into mammalian cells, 20: 31125
SIMPSON, K. M. Jr., Data compilation and evaluation of space shielding problems, 20: 32674 (NP-15697(Vol.3))
SINANOGLU, Oktay, Meson spectrum and internal dynamics, 20: 32203
SINCLAIR, D., Observation and properties of neutral A_2 meson, 20: 31864
SINGH, B. B., Effect of metal ions on free radical formation and reactions in irradiated proteins, 20: 31003
SINGH, M., Measurement of Compton scattering cross section, 20: 32007
SINGH, R. S., Parametric studies of reactivity coefficients for large ^{233}U–TH-fueled fast reactors, 20: 32790 (ANL-6930)
SINGH, R. S., Physics aspects of large thorium-fuelled fast reactors, 20: 32775
SINHA, A. P. B., Synthesis of new europium chelates, 20: 31232
SINNHUBER, R. O., Microbial flora of irradiated Dungeness crabmeat and Pacific oysters, 20: 31626
SIVITSKI, R., Radiation protection at WWRS-type reactor "EWA", 20: 32877
SKADRON, G., Model for origin and properties of cosmic-ray rigidity spectrum, 20: 31954
SKALAFURIS, Angelo J., Radiative shock structure: theory and observations, 20: 32670
SKOLOZDRA, R. V., X-ray structural analysis of some Zr–Fe and Zr–Cr alloys, 20: 31727.
SKOROPOD, Yu. D., Irradiation of head, 20: 31060
SKZHIPCHAK, Z., Irradiation of combined emulsion and spark chamber system, 20: 31569
SLATTERY, G. F., Effect of hydride on thermal expansivity of Zr alloys,

20: 31745
SLODZIAN, Georges, Microanalysis by secondary ion emission, 20: 31200
SLOOTEN, H. S. G., Sol-gel processes for Th fuel production, 20: 31700
SLOVOKHVATOV, L. I., Investigation of neutron counter efficiency at intermediate energies, 20: 31584
SLUIJTER, F. W., Wave propagation through Epstein density profile across inhomogeneous magnetic field, 20: 32625
SLUYTER, M. M., Thermionic power generation from reentry vehicles, 20: 31961 (SC-DC-66-1115)
SMALL, R. L., Plasma injected into B_z guide field from conical theta-pinch accelerator, 20: 32661
SMIRNOV, E. V., Plasma gun for producing high electron-current peaks, 20: 31486
SMITH, A. W., Permeability of zirconia, hafnia, and thoria to O, 20: 31731
SMITH, B. H., Regenerative beam extraction for Berkeley 88-inch cyclotron, 20: 31827 (UCRL-16794)
SMITH, Don W., Growth of foreign nuclear power, 20: 32808 (TID-22973)
SMITH, E. J., Interplanetary magnetic measurements, 20: 31883
SMITH, E. J., Variations in polarity distribution of interplanetary magnetic field, 20: 31860
SMITH, F. A., Neutron diffraction investigation of Au_2Mn under pressure, 20: 31756
SMITH, Harold H., Energy requirements and RBE cytogenetic phenomenon in maize by irradiating seeds, 20: 31092
SMITH, J., Application of modified determinantal method to Yukawa potential scattering, 20: 32135
SMITH, J. S., Metastable transitions of zirconium oxide obtained from decomposition of alkoxides, 20: 31736
SMITH, Kenneth C., ILLIAC III: processor of visual information, 20: 31652 (COO-1018-1057)
SMITH, M. W., Atomic transition probabilities. I., 20: 31942
SMITH, R. D., Fast Reactors, 20: 32818
SMITH, W. L., Defects in natural quartz, 20: 32695
SMOES, S., Thermodynamic and kinetic studies in high-temperature chemistry, 20: 31227
SMULDERS, P. J. M., Doublet (2.8-Mev) in ^{21}Ne, 20: 32474
SMYTH, D. H., Effects of whole-body irradiation on transfer capacity of rat small intestine, 20: 31081
SMYTHE, L. E., Burn-up procedure for HTGCR experimental fuels, 20: 32838
SNELLING, N. J., Strontium isotopes and trace elements in carbonatites and limestones from Ice River, British Columbia, 20: 31406
SNIDER, Dale R., Elastic collisions as Lorentz transformations with application to Compton scattering, 20: 31994
SNOW, E. H., Model for radiation damage in metal-oxide-semiconductor structures, 20: 31615
SNYDER, C. R., Development of Ti pressure vessel for NERVA, 20: 32856
SNYDER, Conway W., Mariner-2 measurements of solar wind, 20: 31881
SNYDER, Conway W., Relation of Mariner-2 plasma data to solar phenomena, 20: 31882
SNYDER, Oscar P. Jr., Cryogenics in food irradiation, 20: 31634
SNYDER, R. E., Decay of ^{94}Nb and ^{94m}Nb, 20: 32518
SNYDER, Thoma M., Future cross section needs of nuclear power industry, 20: 32839
SOBALLA, G., X ray damage after therapeutic irradiations in vicinity of joints, 20: 31163
SOBO, D. J., Optimum power transmission cable weight, 20: 32853 (NAA-SR-Memo-11925)
SODAN, H., Decay of ^{162}Tb and ^{163}Tb, 20: 32462
SODAN, H., Decay $^{157}Eu(\beta^-)^{157}Gd$, 20: 32465
SODAN, H., Decay of ^{163}Er, 20: 32466
SODAN, H., Gamma transitions and energy levels in ^{161}Dy, 20: 32463
SODAN, H., Levels in ^{157}Tb, 20: 32464
SOERENSEN, B., Phenomenological description of anharmonic vibrations, 20: 32480
SOHL, G., Life testing of electron-bombardment cesium ion engines, 20: 31367
SOKOL, G. A., Investigation of neutron counter efficiency at intermediate energies, 20: 31584
SOKOLOV, A. P., Orientation of ^{111}Cd nuclei by 3261 A resonant radiation, 20: 32419
SOLMITZ, Frank T., Y^{89}'s with spin 7/2, 20: 32068
SOMASUNDARAM, R., Metallorgraphic observations of plastic deformation in thermally cycled uranium, 20: 31754
SOMMER, G., Resonant and nonresonant contributions from unphysical regions in dispersion relations, 20: 32192
SONETT, C. P., Evidence for collision-free hydromagnetic shock in interplanetary space, 20: 31891
SONETT, C. P., Interplanetary magnetic measurements, 20: 31883
SONNERUP, B. U. O., Occurrence of topological changes of magnetosphere, 20: 32278
SOOD, B. S., Measurement of Compton scattering cross section, 20: 32007
SOPPET, Frederick E., Method and apparatus for vibratory compaction, 20: 31704
SORENSEN, Raymond A., Structure effects in charge radius of spherical nuclei, 20: 32561
SOSIN, A., Stage IV recovery of Pt after electron irradiation, 20: 31800
SOYBERK, Oezdemir A., Minimum pulse rate and detection limit of apparatus in measurement of radioactive rays, 20: 31512 (SGAE-SS-5/1966)
SPALDING, J. F., Heritable radiation effects on mouse, 20: 31048
SPALEK, G., Polarization of neutrons elastically scattered from ^3He at at 3.33 and 7.90 Mev, 20: 32452
SPARROW, A. H., Effect of irradiation on shoot apex and internodes of Kalanchoe, 20: 31076
SPEISER, R. C., Life testing of electron-bombardment cesium ion engines, 20: 31367
SPENCER, W. J., Defects in natural quartz, 20: 32695
SPERBER, Daniel, Prog. rpt. on effect of high spin on electromagnetic decay of nuclei, annual, 5/65–5/66, 20: 32374 (IITRI-578P25-15)
SPETH, R., Strange-particle production in π^-p and π^+p collisions at 4 Bev/c, 20: 32029
SPICER, B. M., Energy spectra of photoprotons from Al, S, and Si, 20: 32394
SPIELBERG, D., ATHENA: system of FORTRAN programs for radiation transport and heating calculations in complex reactor geometries, 20: 32768 (UNC-5148)
SPITSYN, V. I., Electrochemical properties of radioactive specimens of iron and steel, 20: 31231
SPIVAK, G. V., Determining structure of sintered materials by ionic bombardment, 20: 31765
SPRANG, P. G., Phase relations in the system $CoNb_2O_6$–$CoTa_2O_6$, 20: 31734
SPRECKELS, C., Miniature thermoluminescent dosimetry for application in medicine and biology, 20: 31598
SPRING, K. H., Direct generation of electricity, 20: 31970
SPROTT, J. C., Wide band electrostatic probes for use tenuous plasmas, 20: 32632
SPRUCH, Larry, Relativistic versus nonrelativistic scattering of slow electrons, 20: 31923
SPURNY, Z., Effect of ionizing radiation on glasses, 20: 31283
SRINIVASAN, K. R., Physics calculations of thorium-fuelled heavy-water lattices, 20: 32774
STAB, L., Decay of ^{51}Cr, 20: 32410
STABELL, R., Classification of general relativistic world models, 20: 31863
STAEHLE, R. W., Prog. rpt. on stress corrosion cracking in Fe–Ni–Cr alloy system, 12/17/65–3/16/66, 20: 31676 (COO-1319-39)
STAGG, M. S., Production of metallic and other ions in r-f ion source, 20: 31845
STAKH, V., Xenon stability in absorbing-layer slab reactor, 20: 32771
STAMER, P., Analysis of K and $\eta \to 3\pi$ decay spectra, 20: 32010
STANCHI, L., Solutions for a nuclear counting chain, 20: 31551
STANKIEWICZ, Norbert, Limits of validity of radiationless decay of high-density plasmas, 20: 32575 (NASA-TN-D-3372)
STARK, J. M., Cellular control systems and radiosensitivity, 20: 31064
STARKOV, M. G., NMR studies of solubility H in liquid N and He in liquid H, 20: 31251
STARODUBTSEV, S. V., Loop dose transformer, 20: 32865
START, D. F. H., Investigation of levels in ^{23}Na below 3 Mev by $^{26}Mg(p,\alpha\gamma)^{23}Na$ reaction, 20: 32509
START, D. F. H., Study of the low-lying states of ^{23}Na by $^{26}Mg(p,\alpha\gamma)^{23}Na$ reaction, 20: 32567
STAVISSKII, Yu. Ya., Producing starting pulses in time-of-flight nanosecond, 20: 31579
STEENBECK, M., Calculation of average Lorentz field strength $\overline{v \times B}$ for electrically conducting medium in turbulent motion influenced by Coriolis forces, 20: 32235
STEIN, J. E., Liquid scintillation counting, 20: 30997
STEIN, O. L., Effect of irradiation on shoot apex and internodes of Kalanchoe, 20: 31076
STEINBACH, Gerda, Lead-210, shell model calculations with harmonic oscillator wave functions, 20: 32381 (SGAE-PH-37/1966)
STEINDLER, M. J., Absorption spectrum of neptunium hexafluoride, 20: 31248
STEINER, Albert J., Syntax loader and subscanner for compiler-compiler, 20: 31650 (COO-1018-1031)
STEPANOV, A. P., Double nuclear-electron resonance spectrometer, 20: 32525
STEPANOV, V. G., EPR of Tb in CeO_2, 20: 32723
STEPANOV, V. G., EPR of Gd^{3+} in Y and La double molybdates, 20: 32728
STEPHAN, Richard A., Growth of foreign nuclear power, 20: 32808 (TID-22973)
STEPHANI, H., Two-dimensional spinor fields in Riemannian space,

20: 32109
STEPINSKI, Marian, Apparatus for investigation of directional correlation of γ-rays emitted in cascade, 20: 31595
STERN, H., Foundations of the bootstrap theory, 20: 32212
STERNHEIMER, D., Local representations and mass spectrum, 20: 32161
STEUER, M. F., Elastic scattering of polarized 4.4 Mev neutrons from ^{6}Li and ^{7}Li, 20: 32433
STEVENS, G. G., Circuit hardening using computer techniques, 20: 31621
STEVENSON, M. Lynn, Y*'s with spin 7/2, 20: 32068
STEWART, A. T., Positron annihilation in liquid He, 20: 32346
STEWART, A. T., Positron annihilation in liquefied gases, 20: 32345
STEWART, J. D., Calculation of neutron diffusion parameters of parallel-plate lattice, 20: 32763 (AECL-2543)
STEWART, M. G., Measurements of conversion coefficients for transitions in ^{154}Gd, ^{160}Dy, ^{170}Yb, ^{171}Yb, and ^{141}Pr, 20: 32443
STIHI, M., Regge poles in potential theory. I., 20: 32186
STILL, Ed T., Effects of whole-body 32-Mev proton irradiations on primates, 20: 31097
STILLER, G., Optical model analysis of elastic scattering on deuterons on ^{12}C, 20: 32454
STOBER, A. K., Soft x-ray photoionization detector, 20: 31511 (N-66-16936)
STOECKER, H. J., System U–N, 20: 31230
STOLIN, V. L., Determination of kinematic properties of particles in spark chamber sparks, 20: 31570
STOTSKII, V. M., Double nuclear-electron resonance spectrometer, 20: 32525
STRATHDEE, J., Coupling of noncompact group representations, 20: 32169
STRATTON, R. F., Apparent high-frequency stability of highly anisotropic plasma, 20: 32624
STRELIN, G. S., Possibility of therapeutic application of bone marrow autotransplantation in uneven irradiation, 20: 31133
STRELZOFF, Alan, Radiative decay of the μ meson, 20: 32104
STRIEBEL, H. R., Reaction ^{6}Li(d,n)^{7}Be* with polarized deuterons, 20: 32411
STRIEVA, A. V., Inversion of levels during excitation by a monoenergetic electron beam, 20: 31941
STRINGER, J., Void formation during oxidation of tantalum, 20: 31684
STRINGER, J. L., Digital control for whole-body scanner, 20: 31502 (BNWL-235-4, pp 11-14)
STRITTMATTER, P. A., Gravitational collapse in the presence of a magnetic field, 20: 31862
STROCCHI, F., Electromagnetic interactions and T violation, 20: 32020
STROGANOVA, I. M., Ternary compounds in Be–B–C system, 20: 31257
STRUTSINSKII, V. A., Physical stand for critical assembly of Institute of Physics at Ukrainian Academy of Sciences, 20: 32770
STRYCKMANS, Pierre A., Extracorporeal irradiation of blood in humans, 20: 31000
STUART, J., Spectrometer of high aperture ratio, 20: 31481 (AERE-Trans-1050)
STUBBE, E. J., Electrical conductivity of plasmas, 20: 32668
STUBICAN, V. S., Grain boundary precipitation in oxide systems, 20: 31738
SUAREZ, J. F., Energy levels of ^{106}Pd fed in the ^{106m}Rh decay, 20: 32425
SUBOTOWICZ, M., Determination of matrix elements in first-forbidden β transitions, 20: 32393
SUBRAMANIAN, T. A., Physics calculations of thorium-fuelled heavy-water lattices, 20: 32774
SUCKER, K.-H., Use of uniform half lives of important radionuclides, 20: 32421
SUDARSHAN, E. C. G., Noncompact groups in particle physics, 20: 32210
SUDARSHAN, George, Boson resonances, 20: 32089
SUDARSHAN, George, Conferences on symmetry principles at high energy, 3rd Coral Gables, 1/66, 20: 32195
SUDNITSYN, O. A., Temperature of heated tubes with pulsating flow, 20: 31346
SUESSMANN, G., Surface tension of nuclei according to Fermi-gas model, 20: 32470
SUGAHARA, Tsutomu, Radiosensitivity of bone marrow cells in mouse strains with different LD50, 20: 31071
SUGANO, Reiji, Double octet model of bosons, 20: 32084
SUGIYAMA, Masataka, Properties of WC-20% Co and WC-5% TaC-20% Co alloys, 20: 31760
SUITA, Tokuo, Secondary electron emission-type neutral particle detector, 20: 31533
SUITS, J. C., Preparation and Faraday rotation of divalent europium glasses, 20: 31733
SUMI, Yoshio, Real and imaginary amplitudes in high-energy elastic scattering, 20: 32179
SUN, Ch'ing-ch'i, Effect of γ radiation on survival reproduction and rate of infection of watersnails, 20: 31116
SUPEK, Zlatko, Liberation of 5-hydroxytryptamine in brain stem of adrenalectomized rats after x-irradiation, 20: 31069
SUSCILLON, Michel, Effects of x rays on platelet environment, 20: 31032 (CEA-R-2953)
SUSKI, L., Radiometric determination of solubility of cadmium in molten cadmium chloride, 20: 31237
SUTTON, J., Effect of precipitates on critical current of Ti-32Nb superconductor, 20: 32322
SUWALSKI, W., Progress in reactor kinetics at Swierk, 20: 32781
SUZUKI, Hisashi, Properties of WC-20% Co and WC-5% TaC-20% Co alloys, 20: 31760
SVENNE, J. P., Hartree-Fock calculation for finite nuclei with nonlocal two-body potential, 20: 32496
SVIRIDENKO, V. K., Melting points of V and Nb of high purity, 20: 31721 (AD-630971)
SWANSON, Lynwood W., Applications of field electron microscopy to surface physics problems, 20: 32742
SWIFT, C. D., Atomic fluorescence yields, 20: 31936
SWIFT, P., Quantitative analysis by spark source mass spectrometry, 20: 31202
SWINTH, K. L., Whole-body counting of Pu in dogs, 20: 30968 (BNWL-SA-11)
SYMONS, R. H., Preparation of ^{32}P-labeled nucleoside 5'-monophosphates, 20: 31307
SZAMOSI, G., Composition of degenerate gas of elementary particles, 20: 32044
SZCZECHLA, B., Progress in reactor kinetics at Swierk, 20: 32781
SZECHTER, A., Methods and results of static measurements in zero power reacto: ANNA, 20: 32875
SZEKERES, P., Embedding properties of general relativistic manifolds, 20: 32297
SZENDY, K., Losses caused by Hall effect and their influence on efficiency of thermal cycle in MHD generators, 20: 31962
SZULC, Przemyslaw, Solid-state instrumentation for control and safety of experimental reactors, 20: 32876
SZUTA, M., EWA reactor power ^{16}N activity monitoring, 20: 32870
SZYMENDERA, Lech, Calculations of top shield of critical assembly MARYLA, 20: 32878

T

TABUCHI, Akira, Estimation of exposure dose to fetus from fetal radiography, 20: 31146
TADIC, D., Broken symmetries and nonleptonic hyperon decays, 20: 32651
TADIC, D., Induced terms and partial conservation of axial vector current in β decay, 20: 32479
TAI, Yukimitsu, Mechanism of recovery of irradiated Yoshida ascites tumor cells, 20: 31070
TAJIRI, Masayoshi, C.C.L. approximation for treating collisionless plasma flow, 20: 32649
TAKAGI, Tomoo, Adsorption and electrodeposition of protactinium, 20: 31243
TAKAHASHI, Tan, Measurement of tritium at natural levels, 20: 31398 (NSJ-tr-49)
TAKAHASHI, Yasutaro, Four-particle scattering in nonrelativistic theory. II., 20: 32171
TAKAHASHI, Yoshizo, Computer control of research reactor TTR-1, 20: 32867
TAKAMATSU, Shigeyuki, Computer control of research reactor TTR-1, 20: 32867
TAKAOKA, N., Half life of ^{130}Te double β decay, 20: 32385
TAKEDA, Eizo, Uranium in coal-bearing beds of Mikawa and Akatani area, Niigata Prefecture, 20: 31437
TALBERT, W. L. Jr., Measurements of conversion coefficients for transitions in ^{154}Gd, ^{160}Dy, ^{170}Yb, ^{171}Yb, and ^{141}Pr, 20: 32443
TAMAGAKI, Ryozo, Optical potential for high-energy α-α scattering, 20: 32531
TAMAGNINI, Carlo Monginil, Nuclear codes, 20: 32745
TAMAMURA, Shozo, Effect of green tea and related substances on G-I absorption of ^{90}Sr, 20: 30987
TAMEMASA, Osamu, Effect of green tea and related substances on G-I absorption of ^{90}Sr, 20: 30987
TANAKA, Eiichi, Low-background beta-ray sciatillation spectrometer, 20: 31603
TANAKA, Hojime, Strong interaction of intermediate vector mesons and extremely high-energy phenomena, 20: 32177
TANAKA, Masatoshi, Propagation of low-frequency waves in inhomogeneous plasma column, 20: 32601
TANAKA, Tomizo, Radiosensitivity of bone marrow cells in mouse strains with different LD50, 20: 31071
TANDON, J. N., Wave propagation in rarefied plasma under action of Coriolis force, 20: 32603
T'ANG, Tse-sheng, Biological effect of gamma rays on peas. I., 20: 31170
TANI, S., Complete continuity of kernel in generalized potential scatter-

ing. II., 20: 32118
TANI, S., Complete continuity of kernel in generalized potential scattering. I., 20: 32117
TANIUTI, Tosiya, Nonlinear motion of two ion streams in background of high temperature electrons, 20: 32654
TAO, Atuke, Effect of green tea and related substances on G-I absorption of ^{90}Sr, 20: 30987
T'AO, Tsung-hsin, Adsorption of ^{90}Sr by aged horse manure, 20: 31252
TAOQU, D., Measurement, by gaging, of luminescence pulse forms of organic scintillators, 20: 31529
TARANTIN, N. I., Calculation of magnetic analyzer of mass separator, 20: 31484
TARAS, P., Chlorine-35 and the unified model, 20: 32400
TARASENKO, A. S., Electron beam injection into magnetic quadrant of an accumulator at 100 Mev, 20: 31849
TARUSOV, B. N., Effect of ^{60}Co rays on hyperweak luminescence of root system of malt sprout, 20: 31020
TASSAN, S., Resonance absorption in heavy water lattices development work at Ispra, 20: 32785
TATEVSKII, V. M., Electron diffraction study of structure of neodymium halide molecules, 20: 31222 (ANL-Trans-310)
TATSUNO, Ikuro, Various problems in stomach scanning, 20: 31160
TATU, Vasile, Determination of quadrupole moments of Ba by measurements of isotopic displacements, 20: 32404
TAUPIN, J. L., Energy released at high temperature by irradiated graphite, 20: 31802
TAURIT, Rudolf, Boiling water reactor construction outline of AEG, 20: 32812
TAUSEND, A., Gamma radiation of ^{83}Br, 20: 32413
TAYLOR, A. Joanne, Correlation in the elastic and inelastic S-wave scattering of electrons by H and He^+, 20: 31927
TAYLOR, Lawnie H., Surface physics comparison of ionizer materials, 20: 31388
TAYLOR, R. L., Approximate method for thermoviscoelastic stress analysis, 20: 31334
TAYLOR, S., Analysis of K and $\eta \rightarrow 3\pi$ decay spectra, 20: 32010
TAYLOR, T. I., Enrichment of ^{18}O and ^{13}C by carbon dioxide exchange in amine-solvent systems, 20: 31641 (NYO-755-1, pp 173-208)
TAYLOR, T. I., Exchange between methyl acetylene and water for concentration of deuterium, 20: 31640 (NYO-755-1, pp 130-72)
TAYLOR, T. I., Factors affecting the exchange of ^{15}N between nitric oxide and nitric acid in exchange columns, 20: 31639 (NYO-755-1, pp 77-129)
TAYLOR, T. I., Prog. rpt. on separation of isotopes, annual, 1964, 20: 31637 (NYO-755-1)
TAYLOR, T. I., Solvent carrier system for concentration of ^{15}N by chemical exchange between oxides of N, 20: 31638 (NYO-755-1, pp 12-76)
TEBBLE, R. S., Microwave resonance observations in gadolinium solid solutions, 20: 32716
TEIGER, J., New structure in the K^+-p and K^+-d total cross sections between 0.9 and 2.4 Bev/c, 20: 32067
TEILLAC, J., Polarization and spin correlation parameter measurements in 600-Mev proton-proton scattering, 20: 32016
TEITLER, S., Baryons, leptons, and isotopic spinor modulation, 20: 32215
TEITLER, S., Isotopic space, complex conjugation, and U_3 symmetry for particles, 20: 32213
TEITLER, S., Lorentz equivalence, unitary symmetry, and spin unitary symmetry, 20: 32214
TEITLER, S., Structure of 4-spinors, 20: 32216
TEMMER, G. M., Isobaric analog states of doubly magic ^{208}Pb, 20: 32478
TENTCHEVA-MALINOVA, S., Biochemical changes occurring in apple juice irradiated for storage, 20: 31629
TEODORESCU, Crina, Simultaneous measurement of beam energy in angular distribution studies, 20: 32403
TEPLOV, I. B., Use of magnetic quadrupole lenses for focusing particles passing through stopping foils, 20: 31844
TERASHIMA, Yoshinosuke, Excitations of cyclotron harmonic waves propagating perpendicular to external magnetic field, 20: 32630
TESTA, H., Scintillation scanning in kidneys, 20: 31148 (CNEA-170)
TETENBAUM, S. J., Electron cyclotron harmonic resonance phenomena in an rf-excited discharge, 20: 32236
TETER, M. P., Hornbeck-Molnar cross-sections for the n = 3 states of He, 20: 31947
TEWORDT, L., Effect of spatial variation of order parameter on tunneling density of states of superconducting alloys, 20: 32340
THACKRAY, M., Burn-up procedure for HTGCR experimental fuels, 20: 32838
THAMPY, R. T., Effect of ^{60}Co gamma rays on commercial polypropylene films, 20: 31274
THEMANN, H., Fine structural studies on effect of x rays on retina of guinea pigs, 20: 31118
THIEBLEMONT, Bernard, Absorption spectra of irradiated $KClO_3$, 20: 32686
THIELGES, Bart A., Effects of chronic exposures to ^{60}Co radiation on Pinus rigida seedlings, 20: 31077
THIRRING, W., Predictions of static quark model on boson decays, 20: 32061
THOMAS, D. W., Charge transfer and atom transfer in ion-molecule interactions studied by time-of-flight mass spectrometer, 20: 31224
THOMAS, J. B., Lifetimes of first excited states of ^7Li and ^7Be, 20: 32504
THOMAS, Jess W., Distribution of radioactivity on polydisperse aerosol by diffusion method, 20: 31461
THOMAS, Ruth E., Frequency of x-ray induced crossover-suppressing aberrations recovered from oocytes and sperm of Drosophila, 20: 31047
THOMAS, Scott J., Liquid immersion for reducing damaging effect of laser giant pulses to dielectric mirror coatings, 20: 31787
THOMAS, Scott J., Momentum transfer produced by focused laser giant pulses, 20: 31810
THOMPSON, P. A., FORTRAN listings and flow charts for ZAP31: program to calculate β-γ radiation dose rates, 20: 32675 (ORNL-TM-1160)
THOMPSON, S. A., Factors in life testing ion engines, 20: 31358
THOMPSON, S. A., Ion engines for satellite control, 20: 31366
THOMSON, J., Some thoughts on electron, 20: 32002
THOMSON, John F., Pancreatic lipase activity in deuterium oxide, 20: 30995
THORNDIKE, E. H., Proton-proton bremsstrahlung at 204 Mev, 20: 32062
THORSON, I. M., Normal vibrations of potassium iodide, 20: 32710
THOSAR, B. V., Lifetimes of positronium in polystyrene irradiated by thermal neutrons, 20: 32704
TIBOR, Zh., Polonium-210 determination in human urine samples, 20: 31187
T'IEN, Chi-en, Velocity of turbulent flow of water through a bundle of hollow rods, 20: 31350
TIESINGA, C. J., Light attenuation in scintillation counters, 20: 31546
TIFFANY, O. L., Radionuclide production in Fe targets bombarded with 400-Mev protons, 20: 32560
TILAK, S. P., Direct irradiation of lymph nodes with ^{131}I tagged ethiodol, 20: 31044
TIMOKHIN, L. A., Time-of-flight neutron spectrometer, 20: 31566
TINGUELY, H., Effects of x rays on function and ultrastructure of isolated sympathetic ganglion, 20: 31055
TIPPINS, H. H., Absorption edge spectrum of scandium oxide, 20: 31240
TIPTON, Donald L., Nonequilibrium ionization for MPD power generation, 20: 31963
TITTA, L., Experimental observations on behavior of serum cholesterol after irradiation, 20: 31006
TITTERTON, E. W., States of ^{13}N in 20 to 30 Mev region, 20: 32527
TIWARI, P. N., Efficiencies for well-type NaI(Tl) crystal for cylindrical sources, 20: 31553
TODD, F. C., Ionization in hydrogen plasmas, 20: 32628
TOEFTE, H., Multiple pion production in proton-proton collisions at 24 Bev/c, 20: 32017
TOELGYESSY, J., Simple scintillation device for measuring β absorption in liquids, 20: 31521
TOIVOLA, Ahti, Comparative study of saturation characteristics of air- and hydrogen-filled ionization chambers, 20: 31516
TOKAR, S. S., Relation between nonrelativistic partial wave amplitude and trajectories of its poles in λ plane, 20: 32187
TOLLET, Louis H. J., Nuclear reactor pressure vessel cover, 20: 32758
TOLSTOI, A. E., Electron beam injection into magnetic quadrant of an accumulator at 100 Mev, 20: 31849
TOMBRELLO, T. A., Natural parity states of ^{16}O at 11.09 and 12.05 Mev, 20: 32502
TOMODA, C., Thorium fuel utilization research in Japan, 20: 32828
TOMS, R., Potentials of solar power electric propulsion, 20: 31382
TOMS, Ronald S. H., Development of ion microthrustors for satellite applications, 20: 31362
TOPA, J., Progress in reactor kinetics at Swierk, 20: 32781
TOPA, Jerzy, Progress in reactor detectors design and construction, 20: 31596
TOSIC, D., New mass spectrometer ion source for solids, 20: 31204
TOTH, G., Production of carrier-free ^{131}I-iodate, 20: 31234
TOTH, K. S., Angular distributions of ^{18}F from the reaction $^{16}O(^{14}N,^{18}F)^{12}C$, 20: 32429
TOTH, K. S., Estimates of residual radiation levels induced by high-energy nucleons, 20: 31831
TOUBER, J. L., Treatment of patients with metastasized mammary carcinomas by radioactive Y, 20: 31153
TOUCHE, Jacques, Temporary capture of charged particles in static magnetic bottle, 20: 32582
TOURYAN, K. J., Thermionic power generation from reentry vehicles, 20: 31961 (SC-DC-66-1115)
TRAPP, J. P., Detection efficiency of spark chambers and its exact calculation, 20: 31558
TRAUGER, D. B., Irradiation behavior of Th–U alloys and compounds,

20: 32833
TREIMAN, Marilyn, Bibliography on kinetics of oxidation-reduction reactions of U, Np, Pu, and Am in aqueous solutions, 20: 31215 (LA-3507)
TRET'YAKOV, E. F., Conversion electrons associated with alpha decay of ^{241}Am and level scheme of ^{237}Np, 20: 32375 (ITEF-351)
TRIFTSHAEUSER, Werner, Time independence of charge states produced following electron capture in ^{57}Co, 20: 32713
TROZZI, Marcello, Polarographic investigation on Pu(IV) in sulfuric acid solution, 20: 31302
TRUMP, G. E., Surface tension storage and feed systems for ion engines, 20: 31379
TSAI, S. Y., Semi-leptonic decays ($\Delta S = \Delta Q$) and CP violation, 20: 32184
TSAO, Fu-chuen, Velocity of turbulent flow of water through a bundle of hollow rods, 20: 31350
TSOULFANIDIS, N., Pulse propagation experiments using reactor source, 20: 32362
TSUCHIDA, T., Magnetic characteristics of $ZrNi_5$ and $HfNi_5$ and lanthanide–Ni compounds having Th_7Ni_{13} structure, 20: 32699
TSUKADA, K., Average level width of compound nucleus, 20: 32424
TSUYA, Kazuo, Anisotropy of ductile-brittle transition behavior of Be sheets, 20: 31761
TUNKELO, Eino, Construction and performance of cold neutron source, 20: 32351
TUPLIN, T. A., Thermal ionization of elements of high ionization potential, 20: 31226
TURCK, Bernard, Detection of hard β radiation in water using the Cherenkov effect, 20: 31506 (CEA-R-2915)
TURETSKAYA, E. A., Dependence of luminescence spectra of organic uranyl salt solutions on exciting light wave length, 20: 31305
TURK, Roland, Business pattern of nuclear fuel industry, 20: 32792
TURKAKULOV, Ya. Kh. Effects of γ-irradiation of cottonseeds on change of DNA in succeeding generations, 20: 31019
TURKO, M. N., Vaporization of material from surface of probe in an arc, 20: 32593
TURNBULL, David, Solid state physics. Vol. 18, 20: 32718
TURNER, D. T., ESR study of free radicals formed by γ-irradiation of polyethylene terephthalate, 20: 31306
TURNER, F. Cort, Growth of foreign nuclear power, 20: 32808 (TID-22973)
TURNER, Grenville, Potassium–Ar dating by activation with fast neutrons, 20: 31431
TURNER, J. E., WKB treatment of bound states in an electric-dipole potential, 20: 32295
TURNER, Richard Franklin, Nuclear reactor fuel element, 20: 32793
TYE, R. P., Thermal conductivity of compacted powder carbons, 20: 31777
TYREE, Ella B., Effect of L-triiodothyronine on radiation-induced pulmonary fibrosis in dogs, 20: 31138
TZARENKOV, A. P., Programming operation of JINR synchrophasotron, 20: 31840

U

UDAGAWA, Takeshi, Nonadiabatic effects of nuclear rotational spectra, 20: 32492
UEDA, Kazuo, Properties of polyethylene–vinyl chloride graft copolymers, 20: 31288
UENO, Kaoru, Cross sections and isomer ratios for ^{88}Sr(^{3}He,p)/^{90m,90g}Y reaction, 20: 32430
UHER, Richard A., Structure effects in charge radius of spherical nuclei, 20: 32561
UHLMANN, W., Bibliography on radiation effects on solid, U based nuclear fuel materials, Vol. 6, No. 1, 20: 31783 (FTI-16(6.1))
UKAI, Teiji, Effect of green tea and related substances on G-I absorption of ^{90}Sr, 20: 30987
ULLMANN, J. W., Production of ammonia using electricity from nuclear desalination reactor complex, 20: 32841 (ORNL-3882)
ULRICH, A. J., Thermionic energy converter using film-boiling liquid metal, 20: 31969
ULRICH, Reinhard, Cherenkov radiation of electrons in thick dielectric, 20: 32098
UMEHARA, Eiju, Effects of x radiation on HeLa cells, 20: 31056
UMERJEE, R. K., Polarization and asymmetry in the ^{3}He(d,p)^{4}He reaction, 20: 32475
UNGSTRUP, Eigil, Association between VLF emissions and flickering aurora, 20: 32256
URANO, Muneyasu, Effect of x-irradiated tumor bed on tumor cells. I., 20: 31073
URBAIN, Walter M., Commercial use of radiation preservation, 20: 31635
URBAN, C. W., Thorium-cycle possibilities in Brazilian nuclear power program, 20: 32821
UTAGAWA, Keiji, Effects of x radiation on HeLa cells, 20: 31056

V

VACHASPATI, Harmonics in scattering of electromagnetic radiation by electron current, 20: 32001
VAES, Aime, Nuclear Energy in Belgium, 20: 32890
VAINSHTEIN, E. E., Spectrometer for studying fine structure of x-ray spectra (URS-1I), 20: 31581
VAINSHTEIN, E. E., Valence state of Sm in metal and in its monosulfide, 20: 32720
VAISBERG, O. L., Atomic hydrogen and helium in airglow, 20: 32289
VAL'DNER, O. A., Basic calculations of small energy linear electron accelerators, 20: 31850
VAL'DNER, O. A., Computation of particle dynamics in waveguide separators, 20: 31841
VALSAMAKIS, E. A., Plasma injected into B_z guide field from conical theta-pinch accelerator, 20: 32661
VAN ALLEN, J. A., Absence of a very extended magnetospheric tail, 20: 32258
VAN ALLEN, J. A., Correlation of outer radiation zone electrons with the solar activity cycle, 20: 32260
VAN ATTA, C. M., Vacuum science and engineering, 20: 31391
VANDEN BOUT, Paul A., Hyperfine-structure anomalies of ^{198}Au and ^{199}Au, 20: 32553
VAN DEN BRENK, H. A. S., Mechanisms of chemical radiation protection in vivo. III., 20: 31122
VANDENBUSSCHE, Gerard, Kinetic study of fluorination by F of U and Pu compounds, 20: 31214 (CEA-R-2859)
VAN DER BORGHT, O., Calcium metabolism in freshwater mollusk, 20: 30991
VAN DER KRAAN, A. M., Beta-gamma circular polarization in decay of ^{48}Sc, 20: 32457
VAN DER PLAATS, G. J. Jr., Treatment of patients with metastasized mammary carcinomas by radioactive Y, 20: 31153
VAN DER PLAS, Th., Sol-gel processes for Th fuel production, 20: 31700
VANDER VELDE, J., Observation and properties of neutral A_2 meson, 20: 32064
VAN DER WERF, A. J. M., Treatment of patients with metastasized mammary carcinomas by radioactive Y, 20: 31153
VAN DER WIEL, M. J., Ionization cross-section measurements for 0.6- to 20-kev electrons in atomic and molecular gases, 20: 31906
VAN DER WOUDE, A., Polarizations and differential cross sections for the elastic scattering of 40-Mev protons from ^{12}C, ^{40}Ca, ^{58}Ni, ^{90}Zr, and ^{208}Pb, 20: 32510
VAN DREAL, Paul A., Radiation-induced division delay in Astasia longa, 20: 31085
VAN EEKELEN, H. A. M., Operator method for angular momentum and SU_3, 20: 32166
VAN HAGAN, T. H., SNAP 50/SPUR boiler development, 20: 32857
VAN HOLLEBEKE, M., Antiproton-nuclei scattering at 3 Bev/c, 20: 32467
VAN KERSEN, G. R., Effect of O on impairment of proliferative capacity of human cells by radiations LET, 20: 31123
VAN KOOY, J. G., Mitochondria: increase in oxidative capacity and quantitative recovery after massive doses of radiation, 20: 31633
VAN KRUGTEN, H., Beta-gamma circular polarization in decay of ^{48}Sc, 20: 32457
VAN LOAN, Paul R., Crystal chemistry and dielectric properties in systems $BaTiO_3$–UO_2 and $BaTiO_3$–$BaUO_3$, 20: 31735
VAN NOOIJEN, B., Beta-gamma circular polarization in decay of ^{48}Sc, 20: 32457
VAN OERS, W. T. H., Proton spectra from d+d breakup at 25.3 Mev, 20: 32568
VAN PUYMBROECK, S., Calcium metabolism in freshwater mollusk, 20: 30991
VAN ROYEN, R. P., Dashen-Frautschi method and parity-conserving baryon-meson couplings, 20: 32138
VARLJEN, Thomas C., Post-shutdown generation of photoneutrons in beryllium-moderated systems, 20: 32767 (UCRL-14720)
VASILESCU, A., Isotopic exchange of active methyl hydrogens. II., 20: 31260
VASIL'EV, R. F., Spectrometer of high aperture ratio, 20: 31481 (AERE-Trans-1050)
VAUCHER, B., Excitation of levels of ^{12}C by inelastic scattering of 14.1-Mev neutrons, 20: 32408
VAVILOV, V. S., Electron-bombardment-induced stimulated emission from cadmium selenide, 20: 32730
VAVILOV, V. S., Ionization currents in diamonds during irradiation with 500 to 1000-kev electrons, 20. 32725
VEDEKHIN, A. F., Selection of scintillators for counters recording γ radiation, 20: 31574
VEKSHINA, N. V., Ternary compounds in Be–B–C system, 20: 31257
VELA, P., Behavior of He gas in irradiated Cu–B alloys, 20: 31797
VELA, P., Spontaneous grain boundary swelling in irradiated Cu–B alloys, 20: 31798

detonation in basalt, 20: 31393 (PNE-711F)

VOVCHENKO, V. G., Magnetic analysis of relativistic particles, 20: 31563

VOVENKO, A. S., Irradiation of combined emulsion and spark chamber system, 20: 31569

VUILLEMIN, Michel, Calculation of statistical entropy of plasma during equilibrium, 20: 32583

VUISTER, P. H., Reaction $^{52}Cr(p,\gamma)^{53}Mn$, 20: 32446

VYRUBOVA, A. V., Improved dosimetric technique in alpha therapy, 20: 31157

VYSOTSKII, V. G., Effects of spaceflight factors on wheat seeds, 20: 31058

W

WAGNER, R. J., Sizable proton polarizations in frozen toluene, 20: 31811

WAHLBERG, J. S., Adsorption equilibria between earth materials and radionuclides, 20: 31426 (PNE-481, pp 1121-39)

WAIDELICH, Wilhelm, Defect formation in uv-irradiated silver chloride, 20: 32731

WAINIO, K. M., Radionuclide production in Fe targets bombarded with 400-Mev protons, 20: 32560

WALDRON, M. B., Safety aspects of carbide fast reactor fuels, 20: 31675

WALECKA, J. D., Nuclear spectroscopy in α particle, 20: 32503

WALKER, F. W., Measurement of total neutron cross sections of ^{147}Pm, ^{148}Pm, and ^{148m}Pm, 20: 32376 (KAPL-3090)

WALKER, J. K., Factors affecting resolution of lead scintillator sandwich shower counters, 20: 31587

WALKER, John W., Worldwide geomagnetic disturbances generated by Starfish explosion, 1962, 20: 32264

WALKER, Robert L., Photoproduction of negative pions from hydrogen, 20: 31983 (CALT-68-71)

WALLACE, W. E., Magnetic characteristics of $ZrNi_5$ and $HfNi_5$ and lanthanide–Ni compounds having Th_7Ni_3 structure, 20: 32699

WALLIN, W. R., BORAX-V nuclear superheat operating experience, 20: 32866

WALLIS, Valerie, Inhibition of radiation-induced leukemia by injection of haematopoietic tissue, 20: 31127

WALSH, Robert C., Miniature diamond ultrahigh pressure cell adapted for in-reactor irradiation studies, 20: 32754

WALTER, F. J., Low-background counting of betas and alphas with silicon detectors, 20: 31540

WALTERS, G. P., Effect of neutron irradiation on mechanical properties of hot-pressed and extruded Be, 20: 31794

WALTERSCHEID, Edward C., Nuclear excavation, 20: 31336

WANDERS, G., Sum rules for π-σ scattering, 20: 31999

WANG, Chan-t'ien, Effect of gamma radiation on seeds in second generation, 20: 31113

WANG, Tso-pin, Theory of α matter, 20: 32542

WARBURTON, E. K., Angular correlations in the $^{13}C(^3He,\gamma)^{15}N$ reaction, 20: 32495

WARD, W., Electron-bombardment thrusters using liquid-mercury cathodes, 20: 31368

WARDLEWORTH, D., Interpretation of Doppler and Na reactivity worth measurements in zero power reactors, 20: 32869

WARNER, C., Plasma physics of thermionic converters, 20: 31971

WARNER, Charles, Theory of ignited mode with electron temperature variations T(x), 20: 31974

WARNER, Robert E., Bremsstrahlung production in 48-Mev p-p collisions, 20: 31997

WARREN, Shields, Basis for the limit on whole-body exposure, 20: 31458

WARSCHAUER, K. A., Thorium cycle and homogeneous suspension reactor project, 20: 32829

WARSHAW, S. I., Reaction study of $^{19}F(d,n)^{20}Ne$, 20: 32555

WASLEY, R. J., Propagation of elastic stress disturbances in deformable solids, 20: 31331 (UCRL-14616)

WASSERBAUER, Joseph F., Ion thrustor suitable for spacecraft station keeping and attitude control, 20: 31371

WASSILOPULOS, M., Ternary and quaternary oxides of four, six, and seven valent Tc with alkali earths, 20: 31244

WATAL, Chitra, Production and decay of Ξ^* in one-particle exchange model, 20: 32009

WATANABE, Hiroshi, Operator methods in ligand field theory, 20: 32734

WATANABE, Keiji, Pion-pion correlation effect in two-pion-exchange contribution for nucleon-nucleon scattering, 20: 32073

WATANABE, Tomiya, Determination of electron distribution in magnetosphere using hydromagnetic whistlers, 20: 32290

WATARI, Kazuo, Cesium turnover in man following single administration of ^{132}Cs. I., 20: 30988

WATSON, C. D., Reprocessing methods and costs for selected thorium-bearing fuel types, 20: 31326

WATSON, D. E., Mathematical model of geomagnetic field for 1965,

20: 32255
WATSON, D. G., Radionuclides in terrestrial and freshwater biota, 20: 31428 (PNE-481, pp 1165-1200)
WATSON, D. L., Asymmetries in elastic and inelastic scattering of polarized protons from C and Si, 20: 32440
WATSON, E. C., IDERM: program for intake, distribution and excretion of radionuclides in mammals, 20: 31441 (BNWL-SA-40)
WATSON, H. E., NRL high level radiation laboratory. III., 20: 31337
WATSON, H. H. H., Ion bombardment apparatus for study of interaction of light ions with surfaces, 20: 31937
WATT, D. E., Proportional counting soft beta particles from solid sources, 20: 31548
WEED, Ronald D., Decontamination solution and method, 20: 32747
WEENINK, M. P. H., Wave propagation through Epstein density profile across inhomogeneous magnetic field, 20: 32625
WEHNER, Guenter, Energy distribution of electrons ejected from Mo by 2-, 5-, 10-, and 15-kev He and Ar ions, 20: 31939
WEIDENMUELLER, H. A., Theory of nuclear reactions. II., 20: 32428
WEIERSHAUSEN, W., Influence of O on surface ionization of some rare earth metals on W and Re, 20: 31225
WEIL, Raoul B., Ultrasonic studies in normal and superconducting thallium, 20: 31780
WEISE, Lothar, Applications of Laplace transforms for the calculation of counting losses, 20: 31594
WEISS, E., Prog. rpt. on critical heat flux (burnout) in boiling water, 7–9/65, 20: 31342 (EURAEC-1482)
WEISS, J., Radiolysis of aromatic compounds: toluene, 20: 31291
WEISS, Z., Recent numerical methods in neutron thermalization in reactor elementary cell, 20: 32367
WENT, J. J., Thorium cycle and homogeneous suspension reactor project, 20: 32829
WERNER, L., Decay $^{157}Eu(\beta^-)^{157}Gd$, 20: 32475
WERNER, L., Levels in ^{157}Tb, 20: 32464
WERNLUND, Roger F., In-flight instrumentation for prompt miss distance measurement using gamma ray techniques, 20: 31496
WERNLUND, Roger F., Pulsed x-ray instrument for altitude measurement and terrain identification, 20: 31493
WERNLUND, Roger F., Radioisotope and machine sources of x radiation for aerospace applications, 20: 31339
WERT, C., Clustering of interstitials in dilute Nb–O–N solid solutions, 20: 31774
WESLEY, E. J., Comparison of cesium iodide and sodium iodide for underwater radiation detection systems, 20: 31499 (AD-633752)
WESS, J., Mass splitting as covariant concept in generalized Poincare group, 20: 32114
WESTER, P. O., Trace elements in human myocardial infarction determined by neutron activation analysis, 20: 31175
WESTER, P. O., Trace elements in conductive tissue of beef heart determined by neutron activation analysis, 20: 31176
WESTGAARD, L., Radiochemical determination of ^{235}U abundances by activation analysis, 20: 31189
WESTGAARD, L., Self-supporting metal foils prepared from oxides of separated isotopes of rare earth elements, 20: 31696
WESTLAKE, D. G., Pitfall in preparation of metal–H alloys for transmission electron microscopy, 20: 31691
WEYERS, J., Partially conserved currents and CP violation in K^0-meson decays, 20: 32021
WHEATLEY, J. C., Propagation of zero sound in liquid ^3He at low temperatures, 20: 32329
WHEATLEY, J. C., Techniques for using liquid helium in very low-temperature apparatus, 20: 32336
WHEELER, R. C., Doppler coefficient measurements in Zebra core 5, 20: 32840
WHITE, B. L., Excited states of ^{11}C from n-γ angular correlations and gamma branching ratios, 20: 32395
WHITE, G., Boiling water reactor, 20: 32849
WHITE, J. E., Alloying-element/dispersed-phase interactions in tungsten-base alloys, 20: 31781
WHITE, R. L., Magnetism and magnetic materials, 20: 32738
WHITE, R. Stephen, Energetic electron spectra in radiation belts, 20: 32251
WHITE, R. Stephen, Low-energy proton radiation belts, 20: 32250
WHITE, W. H. Jr., Operating characteristics of ORIC beam extraction system, 20: 31821 (ORNL-P-2239)
WHITESIDE, D., External proton beam at Nimrod, 20: 31823 (RPP-N-5)
WHITMAN, A. M., Stagnation pressure distribution in current-carrying plasma, 20: 32660
WHITMORE, Frank C., Apparatus for radiofrequency surface measurements on single crystal superconductors, 20: 32343
WHITMORE, G. F., Survival of synchronized L cells after uv irradiation, 20: 31084
WHITTEN, L. G., Single-transducer differential measuring device, 20: 31333 (Y-1541)
WHITTLE, I., Effect of irradiated, low-temperature, high pH water on nylon, 20: 31280
WIBBERENZ, Gerd, Measurement of secondary gamma spectrum from 0.2 to 2 Bev in upper atmosphere, 20: 32283
WICKE, E., H/D separation factors in electrolysis and diffusion by use of Pd and Pd/Ag membranes, 20: 31256
WICKERSHEIM, K. A., Magnetism and magnetic materials, 20: 32738
WIEDERSICH, H., Spin orientation determination by linearly polarized, recoil-free γ rays, 20: 31228
WIEGAND, D. A., Schottky disorder and lattice relaxation in single crystals of NaCl due to x irradiation, 20: 32712
WIEGEL, M., Spectral representation for singlet and triplet Green's functions, 20: 32191
WIEGEL, Roger E., Programming manual for ILLIAC III computer, 20: 31653 (COO-1018-1061)
WIENECKE, R., Pressure elevation in H arc discharge in axial magnetic field, 20: 32638
WIESE, W. L., Atomic transition probabilities. I., 20: 31942
WILBER, John A., Programming manual for ILLIAC III computer, 20: 31653 (COO-1018-1061)
WILBER, Robert D., Hyperfunctioning solitary thyroid nodule, 20: 31154
WILBUR, R. L., Animal activity monitor development, 20: 30960 (BNWL-235-4, pp 22-5)
WILHELM, H. E., Closed loop MPD power generation experiment, 20: 31975
WILIMOVSKY, Norman J., Environment of Cape Thompson region, Alaska, 20: 32885 (PNE-481)
WILIP, Elmar K., Electron diffraction study of structure of neodymium halide molecules, 20: 31222 (ANL-Trans-310)
WILKINS, Daniel R., Thermionic converters operating in ignited mode. I., 20: 31967
WILKINS, Daniel R., Thermionic converters operating in ignited mode. II., 20: 31968
WILKINSON, David T., Cosmic background radiation at 3.2 cm—support for cosmic blackbody radiation, 20: 31957
WILKNISS, Peter, Preparation of toluene diisocyanate-^{14}C, 20: 31266
WILKS, R. S., Gas formation by transmutation of MgO and Al_2O_3, 20: 31799
WILLERS, G., Gamma radiation of ^{83}Br, 20: 32413
WILLIAMS, A., Measurement of decay scheme correction in absolute standardization of ^{57}Co, 20: 32414
WILLIAMS, Gwilym H., Proton depth-dose dosimetry, 20: 31467
WILLIAMS, Gwilym H., Whole-body irradiation of primates with protons of energies to 400 Mev, 20: 31096
WILLIAMS, H. J., Localized moments, 20: 32739
WILLIAMS, I. R., Level structure of ^{92}Mo, 20: 32471
WILLIAMS, Lewis Rhoslyn, Improvements in or relating to cermets, 20: 31707
WILLIAMS, M. M. R., Slowing down and thermalization of neutrons, 20: 32361
WILLIAMS, N. L., Canadian heavy-water reactor in a dual-purpose power-desalination plant, 20: 32847
WILLIAMS, P. J. S., Magnetic field within some quasistellar radio sources, 20: 31868
WILLIS, D. M., Motion of isolated charged particle in force-free magnetic field, 20: 31812
WILSON, G. L., Excitation and detection of magnetoacoustic waves in rotating plasma accelerator, 20: 32651
WILSON, H. W., Tandem mass spectrometer for isotopic analysis, 20: 31206
WILSON, I. J., Radiation and supersonic flight, 20: 31468
WILSON, J. P., Tunnel effect measurements on superimposed layers of Pb and Al, 20: 32342
WILSON, R. G., Electrode materials for cesium contact ion thrustors, 20: 31383
WILTSHIRE, L. L., Radiological reclamation performance summary. I., 20: 31454 (USNRDL-TR-967)
WINBORNE, R. A., Brittle failures of carbon steel tubes, 20: 31681 (NAA-SR-Memo-11707)
WINKLE, L. W., Differential spectrophotometric determination of Pu(III), 20: 31170 (ISO-SA-16)
WIRTH, John L., Anomalous photocurrent generation in transistor structures, 20: 31612 (SC-DC-66-1415)
WITKOWSKI, S., Pressure elevation in H arc discharge in axial magnetic field, 20: 32638
WLEZEK, C., Method for determining optimum type of atomic power station and competition between atomic and classical stations, 20: 32814
WOELFER, G., Study of neutron reactions with α-particle emission on ^{23}Na in energy region 12.6 to 18.7 Mev, 20: 32540
WOHL, Charles G., Y*'s with spin 7/2, 20: 32068
WOHLFROMM, Merlis, Previous reproductive history and susceptibility to x-ray-induced congenital anomalies, 20: 31066
WOJTASZEK, Joseph, Boson resonances, 20: 32089
WOJTASZEK, Joseph, Conferences on symmetry principles at high energy,

3rd Coral Gables, 1/66, 20: 32195
WOLFE, J. H., Probe observations of solar wind-geomagnetic field interaction region, 20: 32286
WOLFE, John N., Environment of Cape Thompson region, Alaska, 20: 32885 (PNE-481)
WOLFLE, Thomas L., Edema: delayed complication of total-body 32-Mev proton irradiation, 20: 31098
WOLFRAM, T., Macroscopic quantization in superconducting films, 20: 32324
WOLSTENHOLME, W. A., Quantitative analysis by spark source mass spectrometry, 20: 31202
WOLTERS, J. A., Life testing of electron-bombardment cesium ion engines, 20: 31367
WONG, A. Y., Propagation of ion acoustic waves along cylindrical plasma columns, 20: 32618
WONG, A. Y., Stability limits for longitudinal waves in ion beam-plasma interaction, 20: 32608
WONG, C. Y., Additional evidence of stability of superheavy element $_{310}126$ according to shell model, 20: 32482
WONG, Eugene Y., Temperature dependence of vibronic transitions in crystals and spectroscopic observation of phase transition, 20: 32737
WOO, Ching-Hung, On off-diagonal mass matrix element of neutral K system, 20: 31982 (AD-634703)
WOOD, R. F., Calculation of electronic structure of defects in insulators, 20: 32682 (ORNL-P-2193)
WOOD, R. F., Calculation of force-constant changes for U center, 20: 32683 (ORNL-P-2194)
WOODMAN, Margaret J., Thermal conductivity of compacted powder carbons, 20: 31777
WOODS, J. W., In-reactor mechanical properties experiments, 20: 31785 (ORNL-P-2162)
WOODSON, H. H., Excitation and detection of magnetoacoustic waves in rotating plasma accelerator, 20: 32651
WOODWARD, D. O., Genetics of enzyme locational specificity, 20: 31012
WOOLNER, Lewis B., Hyperfunctioning solitary thyroid nodule, 20: 31154
WORK, G. A., Power conditioning systems for ion engines, 20: 31357
WORK, George A., Ion beam deflection for thrust vector control, 20: 31369
WORLOCK, R. M., Characteristics of micropound range ion thrustors, 20: 31385
WORLOCK, R. M., Surface ionization engine development, 20: 31370
WRIGHT, Edward S., Rogowski coil probes for current density distribution in a plasma pinch, 20: 32574 (N-65-32035)
WU, S. T., Radiative hydrogenic shock structure, 20: 32241
WULFF, J., Electronic structure of transition metal-interstitial atom alloy superconductors, 20: 31747
WYARD, S. J., Electron spin resonance study of thermal effects in irradiated deoxyribonucleic acid, 20: 31009
WYATT, A. F. G., Microwave-enhanced critical supercurrents in constricted tin films, 20: 32328
WYNDHAM, J. D., Radio astronomy observations in relation to solar-wind problem, 20: 31888
WYSOCKI, J. J., Li-doped, radiation-resistant silicon solar cells, 20: 31614

Y

YAGOVOI, P. N., Determination of beta activity in preparations using cylindrical counters, 20: 31536
YAJIMA, Nobuo, Non-linear motion of two ion streams in background of high temperature electrons, 20: 32654
YAKIM, S. M., Effect of radiation on biological activity of penicillin, 20: 31022
YAKOVLEV, V. G., Isolating radiation protection agents on basis of Diche-positive compounds in urine, 20: 31140
YAKOVLEVA, N. I., Radiation resistance of complex organophosphorus resins, 20: 31303
YAKUSHEV, V. P., Pulsed neutron generator, 20: 32358
YAMADA, Shigeharu, ILLIAC III: processor of visual information, 20: 31652 (COO-1018-1057)
YAMAGUCHI, Hikoyuki, Induction of mutations by repeated irradiation of successive generations in barley and rice, 20: 31050
YAMAGUCHI, Junji, Effects of x radiation on HeLa cells, 20: 31056
YAMAKAWA, T., Production of neutral pions from electron-proton collisions, 20: 32038
YAMAKI, Kozo, Reactivity measurements by neutron noise analysis, 20: 32868
YAMAMOTO, Albert S., Equilibrium phase diagram, Nb(Cb)–Al, 20: 31769
YAMAMOTO, Kunio, M(12) and meson-baryon inelastic two-body scattering at high energy, 20: 32079
YAMAMOTO, Takeharu, Properties of WC-20% Co and WC-5% TaC-20% Co alloys, 20: 31760
YAMASHINA, Toshiro, Hydrogen reduction of γ-irradiated NiO, 20: 31285
YAMAZAKI, Toshimitsu, Application of perturbed angular correlation to hot-atom chemistry of Re, 20: 31311
YAMAZAKI, Toshimitsu, New weak beta transition from ^{88}Y, 20: 32453
YANG, Ch'eng-yu, Biological effect of gamma rays on peas. I., 20: 31114
YANTOVSKII, E. I., Computation of magnetic Reynold's numbers, 20: 32700
YARGER, L. L., Secondary electron production from 1-Mev alpha particles from Au, 20: 31918
YAROSHEVICH, O. I., Starting of critical assembly in Nuclear Power Engineering Institute of Belorussian Academy of Sciences, 20: 32769
YAROSHEVICH, V. F., Physical stand for critical assembly of Institute of Physics at Ukrainian Academy of Sciences, 20: 32770
YAROVAYA, S. M., Radiation chemistry of carbohydrates. V., 20: 31304
YASHIN, V. P., Device for measuring charged particle beam parameters, 20: 31838
YASUNO, Masaru, Polarization in elastic pion-nucleon scattering in few-Bev region, 20: 32087
YEH, Chia-fu, Effect of γ radiation on survival reproduction and rate of infection of watersnails, 20: 31116
YEH, K. C., Steady state fluid model of ion-exosphere, 20: 32291
YEH, Tyan, Nonexistence of looping trajectories in hydromagnetic waves of finite amplitude, 20: 32607
YELLIN, J., Meson decay of strongly interacting systems, 20: 32045
YELLIN, Joel, Baryon magnetic moments, 20: 32178
YILDIZ, Musa, Wave propagation and electro-acoustic spectrum in isotropic compressible plasma, 20: 32591
YIOU, F., Relative abundance and production cross sections of lithium isotopes, 20: 31205
YOKOMI, Hiroyuki, Possible determination of $\gamma m\omega$ coupling constant, 20: 32077
YOKOO, Yoshimatsu, Baryon decays and unitary symmetry, 20: 32175
YOKOYAMA, Takamitsu, Stoichiometric number and electrolytic separation factor of deuterium on nickel hydrogen electrode, 20: 31644
YOKOYAMA, Yuji, Application of perturbed angular correlation to hot-atom chemistry of Re, 20: 31311
YOSHIDA, Toshio, Optical absorptions of neutron-irradiated ZnS, 20: 31272
YOSHIKAWA, Kazuko, Radionuclide fractionation in debris from land surface burst, 20: 31460
YOSHINAGA, Haruma, Application of a fluoroglass dosimeter, 20: 31538
YOUNG, R. M., Soft x-ray photoionization detector, 20: 31511 (N-66-16936)
YOUNG, W. A. P., Tandem mass spectrometer for isotopic analysis, 20: 31206
YOVANOVITCH, D. D., Search for Y = 2, S = 0 resonances, 20: 32066
YU, Shao-hua, Biological effect of gamma rays on peas. I., 20: 31114
YUDIN, L. I., Feasibility of operating electron multipliers as h-f amplifiers, 20: 31485
YUDINTSEVA, E. V., Effects of soil fractions on uptake of ^{90}Sr into plants, 20: 30985
YUEN, Man Chuen, Stability of Poiseuille plasma arc in axial magnetic field, 20: 32614
YUKHNOVSKII, I. R., Virial expansions for plasma in collective variable method, 20: 32635
YUNKO, L. M., Melting points of V and Nb of high purity, 20: 31721 (AD-630971)
YURASOVA, V. E., Determining structure of sintered materials by ionic bombardment, 20: 31765
YURKOV, B. Ya., Collective energy losses in electron avalanche, 20: 32727
YUROVA, L. N., Gamma spectrometer measurements of ^{238}U capture-to-fission ratio, 20: 32391

Z

ZABEL, N. R., Containment of fragments from runaway reactor, 20: 32744 (SRIA-1)
ZABIYAKIN, G. I., Multichannel recording devices and computers for low-temperature physics, 20: 31562
ZAITOV, F. N., Creation and destruction of color centers in alkali-halide crystals, 20: 32691
ZAITOV, F. N., Destruction of color centers and recombination luminescence of crystal phosphor NaCl–Ag. I., 20: 32693
ZAITOV, F. N., Destruction of color centers and recombination luminescence of NaCl–Ag : Ca crystal phosphor. II., 20: 32694
ZAITSEVA, N. G., Behavior of radio-iodine recoils produced in isotopic and nonisotopic lattices, 20: 31298
ZALUTSKII, I. I., Crystal structure of $HoAl_3$ and $DyAl_3$ compounds, 20: 31728
ZAMBOTTI, G., Dynamical group of anisotropic harmonic oscillator, 20: 32301
ZAMPIERI, E., Alternative interpretation of the enhancement observed at $M^*pp\pi^+$ 2.52 Bev/c^2, 20: 32040
ZANETTI, Mario, Biological efficiency of 200 kv x rays, ^{60}Co rays and 14-Mev neutrons in Escherichia coli inactivation, 20: 31107
ZAPLESNICHENKO, G. P., Preparation of plastic scintillators in plate form, 20: 31261

ZARETSKII, D. F., Photoabsorption of nuclei in theory of Fermi-liquids, 20: 32639
ZARIN', D., Effect of x rays on extracellular accumulation of amino acids in Mycobacterium cyaneum 416, 20: 31005
ZARIPOV, M. M., EPR of Tb in CeO_2, 20: 32723
ZARIPOV, M. M., EPR of Gd^{3+} in Y and La double molybdates, 20: 32728
ZAVEL'SKII, F. S., Measurements using two-amplitude differential analyzer connected to coincidence scheme, 20: 31585
ZAWISCHA, D., Treatment of pairing in small systems by Green functions, 20: 32094
ZEBROSKI, E. L., Effect of stoichiometry on properties of mixed oxide U–Pu fuel, 20: 31674
ZEBROSKI, E. L., Plutonium and fission product redistribution in mixed oxide fuels, 20: 31804
ZELAZNY, R., New developments in reactor theory and neutron transport, 20: 32366
ZEL'CHINSKI, M., Radiation protection at WWRS-type reactor "EWA", 20: 32877
ZELDOVICH, A. G., Cryogenic developments at Joint Institute for Nuclear Studies, 20: 32318
ZELLE, Max, Advances in radiation biology. II., 20: 31038
ZENKEVICH, P. R., Correcting system for forced oscillations in accelerator with reverse coupling, 20: 31839
ZEPPENFELD, K., Energy loss of 50-kev electrons in Ge and Si, 20: 32732
ZHARNOVETSKII, K., Radiation protection at WWRS-type reactor "EWA", 20: 32877
ZHITNIKOV, R. A., PMR of H atoms formed in frozen acids irradiated at 77 deg K, 20: 32719
ZHUCHKOVA, T. N., Spectrometer of high aperture ratio, 20: 31481 (AERE-Trans-1050)
ZHUKOVA, I. A., Concentration and energy of formation of vacancies in Nb, 20: 32726
ZICHICHI, A., Determination of the $(\omega$-$\phi)$ mixing angle using nucleon electromagnetic form factors, 20: 32058
ZICHICHI, A., One-parameter fit to electromagnetic form factors of nucleon, 20: 32033
ZIEMBA, Francis P., Nuclear particle semiconductor detectors for aerospace applications, 20: 31605
ZIMERMAN, A. M., Equal-time commutators and $\eta \to 3\pi$ decays, 20: 32037
ZIMMERMANN, W., Invariant meson-sextet interactions in relativistic formulation of SU(6) symmetry, 20: 32116
ZIMMERMANN, W., Relativistic extension of SU(6) symmetry, 20: 32115
ZNAMENSKII, V. B., Inversion of levels during excitation by a monoenergetic electron beam, 20: 31941
ZOELLNER, W., Scattering of massive photons with vector-scalar coupling, 20: 32046
ZONTEK, D. E., Enriched uranium scrap assay gage, 20: 31174 (WAPD-T-1905)
ZORSKIE, J., Rotational-velocity and ion-density profiles in plasma vortices, 20: 32644
ZUCKER, A., Polarizations and differential cross sections for the elastic scattering of 40-Mev protons from ^{12}C, ^{40}Ca, ^{58}Ni, ^{90}Zr, and ^{208}Pb, 20: 32510
ZUNKER, Heinz O. H., Ultrastructural alterations in deuterium intoxication, 20: 30975
ZWICKER, H., Measurements of ion and electron temperature in theta-pinch plasma, 20: 32621
ZWOENITZER, Dieter, Emergency power supply in Gundremmingen power plant, 20: 32811

SUBJECT INDEX

Main entries in this index are generally specific materials, things, and processes. These are followed by modifiers that describe the properties of, and processes applied to, the main entries.

The number preceding the colon is the *NSA* volume number, and the number following is the abstract number. The designation (R) following the abstract number indicates that the abstract is of a progress report; (P) indicates a patent; and (T) indicates a translation. Abstracts for reports other than progress reports carry no letter designation. References to report numbers, where appropriate, are included after the abstract number of the citation. Published literature (journal article or book) is identifiable by the absence of a report number.

The user should bear in mind that the ideas presented in the original literature, rather than key words, have been indexed. The indexers have tried to select what seemed the most probable and logical place to look for typical information. Since it is not possible to anticipate where a user would look for information, numerous cross references are included in cumulative indexes to assist him in his search.

Experience in using an index of this type will be the best guide in obtaining the desired information, and a consideration of synonymous or closely related terms will prove valuable.

Information must be so indexed as to be of the greatest use to the greatest number of users. This requires that a topic be indexed to headings that most specifically describe it and not ordinarily to the headings that describe its ultimate use, nor to the general class headings that include the specific headings. For example, information on the treatment of thyroid disease with I-131 would be indexed under Thyroid Gland and under Iodine Isotopes I-131, but not necessarily under Radiotherapy. A study of the effects of x radiation on hair would be indexed under both X Radiation and Hair. However, the information would not be indexed under the experimental animal, e.g., Rats, unless the report discusses the effects on rat hair as compared with the effect on the hair of other animals.

The broad, general class headings are used only for general information or for comprehensive reports or articles.

Subject Heading Styles

Generally, the direct form of subject entry is used rather than inverted headings, e.g., Amino Acids rather than Acids, Amino; Helium Isotopes He-4 rather than Helium—Isotopes He-4 or Helium—He-4 isotopes. Note, however, that in some cases parenthetic modifying terms or inverted headings of the form Neutrons, Fast are used in preference to a direct entry that would result in the scattering of information. Organic compounds are usually entered in the index in the inverted form so that substituted compounds can be listed near the parent compound; e.g., Benzene, Bromo- rather than Bromobenzene. In general, the style of nomenclature used is that of Chemical Abstracts, except that some items listed in that publication as subheadings are elevated to form part of the main heading; e.g., Butyric Acid, Methyl Ester rather than Butyric Acid—methyl ester.

Alphabetization

Main headings are alphabetized word-by-word. A parenthetic qualifier following a main heading is disregarded in alphabetizing unless there are two or more headings identical except for the parenthetic qualifier, in which case the qualifier determines the order. Headings involving Greek letters are arranged as if the names of the letters were spelled out.

Examples:

M-Capture
  see Electron Capture
Magnesium
Magnesium Alloys
Manganese Fluorides
Manganese(II) Fluorides
Mesons
Mesons (π)
Mesons (ρ)
3-Pentanol, 2,4-Dimethyl-
2-Pentanol, 2-Methyl-
2-Pentanol, 4-Methyl-

Nomenclature of Inorganic Compounds

Inorganic compounds are indexed in the direct form, listing cations in the order of increasing valence in the case of polycationic salts of varying valence and in alphabetic order for polycationic salts in which all cations have the same valence; e.g., Sodium Aluminum Silicates and Potassium Sodium Sulfates.

Multicomponent Alloys and Other Systems

Multicomponent alloys, except well-known trade names, are indexed under a main heading in the form "element alloy" for each element in the alloy. The modifier begins with element symbols for each component arranged alphabetically as if the English name for the element were spelled out.

Example: Copper-Gold Alloy is indexed
  Copper Alloys
    Cu-Au...
  Gold Alloys
    Cu-Au...

Well-known alloys such as Zircaloy-2 are indexed directly to the trade name; cross references referring from each component of the alloy to the entry for the trade name appear in cumulative indexes.

Multicomponent systems of non-metallic elements are indexed in a manner similar to alloys except the main heading used contains the word "Systems" in place of "Alloys."

Example: Silicon–Tungsten Systems are indexed
  Silicon Systems
    Si-W...
  Tungsten Systems
    Si-W...

Multicompound systems and mixtures of compounds are indexed under the main heading for each component com-

pound; the modifiers begin with an alphabetical listing of compound formulas.

Example: Lead Titanate–Lead Zirconate is indexed
Lead Titanates
$PbTiO_3$-$PbZrO_3$...
Lead Zirconates
$PbTiO_3$-$PbZrO_3$...

A mixed system of compounds and elements is indexed using a combined form of the above conventions, e.g., a dispersion of copper and alumina would be indexed

Aluminum Oxides
Al_2O_3-Cu...
Copper Systems
Al_2O_3-Cu..

Physical States and Configurations of Materials

Specification of the physical state, if other than normal, or geometric configuration of the material is included in the modifying phrase, i.e., liquid metals would be indexed to the metal with "liquid" in the modifier, and carbon crucibles would be indexed to Carbon with "crucibles" appropriately placed in the modifier and also to Crucibles if appropriate.

Modifying Phrases

The modifiers appearing under a main heading are written specifically to describe the relation of the item being indexed to that main heading. The modifier, therefore, will generally contain more useful information about that relation than will a title or a phrase written to be used under every main heading assigned to the item. Effort is exerted to begin the modifier with the word judged to be of greatest use to the greatest number of users; this, however, does not obviate the need to consider all modifiers under the main heading(s) of interest.

Modifiers are usually intended to form a meaningful phrase when combined with the main heading. Some are intended to be read following the main heading, e.g., the entry Hydrogen—sorption by charcoal is read "hydrogen sorption by charcoal"; however, as a result of placing the important word first, many modifiers must be arranged for smooth reading, e.g., Formaldehyde—yields in radiolysis of ethyl ether, effects of deuterium on is read "effects of deuterium on formaldehyde yields in radiolysis of ethyl ether" and Uranium—crystal structure of, effect of cooling rate on allotropic transformations in is read "effect of cooling rate on allotropic transformations in crystal structure of uranium." Prepositions are sometimes omitted if no ambiguity results.

Special characters are added to modifiers in the field of physics; if the modifier does not establish the experimental or theoretical character of a reference, a symbol (E), (T), or (E/T) is placed immediately after the modifying phrase and before the journal reference number. The value of this identification has been established by the American Institute of Physics.

A

ACCELERATOR TUBES
particle motion in oblique-field, 20: 31842
ACCELERATORS
beam deflection in, method for dispersionless, 20: 31847
beam injection channel for accumulator of 100-Mev electron, 20: 31849
beam monitor for nanosecond pulsed electron, noninterrupting, 20: 31846
design and performance of Kaman, as pulsed neutron generator for nuclear engineering studies, 20: 32360
development and operation of dynamitron, 20: 31786(R) (ORO-2891-5)
radioactivity levels in, induced, 20: 31831
storage ring for Orsay ACO, design of, 20: 31816 (CEA-R-2929)
vacuum system for proton, liquid-nitrogen cooled shield against contamination from oil-pumped, 20: 31848
ACCIDENTS
plutonium, evaluation and treatment of wounds in, 20: 31030 (BNWL-SA-39)
ACETAMIDE, 2-AMINOTHIO-
effects on radiation effects on *Allium cepa* roots, 20: 31137
ACETAMIDE, *N,N*-DIMETHYL-
complexes with neptunium chlorides, preparation and properties of, 20: 31235
ACETAMIDE, IODO-
radiosensitivity effects of, use of activation analysis for determining mechanism of, 20: 31172 (SGAE-BL-17/1966)
ACETIC ACID
determination by xenon trioxide oxidation, titrimetric, 20: 31196
deuterium exchange with active methyl hydrogens of pyrylium and tropylium compounds, 20: 31260
use of carbon-14-labeled, in preparing labeled oxalic acid, 20: 31263
ACETIC ACID, [(CARBOXYMETHYLIMINO) BIS(ETHYLENENITRILO)] TETRA-
use for treatment of plutonium contaminated wounds, 20: 31030 (BNWL-SA-39)
ACETIC ACID, (ETHYLENEDIAMINE) TETRA-, SODIUM SALTS
effects on radioinduced degradation of DNA in *E. coli*, 20: 31144
ACETIC ACID, IODO-
radiosensitivity effects of, use of activation analysis for determining mechanism of, 20: 31172 (SGAE-BL-17/1966)
ACETIC ACID, TRICHLORO-
yields from gamma radiolysis of aqueous carbon tetrachloride and chloroform solutions saturated with carbon dioxide, 20: 31276
ACETIC ACID, TRIFLUORO-, URANIUM SALTS
preparation and chemical properties of, 20: 31236
with carboxylic acids, preparation and chemical properties of, 20: 31236
ACETOACETIC ACID
effects on radioinduced degradation in DNA in *E. coli*, 20: 31144
ACETYLENE
deuterium exchange between water and, factors affecting, 20: 31640(R) (NYO-755-1, pp 130-72)
hydrogen ion reactions at 20 to 120 kev, ionization cross sections for, 20: 31909
ACIDS
reactions with ammonia, NMR studies of, 20: 31218(R) (UCRL-16658, pp 1-9)
ACOUSTIC WAVES
excitation of electro-acoustic lateral, in hot compressible plasma, (T), 20: 32590
propagation of electro-acoustic, in isotropic compressible plasma, (T), 20: 32591
ACRYLIC ACID
radioinduced solid-state polymerization of, with crotonic acid, 20: 31287
ACTINIUM ISOTOPES Ac-227
use in isotopic power generators for space, 20: 31965
ACTIVATION ANALYSIS
of fission products for praseodymium-141, 20: 31167(R) (ANL-7175, pp 217-25)
sensitivity of, effects of variations in isotopic ratio on, 20: 31190
technique for remote-surface, neutron, 20: 31211
use of neutron, for potassium–argon dating, 20: 31431
use of neutron, for mineral exploration and soil analysis, 20: 31434
use of neutron, for determining trace elements in materials, computer program for, 20: 31541
uses of, for determination of radiosensitizers in tissues, 20: 31172 (SGAE-BL-17/1966)
ADAMANTANE
radiation effects on stability of, *y*, 20: 31273
ADENINE, *N*-FURFURYL-
analysis for carbon-14 in agar blocks by liquid scintillation counting, 20: 31179
ADRENAL GLANDS
corticosteroid synthesis by rat, effects of hypophysectomy on, 20: 31011
radiation effects on synthesis of corticosteroids by rat, 20: 31011
radiation effects on goldfish, pathological, 20: 31094
ADSORPTION
study by field emission microscopy, techniques of, 20: 32742
AERIAL SURVEYING
data from radioactivity, over Cape Thompson, Alaska, 1958, 20: 31425 (PNE-481, pp 1115-19)
data from, of Albuquerque–Los Alamos area, 20: 31396 (CEX-61.6.2)
AEROSOLS
distribution in atmosphere of polydisperse, diffusion method for measuring, 20: 31461
fission product deposition on tropospheric, 20: 31459
plutonium-239 distribution from inhaled, in dogs, 20: 30968 (BNWL-SA-11)
AGAR-AGAR
effects on radiation effects with novoembichine on amino acids in *Mycobacterium cyaneum* 416, 20: 31005
effects on x-radiosensitivity of trypsin solutions, 20: 31017
radioactivity of, liquid scintillation measurements of, 20: 31179
AGE
effects on immunogenic efficiency of double vaccination with x-irradiated *Ancylostoma caninum* in dogs, 20: 31043
AGE ESTIMATION
argon–potassium, by activation with fast neutrons, 20: 31431
carbon-14 method for, 20: 31433
carbon-14 methods of, uses of, 20: 31429
use of silicon-32 for ground water, 20: 31432
AGRICULTURE
radioisotope uses in, 20: 31109
AIR
effects of moist, on oxidation of yttrium, 20: 31686
effects on hardness of iron- and nickel-base alloys at 1200 to 1400°F, 20: 31669
effects on radiosensitivity of Kalanchoe, 20: 31076
electron reactions with rarefied, emission spectra from, (E), 20: 31921
microwave propagation in plasma of, 20: 32667
radiation from high-temperature gas of, pressure and temperature dependence of, (E), 20: 32240
reactions with Hastelloy X at 1300 to 1800°F, 20: 31669
reactions with sodium at high temperatures, 20: 31440(R) (ANL-7175, pp 159-83)
separation from plutonium hexafluoride by hydrolysis, 20: 31315(R) (ANL-7175, pp 42-103)
AIRCRAFT
radioactivity measurements in commercial, 20: 31952
radioisotope uses in Army, 20: 31622
ALANINE
analysis for carbon-14 in agar blocks by liquid scintillation counting, 20: 31179
radiation effects combined with novoembichine on accumulation of, in *Mycobacterium cyaneum* 416, 20: 31005
ALASKA
bioenvironment, physical characteristics, and radioactivity of Cape Thompson region, 20: 32885 (PNE-481)
fallout monitoring at Cape Thompson, 1956 through 1962, 20: 31428 (PNE-481, pp 1165-1200)
fallout radionuclide content in ecosystems of, 20: 31442 (BNWL-SA-661)
radioactivity of Cape Thompson-Cape Seppings area, aerial survey of 1958, 20: 31425 (PNE-481, pp 1115-19)
ALBUMINS
radioinduced free radicals in blood serum, effects of metal ions on *y*, 20: 31003
ALBUQUERQUE AREA (N. MEX.)
radiation monitoring of, aerial natural, 20: 31396 (CEX-61.2.2)
ALCOHOLS
mass spectra, 20: 31198
ALGAE
radionuclide uptake by, *in situ* measuring instrument for, 20: 31504(R) (BNWL-235-4, pp 16-18)
uptake and loss of cesium, rubidium, and sodium in relation to active mechanism for sodium extrusion in Scenedesmus cells, 20: 30994
ALKALI METAL HALIDES
color centers in, electronic structure of F, (T), 20: 32682 (ORNL-P-2193)
radioinduced color centers in, x, 20: 32691
ALKALI METAL SILICATES
radioinduced absorption centers at low temperatures in glasses of, gamma, 20: 32733
ALKALI METALS
dissociation energies of, 20: 31221(R) (UCRL-16658, pp 73-87)
effects of liquid, on building materials, bibliography on corrosive,

20: 31680 (NAA-SR-Memo-11652)
ALKENES
mass spectra, 20: 31198
ALLOYS
corrosion of, method for measuring intensity of, 20: 31682 (NP-16003)
vacancy distributions on sublattices of ordered, 20: 31714(R) (UCRL-16658, pp 99-103)
ALPHA DECAY
barrier penetrabilities for even-mass nuclei, 20: 32399
ALPHA PARTICLES
angular distributions from proton reactions (p,α) with zinc-66 and -68 at 17.5 Mev, 20: 32489
angular distribution from proton reactions (p,α) with zinc-66 and zirconium-92 at 28 Mev, 20: 32489
clustering in nuclear matter, (T), 20: 32542
detection and measurement in human blood, 20: 31145
detection of, low-background silicon detector for, 20: 31540
dosimetry in radon-222 baths, 20: 31157
dosimetry of, computer program for, 20: 32674 (NP-15697(Vol.3))
effects of polonium-210, on spermatogenesis in mouse testes, 20: 31063
effects on animal cells in culture, effects of oxygen on biological, 20: 31123
effects on ethylene, polymeric ions from, 20: 31270
effects on inner and outer epidermises of *Allium cepa* and *Mnium cuspidatum*, 20: 31079
effects on water vapor, production of ions from, 20: 31270
emission in proton reactions with gold-197 at 155 Mev, (T), 20: 32455
interactions with alpha particles at high energies, optical potential for, (T), 20: 32531
interactions with alpha particles at high energies, differential cross sections for, 20: 32532
production in deuterium–tritium reactions, deuteron detection by, 20: 32586
reactions (α,α') and (α,d) with nuclei, effects of Coulomb interaction on, (T), 20: 32484
reactions (α,Be-7) with magnesium-27 at 35 to 65 Mev, angular-momentum effects in, (E), 20: 32507
reactions ($\alpha,n\gamma$) with oxygen-18 at 4.43 and 5.5 Mev, neon-21 levels from, (E), 20: 32427
reactions ($\alpha,n\gamma$) with oxygen-18 at 4.7 to 6.0 Mev, neon-21 levels from, (E), 20: 32474
reactions ($\alpha,n\gamma$) with oxygen-18 at 4.15 Mev, neon-21 levels from, (E), 20: 32476
reactions with gold at 1 Mev, secondary electron emission from, 20: 31918
reactions with silver-107 and zinc-64, excitation functions for, (T), 20: 32373(R) (COO-1530-1)
scattering by nuclei, computer program for analysis of inelastic, 20: 32544
scattering by oxygen-16 at 11.09 and 12.05 Mev, level spins and parities from elastic, (E), 20: 32502
scattering by oxygen-16 at 31.8 and 39.5 Mev, inelastic, (E), 20: 32554
scattering losses in plastic and sodium iodide scintillators, 20: 31542
spectra from neutron reactions (n,α), (n,$\alpha n'$), and (n,$n'\alpha$) with sodium-23 at 12.6 to 18.7 Mev, (E), 20: 32540
ALPHA SPECTRA
determination for Lunar and Martian space missions, (T), 20: 32674 (NP-15697(Vol.3))
ALPHA SPECTROMETERS
use for monitoring radon-222 in air, 20: 31157
ALTIMETERS
design of pulsed x-ray, 20: 31493
ALUMINUM
analysis of, by spark-source mass spectrography, background in, 20: 31203
bremsstrahlung reactions (y,p) at 32 Mev proton energy spectra from, (E), 20: 32394
effects on grain size and transformations in alpha-uranium and uranium alloys at 720 to 800°C, 20: 31666
effects on hardness of molybdenum, 20: 31741
effects on radioinduced swelling in uranium irradiated at 400 to 500°C, 20: 31666
electron tunneling in superimposed layers of superconducting lead and normal, (E), 20: 32342
gamma scattering at 0.1 to 8.0 Mev, resonance, (E), 20: 32369 (AECL-2535)
gamma scattering at 0.662 and 1.25 Mev, cross sections for Compton, (E), 20: 32007
hydrogen atom and ion reactions at 10 to 40 kev, secondary electron emission from, (E), 20: 31533
joining to aluminum, parameters for friction, 20: 31670
laser beam reactions on surfaces of, momentum transfer by giant-pulsed, (E), 20: 31810
neutron capture by, average level widths of compound nucleus from, (E), 20: 32424
neutron scattering by, energy spectra from cold, (E), 20: 31567
nucleon reactions at high energies, residual radioactivity from, 20: 31831
proton reactions at 0.05 to 2.9 Bev, induced activity data and cross sections for spallation, 20: 32549
radiation effects on tensile properties of, at cryogenic temperatures, fast-neutron, 20: 31784(R) (NASA-CR-54976)
radiation effects on lattice parameter of, neutron, 20: 31669
reactions with steam at 1400°C, hydrogen evolution from, 20: 31440(R) (ANL-7175, pp 159-83)
specific heat of, effects of pressure on, 20: 32684(R) (UCRL-16658, pp 21-38)
sputtering by cesium ions at 0.5 to 15 kev, yields from, 20: 31948
stacking-fault energies of, 20: 31715(R) (UCRL-16658, pp 105-20)
superconducting energy gap anisotropy in magnetic fields, determination using microwave absorption, 20: 32326
use as electric power transmission cables, for SNAP-8, 20: 32853 (NAA-SR-Memo-11925)
ALUMINUM ALLOY COUPLES
Al–stainless steel, contact thermal conductance of, 20: 31712 (UCRL-14227(Rev.1))
ALUMINUM ALLOYS
tensile properties of type 7178, at cryogenic temperatures, 20: 31784(R) (NASA-CR-54976)
Al–Cr–Fe–Mo–Ni–Ti, radiation effects on tensile properties of Nimonic PE16, thermal-neutron, 20: 31669
Al–Cu, crystal symmetry of, Kikuchi analysis of, 20: 31715(R) (UCRL-16658, pp 105-20)
Al–Cu, radiation effects on electric conductivity of, neutron, 20: 31786(R) (ORO-2891-5)
Al–Dy, crystal structure of $DyAl_3$, 20: 31728
Al–Fe, mechanical properties of, effects of aluminum content and temperature on, 20: 31751
Al–Ho, crystal structure of $HoAl_3$, 20: 31728
Al–Mg, stacking-fault energies of, 20: 31715(R) (UCRL-16658, pp 105-20)
Al–Nb, phase diagram, 20: 31769
Al–Sn–Ti, radiation effects on tensile properties of, at cryogenic temperatures, fast-neutron, 20: 31784(R) (NASA-CR-54976)
ALUMINUM CARBIDES
effects on neutron-induced contraction in graphite, 20: 31667
ALUMINUM ISOTOPES Al-24
energy levels and mass from helium-3 reactions (He-3,t) with magnesium-24 at 37.8 to 40.1 Mev, (E), 20: 32473
ALUMINUM ISOTOPES Al-25
energy levels from beta-delayed proton spectra of silicon-25, (E), 20: 32505
ALUMINUM ISOTOPES Al-27
neutron reactions (n,α) at 13.5 to 14.8 Mev, cross sections for, (E), 20: 32528
proton reactions (p,Be-7) at 35 to 65 Mev, angular-momentum effects in, (E), 20: 32507
ALUMINUM ISOTOPES Al-28
energy level density in, (T), 20: 32432
ALUMINUM NITRIDES
vaporization kinetics, 20: 31718(R) (UCRL-16658, pp 149-54)
ALUMINUM OXIDES
bonding to niobium, method for, 20: 31669
compatibility with cesium vapor at 1800°C, 20: 31669
dehydration of crystalline, 20: 31719(R) (UCRL-16658, pp 155-69)
diffusion of gases in, 20: 31719(R) (UCRL-16658, pp 155-69)
performance in focus electrodes in cesium-contact ion thrustors, 20: 31383
radioinduced transmutations in, calculation of gas volume from neutron, 20: 31799
reactions with bromine pentafluoride mixtures of fission products and uranium chlorides, 20: 31315(R) (ANL-7175, pp 42-103)
strength of hot-pressed, effects of process variables on, 20: 31669
Al_2O_3–BeO–MgO, properties of molten, for fuel matrix for homogeneous thermal nuclear reactors, 20: 31726
Al_2O_3–B_2O_3–EuO, preparation and Faraday rotation of glasses of, 20: 31733
Al_2O_3–MgO, grain boundary precipitation in, 20: 31738
ALUMINUM SYSTEMS
Al–C–Mo, superconductivity of Mo_3Al_2C in, 20: 32312(R) (UCRL-16658, pp 133-43)
Al–PuO_2, fabrication and properties of dispersion fuels of, 20: 31666
Al–Si, crystal structure of eutectic, effects of phosphorus on, 20: 31716(R) (UCRL-16658, pp 121-32)
AMERICIUM
oxidation-reduction reactions of, bibliography on kinetics of, 20: 31215 (LA-3507)

processing of irradiated, by extraction chromatography, 20: 31323
separation of, from berkelium and californium by extraction chromatography, 20: 31323

AMERICIUM ISOTOPES Am-241
alpha decay of, conversion electrons from, (E), 20: 32375 (ITEF-351)
gamma spectra, 20: 31500(R) (BNWL-235-4, pp 4-10)

AMIDE POLYMERS
decomposition of, effects of irradiated water at pH 10.5 and 40 to 45°C on, 20: 31280

AMINES
complexes with uranium tetrafluoride, preparation of, 20: 31236

AMINO ACIDS
radiation effects on composition of, in dog blood serum, 20: 31021
radiation effects on content in meat, γ, 20: 31630
radiosensitivity effects on *Bacillus subtilis*, uv, 20: 31129

AMMETERS
performance of cryotron relaxation oscillators as, in superconducting circuits, 20: 32333

AMMONIA
complexes with uranium tetrafluoride, preparation of, 20: 31236
production for fertilizer, using power from nuclear desalination reactor, economics of, 20: 32841 (ORNL-3882)
radioinduced synthesis of, from nitrogen and water, γ and uv, 20: 31289
reactions with weak acids, NMR studies of, 20: 31218(R) (UCRL-16658, pp 1-9)
solvent properties for calcium, 20: 31220(R) (UCRL-16658, pp 39-72)
NH_3–metal, kinetics and structure of solutions of, 20: 31218(R) (UCRL-16658, pp 1-9)

AMMONIUM BROMIDES
ammonium ion rotational behavior in normal and deuterated, neutron spectrometric studies of, 20: 31241

AMMONIUM CHLORIDES
ammonium ion rotational behavior in normal and deuterated, neutron spectrometric studies of, 20: 31241

AMMONIUM IODIDES
ammonium ion rotational behavior in, neutron spectrometric studies of, 20: 31241

AMMONIUM IONS
rotational behavior in crystal lattices, neutron spectrometric studies of, 20: 31241

AMMONIUM PERCHLORATES
effects of irradiated, on solid propellants, 20: 31286

AMMONIUM SULFATES
crystal structure of ferro- and paraelectric, neutron-diffraction analysis of, 20: 32698

AMMONIUM TIN BROMIDES
ammonium ion rotational behavior in, neutron spectrometric studies of, 20: 31241

AMMONIUM TIN CHLORIDES
ammonium ion rotational behavior in, neutron spectrometric studies of, 20: 31241

AMPLIFIERS
design for radiation detectors for aerospace applications, 20: 31609
design of stable pulsed, for alpha spectrometer, 20: 31580
use to obtain starting pulses for time-of-flight measurements, 20: 31579

ANIMAL CELLS
effects of AET, glutathione, and serotonin mixture on lysosome morphology in mouse stem cells, 20: 30964
nucleic acid synthesis in cultured, from leukemia and myeloma patients, 20: 30971 (ORINS-45)
protein synthesis in cultured, from leukemia and myeloma patients, 20: 30971 (ORINS-45)
radiation effects on, mechanisms of, 20: 31108
radiation effects on DNA synthesis and mitosis in HeLa cell cultures, γ, 20: 31008
radiation effects on reproduction of hamster and HeLa, γ, 20: 31051
radiation effects on function and ultrastructure of isolated rat sympathetic ganglion, x, 20: 31055
radiation effects on cultured HeLa, biological x, 20: 31056
radiation effects on fine structure of Paneth cells in mice, x, 20: 31083
radiation effects on survival of synchronized L cells in mice, uv, 20: 31084
radiation effects on, in flagellate *Astasia longa*, 20: 31085
radioinduced lethality of, role of genetic damage in, 20: 31042
radiosensitivity of cultured, effects of oxygen on α, deuteron, fast-neutron, and x, 20: 31123
radiosensitivity of cultured HeLa, effects of anoxia and *N*-ethylmaleinimide on, 20: 31130
radiosensitivity of, relation of cellular control systems to, 20: 31064

ANIMAL REPRODUCTION
radiation effects on susceptibility of mice exposed *in utero* to congenital anomalies, x, 20: 31066
radiation effects on live births among atomic bomb survivors of Hiroshima and Nagasaki, 20: 31091

ANIMAL RESPIRATION
effects of cystamine on rat, 20: 30984

ANIMALS
body temperature, heartbeat, and respiration of, remote monitoring equipment for, 20: 30961(R) (BNWL-235-4, pp 25-9)
handling and housing of, in radioisotope tracer lab, 20: 31469
movement and position in cages, monitoring equipment for, 20: 30960(R) (BNWL-235-4, pp 22-5)
radiation injuries to, from barium-140 deposited in aortic wall, chemical protection against, 20: 31142
radiation injuries to, effects of bone marrow and chemical compounds on, 20: 31142
radioisotope transfer mechanisms in placentas of, effects of inactive carriers on, 20: 31142
radiosensitivity of mouse intestinal crypt, effects of AET, glutathione, and serotonin on x, 20: 31128
respiration of test, measuring equipment for, 20: 31475(R) (BNWL-235-4, pp 19-20)

ANODES
reactions in porous metal, 20: 31220(R) (UCRL-16658, pp 39-72)

ANOXIA
effects of radioprotective compounds on cellular, 20: 31122
effects on radiation effects on *Allium cepa* roots, 20: 31137
radiosensitivity effects in rat tissues, 20: 31122
radiosensitivity effects on HeLa cells in culture, x, 20: 31130
radiosensitivity effects on *Thiobacillus thiooxidans*, x, 20: 31139

ANTARCTICA
carbon-14 content of atmosphere at Scott Base, 20: 31410

ANTIBARYONS
interactions with mesons, N/D method for multichannel, 20: 32181

ANTIBODIES
radiation effects on formation of thyroglobulin, in euthyroid patients receiving iodine-131, 20: 31161

ANTIGENS
radiation effects on *Treponema pallidum* content in rabbit, 20: 31119

ANTIMONY
determination in conductive tissue of beef heart, activation, 20: 31176
determination in human heart tissue, activation, 20: 31175

ANTIMONY ALLOYS
Bi–Sb, superconducting transitions of amorphous, 20: 32341
Sb–In, sputtering by argon ions at 75 to 600 ev, yields from, (E), 20: 31914

ANTIMONY ISOTOPES Sb-124
radioinduced oxidation of trivalent to pentavalent, effects of ultraviolet radiation on self-, 20: 31300

ANTINEUTRINOS
flux density in universe, upper limits for, 20: 32012
interactions with nucleons, amplitudes and selection rules for inelastic, (T), 20: 32090

ANTIOXIDANTS
effects on inhibition of selected photosensitizers in *Tetrahymena pyriformis*, 20: 31018

ANTIPROTONS
interactions with neutrons at rest in deuterium annihilation, (E), 20: 32015
interactions with protons, nucleon electromagnetic form factors for, 20: 32033
interactions with protons, branching ratios for annihilation, (T), 20: 32045
interactions with protons and neutrons, SU_{6W} predictions for, 20: 32056
interactions with protons, $(\omega$-$\phi)$ mixing angle from, (E/T), 20: 32058
interactions with protons, vector meson exchange for real part of forward amplitude of, (T), 20: 32065
interactions with neutrons, Regge-pole theory for charge-exchange, 20: 32069
interactions with protons at high energies, uncorrelated jet model for elastic, 20: 32028
interactions with protons, Dalitz plot density for $\pi\bar{K}k$ final state from, 20: 32047
scattering by emulsion nuclei at 3 Bev/c, amplitudes for elastic, (E/T), 20: 32467
separation from proton beams in waveguides, 20: 31841

ARGON
cyclotron harmonic radiation from plasma of, in magnetic field, (E/T), 20: 32637
diagnostics of arc plasma of, using laser scattering, (E), 20: 32599
diffusion model for, 20: 32684(R) (UCRL-16658, pp 21-38)
electron-heavy particle nonequilibrium in partially ionized plasma jets of, 20: 32658
electron-ion recombination in dense plasma of, limits of validity of radiationless, 20: 32575 (NASA-TN-D-3372)
heat capacity at 0.4 to 10°K, 20: 32684(R) (UCRL-16658, pp 21-38)

ionization of gases of, by laser beam at low pressure, (E), 20: 32665
ionization of, by electrons at 0.6 to 20 kev, cross sections for, (E/T), 20: 31906
positron annihilation in liquid, angular distribution of photons from, (E), 20: 32345
positron annihilation and elastic scattering in, calculations of, 20: 32105
properties of electrodeless discharge plasma of, probe measurements of, 20: 32655
reactions of, with ions, atom and charge transfer in, 20: 31224
relaxation of potassium-seeded plasma of, to steady state, 20: 32657
relaxations of atoms in solid, during vacancy formation, 20: 32684(R) (UCRL-16658, pp 21-38)
separation of nitrogen from, by titanium gettering, 20: 31314(R) (ANL-7175, pp 1-41)
stability of Poiseuille plasma arc of, in axial magnetic fields, (E/T), 20: 32614

ARGON IONS
reactions of, with molecules, atom and charge transfer in, 20: 31224
reactions with metal surfaces, secondary emission factors for, 20: 31926
reactions with molybdenum at 2 to 15 kev, ejected electron energy distribution from, (E), 20: 31939
reactions with sodium chloride at 40 to 2000 ev, electron emission from, (E), 20: 31912
sputtering on germanium (100) and (110) surfaces, temperature dependence of yields from, 20: 31915
sputtering on semiconducting compounds at 75 to 600 ev, yields from, (E), 20: 31914

ARGON ISOTOPES
abundance in stone meteorites, relative, 20: 31876

ARGON ISOTOPES Ar-36
energy levels from proton reactions (p,γ) with chlorine-35 at 733 to 2595 kev, (E), 20: 32451

ARGON ISOTOPES Ar-40
proton elastic scattering at 18.5 and 20.5 Mev, polarization from, (E/T) 20: 32523

ARGON SYSTEMS
Ar–O, shock layers in, magnetohydrodynamically supported, (E), 20: 32217 (N-65-33713)

ARSENIC
determination in conductive tissue of beef heart, activation, 20: 31176
determination in human heart tissue, activation, 20: 31175

ARSONIUM COMPOUNDS
with neptunium oxychlorides, preparation and properties of, 20: 31235

ASCORBIC ACID
radiation effects on content of, in oranges, γ, 20: 31632

ASPARTIC ACID
determination by xenon trioxide oxidation, titrimetric, 20: 31196
radiation effects combined with novoembichine on accumulation of, in *Mycobacterium cyaneum* 416, 20: 31005

ASTRONAUTS
radiation effects on, in space, hematological, 20: 31029 (BNL-10221)
radiation hazards to, during space flight, proton, 20: 31095

ASTROPHYSICS
elementary-particle composition of superdense matter in, 20: 32044
gravitational collapse of interstellar gas cloud, effect of magnetic field on, 20: 31862
spectral red shift in conformally flat space, (T), 20: 31855

ATLANTIC OCEAN
strontium-90 content in surface waters of, 1961, 20: 31418
strontium-90 distribution in surface waters of, 1960 and 1961, 20: 31420

ATMOSPHERE
airglow in, helium and hydrogen spectra in, 20: 32289
book: *Particles in the Atmosphere and Space*, 20: 32285
carbon-14 content and distribution in, 1963 to 1966, 20: 31397(R) (RLO-1776-2)
carbon-14 content of, in Southern Hemisphere, effects of fallout from nuclear explosions on, 20: 31410
carbon-14 content of, methods for determining, 20: 31433
contamination control techniques for nuclear facility, 20: 31453 (STI-PUB-121)
electron energy spectra in, soft, (E), 20: 32270
fallout in, stratospheric-tropospheric mass exchange mechanism for, 20: 31402
fission product distribution in, 1963 to 1966, 20: 31397(R) (RLO-1776-2)
gamma energy spectra in upper, at 100 to 2000 Mev, (E), 20: 32283
lead-210 content in, effects of local meterological parameters on, 20: 31407
proton acceleration in low-altitude auroral, 20: 32249
radiation monitoring for beta and gamma activity in New Zealand, 1965, 20: 31446(R) (NP-16015)
radiation monitoring of, calibration of unit for continuous, 20: 31528
radioactivity distribution on polydisperse aerosol in, diffusion method for measuring, 20: 31461
radioactivity of, at 500 ft, San Francisco region, California, 20: 31395 (CEX-58.4.5)
radon vertical distributions in, 20: 31404
radon-222 content in, at therapeutic baths, 20: 31157
strontium-90 content of, above continents and oceans, 20: 31421
thoron vertical distribution in, 20: 31404

ATOMIC ENERGY
development in India, 20: 32817
development in, Belgium, review of, 20: 32890

ATOMIC EXPLOSIONS
effects on urban areas, models of, 20: 31332 (URS-651-4)
fallout from USSR underground, Jan. 15, 1965, 20: 31405
fallout monitoring in Israel after Chinese, May, 1965, 20: 31408
radiation effects on human populations, 20: 31091
radioisotope fractionation in fallout particles from, on land, 20: 31460
use for excavation of sea-level canal in Central America, 20: 31336

ATOMIC MASSES
measurement of, developments since 1926 in, 20: 31808

ATOMS
association of neutral, with ions, 20: 31221(R) (UCRL-16658, pp 73-87)
electron scattering at 2 to 200 ev by neutral heavy, relativistic effects in, (T), 20: 31923
energy level fluorescence yields of, 20: 31936
energy levels of beryllium sequence, expectation values for, 20: 31934
energy levels of lithium ^2S sequence, correlation, 20: 31935
perturbation theory for, Brueckner and Goldstone, 20: 31944
scattering in crystal lattices, nonbinary model for, 20: 31920
spectra of, Heisenberg uncertainty principle for determining, (T), 20: 31910

AURORAL STORMS
properties of September 22–3, 1963, 20: 32272
radio wave emission from, v-l-f, 20: 32256

AUSTENITE
microstructure of deformed, 20: 31716(R) (UCRL-16658, pp 121-32)

AUSTRALIA
carbon-14 content of atmosphere at Melbourne, 20: 31410
fallout monitoring, 1961 through 1963, 20: 31403

AUSTRIA
radiation processing of food in, review of, 20: 31628

AUTORADIOGRAPHY
techniques for, of plutonium distribution in plutonium oxide–uranium oxide pellets, 20: 31212

B

BACTERIA
radiation effects on *Thiobacillus thiooxidans*, effects of anoxia, chemicals, and pH on, 20: 31139
radiation effects combined with novoembichine on amino acid accumulation in *Mycobacterium cyaneum* 416, 20: 31005
radiation effects on genetic transcription in Rhodopseudomonas, x, 20: 31033(R) (NASA-CR-59196)
radiation effects on, in Dungeness crabmeat and Pacific oysters, gamma, 20: 31626
radiation injuries in, repair of premutational uv and x, 20: 31040
radiation injury and recovery mechanisms in, uv, 20: 31039
radiosensitivity of *Bacillus subtilis*, effects of amino acids on uv, 20: 31129
radiosensitivity of, genetic control of, 20: 31041
structure of radioresistant *Flexner bacilli*, ultrafine, 20: 30966

BACTERIOPHAGES
radiation injuries to, 20: 31142
radiosensitivity of, genetic control of, 20: 31041
use of dry films of, for radiation dosimetry, 20: 31093

BARIUM
determination in conductive tissue of beef heart, activation, 20: 31176
determination in human heart tissue, activation, 20: 31175
effects on corrosion of graphite by water vapor, 20: 31667
proton reactions at 0.05 to 2.9 Bev, induced activity data and cross sections for spallation, (E/T), 20: 32549
separation from irradiated chromium–uranium alloy by solvent extraction using liquid magnesium, 20: 31320 (UCRL-16108)

BARIUM ALLOYS
Ba–Hg, critical temperatures of intermetallic compounds in, 20: 31757

BARIUM FLUORIDES
vapor pressure, 20: 31718(R) (UCRL-16658, pp 149-54)

BARIUM ISOTOPES Ba-134
nuclear deformation parameter and quadrupole moment of, (E), 20: 32404

BARIUM ISOTOPES Ba-135
nuclear deformation parameter and quadrupole moment of, (E), 20: 32404

BARIUM ISOTOPES Ba-136
nuclear deformation parameter and quadrupole moment of, (E), 20: 32404
BARIUM ISOTOPES Ba-137
nuclear deformation parameter and quadrupole moment of, (E), 20: 32404
radiation hazard from atmospheric, in mixture with cesium-137, 20: 31528
BARIUM ISOTOPES Ba-138
nuclear deformation parameter and quadrupole moment of, (E), 20: 32404
BARIUM ISOTOPES Ba-140
beta decay of, spectra of, (E), 20: 32407
content in fallout in Japan, 1965, 20: 31405
content in fallout particles from high-altitude explosions, 20: 31424
BARIUM OXIDES
$BaO–Li_2O–O–Tc_2O_7$, compound formation in, 20: 31244
$BaO–O–Na_2O–Tc_2O_7$, compound formation in, 20: 31244
$BaO–O–Tc_2O_7$, compound formation in, 20: 31244
BARIUM TITANATES
$BaTiO_3–BaUO_3$, dielectric properties and phase studies of, 20: 31735
$BaTiO_3–UO_2$, dielectric properties and phase studies of, 20: 31735
BARIUM URANATES
$BaTiO_3–BaUO_3$, dielectric properties and phase studies of, 20: 31735
BARLEY
radiation effects on mutations of, x, 20: 31109
radiation effects on roots of, biological, 20: 31052
radioinduced chromosome aberrations in seeds of, effects of Myleran on neutron, 20: 31136
radioinduced mutations in seeds of, γ and x, 20: 31050
radiosensitivity of seedlings of, γ, 20: 31020
BARYONS
decay of, SU(3) symmetry for leptonic and nonleptonic, 20: 32175
decay of, unitary symmetry for $\Delta S = -\Delta Q$ leptonic, 20: 32184
interactions with mesons, experimental status of baryon-exchange, 20: 32027
interactions with mesons in relativistic formulation of SU(6), 20: 32116
interactions with mesons, U(3) × U(3) for amplitudes of collinear, 20: 32131
interactions with mesons, Dashen-Frautschi method for parity-conserving coupling, 20: 32138
interactions with mesons, N/D method for multichannel, 20: 32181
interactions with mesons, bootstrap of 70-plet of SU(6) for, 20: 32151
magnetic moments in SU(3), 20: 32178
mass breaking in SU(3) symmetry in strong-coupling theory, 20: 32128
mass formula for octet of, without symmetry breaking, 20: 32132
mass formulas for spin-½⁺, model for, 20: 32130
mass formulas for, in pole approximation in SU(3), 20: 32129
production of P_{33}, in meson (π)-nucleon interactions, (T), 20: 32023
production of $Y_1^*(1385)$ and $Y_0^*(1660)$, in meson (K^-)-proton interactions, (E/T), 20: 32034
structure of, 20: 32082
structure of, inner symmetry in, 20: 32176
symmetry for, isotropic spinor modulation in, 20: 32215
BARYONS, RESONANCE
decay angular correlations for Y_1^{*-}, from meson (K^-)-proton interactions, (T), 20: 32052
decay of N*, Ξ^*, Y*, and Y_1^*, broken SU(3) for widths of, 20: 32019
decay of Ξ^* in one-particle exchange model, 20: 32009
lifetime of, Heisenberg uncertainty principle for determining, 20: 31910
mass formulas for spin-3/2⁺, model for, 20: 32130
photoproduction of N*(1238) on protons at 0.9 to 1.3 Bev, (E/T), 20: 31983 (CALT-68-71)
production in electron-positron interactions, differential cross sections for, (T), 20: 32018
production in proton-proton interactions at 12.5 Bev/c, upper limit for, 20: 32066
production of $N_{3/2}^*$ in nucleon-photon interactions, T violation in, (T), 20: 32020
production of $N_{\frac{1}{2}}^*$, by meson (π) absorption in nuclei, (T), 20: 32078
production of N_{11}^* and N_{13}^* in meson (π)-nucleon interactions, (T), 20: 32091
production of N* (1236) in meson (π^+)-proton interactions at 38 to 307 Mev, resonance formulas for, (T), 20: 32100
production of N*(3/2⁺) and N**(5/2⁻) in electron-proton interactions, time invariance in, 20: 32042
production of $\Sigma^-\eta$ in meson (K^-) interactions with neutrons at 0.920 to 1.120 Bev/c, 20: 32103
production of Ξ^* in one-particle exchange model, 20: 32009
production of Y*(1385), in meson (π^+)-proton interactions, (E), 20: 32029
production of Y*(J = 3/2), in meson (K^-) interactions with protons at 1.22 to 1.70 Bev/c, (E/T), 20: 32068
production of 3/2⁺ decuplet and 1/2⁻ octet in neutrino-nucleon interactions, 20: 32080
BEANS
radioinduced chromosome aberrations in *Vicia faba* seeds, effects of Myleran on neutron, 20: 31136
radiosensitivity of *Vicia faba* and its hybrid, 20: 31054
BELGIAN REACTOR-2
radioisotope production in, 20: 31643
BELGIUM
atomic energy development in, review of, 20: 32890
radiation processing of food in, review of, 20: 31628
radioisotope production and uses in, 20: 31643
BENZENE
benzene–2,5-diphenyloxazole, scintillation efficiency of, 20: 31290
BENZENE, BROMO-
radiation effects on, reaction of recoil bromine-82 from, 20: 31296
BENZENE, CHLORO-
chlorobenzene–2,5-diphenyloxazole, scintillation efficiency of, 20: 31290
BENZENE, CHLOROPENTAFLUORO-
chloropentafluorobenzene–2,5-diphenyloxazole, scintillation efficiency of, 20: 31290
BENZENE, DICHLOROTETRAFLUORO-
dichlorotetrafluorobenzene–2,5-diphenyloxazole, scintillation efficiency of, 20: 31290
BENZENE, HEXAFLUORO-
hexafluorobenzene–2,2'-p-phenylenebis[5-phenyloxazole], scintillation efficiency of, 20: 31290
2,5-diphenyloxazole–hexafluorobenzene, scintillation efficiency of, 20: 31290
BENZENE, NITRO-
effects on dielectric mirror coating damage resistance for laser pulses, (E), 20: 31787
BENZENE, TRICHLOROTRIFLUORO-
2,5-diphenyloxazole–trichlorotrifluorobenzene, scintillation efficiency of, 20: 31290
BENZOIC ACID
determination by xenon trioxide oxidation, titrimetric, 20: 31196
radiolysis of alkaline aqueous solutions of salts of, spectra of transient species from pulse, 20: 31281
BENZOIC ACID, *p*-CHLORO-, MERCURY SALT
radiosensitivity effects of, use of activation analysis for determining mechanism of, 20: 31172 (SGAE-BL-17/1966)
BENZOIC ACID, *p*-(HYDROXYMERCURI)-
radiosensitivity effects of, use of activation analysis for determining mechanism of, 20: 31172 (SGAE-BL-17/1966)
BENZOIC ACID, IODO-
radiosensitivity effects of, use of activation analysis for determining mechanism of, 20: 31172 (SGAE-BL-17/1966)
BENZOIC ACID, *p*-NITRO-
radiosensitivity effects on Vicia chromosomes, β, γ, and x, 20: 31124
BERKELIUM
separation of, from irradiated americium by extraction chromatography, 20: 31323
BERYLLIUM
content in primary cosmic radiation, at geomagnetic latitude 42° North, 20: 31951
deposition on metals for corrosion protection, method for, 20: 31667
determination of, using sputtering ion source, 20: 31168 (CONF-660611-1)
ductility of sheets of, at 100 to 400°C, effects of rolling direction on, 20: 31761
effects of reflectors of, on thermal neutron flux in horizontal reactor channels, 20: 32765 (IAE-957)
energy level transition probabilities of, data compilation on, 20: 31942
fabrication, 20: 31667
fabrication of sheets of, by gas-pressure bonding, 20: 31670
laser beam reactions on surfaces of, momentum transfer by giant-pulsed, (E), 20: 31810
machining of, damage induced during, 20: 31667
mechanical properties of, effects of impurities on, 20: 31667
performance in accelerating electrodes in cesium-contact ion thrustors, 20: 31383
proton elastic scattering at 17.8 Mev, polarization of, (E), 20: 32439
purification by zone refining, 20: 31667
radiation effects on mechanical properties of, in-reactor, 20: 31785 (ORNL-P-2162)
radiation effects on mechanical properties of hot-pressed and extruded, fast-neutron, 20: 31794
sintering aids for, research on, 20: 31667
texture of rolled sheets of, method for determining, 20: 31671
thermal conductivity of hot-pressed, 20: 31725
BERYLLIUM ALLOYS
Be–Gd, phase studies, 20: 31667
Be–Sc, phase studies, 20: 31667
Be–Ti, phase diagram, 20: 31772
BERYLLIUM BOROCARBIDES

preparation and properties of, 20: 31257
BERYLLIUM CARBIDES
Be_2C–graphite, fabrication and properties of hot-pressed composites of, 20: 31688 (NASA-CR-507)
BERYLLIUM FLUORIDES
BeF_2–LiF, density, specific heat, and thermal conductivity of, calculation of, 20: 32804(R) (ORNL-3936, pp 122-71)
BeF_2–LiF–ZrF_4, separation from rare earth fission products, 20: 32804(R) (ORNL-3936, pp 122-71)
BERYLLIUM IONS
electron reactions with, excitation cross sections for, (T), 20: 31929
BERYLLIUM ISOTOPES Be-7
energy levels of, lifetime of first excited, (E), 20: 32504
energy levels of, intermediate coupling shell-model calculations of, (T), 20: 32436
BERYLLIUM ISOTOPES Be-8
energy levels from boron-11 (p,$\alpha\alpha$) reactions, (E), 20: 32402
energy levels of, isobaric spin mixing in, (T), 20: 32436
energy levels of, intermediate coupling shell-model calculations for, 20: 32436
BERYLLIUM ISOTOPES Be-9
energy levels from deuteron reactions (d,α) with boron-11 at 1.7 Mev, widths of, (E), 20: 32441
energy levels from deuteron reactions (d,He-3) with boron-10 at 11,8 Mev, (E), 20: 32481
energy levels of, intermediate coupling shell-model calculations for, 20: 32436
BERYLLIUM MODERATED REACTORS
neutron buckling and fission ratios for thorium–uranium fueled, 20: 32820
neutron production in, calculational method for delayed, (T), 20: 32767 (UCRL-14720)
BERYLLIUM OXIDES
radiation effects on thermal diffusivity of, fast-neutron, 20: 31667
strength of, effects of glass additions on, 20: 31667
Al_2O_3–BeO–MgO, properties of molten, for fuel matrix for homogeneous thermal nuclear reactors, 20: 31726
BeO–MgO–ZrO_2, properties of molten, for fuel matrix for homogeneous thermal nuclear reactors, 20: 31726
BeO–UO_2, creep properties at high temperatures, 20: 31669
BERYLLIUM OXIDES (IMPREGNATED)
reactivity worth of thoria, 20: 32820
BERYLLIUM SYSTEMS
Be–B–C, sintering of, stable ternary compounds from, 20: 31257
BETA DECAY
coupling constants in, renormalization of axial-vector, 20: 32157
detection of double, 20: 32562
rate of photon-induced, in stars, (T), 20: 31878
transitions in nucleic, PCAC hypothesis for, 20: 32479
transitions in, matrix elements for first-forbidden, 20: 32393
BETA PARTICLES
absorption by liquids, scintillation device for measuring, 20: 31521
detection and measurement in layered preparations, use of cylindrical counters for, 20: 31536
detection in water, using Cherenkov effect, 20: 31506 (CEA-R-2915)
detection of, low-background silicon detector for, 20: 31540
dose rate from slab and spherical sources, computer program for calculating, 20: 32675 (ORNL-TM-1160)
effects on chromosomes in Vicia, genetic, 20: 31124
effects on chromosomes in cultured hamster thyroids, 20: 31053
effects on *E. coli*, mutagenic, 20: 31033(R) (NASA-CR-59196)
effects on hematopoietic tissues of dogs and swine, carcinogenic, 20: 31031 (BNWL-SA-201)
effects on immune reactions in euthyroid patients, 20: 31161
effects on thermal tolerance of fish, 20: 31028 (AECL-2409)
BETA SOURCES
activity of, measurement using liquid scintillators with external standards, 20: 31518
dose rate from slab or spherical, computer program for, 20: 32675 (ORNL-TM-1160)
use for measuring density of liquid hydrogen, 20: 31494
BETA SPECTROMETERS
description of, with space focusing, 20: 31583
design of low-background scintillation, 20: 31603(P)
design of magnetic, with automatic device for conversion-spectrum measurement, 20: 31565
luminosity of double-focusing, improvement of, 20: 31559
performance of lithium-drifted silicon, 20: 31519
BEVERAGES
effects of green tea on intestinal absorption of strontium-90 in rats, 20: 30987
radiation processing of apple juice, biochemical changes in, 20: 31629
BIBLIOGRAPHIES
of atomic energy literature, 20: 32887 (TID-3735)
of computer programs for reactor technology, 20: 32764 (CEA-Bib-17(Pt.2))
on corrosion of structural materials by liquid alkali metals, 20: 31680 (NAA-SR-Memo-11652)
on helium and hydrogen spectra in airglow, 20: 32289
on isotope abundance measurements by mass spectrography, 20: 31399
on kinetics of oxidation-reduction reactions of americium, neptunium, plutonium, and uranium, 20: 31215 (LA-3507)
on mass spectrometry, 20: 31808
on mass spectrometry, Jan. 1961 to Dec. 1962, 20: 31197
on nondestructive testing of reactor fuel elements, 20: 31354
on photobiological damage and reactivation mechanisms, 20: 31039
on positron annihilation, 20: 32101
on radiation effects on tissue transplants, 20: 31120
on radiation effects on solid uranium-based nuclear fuel materials, 20: 31783 (FTI-16(6.1))
on radioecology, 20: 30967 (TID-3910(Suppl.4))
BINDING ENERGY
calculations for nuclear, 20: 32559
BIOLOGICAL MATERIALS
analysis for iodine, neutron activation, 20: 31173 (SGAE-BL-18/1966)
carbon-14 content of, methods for determining, 20: 31433
labile state of molecules in, 20: 30974
BIOLOGICAL MODELS
development for kinetic studies of lethal radiation response, 20: 31087
BIOLOGICAL SYSTEMS
measurement of primary production using carbon-14 as tracer, 20: 30997
radiation effects on, 20: 31038
radiation effects on, model for kinetics of lethal, 20: 31087
BIOMETRY
site distribution parameters for radioinduced chromosome exchanges, 20: 31057
BIOPHYSICS
visual receptor processes, 20: 30963
BIRDS
radiation injury and repair in tissues of, 20: 31045
BISMUTH
corrosive effects on stainless steel at high temperatures, 20: 31959(R) (ANL-7175, pp 184-211)
proton reactions at 0.05 to 2.9 Bev, induced activity data and cross sections for spallation, (E/T), 20: 32549
thermodynamic properties of liquid, Prandtl number at 0 to 700°C for, 20: 31724
BISMUTH ALLOYS
Bi–In, critical currents in superconducting films of, magnetic field effects on, (E), 20: 32317
Bi–Li, thermodynamic properties, 20: 31959(R) (ANL-7175, pp 184-211)
Bi–Na, corrosive effects on stainless steel at high temperatures, 20: 31959(R) (ANL-7175, pp 184-211)
Bi–Na, properties and vapor pressures of, effects of composition and temperature on, 20: 31959(R) (ANL-7175, pp 184-211)
Bi–Na, thermodynamic properties, 20: 31959(R) (ANL-7175, pp 184-211)
Bi–Pb, superconducting transitions of amorphous, 20: 32341
Bi–Pb, thermodynamic properties of liquid, Prandtl number at 0 to 700°C for, 20: 31724
Bi–Sb, superconducting transitions of amorphous, 20: 32341
Bi–Sn, critical currents in superconducting films of, magnetic field effects on, (E), 20: 32317
Bi–Tl, superconducting transitions of amorphous, 20: 32341
BISMUTH ISOTOPES
abundance determination by mass spectrometry, ion production technique for, 20: 31207
meson (μ^-) capture by, x-ray intensity ratios from, (T), 20: 31945
BISMUTH ISOTOPES Bi-207
decay of, lead-207 levels from electron-capture, (E), 20: 32401
BISMUTH ISOTOPES Bi-208
energy levels from proton scattering at 11 to 16 Mev, isobaric analog, 20: 32478
BLADDER
phosphorus-32 absorption by dog, 20: 31149(R) (TID-22969)
BLOOD
effects of injections of whole, on radiation lethality in dogs, 20: 31132
radiation effects on proliferation of human leukocytes in culture, x, 20: 31067
radiation effects on lymphoid cells in dog, x, 20: 31086
radioactivity of human, α, 20: 31145
BLOOD COAGULATION
radiation effects on, x, 20: 31032 (CEA-R-2953)
scintillation photography of intravascular clots using iodine-131-plasminogen as tracer, 20: 31150 (UCRL-16691)
BLOOD PICTURE
effects of age and sex on mouse, 20: 30970 (COO-1170-5)

effects of blood transfusions and bone marrow transplants on, in lethally irradiated dogs, 20: 31132
BLOOD PLASMA
protein metabolism in, tracer study using stable brominated proteins and neutron activation analysis, 20: 30990
radioactivity of human, α, 20: 31145
strontium-90 content of, effects on content in dog hair, 20: 30972 (TID-22027)
BLOOD PLATELETS
radiation effects on, effects of environment on, 20: 31032 (CEA-R-2953)
BLOOD PRESSURE
radiation effects on *Macaca mulatta*, γ and proton, 20: 31104
BLOOD SERUM
analysis for iodine, neutron activation, 20: 31173 (SGAE-BL-18/1966)
radiation effects on cholesterol content in guinea pig, γ, 20: 31006
radiation effects on amino acid composition of dog, 20: 31021
BLOOD VESSELS
barium-140 deposition in aortic wall, chemical protection against radiation injuries from, 20: 31142
radiation effects on, around joints, therapeutic x, 20: 31163
BODY FLUIDS
pathology of proton-induced, in *Macaca mulatta*, 20: 31098
BOILERS
development for SNAP-50/SPUR power system, 20: 32857
tube brittle failure in, carbon steel, 20: 31681 (NAA-SR-Memo-11707)
BOILING
burnout in, effects of tube diameters and flow inlet conditions on, 20: 31342(R) (EURAEC-1482)
heat transfer and thermal fluxes in potassium, in tubes, 20: 31347
BOILING REACTOR EXPERIMENTS
operation experience with BORAX-V, 20: 32866
BOILING REACTORS
development for desalination and power, 20: 32849
heat transfer at coexistence of nucleate and film, 20: 31345(T), (NSJ-tr-471
BONE MARROW
effects of autografts of irradiated, in rats, 20: 31133
effects of fractionated, against lethal irradiation effects on guinea pigs, 20: 31126
effects of sulfhydryl compounds on DNA synthesis in mouse, 20: 31125
effects of transplantation of homologous, on radiation lethality in dogs, 20: 31132
effects on lethally irradiated mammals in combination with radioprotective compounds, 20: 31142
effects on radiation injuries to tissues in mice, 20: 31108
nucleic acid synthesis in cultured, from leukemia and myeloma patients, 20: 30971 (ORINS-45)
protein synthesis in cultured, from leukemia and myeloma patients, 20: 30971 (ORINS-45)
radiation dose to, from fluoroscopy in Japan, 20: 31466
radiation effects on incorporation of dietary linoleic acid in triglycerides in rat, whole-body, 20: 31016
radiation effects on lymphoid cells in dog, x, 20: 31086
radiosensitivity effects of injected, in mice, 20: 31127
radiosensitivity of human, 20: 31029 (BNL-10221)
radiosensitivity of mouse, 20: 31071
sulfur content in human, estimation of, 20: 30982
use of autotransplantation of, in treatment of leukopenia radioinduced in gynecology patients, 20: 31134
use of cadaver, for treatment of radiation injuries in mice, 20: 31135
BONE TUMORS
radioinduced by strontium-90 in dogs and swine, 20: 31031 (BNWL-SA-201)
BONES
cesium-137 and strontium-90 contents of human, in Finland, 20: 31142
lead-210 content in, effects of atmospheric content on, 20: 31407
radiation effects on blood vessels around joints, therapeutic x, 20: 31163
strontium uptake by, mechanism of, 20: 30973
strontium-90 content in sheep, in Australia, 1961 through 1963, 20: 31403
sulfur content in human, estimation of, 20: 30982
BORATE GLASS
radiation effects on color and phosphorescence of, x, 20: 31283
BORIC ACID
corrosive effects on type 304 stainless steel at 600°F, 20: 31669
BORON
content in primary cosmic radiation, at geomagnetic latitude 42° North, 20: 31951
deposition on titanium, 20: 31670
effects on type 304 stainless steel embrittlement by fast neutrons, 20: 31669
energy level transition probabilities of, data compilation on, 20: 31942
energy levels of, hyperfine structure of 2p, (T), 20: 31904 (UCRL-16581)
BORON CARBIDES
B_4C–Co–Dy_2O_3, radiation effects on dispersions of, in soda-potash glass, thermal-neutron, 20: 31668
B_4C–graphite, fabrication and properties of hot-pressed composites of, 20: 31688 (NASA-CR-507)
BORON FLUORIDES
enthalpy of formation of, 20: 31213(R) (ANL-7175, pp 119-58)
BORON ISOTOPES B-8
energy levels of, intermediate coupling shell-model calculations for, 20: 32436
BORON ISOTOPES B-9
deuteron reactions (d,n) with, neutron spectra from, 20: 31786(R) (ORO-2891-5)
energy levels from deuteron reactions (d,t) with boron-10 at 11.8 Mev, (E), 20: 32481
energy levels of, intermediate coupling shell-model calculations for, 20: 32436
BORON ISOTOPES B-10
deuteron reactions (d,nγ) at 800 kev, carbon-11 levels from, (E), 20: 32395
deuteron reactions (d,t) at 11.8 Mev, boron-9 levels from, (E), 20: 32481
deuteron reactions (d,He-3) at 11.8 Mev, beryllium-9 levels from, (E), 20: 32481
energy levels from deuteron reactions (d,α) with carbon-12 at 9 to 12.5 Mev, isospin selection rules for, (E), 20: 32500
helium-3 reactions (He-3,p) at 1.2 to 12 Mev, nitrogen-13 excited levels from, (E), 20: 32527
proton reactions (p,$\alpha\alpha$) at 163 kev, angular and energy correlations from, (E), 20: 32402
BORON ISOTOPES B-11
deuteron reactions (d,α) at 1.7 Mev, beryllium-9 level widths from, (E), 20: 32441
BORON NITRIDES
compatibility with cesium vapor at 1800°C, 20: 31669
enthalpy of formation of, 20: 31213(R) (ANL-7175, pp 119-58)
BORON OXIDES
enthalpy of formation of, 20: 31213(R) (ANL-7175, pp 119-58)
Al_2O_3–B_2O_3–EuO, preparation and Faraday rotation of glasses of, 20: 31733
BORON SYSTEMS
B–Cu, grain boundary swelling in irradiated, mechanisms of, 20: 31798
B–Cu, radioinduced helium bubbles in, effects of annealing on properties of neutron, 20: 31797
Be–B–C, sintering of, stable ternary compounds from, 20: 31257
BOROSILICATE GLASS
radioinduced absorption centers at low temperatures in, gamma, 20: 32733
BOSONS
decays of, predictions of static quark model on, 20: 32061
electromagnetic wave emission in magnetic fields, polarization of, (T), 20: 32120
interactions of intermediate vector, effects on strong interaction theory, 20: 32177
model of, double octet, 20: 32084
theory for spin-one massless, matrices and projection operators for, 20: 32167
virial coefficients for gas of, Faddeev equations for, 20: 32230
BRAIN
effects of radiation sickness on DNA, phosphatase, and RNA activity in nerve cells in rat, 20: 31010
radiation effects on serotonin in rat, relation of barbiturate hypnosis to x, 20: 31007
radiation effects on electrical activity of, in rabbit embryo, effects of developmental stage on x, 20: 31037(T) (JPRS-35315, pp 65-75)
radiation effects on liberation of 5-hydroxytryptamine in stem of, in adrenalectomized rats, x, 20: 31069
sulfur content in human, estimation of, 20: 30982
BRASS
hydrogen atom and molecule reactions at 20 to 45 kev, secondary electron emission from, (E), 20: 31533
BRAZIL
radiation dose to population of Guarapari, measurement of environmental, 20: 31463
radiation dose to population of Guarapari, survey of, 20: 31470
BREEDER REACTORS
breeding coefficient in intermediate-energy uranium–thorium water-moderated, (T), 20: 32831
design and evaluation of molten-salt power, 20: 32805(R) (ORNL-3936, pp 172-92)

economics and role of thorium-fueled, 20: 32832
fuel cycles in heavy-water, burn-up and neutron economy of thorium, (T), 20: 32823
fuel performance for fast, molten plutonium, 20: 32798 (LA-DC-7550)
fuel processing methods for molten-salt, 20: 32806(R) (ORNL-3936, pp 193-211)
fuel slurry development for, homogeneous suspended thorium, 20: 32829
fuels for fast, performance of thorium-232–uranium-233, 20: 32790 (ANL-6930)

BREMSSTRAHLUNG
emission from electrons, analogy with synchrotron radiation, (T), 20: 31992
emission in electron reactions with nuclei, nuclear structure effects on, (T), 20: 32456
emission in electron reactions with oxygen-16, nuclear structure effects on, (T), 20: 32456
emission in proton-proton interactions at 204 Mev, (E), 20: 32062
interactions with protons at 250 to 360 Mev, recoil-proton polarization from pion-photoproduction, (E), 20: 32096
interactions with protons at 360 Mev, recoil-proton polarization from pion-photoproduction, (E), 20: 32097
interactions with protons at 600 to 1000 Mev, cross sections for meson (π^0) production in, (E), 20: 32051
production in proton-proton interactions at 48 Mev, cross sections for, (E), 20: 31997
production in proton-proton interactions, cross sections for, (T), 20: 32059
reactions (γ,n) with helium-3 at threshold to 30 Mev, cross sections for, (E), 20: 32546
reactions (γ,n), (γ,2n), and (γ,pn) with calcium-40 at 15.5 to 62.0 Mev, cross sections for, (E), 20: 32445
reactions (γ,p) with aluminum, silicon, and sulfur at 32 Mev, proton energy spectra from, (E), 20: 32394
reactions in nuclear emulsions, electron pair opening angle in, (E), 20: 32006

BROMINE
determination in conductive tissue of beef heart, activation, 20: 31176
determination in human heart tissue, activation, 20: 31175
determination of, in radiosensitizers in tissues, neutron activation, 20: 31172 (SGAE-BL-17/1966)
use as tracer for neutron activation analysis of plasma proteins, 20: 30990

BROMINE FLUORIDES
reactions with alumina–fission products–uranium chloride mixtures, 20: 31315(R) (ANL-7175, pp 42-103)

BROMINE ISOTOPES Br-82
production of high-specific-activity, for medical use, 20: 31275
reactions with aromatic compounds, recoil, 20: 31296

BROMINE ISOTOPES Br-83
gamma spectra, 20: 32413

BROOKHAVEN ALTERNATING-GRADIENT SYNCHROTRON
magnet power supply of, electronic ripple filter for, 20: 31833

BUBBLE CHAMBERS
data analysis for, computer program for, 20: 31507 (COO-1018-1013)
data analysis for, computer development for, 20: 31645(R) (AD-627094)
design of 100-cm liquid hydrogen, 20: 32318
electron energy loss measurements in heavy-liquid, optimization of, (T), 20: 31568
photographs from, projector for, 20: 31550

BUBBLES
coalescence of gas, by surface diffusion, (T), 20: 31739
data analysis for, computer use for, 20: 31508(R) (COO-1018-1075)

BUILDING MATERIALS
corrosion by liquid alkali metals, bibliography on, 20: 31680 (NAA-SR-Memo-11652)
corrosion of reactor, method for measuring intensity of, 20: 31682 (NP-16003)

BULK SHIELDING FACILITY
experimental facilities for, irradiation, 20: 32862 (ORNL-P-2160)

BUTANE
ionization of, by electrons at 0.6 to 20 kev, cross sections for (E/T), 20: 31906

C

CABLES
development for electric power transmission in SNAP-8, 20: 32853 (NAA-SR-Memo-11925)

CADAVERS
use of bone marrow from, for treatment of radiation injuries in mice, 20: 31135

CADMIUM
determination in conductive tissue of beef heart, activation, 20: 31176
determination in human heart tissue, activation, 20: 31175
neutron capture by, average level widths of compound nucleus from, (E), 20: 32424
proton reactions at 0.05 to 2.9 Bev, induced activity data and cross sections for spallation, (E/T), 20: 32549
solubility in molten cadmium chloride, radiometric techniques for measuring, 20: 31237
vaporization from probe surface in electric arcs, (E), 20: 32593

CADMIUM ALLOYS
Cd–Cu, solvent properties of, for uranium, 20: 31314(R) (ANL-7175, pp 1-41)
Cd–In–Ag, radiation effects on mechanical properties of, thermal-neutron, 20: 31668
Cd–Mg, mechanical properties of intermetallic compound single-crystal, 20: 31714(R) (UCRL-16658, pp 99-103)
Cd–rare earth, crystal structure of, CsCl-type intermediate phases in, 20: 31737
Cd–rare earths, lattice constants, 20: 31167(R) (ANL-7175, pp 217-25)
Cd–rare earths, thermodynamic properties, 20: 31213(R) (ANL-7175, pp 119-58)

CADMIUM CHLORIDES
formation and reactions of, in fused chlorides, 20: 31314(R) (ANL-7175, pp 1-41)
radiation effects on copper- or silver-activated crystals of, EPR spectral studies on gamma, 20: 32685
solvent properties of molten, for cadmium, radiometric techniques for measuring, 20: 31237

CADMIUM ISOTOPES Cd-109
isomeric transitions in, energies and half life of, (E), 20: 32520

CADMIUM ISOTOPES Cd-111
nuclear orientation of, by 3261 A resonant radiant, 20: 32419(T)

CADMIUM ISOTOPES Cd-114
energy levels in, anharmonicity of vibrational, 20: 32480

CADMIUM SELENIDES
radiation effects on photoconductive properties of, thermal neutron, 20: 32736
radioinduced stimulated emission from, electron, 20: 32730(T)

CADMIUM SULFIDES
diffusion of copper in single-crystal, 20: 32684(R) (UCRL-16658, pp 21-38)
evaporation mechanisms, 20: 32684(R) (UCRL-16658, pp 21-38)
radiation effects on photoconductive properties of, thermal neutron, 20: 32736
radiation effects on thin-film solar cells of, proton, 20: 31616
sputtering by argon ions at 75 to 600 ev, yields from, (E), 20: 31914

CADMIUM SYSTEMS
Cd–Mg–UCl_4–Zn, corrosive effects of, on stainless steel at 650°C, 20: 31314(R) (ANL-7175, pp 1-41)

CADMIUM TELLURIDES
properties of diodes of, for particle detection, 20: 31523

CALCIUM
determination in conductive tissue of beef heart, activation, 20: 31176
determination in human heart tissue, activation, 20: 31175
dissolution in liquid ammonia, properties of solutions from, 20: 31220(R) (UCRL-16658, pp 39-72)
effects on adenosine triphosphatase formation in wheat roots, 20: 30992
metabolism by man, tracer studies of effects of thyroid disorders on, 20: 31142
proton reactions at 0.05 to 2.9 Bev, induced activity data and cross sections for spallation, (E/T), 20: 32549
uptake by aquatic snails, role of ionic diffusion in, 20: 30991
Ca–Hg, critical temperatures of intermetallic compounds in, 20: 31757

CALCIUM FERRATES
gamma absorption by $Ca_2[Fe](Fe)O_5$, spin orientation determination by, 20: 31228

CALCIUM FLUORIDES
radiation effects on electric conductivity of crystals of, temperature dependence of x, 20: 32721(T)
use of manganese-doped, for dosimetry, 20: 31598

CALCIUM ISOTOPES Ca-40
binding energy of, Hartree-Fock calculation of, 20: 32496
bremsstrahlung reactions (γ,n), (γ,2n), and (γ,pn) at 15.5 to 62.0 Mev, cross sections for, (E), 20: 32445
deuteron reactions (d,p) with, target excitation effects in, (T), 20: 32497
nuclear charge distribution of, (T), 20: 32534
proton elastic scattering at 40 Mev, differential cross sections and polarization for, (E), 20: 32510
proton elastic scattering at 18.5 and 20.5 Mev, polarization from, (E/T), 20: 32523
proton inelastic scattering at 11.5 Mev, level excitation energies from, (E), 20: 32511

CALCIUM ISOTOPES Ca-42
neutron total cross sections for, level spacings from, (E/T), 20: 32389

CALCIUM ISOTOPES Ca-44
neutron total cross sections for, level spacings from, (E/T), 20: 32389
nuclear charge distribution of, (T), 20: 32534
CALCIUM ISOTOPES Ca-47
determination of, efficiency of Cherenkov counting methods for, 20: 31184
CALCIUM ISOTOPES Ca-48
beta decay of, lower limit for two-neutrino mode of double, (E), 20: 32562
proton inelastic scattering at 11.5 Mev, level excitation energies from, (E), 20: 32511
CALCIUM OXIDES
electron spectra of, 20: 31219(R) (UCRL-16658, pp 11-20)
CaO–MgO, diffusion in, 20: 31719(R) (UCRL-16658, pp 155-69)
CaO–MgO, grain boundary precipitation in, 20: 31738
CaO–O–Te_2O_7, compound formation in, 20: 31244
CaO–UO_2, grain boundary precipitation in, 20: 31738
CaO–Yb_2O_3, grain boundary precipitation in, 20: 31738
CaO–ZrO_2, diffusion at 1700 to 2150°C in, cationic self-, 20: 31732
CALIFORNIA
radioactivity measurements at a height of 500 ft in San Francisco region, 20: 31395 (CEX-58.4.5)
radioisotope content in diet in, 20: 31471
CALIFORNIUM
separation of, from irradiated americium by extraction chromatography, 20: 31323
CALIFORNIUM ISOTOPES
abundance determination by mass spectrometry, ion production technique for, 20: 31207
CALORIMETERS
development of, for use at 0.25 to 25°K, 20: 32684(R) (UCRL-16658, pp 21-38)
CALORIMETRY
equipment for enthalpy-increment, design and performance of, 20: 31213(R) (ANL-7175, pp 119-58)
methods of, for fluid-solid interfaces, 20: 31220(R) (UCRL-16658, pp 39-72)
CAMBRIDGE SYNCHROTRON
magnet power supplies of, feedback system for stabilizing, 20: 31834
CANADA
radiation processing of food in, review of, 20: 31628
CAPE THOMPSON–CAPE SEPPINGS AREA (ALASKA)
bioenvironment, physical characteristics, and radioactivity of, 20: 32885 (PNE-481)
fallout monitoring, 1959 through 1962, 20: 31428 (PNE-481, pp 1165-1200)
radioactivity of, aerial surveying of 1958, 20: 31425 (PNE-481, pp 1115-19)
radionuclide content of Chukchi Sea organisms, 1959 to 1962, 20: 31427 (PNE-481, pp 1141-9)
sorptive properties of soils for cesium, iodine, and strontium, 20: 31426 (PNE-481, pp 1121-39)
CARBON
analysis for uranium in fuel particle coatings of pyrolytic, use of electron microprobe for, 20: 31795
content in primary cosmic radiation, at geomagnetic latitude 42° North, 20: 31951
deposition from carbon monoxide on mild steel surfaces, 20: 31670
determination in sodium by combustion, 20: 31213(R) (ANL-7175, pp 119-58)
effects of impurities of, on thermal expansion of tantalum, 20: 31669
effects on age hardening in vanadium–niobium–tantalum and vanadium–niobium–titanium alloys, 20: 31709(R) (IITRI-B6042-5)
effects on corrosive properties of tantalum alloys by molten plutonium fuels, 20: 31679(R) (LA-3524)
effects on corrosive properties of niobium alloys by molten plutonium alloys, 20: 31679(R) (LA-3524)
effects on corrosion of reactor materials by liquid sodium, 20: 31213(R) (ANL-7175, pp 119-58)
effects on mechanical properties and microstructure of cobalt–tungsten carbide cermets, 20: 31760
electric and thermal conductivity of compacted powders of, effects of fabrication variables on, 20: 31777
energy level transition probabilities of, data compilation on, 20: 31942
energy levels of, hyperfine structure of 2p, (T), 20: 31904 (UCRL-16581)
ionization equation for optically thin plasma of, (T), 20: 32636
laser beam reactions on surfaces of, momentum transfer by giant-pulsed, (E), 20: 31810
neutron capture by, average level widths of compound nucleus from, (E), 20: 32424
nucleon reactions at high energies, residual radioactivity from, 20: 31831
proton reactions at 40 Mev to 25 Bev, lithium isotopes from, (E), 20: 31205
proton scattering at 29 and 49 Mev, asymmetries in elastic and inelastic, (E), 20: 32440
radiation effects on thermal diffusivity of pyrolytic, fast-neutron, 20: 31667
reactions with uranium dioxide, oxygen concentrations from, 20: 31230
solubility in molybdenum, rhenium, and tungsten at high temperatures, 20: 31669
spectra of foil-excited beams of, 20: 31903 (N-66-16702)
CARBON DIOXIDES
effects on radiosensitivity of Kalanchoe, 20: 31076
hydrogen ion reactions at 20 to 120 kev, ionization cross sections for, 20: 31909
radioinduced reactions with formic acid and methanol in aqueous solutions, 20: 31278
reactions with zirconium at 850°C, kinetics of, 20: 31669
CARBON IONS
spectra of negative, coefficient for free-free absorption, 20: 31864
CARBON ISOTOPES C-11
energy levels from deuteron reactions (d,nγ) with boron-10, (E), 20: 32395
CARBON ISOTOPES C-12
alpha cluster model for, 20: 32558
deuteron elastic scattering at 10.6 to 13.9 Mev, optical-model analyses of, (E/T), 20: 32454
deuteron reactions (d,α) at 9 to 12.5 Mev isospin selection rules for, (E), 20: 32500
deuteron reactions (d,p) at 11 and 13 Mev, angular-momentum effects on angular distribution from, (E), 20: 32512
electron inelastic scattering by, cross sections for, (T), 20: 32536
electron scattering by, form factors for 180° inelastic, (T), 20: 32569
model for, three-alpha, 20: 32493
neutron elastic scattering by, polarization in, (E/T), 20: 32359
neutron scattering at 14.1 Mev, level excitation from, (E), 20: 32408
oxygen-16 reactions (O-16,α) at 22 and 32 Mev, magnesium-24 levels from, (E), 20: 32556
photon reactions (γ,π⁻p) at 670 and 700 Mev, angular correlations from, (E/T), 20: 32530
proton elastic and inelastic scattering at 40 Mev, polarization and cross sections for, (E), 20: 32510
proton reactions (p,2p) at 80 to 150 Mev, momentum distribution of recoil nucleus in, 20: 32529
proton reactions (p,pγ) at 5.9 Mev, angular correlations for, (E), 20: 32438
CARBON ISOTOPES C-13
concentration in liquids by exchange with gaseous carbon dioxide, 20: 31641(R) (NYO-755-1, pp 173-208)
helium-3 reactions (He-3 pγ) at 3.0 Mev, nitrogen-15 levels from, (E), 20: 32495
helium-3 reactions (He-3,p) at 4.0 Mev, nitrogen-15 levels from, (E), 20: 32501
CARBON ISOTOPES C-14
content in atmosphere of Southern Hemisphere, effects of fallout from nuclear explosions on, 20: 31410
content in atmosphere, sea water, and biological materials, methods for determining, 20: 31433
content in ocean surface waters, 1960 and 1961, 20: 31419
content of fission product, in atmosphere, May 1, 1963 to April 1, 1966, 20: 31397(R) (RLO-1776-2)
determination in alanine, indoleacetic acid, and kinetin in agar blocks by liquid scintillation counting, 20: 31179
determination in aqueous samples in presence of tritium, computer program for use in, 20: 31182
determination of, in lactate by liquid scintillation counting, 20: 31178
determination of, by oxygen flask method using scintillation counting, equipment for, 20: 31185
distribution between atmosphere and sea water, 1963 to 1966, 20: 31397(R) (RLO-1776-2)
helium-3 reactions (He-3,p) at 4.0 and 4.5 Mev, nitrogen-16 levels from, (E), 20: 32501
incorporation in dimethanesulfonate of 3,3'-(methylimino)di-1-propanol, method for, 20: 31308
incorporation in oxalic acid using labeled acetic acid, 20: 31263
incorporation in toluene diisocyanate, 20: 31266
use as tracer for primary production measurements, 20: 30997
CARBON MONOXIDES
hydrogen ion reactions at 20 to 120 kev, ionization cross sections for, 20: 31909
reactions with zirconium at 850°C, kinetics of, 20: 31669
CARBON STEEL
corrosion by water in operating pressure boilers, 20: 31681 (NAA-SR-Memo-11707)
failure of tubes of, in pressure boilers, 20: 31681 (NAA-SR-Memo-11707)
hardenability of A-212B, effects of uranium alloying additions on,

20: 31669
joining of alloy steel, carbon steel, and stainless steel to, parameters for friction, 20: 31670
reactions of mild, with sodium at high temperatures, 20: 31440(R) (ANL-7175, pp 159-83)
C–Co–Ni, tensile properties of strain-aged, 20: 31716(R) (UCRL-16658, pp 121-32)

CARBON SYSTEMS
Al–C–Mo, superconductivity of Mo_3Al_2C in, 20: 32312(R) (UCRL-16658, pp 133-43)
Be–B–C, sintering of, stable ternary compounds from, 20: 31257
C–Cr–Zr, phase studies, 20: 31669
C–Hf–Ta, phase diagram at 2050°C, 20: 31668
C–Mo–Ti–Zr, fatigue properties of TZC at high temperatures, 20: 31710(R) (NASA-CR-54983)
C–Mo–Zr, phase studies, 20: 31669
C–Re–W, superconductivity of W_3Re_2C in, 20: 32312(R) (UCRL-16658, pp 133-43)
C–Th, phase studies, 20: 31768
C–Uc, electric and thermal conductivity of compacted powders of, effects of fabrication variables on, 20: 31777
C–W–Zr, phase studies, 20: 31669

CARBON TETRACHLORIDE
radiolysis of aqueous solutions of, saturated with carbon dioxide, gamma, 20: 31276
CCl_4–tetrachlorodifluoroethane, solvent carrier for nitrogen-15 concentration, 20: 31638(R) (NYO-755-1, pp 12-76)

CARBONATITES
strontium isotope ratios in, from Ice River, British Columbia, 20: 31406

CARCINOMAS
radiotherapy of maxillary sinus, 20: 31159
radiotherapy of metastasized mammary, using yttrium-90, 20: 31153
radiotherapy of, in mice, effects of chemical radiation protectors on x-ray, 20: 31142

CARTILAGE
sulfur content in human, estimation of, 20: 30982

CATALASES
radiation effects on activities of, in oranges, γ, 20: 31632

CATIONS
spectra of nitrogen-15 in thiotrithiazyl, NMR, 20: 31218(R) (UCRL-16658, pp 1-9)

CATS
krypton-85 metabolism in intestine in, tissue clearance studies on, 20: 30979

CATTLE
analysis for trace elements in conductive tissue in heart of, activation, 20: 31176

CAVES
equipment and operation procedures of Naval High-Level Radiation Laboratory, 20: 31337

CELLOBIOSE
radiolysis of aqueous solutions of, acid formation in, 20: 31304

CELLULOSE PHOSPHATES
properties as ion exchange material for separation of radioisotopes, 20: 31324

CERAMIC COUPLES
ceramics–stainless steel, contact thermal conductivity of, 20: 31712 (UCRL-14227(Rev.1))

CERAMIC MATERIALS
mechanical properties of composite, 20: 31719(R) (UCRL-16658, pp 155-69)

CERIUM
determination in conductive tissue of beef heart, activation, 20: 31176
determination in human heart tissue, activation, 20: 31175
effects on ductility of austenitic stainless steel, 20: 31669
separation from beryllium fluorides and lithium fluorides, 20: 32804(R) (ORNL-3936, pp 122-71)
separation from water by precipitation, kinetics of, 20: 31318 (BMwF-FBK-65-04)
toxicity in laboratory animals, 20: 30970 (COO-1170-5)

CERIUM ALLOYS
Ce–Co–Pu, corrosive effects on carburized and noncarburized tantalum alloys, 20: 31679(R) (LA-3524)
Ce–Co–Pu, corrosive effects on niobium alloys, effects of carbon on, 20: 31679(R) (LA-3524)
Ce–Co–Pu, irradiation testing of molten, reactor performance for, 20: 32799 (LA-DC-7752)
Ce–Co–Pu, performance in fast breeder reactors, 20: 32798 (LA-DC-7550)
Ce–Ni, magnetic properties of intermetallic compounds of, 20: 32699
Ce–Pu, viscosity to 875°C, 20: 31666
Ce–Zn, melting point of $CeZn_2$, 20: 31743

CERIUM FLUORIDES
energy levels in, coupling of negative hydrogen- and deuterium-ion localized modes to, (E), 20: 32709
thermodynamic properties, 20: 31238
vapor pressure, 20: 31718(R) (UCRL-16658, pp 149-54)
vapor pressure of, torsion-effusion method for measuring, 20: 31238

CERIUM ISOTOPES Ce-140
energy level transitions from lathanum-140 decay, K-conversion coefficients for, (E), 20: 32541
energy levels from lanthanum-140 decay, (E), 20: 32407

CERIUM ISOTOPES Ce-141
beta decay of, conversion coefficients for transitions in, (E), 20: 32443
content in fallout particles from high-altitude explosions, 20: 31424

CERIUM ISOTOPES Ce-144
content in fallout particles from high-altitude explosions, 20: 31424
content in marine organisms in Chukchi Sea, Alaska, 1959 to 1962, 20: 31427 (PNE-481, pp 1141-9)
content in ocean surface waters, 1960 and 1961, 20: 31419
deposition on tropospheric aerosols, 20: 31459
determination of, efficiency of Cherenkov counting methods for, 20: 31184

CERIUM OXIDES
terbium ion EPR in crystals of, 20: 32723(T)

CERMETS
fabrication method for, 20: 31707(P)
mechanical properties, 20: 31719(R) (UCRL-16658, pp 155-69)
processing of stainless steel–urania, 20: 31315(R) (ANL-7175, pp 42-103)
reactions of fuel-element, in TREAT, 20: 31440(R) (ANL-7175, pp 159-83)
temperature distribution in irradiated, calculation of, 20: 32791 (NAA-SR-Memo-11731)

CESIUM
atom-electron collisions in plasma of, cross sections for, (E), 20: 32646
corrosive effects on refractory ceramics and metals at 1800°C, 20: 31669
current oscillations in plasma diodes of, (E), 20: 31966
determination in conductive tissue of beef heart, activation, 20: 31176
determination in human heart tissue, activation, 20: 31175
electron-ion recombination in dense plasma of, limits of validity of radiationless, 20: 32575 (NASA-TN-D-3372)
ionization on surfaces of porous refractory metals, 20: 31776
properties of thermionic ignited-mode plasma of, (T), 20: 31974
radiative lifetime of excited electronic states in, 20: 31219(R) (UCRL-16658, pp 11-20)
rare-gas reactions with, ionization cross sections for excited, (T), 20: 31917
separation from strontium by ion exchange on cellulose phosphate, 20: 31324
separation from water by precipitation, kinetics of, 20: 31318 (BMwF-FBK-65-04)
sorption by tungsten, effects of filament treatment on heat of, 20: 31730
sorption on soil from Cape Thompson, Alaska area, 20: 31426 (PNE-481, pp 1121-39)
transport through tungsten capillaries, 20: 31381
uptake and loss in relation to active mechanism for sodium extrusion in Scenedesmus cells, 20: 30994
use of liquid, in thermionic cells, 20: 31969

CESIUM COMPLEXES
with neptunium chlorides and oxychlorides, preparation and properties of, 20: 31235

CESIUM FLUORIDES
effects on fluid-bed fluorination and oxidation of plutonia–urania mixtures, 20: 31315(R) (ANL-7175, pp 42-103)

CESIUM IODIDES
electron emission from transmission dynodes of, attenuation length for secondary, 20: 31916
performance of scintillation detectors of, for underwater use, 20: 31499 (AD-633752)

CESIUM IONS
acceleration for space propulsion engines, electrostatic, 20: 31378
diffusion of, in cesium vapor, 20: 31221(R) (UCRL-16658, pp 73-87)
sputtering on aluminum, copper, and titanium, yields from, 20: 31948
transport in cesium vapor, parameters for, 20: 31972

CESIUM ISOTOPES Cs-129
production in lanthanum-139 (p,3pxn) reactions at 30 to 150 Mev, cross sections for, (E), 20: 32386

CESIUM ISOTOPES Cs-130
production in lanthanum-139 (p,3pxn) reactions at 30 to 150 Mev, cross sections for, (E), 20: 32386

CESIUM ISOTOPES Cs-131
production in lanthanum-139 (p,3pxn) reactions at 30 to 150 Mev, cross sections for, (E), 20: 32386

CESIUM ISOTOPES Cs-132
production in lanthanum-139 (p,3pxn) reactions at 30 to 150 Mev, cross sections for, (E), 20: 32386
uptake and excretion by man, 20: 30988
CESIUM ISOTOPES Cs-133
neutron reactions (n,γ) with, gamma spectra from thermal, (E), 20: 32422
production in lanthanum-139 (p,3pxn) reactions at 30 to 150 Mev, cross sections for, (E), 20: 32386
CESIUM ISOTOPES Cs-134
determination of, from gamma spectrum, 20: 31186
energy levels from cesium-133 (n,γ) reactions, (E), 20: 32422
CESIUM ISOTOPES Cs-137
content in caribou, reindeer, and man, effects of diet on, 20: 31442 (BNWL-SA-661)
content in diet in California, 20: 31471
content in Finnish Lapps, 1966 whole body, 20: 31444 (CONF-660405-15)
content in human bones and tissues in Finland, 20: 31142
content in milk in New Zealand, 1965, 20: 31446(R) (NP-16015)
content in milk in Norway, 1960 through 1964, 20: 31465
content in ocean surface waters, 1960 and 1961, 20: 31419
deposition on tropospheric aerosols, 20: 31459
determination in food and water, gamma spectrometric, 20: 31180
determination in irradiated fuel elements by gamma spectrometry, 20: 31355
determination of, efficiency of Cherenkov counting methods for, 20: 31184
determination of, from gamma spectrum, 20: 31186
distribution and natural carriers of, in sea water, 20: 31422
distribution in man and environment, 20: 31142
distribution of inhaled, in rats, 20: 31111
effects of inhaled, in rats, pathological, 20: 31111
radiation hazard from atmospheric, in mixture with barium-137m, 20: 31528
uses of, in industrial defectoscopy, personnel protection in, 20: 31464
yields in fast neutron fission of thorium, fast-neutron dosimetry using, 20: 31530
CESIUM NEPTUNIUM CHLORIDES
preparation and properties of, 20: 31235
CHARGED PARTICLE BEAMS
current distribution and geometry of axially symmetric, device for measuring, 20: 31838
focusing of, superconducting quadrupole lens for, 20: 31815 (BNL-10144)
CHARGED PARTICLES
capture in static magnetic bottle, temporary, (T), 20: 32582
detection by solid-state detectors, entrance effects on, 20: 31498 (AD-632527)
effects on dry films of bacteriophage, 20: 31093
energy spectra of, single-crystal magnetic spectrometer for determining, (E/T), 20: 31563
energy spectra of, analog-plotting system for recording, 20: 31592
kinematics in spark chambers, use of multiple scattering and secondary sparks in determining, (E), 20: 31570
losses in axisymmetric and multipolar magnetic fields, nonadiabatic, (E/T), 20: 32545
magnetic field effects on propagation and storage of solar injected, in interplanetary space, (E), 20: 31884
motion in plane electromagnetic wave, (T), 20: 32003
motion in simple force-free magnetic fields, (T), 20: 31812
motion in static magnetic fields, first order correction to magnetic moment for, (T), 20: 32669
motion of trapped, in magnetosphere, (T), 20: 32279
motion through plasma, density wake of, (T), 20: 32589
scattering by nuclei, transfer theorem for multichannel, 20: 32409
trapping in ionosphere, first order correction for adiabatic invariant for, (T), 20: 32669
trapping in magnetic field configuration, method for, 20: 32642(P)
CHEMICAL ANALYSIS
methods used at ANL for elements, 20: 31167(R) (ANL-7175, pp 217-25)
CHEMICAL ENGINEERING
control and dynamics of complex process systems in, 20: 31220(R) (UCRL-16658, pp 39-72)
CHEMICAL RADIATION DETECTORS
performance for proton depth-dose measurements, 20: 31467
performance of ferrous-copper, for large doses, 20: 31607
CHERENKOV DETECTORS
design and testing of, with controlled threshold, 20: 31572
design for beta particle detection in water, 20: 31506 (CEA-R-2915)
CHERENKOV RADIATION
emission by electrons in thick dielectric, 20: 32098
CHLORINE
determination of, in radiosensitizers in tissues, neutron activation, 20: 31172 (SGAE-BL-17/1966)
reactions of, with uranium tetrachloride in fused chlorides, 20: 31166(R) (UCRL-16658, pp 89-92)
CHLORINE ISOTOPES Cl-35
energy levels of, unified model for, 20: 32400
neutron inelastic scattering at 4 and 6 Mev, level parities and spins from, (E), 20: 32550
proton reactions (p,γ) at 733 to 3595 kev, argon-36 levels from, (E), 20: 32451
CHLORINE ISOTOPES Cl-36
determination of, efficiency of Cherenkov counting methods for, 20: 31184
exchange between iodine chloride and lithium chloride, 20: 31246
incorporation in iodine chloride, 20: 31246
CHLORINE ISOTOPES Cl-37
neutron inelastic scattering at 4 and 6 Mev, level parities and spins from, (E), 20: 32550
CHLOROFORM
radiolysis of aqueous solutions of, saturated with carbon dioxide, gamma, 20: 31276
CHLORTETRACYCLINE
effects on radioinduced changes in properdin system in dogs, 20: 31013
CHOLESTEROL
radiation effects on content of, in serum of guinea pigs, γ, 20: 31006
CHROMATOGRAPHY
equipment and methods for continuous, 20: 31210
CHROMIUM
compatibility with plutonium–thorium–uranium alloy, 20: 31666
deposition on uranium, electrolytic, 20: 31670
determination in conductive tissue of beef heart, activation, 20: 31176
determination in human heart tissue, activation, 20: 31175
effects on grain size and transformations in alpha-uranium and uranium alloys at 720 to 800°C, 20: 31666
effects on hardness of molybdenum, 20: 31741
effects on radioinduced swelling in uranium irradiated at 400 to 500°C, 20: 31666
grain boundary grooving in, mechanisms of, 20: 31672
neutron capture by, average level widths of compound nucleus from, (E), 20: 32424
performance in accelerating electrodes in cesium-contact ion thrusters, 20: 31383
proton reactions at 0.05 to 2.9 Bev, induced activity data and cross sections for spallation, (E/T), 20: 32549
radiation effects on lattice parameter of, neutron, 20: 31669
solubility in magnesium–zinc alloys, 20: 31314(R) (ANL-7175, pp 1-41)
surface tension and solid surface energy of, effects of alloying additions of rhenium on, 20: 31773
CHROMIUM ALLOYS
Al–Cr–Fe–Mo–Ni–Ti, radiation effects on tensile properties of Nimonic PE16, thermal-neutron, 20: 31669
Cr–Cu, tensile properties of composites of tungsten fibers and, 20: 31770
Cr–Fe–Mo–Ni–W, radiation effects on mechanical properties of Hastelloy X-280, fast-neutron, 20: 31669
Cr–Fe–Ni, corrosion by boiling magnesium chloride solutions and by water, cracking in stress-, 20: 31676(R) (COO-1319-39)
Cr–Fe–Zr, properties of, for use as fuel cladding material, 20: 31677(R) (GEAP-4840)
Cr–Fe–Zr, corrosion by steam at 300, 400, and 500°C, 20: 31677(R) (GEAP-4840)
Cr–Re, antiferromagnetic properties, specific heat, and superconductivity in, 20: 32702
Cr–Re, grain boundary grooving in, mechanisms of, 20: 31672
Cr–Re, surface tension and solid surface energy of, 20: 31773
Cr–U, separation of barium and lanthanum from, by solvent extraction using liquid magnesium, 20: 31320 (UCRL-16108)
Cr–U, separation of, from fission products by extraction using liquid metals, 20: 31166(R) (UCRL-16658, pp 89-92)
Cr–W, decomposition mechanisms in solid solutions of, 20: 31716(R) (UCRL-16658, pp 121-32)
CHROMIUM BROMIDES
heat capacity of ferromagnetic, at 0.3 to 25°K, 20: 32684(R) (UCRL-16658, pp 21-38)
CHROMIUM CARBIDES
fabrication by hot-pressing, 20: 31699
CHROMIUM COMPLEXES
with hydroxyl radicals, ESR spectra of, 20: 31221(R) (UCRL-16658, pp 73-87)
CHROMIUM COMPOUNDS
radiation effects on, reactions of recoil chromium-51 from neutron, 20: 31297
CHROMIUM IONS
polymerization of, hydrolytic, 20: 31218(R) (UCRL-16658, pp 1-9)

CHROMIUM ISOTOPES Cr-50
neutron total cross sections for, level spacings from, (E/T), 20: 32389
CHROMIUM ISOTOPES Cr-51
decay of, gamma spectra from electron-capture, (E), 20: 32410
energy levels from vanadium-51 (p,n) reactions, parity and spin of, (E), 20: 32371 (CEA-R-2832)
production in proton reactions with iron at 400 Mev, (T), 20: 32560
production of high-specific-activity, for medical use, 20: 31275
reactions of recoil, in irradiated chromium compounds, 20: 31297
CHROMIUM ISOTOPES Cr-52
deuteron elastic scattering at 4.3 to 6.5 Mev, optical-model parameters from, (E/T), 20: 32459
deuteron reactions (d,p) at 4.3 to 6.5 Mev, test of distorted-wave stripping theory by, (E/T), 20: 32459
energy levels from vanadium-52 decay, (E), 20: 32564
proton reactions (p,γ) at 1.36 to 2.26 Mev, manganese-53 levels from, (E), 20: 32446
CHROMIUM ISOTOPES Cr-53
proton elastic scattering at 10 to 12 Mev, optical-model parameters from, (E/T), 20: 32459
CHROMIUM ISOTOPES Cr-54
neutron total cross sections for, level spacings from, (E/T), 20: 32389
CHROMIUM OXIDES
effects on neutron-induced contraction in graphite, 20: 31667
CHROMIUM SYSTEMS
C–Cr–Zr, phase studies, 20: 31669
CHROMOSOMES
radiation effects on Drosophila, 20: 31036(R) (SAN-529-3)
radioinduced aberrations of Vicia, effects of p-nitrobenzoic acid and sulfoguanidine on β, γ, and x, 20: 31124
radioinduced aberrations in barley and *Vicia faba*, effects of Myleran on neutron, 20: 31136
radioinduced aberrations in Drosophila, x, 20: 31047
radioinduced aberrations in, in cultured hamster thyroids, 20: 31053
radioinduced aberrations in, mathematical analysis of, 20: 31057
CIRCUITS
design of radiation hardened, using computer techniques, 20: 31621
design of self-recording, for determining stability of radiometric instruments, 20: 31575
CITIES
damage by nuclear explosions, models of debris from, 20: 31332 (URS-651-4)
CIVILIAN DEFENSE
building debris models for urban nuclear explosions, 20: 31332 (URS-651-41
CLOSTRIDIUM
radiation effects on, in meat at low temperatures, 20: 31634
COAL DEPOSITS
uranium content of Jananese, 20: 31437
COBALT
determination in conductive tissue of beef heart, activation, 20: 31176
determination in human heart tissue, activation, 20: 31175
determination of trace amounts of, using cobalt-60 as radioactive indicator, complexometric, 20: 31181
effects on corrosion of graphite by water vapor, 20: 31667
effects on sintering of zirconium diboride, 20: 31668
neutron capture by, average level widths of compound nucleus from, (E), 20: 32424
platinum-195 Mössbauer effect in, g-factor and internal fields from, (E), 20: 32487
proton elastic scattering at 17.8 Mev, polarization of, (E), 20: 32439
proton reactions at 0.05 to 2.9 Bev, induced activity data and cross sections for spallation, (E/T), 20: 32549
separation from water by precipitation, kinetics of, 20: 31318 (BMwF-FBK-65-04)
COBALT ALLOYS
Ce–Co–Pu, corrosive effects on carburized and noncarburized tantalum alloys, 20: 31679(R) (LA-3524)
Ce–Co–Pu, corrosive effects on niobium alloys, effects of carbon on, 20: 31679(R) (LA-3524)
Ce–Co–Pu, irradiation testing of molten, reactor performance for, 20: 32799 (LA-DC-7752)
Ce–Co–Pu, performance in fast breeder reactors, 20: 32798 (LA-DC-7550)
Co–Zr, crystal structure of Zr_6Co_{23}, 20: 31727
COBALT CARBIDES
B_4C–Co–Dy_2O_3, radiation effects on dispersions of, in soda-potash glass, thermal-neutron, 20: 31668
COBALT COMPLEXES
with ammonia, proton magnetic resonance spectra of, 20: 31218(R) (UCRL-16658, pp 1-9)
COBALT IONS
effects on radioinduced free radical formation in proteins, 20: 31003
COBALT ISOTOPES Co-56
production in proton reactions with iron at 400 Mev, (T), 20: 32560
COBALT ISOTOPES Co-57
decay scheme of, correction in absolute standardization of, 20: 32414
Mössbauer effect in cobalt oxide, copper, and nickel oxide, time independence of charge states determination from, (E), 20: 32713
COBALT ISOTOPES Co-60
beta activity of, use of 4π proportional counters for measuring, 20: 31548
production and uses of, 20: 31642 (ORNL-P-2190)
radiation hazard from atmospheric, calculation of, 20: 31528
use in commercial radiopreservation of food, costs of, 20: 31635
use in maxillary sinus cancer therapy, 20: 31159
uses in complexometric microdetermination of heavy metals, 20: 31181
uses of, in industrial defectoscopy, personnel protection in, 20: 31464
COBALT NIOBATES
$CoNb_2O_6$–$CoTa_2O_6$, phase studies, 20: 31734
COBALT OXIDES
cobalt-57 Mössbauer effect in, time independence of charge states determination from, (E), 20: 32713
diffusion in sodium silicate glass, 20: 31719(R) (UCRL-16658, pp 155-69)
CoO–Nb_2O_5–Ta_2O_5, phase studies, 20: 31734
COBALT STEEL
C–Co–Ni, tensile properties of strain-aged, 20: 31716(R) (UCRL-16658, pp 121-32)
Co–Mo–Ni, tensile properties of strain-aged, 20: 31716(R) (UCRL-16658, pp 121-32)
COBALT SULFATES
effects on nitrogen-15 concentration by nitric acid–nitric oxide exchange, 20: 31639(R) (NYO-755-1, pp 77-129)
COBALT SYSTEMS
Co–Dy_2O_3, radiation effects on dispersions of, in soda-potash glass, thermal-neutron, 20: 31668
Co–TaC–WC, mechanical properties of cermets of, effects of composition on, 20: 31760
Co–WC, mechanical properties of cermets of, effects of composition on, 20: 31760
Co–WC, sintering properties of, 20: 31695
COBALT TANTALATES
$CoNb_2O_6$–$CoTa_2O_6$, phase studies, 20: 31734
COCKCROFT-WALTON ACCELERATORS
design of 500-kev proton, 20: 31829
performance as pulsed neutron generator for nuclear engineering studies, 20: 32360
COILS
design and development of Rogowski, for current density measurements in plasma pinch, 20: 32574 (N-65-32035)
COINCIDENCE CIRCUITS
performance of, determination of statistical parameters of, 20: 31547
COINCIDENCE COUNTERS
design of nanosecond, for gamma cascade directional correlation determinations, 20: 31595
COKE
moisture content of, neutron recoil methods of measuring, 20: 31627
COLCHICINE
effects on intestinal mucosa in mice, 20: 31082
COLLIMATORS
design with surface coatings for neutron reflection suppression, 20: 32368(P)
COLUMBIA RIVER
effluent dispersion in northeast Pacific Ocean, 20: 31448 (RLO-1725-15)
effluent dispersion in northeast Pacific Ocean, 20: 31450 (RLO-1725-17)
effluent dispersion in northeast Pacific Ocean, 20: 31451 (RLO-1725-18)
effluent dispersion in northeast Pacific Ocean, 20: 31449 (RLO-1725-16)
effluent from, dispersion in northeast Pacific Ocean, 20: 31452 (RLO-1725-19)
radiobiological monitoring of, 20: 30969 (BNWL-SA-45)
COMETS
solar wind effects on type-1 tails of, (T), 20: 31898
solar wind interactions with tail of, 20: 31874
solar wind interactions with, 20: 31896
solar wind interactions with, MHD aspects of, (T), 20: 31897
COMPTON EFFECT
cross sections for, (E), 20: 32007
scattering relation for, covariant notation of, 20: 31993
wavelength shift in, Lorentz transformations for, 20: 31994
wavelength shift in, Doppler effect analogy to, 20: 31995
COMPUTER PROGRAMS
ATHENA, for radiation heating and transport in complex reactor geometries, 20: 32768 (UNC-5148)
BUBBLE SCAN I, for bubble chamber data analysis, for IBM 7094, 20: 31507 (COO-1018-1013)

DOSE, for alpha, electron, and proton dosimetry, FORTRAN IV for IBM 7094, 20: 32674 (NP-15697(Vol.3))
FLARE, for alpha and proton fluxes from solar flares, FORTRAN IV for IBM 7094, 20: 32674 (NP-15697(Vol.3))
for alpha inelastic scattering data, in FORTRAN II-D for IBM 1620, 20: 32544
for calculation of liquid scintillation spectrometry data from dual-labeled samples in FORTRAN II, 20: 31177
for determining trace elements in neutron-activated materials, FORTRAN-4 for IBM 7090, 20: 31541
for neutron scattering cross section data analysis, 20: 32379 (ORNL-TM-1208)
for neutron thermalization in reactor cell, 20: 32367
for nuclear electricity production costs, 20: 32743 (ORNL-3944)
for reactor computations, bibliography of, 20: 32764 (CEA-Bib-17(Pt.2))
for reactor physics, review of development of, 20: 32745
for use in analysis of aqueous samples containing carbon-14 and tritium, in FORTRAN IV on IBM-7094, 20: 31182
IDERM, for calculation of radiation exposure from ingested radioisotopes in mammals, 20: 31441 (BNWL-SA-40)
library of AECL, for G-20 computer, 20: 31646 (AECL-1744)
library of AECL, for G-20 computer, 20: 31647 (AECL-1744(Pt.A)(Add. 1))
LIZARD-IV, for nonlinear, ordinary differential equations, FORTRAN IV for Philco 2000, 20: 31657 (KAPL-M-6548)
memory device for, input/output signals of transfer, 20: 31649 (COO-1018-1030)
SPENCER, for reconstituting a one-dimensional function from its moments, FORTRAN II, 20: 31658 (NAA-SR-Memo-11653)
SPOON, for reactor fuel element temperatures, FORTRAN IV, 20: 32791 (NAA-SR-Memo-11731)
UCAPP, for machine tool control, 20: 31478 (K-1670)
UCAPP, for machine tool control, 20: 31327 (K-1671)
ZAP31, for beta-gamma dose rates from slab or spherical sources, FORTRAN 63 for CDC 1604A, 20: 32675 (ORNL-TM-1160)

COMPUTERS
compiler for, design of, 20: 31650 (COO-1018-1031)
data processing by ILLIAC III, visual, 20: 31652 (COO-1018-1057)
design for shock pulse calculations, 20: 32219 (SCL-DC-66-2)
development, 20: 31654(R) (COO-1018-1066)
development, 20: 31655(R) (COO-1018-1076)
development, 20: 31660(R) (RISO-M-385)
development, 20: 31662(R) (TID-23020)
development as automatic control systems, 20: 31645(R) (AD-627094)
development for bubble chamber data analysis, 20: 31645(R) (AD-627094)
development of digital, for low-energy physics, 20: 31562
digital processors for, interconnection and packaging of logical units in, 20: 31648 (COO-1018-1021)
instrumentation development for, 20: 31660(R) (RISO-M-385)
language for pattern recognition by, grammar for, 20: 31651 (COO-1018-1054)
logic circuits for, performance of superconductive threshold, 20: 32311 (ORO-2430-27)
programming of ILLIAC III, manual for, 20: 31653 (COO-1018-1061)
switch development for, 20: 31645(R) (AD-627094)
use for bubble chamber data analysis, 20: 31508(R) (COO-1018-1075)
use for evaluation of internal plutonium deposition through wounds, 20: 31030 (BNWL-SA-39)
use for oscillograph data analysis, 20: 31479 (Y-1533)
use for radiation dose calculations for tumor therapy, 20: 31155
use in crystal structure analysis, 20: 32681 (BNL-10238)
use of small, on-line, 20: 31661 (SLAC-PUB-191)

CONCRETES
gamma transport in slabs of, Monte Carlo calculations for secondary, 20: 32671 (AD-633216)
properties of prestressed, in reactor pressure vessels, 20: 32750
shielding calculations for, for cylindrical gamma sources, 20: 32678
shielding properties of iron–serpentine, neutron, 20: 32677
shielding properties for gamma rays and neutrons, review of, 20: 32679
thermal properties of, for use in reactor containment vessels, 20: 31722(T) (ORNL-tr-1227)

CONFERENCES
see also introduction to Report Number Index
Advances in Mass Spectrometry, Vol. III, Paris, Sept. 1964, 20: 31197

CONVERSION ELECTRONS
energy spectra of, magnetic beta spectrometer with automatic device for measuring, 20: 31565

COPPER
cobalt-57 Mössbauer effect in, time independence of charge states determination from, (E), 20: 32713
crystal structure of, electron diffraction and microscopy methods for studying, 20: 31715(R) (UCRL-16658, pp 105-20)
deposition of protactinium on gold-plated, tracer studies of, 20: 31243
deposition on uranium, electrolytic, 20: 31670
determination in conductive tissue of beef heart, activation, 20: 31176
determination in human heart tissue, activation, 20: 31175
determination of traces of, in quartz, activation, 20: 31183
diffusion of, in cadmium sulfide single crystals, 20: 32684(R) (UCRL-16658, pp 21-38)
fractionation in neutron-activated soils, 20: 31325
gamma scattering at 0.662 and 1.25 Mev, cross sections for Compton, (E), 20: 32007
joining to copper, parameters for friction, 20: 31670
neutron capture by, average level widths of compound nucleus from, (E), 20: 32424
neutron reactions above 10 ev, chemical binding effects on total cross sections for, 20: 32392
nucleon reactions at high energies, residual radioactivity from, 20: 31831
performance in accelerating electrodes in cesium-contact ion thrustors, 20: 31383
proton elastic scattering at 17.8 Mev, polarization of, (E), 20: 32439
proton reactions at 0.05 to 2.9 Bev, induced activity data and cross sections for spallation, (E/T), 20: 32549
radiation effects on microstrain in single-crystal, fast-neutron, 20: 31669
radiation effects on lattice parameter of, neutron, 20: 31669
radiative lifetime of excited electronic states in, 20: 31219(R) (UCRL-16658, pp 11-20)
sputtering by cesium ions at 0.5 to 15 kev, yields from, 20: 31948
sputtering by cesium ions at 2 to 7 kev, yields from, 20: 31948
sputtering of, by deuterons, helium ions, and protons at 0.1 to 4.0 Mev, (E), 20: 31905
tensile properties of composites of tungsten fibers and, 20: 31770

COPPER ALLOYS
Al–Cu, crystal symmetry of, Kikuchi analysis of, 20: 31715(R) (UCRL-16658, pp 105-20)
Al–Cu, radiation effects on electric conductivity of, neutron, 20: 31786(R) (ORO-2891-5)
Cd–Cu, solvent properties of, for uranium, 20: 31314(R) (ANL-7175, pp 1-41)
Cr–Cu, tensile properties of composites of tungsten fibers and, 20: 31770
Cu–Mg, solvent properties of, for iron, 20: 31314(R) (ANL-7175, pp 1-41)
Cu–Mg–Zn, liquid miscibility of, at high temperatures, 20: 31314(R) (ANL-7175, pp 1-41)
Cu–Mn, heat capacities at $<0.15^{\circ}K$, 20: 32684(R) (UCRL-16658, pp 21-38)
Cu–Ni, tensile properties of composites of tungsten fibers and, 20: 31770

COPPER COMPLEXES
with glycine, radioinduced deamination of, gamma, 20: 31299

COPPER IONS
effects on radioinduced free radical formation in proteins, 20: 31003

COPPER SULFATES
effects on nitrogen-15 concentration by nitric acid–nitric oxide exchange, 20: 31639(R) (NYO-755-1, pp 77-129)
effects on radioinduced degradation of DNA in *E. coli*, 20: 31144
solvent properties for copper in neutron-activated soils, 20: 31325
$CuSO_4$–$FeSO_4$, use in radiation dosimetry, 20: 31607

COPPER SYSTEMS
B–Cu, grain boundary swelling in irradiated, mechanisms of, 20: 31798
B–Cu, radioinduced helium bubbles in, effects of annealing on properties of neutron, 20: 31797
Cu–$MgCl_2$, corrosive effects on steels, 20: 31314(R) (ANL-7175, pp 1-41)
Cu–$MgCl_2$–KCl–NaCl, corrosive effects on ferrous alloys, 20: 31314(R) (ANL-7175, pp 1-41)

CORTICOSTEROIDS
radiation effects on synthesis of, by rat adrenals, x, 20: 31011
synthesis in rats, effects of hypophysectomy on, 20: 31011

COSMIC MESONS (π)
production spectrum exponent relation with production level at 0.4 to 1 Bev/c, (T), 20: 31956

COSMIC PARTICLES
flux of heavy nuclei $Z \geq 3$ in, at geomagnetic lattitude 42° North, 20: 31951
flux of helium and hydrogen nuclei at balloon altitudes, 20: 31953

COSMIC PROTONS
spectra of primary during solar minimum, (E), 20: 31958

COSMIC RADIATION
composition and energy spectra of primary, conference on, 20: 31950 (CONF-650120)
detection and measurement of, at 3.2 cm, 20: 31957
effects on wheat seeds during space flight, 20: 31058
hazards to aircraft passengers in high-altitude supersonic flight from, 20: 31468

magnetic field effects on high-energy galactic, (E), 20: 31884
measurement in commercial aircraft, 20: 31952
penetration of galactic, in solar system, (T), 20: 31955
rigidity spectra of, model for origin and properties of, 20: 31954
spectra of primary during solar minimum, (E), 20: 31958

COSMIC SHOWERS
conference on EAS, 20: 31950 (CONF-650120)

COSMOLOGY
energy mechanics of semistatic space-times in, 20: 32298
universe models in, general relativistic, 20: 31863

COTTON
radiation effects on DNA in seeds of, γ, 20: 31019

CREATININE
use as index of urinary excretion rate by man, 20: 30983

CRITICAL ASSEMBLIES
criticality parameters for low power, 20: 32773
design and operation of Ukrainian, 20: 32770
design and startup of ROZA, 20: 32769
modification of MARYLA, 20: 32873
neutron kinetics in, unification of theory for, 20: 32779
neutron kinetics in, space-time, (T), 20: 32784
neutron multiplication factors of sub-, measurement using pulsed-neutron technique with distributed neutron absorber, 20: 32787
neutron parameters of ANNA, static, 20: 32875
operating experience with ANNA, 20: 32872
reactivity worth for ZPR VI, sodium, (T), 20: 32869
safety analysis of ZPR-9, 20: 32858 (ANL-7166)
shielding calculations for MARYLA, 20: 32878

CROTONIC ACID
radioinduced solid-state polymerization of, with acrylic monomers, 20: 31287

CRUCIBLES
testing of tungsten, 20: 31314(R) (ANL-7175, pp 1-41)

CRUSTACEA
radiation effects on microbial flora in Dungeness crabmeat, gamma, 20: 31626

CRYOGENICS
design of gamma backscatter quality meter for liquid hydrogen, 20: 32347
equipment testing at liquid helium temperatures, methods and costs of, 20: 32315
use in meat irradiation, 20: 31634
use in 10^{-13} torr pumping system and work chamber, 20: 31392
use of liquid helium-4 in very low temperature apparatus, 20: 32336

CRYOSTATS
design and performance of, for electron irradiation of metals, 20: 32319
design for superconducting solenoids with thermal working volume, 20: 32334
helium transfer system for, using superconducting pump, 20: 32348

CRYSTAL DETECTORS
use in radiation dosimetry, 20: 31560

CRYSTAL STRUCTURE
analysis using automatic acquisition of neutron spectrometer data, 20: 32681 (BNL-10238)
theory of, book on, 20: 32718

CRYSTALS
atom scattering in lattices of, nonbinary model for, 20: 31920
creep behavior and dislocation mobility in, (T), 20: 32696
electron inelastic scattering by, excitation of plasma losses in, (T), 20: 32741
ligand field theory for, operator methods in, 20: 32734
neutron diffraction analysis in, time-of-flight method for, 20: 32701
neutron scattering by, automatic data analysis of, 20: 32681 (BNL-10238)
plastic deformation of metallic, cross-slip mechanisms in, 20: 31713(R) (UCRL-16658, pp 93-8)
positron lifetime in, anomalous long, (E), 20: 32099
spectra of, temperature dependence of vibrational bands in, (E/T), 20: 32737

CURIUM ISOTOPES Cm-242
use in Manned Orbital Research Laboratory propulsion system, 20: 31387

CURIUM ISOTOPES Cm-244
production and uses of, 20: 31642 (ORNL-P-2190)
use in isotopic power generators for space, 20: 31965
use in Manned Orbital Research Laboratory propulsion system, 20: 31387

CURRENT REGULATORS
design of multichannel d-c stabilizer, for ring phasotron, 20: 31837

CYCLOHEPTATRIENONES
deuterium exchange of active methyl hydrogens of, with heavy water and acetic acid, 20: 31260

CYCLOHEXANE, UNDECAFLUORO(TRIFLUOROMETHYL)-
attachment of gaseous electrons to, 20: 31221(R) (UCRL-16658, pp 73-87)

CYCLOTRON RADIATION
emission from electrons, analogy with bremsstrahlung, (T), 20: 31992
production of harmonic resonance phenomena of, in r-f-excited helium discharge, (E), 20: 32236

CYCLOTRONS
beam extraction from heavy ions, 20: 31828
beam extraction system for Berkeley 88-inch, regenerative, 20: 31827 (UCRL-16794)
beam optics for 70-inch, external, 20: 31814 (AD-634300)
beam oscillations in reverse-coupled, correction system for forced, 20: 31839
operation of Davis 76-inch, 20: 31826 (UCD-CNL-47)

CYLINDERS
deformation of rigid-plastic hollow, effects of axial tension and external pressure on, 20: 31335
heat transfer from, liquid helium II, (E), 20: 32349
thermoviscoelastic stress analysis of, 20: 31334
vibration response of cantilever supported, surrounded by annular fluid, (E/T), 20: 31328 (KAPL-M-6539)

CYSTEINE
effects on metabolism in wheat seeds, 20: 31002
effects on radiation effects on *Allium cepa* roots, 20: 31137

CYSTINE
effects on radiation injuries in liver and tumor tissues in mice, 20: 31141

CYTIDINE, 5-BROMO-2'-DEOXY-
radiosensitivity effects of, use of activation analysis for determining mechanism of, 20: 31172 (SGAE-BL-17/1966)

D

DATA RECORDING SYSTEMS
development of digital, 20: 31220(R) (UCRL-16658, pp 39-72)
for fish radiation dose rates, 20: 31501(R) (BNWL-235-4, pp 10-11)
for human body temperature and heart function, 20: 31474 (BNWL-235-4, pp 1-4)
for test animal movement and positions in cages, 20: 30960(R) (BNWL-235-4, pp 22-5)
performance of analog-plotting, for low-energy charged-particle spectra, 20: 31592

DATA TABULATIONS
atomic transition probabilities for $1 \leq Z \leq 10$, 20: 31942
corrosion of structural materials by liquid alkali metals, 20: 31680 (NAA-SR-Memo-11652)
geomagnetic and solar activity parameters for 1965, 20: 32259
neutron resonance parameters for plutonium-239 and uranium-235 and -238, 20: 32551
radionuclide half lives, 20: 32421

DECONTAMINATING SOLUTIONS
development of aqueous, for reactor coolant and moderator systems, 20: 32747(P)

DECONTAMINATION
data on soil surface, 20: 31454 (USNRDL-TR-967)

DECONTAMINATION OF EQUIPMENT
data on, 20: 31454 (USNRDL-TR-967)

DEER
cesium-137 content in caribou and reindeer effects of diet on, 20: 31442 (BNWL-SA-661)
iron-55 content in tissues of reindeer in Finland, 1966, 20: 31444 (CONF-660405-15)
strontium-90 content in, effects of diet on, 20: 31442 (BNWL-SA-661)

DEHYDROGENASES
genetics of locational specificity of malate, in radioinduced mutants of of Neurospora, 20: 31012
radiation effects on activity of, in serum and tissues of monkeys, γ and proton, 20: 31105
radiation effects on activity in mouse gonads, γ and x, 20: 31090

DENMARK
radiation processing of food in, review of, 20: 31628

DENSITOMETERS
design of radiometric, for liquid hydrogen, 20: 31494

DEUTERIUM
concentration in water by exchange with acetylene, 20: 31640(R) (NYO-755-1, pp 130-72)
determination in water by infrared spectroscopy, 20: 31640(R) (NYO-755-1, pp 130-72)
determination of, in helium, chromatograph for continuous, 20: 31210
deuteron reactions (d,p) at 25.3 Mev, proton spectra from, (E), 20: 32568
diffusion of interstitial, in tantalum, 20: 31766
exchange between pyrylium or tropylium compounds and acetic acid or heavy water, 20: 31260
hydrogen atom reactions with molecular, rotational excitation from, (T),

20: 31932
ionization of, by electrons at 0.6 to 20 kev, cross sections for, (E/T), 20: 31906
isotope effects in radioinduced dissociation of hydrogen sulfide, 20: 31271
pinch discharges in, particle temperatures and radiative energy losses in theta, (T), 20: 32610
proton reactions (p,γ) at 156 Mev, cross section for, (E), 20: 32486
reactions of, with ions, atom and charge transfer in, 20: 31224
separation from hydrogen by electrolysis and diffusion using palladium and palladium–silver membranes, 20: 31256
separation from hydrogen on nickel hydrogen electrode, electrolytic, 20: 31644
spectra of foil-excited beams of, 20: 31903 (N-66-16702)

DEUTERIUM IONS
reaction with tritium in accelerated mixed plasma, 20: 32586

DEUTERIUM SYSTEMS
D–H, NMR studies of solid solutions of, 20: 32711

DEUTERONS
binding energy from neutron reactions (n,γ) with hydrogen, (E), 20: 32488
binding energy of, from nucleon-nucleon interactions, (T), 20: 32008
effects on animal cells in culture, effects of oxygen on biological, 20: 31123
interactions with photons, cross section for disintegration, (T), 20: 32004
interactions with photons, cross section for meson (π^0) production from elastic, (T), 20: 32041
interactions with mesons (π^+) at 3.65 Bev/c, A_2 (1300) production and properties from, (E), 20: 32064
interactions with mesons (K^+) at 0.9 and 2.4 Bev/c, total cross sections for, (E), 20: 32067
interactions with protons at 1.0 to 1.5 Bev, backward elastic, (E), 20: 32102
interactions with electrons and mesons (μ), detection of $|\Delta I| = 0$ weak nuclear force from elastic, 20: 32049
production in proton-proton interactions at 12.5 Bev/c, cross sections for, (E), 20: 32066
reactions (d,α) with carbon-12 at 9 to 12.5 Mev, isospin selection rules for, (E), 20: 32500
reactions (d,α) with boron-11 at 1.7 Mev, beryllium-9 level widths from, (E), 20: 32441
reactions (d,He-3) with boron-10 at 11.8 Mev, beryllium-9 levels from, (E), 20: 32481
reactions (d,nγ) with boron-10 at 800 kev, carbon-11 levels from, (E), 20: 32395
reactions (d,n) and (d,p) with nuclei, target-excitation effects in, (T), 20: 32497
reactions (d,n) with fluorine-19 at 1.0 to 2.5 Mev, differential cross sections for, (E), 20: 32555
reactions (d,n) with beryllium and boron-9, neutron spectra from, 20: 31786(R) (ORO-2891-5)
reactions (d,n) with lithium-6 at 200 to 800 Mev, polarization effects on, (E), 20: 32411
reactions (d,pγ) with neon-20 at 2.05 Mev, neon-21 levels from, (E), 20: 32476
reactions (d,p) with calcium-40, target-excitation effects in, (T), 20: 32497
reactions (d,p) with nitrogen-14 at 4 Mev, nitrogen-15 levels from, (E), 20: 32501
reactions (d,p) with sulfur-32 at 3.20 Mev, sulfur-33 low-lying levels from, (E), 20: 32565
reactions (d,p) with deuterium at 25.3 Mev, proton spectra from, (E), 20: 32568
reactions (d,p) with helium-3 at 6.0 and 10.0 Mev, polarization and asymmetry from, (T), 20: 32475
reactions (d,p) with nuclei at 11 at 13 Mev, angular-momentum effects on angular distributions from, (E), 20: 32512
reactions (d,p) with chromium-52 at 4.3 to 6.5 Mev, test of distorted-wave stripping theory by, (E/T), 20: 32459
reactions (d,t) with lead-208 at 8.0 to 9.0 Mev, cross sections for, (E/T), 20: 32485
reactions (d,t) with boron-10 at 11.8 Mev, boron-9 levels from, (E), 20: 32481
reactions with nuclei, many-body nucleon transfer in, (E/T), 20: 32547
scattering by carbon-12 at 10.6 to 13.9 Mev, optical-model analyses of elastic, (E/T), 20: 32454
scattering by chromium-52 at 4.3 to 6.5 Mev, optical-model parameters from elastic, (E/T), 20: 32459
scattering losses in plastic and sodium iodide scintillators, 20: 31542
sputtering on copper and silver at 0.1 to 4.0 Mev, (E), 20: 31905

DIAMONDS
radioinduced ionization currents in, 0.5- to 1-Mev electron, 20: 32725(T)

DIELECTRIC BREAKDOWN
mechanism of, in plastic in uniform electric field, 20: 32692

DIET
effects of irradiated, on Drosophila, 20: 31036(R) (SAN-529-3)
effects on cesium-137 and strontium-90 content in man, caribou, and reindeer, 20: 31442 (BNWL-SA-661)
radioisotope content in California, 20: 31471

DIFFERENTIAL EQUATIONS
solution of Fredholm, numerical techniques for, 20: 31656 (IDO-17175)
solution of nonlinear, ordinary, computer program for, 20: 31657 (KAPL-M-6548)
solutions for partial, containing both flow and diffusion terms, 20: 31659 (ORNL-TM-1497)
solutions with two small parameters, asymptotic representations of, 20: 32640

DIKETONES
complexes with europium, preparation of, for use as laser material, 20: 31232

DIOCTYLAMINE
solvent properties for uranium, 20: 31322

DIODES
electron tunneling in junction, localized magnetic states and Fermi-surface anomalies in, 20: 32715
electron tunneling conductance in junction, model for zero-bias anomalies in, 20: 32714
properties of cadmium telluride, for particle detection, 20: 31523

DIRECT ENERGY CONVERSION DEVICES
book: *Direct Generation of Electricity*, 20: 31970
development of thermal-to-kinetic, for electrostatic propulsion systems, 20: 31384

DISTILLATION
use of flash, for seawater desalination, 20: 31193

DOGS
effects of inhaled plutonium-239 oxide aerosols in, pathological, 20: 31025 (AD-631690)
immunogenic efficiency of double vaccination of, with x-irradiated *Ancylostoma caninum*, effects of age on, 20: 31043
phosphorus-32 uptake by prostate gland and urinary bladder of, effects of carrier solution on, 20: 31149(R) (TID-22969)
plutonium-239 distribution in, after inhalation in aerosols, 20: 30968 (BNWL-SA-11)
radiation effects on lethality in, effects of blood transfusions and bone marrow transplants on, 20: 31132
radiation effects on properdin system in, γ and x, 20: 31013
radiation effects on amino acid composition of blood serum of, 20: 31021
radiation effects on, following head exposure, 20: 31060
radiation effects on lymphoid cells in blood and bone marrow in, x, 20: 31086
radiation effects on pancreatic morphology and physiology in, x, 20: 31089
radiation effects on lymph nodes in, from iodine-131-labeled Ethiodol, 20: 31044
radioinduced hematopoietic tumors in, effects of strontium-90 on, 20: 31031 (BNWL-SA-201)
radioinduced pulmonary fibrosis in, protective effects of L-triiodothyronine against gamma, 20: 31138
strontium-90 content in hair of, effects of dietary content on, 20: 30972 (TID-22027)

DOORS
lockout device for, to ensure evacuation of personnel, 20: 31472(P)

DOSIMETERS
design of portable, for neutron dose-rate measurements, 20: 31600
design of solid-state miniature aural, 20: 31503(R) (BNWL-235-4, pp 14-16)
development of in-pile loop, for VVR-S, 20: 32865
development of miniature thermoluminescent, for use *in vivo*, 20: 31598
development of solid-state, 20: 31560
evaluation of, for personnel protection in industrial gamma and x-ray defectoscopy, 20: 31464
performance of boron trifluoride proportional detector, for fast neutrons, 20: 31561
performance of ferrous-copper, for large doses, 20: 31607
performance of fluoroglass, for diagnostic x rays, 20: 31538
performance of lithium fluorides, tissue-equivalent, 20: 31514(R) (UCRL-14881)
performance of rem, for intermediate energy neutrons, 20: 31514(R) (UCRL-14881)
performance of, calculation of detection limit and minimum pulse rate for determining, 20: 31512 (SGAE-SS-5/1966)
production and properties of thermoluminescent, 20: 31608
properties of biological, using films of bacteriophage, 20: 31093
reader modification of FGD-3B Fluoro Glass, for improved accuracy and

reproducibility, 20: 31527
use for measuring radiation absorbed in vacuum envelopes of Nimrod proton-synchrotron, 20: 31832
DRESDEN POWER REACTOR
design and development, 20: 32849
DROPS
charge and velocity of rain, measuring equipment for, 20: 31476(R) (BNWL-235-4, pp 21)
combustion in hot gas streams, 20: 31220(R) (UCRL-16658, pp 39-72)
evaporation in high-temperature convective environments, 20: 31220(R) (UCRL-16658, pp 39-72)
DROSOPHILA
radiation effects on mutation rates at specific *Autosomal loci* in, 20: 31108
radiation effects on, genetic x, 20: 31049
radiation effects, genetic x, 20: 31047
radiosensitivity of, genetic factors in, 20: 31036(R) (SAN-529-3)
DRUGS
barbiturate hypnosis, relation of radiation effects on brain serotonin in rats to, 20: 31007
DYES
effects of food, on radiosensitivity of agarose jellies, 20: 30998 (BNWL-SA-709)
DYSPROSIUM
proton reactions at 0.05 to 2.9 Bev, induced activity data and cross sections for spallation, (E/T), 20: 32549
toxicity in laboratory animals, 20: 30970 (COO-1170-5)
DYSPROSIUM ALLOYS
Al–Dy, crystal structure of $DyAl_3$, 20: 31728
Dy–Zn, melting point of $DyZn_2$, 20: 31743
DYSPROSIUM ISOTOPES
preparation of self-supporting foils of, 20: 31696
DYSPROSIUM ISOTOPES Dy-157
beta decay of, terbium-157 levels from, (E), 20: 32464
DYSPROSIUM ISOTOPES Dy-160
energy level transitions in, L-subshell ratios of E2 rotational, 20: 32516
energy level transitions from terbium-160 decay, conversion coefficients for, (E), 20: 32443
DYSPROSIUM ISOTOPES Dy-161
energy levels from terbium-161 decay, (E), 20: 32463
DYSPROSIUM ISOTOPES Dy-162
energy levels from terbium-162 beta decay, (E), 20: 32462
DYSPROSIUM ISOTOPES Dy-163
energy levels from terbium-163 beta decay, (E), 20: 32462
DYSPROSIUM MOLYBDATES
preparation and crystal structure of, 20: 31740
DYSPROSIUM OXIDES
B_4C–Co–Dy_2O_3, radiation effects on dispersions of, in soda-potash glass, thermal-neutron, 20: 31668
Co–Dy_2O_3, radiation effects on dispersions of, in soda-potash glass, thermal-neutron, 20: 31668
DYSPROSIUM TUNGSTATES
preparation and crystal structure of, 20: 31740

E

EARTH
isotope abundance ratios in mantle of, 20: 32245(T) (NSJ-tr-48)
ECOLOGY
bibliography on freshwater and terrestrial, 20: 30967 (TID-3910(Suppl.4))
cesium-137 distribution in environment, 20: 31142
ELECTRIC ARCS
maintenance of arc spot, mechanism of, (T), 20: 32648
metal vaporization from probe surfaces in, (E), 20: 32593
performance for plasma jets, 20: 31356 (N-66-12435)
properties of, MGD equations for, 20: 32232
stability of argon Poiseuille plasma, in axial magnetic fields, (E/T), 20: 32614
ELECTRIC CHARGES
measurement on raindrops, equipment for, 20: 31476(R) (BNWL-235-4, pp 21)
ELECTRIC CURRENTS
generation of a-c, by triode-type thermionic converters, 20: 31980(P)
measurement through electrodes in plasma, 20: 32631
source design for constant, for instrument calibration, 20: 31588
ELECTRIC DISCHARGE
electron cyclotron harmonic resonance phenomena in r-f-excited, in helium, (E), 20: 32236
ion surface waves in bounded low-pressure, 20: 32620
pressure elevation in hydrogen arc, in axial magnetic field, (E), 20: 32638
properties of h-f, in magnetic field, (E), 20: 32634
ELECTRIC FIELDS
effects on positron annihilation rates in argon, 20: 32105
theory of magnetospheric, 20: 32287
ELECTRIC GENERATORS
design and performance of self-excited MHD, (E), 20: 31976
efficiency of thermal cycle in MHD, (T), 20: 31962
ELECTRIC PROBES
design and development of Rogowski coil, for plasma current distributions, 20: 32574 (N-65-32035)
metal vaporization from surface of, in electric arcs, (E), 20: 32593
theory of electrostatic, for plasma diagnostics, 20: 32662
use for plasma diagnostics in uniform guide field from theta pinch accelerator, 20: 32661
use of eddy-current, for plasma conductivity measurements, 20: 32668
use of wide-band, for plasma measurements, 20: 32632
ELECTRICITY
production by dual-purpose plants, economics of, 20: 32846
production by dual-purpose heavy water reactors, economics for, 20: 32847
ELECTRODEIONIZATION
use for seawater desalination, properties of, 20: 31194
ELECTRODES
current measurement through, in plasma, 20: 32631
electrolytic current distribution in porous, fissure model of, 20: 31220(R) (UCRL-16658, pp 39-72)
mass transfer and polarization at rotating-disk, 20: 31220(R) (UCRL-16658, pp 39-72)
mass transfer at plane, current and potential distribution in, 20: 31220(R) (UCRL-16658, pp 39-72)
operation of porous gas, 20: 31220(R) (UCRL-16658, pp 39-72)
properties of radioactive, 20: 31231
ELECTROLYTES
electric currents in effects of diffusion on, 20: 31220(R) (UCRL-16658, pp 39-72)
polarography in binary, 20: 31220(R) (UCRL-16658, pp 39-72)
transport properties of concentrated, 20: 31220(R) (UCRL-16658, pp 39-72)
ELECTROMAGNETIC FIELDS
polarization precession in, Thomas-Wigner, (T), 20: 32126
ELECTROMAGNETIC LENSES
field of quadrupole, nonlinearity of, (T), 20: 31836
properties of superconducting quadrupole, 20: 31815 (BNL-10144)
use of quadrupole, for focusing particles passing through stopping foils, 20: 31844
ELECTROMAGNETIC WAVES
charged-particle motion in plane, (T), 20: 32003
diffraction by conducting half-plane in plasma, (T), 20: 32580
diffraction by plasma column, density and column diameter from, (T), 20: 32585
emission of polarized, by bosons and fermions in magnetic fields, (T), 20: 32120
excitation of electro-acoustic lateral, in hot compressible plasma, (T), 20: 32590
interaction between light and spin waves, (T), 20: 32735
interactions with electrons, first and second harmonic, (T), 20: 32000
interactions with electron beams, harmonics for, 20: 32001
propagation in inhomogeneous electron plasma, forward scattering corrections for, (T), 20: 31857
propagation in plasma, nonlinear, 20: 32663
propagation in relativistic electron plasma, stability of, 20: 32606
propagation in space dispersive plasma, absorption cross sections and fluctuation scattering of, (T), 20: 32613
propagation in stratified plasma, across inhomogeneous magnetic field, (T), 20: 32625
propagation of electro-acoustic, in isotropic compressible plasma, (T), 20: 32591
reflection of vertically polarized, from magnetoplasma, (T), 20: 32627
reflection on plasma-vacuum boundary, 20: 32588
ELECTROMETERS
calibration of, constant current source for, 20: 31588
ELECTRON BEAMS
effects on dissociation of hydrogen sulfide, isotope effects in, 20: 31271
effects on electric conductivity of platinum, stage IV recovery from, (E), 20: 31800
effects on electric conductivity of nickel, stage IV recovery from, (E), 20: 31800
effects on silicon at 300 kev, depth distribution of defect introduction rate from, 20: 31791
electromagnetic wave interactions with, harmonics for, 20: 32001
focusing of, trajectories of outermost electrons in uniform magnetic field, 20: 31809
interactions with helium and neon gas, level inversion during excitation from, (E), 20: 31941

interactions with plasma, microwave incoherent scattering by unstable oscillations from, (E), 20: 32622
interactions with plasma, anomalous diffusion from, 20: 31645(R) (AD-627094)
kinetics in low-energy linear accelerators, (T), 20: 31850
monitor for nanosecond pulsed, noninterrupting, 20: 31846
ELECTRON-DIFFRACTION ANALYSIS
uses of, in crystal structure determinations, · 20: 31715(R) (UCRL-16658, pp 105-20)
ELECTRON MICROSCOPY
uses of dark-field, for crystal defects, · 20: 31715(R) (UCRL-16658, pp 105 20)
ELECTRON MULTIPLIER TUBES
operation of thermionic-cathode, as amplifers of h-f oscillations, 20: 31485
ELECTRON PAIRS
photoproduction in nuclear emulsions, opening angle for, (E), 20: 32006
ELECTRON SOURCES
design of high-peak-current plasam-gun, 20: 31486
ELECTRONIC EQUIPMENT
radiation effects on, 20: 31620
radiation hardening of, for ion propulsion system, 20: 31618
radiation vulnerability of, for space applications, 20: 31619
ELECTRONIC FILTERS
design of ripple, for AGS magnet power supply, 20: 31833
ELECTRONICS
research programs on, 20: 31165(R) (HMI-B-46)
ELECTRONS
attachment of, to undecafluoro-(trifluoromethyl)cyclohexane and sulfur hexafluoride, 20: 31221(R) (UCRL-16658, pp 73-87)
capture by protons in hydrogen in electric fields, cross section for, (T), 20: 31901 (N-65-34224)
configurations in iodine $B^3\pi$ o + u state, radiative lifetime of, 20: 31219(R) (UCRL-16658, pp 11-20)
content in cislunar space, effects of coherent density fluctuations on radar determination of, 20: 31857
density distribution in magnetosphere, measurement using hydromagnetic whistlers, · 20: 32290
detection and measurement of extraterrestrial, 20: 31886
distribution in homogeneous Lorentz plasma, nonlinear effects on, 20: 32584
distribution in Van Allen belts, solar wind effects on, · 20: 32260
dosimetry of, computer program for, 20: 32674 (NP-15697(Vol.3))
effects of pulsed, on alkaline aqueous benzoate solutions, 20: 31281
effects on cadmium selenide crystals, stimulated emission from, 20: 32730(T)
effects on dry films of bacteriophage, 20: 31093
effects on lithium-doped silicon in solar cells, 20: 31614
effects on palladium at 1.6 to 3.0 Mev, 20: 31805
electromagnetic wave interactions with, first and second harmonic, (T), 20: 32000
emission and propagation from solar flares, (E), 20: 31869
emission from alpha reactions with gold at 1 Mev, secondary, 20: 31918
emission of secondary, from ion beam reactions with metals, 20: 31645(R) (AD-627094)
energy in ion pair production in gamma-irradiated hydrobromic and hydrochloric acids and sulfur hexafluoride, 20: 31292
energy levels of gases of, exchanged-coupled to localized spin, 20: 32085
energy loss spectra in germanium and silicon at 50 kev, (E), 20: 32732
energy losses in bubble chambers, measurement of, 20: 31568
energy resolution of slow, limitations in, 20: 31981 (AD-634517)
energy spectra in tail of magnetosphere, · 20: 32252
energy spectra in Van Allen belts, · 20: 32251
energy spectra of soft, in atmosphere, (E), · 20: 32270
energy states in electric-dipole potential, WKB treatment of bound, 20: 32295
fixation on electronegative gas, tracer techniques for determination of, 20: 32223
flux distribution in magnetosphere, determination of, 20: 32674 (NP-15697(Vol.3))
flux in transition zone of magnetosphere, (E), · 20: 32280
interactions in gases of, self-consistent equations including exchange and correlation effects for, 20: 31946
interactions of bound, with neutrinos, cross section for, (T), 20: 32005
interactions with photons, covariant notation for Compton, 20: 31993
interactions with photons, Lorentz transformations for Compton, 20: 31994
interactions with photons, analogy between Compton and Doppler effect in, 20: 31995
interactions with photons, circular polarization from Compton, (E/T), 20: 31998
interactions with positrons, differential cross sections for baryon resonance production in, (T), 20: 32018
interactions with phonons in gases, kinetic equations for, · 20: 32239
interactions with electrons at 600 Mev, testing quantum electrodynamics by, (E), 20: 32305
interactions with mesons (μ), universality in, (E/T), 20: 31986 (NEVIS-148)
interactions with protons, nucleon electromagnetic form factors for, (T), 20: 32033
interactions with neutrons, nucleon electromagnetic form factors for, (T), 20: 32033
interactions with protons at 593 Mev, cross section for meson (π^0) production in, (E/T), 20: 32038
interactions with nucleons, (ω-ρ) mixing angle from elastic, (E/T), 20: 32058
interactions with positrons at high energies, anapole effects on meson (μ) pair production in annihilation, (T), 20: 32070
interactions with protons, radiative corrections for coincidence measurements of, 20: 32092
interactions with positrons, neutral vector boson propagator in, 20: 32093
interactions with electrons, positrons, and protons at high energies, electron anapole effects on polarization from, (T), 20: 32070
interactions with deuterons, detection of $|\Delta I| = 0$ weak nuclear force from elastic, 20: 32049
losses from Van Allen zones due to pitch angle scattering by electromagnetic disturbances, 20: 32288
mass of, experiment for measuring transverse electromagnetic, 20: 32071
motion in thick dielectric, Cherenkov radiation from, 20: 32098
motion on surface of superconductors in gravitational field, (T), 20: 32325
polarization of, Foldy-Wouthuysen transformation for, 20: 32088
radiations from, moving in curved path and guided surface waves, (T), 20: 31992
reactions in solids, collective energy losses in avalanche ionization in, 20: 32727(T)
reactions with atoms in cesium plasma, cross sections for, (E), 20: 32646
reactions with diamonds at 0.5 to 1 Mev, ionization currents from, 20: 32725(T)
reactions with excited hydrogen atoms at high energies, cross sections for, (T), 20: 31930
reactions with gases at 0.6 to 20 kev, cross sections for ionization, (E/T), 20: 31906
reactions with helium atoms, correlations effects in ionization from, (T), 20: 31924
reactions with hydrogen atoms and ions, ionization cross section for, (T), 20: 31928
reactions with hydrogen molecules, dissociation from, (T), 20: 31931
reactions with lithium-like ions, excitation cross sections for, (T), 20: 31929
reactions with rarefied molecular gases, energy dependence of emission spectra intensity from, (E), 20: 31921
reactions with thick silver foils at 40 to 80 kev, radiation emission from, (E), 20: 32708
scattering by carbon-12, cross sections for inelastic, (T), 20: 32536
scattering by carbon-12 and oxygen-16, form factors for 180° inelastic, (T), 20: 32569
scattering by crystals, excitation of plasma losses in inelastic, (T), 20: 32741
scattering by helium ions and hydrogen atoms, correlation in s-wave, (T), 20: 31927
scattering by neutral heavy atoms at 2 to 200 ev, relativistic effects in, (T), 20: 31923
scattering by nuclei, form factors for 180° inelastic, (T), · 20: 32569
scattering by nuclei, nuclear property determination using, 20: 32405
scattering by oxygen-16, cross sections and sum rules for inelastic, (T), 20: 32536
scattering by oxygen-16 at high energies, form factors for inelastic, (T), 20: 32442
scattering by oxygen-16, nuclear structure effects on bremstrahlung emission from, (T), 20: 32456
scattering in outer magnetosphere, effects of electrostatic plasma oscillations on, · 20: 32262
temperature measurements in theta-pinch plasmas using laser-beam scattering, (E), 20: 32621
theory of, charge and mass relations in, 20: 32002
thermal release from polyethylene terephthalate films, 20: 31790
trapping in polyethylene terephthalate films, 20: 31790
ELECTROSTATIC ANALYZERS
performance for slow electron energy resolution, limitations of, 20: 31981 (AD-634517)
performance with analog plotting system for low-energy charged particles,

20: 31592
properties of spherical, for nonrelativistic charged particles, 20: 31549
ELECTROSTATIC FIELDS
calculation for pulsed controlled-thermonuclear fusion experiments, 20: 32596
ELEMENTARY PARTICLES
bootstrap conditions in field theory for, 20: 32153
content in superdense matter, 20: 32044
coupling constants and mass shifts in broken SU(3) for, 20: 32156
decay of, symmetry theory for leptonic, · 20: 32197
electromagnetic structure of, vortical-torus model for, 20: 32122
field theory for, structure of 4-spinors in, · 20: 32216
Green functions for many-body systems of spectral representation for singlet and triplet, · 20: 32191
interaction amplitudes and cross section calculations for, using crossing symmetry and holomorphy, 20: 32106 (AD-634706)
interactions at high energies, quark models and universality predictions for, 20: 32144
interactions at high energies, impact parameter formalism for, 20: 32173
interactions in SU(3) symmetry as broken SU(8) symmetry, 20: 32143
interactions of arbitrary spin, form factors and parity conservation for, 20: 32382 (UCRL-14582-T(Rev.1))
interactions of spin-1 with spin-0, M-matrix for elastic, · 20: 32193
interactions of spin-1 with spin-2, M-matrix for elastic, · 20: 32194
interactions of, analytic properties of vertex functions in, · 20: 32190
interactions of, analytic properties of impact parameter amplitude for, 20: 32180
interactions of, bootstrap theory for strong, · 20: 32212
interactions of, contributions from unphysical regions in dispersion relations for, · 20: 32192
interactions of, Cabibbo angle for, 20: 32108 (IC-66/59)
interactions of, compositeness conditions for partial-wave amplitude for, 20: 32137
interactions of, current-commutator constraints on amplitudes of forward, 20: 32163
interactions of, field theoretical formulation of relativistic generalization of Levinson theorem for, 20: 32127
interactions of, impact parameter formalism for, 20: 32174
interactions of, Levinson's theorem for vertex zeros in, 20: 32172
interactions of, nonrelativistic four-body, (T), 20: 32171
interactions of, quark model and symmetry for, · 20: 32202
interactions of, Regge-pole theory for, · 20: 32185
interactions of, symmetry properties of electromagnetic, · 20: 32201
interactions of, SU(n)-invariant amplitudes for elastic, 20: 32136
mass splitting in generalized Poincare group for, 20: 32114
mass splitting in SU(3) for, Gell-Mann-Okubo octuplet rule for, 20: 32139
model for, bound states of quark-antiquark system in, 20: 32147
model for, de Sitter, 20: 32160
model for, in unified nonlinear spinor theory, 20: 32121
model for, reformulation of quark, 20: 32183
models in SU(6) symmetry, quark, · 20: 32205
polarization precession in electromagnetic fields, Thomas-Wigner, (T), 20: 32126
production of, unitary conditions at complex values of angular momentum for three-body, 20: 32113
Regge recurrences for, algebraic descriptions of, · 20: 32204
scattering by nuclei, coupled equations for rearrangement, 20: 32388
scattering by nuclei, transfer theorem for multichannel, 20: 32409
structure of hadrons, 20: 32082
structure of, internal, 20: 32083
symmetry for, algebra of currents in, · 20: 32206
symmetry for, bootstrap model in SU(6), · 20: 32208
symmetry for, Clebsch-Gordan series for semisimple Lie groups in, 20: 32158
symmetry for, complex conjugation and isotopic space in U(3), 20: 32213
symmetry for, Lorentz equivalence in unitary and spin unitary, · 20: 32214
symmetry for, magnetic charge in space-time U(3,3), · 20: 32200
symmetry for, mass spectrum and local representations in, 20: 32161
symmetry for, relativistic extension of SU(6), 20: 32115
symmetry for, Schwinger's operator method for angular momentum in, 20: 32166
symmetry for, $U(6) \times U(6)$, 20: 32133
symmetry for, unitary representations of SL (6,C), · 20: 32199
symmetry group for, generalized nonet representations of SU(3) ⊗ SU(3), 20: 32107 (IC-66/48)
symmetry group SL(ν,C) for, coupling of representations of noncompact, 20: 32169
symmetry group SU_{ms} for, algebra of currents in, 20: 32155
symmetry groups for, quark model with chiral decomposition for, 20: 32198
symmetry groups for, invariance in, · 20: 32210
symmetry groups for, R(n) imbedding in U(n), 20: 32124
symmetry in strong coupling theory of, · 20: 32207
symmetry models for, strong coupling of pseudoscalar-meson octet in SU(3), (T), 20: 32063
symmetry principles for, conference on, · 20: 32195
theory of Hadron, matrix mechanics in, · 20: 32211
theory of, formulation of, 20: 32076
ELEMENTS
abundance and synthesis of, in stars, review of, (T), 20: 31808
determination of light, design of gas flow proportional counter for electron-probe, 20: 31589
EMBRYOS
radiation effects on electrical activity of brain of rabbit, effects of developmental stage on x, 20: 31037(T) (JPRS-35315, pp 65-75)
radiation effects on tissue cultures from *Macaca mulatta*, protective effects of serotonin and thiourea against x, 20: 31121
radiosensitivity of barley, γ, 20: 31020
ENANTHIC ACID, URANIUM SALTS
preparation and chemical properties of, 20: 31236
ENDOXAN
effect on radiotherapy of thymic and splenic tumors in mice, 20: 31131
ENGINEERING
book: *Vacuum Science and Engineering*, 20: 31391
ENZYMES
effects of deuterium oxide on lipase activity, 20: 30995
radiation effects on synthesis of induced β-D-galactosidase in *E. coli*, x, 20: 31004
radiation effects on mouse gonad, γ and x, 20: 31090
radiation effects on activities of, in oranges, γ, 20: 31632
EPITHELIUM
effects of sulfhydryl compounds on DNA synthesis in mouse intestinal, 20: 31125
radiation effects on DNA synthesis in mouse uterine, x, 20: 31088
ERBIUM ALLOYS
Er–Ag, electron paramagnetic resonance in, non-S-state, (E), 20: 31764
Er–Zn, melting point of $ErZn_2$, 20: 31743
ERBIUM ISOTOPES
neon-20 reactions (Ne-20,xn) with, alpha-active platinum isotopes from, (E), 20: 32458
preparation of self-supporting foils of, 20: 31696
ERBIUM ISOTOPES Er-163
beta decay of, holmium-163 levels from, (E), 20: 32466
ERBIUM ISOTOPES Er-166
energy level transitions in, L-subshell ratios of E2 rotational, 20: 32516
ERBIUM MOLYBDATES
preparation and crystal structure of, 20: 31740
ERBIUM TUNGSTATES
preparation and crystal structure of, 20: 31740
ERYTHROCYTES
radiation effects on survival of extracorporeal, γ, 20: 31000
radioactivity of human, α, 20: 31145
radioinduced hemolysis of extracorporeal, γ, 20: 31000
ESCHERICHIA COLI
centrifugation studies, 20: 31033(R) (NASA-CR-59196)
mutations in, induced by tritium decay, 20: 31033(R) (NASA-CR-59196)
phage-resistant mutations in, effects of water-d_2 on, 20: 31033(R) (NASA-CR-59196)
phosphate metabolism by, tracer studies of, 20: 31108
radiation effects on properties of DNA in, x, 20: 31144
radiation effects on synthesis of induced β-D-galactosidase in, x, 20: 31004
radiation effects on degradation of DNA in, x, 20: 31015
radiation effects on nucleic acid content of, x, 20: 31023
radiation effects on lethal damage in growing, site of x, 20: 31068
radiation effects on DNA breakdown and synthesis in, effects of bromouracil on uv, 20: 31062
radioinduced inactivation of, relative biological efficiency of gammas, neutrons, and x rays for, 20: 31107
ESTRADIOL
radiation effects on, in man, 20: 31034(R) (RLO-1780-7)
ESTROGENS
radiation effects on, in man, 20: 31034(R) (RLO-1780-7)
radiation effects on, in man, 20: 31035(R) (RLO-1780-8)
ETHANE
hydrogen ion reactions at 20 to 120 kev, ionization cross sections for, 20: 31909
ionization of, by electrons at 0.6 to 20 kev, cross sections for, (E/T), 20: 31906
labeling with tritium by hydrogenation of ethylene, 20: 31259
ETHANE, TETRACHLORODIFLUORO-
CCl_4–tetrachlorodifluoroethane, solvent carrier for nitrogen-15 concentration, 20: 31638(R) (NYO-755-1, pp 12-76)
ETHANETHIOL, 2-AMINO-
effects on radiation injuries in liver and tumor tissues in mice,

20: 31141
radiosensitivity effects of, relation between cellular anoxia and, 20: 31122
ETHYL ETHER
mass spectra, 20: 31198
ETHYLAMINE, 2,2'-DITHIOBIS-
effects on morphology and respiration in rat tissues, 20: 30984
radiosensitivity effects on rats, 20: 31143
ETHYLENE
hydrogen ion reactions at 20 to 120 kev, ionization cross sections for, 20: 31909
hydrogenation to ethane, labeling with tritium by, 20: 31259
radiation effects on production of polymeric ions from, alpha, 20: 31270
ETHYLENE, CHLORO-
radioinduced graft polymerization of, with polyethylene, 20: 31288
ETHYLENE GLYCOL
dibenzoate, radioinduced free radicals in, ESR study of γ, 20: 31306
neutron scattering by, energy spectra from cold, (E), 20: 31567
ETHYLENE POLYMERS
radiation effects on, uv absorption spectroscopy of, 20: 31268(R) (COO-1088-20)
radiation effects on, effects of selenium, sulfur, and tellurium on, 20: 31279
radioinduced crosslinking, double bond formation, and hydrogen evolution in, 20: 31268(R) (COO-1088-20)
radioinduced free radical formation in, 20: 31268(R) (COO-1088-20)
radioinduced graft polymerization of, with vinyl chloride, 20: 31288
reactions of allyl radicals in irradiated, with oxygen, 20: 31268(R) (COO-1088-20)
ETHYLENE, TETRAFLUORO- POLYMERS
radiation effects on specific volume at 40 to 150°C, gamma, 20: 31284
EULYTITES
molecular structure of, neutron-diffraction analysis of, 20: 31254
EUROPEAN ATOMIC ENERGY COMMUNITY
reactor fuel requirements and industrial resources, 20: 32792
EUROPIUM
separation from beryllium fluorides and lithium fluorides, 20: 32804(R) (ORNL-3936, pp 122-71)
EUROPIUM ALLOYS
Eu–Zn, melting point on $EuZn_2$, 20: 31743
EUROPIUM COMPLEXES
with β-diketones, for use as laser materials, 20: 31232
EUROPIUM ISOTOPES Eu-154
beta decay of, conversion coefficients for transitions in, (E), 20: 32443
EUROPIUM ISOTOPES Eu-157
beta decay of, gadolinium-157 levels from, (E), 20: 32465
beta decay scheme, (E), 20: 32514
EUROPIUM ISOTOPES Eu-158
beta decay scheme, (E), 20: 32514
EUROPIUM ISOTOPES Eu-159
beta decay scheme, (E), 20: 32514
EUROPIUM MOLYBDATES
preparation and crystal structure of, 20: 31740
EUROPIUM OXIDES
magnetic properties of single crystals of, Kerr effect in, 20: 31229
Al_2O_3–B_2O_3–EuO, preparation and Faraday rotation of glasses of, 20: 31733
Eu_2O_3–stainless steel 304L–TiO_2, corrosion by water at high temperatures, 20: 31678 (HIT-3583-24)
Eu_2O_3–TiO_2, corrosion by water at high temperatures, 20: 31678 (HIT-3583-24)
EUROPIUM SULFIDES
magnetic properties of single crystals of, Kerr effect in, 20: 31229
EUROPIUM TUNGSTATES
preparation and crystal structure of, 20: 31740
EVAPORATION
mechanisms of, for cadmium sulfide and sodium chloride, 20: 32684(R) (UCRL-16658, pp 21-38)
EVAPORATORS
development of, for metallurgical uses, 20: 32312(R) (UCRL-16658, pp 133-43)
EXCAVATION
nuclear devices and economics for, of sea-level Isthmian canal, 20: 31336
EXHAUST SYSTEMS
design for nuclear facilities, 20: 31453 (STI-PUB-121)
EXPERIMENTAL BREEDER REACTOR-II
fuel cycle development for, 20: 31314(R) (ANL-7175, pp 1-41)
fuel cycle facility for, temperatures of shielding windows in, 20: 31313 (ANL-6852)
EXPONENTIAL PILES
neutron buckling and fission ratios for thorium–uranium fueled, beryllium oxide moderated, 20: 32820
neutron buckling in HELENA, determination from flux measurements, 20: 32783
neutron kinetics in, space-time, (T), 20: 32784
neutron multiplication factors of, measurement using pulsed-neutron technique with distributed neutron absorber, 20: 32787
EYES
radiation effects on fine structure of guinea pig retina, x, 20: 31118
rubidium-86 uptake and dulcitol distribution in, of galactose-fed rats, 20: 30978

F

FALLOUT
analysis of, from USSR nuclear test on Jan. 15, 1965, 20: 31405
cycling in freshwater and terrestrial ecological systems, 20: 30967 (TID-3910(Suppl.4))
formation in thermonuclear surface bursts, 20: 31409
monitoring at Kanazawa, Japan, January 1963 to May 1965, 20: 31413
monitoring in Australia, 1961 through 1963, 20: 31403
monitoring in Cape Thompson–Cape Seppings area, Alaska, 1959 through 1962, 20: 31428 (PNE-481, pp 1165-1200)
monitoring in Finland, 1966, 20: 31444 (CONF-660405-15)
monitoring in Israel after Chinese nuclear test, May to Nov., 1965, 20: 31408
monitoring in Japan, 1965, 20: 31405
monitoring in Nagaoka City, Japan, 1965, 20: 31411
monitoring in New Zealand, 1965, 20: 31446(R) (NP-16015)
origin of sudden increase of surface, stratospheric-tropospheric mass exchange mechanism for, 20: 31402
particles in, beta activity and radionuclide concentrations of, 20: 31424
properties of giant-particle, 20: 31412
radioisotope fractionation in, from land surface burst, 20: 31460
removal from equipment and soil surfaces, data on, 20: 31454 (USNRDL-TR-967)
FAST REACTORS
development of, engineering problems and fuel economy, 20: 32818
fuel burnup in, methods of determining, 20: 31167(R) (ANL-7175, pp 217-25)
fuel performance for breeder, molten plutonium, 20: 32798 (LA-DC-7550)
fuel processing for 1000-MW(e), cost studies on, 20: 31316(R) (ANL-7175, pp 104-18)
fuel temperature calculation for, computer program for, 20: 32791 (NAA-SR-Memo-11731)
fuels for breeder, performance of thorium-232–uranium-233, 20: 32790 (ANL-6930)
reactivity losses in thorium-fueled sodium-cooled, calculation of, 20: 32775
FECES
strontium-90 excretion in rat, effects of sodium phytate on, 20: 30977
strontium-90 sorption by aged horse, 20: 31252
FERMI FAST BREEDER REACTOR
cooling system of, carbon impurities in primary, 20: 32809 (TID-23101)
FERMIONS
electromagnetic wave emission in magnetic fields, polarization of, (T), 20: 32120
mass of fundamental, in unified nonlinear spinor theory, 20: 32121
pairing interactions in small systems, Green functions for, 20: 32094
FERROMAGNETIC MATERIALS
heat capacities of chromium tribromide at 0.3 to 25°K, 20: 32684(R) (UCRL-16658, pp 21-38)
neutron inelastic scattering in region of ferroacoustic resonance, cross sections for, (T), 20: 32722(T)
FERTILIZERS
effects on maize fertility, tracer studies of, 20: 31109
production of ammonia for, using power from nuclear desalination reactor, economics of, 20: 32841 (ORNL-3882)
FETUSES
radiation dose to human, in radiography, 20: 31146
radiation effects on susceptibility of mouse, exposed *in utero* to congenital anomalies, x, 20: 31066
FIELD EMISSION MICROSCOPY
techniques and uses in surface physics, review, 20: 32742
FIELD THEORY
algebra of moments in, approximate saturation of, 20: 32159
book: *Operator Methods in Ligand Field Theory*, 20: 32734
bootstrap conditions for elementary particles in, 20: 32153
Dirac equation generalization in, 20: 32119
fields with spacelike momentum spectra in, relativistic, 20: 32146
formalism in quantum, four-dimensional symmetric canonical, 20: 32123
formalisms for, conservation equations and invariants in vector and spinor, 20: 32145
formulation of unified nonlinear spinor, for fundamental-fermion particle

model, 20: 32121
functions in quantum, homological study of generalized, 20: 32182
gauge transformations in, operator and third kind, 20: 32111
isotopic spinor modulation in, · 20: 32215
lagrangian in, derivation of conserved quantities from symmetries of, 20: 32110
magnetic charge in relativistic quantum, · 20: 32209
quantization of Bargmann-Wigner fields in, Lagrange formalism for relativistic, 20: 32150
quantum, Edge of the Wedge theorem for, 20: 32142
spinor fields in Riemann space in, equations for two-dimensional, 20: 32109
spinors in, structure of 4-, · 20: 32216

FIJI ISLANDS
carbon-14 content of atmosphere at Lauthala Bay, 20: 31410

FILMS
Debye-Waller factor of very thin, effect of substrate on, 20: 32688
quantization in superconducting, macroscopic, 20: 32324

FILTERS
analysis of air exhaust, for uranium-235, 20: 31174 (WAPD-T-1905)
design for air cleaning in nuclear facilities, 20: 31453 (STI-PUB-121)

FINLAND
cesium-137 and strontium-90 contents of human bones and tissues in, 20: 31142
cesium-137 content in Lapps in, 1966, 20: 31444 (CONF-660405-15)
fallout radionuclide content in ecosystems of, · 20: 31442 (BNWL-SA-661)
potassium content in Lapps in, 1966, · 20: 31444 (CONF-660405-15)

FISH
phosphorus-32 uptake and retention by man from Columbia River, 20: 30969 (BNWL-SA-45)
radiation dose rates in reactor effluents, monitor for, · 20: 31501(R) (BNWL-235-4, pp 10-11)
radiation effects on thermal tolerance of, β, 20: 31028 (AECL-2409)
radiation effects on adrenal glands of, pathological γ, 20: 31094
zinc-65 uptake and retention by man from Columbia River, 20: 30969 (BNWL-SA-45)

FISSION
calculation of effective coefficient of, using Monte Carlo method, 20: 32778

FISSION CHAMBERS
development for neutron detection and measurement in reactors, 20: 31596

FISSION FRAGMENTS
nuclear track registration in glasses for neutron dosimetry in mixed fields, 20: 31462

FISSION PRODUCTS
analysis for praseodymium-141, activation, 20: 31167(R) (ANL-7175, pp 217-25)
cycling in freshwater and terrestrial ecological systems, 20: 30967 (TID-3910(Suppl.4))
deposition in lungs and pulmonary lymph nodes of man, 20: 31142
deposition of stratospheric, on tropospheric aerosols, 20: 31459
diffusion of gaseous, in reactor fuels, (T), 20: 31739
distribution and size in uranium, effects of heating time and temperature on gaseous, 20: 31666
distribution in atmosphere, 1963 to 1966, 20: 31397(R) (RLO-1776-2)
distribution in irradiated plutonium dioxide–uranium dioxide fuel, 20: 31804
distribution in irradiated urania, 20: 31666
reactions with bromine pentafluoride mixtures of alumina and uranium chlorides, 20: 31315(R) (ANL-7175, pp 42-103)
separation of, from reactor fuel alloys by extraction using liquid metals, 20: 31166(R) (UCRL-16658, pp 89-92)
sorption by pyroelastic rocks, 20: 32883

FISSIONABLE MATERIAL
neutron fission coefficient calculations using Monte Carlo method, 20: 32778

FLUID FLOW
analysis of flow past obstacles, 20: 31220(R) (UCRL-16658, pp 39-72)
boiling burnout in, effects of tube diameters and flow inlet conditions on, 20: 31342(R) (EURAEC-1482)
Hamilton's principle for nonrelativistic and relativistic, · 20: 32227
Hamilton's principle for nonrelativistic and relativistic electromagnetic, 20: 32228
heat transfer in two-phase, in multirod geometries, (E), 20: 31343(R) (GEAP-5056)
regime transitions in vertical two-phase, 20: 31340 (ANL-7093)

FLUID FLOW (LAMINAR)
heat transfer in hexagonal channels, 20: 31341 (BNL-9546)
magnetohydrodynamic, in entrance region of flat channel with parabolic velocity, (T), · 20: 32226
stability between concentric rotating cylinders, (T), · 20: 31344 (LA-3497)

FLUID FLOW (TURBULENT)
Lorentz field strength for, influenced by Coriolis forces, (T), · 20: 32235
velocity of, through channels of finite bundles of hollow rods, 20: 31350

FLUID FUEL REACTORS
fuel slurry development for, homogeneous suspended thorium, 20: 32829

FLUIDS
conference on mechanics of, 20: 31351
hydromagnetic wave equation for compressible infinite conducting, Cartesian tensor form of, · 20: 32229

FLUORIDE VOLATILITY PROCESSES
development of, for reactor fuels, 20: 31315(R) (ANL-7175, pp 42-103)

FLUORINE
content in primary cosmic radiation, at geomagnetic latitude 42° North, 20: 31951
energy level transition probabilities of, data compilation on, 20: 31942
energy levels of, hyperfine structure of 2p, (T), 20: 31904 (UCRL-16581)
reactions with plutonium and uranium compounds, kinetics of, 20: 31214 (CEA-R-2859)
spectra of, effects of temperature on near ultraviolet absorption, 20: 31221(R) (UCRL-16658, pp 73-87)

FLUORINE ISOTOPES F-17
energy levels of, low-lying negative parity, (T), 20: 32398

FLUORINE ISOTOPES F-18
angular distributions from oxygen-16 (N-14, F-18) reactions at 20 to 33 Mev, (E), 20: 32429

FLUORINE ISOTOPES F-19
deuteron reactions (d,p) at 11 and 13 Mev, angular-momentum effects on angular distribution from, (E), 20: 32512
deuteron reactions (d,n) at 1.0 to 2.5 Mev, differential cross sections for, (E), 20: 32555
neutron reactions (n,α) at 4.7 Mev, angular and energy distributions from, (E), 20: 32434
reactions (F-19,xn) with thulium-169, alpha-active platinum isotopes from, (E), 20: 32458

FLUOROMETRY
radiation dose from, in Japan, 20: 31466

FONTENAY-AUX-ROSES REACTORS (TRITON)
power production using thermionic conversion, 20: 31964

FOOD
analysis for cesium-137, iodine-131, and strontium-89 and -90, gamma spectrometric, 20: 31180
radiation processing of, in O.E.C.D. member countries, review of, 20: 31628
radiation processing of apple juice, biochemical changes in, 20: 31629
radiation resistance of fungi in, 20: 31108
radiopreservation of, factors in commercial, 20: 31635

FOOD IRRADIATION FACILITIES
neutron source for FIR-1, design and performance of cold, 20: 32351

FORMIC ACID
radioinduced carboxylation of, in aqueous solutions, yields of oxalic acid from gamma, 20: 31278

FRANCE
iodine-131 content in milk in, 1961 to 1963, 20: 31456
nuclear power requirements in, 20: 32889
radiation processing of food in, review of, 20: 31628

FREE RADICALS
radioinduced in albumin and trypsin solutions, effects of metal ions on, 20: 31003
radioinduced in aqueous solutions, model of mechanisms in, 20: 31293
radioinduced in DNA base composition, ESR spectral studies on x, 20: 31014
radioinduced in ethylene glycol dibenzoate and polyethylene terephthalate, ESR spectra of, 20: 31306
radioinduced in water, diffusion-controlled reactions of, 20: 31294

FRUITS
radiation effects on chemistry and histology of freeze-dehydrated apples, γ, 20: 31631
radiation effects on composition and enzymatic activities of flavedo and juice of oranges, γ, 20: 31632
radiation effects on metabolism, mitochondrial yields, and respiration in pear tissues, γ, 20: 31633

FUNGI
radiation resistance of, in food, 20: 31108

FURNACES
design and operation of, for skull reclamation process, 20: 31314(R) (ANL-7175, pp 1-41)

G

GADOLINIUM
specific heat of, effects of pressure on, 20: 32684(R) (UCRL-16658, pp 21-38)

toxicity in laboratory animals, 20: 30970 (COO-1170-5)
GADOLINIUM ALLOYS
Be–Gd, phase studies, 20: 31667
Gd–Ag, thermal capacity of dilute, at low temperatures, (E), 20: 31762
Gd–La, magnetic ordering in, gadolinium-content effects on g factor for, (E), 20: 32716
Gd–La, magnetic ordering in, gadolinium-content effects on g factor for, (E), 20: 32716
Gd–Mg, magnetic properties of, 20: 31758
Gd–Sc, magnetic ordering in, gadolinium-content effects on g factor for, (E), 20: 32716
Gd–Y, magnetic ordering in, gadolinium-content effects on g factor for, (E), 20: 32716
Gd–Zn, melting point of $GdZn_2$, 20: 31743
GADOLINIUM FLUORIDES
enthalpy of formation of, 20: 31213(R) (ANL-7175, pp 119-58)
GADOLINIUM IONS
electron paramagnetic resonance in potassium yttrium molybdate crystals, 20: 32728(T)
GADOLINIUM ISOTOPES
preparation of self-supporting foils of, 20: 31696
GADOLINIUM ISOTOPES Gd-146
internal conversion spectrum, (E), 20: 31565
GADOLINIUM ISOTOPES Gd-154
energy level transitions from europium-154 decay, conversion coefficients for, (E), 20: 32443
GADOLINIUM ISOTOPES Gd-157
energy levels from europium-157 beta decay, (E), 20: 32465
GADOLINIUM MOLYBDATES
preparation and crystal structure of, 20: 31740
GADOLINIUM TUNGSTATES
preparation and crystal structure of, 20: 31740
GALACTOSE
effects on dulcitol distribution and rubidium-86 uptake by lenses in rats, 20: 30978
GALLIUM
proton elastic scattering at 17.8 Mev, polarization of, (E), 20: 32439
x-ray absorption by monocrystalline, extended fine structure of K-edge, (T), 20: 32707
GALLIUM ARSENIDES
radiation effects on semiconducting properties of, fast neutron, 20: 31617(T)
sputtering by argon ions at 75 to 600 ev, yields from, (E), 20: 31914
GALLIUM OXIDES
Ga–Pu, mechanical recovery in, effects of prestrain on, 20: 31753
GALLIUM PHOSPHIDES
sputtering by argon ions at 75 to 600 ev, yields from, (E), 20: 31914
GALVANOMETERS
use in measuring track brightness in spark chambers, 20: 31582
GAMMA CAMERAS
use for scintillation, in photography of intravascular clots using iodine-131-plasminogen as tracer, 20: 31150 (UCRL-16691)
GAMMA RADIATION
absorption of linearly polarized, by antiferromagnetic calcium ferrate, spin orientation determination from, 20: 31228
attenuation in lithium hydride-uranium shields, 20: 32672 (NAA-SR-Memo-11786)
detection and measurement of, from deposited plutonium-239 in dogs, 20: 30968 (BNWL-SA-11)
detection and measurement in man, 20: 30993
detection and measurement using scintillation coincidences, instrument for, 20: 31599
detection and measurement in high neutron flux, 20: 31602
detection of, efficiency of thallium-doped sodium iodide crystals for, 20: 31553
detection of, selection of phosphors for, 20: 31574
detection of, 4π Geiger counter design and performance for, 20: 31593
directional correlations of, apparatus for measuring, 20: 31595
dose measurement in mixed neutron fields, instruments for, 20: 31505(R) (BNWL-235-4, pp 30-4)
dose rate from slab and spherical sources, computer program for calculating, 20: 32675 (ORNL-TM-1160)
dosimetry in mixed fields, tissue-equivalent ionization chamber for in-phantom, 20: 31524
dosimetry using fluoroglass, 20: 31538
effects at cellular level, mechanisms of, 20: 31108
effects on adrenal glands of goldfish, pathological, 20: 31094
effects on adult rice weevils in stored grain, lethal, 20: 31623 (AECD/AG-15)
effects on alkali silicate and borosilicate glasses at low temperatures, absorption centers from, 20: 32733
effects on *Allium cepa* roots, protective effects of anoxia, α-aminothioacetamide, and cysteine against, 20: 31137
effects on amino acid content of meats, 20: 31630
effects on ammonium perchlorate properties in solid propellants, 20: 31286
effects on aqueous solutions of carbon-tetrachloride and chloroform saturated with carbon dioxide, 20: 31276
effects on aqueous oxalate solutions, tracer studies of, 20: 31277
effects on biochemical properties of stored seeds, 20: 31024
effects on biological activity of penicillin, 20: 31022
effects on carboxylation of formic acid and methanol in aqueous solutions, 20: 31278
effects on cellobiose, lactose, and maltose, 20: 31304
effects on chemistry and histology of freeze-dehydrated apples, 20: 31631
effects on cholesterol content in blood serum of guinea pigs, 20: 31006
effects on chromosomes in Vicia, genetic, 20: 31124
effects on chromosomes in cultured hamster thyroids, 20: 31053
effects on composition and enzymatic activities of flavedo and juice of oranges, 20: 31632
effects on copper- or silver-activated cadmium chloride crystals, EPR spectral studies on, 20: 32685
effects on cytology and growth of *Pinus rigida*, 20: 31077
effects on deamination in aqueous glycine–copper solutions, 20: 31299
effects on development of corn and wheat, 20: 31113
effects on development of pea seeds, 20: 31114
effects on DNA synthesis and mitosis in HeLa cell cultures, 20: 31008
effects on dry films of bacteriophage, 20: 31093
effects on electron energy in ion pair production in hydrobromic and hydrochloric acids and sulfur hexafluoride, 20: 31292
effects on enzyme activity in monkeys, 20: 31105
effects on erythrocytes, 20: 31000
effects on *Escherichia coli*, from cobalt-60, relative biological efficiency in, 20: 31107
effects on ESR spectrum of human black hair, 20: 31075
effects on ethylene glycol dibenzoate, ESR study of, 20: 31306
effects on ethylene polymers in presence of small amounts of additive, 20: 31279
effects on free radical formation in albumin and trypsin solutions, effects of metal ions on, 20: 31003
effects on gonads of monkeys, pathological, 20: 31117
effects on growth and development of mice, continuous low-dose, 20: 31074
effects on growth and mutations in Triticum, 20: 31080
effects on hamster and HeLa cells in culture, biological, 20: 31051
effects on human tissue cultures, protective effects of AET, serotonin, and streptomycin against, 20: 31121
effects on hydrogen reduction of nickel oxide, 20: 31285
effects on immune reactions in euthyroid patients, 20: 31161
effects on induction of pulmonary fibrosis in dogs, protective effects of L-triiodothyronine against, 20: 31138
effects on jute seed, genetic, 20: 31027 (AECD/AG-14)
effects on liver and tumor tissues in mice, protective effects of cystine, glutathione, and MEA against, 20: 31141
effects on luminescence of plant embryos, 20: 31020
effects on *Macaca mulatta*, physiological, 20: 31104
effects on magnetic properties of DNA, effects of temperature on, 20: 31009
effects on mice, biological, 20: 31100
effects on mice, biological, 20: 31102
effects on microbial flora in Dungeness crabmeat and Pacific oysters, 20: 31626
effects on microorganisms, genetic control of, 20: 31041
effects on mutation induction in barley and rice seeds, 20: 31050
effects on oxidative enzymes in mouse epididymis and testis, 20: 31090
effects on planar defects in natural quartz crystals, 20: 32695
effects on polyethylene terephthalate, ESR study of, 20: 31306
effects on preservation of apple juice, 20: 31629
effects on properdin system in dogs, 20: 31013
effects on properties of DNA in cotton seeds, 20: 31019
effects on quinone formation in potatoes, quantitative regularities in, 20: 31001
effects on rabbits, chronic-exposure, 20: 31112
effects on rat skin wound healing, effects of hormones on, 20: 31061
effects on rats, biological, 20: 31140
effects on reproduction of Tephritid flies (*Dacus cucurbitae*), 20: 31046
effects on sheep, pathological, 20: 31026 (AD-633606)
effects on sorptive properties of resins based on diallyl esters of phosphoric acid, 20: 31303
effects on specific volume of polytetrafluoroethylene at 40 to 150°C, 20: 31284
effects on stability of adamantanes, 20: 31273
effects on synthesis of ammonia from nitrogen and water, 20: 31289
effects on tensile strength of polypropylene film, 20: 31274

effects on water content of corn and wheat leaves, 20: 31110
effects on water snails, biological, 20: 31116
effects on wheat seeds, metabolic, 20: 31002
effects on window temperature in EBR-II fuel cycle facility, 20: 31313 (ANL-6853)
energy spectra in upper atmosphere at 100 to 2000 Mev, (E), 20: 32283
polarization analyzers for, efficiency of Compton circular, (E/T), 20: 31998
scattering by aluminum, copper, iron, and lead at 0.662 and 1.25 Mev, cross sections for Compton, (E), 20: 32007
scattering by aluminum, gold, and lithium fluorides at 0.1 to 8.0 Mev, resonance, (E), 20: 32369 (AECL-2535)
scattering by lead isotopes at 5.5 to 8.0 Mev, self-absorption in, (E), 20: 32369 (AECL-2535)
shielding against, properties of concretes for, 20: 32679
transport in complex reactor geometries, computer programs for, 20: 32768 (UNC-5148)
transport in concrete slabs, Monte Carlo calculations for secondary, 20: 32671 (AD-633216)
transport in shields, P_3 method for flux calculation from, 20: 32673 (NAA-SR-Memo-11872)
use for reactor noise analysis, (E), 20: 32786
uses in determination of solubility of a metal in its molten salt, 20: 31237

GAMMA SHIELDING
calculations for cylindrical sources, 20: 32678

GAMMA SOURCES
development of Compton scattered neutron capture, 20: 32369 (AECL-2535)
dose rate from slab or spherical, computer program for, 20: 32675 (ORNL-TM-1160)
use in flight instrumentation for rocket target miss distance measurements, 20: 31496
use in missile tracking systems, 20: 31495

GAMMA SPECTROMETERS
performance for activation analysis, 20: 31541
performance of lithium-drifted germanium, 20: 31514(R) (UCRL-14881)
performance of lithium-drifted silicon, 20: 31519
performance of stilbene crystal, for gamma detection in high neutron flux, 20: 31602
sensitivity function of cesium iodide (thallium) crystal scintillation, 20: 31564
velocity drive system for Mössbauer, electromagnetic, 20: 31590

GAMMA SPECTROSCOPY
pulse height distribution in, evaluation of, 20: 31555

GARIGLIANO POWER REACTOR
waste treatment and disposal for, liquid, 20: 32815

GAS COOLED REACTORS
fuel burnup determinations for power, techniques for, 20: 32838
safety systems for graphite-moderated power, 20: 32835

GAS FLOW
magnetohydrodynamic shock relations in nonaligned, 20: 32218 (NYO-1480-29)

GASES
book: *Radiation Gas Dynamics*, 20: 32238
diffusion and solubility in liquids, determination of, by laser interferometry, 20: 31220(R) (UCRL-16658, pp 39-72)
diffusion in alumina, 20: 31719(R) (UCRL-16658, pp 155-69)
effects on reactor building materials, 20: 31682 (NP-16003)
electric discharges in, induction coil for measuring, 20: 32571 (IPP-1/2)
electron fixation on electronegative, tracer technique for determination of, 20: 32223
evolution of, mechanisms of electrolytic, 20: 31220(R) (UCRL-16658, pp 39-72)
kinetic equation for electron-phonon, 20: 32239
laser beam reactions with, plasma production by, 20: 32666
plasma motion in weakly ionized, with strong magnetic field, (T), 20: 32645
properties at low pressures, book on, 20: 31391
shock propagation in spheres of, spherical, (T), 20: 31871
solubility of, in metals, high-temperature technique for determining terminal, 20: 31250
spectra of high-temperature diatomic, electron, 20: 31219(R) (UCRL-16658, pp 11-20)
thermodynamics of nonextensive systems of, statistical, 20: 32237
virial coefficients of Bose-Einstein, Faddeev equations for, 20: 32230
viscosity of, mass dependence of, 20: 32234

GEIGER-MUELLER TUBES
construction and operation of, filled with mercury vapor, 20: 31517
design and performance of 4π, for gamma detection, 20: 31593
development of, for oxygen analyzer using thallium-204 for oceanographic applications, 20: 31171 (ORO-596)
performance for radiation measurements in space, 20: 31610

GENES
radiosensitivity effects in microorganisms, 20: 31041
radiosensitivity effects in cells, 20: 31042

GENETICS
radiation effects on Rhodopseudomonas, x, 20: 31033(R) (NASA-CR-59196)
site distribution parameters for radioinduced chromosome exchanges, 20: 31057

GEOCHEMISTRY
isotope abundance ratios in Earth's mantle, 20: 32245(T) (NSJ-tr-48)

GEOLOGY
mapping of Cape Thompson region, Alaska, 20: 32885 (PNE-481)
terrain identification in, design of pulsed x-ray instrument for aerial, 20: 31493

GEOMAGNETIC FIELDS
disturbances in, from Starfish high altitude explosion on, 20: 32264
intensity variations of, tables for 1965, 20: 32259
intensity variations of, 6-month, 20: 32257
interactions with solar wind, (E), 20: 32286
line-of-force reconnection with interplanetary lines, mechanism for, 20: 32277
neutron decay in, proton spatial distribution from, 20: 32266
properties during 1965, mathematical model for, 20: 32255
proton intensity distribution in, model for, (T), 20: 32292
proton trapping in South Atlantic anomaly, atmospheric effects on 125 Mev, 20: 32265
pulsation band in, 4-second micro-, 20: 32263
pulsations in outer Van Allen belts, micro-, 20: 32248
structure of, Newtonian theory for distortion in, 20: 32282

GEOMAGNETIC STORMS
commencement times and properties of, tables for 1965, 20: 32259
effects on tail of magnetosphere, 20: 32253

GERMAN REACTORS
construction outline of AEG boiling water, 20: 32812
development for heat and power, 20: 32844
fuels for, use of thorium, 20: 32824

GERMANES
synthesis of, procedure for, 20: 31218(R) (UCRL-16658, pp 1-9)

GERMANIUM
description of lithium-compensated detectors of, 20: 31605
efficiency of lithium-drifted detectors of, for gamma rays, 20: 32564
electron energy losses at 50 kev in, spectra of, (E), 20: 32732
fabrication for nuclear spectroscopy, 20: 32373(R) (COO-1530-1)
fabrication technique of lithium-drift, for radiation detection, 20: 31513 (UCRL-14561)
performance of lithium-drifted, for gamma energy spectra, 20: 31500(R) (BNWL-235-4, pp 4-10)
performance of lithium-drifted, for gamma spectroscopy, 20: 31514(R) (UCRL-14881)
performance of p-i-n junction detectors of, 20: 31537
preparation of p-i-n junctions of, using lithium drifting, 20: 31537
reactions of, with iodine, surface kinetics of, 20: 31166(R) (UCRL-16658, pp 89-92)
sputtering by argon and neon ions on (100) and (110) surfaces of, temperature dependence of yields from, 20: 31915

GERMANY
radiation processing of food in, review of, 20: 31628

GLASS
properties of, for use as neutron dosimeters in mixed fields, 20: 31462
reactions of, with metals at interfaces, mechanisms of, 20: 31719(R) (UCRL-16658, pp 155-69)
sorptive properties for krypton and xenon, 20: 31242
sorptive properties for protactinium, tracer studies of, 20: 31243
sorptive properties for manganese, tracer studies of, 20: 31245

GLOBULIN
labeling with iodine-131, separation of α, β, and γ fractions following, 20: 31264

GLOW DISCHARGES
properties of positive column of, effects of small impurities on, (T), 20: 32595

GLUTATHIONE
effects in mixture with AET and serotonin on lysosome morphology of mouse stem cells, 20: 30964
effects on radiation injuries in liver and tumor tissues in mice, 20: 31141
radiosensitivity effects on mouse intestinal crypt cells, x, 20: 31128

GLYCERIDES
radiation effects on incorporation of dietary linoleic acid in, in rat bone marrow, 20: 31016

GLYCEROL
radiosensitivity effects on *Thiobacillus thiooxidans*, x, 20: 31139

GLYCINE
complexes with copper, radioinduced deamination in, gamma, 20: 31299
radioinduced deamination of, in aqueous solutions, gamma, 20: 31299
GLYCOLIC ACID
yields from radioinduced carboxylation of methanol in aqueous solutions, 20: 31278
GOITER
causes of endemic, in Philippines, tracer studies of, 20: 30965
pathology and therapy of, 20: 31162
GOLD
alpha reactions at 1 Mev, secondary electron emission from, 20: 31918
determination in conductive tissue of beef heart, activation, 20: 31176
determination in human heart tissue, activation, 20: 31175
gamma scattering at 0.1 to 8.0 Mev, resonance, (E), 20: 32369 (AECL-2535)
heats of solution in tin-rich alloys, 20: 31717(R) (UCRL-16658, pp 143-9)
neutron reactions at 24 Mev, Monte Carlo capture cross sections for, (T), 20: 32378 (NASA-TR-R-239)
proton reactions at 0.05 to 2.9 Bev, induced activity data and cross sections for spallation, (E/T), 20: 32549
radiation effects on crystal structure defects in annealed and quenched, neutron, 20: 31788
surface structures on faces of single-crystal, 20: 32684(R) (UCRL-16658, pp 21-38)
GOLD ALLOYS
Au–Mn, heat capacities of intermetallic compound in, at 0.14 to 1.18°K, 20: 32684(R) (UCRL-16658, pp 21-38)
Au–Mn, magnetic structure of, neutron diffraction studies of effects of pressure on, 20: 31756
Au–Mo–Ni, performance for bonding graphite to metals, 20: 31683(R) (ORNL-3936, pp 95-121)
Au–Pt, fracture mechanisms of, 20: 31716(R) (UCRL-16658, pp 121-32)
Au–Sn, thermal properties of intermetallic compound in, 20: 31717(R) (UCRL-16658, pp 143-9)
GOLD ISOTOPES Au-197
proton reactions at 155 Mev, alpha emission from, (T), 20: 32455
GOLD ISOTOPES Au-198
determination of, efficiency of Cherenkov counting methods for, 20: 31184
hyperfine-structure anomaly, (E), 20: 32553
production and uses of, 20: 31642 (ORNL-P-2190)
GOLD ISOTOPES Au-199
hyperfine-structure anomaly, (E), 20: 32553
GONADOTROPIC HORMONES
radiation effects on human, from gonadal exposure, 20: 31034(R) (RLO-1780-7)
GONADS
radiation dose to, during hemangiomas therapy, 20: 31156
radiation effects on seminal fluid and sperm counts in human, 20: 31034(R) (RLO-1780-7)
radiation effects on human, 20: 31035(R) (RLO-1780-8)
radiation effects on monkey, pathological γ and x, 20: 31117
radiation effects on orchitis development and *Treponema pallidum* content in antigens in rabbit, 20: 31119
radiation effects from polonium-210 on spermatogenesis in mouse testes, 20: 31063
radiation effects on oxidative enzyme systems in mouse, γ and x, 20: 31090
radiation exposure to human, design of apparatus for, 20: 31034(R) (RLO-1780-7)
sulfur content in human testes, estimation of, 20: 30982
GRAPHITE
bonding to metals, performance of gold–molybdenum–nickel alloy for, 20: 31683(R) (ORNL-3936, pp 95-121)
compatibility with cesium vapor at 1800°C, 20: 31669
corrosion by water vapor, effects of metal additions on, 20: 31667
corrosion of grade CGB, in molten fluoride salts, 20: 31683(R) (ORNL-3936, pp 95-121)
neutron pulse propagation in, (E/T), 20: 32362
oxidation at 450 to 510°C, inhibiting effects of phosphorus oxychloride vapor on, 20: 31667
radiation damage in, energy release at high temperatures from neutron, 20: 31802
radiation damage in, effects of annealing on fast-neutron, 20: 31803
radiation effects on physical properties of, neutron, 20: 31683(R) (ORNL-3936, pp 95-121)
radiation effects on dimensional stability of, at 450 to 1200°C, neutron, 20: 31782 (BNWL-SA-67)
radiation effects on mechanical properties of, in-reactor, 20: 31785 (ORNL-P-2162)
radiation effects on thermal diffusivity of pyrolytic, fast-neutron, 20: 31667
radioinduced contraction in, effects of chemical additions on neutron, 20: 31667
radioinduced dimensional changes in sodium-saturated, neutron, 20: 31667
reactions with hydrogen, kinetics of, 20: 31166(R) (UCRL-16658, pp 89-92)
reactions with lithium vapor, 20: 31223(T) (BNL-tr-78)
B_4C–graphite, fabrication and properties of hot-pressed composites of, 20: 31688 (NASA-CR-507)
Be_2C–graphite, fabrication and properties of hot-pressed composites of, 20: 31688 (NASA-CR-507)
graphite–Mo_2C, fabrication and properties of hot-pressed composites of, 20: 31688 (NASA-CR-507)
graphite–NbC, fabrication and properties of hot-pressed composites of, 20: 31688 (NASA-CR-507)
graphite–TaC, fabrication and properties of hot-pressed composites of, 20: 31688 (NASA-CR-507)
graphite–ThC_2, fabrication and properties of hot-pressed composites of, 20: 31688 (NASA-CR-507)
graphite–ThC_2, phase studies, 20: 31666
graphite–TiC, fabrication and properties of hot-pressed composites of, 20: 31688 (NASA-CR-507)
graphite–UC_2, fabrication and properties of hot-pressed composites of, 20: 31688 (NASA-CR-507)
graphite–ZrC, fabrication and properties of hot-pressed composites of, 20: 31688 (NASA-CR-507)
HfC–graphite, fabrication and properties of hot-pressed composites of, 20: 31688 (NASA-CR-507)
GRAPHITE MODERATED REACTORS
safety systems for gas-cooled power, 20: 32835
GRAVITATION
collapse in cosmological background, (T), 20: 32306
collapse of interstellar gas cloud, effects of magnetic field on, 20: 31862
effects on electron motion on surface of superconductors, (T), 20: 32325
neutrino transport theory in stellar collapse, relativistic, 20: 32296
spectral red shift in conformally flat field of, (T), 20: 31855
theories of, equivalence-principle violation in Nordstroem-type, 20: 32299
GREAT BRITAIN
radiation processing of food in, review of, 20: 31628
GROSSWELZHEIM SUPERHEAT REACTOR
heat transfer systems of, description of, 20: 32812
GROUND WATERS
age estimations on, using silicon-32, 20: 31432
flow direction of, use of neutron source in single-well method for, 20: 31430
motion, mixing, and recharge of, tracer studies of, 20: 31394
GROWTH
radiation effects on Kalanchoe, effects of air, carbon dioxide, and nitrogen atmospheres on x, 20: 31076
radiation effects on *Pinus rigida*, chronic gamma, 20: 31077
radiation effects on Triticum, fast and fission neutron and gamma, 20: 31080
GUANIDINE
sulfo-, radiosensitivity effects on Vicia chromosomes, β, γ, and x, 20: 31124
GUINEA PIGS
radiation effects on fine structure of retina of, x, 20: 31118
radiation effects on, protective effects of fractionated bone marrow against lethal, 20: 31126
radiation effects on cholesterol content in blood serum of, γ, 20: 31006
rare earth toxicity in, 20: 30970 (COO-1170-5)
GUNDREMMINGEN POWER REACTOR
description, 20: 32810
heat transfer systems of, description of, 20: 32812
power supply for, emergency, 20: 32811

H

HAFNIUM
effects on microstructure of tungsten–thoria dispersion-hardened alloys, 20: 31781
radiation effects on mechanical properties of control rods of, neutron, 20: 31668
HAFNIUM ALLOYS
Hf–Ni, magnetic properties of intermetallic compounds of, 20: 32699
Hf–Zr, phase diagram, 20: 31744
HAFNIUM BORIDES
enthalpy of formation of, 20: 31213(R) (ANL-7175, pp 119-58)
HAFNIUM CARBIDES
fabrication by hot-pressing, 20: 31699
HfC–graphite, fabrication and properties of hot-pressed composites of, 20: 31688 (NASA-CR-507)

HfC–Mo, phase diagram, 20: 31729
HAFNIUM OXIDES
compatibility with cesium vapor at 1800°C, 20: 31669
effects on sintering of magnesia, 20: 31669
permeability to oxygen at 1100 to 2050°C, 20: 31731
HAFNIUM SYSTEMS
C–Hf–Ta, phase diagram at 2050°C, 20: 31668
Hf–H–Zr, phase diagrams, 20: 31667
HAIR
radiation effects on ESR spectrum of human black, 20: 31075
spectrum of human black, ESR, 20: 31075
strontium-90 content in dog, effects of dietary content on, 20: 30972 (TID-22027)
HALIDES
electron spectra of group II, 20: 31219(R) (UCRL-16658, pp 11-20)
HALL EFFECT
effects on efficiency of thermal cycle in MHD generators, 20: 31962
plasma acceleration by, analysis of, (T), 20: 32573 (N-65-12780)
HAMSTERS
radioinduced chromosome aberrations in cultured thyroid of, 20: 31053
HANDBOOKS AND MANUALS
radiological safety, 20: 31445 (N-65-12416)
HANFORD WORKS, RICHLAND, WASH.
plastic uses at, review of, 20: 31267 (BNWL-SA-658)
HARWELL SYNCHROTRON
beam extraction system for, 20: 31823 (RPP-N-5)
radiation damage in vacuum systems of, dosimetry techniques for measuring, 20: 31832
HASTELLOY F
hardness of, effects of exposure to air at 1200 to 1400°F on, 20: 31669
HASTELLOY X
hardness of, effects of exposure to air at 1200 to 1400°F on, 20: 31669
oxidation by air at 1300 to 1800°F, 20: 31669
tensile properties of, effects of temperature at 1300 to 2000°F on, 20: 31669
HEAD
radiation effects on, of dogs, 20: 31060
radiotherapy of maxillary sinus of, 20: 31159
HEALTH PHYSICS
handbook on, 20: 31445 (N-65-12416)
HEART
analysis for trace elements in tissues of human, activation, 20: 31175
analysis for trace elements in conductive tissue of beef, activation, 20: 31176
function of animal, remote monitoring equipment for, 20: 30961(R) (BNWL-235-4, pp 25-9)
functioning in man, monitoring telemetry system for, 20: 31474(R) (BNWL-235-4, pp 1-4)
HEAT-RESISTING ALLOYS
bonding to TD nickel, diffusion, 20: 31670
HEAT TRANSFER
boiling, to hydrogen, annular flow model for forced convective, 20: 31348
conference on, 20: 31351
from cylinders in liquid helium II, (E), 20: 32349
from nickel spheres to water at 30 to 94°C, 20: 31440(R) (ANL-7175, pp 159-83)
in boiling potassium in tubes, 20: 31347
in laminar flow in hexagonal channels, 20: 31341 (BNL-9546)
in two-phase flow in multirod geometries, (E), 20: 31343(R) (GEAP-5056)
to water at coexistence of nucleate and film boiling, 20: 31345(T) (NSJ-tr-47)
HEAVY WATER REACTORS
control system development for organic-cooled, 20: 32796(R) (AI-CE-3)
development of organic-cooled, 20: 32796(R) (AI-CE-3)
economics for electric power generation and water desalination, 20: 32847
fuel channel assembly development for organic-cooled, 20: 32796(R) (AI-CE-3)
fuel cycles in, burn-up and neutron economy of thorium, (T), 20: 32823
fuel element development for organic-cooled, 20: 32796(R) (AI-CE-3)
fuel reprocessing for organic-cooled, 20: 31317 (BAW-393-3)
loading system for organic-cooled, development of, 20: 32796(R) (AI-CE-3)
materials development for organic-cooled, 20: 32796(R) (AI-CE-3)
neutron kinetics in thorium-fueled, calculation of, 20: 32774
neutron resonance absorption in lattices of uranium-fueled, organic-cooled, (E/T), 20: 32785
HELIUM
analysis for nitrogen and oxygen, methods for, 20: 31167(R) (ANL-7175, pp 217-25)
analysis of, for impurities, chromatograph for continuous, 20: 31210
content in cosmic radiation at balloon altitudes, 20: 31953
density and order parameter for superfluid, near lambda point, 20: 32323
diffusion of metastable atoms of, in cryogenic plasma, 20: 32602(T)
effects on grain boundary swelling in irradiated boron–copper systems, 20: 31798
electric discharge in, electron cyclotron harmonic resonance phenomena in r-f-excited, (E), 20: 32236
electron beam interactions with gas of, level inversion during excitation by monoenergetic, (E), 20: 31941
electron charge density in, first-order shielding approximation for, 20: 31902 (N-66-16249)
electron reactions with atomic, correlation effects in ionization from, (T), 20: 31924
energy level transition probabilities of, data compilation on, 20: 31942
energy levels of, Hornbeck-Molnar cross sections for n = 3, 20: 31947
flow of liquid II, in narrow channels, 20: 32332
heat capacity of solid, 20: 32684(R) (UCRL-16658, pp 21-38)
heat transfer from cylinders in liquid II, (E), 20: 32349
hydrogen ion reactions at 20 to 120 kev, ionization cross sections for, 20: 31909
ionization equation for optically thin plasma of, (T), 20: 32636
ionization of, by electrons at 0.6 to 20 kev, cross sections for, (E/T), 20: 31906
positron annihilation in liquid, angular distribution of photons from, (E), 20: 32346
properties and uses of liquid, 20: 32314
properties in neutron-irradiated boron–copper systems, effects of annealing on, 20: 31797
spectra in airglow, 20: 32289
stability of plasma column of, sub-threshold study of azimuthal modes of Kadomtsev, (E), 20: 32579
HELIUM IONS
electron scattering by, correlation in s-wave, (T), 20: 31927
reactions of, with molecules, atom and charge transfer in, 20: 31224
reactions with metal surfaces, secondary emission factors for, 20: 31926
reactions with molybdenum at 2 to 15 kev, ejected electron energy distribution from, (E), 20: 31939
reactions with sodium chloride at 40 to 2000 ev, electron emission from, (E), 20: 31912
sputtering on copper and silver at 0.1 to 4.0 Mev, (E), 20: 31905
HELIUM ISOTOPES
abundance in stone meteorites, relative, 20: 31876
HELIUM ISOTOPES He-3
binding energy and wave functions for, 20: 32498
bremsstrahlung reactions (γ,n) 2p at threshold to 30 Mev cross sections for, (E), 20: 32546
deuteron reactions (d,p) at 6.0 and 10.0 Mev, polarization and asymmetry from, (T), 20: 32475
neutron elastic scattering at 3.33 to 7.90 Mev, polarization from, (E), 20: 32452
production in proton reactions (p,γ) with deuterium at 156 Mev, cross section for, (E), 20: 32486
proton scattering by, differential polarization of, (T), 20: 32543
reactions (He-3, pγ) with carbon-13 at 3.0 Mev, nitrogen-15 levels from, (E), 20: 32495
reactions (He-3,α) with iron-56 and nickel-60 at 17.5 Mev, angular momentum effects in, 20: 32508
reactions (He-3,p) with carbon-13 at 4.0 Mev, nitrogen-15 levels from, (E), 20: 32501
reactions (He-3,p) with carbon-14 at 4.0 and 4.5 Mev, nitrogen-16 levels from, (E), 20: 32501
reactions (He-3,p) with boron-10 at 1.2 to 12 Mev, nitrogen-13 excited levels from, (E), 20: 32527
reactions (He-3,p) with strontium-88 at 14 to 19 Mev, isomer pair production cross sections for, (E), 20: 32430
reactions (He-3,p) with uranium-238, half life of neptunium-240 isomeric state from, (E), 20: 32460
reactions (He-3,t) with magnesium-24 at 37.8 to 40.1 Mev, aluminum-24 levels and mass from, (E), 20: 32473
reactions (He-3,t) with silicon-28 at 37.8 to 40.1 Mev, phosphorus-28 levels and mass from, (E), 20: 32473
solubility in liquid hydrogen, NMR studies of, 20: 31251
sound propagation at low temperatures in liquid, zero-, (E), 20: 32329
HELIUM ISOTOPES He-4
energy levels in, properties of negative-parity, (T), 20: 32503
use of liquid, in very low temperature apparatus, 20: 32336
HEMATOPOIETIC SYSTEM
radiation effects on astronaut, during space flight, 20: 31029 (BNL-10221)
radiation effects on dog and swine, carcinogenic beta, 20: 31031 (BNWL-SA-201)
HEME
radiation effects on proteins of, 20: 30999(R) (UCB-34P95-7)
HEMOLYSIS

radioinduced in extracorporeal erythrocytes, γ, 20: 31000
HETEROGENEOUS REACTORS
design and operation of thermal, 20: 32789(P)
HEVEA
latex biochemistry in, tracer studies of, 20: 31109
HEXANE
ionization of, by electrons at 0.6 to 20 kev, cross sections for, (E/T), 20: 31906
1-HEXANOL, 2-ETHYL-
uses of, in sol-gel process for preparing plutonium dioxide, thorium dioxide, and uranium dioxide microspheres, 20: 31689 (ORNL-P-2159)
HIGH-ALTITUDE EXPLOSIONS
fallout from Starfish, activity of, (E), 20: 32271
fallout particles from, radionuclide concentrations in, 20: 31424
geomagnetic effects of Starfish, 20: 32264
seismic surface waves from, second Rayleigh and second and third Love modes in, (E), 20: 32269
HIGH TEMPERATURE SEPARATION PROCESSES
development of, for power reactor fuels, 20: 31314(R) (ANL-7175, pp 1-41)
HIROSHIMA
radiation effects on live births among atomic bomb survivors in, 20: 31091
HOLMIUM ALLOYS
Al–Ho, crystal structure of $HoAl_3$, 20: 31728
Ho–Ag, phase studies, 20: 31749
Ho–Zn, melting point of $HoZn_2$, 20: 31743
HOLMIUM ISOTOPES Ho-163
energy levels from at erbium-163 beta decay, (E), 20: 32466
HOLMIUM MOLYBDATES
preparation and crystal structure of, 20: 31740
HOLMIUM TUNGSTATES
preparation and crystal structure of, 20: 31740
HOMOGENEOUS REACTORS
fuel slurries for, fabrication of glass spheres for, 20: 31702
HORMONES
effects on skin wound healing in γ-irradiated rats, 20: 31061
HUMIDITY
effects on strontium-85 uptake and retention by leaves, 20: 30996
HYDROAROMATIC COMPOUNDS
reactions of recoil bromine-82 with, 20: 31296
HYDROBROMIC ACID
radiation effects on electron energy in ion pair production in, measurement of γ, 20: 31292
HYDROCARBONS
analysis of mixtures of, by field ion mass spectrometry, 20: 31199
HYDROCHLORIC ACID
effects on nitrogen-15 concentration by nitric acid–nitric oxide exchange, 20: 31639(R) (NYO-755-1, pp 77-129)
radiation effects on electron energy in ion pair production in, measurement of γ, 20: 31292
radiation effects on frozen, EPR of hydrogen atoms formed in uv and x, 20: 32719(T)
HYDRODYNAMICS
equations of, general theory for solving, 20: 32220 (UCRL-14912-T)
HYDROFLUORIC ACID
radiation effects on frozen, EPR of hydrogen atoms formed in uv and x, 20: 32719(T)
HF–O, reactions with uranium, 20: 31315(R) (ANL-7175, pp 42-103)
HYDROGEN
content in cosmic radiation at balloon altitudes, 20: 31953
content in man, neutron capture analysis of, 20: 30993
density of liquid, solid state beta gage for measuring, 20: 31494
diffusion from high-temperature reactions of steam with aluminum and stainless steel, 20: 31440(R) (ANL-7175, pp 159-83)
effects on electronic structure of transition metals and alloys, 20: 31747
effects on fracture properties of zirconium-base alloys, 20: 31669
effects on impact properties of zirconium–2.5 niobium and Zircaloy-2, effects of fast neutrons on, 20: 31669
effects on thermal expansion of niobium–zirconium alloy, Zircaloy-2, and Zircaloy-4, 20: 31745
electron capture by protons in, cross section for, (T), 20: 31901 (N-65-34224)
electron reactions with atomic, ionization cross section for, (T), 20: 31928
electron reactions at high energies with excited atomic, cross sections for, (T), 20: 31930
electron reactions with molecular, dissociation from, (T), 20: 31931
electron scattering by atomic, correlation in s-wave, (T), 20: 31927
electron-heavy particle nonequilibrium in partially ionized plasma jets of, 20: 32658
energy level transition probabilities of, data compilation on, 20: 31942
energy levels of, Lamb shift in first excited, 20: 31925
flow in nonlocal thermodynamic equilibrium, Navier-Stokes equation for radiative, 20: 32241
heat transfer to, annular flow model for forced convective boiling, 20: 31348
hydrogen atom reactions with molecular, rotational excitation from, (T), 20: 31932
hydrogen ion reactions at 20 to 120 kev, ionization cross sections for, 20: 31909
ionization density in plasma of, methods for calculating, 20: 32628
ionization equation for optically thin plasma of, (T), 20: 32636
ionization of, by electrons at 0.6 to 20 kev, cross sections for, (E/T), 20: 31906
neutron reactions (n,γ) with, deuteron binding energy from, (E), 20: 32488
pinch discharges in, particle temperatures and radiative energy losses in theta, (T), 20: 32610
positron annihilation in liquid, angular distribution of photons from, (E), 20: 32345
positron scattering by, coupled equations for rearrangement, 20: 32388
pressure elevation in arc discharge plasma of, in superimposed axial magnetic field, (E), 20: 32638
proton reactions at high energies with atomic, excitation cross sections for, (T), 20: 31933
quality meter for liquid, design of gamma backscatter, 20: 32347
radioinduced formation in frozen hydrochloric and hydrofluoric acids, EPR in uv and x, 20: 32719(T)
reactions of, with ions, atom and charge transfer in, 20: 31224
reactions with brass at 20 to 45 kev, secondary electron emission from, (E), 20: 31533
reactions with deuterium and hydrogen molecules, rotational excitation from, (T), 20: 31932
reactions with gamma-irradiated nickel oxide, reduction in, 20: 31285
reactions with graphite, kinetics of, 20: 31166(R) (UCRL-16658, pp 89-92)
reactions with metals at 10 to 40 kev, secondary electron emission from, (E), 20: 31533
separation from deuterium by electrolysis and diffusion using palladium and palladium–silver membranes, 20: 31256
separation from deuterium on nickel hydrogen electrode, electrolytic, 20: 31644
shock wave propagation in, in magnetically driven shock tubes, (E), 20: 32615
solubility in alpha-zirconium, effects of alloying additions on, 20: 31667
solubility in liquid nitrogen, NMR studies of, 20: 31251
solubility in zirconium, effects of dissolved oxygen on, 20: 31667
solvent properties of liquid, for helium-3, 20: 31251
spectra of, zero-point energy and Lamb shift in, 20: 31908
stability of anisotropic plasma of, h-f, (E), 20: 32624
symmetry for atomic, dynamical groups of simple nonrelativistic models in, 20: 31922
HYDROGEN ION CONCENTRATION
radiosensitivity effects on *Thiobacillus thiooxidans*, x, 20: 31139
HYDROGEN IONS
electron reactions with, ionization cross section for, (T), 20: 31928
reactions with gases at 20 to 120 kev, cross sections for ionization and charge-exchange, 20: 31909
reactions with metals at 10 to 40 kev, secondary electron emission from, (E), 20: 31533
reactions with surfaces at 30 kev, design of ultrahigh-vacuum ion-bombardment apparatus for, 20: 31937
HYDROGEN PEROXIDES
spectra of normal and deuterated, in solid state, for infrared, 20: 31247
HYDROGEN SULFIDES
radioinduced dissociation of deuterated and normal, isotope effects in, 20: 31271
HYDROGEN SYSTEMS
D–H, NMR studies of solid solutions of, 20: 32711
Hf–H–Zr, phase diagrams, 20: 31667
H–Nb, phase diagram and tensile properties of, 20: 31667
H–Nb, preparation of, for transmission electron microscopy, hydrogen concentration in electrothinning procedures for, 20: 31691
H–Nb, tensile properties of, effects of temperature and strain rate on, 20: 31669
H–Ne, liquid-vapor phase equilibria in, 20: 32242
H–O, shock recombination of near-stoichiometric, 20: 31216 (LA-DC-7659)
H–O, shock recombination of, post-induction kinetics for, (T), 20: 31217 (LA-DC-7661)
H–Ta, preparation of, for transmission electron microscopy hydrogen concentration in electrothinning procedures for, 20: 31691
H–V, preparation of, for transmission electron microscopy, hydrogen concentration in electrothinning procedures for, 20: 31691

H–Zr, preparation of, for transmission electron microscopy, hydrogen concentration in electrothinning procedures for, 20: 31691
HYDROLOGY
research programs on, uses of tritium in, 20: 31394
HYDROMAGNETIC WAVES
propagation in cold plasma, looping trajectories in, (T), 20: 32607
propagation in compressible infinite conducting fluid, Cartesian tensor form of wave equation for, 20: 32229
propagation in flowing plasma, (E/T), 20: 32651
propagation in warm collisionless plasma, structure of, (T), 20: 32577 (NYO-1480-54)
properties of collision-free shock, in interplanetary space, (E/T), 20: 31891
HYPERFRAGMENTS
decay of $_{\Lambda}H^{4}$ and $_{\Lambda}He^{4}$, final-state interactions in meson ($\pi^{\pm}$), 20: 32477
decay of mesic, from meson (K^{-}) reactions with emulsion nuclei at 1.5 Bev/c, (E), 20: 32491
hyperon (Λ) potential well depth in heavy, 20: 32449
model of $_{\Lambda}Li^{7}$, alpha-deuteron-hyperon (Λ), 20: 32450
production of $_{\Lambda}B^{12}$ in meson (π^{-}) interactions with nuclear emulsions at 300 Bev, (E), 20: 32412
HYPERONS
decay amplitudes of, broken-symmetry predictions for, 20: 32050
decay of, analysis of weak radiative, 20: 32081
decay of, partially conserved axial vector-current hypothesis in non-leptonic, 20: 32196
decay of, SU(3) symmetry for leptonic and nonleptonic, 20: 32175
HYPERONS (Λ)
decay of, analysis of weak radiative, 20: 32081
decay of, SU(3) symmetry for leptonic, 20: 32176
interactions with mesons (π), partially-conserved axial-vector current hypothesis for, 20: 32013
nuclear potential well depth in heavy hyperfragments, 20: 32449
HYPERONS (Ω^{-})
decay of, nonleptonic, (T), 20: 31985 (IC-66/57)
HYPERONS (Σ^{-})
symmetry for bound states of hyperons (Ξ^{0}) with, SU(3), 20: 32170
HYPERONS (Σ^{0})
decay of, analysis of weak radiative, 20: 32081
HYPERONS (Σ^{+})
decay of, analysis of weak radiative, 20: 32081
symmetry for bound states of hyperons (Ξ^{0}) with, SU(3), 20: 32170
HYPERONS (Ξ^{-})
decay of, analysis of weak radiative, 20: 32081
symmetry for bound states of hyperons (Σ^{-}) with, SU(3), 20: 32170
HYPERONS (Ξ^{0})
decay of, analysis of weak radiative, 20: 32081
production in meson (K^{-})-proton interactions at 1.05 to 1.7 Bev/c, (E/T), 20: 31988 (UCRL-11510)
symmetry for bound states of hyperons (Σ^{+}) with, SU(3), 20: 32170
HYPERTHYROIDISM
pathology and radiotherapy of, 20: 31162
pathology and therapy of, 20: 31162

I

IMMUNE REACTIONS
book: *Tissue Grafting and Radiation*, 20: 31120
effects of zinc-65 on, in rabbits, 20: 31112
radiation effects on, in euthyroid patients receiving iodine-131, 20: 31161
IMMUNITY
effects of double vaccination with x-irradiated *Ancylostoma caninum* on dog, effects of age on, 20: 31043
IMPACT SHOCK
testing equipment for, design of gas-operated, 20: 31714(R) (UCRL-16658, pp 99-103)
INCOLOY
hardness of types 800, 801, 804, and 825, effects of exposure to air at 1200 to 1400°F on, 20: 31669
INCONEL
hardness of types 625 and 718, effects of exposure to air at 1200 to 1400°F on, 20: 31669
radiation effects on mechanical properties of, in-reactor, 20: 31785 (ORNL-P-2162)
radiation effects on mechanical properties of type 625, fast-neutron, 20: 31669
radioinduced embrittlement in types 600, 625, and X750, neutron, 20: 31801
INDIA
nuclear power developments in, 20: 32817
INDIAN OCEAN
strontium-90 content in deep waters of, 1960 and 1961, 20: 31417
strontium-90 distribution in surface waters of, 1960 and 1961, 20: 31420
INDIUM
heats of solution in tin-rich alloys, 20: 31717(R) (UCRL-16658, pp 143-9)
proton elastic scattering at 17.8 Mev, polarization of, (E), 20: 32439
proton reactions at 0.05 to 2.9 Bev, induced activity data and cross sections for spallation, (E/T), 20: 32549
radiative lifetime of excited electronic states in, 20: 31219(R) (UCRL-16658, pp 11-20)
superconducting transition in small spheres of, superheating and supercooling in, (E), 20: 32331
INDIUM ALLOYS
Bi–In, critical currents in superconducting films of, magnetic field effects on, (E), 20: 32317
Cd–In–Ag, radiation effects on mechanical properties of, thermal-neutron, 20: 31668
In–Ag, stacking-fault energies in, methods of determining, 20: 31713(R) (UCRL-16658, pp 93-8)
In–Pb, thermal conductivity of superconducting surface sheath of, (E), 20: 32327
In–Pb–Sn, magnetic flux pinning by superconducting tin precipitates in, (E), 20: 32313
In–rare earth, crystal structure of, CsCl-type intermediate phases in, 20: 31737
Sb–In, sputtering by argon ions at 75 to 600 ev, yields from, (E), 20: 31914
INDIUM ISOTOPES In-110
decay scheme for isomeric, (E), 20: 32373(R) (COO-1530-1)
INDIUM ISOTOPES In-116
beta decay of isomeric, spectra from, (E), 20: 32564
INDOLE,3-(2-AMINOETHYL)-
radiation effects on liberation of, in brain stem of adrenalectomized rats, x, 20: 31069
3-INDOLEACETIC ACID
analysis for carbon-14 in agar blocks by liquid scintillation counting, 20: 31179
5-INDOLOL, 3-(2-AMINOETHYL)-
effects in mixture with AET and glutathione on lysosome morphology of mouse stem cells, 20: 30964
effects on gamma radiation effects on human tissue cultures, 20: 31121
effects on x radiation effects on *Macaca mulatta* embryo cell cultures, 20: 31121
radiation effects on, in rat brain, relation of barbiturate hypnosis to x, 20: 31007
radiosensitivity effects of, relation between cellular anoxia and, 20: 31122
radiosensitivity effects on mouse intestinal crypt cells, x, 20: 31128
INOR-8
corrosion by molten fluoride salts, 20: 31683(R) (ORNL-3936, pp 95-121)
radiation effects on physical properties of, neutron, 20: 31683(R) (ORNL-3936, pp 95-121)
radiation effects on mechanical properties of, in-reactor, 20: 31785 (ORNL-P-2162)
radiation effects on stress-rupture properties of, fast-neutron, 20: 31669
welds of, creep-rupture properties of, 20: 31683(R) (ORNL-3936, pp 95-121)
INSECTS
population control of Mediterranean fruit fly, *Ceratitis capitata*, by release of irradiated males, 20: 31109
population control of Queensland fruit fly, *Dacus tryoni*, by release of irradiated males, 20: 31109
population control of Tephritid flies (*Dacus cucurbitae*) by release of sterile males, 20: 31046
radiation control of rice weevil, *Sitophilus oryzae*, in stored grain, γ, 20: 31623 (AECD/AG-15)
INSTRUMENTATION
design and development of nuclear electronics, for aerospace applications, 20: 31609
INSULIN
labeling with technetium-99m, 20: 31265
INTERFEROMETERS
design of microwave, with amplitude modulation, 20: 31490
INTERMETALLIC COMPOUNDS
thermodynamic properties of, effects of composition on, 20: 31717(R) (UCRL-16658, pp 143-9)
INTERNATIONAL ATOMIC ENERGY AGENCY
research programs of, summaries of 1965, 20: 32886(R) (STI-DOC-10/53)
INTESTINE
effects of AET, glutathione, and serotonin mixture on lysosome morphology on stem cells in mouse, 20: 30964
effects of colchicine and x radiation on mucosa in mouse, 20: 31082

krypton-85 metabolism in cat, tissue clearance studies on, 20: 30979
radiation effects on transfer capacity of rat small, whole-body x, 20: 31081
radiosensitivity of crypt cells of mouse, x, 20: 31128
strontium-90 absorption by rat, effects of green tea on, 20: 30987
INVERTEBRATES
meiosis in starfish oocytes, effects of heavy water and hydrostatic pressure on, 20: 30986
IODATES
production of carrier-free iodine-131-labeled, by oxidation of iodine-131 on platinum surfaces, 20: 31234
IODINE
determination in biological materials, activation, 20: 31173 (SGAE-BL-18/1966)
determination of, using sputtering ion source, 20: 31168 (CONF-660611-1)
determination of, in radiosensitizers in tissues, neutron activation, 20: 31172 (SGAE-BL-17/1966)
neutron reactions at 24 Mev, Monte Carlo capture cross sections for, (T), 20: 32378 (NASA-TR-R-239)
radiative lifetime of $B^3\pi$ o + u electronic state of, 20: 31219(R) (UCRL-16658, pp 11-20)
reactions of, with germanium, surface kinetics of, 20: 31166(R) (UCRL-16658, pp 89-92)
sorption on soil from Cape Thompson, Alaska area, 20: 31426 (PNE-481, pp 1121-39)
IODINE CHLORIDES
labeling with chlorine-36 by isotope exchange with lithium chloride, 20: 31246
IODINE ISOTOPES
abundance ratios of, use of sputtering ion source for determining, 20: 31168 (CONF-660611-1)
IODINE ISOTOPES I-125
half life, 20: 32406
IODINE ISOTOPES I-126
production and uses of, 20: 31642 (ORNL-P-2190)
IODINE ISOTOPES I-127
energy levels from tellurium-127 decay, (E), 20: 32396
neutron reactions (n,γ) with, gamma spectra from thermal, (E), 20: 32422
IODINE ISOTOPES I-128
energy levels from iodine-127 (n,γ) reactions, (E), 20: 32422
IODINE ISOTOPES I-129
content in reactor effluents, 20: 32884
production of, in reactors, 20: 32884
IODINE ISOTOPES I-131
content in milk in France, 1961 to 1963, 20: 31456
determination in food and water, gamma spectrometric, 20: 31180
effects on immune reactions in euthyroid patients, 20: 31161
effects on lymph nodes in dogs, 20: 31044
effects on thermal tolerance of fish, 20: 31028 (AECL-2409)
energy levels from tellurium-131 decay, spins for, (E), 20: 32563
incorporation in serum globulin, 20: 31264
oxidation on platinum surfaces to produce carrier-free labeled iodate, 20: 31234
production and uses of, 20: 31642 (ORNL-P-2190)
properties of recoil, in proton-irradiated potassium iodate, 20: 31298
radiation effects from deposited, on chromosomes in cultured hamster thyroids, 20: 31053
uptake by salivary glands and stomach, 20: 31160
uptake from milk by man, method for predicting, 20: 30980
uptake from milk by man, use of counter measures in predicting, 20: 30981
use for therapy of thyrotoxicosis, 20: 31162
use in intravascular blood clot photography, 20: 31150 (UCRL-16691)
use of, for radiotherapy of hyperfunctioning solitary thyroid nodule, dosage and scintigraphy in, 20: 31154
uses in studying cause of endemic goiter in Philippines, 20: 30965
IODINE ISOTOPES I-132
radiation dose from ingested, computer calculation of, 20: 31441 (BNWL-SA-40)
ION BEAMS
extraction of heavy-, from sector-focusing cyclotrons, 20: 31828
interactions with plasmas, stability limits for longitudinal waves in, (T), 20: 32608
production in r-f ion source, 20: 31845
reactions with metals, secondary electron emission from, (E), 20: 31645(R) (AD-627094)
reactions with surfaces at 30 kev, design of ultrahigh-vacuum ion-bombardment apparatus for, 20: 31937
ION PAIR PRODUCTION
electron energy in, in gamma-irradiated hydrobromic and hydrochloric acids and sulfur hexafluoride, 20: 31292
ION SOURCES
design and performance of cathode-sputtering, for mass spectrographic analysis, 20: 31204
design of PIG, for linear accelerators, 20: 31829
design of, for field ion mass spectrometry, using razor blades, 20: 31198
design of, for field ion mass spectrometry, review on, 20: 31199
development for use in mass analysis of nanogram solid samples, 20: 31168 (CONF-660611-1)
performance of r-f, 20: 31845
use of, for mass spectrographic analysis of solids, review of, 20: 31201
IONIZATION
radioinduced in aqueous solutions, energy partition between spurs, blobs, and short tracks during, 20: 31293
radioinduced in water, energy partition between spurs, blobs, and short tracks during, 20: 31294
IONIZATION CHAMBERS
design and performance of high-pressure helium-3, for neutron spectrometry, 20: 31573
design of tissue-equivalent, for in-phantom dosimetry, 20: 31524
development for gamma dose rate measurement in mixed gamma-neutron fields, 20: 31505(R) (BNWL-235-4, pp 30-4)
development of boron-coated, for neutron detection and measurement in reactors, 20: 31596
evaluation of, for personnel dosimetry in industrial defectoscopy, 20: 31464
fabrication and operation of, for soft solar x rays, 20: 31511 (N-66-16936)
performance for radiation measurements in space, 20: 31610
response in neutron detection and measurement, frequency, 20: 31597
saturation properties of air- and hydrogen-filled, (T), 20: 31516
IONOSPHERE
charged-particle trapping in, first order correction for adiabatic invariant for, (T), 20: 32669
model of upper, steady-state fluid, (T), 20: 32291
proton precipitation in auroral, Balmer radiation and ionization rate for, (T), 20: 32246
relaxation time of, solar flare effects on, 20: 32267
solar flare effects on sudden frequency deviations in, 20: 32268
structure irregularities in, spread F and F region, 20: 32273
IONS
association with neutral atoms, mechanisms of, 20: 31221(R) (UCRL-16658, pp 73-87)
detection of, in mass spectrographic analysis, 20: 31201
emission of secondary, microanalysis using, 20: 31200
energy levels of beryllium sequence, expectation values for, 20: 31934
energy levels of lithium ^2S sequence, correlation, 20: 31935
formation and interactions of, in field ion mass spectrometry, mechanisms of, 20: 31199
neutralization of gaseous, mechanisms of, 20: 31221(R) (UCRL-16658, pp 73-87)
oscillation in bounded low-pressure discharge plasma, surface, 20: 32620
production from submicrogram samples for isotopic analysis, 20: 31207
reactions with metals, coefficient of surface ionization of secondary ions from, 20: 31913
reactions with nuclei, method for calculating cross sections for, 20: 32374(R) (IITRI-578P25-15)
sorption by soils, tracer studies of, 20: 32883
sorption of, from solutions by metal surfaces, 20: 31220(R) (UCRL-16658, pp 39-72)
spectra of, Heisenberg uncertainty principle for determining, (T), 20: 31910
temperature measurements in theta-pinch plasmas using laser-beam scattering, (E), 20: 32621
transport in redox systems by free convection, 20: 31220(R) (UCRL-16658, pp 39-72)
velocity distribution in repetitively pulsed coaxial plasma accelerator, 20: 32650
water exchange on metal, NMR studies of, 20: 31218(R) (UCRL-16658, pp 1-9)
IRIDIUM
ionization efficiency of electrodes of, in ion engines, 20: 31386
performance as ionizer material in cesium-contact ion thrustors, 20: 31383
properties of porous, for cesium ionization, 20: 31388
surface structures on faces of single-crystal, 20: 32684(R) (UCRL-16658, pp 21-38)
IRIDIUM ALLOYS
Ir–Fe, magnetic properties of fcc, 20: 32739
Ir–Pt, elastic properties at 23°C, 20: 31748
IRIDIUM ISOTOPES Ir-192
production and uses of, 20: 31642 (ORNL-P-2190)
uses of, in industrial defectoscopy, personnel protection in, 20: 31464

IRON
abundance in solar corona, (T), 20: 31865
abundance in solar corona, (T), 20: 31867
abundance of, natural isotopic, 20: 31401
corrosion by boiling magnesium chloride solutions and by water, dissolution patterns in, 20: 31676(R) (COO-1319-39)
determination in conductive tissue of beef heart, activation, 20: 31176
determination in human heart tissue, activation, 20: 31175
diffusion in single-crystal magnesia, 20: 31719(R) (UCRL-16658, pp 155-69)
effects on corrosion of graphite by water vapor, 20: 31667
effects on grain size and transformations in alpha-uranium and uranium alloys at 720 to 800°C, 20: 31666
effects on neutron shielding properties of serpentine concretes, 20: 32677
effects on radioinduced swelling in uranium irradiated at 400 to 500°C, 20: 31666
effects on sintering of zirconium diboride, 20: 31668
electrochemical properties of radioactive, 20: 31231
gamma scattering at 0.662 and 1.25 Mev, cross sections for Compton, (E), 20: 32007
lutetium-175 magnetic field in, g-factor from internal, 20: 32472
neutron capture by, average level widths of compound nucleus from, (E), 20: 32424
nucleon reactions at high energies, residual radioactivity from, 20: 31831
performance in accelerating electrodes in cesium-contact ion thrustors, 20: 31383
platinum-195 Mössbauer effect in, g-factor and internal fields from, (E), 20: 32487
proton elastic scattering at 17.8 Mev, polarization of, (E), 20: 32439
proton reactions at 0.05 to 2.9 Bev, induced activity data and cross sections for spallation, (E/T), 20: 32549
proton reactions at 400 Mev, radioisotope production in, (T), 20: 32560
radiation effects on lattice parameter of, neutron, 20: 31669
radioinduced interstitials in, neutron, 20: 31789
reactions with steam at 950 to 1400°C, kinetics of, 20: 31669
shielding calculations for, for cylindrical gamma sources, 20: 32678
solubility in copper–magnesium alloys, 20: 31314(R) (ANL-7175, pp 1-41)
solubility in magnesium–zinc alloys, 20: 31314(R) (ANL-7175, pp 1-41)
specific heat of, effects of pressure on, 20: 32684(R) (UCRL-16658, pp 21-38)
vaporization from probe surface in electric arcs, (E), 20: 32593

IRON ALLOYS
corrosion by copper–magnesium chloride–potassium chloride–sodium chloride systems, 20: 31314(R) (ANL-7175, pp 1-41)
Al–Cr–Fe–Mo–Ni–Ti, radiation effects on tensile properties of Nimonic PE16, thermal-neutron, 20: 31669
Al–Fe, mechanical properties of, effects of aluminum content and temperature on, 20: 31751
Cr–Fe–Mo–Ni–W, radiation effects on mechanical properties of Hastelloy X-280, fast-neutron, 20: 31669
Cr–Fe–Ni, corrosion by boiling magnesium chloride solutions and by water, cracking in stress-, 20: 31676(R) (COO-1319-39)
Cr–Fe–Zr, corrosion by steam at 300, 400, and 500°C, 20: 31677(R) (GEAP-4840)
Cr–Fe–Zr, properties of, for use as fuel cladding material, 20: 31677(R) (GEAP-4840)
Fe–Mo, strain-aging effects on, 20: 31716(R) (UCRL-16658, pp 121-32)
Fe–Os, magnetic properties of fcc, 20: 32739
Fe–Pt, magnetic properties of fcc, 20: 32739
Fe–Zr, crystal structure of Zr_2Fe, 20: 31727
Ir–Fe, magnetic properties of fcc, 20: 32739

IRON ANTIMONATES(III)
magnetic structure, 20: 32705

IRON IONS
effects on radioinduced free radical formation in proteins, 20: 31003

IRON ISOTOPES
distribution and natural carriers of, in sea water, 20: 31422

IRON ISOTOPES Fe-54
abundance of, natural isotopic, 20: 31401

IRON ISOTOPES Fe-55
content in tissues of reindeer in Finland, 1966, 20: 31444 (CONF-660405-15)

IRON ISOTOPES Fe-56
abundance of, natural isotopic, 20: 31401
helium-3 reactions (He-3,α) at 17.5 Mev, angular-momentum effects in, (E), 20: 32508
neutron reactions (n,p) at 13.5 to 14.8 Mev, cross sections for, (E), 20: 32528

IRON ISOTOPES Fe-57
abundance of, natural isotopic, 20: 31401
Mössbauer effect in particles of iron(III) oxides, 20: 31779
Mössbauer spectra of stainless steel-incorporated, effects of pressure on, 20: 32684(R) (UCRL-16658, pp 21-38)

IRON ISOTOPES Fe-58
abundance of, natural isotopic, 20: 31401

IRON ISOTOPES Fe-59
production of high-specific-activity, for medical use, 20: 31275
radiation hazard from atmospheric, calculation of, 20: 31528

IRON OXIDES
diffusion in sodium silicate glass, 20: 31719(R) (UCRL-16658, pp 155-69)

IRON(III) OXIDES
magnetic properties of particles of, measurement of, using iron-57 Mössbauer effect, 20: 31779

IRON SULFATES
effects on nitrogen-15 concentration by nitric acid–nitric oxide exchange, 20: 31639(R) (NYO-755-1, pp 77-129)

IRON(II) SULFATES
$CuSO_4$–$FeSO_4$, use in radiation dosimetry, 20: 31607

IRON SYSTEMS
Fe–Si, creep at high temperatures, 20: 31714(R) (UCRL-16658, pp 99-103)

IRRADIATION FACILITIES
catalog of, Atomic Energy of Canada Ltd., 20: 32891
design and calibration of x-ray, for studies on human testes, 20: 31034(R) (RLO-1780-7)
design and performance of x-ray, for studies on human gonads, 20: 31035(R) (RLO-1780-8)
development of, for evaluation of in-reactor mechanical properties, 20: 31785 (ORNL-P-2162)
maintenance and modification of cryogenic, at Plumbrook reactor, 20: 32861 (N-66-12348)
pressure cell for in-pile, design of miniature diamond ultrahigh, 20: 32754

ISOBUTYRIC ACID, URANIUM SALTS
preparation and chemical properties of, 20: 31236

ISOCYANIC ACID
methylphenylene ester of, labeling with carbon-14, 20: 31266

ISOTOPE SEPARATION METHODS
exchange, concentration of carbon-13 and oxygen-18 in amine–solvent systems and aqueous solvents from gaseous carbon dioxide, 20: 31641(R) (NYO-755-1, pp 173-208)
exchange, nitrogen-15 concentration in carbon tetrachloride–freon 112 solvents, 20: 31638(R) (NYO-755-1, pp 12-76)
for deuterium concentration by acetylene–water exchange, 20: 31640(R) (NYO-755-1, pp 130-72)
for nitrogen-15, effects of additives on exchange between nitric acid and nitric oxide, 20: 31639(R) (NYO-755-1, pp 77-129)

ISOTOPES
abundance determination by mass spectrometry, review of, 20: 31399
abundance measurement of, mass spectrometer for, 20: 31206
determination by mass spectrometry, ion production technique for, 20: 31207

ISOTOPIC EXCHANGE
between deuterated acetic acid or heavy water and pyrylium or tropylium compounds, 20: 31260
between iodine chloride and lithium chloride, 20: 31246
of carbon-13 and oxygen-18 between gaseous carbon dioxide and liquids, 20: 31641(R) (NYO-755-1, pp 173-208)
of deuterium between acetylene and water, factors affecting, 20: 31640(R) (NYO-755-1, pp 130-72)
of nitrogen-15 between oxides of nitrogen in carbon tetrachloride–freon 112 solvents, 20: 31638(R) (NYO-755-1, pp 12-76)
of nitrogen-15 between nitric acid and nitric oxide, effects of additives on, 20: 31639(R) (NYO-755-1, pp 77-129)

ISRAEL
fallout monitoring after Chinese nuclear test, May to Nov., 1965, 20: 31408

ITALY
radiation processing of food in, review of, 20: 31628

J

JAPAN
fallout monitoring, 1965, 20: 31405
fallout monitoring at Nagaoka City, 1965, 20: 31411
fallout monitoring in, May 1965, 20: 31412
fallout monitoring at Kanazawa, January 1963 to May 1965, 20: 31413
tritium content in natural waters of, 20: 31398(T) (NSJ-tr-49)
uranium content of coal deposits in, 20: 31437

JOURNAL BEARINGS
analysis of superlaminar flow, for rotors, 20: 31329 (KAPL-M-6543)
analysis of vortex-turbulent flow, friction factors for, 20: 31330 (KAPL-M-6546)

K

KETONES
mass spectra, 20: 31198
KIDNEYS
radiodiagnostic procedure for, using mercury-197- or mercury-203-labeled compounds and scintillation scanning, 20: 31148 (CNEA-170)
KRYPTON
content in silicates from Estherville Mesosiderite meteorites, 20: 31859
cyclotron harmonic radiation from plasma of, in magnetic field, (E/T), 20: 32637
heat capacity at 0.4 to 10°K, 20: 32684(R) (UCRL-16658, pp 21-38)
ionization of, by electrons at 0.6 to 20 kev, cross sections for, (E/T), 20: 31906
sorption on glass and molybdenum films, 20: 31242
KRYPTON IONS
reactions of, with molecules, atom and charge transfer in, 20: 31224
reactions with metal surfaces, secondary emission factors for, 20: 31926
KRYPTON ISOTOPES
abundance in meteorites, fission, neutron capture, and spallation anomalies in, 20: 31875
KRYPTON ISOTOPES Kr-79
production and uses of, 20: 31642 (ORNL-P-2190)
KRYPTON ISOTOPES Kr-85
diffusion from irradiated thorium dioxide–uranium dioxide fuels during processing, 20: 31447 (ORNL-3956)
metabolism in cat intestine, tissue clearance studies on, 20: 30979
production and uses of, 20: 31642 (ORNL-P-2190)
uses in surface area measurements, 20: 31353

L

LA CROSSE BOILING WATER REACTOR
coolant chemistry of, 20: 32795 (ACNP-66538)
LABORATORIES
air pollution control in nuclear, 20: 31453 (STI-PUB-121)
description of JINR cryogenic, 20: 32318
safety procedures for radiochemical, 20: 31469
LACTATES
analysis of, for carbon-14 by liquid scintillation counting, 20: 31178
LACTOSE
radiolysis of aqueous solutions of, acid formation in, 20: 31304
LANTHANUM
determination in conductive tissue of beef heart, activation, 20: 31176
determination in human heart tissue, activation, 20: 31175
effects on ductility of austenitic stainless steel, 20: 31669
separation from beryllium fluorides and lithium fluorides, 20: 32804(R) (ORNL-3936, pp 122-71)
separation from irradiated chromium–uranium alloy by solvent extraction using liquid magnesium, 20: 31320 (UCRL-16108)
LANTHANUM ALLOYS
Gd–La, magnetic ordering in, gadolinium-content effects on g factor for, (E), 20: 32716
La–Ni, magnetic properties of intermetallic compounds of, 20: 32699
La–Zn, melting point of $LaZn_2$, 20: 31743
LANTHANUM FLUORIDES
energy levels in, coupling of negative hydrogen- and deuterium-ion localized modes to, (E), 20: 32709
LANTHANUM ISOTOPES La-139
neutron reactions (n,γ) at 10 kev to 3 Mev, cross sections for, (E), 20: 32370(R) (ANL-7175, pp 212-16)
proton reactions (p,3pxn) at 30 to 150 Mev, cesium isotopes from, (E), 20: 32386
LANTHANUM ISOTOPES La-140
beta decay of, K-conversion coefficients for transitions from, (E), 20: 32541
beta decay of, spectra of, (E), 20: 32407
content in fallout in Japan, 1965, 20: 31405
energy levels from barium-140 decay, (E), 20: 32407
LANTHANUM MOLYBDATES
preparation and crystal structure of, 20: 31740
LANTHANUM OXIDES
effects on xenon diffusion in urania, 20: 31666
electron spectra of, 20: 31219(R) (UCRL-16658, pp 11-20)
LANTHANUM TUNGSTATES
preparation and crystal structure of, 20: 31740
LEAD
corrosive effects on niobium–zirconium alloys at 1400°F, 20: 31683(R) (ORNL-3936, pp 95-121)
corrosive effects on stainless steel at high temperatures, 20: 31959(R) (ANL-7175, pp 184-211)
determination of trace amounts of, using cobalt-60 as radioactive indicator, 20: 31181
electron tunneling in superimposed layers of normal aluminum and superconducting, (E), 20: 32342
gamma and neutron attenuation in shields of, 20: 32672 (NAA-SR-Memo-11786)
gamma scattering at 5.5 to 8.0 Mev, self-absorption in, (E), 20: 32369 (AECL-2535)
gamma scattering at 0.662 and 1.25 Mev, cross sections for Compton, (E), 20: 32007
neutron capture by, average level widths of compound nucleus from, (E), 20: 32424
properties as radiation shielding, 20: 32680
proton reactions at 0.05 to 2.9 Bev, induced activity data and cross sections for spallation, (E/T), 20: 32549
shielding calculations for, for cylindrical gamma sources, 20: 32678
thermodynamic properties of liquid, Prandtl number at 0 to 700°C for, 20: 31724
vapor pressures of alloyed and pure, 20: 31717(R) (UCRL-16658, pp 143-9)
LEAD ALLOYS
properties as radiation shielding, 20: 32680
Bi–Pb, superconducting transitions of amorphous, 20: 32341
Bi–Pb, thermodynamic properties of liquid, Prandtl number at 0 to 700°C for, 20: 31724
In–Pb, thermal conductivity of superconducting surface sheath of, (E), 20: 32327
In–Pb–Sn, magnetic flux pinning by superconducting tin precipitates in, (E), 20: 32313
Pb–Ag, thermodynamic properties, 20: 31717(R) (UCRL-16658, pp 143-9)
Pb–Na, corrosive effects on stainless steel at high temperatures, 20: 31959(R) (ANL-7175, pp 184-211)
Pb–Na, properties at high temperatures, 20: 31959(R) (ANL-7175, pp 184-211)
Pb–Sn, magnetic flux pinning by superconducting tin precipitates in, (E), 20: 32313
LEAD ISOTOPES
meson (μ⁻) capture by, x-ray intensity ratios from, (T), 20: 31945
LEAD ISOTOPES Pb-207
energy levels from bismuth-207 decay, half life of 570-kev, (E), 20: 32401
LEAD ISOTOPES Pb-208
deuteron reactions (d,t) at 8.0 to 9.0 Mev, cross sections for, (E/T), 20: 32485
energy levels in, neutron, 20: 32566
neutron elastic scattering at 0.715 to 1.761 Mev, resonances, (E), 20: 32519
proton elastic and inelastic scattering at 11 to 16 Mev, bismuth-208 analog states of lead-208 from, (E), 20: 32478
proton elastic scattering at 40 Mev, differential cross sections and polarization for, (E), 20: 32510
LEAD ISOTOPES Pb-210
content in atmosphere, effects of meterological parameters on, 20: 31407
content in rain water in New Zealand, 1965, 20: 31446(R) (NP-16015)
energy level splitting in, shell model calculation of, 20: 32381 (SGAE-PH-37/1966)
LEAD SYSTEMS
Pb–H_2O, shielding efficiency for gamma rays and neutrons, (T), 20: 32676
Pb–plastic, use as radiation shielding, 20: 32680
LEAD TELLURIDES
sputtering by argon ions at 75 to 600 ev, yields from, (E), 20: 31914
LEAVES
radiation effects on water content in corn and wheat, γ, 20: 31110
strontium-85 uptake and retention by, effects of relative humidity and temperature on, 20: 30996
LECTURES
on decay and production laws of radioisotopes, 20: 32377 (KFK-117)
LEPTONS
interactions of, symmetry theory for weak, 20: 32197
interactions with nucleons, C-violating effects in electromagnetic inelastic, 20: 32042
symmetry for, isotopic spinor modulation in, 20: 32215
LEUKEMIA
nucleic acid synthesis in cultures from patients with, 20: 30971 (ORINS-45)
protein synthesis in cultures from patients with, 20: 30971 (ORINS-45)
radioinduced in mice, effects of injected parental bone marrow and spleen cells on x, 20: 31127
LEUKOCYTES
radiation effects on proliferation of human, in culture, x, 20: 31067
LEUKOPENIA

radioinduced in gynecology patients, bone marrow autotransplantation treatment of, 20: 31134
LIGHT
attenuation in scintillators, 20: 31546
effects on uranyl salts in organic solutions, luminescence spectra from, 20: 31305
interactions with spin waves, (T), 20: 32735
polarization using Faraday effect at high magnetic fields, 20: 31807 (TID-23030)
reflection in curved pipes, analysis for total, (T), 20: 31818 (ITEF-385)
scattering by plasma, analysis of nonlinear incoherent, (T), 20: 32572 (IPP-6/49)
LIGHT SOURCES
design of nanosecond pulse, 20: 31497(P)
LIMESTONE
strontium isotope ratios in, from Ice River, British Columbia, 20: 31406
LINEAR ACCELERATORS
beam dispersion in proton, 20: 31843
beam phasing of multisection, method for, 20: 31852(P)
book: *Linear Electron Accelerators. (Basic Calculations of Small Energy Linear Electron Accelerators)*, 20: 31850
control systems for LAMPF, development of, 20: 31819 (LA-3521)
design of 5-Mev proton, 20: 31829
power systems for LAMPF, development of r-f, 20: 31819 (LA-3521)
shielding of Frascati, performance of, 20: 31820 (LNF-66/14)
waveguide design for traveling-field, 20: 31851(P)
LINGEN POWER REACTOR
heat transfer systems of, description of, 20: 32812
LINOLEIC ACID
radiation effects on incorporation of dietary, in triglycerides in rat bone marrow, 20: 31016
LIQUID FLOW
magnetohydrodynamic steady, in channel with porous walls, (T), 20: 32221
magnetohydrodynamic steady, in annular channel with porous walls, (T), 20: 32222
stability of liquid conductor model of hard-core pinch for, viscous effects on, 20: 32233
LIQUID METAL COOLED REACTORS
reactivity losses in thorium-fueled fast sodium, calculation of, (T), 20: 32775
LIQUIDS
beta absorption in, scintillation device for measuring, 20: 31521
diffusion and solubility of gases in, laser interferometric studies on, 20: 31220(R) (UCRL-16658, pp 39-72)
neutron scattering by homonuclear diatomic, cold, (T), 20: 32353
neutron scattering by homonuclear diatomic, cold, (T), 20: 32354
viscosity of, mass dependence of, 20: 32234
LITHIUM
content in primary cosmic radiation, at geomagnetic latitude 42° North, 20: 31951
determination of, by activation analysis, effects of variations in isotopic ratio on, 20: 31190
effects on radiation resistance of silicon solar cells, 20: 31614
energy level transition probabilities of, data compilation on, 20: 31942
reactions of gaseous, with graphite, 20: 31223(T) (BNL-tr-78)
thermodynamic properties of liquid, Prandtl number at 0 to 700°C for, 20: 31724
LITHIUM ALLOYS
Bi–Li, thermodynamic properties, 20: 31959(R) (ANL-7175, pp 184-211)
Li–Hg, solubility of intermetallic compound in, in fused lithium halides, 20: 31959(R) (ANL-7175, pp 184-211)
Li–Mg, creep of intermetallic compound single-crystal, 20: 31714(R) (UCRL-16658, pp 99-103)
Li–Sn, thermodynamic properties, 20: 31959(R) (ANL-7175, pp 184-211)
LITHIUM BROMIDES
LiBr–LiH, thermodynamic properties, 20: 31959(R) (ANL-7175, pp 184-211)
LITHIUM CARBIDES
preparation of, by reactions of lithium vapor with graphite, 20: 31223(T) (BNL-tr-78)
LITHIUM CHLORIDES
chlorine-36 exchange with iodine chloride, 20: 31246
LiCl–LiF, solvent properties for lithium–mercury intermetallic compounds, 20: 31959(R) (ANL-7175, pp 184-211)
LiCl–LiH, thermodynamic properties, 20: 31959(R) (ANL-7175, pp 184-211)
LITHIUM FLUORIDES
gamma scattering at 0.1 to 8.0 Mev, resonance, (E), 20: 32369 (AECL-2535)
nuclear spin transitions in crystalline, phonon-induced dipole, (T), 20: 32689
performance of tissue-equivalent, for dosimetry, 20: 31514(R) (UCRL-14881)
use of, as thermoluminescent dosimeters for environmental monitoring, 20: 31526
BeF_2–LiF, density, specific heat, and thermal conductivity of, calculation of, 20: 32804(R) (ORNL-3936, pp 122-71)
BeF_2–LiF–ZrF_4, separation from rare earth fission products, 20: 32804(R) (ORNL-3936, pp 122-71)
LiCl–LiF, solvent properties for lithium–mercury intermetallic compounds, 20: 31959(R) (ANL-7175, pp 184-211)
LiF–LiH, thermodynamic properties, 20: 31959(R) (ANL-7175, pp 184-211)
LITHIUM HYDRIDES
corrosive effects on stainless steels at 900, 1200, and 1400°F, 20: 31669
gamma and neutron attenuation in shields of, 20: 32672 (NAA-SR-Memo-11786)
LiBr–LiH, thermodynamic properties, 20: 31959(R) (ANL-7175, pp 184-211)
LiCl–LiH, thermodynamic properties, 20: 31959(R) (ANL-7175, pp 184-211)
LiF–LiH, thermodynamic properties, 20: 31959(R) (ANL-7175 pp 184-211)
LiH–LiI, thermodynamic properties, 20: 31959(R) (ANL-7175, pp 184-211)
LiH–U, gamma and neutron attenuation in shields of, 20: 32672 (NAA-SR-Memo-11786)
LITHIUM IODIDES
LiH–LiI, thermodynamic properties, 20: 31959(R) (ANL-7175, pp 184-211)
LITHIUM ISOTOPES Li-6
deuteron reactions (d,n) at 200 to 800 Mev, polarization effects on, (E), 20: 32411
energy levels of, intermediate coupling shell-model calculations of, (T), 20: 32436
neutron elastic scattering at 4.4 Mev, polarization in, (E), 20: 32433
production in proton reactions with metals at 40 Mev to 25 Bev, (E), 20: 31205
LITHIUM ISOTOPES Li-7
energy levels of, lifetime of first excited, (E), 20: 32504
energy levels of, intermediate coupling shell-model calculations of, (T), 20: 32436
neutron elastic scattering at 4.4 Mev, polarization in, (E), 20: 32433
production in proton reactions with metals at 40 Mev to 25 Bev, (E), 20: 31205
proton reactions (p,n) at 4.3 and 4.5 Mev, neutron polarization in, (T/E), 20: 32359
LITHIUM ISOTOPES Li-8
emission in meson (K⁻) reactions with emulsion nuclei at 5.0 Bev/c, (E), 20: 32469
energy levels of, intermediate coupling shell-model calculations for, 20: 32436
LITHIUM OXIDES
$BaO–Li_2O–O–Tc_2O_7$, compound formation in, 20: 31244
$Li_2O–O–SrO–Tc_2O_7$, compound formation in, 20: 31244
LITHIUM SULFATES
electric conductivity of natural and lithium-6-enriched, 20: 31255
LITHIUM SYSTEMS
Li–Te, thermodynamic properties, 20: 31959(R) (ANL-7175, pp 184-211)
LIVER
phosphate metabolism in rat, tracer study, 20: 30976
radiation injuries in mouse, protective effects of cystine, glutathione, and MEA against gamma, 20: 31141
radiodiagnosis of diseases of, use of technetium-99 and scintillation scanning for, 20: 31147 (CNEA-168)
sulfur content in human, estimation of, 20: 30982
LIVERWORTS
radiation effects on *Marchantia polymorpha*, effects of apical cell number on x, 20: 31065
radiation effects on inner and outer epidermises of *Mnium cuspidatum*, alpha and uv, 20: 31079
LOADED PLASTICS
fabrication of lead–plastic composites for shielding, 20: 32680
LOS ALAMOS AREA (N. MEX.)
radiation monitoring of, aerial natural, 20: 31396 (CEX-61.6.2)
LOS ALAMOS MOLTEN PLUTONIUM REACTOR EXPERIMENTS
development and research program of FRCTF, 20: 31679(R) (LA-3524)
fuel irradiation testing in, molten plutonium, 20: 32799 (LA-DC-7752)
fuels for, fast transients in molten plutonium, 20: 32797 (LA-DC-7748)
LOS ALAMOS OMEGA WEST REACTOR
fuel irradiation testing in, molten plutonium, 20: 32799 (LA-DC-7752)
LUBRICANTS
properties of liquid metals as high-temperature, 20: 31720(T) (AD-

629415)
LUMINESCENT DETECTORS
performance for long-term measurements of environmental radiation dose, 20: 31463
performance of glass, in γ- and x-ray dosimetry, 20: 31538
LUMINESCENT MATERIALS
use with radioactive isotope in self-luminous signs or patterns, 20: 31636(P)
LUNGS
fission product deposition in human, 20: 31142
radioinduced pulmonary fibrosis in dog, protective effects of L-triiodothyronine against gamma, 20: 31138
sulfur content in human, estimation of, 20: 30982
LUTETIUM ALLOYS
Gd–Lu, magnetic ordering in, gadolinium-content effects on g factor for, (E), 20: 32716
Lu–Zn, melting point of $LuZn_2$, 20: 31743
LUTETIUM ISOTOPES
preparation of self-supporting foils of, 20: 31696
LUTETIUM ISOTOPES Lu-175
magnetic field in iron, g-factor from internal, 20: 32472
neutron reactions (n,γ) at 10 kev to 3 Mev, cross sections for, (E), 20: 32370(R) (ANL-7175, pp 212-16)
LUTETIUM MOLYBDATES
preparation and crystal structure of, 20: 31740
LUTETIUM TUNGSTATES
preparation and crystal structure of, 20: 31740
LYMPH CELLS
radiation effects on, in blood and bone marrow in dogs, x, 20: 31086
LYMPH SYSTEM
fission product deposition in human, 20: 31142
radiation effects on dog, from iodine-131-labeled Ethiodol, 20: 31044
LYSOSOMES
effects of AET, glutathione, and serotonin mixture on morphology of, in stem cells in mice, 20: 30964

M

MACHINE TOOLS
control of, computer program for automatic, 20: 31478 (K-1670)
control of, computer program for automatic, 20: 31327 (K-1671)
measuring device for, single-transducer differential, 20: 31333 (Y-1541)
MAGNESIUM
grain boundaries in high-purity, small-angle tilt motion in, 20: 31714(R) (UCRL-16658, pp 99-103)
proton reactions at 0.05 to 2.9 Bev, induced activity data and cross sections for spallation, 20: 32549
solvent properties of liquid, for barium and lanthanum, 20: 31320 (UCRL-16108)
Gd–Mg, magnetic properties of, 20: 31758
MAGNESIUM ALLOYS
Al–Mg, stacking-fault energies of, 20: 31715(R) (UCRL-16658, pp 105-20)
Cd–Mg, mechanical properties of intermetallic compound single-crystal, 20: 31714(R) (UCRL-16658, pp 99-103)
Cu–Mg, solvent properties of, for iron, 20: 31314(R) (ANL-7175, pp 1-41)
Cu–Mg–Zn, liquid miscibility of, at high temperatures, 20: 31314(R) (ANL-7175, pp 1-41)
Li–Mg, creep of intermetallic compound single-crystal, 20: 31714(R) (UCRL-16658, pp 99-103)
Mg–Hg, superconducting transition temperature of intermetallic compounds in, 20: 31757
Mg–Pu, phase studies, 20: 31314(R) (ANL-7175, pp 1-41)
Mg–Pu–Zn, liquid miscibility of, at high temperatures, 20: 31314(R) (ANL-7175, pp 1-41)
Mg–Zn, solvent properties of, for chromium, iron, niobium, and zirconium, 20: 31314(R) (ANL-7175, pp 1-41)
MAGNESIUM CERIUM NITRATES
use for low-temperature thermometry with liquid helium-4, 20: 32336
MAGNESIUM CHLORIDES
effects on stress corrosion cracking of chromium–iron–nickel alloy, 20: 31676(R) (COO-1319-39)
Cu–$MgCl_2$, corrosive effects on steels, 20: 31314(R) (ANL-7175, pp 1-41)
Cu–$MgCl_2$–KCl–NaCl, corrosive effects on ferrous alloys, 20: 31314(R) (ANL-7175, pp 1-41)
MAGNESIUM FLUORIDES
hydrolysis of, at high temperatures, 20: 31719(R) (UCRL-16658, pp 155-69)
MAGNESIUM ISOTOPES Mg-24
alpha reactions (α,Be-7) at 35 to 65 Mev, angular-momentum effects in, (E), 20: 32507
energy levels from carbon-12 (O-16,α) reactions, parity and spin of, (E), 20: 32556
helium-3 reactions (He-3,t) at 37.8 to 40.1 Mev, aluminum-24 levels and mass from, (E), 20: 32473
MAGNESIUM ISOTOPES Mg-26
proton reactions (p,αγ) at 9.3 to 10.5 Mev, sodium-23 levels from, (E), 20: 32509
proton reactions (p,αγ) at 8.5 to 10.5 Mev, sodium-23 gamma multipole mixing ratios and spins from, (E), 20: 32567
MAGNESIUM NITRIDES
vaporization kinetics, 20: 31718(R) (UCRL-16658, pp 149-54)
MAGNESIUM OXIDES
creep of single-crystal, 20: 31719(R) (UCRL-16658, pp 155-69)
deformation of crystalline, strain-stress curves for, 20: 31719(R) (UCRL-16658, pp 155-69)
dislocation dipoles in crystalline, mechanisms of, 20: 31713(R) (UCRL-16658, pp 93-8)
evaporation at 1800 to 2300°K, rates of polycrystalline, 20: 31669
preparation of polycrystalline, 20: 31719(R) (UCRL-16658, pp 155-69)
radioinduced color centers in, symmetry of neutron, (E), 20: 32717
radioinduced transmutations in, calculation of gas volume from neutron, 20: 31799
sintering properties of, effects of hafnia additions on, 20: 31669
strength of hot-pressed, effects of process variables on, 20: 31669
Al_2O_3–BeO–MgO, properties of molten, for fuel matrix for homogeneous 20: 31726
Al_2O_3–MgO, grain boundary precipitation in, 20: 31738
BeO–MgO–ZrO_2, properties of molten, for fuel matrix for homogeneous thermal nuclear reactors, 20: 31726
CaO–MgO, diffusion in, 20: 31719(R) (UCRL-16658, pp 155-69)
CaO–MgO, grain boundary precipitation in, 20: 31738
MgO–ZrO_2, grain boundary precipitation in, 20: 31738
MAGNESIUM SYSTEMS
Cd–Mg–UCL_4–Zn, corrosive effects of, on stainless steel at 650°C, 20: 31314(R) (ANL-7175, pp 1-41)
MAGNET COILS
development for ultrahigh fields, 20: 32337
use as measuring element in fast high-current gas discharges, 20: 32571 (IPP-1/2)
MAGNETIC FIELDS
calculation for pulsed controlled-thermonuclear fusion experiments, 20: 32596
charged particle motion in simple force-free, (T), 20: 31812
charged-particle motion in static, first order correction to magnetic moment for, (T), 20: 32669
charged-particle trapping in, method for, 20: 32642(P)
detection and measurenets of interplanetary, (E), 20: 31883
effects of minimum, on plasma stability, (T), 20: 32623
effects on gravitational collapse of interstellar gas cloud, 20: 31862
effects on h-f discharge plasma, (E), 20: 32634
effects on high-energy galactic cosmic radiation, (E), 20: 31884
line-of-force reconnection for geo- and interplanetary, mechanism for, 20: 32277
plasma diffusion across, relation to decay along field, (E/T), 20: 32647
plasma flow in aligned, equations for collisionless, 20: 32649
polarity distribution of interplanetary, variations in, 20: 31860
production of ultrahigh, methods for, 20: 32337
properties of interplanetary, (E), 20: 31887
stabilization using broadband EPR field sensor, 20: 31813
structure in solar photosphere, (E), 20: 31892
structure of solar, reconnection and annihilation in, (T), 20: 31895
trapping by niobium–tin superconducting hollow cylinders, temperature dependence of, (E), 20: 32316
use of pulsed, in superconductivity research, 20: 32312(R) (UCRL-16658, pp 133-43)
MAGNETIC MATERIALS
book: *Magnetism and Magnetic Materials*, 20: 32738
photon interactions with spin waves in, (T), 20: 32735
MAGNETIC MIRROR MACHINES
plasma diffusion in Q devices, end plate effects on, (T), 20: 32611
plasma electron and ion density distribution in, (T), 20: 32609
MAGNETIC MIRRORS
charged-particle losses in axisymmetric and multipolar, 20: 32545
charged-particle temporary capture in static, (T), 20: 32582
plasma containment by, first order correction to first adiabatic invariant for, (T), 20: 32669
MAGNETIC PROBES
analysis of induction coil, for fast high-current gas discharges, 20: 32571 (IPP-1/2)
MAGNETIC SEPARATORS
design of double-focusing for mass-number identification of product nuclei, 20: 31484
MAGNETISM
book: *Magnetism and Magnetic Materials*, 20: 32738
MAGNETOHYDRODYNAMIC CELLS

design, 20: 31979(P)
design and performance of self-excited, (E), 20: 31976
design for a-c current production, 20: 31978(P)
development, 20: 32633
development of closed-cycle MPD, 20: 31977
development of liquid-metal a-c, 20: 31973
development of MPD, nonequilibrium ionization studies for, 20: 31963
diagnostics and operation of closed-loop plasma, 20: 31975
efficiency of thermal cycle in, (T), 20: 31962
gas flows in, shock relations in nonaligned, (T), 20: 32118 (NYO-1480-29)
plasma acceleration in, analysis of Hall-current produced, (T), 20: 32573 (N-65-12780)

MAGNETOHYDRODYNAMICS
fluid flow in entrance region of flat channel with parabolic velocity, (T), 20: 32226
fluid motion influenced by Coriolis forces, calculation of Lorentz field strength for turbulent, (T), 20: 32235
gas flow in, book on radiative, 20: 32238
liquid flow in annular channel with porous walls, axial and radial pressure variations for steady, (T), 20: 32222
liquid flow in channel with porous walls, steady, (T), 20: 32221
plasma flow in, nonstationary axisymmetric, (T), 20: 32231
Reynold's number in, calculation of, 20: 32700
shock propagation in argon–hydrogen mixtures, (E), 20: 32217 (N-65-33713)
theory for magnetospheric boundary stability, validity of, 20: 32254

MAGNETOMETERS
design for heterogeneous fields, 20: 31487

MAGNETOSPHERE
charged-particle motion in, trapped, (T), 20: 32279
electric field in, theory of, 20: 32287
electron and proton energy spectra in tail of, 20: 32252
electron and proton flux distribution in, determination of, 20: 32674 (NP-15697(Vol.3))
electron density distribution in, measurement using hydromagnetic whistlers, 20: 32290
electron scattering in outer, effects of electrostatic plasma oscillations on, 20: 32262
geomagnetic storm effects on tail of, 20: 32253
magnetic field at magnetopause, (E), 20: 32281
magnetic field line reconnection in, mechanism for geo- and interplanetary, 20: 32277
solar wind interactions with, fluid dynamics of, (T), 20: 32275
solar wind interactions with, particle aspects of, (T), 20: 32276
solar wind interactions with, shock wave from, (E/T), 20: 32281
solar wind interactions with, simulation of, 20: 32284
solar wind interaction with, (E), 20: 32286
stability of boundary of, validity of hydromagnetic approach to determining, 20: 32254
structure of lunar, (T), 20: 31899
structure of, linear stability in, (T), 20: 32278
structure of, Newtonian theory for, 20: 32282
tail of, length and structure of, 20: 32258
transition zone of, particle flux in, (E), 20: 32280

MAGNETS
properties of superconducting quadrupole, for lens systems, 20: 31815 (BNL-10144)

MAIZE
radiation effects on mutations of, x, 20: 31109
radiation effects on water content of leaves of, γ, 20: 31110
radiation effects on development of, γ, 20: 31113
radiation effects on seeds of, genetic fast-neutrons and x, 20: 31092
reproduction of, tracer studies of effects of fertilizers on, 20: 31109

MALEIC ACID
determination by xenon trioxide oxidation, titrimetric, 20: 31196

MALEIMIDE, *N*-ETHYL-
radiosensitivity effects on HeLa cells in culture, x, 20: 31130
radiosensitivity effects on *Thiobacillus thiooxidans*, x, 20: 31139

MALIC ACID
determination by xenon trioxide oxidation, titrimetric, 20: 31196

MALONIC ACID
determination by xenon trioxide oxidation, titrimetric, 20: 31196

MALTOSE
radiolysis of aqueous solutions of, acid formation in, 20: 31304

MAMMALS
radiation dose to, from internally deposited radioisotopes, computer calculation of, 20: 31441 (BNWL-SA-40)
radiation injury and repair in tissues of, 20: 31045

MAMMARY GLAND
radiotherapy of carcinomas of, using yttrium-90, 20: 31153

MAN
calcium metabolism by, tracer studies of effects of thyroid disorders on, 20: 31142
cesium-132 distribution and excretion, 20: 30988
cesium-137 and strontium-90 contents of bones and tissues in, in Finland, 20: 31142
cesium-137 content in caribou and reindeer, effects of diet on, 20: 31442 (BNWL-SA-661)
cesium-137 content in Finnish Lapps, 1966, 20: 31444 (CONF-660405-15)
cesium-137 distribution in, 20: 31142
diiodotyrosine and triiodothyronine metabolism by, tracer studies of, 20: 30965
excretion of urine by, use of creatinine as index of rate of, 20: 30983
fission product deposition in lungs and pulmonary lymph nodes of, 20: 31142
hydrogen content in, neutron capture measurement of, 20: 30993
phosphorus-32 uptake from Columbia River fish, 20: 30969 (BNWL-SA-45)
polonium-210 content in urine of normal, 20: 31187
potassium content in Finnish Lapps, 1966, 20: 31444 (CONF-660405-15)
radiation effects on gonadal and gonadotropic hormones in, 20: 31034(R) (RLO-1780-7)
radiation effects on function and hormones in gonads of, 20: 31035(R) (RLO-1780-8)
radiation effects on tissue cultures from, protective effects of AET, serotonin, and streptomycin against gamma, 20: 31121
radiation effects on proliferation of leukocytes of, in culture, x, 20: 31067
radiation effects on live births among atomic bomb survivors, 20: 31091
radiation injuries to, from barium-140 deposited in aortic walls, chemical protection against, 20: 31142
radioactivity in, performance of sodium iodide counters for detecting, 20: 31443 (CONF-650673-1)
radioiodine uptake from milk by, method for predicting, 20: 30980
radioiodine uptake from milk by, use of counter measures in predicting, 20: 30981
radioisotope distribution and dose in, method for external measuring of, 20: 31158
radioisotope transfer mechanisms in placentas of, effects of inactive carriers on, 20: 31142
radiotherapy of hemangiomas in children, x radiation dose to gonads from, 20: 31156
radium and strontium-90 metabolism by, 20: 31142
strontium-90 content in, effects of diet on, 20: 31442 (BNWL-SA-661)
sulfur content in tissues in, estimation of, 20: 30982
thorium isotopic content in, 20: 30989
thyroid pathology and physiology in, 20: 31162
zinc-65 uptake from Columbia River fish, 20: 30969 (BNWL-SA-45)

MANGANESE
neutron capture by, average level widths of compound nucleus from, (E), 20: 32424
neutron inelastic scattering to 14 Mev, energy spectra of, (E), 20: 31566
proton reactions at 0.05 to 2.9 Bev, induced activity data and cross sections for spallation, (E/T), 20: 32549
sorption of trace amounts of, by glass, tracer studies of, 20: 31245

MANGANESE ALLOYS
Au–Mn, heat capacities of intermetallic compound in, at 0.14 to 1.18°K, 20: 32684(R) (UCRL-16658, pp 21-38)
Au–Mn, magnetic structure of, neutron diffraction studies of effects of pressure on, 20: 31756
Cu–Mn, heat capacities at <0.15°K, 20: 32684(R) (UCRL-16658, pp 21-38)

MANGANESE ALUMINATES
neutron magnetic inelastic scattering by, filter-cutoff method for, 20: 32706

MANGANESE FLUORIDES
neutron magnetic inelastic scattering by, filter-cutoff method for, 20: 32706

MANGANESE ISOTOPES
distribution and natural carriers of, in sea water, 20: 31422

MANGANESE ISOTOPES Mn-52
beta decay of, matrix elements from β-γ correlations from, (E), 20: 32506
production in proton reactions with iron at 400 Mev, (T), 20: 32560

MANGANESE ISOTOPES Mn-53
energy levels from proton reactions (p,γ) with chromium-52 at 1.36 to 2.26 Mev, (E), 20: 32446

MANGANESE ISOTOPES Mn-54
production in proton reactions with iron at 400 Mev, (T), 20: 32560

MARITIME REACTORS
development and economics of, review of, 20: 32854

MASERS (OPTICAL)
beam reactions on beryllium surfaces, momentum transfer by giant-pulsed, (E), 20: 31810
beam reactions on carbon surfaces, momentum transfer by giant-pulsed, (E), 20: 31810

beam reactions on aluminum surfaces, momentum transfer by giant-pulsed, (E), 20: 31810
beam reactions on zinc surfaces, momentum transfer by giant-pulsed, (E), 20: 31810
beam reactions on silver surfaces, momentum transfer by giant-pulsed, (E), 20: 31810
beam reactions on tungsten surfaces, momentum transfer by giant-pulsed, (E), 20: 31810
beam reactions with argon gas at low pressure, ionization in, (E), 20: 32665
beam reactions with gases and solids, plasma production by, 20: 32666
crystals for, preparation of europium–β-diketone chelate, 20: 31232
intensity of discharge in air, space-time distribution of, · 20: 32224
mirror coatings for, effects of nitrobenzene immersion on damage resistance of dielectric, (E), 20: 31787
pumping of, using nuclear radiation, 20: 32740
use for argon arc plasma diagnostics, (E), 20: 32599
use for plasma diagnostics, 20: 32598
use for theta-pinch plasma diagnostics, 20: 32621

MASS SPECTROGRAPHY
background effects in spark-source, reduction of, 20: 31203
ion source for analysis of low-vapor-pressure materials by, 20: 31204
methods for analysis of solids by, review of, 20: 31201
techniques, theory, and uses of field ion, review on, 20: 31199
theory and uses of, conference on, 20: 31197
use for isotope analysis, ion production technique in, 20: 31207
use in isotope abundance measurements, review of, · 20: 31399
use of spark-source, for quantitative analysis, 20: 31202
use of, in study of composition and thermodynamic properties of non-stoichiometric compounds, 20: 31723

MASS SPECTROMETERS
design and operation of electron-bombardment, 20: 31488
design and performance of tandem, for isotopic analysis, 20: 31206
design and performance of sector-type double-focusing, 20: 31208
design and performance of electrostatic time-of-flight, 20: 31209
design and performance of low-resolution, 20: 31169 (D-1-82-0508)
design of alpha-particle ionization, 20: 31270
developments in, since 1926, 20: 31808
magnetic analyzers of, calculations for, 20: 31484
performance of ultrahigh vacuum, under high argon pressures, 20: 31390
performance of, using razor blades as field ionization sources, 20: 31198
use in detection of molecular beams, 20: 31492
use in high-energy sputtering studies, 20: 31905
use in lithium isotope abundance measurements, 20: 31205
use of, in study of atomic impact phenomena on metal surfaces, 20: 31907
use of, in study of ion–molecule reactions, 20: 31224

MASS TRANSFER
in boundary-layer flows, Blasius series for, 20: 31220(R) (UCRL-16658, pp 39-72)

MATERIALS TESTING
equipment for experiments on in-reactor mechanical properties, 20: 31785 (ORNL-P-2162)
methods for, development of nondestructive, 20: 31670
radiation protection of personnel in gamma and x-ray defectoscopy, evaluation of dosimeters for, · 20: 31464

MATHEMATICS
functions in, computer programs for special, 20: 31646 (AECL-1744)
functions in, computer programs for special, 20: 31647 (AECL-1744 (Pt.A)(ADD.1))
functions of, approximate reconstruction of one-dimensional from its moments, · 20: 31658 (NAA-SR-Memo-11653)
groups in, physical state vector-space representations of noncompact, 20: 31663
Lie groups in, structure of Clebsch-Gordan series for semisimple, 20: 32158
research programs on, 20: 31165(R) (HMI-B-46)

MATTER
alpha clustering in nuclear, (T), 20: 32542

MEATS
radiation effects on heme proteins in, 20: 30999(R) (UCB-34P95-7)
radiation effects on amino acid content of, γ, 20: 31630
radiopreservation of, use of low temperatures in, 20: 31634

MECHANICS
variational principle for quantum and classical, unified, · 20: 32302

MEDICINE
radioisotopes in, survey of, 20: 31152

MEIOSIS
effects of heavy water and hydrostatic pressure on, in starfish oocytes, 20: 30986

MERCAPTO GROUP
effects on DNA synthesis in mouse bone marrow and intestinal epithelium, 20: 31125

MERCHANT VESSELS
reactor development and economics for, review of, 20: 32854

MERCURY
corrosive effects on titanium at 538°C, effects of additives on, 20: 31669
determination in conductive tissue of beef heart, activation, 20: 31176
determination in human heart tissue, activation, 20: 31175
determination of, in radiosensitizers in tissues, neutron activation, 20: 31172 (SGAE-BL-17/1966)
electric conductivity below superconducting transition, temperature effects on surface, (E), 20: 32343
performance in electron-bombardment ion thrustors for space propulsion, durability tests of, 20: 31374
proton reactions at 0.05 to 2.9 Bev, induced activity data and cross sections for spallation, (E/T), 20: 32549
radiative lifetime of excited electronic states in, 20: 31219(R) (UCRL-16658, pp 11-20)
thermodynamic properties of liquid, Prandtl number at 0 to 700°C for, 20: 31724

MERCURY, ACETOXYPHENYL-
radiosensitivity effects of, use of activation analysis for determining mechanism of, 20: 31172 (SGAE-BL-17/1966)

MERCURY ALLOYS
Ba–Hg, critical temperatures of intermetallic compounds in, 20: 31757
Ca–Hg, critical temperatures of intermetallic compounds in, 20: 31757
Hg–rare earth, crystal structure of, CsCl-type intermediate phases in, 20: 31737
Li–Hg, solubility of intermetallic compound in, in fused lithium halides, 20: 31959(R) (ANL-7175, pp 184-211)
Mg–Hg, superconducting transition temperature of intermetallic compounds in, 20: 31757

MERCURY IONS
effects on radioinduced free radical formation in proteins, 20: 31003

MERCURY ISOTOPES
isotope shifts of neutron-deficient, (E), 20: 32517

MERCURY ISOTOPES Hg-192
hyperfine structure and isotope shift of, 20: 32517

MERCURY ISOTOPES Hg-193
hyperfine structure and isotope shift, (E), 20: 32517
hyperfine structure and isotope shift of isomeric, (E), 20: 32517

MERCURY ISOTOPES Hg-197
use for diagnosis of kidney diseases, 20: 31148 (CNEA-170)

MERCURY ISOTOPES Hg-203
use for diagnosis of kidney diseases, 20: 31148 (CNEA-170)

MESIC ATOMS
energy level fluorescence yields of, 20: 31936
x-ray intensity ratios from bismuth and lead μ, (T), 20: 31945

MESON PAIRS
production of μ, in electron-positron annihilation at high energies, (T), 20: 32070

MESONS
coupling of pseudoscalar SU(3) octet, (T), 20: 32063
decay of, unitary symmetry for $\Delta S = -\Delta Q$ leptonic, · 20: 32184
interactions of pseudoscalar, SU(3) octet-octet, 20: 32011
interactions of pseudoscalar with pseudovector, S-matrix elements in neutral theory for, 20: 32168
interactions with baryons, experimental status of baryon-exchange, 20: 32027
interactions with spin-½ baryons in relativistic formulation of SU(6), 20: 32116
interactions with baryons, U(3) × U(3) for amplitudes of collinear, 20: 32131
interactions with baryons, Dashen-Frautschi method for parity-conserving coupling, 20: 32138
interactions with baryons, bootstrap of 70-plet of SU(6) for, 20: 32151
interactions with baryon-antibaryon pairs, N/D method for multi-channel, 20: 32181
mass breaking in SU(3) symmetry in strong-coupling theory, 20: 32128
mass formulas for pseudoscalar, in pole approximation in SU(3), 20: 32129
mass formulas for vector, model for, 20: 32130
mass spectrum of, · 20: 32203
model for, bound states of quark-antiquark system in, 20: 32147
model of, double octet, 20: 32084
properties of 2^+, · 20: 32205
structure of, 20: 32082
theory for vector, currents and sum rules in, 20: 32125

MESONS, RESONANCE
classification of positive-parity, in SU(6), 20: 32148
decay of K*, (T), 20: 32045
decay of K*, current-algebra prediction of SU(3) violation in, 20: 32035
decays of, predictions of static quark model on, 20: 32061

lifetime of, Heisenberg uncertainty principle for determining, 20: 31910
parity and spin of A_2 (1300), 20: 32064
production of K*, in meson (K^-)-proton interactions at 1.455 Bev/c, (E), 20: 31987 (NP-16097)
production of K*(891), in meson (π^+) and (π^-) interactions with protons at 4 Bev/c, (E), 20: 32029
production of neutral A_2 (1300) in deuteron-meson (π^+) interactions at 3.65 Bev/c, (E), 20: 32064
research on, status of, 20: 32089

MESONS (η)
decay of, branching ratios for, 20: 32055
decay spectra of, 3π, 20: 32010

MESONS (η^0)
decay rates of, equal-time commutators for 3π, 20: 32037

MESONS (K)
decay of, neutrino interactions in, (E), 20: 31986 (NEVIS-148)
decay spectra of, 3π, 20: 32010
interactions with nucleons at low energies, N/D methods for s-wave, 20: 32024
separation from proton beams in waveguides, 20: 31841

MESONS (K^-)
interactions with protons at 1.455 Bev/c, K* resonance production in, (E), 20: 31987 (NP-16097)
interactions with protons at 1.05 to 1.7 Bev/c, hyperon (Ξ^0) properties from, (E/T), 20: 31988 (UCRL-11510)
interactions with protons at 1.2 to 2.7 Bev/c, cross sections for, (E/T), 20: 31990 (UCRL-16648)
interactions with protons, decay angular correlation for Y_1^{*-} from, (T), 20: 32052
interactions with protons at high energies, M(12) symmetry for, 20: 32079
interactions with protons at 1.22 to 1.70 Bev/c, $Y^*(J = 3/2)$ production in, (E/T), 20: 32068
interactions with protons, experimental status of baryon-exchange, 20: 32027
interactions with protons $Y_1^*(1385)$ and $Y_0^*(1660)$ production in, (E/T), 20: 32034
interactions with neutrons at 0.920 to 1.120 Bev/c, Σ-η resonances from, (E), 20: 32103
reactions with emulsion nuclei at 1.5 Bev/c, hyperfragment production and mesic decay from, (E), 20: 32491
reactions with emulsion nuclei at 5.0 Bev/c, lithium-8 emission in, (E), 20: 32469

MESONS (K^0)
decay of K_2^0, test of CP violation in, 20: 32060
decay of, CP noninvariance in 2π, 20: 31982 (AD-634703)
decay of, leptonic, (E), 20: 31991 (UCRL-16771)
decay of, partially conserved currents and CP violation for, (T), 20: 32021
decay rate of K_1^0, 2π, (T), 20: 32039
interactions of K_2^0, test of CP violation in, 20: 32060
mass difference of K_1^0 and K_2^0 in S-matrix theory, 20: 32025
mass matrix of K^0–$\bar{K}^0$ system, off-diagonal elements of, 20: 31982 (AD-634703)

MESONS ($\bar{K}^0$)
mass matrix of K^0–$\bar{K}^0$ system, off-diagonal elements of, 20: 31982 (AD-634703)

MESONS (K^+)
decay branching ratios, (E), 20: 32043
decay of, current-current interaction model for 2π, 20: 32075
interactions with deuterons and protons at 0.9 and 2.4 Bev/c, total cross sections for, (E), 20: 32067

MESONS (K_{e3}^+)
decay branching ratio, (E), 20: 32043

MESONS ($K_{\mu 3}^+$)
decay branching ratio, (E), 20: 32043

MESONS ($K_{\pi 2}^+$)
decay branching ratio, (E), 20: 32043

MESONS (μ)
interactions with electrons, universality in, (E/T), 20: 31986 (NEVIS-148)
interactions with deuterons, detection of $|\Delta I| = 0$ weak nuclear force from elastic, 20: 32049
magnetic moment of, NMR equipment for measuring, 20: 31817 (CERN-66-15)
production and polarization from neutrino quasielastic scattering by nuclei, 20: 32468
production of pairs of, in electron-positron annihilation at high energies, (T), 20: 32070

MESONS (μ^-)
capture by bismuth and lead, x-ray intensity ratios from, (T), 20: 31945

MESONS (μ^+)
decay of, radiative, (E/T), 20: 32104

MESONS (ω)
decay of, mixing angles for, 20: 32107 (IC-66/48)
decay rate, (T), 20: 32045
photoproduction on nucleons, analysis of, (T), 20: 31984 (IC-66/54)

MESONS (ϕ)
decay of, mixing angles for, 20: 32107 (IC-66/48)
decay rate, (T), 20: 32045

MESONS (π)
absorption by nuclei up to 800 Mev, cross sections for, (T), 20: 32078
emission in $_{\Lambda}H^4$ and $_{\Lambda}He^4$ decay, final-state interactions in, 20: 32477
exchange in nucleon-nucleon interactions, correlation effects in, (T), 20: 32073
interactions with mesons (π), sum rules for, (T), 20: 31999
interactions with mesons (π), meson (ρ) and photon exchange in inelastic, (T), 20: 32011
interactions with hyperons (Λ), partially conserved axial-vector current hypothesis for, 20: 32013
interactions with nucleons, inelastic unitarity in eigenstates of total angular momentum for, 20: 32014
interactions with protons, absorptive correction to peripheral model for, 20: 32022
interactions with nucleons, boundary condition model for P_{33} resonance in, 20: 32023
interactions with nucleons at high energies, forward dispersion relations for, 20: 32026
interactions with nucleons, asymptotic behavior of amplitudes for elastic, (T), 20: 32032
interactions with protons at high energies, amplitudes for large-angle elastic, 20: 32086
interactions with nucleons, amplitudes for N_{11}^* and N_{13}^* production in, (T), 20: 32091
interactions with nucleons, Mandelstam representation and elastic unitarity for amplitudes of, 20: 32095
kinematics in spark chambers, use of multiple scattering and secondary sparks in determining, (E), 20: 31570
photoproduction of, dispersion relations and $\gamma p\pi$ coupling from, (T), 20: 31996
photoproduction of, determination of $\gamma\pi\omega$ coupling constant from, 20: 32077
production in proton-proton interactions at 24 Bev/c, multiple, (E), 20: 32017

MESONS (π^-)
interactions with protons at 1035 to 1170 Mev/c, meson (K^0) production in, (E), 20: 31991 (UCRL-16771)
interactions with protons, experimental status of baryon-exchange, 20: 32027
interactions with protons at 4 Bev/c, cross sections for strange-particle production in, (E), 20: 32029
interactions with protons at high energies, amplitude and nucleon recoil effects on, (T), 20: 32072
interactions with protons at high energies, M(12) symmetry for, 20: 32079
interactions with protons at 1.7 to 2.5 Bev/c, differential cross sections and polarization in elastic, (T), 20: 32087
photoproduction on protons at 0.9 to 1.3 Bev, (E/T), 20: 31983 (CALT-68-71)
reactions with emulsion nuclei at 300 Bev, $_{\Lambda}B^{12}$ production in, (E), 20: 32412

MESONS (π^0)
photoproduction on protons, C and T violation in, (T), 20: 32074
photoproduction on deuterons, cross section for elastic, (T), 20: 32041
photoproduction on protons at 250 to 360 Mev, recoil-proton polarization from, (E), 20: 32096
photoproduction on protons at 360 Mev, recoil-proton polarization from, (E), 20: 32097
photoproduction on protons at 600 to 1000 Mev, cross sections for, (E), 20: 32051
production in electron-proton interactions at 593 Mev, cross section for, (E/T), 20: 32038

MESONS (π^+)
interactions with protons at 4 Bev/c, cross sections for strange-particle production in, (E), 20: 32029
interactions with protons at high energies, amplitude and nucleon recoil effects on, (T), 20: 32072
interactions with protons at 38 to 307 Mev, resonance formulas for N* (1236) from, (T), 20: 32100
interactions with deuterons at 3.65 Bev/c, A_2 (1300) production and properties from, (E), 20: 32064

MESONS (ρ)
decay of, current-algebra prediction of SU(3) violation in 2π, 20: 32035
decay rate, (T), 20: 32045
exchange in antiproton-proton and proton-proton interactions, (T),

20: 32065
exchange in meson (π)-meson (π) elastic interactions, (T), 20: 32011
mass splitting of, electromagnetic, (T), 20: 32011
photoproduction on nucleons, analysis of, (T), 20: 31984 (IC-66/54)

METABOLISM CAGES
design for animal movement and position monitoring in, 20: 30960(R) (BNWL-235-4, pp 22-5)

METALS
analysis by spark-source mass spectrometry, 20: 31202
bonding to graphite, performance of gold–molybdenum–nickel alloy for, 20: 31683(R) (ORNL-3936, pp 95-121)
cesium ionization on surfaces of porous refractory, 20: 31776
corrosion of, method for measuring intensity of, 20: 31682 (NP-16003)
crystal structure of, electron irradiation experiments at low temperatures for determining, 20: 32319
diffusion of liquid, 20: 31166(R) (UCRL-16658, pp 89-92)
dislocations in fcc and hcp, constriction energy of dissociated, 20: 31714(R) (UCRL-16658, pp 99-103)
dissolution of, methods for high-rate anodic, 20: 31220(R) (UCRL-16658, pp 39-72)
effects of liquid, on reactor building materials, 20: 31682 (NP-16003)
electron energy levels in, exchanged-coupled to localized spin, 20: 32085
electron tunneling conductance in junctions of superconductors and normal, zero-bias anomalies in, 20: 32714
electronic bonding strength theory for, 20: 31219(R) (UCRL-16658, pp 11-20)
ion beam reactions with, secondary electron emission from, (E), 20: 31645(R) (AD-627094)
ion reactions with, coefficient of surface ionization of secondary ions from, 20: 31913
plastic deformation of fcc, cross-slip mechanisms in, 20: 31713(R) (UCRL-16658, pp 93-8)
properties of liquid, as high-temperature lubricants, 20: 31720(T) (AD-629415)
radiative lifetimes of excited states in gaseous, 20: 31219(R) (UCRL-16658, pp 11-20)
reactions of, with glass at interfaces, mechanisms of, 20: 31719(R) (UCRL-16658, pp 155-69)
solvent properties of, for gases, high-temperature technique for determining terminal, 20: 31250
stability of work-hardened fcc, parameters of, 20: 31713(R) (UCRL-16658, pp 93-8)
surface physics of, use of field emission microscopy in study of, 20: 32742
use of liquid, in thermionic cells, 20: 31969
NH_3–metal, kinetics and structure of solutions of, 20: 31218(R) (UCRL-16658, pp 1-9)

METEORITES
krypton isotope abundances in, fission, neutron capture and spallation anomalies in, 20: 31875
rare gas abundance and isotopic composition of, 20: 31876
rare gas content in silicates from Estherville Mesosiderite, heavy, 20: 31859
silver content in Canyon Diablo, isotopic composition of, (E), 20: 31861
xenon isotope abundances in, fission, neutron capture, and spallation anomalies in, 20: 31875

METERS
design of radiometric quality, for hydrogen, 20: 32347

METHACRYLIC ACID, METHYL ESTER
use of dyed, for dosimetry of vacuum envelopes in Nimrod proton synchrotron, 20: 31832

METHANE
hydrogen ion reaction at 20 to 120 kev, ionization cross sections for, 20: 31909
ionization of, by electrons at 0.6 to 20 kev, cross sections for, (E/T), 20: 31906
reactions of, with ions, atom and charge transfer in, 20: 31224

METHANE, TRICHLOROFLUORO-
flow in vertical, rectangular conduit, two-phase, 20: 31340 (ANL-7093)

METHANESULFONIC ACID, TETRAMETHYLENE ESTER
effects on neutron-induced chromosome aberrations in barley and *Vicia faba* seeds, 20: 31136

METHANOL
radioinduced carboxylation of, in aqueous solutions, yields of glycolic acid from gamma, 20: 31278

METHYL SULFOXIDE
radiosensitivity effects of, relation between cellular anoxia and, 20: 31122
solvent properties, 20: 31220(R) (UCRL-16658, pp 39-72)

MICE
blood picture in, effects of age and sex on, 20: 30970 (COO-1170-5)
effects of AET, glutathione, and serotonin mixture on lysosome morphology in stem cells in, 20: 30964
effects of colchicine and x radiation on intestinal mucosa in, comparison of, 20: 31082
effects of ingested deuterium on, pathological, 20: 30975
effects of sulfhydryl compounds on DNA synthesis in, tracer study, 20: 31125
radiation effects on, genetic x, 20: 31048
radiation effects from polonium-210 on spermatogenesis in testes of, 20: 31063
radiation effects on susceptibility of newborn, to congenital anomalies, x, 20: 31066
radiation effects on, RBE for 15-Mev x, 20: 31072
radiation effects on tumor beds in, x, 20: 31073
radiation effects on growth and development of, continuous low-dose gamma, 20: 31074
radiation effects on fine structure of Paneth cells in, x, 20: 31083
radiation effects on survival of synchronized L cells in, uv, 20: 31084
radiation effects on DNA synthesis in uterine epithelium of, x, 20: 31088
radiation effects on, γ and proton, 20: 31100
radiation effects on, γ and proton, 20: 31102
radiation effects on oxidative enzyme systems in gonads of, γ and x, 20: 31090
radiation injuries to tissues in, effects of bone marrow therapy on, 20: 31108
radiation injuries of, use of cadaver bone marrow for treatment of, 20: 31135
radiation injuries in liver and tumor tissues in, protective effects of cystine, glutathione, and MEA against gamma, 20: 31141
radioinduced leukemia in, effects of injected parental bone marrow or spleen cells on, 20: 31127
radiosensitivity of intestinal crypt cells of, x, 20: 31128
radiosensitivity of bone marrow cells in, 20: 31071
radiotherapy of cancer in, effects of chemical radiation protectors on x-ray, 20: 31142
radiotherapy of spleen and thymus of, synergistic effects of Mitomycin C and Endoxan in, 20: 31131
rare earth toxicity in, 20: 30970 (COO-1170-5)

MICROANALYSIS
method of, using secondary ion emission, 20: 31200

MICROWAVE EQUIPMENT
development of, using superconducting point contacts, 20: 31482
particle dynamics in waveguide separators, 20: 31841
performance of short-circuited waveguide as EPR sensor for stabilizing magnetic fields, 20: 31813
waveguide design for traveling-field linear accelerator, 20: 31851(P)

MICROWAVE SPECTROMETERS
design with amplitude modulation, methods for, 20: 31490

MICROWAVES
detection and measurement of, selective receiver for, 20: 32626
effects on critical supercurrents in constricted tin films, (E), 20: 32328
emission by superconducting bridges, 20: 31482
propagation in pure air plasma, 20: 32667
scattering by unstable electron oscillations in plasma, incoherent, (E), 20: 32622

MILK
cesium-137 content in Norwegian, 1960 through 1964, 20: 31465
iodine-131 content in French, 1961 to 1963, 20: 31456
radioactivity from cesium-137 and strontium-90 in New Zealand, 1965, 20: 31446(R) (NP-16015)
radioiodine uptake by man from, method for predicting, 20: 30980
radioiodine uptake by man from, use of counter measures in predicting, 20: 30981
strontium-90 content in Norwegian, 1960-64, 20: 31465

MINERALS
prospecting for, neutron activation methods for, 20: 31434

MINING
radioactive pollution control in uranium, 20: 31457

MIRRORS
radiation effects on coatings of dielectric, protective effects of nitrobenzene immersion on pulsed laser, 20: 31787

MITOCHONDRIA
radiation effects on content in pear tissues, γ, 20: 31633
respiration in rat liver and spleen, effects of cystamine on, 20: 30984

MITOMYCINS
effect on radiotherapy of thymic and splenic tumors in mice, 20: 31131

MITOSIS
radiation effects on HeLa cell, gamma, 20: 31008

MOLECULAR BEAMS
detection of, by electron bombardment method, 20: 31492
detector for, design and operation of electron-bombardment, 20: 31488
uses of, in studies of high-temperature molecules, 20: 31219(R)

(UCRL-16658, pp 11-20)
MOLECULES
ground states of high-temperature, determination of, by molecular beam fluorescence, 20: 31219(R) (UCRL-16658, pp 11-20)
optical excitation of biological, 20: 30974
potential energy functions for, determination from spectral data, 20: 31949
spectra of linear triatomic, Renner effect in, 20: 31943
MOLTEN SALT REACTOR EXPERIMENT
component development for, 20: 32802(R) (ORNL-3936, pp 53-81)
control rod reactivity calculations for, xenon-135 effects on, 20: 32803(R) (ORNL-3936, pp 82-92)
coolant chemistry of, 20: 32804(R) (ORNL-3936, pp 122-71)
fuel analysis for, methods development for, 20: 32804(R) (ORNL-3936, pp 122-71)
materials corrosion testing for, 20: 31683(R) (ORNL-3936, pp 95-121)
operation and maintenance of, 20: 32801(R) (ORNL-3936, pp 7-52)
MOLYBDENUM
cesium ionization on surfaces of, 20: 31776
compatibility with cesium vapor at 1800°C, 20: 31669
determination in conductive tissue of beef heart, activation, 20: 31176
determination in human heart tissue, activation, 20: 31175
dislocation mechanisms of single-crystal, 20: 31714(R) (UCRL-16658, pp 99-103)
effects on grain size and transformations in alpha-uranium and uranium alloys at 720 to 800°C, 20: 31666
effects on microstructure of tungsten–thoria dispersion-hardened alloys, 20: 31781
effects on radioinduced swelling in uranium irradiated at 400 to 500°C, 20: 31666
grain boundary grooving in, mechanisms of, 20: 31672
hardness of, effects of aluminum, chromium, or nickel alloying additions on, 20: 31741
ion reactions at 2 to 15 kev, ejected electron energy distribution from argon and helium, (E), 20: 31939
oxidation by steam at 1100 to 1700°C, 20: 31669
preparation of beta-phase, 20: 31717(R) (UCRL-16658, pp 143-9)
preparation of high-purity, 20: 31741
properties of porous, for cesium ionization, 20: 31388
proton reactions at 0.05 to 2.9 Bev, induced activity data and cross sections for spallation, (E/T), 20: 32549
radiation effects on lattice parameter of, neutron, 20: 31669
solvent properties for carbon at high temperatures, 20: 31669
sorptive properties for krypton and xenon, 20: 31242
surface tension and solid surface energy of, effects of alloying additions of rhenium on, 20: 31773
Mo–Ti–Zr, stress-rupture at 2000°F of TZM, 20: 31669
MOLYBDENUM ALLOYS
Al–Cr–Fe–Mo–Ni–Ti, radiation effects on tensile properties of Nimonic PE16, thermal-neutron, 20: 31669
Au–Mo–Ni, performance for bonding graphite to metals, 20: 31683(R) (ORNL-3936, pp 95-121)
Cr–Fe–Mo–Ni–W, radiation effects on mechanical properties of Hastelloy X-280, fast-neutron, 20: 31669
Fe–Mo, strain-aging effects on, 20: 31716(R) (UCRL-16658, pp 121-32)
Mo–Nb, electronic structure of, at superconducting critical temperatures, 20: 31747
Mo–Nb–W–Zr, hardness of niobium-base, effects of composition on hot-, 20: 31669
Mo–Re, grain boundary grooving in, mechanisms of, 20: 31672
Mo–Re, properties of porous, for cesium ionization, 20: 31388
Mo–Re, surface tension and solid surface energy of, 20: 31773
Mo–Ta, properties of single-crystal, electric and mechanical, 20: 31715(R) (UCRL-16658, pp 105-20)
Mo–Ti–Zr, fatigue properties of TZM, at high temperatures, 20: 31710(R) (NASA-CR-54983)
Mo–U, radiation effects on stainless steel-clad fuel elements of, 20: 31666
MOLYBDENUM CARBIDES
fabrication by hot-pressing, 20: 31699
performance in focus electrodes in cesium-contact ion thrustors, 20: 31383
graphite–Mo_2C, fabrication and properties of hot-pressed composites of, 20: 31688 (NASA-CR-507)
MOLYBDENUM IONS
production of, for mass spectrometry, thermal techniques for, 20: 31226
MOLYBDENUM ISOTOPES Mo-92
proton reactions (p,p'γ) at 10 Mev, energy level structure from, (E), 20: 32471
MOLYBDENUM ISOTOPES Mo-98
neutron reactions (n,γ) at 10 kev to 3 Mev, cross sections for, (E), 20: 32370(R) (ANL-7175, pp 212-16)
MOLYBDENUM ISOTOPES Mo-99
determination in fission product mixtures for calculating uranium-235 abundance in uranium, 20: 31189
MOLYBDENUM OXIDES
growth of single crystals of, (E), 20: 32697
molecular shrinkage effects and vibration mean amplitudes for MoO_2 and MoO_3, (T), 20: 31233
MOLYBDENUM PHOSPHIDES
phase studies of, using mass spectrometry, 20: 31723
MOLYBDENUM SILICIDES
fabrication by slip casting, 20: 31697
oxidation at 450 to 650°C, 20: 31669
performance in focus electrodes in cesium-contact ion thrustors, 20: 31383
MOLYBDENUM STEEL
Co–Mo–Ni, tensile properties of strain-aged, 20: 31716(R) (UCRL-16658, pp 121-32)
MOLYBDENUM SYSTEMS
Al–C–Mo, superconductivity of Mo_3Al_2C in, 20: 32312(R) (UCRL-16658, pp 133-43)
C–Mo–Ti–Zr, fatigue properties of TZC, at high temperatures, 20: 31710(R) (NASA-CR-54983)
C–Mo–Zr, phase studies, 20: 31669
HfC–Mo, phase diagram, 20: 31729
Mo–Ni–ThO_2, development and properties of dispersion-strengthened, 20: 31669
Mo–Si–U, hot hardness and microstructure of, effects of quenching temperature on, 20: 31666
Mo–ZrB_2, sintering of, effects of composition on, 20: 31698
MONKEYS
proton depth-dose measurements in phantom, 20: 31467
proton dosimetry in *Macaca mulatta*, 20: 31096
radiation effects on blood pressure of *Macaca mulatta*, γ and proton, 20: 31104
radiation effects on enzyme activity in serum and tissues of *Macaca mulatta*, γ and proton, 20: 31105
radiation effects on spermatocytes of, pathological γ and x, 20: 31117
radiation effects on *Macaca mulatta*, pathological proton, 20: 31097
radiation effects on *Macaca mulatta*, pathological proton, 20: 31098
radiation effects on *Macaca mulatta*, pathological proton, 20: 31099
radiation effects on *Macaca mulatta*, pathological proton and x, 20: 31101
radiation effects on *Macaca mulatta*, pathological proton and x, 20: 31103
radiation effects on *Macaca mulatta*, proton, 20: 31106
radiation effects on embryo cell tissue cultures of, protective effects of serotonin and thiourea against x, 20: 31121
rare earth toxicity in, 20: 30970 (COO-1170-5)
MONTE CARLO METHOD
use for neutron fission coefficient calculations, 20: 32778
MOON
analysis of surface of, combination neutron technique for, 20: 31211
organic matter on, observability of indigenous, 20: 31854
solar wind interactions with, lunar magnetosphere from, (T), 20: 31899
wake of, structure of, (E), 20: 31900
MÖSSBAUER EFFECT
equipment for studying, electromagnetic velocity drive system for, 20: 31590
on iron-57 in stainless steel, effects of pressure on, 20: 32684(R) (UCRL-16658, pp 21-38)
MULTIPLICATION FACTOR
theory, 20: 32779
MUTATIONS
induced in *E. coli* by water-d_2 for phage resistance, 20: 31033(R) (NASA-CR-59196)
induced in *E. coli* by tritium decay, 20: 31033(R) (NASA-CR-59196)
radiation effects on rates of, at specific *Autosomal loci* in Drosophila, 20: 31108
radiation effects on Triticum, fast and fission neutron and gamma, 20: 31080
radioinduced in barley and rice seeds, γ and x, 20: 31050
radioinduced in Drosophila, x, 20: 31036(R) (SAN-529-3)
radioinduced in Drosophila, x, 20: 31047
radioinduced in Drosophila, x, 20: 31049
radioinduced in jute plants, γ, 20: 31027 (AECD/AG-14)
radioinduced in maize, fast-neutron and x, 20: 31092
radioinduced in mice, x, 20: 31048
radioinduced in Neurospora, uv and x, 20: 31012
radioinduced in oats, frequency of somatic, 20: 31078

N

NAGASAKI
radiation effects on live births among atomic bomb survivors in,

20: 31091
2-NAPHTHOL, 1-BROMO-
radiosensitivity effects of, use of activation analysis for determining mechanism of, 20: 31172 (SGAE-BL-17/1966)
2-NAPHTHOL, 6-BROMO-
radiosensitivity effects of, use of activation analysis for determining mechanism of, 20: 31172 (SGAE-BL-17/1966)
NASA RESEARCH REACTOR
experimental facilities of, maintenance and modification of cryogenic, 20: 32861 (N-66-12348)
NATURAL WATERS
tritium activity in, method for measurement of, 20: 31310
tritium content of, in Japan, 20: 31398(T) (NSJ-tr-49)
NEODYMIUM
ionization on rhenium and tungsten surfaces, effects of adsorbed oxygen on, 20: 31225
separation from molten fluoride salts, 20: 32804(R) (ORNL-3936, pp 122-71)
toxicity in laboratory animals, 20: 30970 (COO-1170-5)
NEODYMIUM ALLOYS
Nd–Zn, melting point of $NdZn_2$, 20: 31743
NEODYMIUM BROMIDES
molecular structure of gaseous, electron diffraction studies of, 20: 31222(T) (ANL-Trans-310)
NEODYMIUM CHLORIDES
molecular structure of gaseous, electron diffraction studies of, 20: 31222(T) (ANL-Trans-310)
NEODYMIUM FLUORIDES
energy levels in, coupling of negative hydrogen- and deuterium-ion localized modes to, (E), 20: 32709
molecular structure of gaseous, electron diffraction studies of, 20: 31222(T) (ANL-Trans-310)
NEODYMIUM IODIDES
molecular structure of gaseous, electron diffraction studies of, 20: 31222(T) (ANL-Trans-310)
NEODYMIUM ISOTOPES
preparation of self-supporting foils of, 20: 31696
NEODYMIUM MOLYBDATES
preparation and crystal structure of, 20: 31740
NEODYMIUM OXIDES
heat of formation on hot metal surfaces, 20: 31225
NEODYMIUM TUNGSTATES
preparation and crystal structure of, 20: 31740
NEON
cyclotron harmonic radiation from plasma of, in magnetic field, (E/T), 20: 32637
electron beam interactions with gas of, level inversion during excitation by monoenergetic, (E), 20: 31941
energy level transition probabilities of, data compilation on, 20: 31942
hydrogen ion reactions at 20 to 120 kev, ionization cross sections for, 20: 31909
ionization of, by electrons at 0.6 to 20 kev, cross sections for, (E/T), 20: 31906
positron annihilation in liquid, angular distribution of photons from, (E), 20: 32345
NEON IONS
electron reactions with, excitation cross sections for, (T), 20: 31929
reactions of, with molecules, atom and charge transfer in, 20: 31224
reactions with metal surfaces, secondary emission factors for, 20: 31926
sputtering on germanium (100) and (110) surfaces, temperature dependence of yields from, 20: 31915
NEON ISOTOPES
abundance in stone meteorites, relative, 20: 31876
NEON ISOTOPES Ne-17
energy levels of, low-lying negative parity, (T), 20: 32398
NEON ISOTOPES Ne-20
deuteron reactions (d,py) at 2.05 Mev, neon-21 levels from, (E), 20: 32476
reactions (Ne-20,xn) with erbium isotopes, alpha-active platinum isotopes from, (E), 20: 32458
NEON ISOTOPES Ne-21
energy levels from oxygen-18 (α,nγ) reactions at 4.43 and 5.5 Mev, (E), 20: 32427
energy levels from deuteron reactions (d,pγ) with neon-20 at 2.05 Mev, (E), 20: 32476
energy levels from alpha reactions (α,nγ) with oxygen-18 at 4.75 Mev, (E), 20: 32476
energy levels from alpha reactions (α,nγ) with oxygen-18 at 4.7 to 6.0 Mev, (E), 20: 32474
NEON SYSTEMS
H–Ne, liquid-vapor phase equilibria in, 20: 32242
NEPTUNIUM
oxidation-reduction reactions of, bibliography on kinetics of, 20: 31215 (LA-3507)
separation from fission products in acid-deficient nitrate system by solvent extraction using 4-methyl-2-pentanone, 20: 31319 (ISO-SA-10)
NEPTUNIUM CHLORIDES
complexes with dimethylacetamide, preparation and properties of, 20: 31235
NEPTUNIUM COMPLEXES
oxychloride, preparation and properties of, 20: 31235
NEPTUNIUM FLUORIDES
chemistry of, 20: 31315(R) (ANL-7175, pp 42-103)
NEPTUNIUM(VI) FLUORIDES
spectra of gaseous, absorption, 20: 31248
NEPTUNIUM ISOTOPES Np-237
energy levels from americium-241 decay, (E), 20: 32375 (ITEF-351)
production in power reactors, fuel cycle for, 20: 32837
NEPTUNIUM ISOTOPES Np-240
half life of isomeric, (E), 20: 32460
NEPTUNIUM OXYCHLORIDES
complexes with arsonium compounds and cesium, preparation and properties of, 20: 31235
NERVE CELLS
effects of radiation sickness on DNA, phosphatase, and RNA in cerebral, in rats, 20: 31010
NERVES
radiation effects on function and ultrastructure of isolated rat sympathetic ganglion, x, 20: 31055
NETHERLANDS
radiation processing of food in, review of, 20: 31628
NEUROSPORA
enzyme locational specificity in, genetic factors in, 20: 31012
radioinduced mutations of, uv and x, 20: 31012
NEUTRINOS
interactions with bound electrons, cross section for, (T), 20: 32005
interactions with neutrons and protons at very-high energies, cross sections for, (T), 20: 32036
interactions with nucleons, baryon resonance production in, 20: 32080
scattering by nuclei, transverse muon polarization from quasielastic, 20: 32468
transport in stellar gravitational collapse, relativistic theory for, 20: 32296
NEUTRON CAPTURE CROSS SECTIONS
measurement of, for reactor materials, (E), 20: 32370(R) (ANL-7175, pp 212-16)
NEUTRON CROSS SECTIONS
data requirements for nuclear power development, 20: 32839
tabulation for 14-Mev neutrons, 20: 32380 (SC-RR-66-229)
NEUTRON-DIFFRACTION ANALYSIS
method for single crystal- and powder-, time-of-flight, 20: 32701
NEUTRON MONOCHROMATORS
design of slow, 20: 31477 (CEA-R-2981)
design with surface coatings for neutron reflection suppression, 20: 32368(P)
NEUTRON SCATTERING CROSS SECTIONS
calculation of cold, in homonuclear diatomic liquids, 20: 32353
calculation of cold, in homonuclear diatomic liquids, 20: 32354
measurement by time-of-flight technique, computer programs for analysis of, 20: 32379 (ORNL-TM-1208)
NEUTRON SHIELDING
properties of iron–serpentine concretes for, 20: 32677
NEUTRON SOURCES
description of pulsed, using deuteron–tritium reactions, 20: 32358
design and performance of cold, 20: 32351
dose conversion factors for, in soft tissue, 20: 32355
dose conversion factors for americium–boron and americium–beryllium, 20: 32356
neutron yields from (radium + mesothorium)–beryllium, time dependence of, 20: 32352
performance of accelerators as pulsed, for nuclear engineering studies, 20: 32360
spectra from boron-9(d,n) reactions, 20: 31786(R) (ORO-2891-5)
use in analysis of remote surfaces, 20: 31211
use of pulsed, for aerospace research, 20: 32365
uses in determining direction of ground-water flow, 20: 31430
uses in equipment for moisture measurements, 20: 31627
NEUTRON SPECTROMETERS
control system for triple axis, programmed automatic, 20: 31543
design and operation of cold-neutron time-of-flight, 20: 31567
design and performance of time-of-flight, 20: 31566
performance of high-pressure helium-3 ionization, 20: 31573
NEUTRON SPECTROSCOPY
uses for studies of rotational behavior of ammonium ions in several salts, 20: 31241

NEUTRONS

absorption in uranium-fueled, heavy water-moderated, organic-cooled lattices, resonance, (T), 20: 32785
attenuation in lithium hydride-uranium shields, 20: 32672 (NAA-SR-Memo-11786)
book: *Slowing Down and Thermalization of Neutrons*, 20: 32361
buckling in thorium–uranium fueled beryllium oxide moderated exponential piles, 20: 32820
capture by hydrogen in man, estimation of total hydrogen content by, 20: 30993
capture by nuclei, average level widths of compound nucleus from, (E), 20: 32424
decay of geomagnetically trapped, spatial distribution of protons from, 20: 32266
decay of, SU(3) symmetry for leptonic, 20: 32176
detection and measurement of, design of stilbene scintillation counter for, 20: 31532
detection and measurement in reactors, instrument development for, 20: 31596
detection and measurement of, frequency response of ionization chambers for, 20: 31597
detection of, rem, dosimeter performance for, 20: 31514(R) (UCRL-14881)
detection of, techniques for, 20: 31606
diffusion theory for wave-type experiments on, 20: 32363
dose measurement in mixed gamma fields, instruments for, 20: 31505(R) (BNWL-235-4, pp 30-4)
dose-rate meter for, design of portable, 20: 31600
effects of 14-Mev, on *Escherichia coli*, relative biological efficiency in, 20: 31107
effects on chromium compounds, 20: 31297
effects on chromosome aberrations in barley and *Vicia faba* seeds, effects of Myleran on, 20: 31136
effects on crystal structure defects in gold, 20: 31788
effects on dimensional stability of graphite at 450 to 1200°C, 20: 31782 (BNWL-SA-67)
effects on dimensions of graphite, effects of chemical additions on, 20: 31667
effects on dimensions of sodium-saturated graphite, 20: 31667
effects on ductility of austenitic stainless steels and nickel alloys, 20: 31801
effects on impact properties of nickel steel, 20: 31669
effects on iron, interstitials from, 20: 31789
effects on lattice parameters of metals, 20: 31669
effects on magnesium oxide crystals, symmetry of color center from, (E), 20: 32717
effects on mechanical properties of hafnium control rods, 20: 31668
effects on physical properties of graphite and Hastelloy N, 20: 31683(R) (ORNL-3936, pp 95-121)
effects on recoil bromination of aromatic compounds, 20: 31296
effects on silicon semiconductors, transient annealing in, 20: 31613 (SC-DC-66-1443)
effects on structure of graphite, energy release at high temperatures from, 20: 31802
energy spectra and flux measurements of accelerator, methods for, 20: 31786(R) (ORO-2891-5)
energy states in local and nonlocal potentials, 20: 32566
energy states in lead-208, 20: 32566
flux distributions in time-dependent media, 20: 32357
flux measurements in reactor cores, method for absolute, 20: 32776
interactions with protons, cross sections for deuteron formation in, (T), 20: 32004
interactions with antiprotons at rest in deuterium annihilation, (E), 20: 32015
interactions with electrons, nucleon electromagnetic form factors for, (T), 20: 32033
interactions with neutrinos at very-high energies, cross sections for, (T), 20: 32036
interactions with protons, direct and charge-exchange, (T), 20: 32048
interactions with antiprotons, SU_{6W} predictions for, 20: 32056
interactions with antiprotons and protons, Regge-pole theory for charge-exchange, 20: 32069
interactions with mesons (K^-) at 0.920 to 1.120 Bev/c, $\Sigma^-\eta$ resonances from, (E), 20: 32103
kinetics in critical, nonmultiplying, and subcritical media, space-time, 20: 32784
kinetics in multiplying systems, unification of theory for, 20: 32779
kinetics in thorium-fueled heavy water reactors, calculation of, 20: 32774
mass relative to protons, model for electromagnetic, 20: 32057
moderation and multiplication in reactors, properties of media for, 20: 32776
photoproduction in beryllium-moderated reactors, calculational method for delayed, (T), 20: 32767 (UCRL-14720)
reactions (n,α) with aluminum-27 at 13.5 to 14.8 Mev, cross sections for, (E), 20: 32528
reactions (n,α), (n,$\alpha n'$), and (n,$n'\alpha$) with sodium-23 at 12.6 to 18.7 Mev, cross sections for, (E), 20: 32540
reactions (n,α) and (n,p) with silicon-28 at 13.95 and 14.6 Mev, angular and energy distributions from, (E), 20: 32431
reactions (n,α) with fluorine-19 at 4.7 Mev, angular and energy distributions from, (E), 20: 32434
reactions (n,α) in alumina and magnesia, calculation of gas volume from, 20: 31799
reactions (n,γ) with hydrogen, deuteron binding energy from, (E), 20: 32488
reactions (n,γ) with nuclei, method for calculating cross sections for, 20: 32374(R) (IITRI-578P25-15)
reactions (n,p) with iron-56 at 13.5 to 14.8 Mev, cross sections for, (E), 20: 32528
reactions with copper above 10 ev, chemical binding effects on total cross sections for, 20: 32392
reactions with even intermediate elements, level spacings from total cross sections for, (E/T), 20: 32389
reactions with gold and iodine at 24 Mev, Monte Carlo capture cross sections for, (T), 20: 32378 (NASA-TR-R-239)
reactions with metals at high energies, residual radioactivity from, 20: 31831
reactions with nuclei at 14 Mev, cross sections, Q-values, and sensitivities for, 20: 32380 (SC-RR-66-229)
reactions with promethium-147 and -148, total cross sections for, (E/T), 20: 32376 (KAPL-3090)
reactions with uranium-238, capture-to-fission ratios for, 20: 32391
scattering by carbon-12, polarization in elastic, (E/T), 20: 32359
scattering by carbon-12 at 14.1 Mev, level excitation from, (E), 20: 32408
scattering by chlorine-35 and -37 at 4 and 6 Mev, level parities and spins from inelastic, (E), 20: 32550
scattering by crystals, automatic data analysis of, 20: 32681 (BNL-10238)
scattering by ferromagnets in region of ferroacoustic resonance, cross sections for inelastic, (T), 20: 32722(T)
scattering by lead-208 at 0.715 to 1.761 Mev, resonances in, (E), 20: 32519
scattering by lithium-6 and -7 at 4.4 Mev, polarization in elastic, 20: 32433
scattering by manganese fluorides and manganese aluminates, magnetic inelastic, 20: 32706
scattering by potassium iodides, dispersion relation for normal-mode vibrations from inelastic, (E), 20: 32710
scattering by solids under pressure, apparatus for measurement of, 20: 31756
scattering by solids, spectroscopy for, 20: 32687
scattering by zirconium-90, zirconium-91 neutron single-particle levels from, (T), 20: 32552
scattering by 302°K water at 0.15 to 1.8 ev, differential cross sections for, (E/T), 20: 32350 (KAPL-M-6536)
shielding against, properties of concretes for, 20: 32679
slowing down of, analysis limitations for, (T), 20: 32363
transport in complex reactor geometries, computer programs for, 20: 32768 (UNC-5148)
transport in reflected multiplying slab, 20: 32782
transport in shields, P_3 method for flux calculation from, 20: 32673 (NAA-SR-Memo-11872)
transport theory for reactor, 20: 32366

NEUTRONS, COLD

scattering by materials, energy spectra from, (E), 20: 31567
source of, design and performance of, 20: 32351

NEUTRONS, FAST

diffusion in parallel-plate lattices, calculation of, 20: 32763 (AECL-2543)
dosimetry in gamma background, performance of boron trifluoride proportional detectors for, 20: 31561
dosimetry in mixed fields, properties of glasses for, 20: 31462
dosimetry in mixed fields, tissue-equivalent ionization chamber for in-phantom, 20: 31524
dosimetry of, using cesium-137 gamma spectrometry following thorium fission, 20: 31530
effects in graphite, effects of annealing on, 20: 31803
effects on animal cells in culture, effects of oxygen on biological, 20: 31123
effects on ductility of type 304 stainless steel, effects of carbon content and titanium additions on, 20: 31669
effects on growth and mutations in Triticum, 20: 31080
effects on impact properties of zirconium–2.5 niobium and Zircaloy-2, effects of hydrogen on, 20: 31669
effects on maize seeds, genetic, 20: 31092

effects on mechanical properties of hot-pressed and extruded beryllium, 20: 31794
effects on mechanical properties of low-alloy pressure vessel steel, 20: 31796
effects on mechanical properties of Hastelloy X-280 and Inconel 625, 20: 31669
effects on microstrain in copper single crystals, 20: 31669
effects on n-type silicon, defect clusters from, (E), 20: 31792
effects on optical transmission spectra of zinc sulfide single crystals, 20: 31272
effects on semiconducting properties of gallium arsenides, 20: 31617(T),
effects on stress relaxation of Nimonic 80A springs, 20: 31669
effects on stress-rupture properties of Hastelloy N, 20: 31669
effects on tensile properties of aluminum, titanium, and titanium-base alloy at cryogenic temperatures, 20: 31784(R) (NASA-CR-54976)
effects on thermal diffusivity of pyrolytic carbon and pyrolytic graphite, 20: 31667
effects on thermal diffusivity of beryllia, 20: 31667
embrittlement of type 304 stainless steel, effects of boron additions on, 20: 31669
reactions with nuclei, survey of, 20: 32535
scattering by helium-3 at 3.33 to 7.90 Mev, polarization from elastic, (E), 20: 32452
scattering by manganese to 14 Mev, energy spectra of inelastic, (E), 20: 31566

NEUTRONS, FISSION
effects on growth and mutations in Triticum, 20: 31080

NEUTRONS, THERMAL
diffusion in parallel-plate lattices, calculation of, 20: 32763 (AECL-2543)
dosimetry in mixed fields, properties of glasses for, 20: 31462
dosimetry in mixed fields, tissue-equivalent ionization chamber for in-phantom, 20: 31524
effects on cobalt–dysprosia dispersed in soda-potash glass, effects of boron carbide additions on, 20: 31668
effects on ductility of type 304 stainless steel, effects of carbon content and titanium additions on, 20: 31669
effects on mechanical properties of silver–15 indium–5 cadmium alloy, 20: 31668
effects on photoconductive properties of cadmium sulfides and selenides, 20: 32736
effects on polystyrene, positronium lifetimes in, (E), 20: 32704
effects on tensile properties of Nimonic PE16, 20: 31669
flux distribution in horizontal reactor channels, beryllium reflector effects on, 20: 32765 (IAE-957)
propagation of pulsed, in absorbing media, (E/T), 20: 32362
reactions (n,γ) with cesium-133 and iodine-127, gamma spectra from, (E), 20: 32422
transport equation for, regular eigenfunctions of time-dependent, 20: 32364

NEW ZEALAND
carbon-14 content of atmosphere at Markara, 20: 31410
radiation monitoring in, 1965, 20: 31446(R) (NP-16015)

NICHROME
vaporization from probe surface in electric arcs, (E), 20: 32593

NICKEL
abundance in solar corona, (T), 20: 31865
deposition on uranium, electrolytic, 20: 31670
diffusion in single-crystal magnesia, 20: 31719(R) (UCRL-16658, pp 155-69)
effects of sintering aids of, on thermal conductivity of uranium and plutonium uranium carbides, 20: 31666
effects on corrosion of graphite by water vapor, 20: 31667
effects on hardness of molybdenum, 20: 31741
effects on sintering of zirconium diboride, 20: 31668
heat transfer from spheres of, to water at 30 to 94°C, 20: 31440(R) (ANL-7175, pp 159-83)
hydrogen atom and ion reactions at 10 to 40 kev, secondary electron emission from, (E), 20: 31533
neutron capture by, average level widths of compound nucleus from, (E), 20: 32424
performance in accelerating electrodes in cesium-contact ion thrustors, 20: 31383
platinum-195 Mössbauer effect in, g-factor and internal fields from, (E), 20: 32487
positron annihilation in ferromagnetic, angular correlations from polarized, (E), 20: 32703
proton reactions at 0.05 to 2.9 Bev, induced activity data and cross sections for spallation, (E/T), 20: 32549
radiation effects on electric conductivity of, stage IV recovery from electron, (E), 20: 31800
vaporization from probe surface in electric arcs, (E), 20: 32593

NICKEL ALLOYS
compatibility of EPE7, with plutonium carbide–uranium carbide, 20: 31675
Al–Cr–Fe–Mo–Ni–Ti, radiation effects on tensile properties of Nimonic PE16, thermal-neutron, 20: 31669
Au–Mo–Ni, performance for bonding graphite to metals, 20: 31683(R) (ORNL-3936, pp 95-121)
Ce–Ni, magnetic properties of intermetallic compounds of, 20: 32699
Cr–Fe–Mo–Ni–W, radiation effects on mechanical properties of Hastelloy X-280, fast-neutron, 20: 31669
Cr–Fe–Ni, corrosion by boiling magnesium chloride solutions and by water, cracking in stress-, 20: 31676(R) (COO-1319-39)
Cu–Ni, tensile properties of composites of tungsten fibers and, 20: 31770
Hf–Ni, magnetic properties of intermetallic compounds of, 20: 32699
La–Ni, magnetic properties of intermetallic compounds of, 20: 32699
Ni–Pr, magnetic properties of intermetallic compounds of, 20: 32699
Ni–Ta, electric conductivity of, anomalies in, 20: 31775
Ni–W, creep properties at high temperatures, 20: 31669

NICKEL FLUORIDES
enthalpy of formation of, 20: 31213(R) (ANL-7175, pp 119-58)

NICKEL ISOTOPES Ni-58
neutron total cross sections for, level spacings from, (E/T), 20: 32389
proton elastic scattering at 40 Mev, differential cross sections and polarization for, (E), 20: 32510

NICKEL ISOTOPES Ni-60
helium-3 reactions (He-3,α) at 17.5 Mev, angular-momentum effects in, (E), 20: 32508
neutron total cross sections for, level spacings from, (E/T), 20: 32389
proton inelastic scattering at 10.5 and 14.0 Mev, spin flip in, (E), 20: 32557
proton reactions (p,p′γ) at 13 Mev, energy levels from, (E), 20: 32490

NICKEL ISOTOPES Ni-62
neutron total cross sections for, level spacings from, (E/T), 20: 32389
proton reactions (p,p′γ) at 13 Mev, energy levels from, (E), 20: 32490

NICKEL ISOTOPES Ni-63
beta activity of, use of 4π proportional counters for measuring, 20: 31548

NICKEL ISOTOPES Ni-64
neutron total cross sections for, level spacings from, (E/T), 20: 32389

NICKEL OXIDES
cobalt-57 Mössbauer effect in, time independence of charge states determination from, (E), 20: 32713
radiation effects on reduction of, by hydrogen, 20: 31285

NICKEL STEEL
fracture toughness of maraging, effects of microstructure on, 20: 31670
radiation effects on impact properties of, neutron, 20: 31669
C–Co–Ni, tensile properties of strain-aged, 20: 31716(R) (UCRL-16658, pp 121-32)
Co–Mo–Ni, tensile properties of strain-aged, 20: 31716(R) (UCRL-16658, pp 121-32)

NICKEL SYSTEMS
Mo–Ni–ThO_2, development and properties of dispersion-strengthened, 20: 31669
Ni–rare earth–Si, crystal structure of $R_3Ni_6Si_2$ compounds in, 20: 31253
Ni–ThO_2—bonding to refractory metals, process for TD Nickel diffusion, 20: 31670
Ni–ThO_2, development and properties of dispersion-strengthened, 20: 31669

NIMONIC-80
compatibility of 80A, with plutonium carbide–uranium carbide, 20: 31675
radiation effects on stress relaxation of springs of, fast-neutron, 20: 31669

NIMONIC-90
compatibility with tantalum at 760 to 900°C, 20: 31675

NIOBIUM
corrosion by various alkaline media at 25 and 98°C, 20: 31669
effects on grain size and transformations in alpha-uranium and uranium alloys at 720 to 800°C, 20: 31666
effects on microstructure of tungsten–thoria dispersion-hardened alloys, 20: 31781
electric conductivity of, effects of impurities and strain on, 20: 31742
electronic structure of, at superconducting critical temperatures, 20: 31747
heat capacity of high-purity, at 0.35 to 25°K, 20: 32684(R) (UCRL-16658, pp 21-38)
melting point of zone-refined, 20: 31721(T) (AD-630971)
oxidation by steam at 1050 to 1500°C, 20: 31669
phase studies on, 20: 32312(R) (UCRL-16658, pp 133-43)
proton reactions at 40 Mev to 25 Bev, lithium isotopes from, (E), 20: 31205
separation from neptunium by solvent extraction using 4-methyl-2-pentanone, 20: 31319 (ISO-SA-10)
solubility in magnesium–zinc alloys, 20: 31314(R) (ANL-7175, pp 1-41)

solvent properties for nitrogen, 20: 31250
superconducting critical current in, effects of lattice defects on, 20: 31759
tensile properties of, effects of temperature and strain rate on, 20: 31669
vacancies in, method of mixtures measurement of concentration and energy of formation of, 20: 32726(T)

NIOBIUM ALLOYS
Al–Nb, phase diagram, 20: 31769
Mo–Nb, electronic structure of, at superconducting critical temperatures, 20: 31747
Mo–Nb–W–Zr, hardness of niobium-base, effects of composition on hot-, 20: 31669
Nb–Os, electronic structure of, at superconducting critical temperatures, 20: 31747
Nb–Re, electronic structure of, at superconducting critical temperatures, 20: 31747
Nb–Ru, electronic structure of, at superconducting critical temperatures, 20: 31747
Nb–Sn, magnetic field trapping by superconducting hollow cylinders of intermetallic compounds of, temperature dependence of, (E), 20: 32316
Nb–Sn, magnetic flux jumping in high-field high-current superconducting, stability against, (T), 20: 32320
Nb–Sn–Zr, corrosion by steam, composition of oxide film formed by, 20: 31669
Nb–Sn–Zr, hardness of zirconium-base, effects of tempering at 400 to 700°C on, 20: 31669
Nb–Ta–V, development and properties of, 20: 31709(R) (IITRI-B6042-5)
Nb–Ta–W–Zr, creep properties of FS-85, 20: 31669
Nb–Ti, superconducting critical field of, spin-orbit effects on upper, (E), 20: 32330
Nb–Ti, superconducting critical current of, effect of precipitates on, 20: 32322
Nb–Ti–V, development and properties of, 20: 31709(R) (IITRI-B6042-5)
Nb–W, corrosion by cerium–cobalt–plutonium alloy fuels, effects of carbon on, 20: 31679(R) (LA-3524)
Nb–W, electronic structure of, at superconducting critical temperatures, 20: 31747
Nb–Zn, phase diagram, 20: 31669
Nb–Zr, corrosion by cerium–cobalt–plutonium alloy fuels, effects of carbon on, 20: 31679(R) (LA-3524)
Nb–Zr, corrosion by lead at 1400°F, 20: 31683(R) (ORNL-3936, pp 95-121)
Nb–Zr, fracture properties of zirconium-base, effects of hydrogen and temperature on, 20: 31669
Nb–Zr, mechanical properties of cold-worked zirconium-base, 20: 31669
Nb–Zr, radiation effects on impact properties of, effects of hydrogen on fast-neutron, 20: 31669
Nb–Zr, reactions with oxygen at 1000 to 1600°F, mechanisms of, 20: 31669
Nb–Zr, superconductivity of, in pulsed magnetic fields, effects of aging on, 20: 32312(R) (UCRL-16658, pp 133-43)
Nb–Zr, thermal expansion of, effects of hydride phase on, 20: 31745

NIOBIUM BORIDES
enthalpy of formation of, 20: 31213(R) (ANL-7175, pp 119-58)

NIOBIUM CARBIDES
fabrication by hot-pressing, 20: 31699
graphite–NbC, fabrication and properties of hot-pressed composites of, 20: 31688 (NASA-CR-507)

NIOBIUM HYDRIDES
ductility of solid-solution, 20: 31716(R) (UCRL-16658, pp 121-32)

NIOBIUM ISOTOPES
distribution and natural carriers of, in sea water, 20: 31422

NIOBIUM ISOTOPES Nb-94
beta decay of, gamma energies and spectrum shape in, 20: 32518

NIOBIUM ISOTOPES Nb-95
content in fractionated fallout particles from land surface burst, 20: 31460
content in large fallout particles in Japan, 20: 31412
deposition on tropospheric aerosols, 20: 31459

NIOBIUM OXIDES
bonding to alumina, method for, 20: 31669
crystal structure of Nb_2O_5, 20: 31746
effects on xenon diffusion in urania, 20: 31666
thermodynamic stability measurements on, using galvanic cells, 20: 31717(R) (UCRL-16658, pp 143-9)
CoO–Nb_2O_5–Ta_2O_5, phase studies, 20: 31734

NIOBIUM SYSTEMS
H–Nb, phase diagram and tensile properties of, 20: 31667
H–Nb, preparation of, for transmission electron microscopy, hydrogen concentration in electrothinning procedures for, 20: 31691
H–Nb, tensile properties of, effects of temperature and strain rate on, 20: 31669
Nb–N–O, internal friction studies of interstitial clusters in, 20: 31774

NITRIC ACID
isotopic exchange with nitric oxide, effects of additives on nitrogen-15 concentration by, 20: 31639(R) (NYO-755-1, pp 77-129)
molecular state of aqueous, NMR studies of, 20: 31221(R) (UCRL-16658, pp 73-87)

NITROGEN
content in primary cosmic radiation, at geomagnetic latitude 42° North, 20: 31951
determination in helium, method for, 20: 31167(R) (ANL-7175, pp 217-25)
determination of, in helium, chromatograph for continuous, 20: 31210
effects on corrosion of chromium–iron–zirconium alloy by steam at 300, 400, and 500°C, 20: 31677(R) (GEAP-4840)
effects on electronic structure of transition metals and alloys, 20: 31747
effects on radiosensitivity of Kalanchoe, 20: 31076
electron reactions with rarefied, emission spectra from, (E), 20: 31921
energy level transition probabilities of, data compilation on, 20: 31942
energy levels of, hyperfine structure of 2p, (T), 20: 31904 (UCRL-16581)
hydrogen ion reactions at 20 to 120 kev, ionization cross sections for, 20: 31909
ionization equation for optically thin plasma of, (T), 20: 32636
ionization of, by electrons at 0.6 to 20 kev, cross sections for, (E/T), 20: 31906
positron annihilation in liquid, angular distribution of photons from, (E), 20: 32345
radiation from high-temperature gas of, pressure and temperature dependence of, (E), 20: 32240
radiolysis of, isotopic exchange in, 20: 31282
radiosensitivity effects on *Thiobacillus thiooxidans*, x, 20: 31139
reactions of atomic, with sulfur compounds, 20: 31218(R) (UCRL-16658, pp 1-9)
reactions of, with ions, atom and charge transfer in, 20: 31224
relaxation of potassium-seeded plasma of, to steady state, 20: 32657
separation of, from argon by titanium gettering, 20: 31314(R) (ANL-7175, pp 1-41)
solubility in niobium, 20: 31250
solvent properties of liquid, for hydrogen, 20: 31251
spectra in airglow, 20: 32289
spectra of foil-excited beams of, 20: 31903 (N-66-16702)
thermal conductivity of high-temperature gas of, pressure and temperature dependence of, (E), 20: 32240

NITROGEN IONS
electron reactions with, excitation cross sections for, (T), 20: 31929
reactions of, with molecules, atom and charge transfer in, 20: 31224

NITROGEN ISOTOPES N-13
energy level from carbon-12 (p,p'γ) reactions, parity and spin of, (E), 20: 32438
energy levels from boron-10 (He-3,p) reactions at 1.2 to 12 Mev, excited, (E), 20: 32527

NITROGEN ISOTOPES N-14
deuteron reactions (d,p) at 4 Mev, nitrogen-15 levels from, (E), 20: 32501
exchange with nitrogen-15 in radiolysis of gaseous nitrogen, 20: 31282
reactions (N-14, F-18) with oxygen-16 at 20 to 33 Mev, angular distributions from, (E), 20: 32429

NITROGEN ISOTOPES N-15
concentration by exchange between nitrogen oxides using carbon tetrachloride–freon 112 solvents, 20: 31638(R) (NYO-755-1, pp 12-76)
concentration by exchange between nitric acid and nitric oxide, effects of additives on, 20: 31639(R) (NYO-755-1, pp 77-129)
energy levels from helium-3 reactions (He-3, pγ) with carbon-13 at 3.0 Mev, (E), 20: 32495
energy levels from deuteron reactions (d,p) with nitrogen-14 at 4 Mev, (E) 20: 32501
energy levels from helium-3 reactions (He-3,p) with carbon-13 at 4.0 Mev, (E), 20: 32501
exchange with nitrogen-14 in radiolysis of gaseous nitrogen, 20: 31282
spectra in thiotrithiazyl cations, NMR, 20: 31218(R) (UCRL-16658, pp 1-9)

NITROGEN ISOTOPES N-16
activity in water coolant of EWA research reactor, power measurement by, 20: 32870
energy levels from helium-3 reactions (He-3,p) with carbon-14 at 4.0 and 4.5 Mev, 20: 32501

NITROGEN ISOTOPES N-17
energy levels of, low-lying negative parity, (T), 20: 32398

NITROGEN MUSTARDS
effects of novoembichine combined with x radiation on amino acid accumulation in *Mycobacterium cyaneum* 416, 20: 31005

NITROGEN OXIDES
isotopic exchange reactions of, nitrogen-15 concentration by, 20: 31638(R) (NYO-755-1, pp 12-76)
isotopic exchange with nitric acid, effects of additives on nitrogen-15

concentration by, 20: 31639(R) (NYO-755-1, pp 77-129)
photolysis of, mechanisms of ultraviolet, 20: 31221(R) (UCRL-16658, pp 73-87)
reactions with tungsten, 20: 31718(R) (UCRL-16658, pp 149-54)

NITROGEN SYSTEMS
$N-H_2O$, radiation effects on production of ammonia in, effects of acidity on γ and uv, 20: 31289
Nb–N–O, internal friction studies of interstitial clusters in, 20: 31774

NORWAY
fallout monitoring, 1960 through 1964, 20: 31465

NUCLEAR CHEMISTRY
research programs on, 20: 31165(R) (HMI-B-46)

NUCLEAR EMULSIONS
antiproton elastic scattering at 3 Bev/c by nuclei in, amplitudes for, (E/T), 20: 32467
bremsstrahlung reactions in, electron pair opening angle in, (E), 20: 32006
meson (K^-) reactions, at 1.5 Bev/c in, hyperfragment production and mesic decay from, (E), 20: 32491
meson (K^-) reactions at 5.0 Bev/c with nuclei in, lithium-8 emission in, (E), 20: 32469
meson (π^-) reactions at 300 Bev, $_{\Lambda}B^{12}$ production in, (E), 20: 32412
particle track structure in, distribution of bundle length in, 20: 31522
performance in system with spark chambers for determining point of incidence of particles, 20: 31569

NUCLEAR MAGNETIC RESONANCE
measurement in paramagnetic materials, ENDOR spectrometer for, 20: 32525
relaxation time of oriented atoms in, effect of surface inhibitors on, (T), 20: 32417
use for magnetic field measurements in CERN storage ring, equipment for, 20: 31817 (CERN-66-15)
use of, in chemical exchange studies, 20: 31218(R) (UCRL-16658, pp 1-9)

NUCLEAR MATERIALS MANAGEMENT
autoradiography of plutonium oxide–uranium oxide compacts, 20: 31212
uranium-235 determination in combustible waste and air filters by gamma counting, gage for, 20: 31174 (WAPD-T-1905)

NUCLEAR PHYSICS
book: *Nuclear Physics. Mechanism of Nuclear Reactions*, 20: 32538
research programs on, 20: 31165(R) (HMI-B-46)

NUCLEAR POWER
development of, neutron cross section data requirements for, 20: 32839
economics of, in France, 20: 32889

NUCLEAR POWER PLANTS
development and economics of, in France, 20: 32889
development in India, 20: 32817
development of, neutron cross section data requirements for, 20: 32839
economics and growth in free world, 20: 32808 (TID-22973)
economics of, calculation method for, 20: 32814
economics of, computer program for calculating, 20: 32743 (ORNL-3944)
energy transformation in, efficiency of, 20: 32813

NUCLEAR REACTIONS
alpha emission in spallation, effect of alpha substructure on, (T), 20: 32455
angular distributions and polarization from, summation and integration of spherical harmonics for, 20: 32437
book: *Nuclear Physics. Mechanism of Nuclear Reactions*, 20: 32538
deuteron stripping, target-excitation effects in, (T), 20: 32497
isospin selection rules for (α,d) and (α,α'), effects of Coulomb interaction on, 20: 32484
nucleon transfer in, many-body, (E/T), 20: 32547
potential barrier model for, parabolic, (T), 20: 32423
Q-value measurements at MIT, review of, 20: 31808
theory for arbitrary spin, 20: 32382 (UCRL-14592-T(Rev.1))
theory of direct and resonance, short-range interaction, 20: 32387
theory of resonance, 20: 32428

NUCLEAR SPECTRA
rotational, nonadiabatic effects of, 20: 32492

NUCLEAR STRUCTURE
theory of, in relation to atomic mass measurements, review, 20: 31808

NUCLEAR THEORY
nucleon pairing interactions in nuclei, number-conserving approximations for, 20: 32494

NUCLEI
alpha clustering in, (T), 20: 32542
alpha inelastic scattering by, computer program for analysis of, 20: 32544
alpha reactions (α,α') and (α,d) with, effects of Coulomb interaction on, (T), 20: 32484
alpha-decay barrier penetrabilities with Igo potential for even-mass, 20: 32399
beta decay in stars, photon-induced, (T), 20: 31878
beta decay of, double, 20: 32562
beta decay of, matrix elements for first-forbidden, 20: 32393
binding energy of, (T), 20: 32559
charge radius of spherical, structure effects in, (T), 20: 32561
decay of, effect of high spin on electromagnetic, (T), 20: 32374(R) (IITRI-578P25-15)
deuteron reactions with, many-body nucleon transfer in, (E/T), 20: 32547
distributions of recoil, device for measuring angular and energy, 20: 32526
electron scattering by, nuclear property determination using, 20: 32405
elementary particle scattering by, coupled equations for rearrangement, 20: 32388
energy level density in, calculation of, 20: 32432
energy level transitions of, competition between M1 and E2 of, (T), 20: 32374(R) (IITRI-578P25-15)
energy level transitions of even, collective M1, (T), 20: 32420(T)
energy level transition probabilities in single closed shell, (T), 20: 32426
energy levels of light, tensor and vector Coulomb energies of, 20: 32499
energy levels of light even-even, systematics of O^+, (T), 20: 32522
energy levels of odd-mass deformed, transverse spin polarization effects on, (T), 20: 32447
energy levels of $6 \leq A \leq 9$, intermediate coupling shell-model calculations for, 20: 32436
energy levels of, rotational, (T), 20: 32492
energy levels of, projection operator for studying isospin of, 20: 32533
energy levels of, spin assignment from triple correlations from, (T), 20: 32372 (COO-1120-43)
energy levels of, macroscopic and microscopic descriptions of dipole, 20: 32448
energy levels of, Heisenberg uncertainty principle for determining, (T), 20: 31910
ion reactions with, method for calculating isomeric cross sections for, 20: 32374(R) (IITRI-578P25-15)
mass of deformed, electromagnetic, (T), 20: 32548
mesons (π) absorption cross sections up to 800 Mev, (T), 20: 32078
moments of inertia of strongly deformed, (T), 20: 32416
neutrino quasielastic scattering by, transverse muon polarization from, 20: 32468
neutron capture by, average level widths of compound nucleus from, (E), 20: 32424
neutron reactions with, survey of fast, 20: 32535
neutron reactions (n,γ) with, method for calculating cross sections for, 20: 32374(R) (IITRI-578P25-15)
neutron reactions at 14 Mev, cross sections, Q-values, and sensitivities for, 20: 32380 (SC-RR-66-229)
nucleon interactions in, integral operators and S-matrix for scalar dispersion in, 20: 32537
nucleon interactions in, two-body matrix element for Gaussian, 20: 32461
nucleon pairing interactions in, number-conserving approximations for theory of, 20: 32494
nucleon pairing interaction in, superconductivity approximation for, 20: 32397
nucleon reactions with, heavy particle stripping in, (T), 20: 32444
orientation of spin-1, 20: 32390
particle inelastic scattering by, matrix elements for heavy-, 20: 32383
particle scattering by, transfer theorem for multichannel, 20: 32409
photon absorption by, Fermi liquid theory for, 20: 32539
photon interactions with Coulomb field of, cross section for two photon production in, (T), 20: 32031
polarization in paramagnetic solutions, ENDOR spectrometer for measuring, 20: 32525
proton elastic scattering at 18.5 and 20.5 Mev, optical-model analysis of polarization from, (E/T), 20: 32523
proton reactions with, nucleon-alpha cascades from, (T), 20: 32455
reactions with nuclei, parabolic potential barrier model for, 20: 32423
stability of $Z = 126$, $A = 310$, shell model calculations for, 20: 32482
surface tension of, Fermi-gas model for, 20: 32470

NUCLEIC ACIDS
radiation effects on content of, in *E. coli*, x, 20: 31023
radiation effects on, uv, 20: 31039
synthesis in cultured bone marrow cells from patients with leukemia, myeloma, or polycythemia, tracer study, 20: 30971 (ORINS-45)

NUCLEONS
coupling to massive photons in elastic scattering, 20: 32046
form factors of, electromagnetic, (T), 20: 32033
interactions in nuclei, integral operators and S-matrix for scalar dispersion in, 20: 32537
interactions in nuclei, two-body matrix element for Gaussian, 20: 32461
interactions of, short-range theory for, 20: 32387
interactions of, S-matrix elements in theory for, 20: 32168
interactions with nucleons, dispersion theory calculations for,

20: 32008
interactions with mesons (π) and nucleons, inelastic unitarity in eigenstates of total angular momentum for, 20: 32014
interactions with photons, T violation in $N^*_{\frac{1}{2}}$ production in, (T), 20: 32020
interactions with mesons (π), boundary-condition model for P_{33} resonance in, 20: 32023
interactions with mesons ($\bar{K}$) at low energies, N/D method for s-wave, 20: 32024
interactions with photons, mesons (ω) and (ρ) production in, (T), 20: 31984 (IC-66/54)
interactions with mesons (π) at high energies, forward dispersion relations for, 20: 32026
interactions with nucleons, charge-dependent effects in $^1S_0$ scattering lengths for, 20: 32030
interactions with mesons (π), asymptotic behavior of amplitudes for elastic, (T), 20: 32032
interactions with photons, asymptotic behavior of amplitudes for elastic, (T), 20: 32032
interactions with leptons, C-violating effects in electromagnetic inelastic, 20: 32042
interactions with photons, high-energy theory for Compton, 20: 32054
interactions with electrons, (ω-ϕ) mixing angle from elastic, (E/T), 20: 32058
interactions with nucleons, meson (π) correlation effects in two meson (π)-exchange contribution for, (T), 20: 32073
interactions with neutrinos, baryon resonance production in, 20: 32080
interactions with mesons (π), amplitudes for N^*_{11} and N^*_{13} production in, (T), 20: 32091
interactions with mesons (π), Mandelstam representation and elastic unitarity for amplitudes of, 20: 32095
interactions with antineutrinos, amplitudes and selection rules for inelastic, (T), 20: 32090
magnetic moment operator in SU(6) for, covariant, 20: 32053
mass difference of, model for electromagnetic, 20: 32057
pairing interactions in nuclei, number-conserving approximations for, 20: 32494
pairing interaction in nuclei, superconductivity approximation for, 20: 32397
reactions with nuclei, heavy particle stripping in, (T), 20: 32444
transfer in deuteron reactions with nuclei, many-body, (E/T), 20: 32547

NUCLEOSIDES
5'-monophosphate, labeling with phosphorus-32, 20: 31307

NUCLEOTIDES
fluorescence of intracellular pyridine, effects of radioprotective compounds on, 20: 31122

O

OATS
radiation effects on somatic mutation frequency induction in, 20: 31078

OCEANOGRAPHY
biological, chemical, and physical characteristics of northeast Pacific Ocean, 20: 31448 (RLO-1725-15)
biological, chemical, and physical characteristics of northeast Pacific Ocean, 20: 31449 (RLO-1725-16)
biological, chemical, and physical characteristics of northeast Pacific Ocean, 20: 31451 (RLO-1725-18)
biological, chemical, and physical characteristics of northeast Pacific Ocean, 20: 31452 (RLO-1725-19)
biological, chemical, and physical characteristics of northeast Pacific Ocean, 20: 31450 (RLO-1725-17)
oxygen analyzer using thallium-204 beta source for use in, 20: 31171 (ORO-596)

ONIONS
radiation effects on *Allium cepa* roots, protective effects of anoxia, α-aminothioacetamide, and cysteine against gamma, 20: 31137
radiation effects on inner and outer epidermises of *Allium cepa*, alpha and uv, 20: 31079

OOCYTES
meiosis in starfish, effects of heavy water and hydrostatic pressure on, 20: 30986

ORGANIC ACIDS
determination by xenon trioxide oxidation, titrimetric, 20: 31196

ORGANIC COOLED REACTORS
control system development for heavy water-moderated, 20: 32796(R) (AI-CE-3)
development of heavy water-moderated, 20: 32796(R) (AI-CE-3)
fuel channel assembly development for heavy water-moderated, 20: 32796(R) (AI-CE-3)
fuel element development for heavy water-moderated, 20: 32796(R) (AI-CE-3)
fuel reprocessing for heavy water-moderated, 20: 31317 (BAW-393-3)
loading system for heavy water moderated, development of, 20: 32796(R) (AI-CE-3)
materials development for heavy water-moderated, 20: 32796(R) (AI-CE-3)
neutron resonance absorption in lattices of uranium-fueled, heavy-water moderated, (E/T), 20: 32785

ORNL RELATIVISTIC ISOCHRONOUS CYCLOTRON
beam analysis of, spectrograph facility for, 20: 31822 (ORNL-P-2260)
beam extraction system for, operation of, 20: 31821 (ORNL-P-2239)

OSCILLATORS
design and properties of cryotron relaxation, with frequency control, 20: 32333

OSCILLOGRAPHS
data analysis from, automatic film reader for, 20: 31479 (Y-1533)

OSMIUM
performance as ionizer material in cesium-contact ion thrustors, 20: 31383

OSMIUM ALLOYS
Fe–Os, magnetic properties of fcc, 20: 32739
Nb–Os, electronic structure of, at superconducting critical temperatures, 20: 31747

OSMIUM ISOTOPES Os-186
energy level transitions in, L-subshell ratios of E2 rotational, 20: 32516

OSMIUM ISOTOPES Os-188
energy level transitions in, L-subshell ratios of E2 rotational, 20: 32516

OXALATES
radiolysis of aqueous solutions of, tracer studies of reformation of oxalic acid in gamma, 20: 31277

OXALIC ACID
determination by xenon trioxide oxidation, titrimetric, 20: 31196
labeling with carbon-14 using labeled acetic acid, 20: 31263
yields from gamma radiolysis of aqueous oxalate solutions, tracer studies of mechanisms in, 20: 31277
yields from radioinduced carboxylation of formic acid in aqueous solutions, 20: 31278

OXAZOLE, DIPHENYL-
benzene–2,5-diphenyloxazole, scintillation efficiency of, 20: 31290
chlorobenzene–2,5-diphenlyoxazole, scintillation efficiency of, 20: 31290
chloropentafluorobenzene–2,5-diphenyloxazole, scintillation efficiency of, 20: 31290
dichlorotetrafluorobenzene–2,5-diphenyloxazole, scintillation efficiency of, 20: 31290
2,5-diphenyloxazole–hexafluorobenzene, scintillation efficiency of, 20: 31290
2,5-diphenyloxazole–toluene, scintillation efficiency of, 20: 31290
2,5-diphenyloxazole–trichlorotrifluorobenzene, scintillation efficiency of, 20: 31290

OXAZOLE, 2,2'-*p*-PHENYLENEBIS[5-PHENYL-
hexafluorobenzene–2,2'-p-phenylenebis[5-phenyloxazole], scintillation efficiency of, 20: 31290
2,2'-p-phenylenebis[5-phenyloxazole]–toluene, scintillation efficiency of, 20: 31290

OXYGEN
content in primary cosmic radiation, at geomagnetic latitude 42° North, 20: 31951
corrosive effects on molybdenum disilicide at 450 to 650°C, 20: 31669
determination in helium, method for, 20: 31167(R) (ANL-7175, pp 217-25)
determination in sea water, thallium-204 beta source and Geiger-Mueller counter for, 20: 31171 (ORO-596)
determination of, in helium, chromatograph for continuous, 20: 31210
effects of adsorbed, on surface ionization of neodymium and tungsten, 20: 31225
effects of dissolved, on solubility of hydrogen in zirconium, 20: 31667
effects on corrosion of vanadium–titanium alloys by sodium at 650°C, 20: 31669
effects on electronic structure of transition metals and alloys, 20: 31747
electron reactions with rarefied, emission spectra from, (E), 20: 31921
energy level transition probabilities of, data compilation on, 20: 31942
energy levels of, hyperfine structure of 2p, (T), 20: 31904 (UCRL-16581)
hydrogen ion reactions at 20 to 120 kev, ionization cross sections for, 20: 31909
ionization of, by electrons at 0.6 to 20 kev, cross sections for, (E/T), 20: 31906
permeation in hafnia, thoria, and zirconia at 1100 to 2050°C, 20: 31731
positron annihilation in liquid, angular distribution of photons from, (E), 20: 32345
radiation from high-temperature gas of, pressure and temperature dependence of, (E), 20: 32240
radiosensitivity effects on cultured human cells, α, deuteron, fast-neutron, and x, 20: 31123

radiosensitivity effects on *Thiobacillus thiooxidans*, x, 20: 31139
reaction kinetics of $^1\Delta g$-state molecular, 20: 31221(R) (UCRL-16658, pp 73-87)
reactions with allyl radicals in irradiated polyethylene, 20: 31268(R) (COO-1088-20)
reactions with graphite at 450 to 510°C, inhibiting effects of phosphorus oxychloride vapor on, 20: 31667
reactions with niobium–1 zirconium at 1000 to 1600°F, mechanisms of, 20: 31669
reactions with urania–yttria solid solutions, kinetics of, 20: 31685
reactions with zirconium at 840 to 1100°C, diffusion kinetics for, 20: 31669
solubility in sodium at 110 to 550°C, equation for, 20: 31669
spectra of foil-excited beams of, 20: 31903 (N-66-16702)
yields from reactions of uranium dioxide with carbon, 20: 31230

OXYGEN IONS
effects on sapphires at 100 kv, dislocation loops from, 20: 31793

OXYGEN ISOTOPES O-16
alpha elastic scattering at 11.09 and 12.05 Mev, level spins and parities from, (E), 20: 32502
alpha inelastic scattering at 31.8 and 39.5 Mev, (E), 20: 32554
binding energy of, Hartree-Fock calculation of, 20: 32496
deuteron reactions (d,p) at 11 and 13 Mev, angular-momentum effects on angular distribution from, (E), 20: 32512
electron inelastic scattering by, cross sections and sum rules for, (T), 20: 32536
electron inelastic scattering at high energies, form factors for, (T), 20: 32442
electron scattering by, form factors for 180° inelastic, (T), 20: 32569
electron scattering by, nuclear structure effects on bremsstrahlung emission from, (T), 20: 32456
energy levels of, two-particle-two-hole, 20: 32524
energy levels of, excitation by alpha particles, (E), 20: 32554
nitrogen-14 reactions (N-14, F-18) at 20 to 33 Mev, angular distributions from, (E), 20: 32429
reactions (O-16,α) with carbon-12 at 22 and 32 Mev, magnesium-24 levels from, (E), 20: 32556
reactions (O-16,xn) with ytterbium isotopes, alpha-active platinum isotopes from, (E), 20: 32458

OXYGEN ISOTOPES O-17
energy levels of, low-lying negative parity, (T), 20: 32398
hyperfine structure of, in $^1\Delta g$-state molecular oxygen, 20: 31221(R) (UCRL-16658, pp 73-87)

OXYGEN ISOTOPES O-18
alpha reactions (α,nγ) at 4.7 to 6.0 Mev, neon-21 levels from, (E), 20: 32474
alpha reactions (α,nγ) at 4.75 Mev, neon-21 levels from, (E), 20: 32476
alpha reactions (α,nγ) at 4.43 and 5.5 Mev, neon-21 levels from, (E), 20: 32427
concentration in liquids by exchange with gaseous carbon dioxide, 20: 31641(R) (NYO-755-1, pp 173-208)

OXYGEN SYSTEMS
Ar–O, shock layers in, magnetohydrodynamically supported, (E), 20: 32217 (N-65-33713)
$BaO–Li_2O–O–Tc_2O_7$, compound formation in, 20: 31244
$BaO–O–Na_2O–Tc_2O_7$, compound formation in, 20: 31244
$BaO–O–Tc_2O_7$, compound formation in, 20: 31244
$CaO–O–Te_2O_7$, compound formation in, 20: 31244
H–O, shock recombination of near-stoichiometric, 20: 31216 (LA-DC-7659)
H–O, shock recombination of, post-induction kinetics for, (T), 20: 31217 (LA-DC-7661)
HF–O, reactions with urania, 20: 31315(R) (ANL-7175, pp 42-103)
$Li_2O–O–SrO–Tc_2O_7$, compound formation in, 20: 31244
Nb–N–O, internal friction studies of interstitial clusters in, 20: 31774
$O–Na_2O–SrO–Tc_2O_7$, compound formation in, 20: 31244
O–Na–U, phase studies at 600 to 1000°C, 20: 31666
O–PuC–UC, stability as fast reactor fuel, 20: 31675
$O–SrO–Tc_2O_7$, compound formation in, 20: 31244

OYSTERS
radiation effects on microbial flora in Pacific, gamma, 20: 31626

OZONE
distribution in atmosphere, 1963 to 1966, 20: 31397(R) (RLO-1776-2)

P

PACIFIC OCEAN
characteristics of northeast, biological, chemical, and physical, 20: 31449 (RLO-1725-16)
characteristics of northeast, biological, chemical, and physical, 20: 31450 (RLO-1725-17)
characteristics of northeast, biological, chemical, and physical, 20: 31451 (RLO-1725-18)
characteristics of northeast, biological, chemical, and physical, 20: 31452 (RLO-1725-19)
characteristics of northeast, biological, chemical, and physical, 20: 31448 (RLO-1725-15)
strontium-90 content in deep waters of central, 1961, 20: 31414
strontium-90 content in South China Sea region of, November, 1962, 20: 31415
strontium-90 content in central, 1962 and 1964, 20: 31416
strontium-90 distribution in surface waters of, 1960 and 1961, 20: 31420

PAINTS
design of luminous, using radioisotopes, 20: 31636(P)

PALLADIUM
radiation effects on, at 1.6 to 3.0 Mev, electron, 20: 31805
use in deuterium–hydrogen separation by diffusion and electrolysis, 20: 31256
vaporization from probe surface in electric arcs, (E), 20: 32593

PALLADIUM ALLOYS
Pd–Ag, use in deuterium–hydrogen separation by diffusion and electrolysis, 20: 31256

PALLADIUM IONS
production of, for mass spectrometry, thermal techniques for, 20: 31226

PALLADIUM ISOTOPES
abundance determination by mass spectrometry, ion production technique for, 20: 31207

PALLADIUM ISOTOPES Pd-99
decay scheme for isomeric, (E), 20: 32373(R) (COO-1530-1)

PALLADIUM ISOTOPES Pd-106
energy levels from rhodium-106 decay, (E), 20: 32425

PANCREAS
radiation effects on dog, morphological and physiological x, 20: 31089

PARAMAGNETIC MATERIALS
neutron inelastic scattering by, filter-cutoff method for, 20: 32706

PARAMECIUM
radiation injuries in, repair of premutational uv and x, 20: 31040

PARTICLE BEAMS
energy measurement in angular distribution studies, method for simultaneous, 20: 32403

PARTICLE STATISTICS
stress tensor for many-body systems, symmetry of, 20: 32165

PARTICLE TRACKS
brightness of spark-chamber, measurement of, 20: 31582
formation in dosimeter glasses for neutron dosimetry in mixed radiation fields, 20: 31462
radical reactions along, in aqueous solutions, 20: 31293
radical reactions in, in water, 20: 31294
structure in nuclear emulsions, distribution of bundle length in, 20: 31522

PARTICLES
book: *Particles in the Atmosphere and Space*, 20: 32285
motion of variable-mass, equations for relativistic, 20: 32294
scattering of heavy, matrix elements for inelastic, 20: 32383
scattering of heavy, matrix elements for inelastic, 20: 32384

PEACH BOTTOM POWER REACTOR
coolant loop and purge system of, 20: 32788
fuel processing flowsheets for, 20: 31314(R) (ANL-7175, pp 1-41)

PEAS
radiation effects on development of seeds of, γ, 20: 31114

PEBBLE BED REACTORS
fuels for, use of thorium, 20: 32825

PENICILLIN
radiation effects on biological activity of, γ, 20: 31022

PENTANES
ionization of, by electrons at 0.6 to 20 kev, cross sections for, (E/T), 20: 31906

2-PENTANONE, 4-METHYL-
solvent properties for neptunium, 20: 31319 (ISO-SA-10)

PERCHLORIC ACID
corrosive effects on zirconium, 20: 31687
effects on nitrogen-15 concentration by nitric acid–nitric oxide exchange, 20: 31639(R) (NYO-755-1, pp 77-129)
molecular state of aqueous, NMR studies of, 20: 31221(R) (UCRL-16658, pp 73-87)

PEROXIDASES
radiation effects on activities of, in oranges, γ, 20: 31632

PERSONNEL
monitoring of, design of aural dosimeter for, 20: 31503(R) (BNWL-235-4, pp 14-16)
radiation hazards to radiologists, limits on whole-body, 20: 31458
radiation monitoring of, 20: 31439 (AECL-2540)
radiation monitoring of laboratory, procedures for, 20: 31469
radiation protection of, in gamma and x-ray defectoscopy, 20: 31464

PERTURBATION THEORY
formalism of Brueckner and Goldstone, for atoms, 20: 31944

vertex functions in, analytic properties of, 20: 32190
PHANTOMS
design of dose-equated plastic, for use in space flight, 20: 31455
radiation dosimetry of, tissue-equivalent ionization chamber for, 20: 31524
use of tissue-equivalent primate, for proton depth-dose measurements, 20: 31467
use of water-equivalent, for measurement of scattered x radiation dose during therapy, 20: 31156
PHENOL, p-BROMO-
radiosensitivity effects of, use of activation analysis for determining mechanism of, 20: 31172 (SGAE-BL-17/1966)
PHENOL, *p*-CHLORO-
radiosensitivity effects of, use of activation analysis for determining mechanism of, 20: 31172 (SGAE-BL-17/1966)
PHENOL, IODO-
radiosensitivity effects of, use of activation analysis for determining mechanism of, 20: 31172 (SGAE-BL-17/1966)
PHENOTHIAZINE, 3-CHLORO-10-(3'-DIMETHYLAMINOPROPYL)-
radiosensitivity effects of, relation between cellular anoxia and, 20: 31122
PHILIPPINE ISLANDS
endemic goiter in population of, tracer studies of causes of, 20: 30965
PHONONS
effects on lithium fluoride crystals, dipole nuclear spin transitions from, (T), 20: 32689
interactions with electrons in gases, kinetic equations for, 20: 32239
PHOSPHATASES
effects of radiation sickness on, in cerebral nerve cells in rats, 20: 31010
synthesis of adenosine, in wheat roots, effects of calcium and strontium on, 20: 30992
PHOSPHATES
effects of carrier, on phosphorus-32 uptake by prostate gland in dogs, 20: 31149(R) (TID-22969)
metabolism in rat liver, tracer study, 20: 30976
PHOSPHINES
synthesis of, in electric discharges, 20: 31218(R) (UCRL-16658, pp 1-9)
PHOSPHONIC ACID, DIALLYL ESTERS
radiation effects on sorptive properties of resins based on, gamma, 20: 31303
PHOSPHORIC ACID
effects on nitrogen-15 concentration by nitric acid–nitric oxide exchange, 20: 31639(R) (NYO-755-1, pp 77-129)
PHOSPHORIC ACID, BIS(2-ETHYLHEXYL) ESTER
solvent properties of, for americium, berkelium, and californium, 20: 31323
PHOSPHORS
charged-particle scattering losses in plastic and sodium iodide in, 20: 31542
efficiency in gamma-ray telescopes, Monte Carlo calculations for, 20: 31554
light attenuation in, 20: 31546
luminescence pulse forms for Naton 136, NE 102 A, and NE 213, (E), 20: 31529
performance of liquid-organic and monocrystalline, in gamma counters, 20: 31574
preparation and scintillation efficiency of liquid, using hexafluorobenzene and chlorine-substituted compounds, 20: 31290
preparation of plastic, with increased heat resistance, 20: 31262
preparation of smooth plates of plastic, without defects, 20: 31261
PHOSPHORUS
determination in conductive tissue of beef heart, activation, 20: 31176
determination in human heart tissue, activation, 20: 31175
effects on eutectic structure of aluminum–silicon systems, 20: 31716(R) (UCRL-16658, pp 121-32)
PHOSPHORUS FLUORIDES
enthalpy of formation of, 20: 31213(R) (ANL-7175, pp 119-58)
PHOSPHORUS ISOTOPES P-28
energy levels and mass from helium-3 reactions (He-3,t) with silicon-28 at 37.8 to 40.1 Mev, (E), 20: 32473
PHOSPHORUS ISOTOPES P-31
energy levels in, Nilsson model calculation of, 20: 32483
PHOSPHORUS ISOTOPES P-32
chemical properties of recoil, in neutron-irradiated sulfur, 20: 31295
determination of, efficiency of Cherenkov counting methods for, 20: 31184
incorporation in nucleoside 5' monophosphates, 20: 31307
radiation hazard from atmospheric, calculation of, 20: 31528
separation from mixtures with sulfur-35, 20: 31309
uptake and retention by man from Columbia River fish, 20: 30969 (BNWL-SA-45)
uptake by prostate gland of dogs, effects of carrier solution on, 20: 31149(R) (TID-22969)
uptake by urinary bladder of dogs, 20: 31149(R) (TID-22969)
PHOSPHORUS ISOTOPES P-33
production and uses of, 20: 31642 (ORNL-P-2190)
PHOSPHORYL CHLORIDES
effects on oxidation of graphite at 450 to 510°C, 20: 31667
PHOTOCHEMISTRY
flash photolysis of biological molecules, 20: 30974
luminescence from, spectrometer for analyzing, 20: 31481(T) (AERE-Trans-1050)
PHOTOCONDUCTIVITY
theory of visual receptor processes, 20: 30963
PHOTOELECTRIC CELLS
use in radiation dosimetry, 20: 31560
PHOTOGRAPHIC FILM DETECTORS
evaluation of, for personnel dosimetry in industrial defectoscopy, 20: 31464
use for personnel monitoring, 20: 31439 (AECL-2540)
PHOTOMULTIPLIER TUBES
light pipes for, optimum curve of rectangular, 20: 31818 (ITEF-385)
operation as amplifiers of h-f oscillations, 20: 31485
time resolution measurements of, 20: 31552
use in measuring track brightness in spark chambers, 20: 31582
PHOTONS
absorption by nuclei, Fermi liquid theory for, 20: 32539
angular correlation from polarized positron annihilation in ferromagnetic nickel, (E), 20: 32703
angular distribution from positron annihilation in liquefied gases, (E), 20: 32345
angular distribution from positron annihilation in liquid helium, (E), 20: 32346
detection and measurement of, sensitivity of analyzer for, 20: 31510 (N-65-33971)
effects on transistors, anomalous current production in, (E/T), 20: 31612 (SC-DC-66-1415)
exchange in meson (π)-meson (π) elastic interactions, (T), 20: 32011
interactions of massive, with vector-scalar coupling, 20: 32046
interactions with nucleons, mesons (ω) and (ρ) production in, (T), 20: 31984 (IC-66/54)
interactions with electrons, covariant notation for Compton, 20: 31993
interactions with electrons, Lorentz transformations for Compton, 20: 31994
interactions with electrons, analogy between Compton and Doppler effect in, 20: 31995
interactions with polarized electrons, circular polarization from Compton, (E/T), 20: 31998
interactions with deuterons, cross section for disintegration, (T) 20: 32004
interactions with nucleons, T violation in $N^*_{3/2}$ production in, (T), 20: 32020
interactions with protons at 0.9 to 1.3 Bev, meson (π^-) and N*(1238) production in, (E/T), 20: 31983 (CALT-68-71)
interactions with spin waves, (T), 20: 32735
interactions with nuclear Coulomb fields, cross section for two photon production in, (T), 20: 32031
interactions with nucleons, asymptotic behavior of amplitudes for elastic, (T), 20: 32032
interactions with deuterons, cross section for meson (π^0) production from elastic, (T), 20: 32041
interactions with protons, meson (π^0) production in, (T), 20: 32074
interactions with nucleons, high-energy theorem for Compton, 20: 32054
production in photon interactions with nuclear Coulomb field, 20: 32031
reactions (γ,π^-p) with carbon-12 at 670 and 700 Mev, angular correlations from, (E/T), 20: 32530
PHOTOSENSITIVITY
effects of antioxidants *Tetrahymena pyriformis*, 20: 31018
PHYSICAL CHEMISTRY
ligand field theory in, operator methods in, 20: 32734
PHYSICS
data analysis in low-energy, digital computers and multichannel analyzers for, 20: 31562
PHYTIC ACID, SODIUM SALTS
effects on strontium-90 excretion by rats, 20: 30977
PIGMENTS
photoconduction in visual, 20: 30963
PINCH EFFECT
charged-particle temperatures in theta, measurement using laser-beam scattering, (E), 20: 32621
model of hard-core, viscous effects in liquid conductor, 20: 32233
plasma kinetics in small theta, (T), 20: 32610
plasma properties from theta, numerical and space-time resolved methods for determining, 20: 32664

PIPES
light reflection in curved, analysis for total, (T), 20: 31818 (ITEF-385)
PITUITARY GLAND
effects on synthesis of corticosteroids in rats, 20: 31011
PLACENTA
radioisotope transfer mechanisms by, effects of inactive carriers on, 20: 31142
PLANETS
radio emission from Jupiter, application of cyclotron radiation emission to decametric, 20: 31870
PLANKTON
distribution and radioactivity in northeast Pacific Ocean, 20: 31448 (RLO-1725-15)
distribution and radioactivity in northeast Pacific Ocean, 20: 31450 (RLO-1725-17)
distribution and radioactivity in northeast Pacific Ocean, 20: 31451 (RLO-1725-18)
distribution and radioactivity in northeast Pacific Ocean, 20: 31452 (RLO-1725-19)
distribution and radioactivity in northeast Pacific Ocean, 20: 31449 (RLO-1725-16)
PLANT METABOLISM
radiation effects on seedling, x, 20: 31115
radiation effects on pear tissue, γ, 20: 31633
PLANT RESPIRATION
radiation effects on seedling, x, 20: 31115
radiation effects on pear tissue, γ, 20: 31633
PLANTS
radiation effects on mutations of economically important, 20: 31109
radiation effects on jute, genetic γ, 20: 31027 (AECD/AG-14)
radiation effects on growth and pigmentation of cucumber, long- and short-wave uv, 20: 31059
radiation effects on growth of Kalanchoe, effects of air, carbon dioxide, and nitrogen atmospheres on x, 20: 31076
radioinduced chromosome aberrations in Vicia, 20: 31124
radioisotope uptake from air by, 20: 31142
strontium-85 uptake and retention by leaves of, effects of relative humidity and temperature on, 20: 30996
strontium-90 uptake by, effects of calcium content and mechanical properties of soil on, 20: 30985
PLASMA
accelerator for, performance of cylindrical traveling wave, 20: 32653
accelerators for, propellant injection devices for coaxial, 20: 31363
atom-electron collisions in cesium, cross sections for, (E), 20: 32646
book: *Physics of High Temperature Plasmas*, 20: 32641
charged-particle motion in, density wake from, (T), 20: 32589
charged-particle motion in, energy loss rate of, (T), 20: 32617
charged-particle temperature measurements in theta-pinch, using laser beam scattering, 20: 32621
containment by magnetic mirrors, first order correction to first adiabatic invariant for, (T), 20: 32669
current density in, design and development of Rogowski coil probes for measuring, 20: 32574 (N-65-32035)
current measurement through electrodes in, 20: 32631
cyclotron harmonic wave propagation in, excitation of, (T), 20: 32630
cyclotron harmonic radiation from, in magnetic field, (E/T), 20: 32637
cyclotron radiation emission from cold magnetoactive, in forward sub-luminous mode, 20: 31870
density and temperature profiles of, electrostatic probe method for measuring, (T), 20: 32662
deuteron acceleration in mixed, 20: 32586
diagnostics in repetitively pulsed coaxial accelerator, 20: 32650
diagnostics of anisotropic, using turnstile multiple-probe polarimeters, 20: 32581
diagnostics of argon arc, using laser scattering, (E), 20: 32599
diagnostics of closed-loop MPD cell, 20: 31975
diagnostics of, tracer techniques for determination of electron fixation on electronegative gas for, 20: 32223
diagnostics using lasers, 20: 32598
diffusion across magnetic fields, relation to decay along field, (E/T), 20: 32647
diffusion in Q devices, end plate effects on, (T), 20: 32611
diffusion of metastable helium atoms in cryogenic, 20: 32602(T)
electric conductivity of, eddy-current type probe for measuring, 20: 32668
electromagnetic wave diffraction by conducting half-plane in, (T), 20: 32580
electromagnetic wave diffraction by, plasma density and column diameter from, (T), 20: 32585
electromagnetic wave reflection on boundary of vacuum with, 20: 32588
electromagnetic wave propagation in relativistic electron, stability of, 20: 32606
electromagnetic wave propagation in space dispersive, absorption cross sections and fluctuation scattering of, (T), 20: 32613
electromagnetic wave propagation in inhomogeneous electron, forward scattering corrections for, (T), 20: 31857
electromagnetic wave propagation in stratified, across inhomogeneous magnetic field, (T), 20: 32625
electromagnetic wave reflection from magneto, vertically polarized, (T), 20: 32627
electromagnetic wave propagation in, nonlinear, 20: 32663
electron and ion density distribution in, contained in magnetic mirror machines, (T), 20: 32609
electron beam interactions with, microwave incoherent scattering by unstable oscillations from, (E), 20: 32622
electron beam interactions with, anomalous diffusion from, 20: 31645(R) (AD-627094)
electron density measurement in pulsed, probe method for, 20: 32597
electron diffusion in low-density, anomalous, 20: 32612
electron distribution in homogeneous Lorentz, nonlinear effects on, 20: 32584
electron wave propagation in, Landau damping of, 20: 31645(R) (AD-627094)
electron-ion recombination in dense, limits of validity of radiationless, 20: 32575 (NASA-TN-D-3372)
energy of, virial expansions for free, 20: 32635
entropy during equilibrium, calculation of statistical, (T), 20: 32583
flow of, nonstationary axisymmetric MHD, (T), 20: 32231
flow of collisionless, in aligned magnetic field, (T), 20: 32649
hydromagnetic wave propagation in warm collisionless, structure of, (T), 20: 32577 (NYO-1480-54)
hydromagnetic wave propagation in cold, looping trajectories in, (T), 20: 32607
interactions with dipole magnetic fields, solar wind–magnetosphere phenomena simulation from, 20: 32284
ion acceleration in low-density, anomalous, 20: 32612
ion acoustic wave propagation in column, boundary effects on, (T), 20: 32618
ion acoustic wave propagation in hot electron, with cold ion streams, 20: 32654
ion beam interactions with, stability limits for longitudinal waves in, (T), 20: 32608
ion surface waves in bounded low-pressure discharge, 20: 32620
ionization density in hydrogen, methods for calculating, 20: 32628
ionization equation for optically thin, (T), 20: 32636
kinetic equations for multicomponent, generalization for Bogoliubov, 20: 32605
kinetic equations for homogeneous nondegenerate fully ionized, linearized Fokker-Planck, 20: 32643
light scattering by, analysis of nonlinear incoherent, (T), 20: 32572 (IPP-6/49)
magnetic neutral point in, study of, 20: 32656
magnetoacoustic wave propagation in flowing, (E/T), 20: 32651
microwave incoherent scattering by unstable electron oscillations in, (E), 20: 32622
microwave propagation in pure air, 20: 32667
microwave radiation from, selective receiver for, 20: 32626
motion in weakly ionized gas with strong magnetic field, (T), 20: 32645
motion of interplanetary streams of, bistatic radar measurements of, 20: 31856
oscillations in inhomogeneous, Landau damping of, (T), 20: 32616
oscillations in, electron avalanche energy losses to, 20: 32727(T)
particle losses in axisymmetric and multipolar magnetic fields, nonadiabatic, (E/T), 20: 32545
performance of cesium thermionic converter, operating in ignited mode, (E/T), 20: 31968
pinch effect in, particle temperatures and radiative energy losses in theta, (T), 20: 32610
potential measurements in, use of wide-band electrostatic probes for, 20: 32632
pressure distribution in current-carrying, stagnation, 20: 32660
pressure elevation in hydrogen arc discharge, in axial magnetic field, (E), 20: 32638
production and control of, MHD plant for, 20: 32633
production by laser beams, 20: 32666
production in laser beam reactions with argon gas, (E), 20: 32665
production of highly ionized, anode-cathode feed of hollow-cathode arc for, 20: 32600
production of high-density, by arc spots, (T), 20: 32648
production of low-pressure, performance of r-f power oscillator for, 20: 32570 (D-1-82-0522)
properties and uses of, 20: 32587
properties in reversed-current cesium-electron bombardment ion engine, 20: 31372
properties in uniform guide field from theta-pinch accelerator, electric probe measurements of, 20: 32661
properties of h-f discharge, in magnetic field, (E), 20: 32634

properties of positive-column glow-discharge, effects of small impurities on, (T), 20: 32595
properties of thermionic converter, 20: 31971
properties of theta pinch, numerical and space-time resolved methods for determining, 20: 32664
properties of, microscopic, (T), 20: 32572 (IPP-6/49)
radiation effects on luminescence of embryos of barley, γ, 20: 31020
relaxation in potassium-seeded argon and nitrogen, to steady state, 20: 32657
shock propagation in, high-field steady-state, (T), 20: 32604
shock structure in, radiative, (E/T), 20: 32670
shock wave propagation in collisionless, (T), 20: 32652
spectra source function of optically dense inhomogeneous layer of, using Ritz variational method, 20: 32594
stability in pulsed-toroidal discharges, (E), 20: 32578(R) (TID-23025)
stability of anisotropic hydrogen, h-f, (E), 20: 32624
stability of guiding center, (T), 20: 32576 (NYO-1480-50)
stability of, magnetic field minimum as criterion for, (T), 20: 32623
stability of Poiseuille arc, in axial magnetic field, (E/T), 20: 32614
stability of, sub-threshold study of azimuthal modes of Kadomtsev, (E), 20: 32579
stability of uniform, composed of streams, (T), 20: 32629
stability theory for, solutions of differential equations in, 20: 32640
theory of thermionic ignited-mode, with electron temperature variations, 20: 31974
thermodynamics of nonextensive systems of, statistical, 20: 32237
vortices in, rotational-velocity and ion-density profiles in, (E), 20: 32644
wave excitation in hot compressible, electro-acoustic lateral, (T), 20: 32590
wave propagation in isotropic compressible, electro-acoustic spectrum for, (T), 20: 32591
wave propagation in inhomogeneous column of, l-f, (T), 20: 32601
wave propagation in inhomogeneous, at singular turning points, (T), 20: 32619
wave propagation in rarefied, effect of Coriolis force on, (T), 20: 32603

PLASMA JETS
analysis of Hall-current produced, (T), 20: 32573 (N-65-12780)
design and performance of pulsed-generator, with laser source, 20: 32639
electron-heavy particle nonequilibrium in partially ionized, 20: 32658
for producing high-peak electron currents, 20: 31486
particle velocities in, Doppler effect measurements of, 20: 32659
performance of cylindrical traveling wave, 20: 32653
performance of electric-arc, 20: 31356 (N-66-12435)
performance of, with interelectrode insert, 20: 32592
properties of argon electrodeless discharge, probe measurements of, 20: 32655

PLASTICS
dielectric breakdown in uniform electric fields, 20: 32692
preparation of scintillators of, with increased heat resistance, 20: 31262
preparation of smooth scintillator plates of, without defects, 20: 31261
radiation effects on, review of, 20: 31267 (BNWL-SA-658)
radioinduced combination of, with wood, economic aspects of, 20: 31624 (BNWL-261)
radioinduced combination of, with wood, economic aspects of, 20: 31625 (NYO-3569-1)
uses of, in Hanford production and research facilities, review of, 20: 31267 (BNWL-SA-658)
Pb–plastic, use as radiation shielding, 20: 32680

PLATES
penetration by projectiles, analysis for, (E/T), 20: 32744 (SRIA-1)

PLATINUM
hydrogen atom and ion reactions at 10 to 40 kev, secondary electron emission from, (E), 20: 31533
performance as ionizer material in cesium-contact ion thrustors, 20: 31383
proton reactions at 0.05 to 2.9 Bev, induced activity data and cross sections for spallation, (E/T), 20: 32549
proton reactions at 40 Mev to 25 Bev, lithium isotopes from, (E), 20: 31205
radiation effects on electric conductivity of, stage IV recovery from electron, (E), 20: 31800
surface structures on faces of single-crystal, 20: 32684(R) (UCRL-16658, pp 21-38)
use of foils of, in plutonium autoradiography, 20: 31212
vaporization from probe surface in electric arcs, (E), 20: 32593

PLATINUM ALLOYS
Au–Pt, fracture mechanisms of, 20: 31716(R) (UCRL-16658, pp 121-32)
Fe–Pt, magnetic properties of fcc, 20: 32739
Ir–Pt, elastic properties at 23°C, 20: 31748
Pt–Ta, phase diagram, 20: 31669

PLATINUM ISOTOPES
alpha decay, (E), 20: 32458
production of alpha-active, in oxygen-16 reactions (O-16,xn) with ytterbium isotopes, (E), 20: 32458
production of alpha-active, in fluorine-19 reactions (F-19,xn) with thulium isotopes, (E), 20: 32458
production of alpha-active, in neon-20 reactions (Ne-20,xn) with erbium isotopes, (E), 20: 32458

PLATINUM ISOTOPES Pt-195
Mössbauer effect in cobalt, iron, and nickel, g-factor and internal fields from, (E), 20: 32487

PLOWSHARE PROJECT
air blast and seismic waves from SULKY in, 20: 31393 (PNE-711F)
excavation of sea-level Isthmian canal, devices and economics for, 20: 31336

PLUTONIUM
creep properties of high-purity, steady-state, 20: 31666
deposition and removal in wounds, 20: 31030 (BNWL-SA-39)
deposition through wounds, evaluation of, 20: 31030 (BNWL-SA-39)
determination of, using colored glass filters, differential spectrophotometric, 20: 31170 (ISO-SA-16)
distribution in irradiated plutonium dioxide–uranium dioxide fuel, 20: 31804
distribution in plutonium oxide–uranium oxide pellets, autoradiography of, 20: 31212
effects of inhaled, in dogs, 20: 31025 (AD-631690)
oxidation-reduction reactions of, bibliography on kinetics of, 20: 31215 (LA-3507)
performance of molten fuels of, fast transients in, 20: 32797 (LA-DC-7748)
phase transformation in, mechanism of beta-to-alpha, 20: 31666
phase transformations in, effects of stress on alpha-beta, 20: 31666
polarographic behavior of, in sulfuric acid solutions, 20: 31302
separation from irradiated urania fuels by fluoride volatility processes, 20: 31315(R) (ANL-7175, pp 42-103)
separation of, from molten uranium by extraction using fused chlorides, 20: 31314(R) (ANL-7175, pp 1-41)
solubility of, in copper–magnesium alloys and magnesium–zinc alloys, 20: 31314(R) (ANL-7175, pp 1-41)
solvent properties for rhenium and tantalum at 700 to 950°C, 20: 31666

PLUTONIUM ALLOYS
Ce–Co–Pu, corrosive effects on carburized and noncarburized tantalum alloys, 20: 31679(R) (LA-3524)
Ce–Co–Pu, corrosive effects on niobium alloys, effects of carbon on, 20: 31679(R) (LA-3524)
Ce–Co–Pu, irradiation testing of molten, reactor performance for, 20: 32799 (LA-DC-7752)
Ce–Co–Pu, performance in fast breeder reactors, 20: 32798 (LA-DC-7550)
Ce–Pu, viscosity to 875°C, 20: 31666
Mg–Pu, phase studies, 20: 31314(R) (ANL-7175, pp 1-41)
Mg–Pu–Zn, liquid miscibility of, at high temperatures, 20: 31314(R) (ANL-7175, pp 1-41)
Pu–Th, economics for thermal reactors, 20: 32822
Pu–Th–U, compatibility with chromium, type 304 stainless steel, and vanadium–20 titanium, 20: 31666
Pu–Ti–U, mechanical properties and phase diagram of, 20: 31666
Pu–U–Zr, compatibility with type 304 stainless steel to 800°C, 20: 31666
Pu–U–Zr, mechanical properties and phase diagram of, 20: 31666

PLUTONIUM CARBIDES
processing of irradiated, flowsheets for pyrochemical, 20: 31314(R) (ANL-7175, pp 1-41)
O–PuC–UC, stability as fast reactor fuel, 20: 31675
PuC–UC, compatibility with type 316L stainless steel up to 900°C, 20: 31675
PuC–UC, compatibility with nickel-base alloys, 20: 31675
PuC–UC, fabrication of fuel elements of, 20: 31675
PuC–UC, preparation of, by hydrocarbon–metal reactions, 20: 31213(R) (ANL-7175, pp 119-58)
PuC–UC, properties as fast reactor fuel, 20: 31675
PuC–UC, temperature distributions in irradiated, 20: 32791 (NAA-SR-Memo-11731)
PuC–UC, thermal conductivity of, effects of nickel sintering aid on, 20: 31666

PLUTONIUM COMPOUNDS
fluorination of, kinetics of, 20: 31214 (CEA-R-2859)

PLUTONIUM(IV) FLUORIDES
fluorination of, kinetics of, 20: 31214 (CEA-R-2859)

PLUTONIUM(VI) FLUORIDES
separation from cell exhaust air by hydrolysis, 20: 31315(R) (ANL-7175, pp 42-103)
PuF_6–UF_6, phase studies, 20: 31315(R) (ANL-7175, pp 42-103)

PLUTONIUM IONS
radioinduced oxidation of trivalent to tetravalent, self-, 20: 31302

PLUTONIUM ISOTOPES Pu-238
production in power reactors, fuel cycle for, 20: 32837
use in Manned Orbital Research Laboratory propulsion system, 20: 31387
PLUTONIUM ISOTOPES Pu-239
distribution of inhaled aerosol of, in dogs, 20: 30968 (BNWL-SA-11)
gamma spectra, 20: 31500(R) (BNWL-235-4, pp 4-10)
neutron Doppler coefficients for Zebra and ZPR VI, (T), 20: 32869
neutron resonance cross sections for, 20: 32551
neutron resonance parameters for, resolved p- and s-wave, 20: 32551
PLUTONIUM ISOTOPES Pu-240
neutron resonance absorption in, in heavy water-moderated organic-cooled reactor lattices, (T), 20: 32785
PLUTONIUM ISOTOPES Pu-241
alpha half life of, (E), 20: 32435
PLUTONIUM NITRATES
denitration of, for preparation of oxide microspheres by sol-gel process, 20: 31689 (ORNL-P-2159)
deposition of, electrolytic, 20: 31670
PLUTONIUM NITRIDES
thermal expansion at 20 to 1000°C, coefficient of, 20: 31666
vapor pressure at 1250 to 1550°C, 20: 31666
PuN–UN, thermal expansion at 20 to 1000°C, coefficient of, 20: 31666
PLUTONIUM OXIDES
fluorination of, kinetics of, 20: 31214 (CEA-R-2859)
Ga–Pu, mechanical recovery in, effects of prestrain on, 20: 31753
PLUTONIUM(IV) OXIDES
preparation of microspheres of, by sol-gel process, 20: 31689 (ORNL-P-2159)
processing of irradiated, flowsheets for pyrochemical, 20: 31314(R) (ANL-7175, pp 1-41)
Al–PuO_2, fabrication and properties of dispersion fuels of, 20: 31666
PuO_2–stainless steel, fabrication of dispersion fuels of, process for, 20: 31666
PuO_2–stainless steel, radiation effects on, effects of sample density on, 20: 31666
PuO_2–ThO_2, preparation of microspheres of, by sol-gel process, 20: 31689 (ORNL-P-2159)
PuO_2–UO_2, burnup in reactor fuel pins, 20: 32836
PuO_2–UO_2, diffusion and segregation in, 20: 31440(R) (ANL-7175, pp 159-83)
PuO_2–UO_2, fluorination and oxidation of, in fluid beds, effects of cesium fluoride on, 20: 31315(R) (ANL-7175, pp 42-103)
PuO_2–UO_2, plutonium and fission-product distributions in irradiated, 20: 31804
PuO_2–UO_2, preparation of microspheres of, by sol-gel process, 20: 31689 (ORNL-P-2159)
PuO_2–UO_2, properties of, as reactor fuel, effect of stoichiometry on, 20: 31674
PuO_2–UO_2, temperature distributions in irradiated, 20: 32791 (NAA-SR-Memo-11731)
POLARISCOPES
use of turnstile multiple-probe, for anisotropic diagnostics plasma, 20: 32581
POLAROGRAPHY
of binary electrolytes, 20: 31220(R) (UCRL-16658, pp 39-72)
POLONIUM ISOTOPES Po-210
content in tobacco in New Zealand, 1965, 20: 31446(R) (NP-16015)
determination in human urine, radiochemical, 20: 31187
effects on spermatogenesis in mouse testes, 20: 31063
use in Manned Orbital Research Laboratory propulsion system, 20: 31387
POLYCYTHEMIA
nucleic acid synthesis in cultures from patients with, 20: 30971 (ORINS-45)
protein synthesis in cultures from patients with, 20: 30971 (ORINS-45)
POLYMERIZATION
hydrolytic mechanisms of chromic ion, 20: 31218(R) (UCRL-16658, pp 1-9)
radioinduced solid-state, of acrylic monomers and crotonic acid, 20: 31287
radioinduced, review of Japanese research on, 20: 31269(T) (NSJ-tr-56)
POLYMERS
radiation effects on, review of Japanese research on, 20: 31269(T) (NSJ-tr-56)
radioinduced formation of, review of Japanese research on, 20: 31269(T) (NSJ-tr-56)
POLYSACCHARIDES
radiation resistance of aqueous jellies of agarose, effects of food colorings on, 20: 30998 (BNWL-SA-709)
POPULATIONS
control of *Ceratitis capitata*, by release of irradiated males, 20: 31109
control of *Dacus tryoni*, by release of irradiated males, 20: 31109
control of Tephritid fly (*Dacus cucurbitae*), by release of sterile male, 20: 31046
radiation dose to Guarapari, Brazil, 20: 31463
radiation dose to, in Guarapari, Brazil, 20: 31470
radiation effects on live births among atomic bomb survivors of Hiroshima and Nagasaki, 20: 31091
PORTLAND CEMENTS
shielding properties of iron–serpentine, neutron, 20: 32677
POSITRONIUM
production and annihilation in polystyrene, thermal neutron effects on, (E), 20: 32704
production in ionic crystals, (E), 20: 32099
POSITRONS
annihilation in argon, calculations of, 20: 32105
annihilation in ferromagnetic nickel, angular correlations from polarized, (E), 20: 32703
annihilation in liquefied gases, angular distribution of photons from, (E), 20: 32345
annihilation in liquid helium, angular distribution of photons from, (E), 20: 32346
annihilation of, physics of, 20: 32101
interactions with electrons, differential cross sections for baryon resonance production in, (T), 20: 32018
interactions with electrons at high energies, electron anapole effects on polarization from, (T), 20: 32070
interactions with electrons at high energies, anapole effects on meson (μ) pair production in annihilation, (T), 20: 32070
interactions with electrons, neutral vector boson propagator in, 20: 32093
lifetime in ionic crystals, anomalous long, (E), 20: 32099
scattering by argon, calculation of elastic cross sections for, 20: 32105
scattering by hydrogen, coupled equations for rearrangement, 20: 32388
POTASSIUM
content in Finnish Lapps, 1966 whole-body, 20: 31444 (CONF-660405-15)
determination in conductive tissue of beef heart, activation, 20: 31176
determination in human heart tissue, activation, 20: 31175
heat transfer and thermal fluxes of boiling, in tubes, 20: 31347
radiative lifetime of excited electronic states in, 20: 31219(R) (UCRL-16658, pp 11-20)
rare-gas reactions with, ionization cross sections for excited, (T), 20: 31917
thermodynamic properties of liquid, Prandtl number at 0 to 700°C for, 20: 31724
use of liquid, in thermionic cells, 20: 31969
POTASSIUM ALLOYS
K–Na, thermodynamic properties, 20: 31213(R) (ANL-7175, pp 119-58)
K–Na, thermodynamic properties of liquid, Prandtl number at 0 to 700°C for, 20: 31724
POTASSIUM BROMIDES
color centers in crystalline, properties of U, 20: 32683 (ORNL-P-2194)
potassium ion reactions at 1 to 6 kev, angular dependence of secondary emission coefficients for, 20: 31938(T)
radioinduced F-center formation in, temperature dependence of x, 20: 32724(T)
POTASSIUM CHLORATES
radioinduced absorption bands in, uv and x, 20: 32686
POTASSIUM CHLORIDES
color centers in crystalline, properties of U, 20: 32683 (ORNL-P-2194)
electron emission from transmission dynodes of, attenuation length for secondary, 20: 31916
radioinduced F-center formation in, temperature dependence of x, 20: 32724(T)
Cu–$MgCl_2$–KCl–NaCl, corrosive effects on ferrous alloys, 20: 31314(R) (ANL-7175, pp 1-41)
POTASSIUM HYDROXIDES
properties of aqueous films of, optical studies on, 20: 31220(R) (UCRL-16658, pp 39-72)
POTASSIUM IODATES
radiation effects on, oxidation and reduction of recoil iodine-131 from proton, 20: 31298
POTASSIUM IODIDES
color centers in crystalline, properties of U, 20: 32683 (ORNL-P-2194)
lattice oscillations in, dispersion relation for normal-mode, (E), 20: 32710
neutron inelastic scattering by, dispersion relation for normal-mode vibrations from, (E), 20: 32710
radioinduced F-center formation in, temperature dependence of x, 20: 32724(T)
POTASSIUM IONS
desorption from tungsten surfaces, mass spectrometric study of, 20: 31907
reactions with potassium bromide single crystals at 1 to 6 kev, angular dependence of secondary emission coefficients for, 20: 31938(T)

POTASSIUM ISOTOPES K-40
determination of, efficiency of Cherenkov counting methods for, 20: 31184
POTASSIUM ISOTOPES K-42
determination of, efficiency of Cherenkov counting methods for, 20: 31184
POTASSIUM YTTRIUM MOLYBDATES
gadolinium ion EPR in crystals of, trivalent, 20: 32728(T)
POTATOES
radiation effects on quinone formation in, quantitative regularities in gamma, 20: 31001
POTENTIOMETERS
design of, for ocean-bottom operation, 20: 31220(R) (UCRL-16658, pp 39-72)
POWDER METALLURGY
fabrication method for, 20: 31707(P)
POWDERS
neutron diffraction analysis in, time-of-flight method for, 20: 32701
POWER CYCLES
development of Brayton, for Manned Orbital Research Laboratory power generation, 20: 31387
POWER PLANTS
economics of, calculation method for, 20: 32814
POWER REACTORS
coolant from, use in soil heating, 20: 32843
design and evaluation of molten-salt breeder, 20: 32805(R) (ORNL-3936, pp 172-92)
development of German, 20: 32844
economics and performance of thorium-fueled, 20: 32834
fuel cycle for production of neptunium-237 and plutonium-238, 20: 32837
fuel processing methods for molten-salt breeder, 20: 32806(R) (ORNL-3936, pp 193-211)
fuels for Brazilian, possibilities of thorium, 20: 32821
fuels for German, utilization of thorium, 20: 32824
fuels for Italian, economics of thorium–uranium, 20: 32827
fuels for Japanese, utilization of thorium, 20: 32828
fuels for Swedish, utilization of thorium-232–uranium-233, 20: 32830
fuels for thermal, performance of thorium, 20: 32822
fuels for, role of thorium, 20: 32826
safety systems for gas-cooled graphite-moderated, 20: 32835
POWER SUPPLIES
design for radiation detectors for aerospace applications, 20: 31609
design of constant-current, for instrument calibration, 20: 31588
design of parallel and series, for spark chambers, 20: 31571
performance of r-f for low-pressure plasma production, 20: 32570 (D-1-82-0522)
PRASEODYMIUM
toxicity in laboratory animals, 20: 30970 (COO-1170-5)
PRASEODYMIUM ALLOYS
Ni–Pr, magnetic properties of intermetallic compounds of, 20: 32699
Pr–Zn, melting point of $PrZn_2$, 20: 31743
PRASEODYMIUM COMPOUNDS
phase studies of, with group V elements, 20: 31723
PRASEODYMIUM FLUORIDES
energy levels in, coupling of negative hydrogen- and deuterium-ion localized modes to, (E), 20: 32709
PRASEODYMIUM ISOTOPES Pr-141
determination in fission products, neutron activation, 20: 31167(R) (ANL-7175, pp 217-25)
energy level transitions from cerium-141 decay, conversion coefficients for, (E), 20: 32443
neutron reactions (n,γ) at 10 kev to 3 Mev, cross sections for, (E), 20: 32370(R) (ANL-7175, pp 212-16)
PRASEODYMIUM ISOTOPES Pr-144
deposition on tropospheric aerosols, 20: 31459
PRASEODYMIUM MOLYBDATES
preparation and crystal structure of, 20: 31740
PRASEODYMIUM PHOSPHIDES
enthalpy-composition function of, mass spectrometric determination of, 20: 31723
PRASEODYMIUM TUNGSTATES
preparation and crystal structure of, 20: 31740
PRESSURE
effects on phase transformations of rare earth sesquioxides, 20: 31258
PRESSURE GAGES
design of high-temperature differential transducer, 20: 31491
PRESSURE VESSELS
development of prestressed concrete, 20: 32750
development of titanium, for NERVA reactors, 20: 32856
fabrication and testing of reactor, 20: 31703
rupture of reactor, missile generation in, (T), 20: 32752
shield plug for, design of, 20: 32758(P)
stress analysis of, using epoxy models, 20: 32751
PROCESS HEAT REACTORS
development of German, 20: 32844
economics for electric power generation and water desalination, 20: 32846
use for desalination, review of, 20: 32845
use in Greece, dual-purpose, 20: 32848
uses for desalination of sea water and ammonia fertilizer production, economics of, 20: 32841 (ORNL-3882)
PROMETHIUM ISOTOPES Pm-147
content in ocean surface waters, 1960 and 1961, 20: 31419
neutron total cross sections for, (E/T), 20: 32376 (KAPL-3090)
use in Manned Orbital Research Laboratory propulsion system, 20: 31387
PROMETHIUM ISOTOPES Pm-148
neutron total cross sections for, (E/T), 20: 32376 (KAPL-3090)
PROPANE
ionization of, by electrons at 0.6 to 20 kev, cross sections for, (E/T), 20: 31906
mass spectra, 20: 31198
1-PROPANOL, 3,3'-(METHYLIMINO)DI-, DIMETHANESULFONATE
preparation of carbon-14-labeled, method for, 20: 31308
PROPENE POLYMERS
radiation effects on tensile strength of films of, gamma and uv, 20: 31274
PROPERDIN
radiation effects on, in dogs, γ and x, 20: 31013
PROPIONIC ACID, URANIUM SALTS
preparation and chemical properties of, 20: 31236
PROPIOPHENONE, p-AMINO-
radiosensitivity effects of, relation between cellular anoxia and, 20: 31122
PROPORTIONAL DETECTORS
design for beta counting, 20: 31509 (EIR-97)
design of boron trifluoride, for integrated neutron fluxes, 20: 31786(R) (ORO-2891-5)
design of gas-flow, for electron-probe light-element analysis, 20: 31589
performance for radiation measurements in space, 20: 31610
performance for soft x-ray spectrometry, 20: 31544
performance for soft x-ray spectrometry, 20: 31545
performance of boron trifluoride, for fast neutron dosimetry, 20: 31561
performance of xenon, for x-ray fluorescence and electron microprobe analyses, 20: 31591
performance of 4π, for soft beta particles from solid sources, 20: 31548
PROPULSION
economic aspects of nuclear, for ships, 20: 32854
electric systems for space, reliability of, 20: 31359
electric systems for space, design of solar powered, 20: 31373
electric systems for space, feasibility of solar power, 20: 31382
electrostatic systems for space, power conversion system for, 20: 31384
geomagnetic thrustor for, development of, 20: 31377
ion engine for space, plasma properties in reversed-current cesium-electron bombardment, 20: 31372
ion engine for space, design of cesium, 20: 31378
ion engine for space, tungsten ionizer structures for cesium, 20: 31381
ion engines for space, power-conditioning systems for, 20: 31357
ion engines for space, testing of, 20: 31358
ion engines for space, power conditioning for contact-ionization, 20: 31360
ion engines for space, development of lightweight, 20: 31364
ion engines for space, development and long-life performance of cesium-contact, 20: 31366
ion engines for space, life testing of electron-bombardment cesium, 20: 31367
ion engines for space, development of electron bombardment-liquid mercury cathode, 20: 31368
ion engines for space, beam deflection for thrust vector control in, 20: 31369
ion engines for space, development of surface ionization, 20: 31370
ion engines for space, development of porous ionizer material for, 20: 31375
ion engines for space, anode losses in Halc-current accelerators in, 20: 31376
ion engines for space, surface tension and feed systems for, 20: 31379
ion engines for space, alloy and metal ionization efficiencies in, 20: 31386
ion microthrustor development for satellite control, 20: 31362
ion thrustor for space, evaluation of two-directional electron-bombardment, 20: 31380
ion thrustors for space, design of mercury electron-bombardment, 20: 31371
ion thrustors for space, durability tests of mercury electron-bombardment, 20: 31374
ion thrustors for space, electrode materials for cesium contact, 20: 31383

ion thrustors for space, characteristics of micropound, 20: 31385
ion thrustors for space, porous metals for cesium-contact, 20: 31389
plasma engine for space, steady-state operation of coaxial pulsed two-stage, 20: 31365
plasma engines for, propellant injection devices for, 20: 31363
radiation hardening of electronic equipment for ion, 20: 31618
systems for space, using radioisotopes for propellant heating, 20: 31361
systems for space, electric and nuclear, 20: 31387

PROPYLENE OXIDE POLYMERS
purification of atactic and isotactic, 20: 31268(R) (COO-1088-20)

PROSTATE GLAND
phosphorus-32 absorption by dog, effects of carrier solution on, 20: 31149(R) (TID-22969)

PROTACTINIUM
deposition of, on gold-plated copper, tracer studies of electrolytic, 20: 31243
separation from beryllium fluorides and lithium fluorides, 20: 32804(R) (ORNL-3936, pp 122-71)
sorption by glass, tracer studies of, 20: 31243

PROTEINS
analysis for iodine, neutron activation, 20: 31173 (SGAE-BL-18/1966)
labeling with technetium-99m, 20: 31265
metabolism of plasma, tracer study using stable brominated proteins and activation analysis, 20: 30990
radiation effects on heme, 20: 30999(R) (UCB-34P95-7)
synthesis in cultured bone marrow cells from patients with leukemia, myeloma, or polycythemia, tracer study, 20: 30971 (ORINS-45)

PROTON BEAMS
extraction from synchrotrons, field nonlinearity in lenses for, (T), 20: 31836
production of polarized, 20: 31835
separation of antiproton and meson (K) beams from, 20: 31841

PROTON SPECTRA
determination for Lunar and Martian space missions, (T), 20: 32674 (NP-15697(Vol.3))

PROTONS
acceleration of low altitude auroral, 20: 32249
angular distributions from deuteron reactions (d,p) with nuclei at 11 and 13 Mev, angular-momentum-effects on, (E), 20: 32512
distribution in Van Allen belts at 0.17 to 3.4 Mev, 20: 32250
dosimetry in monkeys (*Macaca mulatta*), 20: 31096
dosimetry in tissue-equivalent phantoms, 20: 31467
dosimetry of, computer program for, 20: 32674 (NP-15697(Vol.3))
effects on enzyme activity in monkeys, 20: 31105
effects on *Macaca mulatta*, physiological, 20: 31104
effects on mice, biological, 20: 31100
effects on mice, biological, 20: 31102
effects on monkeys, biological, 20: 31106
effects on monkeys, pathological, 20: 31097
effects on monkeys, pathological, 20: 31098
effects on monkeys, pathological, 20: 31099
effects on monkeys, pathological, 20: 31101
effects on monkeys, pathological, 20: 31103
effects on potassium iodate, oxidation and reduction of recoil iodine-131 from, 20: 31298
effects on thin film cadmium sulfide and single crystal silicon solar cells, 20: 31616
effects on tissues, biological, 20: 31095
electron capture in hydrogen, cross section for, (T), 20: 31901 (N-65-34224)
energy spectra in tail of magnetosphere, 20: 32252
flux distribution in magnetosphere, determination of, 20: 32674 (NP-15697(Vol.3))
flux in transition zone of magnetosphere, (E), 20: 32280
flux in Van Allen belts, for space vehicle environment, 20: 32244 (N-66-13126)
flux variations in solar wind, periodic, (E), 20: 31885
intensity distribution in geomagnetic fields, (T), 20: 32292
interactions with mesons (K^-) at 1.455 Bev/c, K^* resonance production in, (E), 20: 31987 (NP-16097)
interactions with protons at 48 Mev, bremsstrahlung production cross sections for, (E), 20: 31997
interactions with neutrons, cross sections for deuteron formation in, (T), 20: 32004
interactions with polarized protons at 600 Mev, polarization and spin correlation parameters from, (E), 20: 32016
interactions with mesons (π), absorptive correction to peripheral model for, 20: 32022
interactions with mesons (K^-) at 1.05 to 1.7 Bev/c, hyperon (Ξ^0) properties from, (E/T), 20: 31988 (UCRL-11510)
interactions with protons at 3 to 7 Bev/c, cross sections for elastic, (E), 20: 31989 (UCRL-16275)
interactions with mesons (K^-) at 1.2 to 2.7 Bev/c, cross sections for, (E/T), 20: 31990 (UCRL-16648)
interactions with mesons (π^-) at 1035 to 1170 Mev/c, meson (K^0) production in, (E), 20: 31991 (UCRL-16771)
interactions with photons at 0.9 to 1.3 Bev, mesons (π^-) and N*(1238) production in, (E/T), 20: 31983 (CALT-68-71)
interactions with protons at 24 Bev/c, multiple meson (π) production from, (E), 20: 32017
interactions with antiprotons at high energies, uncorrelated jet model for elastic, 20: 32028
interactions with electrons, nucleon electromagnetic form factors for, (T), 20: 32033
interactions with antiprotons, nucleon electromagnetic form factors for, 20: 32033
interactions with neutrinos at very-high energies, cross sections for, (T), 20: 32036
interactions with electrons at 593 Mev, cross section for meson (π^0) production in, (E/T), 20: 32038
interactions with protons, $pp\pi^+$ enhancement (2.52 Bev/c²) from, (E/T), 20: 32040
interactions with antiprotons, branching ratios for annihilation, (T), 20: 32045
interactions with antiprotons, Dalitz plot density for $\pi\bar{k}k$ final state from, 20: 32047
interactions with neutrons, direct and charge-exchange, (T), 20: 32048
interactions with bremsstrahlung at 600 to 1000 Mev, cross sections for meson (π^0) production in, (E), 20: 32051
interactions with mesons (K^-), decay angular correlation for Y_1^{*-} from, (T), 20: 32052
interactions with antiprotons, SU_{6W} predictions for, 20: 32056
interactions with antiprotons, (ω-ϕ) mixing angle from, (E/T), 20: 32058
interactions with protons, cross sections for bremsstrahlung production in, (T), 20: 32059
interactions with protons of 204 Mev, bremsstrahlung emission in, (E), 20: 32062
interactions with antiprotons and protons, vector meson exchange for real part of forward amplitude of, (T), 20: 32065
interactions with mesons (K^+) at 0.9 and 2.4 Bev/c, total cross sections for, (E), 20: 32067
interactions with mesons (K^-) at 1.22 to 1.70 Bev/c, $Y^*(J = 3/2)$ production in, (E/T), 20: 32068
interactions with electrons at high energies, electron anapole effects on polarization from, (T), 20: 32070
interactions with mesons ($\pi^\pm$) at high energies, amplitude and nucleon recoil effects on, (T), 20: 32072
interactions with photons, meson (π^0) production in, (T), 20: 32074
interactions with mesons (K^-) and (π^-) at high energies, M(12) symmetry for, 20: 32079
interactions with mesons (π) and protons at high energies, amplitudes for large-angle elastic, 20: 32086
interactions with mesons (π^-) at 1.7 to 2.5 Bev/c, differential cross sections and polarization in elastic, (T), 20: 32087
interactions with electrons, radiative corrections for coincidence measurements of, 20: 32092
interactions with photons at 250 to 360 Mev, recoil-proton polarization from pion-photoproduction, (E), 20: 32096
interactions with photons at 360 Mev, recoil-proton polarization from pion-photoproduction, (E), 20: 32097
interactions with mesons (π^+) at 38 to 307 Mev, resonance formulas for N* (1236) from, (T), 20: 32100
interactions with deuterons at 1.0 to 1.5 Bev, backward elastic, (E), 20: 32102
interactions with protons at 12.5 Bev/c, deuteron-production cross sections from, (E), 20: 32066
interactions with neutrons, Regge-pole theory for charge-exchange, 20: 32069
interactions with mesons (K^-) and (π^-), experimental status of baryon-exchange, 20: 32027
interactions with mesons (π^+) and (π^-) at 4 Bev/c, cross sections for strange-particle production in, (E), 20: 32029
interactions with mesons (K^-), Y_1^0(1385) and Y_3^*(1660) production in, (E/T), 20: 32034
interactions with protons at high energies, impact parameter amplitudes for, (T), 20: 32173
kinematics in spark chambers, use of multiple scattering and secondary sparks in determining, (E), 20: 31570
losses of 125 Mev geomagnetically trapped, in atmosphere at South Atlantic anomaly, 20: 32265
mass relative to neutrons, model for electromagnetic, 20: 32057
origin of space, 20: 31095
photoproduction on aluminum, silicon, and sulfur at 32 Mev, energy spectra from, (E), 20: 32394

polarization in deuteron reactions (d,p) with helium-3 at 6.0 and 10.0 Mev, (T), 20: 32475
polarization in frozen toluene using solid effect, (E), 20: 31811
precipitation in auroral ionosphere, Balmer radiation and ionization rate for, (T), 20: 32246
production from decay of geomagnetically trapped neutrons, 20: 32266
reactions (p,α) with zinc-66 and -68 at 17.5 Mev, J-dependence of angular distributions from, (E), 20: 32489
reactions (p,α) with zinc-66 and zirconium-92 at 28 Mev, J-dependence of angular distributions from, (E), 20: 32489
reactions (p,αγ) with magnesium-26 at 9.3 to 10.5 Mev, sodium-23 levels from, (E), 20: 32509
reactions (p,αγ) with magnesium-26 at 8.5 to 10.5 Mev, sodium-23 gamma multipole mixing ratios and spins from, (E), 20: 32567
reactions (p,αα) with boron-11 at 163 kev, angular and energy correlations from, (E), 20: 32402
reactions (p,Be-7) with aluminum-27 at 35 to 65 Mev, angular-momentum effects in, (E), 20: 32507
reactions (p,γ) with deuterium at 156 Mev, cross section for, (E), 20: 32486
reactions (p,γ) with chromium-52 at 1.36 to 2.26 Mev, manganese-53 levels from, (E), 20: 32446
reactions (p,γ) with chlorine-35 at 733 to 2595 kev, argon-36 levels from, (E), 20: 32451
reactions (p,n) with lithium-7 at 4.3 to 4.5 Mev, neutron polarization in, (E/T), 20: 32359
reactions (p,n) with vanadium-51, cross sections and excitation functions for, (E), 20: 32371 (CEA-R-2832)
reactions (p,p′γ) with nickel-60 and -62, energy levels from, (E), 20: 32490
reactions (p,p′γ) with carbon-12 at 5.9 Mev, angular correlations for, (E), 20: 32438
reactions (p,p′γ) with molybdenum-92 at 10 Mev, energy level structure from, (E), 20: 32471
reactions (p,2p) with carbon-12 at 80 to 150 Mev, momentum distribution of recoil nucleus in, 20: 32529
reactions (p,3pxn) with lanthanum-139 at 30 to 150 Mev, cesium isotopes from, (E), 20: 32386
reactions with gold-197 at 155 Mev, alpha emission from, (T), 20: 32455
reactions with hydrogen atoms at high energies, excitation cross sections for, (T), 20: 31933
reactions with iron at 400 Mev, radioisotope production in, (T), 20: 32560
reactions with metals at high energies, residual radioactivity from, 20: 31831
reactions with metals at 40 Mev to 25 Bev, lithium isotopes from, (E), 20: 31205
reactions with nuclei at 0.05 to 2.9 Bev, induced activity data and cross sections for spallation, (E/T), 20: 32549
reactions with nuclei, nucleon-alpha cascades from, (T), 20: 32455
reactions with radium-226 at 10 to 100 Mev, ratio of asymmetric to symmetric fission by, (E), 20: 32515
scattering by argon-40 and calcium-40 at 18.5 and 20.5 Mev, polarization from, (E/T), 20: 32523
scattering by calcium-40 and -48 at 11.5 Mev, level excitation energies from inelastic, (E), 20: 32511
scattering by carbon and silicon at 29 and 49 Mev, asymmetries in elastic and inelastic, (E), 20: 32440
scattering by chromium-53 at 10 to 12 Mev, optical-model parameters from elastic, (E/T), 20: 32459
scattering by complex nuclei at 18.5 and 20.5 Mev, optical-model analysis of polarization from elastic, (E/T), 20: 32523
scattering by helium-3, differential polarization from, (T), 20: 32543
scattering by lead-207 at 11 to 16 Mev, bismuth-208 analog states of lead-208 from, (E), 20: 32478
scattering by nickel-60 at 10.5 and 14.0 Mev, spin flip in inelastic, (E), 20: 32557
scattering by nuclei at 40 Mev, differential cross sections and polarization for elastic, 20: 32510
scattering by nuclei at 17.8 Mev, polarization of elastic, (E), 20: 32439
scattering losses in plastic and sodium iodide scintillators, 20: 31542
spectra and yields from deuterium (d,p) reactions at 25.3 Mev, (E), 20: 32568
sputtering on copper and silver at 0.1 to 4.0 Mev, (E), 20: 31905
trajectories in Van Allen belts, (T), 20: 32261
trapping in inner radiation belt, losses from, 20: 32243 (AD-634704)

PROTOZOA
effects of antioxidants on inhibition of selected photosensitizers in *Tetrahymena pyriformis*, 20: 31018
radiation effects on cells in flagellate *Astasia longa*, 20: 31085
radiosensitivity of, genetic control of, 20: 31041

PSEUDOUREA, 2-(2-AMINOETHYL)-2-THIO-
effects in mixture with glutathione and serotonin on lysosome morphology of mouse stem cells, 20: 30964
effects on gamma radiation effects on human tissue cultures, 20: 31121
radiosensitivity effects of, relation between cellular anoxia and, 20: 31122
radiosensitivity effects on mouse intestinal crypt cells, x, 20: 31128
radiosensitivity effects on rats, 20: 31143

PULSE ANALYZERS
design and performance of logarithmic, 20: 31577
design for radiation detectors for aerospace applications, 20: 31609
design of time-to-digital code, 20: 31578
design of, combined with spectrometer for biology studies, 20: 31525
development of multichannel, for low-energy physics, 20: 31562
memory system for, analog and digital readout for circulating, 20: 31557
performance of coincidence, 20: 31585
performance of proton, 20: 31510 (N-65-33971)
use in controlling whole-body scanner velocity, 20: 31502(R) (BNWL-235-4, pp 11-14)

PULSE MODIFIERS
design for radiation detectors for aerospace applications, 20: 31609

PULSE TRANSFORMERS
design of 2-Mamp, for coaxial load, 20: 31489

PYRAZINE
coupling constants of anionic radicals of, in solutions, 20: 31221(R) (UCRL-16658, pp 73-87)

PYRIDAZINE
coupling constants of anionic radicals of, in solutions, 20: 31221(R) (UCRL-16658, pp 73-87)

PYRIDINE
spectra of anionic radicals of, ESR, 20: 31221(R) (UCRL-16658, pp 73-87)

PYRYLIUM COMPOUNDS
deuterium exchange of active methyl hydrogens of, with heavy water and acetic acid, 20: 31260

Q

QUANTUM ELECTRODYNAMICS
formalisms for, conservation equations and invariants in vector and spinor, 20: 32145
testing by electron-electron interactions at 600 Mev, (E), 20: 32305
testing of, symmetry, 20: 32201

QUANTUM MECHANICS
hamiltonian path-integral method for, 20: 32310
harmonic oscillator in, Sp(n,R) dynamical group of anistropic, 20: 32301
measurement in, hidden-variable theory for, 20: 32308
operators in, conditions for existence of diagonal representation for, (T), 20: 32304
spin matrices in, scalar products of Pauli, 20: 32300
theory of time-dependent phenomena in, evolution operator technique in, 20: 32293 (N-66-17084)
theory of, existence of hidden variables in, 20: 32309
theory of, problem on hidden variables in, 20: 32307
variational principle for classical and, unified, 20: 32302
wave functions in, random-phase approximation for ground-state, 20: 32303

QUARTZ
analysis for traces of copper, activation, 20: 31183
properties of, for use as thermoluminescence detector, 20: 31520
radioinduced coloration in natural, gamma, 20: 32695
x-ray diffraction by natural, defect structure from, 20: 32695

QUINONES
effects on metabolism in wheat seeds, 20: 31002
radiation effects on formation of, in potatoes, quantitative regularities in gamma, 20: 31001

R

RABBITS
effects of zinc-65 on, pathological, 20: 31112
radiation effects on orchitis development and *Treponema pallidum* content in antigens in, 20: 31119
radiation effects on electric activity of brains of embryonic, x, 20: 31037(T) (JPRS-35315, pp 65-75)

RADAR
use for bistatic measurements of interplanetary shock wave propagation, 20: 31858
use for determining electron content in cislunar space, effects of coherent density fluctuations on, 20: 31857
use in measurements of interplanetary plasma streams, bistatic, 20: 31856

RADIATION
dose to population of Guarapari, Brazil, survey of, 20: 31470
effects of, biological, 20: 31038

effects on amino acid composition of blood serum in dogs, 20: 31021
effects on biological systems, mathematical model for kinetic studies of lethal, 20: 31087
effects on chromosomes, site distribution parameters for exchange, 20: 31057
effects on DNase activity in rat spleen and thymus, 20: 31143
effects on dogs, following head exposure, 20: 31060
effects on electron equipment in space, operational safety margins for, 20: 31619
effects on electronic equipment, 20: 31620
effects on electronic circuitry, hardening against, 20: 31621
effects on guinea pigs, protective effects of fractionated bone marrow against lethal, 20: 31126
effects on hematopoietic system of astronauts during space flight, 20: 31029 (BNL-10221)
effects on heme proteins, 20: 30999(R) (UCB-34P95-7)
effects on incorporation of dietary linoleic acid in triglycerides in rat bone marrow, whole-body, 20: 31016
effects on lethal damage in growing *E. coli* B/r, site of, 20: 31068
effects on lethality in dogs, effects of blood transfusions and bone marrow transplants on, 20: 31132
effects on properties of DNA in *E. coli*, 20: 31144
effects on tissues of birds and mammals, pathological, 20: 31045
effects on toluene, yields of gaseous, liquid, and solid products in, 20: 31291
effects on transistors, surface charges from, 20: 31611 (AD-633468)
effects on transistor properties, 20: 31620
effects on *Vicia faba* and its hybrid, 20: 31054
hazards to radiologists, limits on whole-body, 20: 31458
use of nuclear, for laser pumping, 20: 32740

RADIATION CHEMISTRY
mechanisms in aqueous-solution, 20: 31293
radical reactions in, of water, 20: 31294

RADIATION DETECTION INSTRUMENTS
design for aerospace applications, 20: 31609
design for *in situ* measurement of radionuclide uptake by algae, 20: 31504(R) (BNWL-235-4, pp 16-18)
design of film-type, for measuring angular and energy distributions of recoil nuclei, 20: 32526
design of portable, for radiological monitoring, 20: 31601
development for neutron detection and measurement in reactors, 20: 31596
performance of, time-dependent reliability coefficient for, 20: 31531
sensitivity of proton analyzer, 20: 31510 (N-65-33971)
use of neutron, review of, 20: 31606

RADIATION DETECTION INSTRUMENTS (PULSE TYPE)
description of modular, at Ispra, 20: 31551
design and performance of 4π G-M, for gamma rays, 20: 31593
design of nanosecond, for gamma cascade directional correlation determinations, 20: 31595
design of scintillation, for gamma detection and measurement, 20: 31599
design of, for whole-body counting, 20: 31586
performance of sodium iodide, for whole-body counting, 20: 31443 (CONF-650673-1)
performance of, calculation of detection limit and minimum pulse rate for determining, 20: 31512 (SGAE-SS-5/1966)
pulse shape discrimination for, evaluation of scintillation, 20: 31535

RADIATION DETECTORS
charge release mechanism for ferroelectric, 20: 31539
control system for whole-body scanner-type, 20: 31502(R) (BNWL-235-4, pp 11-14)
design and performance of secondary-electron-type, for neutral particles, 20: 31533
stability of, circuits for determining and improving, 20: 31575

RADIATION INJURIES
effects of cystine, glutathione, and MEA against gamma, in liver and tumor tissues in mice, 20: 31141
pathology of γ, in sheep, 20: 31026 (AD-633606)
pathology of γ-induced, in *Macaca mulatta*, 20: 31101
pathology of proton-induced, in *Macaca mulatta*, 20: 31103
pathology of proton, in monkeys, 20: 31097
pathology of proton-induced, in *Macaca mulatta*, 20: 31098
pathology of proton-induced, in *Macaca mulatta*, 20: 31099
pathology of proton-induced, in *Macaca mulatta*, 20: 31101
recovery from γ and proton, in mice, kinetics of, 20: 31100
recovery from uv, in bacteria and viruses, processes in, 20: 31039
repair in avian and mammalian tissues, mechanisms of, 20: 31045
repair of premutational, in microorganisms and metazoa, uv and x, 20: 31040
therapy of, use of cadaver bone marrow for, in mice, 20: 31135
therapy of, using irradiated bone marrow autografts in rats, 20: 31133

RADIATION MONITORING
equipment for atmospheric, calibration of, 20: 31528
equipment for fish, in reactor effluents, 20: 31501(R) (BNWL-235-4, pp 10-11)
equipment for, design of portable, 20: 31601
handbook on personnel, 20: 31445 (N-65-12416)
use of lithium fluoride thermoluminescent dosimeter for environmental, 20: 31526
use of photographic film detectors for personnel, 20: 31439 (AECL-2540)

RADIATION PROTECTION
effects of fractionated bone marrow on, in guinea pigs, 20: 31126
handbook on, 20: 31445 (N-65-12416)
procedures for, in radiochemical laboratories, 20: 31469

RADIATION SICKNESS
effects on DNA, phosphatase, and RNA in cerebral nerve cells in rats, 20: 31010

RADIATION SOURCES
catalog of, Atomic Energy of Canada Ltd., 20: 32891
dosimetry of high-intensity, ferrous-copper system for, 20: 31607

RADIATION TARGET CANS
design of ultrahigh-pressure, 20: 32754

RADIATION TARGET CHAMBERS
description of, for particle correlation measurements, 20: 31556
design modifications of MIT Rutherford scattering apparatus, 20: 31515

RADIATION TARGETS
design of liquid hydrogen, 20: 32318
development of beryllium, for accelerator production of neutrons, 20: 31786(R) (ORO-2891-5)
preparation of self-supporting foils of separated rare earth isotopes, 20: 31696

RADIO ASTRONOMY
use in solar corona and solar wind structure determination, 20: 31888

RADIO WAVES
emission from auroral storms, v-l-f, 20: 32256

RADIOACTIVE CONTAMINATION
control of, in reactor operation and uranium mining, 20: 31457

RADIOACTIVE MATERIALS
handling and shipping, safety procedures for, 20: 31445 (N-65-12416)

RADIOACTIVITY
content in marine organisms in Chukchi Sea, Alaska, 1959 to 1952, 20: 31427 (PNE-481, pp 11141-9)
determination over unlimited range, table for, 20: 32418
distribution on polydisperse aerosol in atmosphere, diffusion method for measuring, 20: 31461
dosimetry of environmental, in Guarapari, Brazil, 20: 31463
effects on electrochemical properties of iron and steel, 20: 31231
measurement at low sample/background ratios, errors in, 20: 31576
measurement of, in atmosphere, San Francisco region, California, 20: 31395 (CEX-58.4.5)
measurements in New Zealand, environmental, 20: 31446(R) (NP-16015)
monitoring Cape Thompson-Cape Seppings area (Alaska) for, 1958, 20: 31425 (PNE-481, pp 1115-19)

RADIOBIOLOGY
book: *Advances in Radiation Biology*, Vol. 2, 20: 31038
book: *Tissue Grafting and Radiation*, 20: 31120
kinetics of biological radiation response, (T), 20: 31087
relation of cellular control systems to radiosensitivity, 20: 31064

RADIOCHEMICAL PROCESSING PLANTS
krypton-85 and tritium release from, 20: 31447 (ORNL-3956)

RADIOCHEMISTRY
research programs on, 20: 31165(R) (HMI-B-46)

RADIODIAGNOSIS
dose measurement in, using fluoroglass, 20: 31538
uses of, survey of, 20: 31152

RADIOGRAPHY
radiation dose to human fetus in, 20: 31146

RADIOISOTOPES
activity from transported, in commercial aircraft, 20: 31952
activity of beta-emitting, measurement using liquid scintillators with external standards, 20: 31518
activity of, table for determination over unlimited range, 20: 32418
beta activity of, proportional counter for measuring, 20: 31509 (EIR-97)
catalog of, Atomic Energy of Canada Ltd., 20: 32891
decay of lectures on, 20: 32377 (KFK-117)
determination in dual-labeled samples by liquid scintillation spectrometer, computer program for use in, 20: 31177
determination of beta-emitting, by Cherenkov counting methods, 20: 31184
determination of, from gamma spectra, review of, 20: 31186
dispersion in sea water, effects of biological, chemical, and physical processes affecting, 20: 32883
distribution and dose in man, method for external measuring of, 20: 31158

fractionation in fallout particles from land surface burst, 20: 31460
half lives of, tabulation of, 20: 32421
handling and transportation of, in radiochemical laboratories, 20: 31469
production and uses of high-specific-activity, 20: 31642 (ORNL-P-2190)
production and uses in Belgium, 20: 31643
separation by ion exchange on cellulose phosphate, 20: 31324
sorption by marine sediments, 20: 32883
transfer in placentas of animals and humans, effects of inactive carriers on, 20: 31142
uptake by algae, instrument for *in situ* measurement of, 20: 31504(R) (BNWL-235-4, pp 16-18)
uptake from air by plants, 20: 31142
uptake, distribution, and excretion by mammals, computer program for calculation of radiation exposure from, 20: 31441 (BNWL-SA-40)
use for propellant heating in space probes, 20: 31361
use in self-luminous signs, 20: 31636(P)
uses in agriculture, 20: 31109
uses in Army aviation program, 20: 31622

RADIOLOGY
book: *Physics of Industrial Radiology*, 20: 31338
radiation hazards to personnel in, limits on whole-body, 20: 31458

RADIOMETERS
design of selective receiver of microwaves, 20: 32626
stability of, circuits for determining and improving, 20: 31575

RADIOMIMETIC SUBSTANCES
effects of, on tissues, 20: 31108

RADIOPROTECTIVE COMPOUNDS
effects of sulfhydryl, on DNA synthesis in mice, 20: 31125
effects on fluorescence of intracellular pyridine nucleotides, relation between cellular anoxia and, 20: 31122
effects on lethally irradiated mammals in combination with bone marrow, 20: 31142
effects on x-ray therapy of cancer in mice, 20: 31142
efficiency of food colorings for protection of agarose jellies, 20: 30998 (BNWL-SA-709)
efficiency of, review of, 20: 31108
efficiency of, review of, 20: 31142
evaluation of 24, in rats, 20: 31140

RADIOSENSITIVITY
control of microorganism, genetic, 20: 31041
genetic factors in cellular, 20: 31042
monitoring natural, in Albuquerque–Los Alamos area, 20: 31396 (CEX-61.6.2)
relation to cellular control systems, 20: 31064

RADIOSENSITIZERS
effects of, use of activation analysis for determining mechanism of, 20: 31172 (SGAE-BL-17/1966)
effects on antioxidant activity in *Tetrahymena pyriformis*, 20: 31018

RADIOSTERILIZATION
effects on storage life of pears, 20: 31633
effects on wholesomeness of meat, 20: 31630
factors in commercial food, 20: 31635
method for meats, use of low temperatures in, 20: 31634
of male Mediterranean fruit flies for population control, 20: 31109
of male Queensland fruit flies for population control, 20: 31109
of male Tephritid flies (*Dacus cucurbitae*), 20: 31046

RADIOTHERAPY
dose calculations for tumor, use of computer for, 20: 31155
dosimetry for Hodgkin's disease, 20: 31151
effects on blood vessels around joints, 20: 31163
effects on leukopenia development, bone marrow autotransplantation method for treating, 20: 31134
equipment for, Atomic Energy of Canada Ltd. catalog of, 20: 32891
radon-222 baths for, 20: 31157
use of iodine-131 for, of hyperfunctioning solitary thyroid nodule, dosage for, 20: 31154
use of yttrium-90 for, of metastasized mammary carcinomas, 20: 31153
uses of, survey of, 20: 31152

RADIUM
determination of, in river waters, evaluation of methods for, 20: 31191
metabolism by man, 20: 31142

RADIUM ISOTOPES Ra-226
content in diet in California, 20: 31471
proton fission at 10 to 100 Mev, ratio of asymmetric to symmetric, (E), 20: 32515

RADIUM ISOTOPES Ra-228
uses of, in industrial defectoscopy, personnel protection in, 20: 31464

RADON
content in atmosphere, vertical distribution of, 20: 31404

RADON ISOTOPES Rn-220
content in atmosphere, vertical distribution of, 20: 31404

RADON ISOTOPES Rn-222
dosimetry of, in therapeutic baths, 20: 31157

RAIN WATER
charge and velocity of drops of, measuring equipment for, 20: 31476(R) (BNWL-235-4, pp 21)
radioactivity from lead-210 and strontium-90 in New Zealand, 1965, 20: 31446(R) (NP-16015)
radioactivity in, at Nagaoka City, Japan, 1965, 20: 31411

RAPP POWER REACTOR
description, 20: 32816
description, 20: 32817

RARE EARTH ALLOYS
magnetic properties, (E), 20: 31763
Cd–rare earth, crystal structure of, CsCl-type intermediate phases in, 20: 31737
Cd–rare earths, lattice constants, 20: 31167(R) (ANL-7175, pp 217-25)
Cd–rare earths, thermodynamic properties, 20: 31213(R) (ANL-7175, pp 119-58)
Hg–rare earth, crystal structure of, CsCl-type intermediate phases in, 20: 31737
In–rare earth, crystal structure of, CsCl-type intermediate phases in, 20: 31737
rare earth–Zn, crystal structure of, CsCl-type intermediate phases in, 20: 31737
Tl–rare earth, crystal structure of, CsCl-type intermediate phases in, 20: 31737

RARE EARTH COMPOUNDS
toxicity in laboratory animals, 20: 30970 (COO-1170-5)

RARE EARTH ISOTOPES
distribution and natural carriers of, in sea water, 20: 31422

RARE EARTH MOLYBDATES
preparation and crystal structure of, 20: 31740

RARE EARTH OXIDES
phase studies at high pressures, 20: 31258
preparation of microspheres of, by sol-gel process, 20: 31689 (ORNL-P-2159)

RARE EARTH SYSTEMS
Ni–rare earth–Si, crystal structure of $R_3Ni_6Si_2$ compounds in, 20: 31253

RARE EARTH TUNGSTATES
preparation and crystal structure of, 20: 31740

RARE EARTHS
determination in irradiated fuels, methods for, 20: 31167(R) (ANL-7175, pp 217-25)
determination in organic solvent–acid media, spectrophotometric, 20: 31195
separation from beryllium fluorides and lithium fluorides, 20: 32804(R) (ORNL-3936, pp 122-71)
separation from organic solvent–acid media by ion exchange, 20: 31195

RARE GASES
reactions with alkali atoms, ionization cross sections for, 20: 31917
spectra of high-temperature species in matrices of, 20: 31219(R) (UCRL-16658, pp 11-20)

RATE METERS
design of miniature solid-state dose, 20: 31503(R) (BNWL-235-4, pp 14-16)
design of portable, for neutron dose-rate measurements, 20: 31600

RATS
cesium-137 in, pathological effects of inhaled, 20: 31111
corticosteroid synthesis in, effects of hypophysectomy on, 20: 31011
effects of ingested deuterium on normal and pregnant, pathological, 20: 30975
effects of radiation sickness on DNA, phosphatase, and RNA in cerebral nerve cells in, 20: 31010
effects of radioprotective compounds on fluorescence of intracellular pyridine nucleotides in, 20: 31122
morphology of tissues of, effects of cystamine on, 20: 30984
phosphate metabolism in liver of, tracer study, 20: 30976
radiation effects on, effects of uneven exposure and irradiated bone marrow autografts on, 20: 31133
radiation effects on, 20: 31140
radiation effects on brain serotonin in, relation of barbiturate hypnosis to x, 20: 31007
radiation effects on corticosteroid synthesis in, 20: 31011
radiation effects on incorporation of dietary linoleic acid in triglycerides in bone marrow in, whole-body, 20: 31016
radiation effects on function and ultrastructure of isolated sympathetic ganglion in, x, 20: 31055
radiation effects on skin wound healing in, effects of hormones on γ, 20: 31061
radiation effects on liberation of 5-hydroxytryptamine in brain stem of adrenalectomized, x, 20: 31069
radiation effects on Yoshida ascites tumor cells in, recovery mechanism in x, 20: 31070
radiation effects on transfer capacity of small intestine in, whole-body x,

20: 31081
radioprotective agents for, evaluation of 24, 20: 31140
radiosensitivity of, effects of AET and cystamine on, 20: 31143
rare earth toxicity in, 20: 30970 (COO-1170-5)
respiration in tissues of, effects of cystamine on, 20: 30984
rubidium-86 uptake and dulcitol distribution in galactose-fed, 20: 30978
strontium-90 absorption by intestine of, effects of green tea on, 20: 30987
strontium-90 excretion by, effects of sodium phytate on, 20: 30977
REACTOR BREEDING BLANKETS
processing of, for 1000-MW(e) fast reactors, cost studies on, 20: 31316(R) (ANL-7175, pp 104-18)
REACTOR COMPONENTS
instrumentation for control and safety systems of research reactors, solid-state, 20: 32876
REACTOR CONTROL RODS
design with graduated form, for reactivity zone reduction, 20: 32760(P)
positioning of, apparatus for, 20: 32761(P)
REACTOR CONTROL SYSTEMS
development for heavy water-moderated organic-cooled reactors, 20: 32796(R) (AI-CE-3)
instrumentation for research reactors, solid-state, 20: 32876
REACTOR COOLANTS
effects on reactor building materials, 20: 31682 (NP-16003)
loss of water, effects of accidental, 20: 31440(R) (ANL-7175, pp 159-83)
REACTOR COOLING SYSTEMS
design, 20: 32757(P)
valve design for, 20: 32762(P)
REACTOR ENGINEERING
research programs on, 20: 31165(R) (HMI-B-46)
REACTOR FUEL ALLOYS
processing of, equipment and methods for, 20: 31315(R) (ANL-7175, pp 42-103)
processing of, for 1000-MW(e) fast reactors, cost studies on, 20: 31316(R) (ANL-7175, pp 104-18)
reactions with water in TREAT experiments, 20: 31440(R) (ANL-7175, pp 159-83)
separation of, from fission products by extraction using liquid metals, 20: 31166(R) (UCRL-16658, pp 89-92)
REACTOR FUEL ELEMENTS
burnup measurements on, Compton recoil gamma spectrometry for non-destructive, 20: 31355
configuration measurement system for, 20: 32753
design with moderating container and annular fuel compacts, 20: 32793(P)
fabrication in France, industrial, 20: 31693
fabrication in United Kingdom, 20: 31694
fabrication of aluminum-clad, in Belgium, 20: 31692
fabrication of glass sphere, for homogeneous reactors, 20: 31702
fabrication of thorium–uranium, 20: 31690 (ORNL-P-2176)
fabrication of tubular-layer, in Belgium, 20: 31692
handling system for heavy water-moderated organic-cooled reactors, development of, 20: 32796(R) (AI-CE-3)
performance of molten plutonium, fast transients in, (T), 20: 32797 (LA-DC-7748)
testing of, nondestructive, 20: 31354
REACTOR FUEL ELEMENTS (CERAMIC)
burnup testing of plutonium-uranium carbide, 20: 31675
development for heavy water-moderated gas-cooled reactors, 20: 32796(R) (AI-CE-3)
fabrication and burnup testing of uranium carbide, for organic-cooled reactors, 20: 32796(R) (AI-CE-3)
fabrication method for, 20: 31707(P)
fabrication of plutonium carbide–uranium carbide, for fission-gas retention, 20: 31675
fabrication of stainless steel-clad urania pellets, in Belgium, 20: 31692
loading of, apparatus and method for vibratory compaction, 20: 31704(P)
loading of, equation for packing efficiency of vibratory-compaction, 20: 31670
processing of uranium carbide, methods for, 20: 32796(R) (AI-CE-3)
processing of, for 1000-MW(e) fast reactors, cost studies on, 20: 31316(R) (ANL-7175, pp 104-18)
reactions with water in TREAT experiments, 20: 31440(R) (ANL-7175, pp 159-83)
temperature distributions in irradiated plutonium-uranium carbides and oxides, 20: 32791 (NAA-SR-Memo-11731)
REACTOR FUEL ELEMENTS (DISPERSION)
fabrication method for, 20: 31707(P)
radiation effects on, bibliography on, 20: 31783 (FTI-16(6.1))
REACTOR FUEL PINS
burnup of fuel pellets in plutonia–uranias, 20: 32836
REACTOR FUEL PLATES
dimensional stability from fuel growth, 20: 31806
stability of hydraulically collapsed, 20: 32794
REACTOR FUEL RODS
heat flux and temperature distribution in, (T), 20: 31349
vibration in assembly of, coolant-flow-induced, (E), 20: 32746
REACTOR FUEL SPHERES
fabrication method for, 20: 31705(P)
fabrication of silicon carbide-coated uranium carbide, in silicon carbide material, 20: 31706(P)
REACTOR FUELS
breeding in intermediate-energy uranium–thorium water-moderated reactors, (T), 20: 32831
burnup determinations of, techniques for, 20: 32838
burnup of pellets of plutonia–urania, in reactor fuel pins, 20: 32836
burnup of thorium–uranium alloys and compounds, 20: 32833
diffusion and segregation in plutonia–urania, 20: 31440(R) (ANL-7175, pp 159-83)
dimensional stability of, 20: 31806
economics of thorium–uranium, for Italian power reactors, 20: 32827
fabrication technology for thorium–uranium-233, 20: 31701
fission gas migration and bubble coalescence in, (T), 20: 31739
inspection of irradiated coated-particle, use of electron microprobe for, 20: 31795
performance of thorium, for thermal power reactors, 20: 32822
performance of thorium-232–uranium-233, for fast breeders, 20: 32790 (ANL-6930)
processing costs and methods for thorium-bearing, 20: 31326
processing irradiated urania, by fluoride volatility, 20: 31315(R) (ANL-7175, pp 42-103)
processing of irradiated, pyrochemical methods for, 20: 31314(R) (ANL-7175, pp 1-41)
properties of plutonium dioxide–uranium dioxide, effect of stoichiometry on, 20: 31674
radiation effects on uranium-based coated-particle, 20: 31783 (FTI-16(6.1))
use in European Atomic Energy Community in 1970 to 1999, estimation of, 20: 32792
use of thorium-232–uranium-233, in Swedish power reactors, 20: 32830
use of thorium, in Brazilian power plants, 20: 32821
use of thorium, in German power plants, 20: 32824
use of thorium, in pebble bed reactors, 20: 32825
use of thorium, in Japanese power reactors, 20: 32828
use of thorium, review of, 20: 32819
REACTOR FUELS (FUSED SALTS)
processing of, techniques for, 20: 32806(R) (ORNL-3936, pp 193-211)
REACTOR MATERIALS
research progress on, *Technical Progress Review*, Spring 1966, 20: 31665
REACTOR MATRICES
neutron diffusion in parallel-plate, calculation of, 20: 32763 (AECL-2543)
neutron thermalization in cells of, computer programs for, 20: 32367
neutron transport in reflected multiplying slab, 20: 32782
REACTOR REFLECTORS
effects of beryllium, on thermal neutron flux in horizontal columns, 20: 32765 (IAE-957)
REACTOR SAFETY
lockout device for, to ensure evacuation of personnel, 20: 31472(P)
radiation hazards at Polish EWA, 20: 32877
temperature transients in coolant-loss accidents, effects of convection on, 20: 31166(R) (UCRL-16658, pp 89-92)
REACTOR SHIELDING
efficiency of lead–water, 20: 32676
REACTOR SLURRIES
development of homogeneous suspended thorium, 20: 32829
fabrication of glass bead fuels for, 20: 31702
REACTOR TUBES
fuel elements retaining assembly in, design of, 20: 32756(P)
REACTORS
air pollution control at, 20: 31453 (STI-PUB-121)
containment rupture by projectiles during meltdown, (E/T), 20: 32744 (SRIA-1)
containment systems for, analytic model of pressure-temperature transients in, 20: 32748 (BNWL-233)
control of, instrumentation for, 20: 32749
cooling-moderator circuits of, with separate primary circuits, 20: 32757(P)
decontamination solution for, 20: 32747(P)
design of, computer programs for solution of physics problems in, 20: 32745
effluents from, dose monitoring equipment for fish in, 20: 31501(R) (BNWL-235-4, pp 10-11)
fuel assembly vibrations in, coolant-flow-induced, (E), 20: 32746
fuel channels with element retaining assembly for, 20: 32756(P)
gamma and neutron heating and transport in, computer programs for,

20: 32768 (UNC-5148)
iodine-129 production in, 20: 32884
kinetics analysis of, bibliography of computer programs for nuclear, 20: 32764 (CEA-Bib-17(Pt.2))
kinetics research, 20: 32781
loading of, design of machine for horizontal, 20: 32755(P)
neutron detection and measurement in, instrument development for, 20: 31596
neutron flux measurements in, method for absolute, 20: 32776
neutron moderating and multiplying media in, properties of, 20: 32776
neutron poison burnup in plane layer of, 20: 32772
neutron thermalization in cells of, computer programs for, 20: 32367
neutron transport theory for, 20: 32366
operation of, control of radioactive pollution in, 20: 31457
pressure tube failure in liquid-moderated, shock absorbers for, 20: 32759(P)
pressure vessels for, development of prestressed concrete, 20: 32750
pressure vessels for, thermal properties of concrete for, 20: 31722(T) (ORNL-tr-1227)
pressure vessels for, three-dimensional photoelastic stress analysis of, 20: 32751
reactivity noise analysis for, using gamma radiation, (E), 20: 32786
reactivity of subcritical, harmonic effects on, 20: 32777
reactivity transfer functions for, calculation of space-dependent, using statics techniques, 20: 32780
startup with low neutron source, kinetics of, 20: 32766 (KAPL-M-6550)
xenon stability in absorbing-layer slab, absorber effects on, 20: 32771

RELATIVITY THEORY
energy mechanics of semistatic space-times in, 20: 32298
equation of motion for rocket or variable-mass particle, method of derivation, 20: 32294
fields with spacelike momentum spectra in, 20: 32146
gravitational theories in general, equivalence-principle violation in, 20: 32299
neutrino transport in gravitational collapse, 20: 32296
Riemannian manifold in five-dimensional pseudo-Euclidean space in, embedding of, 20: 32297
universe models in general, 20: 31863

RESEARCH REACTORS
control systems of, solid-state instrumentation for, 20: 32876
criticality calculations for EWA, using WWRM-type fuel elements, 20: 32880
experimental facilities of VVR-S, development of dosimeter for in-pile loop, 20: 32865
modification of MARYLA, 20: 32873
modification of VVR-S, 20: 32879
neutron kinetics in Georgia Tech., (E/T), 20: 32863 (TID-23037)
neutron noise analysis for LFR, 20: 32874
power measurement in EWA, using nitrogen-16 activity in water coolant, 20: 32870
radiation hazards at Polish EWA, 20: 32877
reactivity determination for subcritical state of IGR, shot-through method for negative, 20: 32864
reflector of Polish high-flux, use of heavy water in radial, 20: 32871

RESINS
radiation effects on sorptive properties of, based on diallyl esters of phosphoric acid, 20: 31303

RESPIRATION
rate measurement of test-animal, equipment for, 20: 31475(R) (BNWL-235-4, pp 19-20)
rates in test-animals, remote monitoring equipment for, 20: 30961(R) (BNWL-235-4, pp 25-9)

RESPIRATORY TRACTS
cesium-137 accumulation and elimination in rat, 20: 31111
radiotherapy of maxillary sinus of, 20: 31159

RHENIUM
effects on microstructure of tungsten–thoria dispersion-hardened alloys, 20: 31781
effects on surface tension and solid surface energy of chromium, molybdenum, and tungsten, 20: 31773
elastic properties at 25°C, 20: 31748
ionization efficiency of electrodes of, in ion engines, 20: 31386
ionization of neodymium and samarium at surfaces of, effects of adsorbed oxygen on, 20: 31225
performance as ionizer material in cesium-contact ion thrustors, 20: 31383
properties of porous, for cesium ionization, 20: 31388
reactions with steam at 850 to 1700°C, 20: 31669
solubility in plutonium at 700 to 950°C, 20: 31666
solvent properties for carbon at high temperatures, 20: 31669

RHENIUM ALLOY COUPLES
Re–W/Re–W, thermoelectric potential to 3000°C, 20: 31721(T) (AD-630971)

RHENIUM ALLOYS
Cr–Re, antiferromagnetic properties, specific heat, and superconductivity in, 20: 32702
Cr–Re, grain boundary grooving in, mechanisms of, 20: 31672
Cr–Re, surface tension and solid surface energy of, 20: 31773
Mo–Re, grain boundary grooving in, mechanisms of, 20: 31672
Mo–Re, properties of porous, for cesium ionization, 20: 31388
Mo–Re, surface tension and solid surface energy of, 20: 31773
Nb–Re, electronic structure of, at superconducting critical temperatures, 20: 31747
Re–W, deposition of, process development of chemical vapor, 20: 31670
Re–W, fabrication and preparation of, for use in ion engines, 20: 31375
Re–W, grain boundary grooving in, mechanisms of, 20: 31672
Re–W, ionization efficiency of electrodes of, in ion engines, 20: 31386
Re–W, mechanical properties, 20: 31778
Re–W, properties of porous, for cesium ionization, 20: 31388
Re–W, surface tension and solid surface energy of, 20: 31773

RHENIUM ISOTOPES Re-188
decay of, effects of chemical environment on angular correlations in, 20: 31311

RHENIUM SYSTEMS
C–Re–W, superconductivity of W_3Re_2C in, 20: 32312(R) (UCRL-16658, pp 133-43)

RHODIUM
vaporization from probe surface in electric arcs, (E), 20: 32593

RHODIUM ISOTOPES Rh-106
decay of, palladium-106 levels from, (E), 20: 32425
deposition on tropospheric aerosols, 20: 31459

RIBONUCLEASE, DEOXY-
radiation effects on activity of, in rat spleen and thymus, effects of AET and cystamine on, 20: 31143
radiation effects on activity of, in *E. coli*, x, 20: 31144

RIBONUCLEIC ACID
effects of radiation sickness on, in cerebral nerve cells in rats, 20: 31010
metabolism in rat liver, tracer study, 20: 30976

RIBONUCLEIC ACID, DESOXY-
effects of radiation sickness on, in cerebral nerve cells in rats, 20: 31010
radiation effects on properties of, in *Escherichia coli*, 20: 31144
radiation effects on synthesis of, in HeLa cell cultures, γ, 20: 31008
radiation effects on magnetic properties of, effects of temperature on γ, 20: 31009
radiation effects on degradation of, in *E. coli*, x, 20: 31015
radiation effects on properties of cotton-seed, γ, 20: 31019
radiation effects on, repair mechanisms for, 20: 31040
radiation effects on breakdown and synthesis of, in bromouracil-substituted *E. coli*, uv, 20: 31062
radiation effects on synthesis of, in mouse uterine epithelium, x, 20: 31088
radiosensitivity effects in microorganisms, 20: 31041
radiosensitivity of base composition and cells of, ESR spectral studies a 20: 31014
synthesis in mice, effects of sulfhydryl compounds on, 20: 31125

RICE
radiation control of weevils, in, 20: 31623 (AECD/AG-15)
radioinduced mutations in seeds of, γ and x, 20: 31050

ROCKET REACTORS
neutron kinetics in, control of, 20: 32851 (N-65-30544)

ROCKET REACTORS (KIWI)
pressure vessels for NERVA, development of titanium, 20: 32856
propellant for Rover, safety analysis of liquid hydrogen, 20: 32850 (LA-DC-7689)

ROCKETS
motion of variable-mass, equations for relativistic, 20: 32294
tracking at low altitudes using gamma rays, 20: 31495

ROCKS
analysis of, on remote surfaces, combination neutron technique for, 20: 31211
sorptive properties of pyroelastic, for fission products, 20: 32883

RODS
fluid flow velocity through channels of finite bundles of hollow, turbulent, 20: 31350
penetration of steel plates by, analysis for, (E/T), 20: 32744 (SRIA-1)

ROOTS
adenosine triphosphatase synthesis in wheat, effects of calcium and strontium on, 20: 30992
radiation effects on *Allium cepa*, protective effects of anoxia, α-aminothioacetamide, and cysteine against, 20: 31137
radiation effects on barley, biological, 20: 31052

ROTORS
dynamics of, stability and virtual mass effects on, 20: 31329 (KAPL-

M-6543)
RUBIDIUM
determination in conductive tissue of beef heart, activation, 20: 31176
determination in human heart tissue, activation, 20: 31175
radiative lifetime of excited electronic states in, 20: 31219(R) (UCRL-16658, pp 11-20)
rare-gas reactions with, ionization cross sections for excited, (T), 20: 31917
uptake and loss in relation to active mechanism for sodium extrusion in Scenedesmus cells, 20: 30994
use of liquid, in thermionic cells, 20: 31969
RUBIDIUM IONS
desorption from tungsten surfaces, mass spectrometric study of, 20: 31907
diffusion of, in rubidium vapor, 20: 31221(R) (UCRL-16658, pp 73-87)
RUBIDIUM ISOTOPES Rb-85
energy levels in, g-factor, hyperfine structure, and lifetime of $6^2P_{3/2}$, 20: 31940
hyperfine structure of, resonance coherence in, (E), 20: 31911
RUBIDIUM ISOTOPES Rb-86
uptake by lenses in galactose-fed rats, 20: 30978
RUBIDIUM ISOTOPES Rb-87
energy levels in, g-factor, hyperfine structure, and lifetime of $6^2P_{3/2}$, 20: 31940
RUTHENIUM
elastic properties at 25°C, 20: 31748
separation from neptunium by solvent extraction using 4-methyl-2-pentanone, 20: 31319 (ISO-SA-10)
RUTHENIUM ALLOYS
Nb–Ru, electronic structure of, at superconducting critical temperatures, 20: 31747
RUTHENIUM IONS
production of, for mass spectrometry, thermal techniques for, 20: 31226
RUTHENIUM ISOTOPES
abundance determination by mass spectrometry, ion production technique for, 20: 31207
distribution and natural carriers of, in sea water, 20: 31422
RUTHENIUM ISOTOPES Ru-103
content in fractionated fallout particles from land surface burst, 20: 31460
RUTHENIUM ISOTOPES Ru-106
content in ocean surface waters, 1960 and 1961, 20: 31419
deposition on tropospheric aerosols, 20: 31459
determination of, efficiency of Cherenkov counting methods for, 20: 31184

S

SAFETY
criteria for design and use of nuclear devices in space, 20: 32855
SALIVARY GLANDS
iodine-131 uptake by, 20: 31160
SALTS
purification of magnesium chloride-base, equipment and methods for, 20: 31314(R) (ANL-7175, pp 1-41)
SAMARIUM
determination in conductive tissue of beef heart, activation, 20: 31176
determination in human heart tissue, activation, 20: 31175
energy levels in $f^6(^7F)sp$ subconfiguration of, 20: 31919
ionization on rhenium and tungsten surfaces, effects of adsorbed oxygen on, 20: 31225
separation from beryllium fluorides and lithium fluorides, 20: 32804(R) (ORNL-3936, pp 122-71)
valence states of, x-ray spectroscopic analysis of, 20: 32720(T)
SAMARIUM ALLOYS
Sm–Zn, melting point of $SmZn_2$, 20: 31743
SAMARIUM ISOTOPES
preparation of self-supporting foils of, 20: 31696
SAMARIUM MOLYBDATES
preparation and crystal structure of, 20: 31740
SAMARIUM OXIDES
heat of formation on hot metal surfaces, 20: 31225
SAMARIUM SULFIDES
samarium valence states in, x-ray spectroscopic studies of, 20: 32720(T)
SAMARIUM TUNGSTATES
preparation and crystal structure of, 20: 31740
SANDS
moisture content of, neutron recoil methods of measuring, 20: 31627
SAP (SINTERED ALUMINUM PRODUCTS)
fabrication processes for, development of, 20: 32796(R) (AI-CE-3)
mechanical properties, 20: 32796(R) (AI-CE-3)
microstructure of, use of ionic bombardment for determining, 20: 31765
SAPPHIRES
radioinduced dislocation loops in, oxygen-ion, 20: 31793
SATELLITES
performance of Alouette II, experiments and results from, 20: 32247
SAVANNAH RIVER COMPONENTS TEST REACTOR
operation, Oct. 1961–Dec. 1964, 20: 32859 (DP-991)
SCALERS
counting losses for, Laplace transforms for calculating, 20: 31594
SCANDIUM
determination in conductive tissue of beef heart, activation, 20: 31176
determination in human heart tissue, activation, 20: 31175
elastic properties at 25°C, 20: 31748
SCANDIUM ALLOYS
Be–Sc, phase studies, 20: 31667
Gd–Sc, magnetic ordering in, gadolinium-content effects on g factor for, (E), 20: 32716
SCANDIUM ISOTOPES Sc-46
beta decay of, β-γ circular polarization in, (E), 20: 32457
SCANDIUM OXIDES
electron spectra of, 20: 31219(R) (UCRL-16658, pp 11-20)
spectra of monocrystals of, at 80°K and room temperature, uv absorption, 20: 31240
SCATTERING
amplitude and trajectories in lambda plane, nonrelativistic partial wave, 20: 32187
amplitude for nonlocal potential, lambda plane of nonrelativistic partial-wave, 20: 32188
amplitudes and cross section calculations for, using crossing symmetry and holomorphy, 20: 32106 (AD-634706)
amplitudes for elastic, imaginary-mass representations of Poincare group for, 20: 32154
amplitudes for large angular momenta, effect of Coulomb forces on partial-wave, 20: 32141
amplitudes for, compositeness conditions for partial-wave, 20: 32137
amplitudes in complex lambda plane, singularities of partial-wave, 20: 32189
amplitudes in high-energy elastic, real and imaginary, 20: 32179
amplitudes in multichannel, N/D method for, 20: 32181
amplitudes in s-matrix theory with generalized potential, asymptotic behavior of partial-wave, 20: 32140
amplitudes in static approximation for elastic, SU(n)-invariant, 20: 32136
amplitudes of forward, current-commutator constraints on three- and four-point functions for, 20: 32163
amplitudes of, analyticity test for, 20: 32149
amplitudes of, Mandelstam and angular-momentum analyticity of, 20: 32164
potential, analyticity for solution of, 20: 32162
potential, Fourier series expansion for kernel continuity in generalized, 20: 32118
potential, modified determinantal method for Yukawa, 20: 32135
potential, short range interaction without strong singularity for kernel continuity in generalized, 20: 32117
potentials for, inversion in lambda plane for singular, 20: 32152
potentials in, limiting procedures for singular and nonsingular cutt-off, 20: 32134
Regge-pole theory in, status of, 20: 32185
S-matrix for potential, in complex angular momentum plane, analytic properties of, 20: 32186
s-matrix theory in, causality in, 20: 32112
vertex functions in, Levinson's theorem for zeros of, 20: 32172
SCINTILLATION DETECTORS
charged-particle scattering losses in plastic and sodium iodide in, 20: 31542
design of stilbene, for neutrons, 20: 31532
development for measuring beta absorption in liquids, 20: 31521
development for neutron dose rates in mixed gamma-neutron fields, 20: 31505(R) (BNWL-235-4, pp 30-4)
efficiency in gamma-ray telescopes, Monte Carlo calculations for, 20: 31554
efficiency of neutron, at 20 to 70 Mev, 20: 31584
efficiency of thallium-doped sodium iodide crystal, for gamma radiation, 20: 31553
light attenuation in, 20: 31546
performance for detection of γ and x radiation from deposited plutonium-239 in dogs, 20: 30968 (BNWL-SA-11)
performance of cesium iodide and sodium iodide, for underwater use, 20: 31499 (AD-633752)
phosphor selection for gamma, 20: 31574
pulse height distribution from, evaluation of, 20: 31555
pulse shape discrimination for, 20: 31535
resolution of lead-sandwich shower, 20: 31587
stability of, circuit for improving, 20: 31575
use to obtain starting pulses for time-of-flight measurements, 20: 31579

uses in spectrometry of dual-labeled samples, computer program for data analysis in, 20: 31177
SCREENS
use in cylindrical beta counters, 20: 31536
SEA WATER
analysis for dissolved oxygen, thallium-204 beta source and Geiger-Mueller counter for use in, 20: 31171 (ORO-596)
carbon-14 content and distribution in, 1963 to 1966, 20: 31397(R) (RLO-1776-2)
carbon-14 content of, methods for determining, 20: 31433
desalination of, BWR development for, 20: 32849
desalination of, economics of dual purpose plants for, 20: 32846
desalination of, economics of dual-purpose heavy water reactor for, 20: 32847
desalination of, energy requirements and processes for, 20: 31192
desalination of, laser interferometric studies of electrodialytic, 20: 31220(R) (UCRL-16658, pp 39-72)
desalination of, properties of flash distillation for, 20: 31193
desalination of, properties of electrodialysis, 20: 31194
desalination of, review of nuclear, 20: 32845
fission product content in, 1960 and 1961, 20: 31419
fission product distribution in, natural carriers for, 20: 31422
processing for yttrium-90 separation, 20: 31249
radioactive waste disposal in, biological, chemical, and physical processes affecting, 20: 32883
strontium-90 content above and below surfaces of, 20: 31421
strontium-90 content in, errors in analysis for, 20: 31423
strontium-90 distribution in, 1960 and 1961, 20: 31420
SEED
metabolism in wheat, effects of cysteine and quinone on, 20: 31002
radiation effects on corn and wheat, γ, 20: 31110
radiation effects on corn and wheat, γ, 20: 31113
radiation effects on development of pea, γ, 20: 31114
radiation effects on wheat, metabolic γ, 20: 31002
radiation effects on DNA from cotton, γ, 20: 31019
radiation effects on biochemical properties of, effects of storage on γ, 20: 31024
radiation effects on jute, genetic γ, 20: 31027 (AECD/AG-14)
radiation effects on maize, genetic fast-neutron and x, 20: 31092
radioinduced chromosome aberrations in barley and *Vicia faba*, effects of Myleran on neutron, 20: 31136
radioinduced mutations in barley and rice seeds, γ and x, 20: 31050
SEEDLINGS
radiation effects on metabolism in, x, 20: 31115
radiation effects on cytology and growth of *Pinus rigida*, chronic gamma, 20: 31077
SEIGNETTOELECTRIC MATERIALS
use as radiation detectors, 20: 31539
SEISMIC WAVES
propagation of second Rayleigh and second and third Love modes in, from high-altitude explosions, (E), 20: 32269
velocity of, from SULKY underground nuclear explosion, 20: 31393 (PNE-711F)
SELENIUM
determination in conductive tissue of beef heart, activation, 20: 31176
determination in human heart tissue, activation, 20: 31175
effects on radioinduced crosslinking and decomposition of polyethylene, 20: 31279
electron spectra of, 20: 31219(R) (UCRL-16658, pp 11-20)
SELENIUM FLUORIDES
enthalpy of formation of, 20: 31213(R) (ANL-7175, pp 119-58)
SEMICONDUCTOR DETECTORS
design and performance of lithium-drifted germanium, 20: 31500(R) (BNWL-235-4, pp 4-10)
design of silicon p-n, 20: 31604(P)
development for neutron dose rates in mixed gamma-neutron fields, 20: 31505(R) (BNWL-235-4, pp 30-4)
efficiency of lithium-drifted germanium, for gamma rays, 20: 32564
fabrication of germanium and silicon, for nuclear spectroscopy, 20: 32373(R) (COO-1530-1)
fabrication techniques for large-volume lithium-drift germanium, 20: 31513 (UCRL-14561)
performance of lithium-drifted germanium, for gammas, 20: 31514(R) (UCRL-14881)
performance of lithium-drifted silicon, as beta and gamma spectrometer, 20: 31519
performance of silicon, for low-background counting of alpha and beta particles, 20: 31540
preparation and performance of p-i-n junction, 20: 31537
properties of cadmium telluride p-n junction, 20: 31523
pulse amplitude and polarity of charged-particle entrance effects on, 20: 31498 (AD-632527)
use for measuring density of liquid hydrogen, 20: 31494
use in radiation dosimetry, 20: 31560
use in radiation target chambers for particle correlation measurements, 20: 31556
uses in aerospace research, 20: 31605
SEMICONDUCTORS
properties, 20: 31620
radiation effects on silicon, transient annealing from neutron, 20: 31613 (SC-DC-66-1443)
radiation effects on metal-oxide-silicon, x, 20: 31615
superconductivity of thin films of, (T), 20: 32338(T)
surface physics of, use of field emission microscopy in study of, 20: 32742
SHEEP
radiation effects on, γ, 20: 31026 (AD-633606)
strontium-90 content in bones of Australian, 1961 through 1963, 20: 31403
SHELLS
deformation of rigid-plastic hollow, effects of axial tension and external pressure on, 20: 31335
SHIELDED CONTAINERS
catalog of, Atomic Energy of Canada Ltd., 20: 32891
criticality analysis for fissile material, 20: 31514(R) (UCRL-14881)
design of lead, 20: 32680
SHIELDING
calculations for cylindrical gamma sources, 20: 32678
design of lead, 20: 32680
effects on bone marrow in astronauts, 20: 31029 (BNL-10221)
SHIELDING MATERIALS
gamma and neutron flux in, P_3 method for calculating, 20: 32673 (NAA-SR-Memo-11872)
SHIPPING
container for radioactive materials, safety regulations for, 20: 32680
SHOCK WAVES
propagation in collisionless plasma, (T), 20: 32652
propagation in interplanetary space, bistatic-radar measurements of, 20: 31858
propagation in magnetically driven hydrogen shock tubes, (E), 20: 32615
propagation in plasma, high-field steady-state, (T), 20: 32604
propagation of MHD, in argon–oxygen mixtures, (E), 20: 32217 (N-65-33713)
propagation of spherical, in stars, (T), 20: 31871
properties in MHD plasma flow, 20: 32231
properties of collision-free hydromagnetic, in interplanetary space, (E/T), 20: 31891
pulse calculation from, slide rule for, 20: 32219 (SCL-DC-66-2)
structure of radiative, (E/T), 20: 32670
structure of radiative hydrogen, Navier-Stokes equation for, 20: 32241
use for recombination in hydrogen–oxygen mixtures, 20: 31216 (LA-DC-7659)
SILANE
methoxy-, microwave spectra of, 20: 31221(R) (UCRL-16658, pp 73-87)
SILICON
abundance in solar corona, (T), 20: 31865
bremsstrahlung reactions (y,p) at 32 Mev proton energy spectra from, (E), 20: 32394
crystal structure of, electron diffraction and microscopy methods for studying, 20: 31715(R) (UCRL-16658, pp 105-20)
description of lithium-compensated detectors of, 20: 31605
effects on age hardening in vanadium–niobium–tantalum and vanadium–niobium–titanium alloys, 20: 31709(R) (IITRI-B6042-5)
effects on radioinduced swelling in uranium irradiated at 400 to 500°C, 20: 31666
electron energy losses at 50 kev in, spectra of, (E), 20: 32732
fabrication for nuclear spectroscopy, 20: 32373(R) (COO-1530-1)
neutron capture by, average level widths of compound nucleus from, (E), 20: 32424
performance for low-background counting of alpha and beta particles, 20: 31540
performance of p-i-n junction detectors of, 20: 31537
performance of p-n junctions of, for particle detection, 20: 31498 (AD-632527)
photocurrent production in transistors of, anomalous, (E/T), 20: 31612 (SC-DC-66-1415)
preparation of p-i-n junctions of, using lithium drifting, 20: 31537
proton reactions at 0.05 to 2.9 Bev, induced activity data and cross sections for spallation, (E/T), 20: 32549
proton scattering at 29 and 49 Mev, asymmetries in elastic and inelastic, (E), 20: 32440
radiation effects on, transient annealing from neutron, 20: 31613 (SC-DC-66-1443)
radiation effects on lithium-doped, electron, 20: 31614
radiation effects on single-crystal solar cells of, proton, 20: 31616
radioinduced defects in, depth distribution of 340-kev-electron,

20: 31791
radioinduced defect clusters in n-type, fast-neutron, (E), 20: 31792
response of lithium-drifted, for beta and gamma radiation, 20: 31519
SILICON CARBIDES
compatibility with cesium vapor at 1800°C, 20: 31669
enthalpy of formation of, 20: 31213(R) (ANL-7175, pp 119-58)
sputtering by argon ions at 75 to 600 ev, yields from, (E), 20: 31914
use as coating and matrix for uranium carbide spheroids, 20: 31706(P)
SILICON HYDRIDES
synthesis of, procedure for, 20: 31218(R) (UCRL-16658, pp 1-9)
SILICON ISOTOPES Si-25
decay of, aluminum-25 levels from beta-delayed proton, (E), 20: 32505
half life, (E), 20: 32505
SILICON ISOTOPES Si-28
deuteron reactions (d,p) at 11 and 13 Mev, angular-momentum effects on angular distribution from, (E), 20: 32512
helium-3 reactions (He-3,t) at 37.8 to 40.1 Mev, phosphorus-28 levels and mass from, (E), 20: 32473
neutron reactions (n,α) and (n,p) at 13.95 and 14.6 Mev, angular and energy distributions from, (E), 20: 32431
SILICON ISOTOPES Si-32
use for dating ground waters, 20: 31432
SILICON SYSTEMS
Al–Si, crystal structure of eutectic, effects of phosphorus on, 20: 31716(R) (UCRL-16658, pp 121-32)
Fe–Si, creep at high temperatures, 20: 31714(R) (UCRL-16658, pp 99-103)
Mo–Si–U, hot hardness and microstructure of, effects of quenching temperature on, 20: 31666
Ni–rare earth–Si, crystal structure of $R_3Ni_6Si_2$ compounds in, 20: 31253
SILTS
radioisotope sorption by marine, 20: 32883
SILVER
content in Canyon Diablo meteorite, isotopic composition of, (E), 20: 31861
crystal structure of, electron diffraction and microscopy methods for studying, 20: 31715(R) (UCRL-16658, pp 105-20)
determination in conductive tissue of beef heart, activation, 20: 31176
determination in human heart tissue, activation, 20: 31175
electron reactions at 40 to 80 kev with thick foils of, radiation emission from, (E), 20: 32708
hydrogen atom and ion reactions at 10 to 40 kev, secondary electron emission from, (E), 20: 31533
laser beam reactions on surfaces of, momentum transfer by giant-pulsed, (E), 20: 31810
neutron resonance integrals, 20: 32781
proton elastic scattering at 17.8 Mev, polarization of, (E), 20: 32439
proton reactions at 0.05 to 2.9 Bev, induced activity data and cross sections for spallation, (E/T), 20: 32549
sputtering of, by deuterons, helium ions, and protons at 0.1 to 4.0 Mev, (E), 20: 31905
SILVER ALLOYS
crystal symmetry patterns of, Kikuchi analysis of, 20: 31715(R) (UCRL-16658, pp 105-20)
Cd–In–Ag, radiation effects on mechanical properties of, thermal-neutron, 20: 31668
Er–Ag, electron paramagnetic resonance in, non-S-state, (E), 20: 31764
Gd–Ag, thermal capacity of dilute, at low temperatures, (E), 20: 31762
Ho–Ag, phase studies, 20: 31749
In–Ag, stacking-fault energies in, methods of determining, 20: 31713(R) (UCRL-16658, pp 93-8)
Pb–Ag, thermodynamic properties, 20: 31717(R) (UCRL-16658, pp 143-9)
Pd–Ag, use in deuterium–hydrogen separation by diffusion and electrolysis, 20: 31256
SILVER CHLORIDES
radioinduced defect formation in, thermal annealing of uv and x, 20: 32731
SILVER ISOTOPES Ag-107
alpha reactions with, excitation functions for, (T), 20: 32373(R) (COO-1530-1)
SINGLE CRYSTALS
diffusion of iron and nickel in magnesia, 20: 31719(R) (UCRL-16658, pp 155-69)
SKELETON
strontium-90 content of, effects on content in dog hair, 20: 30972 (TID-22027)
thorium-232 content in human, 20: 30989
SKIN
radiation effects on wound healing in rat, effects of hormones on γ, 20: 31061
sulfur content in human, estimation of, 20: 30982
SNAILS
calcium uptake by aquatic, role of ionic diffusion in, 20: 30991
radiation effects on, γ, 20: 31116
SNOW
radioactivity in, at Nagaoka City, Japan, 1965, 20: 31411
SODIUM
analysis for carbon by combustion, 20: 31213(R) (ANL-7175, pp 119-58)
corrosive effects on reactor materials at high temperatures, effects of carbon on, 20: 31213(R) (ANL-7175, pp 119-58)
corrosive effects on vanadium–titanium alloys at 650°C, effects of oxygen content on, 20: 31669
determination in conductive tissue of beef heart, activation, 20: 31176
determination in human heart tissue, activation, 20: 31175
effects on neutron-induced dimension changes in graphite, 20: 31667
purification methods for, 20: 31213(R) (ANL-7175, pp 119-58)
radiative lifetime of excited electronic states in, 20: 31219(R) (UCRL-16658, pp 11-20)
rare-gas reactions with, ionization cross sections for excited, (T), 20: 31917
reactions with air at high temperatures, 20: 31440(R) (ANL-7175, pp 159-83)
reactions with reactor materials at high temperatures, 20: 31440(R) (ANL-7175, pp 159-83)
solvent properties for oxygen at 110 to 550°C, equation for, 20: 31669
thermodynamic properties of liquid, Prandtl number at 0 to 700°C for, 20: 31724
uptake and loss in relation to active mechanism for sodium extrusion in Scenedesmus cells, 20: 30994
SODIUM ALLOYS
Bi–Na, corrosive effects on stainless steel at high temperatures, 20: 31959(R) (ANL-7175, pp 184-211)
Bi–Na, properties and vapor pressures of, effects of composition and temperature on, 20: 31959(R) (ANL-7175, pp 184-211)
Bi–Na, thermodynamic properties, 20: 31959(R) (ANL-7175, pp 184-211)
K–Na, thermodynamic properties, 20: 31213(R) (ANL-7175, pp 119-58)
K–Na, thermodynamic properties of liquid, Prandtl number at 0 to 700°C for, 20: 31724
Pb–Na, corrosive effects on stainless steel at high temperatures, 20: 31959(R) (ANL-7175, pp 184-211)
Pb–Na, properties at high temperatures, 20: 31959(R) (ANL-7175, pp 184-211)
SODIUM CHLORIDES
evaporation mechanisms, 20: 32684(R) (UCRL-16658, pp 21-38)
ion reactions at 40 to 2000 ev, electron emission from argon and helium, (E), 20: 31912
radiation effects on color-center destruction and recombination luminescence in silver-doped, x, 20: 32693
radiation effects on color-center destruction and recombination luminescence in silver–calcium activated, x, 20: 32694
radioinduced F and M color centers in, x, 20: 32691
radioinduced F-center formation in, temperature dependence of x, 20: 32724(T)
radioinduced Schottky disorder and lattice relaxation in single crystals of, x, (E), 20: 32712
Cu–$MgCl_2$–KCl–NaCl, corrosive effects on ferrous alloys, 20: 31314(R) (ANL-7175, pp 1-41)
SODIUM CITRATES
effects on radioinduced degradation of DNA in *E. coli*, 20: 31144
SODIUM FLUORIDES
effects on radioinduced degradation of DNA in *E. coli*, 20: 31144
SODIUM IODIDES
performance of radiation counters for whole-body counting, 20: 31443 (CONF-650673-1)
performance of scintillation detectors of, for underwater use, 20: 31499 (AD-633752)
SODIUM IONS
desorption from tungsten surfaces, mass spectrometric study of, 20: 31907
SODIUM ISOTOPES Na-22
uptake by lenses of galactose-fed rats, 20: 30978
SODIUM ISOTOPES Na-23
energy levels from proton reactions (p,αγ) with magnesium-26 at 9.3 to 10.5 Mev, (E), 20: 32509
energy levels from magnesium-26 (p,αγ) reactions, gamma multipole mixing ratios and spins for, (E), 20: 32567
neutron reactions (n,α),(n,αn′) and (n,n′α) at 12.6 to 18.7 Mev, cross sections for, (E), 20: 32540
SODIUM ISOTOPES Na-24
determination of, efficiency of Cherenkov counting methods for, 20: 31184
SODIUM NITRATES
effects on nitrogen-15 concentration by nitric acid–nitric oxide exchange, 20: 31639(R) (NYO-755-1, pp 77-129)
SODIUM OXIDES

$BaO–O–Na_2O–Tc_2O_7$, compound formation in, 20: 31244
$O–Na_2O–SrO–Tc_2O_7$, compound formation in, 20: 31244

SODIUM PERCHLORATES
corrosive effects on zirconium, 20: 31687

SODIUM SILICATE GLASS
diffusion of iron oxide in, 20: 31719(R) (UCRL-16658, pp 155-69)

SODIUM SULFITES
effects on radioinduced degradation of DNA in *E. coli*, 20: 31144

SODIUM SYSTEMS
O–Na–U, phase studies at 600 to 1000°C, 20: 31666

SOILS
analysis for moisture by neutron probing, 20: 31435
analysis of, neutron activation, 20: 31434
copper fractionation in neutron-activated, 20: 31325
heating of, using coolant from power reactors, 20: 32843
radioactive waste disposal in, hydrodynamics of, 20: 32883
sorption of cesium, iodine, and strontium by, from Cape Thompson, Alaska area, 20: 31426 (PNE-481, pp 1121-39)
sorptive properties for ions, tracer studies of, 20: 32883
strontium-90 content above and on surfaces of, 20: 31421
strontium-90 uptake by plants from, effects of calcium content and mechanical properties on, 20: 30985

SOLAR BATTERIES
development for Manned Orbital Research Laboratory power generation, 20: 31387
radiation effects on thin-film cadmium sulfide and single-crystal silicon, proton, 20: 31616
radiation resistance of lithium-doped silicon, 20: 31614
uses in electric propulsion systems for space, 20: 31382

SOLAR FLARES
alpha fluxes from, computer program for calculating, 20: 32674 (NP-15697(Vol.3))
effects on relaxation time of ionosphere, 20: 32267
effects on sudden frequency deviations in ionosphere, 20: 32268
electron emission and propagation from, (E), 20: 31869
magnetic flux topological variations in, (T), 20: 32656
prediction technique for proton, long-range, 20: 31879
proton fluxes from, computer program for calculating, 20: 32674 (NP-15697(Vol.3))

SOLAR RADIATION
conference on solar wind, 20: 31880
detection and measurement of x, fabrication and operation of ionization chamber for, 20: 31511 (N-66-16936)
effects of solar wind on type-1 comet tails, (T), 20: 31898
effects on electron distribution in Van Allen belts, 20: 32260
electron detection and measurement in, (E), 20: 31886
hazards to aircraft passengers in high-altitude supersonic flight from, 20: 31468
interaction of solar wind with comets, 20: 31896
interaction of solar wind with magnetosphere, simulation of, 20: 32284
interactions of solar wind with comets, MHD aspects of, (T), 20: 31897
interactions of solar wind with magnetosphere, fluid dynamics of, (T), 20: 32275
interactions of solar wind with magnetosphere, particle aspects of, (T), 20: 32276
interactions of solar wind with magnetosphere, shock wave from, (E/T), 20: 32281
interactions of solar wind with geomagnetic fields, (E), 20: 32286
interactions with cometary tails, 20: 31874
interactions with moon, lunar magnetosphere from, (T), 20: 31899
magnetic field polarity of solar wind stream, variations in, 20: 31860
origin of solar wind, (T), 20: 31893
prediction technique for proton, long-range, 20: 31879
properties of solar wind, (E), 20: 31881
properties of solar wind, (E/T), 20: 31889
proton flux variations in, periodic, (E), 20: 31885
solar-wind simulation for Pioneer space vehicle, using plasma sources, 20: 31877
structure of solar wind, models for, 20: 31890
structure of solar-wind, determination using radio astronomy, 20: 31888
velocity of solar wind, correlations with solar phenomena, 20: 31882

SOLENOIDS
cryostat design for superconducting, with thermal working volume, 20: 32334

SOLID PROPELLANTS
burning rates and heats of explosions of, effects of irradiated ammonium perchlorate on, 20: 31286

SOLIDS
analysis by spark-source mass spectrometry, 20: 31202
analysis of low-vapor-pressure, by mass spectrography, 20: 31204
analysis of, by mass spectrometry, review of, 20: 31201
book: *Solid State Physics*, Vol. 18, 20: 32718
electron avalanche formation in, collective energy losses in, (T), 20: 32727(T)
laser beam reactions with, plasma production by, 20: 32666
neutron spectroscopy of, 20: 32687
positron annihilation in, physics of, 20: 32101
stress disturbance propagation in elastic deformable, 20: 31331 (UCRL-14616)
surface area measurements on, using krypton-85, 20: 31353

SOLUBILITY
determination of terminal, of gases in metals, high-temperature technique for, 20: 31250

SOLUTIONS
kinetics and structure of ammonia–metal, 20: 31218(R) (UCRL-16658, pp 1-9)
radioinduced ionization of aqueous, model for radical reaction mechanisms in, 20: 31293

SOLVENT EXTRACTION PROCESSES
development for processing thorium-bearing fuels, 20: 31326

SOLVENTS
analysis for water, chromatographic, 20: 31641(R) (NYO-755-1, pp 173-208)
nuclear polarization of, for measurement of ionic spin-lattice relaxation times, 20: 31221(R) (UCRL-16658, pp 73-87)

SONIC INSPECTION
equipment for elastic moduli determination by, 20: 31708 (ANL-7119)

SOUTHWEST EXPERIMENTAL FAST OXIDE REACTOR
control systems for, development of, 20: 32860(R) (GEAP-5108)
coolant flow testing for, stability of, 20: 32860(R) (GEAP-5108)
core design criteria for, 20: 32860(R) (GEAP-5108)
criticality studies for, 20: 32860(R) (GEAP-5108)
development and research program, Nov. 1965–Jan. 1966, 20: 32860(R) (GEAP-5108)
fuel development for, 20: 32860(R) (GEAP-5108)
fuel handling procedures for, remote, 20: 32860(R) (GEAP-5108)
fuel temperature sensors for, development of, 20: 32860(R) (GEAP-5108)
neutron flux monitoring system for, development of, 20: 32860(R) (GEAP-5108)

SPACE
book: *Particles in the Atmosphere and Space*, 20: 32285
electron content in cislunar region of, effects of coherent density fluctuations on radar determination of, 20: 31857
magnetic field effects on solar-injected charged particle propagation and storage in interplanetary, 20: 31884
magnetic field polarity in interplanetary, variations in, 20: 31860
magnetic fields in interplanetary, measurements of, (E), 20: 31887
shock propagation in interplanetary, collision-free hydromagnetic, (E/T), 20: 31891

SPACE FLIGHT
effects on wheat seeds and plants grown from them, 20: 31058
electronic equipment for, radiation vulnerability of, 20: 31619
phantom for use in, design of dose-equated plastic, 20: 31455
radiation effects on man during, hematological, 20: 31029 (BNL-10221)
radiation hazards from Lunar and Martian, tabulation of, 20: 32674 (NP-15697(Vol.3))
radiation hazards in, proton, 20: 31095

SPACE VEHICLES
ion engines for, power-conditioning systems for, 20: 31357
ion engines for, power conditioning for contact-ionization, 20: 31360
ion-engine systems for, development of lightweight, 20: 31364
plasma engine for, steady-state operation of coaxial pulsed two-stage, 20: 31365
plasma engines for, propellant injection devices for, 20: 31363
propulsion of, feasibility of solar power electric, 20: 31382
propulsion systems for, reliability of electric, 20: 31359
propulsion systems using radioisotopes for propellant heating, 20: 31361
propulsion systems for stability control and station keeping, description of, 20: 31387
radiation flux in Van Allen belts, proton, 20: 32244 (N-66-13126)
reentry of, thermionic power generation from, 20: 31961 (SC-DC-66-1115)
solar-wind simulation for Pioneer, using plasma sources, 20: 31877

SPAIN
radiation processing of food in, review of, 20: 31628

SPARK CHAMBERS
data analysis for, computer use for, 20: 31508(R) (COO-1018-1075)
efficiency of, calculation of, 20: 31558
particle kinematics in, use of multiple scattering and secondary sparks in determining, 20: 31570
particle track brightness in, photomultiplier and galvanometer for measuring, 20: 31582
performance in system with nuclear emulsions for determining point of incidence of particles, 20: 31569
performance of microwave, 20: 31534

power supplies for, parallel and series, 20: 31571
SPECTRA
energy shift of, zero-point and Lamb, 20: 31908
SPECTROMETERS
design and performance of ENDOR, 20: 32525
design of high aperture ratio, 20: 31481(T) (AERE-Trans-1050)
design of high-resolution magnetic, for ORIC, 20: 31822 (ORNL-P-2260)
design of portable, for radiological monitoring, 20: 31601
design of, combined with analyzer for biology studies, 20: 31525
properties of single-crystal magnetic, for relativistic particles, (E/T), 20: 31563
SPECTROPHOTOMETRY
uses of atomic absorption, 20: 31167(R) (ANL-7175, pp 217-25)
SPECTROSCOPY
measurement of short spin-lattice relaxation times by solvent nuclear polarization, 20: 31221(R) (UCRL-16658, pp 73-87)
use of spectral data in determination of anharmonic potential energy constants for molecules, 20: 31949
SPERM
radiation effects on human, after gonadal exposure, 20: 31035(R) (RLO-1780-8)
radiation effects on human, from gonadal exposure, 20: 31034(R) (RLO-1780-7)
radiation injuries in, repair of premutational uv and x, 20: 31040
radiosensitivity of human, tracer study on, 20: 31035(R) (RLO-1780-8)
SPERMATOGENESIS
radiation effects on rate and timing of, in man, 20: 31034(R) (RLO-1780-7)
radiation effects on monkey, γ and x, 20: 31117
radiation effects from polonium-210 on mouse testes, 20: 31063
SPHERES
propagation in gaseous, spherical, (T), 20: 31871
SPLEEN
radiation effects on DNase activity in rat, 20: 31143
radiosensitivity effects of injected, in mice, 20: 31127
radiotherapy of mouse, synergistic effects of Mitomycin C and Endoxan in, 20: 31131
SPUTTERING
study by field emission microscopy, techniques of, 20: 32742
yields from high-energy, mass spectrometric study of, (E/T), 20: 31905
STABLE ISOTOPES
abundance ratios in Earth's mantle, 20: 32245(T) (NSJ-tr-48)
catalog of, Atomic Energy of Canada Ltd., 20: 32891
STAINLESS STEEL
compatibility of type 316L, with plutonium carbide–uranium carbide up to 900°C, 20: 31675
compatibility of type 304, with plutonium–uranium–zirconium alloy to 800°C, 20: 31666
corrosion by copper–magnesium chloride system at 600 to 800°C, 20: 31314(R) (ANL-7175, pp 1-41)
corrosion by liquid metals, 20: 31959(R) (ANL-7175, pp 184-211)
corrosion of type 304, by boric acid at 600°F, 20: 31669
corrosion of types 304, 316, and 17-4 PH, by heavy water at 315°C, 20: 31669
corrosion of types 316, 321, 347, and 19-9DL, by lithium hydride at 900, 1200, and 1400°F, 20: 31669
corrosion of, by fused cadmium chloride-base salts at 650°C, 20: 31314(R) (ANL-7175, pp 1-41)
ductility of austenitic, effects of cerium, lanthanum, and yttrium alloying additions on, 20: 31669
hardness of type 310, effects of exposure to air at 1200 to 1400°F on, 20: 31669
hydrogen atom reactions at 10 to 40 kev, secondary electron emission from, 20: 31533
joining of carbon steel and stainless steel to, parameters for friction, 20: 31670
performance of type 304, in accelerating electrodes in cesium-contact ion thrustors, 20: 31383
radiation effects on mechanical properties of, in-reactor, 20: 31785 (ORNL-P-2162)
radiation effects on ductility of type 304, effects of carbon content on fast- and thermal-neutron, 20: 31669
radioinduced embrittlement in austenitic, neutron, 20: 31801
radioinduced embrittlement in type 304, effects of boron additions on fast-neutron, 20: 31669
radioinduced embrittlement in type 304, effects of titanium additions on fast- and thermal-neutron, 20: 31669
reactions of type 304, with plutonium–thorium–uranium alloy, 20: 31666
reactions of type 304, with steam at 900 to 1500°C, 20: 31669
reactions with sodium at high temperatures, 20: 31440(R) (ANL-7175, pp 159-83)
reactions with steam at 1400 to 1500°C, hydrogen evolution from, 20: 31440(R) (ANL-7175, pp 159-83)
stress-rupture at 1250°F, type 304, 20: 31669
Eu_2O_3–stainless steel 304L–TiO_2, corrosion by water at high temperatures, 20: 31678 (HIT-3583-24)
PuO_2–stainless steel, fabrication of dispersion fuels of, process for, 20: 31666
PuO_2–stainless steel, radiation effects on, effects of sample density on, 20: 31666
STAINLESS STEEL COUPLES
Al–stainless steel, contact thermal conductance of, 20: 31712 (UCRL-14227(Rev.1))
ceramics–stainless steel, contact thermal conductivity of, 20: 31712 (UCRL-14227(Rev.1))
STANFORD LINEAR ACCELERATOR
design and development history and research uses of, 20: 31824 (SLAC-62)
power supplies for, performance of hydrogen thyratron, 20: 31825 (SLAC-PUB-192)
STARS
beta decay in, photon-induced, (T), 20: 31878
carbon negative ion continuous absorption in, free-free, 20: 31864
collapse in expanding universe, gravitational, (T), 20: 32306
collapse of, relativistic neutrino transport theory for gravitational, 20: 32296
evolution of rotating proto-, 20: 31872
formation of, (T), 20: 31873
helium burning in degenerate cores of, model for onset of, 20: 31866
identification of extragalactic radio-source, 20: 31853
magnetic fields in quasars, 20: 31868
shock propagation in polytrope-5, model for spherical, 20: 31871
shock structure in, radiative, (E/T), 20: 32670
STEAM
corrosive effects on niobium–tin–zirconium alloys, composition of oxide film formed by, 20: 31669
effects on chromium–iron–zerconium alloy at 300, 400, and 500°C, 20: 31677(R) (GEAP-4840)
reactions with aluminum, stainless steel, and urania at high temperatures, 20: 31440(R) (ANL-7175, pp 159-83)
reactions with iron at 950 to 1400°C, kinetics of, 20: 31669
reactions with molybdenum, niobium, and tantalum, 20: 31669
reactions with rhenium and tungsten to 1700°C, 20: 31669
reactions with type 304 stainless steel and Zircaloy-2 at 900 to 1500°C, 20: 31669
STEEL
coating with carbon from carbon monoxide, 20: 31670
corrosion of AISI type 1020, by copper–magnesium chloride system at 600 to 800°C, 20: 31314(R) (ANL-7175, pp 1-41)
crystal structures of ausformed, 20: 31715(R) (UCRL-16658, pp 105-20)
electrochemical properties of radioactive, 20: 31231
radiation effects on mechanical properties of low-alloy pressure vessel, fast-neutron, 20: 31796
tensile properties of low-alloy strain-aged, 20: 31716(R) (UCRL-16658, pp 121-32)
STEROIDS
preparation of tritium-labeled estriol-3-glucosiduronate by guinea pig liver homogenate, 20: 31312
structure of, analysis by field ion mass spectrometry, 20: 31199
STEROIDS, 17-KETO-
radiation effects on, in man, 20: 31035(R) (RLO-1780-8)
STILBENE
performance for gamma detection and measurement in high neutron flux, 20: 31602
use in neutron scintillation counters, 20: 31532
STOMACH
iodine-131 uptake by, 20: 31160
STRANGE PARTICLES
production in mesons (π^+)- and (π^-)-proton interactions at 4 Bev/c, cross sections for, (E), 20: 32029
STREPTOMYCIN
effects on radiation effects on human tissue cultures, 20: 31121
STRESS ANALYSIS
of elastic disturbance propagation in deformable solids, 20: 31331 (UCRL-14616)
of projectiles penetrating reactor containment during meltdown, 20: 32744 (SRIA-1)
photoelastic, of reactor pressure vessels, 20: 32751
thermoviscoelastic, approximate method for, 20: 31334
STRONTIUM
effects on adenosine triphosphatase formation in wheat roots, 20: 30992
effects on corrosion of graphite by water vapor, 20: 31667
separation from cesium by ion exchange on cellulose phosphate, 20: 31324
separation from water by precipitation, kinetics of, 20: 31318 (BMwF-FBK-65-04)

sorption on soil from Cape Thompson, Alaska area, 20: 31425 (PNE-481, pp 1121-39)
uptake by bone tissue, mechanism of, 20: 30973

STRONTIUM ISOTOPES Sr-85
uptake and retention by leaves, effects of relative humidity and temperature on, 20: 30996

STRONTIUM ISOTOPES Sr-86
content in carbonatites and limestones from Ice River, British Columbia, 20: 31406

STRONTIUM ISOTOPES Sr-87
content in carbonatites and limestones from Ice River, British Columbia, 20: 31406

STRONTIUM ISOTOPES Sr-88
energy levels from yttrium-88 decay, parity and spin of, (E), 20: 32453
helium-3 reactions (He-3,p) at 14 to 19 Mev, isomer pair production cross sections for, (E), 20: 32430

STRONTIUM ISOTOPES Sr-89
content in fallout in Japan, 1965, 20: 31405
determination in food and water, gamma spectrometric, 20: 31180
determination in presence of strontium-90, beta counting technique for, 20: 31188
radiation hazard from atmospheric, calculation of, 20: 31528

STRONTIUM ISOTOPES Sr-90
content above and on surfaces of land and sea, 20: 31421
content in Atlantic Ocean surface waters, 1961, 20: 31418
content in caribou, reindeer, and man, effects of diet on, 20: 31442 (BNWL-SA-661)
content in central Pacific Ocean, 1961, 20: 31414
content in central Pacific Oacean, 1962 and 1964, 20: 31416
content in deep waters of the Indian Ocean, 1960 and 1961, 20: 31417
content in diet in California, 20: 31471
content in hair, effects of dietary content on, 20: 30972 (TID-22027)
content in human bones and tissues in Finland, 20: 31142
content in marine organisms in Chukchi Sea, Alaska, 1959 to 1962, 20: 31427 (PNE-481, pp 1141-9)
content in milk and rain in New Zealand, 1965, 20: 31446(R) (NP-16015)
content in milk in Norway, 1960 through 1964, 20: 31465
content in ocean surface waters, 1960 and 1961, 20: 31419
content in sea water, errors in determination of, 20: 31423
content in South China Sea surface waters, November, 1962, 20: 31415
depostion on ground, effects of industrial smog on, 20: 31403
determination in food and water, gamma spectrometric, 20: 31180
determination in presence of strontium-89, beta counting technique for, 20: 31188
determination in water, using Cherenkov effect, 20: 31506 (CEA-R-2915)
distribution and natural carriers of, in sea water, 20: 31422
distribution in surface waters of the Atlantic, Indian, and Pacific Oceans, 1960 and 1961, 20: 31420
effects on hematopoietic tissues in dogs and swine, acute- and chronic-exposure carcinogenic, 20: 31031 (BNWL-SA-201)
effects on thermal tolerance of fish, 20: 31028 (AECL-2409)
excretion of, by rats, effects of sodium phytate on fecal and urinary, 20: 30977
metabolism by man, 20: 31142
radiation hazard from atmospheric, in mixture with yttrium-90, 20: 31528
sorption by aged horse manure, 20: 31252
sorption by intestine, effects of green tea on, 20: 30987
uptake by plants, effects of calcium content and mechanical properties of soil on, 20: 30985

STRONTIUM OXIDES
Li_2O–O–SrO–Tc_2O_7, compound formation in, 20: 31244
O–Na_2O–SrO–Tc_2O_7, compound formation in, 20: 31244
O–SrO–Tc_2O_7, compound formation in, 20: 31244

STYRENE POLYMERS
radiation effects on positronium lifetimes in, thermal neutron, (E), 20: 32704

SUCCINIC ACID
determination by xenon trioxide oxidation, titrimetric, 20: 31196

SUGARS
distribution in lenses of galactose-fed rats, 20: 30978
radiation effects on, in oranges, γ, 20: 31632

SULFOXIDES
complexes with uranium tetrafluoride, preparation of, 20: 31236

SULFUR
bremsstrahlung reactions (γ,p) at 32 Mev proton energy spectra from, (E), 20: 32394
content in human tissues, estimation of, 20: 30982
distribution of recoil phosphorus-32 and sulfur-35 in neutron-irradiated, 20: 31295
effects on radioinduced crosslinking and decomposition of polyethylene, 20: 31279
neutron capture by, average level widths of compound nucleus from, (E), 20: 32424
proton elastic scattering at 17.8 Mev, polarization of, (E), 20: 32439
radiation effects on, neutron, 20: 31295

SULFUR COMPOUNDS
reactions of, with atomic nitrogen, 20: 31218(R) (UCRL-16658, pp 1-9)

SULFUR FLUORIDES
attachment of gaseous electrons to, 20: 31221(R) (UCRL-16658, pp 73-87)
enthalpy of formation of, 20: 31213(R) (ANL-7175, pp 119-58)
radiation effects on electron energy in ion pair production in, measurement of γ, 20: 31292

SULFUR ISOTOPES S-32
deuteron (d,p) reactions at 3.20 Mev, sulfur-33 low-lying levels from, (E), 20: 32565
deuteron reactions (d,p) at 11 and 13 Mev, angular-momentum effects on angular distribution from, (E), 20: 32512

SULFUR ISOTOPES S-33
energy levels from sulfur-32 (d,p) reactions, branching and mixing ratios, parities, and spins for low-lying, (E), 20: 32565

SULFUR ISOTOPES S-34
deuteron reactions (d,p) at 11 and 13 Mev, angular-momentum effects on angular distribution from, (E), 20: 32512

SULFUR ISOTOPES S-35
beta activity of, use of 4π proportional counters for measuring, 20: 31548
chemical properties of recoil, in neutron-irradiated sulfur, 20: 31295
separation from mixtures with phosphorus-32, 20: 31309

SULFUR NITRIDES
spectra of nitrogen-15 in cationic thiotrithiazyl, NMR, 20: 31218(R) (UCRL-16658, pp 1-9)

SULFURIC ACID
effects on nitrogen-15 concentration by nitric acid–nitric oxide exchange, 20: 31639(R) (NYO-755-1, pp 77-129)

SUN
activity parameters for 1965, 20: 32259
corona of, diffusion effects on composition of, (T), 20: 31894
corona of, iron abundance in, (T), 20: 31867
corona of, iron, nickel, and silicon relative abundances in, (T), 20: 31865
corona structure determination using radio astronomy, 20: 31888
magnetic field structure of, reconnection and annihilation in, (T), 20: 31895
photosphere of, magnetic field structure in, (E), 20: 31892
prominences of, magnetic flux topological variations in, 20: 32656
properties of, solar wind velocity correlations with, 20: 31882

SUPERCONDUCTIVITY
measurements of, use of liquid helium-4 in low-temperature apparatus for, 20: 32336
theory of thin semiconductor film, 20: 32338(T)

SUPERCONDUCTORS
critical current of niobium–titanium, effect of precipitates on, 20: 32322
critical currents in bismuth–indium and bismuth–tin film, magnetic field effects on, (E), 20: 32317
critical field of titanium alloy, spin-orbit effects on upper, (E), 20: 32330
cryostat design for solenoids of, with thermal working volume, 20: 32334
development of magnets of, for ultrahigh fields, 20: 32337
electron motion on surface of, in gravitational field, (T), 20: 32325
electron tunneling in, spatial variation of order parameter effects on on density of states in, (T), 20: 32340
electron tunneling in superimposed layers of normal aluminum and lead, (E), 20: 32342
electron tunneling conductance in junctions of, model for zero-bias anomalies in, 20: 32714
energy gap anisotropy in aluminum, in magnetic fields, determination using microwave absorption, 20: 32326
magnetic field trapping by niobium–tin hollow cylinders, temperature dependence of, (E), 20: 32316
magnetic flux jumping in high-field high-current, criterion for stability against, 20: 32320
magnetic flux jumping in high-field high-current niobium–tin intermetallic compound, stability against, (T), 20: 32320
magnetic flux penetration into single-crystal, measurement of, (E), 20: 32343
magnetic flux pinning by superconducting tin precipitate in indium–lead–tin and lead–tin alloys, (E), 20: 32313
magnetic moment of type II ellipsoidal, in mixed state, (T), 20: 32321(T)
microwave effects on critical currents in constricted films of tin, (E), 20: 32328
microwave emission by point contacts of, 20: 31482
performance of thin film, for threshold logic circuitry, 20: 32311 (ORO-2430-27)
properties of, 20: 32339
properties of quadrupole magnets of, for lens systems, 20: 31815

(BNL-10144)
properties of type II, research on, 20: 32312(R) (UCRL-16658, pp 133-43)
properties of, effects of metallurgical variables on, 20: 31750
quantization in films of, macroscopic, 20: 32324
quantum interference in multiply connected, (E), 20: 32344
research on, 20: 32339
supercooling and superheating in transition of indium, 20: 32331
thermal conductivity of surface sheath of indium–lead, (E), 20: 32327
ultrasonic attenuation in, (T), 20: 32335
SURFACE WATERS
radium content of, methods for determining, 20: 31191
SURFACES
analysis of remote, combination neutron technique for, 20: 31211
area measurements using krypton-85 adsorption, 20: 31353
SWEDEN
fallout radionuclide content in ecosystems of, 20: 31442 (BNWL-SA-661)
radiation processing of food in, review of, 20: 31628
SWIMMING POOL REACTORS
control of Japanese TTR-1, computer, 20: 32867
reactivity measurements on TTR-1, using neutron noise analysis by two-detector correlation method, 20: 32868
SWINE
radioinduced hematopoietic tumors in, effects of strontium-90 on, 20: 31031 (BNWL-SA-201)
SWITCHES
development for computers, 20: 31645(R) (AD-627094)
development of superconductive threshold, for logic circuits, 20: 32311 (ORO-2430-27)
SWITZERLAND
radiation processing of food in, review of, 20: 31628
SYNCHROCYCLOTRONS
beam for CERN, development of polarized proton, 20: 31835
performance optimization of CERN 600-Mev, 20: 31830
SYNCHROTRONS
beam extraction from proton, field nonlinearily in lenses for, (T), 20: 31836
magnet current stabilizer for, design of multichannel, 20: 31837
operation of JINR, development of programming system for, 20: 31840
storage ring for CERN, NMR field measuring equipment for, 20: 31817 (CERN-66-15)
SYSTEMS FOR NUCLEAR AUXILIARY POWER
safety criteria for design and use of, in space, 20: 32855
SYSTEMS FOR NUCLEAR AUXILIARY POWER (SNAP-8)
power transmission cables for, optimum weight of, 20: 32853 (NAA-SR-Memo-11925)
SYSTEMS FOR NUCLEAR AUXILIARY POWER (SNAP-10)
radiation environment of 10A, equipment hardening against, 20: 31618
shutdown of 10A, electrically actuated band release device for, 20: 32852 (NAA-SR-Memo-11454)
SYSTEMS FOR NUCLEAR AUXILIARY POWER (SNAP-50)
boiler development for SNAP-50/SPUR, 20: 32857

T

TANTALUM
annealing strain-induced point defects in high-purity, 20: 31714(R) (UCRL-16658, pp 99-103)
compatibility with Nimonic-90 at 760 to 900°C, 20: 31675
compatibility with cesium vapor at 1800°C, 20: 31669
corrosion by cerium–cobalt–plutonium alloy fuels, effects of carbon on, 20: 31679(R) (LA-3524)
corrosion by various alkaline media at 25 and 98°C, 20: 31669
diffusion of interstitial deuterium in, 20: 31766
dislocation mechanisms in single-crystal, 20: 31714(R) (UCRL-16658, pp 99-103)
effects on microstructure of tungsten–thoria dispersion-hardened alloys, 20: 31781
elastic properties of, effects of diffusion of interstitial deuterium on, 20: 31766
electronic structure of, at superconducting critical temperatures, 20: 31747
heat capacity of high-purity, at 0.35 to 25°K, 20: 32684(R) (UCRL-16658, pp 21-38)
microstructure and lattice orientations in, technique for revealing, 20: 31673
oxidation by steam at 950 to 1300°C, 20: 31669
oxidation of, void formation in, 20: 31684
oxidation rates at 1450 to 2900°K and 8×10^{-6} to 7×10^{-5} torr oxygen pressure, 20: 31227
properties of porous, for cesium ionization, 20: 31388
proton reactions at 0.05 to 2.9 Bev, induced activity data and cross sections for spallation, (E/T), 20: 32549
proton reactions at 40 Mev to 25 Bev, lithium isotopes from, (E), 20: 31205
solubility in plutonium at 700 to 950°C, 20: 31666
thermal expansion of, effects of carbon contamination on, 20: 31669
TANTALUM ALLOYS
coatings for, oxidation-resistant, 20: 31669
Mo–Ta, properties of single-crystal, electric and mechanical, 20: 31715(R) (UCRL-16658, pp 105-20)
Nb–Ta–V, development and properties of, 20: 31709(R) (IITRI-B6042-5)
Nb–Ta–W–Zr, creep properties of FS-85, 20: 31669
Ni–Ta, electric conductivity of, anomalies in, 20: 31775
Pt–Ta, phase diagram, 20: 31669
Ta–Ti, superconducting critical field of, spin-orbit effects on upper, (E), 20: 32330
Ta–W, corrosion by cerium–cobalt–plutonium alloy fuels, effects of carbon on, 20: 31679(R) (LA-3524)
Ta–W, electronic structure of, at superconducting critical temperatures, 20: 31747
Ta–W, tensile properties of carburized and uncarburized, 20: 31679(R) (LA-3524)
Ta–W–Y, corrosion by cerium–cobalt–plutonium alloy fuels, effects of carbon on, 20: 31679(R) (LA-3524)
TANTALUM BORIDES
enthalpy of formation of, 20: 31213(R) (ANL-7175, pp 119-58)
performance in focus electrodes in cesium-contact ion thrustors, 20: 31383
TANTALUM CARBIDES
fabrication by hot-pressing, 20: 31699
Co–TaC–WC, mechanical properties of cermets of, effects of composition on, 20: 31760
graphite–TaC, fabrication and properties of hot-pressed composites of, 20: 31688 (NASA-CR-507)
TANTALUM ISOTOPES Ta-182
energy level transitions of, spectra from, (E), 20: 32564
TANTALUM OXIDES
thermodynamic stability measurements on, using galvanic cells, 20: 31717(R) (UCRL-16658, pp 143-9)
transformation in, kinetics of avatase-rutile, 20: 31719(R) (UCRL-16658, pp 155-69)
$CoO–Nb_2O_5–Ta_2O_5$, phase studies, 20: 31734
TANTALUM SILICIDES
performance in focus electrodes in cesium-contact ion thrustors, 20: 31383
TANTALUM SYSTEMS
C–Hf–Ta, phase diagram at 2050°C, 20: 31668
H–Ta, preparation of, for transmission electron microscopy hydrogen concentration in electrothinning procedures for, 20: 31691
TARAPUR POWER REACTOR
description, 20: 32816
description, 20: 32817
TARTARIC ACID
determination by xenon trioxide oxidation, titrimetric, 20: 31196
TECHNETIUM IONS
production of, for mass spectrometry, thermal techniques for, 20: 31226
TECHNETIUM ISOTOPES Tc-99
incorporation of, in insulin, proteins, thyroxine, and tyrosine, 20: 31265
preparation of 6-hr isomer of, 20: 31265
use in diagnosis of liver diseases by scintillation scanning, 20: 31147 (CNEA-168)
TECHNETIUM OXIDES
$BaO–Li_2O–O–Tc_2O_7$, compound formation in, 20: 31244
$BaO–O–Na_2O–Tc_2O_7$, compound formation in, 20: 31244
$BaO–O–Tc_2O_7$, compound formation in, 20: 31244
$CaO–O–Te_2O_7$, compound formation in, 20: 31244
$Li_2O–O–SrO–Tc_2O_7$, compound formation in, 20: 31244
$O–Na_2O–SrO–Tc_2O_7$, compound formation in, 20: 31244
$O–SrO–Tc_2O_7$, compound formation in, 20: 31244
TECHNICAL REPORTS
lists of ANL, May 1965 to April 1966, 20: 31164(R) (ANL-7175)
lists of UCRL, on dislocations in metals, 20: 31714(R) (UCRL-16658, pp 99-103)
lists of UCRL, on high-strength materials, 20: 31716(R) (UCRL-16658, pp 121-32)
lists of UCRL, on thermodynamics of metal systems, 20: 31717(R) (UCRL-16658, pp 143-9)
lists of UCRL, on high-temperature reactions, 20: 31718(R) (UCRL-16658, pp 149-54)
lists of UCRL, on ceramics, 20: 31719(R) (UCRL-16658, pp 155-69)
lists of UCRL, on high-field superconductivity, 20: 32312(R) (UCRL-16658, pp 133-43)
lists of UCRL, on solid state chemistry and physics, 20: 32684(R) (UCRL-16658, pp 21-38)
lists of UCRL, on nuclear science, 20: 31166(R) (UCRL-16658, pp 89-92)

lists of UCRL, on inorganic chemistry, 20: 31218(R) (UCRL-16658, pp 1-9)
lists of UCRL, on electrochemistry, 20: 31220(R) (UCRL-16658, pp 39-72)
lists of UCRL, on physical chemistry, 20: 31221(R) (UCRL-16658, pp 73-87)
lists of UCRL, on crystal imperfections, 20: 31713(R) (UCRL-16658, pp 93-8)
lists of UCRL, on structures of metals, 20: 31715(R) (UCRL-16658, pp 105-20)
lists of UCRL, on chemical thermodynamics, 20: 31219(R) (UCRL-16658, pp 11-20)

TELEMETERING SYSTEMS
design for recording physiological functions of free-ranging test animals, 20: 30961(R) (BNWL-235-4, pp 25-9)
design for remote measurements of body temperature and heart function, 20: 31474(R) (BNWL-235-4, pp 1-4)

TELEVISION EQUIPMENT
development for ultrasonic imaging, 20: 31352 (ANL-7042)

TELLURIUM
determination in tellurium ores, 20: 32385
effects on radioinduced crosslinking and decomposition of polyethylene, 20: 31279

TELLURIUM FLUORIDES
enthalpy of formation of, 20: 31213(R) (ANL-7175, pp 119-58)

TELLURIUM ISOTOPES Te-119
decay scheme for isomeric, (E), 20: 32373(R) (COO-1530-1)

TELLURIUM ISOTOPES Te-127
decay of, γ-γ directional correlations in, (E), 20: 32396

TELLURIUM ISOTOPES Te-130
half life of double beta decay of, (E), 20: 32385

TELLURIUM ISOTOPES Te-131
beta decay of isomeric, iodine-131 level spins from, (E), 20: 32563

TELLURIUM ISOTOPES Te-132
radiation dose from ingested, computer calculation of, 20: 31441 (BNWL-SA-40)

TELLURIUM SYSTEMS
Li–Te, thermodynamic properties, 20: 31959(R) (ANL-7175, pp 184-211)

TEMPERATURE
effects on strontium-85 and retention by leaves, 20: 30996
measurement of animal-body, remote equipment for, 20: 30961(R) (BNWL-235-4, pp 25-9)
monitoring human body, telemetering system for, 20: 31474(R) (BNWL-235-4, pp 1-4)

TERBIUM ALLOYS
Tb–Zn, melting point of $TbZn_2$, 20: 31743

TERBIUM FLUORIDES
electron paramagnetic resonance in terbium-doped cerium oxide crystals, 20: 32723(T)

TERBIUM ISOTOPES Tb-157
energy levels from dysprosium-157 beta decay, (E), 20: 32464

TERBIUM ISOTOPES Tb-160
beta decay of, conversion coefficients for transitions in, (E), 20: 32443

TERBIUM ISOTOPES Tb-161
beta decay of, gamma transitions from, (E), 20: 32463

TERBIUM ISOTOPES Tb-162
decay scheme, (E), 20: 32462

TERBIUM ISOTOPES Tb-163
decay scheme, (E), 20: 32462

TERBIUM MOLYBDATES
preparation and crystal structure of, 20: 31740

TERBIUM TUNGSTATES
preparation and crystal structure of, 20: 31740

TEREPHTHALIC ACID, ETHYLENE POLYMER ESTERS
radioinduced free radicals in, ESR studies of gamma, 20: 31306
radioinduced trapping and thermal release in films of, electron, 20: 31790

THALLIUM
determination of trace amounts of, using cobalt-60 as radioactive indicator, complexometric, 20: 31181
radiative lifetime of excited electronic states in, 20: 31219(R) (UCRL-16658, pp 11-20)
ultrasonic attenuation and velocity in single crystals of normal and superconducting, (E/T), 20: 31780
vapor pressures of alloyed and pure, 20: 31717(R) (UCRL-16658, pp 143-9)

THALLIUM ALLOYS
Bi–Tl, superconducting transitions of amorphous, 20: 32341
Tl–rare earth, crystal structure of, CsCl-type intermediate phases in, 20: 31737

THALLIUM ISOTOPES Tl-204
determination of, efficiency of Cherenkov counting methods for, 20: 31184
use in Manned Orbital Research Laboratory propulsion system, 20: 31387
uses in oxygen analyzer for oceanographic applications, 20: 31171 (ORO-596)

THERMAL REACTORS
design and operation of heterogeneous, 20: 32789(P)
fuel matrix for, properties of molten ceramic oxides as, 20: 31726
fuels for, performance of thorium, 20: 32822

THERMIONIC CELLS
current oscillations in cesium plasma diode, (E), 20: 31966
design for generating a-c current, 20: 31980(P)
design using film-boiling liquid metals as electron collector, 20: 31969
development for reentering space vehicles, 20: 31961 (SC-DC-66-1115)
development of cesium vapor-filled, for space uses, 20: 31960 (N-66-16447)
operation in ignited mode, output-current characteristics for, 20: 31967
operation in ignited mode, plasma model for cesium, (E/T), 20: 31968
operation in ignited mode with electron temperature variations, (T), 20: 31974
performance for space applications using actinium-227 and curium-224, 20: 31965
performance of, in-pile, 20: 31964
plasma physics of, 20: 31971

THERMODYNAMICS
statistical, of non-extensive systems, 20: 32237
work equation in relativistic, Lorentz transformation for, 20: 32225

THERMOELECTRIC CELLS
development of liquid metal, 20: 31959(R) (ANL-7175, pp 184-211)

THERMOLUMINESCENT DETECTORS
development of miniature, for *in vivo* dosimetry, 20: 31598
performance and properties of quartz, 20: 31520
production and properties of, for dosimeters, 20: 31608
use in radiation dosimetry, 20: 31560
use of lithium fluoride crystals as, for environmental monitoring, 20: 31526

THERMOMETRY
use of liquid helium-4 in low-temperature, 20: 32336

THERMONUCLEAR EXPLOSIONS
fallout formation in surface, 20: 31409
fallout from Starfish, activity of, (E), 20: 32271

THERMONUCLEAR REACTIONS
research on pulsed-controlled, electrostatic and magnetic field calculations for, 20: 32596

THICKNESS GAGES
development of, using nondestructive testing methods, 20: 31480 (Y-1535)

THORIUM
determination in organic solvent–acid media, spectrophotometric, 20: 31195
mechanical properties of wrought-annealed and cold-worked, at room temperature, 20: 31767
performance as thermal power reactor fuel, 20: 32822
physical properties, 20: 31767
radiation effects on mechanical properties of, effects of annealing on, 20: 31666
separation from organic solvent–acid media by ion exchange, 20: 31195
use as pebble bed reactor fuel, 20: 32825
use as reactor fuel, review of, 20: 32819
use in Brazilian power reactors, 20: 32821
use in breeder reactors, economics and role of, 20: 32832
use in German power reactors, 20: 32824
use in Japanese power reactors, 20: 32828
use in power plants, role of, 20: 32826
use in power reactors, economics and performance for, 20: 32834
use of homogeneous suspended, for breeder reactors, 20: 32829

THORIUM ALLOYS
Th–U-233, fabrication and irradiation testing of fuel elements of, 20: 31690 (ORNL-P-2176)
Pu–Th, economics for thermal reactors, 20: 32822
Pu–Th–U, compatibility with chromium, type 304 stainless steel, and vanadium–20 titanium, 20: 31666
Th–U, economics for thermal reactors, 20: 32822
Th–U, economics for Italian power reactors, 20: 32827
Th–U, mechanical and physical properties of, 20: 31767
Th–U, processing of irradiated, economics of, 20: 31317 (BAW-393-3)
Th–U, processing costs and methods for, 20: 31326
Th–U–Zr, tensile strength of, aging effects on, 20: 31767
Th–U-233, refabrication technology for bred, 20: 31701

THORIUM CARBIDES
mechanical and physical properties of, 20: 31767
phase transformations, 20: 31666

preparation by sol-gel process, 20: 31666
preparation of spherical particles of, 20: 31666
graphite–ThC_2, fabrication and properties of hot-pressed composites of, 20: 31688 (NASA-CR-507)
graphite–ThC_2, phase studies, 20: 31666
ThC_2–UC_2, burnup of, 20: 32833
ThC_2–UC_2, mechanical and physical properties of, 20: 31767
ThC_2–UC_2, preparation of spherical particles of, 20: 31666
ThC–UC, preparation by sol-gel process, 20: 31666

THORIUM ISOTOPES
content in man, 20: 30989

THORIUM ISOTOPES Th-232
content in skeleton and soft tissues of man, 20: 30989
neutron fission of, gamma spectrometric determination of cesium-137 from fast, 20: 31530
use in fuel cycles in heavy-water breeder reactors, (T), 20: 32823
Th-232–U-233, performance as fast breeder reactor fuel, 20: 32790 (ANL-6930)
Th-232–U-233, utilization in Swedish power reactors, 20: 32830

THORIUM NITRATES
denitration of, for preparation of oxide microspheres by sol-gel process, 20: 31689 (ORNL-P-2159)

THORIUM ORES
availability and world reserves of, estimation of, 20: 31436
location in United Arab Republic, 20: 31438

THORIUM(IV) OXIDES
mechanical and physical properties of, 20: 31767
permeability to oxygen at 1100 to 2050°C, 20: 31731
preparation of microspheres of, by sol-gel process, 20: 31689 (ORNL-P-2159)
preparation of spherical, sol-gel processes for, 20: 31700
surface energy at 700 to 1200°C, 20: 31666
Mo–Ni–ThO_2, development and properties of dispersion-strengthened, 20: 31669
Ni–ThO_2—bonding to refractory metals, process for TD Nickel diffusion, 20: 31670
Ni–ThO_2, development and properties of dispersion-strengthened, 20: 31669
PuO_2–ThO_2, preparation of microspheres of, by sol-gel process, 20: 31689 (ORNL-P-2159)
ThO_2–UO_2, burnup and metallography of, 20: 32833
ThO_2–UO_2, preparation of microspheres of, by sol-gel process, 20: 31689 (ORNL-P-2159)
ThO_2–UO_2, processing of irradiated, economics of, 20: 31317 (BAW-393-3)
ThO_2–UO_2, processing of irradiated, release of krypton-85 and tritium in, 20: 31447 (ORNL-3956)
ThO_2–UO_2, processing costs and methods for, 20: 31326
ThO_2–W, microstructure of dispersion-hardened, effects of alloying additions on, 20: 31781

THORIUM PHOSPHIDES
phase studies of, using mass spectrometry, 20: 31723
preparation, 20: 31666

THORIUM SULFIDES
ThS–US, magnetic susceptibilities, 20: 31213(R) (ANL-7175, pp 119-58)

THORIUM SYSTEMS
C–Th, phase studies, 20: 31768

THRESHOLD DETECTORS
design and development of, for fast neutron spectra, 20: 31786(R) (ORO-2891-5)

THULIUM ALLOYS
Tm–Zn, melting point of $TmZn_2$, 20: 31743

THULIUM ISOTOPES Tm-162
conversion electron spectra of, (E), 20: 32415

THULIUM ISOTOPES Tm-164
conversion electron spectra of, (E), 20: 32415

THULIUM ISOTOPES Tm-166
conversion electron spectra of, (E), 20: 32415

THULIUM ISOTOPES Tm-169
energy level transitions in, L-subshell ratios of E2 rotational, 20: 32516
energy levels of, spin g-factors for, (T), 20: 32447
fluorine-19 reactions (F-19,xn) with, alpha-active platinum isotopes from, (E), 20: 32458

THULIUM ISOTOPES Tm-170
beta decay of, conversion coefficients for transitions in, (E), 20: 32443
use in Manned Orbital Research Laboratory propulsion system, 20: 31387

THULIUM ISOTOPES Tm-171
beta decay of, conversion coefficients for transitions in, (E), 20: 32443

THULIUM MOLYBDATES
preparation and crystal structure of, 20: 31740

THULIUM TUNGSTATES
preparation and crystal structure of, 20: 31740

THYMUS GLAND
radiation effects on DNase activity in rat, 20: 31143
radiotherapy of mouse, synergistic effects of Mitomycin C and Endoxan in, 20: 31131

THYROID GLAND
diseases of, effects of, on calcium metabolism, 20: 31142
pathology of diseases of, 20: 31162
physiology of, 20: 31162
radiation effects from deposited iodine-131 on chromosomes in cultured hamster, 20: 31053
radiotherapy of hyperfunctioning solitary nodule of, dosage and scintigraphy in, 20: 31154

THYROID HORMONES
effects on man, physiological, 20: 31162

THYRONINE, TRIIODO-
effects on gamma radioinduced pulmonary fibrosis in dogs, 20: 31138
metabolism by man, tracer studies of, 20: 30965

THYROXINE
labeling with technetium-99m, 20: 31265

TIME MEASUREMENT
production of starting pulses for nanosecond time-of-flight measurements, 20: 31579

TIN
deposition on uranium, electrolytic, 20: 31670
magnetic flux pinning by precipitates of, in indium–lead–tin and lead–tin alloys, (E), 20: 32313
microwave effects on critical currents in superconducting films of, (E), 20: 32328
thermodynamic properties of liquid, Prandtl at 0 to 700°C for, 20: 31724
vaporization from probe surface in electric arcs, (E), 20: 32593

TIN ALLOYS
heats of solution of gold and indium in, 20: 31717(R) (UCRL-16658, pp 143-9)
Al–Sn–Ti, radiation effects on tensile properties of, at cryogenic temperatures, fast-neutron, 20: 31784(R) (NASA-CR-54976)
Au–Sn, thermal properties of intermetallic compound in, 20: 31717(R) (UCRL-16658, pp 143-9)
Bi–Sn, critical currents in superconducting films of, magnetic field effects on, (E), 20: 32317
In–Pb–Sn, magnetic flux pinning by superconducting tin precipitates in, (E), 20: 32313
Li–Sn, thermodynamic properties, 20: 31959(R) (ANL-7175, pp 184-211)
Nb–Sn, magnetic field trapping by superconducting hollow cylinders of intermetallic compounds of, temperature dependence of, (E), 20: 32316
Nb–Sn, magnetic flux jumping in high-field high-current superconducting, stability against, (T), 20: 32320
Nb–Sn–Zr, corrosion by steam, composition of oxide film formed by, 20: 31669
Nb–Sn–Zr, hardness of zirconium-base, effects of tempering at 400 to 700°C on, 20: 31669
Pb–Sn, magnetic flux pinning by superconducting tin precipitates in, (E), 20: 32313

TIN IONS
production of, for mass spectrometry, thermal techniques for, 20: 31226

TIN ISOTOPES Sn-115
isomeric transitions in, energies and half life of, (E), 20: 32520

TIN ISOTOPES Sn-116
energy levels from indium-116 decay, (E), 20: 32564

TISSUE CULTURES
nucleic acid synthesis in, from leukemia and myeloma patients, 20: 30971 (ORINS-45)
protein synthesis in, from leukemia and myeloma patients, 20: 30971 (ORINS-45)
radiation effects on human, protective effects of AET, serotonin, and streptomycin against gamma, 20: 31121
radiation effects on reproduction of hamster and HeLa cells in, γ, 20: 31051
radiation effects on HeLa cells in, biological x, 20: 31056
radiation effects on *Macaca mulatta* embryo cell, protective effects of serotonin and thiourea against x, 20: 31121
radiosensitivity of cells in, effects of oxygen on α, deuteron, fast-neutron, and x, 20: 31123

TISSUE TRANSPLANTS
book: *Tissue Grafting and Radiation*, 20: 31120
use of irradiated bone marrow, in radiation effects therapy in rats, 20: 31133

TISSUES
analysis for radiosensitizers, neutron activation, 20: 31172 (SGAE-BL-17/1966)
cesium-137 and strontium-90 contents of human, in Finland, 20: 31142
dose conversion factors for neutron sources in soft, 20: 32355
dose conversion factors for neutron sources in, 20: 32356

radiation effects on, protection against, 20: 31108
radiation effects on inner and outer epidermises of *Allium cepa* and *Mnium cuspidatum*, alpha and uv, 20: 31079
radiation injuries to, in mice, effects of bone marrow therapy on, 20: 31108
radiation injury and repair in avian and mammalian, 20: 31045
thorium-232 content in human, 20: 30989

TITANIUM
coating with boron, 20: 31670
corrosion by mercury at 538°C, effects of additives on, 20: 31669
joining to titanium, parameters for friction, 20: 31670
neutron capture by, average level widths of compound nucleus from, (E), 20: 32424
performance in accelerating electrodes in cesium-contact ion thrustors, 20: 31383
proton reactions at 0.05 to 2.9 Bev, induced activity data and cross sections for spallation, (E/T), 20: 32549
radiation effects on tensile properties of, at cryogenic temperatures, fast-neutron, 20: 31784(R) (NASA-CR-54976)
reactions with sodium at 2050°C, 20: 31440(R) (ANL-7175, pp 159-83)
sorptive properties for nitrogen, 20: 31314(R) (ANL-7175, pp 1-41)
sputtering by cesium ions at 0.5 to 15 kev, yields from, 20: 31948
Mo–Ti–Zr, stress-rupture at 2000°F of TZM, 20: 31669

TITANIUM ALLOYS
Al–Cr–Fe–Mo–Ni–Ti, radiation effects on tensile properties of Nimonic PE16, thermal-neutron, 20: 31669
Al–Sn–Ti, radiation effects on tensile properties of, at cryogenic temperatures, fast-neutron, 20: 31784(R) (NASA-CR-54976)
Be–Ti, phase diagram, 20: 31772
Mo–Ti–Zr, fatigue properties of TZM, at high temperatures, 20: 31710(R) (NASA-CR-54983)
Nb–Ti, superconducting critical field of, spin-orbit effects on upper, (E), 20: 32330
Nb–Ti, superconducting critical current of, effect of precipitates on, 20: 32322
Nb–Ti–V, development and properties of, 20: 31709(R) (IITRI-B6042-5)
Pu–Ti–U, mechanical properties and phase diagram of, 20: 31666
Ta–Ti, superconducting critical field of, spin-orbit effects on upper, (E), 20: 32330
Ti–V, compatibility with plutonium–thorium–uranium alloy, 20: 31666
Ti–V, corrosion by sodium at 650°C, effects of oxygen content on, 20: 31659
Ti–V, elasticity of, ultrasonic measurements of, as function of temperature, 20: 31708 (ANL-7119)
Ti–V, reactions with sodium at 2100°C, 20: 31440(R) (ANL-7175, pp 159-83)
Ti–V, superconducting critical field of, spin-orbit effects on upper, (E), 20: 32330

TITANIUM CARBIDES
fabrication by hot-pressing, 20: 31699
graphite–TiC, fabrication and properties of hot-pressed composites of, 20: 31688 (NASA-CR-507)

TITANIUM IONS
properties for use in radiation dosimetry, 20: 31301
spectra in sulfuric acid solutions, effects of acid concentration and temperature on extinction coefficient for, 20: 31301

TITANIUM ISOTOPES Ti-46
neutron total cross sections for, level spacings from, (E/T), 20: 32389

TITANIUM ISOTOPES Ti-48
neutron total cross sections for, level spacings from, (E/T), 20: 32389

TITANIUM ISOTOPES Ti-50
neutron total cross sections for, level spacings from, (E/T), 20: 32389

TITANIUM OXIDES
effects on type 304 stainless steel embrittlement by fast and thermal neutrons, 20: 31669
Eu_2O_3–stainless steel 304L–TiO_2, corrosion by water at high temperatures, 20: 31678 (HIT-3583-24)
Eu_2O_3–TiO_2, corrosion by water at high temperatures, 20: 31678 (HIT-3583-24)

TITANIUM PHOSPHIDES
phase studies of, using mass spectrometry, 20: 31723

TITANIUM SYSTEMS
C–Mo–Ti–Zr, fatigue properties of TZC, at high temperatures, 20: 31710(R) (NASA-CR-54983)

TOBACCO
polonium-210 content in New Zealand, 1965, 20: 31446(R) (NP-16015)

TOLUENE
proton polarization in frozen, using solid effect, (E), 20: 31811
radiolysis of, yields of gaseous, liquid, and solid products in, 20: 31291
2,2'-p-phenylenebis[5-phenyloxazole]–toluene, scintillation efficiency of, 20: 31290
2,5-diphenyloxazole–toluene, scintillation efficiency of, 20: 31290

TOMATOES
radiation effects on growth and pigmentation of, long- and short-wave uv, 20: 31059

TRACER TECHNIQUES (BIOLOGY)
stable brominated proteins and neutron activation analysis, for plasma protein metabolism, 20: 30990

TRACER TECHNIQUES (MEDICINE)
development for studies of thyroid physiology, 20: 31162
use in intravascular blood clot photography, 20: 31150 (UCRL-16691)

TRACKING SYSTEMS
development of gamma-ray low-altitude, 20: 31495
development using gamma sources for rocket target miss distance measurements, 20: 31496

TRANSCURIUM ELEMENTS
stability of Z = 126, A ≈ 310, shell model calculations for, 20: 32482

TRANSDUCERS
design of high-temperature differential pressure, 20: 31491

TRANSISTORS
photocurrent production in, anomalous, (E/T), 20: 31612 (SC-DC-66-1415)
radiation effects on silicon, transient annealing from neutron, 20: 31613 (SC-DC-55-1443)
radiation effects on properties of, 20: 31620
radioinduced charge on surface of, operational effects of, 20: 31611 (AD-633468)

TRANSITION METALS
ionic spin-lattice relaxation times of, in solutions, measurement of, 20: 31221(R) (UCRL-16658, pp 73-87)
properties and structure of alloys of, 20: 31219(R) (UCRL-16658, pp 11-20)

TREES
radiation effects on cytology and growth of *Pinus rigida*, chronic gamma, 20: 31077

TRIDODECYLAMINE
solvent properties for uranium, 20: 31322

TRIOCTYLAMINE
solvent properties for uranium, 20: 31322

TRIS(2-ETHYLHEXYL)AMINE
solvent properties for uranium, 20: 31322

TRITIUM
binding energy and wave functions for, 20: 32498
content in natural waters in Japan, 20: 31398(T) (NSJ-tr-49)
content in ocean surface waters, 1960 and 1961, 20: 31419
determination in aqueous samples in presence of carbon-14, computer program for use in, 20: 31182
determination in natural waters, method for, 20: 31310
determination in water by distillation, electrolysis, and scintillation counting, 20: 31398
determination of, by oxygen flask method using scintillation counting, equipment for, 20: 31185
diffusion from irradiated thorium dioxide–uranium dioxide fuels during processing, 20: 31447 (ORNL-3956)
effects on *E. coli*, mutagenic, 20: 31033(R) (NASA-CR-59196)
incorporation in ethane by hydrogenation of ethylene, 20: 31259
reactions with deuterium ions in accelerated mixed plasma, 20: 32586
uses for hydrological studies of ground waters, 20: 31394

TRYPSIN
radioinduced free radicals in solutions of, effects of metal ions on γ, 20: 31003
radiosensitivity of solutions of, effects of agar on x, 20: 31017

TUBES
fluid flow in hexagonal, heat transfer in laminar, 20: 31341 (BNL-9546)
fluid flow in, geometrical effects on boiling burnout in, 20: 31342(R) (EURAEC-1482)
water flow in heated, temperatures for pulsating boiling, 20: 31346

TUMORS
effects of radioprotective compounds on fluorescence of intracellular pyridine nucleotides in, 20: 31122
growth of, transplanted from x-irradiated beds, 20: 31073
nucleic acid synthesis in cultures from myeloma, 20: 30971 (ORINS-45)
protein synthesis in cultures from myeloma, 20: 30971 (ORINS-45)
radiation effects on rat Yoshida ascites, recovery mechanism in x, 20: 31070
radiation effects on transplants of, in mice, x, 20: 31073
radiation injuries in mouse, protective effects of cystine, glutathione, and MEA against gamma, 20: 31141
radioinduced hematopoietic, in dogs and swine exposed to strontium-90, 20: 31031 (BNWL-SA-201)
radiosensitivity and immunoresistance of, 20: 31108
radiosensitivity of cultured HeLa-cell, effects of anoxia and *N*-ethylmaleinimide on, 20: 31130
radiotherapy of hemangiomas in children, radiation dose to gonads from x, 20: 31156
radiotherapy of Hodgkin's disease, x, 20: 31151
radiotherapy of mouse, synergistic effects of Mitomycin C and Endoxan in,

20: 31131
radiotherapy of, use of computer for dose calculations in, 20: 31155
TUNGSTEN
cesium ionization on surfaces of, 20: 31776
cesium transport through capillaries of, 20: 31381
coatings for, factors controlling effectiveness of high-temperature protective, 20: 31669
compatibility with cesium vapor at 1800°C, 20: 31669
deposition of, process development of chemical vapor, 20: 31670
determination in conductive tissue of beef heart, activation, 20: 31176
determination in human heart tissue, activation, 20: 31175
fabrication and preparation of, for use in ion engines, 20: 31375
grain boundary grooving in, mechanisms of, 20: 31672
ion desorption from, mass spectrometric study of, 20: 31907
ionization efficiency of electrodes of, in ion engines, 20: 31386
ionization of neodymium and samarium at surfaces of, effects of adsorbed oxygen on, 20: 31225
laser beam reactions on surfaces of, momentum transfer by giant-pulsed, (E), 20: 31810
oxidation rates at 1450 to 2900°K and 8×10^{-6} to 7×10^{-5} torr oxygen pressure, 20: 31227
performance as ionizer material in cesium-contact ion thrustors, 20: 31383
preparation of beta-phase, 20: 31717(R) (UCRL-16658, pp 143-9)
properties of porous, for cesium ionization, 20: 31388
proton reactions at 0.05 to 2.9 Bev, induced activity data and cross sections for spallation, (E/T), 20: 32549
reactions with nitrous oxide, 20: 31718(R) (UCRL-16658, pp 149-54)
reactions with steam at 1000 to 1700°C, 20: 31669
solvent properties for carbon at high temperatures, 20: 31669
sorptive properties for cesium, effects of filament treatment on, 20: 31730
stress-rupture of wires of, at 1200 to 2500°F, 20: 31711 (NASA-TN-D-3467)
surface tension and solid surface energy of, effects of alloying additions of rhenium on, 20: 31773
testing of crucibles of, 20: 31314(R) (ANL-7175, pp 1-41)
use in porous ionizers for cesium-contact thrustors, 20: 31389
TUNGSTEN ALLOY COUPLES
Re–W/Re–W, thermoelectric potential to 3000°C, 20: 31721(T) (AD-630971)
TUNGSTEN ALLOYS
tensile properties of composites of copper or copper alloys and fibers of, 20: 31770
Cr–Fe–Mo–Ni–W, radiation effects on mechanical properties of Hastelloy X-280, fast-neutron, 20: 31669
Cr–W, decomposition mechanisms in solid solutions of, 20: 31716(R) (UCRL-16658, pp 121-32)
Mo–Nb–W–Zr, hardness of niobium-base, effects of composition on hot-, 20: 31669
Nb–Ta–W–Zr, creep properties of FS-85, 20: 31669
Nb–W, corrosion by cerium–cobalt–plutonium alloy fuels, effects of carbon on, 20: 31679(R) (LA-3524)
Nb–W, electronic structure of, at superconducting critical temperatures, 20: 31747
Ni–W, creep properties at high temperatures, 20: 31669
Re–W, deposition of, process development of chemical vapor, 20: 31670
Re–W, fabrication and preparation of, for use in ion engines, 20: 31375
Re–W, grain boundary grooving in, mechanisms of, 20: 31672
Re–W, ionization efficiency of electrodes of, in ion engines, 20: 31386
Re–W, mechanical properties, 20: 31778
Re–W, properties of porous, for cesium ionization, 20: 13388
Re–W, surface tension and solid surface energy of, 20: 31773
Ta–W, corrosion by cerium–cobalt–plutonium alloy fuels, effects of carbon on, 20: 31679(R) (LA-3524)
Ta–W, electronic structure of, at superconducting critical temperatures, 20: 31747
Ta–W, tensile properties of carburized and uncarburized, 20: 31679(R) (LA-3524)
Ta–W–Y, corrosion by cerium–cobalt–plutonium alloy fuels, effects of carbon on, 20: 31679(R) (LA-3524)
TUNGSTEN CARBIDES
fabrication by hot-pressing, 20: 31699
Co–TaC–WC, mechanical properties of cermets of, effects of composition on, 20: 31760
Co–WC, mechanical properties of cermets of, effects of composition on, 20: 31760
Co–WC, sintering properties of, 20: 31695
TUNGSTEN OXIDES
molecular shrinkage effects and vibration mean amplitudes for WO_2 and WO_3, (T), 20: 31233
TUNGSTEN SILICIDES
performance in focus electrodes in cesium-contact ion thrustors, 20: 31383
TUNGSTEN SYSTEMS
C–Re–W, superconductivity of W_3Re_2C in, 20: 32312(R) (UCRL-16658, pp 133-43)
C–W–Zr, phase studies, 20: 31669
ThO_2–W, microstructure of dispersion-hardened, effects of alloying additions on, 20: 31781
TYROSINE
labeling with technetium-99m, 20: 31265
TYROSINE, 3,5-DIIODO-
metabolism by man, tracer studies of, 20: 30965

U

ULTRASONICS
attenuation and velocity in single crystals of normal and superconducting thallium, (E/T), 20: 31780
use with television systems for materials inspection, 20: 31352 (ANL-7042)
uses for studying elastic moduli as function of temperature, 20: 31708 (ANL-7119)
ULTRAVIOLET RADIATION
effects of long- and short-wave, on growth and pigmentation in cucumber and tomato plants, 20: 31059
effects on *Bacillus subtilis*, effects of amino acids on, 20: 31129
effects on breakdown and synthesis of DNA in *E. coli*, effects of bromouracil on, 20: 31062
effects on cells, role of genetic damage in lethal, 20: 31042
effects on enzyme locational specificity in Neurospora, 20: 31012
effects on inner and outer epidermises of *Allium cepa* and *Munium cuspidatum*, 20: 31079
effects on microorganisms and metazoa, repair mechanisms for, 20: 31040
effects on microorganisms, genetic control of, 20: 31041
effects on oxidation of trivalent antimony-124 to pentavalent, 20: 31300
effects on potassium chlorate crystals at room temperature, absorption bands from, 20: 32686
effects on reproduction of bacteria and viruses, 20: 31039
effects on silver chlorides, defect formation from, 20: 32731
effects on survival of synchronized L cells in mice, 20: 31084
effects on synthesis of ammonia from nitrogen and water, 20: 31289
effects on tensile strength of polypropylene film, 20: 31274
reactions with frozen hydrochloric and hydrofluoric acids, EPR of hydrogen atoms formed in, 20: 32719(T)
ULTRAVIOLET SOURCES
design using plasma oscillations from electron avalanche energy losses, conceptual, 20: 32727(T)
UNDERGROUND EXPLOSIONS
air blast and seismic waves from SULKY, 20: 31393 (PNE-711F)
UNITED STATES
radiation processing of food in, review of, 20: 31628
URACIL, 5-BROMO-
effects on uv radiation effects on DNA breakdown and synthesis in *E. coli*, 20: 31062
radiosensitivity effects of, use of activation analysis for determining mechanism of, 20: 31172 (SGAE-BL-17/1966)
URACIL, 5-CHLORO-
radiosensitivity effects of, use of activation analysis for determining mechanism of, 20: 31172 (SGAE-BL-17/1966)
URACIL, 5-IODO-
radiosensitivity effects of, use of activation analysis for determining mechanism of, 20: 31172 (SGAE-BL-17/1966)
URANIUM
analysis for uranium-235 by neutron activation-induced fission and 20: 31189
coating with chromium, copper, nickel, or tin, electrolytic, 20: 31670
crystal growth of alpha-phase, effects of impurities on orientation of, 20: 31666
deformation processes in thermally cycled, 20: 31754
determination in organic solvent–acid media, spectrophotometric, 20: 31195
determination in pyrolytic carbon fuel particle coatings, use of electron microprobe for, 20: 31795
diffusion in alpha-phase, anisotropy of self-, 20: 31771
effects on hardenability of A-212B carbon steel, 20: 31669
fission gas bubbles in, effects of heating time and temperature on size and distribution of, 20: 31666
gamma and neutron attenuation in shields of, 20: 32672 (NAA-SR-Memo-11786)
grain size and transformations in alpha-phase, effects of alloying additions on, 20: 31666
heat of sublimation, 20: 31227

occurrence in coal-bearing beds of Mikawa and Akatani areas, Niigata Prefecture, Japan, 20: 31437
oxidation-reduction reactions of, bibliography on kinetics of, 20: 31215 (LA-3507)
physical properties, 20: 31767
radiation effects on, bibliography on, 20: 31783 (FTI-16(6.1))
radioinduced swelling in, effects of preirradiation treatments and post-irradiation annealing on, 20: 31666
radioinduced swelling of, at 400 to 500°C, effects of alloying additions on, 20: 31666
radioinduced swelling in, irradiated at 130 to 550°C, 20: 31666
reactions with water, effects of temperature on, 20: 31666
recovery of, from refining crucibles by skull reclamation process, 20: 31314(R) (ANL-7175, pp 1-41)
separation from acid solutions by solvent extraction using aliphatic amines, 20: 31322
separation from irradiated urania fuels by fluoride volatility processes, 20: 31315(R) (ANL-7175, pp 42-103)
separation from organic solvent–acid media by ion exchange, 20: 31195
separation from zirconium by fluidized-bed fluoride volatility process, 20: 31321
separation of molten, from plutonium by fused chloride extraction, 20: 31314(R) (ANL-7175, pp 1-41)
solubility of, in cadmium–copper alloys, 20: 31314(R) (ANL-7175, pp 1-41)
superconductivity of alpha- and beta-, 20: 32684(R) (UCRL-16658, pp 21-38)
use in European Atomic Energy Community in 1970 to 1999, estimation of, 20: 32792
vapor pressure of, mass spectrometric measurement of, 20: 31227

URANIUM ACETATES
preparation and chemical properties of, 20: 31236

URANIUM ALLOYS
radiation effects on, bibliography on, 20: 31783 (FTI-16(6.1))
Cr–U, separation of barium and lanthanum from, by solvent extraction using liquid magnesium, 20: 31320 (UCRL-16108)
Cr–U, separation of, from fission products by extraction using liquid metals, 20: 31166(R) (UCRL-16658, pp 89-92)
Mo–U, radiation effects on stainless steel-clad fuel elements of, 20: 31666
Pu–Th–U, compatibility with chromium, type 304 stainless steel, and vanadium–20 titanium, 20: 31666
Pu–Ti–U, mechanical properties and phase diagram of, 20: 31666
Pu–U–Zr, compatibility with type 304 stainless steel to 800°C, 20: 31666
Pu–U–Zr, mechanical properties and phase diagram of, 20: 31666
Th–U, economics for thermal reactors, 20: 32822
Th–U, economics for Italian power reactors, 20: 32827
Th–U, mechanical and physical properties of, 20: 31767
Th–U, processing of irradiated, economics of, 20: 31317 (BAW-393-3)
Th–U, processing costs and methods for, 20: 31326
Th–U–Zr, tensile strength of, aging effects on, 20: 31767
U–Zr, phase studies, 20: 31666

URANIUM CARBIDES
fabrication and burnup testing of fuel elements of, 20: 32796(R) (AI-CE-3)
fabrication of silicon carbide-coated spheroids of, 20: 31706(P)
fabrication of spheres of, 20: 31705(P)
heat flux and temperature distributions in fuel rods of stainless steel-clad, (T), 20: 31349
heat flux and temperature distributions in fuel rods of aluminum-clad, (T), 20: 31349
preparation of spherical particles of, 20: 31666
preparation of, by hydrocarbon–metal reactions, 20: 31213(R) (ANL-7175, pp 119-58)
processing of irradiated fuel elements of, methods for, 20: 32796(R) (AI-CE-3)
processing of irradiated, flowsheets for pyrochemical, 20: 31314(R) (ANL-7175, pp 1-41)
radiation effects on, bibliography on, 20: 31783 (FTI-16(6.1))
radiation effects on pyrolytic-carbon-coated particles of, 20: 31666
reactions with water, 20: 31666
thermal conductivity of, effects of nickel sintering aid on, 20: 31666
C–UC, electric and thermal conductivity of compacted powders of, effects of fabrication variables on, 20: 31777
graphite–UC_2, fabrication and properties of hot-pressed composites of, 20: 31688 (NASA-CR-507)
O–PuC–UC, stability as fast reactor fuel, 20: 31675
PuC–UC, compatibility with type 316L stainless steel up to 900°C, 20: 31675
PuC–UC, compatibility with nickel-base alloys, 20: 31675
PuC–UC, fabrication of fuel elements of, 20: 31675
PuC–UC, preparation of, by hydrocarbon–metal reactions, 20: 31213(R) (ANL-7175, pp 119-58)
PuC–UC, properties as fast reactor fuel, 20: 31675
PuC–UC, temperature distributions in irradiated, 20: 32791 (NAA-SR-Memo-11731)
PuC–UC, thermal conductivity of, effects of nickel sintering aid on, 20: 31666
ThC_2–UC_2, burnup of, 20: 32833
ThC_2–UC_2, mechanical and physical properties of, 20: 31767
ThC_2–UC_2, preparation of spherical particles of, 20: 31666
ThC–UC, preparation by sol-gel process, 20: 31666

URANIUM CARBONITRIDES
phase studies of, thermodynamic calculations for, 20: 31230

URANIUM CHLORIDE COMPLEXES
with ammonia, amines, and sulfoxides, preparation of, 20: 31236

URANIUM CHLORIDES
reactions with bromine pentafluoride in mixtures with alumina and fission products, 20: 31315(R) (ANL-7175, pp 42-103)

URANIUM(III) CHLORIDES
fluorination of, kinetics of, 20: 31214 (CEA-R-2859)

URANIUM(IV) CHLORIDES
reactions of, with chlorine in fused chlorides, 20: 31166(R) (UCRL-16658, pp 89-92)
Cd–Mg–UCl_4–Zn, corrosive effects of, on stainless steel at 650°C, 20: 31314(R) (ANL-7175, pp 1-41)

URANIUM COMPOUNDS
fluorination of, kinetics of, 20: 31214 (CEA-R-2859)

URANIUM(IV) FLUORIDES
fluorination of, kinetics of, 20: 31214 (CEA-R-2859)

URANIUM(VI) FLUORIDES
PuF_6–UF_6, phase studies, 20: 31315(R) (ANL-7175, pp 42-103)

URANIUM IONS
reactions with uranium(VI) ions in acid perchlorate solutions, kinetics of, 20: 31239
reactions with vanadium(III) ions in acid perchlorate solutions, kinetics of, 20: 31239

URANIUM ISOTOPES
abundance determination by mass spectrometry, ion production technique for, 20: 31207

URANIUM ISOTOPES U-233
Th–U-233, fabrication and irradiation testing of fuel elements of, 20: 31690 (ORNL-P-2176)
Th–U-233, refabrication technology for bred, 20: 31701
Th-232–U-233, performance as fast breeder reactor fuel, 20: 32790 (ANL-6930)
Th-232–U-233, utilization in Swedish power reactors, 20: 32830

URANIUM ISOTOPES U-234
abundance of, natural isotopic, 20: 31400

URANIUM ISOTOPES U-235
determination in uranium by neutron activation-induced fission and counting of molybdenum-99, 20: 31189
determination of, in combustible waste and air exhaust filters, gage for gamma counting for, 20: 31174 (WAPD-T-1905)
neutron resonance cross sections for, 20: 32551
neutron resonance parameters for, resolved p- and s-wave, 20: 32551

URANIUM ISOTOPES U-238
fission of, decay constant and mass-yield curve for spontaneous, 20: 32521
helium-3 reactions (He-3,p) with, half life of neptunium-240 isomeric state from, (E), 20: 32460
neutron capture-to-fission ratio for, method for determining, 20: 32391
neutron resonance absorption in, in heavy water-moderated, organic-cooled reactor lattices, (E/T), 20: 32785
neutron resonance cross sections for, 20: 32551
neutron resonance parameters for, resolved p- and s-wave, 20: 32551

URANIUM NITRATES
denitration of, for preparation of oxide microspheres by sol-gel process, 20: 31689 (ORNL-P-2159)

URANIUM NITRIDES
phase studies of, thermodynamic calculations for, 20: 31230
radiation effects on, bibliography on, 20: 31783 (FTI-16(6.1))
PuN–UN, thermal expansion at 20 to 1000°C, coefficient of, 20: 31666

URANIUM ORES
availability and world reserves of, estimation of, 20: 31436
mining of, control of radioactive pollution in, 20: 31457

URANIUM OXIDES
dissociation energies of, 20: 31227
fluorination of, kinetics of, 20: 31214 (CEA-R-2859)
radiation effects on, bibliography on, 20: 31783 (FTI-16(6.1))

URANIUM(IV) OXIDES
diffusion of xenon in, effects of additions of lanthanum, niobium, or yttrium oxides on, 20: 31666
diffusion of xenon in, at 1330 to 1800°C, effects of radiation dose on, 20: 31666

enthalpy at 900 to 2350°C, equation for, 20: 31666
fission product distribution in irradiated, 20: 31666
heat flux and temperature distributions in fuel rods of stainless steel-clad, (T), 20: 31349
heat flux and temperature distributions in fuel rods of aluminum-clad, (T), 20: 31349
lattice defects in single-crystal, effects of stoichiometry on, 20: 31666
molecular shrinkage effects and vibration mean amplitudes for, (T), 20: 31233
preparation of high-density sintered compacts of, 20: 31666
preparation of microspheres of, by sol-gel process, 20: 31689 (ORNL-P-2159)
preparation of spherical particles of, 20: 31666
processing of irradiated, flowsheets for pyrochemical, 20: 31314(R) (ANL-7175, pp 1-41)
processing of Zircaloy-2-clad, 20: 31315(R) (ANL-7175, pp 42-103)
properties of, effect of stoichiometry on, 20: 31674
reactions with carbon, oxygen concentrations from, 20: 31230
reactions with hydrofluoric acid–oxygen mixtures, 20: 31315(R) (ANL-7175, pp 42-103)
reactions with steam at 1500°C, composition changes from, 20: 31440(R) (ANL-7175, pp 159-83)
$BaTiO_3$–UO_2, dielectric properties and phase studies of, 20: 31735
BeO–UO_2, creep properties at high temperatures, 20: 31669
CaO–UO_2, grain boundary precipitation in, 20: 31738
PuO_2–UO_2, burnup in reactor fuel pins, 20: 32836
PuO_2–UO_2, diffusion and segregation in, 20: 31440(R) (ANL-7175, pp 159-83)
PuO_2–UO_2, fluorination and oxidation of, in fluid beds, effects of cesium fluoride on, 20: 31315(R) (ANL-7175, pp 42-103)
PuO_2–UO_2, plutonium and fission-product distributions in irradiated, 20: 31804
PuO_2–UO_2, plutonium distribution in pellets of, autoradiography of, 20: 31212
PuO_2–UO_2, plutonium distribution in pellets of, autoradiography of, 20: 31212
PuO_2–UO_2, preparation of microspheres of, by sol-gel process, 20: 31689 (ORNL-P-2159)
PuO_2–UO_2, properties of, as reactor fuel, effect of stoichiometry on, 20: 31674
PuO_2–UO_2, temperature distributions in irradiated, 20: 32791 (NAA-SR-Memo-11731)
ThO_2–UO_2, burnup and metallography of, 20: 32833
ThO_2–UO_2, preparation of microspheres of, by sol-gel process, 20: 31689 (ORNL-P-2159)
ThO_2–UO_2, processing of irradiated, economics of, 20: 31317 (BAW-393-3)
ThO_2–UO_2, processing of irradiated, release of krypton-85 and tritium in, 20: 31447 (ORNL-3956)
ThO_2–UO_2, processing costs and methods for, 20: 31326
UO_2–Y_2O_3, oxidation of solid solutions of, kinetics of, 20: 31685
U–UO_2, phase diagrams, 20: 31213(R) (ANL-7175, pp 119-58)
U–UO_2, vapor pressures of, 20: 31227

URANIUM(IV-VI) OXIDES
crystal structure and preparation of delta-phase, 20: 31752

URANIUM(VI) OXIDES
molecular shrinkage effects and vibration mean amplitudes for, (T), 20: 31233

URANIUM SULFIDES
magnetic susceptibility, 20: 31213(R) (ANL-7175, pp 119-58)
ThS–US, magnetic susceptibilities, 20: 31213(R) (ANL-7175, pp 119-58)

URANIUM SYSTEMS
LiH–U, gamma and neutron attenuation in shields of, 20: 32672 (NAA-SR-Memo-11786)
Mo–Si–U, hot hardness and microstructure of, effects of quenching temperature on, 20: 31666
O–Na–U, phase studies at 600 to 1000°C, 20: 31666
U–UO_2, phase diagrams, 20: 31213(R) (ANL-7175, pp 119-58)
U–UO_2, vapor pressures of, 20: 31227

URANYL ACETATES
photoinduced luminescence of, in organic solutions, 20: 31305

URANYL CHLORIDES
separation from acid solutions by solvent extraction using aliphatic amines, 20: 31322

URANYL COMPOUNDS
fluorescence decay at 80 to 500°K, (E), 20: 32690

URANYL NITRATES
denitration of, for preparation of oxide microspheres by sol-gel process, 20: 31689 (ORNL-P-2159)
photoinduced luminescence of, in organic solutions, 20: 31305

UREA, THIO-
effects on x radiation effects on *Macaca mulatta* embryo cell cultures, 20: 31121

URINE
analysis for polonium-210, radiochemical, 20: 31187
excretion rate of human, use of creatinine as index of, 20: 30983
radiation effects on Diche-positive compounds in rat, 20: 31140
strontium-90 excretion in rat, effects of sodium phytate on, 20: 30977

UTERUS
radiation effects on DNA synthesis in epithelium of mouse, x, 20: 31088

V

VACUUM GAGES
design and performance of hot-filament ionization, 20: 31483
performance of, book on, 20: 31391

VACUUM PUMPS
design for 10^{-13} torr, 20: 31392
oil vapor contamination from, shielding of proton accelerators against, 20: 31848
performance of getter-ion, pumping speed measurements for determining, 20: 31645(R) (AD-627094)
performance of, book on, 20: 31391

VACUUM SYSTEMS
design of ultrahigh, for hydrogen ion reactions with surfaces at 30 kev, 20: 31937
design of 10^{-13} torr pumping system and work chamber, 20: 31392
performance of mass-spectrometer ultrahigh, under high argon pressures, 20: 31390
radiation effects on Nimrod proton-synchrotron, dosimetry techniques for measuring, 20: 31832

VACUUM TECHNIQUES
book: *Vacuum Science and Engineering*, 20: 31391

VAK REACTOR
heat transfer systems of, description of, 20: 32812

VALVES
design, 20: 32762(P)

VAN ALLEN RADIATION BELTS
electron distribution in, solar wind effects on, 20: 32260
electron energy spectra in, 20: 32251
electron loss from, due to pitch angle scattering by electromagnetic disturbances, 20: 32288
geomagnetic micropulsations in, 20: 32248
properties, 20: 32274
proton distribution at 0.17 to 3.4 Mev in, 20: 32250
proton flux in environment of earth orbiting vehicles, 20: 32244 (N-66-13126)
proton intensity distribution in, model for, (T), 20: 32292
proton trajectories in, (T), 20: 32261
protons in inner, origin and losses of trapped, 20: 32243 (AD-634704)

VANADIUM
heat capacity of high-purity, at 0.35 to 25°K, 20: 32684(R) (UCRL-16658, pp 21-38)
melting point of zone-refined, 20: 31721(T) (AD-630971)
neutron scattering by, energy spectra from cold, (E), 20: 31567
proton reactions at 0.05 to 2.9 Bev, induced activity data and cross sections for spallation, (E/T), 20: 32549
proton reactions at 40 Mev to 25 Bev, lithium isotopes from, (E), 20: 31205
reactions with sodium at 2200°C, 20: 31440(R) (ANL-7175, pp 159-83)

VANADIUM ALLOYS
Nb–Ta–V, development and properties of, 20: 31709(R) (IITRI-B6042-5)
Nb–Ti–V, development and properties of, 20: 31709(R) (IITRI-B6042-5)
Ti–V, compatibility with plutonium–thorium–uranium alloy, 20: 31666
Ti–V, corrosion by sodium at 650°C, effects of oxygen content on, 20: 31669
Ti–V, elasticity of, ultrasonic measurements of, as function of temperature, 20: 31708 (ANL-7119)
Ti–V, reactions with sodium at 2100°C, 20: 31440(R) (ANL-7175, pp 159-83)
Ti–V, superconducting critical field of, spin-orbit effects on upper, (E), 20: 32330

VANADIUM CARBIDES
fabrication by hot-pressing, 20: 31699

VANADIUM CHLORIDES
spectra of, at liquid helium temperatures, ESR, 20: 31221(R) (UCRL-16658, pp 73-87)

VANADIUM ISOTOPES V-48
beta decay of, matrix elements from β-γ correlations from, (E), 20: 32506
production in proton reactions with iron at 400 Mev, (T), 20: 32560

VANADIUM ISOTOPES V-51
energy levels from chromium-51 decay, (E), 20: 32410
energy levels, static moments, and transition rates of, 20: 32513
proton reactions (p,n) with, cross sections and excitation functions for, (E), 20: 32371 (CEA-R-2832)

VANADIUM ISOTOPES V-52
beta decay of, spectra from, (E), 20: 32564
VANADIUM OXIDES
effects on neutron-induced contraction in graphite, 20: 31667
VANADIUM SYSTEMS
H–V, preparation of, for transmission electron microscopy, hydrogen concentration in electrothinning procedures for, 20: 31691
VELOCITY
of raindrops, equipment for measuring, 20: 31476(R) (BNWL-235-4, pp 21)
VENTILATION
design for nuclear facilities, 20: 31453 (STI-PUB-121)
VIRUSES
radiation injury and recovery mechanisms in, uv, 20: 30139
VISION
visual receptor processes, mechanisms of, 20: 30963

W

WASTE DISPOSAL
iodine-129 content in reactor, limits for, 20: 32884
methods for, review of IAEA research on, 20: 32883
procedures for, at radiochemical laboratories, 20: 31469
WASTE PROCESSING
methods at Karlsruhe Atomic Research Center, 20: 32881
methods at Karlsruhe Atomic Research Center, 20: 32882
WASTE SOLUTIONS
dispersion in northeast Pacific by Columbia River effluent, 20: 31448 (RLO-1725-15)
dispersion in northeast Pacific by Columbia River effluent, 20: 31449 (RLO-1725-16)
dispersion in northeast Pacific by Columbia River effluent, 20: 31450 (RLO-1725-17)
dispersion in northeast Pacific by Columbia River effluent, 20: 31451 (RLO-1725-18)
dispersion in northeast Pacific by Columbia River effluent, 20: 31452 (RLO-1725-19)
evaporation by solar energy, 20: 32883
WATER
analysis for cesium-137, iodine-131, and strontium-89 and -90, gamma spectrometric, 20: 31180
analysis for deuterium by infrared spectroscopy, 20: 31640(R) (NYO-755-1, pp 130-72)
analysis for tritium by distillation, electrolysis, and scintillation counting, 20: 31398(T) (NSJ-tr-49)
analysis of, for radium, evaluation of methods for, 20: 31191
beta particle detection in, using Cherenkov effect, 20: 31506 (CEA-R-2915)
corrosive effects on europia–titania and europia–stainless steel 304L–titania cermets at high temperatures, 20: 31678 (HIT-3583-24)
decontamination of, by precipitation of radioisotopes, 20: 31318 (BMwF-FBK-65-04)
determination in solvents, chromatographic, 20: 31641(R) (NYO-755-1, pp 173-208)
determination in soils by neutron probing, 20: 31435
determination in solids by neutron recoil methods, 20: 31627
determination of, on remote surfaces, combination neutron technique for, 20: 31211
deuterium exchange between acetylene and, factors affecting, 20: 31640(R) (NYO-755-1, pp 130-72)
effects of irradiated, on nylon at pH 10.5 and 40 to 45°C, 20: 31280
effects on carbon steel in operating pressure boilers, 20: 31681 (NAA-SR-Memo-11707)
effects on reactor building materials, 20: 31682 (NP-16003)
effects on stress corrosion cracking of chromium–iron–nickel alloy, 20: 31676(R) (COO-1319-39)
exchange on metal ions, NMR studies of, 20: 31218(R) (UCRL-16658, pp 1-9)
flow in vertical, rectangular conduit, two-phase, 20: 31340 (ANL-7093)
flow of boiling, in heated tubes, 20: 31346
flow velocity through channels of finite bundles of hollow rods, turbulent, 20: 31350
heat transfer to, at coexistence of nucleate and film boiling, 20: 31345 (T) (NSJ-tr-471
neutron scattering at 0.15 to 1.8 ev, differential cross sections for 302°K, (E/T), 20: 32350 (KAPL-M-6536)
neutron scattering by, energy spectra from cold, (E), 20: 31567
potential energy functions for, determination from spectral data, 20: 31949
radioactivity in, performance of scintillation materials for detecting, 20: 31499 (AD-633752)
radioinduced ionization of, diffusion-controlled radical reactions in particle tracks during, 20: 31294
reactions with uranium, effects of temperature on, 20: 31666
reactions with uranium monocarbide, 20: 31666
shielding calculations for, for cylindrical gamma sources, 20: 32678
N–H_2O, radiation effects on production of ammonia in, effects of acidity on γ and uv, 20: 31289
Pb–H_2O, shielding efficiency for gamma rays and neutrons, (T), 20: 32676
WATER-*d*
potential energy functions for, determination from spectral data, 20: 31949
WATER-d_2
corrosive effects on types 304, 316, and 17-4 PH stainless steel at 315°C, 20: 31669
deuterium exchange with active methyl hydrogens of pyrylium and tropylium compounds, 20: 31260
effects of ingested, on normal and pregnant mice and rats, 20: 30975
effects on lipase activity, 20: 30995
effects on meiosis in oocytes of starfish, effects of hydrostatic pressure on, 20: 30986
effects on phage-resistant mutations in *E. coli*, 20: 31033(R) (NASA-CR-59196)
potential energy functions for, determination from spectral data, 20: 31949
use in radial reflector of Polish high-flux research reactor, 20: 32871
WATER COOLED REACTORS
coolant-loss accidents in, analysis of simulated, 20: 31440(R) (ANL-7175, pp 159-83)
WATER MODERATED REACTORS
breeding coefficient in uranium–thorium intermediate-energy, (T), 20: 32831
WATER VAPOR
corrosive effects on graphite, effects of metal additions on, 20: 31667
radiation effects on production of ions from, alpha, 20: 31270
WELL LOGGING
soil-moisture measurements by neutron, 20: 31435
WHEAT
adenosine triphosphatase synthesis in roots of, effects of calcium and strontium on, 20: 30992
effects of space flight on seeds of, 20: 31058
metabolism in seed of, effects of cysteine and quinone on, 20: 31002
radiation effects on water content of leaves of, γ, 20: 31110
radiation effects on development of, γ, 20: 31113
radiation effects on metabolism in seeds of, γ, 20: 31002
radiation effects on seeds of, and plants grown from them, 20: 31058
radiation effects on growth and mutations in Triticum, fast and fission neutron and gamma, 20: 31080
WINDOWS
radioinduced heating of, in EBR-II fuel cycle facility, 20: 31313 (ANL-6853)
WOOD
radioinduced combination of, with plastic, economic aspects of, 20: 31624 (BNWL-261)
radioinduced combination of, with plastic, economic aspects of, 20: 31625 (NYO-3569-1)
WORMS
immunogenic efficiency of double vaccination with x-irradiated *Ancylostoma caninum* in dogs, effects of age on, 20: 31043
WOUNDS
plutonium deposition and removal in, 20: 31030 (BNWL-SA-39)
radiation effects on healing of rat skin, effects of hormones on γ, 20: 31061

X

X RADIATION
absorption by gallium single crystals, extended fine structure of K-edge, (T), 20: 32707
book: *Tissue Grafting and Radiation*, 20: 31120
detection and measurement of, from deposited plutonium-239 in dogs, 20: 30968 (BNWL-SA-11)
detection and measurement of soft solar, fabrication and operation of ionization chamber for, 20: 31511 (N-66-16936)
diffraction by natural quartz, defect structure from, 20: 32695
dose to fetus in radiography, 20: 31146
dose to gonads during therapy of hemangiomas in children, 20: 31156
dose to Japanese people from fluoroscopy, 20: 31466
dosimetry in therapy of Hodgkin's disease, 20: 31151
dosimetry using fluoroglass, 20: 31538
effect on bone marrow cells in mice, 20: 31071
effects combined with novoembichine on amino acid accumulation in *Mycobacterium cyaneum* 416, 20: 31005
effects of 15-Mev, on mice, RBE for, 20: 31072
effects of 200-kv, on *Escherichia coli*, relative biological efficiency in, 20: 31107

effects on animal cells in culture, effects of oxygen on biological, 20: 31123
effects on barley roots, biological, 20: 31052
effects on base composition and cells of DNA, ESR spectral studies on, 20: 31014
effects on blood coagulation, 20: 31032 (CEA-R-2953)
effects on blood vessels around joints, 20: 31163
effects on brain serotonin in rats, relation of barbiturate hypnosis to, 20: 31007
effects on cells in flagellate *Astasia longa*, 20: 31085
effects on cells, role of genetic damage in lethal, 20: 31042
effects on chromosomes in Vicia, genetic, 20: 31124
effects on color and phosphorescence of borate glass, 20: 31283
effects on color centers in alkali-halide crystals, 20: 32691
effects on color-center destruction and recombination luminescence in silver-doped sodium chlorides, 20: 32693
effects on color-center, destruction and recombination luminescence in calcium–silver activated sodium chlorides, 20: 32694
effects on content of nucleic acids in *Escherichia coli*, 20: 31023
effects on degradation of DNA in *E. coli*, 20: 31015
effects on DNA synthesis in uterine epithelium of mice, 20: 31088
effects on DNA, phosphatase, and RNA in cerebral nerve cells in rats, 20: 31010
effects on Drosophila, genetic, 20: 31036(R) (SAN-529-3)
effects on Drosophila, genetic, 20: 31047
effects on Drosophila, genetic, 20: 31049
effects on electrical activity of brain of rabbit embryos, effects of developmental stage on, 20: 31037(T) (JPRS-35315, pp 65-75)
effects on enzyme locational specificity in Neurospora, 20: 31012
effects on F-center formation in ionic crystals, temperature dependence of, 20: 32724(T)
effects on fine structure of guinea pig retina, 20: 31118
effects on fine structure of Paneth cells in mice, 20: 31083
effects on function and ultrastructure of isolated rat sympathetic ganglion, 20: 31055
effects on genetic transcription in Rhodopseudomonas, 20: 31033(R) (NASA-CR-59196)
effects on gonadal and gonadotropic hormones in man, 20: 31034(R) (RLO-1780-7)
effects on gonads of monkeys, pathological, 20: 31117
effects on growth of Kalanchoe, effects of air, carbon dioxide, and nitrogen atmospheres on, 20: 31076
effects on HeLa cells in culture, effects of anoxia and *N*-ethylmaleinimide on, 20: 31130
effects on HeLa cells in culture, biological, 20: 31056
effects on human gonads, 20: 31034(R) (RLO-1780-7)
effects on immunogenic efficiency of double vaccination with *Ancylostoma caninum*, 20: 31043
effects on intestinal mucosa in mice, 20: 31082
effects on liberation of 5-hydroxytryptamine in brain stem of adrenalectomized rats, 20: 31069
effects on liverworts, effects of apical cell number on, 20: 31065
effects on lymphoid cells in blood and bone marrow in dogs, 20: 31086
effects on *Macaca mulatta* embryo cell cultures, protective effects of serotonin and thiourea against, 20: 31121
effects on maize seeds, genetic, 20: 31092
effects on metal-oxide-silicon semiconductors, 20: 31615
effects on mice, effects of injected parental bone marrow or spleen cells on leukemogenic, 20: 31127
effects on mice, genetic, 20: 31048
effects on microorganisms and metazoa, repair mechanisms for, 20: 31040
effects on microorganisms, genetic control of, 20: 31041
effects on monkeys, pathological, 20: 31101
effects on monkeys, pathological, 20: 31103
effects on morphology of mouse intestinal crypt cells, 20: 31128
effects on mouse spleen and thymus, synergistic effects of Mitomycin C and Endoxan in, 20: 31131
effects on mutation rates in Drosophila, 20: 31108
effects on mutations of economically important plants, 20: 31109
effects on mutation induction in barley and rice seeds, 20: 31050
effects on orchitis development and *Treponema pallidum* content in antigens in rabbits, 20: 31119
effects on oxidative enzymes in mouse epididymis and testis, 20: 31090
effects on pancreatic morphology and physiology in dogs, 20: 31089
effects on plant seedlings, metabolic, 20: 31115
effects on potassium chlorate crystals at room temperature, absorption bands from, 20: 32686
effects on preservation of apple juice, 20: 31629
effects on proliferation of human leukocytes in culture, 20: 31067
effects on properdin systems in dogs, 20: 31013
effects on rats, effects of uneven exposure and irradiated bone marrow autografts on, 20: 31133
effects on silver chlorides, defect formation from, 20: 32731
effects on sodium chloride single crystals, Schottky disorder and lattice relaxation from, (E), 20: 32712
effects on somatic mutation frequency induction in oats, 20: 31078
effects on susceptibility of mice exposed *in utero* to congenital anomalies, 20: 31066
effects on synthesis of induced β-D-galactosidase in *E. coli*, 20: 31004
effects on synthesis of corticosteroids in rats, 20: 31011
effects on *Thiobacillus thiooxidans*, effects of anoxia, chemicals, and pH on, 20: 31139
effects on transfer capacity of rat small intestine, whole-body, 20: 31081
effects on trypsin solutions, effects of agar on, 20: 31017
effects on tumor beds in mice, 20: 31073
effects on Yoshida ascites tumor cells in rats, recovery mechanism in, 20: 31070
protection against, manual for, 20: 31445 (N-65-12416)
reactions with frozen hydrochloric and hydrofluoric acids, EPR of hydrogen atoms formed in, 20: 32719(T)
use in commercial radiopreservation of food, costs of, 20: 31635

X-RAY-DIFFRACTION ANALYSIS
uses at ANL, 20: 31167(R) (ANL-7175, pp 217-25)

X-RAY SOURCES
use for altitude measurement and terrain identification, 20: 31493
use of machine and radioisotope, for aerospace applications, 20: 31339

X-RAY SPECTROMETERS
design and testing of URS-II, for spectral fine structure, 20: 31581
performance of proportional counter, 20: 31544
performance of proportional counter, 20: 31545

X-RAY SPECTROSCOPY
uses at ANL, 20: 31167(R) (ANL-7175, pp 217-25)

XENON
content in silicates from Estherville Mesosiderite meteorites, 20: 31859
diffusion in uranium dioxide, effects of additions of, lanthanum, niobium, or yttrium oxides on, 20: 31666
diffusion in urania at 1330 to 1800°C, effects of radiation dose on, 20: 31666
ionization of, by electrons at 0.6 to 20 kev, cross sections for, (E/T), 20: 31906
sorption on glass and molybdenum films, 20: 31242
stability in absorbing-layer slab reactor, absorber effects on, 20: 32771

XENON FLUORIDES
spectra of, effects of temperature on near ultraviolet absorption, 20: 31221(R) (UCRL-16658, pp 73-87)

XENON IONS
reactions with metal surfaces, secondary emission factors for, 20: 31926

XENON ISOTOPES
abundance in meteorites, fission, neutron capture, and spallation anomalies in, 20: 31875

XENON ISOTOPES Xe-129
production and uses of, 20: 31642 (ORNL-P-2190)

XENON ISOTOPES Xe-130
determination in tellurium ores, 20: 32385

XENON ISOTOPES Xe-131
production and uses of, 20: 31642 (ORNL-P-2190)

XENON ISOTOPES Xe-133
production and uses of, 20: 31642 (ORNL-P-2190)

XENON OXIDES
uses in titrimetric determination of organic acids, 20: 31196

Y

YEASTS
phosphate metabolism by, tracer studies of, 20: 31108
radiosensitivity of, genetic control of, 20: 31041

YTTERBIUM
toxicity in laboratory animals, 20: 30970 (COO-1170-5)

YTTERBIUM ALLOYS
Yb–Zn, melting point of $YbZn_2$, 20: 31743

YTTERBIUM ISOTOPES
oxygen-16 reactions (O-16,xn) with, alpha-active platinum isotopes from, (E), 20: 32458
preparation of self-supporting foils of, 20: 31696

YTTERBIUM ISOTOPES Yb-164
conversion electron spectra of, (E), 20: 32415

YTTERBIUM ISOTOPES Yb-170
energy level transitions in, L-subshell ratios of E2 rotational, 20: 32516
energy level transitions from thulium-170 decay, conversion coefficients for, (E), 20: 32443

YTTERBIUM ISOTOPES Yb-171
energy level transitions from thulium-171 decay, conversion coefficients

for, (E), 20: 32443
YTTERBIUM ISOTOPES Yb-176
neutron reactions (n,γ) at 10 kev to 3 Mev, cross sections for, (E), 20: 32370(R) (ANL-7175, pp 212-16)
YTTERBIUM MOLYBDATES
preparation and crystal structure of, 20: 31740
YTTERBIUM OXIDES
$CaO-Yb_2O_3$, grain boundary precipitation in, 20: 31738
YTTERBIUM TUNGSTATES
preparation and crystal structure of, 20: 31740
YTTRIUM
effects on ductility of austenitic stainless steel, 20: 31669
oxidation by moist air, kinetics of, 20: 31686
separation from water by precipitation, kinetics of, 20: 31318 (BMwF-FBK-65-04)
toxicity in laboratory animals, 20: 30970 (COO-1170-5)
YTTRIUM ALLOYS
Gd–Y, magnetic ordering in, gadolinium-content effects on g factor for, 20: 32716
Ta–W–Y, corrosion by cerium–cobalt–plutonium alloy fuels, effects of carbon on, 20: 31679(R) (LA-3524)
YTTRIUM ISOTOPES Y-88
beta transitions in, strontium-88 levels from, (E), 20: 32453
YTTRIUM ISOTOPES Y-89
neutron reactions (n,γ) at 10 kev to 3 Mev, cross sections for, (E), 20: 32370(R) (ANL-7175, pp 212-16)
YTTRIUM ISOTOPES Y-90
determination in presence of strontium-90, beta counting technique for, 20: 31188
production of isomer pairs of, from helium-3 reactions (He-3,p) with strontium-88 at 14 to 19 Mev, (E), 20: 32430
radiation hazard from atmospheric, in mixture with strontium-90, 20: 31528
separation from sea water, 20: 31249
use for radiotherapy of metastasized mammary carcinomas, 20: 31153
YTTRIUM MOLYBDATES
preparation and crystal structure of, 20: 31740
YTTRIUM OXIDES
effects on xenon diffusion in urania, 20: 31666
electron spectra of, 20: 31219(R) (UCRL-16658, pp 11-20)
$UO_2-Y_2O_3$, oxidation of solid solutions of, kinetics of, 20: 31685
YTTRIUM TUNGSTATES
preparation and crystal structure of, 20: 31740

Z

ZEBRA
reactivity Doppler coefficients for, (T), 20: 32869
reactivity Doppler coefficient in core 5, 20: 32840
ZINC
determination in conductive tissue of beef heart, activation, 20: 31176
determination in human heart tissue, activation, 20: 31175
laser beam reactions on surfaces of, momentum transfer by giant-pulsed, (E), 20: 31810
neutron capture by, average level widths of compound nucleus from, (E), 20: 32424
proton elastic scattering at 17.8 Mev, polarization of, (E), 20: 32439
proton reactions at 0.05 to 2.9 Bev, induced activity data and cross sections for spallation, (E/T), 20: 32549
slip mechanisms in, 20: 31714(R) (UCRL-16658, pp 99-103)
vaporization from probe surface in electric arcs, (E), 20: 32593
ZINC ALLOYS
Ce–Zn, melting point of $CeZn_2$, 20: 31743
Cu–Mg–Zn, liquid miscibility of, at high temperatures, 20: 31314(R) (ANL-7175, pp 1-41)
Dy–Zn, melting point of $DyZn_2$, 20: 31743
Er–Zn, melting point of $ErZn_2$, 20: 31743
Eu–Zn, melting point on $EuZn_2$, 20: 31743
Gd–Zn, melting point of $GdZn_2$, 20: 31743
Ho–Zn, melting point of $HoZn_2$, 20: 31743
La–Zn, melting point of $LaZn_2$, 20: 31743
Lu–Zn, melting point of $LuZn_2$, 20: 31743
Mg–Pu–Zn, liquid miscibility of, at high temperatures, 20: 31314(R) (ANL-7175, pp 1-41)
Mg–Zn, solvent properties of, for chromium, iron, niobium, and zirconium, 20: 31314(R) (ANL-7175, pp 1-41)
Nb–Zn, phase diagram, 20: 31669
Nd–Zn, melting point of $NdZn_2$, 20: 31743
Pr–Zn, melting point of $PrZn_2$, 20: 31743
rare earth–Zn, crystal structure of, CsCl-type intermediate phases in, 20: 31737
Sm–Zn, melting point of $SmZn_2$, 20: 31743
Tb–Zn, melting point of $TbZn_2$, 20: 31743
Tm–Zn, melting point of $TmZn_2$, 20: 31743
Yb–Zn, melting point of $YbZn_2$, 20: 31743
ZINC ISOTOPES
distribution and natural carriers of, in sea water, 20: 31422
ZINC ISOTOPES Zn-61
decay scheme for isomeric, (E), 20: 32373(R) (COO-1530-1)
ZINC ISOTOPES Zn-64
alpha reactions with, excitation functions for, (T), 20: 32373(R) (COO-1530-1)
ZINC ISOTOPES Zn-65
effects on immune reactions in rabbits, 20: 31112
effects on rabbits, pathological, 20: 31112
uptake and retention by man from Columbia River fish, 20: 30969 (BNWL-SA-45)
ZINC ISOTOPES Zn-66
proton reactions (p,α) at 17.5 and 28 Mev, J-dependence of angular distributions from, 20: 32489
ZINC ISOTOPES Zn-68
proton reactions (p,α) at 17.5 Mev, J-dependence of angular distributions from, (E), 20: 32489
ZINC SULFIDES
radiation effects on optical transmission spectra of single crystals of, fast-neutron, 20: 31272
ZINC SYSTEMS
Cd–Mg–UCl_4–Zn, corrosive effects of, on stainless steel at 650°C, 20: 31314(R) (ANL-7175, pp 1-41)
ZIRCALOY-2
creep of, activation energy for, 20: 31669
creep properties at high temperatures, 20: 31669
ductility of, effects of zirconium hydride platelets on, 20: 31669
fracture properties of, effects of hydrogen and temperature on, 20: 31669
mechanical properties, 20: 32796(R) (AI-CE-3)
radiation effects on impact properties of, effects of hydrogen on fast-neutron, 20: 31669
reactions with steam at 900 to 1500°C, 20: 31669
thermal expansion of, effects of hydride phase on, 20: 31745
ZIRCALOY-4
thermal expansion of, effects of hydride phase on, 20: 31745
ZIRCONIUM
corrosion by perchlorate solutions, pitting, 20: 31687
creep behavior and dislocation mobility in alpha-, (E/T), 20: 32696
effects on microstructure of tungsten–thoria dispersion-hardened alloys, 20: 31781
fracture properties of, 20: 31667
nucleation of burning droplets of, effects of supercooling on spearpoint formation during, 20: 31664
reactions with carbon monoxide and carbon dioxide at 850°C, kinetics of, 20: 31669
reactions with oxygen at 840 to 1100°C, diffusion kinetics for, 20: 31669
reactions with sodium at 1700 to 2350°C, 20: 31440(R) (ANL-7175, pp 159-83)
separation from neptunium by solvent extraction using 4-methyl-2-pentanone, 20: 31319 (ISO-SA-10)
separation from uranium by fluidized-bed fluoride volatility process, 20: 31321
solubility in magnesium–zinc alloys, 20: 31314(R) (ANL-7175, pp 1-41)
solvent properties for hydrogen, effects of dissolved oxygen on, 20: 31667
solvent properties for hydrogen, effects of alloying additions on, 20: 31667
vacancy formation energy and concentration in, determination from thermal capacity measurements, 20: 32729(T)
Mo–Ti–Zr, stress-rupture at 2000°F of TZM, 20: 31669
ZIRCONIUM ALLOYS
Co–Zr, crystal structure of Zr_6Co_{23}, 20: 31727
Cr–Fe–Zr, corrosion by steam at 300, 400, and 500°C, 20: 31677(R) (GEAP-4840)
Cr–Fe–Zr, properties of, for use as fuel cladding material, 20: 31677(R) (GEAP-4840)
Fe–Zr, crystal structure of Zr_2Fe, 20: 31727
Hf–Zr, phase diagram, 20: 31744
Mo–Nb–W–Zr, hardness of niobium-base, effects of composition on hot-, 20: 31669
Mo–Ti–Zr, fatigue properties of TZM, at high temperatures, 20: 31710(R) (NASA-CR-54983)
Nb–Sn–Zr, corrosion by steam, composition of oxide film formed by, 20: 31669
Nb–Sn–Zr, hardness of zirconium-base, effects of tempering at 400 to 700°C on, 20: 31669
Nb–Ta–W–Zr, creep properties of FS-85, 20: 31669
Nb–Zr, corrosion by cerium–cobalt–plutonium alloy fuels, effects of carbon on, 20: 31679(R) (LA-3524)
Nb–Zr, corrosion by lead at 1400°F, 20: 31683(R) (ORNL-3936, pp 95-

Nb–Zr, fracture properties of zirconium-base, effects of hydrogen and temperature on, 20: 31669
Nb–Zr, mechanical properties of cold-worked zirconium-base, 20: 31669
Nb–Zr, radiation effects on impact properties of, effects of hydrogen on fast-neutron, 20: 31669
Nb–Zr, reactions with oxygen at 1000 to 1600°F, mechanisms of, 20: 31669
Nb–Zr, superconductivity of, in pulsed magnetic fields, effects of aging on, 20: 32312(R) (UCRL-16658, pp 133-43)
Nb–Zr, thermal expansion of, effects of hydride phase on, 20: 31745
Pu–U–Zr, compatibility with type 304 stainless steel to 800°C, 20: 31666
Pu–U–Zr, mechanical properties and phase diagram of, 20: 31666
Th–U–Zr, tensile strength of, aging effects on, 20: 31767
U–Zr, phase studies, 20: 31666

ZIRCONIUM BORIDES
enthalpy of formation of, 20: 31213(R) (ANL-7175, pp 119-58)
sintering of, effects of cobalt, iron, or nickel additions on, 20: 31668
Mo–ZrB_2, sintering of, effects of composition on, 20: 31698

ZIRCONIUM CARBIDES
fabrication by hot-pressing, 20: 31699
performance in focus electrodes in cesium-contact ion thrustors, 20: 31383
graphite–ZrC, fabrication and properties of hot-pressed composites of, 20: 31688 (NASA-CR-507)

ZIRCONIUM FLUORIDES
BeF_2–LiF–ZrF_4, separation from rare earth fission products, 20: 32804(R) (ORNL-3936, pp 122-71)

ZIRCONIUM HYDRIDES
effects on ductility of Zircaloy-2, 20: 31669
fracture properties of, 20: 31667
magnetic properties of ZrH_5, 20: 32699

ZIRCONIUM ISOTOPES
distribution and natural carriers of, in sea water, 20: 31422

ZIRCONIUM ISOTOPES Zr-90
deuteron reactions (d,p) at 11 and 13 Mev, angular-momentum effects on angular distribution from, (E), 20: 32512
neutron scattering by, zirconium-91 neutron single-particle levels from, (T), 20: 32552

proton elastic scattering at 40 Mev, differential cross sections and polarization for, (E), 20: 32510

ZIRCONIUM ISOTOPES Zr-91
energy levels of, neutron single-particle, (T), 20: 32552

ZIRCONIUM ISOTOPES Zr-92
deuteron reactions (d,p) at 11 and 13 Mev, angular-momentum effects on angular distribution from, (E), 20: 32512
proton reactions (p,α) at 28 Mev, J-dependence of angular distributions from, (E), 20: 32489

ZIRCONIUM ISOTOPES Zr-94
deuteron reactions (d,p) at 11 and 13 Mev, angular momentum effects on angular distribution from, (E), 20: 32512

ZIRCONIUM ISOTOPES Zr-95
content in fallout particles from high-altitude explosions, 20: 31424
content in fractionated fallout particles from land surface burst, 20: 31460
content in large fallout particles in Japan, 20: 31412
deposition on tropospheric aerosols, 20: 31459

ZIRCONIUM OXIDES
compatibility with cesium vapor at 1800°C, 20: 31669
microstructure of thin films of, from oxidized zirconium, 20: 31755
permeability to oxygen at 1100 to 2050°C, 20: 31731
phase transformations in submicron, 20: 31736
BeO–MgO–ZrO_2, properties of molten, for fuel matrix for homogeneous thermal nuclear reactors, 20: 31726
CaO–ZrO_2, diffusion at 1700 to 2150°C in, cationic self-, 20: 31732
MgO–ZrO_2, grain boundary precipitation in, 20: 31738

ZIRCONIUM SYSTEMS
C–Cr–Zr, phase studies, 20: 31669
C–Mo–Ti–Zr, fatigue properties of TZC, at high temperatures, 20: 31710(R) (NASA-CR-54983)
C–Mo–Zr, phase studies, 20: 31669
C–W–Zr, phase studies, 20: 31669
Hf–H–Zr, phase diagrams, 20: 31667
H–Zr, preparation of, for transmission electron microscopy, hydrogen concentration in electrothinning procedures for, 20: 31691

ZYMOSAN
effects on radioinduced changes in properdin system in dogs, 20: 31013

REPORT NUMBER INDEX

Reports, conference papers and proceedings, numbered translations, and patents abstracted during the period are included in this index. Each item is listed by report number; this is followed by the abstract number and a brief notation regarding public availability. The index entries show which reports are on file in the depository libraries, which reports have been published in open-literature journals (journal citation given), and which reports can be purchased (source and price). Whenever a report is identified by more than one number, cross references from secondary to primary report numbers are cited.

The report number codes apply to AEC reports unless designated otherwise. Non-AEC reports are identified by parenthetical notes after the report codes; e.g., (non-AEC), (British), (Canadian), (French). The note (Misc.) identifies those codes used for both USAEC and non-AEC reports. Patents are listed under the heading "PATENTS"; the country of origin is included in parentheses.

A comprehensive listing of both AEC and non-AEC report codes is contained in TID-85(5th Rev.), *Report Number Series Used by the Division of Technical Information in Cataloging Reports*. This information is also included in the Cumulative Report Number Index (issued annually).

Public Availability of USAEC Reports

All USAEC reports abstracted in *NSA* are available to the public through one or more of the following sources:

(1) Depository libraries in the United States, in other countries, and in international agencies. A list of these depositories appears on the inside covers of each issue of *NSA*.

(2) Scientific and technical journals or other publications.

(3) Microcard Editions, Inc., in Microcard and micronegative form. Orders and inquiries should be sent to: Accounting and Shipping Department, West Salem, Wisconsin 54669.

(4) Clearinghouse for Federal Scientific and Technical Information, U. S. Department of Commerce, Springfield, Virginia 22151.

(5) Superintendent of Documents, U. S. Government Printing Office, Washington, D. C. 20402.

Public Availability of Non-AEC Reports

U. S. Reports. Many reports of U. S. Government agencies are available to the public from the Clearinghouse for Federal Scientific and Technical Information (CFSTI). This availability is given when known. Such reports should be ordered by AD number or NASA-N number. If availability is not shown, inquiries may be directed to CFSTI. In the case of NP numbers, inquiries should be by title and author.

Non-U. S. Reports. Many reports of atomic energy establishments of other countries are deposited in the libraries listed on the inside covers of each issue of *NSA*.

Additionally, the following have made their reports available as indicated.

AUSTRALIA

Australian Atomic Energy Commission Research Establishment. Available upon request from the Library, Australian Atomic Research Establishment, Private Mail Bag, Sutherland, New South Wales, Australia.

BELGIUM

Centre d'Étude de l'Énergie Nucléaire. Available upon request to individuals and organizations, from the Centre d'Étude de l'Énergie Nucléaire (CEN), 31, Rue Belliard, Bruxelles, Belgium.

CANADA

Atomic Energy of Canada Limited. For sale by the Technical Information Officer, Atomic Energy of Canada Limited, Chalk River, Ontario, Canada. Copies are also deposited in libraries in the United Kingdom.

National Research Council of Canada. Available from the National Research Council of Canada, Ottawa 2, Ontario, Canada.

DENMARK

Atomic Energy Commission Research Establishment, Risø. Available on exchange from the Library, Danish Atomic Energy Commission, Risø, Roskilde, Denmark. Also for sale by Jul. Gjellerup, Booksellers, 87 Sölvgade, København K., Denmark.

Danatom. Available on loan from Research Establishment, Risø, Roskilde, Denmark. Copies are available from Danatom, Aurehøjvej 2, Hellerup, Denmark.

EURATOM

Reports from the Commission of the European Atomic Energy Community are available from: Presses academiques europeennes, 98, chaussee de Charleroi, Brussels 6, Belgium; and Office central de vente des publications des Communautes eurodeennes 2, place de Metz, Luxemburg.

FRANCE

Commissariat à l'Énergie Atomique. Inquiries for reports numbered 1-2199 should be addressed to Commissariat à l'Énergie Atomique, Service Central de Documentation, Centre d'Études Nucléaires de Saclay, Boite Postale No. 2, Gif-sur-Yvette (S. et O.), France. Reports numbered 2200 and above are available from La Documentation Francaise, 16 Rue Lord-Byron, Paris VIII, France.

Service Central de Protection contre les Rayonnements Ionisants. Copies are available from Ministère de la Santé Publique, Service Central de Protection contre les Rayonnements Ionisants, B. P. n° 35—LE VESINET (S. et O.), France.

GERMANY

Deutsches Elektronen-Synchrotron DESY. Copies are available from Deutsches Elektronen-Synchrotron Desy, Dokumentation, 2000 Hamburg-Gr. Flottbek 1, Notkestieg 1, Germany.

Gesellschaft für Kernforschung mbH (KFK). Copies are available from Gesellschaft für Kernforschung mbH, 75 Karlsruhe, Postfach 947, Germany. Copies are also deposited in many national nuclear centers in the world.

Kernforschungsanlage. Copies may be ordered from Zentralbibliothek der Kernforschungsanlage Jülich, Jülich, Bundesrepublik Deutschland.

Hahn-Meitner-Institute für Kernforschung. Available without charge from Hahn-Meitner-Institute für Kernforschung Berlin, Bibliothek, Glienicker Strasse 100, 1 Berlin

39, Germany. Copies are deposited in many national nuclear centers in the world.

Johann-Wolfgang-Goethe Universität, Frankfurt Am Main, Institut für Kernphysik, (IKF). Copies are available from Gmelin Institut, 40-42 Varrentrappstrasse, Frankfurt (Main), West Germany.

ISRAEL

Israel Atomic Energy Commission. Available without charge from Ministry of Defence/Atomic Energy Commission, Soreq Research Establishment, Yavne, Israel. Copies are deposited in libraries in Israel and in other countries.

ITALY

Centro Informazioni Studi Esperienze (CISE). For sale at CISE Press Office, Casella Postale 3986, Milano, Italy. Copies are deposited in libraries in Italy.

Comitato Nazionale per l'Energia Nucleare. Copies are available from Comitato Nazionale per l'Energia Nucleare, Divisione Affari Internazionali e Studi Economici, Ufficio Pubblicazioni, Via Belisario, 15, Roma, Italy.

JAPAN

Japan Atomic Energy Research Institute (JAERI). Available from the Staff Supply Cooperative of Japan Atomic Energy Research Institute (JAERI), 1-1 Tamura-Cho, Shiba, Minato-Ku, Tokyo, Japan. Copies are deposited in depositories in Tokyo, Nagoya, and Osaka.

Nagoya University. Copies are available from Research Information Center, Institute of Plasma Physics, Nagoya University, Nagoya, Japan.

University of Tokyo. Available free of charge from Institute for Nuclear Study, University of Tokyo, Tanashi-Machi, Kitatama-gun, Tokyo, Japan.

NETHERLANDS

Reactor Centrum Nederland. For sale by Reactor Centrum Nederland, 112 Scheveningseweg, 's-Gravenhage, The Netherlands. Copies are deposited in university libraries in Holland and in many national nuclear centers in the world.

NEW ZEALAND

Institute of Nuclear Sciences. Copies are available from Librarian, Institute of Nuclear Sciences, D.S.I.R., Private Bag, Lower Hutt, New Zealand. Copies are deposited in other countries.

NORWAY

Forsvarets Forskningsinstitutt. Copies available from Norwegian Defence Research Establishment, Library, P. O. Box 25, Kjeller, Norway.

Institutt for Atomenergi. "KR" reports are available on an exchange basis from the Library, Institutt for Atomenergi, Box 40, Kjeller, Norway. Other series are not generally available to the public.

Norwegian Reactor School. Copies are available from The Library, Institutt for Atomenergi, P. O. Box 40, Kjeller, Norway.

PAKISTAN

Atomic Energy Center. Copies are available from Atomic Energy Center, P. O. Box 658, Lahore, (West Pakistan).

POLAND

Reports of the Polish nuclear institutes are published by the Nuclear Energy Information Center of the Government Commissioner for Use of Nuclear Energy. Copies are available from Ośrodek Informacji o Energii Jądrowej, Warszawa, PKiN, Poland.

SPAIN

Junta de Energia Nuclear. "JEN" reports are available without charge from Servicio de Documentation, Junta de Energia Nuclear, Ciudad Universitaria, Madrid (3), Spain.

SWEDEN

Aktiebolaget Atomenergi. "AE" reports are for sale from Aktiebolaget Atomenergi, Library Section, Box 43041, Stockholm 43, Sweden. Bibliographies and literature surveys of the VDDIT- series may be obtained from Aktiebolaget Atomenergi, Information Office, Scientific and Technical Information, Box 43041, Stockholm 43, Sweden. Other series are not generally available to the public. Organizations in the atomic energy field may obtain copies from Aktiebolaget Atomenergi. Microcopy of AE reports is available from the International Documentation Centre, Tumba, Sweden.

SWITZERLAND

CERN European Organization for Nuclear Research. Available without charge from CERN European Organization for Nuclear Research, Geneva 23, Switzerland. Copies are deposited in libraries in 13 countries.

Eidgenössisches Institut für Reaktorforschung. "EIR" reports are available from Eidgenössiches Institut für Reaktorforschung, c/o Bibliothek, Würenlingen/Ag, Switzerland.

TURKEY

Turkish Atomic Energy Commission. Copies are available free of charge from T.A.E.C., Çekmece Nuclear Research Center, P. O. Box 1, Airport, İstanbul, Turkey.

UNITED KINGDOM

United Kingdom Atomic Energy Authority. Some reports are for sale in the United States by the British Information Service (BIS), 845 Third Avenue, New York, N. Y. 10022. United Kingdom reports generally may be purchased from Her Majesty's Stationery Office, London. Copies not for sale by Her Majesty's Stationery Office may be purchased in microcopy form from Micro Methods Limited, East Ardsley, Wakefield, Yorks, England. Report copies are deposited in a large number of libraries in England, depositories of the USAEC in the United States and abroad, and in most national nuclear centers throughout the world.

Conferences

Published conference proceedings as well as individual unpublished papers from conferences are included in this index. A CONF number is assigned to the conference if published proceedings are received and also if only a single paper is received. The base number used is year-month-sequence. Thus, the number CONF-650101 would indicate that the conference was held in 1965, in January, and that this was the first January 1965 conference so received. This number would be assigned to complete published proceedings, or if individual papers are received, the base number would be extended to include a paper number, i.e., CONF-650101-1. As additional papers are received, they will be assigned consecutive numbers in the series, CONF-650101-1, 2, 3, 4, etc. This numbering system ensures that all papers received from a conference will be associated with that conference in this index.

If published proceedings are received after the receipt of individual papers, the complete proceedings will be abstracted and the abstract number will appear in this index with the base CONF number.

Abbreviations Used in Availability Column

AECL	For sale by Atomic Energy of Canada Ltd., Chalk River, Ontario, Canada.
BIS	For sale by British Information Service, 845 Third Avenue, New York, N. Y. 10022
CFSTI	For sale by the Clearinghouse for Federal Scientific and Technical Information, U.S. Department of Commerce, Spring-

field, Virginia 22151. The symbol "cy" indicates that the format of the item sold may be either a printed document or a photographic reproduction (two-thirds of original size) depending upon the availability of printed stock. The indicated price is for either format. The symbol "mn" is used to indicate that copy is also available in the form of micronegatives (microfiche).

Dep. — AEC reports: Full-size copy is on deposit in the depository libraries both inside and outside the United States. These reports are also for sale by Microcard Editions, Inc., Accounting and Shipping Department, West Salem, Wisconsin 54669.

Non-AEC reports: Full-size copy on deposit in the depository libraries in the United States only.

Dep.(mc) — Same as for Dep., except copy is in Microcard form.

Dep.(mn) — Same as for Dep., except copy is in micronegative (microfiche) form.

DSIR — For sale by the National Lending Library for Science and Technology (D.S.I.R.), Boston Spa, Yorkshire, England.

DTI Extension — Available from the U. S. Atomic Energy Commission, Division of Technical Information Extension, P. O. Box 62, Oak Ridge, Tennessee 37830.

EM — Blueprints and microcopy of AEC engineering drawings are available from Clearinghouse for Federal Scientific and Technical Information, U. S. Department of Commerce, Springfield, Virginia 22151. Current prices of the CAPE- packages may be obtained from this address. TID-4100, available from the Division of Technical Information Extension, P. O. Box 62, Oak Ridge, Tennessee 37831, contains information on all the CAPE- packages for sale.

Gmelin — Available at a nominal charge and under the AED- number shown from Atomic Energy Documentation Center, Gmelin Institute, 40-42 Varrentrappstrasse Frankfurt (Main), West Germany.

GPO — For sale by the Superintendent of Documents, Government Printing Office, Washington, D. C. 20402.

HMSO — Her Majesty's Stationery Office, London.

IAEA — Available from the International Atomic Energy Agency, Vienna, Austria, and from its sales agencies in various countries throughout the world. A list of these agencies is found in each STI/DOC and STI/PUB publication.

JCL — For sale by the Special Libraries Association Translation Center, John Crerar Library, 35 West 33rd Street, Chicago, Illinois 60616.

LC — For sale by the Library of Congress, Photoduplication Service, Washington, D. C. 20540.

NAS — National Academy of Sciences, National Research Council, Washington, D. C. 20418.

NRC — For sale by the National Research Council of Canada, Ottawa, Ontario, Canada.

ORAU — Available on interlibrary loan from the Library, Oak Ridge Associated Universities, Post Office Box 117, Oak Ridge, Tennessee 37830.

ORINS — See ORAU.

UKAEA, London — Available from United Kingdom Atomic Energy Authority, 11 Charles II Street, London, S. W. 1.

UN — United Nations Bookshop, United Nations Headquarters, New York, New York.

USGS — Available free of charge from the U. S. Geological Survey, Washington, D. C. 20242.

ZLDI — Zentralstelle Für Luftfahrtdokumentation Und-Information, Maria-Theresia-Strasse 21, Munich 27, Germany.

[The symbols "ph," "mf," and "fs" are used to designate that copy is available only in photostat, microfilm, or facsimile form. The symbol "mn" is used to designate that copy is available in micronegative (microfiche) form. The symbol "cy" is used to designate full size or photographically enlarged copy (two-thirds of original size).]

Report No.	Abstract No.	Availability
AC–	**(Non-AEC)**	
3	20-32851	See N-65-30544
ACNP–	**(Misc.)**	
66538	20-32795	Dep. mn; CFSTI $6.00 cy, $1.25 mn
AD–	**(Misc.)**	
627094	20-31645	CFSTI $4.00 cy, $0.75 mn
629415	20-31720	CFSTI $1.00 cy, $0.50 mn
630971	20-31721	CFSTI $1.00 cy, $0.50 mn
631690	20-31025	CFSTI $3.00 cy, $0.50 mn
632527	20-31498	CFSTI $1.00 cy, $0.50 mn
633216	20-32671	CFSTI $4.00 cy, $0.75 mn
633468	20-31611	CFSTI $3.00 cy, $0.75 mn
633606	20-31026	CFSTI $1.00 cy, $0.50 mn
633752	20-31499	CFSTI $1.00 cy, $0.50 mn
634300	20-31814	CFSTI $1.00 cy, $0.50 mn
634517	20-31981	CFSTI $2.00 cy, $0.50 mn
634703	20-31982	CFSTI $1.00 cy, $0.50 mn
634704	20-32243	CFSTI $1.00 cy, $0.50 mn
634706	20-32106	CFSTI $1.00 cy, $0.50 mn
AECD-AG–	**(Pakistani)**	
14	20-31027	Dep. mn
15	20-31623	Dep. mn
AECL–	**(Canadian)**	
1744	20-31646	Dep. mn; AECL $9.00 per set
1744(Pt.A)(Add.1)	20-31647	Dep. mn; AECL $1.50
2409	20-31028	Dep. mn; AECL $0.50
2423	20-32354	Can. J. Phys., 44: 1299-1311(1966)
2427	20-32353	Can. J. Phys., 44: 1279-97(1966)
2535	20-32369	Dep. mn; AECL $3.00
2540	20-31439	Dep. mn; AECL $0.50
2543	20-32763	Dep. mn; AECL $1.00
AERE-R–	**(British)**	
4993	20-31768	Trans. Brit. Ceram. Soc., 65: 207-17(1966)
5143	20-31799	J. Nucl. Mater., 19: 351-3(1966)
AERE-Trans–	**(British)**	
1050	20-31481	Dep.; BIS $0.30; HMSO 1s. 2d.
AFWL-TR–	**(Non-AEC)**	
65-214	20-31025	See AD-631600
AHSB(RP)–	**(British)**	
M-37	20-30983	Health Phys., 12: 843-50(1966)
AI-CE–		
3	20-32796	Dep. mn; CFSTI $8.43 cy, $2.25 mn
ANL–		
6853	20-31313	Dep. mn; CFSTI $2.00 cy, $0.50 mn
6930	20-32790	Dep. mn; CFSTI $2.00 cy, $0.50 mn
7042	20-31352	Dep. mn; CFSTI $2.00 cy, $0.50 mn
7093	20-31340	Dep. mn; CFSTI $4.00 cy, $1.00 mn
7119	20-31708	Dep. mn; CFSTI $1.00 cy, $0.50 mn
7166	20-32858	Dep. mn; CFSTI $1.00 cy, $0.50 mn
7175	20-31164	Dep. mn; CFSTI $6.00 cy, $1.25 mn
ANL-Trans–		
310	20-31222	Dep. mn; CFSTI $1.00 cy, $0.50 mn; JCL $1.10 fs, $0.80 mf
ARL–	**(Non-AEC)**	
66-0061	20-31981	See AD-634517
BAW–	**(Misc.)**	
393-3	20-31317	Dep. mn; CFSTI $5.00 cy, $0.75 mn
BMwF-FBK–	**(German)**	
65-04	20-31318	Dep. mn
BNL–		
9012	20-31088	Radiat. Res., 28: 232-42(1966)
9135	20-31065	Nature, 210: 748-9(1966)
9256	20-31524	Health Phys., 12: 787-92(1966)
9289	20-31087	See BNL-9366
9299	20-31086	Radiat. Res., 28: 166-80(1966)
9320	20-30990	Nature, 210: 547-8(1966)
9366	20-31087	Radiat. Res., 28: 183-202(1966)
9451	20-32388	Ann. Phys. (N. Y.), 37: 264-70(1966)
9484	20-31000	Blood, 27: 831-43(1966)
9546	20-31341	Dep. mn; CFSTI $2.00 cy, $0.50 mn
9550	20-31291	Radiat. Res., 28: 1-12(1966)
9570	20-31076	Radiat. Bot., 6: 187-201(1966)
9579	20-31077	Radiat. Bot., 6: 203-10(1966)
9633	20-31092	Radiat. Res., 28: 302-21(1966)
9706	20-32045	Nuovo Cimento (10), 44A: 120-30(1966)
9712	20-32178	Progr. Theoret. Phys. (Kyoto), 35: 565 (1966)
9792	20-32706	Phys. Rev., 147: 457-62(1966)
9807	20-32497	Phys. Rev., 147: 715-30(1966)
9866	20-31833	Nucl. Instrum. Methods, 42: 157-62(1966)
9874	20-32495	Phys. Rev., 147: 698-709(1966)
9875	20-32698	J. Chem. Phys., 44: 4498-4509(1966)
9994	20-32516	Phys. Rev., 147: 858-60(1966)
10004	20-32705	Phys. Rev., 147: 415-18(1966)
10013	20-32567	See CONF-651118-17
10015	20-32505	Phys. Rev., 147: 781-8(1966)
10078R	20-32067	Phys. Rev. Lett., 17: 102-5(1966)
10144	20-31815	Dep. mn; CFSTI $1.00 cy, $0.50 mn
10221	20-31029	Dep. mn; CFSTI $2.00 cy, $0.50 mn
10238	20-32681	Dep. mn; CFSTI $1.00 cy, $0.50 mn
BNL-tr–		
78	20-31223	Dep. mn; JCL $1.10 fs, $0.80 mf
BNWL–		
233	20-32748	Dep. mn; CFSTI $5.00 cy, $1.00 mn
235-4	20-31473	Dep. mn; CFSTI $2.00 cy, $0.50 mn
261	20-31624	Dep. mn; CFSTI $2.00 cy, $0.50 mn
BNWL-SA–		
11	20-30968	Dep. mn; CFSTI $1.00 cy, $0.50 mn
39	20-31030	Dep. mn; CFSTI $1.00 cy, $0.50 mn
40	20-31441	DEP. mn; CFSTI $1.00 cy, $0.50 mn
45	20-30969	Dep. mn; CFSTI $1.00 cy, $0.50 mn
67	20-31782	Dep. mn; CFSTI $1.00 cy, $0.50 mn
201	20-31031	Dep. mn; CFSTI $1.00 cy, $0.50 mn
208	20-31525	Health Phys., 12: 801-9(1966)
658	20-31267	Dep. mn; CFSTI $1.00 cy, $0.50 mn
661	20-31442	Dep. mn; CFSTI $1.00 cy, $0.50 mn
709	20-30998	Dep. mn; CFSTI $1.00 cy, $0.50 mn
BRL-R–	**(Non-AEC)**	
1307	20-32671	See AD-633216
CALT–		
68-71	20-31983	Dep. mn; CFSTI $1.00 cy, $0.50 mn
CAPE–		
1339	20- 31599	EM
1353	20-31491	EM
1360	20-31600	EM
1361	20-31601	EM
CEA-Bib–	**(French)**	
17(Pt.2))	20-32764	Dep. mn
CEA-R–	**(French)**	
2832	20-32371	Dep. mn
2859	20-31214	Dep. mn
2915	20-31506	Dep. mn
2929	20-31816	Dep. mn
2953	20-31032	Dep. mn
2981	20-31477	Dep. mn
CERN–	**(European Organization for Nuclear Research)**	
66-15	20-31817	Dep. mn
CEX–		
58.4.5	20-31395	Dep. mn; CFSTI $1.00 cy, $0.50 mn
61.6.2	20-31396	Dep. mn; CFSTI $1.00 cy, $0.50 mn
CNEA–	**(Argentinian)**	
168	20-31147	Dep. mn
170	20-31148	Dep. mn
CONF-520–	**20-31197**	**(Conference on Mass Spectrometry, Paris, Sept. 1964)**
CONF-640418–	**20-31880**	**(Conference on the Solar Wind,**

Report No.	Abstract No.	Availability
		Pasadena, Apr. 1–4, 1964) See JPL-TR-32-630
CONF-641005–	20-39893	(Correlation of Particles Emitted in Nuclear Reactions, Gatlinburg, Tenn., Oct. 15–17, 1964)
3	20-32568	ORAU. Gmelin, AED-CONF-64-296-3
CONF-641127–		(American Physical Society, Fall Meeting of the Ohio Section, Oxford, Ohio, Nov. 6–7, 1964)
1	20-32566	ORAU. Gmelin, AED-CONF-64-297-2
2	20-32554	ORAU. Gmelin, AED-CONF-64-297-1
3	20-31602	ORAU. Gmelin, AED-CONF-64-297-4
5	20-32544	ORAU. Gmelin, AED-CONF-64-297-5
CONF-641210–		(American Physical Society Meeting, Berkeley, Calif., Dec. 1964)
22	20-32344	ORAU. Gmelin, AED-CONF-64-236-44
CONF-650120–	20-31950	(Seminar on Cosmic Rays Extensive Air Showers, Lodz, Poland, Jan. 4–8, 1965) Dep.
CONF-650311–		(Conference on Analytical Chemistry and Applied Spectroscopy, Pittsburgh, Mar. 5, 1965)
5	20-31210	ORAU
CONF-650420–	20-32842	(5th Panel Meeting on Use of Nuclear Energy in Saline Water Conversion, Vienna, Apr. 5–9, 1965) See STI-DOC-10/51
CONF-650422–		(American Geophysical Union, Program for Section of Seismology Annual Meeting, Washington, D. C., Apr. 19–22, 1965
20	20-32286	ORAU. Gmelin, AED-CONF-65-118-60
22	20-32287	ORAU. Gmelin, AED-CONF-65-118-62
CONF-650440–		(American Mathematical Society, 622nd Meeting, New York, Apr. 12–15, 1965)
4	20-32576	See NYO-1480-50
CONF-650451–		(American Physical Society, Spring Meeting of the Ohio Section, Athens, Ohio, Apr. 23–24, 1965)
1	20-32552	ORAU. Gmelin, AED-CONF-65-408-2
CONF-650551–	20-31162	(5th International Thyroid Conference, Rome, May 24–27, 1965) $42.00
CONF-650552–		(Institute of Food Technologists, 25th Annual Meeting, Kansas City, Mo., May 16–20, 1965)
5	20-31635	ORAU. Gmelin, AED-CONF-65-111-5
CONF-650571–		(3rd Annual Surface Physics Symposium, Pullman, Wash., May 21–22, 1965)
1	20-32742	ORAU. Gmelin, AED-CONF-65-223-1
CONF-650602–		(American Nuclear Society 11th Annual Meeting, Gatlinburg, Tenn., June 20–24, 1965)
83	20-32838	ORAU. Gmelin, AED-CONF-65-125-111
CONF-650616–		(Health Physics Society, Annual Meeting, Los Angeles, June 14–17, 1965)
3	20-31441	See BNWL-SA-40
19	20-32884	ORAU. Gmelin, AED-CONF-65-153-43
20	20-31470	ORAU. Gmelin, AED-CONF-65-153-44
26	20-31424	ORAU
30	20-31471	ORAU
CONF-650632–		(7th Biennial Conference on Carbon, Cleveland, June 21–25, 1965)
11	20-31803	ORAU. Gmelin, AED-CONF-65-149-20
12	20-31777	ORAU. Gmelin, AED-CONF-65-149-23
17	20-31802	ORAU. Gmelin, AED-CONF-65-149-31
CONF-650634–		(16th Annual Mid-America Symposium on Spectroscopy, Chicago, June 14–17, 1965)
5	20-31949	ORAU. Gmelin, AED-CONF-65-155-12
CONF-650637–		(International Conference on Luminescent Dosimetry, Palo Alto, Calif., June 21–23, 1965)
8	20-31608	ORAU. Gmelin, AED-CONF-65-151-9
CONF-650638–	20-27251	(Physics of Quantum Electronics Conference, San Juan, Puerto Rico, June 28–30, 1965) $24.00
7	20-32735	ORAU. Gmelin, AED-CONF-65-156-12
CONF-650653–		(American Physical Society, Summer Meeting, New York, June 23–25, 1965)
13	20-32564	ORAU. Gmelin, AED-CONF-65-170-46
14	20-32569	ORAU. Gmelin, AED-CONF-65-170-47
20	20-32214	ORAU
21	20-32213	ORAU
22	20-32215	ORAU
23	20-32216	ORAU
24	20-32562	ORAU. Gmelin, AED-CONF-65-170-50
26	20-32288	ORAU. Gmelin, AED-CONF-65-170-52
27	20-32739	ORAU. Gmelin, AED-CONF-65-170-61
CONF-650663–		(73rd Annual Meeting and World Congress on Engineering Education, Chicago, June 21–25, 1965)
1	20-32779	ORAU. Gmelin, AED-CONF-65-209-5
CONF-650664–		(Canadian Assn. of Physicists Congress, Vancouver, B. C., June 9–12, 1965)
9	20-31943	ORAU. Gmelin, AED-CONF-65-288-12
CONF-650673–		(Meeting on Clinical Uses of Whole-Body Radioactivity Counting, Vienna, June 28–July 2, 1965)
1	20-31443	Dep. mn; CFSTI $1.00 cy, $0.50 mn
CONF-650707–	20-21164	(IEEE Annual Conference on Nuclear and Space Radiation Effects, Ann Arbor, Mich., July 12–15, 1965) Trans. Nucl. Sci., NS-12: 1-155(Oct. 1965)
25	20-31621	ORAU
CONF-650721–		(Positron Annihilation Conference, Detroit, July 27–29, 1965)
3	20-32345	ORAU. Gmelin, AED-CONF-65-211-11
4	20-32105	ORAU. Gmelin, AED-CONF-65-211-10
5	20-32346	ORAU. Gmelin, AED-CONF-65-211-12
14	20-32101	ORAU. Gmelin, AED-CONF-65-211-14
18	20-32099	ORAU. Gmelin, AED-CONF-65-211-18
CONF-650802–		(Cryogenic Engineering Conference, Houston, Tex., Aug. 23–25, 1965)
10	20-32348	ORAU. Gmelin, AED-CONF-65-193-24
11	20-32242	ORAU. Gmelin, AED-CONF-65-193-22
12	20-32349	ORAU. Gmelin, AED-CONF-65-193-22
CONF-650806–		(7th International Conference on Phenomena in Ionized Gases, Belgrade, Aug. 22–27, 1965)
16	20-32647	ORAU
CONF-650826–		(International Conference on Energetics, Rochester, N. Y., Aug. 18–20, 1965)
3	20-31977	ORAU. Gmelin, AED-CONF-65-210-9
5	20-31976	ORAU
CONF-650834–		(Alberta Symposium on Quantum Chemistry, Edmonton, Aug. 23–27, 1965)
2	20-31944	ORAU. Gmelin, AED-CONF-65-230-3
CONF-650835–		(Aeronomy Symposium, Boston, Aug. 16–20, 1965)
1	20-32289	ORAU. Gmelin, AED-CONF-65-234-3
CONF-650840–		(International Conference on Electron Diffraction and the Nature of Defects in Crystals, Melbourne, Aug. 16–21, 1965)
1	20-32741	ORAU. Gmelin, AED-CONF-65-316-1
CONF-650841–		(Conference of Metallurgists, Ottawa, Aug. 30–Sept. 1, 1965)
1	20-31212	ORAU. Gmelin, AED-CONF-65-277-3
CONF-650902–		(American Chemical Society, 150th National Meeting, Atlantic City, Sept. 12–17, 1965)
28	20-31607	ORAU. Gmelin, AED-CONF-65-235-62
29	20-31306	ORAU. Gmelin, AED-CONF-65-235-61
30	20-31258	ORAU. Gmelin, AED-CONF-65-235-63
CONF-650905–		(American Institute of Chemical Engineers Symposia,

Report No.	Abstract No.	Availability
	Minneapolis, Sept. 26–29, 1965)	
3	20-31634	ORAU. Gmelin, AED-CONF-65-382-4
CONF-650923–	**(5th International Conference on High Energy Accelerators, Frascati, Italy, Sept. 9–16, 1965)**	
30	20-31816	See CEA-R-2929
31	20-31823	See RPP-N-5
CONF-650927–	**(American Physical Society, Honolulu, Hawaii, Sept. 2–4, 1965)**	
5	20-31946	ORAU. Gmelin, AED-CONF-65-222-31
14	20-31779	ORAU. Gmelin, AED-CONF-65-222-24
15	20-32652	ORAU. Gmelin, AED-CONF-65-222-22
16	20-32737	ORAU. Gmelin, AED-CONF-65-222-10
17	20-31878	ORAU. Gmelin, AED-CONF-65-222-14
18	20-32654	ORAU. Gmelin, AED-CONF-65-222-9
19	20-32553	ORAU. Gmelin, AED-CONF-65-222-15
22	20-32649	ORAU. Gmelin, AED-CONF-65-222-44
26	20-32736	ORAU. Gmelin, AED-CONF-65-222-51
27	20-32565	ORAU. Gmelin, AED-CONF-65-222-58
CONF-650961–	**(American Geophysical Union, 5th Western National Meeting, Dallas, Sept. 1–3, 1965)**	
1	20-32560	ORAU. Gmelin, AED-CONF-65-224-5
2	20-32292	ORAU. Gmelin, AED-CONF-65-224-1
3	20-32291	ORAU. Gmelin, AED-CONF-65-224-9
4	20-31958	ORAU. Gmelin, AED-CONF-65-224-6
5	20-32290	ORAU. Gmelin, AED-CONF-65-224-2
8	20-31879	ORAU. Gmelin, AED-CONF-65-224-15
CONF-651009–	**(Conference on Safety, Fuels and Core Design in Large Fast Power Reactors, Argonne, Oct. 11–14, 1965)**	
22	20-31804	ORAU. Gmelin, AED-CONF-65-307-40
24	20-32840	ORAU. Gmelin, AED-CONF-65-307-41
26	20-31674	ORAU. Gmelin, AED-CONF-65-307-39
27	20-31675	ORAU. Gmelin, AED-CONF-65-307-44
28	20-32869	ORAU. Gmelin, AED-CONF-65-307-46
CONF-651015–	**(American Physical Society, Chicago, Oct. 7, 1965)**	
15	20-32104	ORAU. Gmelin, AED-CONF-65-312-38
16	20-31805	ORAU. Gmelin, AED-CONF-65-312-37
17	20-32555	ORAU. Gmelin, AED-CONF-65-312-34
20	20-32643	ORAU
22	20-32341	ORAU. Gmelin, AED-CONF-65-312-47
24	20-32561	ORAU. Gmelin, AED-CONF-65-312-54
CONF-651046–	**(12th National Symposium of the American Vacuum Society, New York, Oct. 1, 1965)**	
4	20-31392	ORAU. Gmelin, AED-CONF-65-403-1
CONF-651049–	**(IEEE Thermionic Conversion Specialist Conference, San Diego, Calif., Oct. 25–27, 1965)**	
14	20-31972	ORAU. Gmelin, AED-CONF-65-324-9
17	20-31974	ORAU. Gmelin, AED-CONF-65-324-12
19	20-31971	ORAU. Gmelin, AED-CONF-65-324-15
CONF-651062–	**(Metallurgical Society Fall Meeting, Detroit, Oct. 17–21, 1965)**	
6	20-31778	ORAU. Gmelin, AED-CONF-65-325-14
8	20-31781	ORAU. Gmelin, AED-CONF-65-325-18
CONF-651070–	**(18th Annual Gaseous Electronics Conference, Minneapolis, Oct. 20–22, 1965)**	
1	20-32646	ORAU. Gmelin, AED-CONF-65-395-3
3	20-32648	ORAU. Gmelin, AED-CONF-65-395-1
4	20-31947	ORAU. Gmelin, AED-CONF-65-395-4
CONF-651101–	**20-3647 20-9102**	**(American Nuclear Society, Winter Meeting, Washington, D. C., Nov. 15–18, 1965. Revised 11-8-65)**
65	20-32837	ORAU. Gmelin, AED-CONF-65-332-15
66	20-31806	ORAU. Gmelin, AED-CONF-65-332-13
67	20-32794	ORAU. Gmelin, AED-CONF-65-332-14
70	20-32780	ORAU. Gmelin, AED-CONF-65-332-21
71	20-32836	ORAU. Gmelin, AED-CONF-65-332-58
72	20-32857	ORAU. Gmelin, AED-CONF-65-332-22
74	20-32549	ORAU. Gmelin, AED-COND-65-332-100
76	20-32787	ORAU. Gmelin, AED-CONF-65-332-106
77	20-32364	ORAU. Gmelin, AED-CONF-65-332-45
CONF-651113–	**(18th Annual Conference on Engineering in Medicine and Biology, Philadelphia, Nov. 10–12, 1965)**	
2	20-31598	ORAU. Gmelin, AED-CONF-65-322-1
CONF-651118–	**(American Physical Society, Gatlinburg, Tenn., Nov. 11–13, 1965)**	
10	20-32563	ORAU. Gmelin, AED-CONF-65-329-9
16	20-32550	ORAU. Gmelin, AED-CONF-65-329-20
17	20-32567	ORAU. Gmelin, AED-CONF-65-329-21
CONF-651123–	**(Conference on Reactor Physics and Engineering, Budapest, Nov. 1965)**	
1	20-32879	ORAU
2	20-32875	ORAU
3	20-32781	ORAU
5	20-32870	ORAU
6	20-32871	ORAU
7	20-32783	ORAU
8	20-31597	ORAU
9	20-31596	ORAU
10	20-32876	ORAU
11	20-32880	ORAU
12	20-32782	ORAU
13	20-32878	ORAU
14	20-32367	ORAU
15	20-32366	ORAU
16	20-32873	ORAU
17	20-32872	ORAU
18	20-32877	ORAU
CONF-651126–	**(American Physical Society, 7th Annual Meeting of the Division of Plasma Physics, San Francisco, Nov. 8–11, 1965)**	
2	20-32645	ORAU. Gmelin, AED-CONF-65-353-19
3	20-32545	ORAU. Gmelin, AED-CONF-65-353-2
5	20-32644	ORAU. Gmelin, AED-CONF-65-353-13
9	20-32236	ORAU. Gmelin, AED-CONF-65-353-8
16	20-32669	ORAU. Gmelin, AED-CONF-65-353-39
CONF-651135–	**(American Physical Society, Southeastern Section, Charlottesville, Va., Nov. 1–3, 1965)**	
3	20-32543	ORAU. Gmelin, AED-CONF-65-402-4
CONF-651136–	**(International Space Electronics Symposium, Miami Beach, Fla., Nov. 2–4, 1965)**	
1	20-31618	ORAU. Gmelin, AED-CONF-65-343-11
2	20-31619	ORAU. Gmelin, AED-CONF-65-343-3
CONF-651140–	**(Society of Exploration Geophysicists, 35th Annual International Meeting, Dallas, Nov. 14–18, 1965)**	
1	20-31211	ORAU. Gmelin, AED-CONF-65-399-1
CONF-651141–	**(16th Annual Meeting of the Animal Care Panel, Philadelphia, Nov. 15–19, 1965)**	
1	20-31469	ORAU. Gmelin, AED-CONF-65-398-1
CONF-651145–	**(Symposium on Effect of Nuclear Radiations on Electronic Components, Lyon, France, Nov. 22–25, 1965)**	
Vol. 1	20-31620	
CONF-651212–	**(Ultrasonics Symposium, Boston, Dec. 1–4, 1965)**	
1	20-31780	ORAU. Gmelin, AED-CONF-65-348-2
CONF-651213–	**(American Physical Society, Winter Meeting in the West, Los Angeles, Dec. 20–22, 1965)**	
2	20-31492	ORAU. Gmelin, AED-CONF-65-400-15
8	20-32343	ORAU. Gmelin, AED-CONF-65-400-8
9	20-32542	ORAU. Gmelin, AED-CONF-65-400-16
11	20-32237	ORAU. Gmelin, AED-CONF-65-400-24
CONF-660105–	**20-32195**	**(3rd Conference on Symmetry Principles, Coral Gables, Jan. 19–21, 1966) $6.50**
CONF-660107–	**(American Physical Society Meeting, New York, Jan. 26–29, 1966)**	
2	20-32102	ORAU. Gmelin, AED-CONF-66-003-7
3	20-32547	ORAU. Gmelin, AED-CONF-66-003-13
4	20-32342	ORAU. Gmelin, AED-CONF-66-003-14
8	20-32548	ORAU. Gmelin, AED-CONF-66-003-12
14	20-32546	ORAU. Gmelin, AED-CONF-65-003-30
26	20-32239	ORAU. Gmelin, AED-CONF-66-003-55
32	20-32558	ORAU. Gmelin, AED-CONF-66-003-64
34	20-32556	ORAU. Gmelin, AED-CONF-66-003-57
37	20-31957	ORAU. Gmelin, AED-CONF-66-003-60

Report No.	Abstract No.	Availability
41	20-32103	ORAU. Gmelin, AED-CONF-66-003-91
42	20-32559	ORAU. Gmelin, AED-CONF-66-003-85
44	20-32212	ORAU. Gmelin, AED-CONF-66-003-103
45	20-32557	ORAU. Gmelin, AED-CONF-66-003-93
CONF-660108–	**(IEEE Winter Power Meeting, New York, Jan. 30–Feb. 4, 1966)**	
5	20-31973	ORAU
CONF-660109–	**(AIAA 3rd Aerospace Sciences Meeting, New York, Jan. 24–26, 1966)**	
1	20-31362	ORAU
CONF-660204–	**(American Nuclear Society Meeting, San Diego, Calif., Feb. 7–9, 1966)**	
9	20-32785	ORAU. Gmelin, AED-CONF-66-017-7
11	20-32551	ORAU. Gmelin, AED-CONF-66-017-10
CONF-660206–	**(Symposium on Neutron Noise, Waves, and Pulse Propagation, Gainesville, Feb. 14–16, 1966)**	
6	20-32363	ORAU. Gmelin, AED-CONF-66-014-2
7	20-32874	ORAU. Gmelin, AED-CONF-66-014-1
9	20-32786	ORAU. Gmelin, AED-CONF-66-014-6
10	20-32362	ORAU. Gmelin, AED-CONF-66-014-8
13	20-32784	ORAU. Gmelin, AED-CONF-66-014-13
14	20-32868	ORAU. Gmelin, AED-CONF-66-014-12
CONF-660207–	**(Radioisotope Applications in Aerospace Symposium, Dayton, Ohio, Feb. 15–17, 1966)**	
6	20-31622	ORAU. Gmelin, AED-CONF-66-011-9
7	20-31339	ORAU. Gmelin, AED-CONF-66-011-12
8	20-31496	ORAU. Gmelin, AED-CONF-66-011-10
10	20-31610	ORAU. Gmelin, AED-CONF-66-011-15
11	20-31494	ORAU. Gmelin, AED-CONF-66-011-5
12	20-31495	ORAU. Gmelin, AED-CONF-66-011-14
13	20-32347	ORAU. Gmelin, AED-CONF-66-011-16
16	20-31493	ORAU. Gmelin, AED-CONF-66-011-11
17	20-31609	ORAU. Gmelin, AED-CONF-66-011-20
18	20-31606	ORAU. Gmelin, AED-CONF-66-011-29
19	20-32365	ORAU. Gmelin, AED-CONF-66-011-28
20	20-31605	ORAU. Gmelin, AED-CONF-66-011-19
21	20-32740	ORAU
CONF-660209–	**(Conference on Intermediate Energy Physics, Williamsburg, Va., Feb. 9–11, 1966)**	
5	20-32100	ORAU. Gmelin, AED-CONF-66-023-5
10	20-31945	ORAU. Gmelin, AED-CONF-66-023-10
CONF-660211–	**(1st Midwest Symposium on Nondestructive Testing of Welds, Chicago, Feb. 1–4, 1966)**	
1	20-31713	ORAU. Gmelin, AED-CONF-66-010-1
CONF-660217–	**(Symposium on Interdisciplinary Aspects of Radiative Energy Transfer, Philadelphia, Feb. 24–26, 1966)**	
1	20-32670	ORAU. Gmelin, AED-CONF-66-013-3
2	20-32241	ORAU. Gmelin, AED-CONF-66-013-4
CONF-660303–	**(American Physical Society, Conference of Neutron Cross Section Technology, Washington, D. C., Mar. 22–24, 1966)**	
32	20-32839	ORAU. Gmelin, AED-CONF-66-034-3
33	20-32378	See NASA-TR-R-239
CONF-660304–	**(Institute of Electrical and Electronics Engineers, Scintillation and Semiconductor Counter Symposium, Washington, D. C., Mar. 2–4, 1966)**	
15	20-31513	See UCRL-14561
CONF-660310–	**(AIAA 5th Electric Propulsion Conference, San Diego, Calif., Mar. 7–9, 1966)**	
1	20-31385	ORAU
2	20-31387	ORAU
3	20-31386	ORAU
4	20-31388	ORAU
5	20-31375	ORAU
6	20-31776	ORAU
7	20-31389	ORAU
8	20-31364	ORAU
9	20-31373	ORAU
11	20-31384	ORAU
12	20-31382	ORAU
13	20-31383	ORAU
14	20-31381	ORAU
15	20-31369	ORAU
16	20-31948	ORAU
17	20-31376	ORAU
19	20-32650	ORAU
20	20-31377	ORAU
21	20-31378	ORAU
22	20-31379	ORAU
23	20-31380	ORAU
24	20-31371	ORAU
25	20-31372	ORAU
26	20-32653	ORAU
27	20-31363	ORAU
28	20-31365	ORAU
29	20-31370	ORAU
30	20-31366	ORAU
31	20-31367	ORAU
32	20-31368	ORAU
33	20-31374	ORAU
CONF-660311–	**(Symposium on Water Production Using Nuclear Energy, Tucson, Ariz., Mar. 30–Apr. 1, 1966)**	
3	20-32849	ORAU. Gmelin, AED-CONF-66-037-2
CONF-660315–	**(AIAA Plasmadynamics Conference, Monterey, Calif., Mar. 2–4, 1966)**	
1	20-32655	ORAU
2	20-32657	ORAU
3	20-32658	ORAU
4	20-32240	ORAU
5	20-32668	ORAU
6	20-32660	ORAU
7	20-32659	ORAU
8	20-32665	ORAU
9	20-32666	ORAU
10	20-32667	ORAU
11	20-32651	ORAU
12	20-32663	ORAU
13	20-31975	ORAU
14	20-32662	ORAU
15	20-32661	ORAU
16	20-32284	ORAU
17	20-31877	ORAU
18	20-32656	ORAU
19	20-32664	ORAU
CONF-660405–	**(Symposium on Radioecological Concentration Processes, Stockholm, Apr. 25–29, 1966)**	
13	20-31442	See BNWL-SA-661
15	20-31444	Dep. mn; CFSTI $1.00 cy, $0.50 mn
CONF-660411–	**(American Physical Society Meeting, Washington, D. C., Apr. 25–28, 1966)**	
3	20-31983	See CALT-68-71
CONF-660417–	**(International Symposium on the Structure of Low-Medium Mass Nuclei, Wright-Patterson AFB, Apr. 1966)**	
1	20-32372	See COO-1120-43
CONF-660502–	**(British Nuclear Energy Society Conference on Fast Breeder Reactors, London, May 1966)**	
1	20-32798	See LA-DC-7550
CONF-660503–	**(7th Japanese Conference on Radioisotopes, Tokyo, May 16–19, 1966)**	
3	20-31642	See ORNL-P-2190
CONF-660510–	**(International Conference on Isochronous Cyclotrons, Gatlinburg, Tenn., May 2–5, 1966)**	
6	20-31826	See UCD-CNL-47
7	20-31821	See ORNL-P-2239
8	20-31822	See ORNL-P-2260
10	20-31827	See UCRL-16794
CONF-660511–	**(International Symposium on Capsule Irradiation Experiments, Pleasanton, Calif., May 3–5, 1966)**	
5	20-32862	See ORNL-P-2160
7	20-31785	See ORNL-P-2162
CONF-660524–	**(2nd International Thorium Fuel Cycle Symposium, Gatlinburg, Tenn., May 3–6, 1966)**	
3	20-31690	See ORNL-P-2176

Report No.	Abstract No.	Availability
4	20-31689	See ORNL-P-2159
CONF-660527–	**(Symposium on Use of Computers in Analysis of Experimental Data and Control of Nuclear Facilities, Argonne, Ill., May 3–6, 1966)**	
2	20-32681	See BNL-10238
3	20-31661	See SLAC-PUB-191
CONF-660528–	**(9th Modulator Symposium, Fort Monmouth, N. J., May 12, 1966)**	
2	20-31825	See SLAC-PUB-192
CONF-660529–	**(Conference on the Calculation of the Properties of Vacancies and Interstitials, Skyland, Va., May 1–5, 1966)**	
1	20-32682	See ORNL-P-2193
2	20-32683	See ORNL-P-2194
CONF-660605–	**(Cryogenic Engineering Conference, Boulder, Colo., June 13–15, 1966)**	
2	20-32850	See LA-DC-7689
CONF-660611–	**(Society of Applied Spectroscopy Meeting, Chicago, June 14–15, 1966)**	
1	20-31168	Dep. mn; CFSTI $1.00 cy, $0.50 mn
CONF-660615–	**(American Chemical Society, Northwest Regional Meeting, Vancouver, B. C., June 16–17, 1966)**	
1	20-31319	See ISO-SA-10
2	20-31170	See ISO-SA-16
3	20-30998	See BNWL-SA-709
CONF-660616–	**(7th Annual Inst. of Nuclear Materials Management, Columbus, Ohio, June 15, 1966)**	
1	20-31174	See WAPD-T-1905
CONF-660618–	**20-31351**	**(Heat Transfer and Fluid Mechanics Inst. Conference, Santa Clara, Calif., June 22–24, 1966) $12.50**
CONF-660705–	**(IEEE Annual Conference, Palo Alto, Calif., July 18–22, 1966)**	
1	20-31613	See SC-DC-66-1443
2	20-31612	See SC-DC-66-1415
CONF-660801–	**(3rd International Heat Transfer Conference, Chicago, Aug. 8–12, 1966)**	
1	20-31341	See BNL-9546
CONF-660802–	**(11th International Symposium on Combustion, Berkeley, Calif., Aug. 14–20, 1966)**	
1	20-31216	See LA-DC-7659
2	20-31217	See LA-DC-7661
COO–		
7-0392	20-32433	Nucl. Phys., 83: 401-6(1966)
38-396	20-31294	Radiat. Res., 28: 215-31(1966)
38-395	20-31293	Radiat. Res., 28: 203-14(1966)
881-56	20-32043	Nuovo Cimento (10), 44A: 90-108(1966)
1018-1013	20-31507	Dep. mn; CFSTI $2.00 cy, $0.50 mn
1018-1021	20-31648	Dep. mn; CFSTI $2.00 cy, $0.50 mn
1018-1030	20-31649	Dep. mn; CFSTI $1.00 cy, $0.50 mn
1018-1031	20-31650	Dep. mn; CFSTI $3.00 cy, $0.75 mn
1018-1054	20-31651	Dep. mn; CFSTI $3.00 cy, $0.75 mn
1018-1057	20-31653	Dep. mn; CFSTI $1.00 cy, $0.50 mn
1018-1061	20-31653	Dep. mn; CFSTI $2.00 cy, $0.50 mn
1018-1066	20-31654	Dep. mn; CFSTI $6.00 cy, $1.25 mn
1018-1075	20-31508	Dep. mn; CFSTI $3.00 cy, $0.75 mn
1018-1076	20-31655	Dep. mn; CFSTI $5.00 cy, $1.00 mn
1088-20	20-31268	Dep. mn; CFSTI $1.00 cy, $0.50 mn
1120-43	20-32372	Dep. mn; CFSTI $2.00 cy, $0.50 mn
1170-5	20-30970	ORAU
1198-324	20-32336	Rev. Sci. Instrum., 37: 819-31(1966)
1198-375	20-32329	Phys. Rev. Lett., 17: 74-8(1966)
1233-26	20-32632	Rev. Sci. Instrum., 37: 897-900(1966)
1319-39	20-31676	Dep. mn; CFSTI $2.00 cy, $0.50 mn
1469-0012	20-31654	See COO-1018-1066
1469-0017	20-31655	See COO-1018-1076
1530-1	20-32373	Dep. mn; CFSTI $2.00 cy, $0.50 mn
CRRP–	**(Canadian)**	
1233	20-32763	See AECL-2543
CRT–	**(Canadian)**	
1149	20-31646	See AECL-1744
1149(Pt.A)(Add.1)	20-31647	See AECL-1744(Pt.A)(Add.1)
CU–	**(Misc.)**	
17-64	20-31637	See NYO-755-1
254	20-31986	See NEVIS-148
D–	**(Misc.)**	
1-82-0508	20-31169	
1-82-0522	20-32570	
DP–		
991	20-32859	Dep. mn; CFSTI $3.00 cy, $0.75 mn
ECOM–	**(Non-AEC)**	
2680	20-31498	See AD-632527
EIR–	**(Swiss)**	
97	20-31509	Dep. mn
ER–	**(Misc.)**	
7777(Vol.3)	20-32674	See NP-15697(Vol.3)
8207	20-32861	See N-66-12348
EUR–	**(European Atomic Energy Community)**	
2650	20-31342	See EURAEC-1482
EURAEC–		
1460	20-31677	See GEAP-4840
1482	20-31342	Dep. mn; CFSTI $2.00 cy, $0.50 mn
FRPC-FEWP–	**(British)**	
P(65)298	20-31675	See CONF-651009-27
FTD-TT–	**(Non-AEC)**	
65-1447	20-31720	For translation see AD-629415
65-1888	20-31721	For translation see AD-630971
FTI–	**(Non-AEC)**	
16(6.1)	20-31782	Dep. mn
GEAP–	**(Misc.)**	
4840	20-31677	Dep. mn; CFSTI $3.00 cy, $0.75 mn
5056	20-31343	Dep. mn; CFSTI $2.00 cy, $0.50 mn
5108	20-32860	Dep. mn; CFSTI $3.00 cy, $0.75 mn
HIT–		
3583-24	20-31678	Dep. mn; CFSTI $1.00 cy, $0.50 mn
HMI-B–	**(German)**	
46	20-31165	Dep. mn
IAE–	**(Non-AEC)**	
957	20-32765	Dep. mn
IC–	**(Misc.)**	
66/48	20-32107	Dep. mn
66/54	20-31984	Dep. mn
66/57	20-31985	Dep. mn
66/59	20-32108	Dep. mn
IDO–		
17175	20-31656	Dep. mn; CFSTI $2.00 cy, $0.50 mn
IITRI–	**(Misc.)**	
578P25-15	20-32374	Dep. mn; CFSTI $1.00 cy, $0.50 mn
B6042-5	20-31709	
IPP–	**(Non-AEC)**	
1/2	20-32571	Dep. mn
6/49	20-32572	Dep. mn
IS–		
1253	20-32445	Nucl. Phys., 83: 584-92(1966)
1273	20-32443	Nucl. Phys., 83: 545-74(1966)
ISO-SA–		
10	20-31319	Dep. mn; CFSTI $1.00 cy, $0.50 mn
16	20-31170	Dep. mn; CFSTI $1.00 cy, $0.50 mn

Report No.	Abstract No.	Availability
ITEF–	**(Russian)**	
351	20-32375	Dep. mn
385	20-31818	Dep. mn
JPL-TR–	**(Non-AEC)**	
32-630	20-31880	
JPRS–	**(Non-AEC)**	
35315	20-30962	CFSTI $3.00 cy, $0.75
K–		
1670	20-31478	Dep. mn; CFSTI $2.00 cy, $0.50 mn
1671	20-31327	Dep. mn; CFSTI $4.00 cy, $1.00 mn
KAPL–		
3090	20-32376	Dep. mn; CFSTI $2.00 cy, $0.50 mn
KAPL-M–		
6536	20-32350	Dep. mn; CFSTI $2.00 cy, $0.50 mn
6539	20-31328	Dep. mn; CFSTI $2.00 cy, $0.50 mn
6543	20-31329	Dep. mn; CFSTI $1.00 cy, $0.50 mn
6546	20-31330	Dep. mn; CFSTI $1.00 cy, $0.50 mn
6548	20-31657	Dep. mn; CFSTI $1.00 cy, $0.50 mn
6550	20-32766	Dep. mn; CFSTI $1.00 cy, $0.50 mn
KFK–	**(German)**	
117	20-32377	Dep. mn
LA–		
3497	20-31344	Dep. mn; CFSTI $5.00 cy, $1.00 mn
3507	20-31215	Dep. mn; CFSTI $1.00 cy, $0.50 mn
3521	20-31819	Dep. mn; CFSTI $3.00 cy, $0.75 mn
3524	20-31679	Dep. mn; CFSTI $3.00 cy, $0.75 mn
LA-DC–		
7460	20-32596	J. Appl. Phys., 37: 2541-50(1966)
7479	20-32406	Health Phys., 12: 865(1966)
7550	20-32798	Dep. mn; CFSTI $1.00 cy, $0.50 mn
7588	20-31048	Genetics, 53: 875-82(1966)
7633	20-31239	J. Phys. Chem., 70: 1943-9(1966)
7638	20-32514	Phys. Rev., 147: 845-52(1966)
7659	20-31216	Dep. mn; CFSTI $2.00 cy, $0.50 mn
7661	20-31217	Dep. mn; CFSTI $2.00 cy, $0.50 mn
7689	20-32850	Dep. mn; CFSTI $1.00 cy, $0.50 mn
7748	20-32797	Dep. mn; CFSTI $1.00 cy, $0.50 mn
7752	20-32799	Dep. mn; CFSTI $1.00 cy, $0.50 mn
7785	20-32314	Cyrog. Eng. News, 1: No. 8, 32-6(1966)
7872	20-31748	J. Less-Common Metals, 11: 135-40(1966)
LAC-ER–	**(Non-AEC)**	
8538	20-31784	See NASA-CR-54976
LNF–	**(Italian)**	
66/14	20-31820	Dep. mn
M–	**(Misc.)**	
65-30	20-31448	See RLO-1725-15
65-31	20-31449	See RLO-1725-16
65-32	20-31450	See RLO-1725-17
65-33	20-31451	See RLO-1725-18
65-34	20-31452	See RLO-1725-19
MATT–		
423	20-32611	Phys. Fluids, 9: 1110-14(1966)
MF–	**(Misc.)**	
47	20-32218	See NYO-1480-29
48	20-32576	See NYO-1480-50
50	20-32577	See NYO-1480-54
MIT–	**(Misc.)**	
2098-225	20-32496	Phys. Rev., 147: 710-14(1966)
N–	**(Misc.)**	
65-12416	20-31445	CFSTI $4.00 cy, $0.75 mn
65-12780	20-32573	
65-30544	20-32851	CFSTI $2.00 cy, $0.50 mn
65-32035	20-32574	CFSTI $2.00 cy, $0.50 mn
65-33713	20-32217	CFSTI $2.00 cy, $0.50 mn
65-33971	20-31510	CFSTI $1.00 cy, $0.50 mn
65-34224	20-31901	CFSTI $2.00 cy, $0.50 mn
66-12348	20-32861	CFSTI $5.00 cy, $1.00 mn
66-12435	20-31356	
66-13126	20-32244	CFSTI $2.00 cy, $0.50 mn
66-16249	20-31902	CFSTI $1.00 cy, $0.50 mn
66-16447	20-31960	CFSTI $4.00 cy, $1.25 mn
66-16702	20-31903	CFSTI $3.00 cy, $0.75 mn
66-16936	20-31511	CFSTI $1.00 cy, $0.50 mn
66-17084	20-32293	CFSTI $3.00 cy, $0.50 mn
NAA-SR-Memo–		
11454	20-32852	Dep. mn; CFSTI $3.00 cy, $0.75 mn
11652	20-31680	Dep. mn; CFSTI $4.00 cy, $1.00 mn
11653	20-31658	Dep. mn; CFSTI $2.00 cy, $0.50 mn
11707	20-31681	CFSTI $1.00 cy, $0.50 mn
11731	20-32791	Dep. mn; CFSTI $2.00 cy, $0.50 mn
11786	20-32672	Dep. mn; CFSTI $1.00 cy, $0.50 mn
11872	20-32673	Dep. mn; CFSTI $1.00 cy, $0.50 mn
11925	20-32853	Dep. mn; CFSTI $2.00 cy, $0.50 mn
NASA-CR–	**(Misc.)**	
507	20-31688	CFSTI $3.00 cy, $0.50 mn
54770	20-32861	See N-66-12348
54905	20-32768	See UNC-5148
54976	20-31784	
54983	20-31710	
58153	20-32217	See N-65-33713
59196	20-31033	CFSTI $2.00 cy, $0.50 mn
64248	20-32851	See N-65-30544
64582	20-32574	See N-65-32035
67078	20-31510	See N-65-33971
69849	20-31902	See N-66-16249
69861	20-31960	See N-66-16447
70036	20-31903	See N-66-16702
70301	20-32293	See N-66-17084
NASA-TM–	**(Misc.)**	
X-53351	20-32244	See N-66-13126
X-54859	20-31445	See N-65-12416
X-55289	20-31901	See N-65-34224
NASA-TN–	**(Misc.)**	
D-3169	20-31511	See N-66-16936
D-3372	20-32575	CFSTI $0.35 cy, $0.50 mn
D-3467	20-31711	CFSTI $1.00 cy, $0.50 mn
NASA-TR–	**(Non-AEC)**	
R-239	20-32378	CFSTI $1.00 cy, $0.50 mn
NE–	**(Misc.)**	
5	20-32863	See TID-23037
NEVIS–	**(Misc.)**	
148	20-31986	Dep. mn; CFSTI $3.00 cy, $0.75 mn
NP–	**(AEC File No. for Non-AEC Reports)**	
15697(Vol.3)	20-32674	
15930	20-31954	Rev. Geophys., 4: 177-221(1966)
16003	20-31682	
16015	20-31446	Dep. mn
16097	20-31987	Dep. mn
NRL–	**(Misc.)**	
F19	20-31446	See NP-16015
NSJ-tr–	**(Japanese)**	
47	20-31345	Dep. mn; JCL $1.60 fs, $0.80 mf; JAERI
48	20-32245	Dep. mn; JCL $1.10 fs, $0.80 mf; JAERI
49	20-31398	Dep. mn; JCL $1.10 fs, $0.80 mf; JAERI
56	20-31269	Dep. mn; JCL $1.60 fs, $0.80 mf; JAERI
NYO–		
755-1	20-31637	Dep. mn; CFSTI $6.00 cy, $1.25 mn
901-34	20-31458	Health Phys., 12: 737-41(1966)
1480-29	20-32218	Dep. mn; CFSTI $4.00 cy, $0.75 mn
1480-50	20-32576	Dep. mn; CFSTI $5.00 cy, $1.00 mn
1480-54	20-32577	Dep. mn; CFSTI $2.00 cy, $0.50 mn
2262-110	20-32111	Amer. J. Phys., 34: 597-601(1966)
2581-100	20-31743	J. Less-Common Met., 11: 67-9(1966)
3454-2	20-32699	J. Chem. Phys.. 44: 4651-2(1966)
3569-1	20-31625	Dep. mn; CFSTI $1.75 cy, $1.00 mn
ORINS–		
45	20-30971	Dep. mn; CFSTI $1.00 cy, $0.50 mn

Report No.	Abstract No.	Availability
ORNL–		
3882	20-32841	Dep. mn; CFSTI $3.00 cy, $0.50 mn
3936	20-32800	Dep. mn; CFSTI $6.00 cy, $1.25 mn
3944	20-32743	Dep. mn; CFSTI $3.00 cy, $0.75 mn
3956	20-31447	Dep. mn; CFSTI $2.00 cy, $0.50 mn
ORNL-P–	**(Misc.)**	
118	20-31085	Radiat. Res., 28: 157-65(1966)
983	20-31040	Advance. Radiat. Biol., 2: 135-66(1966)
1012	20-31041	Advance. Radiat. Biol., 2: 167-91(1966)
1654	20-31047	Genetics, 53: 855-62(1966)
1746	20-32295	Amer. J. Phys., 34: 606-10(1966)
1780	20-32356	Health Phys., 12: 856-7(1966)
1838	20-31831	Nucl. Instrum. Methods, 42: 128-33(1966)
1995	20-32429	Nucl. Phys., 83: 353-63(1966)
1997	20-32708	Phys. Rev., 147: 515-17(1966)
2012	20-32519	Phys. Rev., 147: 870-80(1966)
2055	20-32510	Phys. Rev., 147: 812-25(1966)
2144	20-32624	Phys. Rev. Lett., 16: 1152-3(1966)
2159	20-31689	Dep. mn; CFSTI $2.00 cy, $0.50 mn
2160	20-32862	Dep. mn; CFSTI $2.00 cy, 0.50 mn
2162	20-31785	Dep. mn; CFSTI $2.00 cy, $0.50 mn
2176	20-31690	Dep. mn; CFSTI $2.00 cy, $0.50 mn
2190	20-31642	Dep. mn; CFSTI $1.00 cy, $0.50 mn
2193	20-32682	Dep. mn; CFSTI $1.00 cy, $0.50 mn
2194	20-32683	Dep. mn; CFSTI $1.00 cy, $0.50 mn
2229	20-32471	Phys. Lett., 21: 657-9(1966)
2239	20-31821	Dep. mn; CFSTI $1.00 cy, $0.50 mn
2260	20-31822	Dep. mn; CFSTI $1.00 cy, $0.50 mn
ORNL-TM–		
1160	20-32675	Dep. mn; CFSTI $3.00 cy, $0.75 mn
1208	20-32379	Dep. mn; CFSTI $1.00 cy, $0.50 mn
1337	20-31588	Rev. Sci. Instrum., 37: 919-22(1966)
1497	20-31659	Dep. mn; CFSTI $4.00 cy, $0.75 mn
ORNL-tr–		
1227	20-31722	Dep. mn; JCL $2.60 fs, $1.07 mf
ORO–		
596	20-31171	Dep. mn; CFSTI $3.00 cy, $0.50 mn
2430-27	20-32311	Dep. mn; CFSTI $4.00 cy, $1.00 mn
2891-5	20-31786	Dep. mn; CFSTI $2.00 cy, $0.50 mn
PATENTS–	**(British)**	**(4s. 6d. each, U. K. Patent Office)**
1,026,694	20-32761	
1,030,543	20-31472	
1,030,951	20-31636	
1,031,153	20-31705	
1,031,154	20-31706	
1,031,515	20-32762	
1,031,678	20-31707	
1,031,862	20-31980	
1,031,921	20-31979	
PATENTS–	**(Canadian)**	
733,608	20-32758	
733,609	20-32759	
734,864	20-31702	
735,057	20-31603	
735,587	20-32756	
735,588	20-32755	
PATENTS–	**(German)**	
1,213,539	20-31604	
1,213,542	20-32793	
1,213,543	20-32642	
1,213,544	20-32757	
1,213,545	20-32789	
1,213,546	20-31851	
PATENTS–	**(U. S.)**	**($0.50 each, U. S. Patent Office)**
3,252,046	20-31497	
3,255,086	20-32760	
3,257,560	20-32368	
3,257,571	20-31978	
3,257,577	20-31852	
3,258,429	20-32747	
3,261,378	20-31704	
PIBAL–	**(Non-AEC)**	
860	20-32573	See N-65-12780
PNE–		
481	20-32885	CFSTI $9.25 cy
711F	20-31393	Dep. mn; CFSTI $1.50 cy, $0.50 mn
PUR–	**(Non-AEC)**	
937-177	20-32520	Phys. Rev., 147: 881-3(1966)
R–	**(Misc.)**	
2-66	20-31660	See RISO-M-385
548	20-31986	See NEVIS-148
RCN-INT–	**(Dutch)**	
66-013	20-32874	See CONF-660206-7
RHEL/R–	**(British)**	
106	20-31832	Nucl. Instrum. Methods, 42: 141-53(1966)
RISO-M–	**(Danish)**	
385	20-31660	Dep. mn
RLO–		
1725-15	20-31448	Dep. mn; CFSTI $5.00 cy, $1.00 mn
1725-16	20-31449	Dep. mn; CFSTI $5.00 cy, $1.00 mn
1725-17	20-31450	Dep. mn; CFSTI $6.00 cy, $1.50 mn
1725-18	20-31451	Dep. mn; CFSTI $5.00 cy, $1.00 mn
1725-19	20-31452	Dep. mn; CFSTI $6.00 cy, $1.50 mn
1776-2	20-31397	Dep. mn; CFSTI $4.00 cy, $0.75 mn
1780-7	20-31034	Dep. mn; CFSTI $3.00 cy, $0.75 mn
1780-8	20-31035	Dep. mn; CFSTI $2.00 cy, $0.50 mn
RPP-N–	**(British)**	
5	20-31823	Dep. mn
SAN–		
529-3	20-31036	Dep. mn; CFSTI $1.00 cy, $0.50 mn
SC-DC–		
66-1115	20-31961	Dep. mn; CFSTI $3.00 cy, $0.50 mn
66-1415	20-31612	Dep. mn; CFSTI $1.00 cy, $0.50 mn
66-1443	20-31613	Dep. mn; CFSTI $1.00 cy, $0.50 mn
SC-RR–		
66-229	20-32380	Dep. mn; CFSTI $2.00 cy, $0.50 mn
SCL-DC–		
66-2	20-32219	CFSTI $1.95
SGAE-BL–	**(Austrian)**	
17/1966	20-31172	Dep. mn
18/1966	20-31173	Dep. mn
SGAE-PH–	**(Austrian)**	
37/1966	20-32381	Dep. mn
SGAE-SS–	**(Austrian)**	
5/1966	20-31512	Dep. mn
SLAC–		
62	20-31823	Dep. mn; CFSTI $4.00 cy, $0.75 mn
SLAC-PUB–		
154	20-31916	J. Appl. Phys., 37: 2916-17(1966)
160	20-32503	Phys. Rev., 147: 763-73(1966)
191	20-31661	Dep. mn; CFSTI $1.00 cy, $0.50 mn
192	20-31825	Dep. mn; CFSTI $1.00 cy, $0.50 mn
SRIA–		
1	20-32744	Dep. mn; CFSTI $3.00 cy, $0.75 mn
STI-DOC–	**(International Atomic Energy Agency)**	
10/51	20-32842	IAEA $3.00; S63,-; 18/-stg; F.Fr 12,-; DM 10,50
10/52	20-32807	IAEA $8.00; S168,-; £2.8.0; F.Fr 32,-; DM 28,-
10/53	20-32886	IAEA $1.00; S21,-; 6/-stg; F.Fr 4,-; DM 3,20
STI-PUB–	**(International Atomic Energy Agency)**	
121	20-31453	IAEA $2.50; S52,50; 15/-stg; F.Fr 10,-; DM 8,-

Report No.	Abstract No.	Availability
TID–		
3735	20-32887	Dep.; DTI Extension Free
3910(Suppl.4)	20-30967	Dep. mn; CFSTI $1.50 cy, $1.00 mn
21416	20-32459	Nucl. Phys., 84: 398-410(1966)
22027	20-30972	Dep. mn; CFSTI $1.00 cy, $0.50 mn
22413	20-31526	Health Phys., 12: 851-2(1966)
22556	20-32030	Nuovo Cimento (10), 43A: 1047-61(1966)
22640	20-31091	Radiat. Res., 28: 278-88(1966)
22641	20-31589	Rev. Sci. Instrum., 37: 934-8(1966)
22804	20-32059	Phys. Lett., 21: 669-71(1966)
22969	20-31149	Dep. mn; CFSTI $1.00 cy, $0.50 mn
22973	20-32808	Dep. mn; CFSTI $4.00 cy, $0.75 mn
23020	20-31662	Dep. mn; CFSTI $3.00 cy, $0.75 mn
23025	20-32578	Dep. mn; CFSTI $1.00 cy, 0.50 mn
23030	20-31807	Dep. mn; CFSTI $2.00 cy, $0.50 mn
23037	20-32863	Dep. mn; CFSTI $3.00 cy, $0.75 mn
23101	20-32809	Dep. mn; CFSTI $2.00 cy, $0.50 mn
TLW–	**(Misc.)**	
1105	20-31424	See CONF-650616-26
TN–	**(Non-AEC)**	
100	20-32293	See N-66-17084
TT–	**(Canadian)**	
66-31751	20-30962	See JPRS-35315
UCB–	**(Misc.)**	
34P95-7	20-30999	Dep. mn; CFSTI $1.00 cy, $0.50 mn
UCD-CHL–		
47	20-31826	Dep. mn; CFSTI $1.00 cy, $0.50 mn
UCRL–		
11510	20-31988	Dep. mn; CFSTI $3.00 cy, $0.75 mn
14227(Rev.1)	20-31712	Dep. mn; CFSTI $1.00 cy, $0.50 mn
14327	20-31936	Rev. Mod. Phys., 38: 513-40(1966)
14519-T	20-32012	Nuovo Cimento (10), 43A: 591-6(1966)
14533-T	20-32139	Nuovo Cimento (10), 43A: 995-1009(1966)
14561	20-31513	Dep. mn; CFSTI $1.00 cy, $0.50 mn
14563	20-31810	J. Appl. Phys., 37: 2787-9(1966)
14582-T(Rev.1)	20-32382	Dep. mn; CFSTI $3.00 cy, $0.75 mn
14616	20-31331	Dep. mn; CFSTI $6.00 cy, $1.25 mn
14663	20-31846	Rev. Sci. Instrum., 37: 964(1966)
14708	20-32506	Phys. Rev., 147: 789-92(1966)
14720	20-32767	Dep. mn; CFSTI $3.00 cy, $0.50 mn
14777	20-31787	Appl. Phys. Lett., 8: 316-18(1966)
14881	20-31514	Dep. mn; CFSTI $1.00 cy, $0.50 mn
14912-T	20-32220	Dep. mn; CFSTI $2.00 cy, $0.50 mn
16108	20-31320	Dep. mn; CFSTI $5.00 cy, $1.00 mn
16150(Rev.)	20-31238	J. Phys. Chem., 70: 1762-6(1966)
16275	20-31989	Dep. mn; CFSTI $4.00 cy, $0.75 mn
16335	20-32015	Nuovo Cimento (10), 43A: 684-700(1966)
16361	20-32185	Rev. Mod. Phys., 38: 476-82(1966)
16465	20-32011	Nuovo Cimento (10), 43A: 553-75(1966)
16474	20-32025	Nuovo Cimento (10), 43A: 865-74(1966)
16548	20-32453	Nucl. Phys., 84: 302-4(1966)
16581	20-31904	Dep. mn; CFSTI $1.00 cy, $0.50 mn
16592	20-32265	J. Geophys. Res., 71: 2791-8(1966)
16648	20-31990	Dep. mn; CFSTI $3.00 cy, $0.75 mn
16658	20-32888	Dep. mn; CFSTI $5.00 cy, $1.00 mn
16673	20-32458	Nucl. Phys., 84: 385-97(1966)
16691	20-31150	Dep. mn; CFSTI $1.00 cy, $0.50 mn
16771	20-31991	Dep. mn; CFSTI $3.00 cy, $0.50 mn
16794	20-31827	Dep. mn; CFSTI $1.00 cy, $0.50 mn
16799	20-32069	Phys. Rev. Lett., 17: 113-15(1966)
16868	20-32068	Phys. Rev. Lett., 17: 107-13(1966)
UNC–	**(Misc.)**	
5148	20-32768	
UR–		
875-109	20-32127	Nuovo Cimento (10), 43A: 597-614(1966)
URS–	**(Non-AEC)**	
651-4	20-31332	
USNRDL-TR–	**(Misc.)**	
967	20-31454	CFSTI $4.00 cy, $0.75 mn
997	20-31611	See AD-633468
998	20-31026	See AD-633606
1008	20-31814	See AD-634300
1012	20-31499	See AD-633752
WAPD-T–		
1866	20-31739	J. Appl. Phys., 37: 2805-8(1966)
1905	20-31174	Dep. mn; CFSTI $2.00 cy, $0.50 mn
WIS-TCI–	**(Misc.)**	
145	20-31902	See N-66-16249
WNY–	**(Misc.)**	
021	20-31625	See NYO-3569-1
X–	**(Misc.)**	
641-65-306	20-31901	See N-65-34224
Y–		
1533	20-31479	Cep. mn; CFSTI $2.00 cy, $0.50 mn
1535	20-31480	Dep. mn; CFSTI $1.00 cy, $0.50 mn
1541	20-31333	Dep. mn; CFSTI $1.00 cy, $0.50 mn
YALE–		
1807-30	20-32423	Nucl. Phys., 83: 259-73(1966)

DEPOSITORIES OF USAEC REPORTS

In Countries Other than the U.S.

ARGENTINA
Buenos Aires, Comisión Nacional de Energía Atómica
AUSTRALIA
Canberra, Australian National Library
Sutherland, New South Wales, Australian Atomic Energy Commission
AUSTRIA
Vienna, Zentral Bibliothek der Physikalischen Institute der Universität
BELGIUM
Mol-Donk, Centre d'Etude de l'Energie Nucleaire
BOLIVIA
La Paz, Comisión Nacional de Energiá Nuclear
BRAZIL
Rio de Janeiro, Instituto Brasileiro de Bibliografia e Documentacao
São Paulo, Instituto de Energia Atomica, Cidade Universitaria São Paulo
BURMA
Rangoon, Union of Burma Applied Research Institute, Atomic Energy Center Library
CANADA
Hamilton, McMaster University
Ottawa, National Research Council Library
Vancouver, University of British Columbia
CHILE
Santiago, Departamento de Fisica, Universidad de Chile
CHINA
Hsinchu, Taiwan, Free China, National Tsing Hua University
COLOMBIA
Bogota, Instituto De Asuntos Nucleares
COSTA RICA
San Pedro, University of Costa Rica Library
DENMARK
Risö, Danish Atomic Energy Commission
ECUADOR
Quito, Escuela Politécnica Nacional
EL SALVADOR
San Salvador, Universidad de El Salvador, Biblioteca de Energia Nuclear
FINLAND
Helsinki, Teknillisen Korkeakoulun Kirjasto
FRANCE
Gif-sur-Yvette, Centre d'Etudes Nucléaires de Saclay
Paris, Académie des Sciences
GERMANY
Berlin, Hahn-Meitner-Institut für Kernforschung Berlin
Frankfurt/Main, Gmelin-Institut
Munich, Technische Hochschule, Bibliothek
GHANA
Accra, University College of Ghana
GREECE
Athens, Nuclear Research Center "Democritus"
GUATEMALA
Guatemala, Comisión Nacional de Energía Nuclear
INDIA
Bombay, Department of Atomic Energy
IRAN
Tehran, Tehran University Nuclear Centre
IRAQ
Baghdad, Iraqi Atomic Energy Commission
IRELAND
Dublin, University College
ISRAEL
Rehovoth, Israel Atomic Energy Commission
ITALY
Rome, Centro di Studi Nucleari della Casaccia
Rome, Comitato Nazionale per l'Energia Nucleare
JAPAN
Tokyo, National Diet Library
KOREA
Seoul, Office of Atomic Energy
LEBANON
Beirut, Lebanese National Council for Scientific Research
LUXEMBOURG
Luxembourg, Ministry of Transport and Electricity
MALAYSIA
Kuala Lumpur, University of Malaysia
MEXICO
Mexico, D.F., Comisión Nacional de Energía Nuclear
NETHERLANDS
The Hague, Reactor Centrum Nederland
NEW ZEALAND
Lower Hutt, Institute of Nuclear Sciences
NIGERIA
Ibadan, University of Ibadan
NORWAY
Lilleström, Institutt för Atomenergi
PAKISTAN
Lahore, West Pakistan, Atomic Energy Centre
PERU
Lima, Junta de Control de Energia Atomica
PHILIPPINE REPUBLIC
Manila, Philippine Atomic Energy Commission
POLAND
Warsaw, Biura Pelnomocnika Rzadu do Spraw Wykorzystania Energii Jadrowej
PORTUGAL
Sacavem, Junta de Energía Nuclear
REPUBLIC OF SOUTH AFRICA
Pretoria, Atomic Energy Board Library
REPUBLIC OF THE CONGO
Leopoldville, Université Lovanium
SPAIN
Madrid, Junta de Energía Nuclear, Biblioteca Documentación y Publicaciones, Ciudad Universitaria
SWEDEN
Nyköping, Aktiebolaget Atomenergi
SWITZERLAND
Zürich, Eidgenössische Technische Hochschule, Bibliothek
THAILAND
Bangkok, Office of the Thai Atomic Energy Commission, Department of Science
TURKEY
Ankara, Turkish Atomic Energy Commission, Atomic Energy Library
UNITED ARAB REPUBLIC
Cairo, Atomic Energy Commission
UNITED KINGDOM
Birmingham, Central Library
Boston Spa, National Lending Library for Science and Technology
Kingston upon Hull, Central Library
Liverpool, Central Library
London, Central Library, Acton
London, National Reference Library
London, Science Museum Library, South Kensington
Manchester, Central Library
Newcastle upon Tyne, Central Library
Nottingham, Central Library
Sheffield, Central Library
URUGUAY
Montevideo, Comision Nacional de Energia Atomica
VENEZUELA
Caracas, Instituto Venezolano de Investigaciones Científicas
VIET-NAM
Saigon, Atomic Energy Office
YUGOSLAVIA
Belgrade, Federal Commission for Nuclear Energy

In International Agencies

AUSTRIA
Vienna, International Atomic Energy Agency
BELGIUM
Brussels, La Bibliotheque EURATOM
FRANCE
Paris, European Nuclear Energy Agency, O.E.C.D.
ITALY
Ispra, EURATOM Research Center
SWITZERLAND
Geneva, United Nations Library

UNITED STATES
GOVERNMENT PRINTING OFFICE
DIVISION OF PUBLIC DOCUMENTS
WASHINGTON, D.C. 20402

OFFICIAL BUSINESS

POSTAGE AND FEES PAID
U.S. GOVERNMENT PRINTING OFFICE

TECHNICAL PROGRESS REVIEWS

The Division of Technical Information, U. S. Atomic Energy Commission, also publishes the Technical Progress Reviews, a series of five quarterly journals on nuclear technology. These journals, compiled by specialists and recognized authorities, summarize, evaluate, and reference the progress of development in five important fields.

Isotopes and Radiation Technology P. S. Baker, A. F. Rupp, and associates, Oak Ridge National Laboratory. Reviews AEC-sponsored projects and related significant worldwide developments in radioisotopes and radiation technology.

Nuclear Safety Wm. B. Cottrell, W. H. Jordan, and associates, Oak Ridge National Laboratory. Covers topics relevant to the analysis and control of hazards associated with nuclear reactors and with operations involving fissionable materials and the products of nuclear fission.

Power Reactor Technology Argonne National Laboratory. Reviews research, development, design practices, and operating experiences associated with power reactors, including aerospace applications.

Reactor Fuel Processing Stephen Lawroski and associates, Argonne National Laboratory. Reviews all aspects of the fuel-processing field, including aqueous and nonaqueous processing and waste disposal.

Reactor Materials R. W. Dayton, E. M. Simons, and associates, Battelle Memorial Institute. Covers the properties, behavior, and fabrication processes of materials used in nuclear reactors and associated equipment.

Availability

SUBSCRIPTION RATE: The Technical Progress Reviews may be purchased from the Superintendent of Documents, U. S. Government Printing Office, Washington, D. C. 20402, at $2.50 per year for each subscription or $0.70 per issue.

POSTAGE: Postpaid within the United States, Canada, Mexico, and all Central and South American countries except Argentina, Brazil, British and French Guiana, Surinam, and British Honduras. For these Central and South American countries and all other countries, add $0.75 per year or $0.20 per single issue.

REMITTANCE: Payment should be by check, money order, or document coupons and MUST accompany order. Remittances from foreign countries should be made by international money order or draft on an American bank payable to the Superintendent of Documents or by UNESCO book coupons.